Christophe Hendrickx

BSc in Geology, MSc in Paleobiology

Evolution of Teeth and Quadrate in Non-avian Theropoda (Dinosauria: Saurischia), with the Description of *Torvosaurus* Remains from Portugal

Dissertação para obtenção do Grau de Doutor em Geologia, especialidade de Paleontologia

Orientador: Prof. Octávio Mateus,
Faculdade de Ciências e Tecnologia, Universidade Nova de Lisboa

Júri:

Presidente:	Prof. Doutora Maria Paula Diogo
Arguentes:	Doutor Stephen Brusatte
	Prof. Doutor Martin Sander
Vogais:	Prof. Doutor Miguel Telles Antunes

FACULDADE DE CIÊNCIAS E TECNOLOGIA
UNIVERSIDADE NOVA DE LISBOA

May 2015

2015

Evolution of Teeth and Quadrate in non-avian Theropoda (Dinosauria: Saurischia) with the Description of *Torvosaurus* Remains from Portugal

Christophe Hendrickx

Artistic reconstruction of adult *Torvosaurus gurneyi* with two hatchlings. © Sergey Krasovskiy.

Kurt Schwenk (2000: p. 9): "Good descriptive morphology is as rare as it is beautiful, virtually an art. Unfortunately, it may be a dying art because it is little valued within the context of modern science. [...] it may represent the only truly hard, objective data in morphological research, as free of fashion and interpretation as possible. It is, therefore, timeless."

John H. Ostrom and Peter Wellnhofer (1986: p. 148): "The single greatest source of frustration in taxonomic studies of fossil organisms is morphologic variation and its causes. Yet, in the absence of any other taxonomic criteria, we are dependent on morphologic differences in distinguishing between different taxa. Our assumption is that such anatomical differences reflect genetic distinction. Unhappily, that assumption cannot be tested. And even though everyone knows that there will be anatomical differences between any two individuals, a long standing paleontological tradition emphasises these differences in establishing new taxa while underrating morphological similarities."

Richard Owen (1842: p. 103): "The combination of such characters, some, as the sacral ones, altogether peculiar among Reptiles, others borrowed, as it were, from groups now distinct from each other, and all manifested by creatures far surpassing in size the largest of existing reptiles, will, it is presumed, be deemed sufficient ground for establishing a distinct tribe or sub-order of Saurian Reptiles, for which I would propose the name of *Dinosauria**."
"* Gr. δεινός, fearfully great; σαῦρος, a lizard."

Henry Jones Jr. (1984): "Nothing shocks me. I'm a scientist."

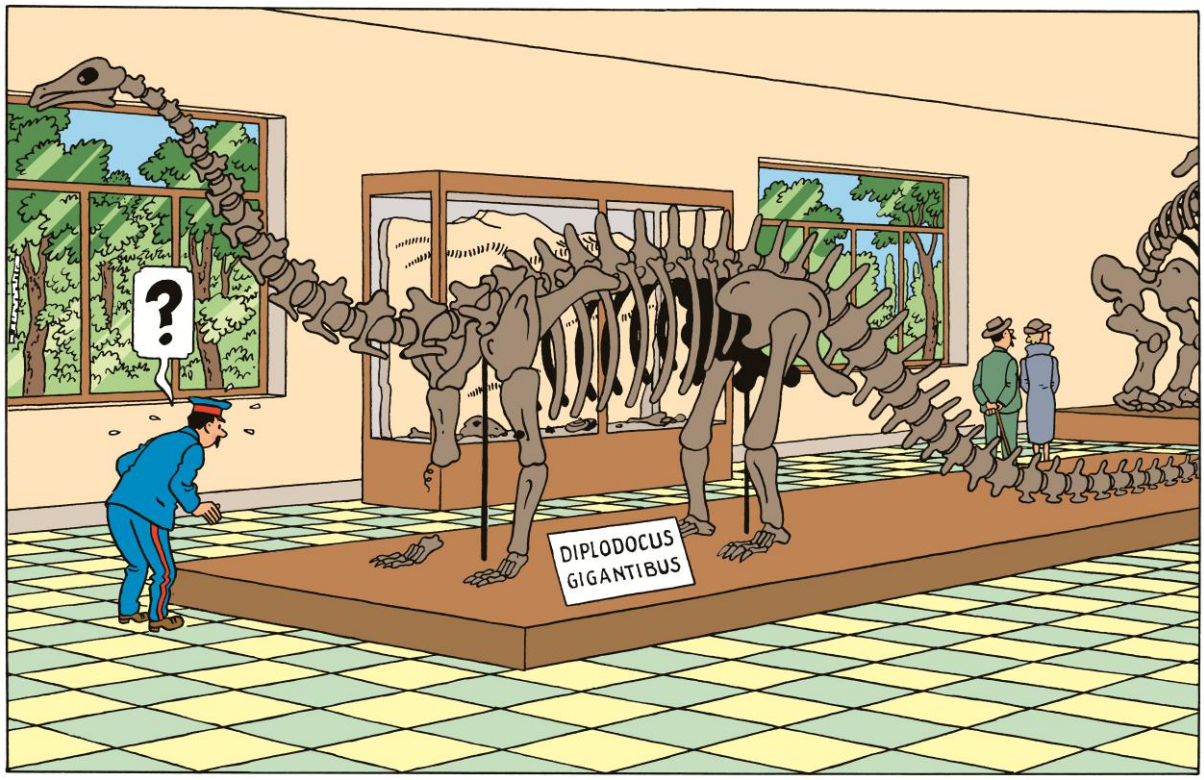

Hergé's reconstruction of *Diplodocus* '*gigantibus*' in King Ottokar's Sceptre (1939).
Courtesy shared by © Hergé/Moulinsart 2014.

Dedicated to
J. Hendrickx,
D. Hendrickx-Ernst,
J. Ernst-Lambert,
and G.A. Martin,
those who built me,
trusted me, supported me,
and made my dream come true.

AUTHOR'S NOTE

The present thesis was submitted to the jury members in October 2014 and was defended in Caparica, Portugal, by the end of February 2015. This final version of the thesis was submitted to the Universidade Nova de Lisboa in May 2015 and, at this stage, includes three published papers (chapters 4, 9, 10), three in press articles (chapters 1, 2, 5), and four manuscripts which have been reviewed a first time and accepted with minor/ major revisions (chapters 3, 6, 7, 8). Due to time constraints, chapters 3, 7 and 8 were not updated following reviewer's suggestions so that a different version of these three chapters will be published. Following a recent reviewer's recommendation, it was decided to favor the terms 'mesial dentition' instead of 'mesialmost dentition'. In this thesis, mesial teeth therefore refer to those of the premaxilla as well as the mesialmost dentary and sometimes maxillary teeth. References in the text were added using the open-source management Zotero, which also created the bibliography. Given the fact that the present work includes more than 950 references, this software had serious issues updating the bibliography, and some references in the text might therefore be incorrectly written and/or uncited in the bibliography. Likewise, only some chapters could be corrected by an English speaker and many spelling mistakes and grammatical errors must remain in the other sections of the thesis. If you were to notice spelling and/or grammatical mistakes as well as misspelled references, please do not hesitate to inform me at this subject by contacting me at this address: christophe.hendrickx@hotmail.com.

Christophe Hendrickx
San Miguel de Tucumán, the 19th of May 2015

ACKNOWLEDGEMENTS

This journey started four years ago and an immense part of it consisted of travelling, visiting collections, asking for information, hundreds of photos and papers, and mostly sitting on a desk in front of a computer, often when the food was being prepared. Without the help of a large number of people, each of them with a different level of contribution, this journey would not have even started. If this thesis and each of its chapters are the fruits of a research tree that grew up for four years, these people are the branches that support the fruits, the soil and the sap that fed them. And if we go further in the metaphor, I cannot find a better way to illustrate my supervisor Octávio Mateus and his contribution as the trunk of this tree. Octávio helped me in so many different ways, from sharing a huge number of photos and publications on theropods to giving me opportunities of working on extremely interesting material of the Museu of Lourinhã and elsewhere. As my colleague Emanuel Tschopp said it very well, our supervisor found the perfect balance between tight guidance and freedom in working the way we liked, whenever and wherever we wanted. Beyond his general advising and the duties expected from a PhD advisor, Octávio was an excellent supervisor in teaching us how to prospect, dig, conduct paleontological expeditions, write articles, teach, and give talks. For proposing such an interesting research project, introducing me to many important people from the paleontological sphere, and being there whenever I needed his help, I thank him deeply, knowing that if I become a paleontologist one day, he was the one who shaped me for this profession.

Family always plays an important role in the task of writing a thesis, yet members of this family are typically thanked at the end of this section. My father must, however, be an exception to this tendency. Because he was the protagonist that helped me visiting collections of museums and universities all over the world, it would sound indecent and illogical to me not to include him among the first people to thank. My father was the pilot who drove me to Chicago, New York, and Buenos Aires, giving me the immense chance and the great opportunity to examine dozens of theropod specimens housed in more than twenty institutions outside Europe. I also thank him warmly for providing the best place I could have imagined in one of the most beautiful regions of the world to finish writing my thesis. In the very same way, I thank my lovely girlfriend Graciela Apud Martin for her support and her help in correcting the English spelling mistakes of many papers constituting this thesis. Because she was far from me, I often had to delay my trip to Argentina to join her because of my work, and I cannot thank her enough for her patience and open-mindedness in considering living her life with a workaholic perfectionist boyfriend who prefers being a nomad than a sedentary.

I am particularly thankful of Ricardo Araújo (Uni. Lisbon) for his help in correcting the English style and spelling mistakes of most of the chapters of this thesis, but also for proposing me to participate to an awesome project on theropod embryos, and for providing all the tools and knowledge to perform phylogenetic morphometric analyses. Ricardo was the one who helped me improving my scientific writing, and I thank him for his availability, thoughtfulness, and hospitality in Dallas where he was kind enough to give Emanuel and I a class on FEA analysis for two weeks at the Southern Methodist University. A special thanks goes also to Steve Brusatte for being the reviewer of several of these chapters, for his general help and advice, and for his tremendous generosity and humbleness. Steve is certainly one of the best vertebrate paleontologists I know, and I thank him for being so inspiring.

In addition to these people, my research on theropods has benefited greatly from the help of scientists who provided me access to theropod material in their care. By chronological order, I thank Octávio Mateus (ML), Simão Mateus (ML), Hans-Jacob Siber (SMA), Louis Jacobs (SMU), Dale Winkler (SMU), Anthony Fiorillo (DMNH), Ronald Tykoski (DMNH), Paul Sereno (UC), Peter Makovicky (FMNH), William Simpson (FMNH), Matthew Lamanna (CMNH), Amy Henrici (CMNH), Matthew Carrano (NMNH), Michael Brett-Surman (NMNH), Ronan Allain (MNHN), Sandra Chapman (NHM), Paul Barrett (NHM), Paul Jeffery (OUMNH), Stephen Hutt (MIW), Jorge Calvo (CePaLB), Juan D. Porfiri (UNDC), Rainer Schoch (SMNS), Christiano Dal Sasso (MSNM), Alejandro Kramarz (MACN), Fernando Novas (MACN), Marcello Reguero (MLP), Juan Ignacio Canale (MUCPv-CH), Ruben Barbieri (MPCA), Rodolfo Coria (MCF-PVPH), Cecilia Succar (MCF-PVPH), Ricardo Martínez (PVSJ), Carl Mehling (AMNH), Mark Norell (AMNH), David Krauze (SBU), Joseph Groenke (SBU), Paul Brinkman (NCSM), Lindsay Zanno (NCSM), Jorge Sequeira (LNEG), Fareed Krupp (QMA), Khalid Hassan Al-Jaber (QMA), Sanker S.B (QMA), Yves Dutour (MHNA), Thierry Tortosa (MHNA), and Jaime Powell (PVL) for allowing me to examine theropod specimens belonging to their respective institutions. I am particularly thankful to Paul Sereno, Fernando Novas, Mark Norell, Fareed Krupp, Khalid Hassan Al-Jaber, and Sanker S.B. who gave me access to unpublished material, and to François Escuillié for donating five spinosaurid quadrates from the Kem Kem beds to a scientific institution for study.

All along these four years, I continually and without reserve asked for photos of theropod cranial material I could not examine myself to many colleagues, sometimes in an undeterred way. For providing these illustrations, I acknowledge the great generosity of Martín Ezcurra (MACNBR), Matthew Lamanna (CMNH), Christian Foth (Ludwig-Maximilians-Uni.), Stephen Brusatte (Uni. Edinburgh), Mick Ellison (AMNH), Matthew Carrano (NMNH), Philip Currie (Uni. of Alberta), Juan Canale (MUCPv-CH), Lindsay Zanno

(NCSM), Vince Shneider (NCSM), Sterling Nesbitt (Uni. Texas), Cristiano Dal Sasso (MSNM), Simone Maganuco (MSNM), Randall Irmis (UMNH), Yoshitsugu Kobayashi (Hokkaido University), Diego Pol (MPEF), Mattia Antonio Baiano (UAB), Roger Benson (Uni. Oxford), Oliver Rauhut (Ludwig-Maximilians-Uni.), Lawrence Witmer (Ohio Uni.), Pablo Asaroff (MACN), Paul Barrett (NHM), Éric Buffetaut (CNRS), Ronald Tykoski (DMNH), Elisabete Malafaia (MNHNC), Ralph Molnar (MNA), Emanuel Tschopp (UNL), Drew Eddy (Uni. Texas), Ricardo Araújo (SMU), Fernando Novas (MACN), Nathan Smith (Howard Uni.), Karine Peyer (MNHN), Rui Pei (AMNH), Mickey Mortimer, Derek Larson (Uni. Toronto), Andrea Cau (MGG), Jonah Choiniere (Uni. of the Witwatersrand), Darren Naish (Uni. of Portsmouth), Carol Abraczinskas (UC), Stephan Lautenschlager (Uni. Bristol), and David Burnham (Uni. of Kansas), and I address my sincere thanks to all these people.

Morphometric data on theropod teeth were generously provided by Carlos R. Candeiro (UFB), Lisa Buckley (Uni. Alberta), James Farlow (IPFW), Julia Sankey (CSU), Federico Fanti (MGPGC), Martín Ezcurra (MACNBR), and Steven Sweetman (Uni. of Portsmouth). As for missing papers, they were kindly shared by Jorge Bar (National University of Salta), Paul Sereno (UC), Stephen Brusatte (Uni. of Edinburgh), Cristiano Dal Sasso (MSNM), Andrea Cau (MGG), Pascal Godefroit (IRSNB), Ricardo Araújo (Uni. Lisbon), and Mickey Mortimer. A special thanks goes to Jorge Bar and the Wikipaleo group on Facebook, which kindly provide a huge number of books and papers every day, and to Cristiano Dal Sasso, who gave me the opportunity of including a spinosaurid quadrate in my research project and provided measurements for this specimen.

I acknowledge the use of the Willi Hennig Society edition of TNT for the cladistic analyses and Phylopic for the theropod silhouettes. I thank Scott Hartman, Funkmonk, Gregory Paul, Travis R. Tischler, Fonty, and Traver for accepting to use their artworks on Phylopic. Likewise, artworks on the *Torvosaurus* skull and the embryo material of *Lourinhanosaurus* and *Torvosaurus*, the *Torvosaurus* skeleton, and the human scale were very kindly provided by Simão Mateus (ML), Scott Hartman, and Carol Abraczinskas (UC), respectively, and I deeply thank them for their generosity. I would especially like to express my utmost thanks to Sergey Krasovsky for his wonderful illustration on *Torvosaurus gurneyi*, and to Jaime Headden for his reconstruction of the jaw mechanic of *Spinosaurus*, both carried out from personal demands. I thank Aart Walen who discovered *Torvosaurus* material (both adult and embryos) and prepared the *Torvosaurus* maxilla from Portugal. I am also thankful to Ronald Tykoski for the information shared on *Dilophosaurus* stratigraphic position and interdental plates morphology, Mickey Mortimer for the precious information on *Dilophosaurus* '*breedorum*' posted on his blog and for reviewing the English of the manuscript on the *Spinosaurus* quadrates, and Jaime Headden for his inspiring blog and the information given on the nature of some pneumatic openings in the maxilla of oviraptorids.

I am particularly thankful for the help given during the process of publications of several papers that form this thesis. Comments on an early version of these papers by reviewers Derek Larson (Uni. Toronto), Steve Brusatte (AMNH), Julia Sankey (CSU), Oliver Rauhut (Ludwig-Maximilians-Uni.), Joshua B. Smith, Jonah Choiniere (Uni. of the Witwatersrand), Thomas Carr (Carthage College), Federico Agnolin (MACN), and six anonymous reviewers, as well as editors Roger Benson (Uni. of Oxford), Paul Barrett (NHM), Mike J. Benton (Uni. of Bristol), Brian Beatty (NYIT), Sylvain Gerber (Uni. of Cambridge) and Andrew Farke (Raymond M. Alf Museum of Paleontology), and my colleague Emanuel Tschopp, considerably improved the quality of these articles and the thesis as a whole. I, therefore, thank them deeply for their precious advices and the time they spent for helping me. In the same way, I thank the members of the doctoral committee Stephen Brusatte, Martin Sander, Miguel Telles Antunes and Maria Paula Diogo for the time spent to read my thesis and/or for accepting to be present during its defense.

This research was supported by several scholarships and grants that were kindly awarded by different institutions throughout those last four years. First and foremost, I acknowledge the Fundação para a Ciência e a Tecnologia (FCT) scholarship SFRH/BD/62979/2009 from the Ministério da Ciência, Tecnologia e Ensino superior, Portugal for their financial help for four years, as well as an external help for following a class at the Southern Methodist University. Travel subsidies were also provided by the European Science Foundation (ESF) and the Palaeontological Association (Palass) for a histology course at the University of Bonn and the attendance of the Annual Meeting of the Palaeontological Association, respectively.

I extend my greatest thank to the Museu of Lourinhã and all my colleagues from that institution and elsewhere. I particularly thank João Marinheiro, João Russo, Emanuel Tschopp, Femke Holwerda, Veronica Duarte, Nury Lopez, Alexandre Audigane, Simão Mateus, Vasco Ribeiro, and Armando in Portugal, as well as Guillaume Hougardy, Damien Pas and many other Belgian friends that I could not see much during these last four years. Last but not least, I thank my whole family which I see so rarely: my three sisters Aurélie, Laure, and Suzanne, my little brother Gabriel, Ania, Oma, and particularly Mami, for her help, kindness, and affection.

I dedicated each of these chapters to people, or to the memory of people that played an important role in my life, namely Jean Hendrickx, Dominique Hendrickx-Ernst, Jacqueline Ernst-Lambert, José Ernst, Marianne Hendrickx-Alexandre, Rose Alexandre, Graciela Apud Martin, Roger Bec, Eric Buffetaut, and Edouard Poty. This thesis is dedicated to four of them in particular: my father, my mother, Mami, and my girlfriend Grace.

RESUMO

Os dinossauros terópodes formam um grupo morfologicamente diversificado e bem-sucedido, do qual se originaram as aves. Estes incluem a maior parte, porventura todos, os dinossauros carnívoros, mas muitos clados de terópodes adaptaram-se secundariamente a uma dieta piscívora, omnívora e herbívora, e os terópodes demonstram um amplo espectro de morfologias cranianas e dentárias. Este trabalho pretende investigar a evolução dos dinossauros terópodes através da análise detalhada da anatomia e ontogenia dos dentes e quadrados nos dinossauros não-avianos, e estudar os vestígios embriónicos e de adultos de uma nova espécie descoberta em Portugal.

Uma lista padronizada de termos e notações para cada acidente anatómico do dente, quadrado e maxilar é aqui proposta com o objectivo de facilitar descrições destes importantes elementos cranianos e dentários. Foi investigada a distribuição de trinta caracteres dentários em 113 táxones de terópodes, sendo apresentada uma lista de caracteres diagnósticos dos dentes. Por exemplo, quatro dentes de terópodes da formação de Lourinhã (Kimeridgiano-Titoniano) de Portugal são descritos e identificados com base numa análise cladística usando 141 caracteres dentários codificados para 60 táxones. Dois dentes são atribuídos a abelissaurídeos, tornando-se no primeiro registo de Abelisauridae no Jurássico da Laurásia e um dos mais antigos registos deste clado no mundo, sugerindo uma possível radiação dos Abelisauridae na Europa bem antes do Cretácico Superior. O cladograma de consenso resultante da análise filogenética – o mais extenso em dentes de terópode – indica que estes possuem informação taxonómica confiável até ao nível da família e este método ajuda a identificar dentes de terópode com maior confiança. Também é apresentada uma descrição detalhada dos dentes de Megalosauridae. Uma análise discriminante numa matriz de informação morfométrica recolhida para 62 táxones revela que os dentes de megalossaurídeos são dificilmente distinguíveis de outros terópodes com dentição zifodonte. Este estudo realça a importância de descrições anatómica detalhadas e fornece informação morfométrica adicional com o propósito de identificar dentes isolados de terópodes.

De modo a avaliar o potencial filogenético e investigar as transformações evolutivas do osso quadrado foi feita uma análise filogenética morfométrica bem como uma análise cladística usando 98 caracteres discretos. A morfologia do quadrado por si só contém uma ampla riqueza de informação com um sinal filogenético e a análise morfométrica revela dois morfotipos principais de articulação mandibular do quadrado relacionada com o seu funcionamento em vida. Por exemplo, seis quadrados isolados das Kem Kem beds do Cenomaniano de Marrocos foram determinados como pertencendo a juvenis e adultos de Spinosaurinae baseado em análises filogenéticas, morfométricas, e filogenética-morfométricas. A análise morfofuncional das mandíbulas de spinossaurídeos demonstrou que a parte posterior dos dois ramos da mandíbula deslocava-se lateralmente quando a boca abria, graças à orientação mediolateral do sulco intercondilar do quadrado. Esse movimento lateral da ramo mandibular foi possível graças a uma sínfise mandibular livre e cinética nos spinossaurídeos, permitindo uma maior abertura da faringe.

É descrita uma nova espécie de terópode, *Torvosaurus gurneyi*, da formação de Lourinhã, o Jurássico Superior de Portugal, sendo o holótipo baseado numa maxilar direito e num corpo vertebral caudal incompleto. Este táxon é coerente com a hipótese de vicariância ocorrida durante o Jurássico Superior quando o proto-Atlântico estava em formação. Um ninho de terópodes descoberto em Porto das Barcas, Lourinhã, contendo vários ovos esmagados e material embrionário é também atribuído a esta nova espécie de *Torvosaurus.* A investigação sobre a ontogenia do maxilar nos tetanuros basais revela que os dentículos da coroa, o alongamento do ramo anterior, e a fusão das placas interdentárias aparece num estágio pós-eclosão. Por outro lado, a pneumaticidade está presente logo nos estágios embrionários nos terópodes não-avianos.

Palavras-chave: dentes; quadrado; filogenética; morfométrica; filogenética morfométrica; embrião; Megalosauroidea; terópode, dinossauros.

ABSTRACT

Theropods form a highly successful and morphologically diversified group of dinosaurs that gave rise to birds. They include most, if not all, carnivorous dinosaurs, yet many theropod clades were secondarily adapted to piscivory, omnivory and herbivory, and theropods show a large array of skull and dentition morphologies. This work aims to investigate aspects of the evolution of theropod dinosaurs by analyzing in detail both the anatomy and ontogeny of teeth and quadrates in non-avian theropods, and by studying embryonic and adult material of a new species of theropod.

A standardized list of terms and notations for each anatomical entity of the tooth, quadrate, and maxilla is here proposed with the goal of facilitating descriptions of these important cranial and dental elements. The distribution of thirty dental characters among 113 theropod taxa is investigated, and a list of diagnostic dental characters is proposed. As an example, four isolated theropod teeth from the Lourinhã Formation (Kimmeridgian–Tithonian) of Portugal are described and identified based on a cladistic analysis performed on a data matrix of 141 dentition-based characters coded in 60 taxa. Two shed teeth are referred to an abelisaurid, providing the first record of Abelisauridae in the Jurassic of Laurasia and the one of the oldest records of this clade in the world, suggesting a possible radiation of Abelisauridae in Europe well before the Upper Cretaceous. The consensus tree resulting from this phylogenetic analysis, the most extensive on theropod teeth, indicates that theropod teeth provide reliable data for identification at approximately family level, and this method will help identifying theropod teeth with more confidence. A detailed description of the dentition of Megalosauridae is also provided, and a discriminant analysis performed on a dataset of numerical data collected on the teeth of 62 theropod taxa reveals that megalosaurid teeth are hardly distinguishable from other theropod clades with ziphodont dentition. This study highlights the importance of detailing anatomical descriptions and providing additional morphometric data on teeth with the purpose of helping to identify isolated theropod teeth.

In order to evaluate the phylogenetic potential and investigate the evolutionary transformations of the quadrate, a phylogenetic morphometric analysis as well as a cladistic analysis using 98 discrete quadrate related characters were conducted. The quadrate morphology by its own provides a wealth of data with strong phylogenetic signal, and the phylogenetic morphometric analysis reveals two main morphotypes of the mandibular articulation of the quadrate linked to function. As an example, six isolated quadrates from the Kem Kem beds (Cenomanian) of Morocco are determined to be from juvenile and adult individuals of Spinosaurinae based on phylogenetic, morphometric, and phylogenetic morphometric analyses. Morphofunctional analysis of the spinosaurid mandibular articulation has shown that the posterior parts of the two mandibular rami displaced laterally when the jaw was depressed due to a mediolaterally oriented intercondylar sulcus of the quadrate. Such lateral movement of the mandibular ramus was possible due to a movable mandibular symphysis in spinosaurids, allowing the pharynx to be widened.

A new species of theropod from the Lourinhã Formation of Portugal, *Torvosaurus gurneyi*, is erected based on a right maxilla and an incomplete caudal centrum. This taxon supports the mechanism of vicariance that occurred in the Iberian Meseta during the Late Jurassic when the proto-Atlantic was already well formed. A theropod clutch containing several crushed eggs and embryonic material is also assigned to this new species of *Torvosaurus*. Investigation on the maxilla ontogeny in basal tetanurans reveals that crown denticles, elongation of the anterior ramus, and fusion of interdental plates appear at a posthatchling stage. On the other hand, maxillary pneumaticity is already present at an embryonic stage in non-avian theropods.

Keywords: teeth; quadrate; phylogenetics; morphometrics; phylogenetic morphometrics; embryo; Megalosauroidea; theropod.

TABLE OF CONTENTS

Author's note IV
Acknowledgements V
Resumo VII
Abstract VIII
Table of contents IX
Figures and tables captions XI
Abbreviations XXXI
I. Introduction 1
Chapter 1: An overview on non-avian theropod discoveries and classification 6
Abstract 6
Historical background 6
Origin, evolution, and current classification 18
Conclusions 50
State of art 51
Objectives 54
Structure of the thesis 54
Materials and methods 55
Case of study 57
Sedimentology and chronostratigraphy of the Lourinhã Formation and the Kem Kem beds 58
II. Evolution of teeth 65
Chapter 2: A proposed terminology of theropod teeth (Saurischia: Dinosauria) 65
Abstract 65
Introduction 65
Positional nomenclature 66
Anatomical nomenclature 68
Morphological nomenclature 77
Morphometric nomenclature 82
Methodology to describe isolated theropod teeth 91
Conclusions 95
Chapter 3: The distribution of dental features in non-avian theropods 97
Abstract 97
Introduction 97
Materials and Methods 98
Results and Discussion 103
Chapter 4: Abelisauridae (Dinosauria: Theropoda) from the Late Jurassic of Portugal and dentition-based phylogeny as a contribution for the identification of isolated theropod teeth 152
Abstract 152
Introduction 153
Methodology 155
Results 157
Systematic Palaeontology 168
Conclusions 190
Chapter 5: The dentition of megalosaurid theropods 191
Abstract 191
Introduction 191
Material and methods 192
The dentition of Megalosauridae 197
Comparison to the dentition of other theropods 205
Conclusions 215
III. Evolution of the quadrate 217
Chapter 6: The non-avian theropod quadrate I: standardized terminology and overview of the anatomy, function and ontogeny 217
Abstract 217
Introduction 217
Proposed terminology of the quadrate anatomy 218
Inter-taxic Topological Homologies 228
Overview of the function, pneumaticity and ontogeny 234
Conclusions 246

Chapter 7: The non-avian theropod quadrate II: systematic usefulness, major trends and cladistic and phylogenetic morphometrics analyses....248
Abstract....248
Introduction....248
Materials and methods....249
Results....255
Anatomy of the non-avian theropod quadrate....260
Discussion....308
Conclusion....312
Chapter 8: Morphofunctional analysis of the quadrate of Spinosauridae (Dinosauria: Theropoda) and the first definitive evidence of two cohabiting *Spinosaurus* in the Upper Cretaceous of North Africa....314
Abstract....314
Introduction....314
Material and methods....317
Systematic Paleontology....321
Results....331
Discussion....335
Conclusion....356
IV. *Torvosaurus* remains from Portugal....358
Chapter 9: *Torvosaurus gurneyi* n. sp., the largest terrestrial predator from Europe, and a proposed terminology of the maxilla anatomy in non-avian theropods....358
Abstract....358
Introduction....358
Proposed terminology of the maxilla anatomy in non-avian theropods....360
Results....375
Discussion....391
Chapter 10: Late Jurassic *Torvosaurus* clutch with embryos from Portugal and the ontogeny of the maxilla in non-avian theropods....405
Abstract....405
Introduction....405
Material....406
Description....408
Method and Results....413
Discussion....418
Ontogeny of the maxilla in basal tetanurans....421
V. Conclusions....427
Future developments....431
References....433
Appendices....472
A1. Silhouette attribution and examined taxa....472
A2. Visited institutions....475
A3. Non-avian theropod taxa included in this study....478
A4. Phylogenetic analysis on dentition-based characters....489
A5. Morphometric data on theropod teeth....516
A6. Function of quadrate sub-entities....537
A7. Analyses on the non-avian theropod quadrate (Chapter 7)....538
A8. Analyses on the *Spinosaurus* quadrate (Chapter 8)....565
A9. Phylogenetic analysis including *Torvosaurus gurneyi* (ML 1100)....584
A10. Phylogenetic analysis including *Torvosaurus* embryos (ML 1188)....592

FIGURES AND TABLES CAPTIONS

Figures

FIGURE 1.1. Phylogeny and stratigraphic distribution of theropod clades. The phylogenetic classification of theropods follows the results of the cladistic analyses obtained by Sues et al. (2011) for non-neotheropod Theropoda, Smith et al. (2007) and Ezcurra and Brusatte (2011) for non-averostran Neotheropoda, Pol and Rauhut (2012) and Tortosa et al. (2014) for Ceratosauria, Carrano et al. (2012) for non-coelurosaur Tetanurae, Loewen et al. (2013), Lü et al. (2014) and Porfiri et al. (2014) for Tyrannosauroidea, Lee et al. (2014) for Ornithomimosauria, Lamanna et al. (2014) for Oviraptorosauria, and Turner et al. (2012), Godefroit et al. (2013a) and Choiniere et al. (2014*b*) for non-tyrannosauroid Coelurosauria. Silhouettes by Funkmonk (Coelophysoidea, Dilophosauridae, and Alvarezsauroidea), Jaime Headden (Caenagnathidae), T. Michael Keesey (Deinocheiridae), Conty (*Eodromaeus*), T. Tischler (Megaraptora), and S. Hartman (all others).

FIGURE 1.2. Earliest historical records of theropod remains in the world. **A–B**, Distal part of a left femur of *Megalosaurus* from Cornwell, U.K., in posterior view, and first reported by Plot (1677); **A**, illustrations by Plot (1677: table 8, fig.4); and **B**, Brookes (1763, p. 312: fig. 317) showing the label 'Scrotum Humanum'; **C**, isolated theropod tooth (likely *Megalosaurus*) from the Stonesfield, U.K., illustrated by Lhuyd (1699: plate 16, fig. 1328); **D**, right femur of *Megalosaurus* from Stonesfield, U.K., in anterior view, illustrated by Platt (1758: table 19); **E**, right dentary of *Megalosaurus bucklandii* from Stonesfield, U.K., in medial and posterior views, illustrated by Buckland (1824: plate 40).

FIGURE 1.3. Earliest historical records of theropod remains in **A–B**, North America; **C**, Asia; **D**, Africa; **E–F**, South America; **G**, Oceania; and **H**, Antarctica. Isolated teeth of **A**, *Troodon formosus*; and **B**, *Deinodon horridus* (= *Albertosaurus sarcophagus*) from the Upper Cretaceous Judith River of Colorado and first reported by Leidy (1856; modified from Leidy 1860: plate 9); **C**, isolated theropod tooth of '*Massospondylus rawesi*', an abelisaurid from the Upper Cretaceous of India (localities of Takli and Maleri) first reported by Hislop (1861, 1864, illustration by Lydekker 1890: fig. 1); **D**, isolated teeth of the abelisaurid *Majungasaurus crenatissimus* first reported and originally described by Depéret (1896*a*, *b*; illustration by Depéret 1896*a*: table 24, plate 6); **E–F**, isolated theropod tooth from the Upper Cretaceous of Par-Aík, India, referred to *Loncosaurus argentines* and first reported by Ameghino (1899); **E**, illustration by Ameghino (1900, p. 160) and Ameghino (1906: fig. 8); and **F**, Huene (1929*a*: plate 41); **G**, pedal ungual of an indeterminate theropod from the Upper Cretaceous of Cape Patterson, Australia, and first reported by Woodward (1906); **H**, distal part of a tibia of a megalosauroid? theropod from the Upper Cretaceous of Col Crame, Antarctica, discovered in 1988 (modified from Molnar et al. 1996).

FIGURE 1.4. Cladogram of basal Theropoda showing the relationships of 'non-neocoelurosaur' theropod taxa. The phylogenetic classification follows the results of the cladistic analyses obtained by Sues et al. (2011) for non-neotheropod Theropoda, Smith et al. (2007) and Ezcurra and Brusatte (2011) for non-averostran Neotheropoda, Pol and Rauhut (2012) and Tortosa et al. (2014) for Ceratosauria, Carrano et al. (2012) for non-coelurosaur Tetanurae, Loewen et al. (2013), Lü et al. (2014) and Porfiri et al. (2014) for Tyrannosauroidea, and Choiniere et al. (2014*b*) for basal Coelurosauria.

FIGURE 1.5. Cladogram of 'neocoelurosaur' Theropoda showing the relationships of non-tyrannosauroid coelurosaurs. The phylogenetic classification follows the results of the cladistic analyses obtained by Choiniere et al. (2014*b*) for basal Coelurosauria and Compsognathidae, Longrich and Currie (2009*a*) and Choiniere et al. (2010*b*) for Alvarezsauroidea, Lee et al. (2014) for Ornithomimosauria, Senter et al. (2012*a*) and Pu et al. (2013) for Therizinosauria, Lamanna et al. (2014) for Oviraptorosauria, Turner et al. (2012) for Paraves, and Foth et al. (2014) for Avialae.

FIGURE 1.6. Skeletal reconstructions of three non-neotheropod saurischians (and possibly three basalmost theropods). **A**, the possible primitive sauropodomorph *Eoraptor lunensis*; **B**, the herrerasaurid *Herrerasaurus ischigualastensis*; and **C**, the very basal theropod *Tawa hallae*. Reconstructions by Scott Hartman.

FIGURE 1.7. Skeletal reconstructions of two non-averostran neotheropod and one basal ceratosaurs. **A**, the coelophysoid *Coelophysis bauri*; **B**, the dilophosaurid *Dilophosaurus wetherilli*; and **C**, the 'elaphrosaurid' *Limusaurus inextricabilis*. Reconstructions by Gregory Paul for *Coelophysis* and *Dilophosaurus* (modified), and Ville Sinkkonen for *Limusaurus* (modified).

FIGURE 1.8. Skeletal reconstructions of three ceratosaurs. **A**, the ceratosaurid *Ceratosaurus nasicornis*; **B**, the noasaurid *Masiakasaurus knopfleri*; **C**, the abelisaurid *Majungasaurus crenatissimus*. Reconstructions by Scott Hartman.

FIGURE 1.9. Skeletal reconstructions of three megalosauroids. **A**, the piatnitzkysaurid *Marshosaurus bicentissimus*; **B**, the megalosaurid *Megalosaurus bucklandii*; and **C**, the spinosaurid *Baryonyx walkeri*. Reconstructions by Scott Hartman.

FIGURE 1.10. Skeletal reconstructions of three allosauroids. **A**, the allosaurid *Allosaurus* '*jimmadseni*'; **B**, the neovenatorid *Neovenator salerii*; and **C**, the carcharodontosaurid *Giganotosaurus carolinii*. Reconstructions by Scott Hartman.

FIGURE 1.11. Skeletal reconstructions of three tyrannosauroids. **A**, the proceratosaurid *Guanlong wucaii*; **B**, the basal tyrannosauroid *Eotyrannus lengi*; and **C**, the tyrannosaurid *Tyrannosaurus rex*. Reconstructions by Scott Hartman.

FIGURE 1.12. Skeletal reconstructions of three basal maniraptoriforms. **A**, the compsognathid *Compsognathus longipes*; **B**, the ornithomimid *Gallimimus bullatus*; and **C**, the basal maniraptoran *Ornitholestes hermanni*. Reconstructions by Scott Hartman.

FIGURE 1.13. Skeletal reconstructions of three basal maniraptorans. **A**, the alvarezsauroid *Shuvuuia deserti*; **B**, the therizinosauroid *Nothronychus graffami*; and **C**, the oviraptorosaur *Khaan mangas*. Reconstructions by Ville Sinkkonen for *Shuvuuia* and Scott Hartman for *Nothronychus* and *Khaan*.

FIGURE 1.14. Skeletal reconstructions of three basal paravians. **A**, the unenlagiine dromaeosaurid *Buitreraptor gonzalezorum*; **B**, the velociraptorine dromaeosaurid *Deinonychus antirrhopus*; and **C**, the troodontid *Troodon formosus*. Reconstructions by Scott Hartman.

FIGURE 1.15. Skeletal reconstructions of three basal avialan? theropods. **A**, the basal avialan *Anchiornis huxleyi*; **B**, the archaeopterygid *Archaeopteryx* sp.; and **C**, the scansoriopterygid *Epidendrosaurus ninchengensis*. Reconstructions by Ville Sinkkonen for *Anchiornis* and Scott Hartman for *Archaeopteryx* and *Epidendrosaurus*.

FIGURE 1.16. Geology and chronostratigraphy of Portugal. **A**, Sedimentary basins of Portugal. The Lusitanian Basin covers the central-west part of Portugal, including Lisbon and the region of Lourinhã (modified after Taylor et al. 2014); **B**, Simplified chronostratigraphic map of the Lourinhã region. The Late Jurassic deposits (in light blue) are mostly comprised in the Lourinhã Formation which covers most of the Lourinhã area (modified after Mateus et al. 2014).

FIGURE 1.17. Geological map and sections of the Lourinhã area. **A**, Simplified chronostratigraphic map of the areas of Peniche, Lourinhã and Santa Cruz; **B**, Lithostratigraphic map of the coast of Porto das Barcas, Areia Branca, San Bernardino and Consolação, with location of sites where *Ceratosaurus*, *Torvosaurus*, *Allosaurus*, and *Lourinhanosaurus* were found. Colors of the different units are given in C; **C**-**D**, Stratigraphic columns of the Lusitanian Basin; **E**, Cliff section between Consolação (A) Areia Branca (B), and Ribamar (C), with location of sites where *Ceratosaurus*, *Torvosaurus*, *Allosaurus*, and *Lourinhanosaurus* were found (modified from Taylor et al. 2014 for A–C, and E; and from Araújo et al. 2013 for D).

FIGURE 1.18. Geographical location and stratigraphy of the Kem Kem beds. **A**, Location of Morocco (in black) in Africa (left corner), the Kem Kem region (in red) in Morocco (middle left), and the Kem Kem beds (in black) in the Kem Kem plateau (right); **B**, Stratigraphic column of the Kem Kem beds of South-Eastern Morocco. Modified from Sereno et al. (1996) and Ibrahim et al. (2014*a*).

FIGURE 1.19. Stratigraphic column of the Kem Kem beds of South-Eastern Morocco. Modified from Ibrahim et al. (2014*a*).

FIGURE 2.1. Anatomical terminology used in this study. **A**, mid-height cross-section of crown in C, in apical view; **B**, basal cross-section of crown in C, in basal view; **C**, idealized lateral theropod tooth in labial view; **D**, idealized lateral theropod tooth in distal view; **E**, idealized distal denticles of theropod crown; **F**, idealized lateral theropod tooth in labial view showing the crown ornamentations and attributes; **G**, idealized fluted theropod tooth, in labial view; **H**, idealized distal denticles showing denticle structures, in labial view. **Abbreviations**: **bst**, basal striation; **ca**, carina; **cap**, crown apex; **cau**, cauda; **ce**, cervix; **co**, crown; **dca**, distal carina; **de**,

denticle; **del**, dentine layer; **enl**, enamel layer; **ema**, external margin; **flu**, flute; **idd**, interdenticular diaphysis; **ids**, interdenticular sulci; **idsl**, interdenticular slit; **idsp**, interdenticular space; **lid**, lingual depression; **mun**, marginal undulation; **mca**, mesial carina; **ope**, operculum; **puc**, pulp cavity; **ro**, root; **sps**, spalled surface; **tun**, transverse undulation; **wfa**, wear facet.

FIGURE 2.2. Crown, root and denticle anatomy of an isolated tooth of *Alioramus altai*, IGM 100–1844. **A-D**, Tooth in **A**, lingual; **B**, distal; **C**, labial; **D**, mesial views, and close up on; **E**, disto-central denticles; **F**, crown, and; **G**, enamel surface, in labial views (courtesy of Mick Ellison © AMNH). **Abbreviations**: **ca**, carina; **cap**, crown apex; **ce**, cervix; **co**, crown; **dca**, distal carina; **de**, denticle; **ema**, external margin; **ent**, enamel texture; **idd**, interdenticular diaphysis; **ids**, interdenticular sulci; **idsl**, interdenticular slit; **idsp**, interdenticular space; **lid**, lingual depression; **mca**, mesial carina; **ro**, root; **sps**, spalled surface; **tun**, transverse undulation. Scale bars equals 1 cm (A–D, F), and 1 mm (E, G).

FIGURE 2.3. Internal anatomy of mesial denticles of an indeterminate tyrannosaurid, ROM 57981, from the Oldman Formation? of Alberta, Canada (courtesy of Kirstin Brink). **Abbreviations**: **ampu**, ampulla; **ema**, external margin; **idd**, interdenticular diaphysis; **idsl**, interdenticular slit; **ope**, operculum; **rad**, radix. Scale bar equals 100 µm.

FIGURE 2.4. Crown ornamentations and attributes in non-avian theropods. **A**, Shed crown of *Troodon formosus*, DMNH 22337, in lingual view; **B**, Distal denticles of an indeterminate Abelisauridae, ML 327, in lingual view; **C**, Disto-central part of an isolated crown of cf. *Megalosaurus bucklandii*, OUMNH J.23014, in labial view; **D**, Disto-central part of an isolated crown of *Carcharodontosaurus saharicus*, UCRC PV6, in lingual view; **E**, Isolated crown of *Megalosaurus bucklandii*, OUMNH J.29866, in lingual view; **F**, Sixth right maxillary tooth of *Acrocanthosaurus atokensis*, NCSM 14345, in labial view; **G**, Shed tooth of *Paronychodon* sp., NHM R8405, in lingual view (Cillari 2010); **H**, Shed tooth of an indeterminate baryonychine (formerly *Suchosaurus cultridens* nomen dubium), NHM R.36536, in labial? view; **I**, Third right dentary tooth of *Masiakasaurus knopfleri*, UA 8680, in linguodistal view; **J**, Shed tooth of an indeterminate Abelisauridae, ML 327, in lingual view; **K**, Close up on the apicolingual portion of the shed tooth of an indeterminate Abelisauridae, ML 327, in lingual view; **L**, Fifth left maxillary crown of *Bambiraptor feinbergi*, AMNH 30556, in labial view; **M**, Fourth left maxillary tooth of *Velociraptor mongoliensis*, AMNH 6515, in labial view; **N**, First right premaxillary tooth of *Proceratosaurus bradleyi*, NHM R.4860, in labial view; **O**, Eight left maxillary tooth of *Allosaurus fragilis*, UMNH VP 5393, in lingual view (courtesy of Stephen Brusatte); **L**, Isolated tooth of *Eocarcharia*, MNN GAD15, in mesial view (courtesy of Juan Canale). **Abbreviations**: **bst**, basal striation; **cau**, cauda; **flu**, flute; **ids**, interdenticular sulci; **lid**, lingual depression; **lgr**, longitudinal groove; **lri**, longitudinal ridge; **mun**, marginal undulation; **spc**, split carina; **sps**, spalled surface; **tun**, transverse undulation; **wfa**, wear facet. Scale bars equals 1 cm (A, C–H, J–K, O–P), and 1 mm (B, I, L–N).

FIGURE 2.5. Crown types and cross-section outlines of the crown base at the cervix in non-avian theropods. **A**, ziphodont (blade-shaped) crown type; **B**, recurved folidont (lanceolate) crown type; **C**, straight folidont (lanceolate) crown type; **D**, pachydont (incrassate) crown type; **E**, conidont (cone-shaped) crown type; **F**, subcircular cross-section; **G**, elliptical cross-section; **H**, subrectangular cross-section; **I**, oval cross-section; **J**, lanceolate cross-section; **K**, lenticular cross-section; **L**, eight-shaped cross-section; **M**, reniform cross-section; **N**, U-shaped cross-section with central ridge on the labial margin; **O**, U-shaped cross-section with convex lingual margin; **P**, symmetrical D-shaped cross-section; **Q**, asymmetrical D-shaped cross-section; **R**, salinon-shaped cross-section; **S**, parlinon-shaped cross-section; **T**, J-shaped cross-section.

FIGURE 2.6. Diversity of enamel texture in non-avian theropods in lateral views. **A**, Irregular enamel texture of the sixth right maxillary tooth of *Majungasaurus crenatissimus*, FMNH PR 2278; **B**, Braided enamel texture of an isolated tooth of *Acrocanthosaurus atokensis*, SMU 7646; **C**, Veined enamel texture of an isolated tooth of *Baryonyx walkeri*, NHM R.9151–26; **D**, Anastomosed enamel texture of an isolated tooth of *Spinosaurus* sp., MSNM V6422. Scale bars equals 1 mm.

FIGURE 2.7. Anatomical and morphometric terminology used in this study. **A**, Mid-height cross-section of crown C showing MCW (mid-crown width) and MCL (mid-crown length), in apical view; **B**, Basal cross-section of crown in C showing CBL (crown-base length), DMT (dentine thickness mesially), DDT (dentine thickness distally), DLAT (dentine thickness labially), and DLIT (dentine thickness lingually), in basal view; **C**, Idealized lateral theropod tooth showing general theropod anatomy and AL (apical length), CA (crown angle), CBL (crown-base length), CH (crown height), and MCL (mid-crown length), in labial view; **D**, Idealized lateral theropod tooth showing MCW (mid-crown width) and CBW (crown-base width), in distal view; **E**, Idealized distal denticles showing DDH (distal denticle height) and DDL (distal denticle length), in labial view; **F**,

Idealized distal denticles showing DDW (distal denticle width), in distal view; **G**, Idealized lateral theropod tooth showing several crown ornamentations morphology and CMU (crown marginal undulation density) and CTU (crown transverse undulation density), in labial view; **H**, Idealized fluted theropod tooth showing DA (disto-apical denticle density), DB (disto-basal denticle density), DC (disto-central denticle density), LAF (number of labial flutes), MA (mesio-apical denticle density), MB (mesio-basal denticle density), and MC (mesio-central denticle density), in labial view; **I**, Idealized lateral theropod tooth showing MDE (mesial denticle extension), MSL (mesial serrated carina length), and DSL (distal serrated carina length), in distal view.

FIGURE 2.8. Morphological diversity of denticles in non-avian theropods in lateral views. **A**, Baso-apically subrectangular distocentral denticles of the fourth left maxillary tooth (Lmx4) of *Eodromaeus murphi*, PVSJ 561; **B**, Subquadrangular distocentral denticles of an isolated maxillary tooth of *Carcharodontosaurus saharicus*, SGM Din-1; **C**, Mesiodistally subrectangular distocentral denticles of an isolated tooth of *Afrovenator abakensis*, MNN TIG1; **D**, Apically inclined and bilobate mesioapical denticles of an isolated tooth of *Megalosaurus bucklandi*, NHM R.234; **E**, Minute subquadrangular distocentral denticles with a regular morphological variation of an isolated tooth of *Suchomimus tenerensis*, MNN G73–3; **F**, Subquadrangular mesioapical denticles with planar external margins of an isolated tooth of *Acrocanthosaurus atokensis*, SMU 74646; **G**, Distocentral denticles with short interdenticular sulci and shallow interdenticular slits of the first left maxillary tooth (Lmx1) of *Erectopus superbus*, MNHN 2001–4; **H**, Large and apically hooked distocentral denticles with dramatic size variation of an isolated tooth of *Troodon formosus*, DMNH 22837; **I**, Weakly apically hooked distocentral denticles of an isolated tooth of an indeterminate Abelisauridae, ML 327; **J**, Subquadrangular distocentral denticles with wide interdenticular chambers of an isolated tooth of an indeterminate Tyrannosauridae, DMNH 21030; **K**, Baso-apically subrectangular and apically hooked distocentral denticles of an isolated tooth of *Masiakasaurus knopfleri*, FMNH PR2221; **L**, Minute subrectangular distocentral denticles with an irregular morphological variation of an isolated tooth of *Baryonyx walkeri*, NHM R.9951–278. Scale bars equals 1 mm.

FIGURE 3.1. Distribution of dental features in non-coelurosaurian theropods. Phylogenetic tree based on the results obtained by Yates (2005), Smith et al. (2007), Brusatte et al. (2010b), Sues et al. (2011), Pol and Rauhut (2012), Carrano et al. (2012), Turner et al. (2012), and Tortosa et al. (2014). The branch colors represent the dentition types and the presence or absence of constricted crowns: ziphodont taxa with unconstricted crowns are in red, ziphodont taxa with a few constricted crowns are in green, conidont taxa are in turquoise, and pachydont taxa are in violet. The colors of taxa represent the presence or absence of serrations on the mesial and distal carinae for both mesial (left column) and lateral dentition (right column): toothless taxa are in grey, taxa with unserrated crown are in green, taxa with a serrated distal carina and a serrated mesial carina not reaching the cervix are in red, taxa with a serrated distal carina and a serrated mesial carina reaching the cervix are in blue, and taxa with a serrated distal carina and an unserrated mesial carina are in yellow. Taxa with distal denticles larger than mesial ones are boxed in green. Some compsognathid taxa possess a double condition in their mesial and lateral dentition: *Juravenator* bears mesial crowns with serrated and unserrated distal carina, *Compsognathus* shows lateral crowns with unserrated and serrated distal carina, and *Sinocalliopteryx* possesses serrated and unserrated mesial carinae in the lateral teeth. **Abbreviations**: **8**, eight-shaped cross-section of lateral teeth; **D**, D-shaped cross-section of mesial teeth; **J**, J-shaped cross-section of mesial teeth; **O**, subcircular/lanceolate cross-section of mesial teeth; **P**, parlinon-shaped cross-section of mesial teeth; **U**, U-shaped cross-section of mesial teeth.

FIGURE 3.2. Distribution of dental features in Coelurosauria. Phylogenetic tree of Turner et al. (2012). The branch colors represent the dentition types: ziphodont taxa with unconstricted crowns are in red, ziphodont taxa with a few constricted crowns are in green, taxa with both folidont and ziphodont lateral dentition are in orange, folidont taxa with unconstricted mesial crowns are in pink, folidont taxa with constricted crowns only are in blue, conidont taxa are in turquoise, and pachydont taxa are in violet. Colors of taxa represent the presence or absence of serrations on the mesial and distal carinae for both mesial (left) and lateral dentition (right): toothless taxa are in grey, taxa with unserrated crowns are in green, taxa with a serrated distal carina and an unserrated mesial carina are in yellow, taxa with serrated mesial and distal carinae are in red, and taxa with both serrated mesial and distal carinae not reaching the cervix are in blue. Taxa showing both conditions (e.g., mesial dentition with unserrated teeth and lateral dentition with serrated teeth) are bicolored. Some deinonychosaurs such as *Troodon*, *Velociraptor* and *Saurornitholestes* possess a lateral dentition with serrated and unserrated carinae. Taxa with distal denticles larger than mesial ones are boxed in green, and taxa with large typically hooked denticles are boxed in purple. **Abbreviations**: **8**, eight-shaped cross-section of lateral teeth; **D**, D-shaped cross-section of mesial teeth; **J**, J-shaped cross-section of mesial teeth; **O**, subcircular/lanceolate cross-section of mesial teeth; **U**, U-shaped cross-section of mesial teeth.

FIGURE 3.3. Basal constriction in non-avian Theropoda. **A**, Fourth right premaxillary tooth of the basal saurischian *Eoraptor lunensis* (PVSJ 512) in labial view; **B**, Isolated tooth of the troodontid *Troodon formosus* (DMNH 22837) in labial view; **C**, Isolated tooth of the therizinosaurid *Erlikosaurus andrewsi* (IGM 100-111) in lateral view (Clark et al. 1994); **D**, Fourth right premaxillary tooth of the proceratosaurid *Proceratosaurus bradleyi* (NHM R.4860) in labial view. Scale bars = 5 mm.

FIGURE 3.4. Distribution of dental features in non-avian theropods. Phylogenetic tree based on Smith et al. (2007), Brusatte et al. (2010b), Sues et al. (2011), Carrano et al. (2012), Turner et al. (2012), and Tortosa et al. (2014). Letters and numbers between brackets represent polymorphic features. The asterisk refers to the basal ceratosaur *Limusaurus*. **Clade numbers**: **A**, Neotheropoda; **B**, Ceratosauria; **C**, Megalosauroidea; **D**, Averostra; **E**, Tetanurae; **F**, Allosauroidea; **G**, Avetheropoda; **H**, Tyrannosauroidea; **I**, Coelurosauria; **J**, Neotheropoda; K, Maniraptoriformes; **L**, Maniraptora; **M**, Paraves; **N**, Deinonychosauria. **Abbreviations**: **0**, absent; **1**, present at least in some teeth or some taxa; **8**, eight-shaped cross-section at the cervix; **?**, unknown; **-**, inapplicable; **~**, medium-sized denticles (i.e., between 15 and 250 denticles on the carina); **<<**, minute denticles (more than 250 denticles on the carina); **>>**, large denticles (less than 15 denticles on the carina); **A**, anastomosed oriented texture; **B**, braided oriented texture; **bco**, basal constriction at the cervix; **bst**, basal striations; **C**, conidonty (dentition with conical crowns); **CBR**, crown base ratio; **CH**, crown height in the largest teeth, in centimetres; **codm**, convex distal margin; **cos**, concave surface adjacent to carinae; **D**, D-shaped cross-section; **ddca**, displaced distal carina; **den**, dentition; **des**, denticle size; **ent**, enamel texture; **edg**, edentulous jaw; **F**, folidonty (dentition with lanceolate crowns); **flu**, fluted teeth; **hd**, hooked denticles; **I**, irregular, non-oriented, texture; **ids**, interdenticular sulci; **L**, present in lateral teeth; **lgr**, longitudinal groove; **lri**, longitudinal ridges; **M**, present in mesial teeth; **Mcs**, mesial teeth, cross-section at the cervix; **md<dd**, mesial denticles smaller than distal denticles (DSDI > 1.2); **mdrc**, mesial denticles reaching the cervix; **mun**, marginal undulations; **O**, subcircular/lanceolate cross-section; **P**, parlinon-shaped cross-section; **Pa**, pachydonty (dentition with banana-shaped crowns); **pct**, procumbent teeth; **tmca**, twisted mesial carina; **tun**, transverse undulations; **U**, U-shaped cross-section; **udca**, unserrated distal carina; **umca**, unserrated mesial carina; **V**, veined and anastomosed oriented texture; **W**, present in both mesial and lateral teeth; **Z**, ziphodonty (dentition with blade-shaped crowns).

FIGURE 3.5. Unserrated teeth in non-avian Theropoda. **A**, Right maxillary tooth of the spinosaurid *Irritator challengeri* (SMNS 58022) in labial view; **B**, Right maxillary teeth of the alvarezsaurid *Shuvuuia deserti* (IGM 100-977) in labial view; **C**, Second left dentary tooth of the dromaeosaurid *Buitreraptor gonzalezorum* (MPCA 245) in labial view; **D**, Right maxillary tooth of an undescribed troodontid (IGM 100-1323) in labial view. Scale bars = 1 mm (B–D), 1 cm (A).

FIGURE 3.6. Concave surface adjacent to carinae in non-avian Theropoda. **A**, Third left maxillary tooth of the dilophosaurid *Dilophosaurus wetherilli* (UCMP 37303) in lingual view; **B**, Isolated tooth of the megalosaurid *Afrovenator abakensis* (MNN UBA1) in labial view; **C**, Isolated tooth of the neovenatorid *Neovenator salerii* (MIWG 6348) in labial view; **D**, Fifth left maxillary tooth of *Sinraptor dongi* (IVPP 10600) in labial view (courtesy of Roger Benson). Scale bars = 1 cm.

FIGURE 3.7. Cross-section of mesial teeth in non-avian Theropoda. **A**, First right premaxillary tooth of the abelisaurid *Majungasaurus crenatissimus* (FMNH PR.2008) in apical view; **B**, Isolated premaxillary tooth of the basal tyrannosauroid *Eotyrannus lengi* (MIWG 1997.550) in apical view; **C**, First right premaxillary tooth of the allosaurid *Allosaurus fragilis* (CMNH 1234) in apical view; **D**, Isolated right premaxillary tooth of the dromaeosaurid *Dromaeosaurus albertensis* (AMNH 5356) in apical view. Scale bars = 5 mm (B,D), 1 cm (A,C).

FIGURE 3.8. Hooked denticles in non-avian Theropoda. **A**, Distal carina of third right premaxillary tooth of the basal saurischian *Eoraptor lunensis* (PVSJ 512) in labial view; **B**, Distal carina of an isolated tooth of the noasaurid *Masiakasaurus knopfleri* (FMNH PR.2696) in lateral view; **C**, Distal carina of an isolated tooth of the dromaeosaurid *Saurornitholestes* sp. (DMNH 22870) in lateral view; **D**, Distal carina of an isolated tooth of the troodontid *Troodon formosus* (DMNH 22337) in lateral view. Scale bars = 1 mm.

FIGURE 3.9. Denticles and carinae in Spinosauridae. **A**, Carina of an isolated tooth of *Baryonyx walkeri* (NHM R.9951 R.278) in lateral view; **B**, Carina of an isolated tooth of *Suchomimus tenerensis* (MNN G26-5b) in lateral view; **C**, Carina of a maxillary tooth of *Irritator challengeri* (SMNS 58022) in labial view; **D**, Carina of an isolated tooth of *Spinosaurus* cf. *aegyptiacus* (MSNM V6422) in lateral view. Scale bars = 5 mm (C), 1 mm (A–B, D).

FIGURE 3.10. Bilobate denticles in non-avian Theropoda. **A**, Mesial carina of an isolated crown of the abelisaurid *Aucasaurus garridoi* (MCF-PVPH 236) in lateral view; **B**, Mesial carina of the sixth right maxillary

tooth of the megalosaurid *Duriavenator hesperis* (NHM R.332) in lateral view; **C**, Mesial carina of the third left maxillary tooth of the possible metriacanthosaurid *Erectopus superbus* (MNHN 2001–4) in labial view; **D**, Mesial carina of the tenth maxillary tooth of the tyrannosaurid *Tyrannosaurus rex* (FMNH PR.2081) in labial view. Scale bars = 1 mm.

FIGURE 3.11. Fluted teeth in non-avian Theropoda. **A**, Second left dentary tooth of the ceratosaurid *Ceratosaurus nasicornis* (formerly *C. dentisulcatus*; UMNH VP 5278 = UUVP 158) in lingual view (courtesy of Roger Benson); **B**, Isolated mesial tooth of noasaurid *Masiakasaurus knopfleri* (FMNH PR.2696) in mesio-lingual view; **C**, Isolated tooth of the spinosaurid *Baryonyx* cf. *walkeri* (= *Suchosaurus cultridens*; NHM R.36536) in labial view; **D**, First right premaxillary tooth of the dromaeosaurid *Velociraptor mongoliensis* (AMNH 6515) in labial view. Scale bars = 1 cm (A, C), 1 mm (B, D).

FIGURE 3.12. Transverse undulations in the teeth of most basal and most derived non-avian Theropoda. **A**, Fifth? left maxillary tooth of the herrerasaurid *Herrerasaurus ischigualastensis* (formerly *Sanjuansaurus gordilloi*, PVSJ 605) in labial view; **B**, Second left maxillary tooth of the abelisaurid *Majungasaurus crenatissimus* (FMNH PR.2278) in labiodistal view; **C**, Isolated tooth of a velociraptorine Dromaeosauridae (DMNH unknown) in labial view; **D**, Isolated tooth of the troodontid *Troodon formosus* (DMNH 22337) in labiobasal view. Scale bars = 1 cm (A–B), 5 mm (C–D).

FIGURE 3.13. Marginal undulations in the teeth of non-avian Theropoda. **A**, Fourth left maxillary tooth of the ceratosaurid *Ceratosaurus nasicornis* (USNM 4735) in mesial view; **B**, Second left maxillary tooth of the abelisaurid *Majungasaurus crenatissimus* (FMNH PR.2278) in labiodistal view; **C**, Mesial carina of a left maxillary tooth of the spinosaurid *Irritator challengeri* (SMNS 58022) in mesiolabial view; **D**, Isolated crown of the neovenatorid *Neovenator salerii* (MIWG 6348) in lingual view. Scale bars = 1 cm (A, D), 5 mm (C), 1 mm (B).

FIGURE 3.14. Well-developed interdenticular sulci in non-avian Theropoda. **A**, Distal carina of sixth right maxillary tooth of the abelisaurid *Majungasaurus crenatissimus* (FMNH PR.2278) in lateral view; **B**, Distal carina of an isolated tooth of the megalosaurid *Megalosaurus bucklandi* (NHM R.234) in labial view; **C**, Distal carina of an isolated tooth of the carcharodontosaurid *Giganotosaurus carolinii* (MUCPv CH1 L2) in lateral view; **D**, Distal carina of the fifth maxillary tooth of the tyrannosaurid *Tyrannosaurus rex* (FMNH PR.2081) in lateral view. Scale bars = 1 mm.

FIGURE 3.15. Longitudinal ridges in the teeth of non-avian Theropoda. **A**, Isolated tooth of the metriacanthosaurid *Orkoraptor* burkei (MPM-Pv 3458) in lateral view (courtesy of Martín Ezcurra); **B**, Third and fourth premaxillary teeth of the tyrannosaurid *Raptorex kriegsteini* (LH PV18) in labial view; **C**, Fifth left maxillary tooth of the dromaeosaurid *Bambiraptor feinbergi* (AMNH 30556) in labial view; **D**, Second? maxillary tooth of the dromaeosaurid *Acheroraptor temertyorum* (ROM 63777) in labial view (courtesy of Derek Larson). Scale bars = 1 cm (A–B, D), 1 mm (C).

FIGURE 3.16. Irregular enamel texture of non-avian Theropoda. **A**, Tenth left maxillary tooth of the non-neotheropod theropod *Herrerasaurus ischigualastensis* (PVSJ 407) in labial view; **B**, Isolated tooth of the abelisaurid *Aucasaurus garridoi* (MCF-PVPH-236) in lateral view; **C**, Second premaxillary tooth of the allosaurid *Allosaurus* '*jimmadseni*' (NHFO 455) in labial view; **D**, Tenth maxillary tooth of the tyrannosaurid *Tyrannosaurus rex* (FMNH PR.2081) in labial view.

FIGURE 3.17. Braided enamel texture of non-avian Theropoda. **A**, Isolated tooth of the basal ceratosaur *Berberosaurus liassicus* (MNHN To 339) in lateral view; **B**, Isolated tooth of the neovenatorid *Neovenator salerii* (MIWG 6348) in lateral view; **C**, Fourteenth dentary tooth of the tyrannosaurid *Gorgosaurus libratus* (USNM 12814) in lateral view; **D**, Isolated premaxillary tooth of the dromaeosaurid *Dromaeosaurus albertensis* (AMNH 5356) in lingual view. Scale bars = 1 mm.

FIGURE 3.18. Enamel texture of spinosaurid teeth. **A**, Veined enamel texture of an isolated tooth of the baryonychine *Baryonyx walkeri* (NHM R.9951 278) in lateral view; **B**, Veined enamel texture of an isolated tooth of the baryonychine *Suchomimus tenerensis* (MNN G43–4) in lateral view; **C**, Smooth enamel texture of a maxillary tooth of the spinosaurine *Irritator challengeri* (SMNS 58022) in lateral view; **D**, Anastomosed enamel texture of an isolated tooth of the spinosaurine *Spinosaurus aegyptiacus* (MSNM V6422) in lateral view. Scale bars = 1 mm.

FIGURE 4.1. Strict consensus cladogram of seven most parsimonious trees recovered from analysis of dentition based characters. Initial analysis was a New Technology Search using TNT v.1.1 of a data matrix comprising 141 dentition-based characters for one outgroup (*Eoraptor*), 59 non-avian theropod taxa, as well as ML 327, ML 939, ML 962 and ML 966. Tree length = 703 steps; CI = 0.331; RI = 0.564. Bremer support values are in bold and bootstrap values are in italic. For silhouette attribution, see Appendices A1.1.

FIGURE 4.2. Strict consensus cladogram of 49 most parsimonious trees recovered from analysis of a supermatrix of 1972 discrete characters after the deletion of the two wildcard taxa *Erectopus* and *Piatnitzkysaurus*. The supermatrix includes a dentition-based data matrix of 141 discrete characters and six recent datasets based on whole theropod skeleton (Xu et al. 2009; Brusatte et al. 2010*d*; Martinez et al. 2011; Senter 2011; Carrano et al. 2012; Pol and Rauhut 2012). Initial analysis was a New Technology Search using TNT v.1.1 for one outgroup (*Eoraptor*), 57 non-avian theropod taxa and ML 327, ML 966, ML 939 (coded as lateral teeth), and ML 962 (coded as a mesial tooth). Tree length = 3552 steps; CI = 0.563; RI = 0.628.

FIGURE 4.3. Isolated tooth (ML 327) of an Abelisauridae in **A**, lingual; **B**, mesial; **C**, labial; **D**, distal; **F**, apical; **G**, basal; **H**, mesio-lingual; and **E**, labio-distal views: **E**, apical denticles of the distal carina in labial view. **Abbreviations**: **dca**, distal carina; **esp**, enamel spalling; **ids**, interdenticular sulcus; **idsp**, interdenticular space; **lgr**, longitudinal groove; **mca**, mesial carina; **tun**, transverse undulation; **wfa**, wear facet.

FIGURE 4.4. Isolated tooth (ML 966) of an Abelisauridae in **A**, lingual; **B**, mesial; **C**, labial; **D**, distal; **F**, apical; **G**, basal; and **H**, linguo-distal views; **E**, **I**, mid-crown denticles of the distal carina in lingual view. **Abbreviations**: **dca**, distal carina; **esp**, enamel spalling; **ids**, interdenticular sulcus; **idsp**, interdenticular space; **lgr**, longitudinal groove; **mca**, mesial carina; **mun**, marginal undulation; **tun**, transverse undulation.

FIGURE 4.5. Plots of CBR versus CHR of ML 962, ML 327, ML 966 and 23 theropod taxa comprising the data set. For reasons of clarity, only taxa with CBR of less than 1 were considered.

FIGURE 4.6. Plots of CHR versus DAVG of ML 962, ML 327, ML 966 and 21 theropod taxa comprising the data set. For reasons of clarity, only taxa with serration of less than 20 denticles were considered.

FIGURE 4.7. Plots of MAVG versus DAVG of ML 962, ML 327, ML 966 and 19 theropod taxa comprising the data set. For reasons of clarity, only taxa with serration of less than 20 denticles were considered.

FIGURE 4.8. Plots of CBR versus DAVG of ML 962, ML 327, ML 966 and 21 theropod taxa comprising the data set. For reasons of clarity, only taxa with serration of less than 22 denticles were considered.

FIGURE 4.9. Isolated tooth of *Torvosaurus tanneri* (ML 962) in **A**, labial; **B**, distal; **C**, lingual; **D**, mesial; and **F**, basal views; **E**, apical denticles of the distal carina in labial view. **Abbreviations**: **ce**, cervix; **dca**, distal carina; **idsp**, interdenticular space; **mca**, mesial carina.

FIGURE 4.10. Isolated tooth (ML 939) of *Richardoestesia* aff. *gilmorei* in **A**, lingual; **B**, distal; **C**, labial; **D**, mesial; **F**, apical; and **G**, basal views; **E, I**, mid-crown denticles of the distal carina in labial views; and **H**, enamel texture in lingual view. **Abbreviations**: **cs**, concave surface; **dca**, distal carina; **ent**, enamel texture; **esp**, enamel spalling; **ids**, interdenticular sulcus; **idsp**, interdenticular space; **lad**, labial depression; **lgr**, longitudinal groove.

FIGURE 5.1. Dentition of Afrovenatorinae from the Middle Jurassic of France and Niger. **A–I**, Teeth and denticles of *Dubreuillosaurus valesdunensis* (Allain 2002; MNHN 1998-13); **A–C**, First and second left premaxillary teeth in **A**, anterior; and **C**, palatal views; and **B**, second left premaxillary tooth in distal view; **D–G**, Isolated lateral tooth in **D**, lingual; **E**, distal; and **F**, mesial views; **G**, detail of mesial denticles in lateral view; **H**, Distal denticles of sixth right dentary tooth in lateral view; **I**, Enamel texture of sixth right maxillary tooth; **J–R**, Isolated tooth of *Afrovenator abakensis* (Sereno et al. 1996; MNN UBA1) in **J**, lingual; **K**, labial; **L**, mesial; **M**, distal; and **O**, basal views; with **N**, details of enamel texture; **P**, mesial; and **Q**, distal denticles; and **R**, marginal undulations adjacent to the mesial carina. Scale bars = 5 cm (J–M); 2 cm (O); 1 cm (A–F); 5 mm (R); 2 mm (I, N); 1 mm (G–H, P-Q).

FIGURE 5.2. Dentition of *Eustreptospondylus* and *Magnosaurus* from the Middle Jurassic of England. **A–D**, crown and denticles of *Eustreptospondylus oxoniensis* (Walker 1964; OUMNH J.13558); **A, C–D**, Third right premaxillary tooth in lingual views; **A**, details of crown; **C**, distal serration and enamel texture; **D**, apicodistal denticles; **B**, Apicomesial denticles of the sixth left maxillary tooth in lingual view; **E–H**, Crown and denticles

of *Magnosaurus nethercombensis* (Huene 1923; OUMNH J12143); **E**, Crown of fifth dentary tooth in lingual view; **F**, Mesial denticles of the third dentary tooth in lingual view; **G–H**, Distal denticles of the ninth right dentary tooth in lingual views. Scale bars = 1 cm (E); 5 mm (A, C); 1 mm (B, D, F–H).

FIGURE 5.3. Dentition of Megalosaurinae from the Middle and Late Jurassic of Europe. **A–C**, Sixth right maxillary tooth of *Duriavenator hesperis* (Waldman 1974; NHMUK R.332); with details on **A**, crown; **B**, mesial; and **C**, distal denticles in lingual views; **D–G**, Sixth right dentary tooth of *Megalosaurus bucklandi* (Mantell 1827; OUMNH J13505); with details on **D**, crown; **E**, mesial; and **F**, distal denticles in labial views; and **G**, enamel texture; **H–K**, Isolated tooth of *Torvosaurus* cf. *gurneyi* (Hendrickx and Mateus 2014*a*; ML 500) in **H**, lingual; **I**, labial; **J**, mesial; **K**, and distal views; with details of **L**, mesial; and **M**, distal denticles; and **N**, enamel texture in lateral views. Scale bars = 5 cm (H–K); 2 cm (A, D); 3 mm (G); 2 mm (L–N); 1 mm (B–C, E–F).

FIGURE 5.4. Graphical results of the discriminant analysis of 995 teeth belonging to 62 theropod taxa and 19 groupings along the first two canonical axes of maximum discrimination in the dataset (Eigenvalue of Axis 1 = 7.561, which accounted for 61.52% of the variation; Eigenvalue of Axis 2 = 2.62, which accounted for 21.38 % of the variation). Log-transformed CBL, CBW, CH, AL, MCL, MCW, MC, and DC were used in the analysis, and 70.97% of the specimens of non-avian theropods were correctly classified (see SOM 5.1 available at http://app.pan.pl/SOM/appXX-Hendrickx_etal_SOM.pdf). Morphospace occupation of megalosaurid teeth is delimited by a dashed line.

FIGURE 5.5. Graphical results of the discriminant analysis of 393 teeth belonging to 33 taxa and 11 groupings of large ziphodont theropods along the first two canonical axes of maximum discrimination in the dataset (Eigenvalue of Axis 1 = 2.52, which accounted for 65.75% of the variation; Eigenvalue of Axis 2 = 0.89, which accounted for 23.24% of the variation). Log-transformed CBL, CBW, CH, AL, MCL, MCW, MC, and DC were used in the analysis, and 68.19% of the specimens were correctly classified to their respective clades (see SOM 5.2). Morphospace occupation of megalosaurid teeth is delimited by a dashed line.

FIGURE 5.6. Graphical results of the discriminant analysis of 232 teeth belonging to 7 taxa whose dentition was separated into mesial and lateral teeth, along the first two canonical axes of maximum discrimination in the dataset (Eigenvalue of Axis 1 = 7.99, which accounted for 50.73% of the variation; Eigenvalue of Axis 2 = 4.52, which accounted for 28.73% of the variation). Log-transformed CBL, CBW, CH, AL, MCL, MCW, MC, and DC were used in the analysis, and 84.48% of the specimens were correctly classified to their respective taxa and dentition type (see SOM 5.3).

FIGURE 5.7. Graphical results of the discriminant analysis of 81 teeth belonging to 7 taxa of Megalosauridae, and one indeterminate tetanuran (‘*Megalosaurus dunkeri*’), along the first two canonical axes of maximum discrimination in the dataset (Eigenvalue of Axis 1 = 5.8, which accounted for 71% of the variation; Eigenvalue of Axis 2 = 1, which accounted for 12.36% of the variation). Raw data of CBL, CBW, CH, AL, MCL, MCW, MDE, TUD, DMT, DDT, DLAT, DLIT, MA, MC, MB, DA, DC, and DB were used in the analysis, and 65.48% of the specimens were correctly classified to their a priori genera (see SOM 5.4).

FIGURE 6.1. Avian and non-avian theropod terminology of the quadrate bone. Left quadrate of the common ostrich *Struthio camelus* (NH.11.75; courtesy of Paolo Viscardi, Horniman Museum & Gardens) annotated with **A-F**, Baumel and Witmer (1993), Elzanowski et al. (2001) and Elzanowski and Stidham (2010) terminologies; and **G-L**, the here proposed terminology for the non-avian theropod quadrate. Quadrate in **A, G**, anterior; **B, H**, lateral; **C, I**, posterior; **D, J**, medial; **E, K**, dorsal; and **F, L**, ventral views.

FIGURE 6.2. Anatomy of non-avian theropod quadrates. **A–E**, Line drawings of the right quadrate of *Tsaagan mangas* (IGM 100-1015) in **A**, anterior; **B**, lateral; **C**, posterior; **D**, medial; and **E**, ventral views; **F–I**, left and **J–K**, right quadrates of **F**, *Baryonyx walkeri* (NHM R9951); **G**, *Aerosteon riocoloradensis* (MCNA-PV-3137); **H**, an indeterminate Oviraptoridae (IGM A; Maryańska and Osmólska 1997); **I**, *Tyrannosaurus rex* (BHI 3333; Larson 2008*b*); **J**, *Allosaurus* sp. (SMA 005/02); and **K**, *Majungasaurus crenatissimus* (FMNH PR 2100) in **F–I**, posterior; and **J–K**, ventral views. **Abbreviations**: **dqjc**, dorsal quadratojugal contact; **ecc**, ectocondyle; **enc**, entocondyle; **icn**, intercondylar notch; **ics**, intercondylar sulcus; **lpq**, lateral process of the quadrate; **lvp**, lateroventral process; **mar**, mandibular articulation (in red); **mfq**, medial fossa of the quadrate; **oca**, otic capitulum; **pfl**, pterygoid flange (in green); **pfq**, posterior fossa of the quadrate; **ppne**, posterior pneumatic foramen; **qb**, quadrate body (in light and dark blue); **qf**, quadrate foramen (delimited by a broader line); **qh**, quadrate head (in yellow); **qj**, quadratojugal; **qjp**, quadratojugal process; **qr**, quadrate ridge; **qrg**, quadrate ridge

groove; **qs**, quadrate shaft (in light blue); **sqc**, squamosal contact; **sca**, squamosal capitulum; **vqjc**, ventral quadratojugal contact; **vpdq**, ventral projection of the dorsal quadratojugal contact; **vsh**, ventral shelf.

FIGURE 6.3. Topological homologies in the non-averostran theropod quadrate. **A, C, F**, Left; and **B, D, E**, right (reversed) quadrates of *Dilophosaurus wetherilli* (UCMP 37302) in **A**, anterior; **B**, lateral; **C**, posterior; **D**, medial; **E**, dorsal; and **F**, ventral views (courtesy of Randall Irmis and Matthew Carrano); **G–L**, Right quadrate (reversed) of *Majungasaurus crenatissimus* (FMNH PR 2100) in **G** anterior; **H**, lateral; **I**, posterior; **J**, medial; **K**, dorsal; and **L**, ventral views; **M–R**, Left quadrate of *Baryonyx walkeri* (NHM R9951) in **M**, anterior; **N**, lateral; **O**, posterior; **P**, medial; **Q**, dorsal; and **R**, ventral views. **S–W**, Right quadrate of *Eustreptospondylus oxoniensis* (OUMNH J.13558; reversed) in **S**, anterior; **T**, lateral; **U**, posterior; **V**, medial; and **W**, ventral views (courtesy of Paul Barrett). **Abbreviations**: **afq**, anterior fossa; **dqjc**, dorsal quadratojugal contact; **ecc**, ectocondyle; **enc**, entocondyle; **icn**, intercondylar notch; **ics**, intercondylar sulcus; **lpq**, lateral process; **mfq**, medial fossa; **pfq**, posterior fossa; **pfl**, pterygoid flange; **qf**, quadrate foramen; **qh**, quadrate head; **qjp**, quadratojugal process; **qr**, quadrate ridge; **vpdq**, ventral projection of the dorsal quadratojugal contact; **vqjc**, ventral quadratojugal contact; **vsh**, ventral shelf of the pterygoid flange.

FIGURE 6.4. Topological homologies in the non-avian averostran quadrate. **A–F**, Left quadrate of *Aerosteon riocoloradensis* (MCNA-PV-3137) in **A**, anterior; **B**, lateral; **C**, posterior; **D**, medial; **E**, dorsal; and **F**, ventral views (courtesy of Martin Ezcurra); **G–K**, Left quadrate of *Alioramus altai* (IGM 100-1844) in **G**, anterior; **H**, lateral; **I**, posterior; **J**, medial; and **K**, dorsal views (courtesy of Mick Ellison © AMNH). **L**, Right quadrate of *Qianzhousaurus sinensis* (GM F10004-1; reversed) in ventral views (courtesy of Stephen Brusatte); **M–Q**, Right quadrate of *Falcarius utahensis* (UMNH VP 14559; reversed) in **M**, anterior; **N**, lateral; **O**, posterior; **P**, medial; and **Q**, ventral views (courtesy of Lindsay Zanno); **R–W**, Left quadrate of *Bambiraptor feinbergi* (AMNH 30556) in **R**, anterior; **S**, lateral; **T**, posterior; **U**, medial; **V**, dorsal; and **W**, ventral views. **Abbreviations**: **afq**, anterior fossa; **dqjc**, dorsal quadratojugal contact; **ecc**, ectocondyle; **enc**, entocondyle; **icn**, intercondylar notch; **ics**, intercondylar sulcus; **lpq**, lateral process; **mfq**, medial fossa; **mpne**, medial pneumatic foramen; **pfq**, posterior fossa; **ppne**, posterior pneumatic foramen; **pfl**, pterygoid flange; **qf**, quadrate foramen; **qh**, quadrate head; **qjp**, quadratojugal process; **qr**, quadrate ridge; **vpdq**, ventral projection of the dorsal quadratojugal contact; **vpne**, ventral pneumatic foramen; **vqjc**, ventral quadratojugal contact; **vsh**, ventral shelf of the pterygoid flange.

FIGURE 6.5. Distribution of quadrate pneumaticity in Theropoda. Cladogram of non-avian theropods based on the most recent cladistic analyses on theropods (see Chapter 1) and showing the phylogenetic distribution of quadrate pneumatic foramina in non-avian theropods.

FIGURE 6.6. Morphology and position of pneumatic openings in the quadrate of non-avian Theropoda. Right quadrate (**A**) of the carcharodontosaurid *Acrocanthosaurus atokensis* (NCSM 14345; reversed) in medial view. Left quadrate (**B**) of the carcharodontosaurid *Mapusaurus roseae* (MCF-PVPH-108) in medial view. Left quadrate (**C**) of the carcharodontosaurid *Giganotosaurus carolinii* (MUCPv CH 1) in medial view. Right quadrate (**D**) of the therizinosauroid *Falcarius utahensis* (UMNH VP 14559; reversed) in medial view (courtesy of Lindsay Zanno). Right quadrate (**E**) of the metriacanthosaurid *Sinraptor dongi* (IVPP 10600; reversed) in posterior view (courtesy of Philip Currie). Left quadrate (**F**) of the neovenatorid *Aerosteon riocoloradensis* (MCNA PV 3137) in posterior view (courtesy of Martín Ezcurra). Left quadrate (**G**) of the ornithomimid *Garudimimus brevipes* (IGM 100–13) in posterior view (courtesy of Yoshitsugu Kobayashi). Right quadrate (**H**) of the dromaeosaurid *Buitreraptor gonzalezorum* (MPCA 245; reversed) in posterior view. Right quadrate (**I**) of the tyrannosaurid *Alioramus altai* (IGM 100–844) in ventral view (courtesy of Mick Ellison). Left quadrate (**J**) of the tyrannosaurid *Tyrannosaurus rex* (FMNH PR2081; cast, reversed) in ventral view. Left quadrate (**K**) of the carcharodontosaurid *Mapusaurus roseae* (MCF-PVPH-108) in anterior view. Left quadrate (**L**) of the neovenatorid *Aerosteon riocoloradensis* (MCNA PV 3137) in lateral view (courtesy of Martín Ezcurra). **Abbreviations**: **apne**, anterior pneumatic foramen; **lpq**, lateral process; **lpne**, lateral pneumatic foramen; **mpne**, medial pneumatic foramen; **ppne**, posterior pneumatic foramen; **qf**, quadrate foramen; **vpne**, ventral pneumatic foramen. Scale bars = 10 cm (A–C, J, K), 5 cm (E–G,L), 1 cm (D,H, I).

FIGURE 6.7. Quadrate of embryonic specimen of *Lourinhanosaurus antunesi* (ML565-150). **A–H**, Incomplete left quadrate in **A**, anterior; **B**, lateral; **C**, posterior; **D**, medial; **E**, ventral; **F**, dorsal; **G**, posteromedial; and **H**, ventromedial views (the quadrate in **G** and **H** was photographed before preparation). **Abbreviations**: **dqjc**, dorsal quadratojugal contact; **ecc**, ectocondyle; **enc**, entocondyle; **mfq**, medial fossa; **pfl**, pterygoid flange; **pfq**, posterior fossa; **qjp**, quadratojugal process; **qr**, quadrate ridge; **vqjc**, ventral quadratojugal contact.

FIGURE 6.8. Incomplete left quadrate of *Lourinhanosaurus antunesi* embryo (ML565-10; lost) in **A, C**, anterior; and **B**, lateral views. **Abbreviations**: **dqjc**, dorsal quadratojugal contact; **ecc**, ectocondyle; **enc**, entocondyle; **pfl**, pterygoid flange; **vqjc**, ventral quadratojugal contact (drawings by and courtesy from Simão Mateus).

FIGURE 6.9. Quadrates of juvenile and adult specimens of *Shuvuuia deserti*. **A**, Skull of the juvenile *Shuvuuia deserti* (IGM 100-1001; reversed) in lateral view; **B–C**, comparison between the left quadrate of the juvenile specimen of *Shuvuuia deserti* (IGM 100-1001) in **B**, posterior; and **C**, lateral view; and **D–E**, the right quadrate of the adult specimen of *Shuvuuia deserti* (IGM 100-977) in **D**, posterior; and **E**, posterolateral views. **Abbreviations**: **j**, jugal; **jc**, jugal contact; **lpq**, lateral process; **oca**, otic capitulum; **pfl**, pterygoid flange; **po**, postorbital; **poc**, postorbital contact; **qf**, quadrate foramen; **sq**, squamosal; **sca**, squamosal capitulum. Scale bars = 2 cm (1-2), 1 cm (5-6), and 5 mm (3-4).

FIGURE 7.1. Strict consensus cladogram from 13 most parsimonious trees. Initial analysis was a New Technology Search using TNT v.1.1 of a data matrix comprising 98 quadrate based characters for one outgroup (*Herrerasaurus ischigualastensis*) and 54 non-avian theropod taxa. Tree length = 589 steps; CI = 0.282; RI = 0.556. Bremer support values are in bold and bootstrap values are in italic.

FIGURE 7.2. Strict consensus cladogram from 34 most parsimonious trees. Initial analysis was a New Technology Search using TNT v.1.1 of a supermatrix comprising 98 quadrate based characters combined with six recent datasets based on the whole skeleton (Brusatte et al. 2010*d*; Choiniere et al. 2010*b*; Martinez et al. 2011; Carrano et al. 2012; Pol and Rauhut 2012) for one outgroup (*Eoraptor lunensis*) and 54 non-avian theropod taxa. Tree length = 3616 steps; CI = 0.562; RI = 0.63113. Bremer support values are in bold and bootstrap values are in italic.

FIGURE 7.3. **A**, Cladogram resulting from the phylogenetic morphometrics analysis of the quadrate body shape in posterior view using 12 landmarks (tree score: 3.25, by using RFTRA) and revealing two morphotypes: low and stout quadrate with well-delimited and relatively broad lateromedially quadrate foramen (morphotype A; Spinosauridae and Coelurosauria) versus tall and slender quadrate with a lateromedially narrow or completely absent quadrate foramen (morphotype B; Ceratosauria and Megalosauridae); **B**, Cladogram resulting from the phylogenetic morphometrics analysis of the mandibular articulation in ventral view using 8 landmarks (tree score: 2.92; by using RFTRA) and revealing two morphotypes: anteroposteriorly broad mandibular articulation with two ovoid/subcircular condyles roughly subequal in size (Morphotype A; Ceratosauria, Tyrannosauroidea and Oviraptorosauria) versus elongate and anteroposteriorly narrow mandibular articulation with a long and parabolic/sigmoid ectocondyle (Morphotype B; Megalosauroidea, Carcharodontosauridae and Dromaeosauridae).

FIGURE 7.4. Quadrate diversity in non-neotheropod Theropoda. **A–D**, Right quadrate of *Herrerasaurus ischigualastensis* (PVSJ 53, formerly *Frenguellisaurus ischigualastensis*) in **A**, posterior; **B**, medial; **C**, anterior; and **D**, ventral views; **E**, Right quadrate of *Eoraptor lunensis* (PVSJ 512) in posterolateral view; **F–J**, Left quadrate of *Eodromaeus murphi* (PVSJ 562) in **F**, lateral; **G**, medial; **H**, posterior; **I**, dorsal; and **J**, ventral views; **K–M**, Left and **N–P**, right quadrates of *Tawa hallae* (GR 241) in **K**, lateral; **L, N**, posterior; **M, O**, medial; and **P**, ventral views (courtesy of Sterling Nesbitt). **Abbreviations**: **ecc**, ectocondyle; **enc**, entocondyle; **lpq**, lateral process; **mfq**, medial fossa; **pfl**, pterygoid flange; **pfq**, posterior fossa; **qf**, quadrate foramen; **qjp**, quadratojugal process; **qr** quadrate ridge; **vsh**, ventral shelf of the pterygoid flange.

FIGURE 7.5. Quadrate diversity in Coelophysoidea. **A–F**, Right quadrate of *Liliensternus liliensterni* (MB R.2175) in **A**, anterior; **B**, lateral; **C**, posterior; **D**, medial; **E**, dorsal; and **F**, ventral views (courtesy of Martín Ezcurra). **G–H**, Right and **H–I**, left quadrates of *Megapnosaurus kayentakatae* (MNA V2623) in **I**, lateral; and **G, H**, posterior views (courtesy of Ronald Tykoski); **J, L, O**, Left and **K, M–N**, right quadrates of *Dilophosaurus wetherilli* (UCMP 37302) in **J**, anterior; **K**, lateral; **L**, posterior; **M**, medial; **N**, dorsal; and **O**, ventral views (courtesy of Randall Irmis). **Abbreviations**: **ecc**, ectocondyle; **enc**, entocondyle; **lpq**, lateral process; **mfq**, medial fossa; **pfl**, pterygoid flange; **pfq**, posterior fossa; **qf**, quadrate foramen; **qh**, quadrate head; **qjp**, quadratojugal process; **qr** quadrate ridge; **vsh**, ventral shelf of the pterygoid flange.

FIGURE 7.6. Quadrate diversity in Ceratosauridae and Noasauridae. **A, C**, Coosified right and **B, D–E**, left quadrates and quadratojugals of *Ceratosaurus nasicornis* (MWC 1; formerly known as *C.* '*magnicornis*') in **A**, anterior; **B**, lateral; **C**, posterior; **D**, medial; and **E**, ventral views; **F–I**, Right quadrate of *Masiakasaurus knopfleri* (FMNH PR 2496) in **F**, lateral; **G**, posterior; **H**, medial; and **I**, ventral views (courtesy of Matthew Carrano); **J–O**, Right quadrate of *Noasaurus leali* (PVL 4061) in **J**, anterior; **K**, lateral; **L**, posterior; **M**, medial,

dorsal; and **N, O**, ventral views. **Abbreviations**: **ecc**, ectocondyle; **enc**, entocondyle; **ics**, intercondylar sulcus; **lpq**, lateral process; **mfq**, medial fossa; **pfl**, pterygoid flange; **qh**, quadrate head; **qjc**, quadratojugal contact; **qr** quadrate ridge; **vsh**, ventral shelf of the pterygoid flange; **pfq**, posterior fossa.

FIGURE 7.7. Quadrate diversity in Abelisauridae. **A–F**, Right quadrate of *Ilokelesia aguadagrandensis* (PVPH 35) in **A**, anterior; **B**, lateral; **C**, posterior; **D**, medial; **E**, dorsal; and **F**, ventral views (courtesy of Matthew Lamanna); **G–L**, Right quadrate of *Majungasaurus crenatissimus* (FMNH PR 2100) in **G**, anterior; **H**, lateral; **I**, posterior; **J**, medial; **K**, dorsal; and **L**, ventral views (courtesy of Lawrence Witmer); **M, N, O, P**, Right; and **O, Q**, left quadrates of *Carnotaurus sastrei* (MACN CH 894) in **M**, anteroventral; **N**, lateral; **O**, posterior; **P**, anteromedial; and **Q**, ventral views (courtesy of Pablo Asaroff). **Abbreviations**: **ecc**, ectocondyle; **enc**, entocondyle; **icn**, intercondylar notch; **ics**, intercondylar sulcus; **lpq**, lateral process; **mfq**, medial fossa; **pfq**, posterior fossa; **qh**, quadrate head; **qjc**, quadratojugal contact; **qr** quadrate ridge; **ri**, ridge on the ventrolateral surface of the quadrate body; **vsh**, ventral shelf of the pterygoid flange.

FIGURE 7.8. Quadrate diversity in Megalosauridae. **A–E**, Right quadrate of *Eustreptospondylus oxoniensis* (OUMNH J.13558) in **A**, anterior; **B**, lateral; **C**, posterior; **D**, medial and **E**, ventral views (courtesy of Paul Barrett); **F–K**, Right quadrate of *Torvosaurus tanneri* (BYU-VP 9246) in **F**, anterior; **G**, lateral; **H**, posterior; **I**, medial; **J**, dorsal; and **K**, ventral views (courtesy of Matthew Lamanna); **L–Q**, Left quadrates of *Afrovenator abakensis* (UC OBA1) in **L**, anterior; **M**, lateral; **N**, posterior; **O**, medial; **P**, dorsal; and **Q**, ventral views (courtesy of Roger Benson). **Abbreviations**: **ecc**, ectocondyle; **enc**, entocondyle; **fo1**, medial foramen 1; **fo2**, medial foramen 2; **ics**, intercondylar sulcus; **mfq**, medial fossa; **pfq**, posterior fossa; **qh**, quadrate head; **qjc**, quadratojugal contact; **qjp**, quadratojugal process; **vmfo**, ventromedial foramen.

FIGURE 7.9. Quadrate diversity in Spinosauridae. **A–F**, Left quadrate of *Baryonyx walkeri* (NHM R9951) in **A**, anterior; **B**, lateral; **C**, posterior; **D**, medial; **E**, dorsal; and **F**, ventral views; **G–L**, Left quadrate of *Suchomimus tenerensis* (MNN GAD 502) in **G**, anterior; **H**, lateral; **I**, posterior; **J**, medial; **K**, dorsal; and **L**, ventral views; **M–R**, Left quadrate of and indeterminate Spinosaurinae from the Kem Kem beds (MSNM V6896) in **M**, anterior; **N**, lateral; **O**, posterior; **P**, medial; **Q**, dorsal; and **R**, ventral views. **Abbreviations**: **ecc**, ectocondyle; **enc**, entocondyle; **icp**, intercondylar pit; **lfo**, lateral foramen; **mfq**, medial fossa; **pfl**, pterygoid flange; **qf**, quadrate foramen; **qh**, quadrate head; **qjp**, quadratojugal process; **qr**, quadrate ridge; **vpdq**, ventral projection of the dorsal quadratojugal contact; **vsh**, ventral shelf of the pterygoid flange.

FIGURE 7.10. Quadrate diversity in non-carcharodontosaurid Allosauroidea. **A–F**, Left coosified quadrate and quadratojugal of *Allosaurus* '*jimmadseni*'. (SMA 005/02) in **A**, anterior; **B**, lateral; **C**, posterior; **D**, medial; **E**, dorsal; and **F**, ventral views; **G–L**, Left quadrate of *Aerosteon riocoloradensis* (MCNA-PV-3137) in G, anterior; **H**, lateral; **I**, posterior; **J**, medial; **K**, dorsal, and **L**, ventral views (courtesy of Martin Ezcurra); **M–Q**, Right quadrate of *Sinraptor dongi* (IVPP 10600) in **M**, anterior; **N**, lateral; **O**, posterior; **P**, medial; and **Q**, ventral views (Currie 2006 for M, P–Q; courtesy of Philip Currie for N–O). **Abbreviations**: **ecc**, ectocondyle; **enc**, entocondyle; **dqjc**, dorsal quadratojugal contact; **icp**, intercondylar pit; **lpq**, lateral process; **pfq,** posterior fossa; **ppne**, posterior pneumatic foramen; **qf**, quadrate foramen; **qr**, quadrate ridge; **qrg**, quadrate ridge groove; **vqjc**, ventral quadratojugal contact; **vsh**, ventral shelf of the pterygoid flange.

FIGURE 7.11. Quadrate diversity in Carcharodontosauridae. **A, E**, Right and **B–D**, left coosified quadrate and quadratojugal of *Acrocanthosaurus atokensis* (NCSM 14345) in **A**, anterior; **B**, lateral; **C**, posterior; **D**, medial; and **E**, ventral views (courtesy of Drew Eddy and Vince Shneider); **F–K**, Right quadrate of *Shaochilong moartuensis* (IVPP V2885.3) in **F**, anterior; **G**, lateral; **H**, posterior; **I**, medial; **J**, dorsal; and **K**, ventral views (courtesy of Steve Brusatte); **L–Q**, Left quadrate of *Mapusaurus rosea* (MCFPVPH-108.102) in **L**, anterior; **M**, lateral; **N**, posterior; **O**, medial; **P**, dorsal; and **Q**, ventral views (courtesy of Matthew Lamanna). **Abbreviations**: **apne**, anterior pneumatic foramen; **lpq**, lateral process; **mfq**, medial fossa; **mpne**, medial pneumatic foramen; **pfq**, posterior fossa; **ppne**, posterior pneumatic foramen; **qf**, quadrate foramen; **qrg**, quadrate ridge groove; **vsh**, ventral shelf of the pterygoid flange.

FIGURE 7.12. Quadrate diversity in Tyrannosauroidea. **A–C**, Left and right quadrates of *Proceratosaurus bradleyi* (NHM R 4860) in A, posterior; and **B–C**, posteromedial views; **D–I**, Ventral part of the right quadrate of *Eotyrannus lengi* (MIWG 1997.550) in **D**, anterior; **E**, lateral; **F**, posterior; **G**, medial; **H**, dorsal; and **I**, ventral views; **J–O**, Left quadrate of *Alioramus altai* (IGM 100-1844) in **J**, anterior; **K**, lateral; **L**, posterior; **M**, medial; **N**, dorsal; and **O**, ventral views (courtesy of Mick Ellison © AMNH). **Abbreviations**: **dqjc**, dorsal quadratojugal contact; **ecc**, ectocondyle; **enc**, entocondyle; **mfq**, medial fossa; **pfl**, pterygoid flange; **pfq**, posterior fossa; **qf**, quadrate foramen; **qh**, quadrate head; **qr**, quadrate ridge; **vqjc**, ventral quadratojugal contact; **vpne**, ventral pneumatic foramen.

FIGURE 7.13. Quadrate diversity in Ornithomimosauria and Therizinosauria. **A**, Left quadrate of *Struthiomimus altus* (AMNH 5339) in lateral view; **B**, Left quadrate of *Gallimimus bullatus* (IGM 100-1133) in ventral view; **C–D**, Right coosified quadrates and quadratojugal of *Ornithomimus edmontonicus* (RTMP 95.110.1) in **A, C**, lateral; and **B, D**, lateroposterior views (courtesy of Rui Tahara and Yoshitsugu Kobayashi); **E**, Left coosified quadrate and quadratojugal of *Sinornithomimus dongi* (IVPP−V11797−10) in posterior view (courtesy of Yoshitsugu Kobayashi, modified); **F**, Left and **G**, right coosified quadrates and quadratojugals of *Garudimimus brevipes* (IGM 100-13) in posterior view (courtesy of Yoshitsugu Kobayashi, modified); **H**–**L**, Right quadrate of *Falcarius utahensis* (UMNH VP 14559) in **H**, anterior; **I**, lateral; **J**, posterior; **K**, medial; and **L**, ventral views (courtesy of Lindsay Zanno). **Abbreviations**: **dqjc**, dorsal quadratojugal contact; **ecc**, ectocondyle; **enc**, entocondyle; **exo**, exoccipital; **j**, jugal; **la**, lacrimal; **mpne**, medial pneumatic foramen; **pfq**, posterior fossa; **po**, postorbital; **ppne**, posterior pneumatic foramen; **qf**, quadrate foramen; **qh**, quadrate head; **qj**, quadratojugal; **pfq**, posterior fossa; **ppne**, posterior pneumatic foramen; **sq**, squamosal; **vqjc**, ventral quadratojugal contact.

FIGURE 7.14. Quadrate diversity in basal Coelurosauria and Alvarezsauroidea. **A**–**B**, **F**, Right; and **C**–**E**, left quadrates of *Bicentenaria argentina* (MPCA 865) in **A**, anterior; **B**, lateral; **C**, posterior; **D**, medial; **E**, dorsal; and **F**, ventral views; **G**–**H**, Right quadrate of *Ornitholestes hermanni* (AMNH FARB 619) in **G**, lateral; **H, J**, posterior; **I**, posterolateral; and **K**, ventral views; **J**, details of the central part of the quadrate body (photo courtesy shared by Mickey Mortimer); **L**–**M**, Right and **N**–**P**, left quadrates of *Shuvuuia deserti* (L–M: IGM 100-977; N–P: IGM 100-1001) in **L**, **N**, posterior; **M**, posteromedial; **O**, lateral; and **P**, ventral views. **Abbreviations**: **dpvq**, dorsal projection of the ventral quadratojugal contact; **ecc**, ectocondyle; **enc**, entocondyle; **ics**, intercondylar sulcus; **lpq**, lateral process; **mfq**, medial fossa; **oca**, ootic capitulum; **pfl**, pterygoid flange; **pfq**, posterior fossa; **po**, postorbital; **poc**, postorbital contact; **pt**, pterygoid; **ptc**, pterygoid contact; **qf**, quadrate foramen; **qh**, quadrate head; **qj**, quadratojugal; **qjc**, quadratojugal contact; **qr**, quadrate ridge; **sca**, squamosal capitulum; **sq**, squamosal; **vpdq**, ventral projection of the dorsal quadratojugal contact; **vpne**, ventral pneumatic foramen; **vqjc**, ventral quadratojugal contact; **vsh**, ventral shelf.

FIGURE 7.15. Quadrate diversity in Oviraptorosauria. **A–D**, Occipital part of the cranium of *Avimimus portentosus* (cast of PIN 3907/1) in **A**, lateral; **B**, posterior; **C**, anterolateral, and **D**, ventral views (courtesy of Lawrence Witmer); **E–H**, Right quadrate of *Citipati osmolskae* (IGM 100-978) in **E**, lateral; **F**, posterior; **G**, medioposterior; and **H**, ventral views; **I–L**, Right quadrate of *Khaan mckennai* (IGM 100-1127 for I–J, IGM 100-1002 for L) in **I**, **L**, lateral; **J**, posterolateral; and **K**, anterolateral views. **Abbreviations**: **brc**, braincase contact; **dptc**, dorsal pterygoid contact; **dqjc**, dorsal quadratojugal contact; **ecc**, ectocondyle; **enc**, entocondyle; **pfl**, pterygoid flange; **pfq**, posterior fossa; **pt**, pterygoid; **ptc**, pterygoid contact; **qf**, quadrate foramen; **qj**, quadratojugal; **qjc**, quadratojugal contact; **qr**, quadrate ridge; **sq**, squamosal; **sqc**, squamosal contact; **vptc**, ventral pterygoid contact; **vqjc**, ventral quadratojugal contact.

FIGURE 7.16. Quadrate diversity in Dromaeosauridae. **A–F**, Left quadrate of *Bambiraptor feinbergi* (AMNH 30556) in **A**, anterior; **B**, lateral; **C**, posterior; **D**, medial; **E**, dorsal; and **F**, ventral views; **G**–**K**, Right quadrate of *Tsaagan mangas* (IGM 100-1015) in **G**, anterior; **H**, lateral; **I**, posterior; **J**, medial; and **K**, ventral views (courtesy of Mick Ellison); **L–Q**, Right quadrate of *Dromaeosaurus albertensis* (AMNH 5356) in **L**, anterior; **M**, lateral; **N**, posterior; **O**, medial; **P**, dorsal; and **Q**, ventral views. **Abbreviations**: **dqjc**, dorsal quadratojugal contact; **ecc**, ectocondyle; **enc**, entocondyle; **ics**, intercondylar sulcus; **lpq**, lateral process; **mfq**, medial fossa; **pfl**, pterygoid flange; **pfq**, posterior fossa; **pt**, pterygoid; **qf**, quadrate foramen; **qh**, quadrate head; **qjp**, quadratojugal process; **qr**, quadrate ridge; **sqc**, squamosal contact; **vqjc**, ventral quadratojugal contact; **vptc**, ventral pterygoid contact.

FIGURE 8.1. Geographical location and stratigraphy of the Kem Kem beds. **A**, Location of Morocco (in black) in Africa (left corner), the Kem Kem and Tafilalt regions (in red) in Morocco (middle left), and the Kem Kem beds (in black) in the Kem Kem plateau (right). The black star indicates the site in which two quadrates were found; **B**, Stratigraphic column of the Kem Kem beds of South-Eastern Morocco. Stratigraphic position of the type remains of **1**, *Carcharodontosaurus saharicus* (neotype; Sereno et al. 1996; Brusatte and Sereno 2007); **2**, *Spinosaurus aegyptiacus* (neotype; Ibrahim et al. 2014*b*); and **3**, *Deltadromeus agilis* (holotype; Sereno et al. 1996); and **4**, probable stratigraphic position of the here studied material. The presence of *Carcharodontosaurus* material in the 'upper unit' is here questioned. Modified from Sereno et al. (1996) and Ibrahim et al. (2014*a*).

FIGURE 8.2. Quadrate position and quadrate morphotypes in Spinosaurinae from the Kem Kem beds. **A–B**, Position of the quadrate bone in the *Spinosaurus* skull in **A**, left lateral; and **B**, occipital views; **C–F**, Morphotype 1; and **G–J**, reconstructed morphotype 2 of an idealized left quadrate of *Spinosaurus* in **C,G**, anterior; **D, H**, lateral; **E, I**, posterior; and **F, J**, ventral views. **Abbreviations**: **an**, angular; **bo**, basioccipital; **bs**,

basisphenoid; **d**, dentary; **dqjc**, dorsal quadratojugal contact; **ecc**, ectocondyle; **ecd**, ectocondyle depression; **enc**, entocondyle; **ics**, intercondylar sulcus; **j**, jugal; **l**, lacrimal; **m**, maxilla; **n**, nasal; **oc**, occipital condyle; **p**, parietal; **pm**, premaxilla; **pop**, paroccipital process; **pt**, pterygoid; **q**, quadrate; **qf**, quadrate foramen; **qj**, quadratojugal; **qr**, quadrate ridge; **sa**, surangular; **so**, supraoccipital; **sq**, squamosal; **vqjc**, ventral quadratojugal contact.

FIGURE 8.3. Quadrates of Morphotype 1 referred to *Spinosaurus aegyptiacus*. **A–N**, Left quadrates of specimens **A–F**, MHNM.KK374; **G–L**, MHNM.KK375; and **M–N**, MSNM V6896, in **A, G, M**, anterior; **B, H, N**, lateral; **C, O**, posterior; **I**, posteromedial; **D**, posterolateral; **J, P**, lateral; **E, K, P**, dorsal; and **F, L, R**, ventral views. **Abbreviations**: **dqjc**, dorsal quadratojugal contact; **ecc**, ectocondyle; **enc**, entocondyle, **ics**, intercondylar sulcus; **mfq**, medial fossa; **pfl**, pterygoid flange; **pgq**, posterior groove; **qf**, quadrate foramen; **qh**, quadrate head; **qr**, quadrate ridge; **vpdq**, ventral projection of the dorsal quadratojugal contact; **vqjc**, ventral quadratojugal contact.

FIGURE 8.4. Quadrate of Morphotype 2 referred to *Spinosaurus maroccanus*. **A–F**, Right quadrate MHNM.KK376 in **A**, anterior; **B**, lateral; **C**, posterior; **D**, medial; **E**, ventral; **F**, ventromedial; and **G**, dorsal views. **Abbreviations**: **dqjc**, dorsal quadratojugal contact; **ecc**, ectocondyle; **ecd**, depression of the ectocondyle; **enc**, entocondyle, **ics**, intercondylar sulcus; **mfq**, medial fossa; **pfl**, pterygoid flange; **qf**, quadrate foramen; **qr**, quadrate ridge; **vpdq**, ventral projection of the dorsal quadratojugal contact; **vqjc**, ventral quadratojugal contact.

FIGURE 8.5. **A–D**, Measurements taken on the six spinosaurine quadrates from the Kem Kem beds of Morocco in **A**, lateral; **B**, posterior, **C**, medial; and **D**, ventral views; **E**, location of the ten landmarks used in the morphometric analyses in an idealized mandibular articulation of a non-avian theropod in ventral view. **Abbreviations**: **ecc**, ectocondyle; **enc**, entocondyle, **ics**, intercondylar sulcus.

FIGURE 8.6. Quadrate based phylogeny of non-avian theropods. Strict consensus cladogram from most parsimonious trees after the a posteriori deletion of *Monolophosaurus*. Initial analysis was a New Technology Search using TNT v.1.1 of a supermatrix comprising 98 quadrate based characters combined with seven recent datasets (i.e., Brusatte et al. 2010*d*; Martinez et al. 2011; Carrano et al. 2012; Pol and Rauhut 2012; Novas et al. 2013; Choiniere et al. 2014*b*) based on the whole skeleton, for one outgroup (*Eoraptor lunensis*) and 58 non-avian theropod taxa. Tree length = 4994; CI = 0.522, RI = 0.61. For silhouette attribution, see Appendices A1.1.

FIGURE 8.7. Results of the geometric morphometric analysis performed on the mandibular articulation of non-avian theropods. PCA plot of the principal component analysis performed on 37 theropod taxa and 10 landmarks along the first two principal axes explaining 35.8% and 20.04% of the variation in the sample. Colors refer to theropod clades and correspond to those in Figure 8.6. Major groupings at family level are delimited and outline images are associated with taxa of hypothetical extremes.

FIGURE 8.8. Results of the phylogenetic morphometric analysis. **A–B**, Phylogenetic morphometric analysis of the mandibular articulation of 36 non-avian taxa performed with a degree of thoroughness of one, and using **A**, 10 landmarks on the quadrate in ventral view (Tree score = 5.18); and **B**, a combination of the phylogenetic morphometric character based on 10 landmarks of the mandibular articulation in ventral view and 2377 discrete characters from the supermatrix (Tree score = 6.61).

FIGURE 8.9. Quadrate morphology in Baryonychinae and *Irritator*. **A–L**, Left quadrates of **A–F**, *Baryonyx walkeri* (NHM R9951); and **G–L**, *Suchomimus tenerensis* (MNN GAD 502) in **A, G**, anterior; **B, H**, lateral; **C, I**, posterior; **D, J**, medial; **E, K**, dorsal; and **F, L**, ventral views. **M–N**, Right and **O–Q**, left quadrates of *Irritator challengeri* (SMNS 58022) with **M**, close up on the lateral portion of the quadrate body; **N**, quadrate foramen; **O**, anteromedial surface of the pterygoid flange; and **P–Q**, quadrate head in **M–N, P**, posterolateral, **O**, anterior; **Q**, and dorsal views. **Abbreviations**: **ecc**, ectocondyle; **enc**, entocondyle; **icp**, intercondylar pit; **lfo**, lateral foramen; **lpq**, lateral process; **mfq**, medial fossa; **pfl**, pterygoid flange; **qf**, quadrate foramen; **qh**, quadrate head; **qjp**, quadratojugal process; **qr**, quadrate ridge; **qs**, quadrate shaft; **vpdq**, ventral projection of the dorsal quadratojugal contact; **vsh**, ventral shelf of the pterygoid flange.

FIGURE 8.10. Ontogenetical changes in the quadrates of *Spinosaurus aegyptiacus* (Morphotype 1). **A–C**, Left quadrate MHNM.KK374 representing ontogenetic stage 1 (juvenile) with **A**, close up on the smooth lateral surface of the dorsal quadratojugal contact in lateral view; **B**, quadrate foramen and absence of a ventral projection of the dorsal quadratojugal contact in posterior view; **C**, and non-delimited mandibular condyles in ventral view. **D–E**, Left quadrates of specimens **D, F**, MHNM.KK377; and **E**, MSNM V6896 representing ontogenetic stage 2 and 3 (immature to subadult) with **D**, close up on the ridged dorsal quadratojugal contact in lateral view; **E**, quadrate foramen and a ventral projection of the dorsal quadratojugal contact in posterior view;

and **F**, poorly delimited mandibular condyles in ventral view. **G–I**, Left quadrate MHNM.KK375 representing ontogenetic stage 4 (adult) with **G**, close up on the irregular and ridged lateral surface of the dorsal quadratojugal contact in lateral view; **H**, deeply excavated ventral quadratojugal contact in lateral view; and **I**, well-delimited mandibular condyles in ventral view. **J–L**, Left quadrate MHNM.KK378 representing ontogenetic stage 4 (large fully mature) with **J**, close up on the protuberant squamosal capitulum in ventral view; **K**, second dorsal quadrate ridge extending to the quadrate head in posterior view; and **L**, well-delimited entocondyle with deep intercondylar sulcus in ventral view. **Abbreviations**: **enc**, entocondyle; **ics**, intercondylar sulcus; **qr**, quadrate ridge; **ri**, ridge of the dorsal quadratojugal contact; **vpdq**, ventral projection of the dorsal quadratojugal contact. Quadrates not to scale.

FIGURE 8.11. Comparison of the snout of two specimens of *Spinosaurus* from the 'Continental intercalaire' of Northwestern Africa. **A–H**, Fused maxillae and premaxillae of **A–B, E, G**, MSNM V4047 referred to *Spinosaurus aegyptiacus* by Dal Sasso et al. (2005) (courtesy of Simone Maganuco); and **C–D, F, H**, MNHM SAM 124 referred to *Spinosaurus maroccanus* by Taquet and Russell (1998) in **A, C**, lateral; **B, D**, anterior; **E, F**, ventral; and **G, H**, dorsal views. Abbreviation: **mx9**, ninth maxillary alveolus; **pmx6**, sixth premaxillary alveolus, **pmx7**, seventh premaxillary alveolus. Scale = 20 cm (A, E, G), 10 cm (C, F, H), 5 cm (B), 2 cm (D).

FIGURE 8.12. Morphological diversity of the mandibular articulation in non-avetheropod theropods. **A–P**, **R–T**, right quadrate (unless indicated) in ventral view in; **A**, *Herrerasaurus ischigualastensis* (formerly '*Frenguellisaurus*' *ischigualastensis*; PVSJ 053; left reversed); **B**, *Eodromaeus murphi* (PVSJ 562); **C**, *Tawa hallae* (GR 241; courtesy of Sterling Nesbitt); **D**, *Dilophosaurus wetherilli* (UCMP 37302; left reversed; courtesy of Juan Canale); **E**, *Ceratosaurus nasicornis* (MWC 1; left reversed); **F**, *Masiakasaurus knopfleri* (FMNH PR 2496); **G**, *Noasaurus leali* (PVL 4061); **H**, *Ilokelesia aguadagrandensis* (MCF-PVPH 35); **I**, *Abelisaurus comahuensis* (MPCA 11098; left reversed; in posteroventral view); **J**, *Aucasaurus garridoi* (MCF-PVPH 236); **K**, *Majungasaurus crenatissimus* (FMNH PR 2100; left reversed); **L**, *Carnotaurus sastrei* (MACN-CH 894; left reversed; courtesy of Pablo Asaroff); **M**, *Baryonyx walkeri* (NHM R.9951; left reversed); **N**, *Suchomimus tenerensis* (MNN GAD502; left reversed); **O**, *Spinosaurus aegyptiacus* Morphotype 1 (MHNM.KK375; left reversed); **P**, *Spinosaurus maroccanus* Morphotype 2 (MHNM.KK376; left reversed); **Q**, anatomy and orientation of an idealized right quadrate in ventral view; **R**, *Eustreptospondylus oxoniensis* (OUMNH J.13558; courtesy of Paul Barrett); **S**, *Afrovenator abakensis* (MNN UBA1; left reversed; courtesy of Roger Benson); **T**, *Torvosaurus tanneri* (BYU-VP 5110). **Abbreviations**: **ecc**, ectocondyle; **enc**, entocondyle; **ics**, intercondylar sulcus. Taxa framed in blue are those belonging to morphoclade 2 retrieved in the phylogenetic morphometric analysis. Quadrates not to scale.

FIGURE 8.13. Morphological diversity of the mandibular articulation in non-avian Avetheropoda. **A–T**, Right quadrate (unless indicates) in ventral view in; **A**, *Allosaurus* '*jimmadseni*' (SMA 05/002); **B**, *Aerosteon riocoloradensis* (MCNA-PV-3137; left reversed; courtesy of Martin Ezcurra); **C**, *Acrocanthosaurus atokensis* (NCSM 14345); **D**, *Giganotosaurus carolinii* (MUCPv-CH-1; left reversed); **E**, *Guanlong wucaii* (IVPP V14531; left reversed; courtesy of Oliver Rauhut); **F**, *Eotyrannus lengi* (MIWG 1997.550); **G**, *Qianzhousaurus sinensis* (GM F10004-1; left reversed; courtesy of Stephen Brusatte); **H**, *Tyrannosaurus rex* (BHI l013; from Larson 2008*b*, modified); **I**, *Bicentenaria argentina* (MPCA 865; left reversed); **J**, *Ornitholestes hermanni* (AMNH FARB 619); **K**, *Shuvuuia deserti* (IGM 100-1001; left reversed); **L**, *Gallimimus bullatus* (IGM 100-1133; left reversed); **M**, *Falcarius utahensis* (UMNH VP 14559; left reversed; courtesy of Lindsay Zanno); **N**, *Avimimus portentosus* (cast of PIN 3907-3; left reversed; courtesy of Lawrence Witmer); **O**, Indeterminate Oviraptoridae (?*Ingenia yanshini* or ?*Conchoraptor gracilis*; IGM A; left reversed; Maryańska and Osmólska 1997); **P**, *Citipati osmolskae* (IGM 100-978); **Q**, Indeterminate Oviraptoridae (?*Saurornithoides mongoliensis*; IGM 100-1083; Norell and Hwang 2004, modified); **R**, *Dromaeosaurus albertensis* (AMNH FARB 5356); **S**, *Bambiraptor feinbergi* (AMNH FARB 30556; left reversed); **T**, *Tsaagan mangas* (IGM 100-1015; Norell et al. 2006; courtesy of Mick Ellison). Quadrates not to scale. Taxa framed in blue are those belonging to morphoclade 2 retrieved in the phylogenetic morphometric analysis. Quadrates not to scale.

FIGURE 8.14. Morphology of the left articular in Spinosauridae. **A–B**, *Baryonyx walkeri* (NHM R.9951); and **C**, *Irritator challengeri* (SMNS 58022) in **A, C**, medial; and **B**, dorsal views. **Abbreviations**: **igr**, interglenoid ridge; **gfo**, glenoid fossa; **lgd**, lateral glenoid depression; **mgd**, medial glenoid depression; **retp**, retroarticular process.

FIGURE 8.15. Jaw mechanic in the spinosaurid *Spinosaurus*. **A–D**, Mandibular articulation; and **F, G**, skull in **A, C, F–G**, lateral; and **B, D**, anterior views; when **A–B, F**, the mouth is closed; and **C–D, G**, fully open, illustrating the lateral movement (in red) of the mandibular ramus for a 45° rotation of the lower jaw (courtesy of © Jaime A. Headden); **E**, skeletal reconstruction of *Spinosaurus aegyptiacus* by Ibrahim et al. (2014*b*) in

swimming position in lateral view with a human (1.8 m) as a scale (modified from Ibrahim et al. 2014*b*). This model is based on all spinosaurid cranial and postcranial material (in red color) known from the Cenomanian of North Africa, and which likely belong to two spinosaurine taxa; **H**, reconstruction of a semi-aquatic *Spinosaurus* in fishing position (i.e., jaws wide open) in anterolateral view (courtesy of © Jason Poole). **Abbreviations**: **an**, angular; **ar**, articular; **d**, dentary; **ecc**, ectocondyle; **enc**, entocondyle; **j**, jugal; **m**, maxilla; **n**, nasal; **p**, parietal; **pm**, premaxilla; **po**, postorbital; **pt**, pterygoid; **ptf**, pterygoid flange; **q**, quadrate; **qf**, quadrate foramen; **qj**, quadratojugal; **retp**, retroarticular process of the articular; **sa**, surangular; **sq**, squamosal.

FIGURE 8.16. Morphological diversity of the mandibular symphysis in non-avian theropods in medial view. **A–B**, left dentary of *Spinosaurus* cf. *aegyptiacus* (NHM R.16421); **A**, Anterior portion; and **B**, close up on the well-developed anterior ridges of the mandibular symphysis. **C–E**, left dentary of *Baryonyx walkeri* (NHM R.9951 and ML 1190); **C**, anterior portion; and **D**–**E**, close up on the weakly developed anterior ridges of the mandibular symphysis in **D**, NHM R.9951; and **E**, ML 1190. **F–G**, right dentary of *Majungasaurus crenatissimus* (FMNH PR 2100; reversed); **F**, anterior portion; and **G**, close up on the irregular surface of the mandibular symphysis. **H–I**, right dentary of *Megalosaurus bucklandii* (OUMNH J13505; reversed); **H**, anterior portion; and **I**, close up on the smooth surface of the mandibular symphysis. **J–K**, right dentary of *Tyrannosaurus rex* (NHM R.7994); **J**, anterior portion; and **K**, close up on the poorly developed anterodorsal ridges of the mandibular symphysis. The symphyseal surface is colored in light grey. **Abbreviation**: **ri**, anteroposterior ridges of the mandibular symphysis.

FIGURE 9.1. Proposed terminology and annotation of the non-avian theropod maxilla. Right maxilla of *Allosaurus fragilis* (USNM 8335) in **A**, lateral; **B**, anterior; **C**, medial and **D**, posterior views, with details of **E**, promaxillary recess and maxillary antrum in medial view; and **F**, ascending ramus and dorsal margin of vestibular bulla in dorsal view. **Abbreviations**: **ammf**, anteromedial maxillary fenestra; **amp**, anteromedial process; **anr**, anterior ramus; **aor**, antorbital ridge; **asr**, ascending ramus; **idw**, interdental wall; **ifs**, interfenestral strut; **juc**, jugal contact; **lac**, lacrimal contact; **laof**, lateral antorbital fossa; **law**, lateral wall; **maf**, maxillary alveolar foramina; **man**, maxillary antrum; **maof**, medial antorbital fossa; **mbo**, maxillary body; **mcf**, maxillary circumfenestra foramina; **mes**, medial shelf; **mew**, medial wall; **mfe**, maxillary fenestra; **mfo**, maxillary fossa; **mmf**, medial maxillary foramina; **mx1**, first maxillary tooth; **nac**, nasal contact; **nuf**, nutrient foramina; **nug**, nutrient groove; **pac**, palatine contact; **pmc**, premaxillary contact; **pmmf**, posteromedial maxillary fenestra; **pmr**, promaxillary recess; **pne**, pneumatic excavation; **poas**, postantral strut; **pras**, preantral strut; **snf**, subnarial foramen; **suas**, suprantral strut; **veb**, vestibular bulla. Scale bars = 5 cm.

FIGURE 9.2. Proposed terminology and annotation of the non-avian theropod maxilla. Left maxillae of *Tyrannosaurus rex* in **A**-**B**, lateral view (CMNH 9380, reversed); and **C**, medial view (BHI 3033; modified from Hurum and Sabath 2003). **Abbreviations**: **ammf**, anteromedial maxillary fenestra; **amp**, anteromedial process; **anb**, anterior body; **aofe**, antorbital fenestra; **asr**, ascending ramus; **ear**, epiantral recess; **idg**, interdental gap; **idp**, interdental plate; **ifs**, interfenestral strut; **juc**, jugal contact; **jur**, jugal ramus; **lac**, lacrimal contact; **laof**, lateral antorbital fossa; **law**, lateral wall; **maf**, maxillary alveolar foramina; **man**, maxillary antrum; **mbo**, maxillary body; **mcf**, maxillary circumfenestra foramina; **mes**, medial shelf; **mew**, medial wall; **mfe**, maxillary fenestra; **mx9**, ninth maxillary tooth; **nac**, nasal contact; **nuf**, nutrient foramina; **nug**, nutrient groove; **pab**, preantorbital body; **pac**, palatine contact; **pmc**, premaxillary contact; **pmf**, promaxillary fenestra; **pmmf**, posteromedial maxillary fenestra; **pmr**, promaxillary recess; **pne**, pneumatic excavation; **poas**, postantral strut; **pras**, preantral strut; **prms**, promaxillary strut; **snf**, subnarial foramen. Scale bars = 5 cm.

FIGURE 9.3. Proposed terminology and annotation of the non-avian theropod maxilla. **A**, Right maxilla of *Allosaurus fragilis* (AMNH 600) in posteromedial view; **B**, lateral antorbital fossae of *Ceratosaurus* in lateral view; **B1**, right maxilla of *Ceratosaurus magnicornis* (MWC 1) and; **B2**, left maxilla of *Ceratosaurus dentisulcatus* (UMNH VP 5278; courtesy of Roger Benson); **C**, left maxilla of *Tyrannosaurus rex* (CMNH 9380) in posterodorsal (**C1**) and dorsal (**C2**) views; **D**, left maxilla of *Tarbosaurus baatar* (ZPAL MgD-I/4; courtesy of Stephen Brusatte) in lateral view; **E**, right maxilla of *Duriavenator hesperis* (NHM R332) in dorsomedial view; and **F**, left maxilla of *Piatnitzkysaurus floresi* (PVL 4073) in dorsomedial view (courtesy of Martin Ezcurra). **Abbreviations**: **amf**, accessory maxillary fenestra; **ammf**, anteromedial maxillary fenestra; **ampr** anteromedial pneumatic recess; **iar**, interalveolar recess; **mal**, maxillary alveoli; **mes**, medial shelf; **mfe**, maxillary fenestra; **mfo**, maxillary fossa; **pmf**, promaxillary fenestra; **pmmf**, posteromedial maxillary fenestra; **pmr**, promaxillary recess; **pne**, pneumatic excavation; **poas**, postantral strut; **pras**, preantral strut; **ptmf**, postmaxillary fenestra; **ptms**, postmaxillary strut; **trb**, tooth root bulge; **vmpr**, ventromedial pneumatic recess. Scale bars = 5 cm.

FIGURE 9.4. Reconstruction of *Torvosaurus gurneyi* in lateral view. **A**, Skeletal reconstruction of *Torvosaurus gurneyi* in lateral view illustrating, in red, the elements present in the holotype specimen (ML 1100) and, in blue, the elements tentatively assigned to this species (artwork by Scott Hartman, used with permission and modified; drawing of man by Carol Abraczinskas, University of Chicago, used with permission); **B**, Skull reconstruction of *Torvosaurus gurneyi* in lateral view illustrating the incomplete left maxilla (ML 1100) of the holotype specimen (artwork by Simão Mateus, used with permission and modified); **C**, Skeletal reconstruction of *Torvosaurus gurneyi* in lateral view by Scott Hartman (courtesy of Scott Hartman). Scale bars = 1 m (A, C) and 10 cm (B).

FIGURE 9.5. Maxilla of *Torvosaurus gurneyi* (ML 1100) and comparison with *T. tanneri*. Incomplete left maxilla of the holotype specimen of *Torvosaurus gurneyi* (ML 1100) in **A**, lateral; **B**, medial; **C**, ventral; **D**, dorsal; **E**, anterior; **F**, posterior views with details of **G**, Anterodorsal margin of jugal ramus in dorsomedial view; and **H**, Posterior part of jugal ramus in dorsal view. **I-J**, Anterior part of interdental wall of **I**, *T. gurneyi*; and **J**, *T. tanneri* (BYU-VP 9122) in medial view. **K-L**, Anteromedial process of **K**, *T. gurneyi*; and **L**, *T. tanneri* (BYU-VP 9122) in medial views. Scale bars = 10 cm (A-H), 5 cm (G-L).

FIGURE 9.6. Maxilla of *Torvosaurus gurneyi* (ML 1100) and comparison with *T. tanneri*. Interpretive line drawing of the left maxilla of the holotype specimen of *Torvosaurus gurneyi* (ML 1100) in **A**, lateral; **B**, medial; **C**, ventral; **D**, dorsal; **E**, anterior; **F**, posterior views with details of **G**, anterodorsal margin of jugal ramus in dorsomedial view; and **H**, posterior part of jugal ramus in dorsal view. **I-J**, Interpretive line drawing of the anterior part of interdental wall of **I**, *T. gurneyi*; and **J**, *T. tanneri* (BYU-VP 9122) in medial view. **K-L**, Interpretive line drawing of the anteromedial process of **K**, *T. gurneyi*; and **L**, *T. tanneri* (BYU-VP 9122) in medial views. Hatched areas represents missing parts, light grey tone indicates reconstructed part, and dark grey tone corresponds to the foramina, and alveoli, with alveoli 9 and 10 being reconstructed. **Abbreviations**: **adc**, anterodorsal crest; **adr**, anterodorsal ridge of the anteromedial process; **afo**, anterior foramina; **al**, alveolus; **amg**, anteromedial groove of the anteromedial process; **amp**, anteromedial process; **amr**, anteromedial ridge; **anr**, anterior ramus; **aor**, antorbital ridge; **asr**, ascending ramus; **avg**, anteroventral groove of the anteromedial process; **avr**, anteroventral ridge on the anteromedial process; **dmg**, dorsomedial groove; **idw**, interdental wall; **juc**, jugal contact; **lac**, lacrimal contact; **laof**, lateral antorbital fossa; **law**, lateral wall; **maf**, maxillary alveolar foramina; **mcf**, maxillary circumfenestra foramina; **mes**, medial shelf; **mew**, medial wall; **mfo**, maxillary fossa; **mx**, maxillary teeth; **nac**, nasal contact; **nuf**, nutrient foramina; **nug**, nutrient groove; **nvo**, neurovascular opening; **pmc**, premaxillary contact; **snf**, subnarial foramen. Scale bars = 10 cm (A-H), 5 cm (G-L).

FIGURE 9.7. Dentition of *Torvosaurus gurneyi* (ML 1100). **A, C, E-H**, Second maxillary tooth; and **B, D**, third non-erupted maxillary tooth of the holotype specimen of *Torvosaurus gurneyi* in **A-B**, labial; **C-D**, lingual; **E**, mesial; **F**, distal; **G**, basal; and **H**, apical views. **I-J**, Distal; and **K-M**, mesial denticles of the second maxillary tooth in lateral view. **M**, Distal serrations showing the interdenticular sulci; and **N**, enamel texture of the third non-erupted tooth in labial view. **Abbreviations**: **ce**, cervix; **dca**, distal carina; **del**, dentine layer; **ent**, enamel texture; **ids**, interdenticular sulci; **idsp**, interdenticular space; **mca**, mesial carina; **lic**, lingual concavity for the erupting tooth; **puc**, pulp cavity; **ro**, root; **uet**, unerupted tooth; **tun**, transverse undulation. Scale bars = 5 cm (A-F), 3 cm (G-H), 3 mm (I, K, M-N), 1 mm (J, L).

FIGURE 9.8. Caudal vertebra of *Torvosaurus gurneyi* (ML 1100). **A-F**, Posterior part of an anterior caudal centrum of the holotype specimen of *Torvosaurus gurneyi* (ML 1100) in **A**, anterior; **B**, posterior; **C**, right lateral; **D**, left lateral; **E**, dorsal; and **F**, ventral views. **Abbreviations**: **nc**, neural canal; **st**, striation. Scale bar = 5 cm.

FIGURE 9.9. Cladogram of basal Theropoda and phylogenetic position of *Torvosaurus gurneyi*. Strict consensus cladogram from 71 most parsimonious trees after pruning *Magnosaurus*, *Poekilopleuron*, *Streptospondylus* and *Xuanhanosaurus* from the full set of most parsimonious trees. Initial analysis used New Technology Search using TNT v.1.1 of a data matrix comprising 353 characters for two outgroup (*Eoraptor* and *Herrerasaurus*) and 60 non-avian theropod taxa. Tree length = 1022 steps; CI = 0.414, RI = 0.685. Bremer support values are in regular and bootstrap values are in bold. For silhouette attribution, see Appendices A1.1.

FIGURE 9.10. Comparison of the maxillae of *Torvosaurus gurneyi* and *Torvosaurus tanneri*. Left maxillae of the holotype specimen of *Torvosaurus gurneyi* (ML 1100) in **A**, lateral; **B**, medial; **E**, ventral; **F**, dorsal; **I**, anterior; and **K**, posterior views. Left maxillae of a specimen referred to *Torvosaurus tanneri* (BYU-VP 9122) in **C**, lateral; **D**, medial; **G**, ventral; **H**, dorsal; **J**, anterior; and **L**, posterior views. **Abbreviations**: **adc**, anterodorsal crest; **adr**, anterodorsal ridge of the anteromedial process; **afo**, anterior foramina; **al1**, first alveolus; **al8**, eighth alveolus; **al10**, tenth alveolus; **amp**, anteromedial process; **aor**, antorbital ridge; **avg**, anteroventral groove of the anteromedial process; **avr**, anteroventral ridge on the anteromedial process; **idw**, interdental wall; **ldr**,

laterodorsal ridge within the anterior corner of the lateral antorbital fossa; **mfo**, maxillary fossa; **nuf**, nutrient foramina; **nug**, nutrient groove; **nvo**, neurovascular opening. Scale bars = 5 cm.

FIGURE 9.11. Incomplete maxilla of *Torvosaurus gurneyi* (ALT-SHN.116; courtesy of Elisabete Malafaia). **A–B**, Anterior portion of a right maxilla in **A**, lateral; and **B**, medial view. **Abbreviations**: **amp**, anteromedial process; **anr**, anterior ramus; **asr**, ascending ramus; **erao**, external rim of antorbital fossa; **idp**, interdental plates; **laof**, lateral antorbital fossa; **maf**, maxillary alveolar foramina.

FIGURE 9.12. Femur and tibia of Megalosauridae from the Late Jurassic of Portugal. Distal portion of a left femur (ML 632) of a megalosaurid tentatively referred to *Torvosaurus gurneyi* in **A**, anterior; **B**, lateral; **C**, posterior; **D**, medial; **E**, proximal; and **F**, distal views. Incomplete left tibia (ML 430) of *Torvosaurus* sp. (and tentatively referred to *Torvosaurus gurneyi*), with reconstruction of missing part of cnemial crest, in **A**, anterior; **B**, lateral; **C**, posterior; **D**, medial; **E**, proximal; and **F**, distal views. **Abbreviations**: **asc**, contact with astragalus; **ccr**, cnemial crest ridge; **cnc**, basal part of cnemial crest; **ctf**, crista tibiofibularis; **dep**, anterodistal depression; **dir**, distal ridges; **exg**, extensor groove; **ffl**, fibular flange; **flg**, flexor groove; **lc**, lateral condyle; **mc**, medial condyle; **mdc**, mediodistal crest; **sab**, supracetabular buttress. Scale bars = 10 cm.

FIGURE 10.1. The known record of embryos and associated eggshell structure explicit the phylogenetic position of the *Torvosaurus* embryos (ML1188), which occupies a gap at the base of the Theropoda cladogram. Dashed lines indicate the dubious position of *Lourinhanosaurus* as an Allosauroidea or as a basal Coelurosauria in the light of the most recent analysis (see Chapter 1). Major clades in bold indicate the presence of associated embryo-eggshell fossils. For silhouette attribution, see Appendices A1.1.

FIGURE 10.2. *Torvosaurus* eggs, eggshells, and embryos from the Lourinhã Formation (early Tithonian) of Portugal. **A**, Clutch of *Torvosaurus* eggs (ML1188); **B**, Dentary and maxilla in medial view of *Torvosaurus* sp.; **C**, Second and third dentary teeth, separated by interdental plate in medial view; **D**, Second and third maxillary teeth, separated by interdental plate in medial view; **E**, Eggshell external morphology in lateral view; **F**, Eggshell internal morphology in medial view; **G**, SEM micrograph of the eggshell radial section showing acicular crystals and a single layer; **H**, Eggshell radial section; **I**, Eggshell external morphology SEM photograph; **J**, Eggshell internal morphology SEM photograph; **K**, SR-µCT image of an eggshell radial section. Scale bars 10 cm (A), 5 mm (B), 2 mm (C, D), 500 µm (E, F, H, I), 200 µm (G, J).

FIGURE 10.3. Embryonic material of *Torvosaurus* sp. (ML 1188). **A**, Right maxilla, dentary and jugal in medial view; **B-C**, Close up on the anterior part of the right maxilla in medial view; **D**, Indeterminate postcranial bones; and **E**, Articulated vertebrae. **Abbreviations**: **amp**, anteromedial process; **anr**, anterior ramus; **aofe,** antorbital fenestra; **j**, jugal; **jur**, jugal ramus; **lac**, lacrimal contact of the maxilla; **m**, maxilla; **mx1**, first maxillary tooth; **mx2**, second maxillary tooth; **mx5**, fifth maxillary tooth; **nug**, nutrient groove. Scale: 10 mm (A, D, E), 5 mm (B–D).

FIGURE 10.4. **A**, Incomplete right maxilla of *Torvosaurus* sp. embryo (ML 1188) in articulation with the jugal in medial view; **B**, Anterior part of maxilla (jugal ramus not included); **C**, Anterior part of anterior ramus; **D**, Ventral part of ascending ramus; **E**, Anteriormost maxillary teeth; **F**, Dorsal part of ascending ramus; **G.** Apex of the crown of first maxillary tooth; **H**, Medial part of the crown of second maxillary tooth; **I**, Roots of first and second maxillary teeth; **J**, Interdental plate in between second and fourth maxillary tooth. **Abbreviations**: **amp**, anteromedial process; **anr**, anterior ramus; **aofe,** antorbital fenestra; **asr**, ascending ramus; **ce**, cervix; **dca**, distal carina; **idp**, interdental plate; **j**, jugal; **jur**, jugal ramus; **lac**, lacrimal contact of the maxilla; **mca**, mesial carina; **mx1**,first maxillary tooth; **mx2**, second maxillary tooth; **mx4**, fourth maxillary tooth; **nug**, nutrient groove; **vac**, vascular canals. Scale: 10 mm (A); 5 mm (B and C); 2 mm (D to G, K); 1 mm (H to J).

FIGURE 10.5. **A**, Incomplete right dentary of *Torvosaurus* sp. embryo (ML 1188) in medial view; **B**, Anterior part of medial wall of dentary; **C**, Mesial part of medial wall of dentary; **D**, Posterior part of medial wall of dentary; **E**, Anteriormost interdental plates and dentary teeth; **F**, Mesial interdental plate and tooth; **G**, Apex of the crown of seventh dentary tooth. **Abbreviations**: **dca**, distal carina; **dt1**, first dentary tooth; **dt2**, second dentary tooth; **dt3**, third dentary tooth; **dt5**, fifth dentary tooth; **dt7**, seventh dentary tooth; **dt8**, height dentary tooth; **idp**, interdental plate; mca, mesial carina; **mf**, Meckelian fossa; **mef**, Meckelian foramina; **mg**, Meckelian groove; **ms**, mandibular symphysis; **pdg**, paradental groove; **spl**, splenial contact. Scale: 5 mm (A); 2 mm (B to F), 1 mm (G).

FIGURE 10.6. **A**, Set of three amphiplatyan centra in articulation in dorsal view; **B**, Mesial part of the first centrum in dorsal view; **C**, Fourth isolated centrum in dorsal view. **Abbreviation**: **nf**, neurovascular foramina. Scale: 10 mm (A), 2 mm (B, C).

FIGURE 10.7. Strict consensus cladogram from 96 most parsimonious trees. Initial analysis used New Technology Search using TNT v.1.1 of a data matrix comprising 361 characters for two outgroup (*Eoraptor* and *Herrerasaurus*) and 62 non-avian theropod taxa. Tree length = 1094 steps; CI = 0.371; RI = 0.632. Bremer support values are in bold and above the stem. Bootstrap values, in italic, and unambiguous character support are below the stem of each clade.

FIGURE 10.8. 50% Majority Rule cladogram from 96 most parsimonious trees. Initial analysis was a New Technology Search using TNT v.1.1 of a data matrix comprising 363 characters for two outgroup (*Eoraptor* and *Herrerasaurus*) and 62 non-avian theropod taxa. Tree length = 1094 steps; CI = 0.394; RI = 0.665. Clade number, in bold, and above the stem of each clade, is used in the synapomorphy list below. The percentage of clade occurrence is below each clade and in italic. For silhouette attribution, see Appendices A1.1.

FIGURE 10.9. Maxillae of non-avian theropods in medial view. **A**, Embryo of *Torvosaurus* sp. **(**ML 1188, reconstructed); **B**, Hatchling of *Allosaurus* (MG 27804); **C**, *Torvosaurus tanneri* (ML1100); **D**, *Afrovenator abakensis* (MNN UBA1; courtesy of Juan Canale); **E**, *Dubreuillosaurus valesdunensis* (MNHN 1998-13); **F**, *Duriavenator hesperis* (NHM R.332); **G**, *Marshosaurus bicentesimus* (DINO 16455; courtesy of Matt Carrano); **H**, *Piatnitzkysaurus floresi* (PVL 4073; courtesy of Martín Ezcurra); **I**, *Dilophosaurus wetherilli* (UCMP 37303; courtesy of Martín Ezcurra); **J**, *Ceratosaurus magnicornis* (USNM 4735); **K**, *Noasaurus leali* (PVL 4061); **L**, *Masiakasaurus knopfleri* (FMNH PR 2183); **M**, *Kryptops palaios* (MNN GAD1−1); **N**, *Rugops primus* (MNN IGU1); **O**, *Indosuchus raptorius* (AMNH 1955); **P**, *Majungasaurus crenatissimus* (FMNH PR 2100); **Q**, *Allosaurus fragilis* (USNM 8335); **R**, *Neovenator salerii* (MIWG 6348); **S**, *Acrocanthosaurus atokensis* (NCSM 14345; courtesy of Drew Eddy); **T**, *Eocarcharia dinops* (MNN GAD2); **U**, *Eotyrannus lengi* (MIWG 1997.550); **V**, *Alioramus altai* (IGM 100-1844; courtesy of Mick Ellison ©AMNH); **W**, *Raptorex kriegsteini* (LH PV18); **X**, *Tyrannosaurus rex* (CMNH 9380). **Abbreviations**: **amp**, anteromedial process; **ampr**, anteromedial pneumatic recess; **anr**, anterior ramus; **aofe,** antorbital fenestra; **asr**, ascending ramus; **ear**, epiantral recess; **idp**, interdental plate; **juc**, jugal contact; **jur**, jugal ramus; **lac**, lacrimal contact; **mes**, medial shelf; **mfe**, maxillary fenestra; **man**, maxillary antrum; **nuf**, nutrient foramen; **nug**, nutrient groove; **pac**, palatal contact; **pmmf**, posteromedial maxillary fenestra; **pmf**, promaxillary fenestra; **pnf**, pneumatic fenestra; **snf**, subnarial foramen; **vmpr**, ventromedial pneumatic recess. Scale: 5 mm (A, B), 2 cm (L), 5 cm (C to K; M to X).

FIGURE 10.10. Dentaries of non-avian theropods in medial view. **A**, Embryo of *Torvosaurus* sp. (ML 1188, reconstructed); **B**, *Torvosaurus tanneri* (BYU-VP 2003); **C**, *Megalosaurus bucklandii* (OUMNH J13505); **D**, *Magnosaurus nethercombensis* (OUMNH J.12143); **E**, *Dubreuillosaurus valesdunensis* (MNHN 1998-13); **F**, *Eustreptospondylus oxoniensis* (OUMNH J.13558); **G**, *Piatnitzkysaurus floresi* (PVL 4073); **H**, *Dilophosaurus wetherilli* (UCMP 37303; courtesy of Martín Ezcurra); **I**, *Marshosaurus bicentesimus* (AMNH 27641); **J**, *Baryonyx walkeri* (NHM R.9951); **K**, *Ceratosaurus nasicornis* (USNM 4735); **L**, *Ceratosaurus dentisulcatus* (UUVP 158); **M**, *Genyodectes serus* (MLP 26-39); **N**, *Masiakasaurus knopfleri* (FMNH PR 2471); **O**, *Ekrixinatosaurus novasi* (MUCPv 294; courtesy of Matthew Lamanna); **P**, *Majungasaurus crenatissimus* (FMNH PR 2100); **Q**, *Allosaurus fragilis* (UUVP 10.093; courtesy of Stephen Brusatte); **R**, *Sinraptor dongi* (Currie and Zhao 1993*a*; fig. 11B); **S**, *Neovenator salerii* (NHM R10001; courtesy of Roger Benson); **T**, *Acrocanthosaurus atokensis* (NCSM 14345; courtesy of Drew Eddy); **U**, *Giganotosaurus carolinii* (MUCPv-CH-1; courtesy of Matthew Lamanna); **V**, *Tyrannotitan chubutensis* (MPEF-PV 1157; courtesy of Juan Canale); **W**, *Eotyrannus lengi* (MIWG 1997.550); **X**, *Alioramus altai* (IGM 100-1844; courtesy of Mick Ellison © AMNH); **Y**, *Tyrannosaurus rex* (CMNH 9380). **Abbreviations**: **abr**, articular brace; **ac**, angular contact; **emf**, external mandibular fenestra; **idp**, interdental plate; **mf**, Meckelian fossa; **mfr**, Meckelian foramen; **mg**, Meckelian groove; **ms**, mandibular symphysis; **pdg**, paradental groove; **sd**, supradentary; **sdc**, supradentary contact; **sp**, splenial; **spl**, splenial contact; **step**, step between Meckelian fossa and Meckelian groove. Scale: 5 mm (A), 5 cm (B to Y).

FIGURE 10.11. Isolated maxilla of an hatchling specimen of *Allosaurus* sp. (MG 27804). Left maxilla in **A**, lateral; and **B**, medial views; with close up on **C**, the anterolateral pneumatic complex of the maxilla in lateral view; **D**, the jugal ramus in dorsal view; **E**, the maxillary teeth in anteroventral view; **F**, the ascending ramus in posteromedial view; and **G**, the promaxillary recess in posteromedial view. **Abbreviations**: **amp**, anteromedial process; **asr**, ascending ramus; **idp**, interdental plates; **ifs**, interfenestral strut; **juc**, jugal contact; **jur**, jugal ramus; **lac**, lacrimal contact; **maof**, medial antorbital fossa; **mes**, medial shelf; **mfe**, marillary fenestra; **mx6**,

sixth maxillary tooth; **pmf**, promaxillary fenestra; **pmr**, promaxillary recess; **pne**, pneumatic excavation; **pnef**, pneumatic foramen.

FIGURE 10.12. Isolated maxillae of an embryonic specimen of *Lourinhanosaurus antunesi* (ML 565-122). Left and right maxilla in **A–B**, right lateral; and **C**, ventral views; with close up on **D**, the ascending ramus and the anterior portion of the lateral antorbital fossa, and **E**, the fifth? maxillary crown of the right maxilla in lateral view. **Abbreviations**: **anr**, anterior ramus; **aor**, antorbital ridge; **asr**, ascending ramus; **dde**, distal denticles; **mal**, first maxillary alveolus; **mcf**, maxillary circumfenestra foramina; **mfe**, marillary fenestra; **snf**, subnarial foramen. Artwork in B courtesy of Simão Mateus.

FIGURE 10.13. Size comparison of the maxilla of embryonic, hatchling and adult specimens of basal tetanurans in lateral view. **A**, Size comparison of embryonic and adult maxilla of *Torvosaurus gurneyi*; **B**, size comparison of hatchling and adult maxilla of *Allosaurus* sp.; **C-E**, size comparison of embryonic maxillae of **C**, *Lourinhanosaurus antunesi*; **D**, *Torvosaurus gurneyi*; and **E**, hatchling maxilla of *Allosaurus* sp. Scale: 10 cm (A–B), and 1 cm (C–E).

Tables

TABLE 1.1. Phylogenetic definition for non-avian theropod clades up to the ‘subfamily’-level. For each taxon, the original author(s) of the first associated name is given in brackets immediately after the name, followed by the author(s) who first created the name without brackets when different. A phylogenetic definition is provided for taxa that have not already been defined phylogenetically.

TABLE 2.1A. Abbreviations of measurement variables used by previous authors reporting isolated theropod teeth.

TABLE 2.1B. (Continued).

TABLE 3.1. Dentition of the 112 non-avian theropod taxa included in this study.

TABLE 4.1. Teeth and tooth bearing bones of non-avian theropod specimens examined and included in this study.

TABLE 4.2. List of ambiguous and unambiguous dentition-based synapomorphies by theropod clades for results of the cladistic analysis of the dentition-based dataset.

TABLE 4.3. Morphometric measurements of four isolated theropod teeth from the Lourinhã Formation of Portugal.

TABLE 5.1. Morphometric data of megalosaurid teeth.

TABLE 5.2. Tooth-count and tooth-count estimation of the tooth bearing bones of Megalosauridae.

TABLE 5.3. Table of misclassification for the whole dataset grouped by clades (ratios excluded).

TABLE 5.4. Table of misclassification for the reduced dataset (large ziphodont teeth) grouped by clades (ratios excluded).

TABLE 5.5. Table of misclassification for the reduced dataset (megalosaurid teeth only) grouped by taxa (ratios excluded).

TABLE 6.1. Terminology of non-avian theropod quadrate sub-unit by authors.

TABLE 6.2. Standardized terminology and abbreviation of the non-avian theropod quadrate and comparison with the terminology of the avian quadrate based on Baumel and Witmer (1993), Elzanowski et al. (2001) and Elzanowski and Stidham (2010).

TABLE 7.1. Non-avian theropod specimens and clades examined and scored in the cladistic analysis. Taxa and clades with an asterisk were used in the phylogenetic morphometric analysis. **Abbreviations**: **Y**, Yes; **N**, No.

TABLE 8.1. Measurements of five quadrates of Spinosaurinae from the Kem Kem beds of Morocco. Values are given in millimeters. [1]Distance taken from the posterior margin of the squamosal capitulum to the ventral margin of the entocondyle. [2]Distance taken from the dorsalmost point of the dorsal quadratojugal contact to the anterior surface of the pterygoid flange. [3]Distance taken from the apex of the anterodorsal curvature of the pterygoid flange to the apex of the anteroventral curvature. * Distance taken from the base of the mandibular condyles to the dorsal extremity of the broken shaft.

TABLE 8.2. Quadrate size and estimated skull length. *Estimations. **Considering that MNN GAD 502 (quadrate) and MNN GAD 501 (articulated premaxillae and maxillae) pertain to the same individual of *Suchomimus*.

TABLE 9.1. Measurements of left maxilla of the holotype of *Torvosaurus gurneyi* (ML 1100).

TABLE 9.2. Measurements of maxillary teeth of the holotype of *Torvosaurus gurneyi* (ML 1100).

TABLE 9.3. Number of denticles in maxillary teeth of the holotype of *Torvosaurus gurneyi* (ML 1100).

TABLE 9.4. Measurements of proximal caudal vertebra of the holotype of *Torvosaurus gurneyi* (ML 1100).

TABLE 9.5. Measurements of limb bones tentatively referred to *Torvosaurus gurneyi*.

TABLE 10.1. Maxilla, skull and body lengths of juvenile and adult individuals in non-avian tetanurans. Values are given in millimeters for the maxilla, the skull and the body lengths of juvenile individuals, and in metres for the body lengths of adult individuals. *Estimated values. § In adults. **Abbreviations**: **Juv**., juvenile; **max**, maxilla.

Supplementary Material

SOM 5.1. Morphometric data on theropod teeth (whole dataset):
http://app.pan.pl/SOM/appXX-Hendrickx_etal_SOM/SOM_1.xlsx (1.89 MB)

SOM 5.2. Morphometric data on large ziphodont theropod teeth (reduced dataset):
http://app.pan.pl/SOM/appXX-Hendrickx_etal_SOM/SOM_2.xlsx (367 KB)

SOM 5.3. Morphometric data on theropod teeth separatedinto mesial and lateral dentition:
http://app.pan.pl/SOM/appXX-Hendrickx_etal_SOM/SOM_3.xlsx (179 KB)

SOM 5.4. Morphometric data on megalosaurid teeth:
http://app.pan.pl/SOM/appXX-Hendrickx_etal_SOM/SOM_4.xlsx (73.5 KB)

SOM 5.5. Graphical results of the discriminant analysis on theropod teeth by clades, ratios included:
http://app.pan.pl/SOM/appXX-Hendrickx_etal_SOM/SOM_5.pdf (89.9 KB)

SOM 5.6. Graphical results of the discriminant analysis on theropod teeth by taxa, ratios included:
http://app.pan.pl/SOM/appXX-Hendrickx_etal_SOM/SOM_6.pdf (76.2 KB)

SOM 5.7. Graphical results of the discriminant analysis on theropod teeth by taxa, ratios excluded:
http://app.pan.pl/SOM/appXX-Hendrickx_etal_SOM/SOM_7.pdf (75.7 KB)

SOM 5.8. Graphical results of the discriminant analysis on large ziphodont theropod teeth by clades, ratios included:
http://app.pan.pl/SOM/appXX-Hendrickx_etal_SOM/SOM_8.pdf (66.2 KB)

SOM 5.9. Graphical results of the discriminant analysison theropod teeth separated into mesial and lateral dentition, ratios included:
http://app.pan.pl/SOM/appXX-Hendrickx_etal_SOM/SOM_9.pdf (49.9 KB)

SOM 5.10. Graphical results of the discriminant analysis on megalosaurid teeth by taxa, ratios included:
http://app.pan.pl/SOM/appXX-Hendrickx_etal_SOM/SOM_10.pdf (32.4 KB)

ABBREVIATIONS

Institutional Abbreviations

ALT–SHN, Laboratorio de la Associação Leonel Trindade, Sociedade de História Natural Sociedade de História Natural, Torres Vedras, Portugal; **AMNH**, American Museum of Natural History, New York, USA; **ANSP**, Academy of Natural Sciences of Drexel University, Philadelphia, Pennsylvania, USA; **AODF**, Australian Age of Dinosaurs Fossil, Winton, Queensland, Australia; **BHI**, Black Hills Institute, Hill City, South Dakota, USA; **BMMS**, Bürgermeister Müller Museum Solnhofen, Germany; **BMNHC**, Beijing Museum of Natural History, Beijing, China; **BSPG**, Bayerische Staatssammlung für Paläontologie und historische Geology, München, Germany; **BYU-VP**, Brigham Young University Vertebrate Paleontology, Provo, Utah, USA; **CAGS**, Chinese Academy of Geological Sciences, Beijing, China; **CMNH**, Carnegie Museum of Natural History, Pittsburgh, USA; **CV**, Chongqing Museum of Natural History, Chongqing, China; **DMNH**, Perot Museum of Nature and Science, Dallas, Texas, USA; **DMR-TF**, Department of the Mineral Resources, Palaeontological collection, Bangkok, Thailand; **FMNH**, Field Museum of Natural History, Chicago, Illinois, USA; **FPDM**, Fukui Prefectural Dinosaur Museum, Katsuyama, Fukui, Japan; **FRDC-GS**, Fossil Research and Development Center, Gansu Bureau of Geology and Mineral Resources Exploration, Lanzhou, China; **FUB PB**, Freie Universität Berlin, Berlin, Germany; **GM**, Ganzhou Museum, Ganzhou City, Jiangxi Province, China; **GR**, Ghost Ranch Ruth Hall Museum of Paleontology, Ghost Ranch, New Mexico, USA; **HIII**, Henan Geological Museum, Zhengzhou, Henan Province, China; **IGM**, Institute of Geology, Ulaan Baatar, Mongolia; **IPFUB**, Institute for Paleontology of the Freie Universität, Berlin, Germany; **ISIR**, Indian Statistical Institute, Kolkata, India; **IVPP**, Institute for Vertebrate Paleontology and Paleoanthropology, Beijing, China; **JME**, Jura Museum Eichstätt, Eichstätt, Germany; **KMV**, Kunming Municipal Museum, Guandu district, China; **LACM**, Los Angeles County Museum of Natural History, Los Angeles, California, USA; **LDM-LCA**, Lufeng Dinosaur Museum-Lufeng Chuanjie A'na, A'na, China; **LH PV**, Long Hao Institute of Geology and Paleontology, Hohhot, Nei Mongol, China; **LPMB**, Liaoning Paleontological Museum, Liaoning, China; **MACN**, Museo Argentino de Ciencias Naturales 'Bernardino Rivadavia,' Buenos Aires, Argentina; **MB**, Museum für Naturkunde der Humboldt Universität, Berlin, Germany; **MCF PVPH**, Museo Municipal Carmen Funes, Paleontologia de Vertebrados, Plaza Huincul, Argentina; **MCNA**, Museo de Ciencias Naturales y Antropológicas de Mendoza, Mendoza, Argentina; **MCZ**, Museum of Comparative Zoology, Harvard University, Cambridge, Massachusetts, USA; **MG GUI**, Museu Geológico (Guimarota collection), Lisbon, Portugal; **MHNA-PV**, Muséum d'Histoire Naturelle d'Aix-en-Provence, France; **MIWG**, Dinosaur Isle, Isle of Wight Museum Services, Sandown, UK; **ML**, Museu da Lourinhã, Lourinhã, Portugal; **MLP**, Museo de La Plata, La Plata, Argentina; **MMCH-PV**, Museo Municipal 'Ernesto Bachmann,' Villa El Chocón, Neuquén, Argentina; **MML**, Museo Municipal de Lamarque, Río Negro, Argentina; **MN**, Museu Nacional, Universidade Federal do Rio de Janeiro, Brazil; **MNA**, Museum of Northern Arizona, Flagstaff, Arizona, USA; **MNHN**, Muséum national d'Histoire naturelle, Paris, France; **MNN**, Musée National du Niger, Niamey, Niger; **MPCA**, Museo Provincial Carlos Ameghino, Cipolletti, Río Negro, Argentina; **MPEF-PV**, Museo Paleontológico 'Egidio Feruglio,' Trelew, Argentina; **MPM-Pv**, Museo Padre Molina Paleontología de Vertebrados, Río Gallegos, Santa Cruz, Argentina; **MSNM**, Museo di Storia Naturale di Milano, Milan, Italy; **MUCPv**, Museo de Ciencias Naturales de la Universidad Nacional de Comahue, Lago Barreales, Argentina; **MUCPv-CH**, Museo de Ciencias Naturales de la Universidad Nacional de Comahue, El Chocón collection, Villa El Chocón, Argentina; **MWC**, Museum of Western Colorado, Fruita, Colorado, USA; **NCSM**, North Carolina Museum of Natural Sciences, Raleigh, North Carolina, USA; **NH**, Horniman Museum & Gardens, London, UK; **NHFO**, Natural History Fossil Collection, Qatar Museum Authority, Doha, Qatar; **NHM**, The Natural History Museum, London, UK; **NIGP**, Nanjing Institute of Geology and Palaeontology, Nanjing, China; **NMC**, Canadian Museum of Nature, Ottawa, Ontario, Canada; **OUMNH**, Oxford University Museum, Oxford, UK; **PIN**, Paleontological Institute of the Russian Academy of Sciences, Moscow, Russia; **PMAA**, Provincial Museum and Archives of Alberta, Paleontological Collections, Drumheller, Alberta, Canada; **PST**, Paleontological and Stratigraphic Section of the Geological Institute, Mongolian Academy of Sciences, Ulaan Baatar, Mongolia; **PULR**, Paleontología, Universidad Nacional de La Rioja, La Rioja, Argentina; **PVL**, Fundación 'Miguel Lillo,' San Miguel de Tucumán, Argentina; **PVSJ**, Museo de Ciencias Naturales, Universidad Nacional de San Juan, San Juan, Argentina; **QW**, Giant Buddha Temple Museum, Leshan, China; **ROM**, Museum of the Rockies, Bozeman, Montana, USA; **RTMP**, Royal Tyrrell Museum of Palaeontology, Drumheller, Alberta, Canada; **SBA-SA**, Soprintendenza per i Beni Archeologici di Salerno Avellino Benevento e Caserta, Salerno, Italy; **SGM**, Ministère de l'Énergie et des Mines, Rabat, Morocco; **SMA**, Sauriermuseum Aathal, Aathal, Switzerland; **SMNS**, Staatliches Museum für Naturkunde, Stuttgart, Germany; **SMU**, Southern Methodist, University, Dallas, Texas, USA; **TATE**, Tate Museum, Casper College, Casper, USA; **TMM**, Texas Memorial Museum, Austin, Texas, USA; **UA**, Université d'Antananarivo, Antananarivo, Madagascar; **UC**, University of Chicago

Paleontological Collection, Chicago, USA; **UCMP**, University of California Museum of Paleontology, Berkeley, California, USA; **UCPC**, University of Chicago Paleontological Collection, Chicago, USA; **UMNH**, Natural History Museum of Utah, University of Utah, Salt Lake City, USA; **USNM VP**, United State National Museum Vertebrate Paleontology, Washington, District of Columbia, USA; **USNM**, United State National Museum Vertebrate Paleontology, Washington D. C., USA; **UUVP**, Utah Museum of Natural History, Salt Lake City, Utah, USA; **WDC**, Wyoming Dinosaur Center, Thermopolis, Wyoming, USA; **WDIS**, Wyoming Dinamation International Society, Casper, Wyoming, USA; **ZDM**, Zigong Dinosaurian Museum, Zigong, Sichuan, China; **ZLJ**, Lufeng World Dinosaur Valley Park, Yunnan, China; **ZPAL**, Institute of Palaeobiology of the Polish Academy of Sciences, Warsaw, Poland.;

Anatomical Abbreviations

aafe, accessory antorbital fenestra; **abr**, articular brace; **ac**, angular contact; **acf**, accessory fenestra; **adc**, anterodorsal crest; **adf**, anterodorsal foramen; **adr**, anterodorsal ridge of the anteromedial process; **afo**, anterior foramina; **afq**, anterior fossa; **a**l, alveolus; **al1**, first alveolus; **al10**, tenth alveolus; **al8**, eighth alveolus; **alm**, alveolar margin; **amf**, accessory maxillary fenestra; **amg**, anteromedial groove of the anteromedial process; **ammf**, anteromedial maxillary fenestra; **amp**, anteromedial process; **ampr**, anteromedial pneumatic recess; **ampu**, ampulla; **amr**, anteromedial ridge; **an**, angular; **anb**, anterior body; **anr**, anterior ramus; **aofe**, antorbital fenestra; **aofo**, antorbital fossa; **aor**, antorbital ridge; **ap**, apex; **apne**, anterior pneumatic foramen; **ar**, articular; **asc**, contact with astragalus; **asc**, contact with astragalus; **asr**, ascending ramus; **avg**, anteroventral groove of the anteromedial process; **avr**, anteroventral ridge on the anteromedial process; **brc**, braincase contact; **bst**, basal striation; **ca**, carina; **cap**, crown apex; **cau**, cauda; **ccr**, cnemial crest ridge; **ccr**, cnemial crest ridge; **ce**, cervix; **ci**, cingulum; **cnc**, basal part of cnemial crest; **cnc**, basal part of cnemial crest; **co**, crown; **cob**, crown base; **cs**, concave surface; **ctf**, crista tibiofibularis; **ctf**, crista tibiofibularis; **d**, dentary; **d1**, isolated first dentary tooth; **d2**, second dentary tooth; **d3**, third dentary tooth; **d5**, fifth dentary tooth; **dca**, distal carina; **dde**, distal denticle; **de**, denticle; **del**, dentine layer; **dep**, anterodistal depression; **dep**, anterodistal depression; **dir**, distal ridges; **dir**, distal ridges; **dmg**, dorsomedial groove; **dmmf**, dorsomedial maxillary fenestra; **dpne**, dorsal pneumatic foramen; **dptc**, dorsal pterygoid contact; **dpvq**, dorsal projection of the ventral quadratojugal contact; **dqjc**, dorsal quadratojugal contact; **dr**, dorsal recess; **dt**, dentary; **dt1**, first dentary tooth; **dt2**, second dentary tooth; **dt3**, third dentary tooth; **dt5**, fifth dentary tooth; **dt7**, seventh dentary tooth; **dt8**, height dentary tooth; **ear**, epiantral recess; **ecc**, ectocondyle; **ecd**, depression of the ectocondyle; **ema**, external margin; **emf**, external mandibular fenestra; **enc**, entocondyle; **enl**, enamel layer; **ent**, enamel texture; **enu**, enamel undulation; **erao**, external rim of antorbital fossa; **esp**, enamel spalling; **exg**, extensor groove; **exg**, extensor groove; **ffl**, fibular flange; **ffl**, fibular flange; **flg**, flexor groove; **flg**, flexor groove; **flu**, flute; **gfo**, glenoid fossa; **hd**, hooked denticles; **iar**, interalveolar recess; **icas**, intercapitular sulcus; **icn**, intercondylar notch; **icp**, intercondylar pit; **ics**, intercondylar sulcus; **idd**, interdenticular diaphysis; **idg**, interdental gap; **idp**, interdental plate; **ids**, interdenticular sulcus; **idsl**, interdenticular slit; **idsp**, interdenticular space; **idw**, interdental wall; **ifs**, interfenestral strut; **igr**, interglenoid ridge; **j**, jugal; **juc**, jugal contact; **jur**, jugal ramus; **lac**, lacrimal contact; **lad**, labial depression; **laof**, lateral antorbital fossa; **law**, lateral wall; **lc**, lateral condyle; **lc**, lateral condyle; **ldr**, laterodorsal ridge within the anterior corner of the lateral antorbital fossa; **lfo**, lateral foramen; **lgd**, lateral glenoid depression; **lgr**, longitudinal groove; **lic**, lingual concavity for the erupting tooth; **lid**, lingual depression; **liw**, lingual wall; **lpne**, lateral pneumatic foramen; **lpq**, lateral process of the quadrate; **lri**, longitudinal ridge; **lvp**, lateroventral process; **m**, maxilla; **maf**, maxillary alveolar foramina; **mal**, maxillary alveoli; **man**, maxillary antrum; **maof**, medial antorbital fossa; **mar**, mandibular articulation; **mbo**, maxillary body; **mc**, medial condyle; **mc**, medial condyle; **mca**, mesial carina; **mcf**, maxillary circumfenestra foramina; **mdc**, mediodistal crest; **mdc**, mediodistal crest; **mde**, mesial denticle; **mef**, Meckelian foramina; **mes**, medial shelf; **mew**, medial wall; **mf**, Meckelian fossa; **mfe**, maxillary fenestra; **mfo**, maxillary fossa; **mfq**, medial fossa of the quadrate; **mfr**, Meckelian foramen; **mg**, Meckelian groove; **mgd**, medial glenoid depression; **mmf**, medial maxillary foramina; **mnf**, maxillary neurovascular foramina; **mpc**, medial pneumatic complex; **mpne**, medial pneumatic foramen; **ms**, mandibular symphysis; **mun**, marginal undulation; **mx**, maxillary teeth; **mx1**, first maxillary tooth; **mx2**, second maxillary tooth; **mx4**, fourth maxillary tooth; **mx5**, fifth maxillary tooth; **mx9**, ninth maxillary tooth; **n**, nasal; **nac**, nasal contact; **nc**, neural canal; **nf**, neurovascular foramina; **nuf**, nutrient foramina; **nug**, nutrient groove; **nvo**, neurovascular opening; **oca**, ootic capitulum; **ope**, operculum; **pab**, preantorbital body; **pac**, palatine contact; **pdg**, paradental groove; **pfl**, pterygoid flange; **pfq**, posterior fossa of the quadrate; **pgq**, posterior groove; **pm**, premaxilla; **pmc**, premaxillary contact; **pmf**, promaxillary fenestra; **pmfo**, promaxillary fossa; **pmmf**, posteromedial maxillary fenestra; **pmr**, promaxillary recess; **pne**, pneumatic excavation; **pnf**, pneumatic fenestra; **po**, postorbital; **poas**, postantral strut; **poc**, postorbital contact; **ppne**, posterior pneumatic foramen; **pras**, preantral strut; **prms**, promaxillary strut; **pt**, pterygoid; **ptc**, pterygoid contact; **ptmf**, postmaxillary fenestra; **ptms**, postmaxillary strut; **puc**, pulp cavity; **qb**, quadrate body; **qdi**, quadrate diverticulum; **qf**, quadrate foramen; **qh**, quadrate head; **qj**, quadratojugal; **qjc**, quadratojugal contact; **qjp**,

quadratojugal process; **qr**, quadrate ridge; **qrg**, quadrate ridge groove; **qs**, quadrate shaft; **rad**, radix; **rep**, resorption pit; **retp**, retroarticular process; **ri**, ridge; **ro**, root; **rob**, root base; **sa**, surangular; **sab**, supracetabular buttress; **sab**, supracetabular buttress; **sca**, squamosal capitulum; **sca**, squamosal contact; **sd**, supradentary; **sdc**, supradentary contact; **se**, serration; **snf**, subnarial foramen; **sp**, splenial; **spc**, split carina; **spl**, splenial contact; **sps**, spalled surface; **sq**, squamosal; **sqc**, squamosal contact; **st**, striation; **step**, step between Meckelian fossa and Meckelian groove; **suas**, suprantral strut; **trb**, tooth root bulge; **tun**, transverse undulation; **uet**, unerupted tooth; **vac**, vascular canals; **veb**, vestibular bulla; **vem**, ventral margin; **vmf**, ventral maxillary fenestra; **vmpr**, ventromedial pneumatic recess; **vpdq**, ventral projection of the dorsal quadratojugal contact; **vpne**, ventral pneumatic foramen; **vptc**, anteroventral pterygoid contact; **vptc**, ventral pterygoid contact; **vqjc**, ventral quadratojugal contact; **vsh**, ventral shelf of the pterygoid flange; **wfa**, wear facet.

Morphological and Positionnal Abbreviations

8, eight-shaped cross-section at the cervix; **~**, medium-sized denticles (i.e., between 15 and 250 denticles on the carina); **<<**, minute denticles (more than 250 denticles on the carina); **>>**, large denticles (less than 15 denticles on the carina); **A**, anastomosed oriented texture; **B**, braided oriented texture; **bco**, basal constriction at the cervix; **C**, conidonty (dentition with conical crowns); **den**, dentition; **des**, denticle size; **codm**, convex distal margin; **cos**, concave surface adjacent to carinae; **D**, D-shaped cross-section; **ddca**, displaced distal carina; **edg**, edentulous jaw; **F**, folidonty (dentition with lanceolate crowns); **I**, irregular, non-oriented, texture; **L**, left; **La**, present in lateral teeth; **M**, mesial teeth, or present in mesial teeth; **Mcs**, mesial teeth, cross-section at the cervix; **mdrc**, mesial denticles reaching the cervix; **O**, subcircular/lanceolate cross-section; **P**, parlinon-shaped cross-section; **Pa**, pachydonty (dentition with banana-shaped crowns); **pct**, procumbent teeth; **R**, right; **tmca**, twisted mesial carina; **U**, U-shaped cross-section; **udca**, unserrated distal carina; **umca**, unserrated mesial carina; **V**, veined and anastomosed oriented texture; **W**, present in both mesial and lateral teeth; **Z**, ziphodonty (dentition with blade-shaped crowns).

Morphometric Abbreviations

AAD, anterior apical carina denticles; **ABD**, anterior basal carina denticle; **ACDL**, anterior carina denticulate length; **ACL**, anterior carina length; **AD**, denticle height; **ADC**, anterior carina denticle count; **ADCL**, anterior denticulate carina length; **ADD**, anterior denticle density; **ADM**, anterior denticles per millimeter density; **AL**, apical length; **AMD**, anterior medial carina denticles; **ANTSERR**, anterior serration density; **BCR**, basal compression ratio; **BW**, tooth basal width; **CA**, crown angle; **CBL**, crown base length; **CBR**, crown base ratio; **CBW**, crown base width; **CD**, denticle length; **CH**, crown height; **CHR**, crown height ratio; **CST**, cross-sectional thickness; **CTU**, crown transverse undulation density; **DA**, distoapical denticle density; **DAVG**, average distal denticle density; **DB**, distobasal denticle density; **DBR**, distal denticle base ratio; **DC**, distocentral denticle density; **DCAL**, distal carina length; **DCD**, denticle density for the distal carina; **DCM**, denticle density on the mesial carina; **dd**, denticles on the distal carina; **DDC**, distal carina denticle count; **DDH**, distal denticle height; **DDHM**, distal denticle height of middle denticles; **DDL**, distal denticle length; **DDT**, dentine thickness distally; **DDW**, distal denticle width; **Dent. Ht**, denticle height; **Dent. W**, denticle weight; **Dent/mm**, number of denticles per millimeters; **DH**, denticle height; **DHR**, distal denticle height ratio; **DLAT**, dentine thickness labially; **DLIT**, dentine thickness lingually; **dm**, denticles on the mesial carina; **DMCTOB**, mesial carina and the base of the tooth crown; **DMT**, dentine thickness mesially; **DSDI**, denticle size density index; **DSL**, distal serrated carina length; **DW**, denticle width; **ER**, elongation ratio; **FABL**, fore-aft basal length; **Ht**, tooth height; **LAD-H**, largest anterior denticle height; **LAD-L**, largest anterior denticle length; **LAD-W**, largest anterior denticle width; **LAF**, labial flutes; **LCI**, lateral compression index; **LIF**, lingual flutes; **LPD-H**, largest posterior denticle height; **LPD-L**, largest posterior denticle length; **LPD-W**, largest posterior denticle width; **MA**, mesioapical denticle density; **MAVG**, average mesial denticle density; **MB**, mesiobasal denticle density; **MBR**, mesial denticle base ratio; **MC**, mesiocentral denticle density; **MCAL**, mesial carina length; **MCE**, mesiobasal carina extension; **MCL**, mid-crown length; **MCR**, mid-crown ratio; **MCW**, mid-crown width; **MDC**, mesial carina denticle count; **MDE**, mesiobasal denticle extension; **MDH**, mesial denticle height; **MDH**, mesial denticle height; **MDHM**, mesial denticle height of middle denticles; **MDL**, mesial denticle length; **MDL**, mesial denticle length; **MDW**, mesial denticle width; **MDW**, mesial denticle width; **MDWM**, mesial denticle width of middle denticles; **MHR**, mesial denticle height ratio; **MHR**, mesial denticle height ratio; **MSH**, length of the mesial serration; **MSL**, mesial serrated carina length; **MUD**, marginal undulation density; **NDPMa**, number of denticles per millimeter on anterior carina; **NDPMp**, number of denticles per millimeter on posterior carinae; **PAD**, posterior apical carina denticles; **PBD**, posterior basal carina denticles; **PCDL**, posterior carina denticulate length; **PCL**, posterior carina length; **PDC**, posterior carina denticle count; **PDD**, posterior denticle density; **PDM**, posterior denticles per millimeter; **PMD**, posterior medial carina denticles; **POSTSERR**,

posterior serration density; **SI**, slenderness index; **TCH**, tooth crown height; **TCW**, tooth crown width; **THEIGHT**, tooth crown height; **TUD**, transverse undulation density; **XSTHICK**, cross-sectional thickness.

Other Abbreviations

0, absent; **1**, present at least in some teeth or some taxa; **?**, unknown; **-**, inapplicable; **c**, photos of cast provided; **C/**, cast or composite examined; **CI** consistency index; **CVA**, canonical variant analysis; **DFA**, discriminant analysis; **E**, original material examined; **f**, photos of original material provided; **IP**, impact factor; **K–Pg**, Cretaceous–Paleogene; **MPTs**, most parsimonious trees; **OTU**, operational taxonomic units; **p**, publication; **PCA**, principal component analysis; **SEM**, scanning electron microscope; **SI**, retention index; **SOM**, supplementary online material.

Lifesize model of *Torvosaurus gurneyi* displayed at the Belgian TV show Hotel M (Chanel Eén, broadcasted on the 23rd of June 2014).

I. INTRODUCTION

Theropods form a clade of bipedal tetrapods among which birds and all strictly carnivorous dinosaurs are found (e.g., Gauthier 1986; Sereno 1997; Holtz and Osmólska 2004; Holtz 2012; Naish 2012). Along with sauropodomorph and ornithischian clades, they appeared in the Late Triassic (Fig. 1.1) and rapidly acquired a worldwide distribution, being present on every continent by the Lower Jurassic (Tykoski and Rowe 2004). In the Jurassic (possibly as early as the Middle Jurassic, based on ghost ranges; e.g., Hu et al. 2009; Godefroit et al. 2013*a*, *b*), small theropods gave rise to birds, the only dinosaurs to survive the Cretaceous-Paleocene (K-Pg) mass extinction event 66 million years ago (Fig. 1.1). After surviving the K–Pg extinction event, birds radiated into ecological niches left by non-avian dinosaurs (Padian and Chiappe 1998; Chiappe and Witmer 2002; Naish 2012). As a result theropods are one of the most successful groups of tetrapods, and the most morphologically and taxonomically diverse clade of dinosaurs (Rauhut 2003*a*; Holtz 2012; Foth and Rauhut 2013).

Non-avian theropods (i.e., Theropoda excluding Avialae) were the dominant terrestrial predators in Jurassic and Cretaceous ecosystems worldwide (Rauhut 2003*a*; D'Amore 2009). Though their diversity and disparity remained high through the end of the Cretaceous, they became extinct at the end of the Cretaceous concurrent with all other clades of non-avian dinosaurs (Rauhut 2003*a*; Holtz et al. 2004; Upchurch et al. 2011; Brusatte et al. 2012*b*, 2014*b*). While non-avian theropods include the majority (if not all) of meat-eating dinosaurs, many theropod clades became secondarily adapted to herbivorous diets (Barrett 2005; Xu et al. 2009*b*; Zanno et al. 2009; Zanno and Makovicky 2011), and several taxa have been described as omnivores (Holtz et al. 1998; Lee et al. 2014), insectivores (Senter 2005) or filter feeders (Norell et al. 2001). The non-avian theropod body plan underwent relatively little modification during the evolution of the clade, being exclusively bipedal and exhibiting, for the large majority of them, elongated necks and a long, horizontally projecting tail (n.b., some theropods such as tyrannosaurids and caudipterids had short neck and short tail, respectively). Variation in the postcranium mostly occurs in the forelimb, manual and pelvic morphology, hind limbs proportion as well as the vertebral counts, ossification, and elongation of the neural spine. Some theropods like abelisaurids had short stubby arms bearing four short fingers (e.g., Ruiz et al. 2011; Burch and Carrano 2012) whereas others like therizinosaurids possess elongated forelimbs with three slender fingers bearing large claws (Clark et al. 2004; Zanno 2010*a*). Likewise, although the large majority of theropods show short neural spines, some spinosaurids, allosauroids and deinocheirids have developed hypertrophied spines forming a hump or a sail on the back of these animals (Bailey 1997; Lee et al. 2014). Unlike the postcranial skeleton, there is a tremendous diversity of skull morphology in non-avian theropods, from the elongated skull of spinosaurids showing a terminal spatulate rosette (Charig and Milner 1997; Dal Sasso et al. 2005) to the short parrot-like skull and edentulous jaws of oviraptorids (Xu and Han 2010). Recent discoveries of non-avian theropods such as the rodent-like *Incisivosaurus* (Xu et al. 2002*a*), the beaked *Limusaurus* (Xu et al. 2009*b*), the

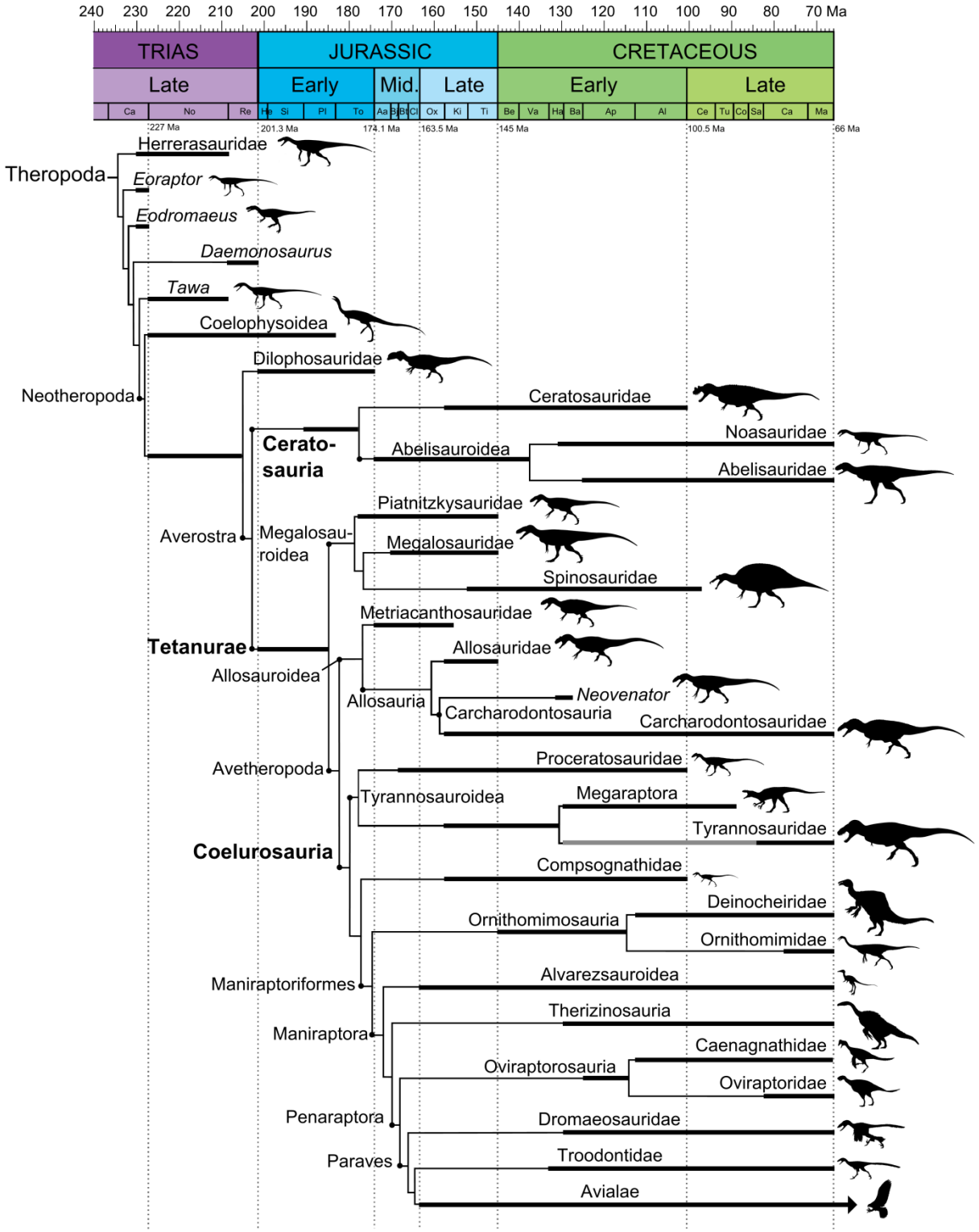

FIGURE 1.1. Phylogeny and stratigraphic distribution of theropod clades. The phylogenetic classification of theropods follows the results of the cladistic analyses obtained by Sues et al. (2011) for non-neotheropod Theropoda, Smith et al. (2007) and Ezcurra and Brusatte (2011) for non-averostran Neotheropoda, Pol and Rauhut (2012) and Tortosa et al. (2014) for Ceratosauria, Carrano et al. (2012) for non-coelurosaur Tetanurae, Loewen et al. (2013), Lü et al. (2014) and Porfiri et al. (2014) for Tyrannosauroidea, Lee et al. (2014) for Ornithomimosauria, Lamanna et al. (2014) for Oviraptorosauria, and Turner et al. (2012), Godefroit et al. (2013a) and Choiniere et al. (2014*b*) for non-tyrannosauroid Coelurosauria. For silhouette attribution, see Appendices A1.1.

crested *Guanlong* (Xu et al. 2006), the long snouted *Buitreraptor* (Makovicky et al. 2005) and the duck-billed *Deinocheirus* (Lee et al. 2014) indicate a particularly high variety of skull morphologies among theropod dinosaurs (Brusatte et al. 2012*c*; Foth and Rauhut 2013).

This work aims to investigate aspects of the evolution of theropod skulls by analyzing in detail both the anatomy and ontogeny of teeth and quadrates in non-avian theropods. A special attention was accorded to Megalosauroidea, as the large majority of megalosauroid taxa were examined first hand, so that the anatomy of teeth and quadrates was exhaustively studied in Megalosauridae and Spinosauridae, respectively. Undescribed (or briefly described) embryonic and adult cranial material referred to the megalosaurid *Torvosaurus* from the Kimmeridgian-Tithonian of Portugal, and the spinosaurid *Spinosaurus* from the Cenomanian of Morocco, also allowed to investigate the ontogenetic variations occurring in the teeth and quadrates of these taxa.

Theropod teeth are typically seen as ziphodont, i.e., they are blade shaped, serrated and laterally compressed, which is the plesiomorphic condition for dinosaurs and archosaurs (Holtz and Osmólska 2004; Holtz 2012). Yet, variation of this ancestral morphology occurred in many clades of theropods such as basal ornithomimosaurs and alvarezsauroids with small, conical or lanceolate, and unserrated teeth, and derived therizinosaurs and troodontids with leaf-shaped crowns bearing large pointed denticles (Currie 1987; Barrett 2000). Because theropods were polyphyodont animals (i.e., they continuously replaced their teeth, therefore producing shed teeth through their life) and enamel covering crowns is one of the hardest skeletal structure (Martin 1999), isolated teeth are certainly one of the most common theropod remains in the dinosaur fossil record. As a result, theropod teeth are constantly reported in the literature, with three to four papers describing these dental remains being published each year. Identification of isolated theropod teeth typically rely on diagnostic features and/or quantitative data through morphometric analyses such as principal coordinate and discriminant analyses (PCA and DFA). Given their abundance, isolated theropod teeth provide crucial information on the paleostratigraphic and paleogeographic distribution of theropod clades, and a single theropod tooth can push back the first occurrence of a clade to dozens of millions of years (e.g., *Ostafrikasaurus*; Buffetaut 2011), and extend its geographic range by nearly 10,000 km (e.g., troodontid tooth from India; Goswami et al. 2013).

Whereas the primary role of teeth is to cut and process food before deglutition, the quadrate of non-avian theropods and the large majority of vertebrates plays many important functions such as a structural support for the basicranium, articulatory element with the lower jaws, attachment for several muscles allowing the mandible to be depressed and to mouth to close, and hosting important nerves, pneumatic sinuses, and vascular passages (e.g., Witmer 1990, 1997*a*; Bakker 1998; Sedlmayr 2002; Kundrát and Janáček 2007; Holliday and Witmer 2008; Tahara and Larsson 2011). In avian theropods, the quadrate is a kinetic bone and its rotation at its dorsal articulation, known as streptostyly, allows upward and downward movements of the rostrum (Bock 1964; Bühler 1981; Zusi 1984; Meekangvan et al. 2006). Due to the important morphofunctional aspect of the quadrate, and because this cranial

bone also articulates with no less than four other bones of the skull (i.e., quadratojugal, squamosal, pterygoid, and articular), the quadrate morphology is particularly complex and significantly differs in each theropod subclades. Despite this morphological variation, the theropod quadrate always corresponds to a ventrodorsally tall body bearing an anteriorly projected and mediolaterally thin ala known as the pterygoid flange, and typically ended by a single dorsal condyle (the squamosal capitulum) and two mandibular condyles (the ecto- and entocondyles). The morphology of the mandibular condyles and the furrow separating them provide crucial information on the biomechanics of the articulation between the mandible and the cranium.

Due to different feeding strategies and lifestyles between Megalosauridae and Spinosauridae, the morphological diversity of the quadrate and teeth is particularly high in the clade of Megalosauria (Megalosauridae + Spinosauridae). Megalosauridae were typical meat-eating theropods from the Middle to Late Jurassic primarily known in Europe. They show a tall and relatively robust skull bearing ziphodont and coarsely serrated teeth and no extravagant cranial ornamentations on the top of the head (Benson 2008*a*, 2010*a*; Sadleir et al. 2008; Carrano et al. 2012). On the other hand, spinosaurids, from the Early and Late Cretaceous of Eurasia and Gondwana, were opportunistic animals feeding on dinosaurs, pterosaurs, and fishes, and showing a longirostrine skull possessing conical fluted teeth and bony crests on the dorsal margin of the cranium (Charig and Milner 1997; Sues et al. 2002; Buffetaut et al. 2004; Dal Sasso et al. 2005; Ibrahim et al. 2014*b*). As for the quadrate, it is ventrodorsally tall and lack a quadrate foramen in megalosaurids, whereas the bone is ventrodorsally short and shows, in some cases, a large quadrate 'fenestra' in spinosaurids. Comparison between the most recent and largest members of both megalosauroid clades, *Spinosaurus* and *Torvosaurus*, reveals some major morphological differences between derived Spinosauridae and Megalosauridae.

Spinosaurus from the Cenomanian (Upper Cretaceous) of North Africa possesses an extremely elongated, crocodile-like snout with a sigmoid alveolar margin and retracted nares. The premaxillae are mediolaterally constricted in their posterior part and include six to seven teeth (Taquet and Russell 1998; Milner 2003; Dal Sasso et al. 2005). The latter are conical, fluted, and unserrated, and surprisingly large in the anterior part of the dentary (Stromer 1915). The body shows very reduced hind limbs and extremely elongated neural spines forming a bony sail in the middle of the back (Ibrahim et al. 2014*b*). *Spinosaurus* remains were first discover in the Bahariya Oasis of Egypt in 1912 by German collector Richard Markgraf, and first described by German paleontologist Ernst Freiherr Stromer von Reichenbach in 1915. The holotype was, however, destroyed in a British bombing raid of Munich in April 1944 (Nothdurft 2003; Smith et al. 2006). Additional material of *Spinosaurus* were later found in the Kem Kem beds of Morocco and the Tademaït of Algeria (Russell 1996; Taquet and Russell 1998; Dal Sasso et al. 2005), and associated cranial and postcranial remains of a new individual has been recently unearthed in the Northern part of Morocco (Ibrahim et al. 2014*b*).

On the other hand, *Torvosaurus* from the Kimmeridgian-Tithonian (Upper Jurassic) of Europe and North America has tall and robust upper and lower jaws bearing four premaxillary teeth and large ziphodont maxillary teeth with no more than 8 denticles per 5 mm (Galton and Jensen 1979; Britt 1991; Mateus et al. 2006; Hendrickx and Mateus 2014*a*). The hind limbs are relatively elongated and powerful in this taxon, and the vertebral column possesses short neural spines (Britt 1991). *Torvosaurus tanneri* is currently the most-recent and the only megalosaurid that lived in North America (Holtz et al. 2004; Carrano et al. 2012; Hanson and Makovicky 2013). It was coined by Galton and Jensen in 1979 to refer to a very large form of theropod from the Morrison Formation based on postcranial material from the Uncompahgre Plateau of Colorado (Galton and Jensen 1979). Additional cranial and postcranial material from Colorado were latter assigned to this taxon by Jensen (1985), and Britt (1991) gave a detailed description of its osteology, referring a dorsal vertebra from Utah and several large isolated teeth from Wyoming to the species *T. tanneri*. In the beginning of the 21st century, cranial and postcranial material from the Lourinhã Formation of Portugal were also identified as belonging to *Torvosaurus*, evidencing the presence of this taxon in Europe by the Late Jurassic (Mateus and Antunes 2000*a*; Mateus et al. 2006; Malafaia et al. 2008).

Chapter 1: An overview on non-avian theropod discoveries and classification

Prepared for ***PalArch's Journal of Vertebrate Palaeontology***:
Hendrickx, C., Hartman, S. and Mateus, O. in press. An overview on non-avian theropod discoveries and classification. *PalArch's Journal of Vertebrate Palaeontology*.

Abstract

Theropods form a taxonomically and morphologically diverse group of dinosaurs that include extant birds. Inferred relationships between theropod clades are complex and have changed dramatically over the past thirty years with the emergence of cladistic techniques. Here, we present a brief historical perspective of theropod discoveries and classification, as well as an overview on the current systematics of non-avian theropods. The first scientifically recorded theropod remains dating back to the 17th and 18th centuries come from the Middle Jurassic of Oxfordshire and most likely belong to the megalosaurid *Megalosaurus*. The latter was the first theropod genus to be named in 1824, and subsequent theropod material found before 1850 can all be referred to megalosauroids. In the fifty years from 1856 to 1906, theropod remains were reported from all continents but Antarctica. The clade Theropoda was erected by Othniel Charles Marsh in 1881, and in its current usage corresponds to an intricate ladder-like organization of 'family' to 'superfamily' level clades. The earliest definitive theropods come from the Carnian of Argentina, and coelophysoids form the first significant theropod radiation from the Late Triassic to their extinction in the Early Jurassic. Most subsequent theropod clades such as ceratosaurs, allosauroids, tyrannosauroids, ornithomimosaurs, therizinosaurs, oviraptorosaurs, dromaeosaurids, and troodontids persisted until the end of the Cretaceous, though the megalosauroid clade did not extend into the Maastrichtian. Current debates are focused on the monophyly of deinonychosaurs, the position of dilophosaurids within coelophysoids, and megaraptorans among neovenatorids. Some recent analyses have suggested a placement of dilophosaurids outside Coelophysoidea, megaraptorans within Tyrannosauroidea, and a paraphyletic Deinonychosauria with troodontids placed more closely to avialans than dromaeosaurids.

Historical background

First Discoveries

The description of the first theropod remains and the first dinosaur material go hand in hand, as the first dinosaur bones and teeth reported in the literature belong to theropods (Lebrun 2004). All theropod material reported in the 17th, 18th, and the first half of the 19th century came from England and France, and has been referred to megalosauroid theropods, with most remains being assigned to Megalosauridae. This coincidence can be explained by two independent factors: 1) the emergence of

vertebrate paleontology in the Early modern period and early 19th century in Western Europe, with scientists like Georges Cuvier, Gideon Mantell, and Richard Owen; and 2) the excavation, at that time, of vertebrate remains from Middle Jurassic limestone quarries of Stonesfield (Oxfordshire) and Caen (Normandy), a period of time when megalosaurids were the dominant theropods in Europe.

Theropod fossils were almost certainly found by prescientific societies prior to the 17th century, but the discovery of these unusual remains were interpreted in ways that gave rise to myths and legends (Buffetaut 1994; Lebrun 2004; Spalding and Sarjeant 2012). Theropod tracks from the Lower Cretaceous sandstones of Paraíba in north-eastern Brazil were, for instance, considered by Amerindians to pertain to giant running birds (Leonardi 1984; Mayor and Sarjeant 2001). Likewise, a set of theropod tracks visible on Cenomanian limestone in the south of Algeria was believed by Arabs to belong to a giant ostrich, property of a venerated man buried nearby (Taquet 2010).

The first published record of a theropod bone is of an incomplete left femur described and figured by Robert Plot in his 1677 *Natural History of Oxfordshire* (Fig. 1.2A). The fossil was dug up from a quarry in the Parish of Cornwell, Oxfordshire, and probably pertains to the megalosaurid *Megalosaurus* (Delair and Sarjeant 1975, 2002). Plot (1677) correctly identified the bone as a distal femoral condyle (*capita femoris inferiora*), and wondered whether this partial femur belonged to an elephant brought to Britain by the Romans. Plot (1677), however, noted many differences with the femur of elephants and instead referred the bone to a human giant also brought by the Romans (Evans 2010). This portion of femur was reillustrated by English naturalist Richard Brookes (1763) who labeled the figure ‘Scrotum Humanum’, given the superficial similarity of the distal condyle to human testicles (Fig. 1.2B). Although this binomial term was clearly used as a descriptive appellation by Brookes (Spalding and Sarjeant 2012), some have proposed its use as a valid scientific name. That would make ‘Scrotum humanum’ the first formal binomial name given to a dinosaur and a senior synonym of *Megalosaurus bucklandii* (Halstead 1970; Delair and Sarjeant 1975), a proposition which was rejected by the International Zoological Commission (Halstead and Sarjeant 1993; Delair and Sarjeant 2002).

Isolated theropod teeth were first described and figured in 1699 by Welsh naturalist Edward Lhuyd in his catalogue of fossils and minerals *Lithophylacii Britannici Ichnographica* (Lhuyd 1699). The specimen number 1328 (Lhuyd 1699: plate 16), originally ascribed to a fish by Lhuyd (1699), corresponds to an isolated tooth from the Middle Jurassic Great Oolite of Stonesfield (Fig. 1.2C). This shed tooth greatly resembles *Megalosaurus* and most likely belongs to that taxon (Delair and Sarjeant 2002). Additional theropod findings reported in the 18th century include a limb bone from Stonesfield labeled specimen a.1 by John Woodward (1729) in his catalogue of British fossils from his personal collection. This section of limb bone is currently preserved in the Sedgwick Museum of Cambridge (specimen D.30.1) and, once again, likely pertains to *Megalosaurus* (Delair and Sarjeant 1975, 2002). It may, therefore, be the earliest-discovered bone that can still be identified as belonging to a theropod with confidence (Delair and Sarjeant 1975, 2002). Later, an incomplete femur described and illustrated

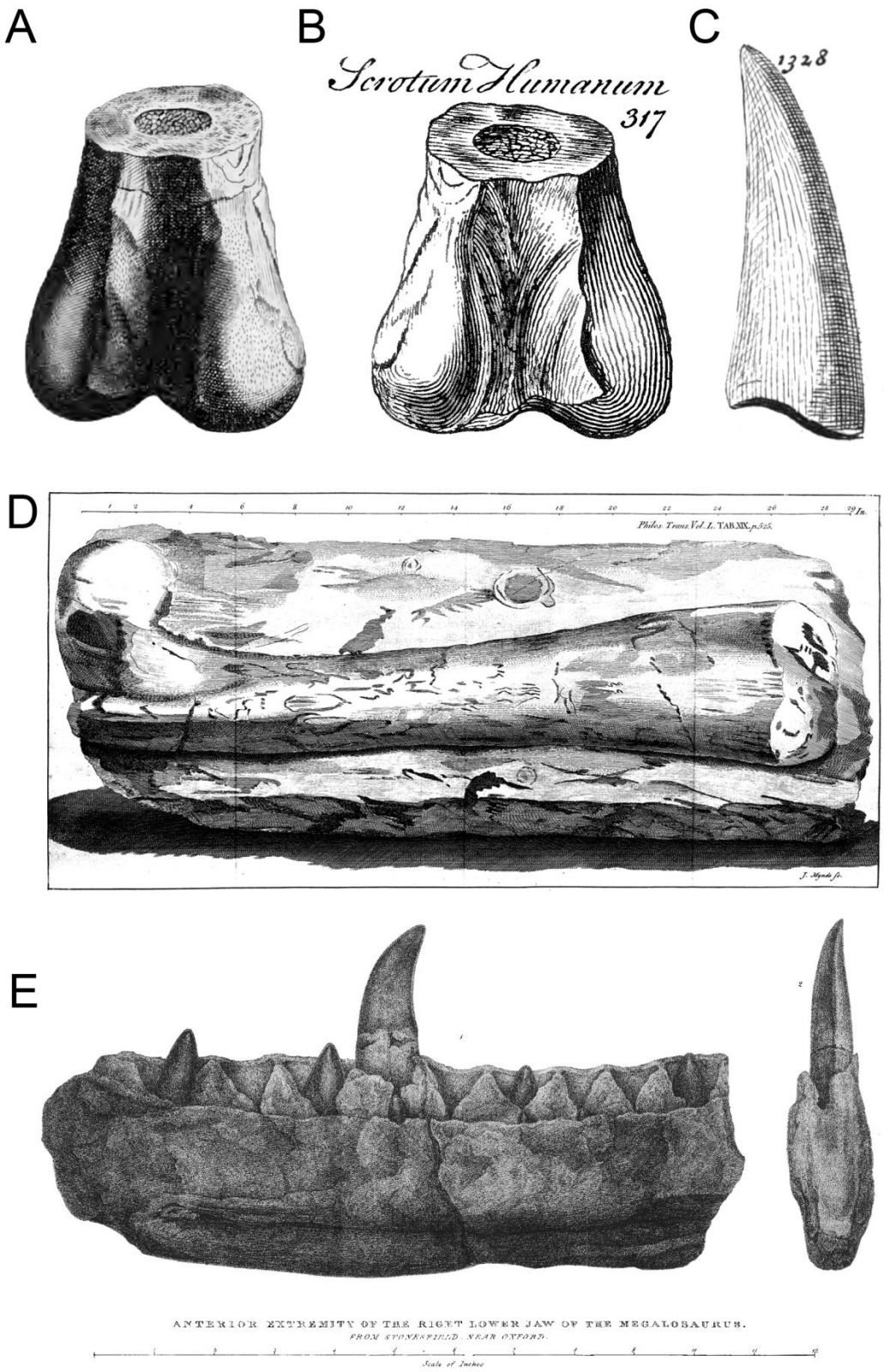

FIGURE 1.2. Earliest historical records of theropod remains in the world. **A–B**, Distal part of a left femur of *Megalosaurus* from Cornwell, U.K., in posterior view, and first reported by Plot (1677); **A**, illustrations by Plot (1677: table 8, fig.4); and **B**, Brookes (1763, p. 312: fig. 317) showing the label 'Scrotum Humanum'; **C**, isolated theropod tooth (likely *Megalosaurus*) from the Stonesfield, U.K., illustrated by Lhuyd (1699: plate 16, fig. 1328); **D**, right femur of *Megalosaurus* from Stonesfield, U.K., in anterior view, illustrated by Platt (1758: table 19); **E**, right dentary of *Megalosaurus bucklandii* from Stonesfield, U.K., in medial and posterior views, illustrated by Buckland (1824: plate 40).

by Platt (1758) was identified as belonging to a hippopotamus, a rhinoceros, or an unknown animal of large size (Fig. 1.2D). This large femur, which is also from Stonesfield, was recently referred to *Megalosaurus bucklandii* (Evans 2010).

The first theropod taxon to be recognized as reptilian and formally described in the literature is, in fact, *Megalosaurus*, coined by William Buckland in 1824 (although the generic name was already announced by James Parkinson in 1822). Material originally ascribed to *Megalosaurus* included a right dentary with a well-preserved erupted tooth (Fig. 1.2E), ribs, hind-limb elements, pelvic bones, and sacral and caudal vertebrae, all collected in the Taynton Limestone Formation (middle Bathonian) of Stonesfield, Oxfordshire. As Buckland (1824) did not provide a species name for *Megalosaurus*, the type species *Megalosaurus conybeari* was proposed by Ferdinand von Ritgen in 1826 (von Ritgen 1826). This author failed to provide a description and diagnosis for the species, allowing Mantell (1827) to be the first scientist to name and diagnose a theropod species, i.e., *Megalosaurus bucklandii*, which is the name currently accepted by the scientific community.

Streptospondylus altdorfensis (Meyer 1832) and *Poekilopleuron bucklandii* (Eudes-Deslongchamps 1837) from France were the first non-avian theropods to be described in the literature outside England, and the second and third Mesozoic theropods to be formally named. These two megalosauroids, considered valid species (Carrano et al. 2012), are only known from postcranial remains. The material of *Streptospondylus*, discovered in the Callovian Vaches Noires cliffs around 1770, was mixed with crocodilian remains, and interpreted as a crocodile by Cuvier (1808, 1812, 1824). The remains of *Poekilopleuron* from the Calcaire de Caen Formation (middle Bathonian) in Caen, Normandy, were correctly identified as belonging to a large reptile closely related to *Megalosaurus*. Unfortunately, the material was lost during World War II and, besides the original illustrations provided by Eudes-Deslongchamps (1837), only casts of some bones remain (Allain and Chure 2002).

Although Buckland (1824) and Mantell (1827) were the first to give a relatively good description of the dentition of *Megalosaurus*, Richard Owen was the first scientist to exhaustively investigate the tooth anatomy of theropods and many other vertebrates. In his treatise on vertebrate teeth, *Odontography* (Owen 1840-1845), and his richly illustrated four volume *A History of British Fossil Reptiles* (Owen 1849-1884), Owen provided a comprehensive description and illustration of the crowns, denticles, and internal structure of the teeth of *Megalosaurus bucklandii* and *Suchosaurus cultridens*. The latter was erected by Owen (1840-1845) based on isolated teeth from the Wealden of Tilgate Forest, near Cuckfield (Sussex). Interestingly, the teeth of *Suchosaurus* were discovered by Mantell, and were first described and illustrated by Mantell (1822) and Cuvier (1824), respectively (Buffetaut 2010). Cuvier (1824), Mantell (1827, 1833), and Owen (1840-1845; 1849-1884) all referred these isolated teeth to crocodilians, yet they closely resemble those of the spinosaurid *Baryonyx walkeri* discovered much later. *Suchosaurus* teeth are now considered as belonging to either *Baryonyx* or an unnamed member of Baryonychinae (Milner 2003; Buffetaut 2007; Mateus et al. 2011).

The first non-megalosauroid theropod to be formally described is *Nuthetes destructor* from the Purbeck Formation (Berriasian, Early Cretaceous) of Durlston Bay, Dorset. This tentative dromaeosaurid was erected by Owen (1854) based on an incomplete dentary and some isolated teeth originally assigned to a lizard or a varanid (Milner 2002). A few years later, *Compsognathus longipes* (Wagner 1861), from the Solnhofen Limestone of Germany, was the first non-avian theropod preserving a nearly complete and slightly disarticulated skull and skeleton to be reported in the literature. This theropod was discovered in Germany around 1859 (Wellnhofer 2008) and was reported by Wagner (1859) the same year. It remained one of the most completely known theropods for more than a century (Ostrom 1978).

After Europe, North America became the second continent to yield theropod remains described by paleontologists. The first theropod fossils reported were isolated teeth discovered in 1855 by eminent American scientist Ferdinand Vandiveer Hayden from the Upper Cretaceous of Montana, at the confluence of the Missouri and Judith rivers (Breithaupt 1999). The dental material was briefly described one year later by Leidy (1856) who erected two new species, *Deinodon horridus* based on several fragment of teeth (Fig. 1.3A) and *Troodon formosus* based on a single shed tooth (Fig. 1.3B). *Troodon* and *Deinodon* were originally thought to belong to a 'lacertian' (a large Monitor according to Leidy 1860) and a relative of *Megalosaurus*, respectively (Leidy 1856, 1860). *Troodon* is now considered to be a valid species of troodontid (Currie 1987), whereas *Deinodon* has been recognized as belonging to an unidentified tyrannosaurid, probably *Albertosaurus* known from the same deposits (Breithaupt 1999; Breithaupt and Elizabeth 2008).

Shortly after Leidy's description of theropod teeth from North America, the Reverend Stephen Hislop (1861, 1864) reported the discovery of isolated theropod teeth from the Upper Cretaceous of India. One of them was discovered by Mr. Rawes in the locality of Takli, in the Nagpur area of Maharashtra, and represents the earliest historical record of theropod dinosaurs in Asia (Carrano et al. 2010). The shed tooth was sent to the Geological Society's Museum of London (which is now part of the Natural History Museum) and studied and illustrated by English naturalist Richar Lydekker (1879, 1885, 1890*;* Fig. 1.3C). Although the latter recognized the theropod affinity of the tooth, he assigned it to a new species of basal sauropodomorph, *Massospondylus rawesi* (Lydekker 1890). The tooth was later referred to *Megalosaurus* (Vianey-Liaud et al. 1988) and is currently assigned to an indeterminate theropod, almost certainly an abelisaurid (Carrano et al. 2010, 2012; pers. obs.).

In the span of a decade, between the latest part of the 19th century and the first part of the 20th century, theropod material was reported on three continents of the Southern Hemisphere, Africa, South America and Australia. The French were the first to collect and describe material belonging to Gondwanan theropods. The first definitive theropod material to be reported in the Southern Hemisphere, in fact, belongs to the well-known abelisaurid *Majungasaurus crenatissimus* unearthed in the Maevarano Formation (Maastrichtian) of Madagascar. The species was erected as *Megalosaurus crenatissimus* by French paleontologist Charles Depéret in 1896, based on fossils collected by Mr.

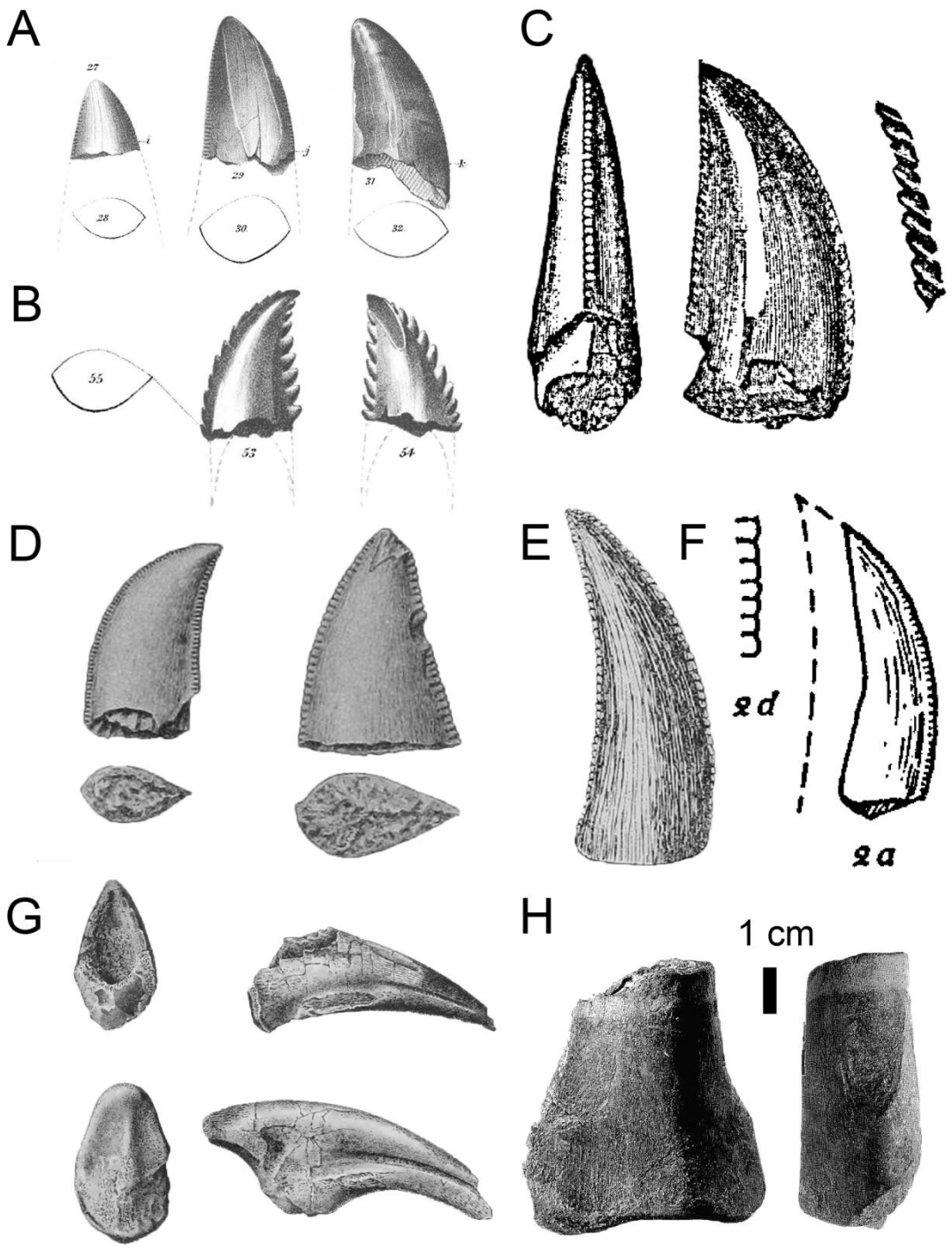

FIGURE 1.3. Earliest historical records of theropod remains in **A–B**, North America; **C**, Asia; **D**, Africa; **E–F**, South America; **G**, Oceania; and **H**, Antarctica. Isolated teeth of **A**, *Troodon formosus*; and **B**, *Deinodon horridus* (= *Albertosaurus sarcophagus*) from the Upper Cretaceous Judith River of Colorado and first reported by Leidy (1856; modified from Leidy 1860: plate 9); **C**, isolated theropod tooth of '*Massospondylus rawesi*', an abelisaurid from the Upper Cretaceous of India (localities of Takli and Maleri) first reported by Hislop (1861, 1864, illustration by Lydekker 1890: fig. 1); **D**, isolated teeth of the abelisaurid *Majungasaurus crenatissimus* first reported and originally described by Depéret (1896*a*, *b*; illustration by Depéret 1896*a*: table 24, plate 6); **E–F**, isolated theropod tooth from the Upper Cretaceous of Par-Aík, India, referred to *Loncosaurus argentines* and first reported by Ameghino (1899); **E**, illustration by Ameghino (1900, p. 160) and Ameghino (1906: fig. 8); and **F**, Huene (1929*a*: plate 41); **G**, pedal ungual of an indeterminate theropod from the Upper Cretaceous of Cape Patterson, Australia, and first reported by Woodward (1906); **H**, distal part of a tibia of a megalosauroid? theropod from the Upper Cretaceous of Col Crame, Antarctica, discovered in 1988 (modified from Molnar et al. 1996).

Landillon in the Mahajanga Basin one year before (Depéret 1896*a*, *b*; Krause et al. 2007; Fig. 1.3D). In Northern Africa, theropod tracks discovered in Cenomanian limestone in the Jebel Bou-Khaïl (near the city of Laghouat), Algeria, by French geologist G. Le Mesle were first reported by Le Mesle and Peron (1880) and account for the first reported theropods (and dinosaurs) in North Africa (Taquet 2010; Chabou et al. 2015). Almost twenty years later, a theropod vertebra and isolated teeth assigned to Spinosauridae were discovered in the Djoua country (near Timassânine), Algeria, during a mission led by French officer François Lami and explorer Fernand Foureau in 1898 (Buffetaut 2010; Taquet 2010). Based on the material collected by the latter, French paleontologist Emile Haug (1904, 1905) reported on and illustrated the first skeletal material of a theropod (and a dinosaur) from the Sahara, though the teeth were interpreted as belonging to an ichthyodectid fish (Buffetaut 2005, 2010).

The first theropod material to be reported in South America was an isolated tooth described by famous Argentinian paleontologist Florentino Ameghino in 1899 (Ameghino 1899; Coria and Salgado 1996; Fig. 1.3E–F). Based on this fragmentary tooth and a partial femur found in the Upper Cretaceous of Par-Aík, Santa Cruz Province of Argentina, Ameghino erected the taxon *Loncosaurus argentines* which was initially classified as a megalosaurid (Ameghino 1899). Although the partial tooth most likely belongs to a theropod, the femur of *Loncosaurus* is that of an ornithopod (Coria and Salgado 1996). *Genyodectes serus*, named and described by Woodward only two years later, is the first valid theropod (and dinosaur) to be reported from Argentina (Woodward 1901; Rauhut 2004*b*). Until the 1970s, this ceratosaurid remained one of the most complete theropods known from that continent (Rauhut 2004*b*).

Theropod material is scarcer in Oceania, yet the first representative fossil was reported in Australia by the beginning of the 20th century (Agnolín et al. 2010). Woodward (1906) described a theropod ungual unearthed from Cape Patterson, on the south coast of Victoria (Fig. 3G). This claw, the first dinosaur material reported from Australia, was collected by Mr. W. H. Ferguson in the Wonthaggi Formation (early Aptian; Agnolín et al. 2010). The pedal ungual was initially referred to a taxon closely related to *Megalosaurus*, and sometimes as *Megalosaurus* itself (Woodward 1906; Huene 1926*a*). It is now considered to belong to an indeterminate theropod (Agnolín et al. 2010; Carrano et al. 2012). Four years later, Woodward (1910) briefly reported the discovery of a tooth and a posterior caudal vertebra of what he assumed to be a small megalosaurian theropod. The material was found by T.C. Wollaston and comes from the Griman Creek Formation (Albian) of Lightning Ridge near Walgett, New South Wales. Huene (1932) described and referred the vertebra to the new taxon *Walgettosuchus woodwardi*, an indeterminate theropod currently considered a *nomen dubium* (Agnolín et al. 2010).

Antarctica is the last continent to have yielded non-avian theropod material. The first discovery of theropod remains occurred in 1988 when Agelandro Lopez Angriman found the distal part of a tibia in the Coniacian–Santonian Hidden Lake Formation of Antarctica (Molnar et al. 1996; Fig. 3H). The bone, known as the Hidden Lake specimen (Carrano et al. 2012), comes from the north

of Col Crame in the Cape Lachman region, north-western James Ross Island. This tibia was assigned to an indeterminate tetanuran by Molnar et al. (1996), and to a megalosauroid by Carrano et al. (2012), which makes it the latest surviving member of this clade found to date. Although the Hidden Lake specimen was the first theropod material to be found in Antarctica, this partial tibia was only described in 1996, and the first theropod to be reported in the literature is, in fact, *Cryolophosaurus ellioti*, described by Hammer and Hickerson (1994) two years earlier. *Cryolophosaurus* material was collected during the 1990–91 and 2003–04 field seasons, and this taxon is the most complete theropod from Antarctica, one of the largest from the Early Jurassic, and possibly one of the earliest tetanurans hitherto discovered (Smith et al. 2007; Carrano et al. 2012).

History of Classification

The clade Dinosauria was erected as a tribe (or a sub-order) by Richard Owen in 1842 to contain three taxa of large reptiles, *Megalosaurus*, *Iguanodon*, and *Hylaeosaurus*. Owen (1842) did not include the already named theropods *Poekilopleuron*, *Streptospondylus*, and *Suchosaurus*, all considered to be crocodilian taxa at the time. 'Goniopoda' was the first clade of dinosaurs to gather two valid theropod dinosaurs. This order was erected by Edward Drinker Cope in 1866 to encompass *Laelaps* (now known as *Dryptosaurus*; Brusatte et al. 2011) and 'probably' *Megalosaurus*. 'Goniopoda' was, by then, opposed to the 'Orthopoda' consisting of *Scelidosaurus*, *Hylaeosaurus*, *Iguanodon*, and *Hadrosaurus* (Cope 1866).

Although the taxa 'Goniopoda' and 'Orthopoda' were used in Matthew and Brown's (1922) classification of theropods in the 20th century, these two groups were abandoned in favor of clades coined by Othniel Charles Marsh by the end of the 19th century. Marsh (1881) first erected the taxon Theropoda to contain the family Allosauridae, initially represented by the North American genera *Allosaurus*, *Creosaurus*, and *Labrosaurus*. The term 'Theropoda' derived from the old Greek words θηρίον, *thérion* meaning 'wild beast, animal', and ποδος, *pous*, *podos* meaning 'foot'. Theropods, with 'beast feet' were, at that time, separated from ornithopods, meaning 'bird feet', and sauropods, meaning 'reptiles feet', which were coined by Marsh in 1871 and 1878, respectively. A year after naming the taxon Theropoda, Marsh (1882) already included six 'families' in this clade, namely Megalosauridae, Zanclodontidae, Amphisauridae, Labrosauridae, Coeluridae, and Compsognathidae. A few years later, Seeley (1887) used the orientation and morphology of the pubis to divide the clade of Dinosauria into two major groups, the Saurischia and the Ornithischia. Theropods and sauropodomorphs were grouped among saurischian dinosaurs with reptile-like pelves, whereas ornithischians with bird-like pelves included Stegosauria and Ornithopoda. Ironically, saurischian theropods with beast-like feet and a reptile-like pelvis ultimately give rise to birds, instead of the ornithischians with a bird-like pelvis, and the ornithopods with bird-like feet. By the end of the 19th century, four currently valid theropod clades (Ceratosauridae, Megalosauridae, Compsognathidae, Omithomimidae), two sauropodomorph (Plateosauridae, Anchisauridae) and four unrecognized

archosaur clades (i.e., Labrosauridae, Dryptosauridae, Coeluridae, and Hallopidae) were gathered into Theropoda by Marsh (1895, 1896).

The classification of theropods was markedly affected by the work of German paleontologist Friedrich von Huene (1909, 1914*a*, *b*, 1923, 1926*a*, *b*, 1929*b*, 1932) in the first half of the 20th century. Up until 1932, Huene ignored the name Theropoda and erected two new clades to encompass all saurischian dinosaurs, Coelurosauria and 'Pachypodosauria'. In Huene's earlier classifications, coelurosaurs comprised theropods such as *Coelophysis*, *Ceratosaurus*, *Compsognathus*, *Proceratosaurus*, *Tyrannosaurus*, and *Ornithomimus*, whereas pachypodosaurs included the Carnosauria, consisting of *Megalosaurus*, *Spinosaurus*, and *Allosaurus* (formerly known as *Antrodemus*), as well as the Prosauropoda and the Sauropoda, two clades currently classified as sauropodomorphs. In the 1930s, Huene (1932) modified his view on theropod systematics and abandoned the taxon 'Pachypodosauria'. At that time, saurischian dinosaurs included Coelurosauria, Carnosauria, Prosauropoda, and Sauropoda, and the separation between coelurosaurs and carnosaurs was mostly based on size (Rauhut 2003*a*). Among carnivorous saurischians, coelurosaurs were assigned to relatively small, slenderly built, predaceous theropod clades such as Coelophysidae (formerly known as 'Podokesauridae'), Compsognathidae, and Ornithomimidae, whereas carnosaurs encompassed large, heavily built predators with massive skulls such as Megalosauridae, Spinosauridae, Tyrannosauridae (formerly known as 'Dinodontidae'), and Allosauridae (Huene 1932).

In the beginning of the second half of the 20th century, Alfred Sherwood Romer (1956), in his authoritative book *Osteology of the Reptiles*, proposed a slightly modified version of the saurischian classification. Romer separated saurischian dinosaurs into Theropoda and Sauropoda, and included all bipedal saurischians within theropods, including Prosauropoda, Coelurosauria, and Carnosauria. Romer (1956) adopted the size criteria followed by Huene (1932) and restricted carnosaurs to Teratosauridae (now considered to be a clade of rauisuchian archosaurs; e.g., Benton 1986), Megalosauridae (represented at that time by theropods such as *Ceratosaurus*, *Megalosaurus*, *Spinosaurus*, *Allosaurus*, *Carcharodontosaurus*, and *Proceratosaurus*), and Tyrannosauridae. From the 1960s to the beginning of the 1980s, authors working on theropods, including Walker (1964), Colbert (1964), Colbert and Russell (1969), Ostrom (1976*a*), and Russell (1984) did not deviate significantly from the classification scheme of Romer (1956). Most of them, however, did acknowledge that coelurosaurs and carnosaurs were likely to be grades rather than clades (Thulborn 1984). A few authors like Ostrom (1972), Barsbold (1977), Welles (1984) and Carroll (1988) did abandon the size-based dichotomy between coelurosaurs and carnosaurs, and Barsbold (1977) included newly erected clades such as Oviraptorosauria (with Oviraptoridae), Deinonychosauria (with Dromaeosauridae and Troodontidae, formerly known as 'Saurornithoididae'), and Therizinosauria (formerly known as 'Deinocheirosauria' by Barsbold (1977), then 'Segnosauria' by Barsbold and Perle (1980)) among theropods.

The adoption in the early 1980s of phylogenetic methodology developed by German entomologist Willi Hennig (1950) in the beginning of the second half of the 20th century, was a major step in the history of theropod systematics, and the results of those cladistic analyses radically changed prevailing views on theropod phylogeny. Thulborn (1984) was the first to investigate theropod interrelationships through a cladistic approach by addressing the systematics of *Archaeopteryx* and other stem-group birds. Gauthier's (1986) work on saurischian interrelationships was the first to outline the current phylogenetic classification of non-avian theropods. Based on a cladistic analysis performed on a data matrix of 84 characters, the American paleontologist confirmed the monophyly of dinosaurs and corroborated Seeley's idea that Sauropodomorpha and Theropoda were sister-groups within Saurischia. Gauthier (1986) recovered Theropoda as a well-supported clade divided into Ceratosauria and Tetanurae, and provided the modern phylogenetic definition of theropods as birds and all saurischians closer to birds than to sauropodomorphs. He recognized a dichotomy between Carnosauria and Coelurosauria within tetanuran theropods, and erected the clade Maniraptora to encompass coelurosaurs more derived than Ornithomimidae. At that time, Ceratosauria contained *Coelophysis*, *Dilophosaurus*, and *Ceratosaurus*, carnosaurs included *Allosaurus*, *Acrocanthosaurus* and tyrannosaurids, and non-avian coelurosaurs comprised *Compsognathus*, *Ornitholestes*, and the Ornithomimidae, Caenagnathidae, and Deinonychosauria (Gauthier 1986).

Since the pioneering work of Gauthier (1986), the availability of parsimony-based phylogenetic software has enabled a large number of authors to investigate theropod interrelationships via cladistic analysis, resulting in major revisions in theropod systematics. Novas (1992) was the first to include abelisaurids and tyrannosaurids among ceratosaurs and coelurosaurs, respectively (Rauhut 2003*a*), and Holtz (1994) was the first major phylogenetic analysis that recovered the clade Avetheropoda (erected by Paul 1988 and also known as 'Neotetanurae') to include Allosauridae and Coelurosauria (Fig. 1.4). The same year, Sereno et al. (1994) found that Megalosauroidea (formerly known as 'Torvosauroidea' and 'Spinosauroidea') formed the sister group of Avetheropoda and was divided into Megalosauridae (formerly known as 'Torvosauridae') and Spinosauridae (Fig. 1.4). Two years later, Sereno et al. (1996) found the new clade Allosauroidea (also termed 'Carnosauria' *sensu* Padian et al. 1999), which gathered *Allosaurus*, Sinraptoridae, and Carcharodontosauridae, to be the sister-group of Coelurosauria. Following these preliminary analyses, Sereno's (1997, 1998, 1999) major phylogenetic analyses of dinosaurs proceeded to define major theropod clades such as Neotheropoda, Coelophysoidea, Megalosauroidea, Allosauroidea, Tyrannosauroidea, Ornithomimosauria ('Ornithomimoidea' *sensu* Sereno 1998), Therizinosauroidea, Paraves, and Deinonychosauria (Fig. 1.5).

Subsequent studies on theropod systematics, whose results are summarized by Holtz (1998), Rauhut (2003*a*), Senter (2007), Carrano and Sampson (2008) and Carrano et al. (2012), better resolved the relationships of non-avian theropods and defined additional clades such as Noasauridae (Coria and Salgado 1998), Piatnitzkysauridae (Carrano et al. 2012), Megaraptora (Benson et al. 2010), and

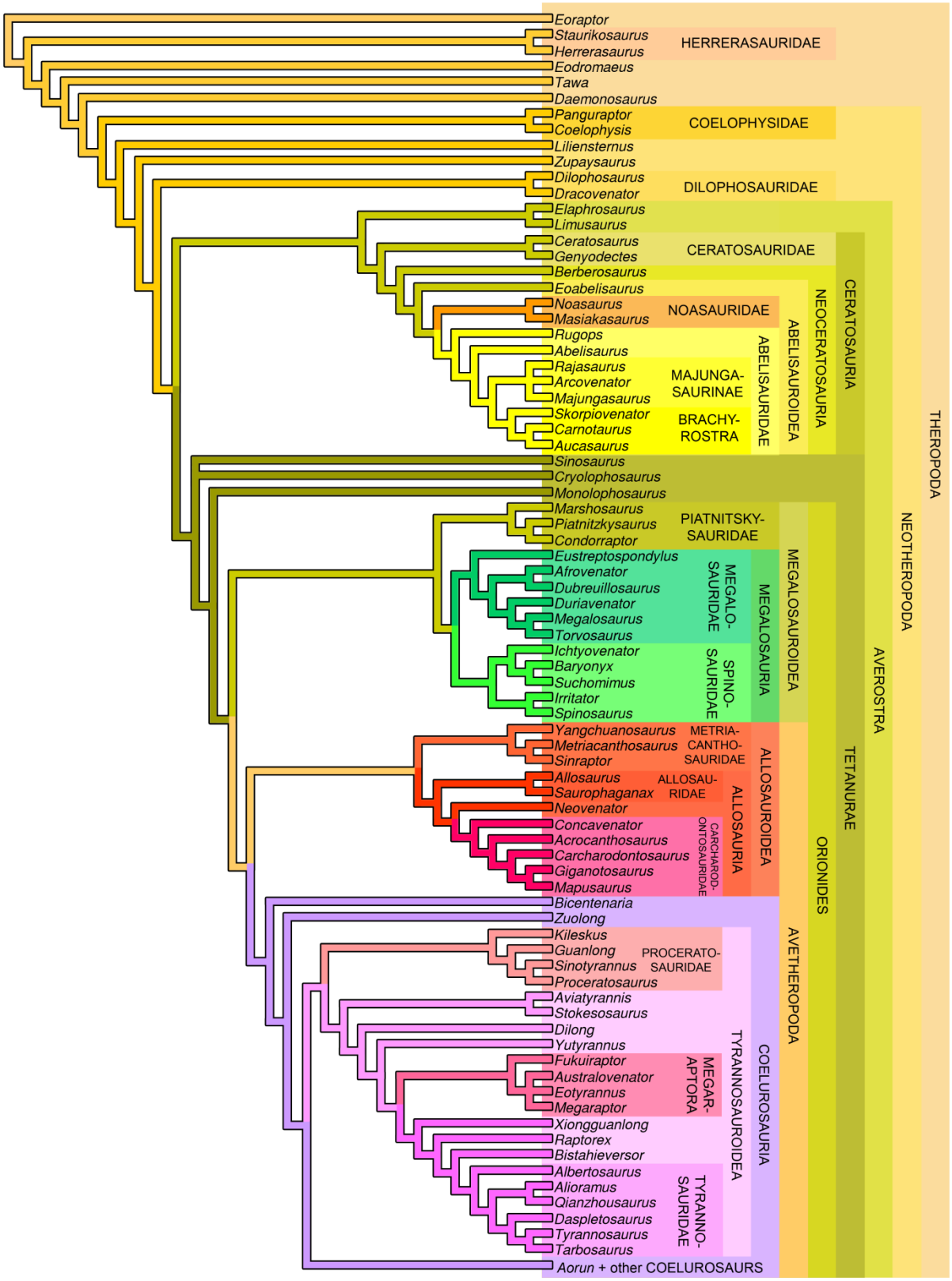

FIGURE 1.4. Cladogram of basal Theropoda showing the relationships of 'non-neocoelurosaur' theropod taxa. The phylogenetic classification follows the results of the cladistic analyses obtained by Sues et al. (2011) for non-neotheropod Theropoda, Smith et al. (2007) and Ezcurra and Brusatte (2011) for non-averostran Neotheropoda, Pol and Rauhut (2012) and Tortosa et al. (2014) for Ceratosauria, Carrano et al. (2012) for non-coelurosaur Tetanurae, Loewen et al. (2013), Lü et al. (2014) and Porfiri et al. (2014) for Tyrannosauroidea, and Choiniere et al. (2014*b*) for basal Coelurosauria.

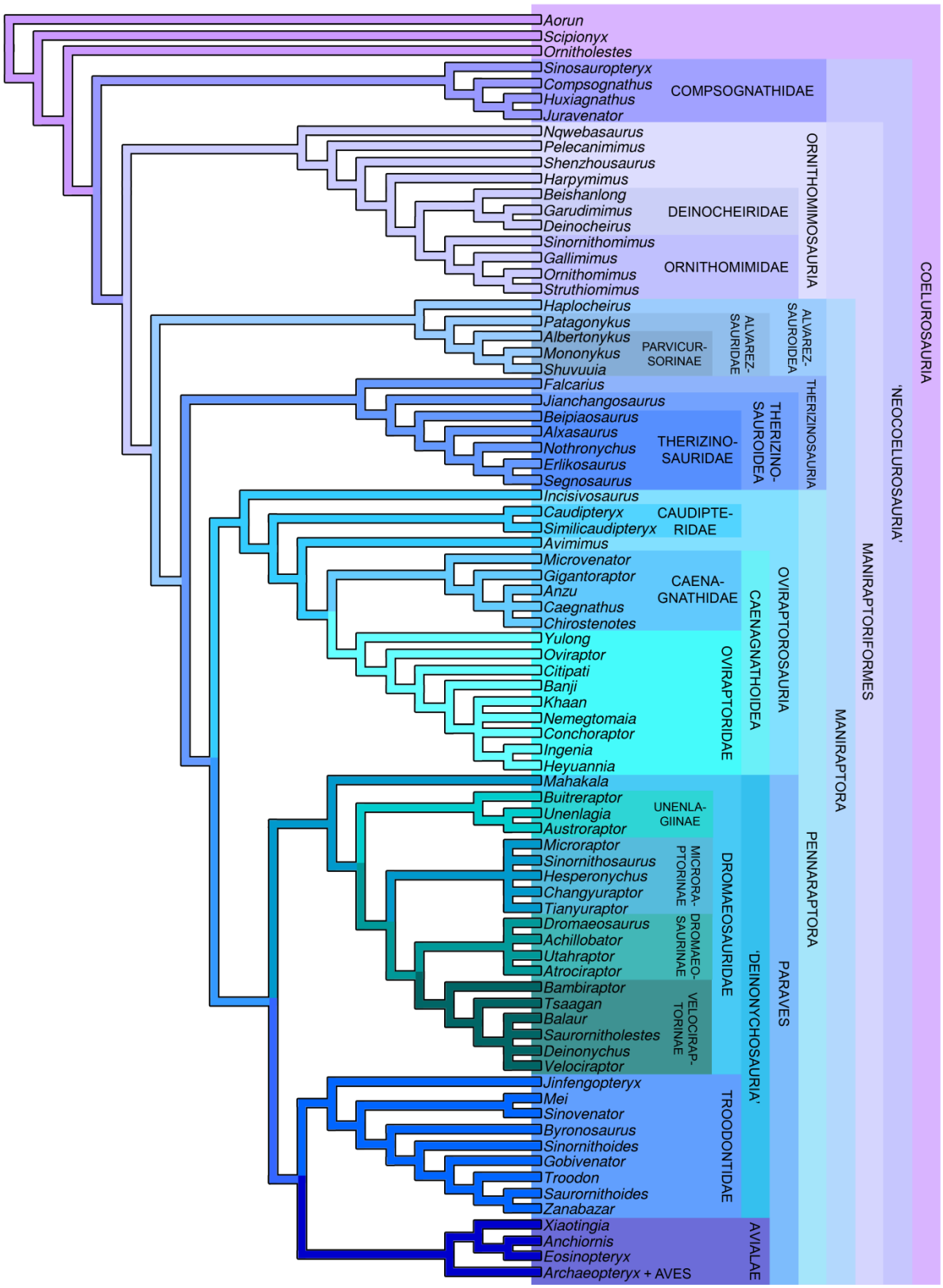

FIGURE 1.5. Cladogram of 'neocoelurosaur' Theropoda showing the relationships of non-tyrannosauroid coelurosaurs. The phylogenetic classification follows the results of the cladistic analyses obtained by Choiniere et al. (2014*b*) for basal Coelurosauria and Compsognathidae, Longrich and Currie (2009*a*) and Choiniere et al. (2010*b*) for Alvarezsauroidea, Lee et al. (2014) for Ornithomimosauria, Senter et al. (2012*a*) and Pu et al. (2013) for Therizinosauria, Lamanna et al. (2014) for Oviraptorosauria, Turner et al. (2012) for Paraves, and Foth et al. (2014) for Avialae.

Proceratosauridae (Rauhut et al. 2010; Figs. 1.4–1.5). In 2015, the current consensus on non-avian theropod classification is based on the results of the most recent large scaled phylogenetic analyses obtained by Sues et al. (2011) for non-neotheropod Theropoda, Smith et al. (2007) and Ezcurra and Brusatte (2011) for non-averostran Neotheropoda, Pol and Rauhut (2012) and Tortosa et al. (2014) for Ceratosauria, Carrano et al. (2012) for non-coelurosaur Tetanurae, Loewen et al. (2013), Lü et al. (2014; which is based on Brusatte et al. (2010*d*) and Porfiri et al. (2014) for Tyrannosauroidea, and Godefroit et al. (2013*a*), Choiniere et al. (2014*b*) and Brusatte et al. (2014*a*; the most updated version of the Theropod Working Group (TWIG) dataset) for non-tyrannosauroid Coelurosauria (Figs. 1.4–1.5).

As noted by Turner et al. (2012), Theropoda is now comprised of numerous well-supported 'family' or 'super-family'-level subclades that form a pectinate, ladder-like organization, with each rung corresponding to a node-based clade that has not always received a name. Although the relationships between most theropod clades are currently well understood, several aspects of theropod systematics remain controversial. Current debate occurs over the phylogenetic placement of *Eoraptor* and/or herrerasaurids within non-theropod saurischians (e.g., Langer and Benton 2006; Alcober and Martinez 2010; Ezcurra 2010; Martinez et al. 2011; Sereno et al. 2013) or at the base of Theropoda (Nesbitt et al. 2009; Ezcurra and Brusatte 2011; Nesbitt 2011; Sues et al. 2011; Langer and Ferigolo 2013; Fig. 4), and over the monophyly or paraphyly of Coelophysoidea (i.e., Coelophysidae + Dilophosauridae; e.g., Tykoski 2005; Yates 2005; Ezcurra and Cuny 2007; Ezcurra and Novas 2007; Smith et al. 2007; Nesbitt et al. 2009; Ezcurra and Brusatte 2011; Xing 2012), as well as Deinonychosauria (i.e., Dromaeosauridae + Troodontidae; e.g., Senter 2011; Turner et al. 2012; Godefroit et al. 2013*a*, *b*; Brusatte et al. 2014*a*; Choiniere et al. 2014*b*; Foth et al. 2014; Tsuihiji et al. 2014). Recent debate also focuses on the position of megaraptorans within neovenatorid allosauroids (Benson et al. 2010; Carrano et al. 2012) or among tyrannosauroid coelurosaurs (Novas et al. 2013; Porfiri et al. 2014; Fig. 1.4).

Origin, evolution, and current classification

First Theropods

Theropoda can be defined as the most inclusive clade containing the house sparrow *Passer domesticus* (Linnaeus 1758) but not the titanosaurid sauropod *Saltasaurus loricatus* Bonaparte and Powell 1980 (Sereno 2005; Table 1.1). Regardless of the status of inclusion of *Eoraptor* and herrerasaurids within Theropoda, the oldest definitive theropod remains come from the mid-Carnian (early Late Triassic; ~231 Ma) of Argentina (Fig. 1.1). Similar in age to *Eoraptor lunensis* (Sereno et al. 2013; Fig. 1.6A) and the herrerasaurids *Herrerasaurus ischigualastensis* (Sereno and Novas 1994; Fig. 1.6B) and *Sanjuansaurus gordilloi* (Alcober and Martinez 2010), the oldest unquestioned theropod taxon *Eodromaeus murphi* (Martinez et al. 2011) is from the Ischigualasto Formation of San

Table 1.1. Phylogenetic definition for non-avian theropod clades up to the 'subfamily'-level. For each taxon, the original author(s) of the first associated name is given in brackets immediately after the name, followed by the author(s) who first created the name without brackets when different. A phylogenetic definition is provided for taxa that have not already been defined phylogenetically.

Taxon	First definitional author	First phylogenetic definition	Definition type	Definition	Definitional author
Abelisauridae Bonaparte and Novas 1985	Novas 1997*b*	*Abelisaurus comahuensis*, *Carnotaurus sastrei*, *Xenotarsosaurus bonapartei*, *Indosaurus matleyi*, *Indosuchus raptorius*, *Majungasaurus crenatissimus* and all descendants of their common ancestor	Stem-based	The most inclusive clade containing *Carnotaurus sastrei* but not *Noasaurus leali*	Wilson et al. 2003
Abelisauroidea (Bonaparte and Novas 1985) Bonaparte 1991*a*	Holtz 1994	Abelisaurids and those members of the *Ceratosaurus*-Abelisauridae clade which shared a more recent common ancestry than with the North American genus [*Ceratosaurus*]	Node-based	The least inclusive clade containing *Carnotaurus sastrei* and *Noasaurus leali*	Sereno 2005
Afrovenatorinae Carrano et al. 2012	Carrano et al. 2012	All megalosaurids more closely related to *Afrovenator* than to *Megalosaurus*	Stem-based	The most inclusive clade containing *Afrovenator abakensis* but not *Megalosaurus bucklandii*	Carrano et al. 2012
Allosauria (Marsh 1878) Paul 1988	/	/	Stem-based	The most inclusive clade containing *Allosaurus fragilis* and *Carcharodontosaurus saharicus* but not *Sinraptor dongi*	New
Allosauridae Marsh 1878	Padian and Hutchinson 1997	*Allosaurus* and all Allosauroidea closer to it than to *Sinraptor*	Stem-based	The most inclusive clade containing *Allosaurus fragilis* but not *Sinraptor dongi*, *Carcharodontosaurus saharicus*, and *Passer domesticus*	Sereno 2005
Allosauroidea (Marsh 1878) Currie and Zhao 1993*a*	Padian and Hutchinson 1997	*Allosaurus* and *Sinraptor* and all descendants of their most recent common ancestor (Node-based definition)	Stem-based	The most inclusive clade containing *Allosaurus fragilis* but not *Passer domesticus*	Sereno 2005
Alvarezsauridae Bonaparte 1991*b*	Sereno 1998	All ornithomimosaurs closer to *Shuvuuia* than to *Ornithomimus* (Stem-based definition)	Node-based	The least inclusive clade containing *Alvarezsaurus calvoi* and *Mononykus olecranus*	Modified from Choiniere et al. 2010*b*
Alvarezsauroidea Bonaparte 1991*b*	Livezey and Zusi 2007	Clade containing *Patagonykus*, *Alvarezsaurus* and *Mononykus*	Stem-based	The most inclusive clade containing *Alvarezsaurus calvoi* but not *Passer domesticus*	Modified from Choiniere et al. 2010*b*
Averostra Paul 2002 (*sensu* Ezcurra 2006)	Paul 2002	[All] ceratosaurs, megalosaurs, and abelisaurs	Node-based	The least inclusive clade containing *Ceratosaurus nasicornis* and *Passer domesticus*	Allain et al. 2012
Avetheropoda Paul 1988	Padian et al. 1999	The most recent common ancestor of Neornithes and *Allosaurus* and all descendants of that ancestor.	Node-based	The least inclusive clade containing *Allosaurus fragilis* and *Passer domesticus*	Modified from Holtz et al. 2004
Avialae Gauthier 1986	Gauthier 1986	Ornithurae plus all extinct maniraptorans that are closer to Ornithurae than they are to Deinonychosauria	Stem-based	The most-inclusive clade containing *Passer domesticus* but not *Dromaeosaurus albertensis* or *Troodon formosus*	Maryańska et al. 2002

Baryonychinae (Charig and Milner 1986) Sereno et al. 1998	Sereno et al. 1998	All spinosaurids that are more closely related to *Baryonyx* than to *Spinosaurus*	Stem-based	The most inclusive clade containing *Baryonyx walkeri* but not *Spinosaurus aegyptiacus*	Holtz et al. 2004
Brachyrostra Canale et al. 2009	Canale et al. 2009	All the abelisaurids more closely related to *Carnotaurus sastrei* than to *Majungasaurus crenatissimus*	Stem-based	The most inclusive clade containing *Carnotaurus sastrei* but not *Majungasaurus crenatissimus*	Modified from Canale et al. 2009
Caenagnathidae Sternberg 1940	Sues 1997	*Caenagnathus pergracilis*, *Chirostenotes elegans*, '*Elmisaurus rarus*', *Caenagnathasia martinsoni*, and the most recent common ancestor of the aforementioned taxa (Node-based definition)	Stem-based	The most inclusive clade containing *Caenagnathus collinsi* but not *Oviraptor philoceratops*	Maryańska et al. 2002
Caenagnathoidea (Sternberg 1940) Sereno 1998	Sereno 1998	*Oviraptor*, *Caenagnathus*, their most recent common ancestor and all descendants	Node-based	The least inclusive clade containing *Oviraptor philoceratops* and *Caenagnathus collinsi*	Modified from Sereno 2005
Carcharodontosauria (Stromer 1931) Benson et al. 2010	Benson et al. 2010	The most inclusive clade comprising *Carcharodontosaurus saharicus* and *Neovenator salerii* but not *Allosaurus fragilis* or *Sinraptor dongi*	Stem-based	The most inclusive clade containing *Carcharodontosaurus saharicus* and *Neovenator salerii* but not *Allosaurus fragilis* or *Sinraptor dongi*	Benson et al. 2010
Carcharodontosauridae Stromer 1931	Sereno 1998	All allosauroids closer to *Carcharodontosaurus* than to either *Allosaurus*, *Monolophosaurus*, *Cryolophosaurus*, or *Sinraptor*	Stem-based	The most inclusive clade containing *Carcharodontosaurus saharicus* but not *Neovenator dongi*, *Allosaurus fragilis* or *Sinraptor dongi*	Benson et al. 2010
Carcharodontosaurinae (Stromer 1931) Carrano et al. 2012	Brusatte and Sereno 2008	The least inclusive clade containing *Carcharodontosaurus saharicus* and *Giganotosaurus carolinii*	Node-based	The least inclusive clade containing *Carcharodontosaurus saharicus* and *Giganotosaurus carolinii*	Brusatte and Sereno 2008
Carnotaurinae Sereno 1998	Sereno 1998	All abelisaurids closer to *Carnotaurus* than to *Abelisaurus*	Stem-based	The most inclusive clade containing *Carnotaurus sastrei* but not *Skorpiovenator bustingorryi*	Modified from Sereno 1998
Caudipteridae Zhou and Wang 2000	/	/	Stem-based	The most inclusive clade containing *Caudipteryx zoui* but not *Oviraptor philoceratops* and *Caenagnathus collinsi*	New
Ceratosauria Marsh 1884*b*	Rowe and Gauthier 1990	The group including *Ceratosaurus nasicornis*, *Dilophosaurus wetherilli*, *Liliensternus liliensterni*, *Coelophysis bauri*, *Syntarsus rhodesiensis*, *Syntarsus kayentakatae*, *Segisaurus halli*, *Sarcosaurus woodi*, and all other taxa stemming from their most recent common ancestor	Stem-based	The most inclusive clade containing *Ceratosaurus nasicornis* but not *Passer domesticus*	Sereno 2005 *sensu* Holtz and Padian 1995
Ceratosauridae Marsh 1884*b*	Rauhut 2004*b*	Clade containing all ceratosaurs that are more closely related to *Ceratosaurus* than to abelisaurids	Stem-based	The most inclusive clade containing *Ceratosaurus nasicornis* but not *Carnotaurus sastrei* and *Noasaurus leali*	Modified from Rauhut 2004*b*
Coelophysidae (Nopcsa 1928) Paul 1988	Sereno 1998	*Coelophysis*, *Procompsognathus*, their most recent common ancestor and all descendants	Node-based	The least inclusive clade containing *Coelophysis bauri* and *Procompsognathus triassicus*	Sereno 1998
Coelophysoidea (Nopcsa 1928) Holtz 1994	Sereno 1998	All ceratosaurs closer to *Coelophysis* than to *Carnotaurus*	Stem-based	The most inclusive clade containing *Coelophysis bauri* but not *Carnotaurus sastrei*, *Ceratosaurus nasicornis*, and *Passer domesticus*	Sereno 2005

Coeluridae Marsh 1881	/	/	Stem-based	The most inclusive clade containing *Coelurus fragilis* but not *Proceratosaurus bradleyi*, *Tyrannosaurus rex*, *Allosaurus fragilis*, *Compsognathus longipes*, *Ornithomimus edmontonicus* and *Deinonychus antirrhopus*	New
Coelurosauria Huene 1914*c*	Gauthier 1986	Birds and all other theropods that are closer to birds than they are to Carnosauria	Stem-based	The most inclusive clade containing *Passer domesticus* but not *Allosaurus fragilis*, *Sinraptor dongi* and *Carcharodontosaurus saharicus*	Sereno 2005
Compsognathidae Cope 1871	Holtz et al. 2004	*Compsognathus longipes* and all taxa sharing a more recent common ancestor with it than with *Passer domesticus*	Stem-based	The most inclusive clade containing *Compsognathus longipes* but not *Passer domesticus*	Holtz et al. 2004
Deinocheiridae Osmólska and Roniewicz 1970	Lee et al. 2014	*Deinocheirus mirificus* and all taxa sharing a more recent common ancestor with it than with *Ornithomimus velox*	Stem-based	The most inclusive clade containing *Deinocheirus mirificus* but not *Ornithomimus velox*	Lee et al. 2014
Deinonychosauria Colbert and Russell 1969	Padian 1997	All maniraptorans closer to *Deinonychus* than to birds (Stem-based definition)	Node-based	The least inclusive clade containing *Troodon formosus* and *Velociraptor mongoliensis* but not *Passer domesticus*	Modified from Sereno 2005
Dilophosauridae (Paul 1988) Charig and Milner 1990	/	/	Stem-based	The most-inclusive clade containing *Dilophosaurus wetherilli* but not *Coelophysis bauri*, *Ceratosaurus nasicornis* and *Passer domesticus*	New
Dromaeosauridae (Matthew and Brown 1922) Colbert and Russell 1969	Sereno 1998	All deinonychosaurs closer to *Velociraptor* than to *Troodon*	Stem-based	The most inclusive clade containing *Dromaeosaurus albertensis* but not *Troodon formosus*, *Ornithomimus edmontonicus*, and *Passer domesticus*	Sereno 2005
Dromaeosaurinae Matthew and Brown 1922	Sereno 1998	All dromaeosaurids closer to *Dromaeosaurus* than to *Velociraptor*	Stem-based	The most inclusive clade containing *Dromaeosaurus albertensis* but not *Velociraptor mongoliensis*, *Microraptor zhaoianus*, *Unenlagia comahuensis* and *Passer domesticus*	Sereno 2005
Eudromaeosauria Longrich and Currie 2009*b*	Turner et al. 2012	The node-based monophyletic group containing the last common ancestor of *Saurornitholestes langstoni*, *Deinonychus antirrhopus*, *Dromaeosaurus albertensis*, and *Velociraptor mongoliensis*, and all its descendants	Node-based	The least inclusive clade containing *Saurornitholestes langstoni*, *Deinonychus antirrhopus*, *Dromaeosaurus albertensis*, and *Velociraptor mongoliensis*	Modified from Turner et al. 2012
Herrerasauridae Benedetto 1973	Novas 1992	*Herrerasaurus* and *Staurikosaurus* and their most recent common ancestor	Stem-based	The most inclusive clade containing *Herrerasaurus ischigualastensis* but not *Passer domesticus*	Sereno 2005
Jinfengopteryginae Turner et al. 2012	Turner et al. 2012	A stem-based monophyletic group containing *Jinfengopteryx elegans*, and all coelurosaurs closer to it than to *Troodon formosus*, *Passer domesticus*, and *Sinovenator changii*	Stem-based	The most inclusive clade containing *Jinfengopteryx elegans* but not *Troodon formosus*, *Sinovenator changii* and *Passer domesticus*	Modified from Turner et al. 2012
Majungasaurinae Tortosa et al. 2014	Tortosa et al. 2014	All the abelisaurids more closely related to *Majungasaurus crenatissimus* than to *Carnotaurus sastrei*	Stem-based	The most inclusive clade containing *Majungasaurus crenatissimus* but not *Carnotaurus sastrei*	Modified from Tortosa et al. 2014
Maniraptora Gauthier 1986	Gauthier	All coelurosaurs that are closer to birds than they are	Stem-	The most-inclusive clade containing *Passer*	Maryańska et

	1986	to Ornithomimidae	based	*domesticus* but not *Ornithomimus velox*	al. 2002
Maniraptoriformes Holtz 1995	Holtz 1996	The most recent common ancestor of *Ornithomimus* and birds (i.e., The most recent common ancestor of Arctometatarsalia and Maniraptora), and all descendants of that common ancestor	Node-based	The least-inclusive clade containing *Passer domesticus* and *Ornithomimus velox*	Maryańska et al. 2002
Megalosauria (Fitzinger 1843) Bonaparte 1850	Allain et al. 2012	The most inclusive clade containing *Spinosaurus aegyptiacus* and *Torvosaurus tanneri* but not *Allosaurus fragilis*, and *Passer domesticus* (Stem-based definition)	Node-based	The least inclusive clade containing *Megalosaurus bucklandii* and *Spinosaurus aegyptiacus*	Modified from Allain et al. 2012
Megalosauridae (Fitzinger 1843) Bonaparte 1850	Allain 2002	*Poekilopleuron*? *valesdunensis*, *Torvosaurus* and *Afrovenator*, and all descendants of their common ancestor (node-based definition)	Stem-based	The most inclusive clade containing *Megalosaurus bucklandii* but not *Allosaurus fragilis*, *Spinosaurus aegyptiacus*, and *Passer domesticus*	Holtz et al. 2004
Megalosaurinae (Fitzinger 1843) Carrano et al. 2012	Carrano et al. 2012	All megalosaurids closer to *Megalosaurus* than to *Afrovenator*	Stem-based	The most inclusive clade containing *Megalosaurus bucklandii* but not *Afrovenator abakensis*	Carrano et al. 2012
Megalosauroidea (Fitzinger 1843) Walker 1964	Sereno 1998	*Spinosaurus*, *Torvosaurus*, their most recent common ancestor and all descendants (Definition given to Spinosauroidea)	Stem-based	The most inclusive clade containing *Megalosaurus bucklandii* but not *Passer domesticus*	Modified from Holtz et al. 2004
Megaraptora Benson et al. 2010	Benson et al. 2010	The most inclusive clade comprising *Megaraptor namunhuaiquii* but not *Chilantaisaurus tashuikouensis*, *Neovenator salerii*, *Carcharodontosaurus saharicus* or *Allosaurus fragilis*	Stem-based	The most inclusive clade containing *Megaraptor namunhuaiquii* but not *Chilantaisaurus tashuikouensis*, *Neovenator salerii*, *Carcharodontosaurus saharicus* or *Allosaurus fragilis*	Benson et al. 2010
Megaraptoridae (Benson et al. 2010) Novas et al. 2013	Novas et al. 2013	A stem based clade including all theropods closer to *Megaraptor namunhuaiquii* than to *Fukuiraptor kitadaniensis*, *Chilantaisaurus tashuikouensis*, *Neovenator salerii*, *Carcharodontosaurus saharicus*, *Allosaurus fragilis*, *Baryonyx walkeri*, *Tyrannosaurus rex*, and *Passer domesticus*	Stem-based	The most inclusive clade containing *Megaraptor namunhuaiquii* but not *Fukuiraptor kitadaniensis*, *Chilantaisaurus tashuikouensis*, *Neovenator salerii*, *Carcharodontosaurus saharicus*, *Allosaurus fragilis*, *Baryonyx walkeri*, *Tyrannosaurus rex*, and *Passer domesticus*	Modified from Novas et al. 2013
Metriacanthosauridae Paul 1988	Padian and Hutchinson 1997	*Sinraptor* and all Allosauroidea closer to it than to *Allosaurus* (Definition given to Sinraptoridae)	Stem-based	The most inclusive clade containing *Metriacanthosaurus parkeri* but not *Allosaurus fragilis*, *Carcharodontosaurus saharicus*, or *Passer domesticus*	Modified from Sereno 2005
Metriacanthosaurinae (Paul 1988) Carrano et al. 2012	Carrano et al. 2012	All metriacanthosaurids more closely related to *Metriacanthosaurus* than to *Yangchuanosaurus*	Stem-based	The most inclusive clade containing *Metriacanthosaurus parkeri* but not *Yangchuanosaurus shangyouensis*	Modified from Carrano et al. 2012
Microraptorinae Senter et al. 2004	Sereno 2005	The most inclusive clade containing Microraptor zhaoianus but not *Dromaeosaurus albertensis*, *Velociraptor mongoliensis*, *Unenlagia comahuensis*, *Passer domesticus*	Stem-based	The most inclusive clade containing *Microraptor zhaoianus* but not *Dromaeosaurus albertensis*, *Velociraptor mongoliensis*, *Unenlagia comahuensis*, and *Passer domesticus*	Sereno 2005
Mononykinae Chiappe et al. 1998	Chiappe et al. 1998	The common ancestor of *Mononykus*, *Shuvuuia*, and *Parvicursor*, plus all their descendants	Node-based	The least inclusive clade containing *Mononykus olecranus* and *Shuvuuia deserti*	Sereno 2005

Neoceratosauria Novas 1991	Holtz 1994	The most recent common ancestor of *Ceratosaurus* and Abelisauridae and all of its descendants	Node-based	The least inclusive clade containing *Ceratosaurus nasicornis* and *Carnotaurus sastrei*	Modified from Holtz 1994
Neotheropoda Bakker 1986	Sereno 1998	*Coelophysis*, Neornithes, their most recent common ancestor and all descendants	Node-based	The least inclusive clade containing *Coelophysis bauri* and *Passer domesticus*	Sereno 2005
Neovenatoridae Benson et al. 2010	Benson et al. 2010	The most inclusive clade comprising *Neovenator salerii* but not *Carcharodontosaurus saharicus*, *Allosaurus fragilis* or *Sinraptor dongi*	Stem-based	The most inclusive clade containing *Neovenator salerii* but not *Carcharodontosaurus saharicus*, *Allosaurus fragilis* or *Sinraptor dongi*	Benson et al. 2010
Noasauridae Bonaparte and Powell 1980	Wilson et al. 2003	The most inclusive clade containing *Noasaurus leali* but not *Carnotaurus sastrei*	Stem-based	The most inclusive clade containing *Noasaurus leali* but not *Carnotaurus sastrei*	Wilson et al. 2003
Orionides Carrano et al. 2012	Carrano et al. 2012	Megalosauroidea, Avetheropoda, their most recent common ancestor, and all its descendants	Node-based	The least-inclusive clade containing *Megalosaurus bucklandii*, *Allosaurus fragilis* and *Passer domesticus*	Modified from Carrano et al. 2012
Ornithomimidae Marsh 1890	Sereno 1998	All ornithomimosaurs closer to *Ornithomimus* than to *Erlikosaurus*	Stem-based	The most inclusive clade containing *Ornithomimus velox* but not *Deinocheirus mirificus*	Lee et al. 2014
Ornithomimosauria (Marsh 1890) Barsbold 1976*a*	Osmólska 1997	All bullatosaurs closer to *Ornithomimus* than to *Troodon*	Stem-based	The most inclusive clade containing *Ornithomimus velox* but not *Allosaurus fragilis*, *Tyrannosaurus rex*, *Compsognathus longipes*, *Alvarezsaurus calvoi*, *Therizinosaurus cheloniformis*, *Deinonychus antirrhopus*, *Troodon formosus*, and *Passer domesticus*	Lee et al. 2014
Oviraptoridae Barsbold 1976*b*	Sereno 1998	All oviraptorosaurs closer to *Oviraptor* than to *Caenagnathus*	Stem-based	The most inclusive clade containing *Oviraptor philoceratops* but not *Caenagnathus collinsi*	Maryańska et al. 2002
Oviraptorinae (Barsbold 1976*b*) (Barsbold 1981)	Osmólska et al. 2004	*Oviraptor philoceratops*, *Citipati osmolskae*, their most recent common ancestor, and all descendants.	Node-based	The least inclusive clade containing *Oviraptor philoceratops* and *Citipati osmolskae*	Osmólska et al. 2004
Oviraptorosauria Barsbold 1976*a*	Barsbold 1997	Oviraptoridae and all taxa closer to *Oviraptor* than to birds	Stem-based	The most-inclusive clade containing *Oviraptor philoceratops* but not *Passer domesticus*	Maryańska et al. 2002
Paraves Sereno 1997	Sereno 1998	All maniraptorans closer to Neornithes than to *Oviraptor*	Stem-based	The most inclusive clade containing *Passer domesticus* but not *Oviraptor philoceratops*	Holtz and Osmólska 2004
Parvicursorinae Karhu and Rautian 1996	Choiniere et al. 2010*b*	The least inclusive clade containing *Parvicursor*, *Mononykus* and their most recent common ancestor (Node-based definition)	Stem-based	The most inclusive clade containing *Parvicursor remotus* but not *Patagonykus puertai*	Xu et al. 2011*b*
Pennaraptora Foth et al. 2014	Foth et al. 2014	Clade including Oviraptor philoceratops, *Deinonychus antirrhopus* and *Passer domesticus* and all descendants of their most recent common ancestor	Node-based	The least inclusive clade containing *Oviraptor philoceratops*, *Deinonychus antirrhopus* and *Passer domesticus*	Foth et al. 2014
Piatnitzkysauridae Carrano et al. 2012	Carrano et al. 2012	All megalosauroids more closely related to *Piatnitzkysaurus* than to either *Spinosaurus* or *Megalosaurus*	Stem-based	The most inclusive clade containing *Piatnitzkysaurus floresi* but not *Spinosaurus aegyptiacus* and *Megalosaurus bucklandii*	Carrano et al. 2012
Proceratosauridae Rauhut et al. 2010	Rauhut et al. 2010	All theropods that are more closely related to *Proceratosaurus* than to *Tyrannosaurus*, *Allosaurus*, *Compsognathus*, *Coelurus*, *Ornithomimus*, or *Deinonychus*	Stem-based	The most inclusive clade containing *Proceratosaurus bradleyi* but not *Tyrannosaurus rex*, *Allosaurus fragilis*, *Compsognathus longipes*, *Coelurus fragilis*, *Ornithomimus edmontonicus* and *Deinonychus antirrhopus*	Rauhut et al. 2010

Scansoriopterygidae Czerkas and Yuan 2002	Zhang et al. 2008	The least-inclusive clade containing *Epidendrosaurus ningchengensis* and *Epidexipteryx hui*	Node-based	The least-inclusive clade containing *Epidendrosaurus ningchengensis* and *Epidexipteryx hui*	Zhang et al. 2008
Spinosauridae Stromer 1915	Sereno 1998	All spinosauroids closer to *Spinosaurus* than to *Torvosaurus*	Stem-based	The most inclusive clade containing *Spinosaurus aegyptiacus* but not *Torvosaurus tanneri*, *Allosaurus fragilis*, and *Passer domesticus*	Sereno 2005
Spinosaurinae (Stromer 1915) Sereno et al. 1998	Holtz et al. 2004	*Spinosaurus aegyptiacus* and all taxa sharing a more recent common ancestor with it than with *Baryonyx walkeri*	Stem-based	The most inclusive clade containing *Spinosaurus aegyptiacus* but not *Baryonyx walkeri*	Holtz et al. 2004
Tetanurae Gauthier 1986	Gauthier 1986	Birds and all other theropods closer to birds than they are to Ceratosauria	Stem-based	The most inclusive clade containing *Passer domesticus* but not *Ceratosaurus nasicornis*	Allain et al. 2012
Therizinosauria (Maleev 1954) Russell 1997	Russell 1997	*Alxasaurus*, *Enigmosaurus*, *Erlikosaurus*, *Nanshiungosaurus*, *Segnosaurus*, *Therizinosaurus* and all others closer to them than to oviraptorosaurs, ornithomimids, and troodontids	Stem-based	The most inclusive clade containing *Therizinosaurus cheloniformis* but not *Tyrannosaurus rex*, *Ornithomimus edmontonicus*, *Mononykus olecranus*, *Oviraptor philoceratops* or *Troodon formosus*	Zanno 2010*b*
Therizinosauridae Maleev 1954	Sereno 1998	All ornithomimosaurs closer to *Erlikosaurus* than to *Ornithomimus* (Stem based definition)	Node-based	The least inclusive clade containing *Nothronychus graffami*, *Segnosaurus galbinensis*, *Erlikosaurus andrewsi* and *Therizinosaurus cheloniformis*	Modified from Zanno et al. 2009
Therizinosauroidea (Maleev 1954) Russell and Dong 1993	Zhang et al. 2001	All coelurosaurs closer to Therizinosaurus than to either *Ornithomimus*, *Oviraptor*, *Velociraptor*, or Neornithes (Stem based definition)	Node-based	The least inclusive clade containing *Beipiaosaurus inexpectus* and *Therizinosaurus cheloniformis*	Clark et al. 2004
Theropoda Marsh 1881	Gauthier 1986	Birds and all saurischians that are closer to birds than they are to sauropodomorphs	Stem-based	The most inclusive clade containing *Passer domesticus* but not *Saltasaurus loricatus*	Sereno 2005
Troodontidae Gilmore 1924	Varricchio 1997	*Troodon*, *Sinornithoides*, *Saurornithoides*, *Borogovia*, and all coelurosaurs closer to them than to ornithomimids, oviraptorosaurs, or other well-defined taxa	Stem-based	The most inclusive clade containing *Troodon formosus* but not *Velociraptor mongoliensis*, *Ornithomimus edmontonicus*, and *Passer domesticus*	Sereno 2005
Tyrannosauridae Osborn 1906	Holtz 2001	All descendants of the most recent common ancestor of *Tyrannosaurus* and *Aublysodon*	Node-based	The least inclusive clade containing *Tyrannosaurus rex*, *Gorgosaurus libratus* and *Albertosaurus sarcophagus*	Sereno 2005
Tyrannosaurinae (Osborn 1906) Matthew and Brown 1922	Sereno 1998	All tyrannosaurids closer to *Tyrannosaurus* than to either *Albertosaurus*, *Daspletosaurus*, or *Gorgosaurus*	Stem-based	The most inclusive clade containing *Tyrannosaurus rex* but not *Gorgosaurus libratus* and *Albertosaurus sarcophagus*	Sereno 2005
Tyrannosauroidea (Osborn 1906) Walker 1964	Sereno 1998	All maniraptorans closer to *Tyrannosaurus* than to Neornithes	Stem-based	The most inclusive clade containing *Tyrannosaurus rex* but not *Ornithomimus edmontonicus*, *Troodon formosus*, or *Velociraptor mongoliensis*	Sereno 2005
Unenlagiinae Bonaparte 1999	Makovicky et al. 2005	All taxa closer to *Unenlagia comahuensis* than to *Velociraptor mongoliensis*	Stem-based	The most inclusive clade containing *Unenlagia comahuensis* but not *Velociraptor mongoliensis*, *Dromaeosaurus albertensis*, *Microraptor zhaoianus* and *Passer domesticus*	Sereno 2005

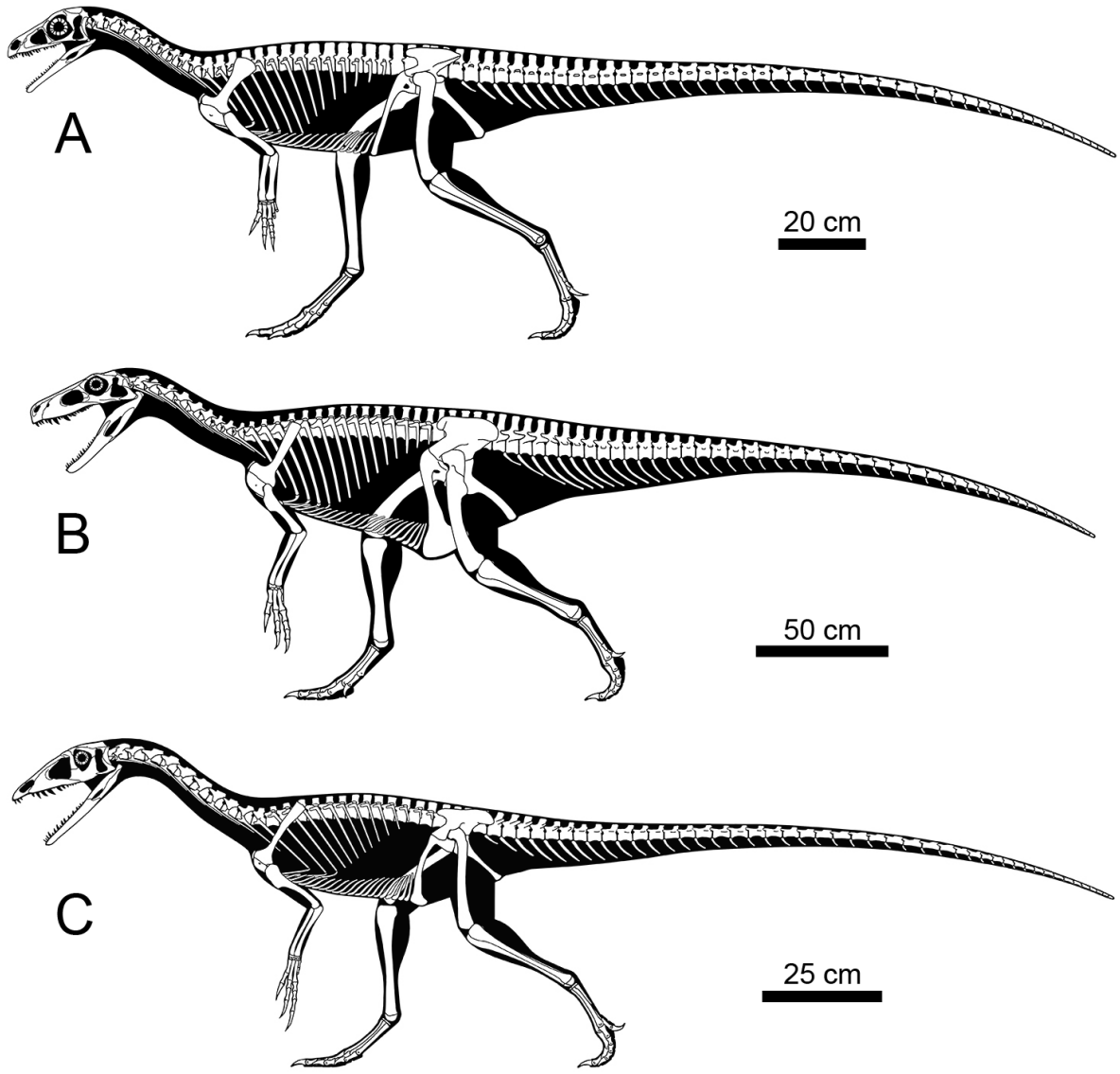

FIGURE 1.6. Skeletal reconstructions of three non-neotheropod saurischians (and possibly three basalmost theropods). **A**, the possible primitive sauropodomorph *Eoraptor lunensis*; **B**, the herrerasaurid *Herrerasaurus ischigualastensis*; and **C**, the very basal theropod *Tawa hallae*. Reconstructions by Scott Hartman.

Juan Province. *Eodromaeus*, *Eoraptor* and herrerasaurids were small to large sized (1-6m long; Sereno and Novas 1992) bipedal saurischians with relatively elongated skulls. These primitive saurischians retained the ancestral dinosauromorph habit of obligate bipedality and the ziphodont dentition present in more primitive archosauriforms (Holtz et al. 1998; Barrett et al. 2010; Holtz 2012), leading to their consideration as carnivorous dinosaurs. Nevertheless, *Eoraptor*, recently interpreted to be a basal sauropodomorph (Martinez et al. 2011; Sereno et al. 2013), exhibits constricted crowns and pointed denticles that suggest that this primitive saurischian, as well as the first dinosaurs, might have been omnivorous (Barrett et al. 2010; Langer et al. 2010; Sereno et al. 2013).

Tawa hallae (Nesbitt et al. 2009; Fig. 1.6C) and *Daemonosaurus chauliodus* (Sues et al. 2011) from the Norian and possibly Rhaetian of New Mexico, respectively, are currently recovered between *Eodromaeus* and neotheropods (Fig. 1.4). Unlike *Eoraptor*, these two recently reported taxa possess

the short subnarial gap present in basal neotheropods and an antorbital fossa restricted to the vicinity of the antorbital fenestra, as seen in *Herrerasaurus* (Nesbitt et al. 2009; Sues et al. 2011; Langer 2014). This condition contrasts with the expanded antorbital fossa of *Eoraptor* and *Eodromaeus*. *Daemonosaurus* is unique in having a short and tall skull filled with procumbent premaxillary and dentary teeth (Sues et al. 2011). *Tawa* is closer to coelophysoids than *Daemonosaurus* and other primitive theropods in having an elongated snout and a more gracile body. *Tawa* shares with *Daemonosaurus* greatly enlarged maxillary teeth as well as pneumatic fossae (pleurocoels) in the cervical vertebrae (Nesbitt et al. 2009; Sues et al. 2011).

Coelophysoidea and Dilophosauridae

Neotheropoda (Bakker 1986), the least inclusive clade containing *Coelophysis bauri* (Cope 1889) and *Passer domesticus* (Linnaeus 1758) (Sereno 2005), currently comprises theropods more derived than *Tawa* (Nesbitt et al. 2009; Nesbitt 2011; Sues et al. 2011). Among their derived features, neotheropods are characterized by an intramandibular joint, a hinge between the dentary and the postdentary bones (Holtz 2012). Current consensus on basal theropod phylogeny suggests neotheropods encompass a basal clade that can be referred to Coelophysoidea and a slightly more derived clade named Dilophosauridae (*sensu* Charig and Milner 1990; Fig. 1.4; the clade Dilophosauridae is here defined phylogenetically for the first time, see Table 1.1). *Dilophosaurus* is thought to belong to Coelophysoidea by some authors (e.g., Carrano et al. 2005; Tykoski 2005; Ezcurra and Cuny 2007; Ezcurra and Novas 2007; Xing 2012). However, results of more recent and/or larger scale analyses recover Dilophosauridae as a more derived clade of neotheropods, and the sister-group of Averostra (e.g., Smith et al. 2007; Nesbitt et al. 2009; Ezcurra and Brusatte 2011; Sues et al. 2011; Ezcurra 2012). Consequently, though the phylogenetic relationships of dilophosaurids remains unresolved, these basal theropods seem to be more derived than coelophysoids.

Coelophysoidea (*sensu* Sereno 2005; Table 1.1) encompasses small to medium sized theropods (2-6m long) with slender skulls, and lightly built, gracile, and elongated bodies characterized by elongated cervical centra (Tykoski and Rowe 2004; Brusatte et al. 2010*c*; Holtz 2012). The first coelophysoids are already present in the Norian of Europe (*Procompsognathus triassicus*, *Camposaurus arizonensis*; Sereno and Wild 1992; Rauhut and Hungerbühler 1998; Ezcurra and Brusatte 2011) and North America (*Coelophysis bauri*; Colbert 1989; Fig. 1.7A). Although coelophysoids form the first radiation of neotheropods, they were not apex terrestrial predators in the Late Triassic, as pseudosuchian carnivores such as rauisuchians and phytosaurs were larger and more abundant at that time (Brusatte et al. 2010*c*; Holtz 2012). Unlike most large pseudosuchian archosaurs, coelophysoids survived the Triassic/Jurassic boundary, and Jurassic coelophysoids are known from the Hettangian–Pliensbachian of China (*Panguraptor lufengensis*; You et al. 2014), South Africa (*Coelophysis rhodesiensis*; Raath 1969, 1977; Bristowe and Raath 2004), and North America (*Coelophysis kayentakatae*; Rowe 1989; n.b., this taxon was originally coined '*Syntarsus*' by

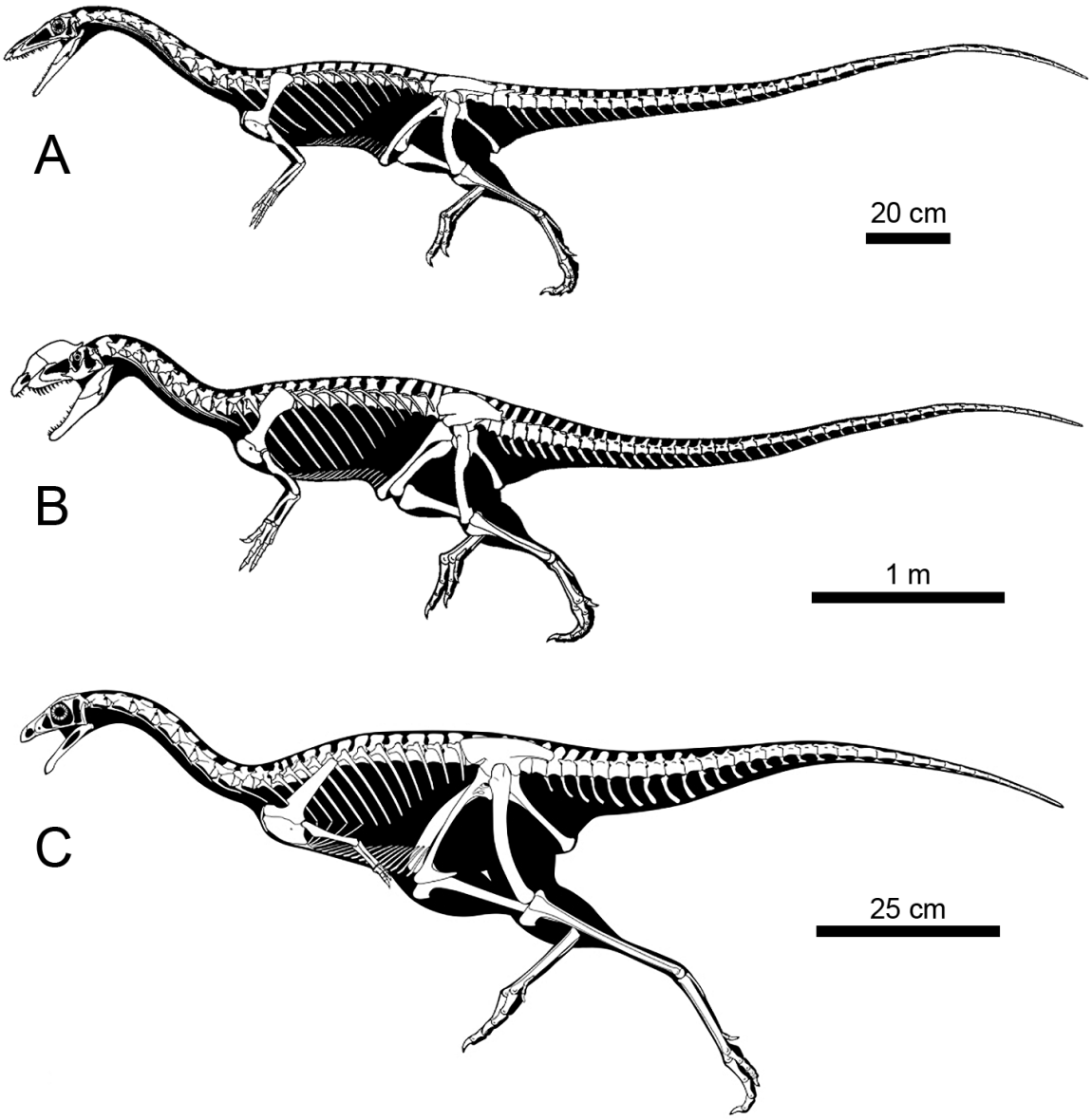

FIGURE 1.7. Skeletal reconstructions of two non-averostran neotheropod and one basal ceratosaurs. **A**, the coelophysoid *Coelophysis bauri*; **B**, the dilophosaurid *Dilophosaurus wetherilli*; and **C**, the 'elaphrosaurid' *Limusaurus inextricabilis*. Reconstructions by Gregory Paul for *Coelophysis* and *Dilophosaurus* (modified), and Ville Sinkkonen for *Limusaurus* (modified).

Rowe (1989); it is also referred as *Megapnosaurus* by some authors as the genus name '*Syntarsus*' was preoccupied by a beetle, and the entomologists Ivie et al. (2001) replaced it with *Megapnosaurus*; '*Syntarsus*' is thought to be a junior synonym of *Coelophysis* by many authors such as Downs (2000), Bristowe and Raath (2004) and Carrano et al. (2012)). *Zupaysaurus rougieri* (Arcucci and Coria 2003; Ezcurra 2007) and *Liliensternus liliensterni* (Huene 1934) from the Norian of Argentina and Germany, respectively, are either classified as coelophysoids (e.g., You et al. 2014) or recovered as more derived neotheropods positioned between Coelophysoidea and Dilophosauridae (Nesbitt et al. 2009; Ezcurra and Brusatte 2011; Sues et al. 2011; Ezcurra 2012; Fig. 1.4).

Dilophosauridae is a poorly supported clade that may contain medium to large sized (4-7m long) theropods, such as *Dilophosaurus wetherilli* (Welles 19841; Fig. 1.7B) and *Dracovenator regenti* (Yates 2005) from the Early Jurassic of North America and South Africa, respectively. Similar to coelophysoids, these two taxa possess a subnarial gap and anteriormost maxillary teeth facing anteroventrally, yet they share with averostrans a promaxillary fenestra and a reduced number of maxillary teeth (Holtz 2012). The clade has been recovered by some authors (Yates 2005; Smith et al. 2007; Xu et al. 2009*b*); however, an over-atomization of cranial crest characters may have been leading phylogenetic analyses to artificially find such dilophosaurid clade (Brusatte et al. 2010*a*). In fact, '*Dilophosaurus*' *sinensis* (Hu 1993), considered to be a junior synonym of *Sinosaurus triassicus* (Dong 2003; Xing et al. 2013*a*, 2014), and *Cryolophosaurus ellioti* (Smith et al. 2007) from the Early Jurassic of China and Antarctica, respectively, were formerly interpreted as dilophosaurid taxa and are now classified among basal tetanurans (Benson 2010*a*; Brusatte et al. 2010*a*; Carrano et al. 2012; Xing 2012). The cranial crest of *Dilophosaurus*, *Cryolophosaurus*, and '*Dilophosaurus*' *sinensis* was convergently acquired in these taxa and evolved independently in dilophosaurids and basal tetanurans (Brusatte et al. 2010*a*; Xing 2012), or was a derived feature present in the common ancestor of dilophosaurids and basal averostrans. Although relatively common and diverse entering the Jurassic, coelophysoids and dilophosaurids became extinct at or near the end of Early Jurassic (Carrano and Sampson 2004; Ezcurra and Novas 2007; Langer et al. 2010).

Ceratosauria

Averostra (Paul 2002), the least inclusive clade containing *Ceratosaurus nasicornis* Marsh 1884*a* and *Passer domesticus* (Linnaeus 1758) (Allain et al. 2012; Table 1.1), radiated into two main clades, Ceratosauria and Tetanurae (Fig. 1.4). Basal averostrans are characterized by the oreinirostral condition of their head, defined as a transversally narrow and dorsoventrally high skull (Holtz 2012). According to Carrano et al. (2012), the derived features shared by averostrans include a reduced prefrontal which remains unfused to the postorbital in adults, the moderate size of the acromion process of the scapula, a ridge-like medial epicondyle on the femur, an interpubic fenestra, the subtriangular morphology of the distal end of the ischium, and a centrally positioned fibular fossa on the medial surface of the fibula. The first averostrans are known from the Early Jurassic and are distributed widely across the globe with remains found in China ('*Dilophosaurus*' *sinensis*; Hu 1993), Antarctica (*Cryolophosaurus ellioti*; Smith et al. 2007), Africa (*Berberosaurus liassicus*; Allain et al. 2007), South America (*Tachiraptor admirabilis*; Langer et al. 2014), and possibly Europe ('*Saltriosaurus*'; Dal Sasso 2003; Benson 2010*a*). Ceratosaurs currently include a basal clade informally referred to as 'elaphrosaurs', a more derived family named Ceratosauridae, and a major clade known as the Abelisauroidea (Wilson et al. 2003; Sereno et al. 2004; Carrano and Sampson 2008; Pol and Rauhut 2012; Tortosa et al. 2014). 'Elaphrosaurs' are a poorly known group of primitive ceratosaurs including *Elaphrosaurus bambergi* from the Kimmeridgian–Tithonian of

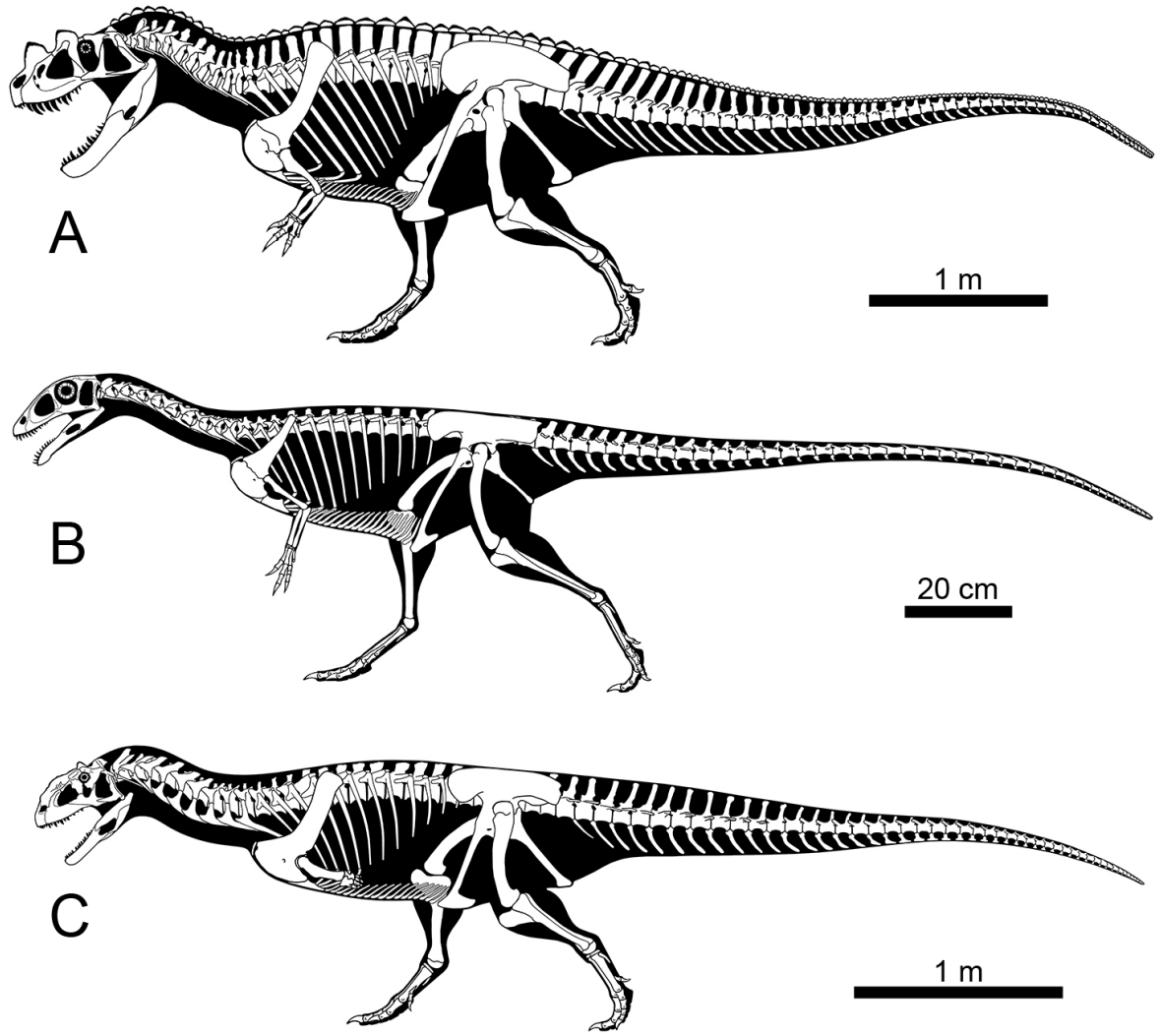

FIGURE 1.8. Skeletal reconstructions of three ceratosaurs. **A**, the ceratosaurid *Ceratosaurus nasicornis*; **B**, the noasaurid *Masiakasaurus knopfleri*; **C**, the abelisaurid *Majungasaurus crenatissimus*. Reconstructions by Scott Hartman.

Tendaguru (Carrano and Sampson 2008), *Limusaurus inextricabilis* from the Oxfordian of China (Xu et al. 2009*b*; Fig. 1.7C), and *Spinostropheus gauthieri* from the Middle Jurassic of Niger (Carrano and Sampson 2008; Rauhut and López-Arbarello 2009; Remes et al. 2009). The 'elaphrosaur' clade was retrieved in all recent cladistic analyses on ceratosaurs (Xu et al. 2009*b*; Pol and Rauhut 2012; Farke and Sertich 2013; Tortosa et al. 2014) and always gathers the taxa *Elaphrosaurus* and *Limusaurus*. The latter is the only 'elaphrosaur' known from cranial material and the only non-maniraptoriform theropod to possess an edentulous skull convergent with that of ornithomimids (Fig. 1.7C). Although recovered as 'elaphrosaurs' in all recent large scaled cladistic analyses on ceratosaurs (Pol and Rauhut 2012; Tortosa et al. 2014), *Elaphrosaurus* and *Limusaurus* have also been suggested to belong to Noasauridae (Canale et al. 2009; Stiegler et al. 2014).

Ceratosauridae only contains two taxa, the eponymous *Ceratosaurus* from the Kimmeridgian–Tithonian of North America (*C. nasicornis*; Gilmore 1920; Madsen and Welles 2000; Carrano and

Sampson 2008; Fig. 1.8A) and Europe (*Ceratosaurus* sp.; Mateus and Antunes 2000; Malafaia et al. 2014), and *Genyodectes serus* from the Aptian–Albian of Argentina (Rauhut 2004*b*). Ceratosaurids were large theropods (6-8m long) characterized by strongly elongated maxillary teeth longer than the dentary height, and at least *Ceratosaurus* showed a fused nasal horn, two lacrimal horns, and osteoderms on the dorsal midline of the animal (Marsh 1884*a*; Gilmore 1920; Madsen and Welles 2000; Rauhut 2004*b*). Along with megalosaurids and allosaurids, ceratosaurids were apex predators in the Late Jurassic (Kimmeridgian–Tithonian) ecosystems of Europe, North America, and possibly South America and Africa (Henderson 1998; Bakker and Bir 2004; Soto and Perea 2008; Rauhut 2011).

Abelisauroidea falls into two divergent subclades, the Noasauridae and Abelisauridae (Wilson et al. 2003; Sereno et al. 2004; Carrano and Sampson 2008; Pol and Rauhut 2012; Tortosa et al. 2014; Fig. 1.4). Noasaurids form a relatively poorly known group of small, slender abelisauroids with forelimbs bearing well-developed claws (Bonaparte 1991*a*; Carrano and Sampson 2008; Agnolín and Chiarelli 2010; Carrano et al. 2011). They are only known from the Cretaceous and may have already been present in the Barremian–early Aptian of Argentina (*Ligabueino andesi*; Bonaparte 1996; Carrano and Sampson 2008). Noasaurids are well-known in the latest part of the Cretaceous of Gondwana, having been unearthed in Santonian–Maastrichtian deposits in Argentina (*Noasaurus leali*, *Velocisaurus unicus*; Bonaparte and Powell 1980; Bonaparte 1991*b*, 1996), Madagascar (*Masiakasaurus knopfleri*; Carrano et al. 2002, 2011) and India (*Laevisuchus*; Huene and Matley 1933). *Masiakasaurus knopfleri* (Fig. 1.8B), the best known noasaurid taxon, shows the peculiarity of having procumbent dentary teeth with a constriction at the crown base and flutes on the lingual surface (Carrano et al. 2002, 2011).

Abelisauridae is a well-supported clade of medium to large (5-9m long) stubby-armed theropods with short rounded snouts, deep, heavily sculptured skulls bearing bony protuberances and poorly recurved teeth (Bonaparte 1991*a*; Wilson et al. 2003; Carrano and Sampson 2008; Canale et al. 2009; Pol and Rauhut 2012). The inclusion of *Eoabelisaurus mefi* (Pol and Rauhut 2012) from the Aalenian-Bajocian of Patagonia within abelisaurids is subject of debate (Pol and Rauhut 2012; Tortosa et al. 2014) and the first definitive Abelisauridae, *Kryptops palaios*, comes from the Aptian–Albian of North Africa (Sereno and Brusatte 2008). Abelisaurids were not the dominant predators in Gondwanian ecosystems in the Early Cretaceous and early Late Cretaceous of South America and North Africa, as they were dominated by the larger spinosaurids and carcharodontosaurids during that time (Holtz 2012; Novas et al. 2013). Following the extinction and/or decline of Spinosauridae and Carcharodontosauridae after the Cenomanian-Turonian transition, abelisaurids became apex predators in Africa, Western Europe, and South America in the latest part of the Cretaceous (Buffetaut et al. 2005; Candeiro and Martinelli 2005; Carrano et al. 2012; Novas et al. 2013; Tortosa et al. 2014; Csiki-Sava et al. 2015). The best-known taxa are from the Campanian-Maastrichtian of Europe and Gondwana, including *Majungasaurus crenatissimus* (Sampson et al. 1998; Sampson and Witmer

2007; Fig. 1.8C) from Madagascar, *Aucasaurus garridoi* (Coria et al. 2002), *Skorpiovenator bustingorryi* (Canale et al. 2009) and *Carnotaurus sastrei* (Bonaparte et al. 1990; Carabajal 2011) from Argentina, *Rajasaurus narmadensis* (Wilson et al. 2003) from India, and *Arcovenator escotae* (Tortosa et al. 2014) from France.

Megalosauroidea

Tetanurae (Gauthier 1986), the most inclusive clade containing *Passer domesticus* (Linnaeus 1758) but not *Ceratosaurus nasicornis* Marsh 1884*a* (Allain et al. 2012; Table 1), is diagnosed by an antorbital tooth row, a moderately extended anterior ramus of the maxilla, a maxillary fenestra piercing the lateral wall of the maxilla, separated interdental plates, and a prominent deltopectoral crest of the humerus (Carrano et al. 2012). Several relatively complete basal tetanurans are known from the Early and Middle Jurassic of China and Antarctica (i.e., '*Dilophosaurus*' *sinensis*, *Cryolophosaurus*, and *Monolophosaurus*). These primitive tetanurans are recovered between basal averostrans and the recent clade Orionides which comprises two major radiations, the Megalosauroidea and Avetheropoda (Carrano et al. 2012). The first one, Megalosauroidea, currently gathers three subclades, namely the Piatnitzkysauridae, Megalosauridae, and Spinosauridae (Fig. 1.4). Piatnitzkysauridae is the sister group of Megalosauria, which is divided into Megalosauridae and Spinosauridae. Piatnitzkysaurids as currently known comprise medium sized (5-6m long) American forms such as *Marshosaurus bicentesimus* (Madsen 1976*a*; Fig. 1.9A) from the Kimmeridgian-Tithonian of North-America, and *Piatnitzkysaurus floresi* (Bonaparte 1986; Rauhut 2004*a*) and *Condorraptor currumili* (Rauhut 2005) from the Toarcian–Bajocian of Argentina (Cúneo et al. 2013). These basal megalosauroids are characterized by a maxilla with a short anterior ramus and vertically ridged interdental plates (Carrano et al. 2012).

Megalosauridae is a diversified clade of theropods restricted to the Middle to Late Jurassic, which suggests they went extinct at the Jurassic-Cretaceous boundary (Carrano et al. 2012). Megalosaurids are medium to very large (4-10m long) theropods exhibiting relatively elongate skulls that lack cranial protuberances, and powerful arms possibly bearing a large claw at digit one (Hendrickx et al. in press*a*; Sadleir et al. 2008; Benson 2010*a*; Allain et al. 2012; Carrano et al. 2012). The most primitive and one of the oldest theropod embryos, found to date, from the Late Kimmeridgian–Early Tithonian of Portugal have been ascribed to this clade (Araújo et al. 2013). Megalosaurids are known as early as the Bajocian of England (*Magnosaurus nethercombensis*, *Duriavenator hesperis*; Benson 2008*a*, 2010*b*) and include forms from the Bajocian-Callovian of England and France (*Megalosaurus bucklandii*, Fig. 1.9B; *Dubreuillosaurus valesdunensis*; Allain 2002; Benson et al. 2008; Benson 2010*a*), the Middle Jurassic of Africa (*Afrovenator abakensis*; Sereno et al. 1996), the Late Jurassic of China (*Leshansaurus qianweiensis*; Li et al. 2009), and the Kimmeridgian-Tithonian of North-America and Portugal (*Torvosaurus tanneri*, *Torvosaurus gurneyi*; Britt 1991; Hendrickx and Mateus 2014*a*). *Sciurumimus albersdoerferi*, a possible megalosaurid from

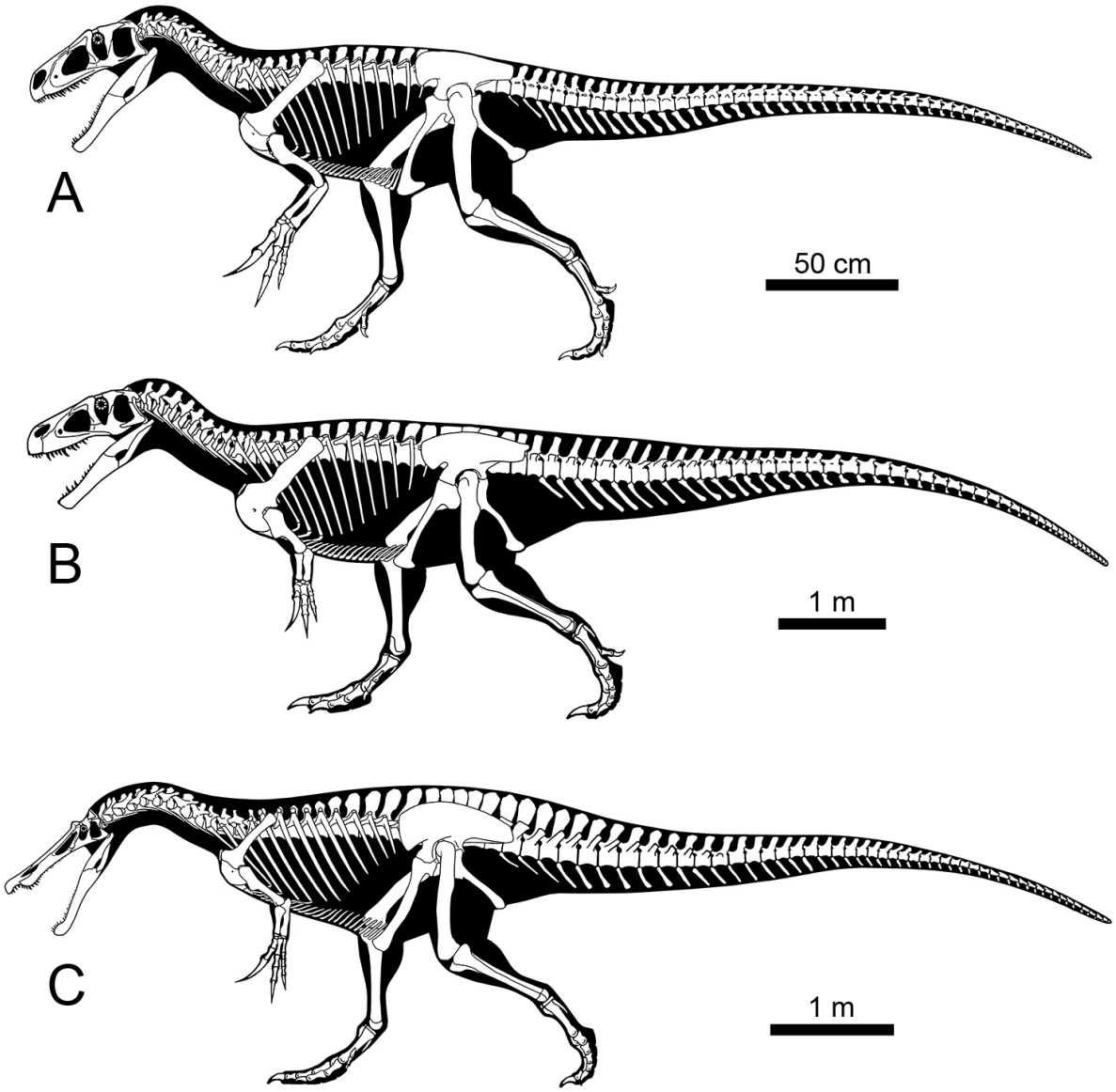

FIGURE 1.9. Skeletal reconstructions of three megalosauroids. **A**, the piatnitzkysaurid *Marshosaurus bicentissimus*; **B**, the megalosaurid *Megalosaurus bucklandii*; and **C**, the spinosaurid *Baryonyx walkeri*. Reconstructions by Scott Hartman.

the Kimmeridgian of Germany, is the most complete megalosauroid discovered so far (Rauhut et al. 2012). It is also currently the most primitive theropod preserved with direct evidence of filamentous integument, indicating that protofeathers were already covering some tetanurans early in their evolution (Rauhut et al. 2012).

Spinosauridae, the sister group of Megalosauridae, is a well-supported clade of highly specialized theropods united by an elongated crocodile-like skull, spatulate snout with sigmoid alveolar margins, fluted conical teeth with minute or no denticles, and an hypertrophied manual ungual (Charig and Milner 1997; Sereno et al. 1998; Sues et al. 2002; Bertin 2010; Allain et al. 2012; Ibrahim et al. 2014*b*). These derived anatomical features, associated with computer modeling of the skull (Rayfield et al. 2007; Cuff and Rayfield 2013), oxygen isotope (Amiot et al. 2010*b*), morphofunctional

analysis of the mandibular articulation (Hendrickx et al. in press*b*) and gut contents (Charig and Milner 1997; Buffetaut et al. 2004), suggest that spinosaurids were at least partially piscivorous, while feeding also on dinosaurs and pterosaurs. Spinosaurids were large to very large theropods (8-17m long) and include the largest terrestrial predators discovered hitherto. They were also characterized by elongated neural spines which evolved into a bony sail in some members (e.g., *Spinosaurus aegyptiacus*, *Ichthyovenator laosensis*; Stromer 1915; Allain et al. 2012; Ibrahim et al. 2014*b*). Spinosaurid teeth seem to be already present in the Kimmeridgian–Tithonian of Tanzania (Buffetaut 2011; but for a different opinion see Rauhut 2011), yet the earliest definitive spinosaurid is currently *Baryonyx walkeri* (Fig. 1.9C) from the Barremian of England and Portugal (Charig and Milner 1986, 1997; Mateus et al. 2011). Spinosauridae are also known from the Aptian and/or Albian of Niger (*Suchomimus tenerensis*; Sereno et al. 1998; n.b., *Suchomimus tenerensis* most likely represents the same animal than the non-diagnostic *Cristatusaurus lapparenti* Taquet and Russell 1998 from the same deposits; Carrano et al. 2012), Brazil (*Angaturama limai*, *Irritator challengeri*; Kellner and Campos 1996; Sues et al. 2002; n.b., these two taxa known from non-overlapping cranial material recovered from the same deposits may in fact represent the same taxon/individual; Sereno et al. 1998; Sues et al. 2002; Dal Sasso et al. 2005) and South-eastern Asia (*Ichthyovenator laosensis*; Allain et al. 2012). The most derived spinosaurid, *Spinosaurus aegyptiacus*, comes from the Albian–Cenomanian of North Africa (e.g., Stromer 1915; Taquet and Russell 1998; Buffetaut and Ouaja 2002; Dal Sasso et al. 2005; Ibrahim et al. 2014*b*). Recent studies have shown that this taxon had many adaptations for a semi-aquatic lifestyle, including short hind-limbs, downsized pelvic girdle, flat-bottomed pedal claws and solid long bones (Ibrahim et al. 2014*b*).

Despite the presence of the tetanuran *Chilantaisaurus* from the Turonian (or younger stage) of China and considered to be a spinosaurid by Allain et al. (2012; n.b., *Chilantaisaurus* is recovered as a neovenatorid allosauroid by Benson et al. 2010 and Carrano et al. 2012) as well as isolated teeth tentatively assigned to Spinosauridae from post-Cenomanian deposits of South America and Asia (Salgado et al. 2009; Hone et al. 2010; for a different opinion see Hasegawa et al. 2010), spinosaurids seem to go extinct in the early Late Cretaceous.

Allosauroidea

Avetheropoda (also known as ‘Neotetanurae’; e.g., Sereno et al. 1994; Sereno 1998, 1999; Allain et al. 2012; Table 1), the least inclusive clade containing *Allosaurus fragilis* Marsh 1877 and *Passer domesticus* (Linnaeus 1758) (Allain et al. 2012), is comprised of two major subclades: the Allosauroidea, and the Coelurosauria (Fig. 1.4). According to Carrano et al. (2012), avetheropods differ from more primitive theropods by possessing strongly curved chevrons, a poorly developed ridge on the medial surface of the ilium, and a subtriangular flange-like accessory trochanter on the femur. Allosauroids were dominant terrestrial predators in the Late Jurassic, Early Cretaceous, and early Late Cretaceous worldwide. Allosauroids are currently divided into four subclades: the

Metriacanthosauridae, Allosauridae, Neovenatoridae, and Carcharodontosauridae (Fig. 1.4). Metriacanthosauridae (formerly known as 'Sinraptoridae'; Carrano et al. 2012) is the most primitive and contains forms from the Middle and Late Jurassic of China such as *Sinraptor dongi* (Currie and Zhao 1993*a*), '*Yangchuanosaurus*' *hepigensis*, and *Yangchuanosaurus shangyouensis* (Dong et al. 1983). These taxa, which are known from exceptionally well-preserved skeletons, share a maxilla with a promaxillary fenestra larger than the maxillary fenestra, a pneumatic recess on the lateral surface of the ascending ramus, and the absence of an anterior ramus (Currie and Zhao 1993*a*; Carrano et al. 2012). *Metriacanthosaurus parkeri* (Huene 1923) from the Oxfordian of England is the only definitive non-Asian metriacanthosaurid reported to date (though *Lourinhanosaurus antunesi* from the Kimmeridgian-Tithonian of Portugal may also be referred to this clade; see Benson 2010*a*), and *Siamotyrannus isanensis* (Buffetaut et al. 1996) from the Barremian–Aptian of Thailand is the only known metriacanthosaurid that survived into the Cretaceous (Carrano et al. 2012).

Allosauridae, a more derived clade of allosauroids and the sister-clade of Carcharodontosauria, is a small group of Kimmeridgian-Tithonian tetanurans comprising several North American and Portuguese taxa, namely *Allosaurus fragilis* (Gilmore 1920; Madsen 1976*b*; Chure 2000; Loewen 2010; Fig. 1.10A), *Allosaurus europaeus* (Mateus et al. 2006), *Allosaurus* n. sp. (*Allosaurus jimmadseni sensu* Chure 2000; Chure et al. 2006; Loewen 2010), and *Saurophaganax maximus* (Chure 1995). Allosaurids were medium to large (8-10m long) theropods with thin and dorsally-developed lacrimal horns, and were one of the dominant predators in Late Jurassic ecosystems of North America and Europe (Chure 2000; Loewen 2010).

Carcharodontosauria falls into two subclades, the Neovenatoridae and the Carcharodontosauridae (Carrano et al. 2012). It has been debated whether Neovenatoridae is a monospecific clade including the taxon *Neovenator salerii* (Brusatte et al. 2008; Fig. 1.10B) from the Hauterivian–Barremian of England (Novas et al. 2013; Porfiri et al. 2014), or a more inclusive clade including *Neovenator* and megaraptorans (Benson et al. 2010; Carrano et al. 2012; Zanno and Makovicky 2013). According to Benson et al. (2010), neovenatorids are united by postcranial synapomorphies such as a short and broad scapula and a pneumatic ilium. The recent discovery of a relatively well-preserved megaraptoran with cranial material, however, seems to suggest a placement of megaraptorans within Tyrannosauroidea (Porfiri et al. 2014). Though this is still an active debate in theropod systematics, megaraptorans will be described in the next section.

Carcharodontosauridae, on the other hand, forms a well-supported clade comprising medium to very large theropods (6-14m long) characterized by a massive and deep skull with sculptured facial bones, and cranial protuberances on the lacrimals and postorbitals (Novas et al. 2005, 2013; Coria and Currie 2006; Brusatte and Sereno 2007; Ortega et al. 2010; Cau et al. 2013). The earliest carcharodontosaurid is currently *Veterupristisaurus milneri* (Rauhut 2011) known from caudal vertebrae from the Kimmeridgian-Tithonian of Tanzania. In the Cretaceous, carcharodontosaurids became a diversified clade of allosauroids distributed worldwide. Due to their very large sized,

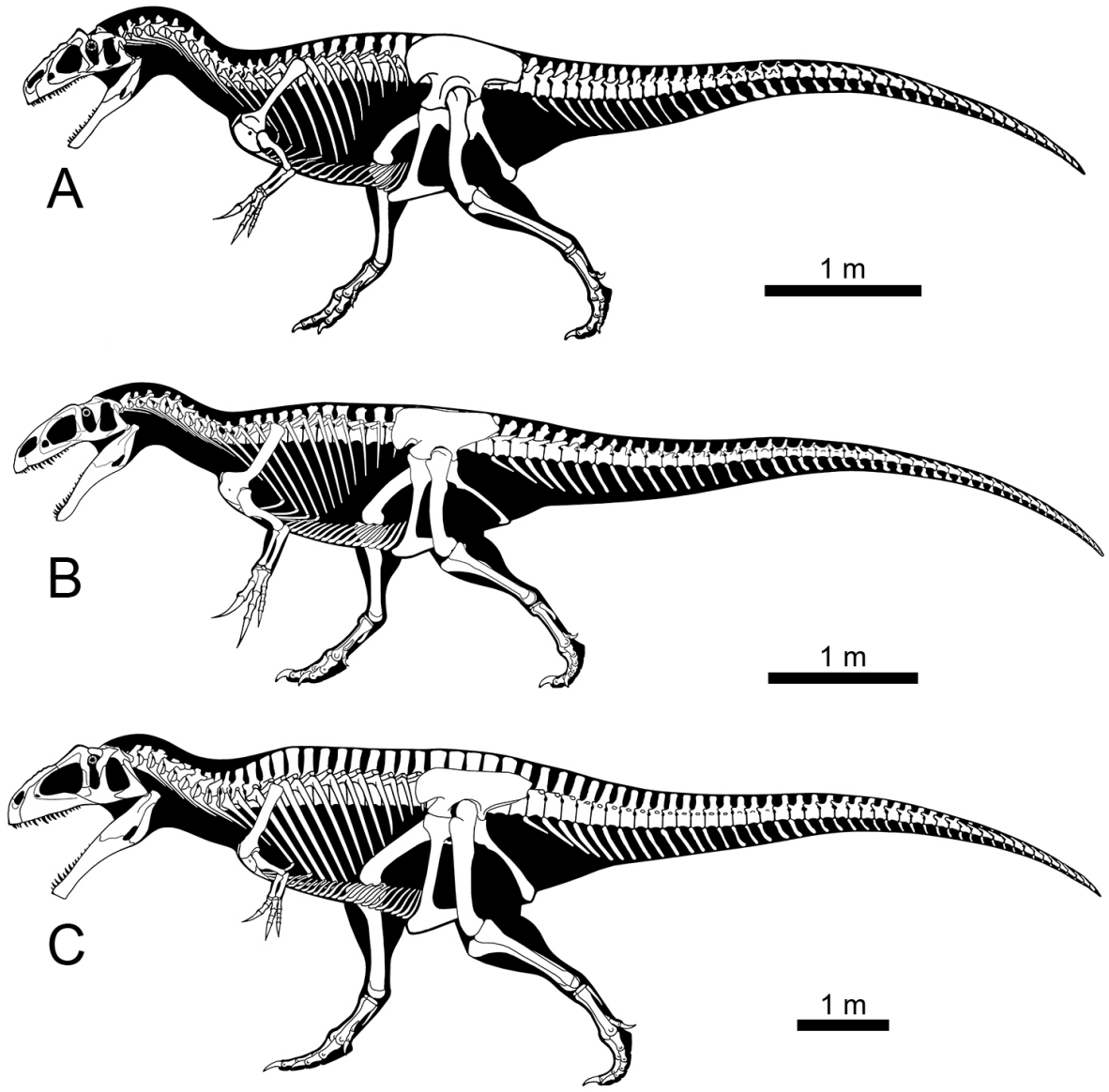

FIGURE 1.10. Skeletal reconstructions of three allosauroids. **A**, the allosaurid *Allosaurus 'jimmadseni'*; **B**, the neovenatorid *Neovenator salerii*; and **C**, the carcharodontosaurid *Giganotosaurus carolinii*. Reconstructions by Scott Hartman.

carcharodontosaurids were at the apex of the food chain in most 'mid' Cretaceous ecosystems. The best preserved carcharodontosaurids are *Concavenator corcovatus* (Ortega et al. 2010) from the Barremian of Spain, *Acrocanthosaurus atokensis* (Harris 1998; Currie and Carpenter 2000; Eddy and Clarke 2011) and *Tyrannotitan chubutensis* (Novas et al. 2005; Canale et al. 2014) from the Aptian-Albian of North America and Argentina, respectively, *Carcharodontosaurus saharicus* (Rauhut 1995; Brusatte and Sereno 2007) from the Cenomanian of North Africa, *Giganotosaurus carolinii* (Coria and Salgado 1995; Calvo and Coria 1998; Fig. 1.10C) and *Mapusaurus roseae* (Coria and Currie 2006) from the Cenomanian-?Santonian of Argentina, and *Shaochilong maortuensis* (Brusatte et al. 2009*c*, 2010*b*) from the Turonian of China (Carrano et al. 2012). The carcharodontosaurid lineage may have extended to the latest part of the Cretaceous in South America as material assigned to

Carcharodontosauridae have been reported from the Campanian-Maastrichtian of Brazil (e.g., Candeiro et al. 2012; Azevedo et al. 2013).

Basal Coelurosauria and Tyrannosauroidea

Coelurosauria (Huene 1914*a*), the most inclusive clade containing *Passer domesticus* (Linnaeus 1758) but not *Allosaurus fragilis* Marsh 1877, *Sinraptor dongi* Currie and Zhao 1993*a*, and *Carcharodontosaurus saharicus* (Depéret and Savornin 1927) (Sereno 2005), is a well-supported clade that contains a large diversity of herbivorous and carnivorous non-avian theropods as well as living birds. According to Turner et al. (2012), members of this group differ from more basal theropods by possessing a well-developed medial shelf on the maxilla, a reversed L-shaped quadratojugal and amphiplatyan cervical and anterior dorsal vertebrae. Coelurosaur interrelationships are complex, including several well-defined coelurosaur groups nested in different subclades (Figs. 1.4–1.5). The oldest definite coelurosaurs are known from the Bathonian of Eurasia (Averianov et al. 2010; Rauhut et al. 2010), though putative coelurosaur remains have been described from the Early Jurassic of China (Zhao and Xu 1998; Barrett 2009). The majority of recent cladistic analyses on coelurosaurs recovered Tyrannosauroidea as the basalmost clade of Coelurosauria (e.g., Dal Sasso and Maganuco 2011; Senter et al. 2012*b*; Turner et al. 2012; Godefroit et al. 2013*a*; Loewen et al. 2013; Brusatte et al. 2014*a*; Choiniere et al. 2014*b*; n.b., Tyrannosauroidea are found more derived than Compsognathidae in Zanno et al. 2009, Rauhut et al. 2010 and Novas et al. 2013). There are, however, several coelurosaur taxa that fall outside Tyrannosauroidea, at the very base of Coelurosauria (Fig. 1.4). These include *Aorun zhaoi* (Choiniere et al. 2014*b*) and *Zuolong sallei* (Choiniere et al. 2010*a*) from the Oxfordian-Callovian of China, *Bicentenaria argentina* from the Cenomanian of Argentina (Novas et al. 2012), and possibly *Tanycolagreus topwilsoni* from the Kimmeridgian-Tithonian of Wyoming and *Tugulusaurus faciles* from the ?Valanginian–Albian of China (Rauhut and Xu 2005). The latter two are also recovered as sister-taxa among the Coeluridae, a clade recovered at the base of Coelurosauria by Li et al. (2010), but also at the base of the tyrannosauroid clade (e.g., Dal Sasso and Maganuco 2011; Novas et al. 2012; Senter et al. 2012*b*; Brusatte et al. 2014*a*), or slightly more derived than tyrannosauroids (Choiniere et al. 2014*b*).

Due to the iconic status of *Tyrannosaurus rex* and numerous tyrannosauroid specimens, tyrannosauroids are the most studied and best known non-avian theropods (Brusatte et al. 2010*d*). The recent discovery of a large number of basal and derived tyrannosauroids has dramatically increased the known diversity of this group, resulting in a well-characterized phylogenetic sequence. Tyrannosauroids encompass small to very large-bodied theropods (3-13m long) diagnosed by premaxillary teeth significantly smaller than anterior maxillary teeth and with a U-shaped cross-section, small premaxillae with elongated nasal and maxillary (subnarial) processes, and fused nasals (Holtz 2004, 2012; Brusatte et al. 2010*d*). The discovery of several well-preserved tyrannosauroids from China has revealed that small to large bodied primitive forms such as *Dilong paradoxus* (Xu et

al. 2004) and *Yutyrannus huali* (Xu et al. 2012) were covered with filamentous integument. Some recent phylogenetic analyses of Tyrannosauroidea suggest that three main subclades radiated independently: the Proceratosauridae, Megaraptora, and Tyrannosauridae (Fig. 1.4).

The most basal clade, the Proceratosauridae, comprises small-bodied tyrannosauroids characterized by elaborated cranial crests (Brusatte et al. 2010*d*; Fig. 1.11A). Proceratosaurids originated in the Middle Jurassic of Eurasia, including the taxa *Proceratosaurus bradleyi* (Rauhut et al. 2010) and *Kileskus aristotocus* (Averianov et al. 2010) from the Bathonian of England and Siberia, respectively. Proceratosaurids are also known from the Oxfordian of China (*Guanlong wucaii*; Xu et al. 2006; Fig. 11A), and the youngest member is *Sinotyrannus kazuoensis* (Ji et al. 2009) from the Aptian of China (Brusatte et al. 2010*d*).

Primitive non-proceratosaurid tyrannosauroids (i.e., non-proceratosaurid tyrannosauroids more basal than Tyrannosauridae) encompass several small to medium sized forms from the Late Jurassic of Europe (*Aviatyrannis jurassica*, *Juratyrant langhami*; Rauhut 2003*b*; Benson 2008*b*; Brusatte and Benson 2013) and North America (*Stokesosaurus clevelandi*; Benson 2008*b*; Brusatte and Benson 2013), and the Early Cretaceous of Europe (*Eotyrannus lengi*; Hutt et al. 2001; Fig. 1.11B) and China (*Dilong paradoxus*, *Yutyrannus huali*, *Xiongguanlong baimoensis*; Xu et al. 2004, 2012; Li et al. 2010). They are also known in the Late Cretaceous of North America (e.g., *Dryptosaurus aquilunguis*, *Appalachiosaurus montgomeriensis*, *Bistahieversor sealeyi*; Carr et al. 2005; Carr and Williamson 2010; Brusatte et al. 2011) and Asia (e.g., *Raptorex kriegsteini*, *Alectrosaurus olseni*; Mader and Bradley 1989; Sereno et al. 2009).

Based on the recent description of a relatively complete juvenile specimen of *Megaraptor namunhuaiquii*, megaraptorans are thought to have evolved from primitive tyrannosauroids more derived than proceratosaurids (Novas et al. 2013; Porfiri et al. 2014). Megaraptorans are gracile theropods characterized by an elongated skull, and elongated and robust forelimbs with enlarged thumb claws on digits I and II (Benson et al. 2010; Porfiri et al. 2014). They were distributed widely across the globe as they encompass *Fukuiraptor kitadaniensis* (Azuma and Currie 2000; Currie and Azuma 2006) from the Barremian of Japan, *Australovenator wintonensis* (Hocknull et al. 2009) from the Albian of Australia, and *Aerosteon riocoloradensis* (Sereno et al. 2008) from the Campanian of North Argentina. Megaraptorans seem also to extend to the end of the Cretaceous, with *Orkoraptor burkei* (Novas et al. 2008) from the Maastrichtian of Patagonia as the most recent member of this clade.

Tyrannosaurids are the most derived and the largest tyrannosauroids. Within Tyrannosauroidea, they show the derived features of large body size (6-13m long), robust and broad skulls with powerful jaws bearing incrassate teeth with long roots, and reduced forelimbs ending in two functional fingers (the third digit is vestigial and does not carry phalanges; Currie 2003; Holtz 2004, 2012; Brusatte et al. 2010*d*). Tyrannosaurids were apex predators in all Late Cretaceous ecosystems of North America and Asia. They were hypercarnivores and were able to produce

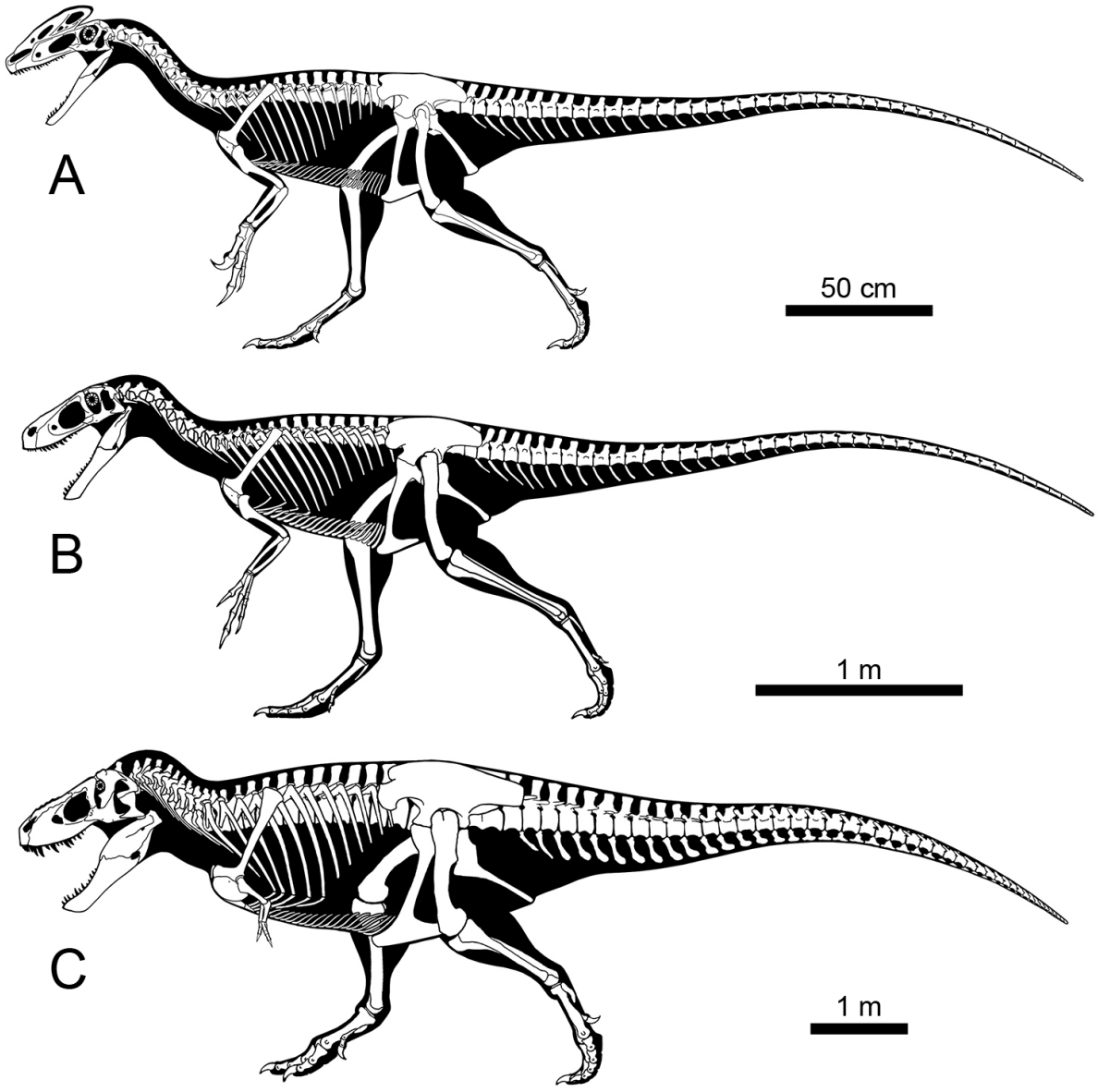

FIGURE 1.11. Skeletal reconstructions of three tyrannosauroids. **A**, the proceratosaurid *Guanlong wucaii*; **B**, the basal tyrannosauroid *Eotyrannus lengi*; and **C**, the tyrannosaurid *Tyrannosaurus rex*. Reconstructions by Scott Hartman.

extremely powerful bite forces capable of crushing bone (Erickson et al. 1996; Bates and Falkingham 2012). Tyrannosaurids also possessed a higher degree of stereoscopic vision than other non-avian theropods, and their olfactory ratios are particularly high, suggestive of a keen sense of smell (Stevens 2006; Witmer and Ridgely 2009; Zelenitsky et al. 2009). Studies have shown that they had accelerated grow rates and underwent well-characterized changes during ontogeny (Carr 1999; Erickson et al. 2004; Horner and Padian 2004). The best known tyrannosaurids are from the Campanian–Maastrichtian of Asia and North-America and include *Albertosaurus sarcophagus*, *Gorgosaurus libratus*, *Daspletosaurus torosus*, and *Tyrannosaurus rex* (Fig. 1.11C) from USA and Canada (e.g., Russell 1970; Molnar 1991; Brochu 2003; Currie 2003), and *Alioramus altai* and *Tarbosaurus baatar* from Mongolia (e.g., Hurum and Sabath 2003; Tsuihiji et al. 2011; Brusatte et al. 2012*a*).

Compsognathidae and Ornithomimosauria

Compsognathidae and Ornithomimosauria are typically recovered as more derived than Tyrannosauroidea and more basal than Alvarezsauroidea, Therizinosauria, and Oviraptorosauria. Several recent large scale cladistic analyses have placed Compsognathidae and Ornithomimosauria as the second and third basalmost clades of coelurosaurs, respectively (e.g., Csiki et al. 2010; Senter 2011; Turner et al. 2012; Godefroit et al. 2013*a*; Choiniere et al. 2014*b*; Fig. 1.5). Compsognathids are characterized by small body size (1-2.5m long), a gracile and slender body, and an elongated skull with slender jaws bearing ziphodont teeth (Fig. 1.12A). Many specimens are immature individuals retaining a primitive and unspecialized anatomy, and Compsognathidae have sometimes been thought to be paraphyletic, with some compsognathid taxa recovered outside the clade in phylogenetic analyses by Butler and Upchurch (2007), Godefroit et al. (2013*a*), Choiniere et al. (2014*b*) and others. Nevertheless, the clade is strongly supported (i.e., united by 18 unambiguous synapomorphies in Brusatte et al. (2014*a*), which is currently the largest and most recent cladistic analyses performed on coelurosaurs. According to Brusatte et al. (2014*a*), compsognathids are diagnosed by a dentition with some unserrated teeth, premaxillary teeth with a subcircular cross-section, the presence of an anterior ramus on the maxilla, a vertically oriented pubis shaft, and ossified sternal plates. In this study, compsognathids include *Juravenator starki* (Chiappe and Göhlich 2010) and *Compsognathus longipes* (Bidar et al. 1972; Ostrom 1978; Peyer 2006; Fig. 1.12A) from the Kimmeridgian-Tithonian of Germany and Germany and France, respectively, *Mirischia asymmetrica* (Naish et al. 2004) from the Albian of Brazil, as well as *Huxiagnathus orientalis* (Hwang et al. 2004), *Sinocalliopteryx gigas* (Ji et al. 2007*a*) and *Sinosauropteryx prima* (Currie and Chen 2001; Ji et al. 2007*b*) from the Barremian–early Aptian Yixian Formation of China. *Aristosuchus pusillus*, from the Barremian of England, and *Scipionyx samniticus*, from the Albian of Italy, are also considered as compsognathids by some authors (e.g., Naish 2002, 2011; Dal Sasso and Maganuco 2011; Loewen et al. 2013; Choiniere et al. 2014*b*). The latter taxon is remarkable for being a hatchling specimen preserving exquisitely fossilized soft tissues and internal organs such as intestines, muscles, and blood vessels (Dal Sasso and Maganuco 2011). Compsognathid feeding behavior is among the best known in non-avian theropods, as stomach contents are preserved in both specimens of *Compsognathus* (Bidar et al. 1972; Ostrom 1976*a*; Evans 1994; Peyer 2006), *Huxiagnathus* (Hwang et al. 2004), *Scipionyx* (Dal Sasso and Maganuco 2011), and two specimens of *Sinosauropteryx* (Currie and Chen 2001; Ji et al. 2007*b*) and *Sinocalliopteryx* (Xing et al. 2012). These reveal that compsognathids ingested gastroliths and had an extremely diverse diet composed of fish, lizards, non-avian theropods (dromaeosaurids), primitive birds, and mammals. Similar to more basal tetanurans, evidences of filamentous integument in well-preserved compsognathids such as *Sinosauropteryx* (Currie and Chen 2001) and *Juravenator* (Chiappe and Göhlich 2010) suggest that protofeathers partially or extensively covered the body of these basal coelurosaurs. A recent study on the fossilized melanosomes in *Sinosauropteryx* has also revealed that

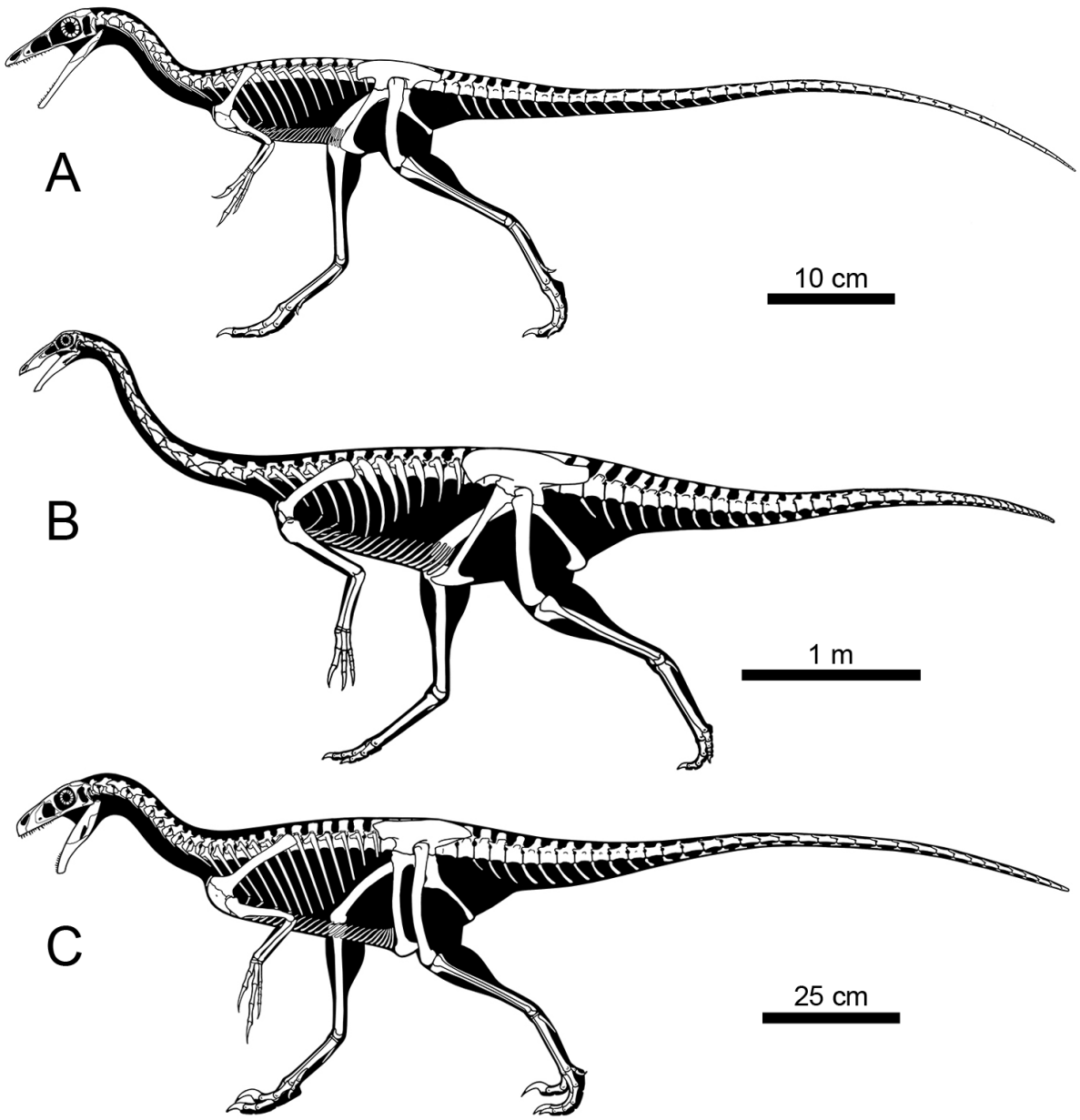

FIGURE 1.12. Skeletal reconstructions of three basal maniraptoriforms. **A**, the compsognathid *Compsognathus longipes*; **B**, the ornithomimid *Gallimimus bullatus*; and **C**, the basal maniraptoran *Ornitholestes hermanni*. Reconstructions by Scott Hartman.

the tail of this animal had stripes which exhibited chestnut to rufous (reddish-brown) tones (Zhang et al. 2010).

Maniraptoriformes (Holtz 1995), the least inclusive clade containing *Passer domesticus* (Linnaeus 1758) and *Ornithomimus velox* Marsh 1890 (Maryańska et al. 2002), is largely composed of non-strictly-carnivorous theropods that are partially or fully edentulous and/or possess reduced lanceolate crowns, with a few derived maniraptoriforms (i.e., dromaeosaurids) being secondarily carnivorous (Holtz 2012). The first radiation of non-strictly carnivorous (i.e., herbivorous to omnivorous; see Barrett 2005; Zanno and Makovicky 2011; Lee et al. 2014) coelurosaurs were ornithomimosaurs. The latter are small to very large (2-10m long) lightly to heavily built theropods

characterized by a low and delicate skull, slender neck, elongate forehands bearing three non-raptorial clawed fingers, and in the ostrich-like ornithomimids long powerful legs that were adapted for rapid locomotion (Russell 1972; Nicholls and Russell 1981; Makovicky et al. 2004; Barrett 2005; Kobayashi and Barsbold 2005*a*; Liyong et al. 2012; Fig. 1.12B). The jaws of basal ornithomimosaurs bear a large number of small conical teeth, intermediate taxa possess small teeth restricted to the anterior extremity of the dentary and derived forms are fully edentulous, possessing only a rhamphotheca (some exhibit columnar structures that may have been used as a filter-feeding system; Norell et al. 2001; for an alternative hypothesis, see Barrett 2005). Some derived ornithomimids possessed filamentous protofeathers and possibly long shafted feathers (pennibrachium) on the forearms, forming wings (Zelenitsky et al. 2012; for a different opinion see Foth et al. 2014). Ornithomimosaurs originated in the earliest part of the Cretaceous and the oldest and basalmost member of the clade is *Nqwebasaurus thwazi* from the Berriasian–Valanginian of South Africa (Choiniere et al. 2012). *Pelecanimimus polyodon* (Pérez-Moreno et al. 1994), another basal ornithomimosaur taxon from the Hauterivian of Spain, possessed more than 200 unserrated teeth on the jaws, which makes it the theropod bearing the largest number of teeth. More derived ornithomimosaurs with dentulous lower jaws are mostly known from the Valanginian-Albian of China such as *Hexing qingyi* (Liyong et al. 2012), *Beishanlong grandis* (Makovicky et al. 2010), *Shenzhousaurus orientalis* (Ji et al. 2003), and *Harpymimus okladnikovi* (Kobayashi and Barsbold 2005*b*). Edentulous ornithomimosaurs are only known from the Upper Cretaceous of Asia and North America, and the best known taxa are *Garudimimus brevipes* (Kobayashi and Barsbold 2005*a*) and *Sinornithomimus dongi* (Kobayashi and Lü 2003) from the early Late Cretaceous of China, *Ornithomimus edmontonicus* and *Struthiomimus altus* (Russell 1972) from the Campanian-Maastrichtian of Canada, and *Gallimimus bullatus* (Osmólska et al. 1972; Fig. 1.12B) and *Deinocheirus mirificus* (Lee et al. 2014) from the Maastrichtian of Mongolia. The latter was recently revealed to be a very large omnivorous ornithomimosaur with a deep jaw, tall neural spines, elongated forelimbs and short hind limbs. It was recovered as a derived member of a new lineage of Asian ornithomimosaurs named Deinocheiridae (Lee et al. 2014). Deinocheirids, which include *Beishanlong*, *Garudimimus* and *Deinocheirus*, do not seem to be adapted for speed, in contrast to cursorial ornithomimids such as *Gallimimus*, *Struthiomimus* and *Ornithomimus* that are widely interpreted as fast runners (Russell 1972; Thulborn 1990; Lee et al. 2014).

Therizinosauria, Alvarezsauroidea and Oviraptorosauria

Maniraptora (Gauthier 1986), the most-inclusive clade containing *Passer domesticus* (Linnaeus 1758) but not *Ornithomimus edmontonicus* Marsh 1890 (Maryańska et al. 2002), includes theropods characterized by a well-developed lateral process of the quadrate, a large bony sternum with co-ossified sternal plates, and a semilunate carpal (Holtz 2012; Turner et al. 2012). Many maniraptorans convergently acquired a retroverted pubis superficially similar to ornithischians (Holtz

2012). *Ornitholestes hermanni* (Osborn 1903; Carpenter et al. 2005; Fig. 1.12C) from the Upper Jurassic of North America is either recovered as the basalmost maniraptoran (e.g., Dal Sasso and Maganuco 2011; Novas et al. 2012; Senter et al. 2012*b*; Turner et al. 2012; Foth et al. 2014) or as a basal coelurosaur closely related to some compsognathids (e.g., Godefroit et al. 2013*a*; Choiniere et al. 2014*b*). The basalmost clade within Maniraptora is the Alvarezsauroidea (Fig. 1.5). Alvarezsauroids were small (1-2.5m long) coelurosaurs characterized by a gracile and low skull with large cranial openings, elongate rostrum, and slender jaws bearing a large number of teeth that are, at least for some crowns, lanceolate (Fig. 1.13A). The forelimbs of alvarezsauroids bear three fingers in which digit II and III are reduced in size and were even lost in some derived taxa (Perle et al. 1993; Chiappe et al. 1998; Longrich and Currie 2009*a*; Choiniere et al. 2010*b*, 2014*a*; Nesbitt et al. 2011; Xu et al. 2011*b*). The basalmost member is *Haplocheirus sollers* from the Oxfordian of China; all alvarezsauroids more derived than *Haplocheirus* belong to Alvarezsauridae (Choiniere et al. 2010*b*, 2014*a*). Alvarezsaurids are restricted to the Late Cretaceous of North-America, South-America, Asia, and Europe (Naish and Dyke 2004; Longrich and Currie 2009*a*; Agnolín et al. 2012; Xu et al. 2013). They comprise taxa with a large number of minute and lanceolate crowns, short forelimbs bearing either a single first digit, or much larger thumb with a massive claw, a pubis oriented backward, and elongated hind limbs adapted for cursoriality. The best known members are *Patagonykus puertai* (Novas 1997*a*) from the Turonian–Coniacian of Argentina, and the parvicursorines *Xixianykus zhengi* (Xu et al. 2011*b*) and *Linhenykus monodactylus* (Xu et al. 2013) from the Coniacian–Santonian and Campanian of China, respectively, and *Mononykus olecranus* (Perle et al. 1993, 1994), *Shuvuuia deserti* (Chiappe et al. 1998; Suzuki et al. 2002; Fig. 1.13A), and *Ceratonykus oculatus* (Alifanov and Barsbold 2009) from the Campanian-Maastrichtian of Mongolia. At least one member of this group (i.e., *Shuvuuia*) possessed filamentous integuments similar to those of more primitive tetanurans (Schweitzer et al. 1999).

Therizinosaurs are small to very large (2-10m long) ‘prosauropod’-like theropods characterized by a small head bearing reduced and basally constricted crowns, an elongated neck, long and robust arms terminated by large claws, broad abdomen and pelvis, and a relatively vertical position of the body (Barsbold and Perle 1980; Clark et al. 2004; Zanno 2010*a*, *b*; Lautenschlager et al. 2014; Fig. 1.13B). Therizinosaurs seem to be restricted to North America and Asia in the Cretaceous, yet the therizinosaur *Eshanosaurus deguchiianus*, said to be found in the Lower Lufeng Formation of the Yunnan Province, China, may attest to the presence of the clade back to the Lower Jurassic (Zhao and Xu 1998; Xu et al. 2001*a*). However, given the fact that the time separating this taxon from the most basal therizinosaur is anomalous, an Early Jurassic age of *Eshanosaurus* requires confirmation (Kirkland et al. 2005; Barrett 2009). The most primitive known member is currently *Falcarius utahensis* (Zanno 2006, 2010*b*) from the Barremian of Utah. *Jianchangosaurus yixianensis* (Pu et al. 2013) and *Beipiaosaurus inexpectus* (Xu et al. 1999*a*) are two basal therizinosaurs from the Early Cretaceous (Barremian?) of China that are slightly more derived than *Falcarius*. The body of these two primitive therizinosaurs was covered with filamentous integument (Xu et al. 2009*a*; Pu et al.

2013), which suggests that most, if not all, therizinosaurs had protofeathers. Therizinosaur taxa more derived than *Jianchangosaurus* form the clade Therizinosauroidea (Pu et al. 2013). *Jianchangosaurus* and therizinosauroids share a downturned anterior extremity of the dentary, large apically inclined denticles of the crowns, and an edentulous premaxilla bearing a rhamphotheca (which may not be present in *Falcarius*). Derived therizinosauroids (therizinosaurids *sensu* Zanno et al. 2009; Table 1.1) possess important basicranial pneumaticity, long scythe-like manual unguals, and a flattened pubic shaft (Zanno 2010*a*). The best known therizinosauroids are *Alxasaurus elesitaiensis* (Russell and Dong 1993) from the Albian of China, *Nothronychus graffami* (Zanno et al. 2009; Fig. 13B) from the Turonian of Utah, *Erlikosaurus andrewsi* and *Segnosaurus galbinensis* (Barsbold and Perle 1980; Barsbold 1983; Clark et al. 1994; Lautenschlager et al. 2014) from the Cenomanian-Turonian of Mongolia, and *Neimongosaurus yangi* (Zhang et al. 2001) from the Campanian-Maastrichtian of China (Zanno 2010*a*).

The clade containing theropods more derived than therizinosaurs, including Oviraptorosauria and Paraves, has recently been named Pennaraptora based on definitive evidence of pennaceous feathers in multiple pennaraptoran taxa (Foth et al. 2014). Oviraptorosauria is a well-supported clade of small to large (1-8m long) theropods easily recognized by their short skulls with parrot-like beaks, forelimbs with elongated manual fingers, and short tails (Clark et al. 2001; Osmólska et al. 2004; Balanoff et al. 2009; Longrich et al. 2010; Balanoff and Norell 2012; Lamanna et al. 2014; Fig. 1.13C). Oviraptorosaurs are restricted to the Cretaceous of Asia, North America and possibly South America (Frey and Martill 1995; Frankfurt and Chiappe 1999; for a different opinion, see Agnolín and Martinelli 2007), and most taxa come from Campanian-Maastrichtian deposits. Members of this clade were partially to strictly herbivorous coelurosaurs who adopted an avian-like brooding posture on their nests (Clark et al. 1999; Varricchio et al. 2008; Zanno and Makovicky 2011). Similar to ornithomimosaurs, basal oviraptorosaurs retained teeth that were subsequently lost in more derived taxa; the majority of oviraptorosaur taxa, which form the clade Caenagnathoidea, were edentulous. The basalmost oviraptorosaur is currently *Incisivosaurus gauthieri* from the Aptian of China (Balanoff et al. 2009). *Incisivosaurus* shows the primitive condition of having dentulous maxillae and dentaries, and the peculiarity of bearing premaxillary teeth that are much larger than the lateral teeth (Xu et al. 2002*a*; Balanoff et al. 2009). Contemporaneous, yet more derived, non-caenagnathoid oviraptorosaurs such as *Caudipteryx zoui* and *Similicaudipteryx yixianensis* from China retained only premaxillary teeth, and several well-preserved specimens possessed branching feathers such as remiges on the forelimbs, and rectrices on the caudal vertebrae (Ji et al. 1998; Zhou et al. 2000; He et al. 2008; Xu et al. 2010). This suggests that some, if not all oviraptorosaurs had feathered bodies and wings, yet they appear entirely flightless. Caenagnathoidea is divided into two main subclades, Oviraptoridae and Caenagnathidae (Osmólska et al. 2004; Longrich et al. 2013; Lamanna et al. 2014). Caenagnathids are characterized by fused dentaries and long, shallow pneumatized mandibles, whereas oviraptorids had deep lower jaws and an external naris extending back and over the antorbital fenestra

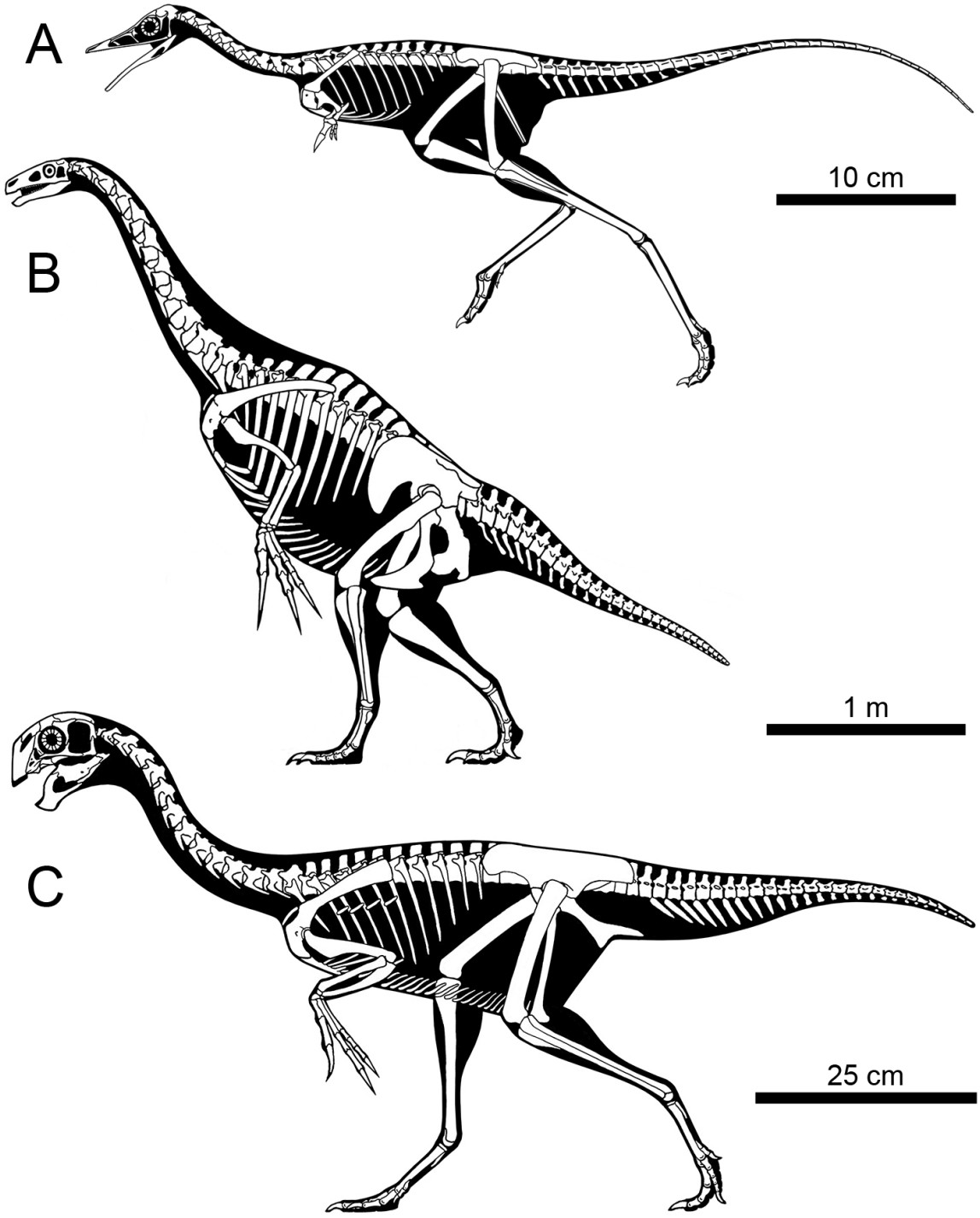

FIGURE 1.13. Skeletal reconstructions of three basal maniraptorans. **A**, the alvarezsauroid *Shuvuuia deserti*; **B**, the therizinosauroid *Nothronychus graffami*; and **C**, the oviraptorosaur *Khaan mangas*. Reconstructions by Ville Sinkkonen for *Shuvuuia* and Scott Hartman for *Nothronychus* and *Khaan*.

(Longrich et al. 2013). Oviraptorids such as *Khaan mckennai* (Clark et al. 1999; Balanoff and Norell 2012; Fig. 13C) inhabited xeric environments (i.e., deserts) whereas caenagnathids occurred in fluvial-dominated and costal floodplain environments (Longrich et al. 2013). Taxa from both clades

convergently acquired cranial crests, as shown in *Citipati osmolskae* (Clark et al. 2002), *Nemegtomaia barsboldi* (Lü et al. 2004), and *Anzu wyliei* (Lamanna et al. 2014).

Paraves

The remaining maniraptorans, comprising birds and two non-avian theropod clades traditionally labeled deinonychosaurs, are grouped within Paraves (Fig. 1.5). The latter is defined as the most inclusive clade including *Passer domesticus* (Linnaeus 1758) but not *Oviraptor philoceratops* (Holtz and Osmólska 2004). Deinonychosauria, on the other hand, is either defined as a node-based clade containing the last common ancestor of *Troodon formosus* and *Velociraptor mongoliensis* and all of its descendants (Turner et al. 2012), or the most-inclusive clade containing *Dromaeosaurus albertensis* but not *Passer domesticus* (Linnaeus 1758) (Godefroit et al. 2013*a*). Deinonychosaurs are typically divided into Dromaeosauridae and Troodontidae, theropods that share a raptorial sickle-shaped claw on the hyperextendable pedal digit II (Holtz 2012; Turner et al. 2012). Deinonychosauria was considered a well-supported clade until recently (e.g., Turner et al. 2012), but newly discovered basal paravians and the description of additional specimens of *Archaeopteryx* (Mayr et al. 2005; Foth et al. 2014) have led to analyses that find troodontids more closely related to avialans than to dromaeosaurids, rendering the taxon Deinonychosauria paraphyletic or equivalent to Dromaeosauridae, depending on the phylogenetic definition given to this clade (e.g., Godefroit et al. 2013*a*; Brusatte et al. 2014*a*; Choiniere et al. 2014*b*; Foth et al. 2014; Fig. 1.5).

Dromaeosaurids are the only definitively carnivorous maniraptoriforms (with perhaps the exception of *Ornitholestes*). They share unconstricted ziphodont teeth and a hinge joint (ginglymus) on the distal end of metatarsal II that permits an extended range of motion in the second toe and its hypertrophied and highly modified claw (Norell and Makovicky 2004; Turner et al. 2012). Dromaeosaurids are a widespread group of very small to large bodied (0.6-7m long) paravians that were present on all continents by the Late Cretaceous. Although isolated teeth from the Late Jurassic of Europe have been assigned to members of this clade (e.g., Zinke 1998; Lubbe et al. 2009; Hendrickx and Mateus 2014*b*) and the presence of dromaeosaurids in the Jurassic is evidenced by the appearance of closely related paravians in the Late Jurassic (Fig. 1.1), definitive dromaeosaurids currently range from the Barremian (China) to the Maastrichtian (North America). A large array of evidence indicates that some, and most likely all Dromaeosauridae were covered with filamentous integuments, and at least two dromaeosaurid taxa (i.e., *Microraptor* and *Changyuraptor*) possessed four wings (i.e., pennaceous fore- and hind limbs) with branching feathers like those seen in extant birds (Xu et al. 1999*b*, 2001*b*, 2003; Ji et al. 2001; Turner et al. 2007; Han et al. 2014). The majority of recent phylogenetic analyses performed on paravians typically recover three dromaeosaurid subclades: Unenlagiinae, Microraptorinae, and Eudromaeosauria (e.g., Senter et al. 2012*b*; Turner et al. 2012; Brusatte et al. 2014*a*; Choiniere et al. 2014*b*; Foth et al. 2014). A different topology was obtained by Agnolín and Novas (2013) who found Microraptorinae and Unenlagiinae outside

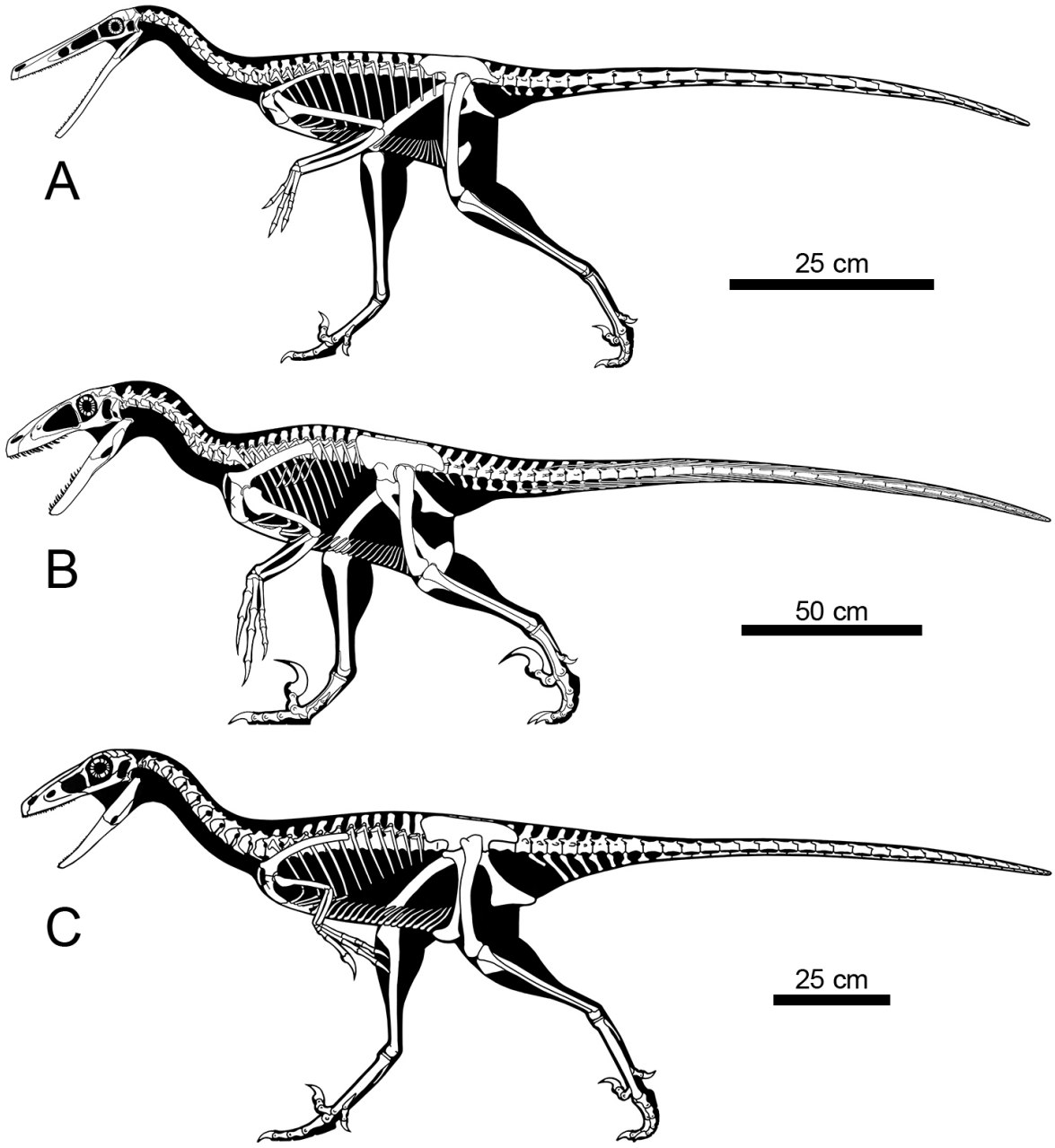

FIGURE 1.14. Skeletal reconstructions of three basal paravians. **A**, the unenlagiine dromaeosaurid *Buitreraptor gonzalezorum*; **B**, the velociraptorine dromaeosaurid *Deinonychus antirrhopus*; and **C**, the troodontid *Troodon formosus*. Reconstructions by Scott Hartman.

Dromaeosauridae and gathered within the new clade 'Averaptora' with Avialae, a configuration not recovered by other theropod workers.

Although Agnolín and Novas (2011, 2013) have defended an avialan affinity of unenlagiines, it is commonly accepted that Unenlagiinae was the first dromaeosaurid radiation and is the most basal lineage of Dromaeosauridae. These primitive dromaeosaurids are characterized by an elongate rostrum, unserrated teeth, and a vertically oriented pubis (Gianechini and Apesteguía 2011; Gianechini et al. 2011; Turner et al. 2012; Fig. 1.14A). They are exclusively found in the Upper Cretaceous of Gondwana, and are mostly known from South America, and the best preserved forms are *Buitreraptor*

gonzalezorum from the Cenomanian (Makovicky et al. 2005; Fig. 13A), *Unenlagia comahuensis* from the Turonian–Coniacian (Novas and Puerta 1997), *Austroraptor cabazai* from the Maastrichtian of Argentina (Novas et al. 2009), and *Rahonavis ostromi* from the Maastrichtian of Madagascar (Forster et al. 1998; Turner et al. 2012).

The remaining dromaeosaurids are distributed among three subclades, Microraptorinae ('Microraptoria' *sensu* Senter et al. 2004, 2012*b*), Velociraptorinae and Dromaeosaurinae (Turner et al. 2012; Fig. 1.5). As suggested by the etymology, microraptorines were small to very small (0.6–2m long) dromaeosaurids thought to have aerial or subaerial abilities (i.e., gliding, powered flight, or other semi-aerial locomotion) that are known from the Early to Late Cretaceous of China and North America (Xu et al. 2003; Longrich and Currie 2009*b*; Han et al. 2014). The best preserved members of this clade, all from the Early Cretaceous of Liaoning in China, are *Microraptor* sp. (Hwang et al. 2002; Xu et al. 2003; O'Connor et al. 2011; Xing et al. 2013*b*), *Sinornithosaurus millenii* (Xu et al. 1999*b*; Xu and Wu 2001; Gong et al. 2010), *Tianyuraptor ostromi* (Zheng et al. 2010), and *Changyuraptor yangi* (Han et al. 2014). *Hesperonychus elizabethae*, from the Campanian of Alberta, is the youngest known microraptorine, and the only one found outside China (Longrich and Currie 2009*b*). Velociraptorinae includes North American, Asian and possibly European dromaeosaurids, which are characterized by pleurocoels in all dorsal vertebrae (Turner et al. 2012). Velociraptorines encompass the famous theropods *Velociraptor mongoliensis* from the Campanian of Mongolia (Sues 1977; Norell and Makovicky 1997, 1999; Barsbold and Osmólska 1999), *Deinonychus antirrhopus* from the Aptian–Albian of Montana (Ostrom 1969, 1976*b*), and *Bambiraptor feinbergi* from the Campanian of Montana (Burnham et al. 2000; Burnham 2004). While *Balaur bondoc*, from the Maastrichtian of Romanian, may represent the only definitive velociraptorine from Europe (Csiki et al. 2010; Brusatte et al. 2013, 2014*a*), two recent large scale phylogenetic analyses on coelurosaurs recovered it as a basal avialan (i.e., Godefroit et al. 2013*a*; Foth et al. 2014) and the position of this taxon among paravians remains unclear. Dromaeosaurinae, the remaining subclade of dromaeosaurids, includes small to large-sized theropods with a lateral dentition bearing mesial denticles, a ventrodorsally tall jugal process of the maxilla, and a vertically oriented pubis (Turner et al. 2012). This clade is mostly comprised by North American dromaeosaurid taxa such as *Utahraptor ostrommaysi* from the Barremian of Utah (Kirkland et al. 1993), *Dromaeosaurus albertensis* (Colbert and Russell 1969; Currie 1995; Fig. 1.14B) and *Atrociraptor marshalli* (Currie and Varricchio 2004) from the Campanian of Alberta. *Achillobator gigantibus* (Perle et al. 1999) from the Cenomanian–Santonian of Mongolia also attests the presence of dromaeosaurines in central Asia in the Late Cretaceous.

Troodontidae is a clade of lightly built non-avian maniraptorans with taxa that rank among the smallest non-avian body sizes and the highest encephalization quotients (Makovicky and Norell 2004; Lü et al. 2010; Zanno et al. 2011; Tsuihiji et al. 2014). Troodontids share an anteroventrally inclined quadrate and jaws with a large number of small, constricted teeth set in an open groove in the dentary

(Makovicky and Norell 2004; Turner et al. 2012). The crowns are unserrated in basalmost forms and bear very large hooked denticles in derived taxa, which suggests an herbivorous diet in primitive troodontids and a carnivorous or omnivorous diet in advanced forms bearing serrated teeth (Currie 1987; Holtz et al. 1998; Currie and Dong 2001; Lü et al. 2010; Zanno and Makovicky 2011). Troodontids are known from the Cretaceous of Asia, North America, Europe, and possibly from the Late Jurassic of China, depending on the troodontid affinities of newly discovered forms such as *Anchiornis*, *Xiaotingia*, and *Eosinopteryx* (Makovicky and Norell 2004; Hu et al. 2009; Vullo and Néraudeau 2010; Xu et al. 2011*a*; Turner et al. 2012; Godefroit et al. 2013*b*; Brusatte et al. 2014*a*). Isolated teeth from the Late Jurassic of North America and Portugal and the Late Cretaceous of India have also been assigned to Troodontidae (Chure 1994; Zinke 1998; Goswami et al. 2013). If *Troodon formosus* from the Campanian of Canada is the most famous troodontid and the first to be discovered (Russell 1948; Currie 1985, 1987; Currie and Zhao 1993*b*; Fig. 1.14C), the best preserved troodontid taxa all come from the Cretaceous of Asia. They include *Sinusonasus magnodens* (Xu and Wang 2004), *Mei long* (Xu and Norell 2004; Gao et al. 2012), and *Sinovenator changii* (Xu et al. 2002*b*) from the Early Cretaceous of China, and *Byronosaurus jaffei* (Norell et al. 2000; Makovicky et al. 2003), *Gobivenator mongoliensis* (Tsuihiji et al. 2014), *Saurornithoides mongoliensis* and *Zanabazar junior* (Barsbold 1974; Norell et al. 2009) from the Campanian of Mongolia.

The recent discovery of a large number of paravian taxa closely related to birds such as *Anchiornis huxleyi* (Hu et al. 2009; Fig. 1.15A), *Xiaotingia zhengi* (Xu et al. 2011*a*), *Aurornis xui* (Godefroit et al. 2013*a*), and *Eosinopteryx brevipenna* (Godefroit et al. 2013*b*), all from the Middle to Late Jurassic of the Tiaojishan Formation of China, have brought new data to bear on the relationships of the earliest avian theropods. According to two of the most recent phylogenetic analyses (e.g., Godefroit et al. 2013*a*; Foth et al. 2014), the latter taxa are gathered within Avialae, the most-inclusive clade containing *Passer domesticus* (Linnaeus 1758) but not *Dromaeosaurus albertensis* Matthew and Brown 1922 or *Troodon formosus* Leidy 1856 (Godefroit et al. 2013*a*). Yet, these taxa were recovered in the same clade at the base of Troodontidae in another large scaled phylogenetic analyses (i.e., Brusatte et al. 2014*a*), and their exact position among paravians remains unsettled. For decades the most basal and earliest avialan taxon was considered to be *Archaeopteryx* sp. (Fig. 1.15B), but with the inclusion of these recently reported paravians from the Tiaojishan Formation into cladistic analyses *Archaeopteryx*'s systematic position has become uncertain. Currently, *Archaeopteryx* is either recovered as the basalmost avialan (e.g., Turner et al. 2012; Agnolín and Novas 2013; Brusatte et al. 2014*a*; Choiniere et al. 2014*b*), a deinonychosaur closely related to troodontids and dromaeosaurids (e.g., Xu et al. 2011*a*; Godefroit et al. 2013*b*; Xu and Pol 2014), or an avialan theropod more derived than basalmost avialans *Aurornis* and *Anchiornis* (e.g., Godefroit et al. 2013*a*; Foth et al. 2014). The anatomical distinctions between non-avian and avian theropods are, therefore, particularly subtle and vary according to the phylogenetic analysis performed by authors. For instance, in one of the largest and most recent cladistic analyses provided by Foth et al. (2014) on coelurosaurs,

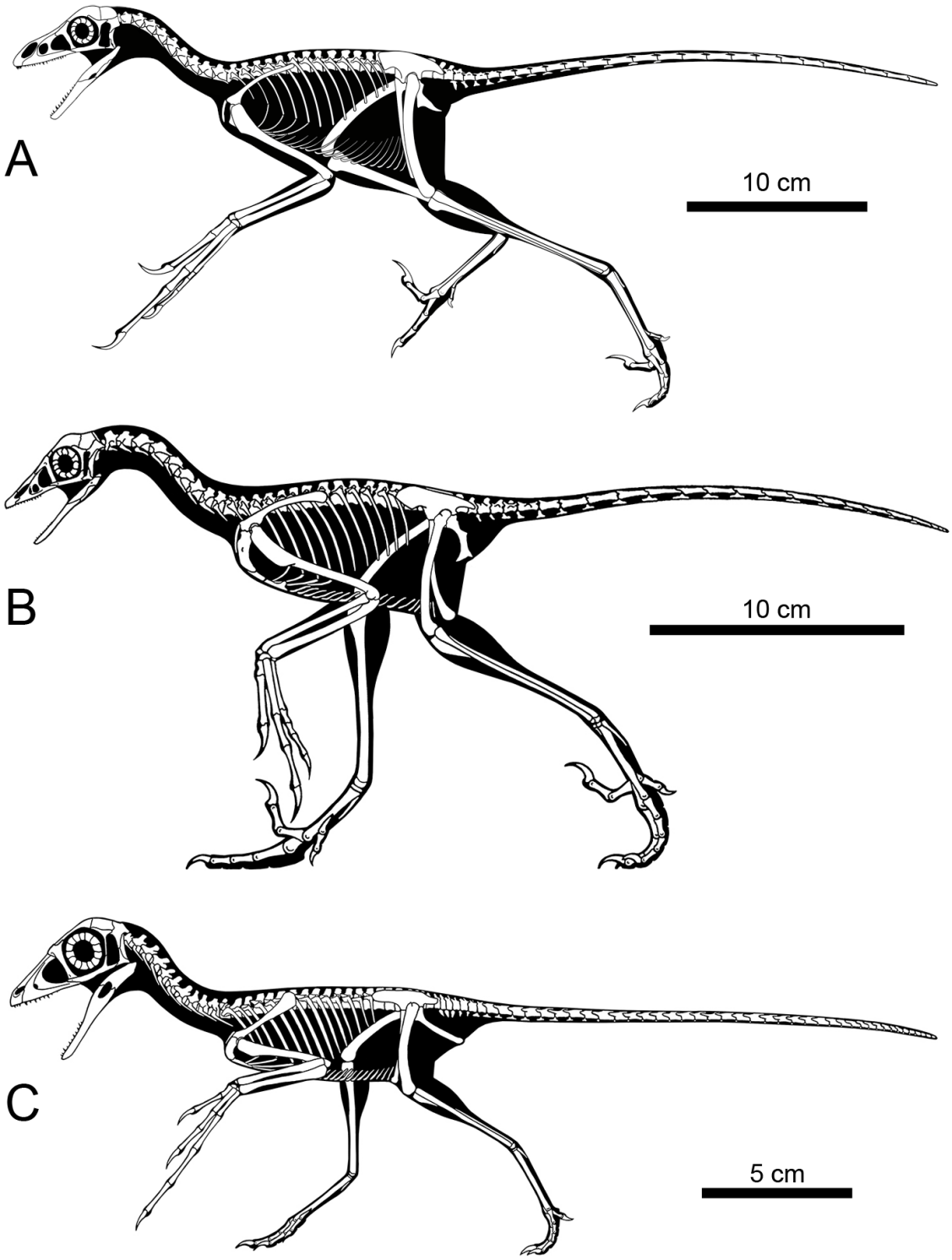

FIGURE 1.15. Skeletal reconstructions of three basal avialan? theropods. **A**, the basal avialan *Anchiornis huxleyi*; **B**, the archaeopterygid *Archaeopteryx* sp.; and **C**, the scansoriopterygid *Epidendrosaurus ninchengensis*. Reconstructions by Ville Sinkkonen for *Anchiornis* and Scott Hartman for *Archaeopteryx* and *Epidendrosaurus*.

avialan synapomorphies include the presence of roots of dentary teeth subcircular in cross-section, extensive contact between pubes, humerus and femur subequal in thickness, and dorsal margin of the antorbital fossa formed by lacrimal and nasal. In another large scaled phylogenetic analysis on

coelurosaurs performed by Brusatte et al. (2014*a*), Avialae are diagnosed by asymmetrical feathers on forelimbs, unfused parietals, less than 26 caudal vertebrae, a dorsal margin of the antorbital fossa formed by lacrimal and nasal, and a humerus longer than the femur.

A similar situation occurs with Scansoriopterygidae and their unsettled phylogenetic position within Pennaraptora. Scansoriopterygids form an aberrant subclade of very small-sized maniraptorans (the only subadult specimen of Scansoriopterygidae has a body length of less than 30 centimeters; Zhang et al. 2008) characterized by a short and high skull bearing a small number of procumbent teeth restricted to the anterior portion of the jaws, propubic pelvis, and elongated ribbon-like tail-feathers (Zhang et al. 2002, 2008; Agnolín and Novas 2013). Their distinctive feature is, however, the slender and hypertrophied manual digit III which suggests climbing ability and arboreal habits (Zhang et al. 2008) or gathering strategy (as the living Ayes Ayes which uses its elongated fingers to pull bugs out of trees; Lhota et al. 2008). This clade currently includes two or three taxa from the Middle Jurassic Daohugou beds (Tiaojishan Formation; Zhou et al. 2013) of Ningcheng, Inner Mongolia, China: *Epidendrosaurus ninchengensis* (= *Scansoriopteryx heilmanni*; Padian 2004; Fig. 1.15C) known from a partial skeleton (Zhang et al. 2002), *Epidexipteryx hui*, the most complete scansoriopterygid preserving a complete skull (Zhang et al. 2008), and possibly *Pedopenna daohugouensis* known from a partial right leg covered with pennaceous feathers (Xu and Zhang 2005). Scansoriopterygids are currently recovered as basal Oviraptorosauria (Agnolín and Novas 2013; Brusatte et al. 2014*a*), basal Paraves (Godefroit et al. 2013*a*, *b*), and basal Avialae (Zhang et al. 2008; Choiniere et al. 2010*b*; Novas et al. 2012; Senter et al. 2012*b*). The clade is also found unresolved by some workers (e.g., Turner et al. 2012).

Conclusions

Theropod dinosaurs form one of the most successful and morphologically diverse groups of tetrapods, surviving the Cretaceous-Paleogene extinction event and radiating as birds in the Cenozoic. Even before the K-Pg extinction non-avian theropods were an extremely diverse group of archosaurs with complex interrelationships. The adoption of cladistic techniques in the 1980s was a major step in the study of theropod phylogenetics; modern analyses currently recover around 25 non-avian theropod subclades, most in a ladder-like organization. While a consensus of higher-level theropod relationships has emerged and the systematics of non-avian theropods seems to be relatively well understood, some significant points of contention remain. Newly discovered non-avian theropods will hopefully shed light on the systematic position of herrerasaurids within saurischians, megaraptorans within avetheropods, scansoriopterygids within pennaraptorans, and troodontids within paravians. Though one might expect few major changes in theropod relationships in the future, large portions of theropod phyletic history remain obscure; future discoveries of theropods in the Jurassic of Australia or the Cretaceous of Antarctica, where theropod faunas are almost unknown, may change the current view of non-avian theropod systematics dramatically.

State of art

Due to their position as ancestors to birds, non-avian theropod dinosaurs have received much interest from vertebrate paleontologists over the past 30 years. However, many aspects of theropod biology, paleogeography and ontogeny remain poorly understood (Rauhut and Fechner 2005). A large number of cladistic analyses have addressed non-avian theropod relationships in great detail (e.g., Rauhut 2003*a*; Holtz et al. 2004; Senter 2007; Smith et al. 2007; Carrano and Sampson 2008; Benson 2010*a*; Benson et al. 2010; Brusatte et al. 2010*d*; Carrano et al. 2012; Senter et al. 2012*a*; Turner et al. 2012; Godefroit et al. 2013*a*; Choiniere et al. 2014*b*; Porfiri et al. 2014) and the phylogeny of this clade is currently relatively well-known. Yet these analyses have focused broadly on the entire skeleton, and none of them has investigated the detailed morphology and evolutionary trends occurring in teeth or in a single bone such as the quadrate.

Since the pioneer work of Owen (1840-1845) on the dentition of the first discovered theropods in the mid-19th century, a large number of studies have been conducted on the systematic paleontology of non-avian theropods teeth (e.g., Buffetaut and Ingavat 1986; Zinke and Rauhut 1994; Rauhut and Kriwet 1994; Rauhut and Werner 1995; Buscalioni et al. 1997; Zinke 1998; Maisch and Matzke 2003; Sweetman 2004; Smith et al. 2005; Smith and Lamanna 2006; Vullo et al. 2007; Fanti and Therrien 2007; Casal et al. 2009; Ősi et al. 2010; Han et al. 2011; Richter et al. 2013; Kear et al. 2013; Tavares et al. 2014; Fanti et al. 2014), with a special interest in the Late Cretaceous theropod fauna of North America (e.g., Gates et al. in press; Currie et al. 1990; Fiorillo and Currie 1994; Baszio 1997; Fiorillo and Gangloff 2001; Sankey et al. 2002; Brinkman 2008; Larson 2008*a*; Longrich 2008; Sankey 2008; Larson and Currie 2013; Williamson and Brusatte 2014). Whereas tooth measurements were first utilized by Currie et al. (1990) for systematic identification of theropod teeth, the first thorough morphometric analyses on theropod teeth were performed by Farlow et al. (1991). These authors used bivariate plots to investigate the relationships between crown size and denticles density, a methodology later followed by Sankey et al. (2002). Smith (2005) and Smith et al. (2005) were, however, the first paleontologist who successfully discriminate theropod teeth to the genus level based on a quantitative methodology and discriminant analyses. Smith et al.'s (2005) methodology was followed by a large number of authors who either performed multivariate analyses based on Smith et al. (2005) dataset (e.g., Smith and Dalla Vecchia 2006; Smith and Lamanna 2006; Ősi et al. 2010; Kear et al. 2013; Richter et al. 2013; Fanti et al. 2014) or on personally created datasets (e.g., Fanti and Therrien 2007; Larson 2008*a*; Larson and Currie 2013; Williamson and Brusatte 2014). The clade of Tyrannosauridae has received a particular attention regarding the morphological variation and function of their teeth. Abler (1992, 1999, 2013) examined the biological function of serrations in tyrannosaurid teeth whereas Erickson (1995) and Schubert and Ungar (2005) discussed the presence of split carinae and wear facets in Tyrannosauridae, respectively. In addition, Samman et al. (2005) used discriminant analysis to quantify the positional and taxonomic variation of tyrannosaurid teeth, and

Smith (2005) explored the heterodonty of *Tyrannosaurus*. More recently, Miyashita et al. (2010) investigated the variation of premaxillary tooth count in Tyrannosauridae, while Buckley et al. (2010) analyzed the intraspecific variation in the dentition of *Albertosaurus*, and Reichel (2010) performed a FEA analysis to examine the effects of heterodonty on tyrannosauroid tooth function.

Although the dental morphology of several theropods such as *Majungasaurus* (Fanti and Therrien 2007; Smith 2007), *Tyrannosaurus* (Smith 2005), *Troodon* (Currie 1987) and *Buitreraptor* (Gianechini et al. 2011*a*) has been described in detail, the anatomy of the dentition of the vast majority of theropods is poorly documented, and sometimes even lack of a description (e.g., Madsen 1976*a*, *b*; Welles 1984; Currie and Zhao 1993*a*; Currie and Carpenter 2000; Madsen and Welles 2000; Allain 2002; Benson 2010*b*; Brusatte et al. 2010*a*; Eddy and Clarke 2011). As noted by Smith (2005), Smith et al. (2005), and Buckley et al. (2010), the morphology and size of denticles, the length of the carinae, and the variation of tooth size and curvature along the tooth row among other anatomical features should be explored further in many theropod taxa, and additional morphometrical data on teeth need to be collected from a large number of theropods. Consequently, a detailed study of the dental anatomy and repartition of dental features in many clades of theropods remains to be done and would greatly facilitate the taxonomic identification of isolated teeth.

If the first detailed studies on theropod teeth by Owen (1840-1845) and Currie et al. (1990) served as a nomenclatural basis to describe theropod teeth, Abler (1992) and Buscalioni et al. (1997) were the first authors to define terms for different theropod tooth sub-units as a standardized nomenclature. Yet, Smith and Dodson (2003) were the only ones to propose a standard terminology on the dentition of theropods and other vertebrates, focusing, however, on anatomical notations and orientation of the dentition and teeth, and omitting to provide a standard nomenclature of their anatomy and morphology. Likewise, terms and notations of measurements variables were first used by Currie et al. (1990) and Farlow et al. (1991) to discriminate theropod teeth, but Smith et al. (2005) were the only ones to thoroughly define and illustrate each measurements variables employed in their morphometric analyses on theropod teeth as a way of standardizing them.

Whereas official standardized anatomical terminologies have been provided by international committees for humans (the *Terminologia Anatomica* by the International Federation of Associations of Anatomists; FIPAT 2011), domesticated mammals (the *Nomina Anatomica Veterinaria* by the International Committee on Veterinary Anatomical Nomenclature; ICVGAN 2012) and birds (the *Nomina Anatomica Avium* by the International Committee on Avian Anatomical Nomenclature; Baumel 1993), the anatomy of most fossil vertebrates typically follows a non-standardized traditional system erected by Sir Richard Owen and elaborated by Alfred Romer (Harris 2004; Wilson 2006). Nevertheless, a large amount of terms describing specific anatomical units of the cranial and postcranial skeleton have not been proposed by these authors, or are simply not followed. Consequently, the terminology and abbreviations used to describe the majority of bones and teeth have been inconsistent in fossil tetrapods, several different anatomical terms for the same sub-entity being

often used. In saurischian dinosaurs, Wilson (1999), followed by Wilson et al. (2011), were the first to present a nomenclature and standardized terminology for the vertebrate laminae and fossae. Besides the standard terminology proposed by Smith and Dodson (2003) for the fossil vertebrate dentitions, no other author has tried to standardize terms employed for teeth and other bones of the skull such as the quadrate and the maxilla. Despite the groundwork on the quadrate of Oviraptoridae by Maryańska and Osmólska (1997), and the antorbital cavity of archosaurs by Witmer (1997*a*), each of them following a well-illustrated terminology to describe the quadrate and maxilla morphology in non-avian theropods, a standardized nomenclature of the quadrate and maxilla anatomy remains to be proposed.

Despite several recent finds of embryonic and hatchling theropods (e.g. Kundrát et al. 2008; Weishampel et al. 2008; Bever and Norell 2009), the ontogeny of the non-avian theropod skull has been particularly poorly studied (Rauhut et al. 2005; Bever and Norell 2009). Ontogenetic variations occurring in the rostrum was investigated by Rauhut and Fechner (2005) in basal Tetanurans based on an isolated maxilla of a hatchling *Allosaurus*, and by Bever and Norell (2009) in Troodontidae based on an incomplete skull of *Byronosaurus*. In Tyrannosauridae, Carr (1999) and Carr and Williamson (2004) examined the general development of tyrannosaurid skull and teeth, whereas Tsuihiji et al. (2011) briefly studied the ontogenetical changes in the cranial morphology of *Tarbosaurus* based on a well-preserved skull of a juvenile individual. Variation of theropod teeth due to ontogenetic change within a single taxon has also been explored by Buckley (2009) and Buckley et al. (2010) for *Coelophysis* and *Albertosaurus*, respectively. Despite the ground work on the ontogeny of the theropod skull, little is known about ontogenetic variation in the dentition, quadrate and maxilla of non-avian theropod and a global view of the ontogeny of these cranial and dental elements is needed.

Objectives

This work aims to thoroughly investigate the anatomy and ontogeny of teeth and quadrates in non-avian theropod dinosaurs with the goal of illuminating evolutionary patterns and processes related to these cranial and dental elements in this particular group of dinosaurs. Several achievements are expected to result from this research project:

- Standardization of the terminology and nomenclature of teeth and quadrate in non-avian theropods.

- Development of a phylogeny of non-avian theropods based on teeth- and quadrate-related characters, useful for an identification key. These cladistic analyses do not aim to clarify non-avian theropod relationships, which are already well understood, but rather to help resolve the phylogenetic position of many indeterminate non-avian theropods based on a single quadrate or one or several isolated teeth in order to clarify the paleogeographical and stratigraphical distribution of many theropod clades.

- Distribution of dental features in non-avian theropods, and examination and evaluation of their functional aspects and phylogenetic potential.

- Identification of the conspicuous major trends observable in the evolution of the quadrate within non-avian theropods, and interpretation of these trends from both biological, biomechanical and paleoenvironmental perspectives.

- Determination of the ontogenetic developments and changes of teeth and quadrate in non-avian theropods.

Structure of the thesis

This thesis is divided in five sections and ten chapters. The first and last sections are the introduction and conclusions, and the three remaining sections concern the evolution of teeth and quadrate in non-avian theropods, as well as the description of *Torvosaurus* remains from the Late Jurassic of Portugal. The present work is an article-based thesis and each chapter corresponds to a manuscript submitted to a scientific journal. A citation of the published or in press/in review article, followed by the 2013 impact factor, is given below the title of the corresponding chapter. At the final stage of the submitted thesis (May 2015), the latter includes four publications, two in press articles, and five manuscripts in review (with all reviewed a first time). All papers but one have been written as a first author. The published papers comprise a single monograph and three scientific articles published in journals with an impact factor ranging from 1.1 (*Zootaxa*) to 5.1 (*Scientific Report*).

Materials and methods

A database of discrete anatomical characters was coded primarily through personal observation of teeth and quadrates in 97 non-avian theropods, and one outgroups (*Eoraptor*) belonging to the palaeontological collections of 28 museums from Argentina, Italy, France, Germany, Portugal, Qatar, Switzerland, United Kingdom, and the United States (Appendices A1.1–2). Teeth and tooth-bearing bones were examined in embryos, juvenile and adult individuals. Denticles and crown ornamentation were viewed under a digital microscope AM411T-Dino-Lite Pro and photographs of the specimens were taken with a digital camera Canon Power Shot SX20 IS and the digital microscope.

A phylogenetic analysis was performed on the data matrix of dentition and quadrate related characters based on more than 60 operational taxonomic units (OTUs) of non-avian theropods examined first hand or from photos and the literature (Appendices A3). TNT v1.1 (Goloboff et al. 2008; freely available at http://www.lillo.org.ar/phylogeny/tnt/) was employed to search for most-parsimonious trees (MPTs). The matrix was analysed under the 'New Technology search' with the 'driven search' option, TreeDrift, Tree Fusing, Ratchet, and Sectorial Searches selected with default parameters, and stabilizing the consensus twice with a factor of 75. The generated trees were then analysed under traditional TBR (tree bisection and reconnection) branch with the 'bbreak = tbr safe' command (Goloboff et al. 2008). Bremer support (Bremer 1994) and Reduced Cladistic Consensus Support Trees (Wilkinson 1994) were calculated with TNT by saving 10,000 suboptimal trees up to 10 steps longer than the MPTs. The consistency and retention indexes as well as the Bremer and relative Bremer supports was calculated using the 'stats' and the 'aquickie' commands, respectively. A bootstrap analysis was also performed with the standard options, and synapomorphies for the consensus tree were listed with the 'list synapomorphies' (Optimize > Synapomorphies) and 'print display buffer' (File > Output) options. The strict consensus tree was then arranged and colored using Dendroscope 2.7.4 (http://dendroscope.org/).

In order to visualize ambiguous and unambiguous synapomorphies on the strict consensus tree, the datasets was also analyzed with WinClada 1.00.08 (Nixon 2002; freely available at http://www.cladistics.com/wincDownload.htm) after making characters non-additive (*fitch*). MPTS were searched by using the Ratchet (Island Hopper) option with default settings. Consensus trees resulting from the cladistic analysis were used to interpret the evolutionary trends of the teeth and quadrate evolution in non-avian theropods.

Measures on teeth were taken with a digital caliper following the methodology proposed by Smith et al. (2005) for teeth. In order to better reflect a normally distributed multivariate dataset, all values were first log-transformed for each variables. Multivariate analyses included a principal component analysis (PCA) and a stepwise discriminant analysis (DFA), and were conducted on the

dataset (grouped by taxa, then by clades) using the program PAST3 (freely available at http://folk.uio.no/ohammer/past/index.html).

The morphometric and phylogenetic morphometric analyses using landmarks on photographs of the quadrate were performed with the software MorphoJ (Klingenberg 2011; available at http://www.flywings.org.uk/morphoj_page.htm) and TNT v1.1, respectively. Photos were compiled using tpsUtil (freely available at http://life.bio.sunysb.edu/morph/soft-utility.html) and the digitization of the landmarks on the pictures was done with tpsDig2 (freely available at http://life.bio.sunysb.edu/morph/soft-dataacq.html). In the morphometric analysis, each landmarks were aligned by a procrustes fit (Preliminaries > New Procrustes Fit) with MorphoJ, once a new project was created from the *.tps file. A principal component analysis (Variation > Principal Component Analysis) was then conducted after generating a covariance matrix (Preliminaries > Generate Covariance Matrix). A wireframe of the quadrate was added (Preliminaries > Create or Edit Wireframe), and the morphospace occupation for each taxon was mapped onto phylogeny (File > Import Phylogeny Files, then Preliminaries > Extract New Classifier From ID Strings, and Comparison > Map onto phylogeny) along the two principal axes of the PCA, after importing a .nex file of the consensus classification of non-avian theropods created with Mesquite (freely available at http://mesquiteproject.org/mesquite/download/download.html).

As for the phylogenetic morphometric analysis, the file resulting from the digitization of the landmarks with tpsDig2 was taken to tpsRelw (freely available at http://life.bio.sunysb.edu/morph/soft-tps.html) in which the alignments was saved by using the 'Save aligned specimens' option (Data > select the .tps file, then comput Consensus, Partial warps and Relative warps, then File > Save > Aligned specimen). The resulting *.tps file was then converted into a *.tnt file with the program tps2tnt.exe (available at https://app.box.com/shared/dnheogzd2q) in order to run on TNT. To reconstruct a phylogeny from landmark data alone, the TNT script LandschW.run (available at http://tnt.insectmuseum.org/index.php/Scripts/LandschW.run) was used, and the commands 'landsch' and 'lmark map' allowed to perform the analysis and display the results, respectively. Using the same commands, the TNT script Landcombsch.run (available at http://tnt.insectmuseum.org/index.php/Scripts/Landcombsch.run) was used to run the search combining discrete characters and landmarks data.

Case of study

Cladistic and morphometric analyses performed as a mean to assess the phylogenetic potential of teeth and quadrate were applied on isolated theropod teeth stored at the Museu of Lourinhã (Portugal) and isolated quadrates deposited in the Wyoming Dinosaur Center (USA) and the Museo di Storia Naturale di Milano (Italy). Isolated theropod teeth are abundant in the Lourinhã Formation (Kimmeridgian–Tithonian, Upper Jurassic) of Portugal and show a large variety of morphology. As a case of study, four isolated theropod teeth stored at the Museu of Lourinhã (ML 327, 939, 962 and 966) were selected and identified based on morphometric and anatomical data collected on theropod teeth (chapter 4). The shed teeth were thoroughly described following the 'modus operandi' given to describe theropod teeth. They were included in the cladistic analysis performed on the data matrix of dentition-based characters and the supermatrix, as well as a morphometric analysis using bivariate plots. A maxilla preserving in situ teeth (ML 1100) from the Lourinhã Formation and referred to the megalosaurid *Torvosaurus*, allowed to thoroughly describe the crown, root, and denticle morphology in *Torvosaurus* (chapter 9). A comparison between the teeth of the Portuguese specimen of *Torvosaurus* and the dentition of six other megalosaurid taxa examined first hand (i.e., *Afrovenator*, *Megalosaurus*, *Duriavenator*, *Magnosaurus*, *Eustreptospondylus*, and *Dubreuillosaurus*) gave us the opportunity to provided a detailed description of the dentition of Megalosauridae (chapter 5).

As a second case of study, six isolated quadrates (WDC-CSG Q1 to Q5, and MSNM V6896) from the Kem Kem beds of Morocco (Cenomanian, Upper Cretaceous) were identified based on the cladistic analysis performed on the quadrate-related data matrix (chapter 8). Due to the peculiar morphology of the mandibular articulation, a morphofunctional analysis of the quadrates from Morocco was conducted based on geometric morphometric and phylogenetic morphometric techniques. Five bones were determined to be from juvenile, immature, subadult and adult individuals of the same species, allowing to explore ontogenetic changes occurring in the quadrate of this taxon.

Investigation on the dental morphology of the *Torvosaurus* maxilla from Portugal resulted in the description of the bones referred to the specimen ML 1100 (a left maxilla and a caudal vertebra) as well as other cranial and postcranial material found in Portugal and assigned to *Torvosaurus* (i.e., anterior portion of a right maxilla, a left femur, and a left a tibia; Chapter 9). Following the proposed terminology on theropod teeth and quadrate, a standard terminology on the theropod maxilla was given as a mean to describe in detail the maxilla of *Torvosaurus*. Description of embryonic remains of a new theropod (ML 1188) preserving in situ teeth, combined with the examination of the maxilla of embryonic and hatchling specimens of *Lourinhanosaurus* (ML 565), *Allosaurus* (MG 27804), and *Byronosaurus* (IGM 100-972), finally leaded to examine the early development of the maxilla and teeth in basal theropods (chapter 10).

Sedimentology and chronostratigraphy of the Lourinhã Formation and the Kem Kem beds

Material used as cases of study comes from two rich Mesozoic fossil sites known for their abundance in dinosaur remains, namely the Lourinhã Formation and the Kem Kem beds. Both areas show a particularly high diversity of theropods, with no less than five coexisting theropod clades. The Kimmeridgian–Tithonian Lourinhã Formation of Central-West Portugal (Figs. 1.15–1.16) is contemporaneous to and similar with the Morrison Formation of North America in terms of paleoenvironment and sedimentology (Mateus 2006). The Late Jurassic theropod fauna of Portugal is represented by at least six clades, namely Ceratosauridae, Megalosauridae, Allosauridae, Tyrannosauroidea, basal Coelurosauria, and Dromaeosauridae (Mateus 1998; Zinke 1998; Rauhut 2003*b*; Mateus et al. 2006; Hendrickx and Mateus 2014*a*, *b*; Malafaia et al. 2014). The Kem Kem beds of South-eastern Morocco (Fig. 1.17-1.18), dated to the Cenomanian (Lower part of the Upper Cretaceous), is contemporaneous to the Bahariya Formation of Western Egypt, and both units also show the same geology and paleoenvironment (Cavin et al. 2010). Theropod clades from the Kem Kem beds include non-abelisaurid Ceratosauria, Abelisauridae, Spinosauridae, Carcharodontosauridae, and Dromaeosauridae (Russell 1996; Sereno et al. 1996; Amiot et al. 2004*a*; Dal Sasso et al. 2005; Mahler 2005; Cau et al. 2012; McFeeters et al. 2013; Ibrahim et al. 2014*a*, *b*). A brief overview on the sedimentology and chronostratigraphy is here provided for these two theropod-dominated units.

Lourinhã Formation

The Lourinhã Formation is a clastic continental succession that occurs throughout the Lusitanian Basin of central west Portugal (Fig. 1.15A; Taylor et al. 2014). First coined by Hill (1988) and Wilson (1988), the Lourinhã Formation is a laterally extensive unit mostly from the Late Jurassic (Late Kimmeridgian to early Berriasian) and ranging in thickness from 200 to 1100 meters (Hill 1988; Mateus et al. 2014; Taylor et al. 2014 and references therein). The Lourinhã Formation comprises most of Late Jurassic deposits of the Lourinhã area (Figs. 1.15-1.16) and overlies conformably the Alcobaça Formation, a shallow marine to transitional (deltaic and estuarine) sequence with occasional carbonate levels dated to the Kimmeridgian (Mateus et al. 2014). The Alcobaça Formation has yielded a very diversified fauna which was revealed during fieldworks by the Germans in the coal mine of Guimarota, near the city of Leiria in Central Portugal, in the second half of the 20th century (Martin and Krebs 2000). The Guimarota ecosystem includes fishes, turtles, crocodiles, pterosaurs, mammals, ornithischians, sauropods, and theropods such as the tyrannosauroid *Aviatyrannis*, and the possible paravians *Paronychodon* (Zinke and Rauhut 1994; Martin and Krebs 2000; Rauhut 2003*b*).

A number of published lithostratigraphic schemes have attempted to sub-divide the Lourinhã Formation into members and beds, so that different terms have been proposed for similar

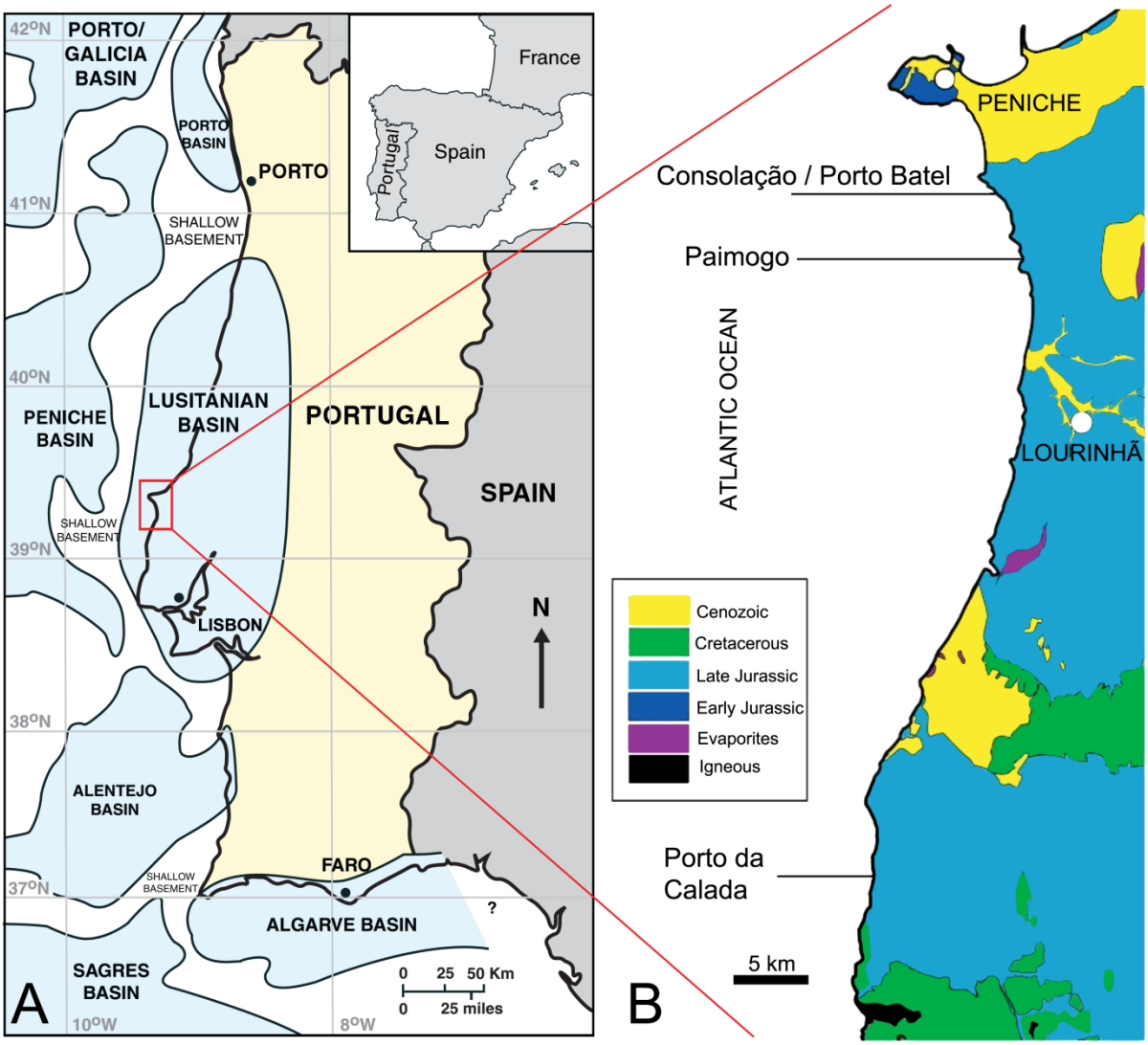

FIGURE 1.15. Geology and chronostratigraphy of Portugal. **A**, Sedimentary basins of Portugal. The Lusitanian Basin covers the central-west part of Portugal, including Lisbon and the region of Lourinhã (modified after Taylor et al. 2014); **B**, Simplified chronostratigraphic map of the Lourinhã region. The Late Jurassic deposits (in light blue) are mostly comprised in the Lourinhã Formation which covers most of the Lourinhã area (modified after Mateus et al. 2014).

lithostratigraphic units of the Lourinhã Formation (Mateus et al. 2014; Taylor et al. 2014). This work follows the lithostratigraphic framework given by Mateus et al. (2014) which mainly adheres to the subdivisions proposed by Hill (1989) for the Lusitanian Basin. Mateus et al. (2014) recognize three main lithostratigraphic divisions within the Lourinhã Formation, from lower to upper: the Praia da Amoreira and Porto Novo members, the Praia Azul Member, and the Assenta Member.

The Praia da Amoreira Member corresponds to sand and mudrock heterolithic facies with frequent bioturbation and soft-sediment deformations, lenses of meter-thick sandstone, and massive mudrock with calcrete horizons (Mateus et al. 2014). The overlaying Porto Novo Member is defined by larger bodies of cross-bedded sandstone composed of laminae rich in Carbonaceous particles, and mudrocks rich in calcrete soils. The Praia da Amoreira Member was deposited by a meandering river system, and the Porto Novo Member corresponds to a fluvial meander system grading laterally to tide-

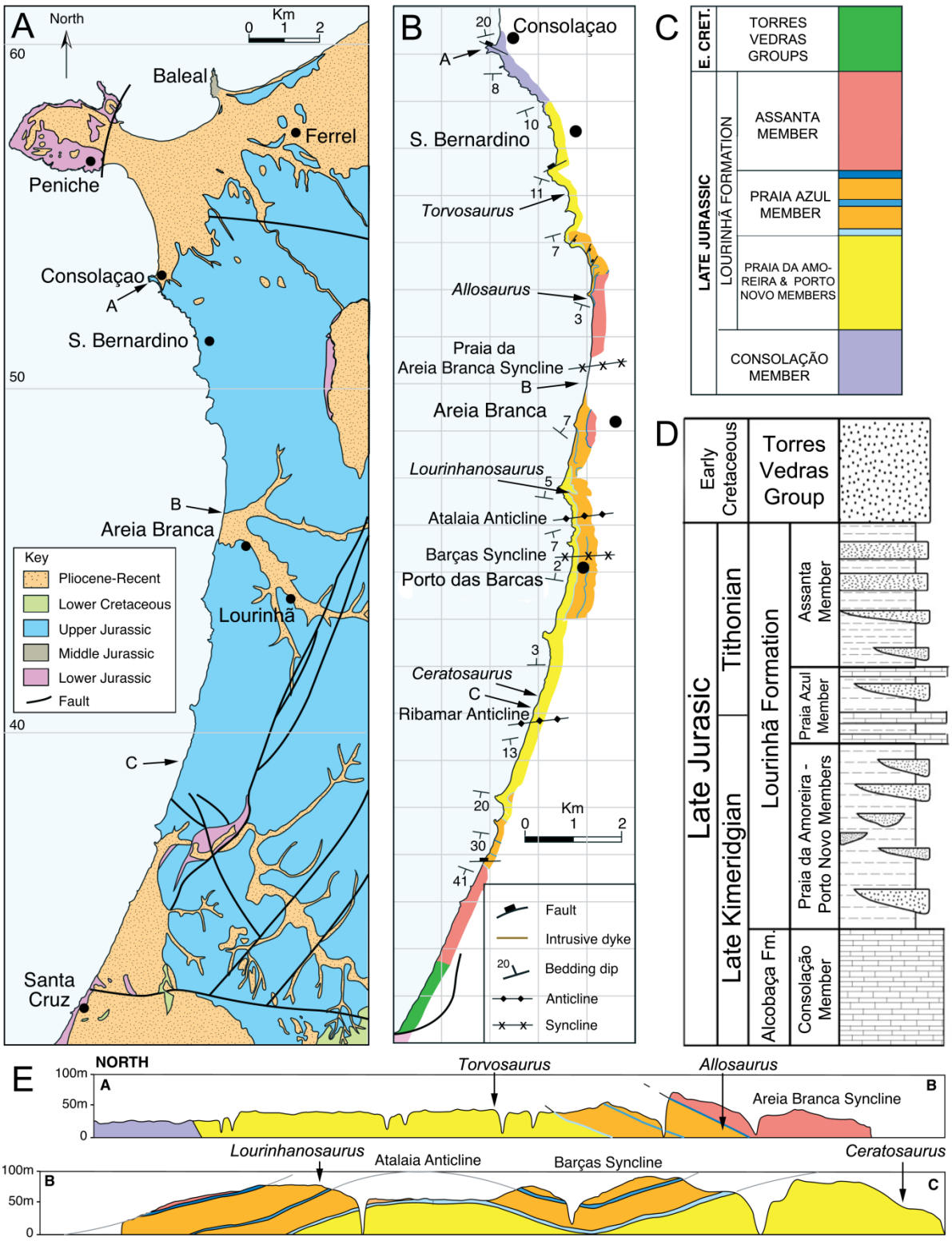

FIGURE 1.16. Geological map and sections of the Lourinhã area. **A**, Simplified chronostratigraphic map of the areas of Peniche, Lourinhã and Santa Cruz; **B**, Lithostratigraphic map of the coast of Porto das Barcas, Areia Branca, San Bernardino and Consolação, with location of sites where *Ceratosaurus*, *Torvosaurus*, *Allosaurus*, and *Lourinhanosaurus* were found. Colors of the different units are given in C; **C**-**D**, Stratigraphic columns of the Lusitanian Basin; **E**, Cliff section between Consolação (A) Areia Branca (B), and Ribamar (C), with location of sites where *Ceratosaurus*, *Torvosaurus*, *Allosaurus*, and *Lourinhanosaurus* were found. (Modified from Taylor et al. 2014 for A–C, and E; and from Araújo et al. 2013 for D).

influenced deltas (Mateus et al. 2014; Taylor et al. 2014). Both members are dated as latest Kimmeridgian and have yielded the theropods *Ceratosaurus* sp., and *Torvosaurus gurneyi* (Mateus et al. 2014; Fig. 1.16B, E).

The Praia Azul Member is defined by marls and mudstones, as well as rare sandstone bodies that sometimes display intense bioturbation, ripple marks, cross-beddings, and carbonaceous debris. This unit also comprises three levels of limestone with a brackish bivalve association and some bivalve patch-reefs (blue layers in Fig. 1.16C, E), the lowermost and the uppermost layers making the lithostratigraphic boundary with the Porto Novo and Assenta members (Fig. 1.16D). The Praia Azul Member is dated with confidence to the latest Kimmeridgian to earliest Tithonian, and has yielded the theropods *Allosaurus europaeus* and *Lourinhanosaurus antunesi* (Mateus et al. 2014; Fig. 1.16B, E). It was deposited by fluvial meandering systems flowing in a coastal plain, and connected with transitional systems such as deltas, sandy bay shorelines and brackish lagoons due to marine incursions (Mateus et al. 2014; Taylor et al. 2014). Finally, the Assenta Member is a mudstone dominated unit intercalated with cross-bedded sandstones, some levels of caliche (pedogenic carbonate concretions), and nodular and marly bioclastic limestone. The Assenta Member is late Early Tithonian to earlier Berriasian in age and was formed by upper fluvial-dominated delta to meandering fluvial systems with occasional transgressions. The latter allowed the establishment of inner and restricted lagoons and the formation of shallow carbonate platforms (Mateus et al. 2014). So far, theropod remains have not been found in the Assenta Member (Mateus pers. comm.).

Kem Kem beds

The Kem Kem is a vast tabular rocky plateau (or hamada) bounding the Algerian boundary in south-eastern Morocco. This region has yielded a large number of vertebrate remains all originating from a continental unit referred as the Kem Kem beds (Sereno et al. 1996; Fig. 1.17). Formerly known as the ‘Continental Intercalaire’ (*sensu* Kilian 1931; Lavocat 1954*a*; de Lapparent 1960), the Kem Kem beds form a 150 to 200 meters thick continental succession exposed along the face of a limestone-capped escarpment, which extends some 250 km in length along, or close by, the Algerian border of Morocco (e.g., Lavocat 1954*a*; Russell 1996; Cavin et al. 2010; Belvedere et al. 2013; Ibrahim et al. 2014*a*). The Kem Kem beds overlie Paleozoic (Cambrian to Silurian) sediments unconformably, and are currently dated to the Cenomanian (Sereno et al. 1996; Dutheil 1999; Cavin et al. 2010). They comprise fluvial to coastal deposits typically divided into two main units, the Ifezouane and Aoufous formations (Ettachfini and Andreu 2004; Cavin et al. 2010; Fig. 1.18).

The Ifezouane Formation, which corresponds to the ‘Grès Infracénomaniens’ of Choubert (1948), the ‘Grès rouges infracénomaniens’ of Joly (1962) and the ‘lower unit’ of Sereno et al. (1996), consists of reddish detritic sandstones with cross-stratified structures alternating with pinkish sands, occasional conglomeratic layers of quartz pebbles, and some calcareous layers containing bivalves and gastropods (Joly 1962; Abramovich et al. 2003; Ettachfini and Andreu 2004; Cavin et al. 2010). The

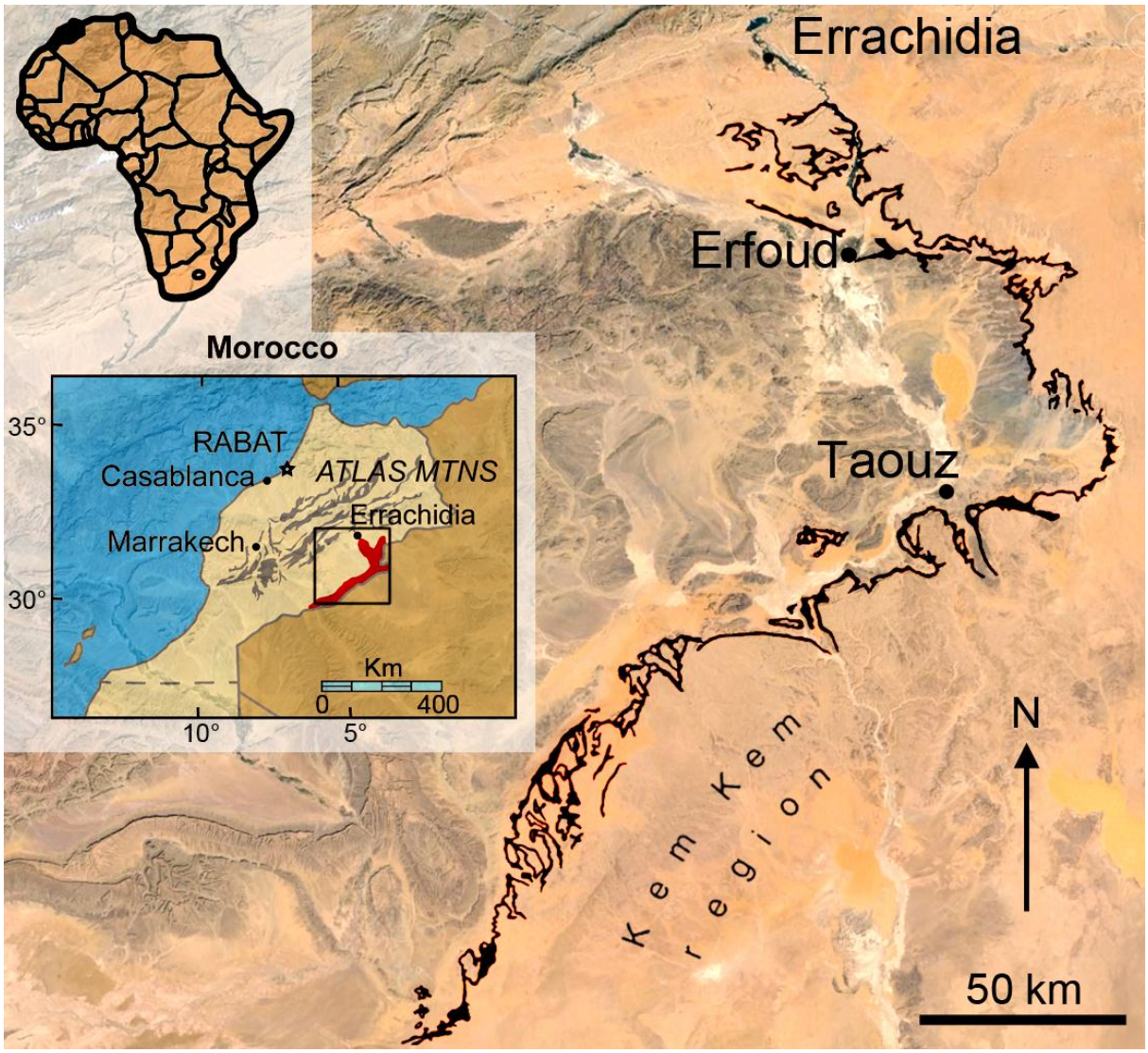

FIGURE 1.17. Geographical location and stratigraphy of the Kem Kem beds. **A**, Location of Morocco (in black) in Africa (left corner), the Kem Kem region (in red) in Morocco (middle left), and the Kem Kem beds (in black) in the Kem Kem plateau (right); **B**, Stratigraphic column of the Kem Kem beds of South-Eastern Morocco. Modified from Sereno et al. (1996) and Ibrahim et al. (2014*a*).

thickness of this unit is extremely variable (from 0 to 250 meters) and typically decreases from the south to the north (Choubert 1948; Cavin et al. 2010). The base of the Ifezouane Formation is made of conglomerates and breccia intercalated with poorly cemented reddish sandstones, whereas the upper part comprises finer-grained, better calibrated, and uniform sandstones with lighter colors that can become yellow (Joly 1962). According to Belvedere et al. (2013), the reddish fluvial sandstones are organized in meter-thick beds, and show high-angled cross-bedding, representative of channel belt successions, with subordinate intercalations of pedogenized overbank mudstones. This facies was interpreted by the authors "as a braided fluvial system [and] a fully continental depositional environment characterized by high-energy deposits" (Belvedere et al. 2013, p. 53). The Ifezouane Formation is the richest unit in terms of skeletal elements and has yielded articulated specimens of *Spinosaurus*, *Deltadromeus* and *Rebachisaurus* (Cavin et al. 2010; Ibrahim et al. 2014*b*).

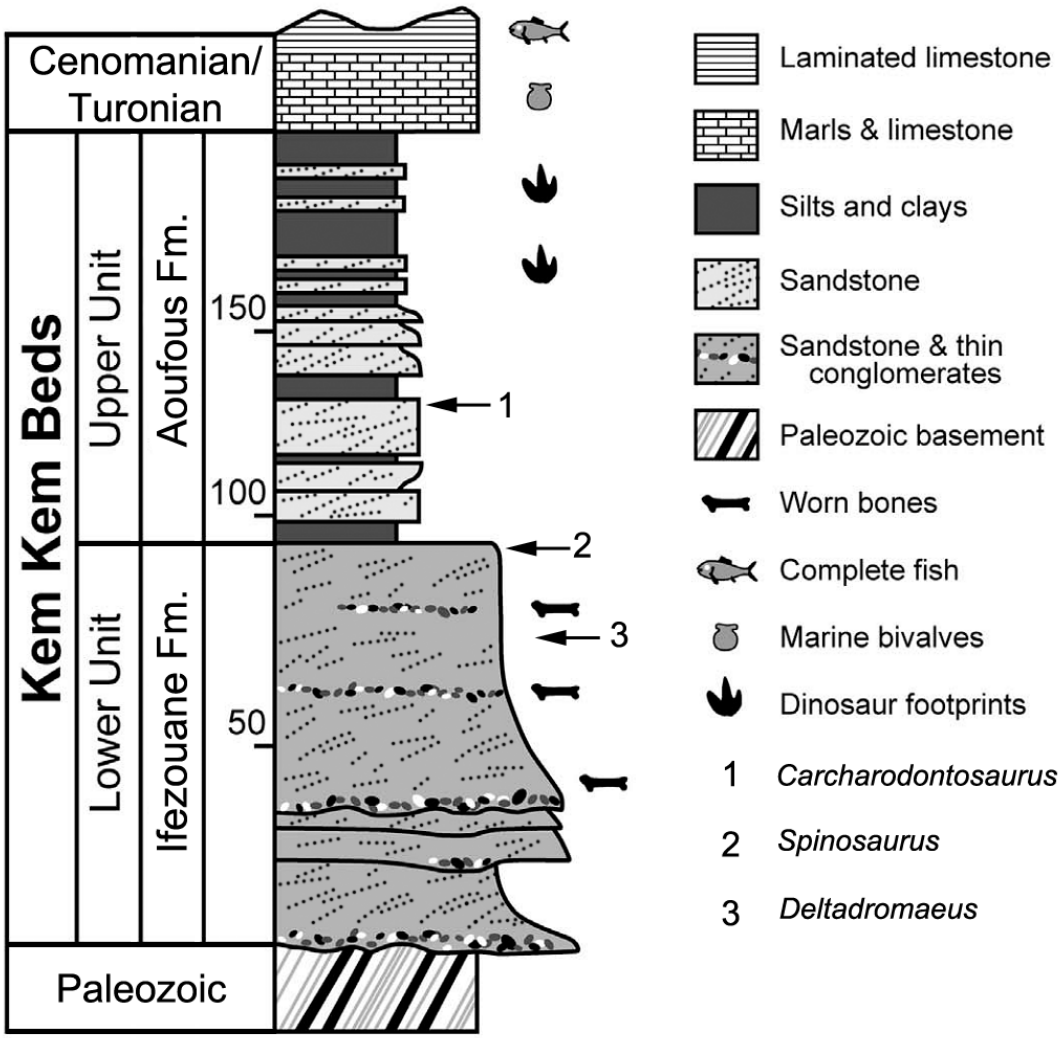

FIGURE 1.18. Stratigraphic column of the Kem Kem beds of South-Eastern Morocco. Modified from Ibrahim et al. (2014*a*).

The Aoufous Formation, also known as the 'Marnes à gypses cénomaniennes' (Choubert 1948), the 'Marnes versicolores à gypse' (Joly 1962) and the 'upper unit' (Sereno et al. 1996), varies in thickness from 100 to 200 meters (Cavin et al. 2010). This unit is mostly comprised of multi-colored sandstone marls, with intercalations of thinly-bedded detritic sandstones, microconglomerates, calcitic palaeosols, thin intercalations of evaporites (fibrous and saccharoïd gypsum), and yellowish dolomitic layers (Joly 1962; Ettachfini and Andreu 2004; Cavin et al. 2010; Belvedere et al. 2013; Ibrahim et al. 2014*a*; Fig. 1.18). According to Belvedere et al. (2013) and Cavin et al. (2010), this facies association represents a coastal lagoon/mudflat deposited in a medio to supralittoral paleoenvironment, and a low-energy environment close to the shoreline with local development of sabkhas and marginal ponds of water. The sandstone layers of the Aoufous Formation have yielded a large diversity of theropod footprints (Sereno et al. 1996; Belvedere et al. 2013; Ibrahim et al. 2014*a*; Fig. 1.18), and skeletal remains from the Aoufous Formation are mostly comprised of *Onchopristis* teeth. According to Cavin et al. (2010), vertebrate remains are only abundant in the Aoufous

Formation in the northern part of the Kem Kem, such as in the Douira locality, north of Erfoud. Yet fossiliferous levels from Douira essentially include microfossils, and classical vertebrate remains found in this locality most likely come from the upper part of the Ifezouane Formation (Cavin pers. comm.). It is, therefore, very likely that most, if not all dinosaur remains reported from the upper unit, such as the *Carcharodontosaurus* cranial material described by Sereno et al. (1996) and Brusatte and Sereno (2007), come from the upper part of the Ifezouane Formation. It is, however, possible that the upper and lower units defined by Sereno et al. (1996) do not exactly correspond to the Aoufous and Ifezouane formations (Cavin pers. comm.), and that the thick layer of sandstone which yielded *Carcharodontosaurus* remains (Sereno et al. 1996: fig. 1C) might in fact be considered as belonging to the Ifezouane Formation by Cavin et al. (2010).

II. EVOLUTION OF TEETH

Chapter 2: A proposed terminology of theropod teeth (Saurischia: Dinosauria)

Accepted in ***Journal of Vertebrate Paleontology*** (IP 2.079):
Hendrickx, C., Mateus, O. and Araújo, R. in press. A proposed terminology of theropod teeth (Saurischia: Dinosauria). *Journal of Vertebrate Paleontology*.

Abstract

Theropod teeth are typically not described in detail, yet these abundant vertebrate fossils are not only frequently reported in the literature, but also preserve extensive anatomical information. Often in descriptions, important characters on the crown and ornamentation are omitted, and in many instances, authors do not include a description of theropod dentition altogether. The paucity of information makes identification of isolated teeth difficult and taxonomic assignments uncertain. Therefore, we here propose a standardization of the anatomical and morphometric terms for tooth anatomical sub-units, as well as a methodology to describe isolated teeth comprehensively. As a corollary, this study exposes the importance of detailed anatomical descriptions with the utilitarian purpose of clarifying taxonomy and identifying isolated theropod teeth.

Introduction

Theropod shed teeth are abundant in the terrestrial fossil record and are frequently described (e.g., Currie et al. 1990; Rauhut and Werner 1995; Baszio 1997; Zinke 1998; Ősi et al. 2010; Han et al. 2011; Larson and Currie 2013; Sues and Averianov 2013), yet their morphology is surprisingly poorly known. The theropod dentition has been thoroughly described for only a few taxa, e.g., *Coelophysis*, *Majungasaurus*, *Tyrannosaurus*, *Troodon*, and *Buitreraptor*, and some Upper Cretaceous theropods of North America (e.g., Gates et al. in press; Currie 1987; Currie et al. 1990; Fiorillo and Currie 1994; Baszio 1997; Fiorillo and Gangloff 2001; Sankey et al. 2002; Smith 2005, 2007; Fanti and Therrien 2007; Brinkman 2008; Longrich 2008; Sankey 2008; Buckley 2009; Larson et al. 2010; Gianechini et al. 2011*a*; Larson and Currie 2013). Yet, several pivotal theropod taxa with well-preserved dentitions still lack a thorough dental description (e.g., *Allosaurus*, *Ceratosaurus*, *Sinraptor*, and *Yangchuanosaurus*), leading numerous authors to identify isolated theropod teeth to broad clades with uncertainty (e.g., Madzia in press; Ősi et al. 2010; Amiot et al. 2011; Carrano et al. 2012; Ruiz-Omeñaca et al. 2012). Nevertheless, due to the elevated apatite concentration, teeth are the hardest known skeletal structures (Martin 1999). Thus, isolated teeth are key pieces of evidence to assess vertebrate paleoecological diversity, and are often used for stable isotopic studies with various applications (e.g., Amiot et al. 2004*b*, 2006, 2010*b*, 2011). A better understanding of theropod

anatomy and morphological variation is, therefore, central to help resolving systematic relationships and to provide paleoecological clues. Tooth morphology is tied to diet, which has extensive evolutionary repercussions such as morphological convergence more than other parts of the skeleton. Yet theropod teeth have been shown to possess many diagnostic features of taxonomic value (e.g., Currie et al. 1990; Smith 2005, 2007; Smith et al. 2005; Hendrickx and Mateus 2014*b*). Although theropod teeth seem simple at first sight, this is effectively a result of the absence of comprehensive studies on tooth anatomy and morphological variation among theropods, as well as the lack of a uniform anatomical nomenclature.

This contribution proposes a standardized list of anatomical, morphological and morphometric terms and abbreviations for each tooth anatomical sub-unit and each measurement previously taken in theropod teeth. Additionally, we propose a methodology to describe isolated teeth thoroughly.

Positional nomenclature

Although the taxonomic and systematic value of theropod dentitions is less important than mammalian dentitions, theropod teeth are usually recognized at the family level, but some isolated teeth are identified to the species level (e.g., Currie et al. 1990; Smith et al. 2005; Fanti and Therrien 2007; Larson and Currie 2013; Hendrickx and Mateus 2014*b*). The crown, carinae, denticles and enamel structures exhibit taxonomically informative morphological variability among theropods (Currie et al. 1990; Smith et al. 2005; Larson and Currie 2013; Hendrickx and Mateus 2014*b*). Unfortunately, the directional, orientation, and anatomical terminology used to refer to theropod teeth in the literature has been inconsistent. As such, we hereby propose standardizing this terminology. Each term is illustrated (Figs. 2.1–2.6) and followed by a definition, and each anatomical and morphometric term is associated with a two to four letters abbreviation to be used in illustrations (Figs. 2.1–2.4, 2.7).

Positional nomenclature largely follows the dental orientation proposed by Smith and Dodson (2003). This positional nomenclature works by identifying the side of the jaw (i.e., left = L; right = R), followed by the abbreviation of the tooth-bearing bone (i.e., premaxilla = pm; maxilla = mx; dentary = dt) and then, the position occupied along the tooth-bearing bone. The first tooth is the mesial one. As an example, Lpm2 refers to the second left premaxillary tooth, and Rdt7, seventh right dentary tooth.

Tooth Orientation

Apical—The direction from the cervix to the apex (Fig. 2.1C, E). This term is bidirectional and can refer to the direction towards the crown apex for the crown, or towards the root apex for the root (Smith and Dodson 2003).

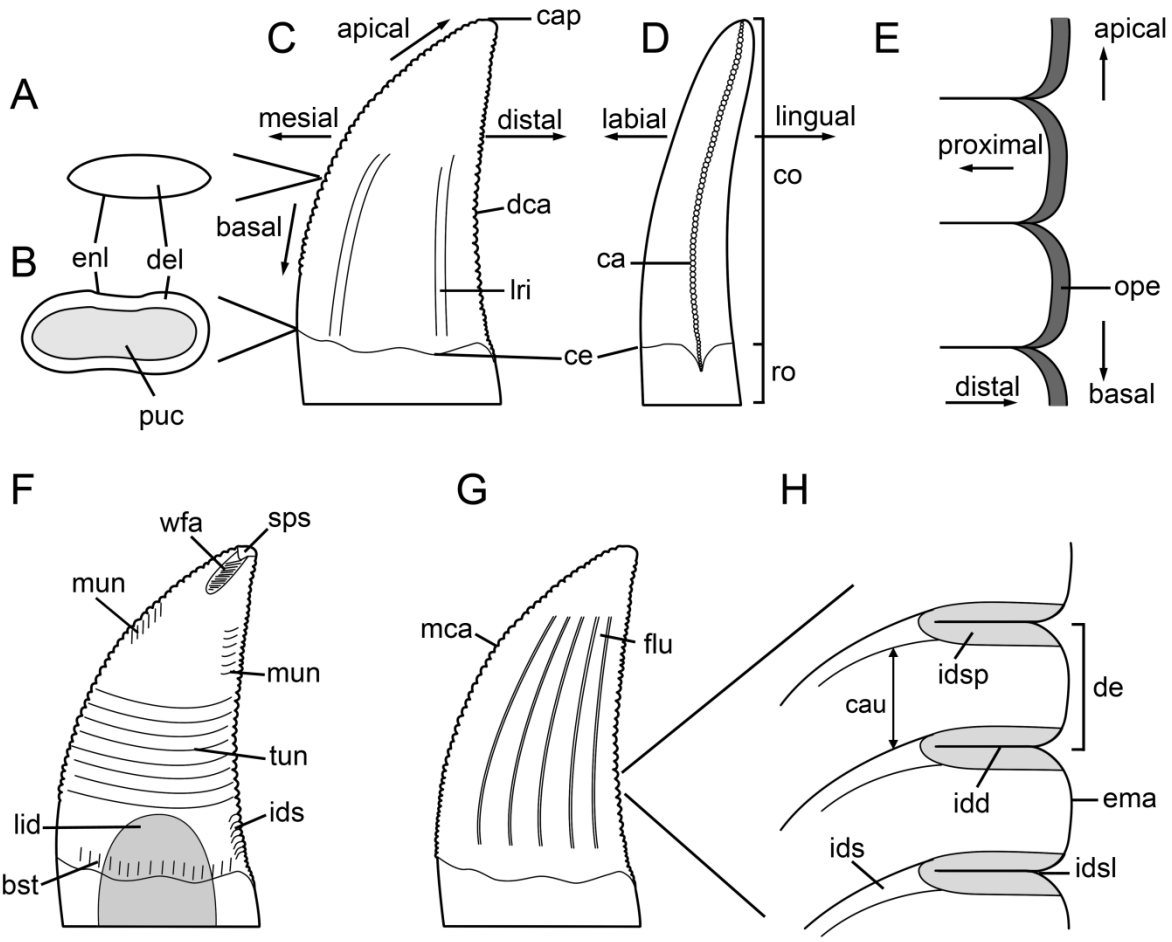

FIGURE 2.1. Anatomical terminology used in this study. **A**, mid-height cross-section of crown in C, in apical view; **B**, basal cross-section of crown in C, in basal view; **C**, idealized lateral theropod tooth in labial view; **D**, idealized lateral theropod tooth in distal view; **E**, idealized distal denticles of theropod crown; **F**, idealized lateral theropod tooth in labial view showing the crown ornamentations and attributes; **G**, idealized fluted theropod tooth, in labial view; **H**, idealized distal denticles showing denticle structures, in labial view. **Abbreviations**: **bst**, basal striation; **ca**, carina; **cap**, crown apex; **cau**, cauda; **ce**, cervix; **co**, crown; **dca**, distal carina; **de**, denticle; **del**, dentine layer; **enl**, enamel layer; **ema**, external margin; **flu**, flute; **idd**, interdenticular diaphysis; **ids**, interdenticular sulci; **idsl**, interdenticular slit; **idsp**, interdenticular space; **lid**, lingual depression; **mun**, marginal undulation; **mca**, mesial carina; **ope**, operculum; **puc**, pulp cavity; **ro**, root; **sps**, spalled surface; **tun**, transverse undulation; **wfa**, wear facet.

Basal—The direction from the apex to the cervix (Fig. 2.1C, E). The term is also bidirectional and refers to the direction towards the cervix for both the crown and root (Smith and Dodson 2003).

Mesial—The direction towards the jaw symphysis (Smith and Dodson 2003; Fig. 2.1C). Mesial can refer also to the surface facing the jaw symphysis.

Distal—This term is used slightly differently for teeth versus denticles. For the tooth, distal refers to the direction away from the jaw symphysis and towards the posterior end of the jaw (Smith and Dodson 2003; Fig. 2.1C). For the denticle, distal refers to the direction away from the crown, from the denticle base to the denticle apex (Fig. 2.1E).

Proximal—From the denticle apex to the base, proximal refers to the direction towards the crown (Smith and Dodson 2003; Fig. 2.1E).

Labial—The surface or direction pointing from the skull outwards, thus towards the lips or cheeks (Smith and Dodson 2003; Buckley 2009; Fig. 2.1D).

Lingual—The surface and direction towards the skull midline, thus facing the tongue (Smith and Dodson 2003; Buckley 2009; Fig. 2.1D).

Tooth Situation and Position

Isolated—Tooth shed or non-articulated with the tooth-bearing bone (Buckley 2009).

Shed tooth—Tooth lost in vivo, either falling out by the eruption of the replacement tooth or when processing food (e.g., biting, impaling, shearing, chewing), and, therefore, only preserving the crown and the basalmost part of the root (Fiorillo and Currie 1994).

In Situ—Tooth within the alveolus of the tooth-bearing bone (Buckley 2009).

Erupted—Crown that grew outside the tooth-bearing bone, thus fully visible in the mouth.

Unerupted—Crown within the alveolus and still inside the jaw, and therefore not visible or only partially visible in the mouth.

Mesial Dentition—Premaxillary teeth as well as mesialmost dentary and, in some cases, maxillary teeth that share a morphology similar or closer to this of premaxillary teeth than more distal dentary and maxillary teeth (Hendrickx and Mateus 2014*b*).

Lateral Dentition—Maxillary and dentary teeth that share a morphology significantly differing from this of mesial teeth (Hendrickx and Mateus 2014*b*). Because the morphology of mesial teeth gradually changes to that of the lateral teeth, there is no precise boundary, and a transitional zone between mesial and lateral dentition may exist. The boundary between these two dentition types is arbitrary. In some theropods such as spinosaurids, premaxillary and lateral maxillary/dentary teeth share a similar morphology so that the distinction between mesial and lateral dentition is not relevant in these taxa.

Anatomical nomenclature

The anatomical terms of the theropod dentition were grouped in three main sections: tooth anatomy, denticle anatomy, and crown and enamel ornamentations. The terms for each tooth sub-unit were selected by their relevance in the theropod literature, and a reference of the first occurrence of each term was given, except for those referring to other part of the skeleton or to non-vertebrate organisms (e.g., apex, cervix, carina, denticle), or whose origin is prior to the 19th century. The anatomical terminology follows the nomenclature proposed by Smith and Dodson (2003) and Smith et al. (2005) for the general tooth anatomy, Abler (1992), Buscalioni et al. (1997) and Smith (2007) for the denticle anatomy, and Schubert and Ungar (2005) and Hendrickx and Mateus (2014*b*) for the crown structures and enamel textures. The large majority of terms have already been used by these authors and only interdenticular diaphysis, and enamel undulation are here proposed for the first time.

Tooth Anatomy

Crown (co)—Portion of the tooth covered with enamel, typically situated above the gum and protruding into the mouth (Schwenk 2000; Licker 2003; Figs. 2.1D, 2.2A). The crown (‘couronne’ of Fauchard 1728; Cuvier 1805; ‘corona dentis’ of Illiger 1811; Owen 1840) is composed of a layer of hard, shiny enamel, and an inner core of resilient dentine, and is excavated by the pulp chamber internally (Hillson 2005). In theropods with labiolingually narrow teeth, the crown includes two wide labial and lingual surfaces, and two narrow mesial and distal surfaces, which often have carinae.

Crown base (cob)—Region of the tooth immediately above and adjacent to the basal limit of the enamel layer.

Root (ro)—Portion of the tooth beneath the gum and embedded in an alveolus or an open alveolar groove (‘racine’ of Fauchard 1728; Cuvier 1805; ‘radix dentis’ of Illiger 1811; Owen 1840; Hillson 2005; Figs. 2.1D, 2.2A). In dinosaurs, the root is composed of a layer of dentine delimiting the outer limit of the pulp cavity. Peyer (1968) considered the root as the part of the tooth embedded in the jawbone and covered with cementum. Because this definition only applies to mammals, Peyer (1968) suggested to use the term root only to mammals, and proposed the terms ‘basal portion,’ or ‘base,’ for non-mammal vertebrates. Smith et al. (2005) and Smith (2005) followed Peyer (1968)‘s suggestion for theropods, and used the terms ‘tooth base’ to describe the portion of the tooth beneath the crown. Because this portion is roughly analogous to the mammal root (Smith et al. 2005) and corresponds to the part of the tooth anchored in an alveolus, the term root, which is the most commonly used by authors describing theropod teeth (pers. obs.), is favored instead of ‘tooth base’.

Root base (rob)—Region of the tooth immediately below and adjacent to the basal limit of the enamel layer.

Apex (ap)—Tip of the crown (crown apex; Figs. 2.1C, 2.2C) or the root (root apex; Fig. 2.2C–D) of a tooth (Schwenk 2000; Licker 2003; Smith and Dodson 2003). The word apex gives the name ‘apical’ to the direction towards crown tips and ‘root apical’ to the direction towards root tips (Smith and Dodson 2003). The crown apex can be serrated, smooth or worn, showing spalled surfaces or wear facets.

Cervix (ce)—Transition between the crown and the root and corresponding to the basal extension of the enamel layer (‘colet’ of Fauchard 1728; Cuvier 1805; Smith and Dodson 2003; Hillson 2005; Nelson and Ash 2009; Figs. 2.1C–D, 2.2B–C). The cervix is short for ‘cervix dentis’, also known as the ‘tooth neck’ (Smith and Dodson 2003).

Cingulum (ci)—Mesiodistal and labiolingual expansions of the crown base, just above the cervix, and forming a shelf surrounding the crown (Illiger 1811; Owen 1840; Sander 1997; Langer and Ferigolo 2013). Although a cingulum was noticed in some isolated teeth of *Paronychodon* (Sankey et al. 2002), theropods do not usually possess a cingulum at the base of their crown. The

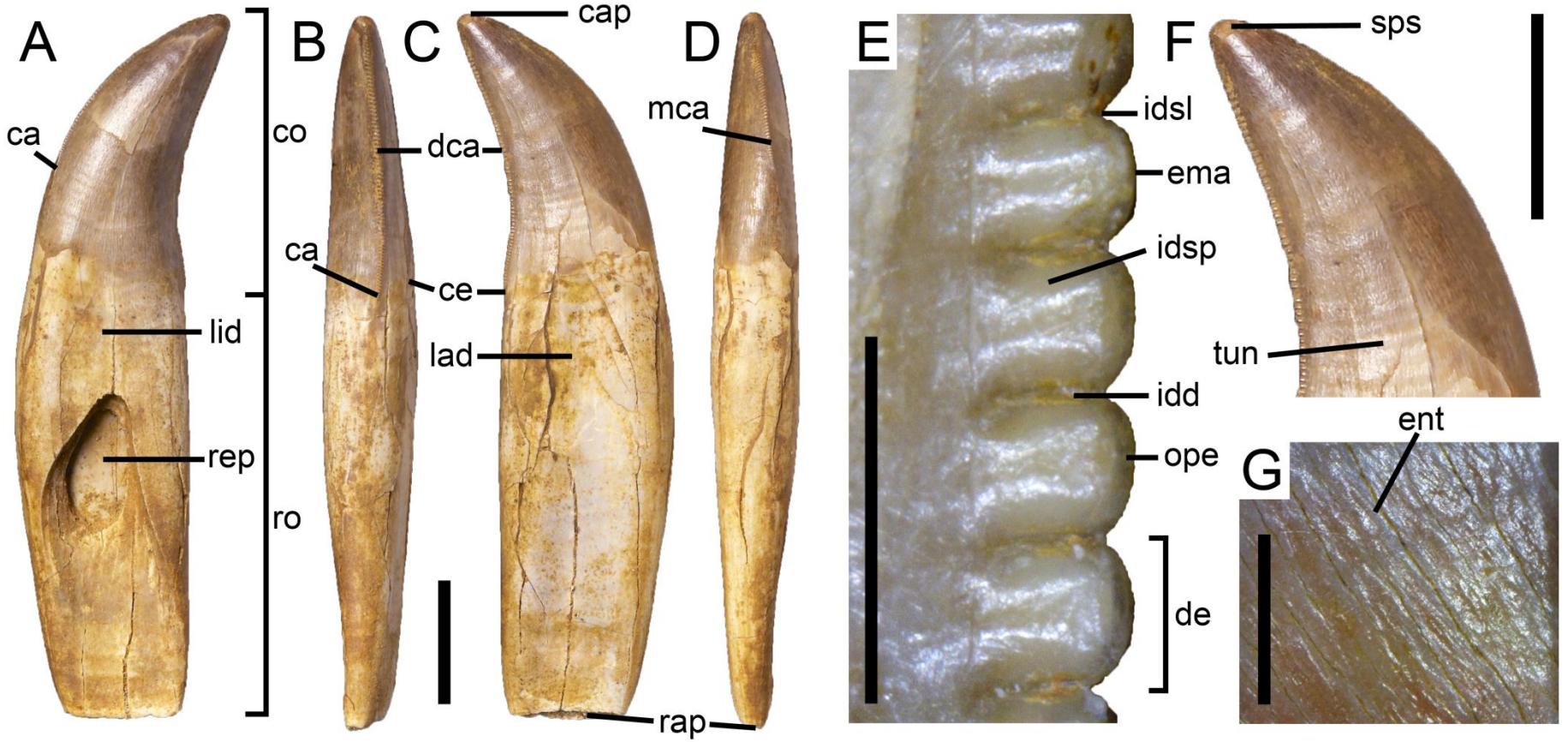

FIGURE 2.2. Crown, root and denticle anatomy of an isolated tooth of *Alioramus altai*, IGM 100–1844. **A-D**, Tooth in **A**, lingual; **B**, distal; **C**, labial; **D**, mesial views, and close up on; **E**, disto-central denticles; **F**, crown, and; **G**, enamel surface, in labial views (courtesy of Mick Ellison © AMNH). **Abbreviations**: **ca**, carina; **cap**, crown apex; **ce**, cervix; **co**, crown; **dca**, distal carina; **de**, denticle; **ema**, external margin; **ent**, enamel texture; **idd**, interdenticular diaphysis; **ids**, interdenticular sulci; **idsl**, interdenticular slit; **idsp**, interdenticular space; **lid**, lingual depression; **mca**, mesial carina; **ro**, root; **sps**, spalled surface; **tun**, transverse undulation. Scale bars equals 1 cm (A–D, F), and 1 mm (E, G).

therizinosauroid *Eshanosaurus* seems, however, to be an exception (Barrett 2009).

Carina (ca)—A sharp, narrow, and well-delimited ridge or keel-shaped structure running apicobasally on the crown and, in some case, on the root base, and typically corresponding to the cutting edge of the tooth (Licker 2003; Brink and Reisz 2014; Figs. 2.1D, 2.2A–B). The carina (used back to the 19th century, e.g., Eastman 1899) differs from flutes and longitudinal ridges by being a much smaller and better delimited ridge with acute corners. It can be serrated or not, straight or twisted. The carina can either extend to the crown apex or below it, and can reach the cervix or terminate above or below it. The carina can also be split, which is usually caused by trauma, aberrant tooth replacement or genetic factors (Erickson 1995). The carina is referred as the 'keel' by some authors (e.g., Farlow et al. 1991; Abler 1992; Holtz et al. 1998).

Mesial Carina (mca)—Ridge located on the mesial margin of the crown (Smith and Dodson 2003; Figs. 2.1G, 2.2D). The mesial carina usually faces mesially, but this keel can also face labially, mesiolingually or completely lingually in mesial teeth.

Distal Carina (dca)—Ridge located on the distal margin of the crown (Smith and Dodson 2003; Figs. 2.1C, 2.2B–C). The distal carina usually faces distally, but can also be displaced labiodistally or completely lingually in mesial teeth. The distal carina usually reaches the cervix, and sometimes extends onto the base root.

Split Carina (spc)—Abnormality of the crown consisting of a bifurcation of the carina into two serrated/unserrated segments (Erickson 1995; Fig. 2.4P). Split carinae are frequent in tyrannosaurid teeth (Currie et al. 1990; Erickson 1995) and have also been reported in other theropod taxa such as *Allosaurus* (Erickson 1995) and a carcharodontosaurid (Brusatte and Sereno 2007).

Enamel Layer (enl)—Outer hard mineralized surface covering the crown and mostly composed of hydroxyapatite ('émail' of Fauchard 1728; Cuvier 1805; Owen 1840; Reid 1997; Sander 1997, 1999; Stokosa 2005; Fig. 2.1A–B). The enamel layer is acellular and almost entirely inorganic as it includes 96% of inorganic material approximating hydroxyapatite $Ca_{10}(PO_4)_6(OH)_2$. The enamel layer is composed of long crystallites, much longer than those of the dentine, that are packed together to make a dense, very finely crystalline mass, so that enamel is a particularly hard substance (Hillson 2005). Enamel is formed by cells called ameloblasts that are located in the internal enamel epithelium, at the enamel-dentine junction (Sander 1999; Hillson 2005).

Dentin Layer (del)—Hard bonelike tissue composing the bulk of a tooth beneath the enamel layer (Owen 1840; Currie and Padian 1997; Licker 2003; Fig. 2.1A–B). The dentine layer is composed of mineral and organic matter. It is composed of 20% organic material (including 85-95% of collagen), 10% water, and 70% inorganic material formed by crystallites shorter than those of enamel and mostly composed of hydroxyapatite (Avery 2001). Dentine is a living tissue formed by odontoblasts, long and narrow cells that occupy closely spaced tunnels called dentine tubules and line the sides of the pulp cavity (Hillson 2005).

Pulp Cavity (puc)—The space within the central part of a tooth containing the dermal pulp and made up of the pulp chamber and a root canal (‘pulpe centrale’ of Cuvier 1805; Owen 1840; Licker 2003; Fig. 2.1B).

Resorption pit (rep)—Depression or shallow concavity centrally positioned on the lingual side of the root that receives a replacement tooth (Fig. 2.2A). The resorption pit (Hopson 1964) is equivalent to the ‘replacement pit’ of Norell and Hwang (2004), and the ‘unerupted tooth fossa’ of Hendrickx and Mateus (2014*b*).

Denticle Anatomy

Serration (se)—A projection along the carina of a tooth, whether composed of enamel or by both enamel and dentine (Brink and Reisz 2014). (Sander 1997) defined the serrations as the line of denticles along the cutting edge of the crown, yet this definition applies to the carina instead.

Denticle (de)—An elaborate type of serration corresponding to a projection of dentine covered with enamel along the carina (‘dentelure’ of Cuvier 1805; Owen 1840; Currie and Padian 1997; Licker 2003; Brink and Reisz 2014; Figs. 2.1H, 2.2E, 2.8). The denticles are known as serrations by many authors (e.g., Farlow et al. 1991; Abler 1992; Holtz et al. 1998). Yet a serration is, for some of them (e.g., Holtz 1998*a*), a smaller version of a denticle, the serrations being the small and sharp projections on the carinae of theropod teeth and teeth of other carnivores, whereas the denticles are the larger and coarser projections on the constricted teeth of plant eaters. (Brink and Reisz 2014) gave, however, a different definition of serration and denticle, the latter being an elaborate version of a serration characterized by a core of dentine. Because the carina of theropod crowns always seems to bear well-delimited serrations showing an external layer of enamel (pers. obs.), the term denticles is to be preferred for theropod teeth. The denticles are always located on the carinae, the smallest denticles being typically at the base and top of the carinae. The morphology of denticles varies significantly within the tooth and among theropods (Fig. 2.8). Yet, it usually corresponds to a rounded bump with an symmetrical or asymmetrical convex margin, in some cases strongly apically recurved. The denticles project either perpendicularly from the crown margin or are apically inclined with a main axis diagonally-oriented from the carina.

Mesial Denticle (mde)—A projection of dentine covered with enamel along the mesial carina. The mesial denticles tend to be lower than the distal ones, and typically devoid of interdenticular sulci. The shape of mesial denticles is usually subrectangular, with a basoapical elongation axis, to subquadrangular.

Distal Denticle (dde)—A projection of dentine covered with enamel along the distal carina (Fig. 2.2E). The shape of distal denticles is typically subquadrangular to subrectangular, with a mesiodistal elongation axis.

External Margin (ema)—Distalmost border of a denticle (Figs. 2.1H, 2.2E, 2.3). The external margin (ema) typically corresponds to the outer edge of the operculum and is equivalent to

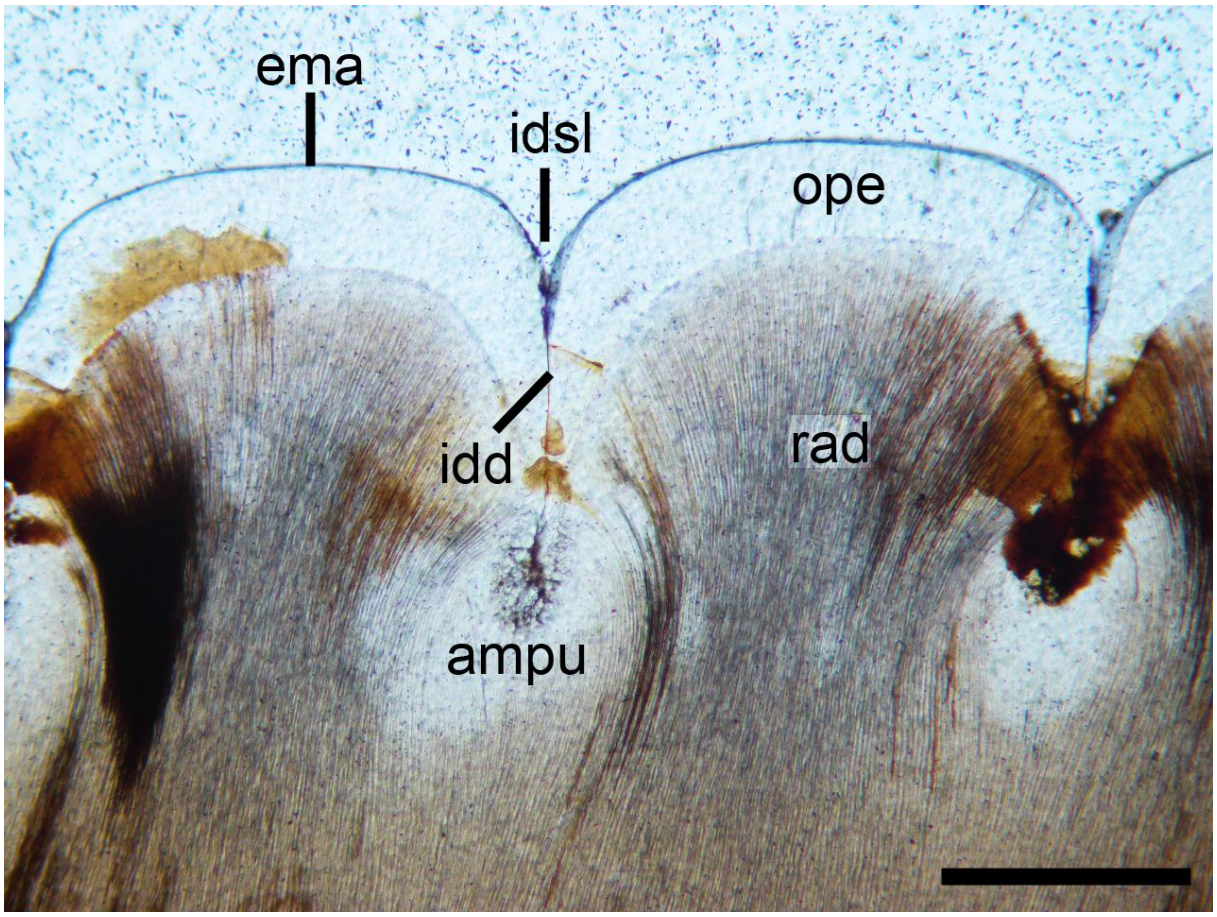

FIGURE 2.3. Internal anatomy of mesial denticles of an indeterminate tyrannosaurid, ROM 57981, from the Oldman Formation? of Alberta, Canada (courtesy of Kirstin Brink). **Abbreviations**: **ampu**, ampulla; **ema**, external margin; **idd**, interdenticular diaphysis; **idsl**, interdenticular slit; **ope**, operculum; **rad**, radix. Scale bar equals 100 µm.

the outer margin/end of Buscalioni et al. (1997).

Interdenticular Diaphysis (idd)—Junction between two neighboring denticles ('diaphysis' of Abler 1992; Buscalioni et al. 1997; Figs. 2.1H, 2.2E, 2.3).

Interdenticular Space (idsp)—Narrow gap between two neighboring denticles, and forming a chamber (Abler 1992; Buscalioni et al. 1997; Figs. 2.1H, 2.2E). The interdenticular space (Zhang and Barnes 2000) is also known as 'cella' (Abler 1992; Buscalioni et al. 1997; Canudo et al. 2009; Fanti et al. 2014) and 'interdenticle space' (Sankey et al. 2002). It varies in length relative to the denticle shape, and is particularly large with apically recurved denticles.

Interdenticular Slit (idsl)—Narrow opening on the distal end of the interdenticular space and separating two neighboring denticles (Cillari 2010; 'interdenticle slit' of Currie et al. 1990; Buscalioni et al. 1997; Sankey et al. 2002; Figs. 2.1H, 2.2E, 2.3).

Interdenticular Sulcus (ids)—Fine groove that continues a short distance onto the labial and lingual surfaces of the crown arising from between two neighboring denticles (Smith 2007; Benson 2009; Figs. 2.1H, 2.4B). The interdenticular sulci (*sensu* Smith 2007), also known as 'blood grooves'

(e.g., Currie et al. 1990; Zinke 1998; Azuma and Currie 2000; Fanti and Therrien 2007; Fanti et al. 2014), can be short or well-developed, perpendicular to the carina or curving basally.

Cauda (cau)—Raised, paddle-shaped tail delimited by two neighboring interdenticular sulci and running a short distance onto the labial and lingual surfaces of the crown from the base of a denticle (Abler 1992; Figs. 2.1H, 2.4B). Caudae and interdenticular sulci form a complex on the crown surface referred as the caudae/ interdenticular sulci complex by Smith and Lamanna (2006), Smith and Dalla Vecchia (2006) and Smith (2007).

Radix (rad)—Cylindrical core of enamel and dentine beneath the operculum and composing most of the internal structure of the denticle (Abler 1992; Fig. 2.3). The radix (*sensu* Abler 1992) is made of hexagonal enamel layers invaded by thin radiating structures of the tooth's dentine interior (Abler 1992).

Operculum (ope)—Dome-shaped outer layer of the denticle composed of enamel (Abler 1992; Figs. 2.2E, 2.3).

Ampulla (ampu)—Flask-shaped space in enamel structure at the junction of each pair of opercula, beneath the interdenticular diaphysis (Abler 1992; Fig. 2.3).

Crown Ornamentations and Attributes

Wear Facet (wfa)—Typically elliptical surface in outline evinced of parallel striations, occurring on the lingual or labial surfaces of the crown, but not both, and formed by repeated tooth-to-tooth contact (Schubert and Ungar 2005; Figs. 2.1F, 2.4K). Wear facets are uniformly flat surfaces that follow the long axis of the crown and never occur on the mesial and distal surfaces of the crown (Schubert and Ungar 2005).

Spalled surface (sps)—Irregular surface of enamel flaking, typically extending to the apex of the tooth (Figs. 2.1F, 2.2F, 2.4A). The spalled surfaces (*sensu* Schubert and Ungar 2005) are usually short and squat, and irregularly shaped. They occur on all surface of the crown and result from forces produced during contact between crown and food (Schubert and Ungar 2005)**.**

Flute (flu)—Narrow apicobasally oriented groove separated by two subparalell and acute ridges (Figs. 2.1G, 2.4H–I). Flutes (from the term 'fluting' of Owen 1840) are also referred as 'striations' (Carrano et al. 2002), 'ribs' (Buffetaut 2007; Buffetaut et al. 2008), 'longitudinal grooves' (Madsen and Welles 2000), 'longitudinal ridges' (e.g., Currie et al. 1990; Sankey 2008; Buckley 2009) or 'ridges' (e.g., Charig and Milner 1997; Buffetaut 2011; Fanti et al. 2014).

Longitudinal Groove (lgr)—Long and shallow apicobasally-oriented channel along the crown and delimited by two convexities (Fig. 2.4J). There is usually only a single longitudinal groove on the crown, typically restricted to the vicinity of the mesial carina. These grooves should not be confused with the narrow flutes bounded by acute ridges and the wide labial/lingual depression centrally positioned on the crown (e.g., Fig. 2.4O).

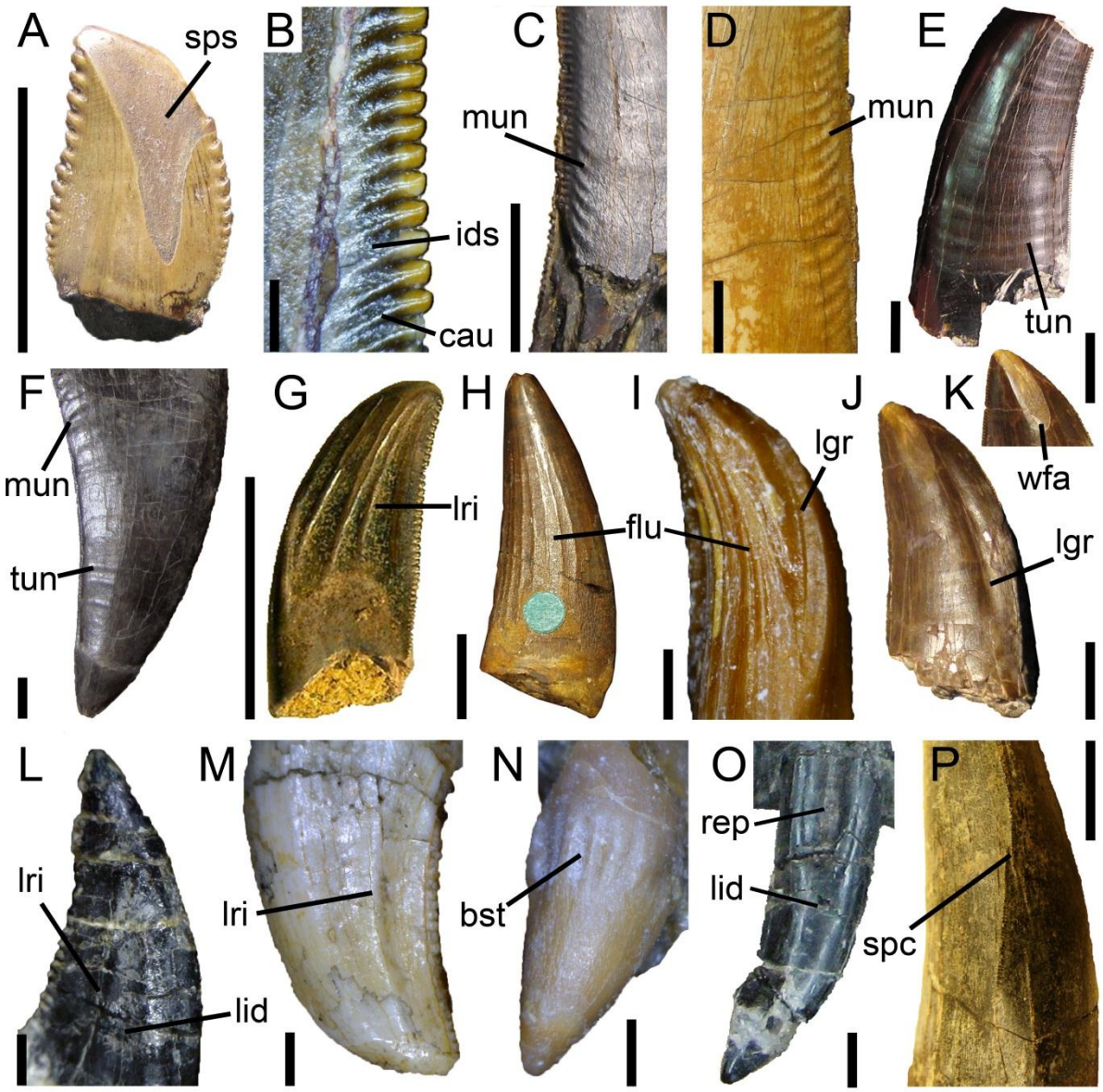

FIGURE 2.4. Crown ornamentations and attributes in non-avian theropods. **A**, Shed crown of *Troodon formosus*, DMNH 22337, in lingual view; **B**, Distal denticles of an indeterminate Abelisauridae, ML 327, in lingual view; **C**, Disto-central part of an isolated crown of cf. *Megalosaurus bucklandii*, OUMNH J.23014, in labial view; **D**, Disto-central part of an isolated crown of *Carcharodontosaurus saharicus*, UCRC PV6, in lingual view; **E**, Isolated crown of *Megalosaurus bucklandii*, OUMNH J.29866, in lingual view; **F**, Sixth right maxillary tooth of *Acrocanthosaurus atokensis*, NCSM 14345, in labial view; **G**, Shed tooth of *Paronychodon* sp., NHM R8405, in lingual view (Cillari 2010); **H**, Shed tooth of an indeterminate baryonychine (formerly *Suchosaurus cultridens* nomen dubium), NHM R.36536, in labial? view; **I**, Third right dentary tooth of *Masiakasaurus knopfleri*, UA 8680, in linguodistal view; **J**, Shed tooth of an indeterminate Abelisauridae, ML 327, in lingual view; **K**, Close up on the apicolingual portion of the shed tooth of an indeterminate Abelisauridae, ML 327, in lingual view; **L**, Fifth left maxillary crown of *Bambiraptor feinbergi*, AMNH 30556, in labial view; **M**, Fourth left maxillary tooth of *Velociraptor mongoliensis*, AMNH 6515, in labial view; **N**, First right premaxillary tooth of *Proceratosaurus bradleyi*, NHM R.4860, in labial view; **O**, Eight left maxillary tooth of *Allosaurus fragilis*, UMNH VP 5393, in lingual view (courtesy of Stephen Brusatte); **L**, Isolated tooth of *Eocarcharia*, MNN GAD15, in mesial view (courtesy of Juan Canale). **Abbreviations**: **bst**, basal striation; **cau**, cauda; **flu**, flute; **ids**, interdenticular sulci; **lid**, lingual depression; **lgr**, longitudinal groove; **lri**, longitudinal ridge; **mun**, marginal undulation; **spc**, split carina; **sps**, spalled surface; **tun**, transverse undulation; **wfa**, wear facet. Scale bars equals 1 cm (A, C–H, J–K, O–P), and 1 mm (B, I, L–N).

Longitudinal Ridge (lri)—Apicobasally long and narrow convexity on the crown (Figs. 2.1A, 2.4G, L–M). Longitudinal ridges can be labiolingually wide/shallow or acute/prominent and forming a crest. Longitudinal ridges should not be confused with ridges delimiting flutes because they are widely spaced, strongly divergent and in some cases bifurcated. Longitudinal ridges are usually unique and centrally positioned on the crown, double (Fig. 2.1N), or numerous and widespread. They can either follow the main axis of the tooth or extend diagonally on the crown (see below).

Basal Striation (bst)—Short apicobasally-oriented furrow restricted to the base of the crown (Gilmore 1942; Figs. 2.1F, 2.4N).

Enamel undulation (enu)—Mesiodistally oriented corrugated structure on the external surface of the tooth and typically on the labial and lingual margins, comprised of parallel ridges and grooves of varying strength and length (Brusatte et al. 2007). Enamel undulation encompasses transverse and marginal undulations. The term 'enamel wrinkle' (Hellman 1928) is commonly employed to describe transverse and marginal undulations (e.g., Brusatte and Sereno 2007). However, we favor the use of 'undulations' rather than 'wrinkle' for these two types of enamel structures because wrinkle can also refer to the millimeter scale wrinkling of the enamel texture (e.g., Buffetaut et al. 2008; Buffetaut 2011; Mateus et al. 2011), so the term 'undulation' is less confusing and also better illustrates these enamel ornamentations.

Transverse undulation (tun)—Band like enamel wrinkle extending along most of the crown width, typically from the mesial to distal carinae (Figs. 2.1F, 2.2F, 2.4E–F). Transverse undulations (Cope 1877), also known as 'bands' (Fanti et al. 2014), 'bands of growth' (Ősi et al. 2010), 'transverse wrinkles' (e.g., Benson et al. 2008), 'transverse bands' (Sereno et al. 1996) and 'transversal undulation' (Hendrickx et al. in press*a*; Araújo et al. 2013; Hendrickx and Mateus 2014*a*, *b*), appear on the crown, and more rarely on the root (e.g., *Baryonyx*, *Neovenator*). Transverse undulations do not necessarily contact both mesial and distal carinae as they can also be restricted to the medial part of the tooth. Transverse undulations can be well-visible or subtle, numerous and closely packed or, just a few and widely separated (Brusatte et al. 2007; Hendrickx and Mateus 2014*b*). Their mesial and distal extremities can curve apically adjacent to the carinae (Brusatte et al. 2007).

Marginal undulation (mun)—Mesiodistally elongated wrinkles restricted to the vicinity of the crown and adjacent to the mesial and/or distal carinae (Figs. 2.1F, 2.4C–D, F). Marginal undulations (*sensu* Hendrickx et al. in press*a*; Hendrickx and Mateus 2014*a*, *b*) are also referred as 'enamel folds' (Buffetaut et al. 2005*b*; Vullo and Néraudeau 2010), 'marginal wrinkles' (Kocsis et al. 2002; Brusatte et al. 2007), 'crenulations' (Coria and Currie 2006; Molnar et al. 2009), 'arcuate wrinkles' (Sereno et al. 1996), 'arcuate enamel wrinkles' (Canale et al. 2009), 'arcuate marginal enamel wrinkles' (Novas et al. 2005*b*; Brusatte and Sereno 2007), or 'enamel wrinkles' (Fanti et al. 2014). Marginal undulations can extend perpendicular to the crown margins or be strongly diagonally-oriented, forming closely packed diagonal ridges.

Labial/Lingual Depression (lad/lid)—Wide concavity centrally-positioned on the labial and/or the lingual side of the tooth, and extending typically along more than one half of the width of the tooth surface (Figs. 2.1F, 2.2A, C, 2.4O). The labial and lingual depressions (Elzanowski and Wellnhofer 1993), also referred as 'furrows' (Novas et al. 2008), 'supradental groove' (Gong et al. 2010, 2011) and 'labial grooves' for the labial depression (e.g., Gianechini et al. 2011*b*; Gong et al. 2011), are typically weakly delimited, yet they can be bounded by two well-marked longitudinal ridges like in *Buitreraptor* and *Bambiraptor* (Gianechini et al. 2011*a*; pers. obs.). On the crown, the basoapical extension of the depression is variable, but this concavity is, in most cases, restricted to the basal part of the crown. On the root, the basoapical extension of the lingual, and sometimes labial, depression is much more prominent, the concavity covering more than two thirds of the root.

Enamel Texture (ent)—Pattern of sculpturing on the crown surface at a sub-millimeter scale (Figs. 2.2G, 2.6). In theropods, the enamel texture (Kohn 1942) can be irregular, braided, veined, or anastomosed (see below).

Morphological nomenclature

Tooth and Dentition Type

Four types of tooth morphology in Theropoda are here defined based on the following dental features: the presence or absence of a constriction between crown and root, the labiolingual narrowness of the crown, the presence or absence of denticles, and the lingual curvature of the tooth. Although the first dental type 'ziphodont' was coined by Langston (1975) and is commonly used in the scientific literature; the others are new. These dental types define four types of dentition based on the morphology of the most common teeth composing the lateral dentition, and each of them is related to a particular feeding mechanism and diet.

Ziphodont—Strongly labiolingually narrow crown (i.e., crown in which the labiolingual width is lower than 60 % of the mesiodistal length) with a distal curvature, typically serrated carinae, and no constriction at the cervix (Fig. 2.5A). The term ziphodont comes from the Ancient Greek ξίφος (ksífos, 'sword') and δόντι (dónti, 'tooth') meaning 'blade-shaped teeth,' and derives from the taxon *Crocodilus ziphodon* erected by Marsh (1871*a*). The species received this name because the crocodile "was remarkable in having smooth compressed teeth, with serrated edges, resembling the teeth of some of the carnivorous dinosaurs." (Marsh 1871*b*: p. 104). (Langston 1975) was the first to propose the term ziphodont to gather crocodiles sharing this tooth morphology. This term is now sometimes very restrictive as it refers to serrated crown only (e.g., D'Amore 2009; Brink and Reisz 2014). Yet, we do not consider the presence of denticles as a compulsory feature for the ziphodont type of crown as unserrated blade-shaped teeth born by some compsognathids and unenlagiines are here described as ziphodont.

Folidont—Crown with a pronounced constriction (i.e., base of crown occupying 85 % or less of largest crown width; Hendrickx and Mateus 2014*b*) at the level of the cervix, thus displaying a lanceolate leaf-shaped outline in lateral view (Fig. 2.5B–C). The term folidont comes from the Latin *folium* ('leaf') and the Ancient Greek δόντι (dónti, 'tooth') meaning 'leaf-shaped tooth.' Folidont crowns can be distally recurved as in Troodontidae, or straight as in Therizinosauria and Alvarezsauroidea (Xu et al. 2001*b*; pers. obs.). Folidont teeth can also be unserrated, or bear minute to large apically recurved denticles as in Therizinosauria and Troodontidae. In *Carcharodontosaurus* (SGM Din 1), *Proceratosaurus* (Rauhut et al. 2010), *Compsognathus* (Zinke and Rauhut 1994), *Haplocheirus* (Choiniere et al. 2010*b*:fig. S4), *Microraptor* (Xu et al. 2000; Hwang et al. 2002), and *Richardoestesia* some teeth also have a constricted crown at the cervix, but the constriction is not significant enough to provide the crown with an overall lanceolate shape; these theropods, therefore, possess a ziphodont dentition.

Pachydont—Labiolingually expanded, non-constricted, and distally recurved crown in which the labiolingual width is greater than 60 % of the mesiodistal length, from cervix to apex (modified from Holtz 2001; Fig. 2.5D). The term pachydont comes from the Ancient Greek παχύς (pakhus, 'thick') and δόντι (dónti, 'tooth') meaning 'thick tooth.' Pachydont crowns occur in the mesial dentition of many non-maniraptoriform and dromaeosaurid theropods, yet they characterized the whole dentition of Tyrannosauridae. Pachydont teeth are also present anteriorly in the lateral dentition of *Allosaurus* and *Acrocanthosaurus* (pers. obs.), and in some notosuchians like *Notosuchus terrestris* (Lecuona and Pol 2008).

Conidont—Conical crown that have minute denticles or no denticles at all, and typically fluted surface (Fig. 2.5E). The term conidont comes from the Ancient Greek κώνος (konos, 'cone, spinning top, pine cone') and δόντι (dónti, 'tooth') meaning 'cone-shaped tooth.' Conidont teeth differ from pachydont teeth by acutely pointed apices, weakly distally recurved crowns, and minute denticles or unserrated carinae. Conidont crowns forming the whole dentition are present in Spinosauridae, and possibly the dromaeosaurid *Austroraptor* (Novas et al. 2009). Because we do not consider the presence of flutes as a mandatory feature for the conidont condition, conidont crowns are also born by basal ornithomimosaur, and constitute the mesial dentition of therizinosaurs and basal oviraptorosaurs.

Ziphodonty—Lateral dentition mostly composed of ziphodont teeth. (De Andrade et al. 2010) differently define ziphodont dentitions as dentitions where all teeth possess denticulate carinae. However, if the large majority of ziphodont theropods show serrated teeth, some of them such as *Buitreraptor* and *Compsognathus*, whose teeth do not always bear denticles, are considered as having a ziphodont dentition. Ziphodonty is common in meat-eating dinosaurs and can be seen in non-neotheropod Theropoda, Coelophysoidea, Dilophosauridae, Ceratosauria, non-spinosaurid Megalosauroidea, Allosauroidea, non-tyrannosaurid Tyrannosauroidea, Compsognathidae, and Dromaeosauridae. A ziphodont dentition is also present in non-theropod amniotes such as

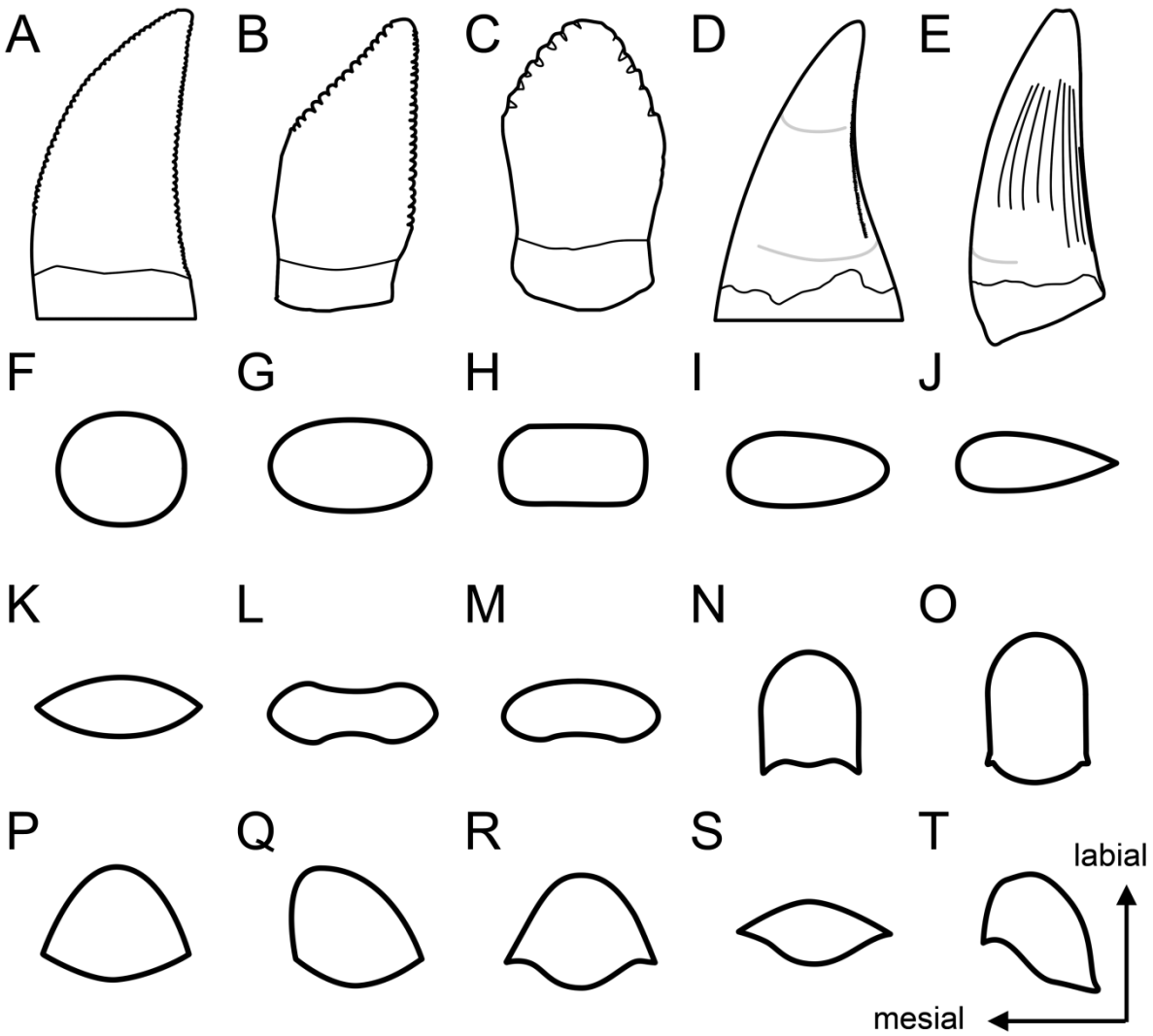

FIGURE 2.5. Crown types and cross-section outlines of the crown base at the cervix in non-avian theropods. **A**, ziphodont (blade-shaped) crown type; **B**, recurved folidont (lanceolate) crown type; **C**, straight folidont (lanceolate) crown type; **D**, pachydont (incrassate) crown type; **E**, conidont (cone-shaped) crown type; **F**, subcircular cross-section; **G**, elliptical cross-section; **H**, subrectangular cross-section; **I**, oval cross-section; **J**, lanceolate cross-section; **K**, lenticular cross-section; **L**, eight-shaped cross-section; **M**, reniform cross-section; **N**, U-shaped cross-section with central ridge on the labial margin; **O**, U-shaped cross-section with convex lingual margin; **P**, symmetrical D-shaped cross-section; **Q**, asymmetrical D-shaped cross-section; **R**, salinon-shaped cross-section; **S**, parlinon-shaped cross-section; **T**, J-shaped cross-section.

sphenacodontids, basal archosaurs, crurotarsians, and living varanids like the Komodo Dragon (e.g., Langston 1975; Auffenberg 1981; Farlow et al. 1991; Senter 2003; D'Amore 2009; De Andrade et al. 2010; Young et al. 2010).

Folidonty—Lateral dentition mostly composed of folidont teeth. Folidonty should not be confused with phyllodonty (Ancient Greek φύλλο fýllo, 'leaf' and δόντι dónti, 'tooth') which also means 'leaf-shaped tooth' yet refer to tooth plates with multiple superimposed sets of replacement teeth in fishes (Estes 1969). A folidont dentition occurs in derived theropods such as Therizinosauria, Alvarezsauroidea, Oviraptorosauria, Troodontidae, and Avialae (Zanno and Makovicky 2011). It is

also present in ornithischians, some sauropodomorphs, and iguanas (e.g., Barrett 2000; Araújo et al. 2011; Becerra et al. 2013).

Pachydonty—Lateral dentition mostly composed of pachydont teeth. In theropods, pachydonty is seen in mature Tyrannosauridae such as *Gorgosaurus*, *Tarbosaurus* and *Tyrannosaurus* which possess typical incrassate/banana-like crowns all along the dentition (Holtz 2003, 2008).

Conidonty—Lateral dentition mostly composed of conidont teeth. Conidont theropods include spinosaurids, basal ornithomimosaurs, and perhaps some dromaeosaurids. The conidont dentition of Spinosauridae includes large fluted teeth with minute or no denticles whereas the conidont dentition of basal ornithomimosaurs shows reduced and unserrated crowns. Among non-theropod tetrapods, conidonty is also seen in many crocodilians, pliosaurs, plesiosaurs, and mosasaurs (Owen 1840; Massare 1987; Prasad and de Lapparent de Broin 2002; Longrich 2008).

Pseudoheterodonty—Dentition in which the crown morphology gradually changes along the jaw so that mesial and lateral teeth differ significantly in their morphology. A pseudoheterodont dentition differs from the heterodont dentition by the absence of a clear distinction of the crowns morphologies along the jaw (e.g., incisors, canines, molars), and the teeth of a pseudoheterodont dentition can only be identified as belonging to the mesial or the lateral part of the jaw. Toothed theropod other than some derived tyrannosaurids (see Smith 2005) are pseudoheterodont as the crown morphology gradually changes from a lateral dentition to a mesial dentition. Pseudoheterodonty can also occur within the lateral dentition as in *Byronosaurus* and *Xixiasaurus* which bear folidont teeth that gradually change into ziphodont teeth distally.

Cross-section Type

The cross-section outline of a crown is an important feature bearing information on the crown position along the tooth row as well as important systematic value. The possible shapes of the cross-section of a crown is diverse (Fig. 2.5F–T) and can be used not only to assign the tooth to the mesial or lateral dentition, but also to a certain clade of theropods. This is particularly the case for mesial teeth in which the large variety of cross-section types can be used as a diagnostic feature in theropods (pers. obs.). Because the cross-section outline varies along the crown height, the cross-section type here refers to the basal cross-sectional shape taken at the cervix. Different cross-section outlines are usually termed ‘D-shaped’ by many authors, and we decided to make a distinction between a U-shaped, D-shaped, J-shaped, and salinon-shaped outlines of the crown base in cross-section (Fig. 2.5N–T). Gradational changes across the premaxillary and dentary arcade between D-shaped/salinon-shaped and J-shaped outline may occur in a single specimen, the D-shaped/salinon-shaped cross section being present in the mesial teeth whereas the J-shaped cross-section outline occurring in more distal teeth of the mesial dentition (e.g., Fanti and Therrien 2007:fig. 7).

Subcircular Cross-section—Circle-shaped outline of the transversal section of a conical or subconical crown with subsymmetrical and convex mesial, distal, labial and lingual margins (Fig. 2.5F).

Elliptical Cross-section—Ellipse-shaped outline of the transversal section of a laterally narrow crown with labiolingually convex and sub-symmetrical mesial and distal margins, and wide labiolingually convex and sub-symmetrical labial and distal surfaces (Fig. 2.5G).

Subrectangular Cross-section—Rectangle-shaped outline of the transversal section of a laterally narrow crown with subparallel lingual and labial sides, and mesial and distal margins, all separated by four rounded angle (Fig. 2.5H).

Oval Cross-section—Egg-shaped outline of the transversal section of a laterally narrow crown with a wide labiolingually convex mesial margin and a narrow labiolingually convex distal surface (Fig. 2.5I).

Lanceolate Cross-section—Lance-shaped outline of the transversal section of a laterally narrow crown with a labiolingually convex mesial margin and a sharp distal edge or carina (Fig. 2.5J).

Lenticular Cross-section—Lens-shaped outline of the transversal section of a laterally narrow crown with sharp and subsymmetrical distal mesial and distal edges or carinae (Fig. 2.5K).

Eight-shaped Cross-section—Hippopede-shaped outline of the transversal section of a laterally narrow crown with labiolingually convex mesial and distal margins, and labial and lingual surfaces with centrally positioned concavities (Fig. 2.5L).

Reniform Cross-section—Bean or kidney-shaped outline of the transversal section of a laterally narrow crown with labiolingually convex mesial and distal margins, and one labial or lingual surface with a centrally positioned concavity, the opposite surface being convex (Fig. 2.5M).

U-shaped Cross-section—Outline of the transversal section of a mesial crown with both carinae facing lingually, subsymmetrical mesial and distal margins, a convex labial surface, and a concave, convex (Fig. 2.5N), or biconcave lingual surface (Fig. 2.5O). The U-shaped condition, also designated as ‘D-shaped,’ ‘incisiform’ or ‘sub-incisiform’ (e.g., Currie et al. 1990; Carr and Williamson 2004; Holtz 2004), is shared by most tyrannosauroids, and perhaps some other basal coelurosaurs such as *Zuolong* (Choiniere et al. 2010*a*).

D-shaped Cross-section—Outline of the transversal section of a mesial crown with both mesial and distal carinae facing linguo-mesially and linguo-distally, respectively, and a wide mesiodistally convex labial and lingual surfaces (Fig. 2.5P). This outline is, in some cases, asymmetrical if the convexity of the labial surface is displaced mesially (Fig. 2.5Q). A D-shaped cross-section is present in some allosauroids.

Salinon-shaped Cross-section—Outline of the transversal section of a mesial crown with both mesial and distal carinae facing linguo-mesially and linguo-distally, respectively, subsymmetrical mesial and distal crown sides, a convex labial margin, and a biconcave lingual margin (Fig. 2.5R). A cross-section with a labiolingually narrow salinon-shaped outline (salinon *sensu* Khelif 2010), here

described as a parlinon-shaped cross-section (parlinon *sensu* Khelif 2010), occurs in lateral teeth, with the biconcave surface facing either lingually or labially (Fig. 2.5S).

J-shaped Cross-section—Comma-shaped outline of the transversal section of a mesial crown with a mesial carina facing mesio-lingually, a convex labial surface, and a sigmoid lingual surface due to a concavity marginal to the mesial carina (Fig. 2.5T).

Enamel Texture Type

The morphology of the enamel texture is often omitted in the description of theropod dentitions and isolated theropod teeth, yet the enamel texture seem to have some phylogenetic potential in non-avian theropods (Hendrickx et al. in press*a*; Buffetaut et al. 2008; Hendrickx and Mateus 2014*b*). The nomenclature of enamel texture type follows the terminology of Hendrickx and Mateus (2014*b*), and an additional type of texture, the anastomosed enamel texture, is here defined for the first time.

Smooth—Absence of enamel texture so that the enamel surface does not show any irregularity.

Irregular—Non-oriented enamel texture with no pattern (Fig. 2.6A).

Braided—Oriented enamel texture made of alternating and interweaving grooves and sinuous ridges (Fig. 2.6B). The ridges can be short, moderately elongated or very long, but always baso-apically oriented on the crown and never convergent.

Veined—Oriented enamel texture made of deep alternating grooves and long sinuous and/or dichotomized ridges obliquely oriented and converging baso-mesially or baso-distally on the crown (Fig. 2.6C). The veined enamel texture has also been refer as a ‘granular texture’ (Charig and Milner 1997; Sues et al. 2002; Hasegawa et al. 2010), ‘textured enamel’ (Sereno et al. 1998), ‘fine wrinkling’ or ‘wrinkles’ (Buffetaut et al. 2008; Buffetaut 2011), and ‘sculptures’ (Hasegawa et al. 2010; Mateus et al. 2011).

Anastomosed—Enamel texture consisting of multiple ridges dividing and reconnecting in an irregular way (Fig. 2.6D). These multiple ridges can connect at a sub-millimeter scale, giving an almost foraminate texture of the enamel (pers. obs.).

Morphometric nomenclature

Measurement variables and associated terms and abbreviations (Fig. 2.1) follow (Smith et al. 2005) nomenclature, and additional measurements (with their respective terms and abbreviations) are proposed.

Crown Morphometry

Crown Base Length (CBL)—Maximum mesiodistal extent of the crown base at the level of the cervix (Smith et al. 2005; Fig. 2.7C). The crown base length, taken along the long axis of the

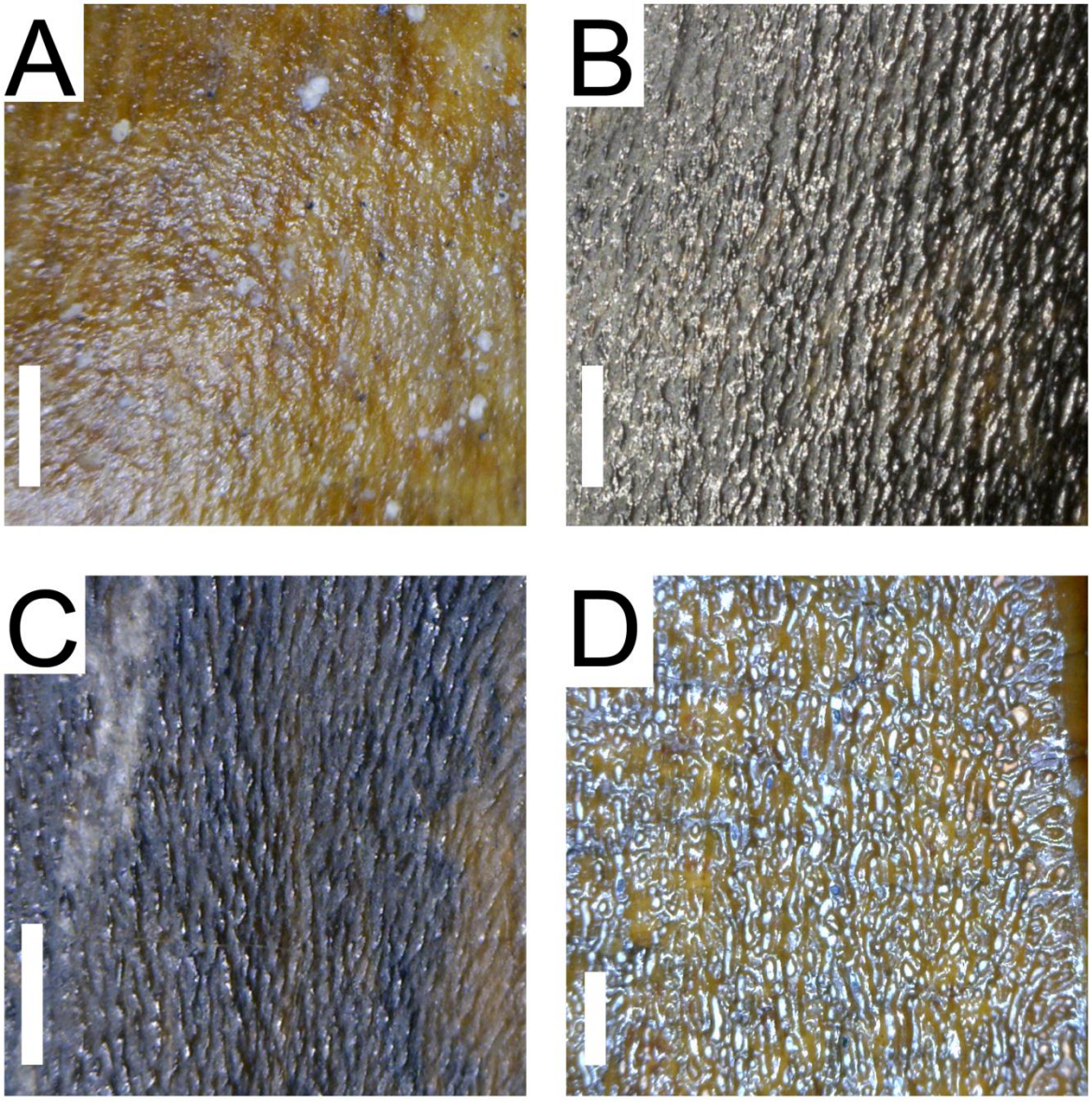

FIGURE 2.6. Diversity of enamel texture in non-avian theropods in lateral views. **A**, Irregular enamel texture of the sixth right maxillary tooth of *Majungasaurus crenatissimus*, FMNH PR 2278; **B**, Braided enamel texture of an isolated tooth of *Acrocanthosaurus atokensis*, SMU 7646; **C**, Veined enamel texture of an isolated tooth of *Baryonyx walkeri*, NHM R.9151–26; **D**, Anastomosed enamel texture of an isolated tooth of *Spinosaurus* sp., MSNM V6422. Scale bars equals 1 mm.

crown base, between the basalmost point of the enamel layer on both mesial and distal surfaces of the crown, is equivalent to the fore-aft basal length (FABL) of some authors (e.g., Currie et al. 1990; Farlow et al. 1991; Sankey et al. 2002; Samman et al. 2005; Larson and Currie 2013).

Crown Base Width (CBW)—Labiolingual extent of the crown base at mid-length of the crown base, perpendicular to the CBL, and at the level of the cervix (Smith et al. 2005; Fig. 2.7B, D). The crown base width (Sweetman 2004), taken from the basalmost point of the enamel layer on both labial and lingual surfaces of the crown, is roughly similar to the cross-sectional thickness (CST) of Sankey et al. (2002) and Sankey (2008), the cross-sectional thickness (XSTHICK) of Samman et al.

(2005), and the tooth basal width (BW) of Farlow et al. (1991), Fanti and Therrien (2007), Larson and Currie (2013), and many other authors (Table 2.1).

Crown Height (CH)—Maximum basoapical extent of the distal margin of the crown. The crown height is taken from the distalmost point at the cervix to the apicalmost point of the crown (Smith et al. 2005; Fig. 2.7C). The crown height is equivalent to the tooth crown height (THEIGHT) of Samman et al. (2005). It is also roughly equivalent, but slightly different from the tooth height (Ht) of Sankey et al. (2002) and Sankey (2008), and the tooth crown height (TCH) of Farlow et al. (1991), Fanti and Therrien (2007) and many other authors (Table 2.1), which are taken from the cervix to the crown apex, perpendicular to CBW, without taking into account the crown curvature.

Apical Length (AL)—Maximum basoapical extent of the mesial margin of the crown (Fig. 2.7C). The apical length, equivalent to the apical distance (AD) of Canudo et al. (2006), is taken from the mesial point at the cervix to the apicalmost point of the crown (Smith et al. 2005).

Crown Angle (CA)—Angle created by the apical length AL and the crown base length (Smith et al. 2005; Fig. 2.7C). The crown angle, which can be calculated using the law of cosines, corresponds to CA = arcos $(((CBL)^2 + (AL)^2 – (CH)^2) / 2 * CBL * AL)$. As the cervix is not always parallel to the jaw margin, Buckley et al. (2010) propose to measure a different crown angle (CA2) on images of teeth in lateral view. This angle is created by a mesiodistal line on the tooth, perpendicular to the jaw margin and passing by the distalmost point of the cervix, and a second line passing by the intersection of the previous one with the mesial margin of the tooth, and the crown apex (i.e., apicalmost point of the crown).

Crown Base Ratio (CBR)—Ratio expressing the labiolingual narrowness of the base crown and corresponding to the quotient of CBL by CBW (CBR = CBL ÷ CBW; Smith et al. 2005). The crown base ratio (CBR) is equivalent to the basal compression ratio (BCR) of Maganuco et al. (2005, 2007), the basal cross-sectional ratio (BCR) of Larson (2008*a*), the slenderness index (SI) of Vullo et al. (2007), and the lateral compression index (LCI) of Amiot et al. (2010*a*). A strongly labiolingually narrow crown has a quotient of less than 0.4, a moderately narrow tooth is around 0.5-0.6, a weakly narrow crown, with an ovoid cross-section, has a ratio fluctuating from 0.6 to 0.7, which usually corresponds to the CBR of a mesial tooth, and a subcircular crown has a ratio in between 0.9 and 1.1 (Smith et al. 2005).

Crown Height Ratio (CHR)—Ratio expressing the crown elongation and corresponding to the quotient of CH by CBL (CHR = CH ÷ CBL; Smith et al. 2005). The crown height ratio (CHR) is equivalent to the elongation ratio (ER) of Maganuco et al. (2005, 2007). A short tooth has a CHR value of less than 1.5, a moderately elongated crown has a CHR varying from 1.5 to 2.5, and a strongly elongated crown has a ratio higher to 2.5.

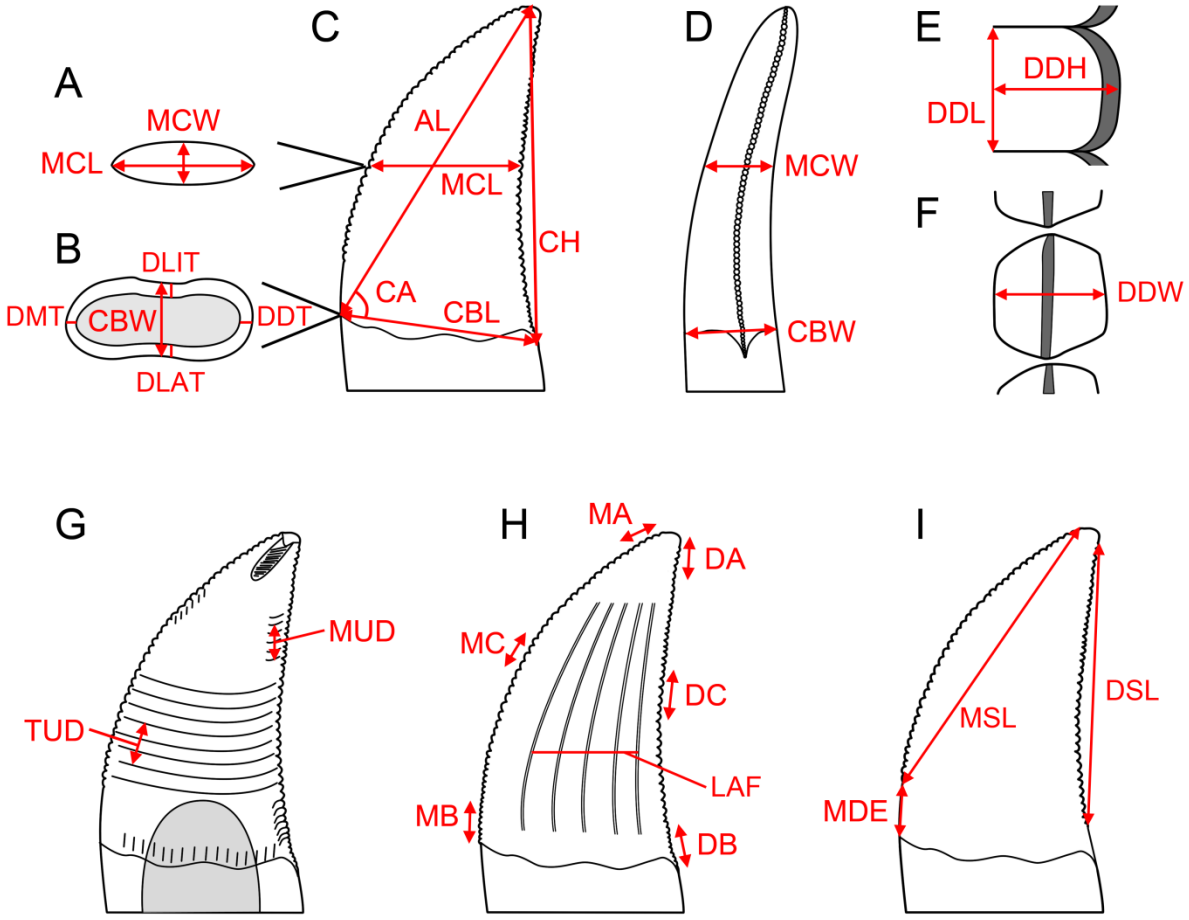

FIGURE 2.7. Anatomical and morphometric terminology used in this study. **A**, Mid-height cross-section of crown C showing MCW (mid-crown width) and MCL (mid-crown length), in apical view; **B**, Basal cross-section of crown in C showing CBL (crown-base length), DMT (dentine thickness mesially), DDT (dentine thickness distally), DLAT (dentine thickness labially), and DLIT (dentine thickness lingually), in basal view; **C**, Idealized lateral theropod tooth showing general theropod anatomy and AL (apical length), CA (crown angle), CBL (crown-base length), CH (crown height), and MCL (mid-crown length), in labial view; **D**, Idealized lateral theropod tooth showing MCW (mid-crown width) and CBW (crown-base width), in distal view; **E**, Idealized distal denticles showing DDH (distal denticle height) and DDL (distal denticle length), in labial view; **F**, Idealized distal denticles showing DDW (distal denticle width), in distal view; **G**, Idealized lateral theropod tooth showing several crown ornamentations morphology and CMU (crown marginal undulation density) and CTU (crown transverse undulation density), in labial view; **H**, Idealized fluted theropod tooth showing DA (disto-apical denticle density), DB (disto-basal denticle density), DC (disto-central denticle density), LAF (number of labial flutes), MA (mesio-apical denticle density), MB (mesio-basal denticle density), and MC (mesio-central denticle density), in labial view; **I**, Idealized lateral theropod tooth showing MDE (mesial denticle extension), MSL (mesial serrated carina length), and DSL (distal serrated carina length), in distal view.

Mid-Crown Length (MCL)—Maximum mesiodistal extent of the tooth at mid-height of the crown (Hendrickx et al. in press*a*; Fig. 2.7A, C). The mid-crown length (MCL) is roughly similar to the ML of Hocknull et al. (2009:table S16).

Mid-Crown Width (MCW)—Maximum labiolingual extent of the tooth, perpendicular to the MCL, at mid-height of the crown (Hendrickx et al. in press*a*; Fig. 2.7A, D).

Mid-Crown Ratio (MCR)—Thickness of the mid-crown corresponding to the quotient of MCL by MCW (MCR = MCL ÷ MCW; Hendrickx et al. in press*a*). The mid-crown ratio is equivalent

or close to the crown base ratio (CBR) in most theropods, but differs from CBR in many folidont theropods in which the labio-lingual narrowness of the crown is more important at mid-crown than at the base (pers. obs.).

Mesiobasal Denticles Extension (MDE)—Distance separating the basalmost mesial denticle from the cervix (Hendrickx et al. in press*a*; Fig. 2.7I). This measure is taken from the basalmost mesial denticle to a point situated on the same plane as the basalmost denticles, at the level of the cervix. The mesiobasal denticles extension is null when the mesial denticulate carina reaches the cervix.

Mesiobasal Carina Extension (MCE)—Distance separating the basalmost part of the mesial carina from the cervix. This measure is taken from the basalmost point of the mesial carina to a point situated on the same plane of that point, at the level of the cervix. The mesiobasal carina extension (MCE) is equivalent to the distance between the base of the mesial carina and the base of the tooth crown (DMCTOB) of Samman et al. (2005).

Mesial Serrated Carina Length (MSL)—Maximum basoapical extent of the mesial serrated carina (Buckley 2009; Buckley et al. 2010; Fig. 2.7I). The mesial serrated carina length (MSL), taken between the basalmost and the apicalmost denticles along the mesial carina, is equivalent to the anterior denticulate carina length (ADCL) of Buckley (2009) and Buckley et al. (2010), and roughly equivalent to the length of the mesial serration (MSH) of Cillari (2010) which is measured perpendicular to CBL. It corresponds to the difference between the mesiobasal denticles extension (MDE) and the apical length (AL) in the large majority of theropods, but differ from the result of this calculation in a few theropods whose mesial serrated carina does not reach the apex (e.g., *Troodon*).

Distal Serrated Carina Length (DSL)—Maximum basoapical extent of the distal serrated carina (Buckley 2009; Buckley et al. 2010; Fig. 2.7I). The distal serrated carina length (DSL), taken between the basalmost and the apicalmost denticles along the distal carina, is equivalent to the posterior carina denticulate length (PCDL) of Buckley (2009) and Buckley et al. (2010). It is also similar to the crown height in most theropods, but shorter than CH in some coelurosaurs such as compsognathids, therizinosaurs and troodontids (pers. obs.).

Mesial Carina Length (MCAL)—Maximum basoapical extent of the mesial carina along the crown (Buckley 2009; Buckley et al. 2010). The mesial carina length, taken from the basalmost point to the apicalmost point of the mesial carina, is equivalent to the anterior carina length (ACL) of Buckley (2009) and Buckley et al. (2010). The mesial carina length is similar to the mesial denticulate carina length in the serrated crown of most theropods, yet some of them have a denticulate carina that becomes unserrated basally and/or apically like in tyrannosaurids (Buckley et al. 2010).

Distal Carina Length (DCAL)—Maximum basoapical extent of the distal carina (Buckley 2009; Buckley et al. 2010). The distal carina length, taken from the basalmost point to the apicalmost point of the distal carina, is equivalent to the posterior carina length (PCL) of Buckley (2009) and Buckley et al. (2010). The distal carina length is also similar to the distal serrated carina length (DSL)

TABLE 2.1A. Abbreviations of measurement variables used by previous authors reporting isolated theropod teeth.

Publication	CBL	CBW	CH	AL	CBR	CHR	CA	MSL	DSL	MCAL	DCAL	MB	MC	MA
Currie et al. 1990	FABL													
Farlow et al. 1991	FABL	BW	TCH										ANTSERR	
Rauhut and Werner 1995	FABL	BW	TCH											
Zinke 1998	FABL	BW	TCH											
Park et al. 2000	FABL	BW	TCH											
Sankey et al. 2002	FABL	CST	Ht											
Rauhut 2002	FABL	BW	TCH											
Sweetman 2004	CBL	CBW	TCW										MDC	
Smith et al. 2005	CBL	CBW	CH	AL	CBR	CHR	CA					MB	MC	MA
Smith 2005	CBL	CBW	CH	AL	CBR	CHR	CA					MB	MC	MA
Samman et al. 2005	FABL	XSTHICK	THEIGHT											
Maganuco et al. 2005	FABL	BW	TCH		BCR	ER								
Smith and Lamanna 2006	CBL	CBW	CH	AL	CBR	CHR	CA					MB	MC	MA
Canudo et al. 2006	FABL	CBW	CH	AD	CBR	CHR	CA					MB	MC	MA
Fanti and Therrien 2007	FABL	BW	TCH										NDPMa	
Smith and Dalla Vecchia 2006	CBL	CBW	CH	AL	CBR	CHR	CA					MB	MC	MA
Maganuco et al. 2007	FABL	BW	TCH		BCR	ER								
Vullo et al. 2007	FABL	BW			SI									
Sankey 2008	FABL	CST	Ht											
Larson 2008*a*	FABL	BW	TCH		BCR								ADD	
Canudo et al. 2009	FABL	CBW	CH		CBR	CHR	CA						dm	
Buckley 2009	FABL	CBW	CH					ACDL	PCDL	ACL	PCL	ABD	AMD	AAD
Casal et al. 2009	FABL	CBW	CH	AL									DCM	
Molnar et al. 2009	CBL	CBW	CH				CA	MAVG	DAVG					
Lubbe et al. 2009	CBL	CBW	CH	AL	CBR	CHR	CA					MB	MC	MA
Averianov and Skutschas 2009	FABL	BW	TCH										ADC	
Cillari 2010	CBL	CBW	CH	AL			CA	MSH						
Buckley et al. 2010	FABL	CBW	CH	AL			CA	ACDL	PCDL	ACL	PCL	ABD	AMD	AAD
Amiot et al. 2010*a*	FABL	BW			LCI								MDC	
Ősi et al. 2010	CBL	CBW	CH	AL	CBR		CA							
Gianechini et al. 2011*a*	CBL	CBW	CH	AL	CBR	CHR	CA							
Han et al. 2011	CBL	CBW	CH	AL	CBR	CHR	CA							
Richter et al. 2013	CBL	CBW	CH	AL	CBR	CHR	CA							
Larson and Currie 2013	FABL	BW	CH	AL									ADM	
Kear et al. 2013	CBL	CBW	CH	AL	CBR	CHR	CA							
Cobos et al. 2014	CBL	CBW	CH	AL	CBR	CHR	CA						MC	MA
Tavares et al. 2014	CBL	CBW	CH	AL	CBR	CHR	CA					MB	MC	MA
Serrano-Brañas et al. 2014	CBL	CBW	CH	AL	CBR	CHR						MB	MC	MA
Williamson and Brusatte 2014	FABL	BW	CH										ADM	
Fanti et al. 2014	FABL	BW	TCH										NDPMa	
Madzia in press	CBL	CBW	CH	AL	CBR	CHR	CA					MB	MC	MA

TABLE 2.1B. (Continued).

Publication	DB	DC	DA	MAVG	DAVG	DSDI	MDH	MDL	MDW	DDH	DDL	DDW	MDE
Currie et al. 1990													
Farlow et al. 1991		POSTSERR											
Rauhut and Werner 1995						DSDI							
Zinke 1998						DSDI							
Park et al. 2000						DSDI							
Sankey et al. 2002		Dent/mm								Dent. Ht	Dent. W		
Rauhut 2002						DSDI							
Sweetman 2004		DDC				DSDI							
Smith et al. 2005	DB	DC	DA	MAVG	DAVG	DSDI							
Smith 2005	DB	DC	DA	MAVG	DAVG	DSDI							
Samman et al. 2005							DH/MDHM	DW/MDWM		DH/DDHM	DW/DDWM		DMCTOB
Maganuco et al. 2005						DSDI							
Smith and Lamanna 2006	DB	DC	DA	MAVG	DAVG	DSDI							
Canudo et al. 2006	DB	DC	DA	MAVG	DAVG	DSDI							
Fanti and Therrien 2007		NDPMp				DSDI							
Smith and Dalla Vecchia 2006						DSDI							
Maganuco et al. 2007	DB	DC	DA	MAVG	DAVG	DSDI							
Vullo et al. 2007						DSDI							
Sankey 2008		Dent/mm								Dent. Ht	Dent. W		
Larson 2008*a*		PDD				DSDI							
Canudo et al. 2009		dd				DSDI							
Buckley 2009	PBD	PMD	PAD				LAD-H	LAD-L	LAD-W	LPD-H	LPD-L	LPD-W	
Casal et al. 2009		DCD				DSDI				CD	AD		
Molnar et al. 2009													
Lubbe et al. 2009	DB	DC	DA	MAVG	DAVG	DSDI							
Averianov and Skutschas 2009		PDC				DSDI							
Cillari 2010				MAVG	DAVG	DSDI							
Buckley et al. 2010	PBD	PMD	PAD										
Amiot et al. 2010*a*		DDC				DSDI							
Ősi et al. 2010					DAVG								
Gianechini et al. 2011*a*													
Han et al. 2011						DSDI							
Richter et al. 2013	DB	DC	DA	MAVG	DAVG	DSDI							
Larson and Currie 2013		PDM											
Kear et al. 2013	DB	DC	DA		DAVG								
Cobos et al. 2014	DB	DC	DA	MAVG	DAVG								
Tavares et al. 2014	DB	DC	DA	MAVG	DAVG	DSDI							
Serrano-Brañas et al. 2014	DB	DC	DA										
Williamson and Brusatte 2014		PDM											
Fanti et al. 2014		NDPMp											
Madzia in press	DB	DC	DA	MAVG	DAVG	DSDI	DH	DW		DH	DW		

in the large majority of theropods, and only a few of them, like tyrannosaurids, seem to have different DSL and DCAL (Buckley et al. 2010).

Denticle Morphometry

Distal Denticle Height (DDH)—Maximum proximodistal extent of a denticle on the distal carina at mid-crown (Samman et al. 2005; Fig. 2.7E). The distal denticle height corresponds to the distal denticle height of middle denticles (DDHM) of Samman et al. (2005), the greatest denticle height (Dent. Ht) of Sankey et al. (2002) and Sankey (2008), the denticle length (CD) of Casal et al. (2009), the largest posterior denticle height (LPD-H) of Buckley (2009), and the height of denticle (DH) of Madzia (in press).

Distal Denticle Length (DDL)—Maximum basoapical extent of a denticle on the distal carina at mid-crown, taken perpendicular to the DDH at the base of the denticle (Fig. 2.7E). The distal denticle length corresponds to the distal denticle width of middle denticles (DDWM) of Samman et al. (2005), the greatest denticle width (Dent. W) of Sankey et al. (2002) and Sankey (2008), the denticle height (AD) of Casal et al. (2009), and the largest posterior denticle length (LPD-L) of Buckley (2009).

Distal Denticle Width (DDW)—Maximum labiolingual extent of a denticle on the distal carina at mid-crown, taken perpendicular to the DDL at the base of the denticle (Fig. 2.7F). The distal denticle width corresponds to the largest posterior denticle width (LPD-W) of Buckley (2009).

Mesial Denticle Height (MDH)—Maximum proximodistal extent of a denticle on the mesial carina at two thirds of the crown (Samman et al. 2005). The mesial denticle height corresponds to the mesial denticle height of middle denticles (MDHM) of Samman et al. (2005), and the largest anterior denticle height (LAD-H) of Buckley (2009).

Mesial Denticle Length (MDL)—Maximum basoapical extent of a denticle on the mesial carina at two thirds of the crown, taken perpendicular to the MDH at the base of denticle. The mesial denticle length corresponds to the mesial denticle width of middle denticles (MDWM) of Samman et al. (2005), and the largest anterior denticle length (LAD-L) of Buckley (2009).

Mesial Denticle Width (MDW)—Maximum labiolingual extent of a denticle on the mesial carina at mid-crown, taken perpendicular to the MDL at the base of the denticle. The mesial denticle width corresponds to the largest anterior denticle width (LAD-W) of Buckley (2009).

Distal Denticle Height Ratio (DHR)—Ratio expressing the distal denticle elongation and corresponding to the quotient of DDH by DDL (DHR = DDH ÷ DDL).

Distal Denticle Base Ratio (DBR)—Ratio expressing the distal denticle thickness at the base of the denticle, and corresponding to the quotient of DDL by DDW (DBR = DDL ÷ DDW).

Mesial Denticle Height Ratio (MHR)—Ratio expressing the mesial denticle elongation and corresponding to the quotient of MDH by MDL (MHR = MDH ÷ MDL).

Mesial Denticle Base Ratio (MBR)—Ratio expressing the mesial denticle thickness at the base of the denticle, and corresponding to the quotient of MDL by MDW (MBR = MDL ÷ MDW).

Distoapical Denticle Density (DA)—Number of denticles per five millimeters at the apicalmost part of the distal carina (Smith et al. 2005; Fig. 2.7H). Given the fact that the serrated distal carina does not always reach the apex of the crown (e.g. *Sciurumimus*, *Compsognathus*, *Scipionyx*), the measurement is inapplicable if the apicalmost part of the distal surface of the crown is unserrated. The distoapical denticle density corresponds to five times the posterior apical carina denticles per millimeter (PAD/mm) of Buckley et al. (2010).

Distocentral Denticle Density (DC)—Number of denticles per five millimeters on the distal carina at mid-crown, regardless the position of the carina on the crown (Smith et al. 2005; Fig. 2.7H). The distocentral denticle density corresponds to five times the posterior medial carina denticles per millimeter (PMD/mm) of Buckley et al. (2010).

Distobasal Denticle Density (DB)—Number of denticles per five millimeters in the basalmost part of the distal carina, regardless the position of the carina on the crown or the root (Smith et al. 2005; Fig. 2.7H). The distobasal denticle density corresponds to five times the posterior basal carina denticles per millimeter (PBD/mm) of Buckley et al. (2010).

Mesioapical Denticle Density (MA)—Number of denticles per five millimeters at the apicalmost part of the mesial carina (Smith et al. 2005; Fig. 2.7H). Similarly to the distal carina, the serrated mesial carina does not always reach the apex of the crown so that the measurement is inapplicable when the apicalmost part of the mesial margin of the crown is unserrated. The mesioapical denticle density corresponds to five times the anterior apical carina denticles per millimeter (AAD/mm) of Buckley et al. (2010).

Mesiocentral Denticle Density (MC)—Number of denticles per five millimeters on the mesial carina at mid-crown, regardless the position of the carina on the crown (Smith et al. 2005; Fig. 2.7H). The mesiocentral denticle density corresponds to five times the anterior medial carina denticles per millimeter (AMD/mm) of Buckley et al. (2010).

Mesiobasal Denticle Density (MB)—Number of denticles per five millimeters at the basalmost part of the mesial carina, regardless the position of the carina on the crown or the root (Smith et al. 2005; Fig. 2.7H). The mesiobasal denticle density corresponds to five times the anterior basal carina denticle per millimeter (ABD/mm) of Buckley et al. (2010). In many cases, the mesial carina does not reach the cervix, and the measurement is, therefore, inapplicable if the basalmost part of the mesial margin of the crown is unserrated.

Average Mesial Denticle Density (MAVG)—Average number of denticles per five millimeters along the mesial carina (Smith et al. 2005). MAVG = ((MA + MC + MB) ÷ 3).

Average Distal Denticle Density (DAVG)—Average number of denticles per five millimeters along the distal carina (Smith et al. 2005). DAVG = ((DA + DC + DB) ÷ 3).

Denticle Size Density Index (DSDI)—Ratio expressing the size difference between mesial and distal denticles (Rauhut and Werner 1995), and corresponding to the quotient of MC by DC (DSDI = MC ÷ DC). This measurement is similar to this of Rauhut and Werner (1995) and slightly differ from that of Smith et al. (2005) as it does not take into consideration the average number of denticles along both carinae, but only the mid-crown denticles on each carina. This reduces sampling errors when basal and/or apical denticles, typically smaller than denticles at the mid-crown, are not entirely preserved due to wearing.

Enamel Morphometry

Transverse Undulation Density (TUD)—Number of transverse undulations per five millimeters on the crown (Fig. 2.7G). The transverse undulation density (TUD) is equivalent to the crown transverse undulation density (CTU) of Hendrickx et al. (in press*a*).

Marginal Undulation Density (MUD)—Number of marginal undulations per five millimeters on the crown (Fig. 2.7G).

Labial Flutes (LAF)—Number of flutes on the labial surface of the crown.

Lingual Flutes (LIF)—Number of flutes on the lingual surface of the crown (Fig. 2.7H).

Dentine Morphometry

Dentine Thickness Mesially (DMT)—Mesiodistal extent of the dentine layer in the most mesial part of the tooth, at the level of the cervix or in the basal part of the root (Hendrickx et al. in press*a*; Fig. 2.7B).

Dentine Thickness Distally (DDT)—Mesiodistal extent of the dentine layer in the most distal part of the tooth, at the level of the cervix or in the basal part of the root (Hendrickx et al. in press*a*; Fig. 2.7B).

Dentine Thickness Lingually (DLIT)—Labiolingual extent of the dentine layer in the medial part of the lingual side of the tooth, at the level of the cervix or in the basal part of the root (Hendrickx et al. in press*a*; Fig. 2.7B).

Dentine Thickness Labially (DLAT)—Mesiodistal extent of the dentine layer in the medial part of the lingual side of the tooth, at the level of the cervix or in the basal part of the root (Hendrickx et al. in press*a*; Fig. 2.7B).

Methodology to describe isolated theropod teeth

Future authors may use the methodology below to facilitate the description of theropod teeth. This procedure is divided in five sections: tooth condition, crown, denticles, enamel, and root.

Condition

The preservation state of the tooth is a first assessment of the quality of the data to be extracted. Therefore details on fractures, eroded surfaces, taphonomic deformation (e.g., compression, tension, shear, torsion and bending) is fundamental to explicit because it may affect the original tooth morphology. Antemortem tooth deformation such as wear facets and spalled surfaces, should not be included in this section, and rather under tooth ornamentation.

Crown

Each tooth needs to be correctly labeled and oriented, with respect to the tooth row. In the case of isolated teeth, it is usually impossible to determine the actual position of the crown within its previous tooth row using curvature, carina orientation, and labial and lingual depression. Yet, these features can help determining the relative orientation of the tooth (i.e., mesial, distal, labial and distal sides of the tooth), and whether the isolated tooth belongs to the mesial or lateral dentition and, in some rare cases of theropods with significantly different dentition on the upper and lower jaws (e.g., *Byronosaurus*), to the left/right side of the cranium or mandible.

Most theropods have a distally curved crown; the mesial profile is thus more convex than the distal one. Theropod crowns like those of Spinosaurinae and some indeterminate coelurosaurs such as *Richardoestesia isosceles* (Baszio 1997; Sankey 2001; Sankey et al. 2002) may however lack curvature, so it is difficult, if not impossible, to know their exact mesiodistal orientation when found isolated. Orienting the labial and lingual surfaces of the crown can also be problematic. Most theropod teeth have a depression on the basal part of the crown. This depression represents the track of the erupting replacement crown lingually located from the erupted crown, therefore the side displaying this basal depression corresponds to the lingual margin, and the concavity is then the lingual depression. This sub-unit of the tooth is sometimes planar, and the basal part of the crown that displays a stronger convexity is typically the basolabial surface of the crown. Some avetheropods have a biconcave cross-section at the crown base, giving a figure-8 shape (e.g., Gianechini et al. 2011*a*; Hendrickx and Mateus 2014*b*; Fig. 2.5L), but the more concave surface is usually on the lingual side of the crown (pers. obs.). The orientation of the carinae also helps determining the labiolingual orientation of an isolated crown. The distal carina is deflected labially in theropods when offset. Likewise, the mesial carina is displaced lingually, or curves towards the lingual side basally if not centrally positioned on the tooth (pers. obs.).

The heterodonty noticed by many authors for the theropod dentition (e.g., Carrano et al. 2002; Smith et al. 2005; Rauhut et al. 2010; Reichel 2010) derives mostly from the morphological difference between mesial and lateral teeth. The position of an isolated tooth along the tooth row is, therefore, often determinable, if they are the mesial teeth, or if they are located posteriorly (i.e., non-mesial teeth) within the lateral dentition. Despite inter-taxic variation in mesial tooth morphology, there are several features that can be used to differentiate mesial from lateral teeth: the crown-base ratio (CBR, *sensu* Smith et al. 2005), the asymmetrical profile of the crown in cross-section, and the presence of

crown ornamentations. In ziphodont theropods, mesial teeth are typically broader than lateral teeth (i.e., CBR is above 0.64). This is, however, not the case in folidont, pachydont and conidont theropods in which the crown-base ratio of lateral teeth is often as high as those of the mesial dentition (pers. obs.). In some ziphodont and folidont theropods bearing serrated teeth (e.g., Non-neotheropod Theropoda, Compsognathidae, Therizinosauroidea, some Deinonychosauria) mesial teeth are not denticulate, or display a mesial margin devoid of carina. The mesial carina of many ziphodont and pachydont theropods typically spirals lingually or faces lingually when present. In these theropods, the distal carina remains either centrally positioned on its distal margin or is deflected labially (and very rarely lingually, pers. obs.). There are few cases of ziphodont theropods (e.g., Megalosauridae) in which both carinae remains centrally positioned so that the mesial crowns are subsymmetrical, but the significant elongation (crown height ratio, or CHR *sensu* Smith et al. 2005), above 2.5) and subcircular/elliptical cross-section of the crown base differentiate them from lateral crowns. Likewise, mesial teeth of some ziphodont theropods present a concave surface adjacent to one or both carinae (e.g., Abelisauridae, Allosauridae), fluted surface (e.g., Coelophysidae, Ceratosauridae, Noasauridae, Compsognathidae, Dromaeosauridae), longitudinal ridges or grooves (e.g., Tyrannosauroidea), or a small mesiodistal constriction at the level of the cervix (e.g., Tyrannosauroidea, Compsognathidae), several features that are typically absent in the lateral dentition.

Teeth can also vary in their crown shape (e.g., ziphodont, folidont, conidont, pachydont; Fig. 2.5), thickness (e.g., strongly, moderately or weakly narrow; arbitrary divisions based on the CBR value), elongation (e.g., short, moderately or strongly elongated; arbitrary divisions based on the CHR value), curvature (e.g., labiodistal, distal or labiolingual orientation of the crown apex), and mesial and distal profiles in lateral (e.g., strongly convex, weakly convex, straight, concave) and distal views (e.g., straight, recurved labially/lingually, sigmoid). Details on the curvature of the labial and distal surface should be added (e.g., strongly or slightly convex, planar), and also the extension of the crown enamel on each side of the crown (e.g., enamel extending more basally in the mesial/distal and labial/lingual part of the crown, symmetrical extension of the enamel on the crown). Additionally, we recommend to add details on the mesial and distal carinae, their morphology (e.g., serrated/unserrated, split, low/markedly developed), position (e.g., centrally positioned on the mesial/distal margin, deflected labially/lingually, facing labially/lingually, symmetrically positioned or not), extension (e.g., reaching the cervix, crossing the apex, terminating well-above the cervix and/or well-below the apex, extending on the root), and orientation (e.g., straight, diagonally-oriented, twisted). The presence of concave surfaces adjacent to the carinae, as well as any labial and/or lingual depressions should also be reported, with further details on the position and extension on the crown surface, both labially and lingually. Finally, it is important to describe the cross-section outline of the base-crown (e.g., subcircular, elliptical, lenticular, lanceolate, reniform, U-shaped, D-shaped, J-shaped; see above) at the level of the cervix (Fig. 2.5F–T) and at mid-height of crown.

Denticles

Important features to describe denticles include the denticle morphology, and the number of denticles per unit distance (typically, one or five millimeters) on both carinae as well as in different locations on the crown, i.e., basally, at mid-crown and apically. A description of the denticle size density index should also be reported (e.g., mesial and distal denticles of similar size, distal denticles larger/smaller than mesial ones; based on denticle size density index value, or DSDI *sensu* Rauhut and Werner (1995) as well as information on the denticle size variation (e.g., regular/irregular, changing smoothly/ dramatically along the carinae). Denticle morphology is relatively diverse in non-avian theropods (Fig. 2.8) and the mesial and distal denticle morphology should be described in terms of its shape (e.g., chisel-shaped, lanceolate), elongation (e.g., subquadrangular, baso-apically subrectangular, proximo-distally subrectangular), inclination (e.g., perpendicular to carina, apically inclined), outline of the external margin (e.g., symmetrically convex, asymmetrically convex, parabolic, subrectangular with planar surface, semi-circular, bilobate, apically hooked), interdenticular

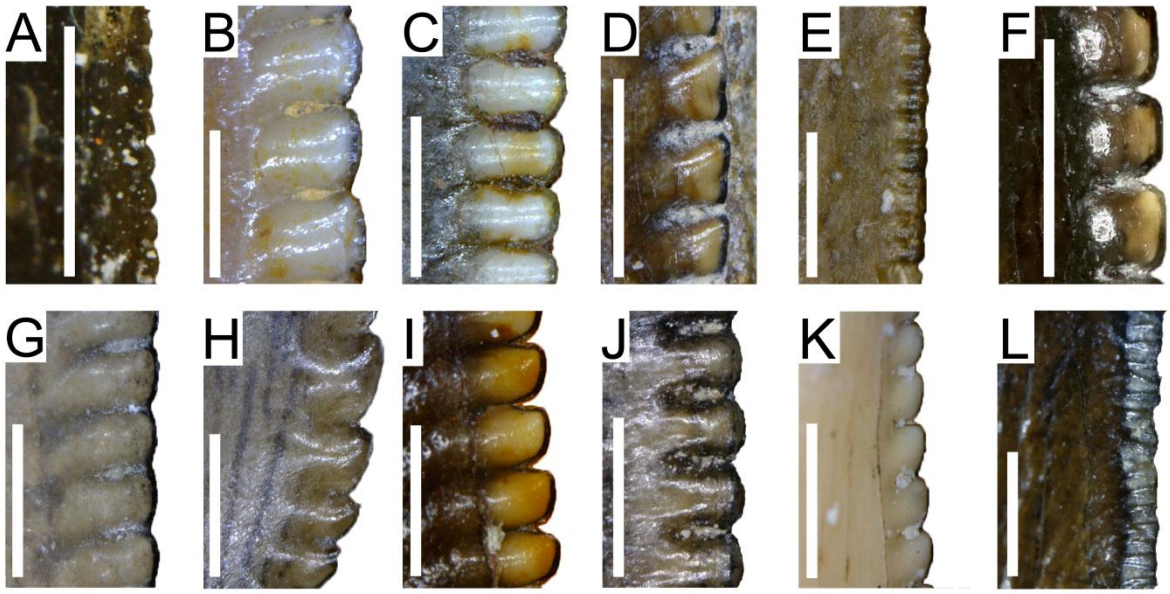

FIGURE 2.8. Morphological diversity of denticles in non-avian theropods in lateral views. **A**, Baso-apically subrectangular distocentral denticles of the fourth left maxillary tooth (Lmx4) of *Eodromaeus murphi*, PVSJ 561; **B**, Subquadrangular distocentral denticles of an isolated maxillary tooth of *Carcharodontosaurus saharicus*, SGM Din-1; **C**, Mesiodistally subrectangular distocentral denticles of an isolated tooth of *Afrovenator abakensis*, MNN TIG1; **D**, Apically inclined and bilobate mesioapical denticles of an isolated tooth of *Megalosaurus bucklandi*, NHM R.234; **E**, Minute subquadrangular distocentral denticles with a regular morphological variation of an isolated tooth of *Suchomimus tenerensis*, MNN G73–3; **F**, Subquadrangular mesioapical denticles with planar external margins of an isolated tooth of *Acrocanthosaurus atokensis*, SMU 74646; **G**, Distocentral denticles with short interdenticular sulci and shallow interdenticular slits of the first left maxillary tooth (Lmx1) of *Erectopus superbus*, MNHN 2001–4; **H**, Large and apically hooked distocentral denticles with dramatic size variation of an isolated tooth of *Troodon formosus*, DMNH 22837; **I**, Weakly apically hooked distocentral denticles of an isolated tooth of an indeterminate Abelisauridae, ML 327; **J**, Subquadrangular distocentral denticles with wide interdenticular chambers of an isolated tooth of an indeterminate Tyrannosauridae, DMNH 21030; **K**, Baso-apically subrectangular and apically hooked distocentral denticles of an isolated tooth of *Masiakasaurus knopfleri*, FMNH PR2221; **L**, Minute subrectangular distocentral denticles with an irregular morphological variation of an isolated tooth of *Baryonyx walkeri*, NHM R.9951–278. Scale bars equals 1 mm.

space (e.g., shallow/deep, narrow/large), diaphysis (e.g., present/absent, shallow/deep) and slit (e.g., shallow/deep, concave/subtriangular, with or without a lamina joining two neighboring denticles). Finally, details on the interdenticular sulci should be reported for both sides and carinae, such as their curvature (e.g., straight or curving basally), inclination (e.g., horizontal or inclined basally) and extension (e.g., short, medium or long and well-developed). Because caudae are the result of interdenticular sulci, and the latter are more distinct and better visible than caudae (Smith 2007; pers. obs.), we suggest to favour the description of interdenticular sulci instead of caudae.

Ornamentations and Other Attributes

A thorough description on the crown ornaments/attributes should include details on spalled surfaces, wear facets, flutes, transverse and marginal undulations, labial and lingual depressions, longitudinal grooves and ridges, and basal striations. These details should be given for both labial and lingual surfaces. It is important to specify details on the number of flutes, striations, longitudinal grooves and ridges on the crown. Concerning transverse and marginal undulations, it is central to describe details on its density (e.g., numerous, just a few), orientation (e.g., horizontal, diagonal), extension (e.g., transverse undulations covering the crown, restricted to the crown center/vicinity) and discernibility (e.g., only visible in certain angle, well-visible in all crown orientations). To complete the description, details on the enamel texture should be provided, with information on the texture pattern (smooth, irregular, braided, or deeply veined; Fig. 2.8) and orientation in the middle of the crown and marginal to the carinae.

Root

Isolated theropod teeth are typically shed teeth, thus only preserving portions of the basal part of the root. However, isolated teeth may also include the whole root, indicating postmortem disarticulation of the teeth from the jaws and distancing from the tooth-bearing bones before burial. A description on the preserved root should include details on its morphology (e.g., labiolingually narrow, sub-cylindrical, tapered at the apex, with parallel/convex mesial and distal margins), ornamentations (e.g., transverse undulations, labial/lingual depressions), and cross-section at mid-height of the root (e.g., subcircular, oval, 8-shaped, reniform). Morphology and depth of the resorption pit should also be provided. In shed teeth preserving the basal portion of the root, it is important to describe the thickness of the dentine layer medially, distally, labially and lingually in basal view as the transversal extension of the dentine layer varies along the tooth jaw and between taxa (pers. obs.).

Conclusions

This study reveals the taxonomic value of theropod teeth and contributes to better understanding the phylogenetic potential of isolated theropod teeth. Many features including the

extension and position of carinae, cross-section outline, size and morphology of denticles, and crown ornamentation and texture are all diagnostic features that help identify the position of isolated teeth along the tooth row as well as the taxa to which they belong to. A detailed description of the dentition of many pivotal theropods such as *Dilophosaurus*, *Ceratosaurus*, *Allosaurus*, *Monolophosaurus*, *Sinraptor*, *Yangchuanosaurus*, *Dilong*, and *Guanlong* is, therefore, critically required in order to help clarify the distribution of the numerous morphologies present in theropod clades with superficially similar dentitions (e.g., Ceratosauridae, Allosauridae, Metricanthosauridae, Neovenatoridae and Proceratosauridae). Likewise, the comprehensive description of isolated theropod teeth, typically abundant in dinosaur fossil sites, is crucial to help resolving their systematic position. The adoption of a methodology, and a standard positional, morphological, anatomical and morphometric nomenclature, such as the ones proposed here for the theropod dentition, will certainly help with description, measurement, and ultimately identification of isolated theropod teeth which can be helpful for paleobiogeographic and stratigraphic purposes.

Chapter 3: The distribution of dental features in non-avian theropods

Submitted to ***Palaeontologia Electronica*** (IP 1.4):
Hendrickx, C., Mateus, O. and Araújo, R. in review. The distribution of dental features in non-avian theropods. *Palaeontologia Electronica*.

Abstract

Isolated theropod teeth are some of the most common fossils in the dinosaur fossil record and are constantly reported in the literature. Although recently developed quantitative methods potentiate the assessment of the phylogenetic relationships of isolated theropod teeth, they are typically assigned to diagnose taxa on the basis of qualitative characters with questionable phylogenetic potential. As a result, the distribution of a large number of dental features is still poorly known. Furthermore, the paucity of comprehensive information in the literature makes identification of isolated teeth problematic. We, therefore, investigated the distribution of thirty dental characters among 113 theropod taxa, and propose a list of diagnostic dental characters in order to facilitate future study on the systematic paleontology of isolated teeth. Functional clues for each dental feature were also added in order to provide context on the degree of homoplasy relating to function.

Introduction

Theropods form a group of bipedal dinosaurs that are the common ancestors to birds (e.g., Padian and Chiappe 1998; Gauthier and Gall 2002; Currie 2004; Padian 2004; Brusatte 2012; Naish 2012). The majority are carnivorous, yet not all of non-avian theropods were meat-eaters (e.g., Kobayashi et al. 1999; Zanno et al. 2009; Sander et al. 2010; Zanno and Makovicky 2011). The diversity of feeding strategies in theropods is particularly relevant among dinosaurs, resulting in a large array of tooth shape and dentition morphology (Currie et al. 1990; Hendrickx and Mateus 2014*b*). Like fishes, crocodiles, squamates and other group of dinosaurs, theropods are polyphyodont animals, i.e., they continuously replaced their teeth, therefore producing shed teeth through their life (Hendrickx et al. in press*c*). Teeth are robust skeletal elements (Hillson 2005), and most toothed theropods had 50 or more teeth that were replaced once every one to two years (Fiorillo and Currie 1994; Erickson 1996), thus theropods teeth are one of the most common fossils in terrestrial Mesozoic formations (e.g., Erickson 1996; Smith et al. 2005; Blob and Badgley 2007) and are constantly reported in the literature (e.g., Madzia in press; Torices et al. in press; Currie et al. 1990; Rauhut and Werner 1995; Baszio 1997; Zinke 1998; Sankey et al. 2002; Sweetman 2004; Maganuco et al. 2005; Vullo et al. 2007; Larson 2008*a*; Lubbe et al. 2009; Casal et al. 2009; Ősi et al. 2010; Han et al. 2011; Richter et al. 2013; Sues and Averianov 2013; Kear et al. 2013; Larson and Currie 2013; Cobos et al. 2014; Hendrickx and Mateus 2014*b*).

Although isolated theropod teeth provide taphonomical, paleoenvironmental and paleoecological data (e.g., Briggs and Crowther 2001; Amiot et al. 2004*b*, 2006, 2009, 2011; Rogers et

al. 2007), they also record the theropod paleodiversity, and extend the temporal and geographic ranges of theropod taxa and clades (Brusatte et al. 2007). Despite the importance of theropod teeth, their morphology is poorly known, leading numerous authors to assign isolated theropod teeth to broad clades (e.g., Madzia in press; Ősi et al. 2010; Amiot et al. 2011; Carrano et al. 2012; Ruiz-Omeñaca et al. 2012), failing to provide useful information on paleogeographic and stratigraphic distributions of theropod clades.

Although morphometric analyses were proven to be successful technique to identify isolated teeth (Smith et al. 2005), recent studies revealed that theropods with similar dentition can only be differentiated based on qualitative characters (Hendrickx et al. in press*a*; Hendrickx and Mateus 2014*b*). Nonetheless, the dentition of the large majority of theropods is briefly described, with very few details provided on the crown, carina, and denticle morphology (Hendrickx et al. in press*a*). Although a few theropod such as *Coelophysis* (Buckley 2009), *Majungasaurus* (Fanti and Therrien 2007; Smith 2007), *Tyrannosaurus* (Smith 2005) *Troodon* (Currie 1987) and *Buitreraptor* (Gianechini et al. 2011*a*) have received a thorough description of their dentition, details on the denticle shape, cross-section outline, extension of the mesial carina and presence of crown ornamentations are often omitted. This scarcity of information on theropod teeth morphology leads to taxonomic assignments on the basis of *a priori* assumptions of their phylogenetic affinities (Smith 2005). As an example, the marginal undulations (*sensu* Hendrickx et al. in press*c*) visible on the crown of some carcharodontosaurids are often considered as a key character of this clade, leading many authors to assign isolated teeth to Carcharodontosauridae solely based on this feature (Brusatte et al. 2007).

This paper aims to investigate the distribution of a certain number of dental features in non-avian theropods, with the goal of facilitating future study on the systematic paleontology of isolated teeth.

Materials and Methods

We investigated the distribution of dental features based on *in situ* and isolated teeth belonging to 113 non-avian theropod taxa (Table 3.1). 73 taxa deposited in 30 scientific collections from Argentina, France, Germany, Italy, Portugal, Qatar, Switzerland, United Kingdom, and the United States of America were examined first hand. Denticles and enamel texture were observed with a digital microscope AM411T-Dino-Lite Pro. High-resolution photos of the dentition were provided for 27 additional theropod taxa, and publications with well-illustrated and/or well-described teeth were used for 13 taxa (Table 3.1). The anatomical nomenclature used in this study follows the terminology proposed by Smith and Dodson (2003) and Hendrickx et al. (in press*c*; see Chapter 1) for theropod teeth (Figs. 2.1– 2.5). The topological definitions proposed by Smith and Dodson (2003) and Hendrickx et al. (in press*c*; see Chapter 1) were followed for the directional and positional nomenclature (Fig. 2.1). Morphometric terms and abbreviations used in this paper follow Smith et al. (2005) nomenclature (Fig. 2.6).

TABLE 3.1. Dentition of the 112 non-avian theropod taxa included in this study.

Taxa	Specimens	Examined	Photo credits	Literature
Abelisaurus comahuensis	MPCA 1, 5, 229, 267, 687, 689, 709	Yes		
Acheroraptor temertyorum	ROM 63777, 63778	No/photos	Derek Larson	Evans et al. 2013
Acrocanthosaurus atokensis	NCSM 14345; SMU 74646	Yes	Drew Eddy; Vince Shneider; Ricardo Araújo	
Aerosteon riocoloradensis	MCNA-PV 3137 UC unnumbered, cast	Cast/photos	Martín Ezcurra	
Afrovenator abakensis	UC UBA1	Yes		
Albertosaurus sarcophagus	DMNH 22019	Yes		Currie 2003
Alioramus altai	IGM 100-1844	Yes	Mick Ellison	Brusatte et al. 2012*a*
Allosaurus 'jimmadseni'	SMA 0005/02; NHFO 455	Yes		
Allosaurus fragilis	AMNH 600, 851; BYU-VP 2028; MWC 5440; USNM 8335; UMNH VP 5427 10.093, 40.585; CMNH 1254, 11844, 21703	Yes		
Anchiornis huxleyi	LPMB 00169	No/photos	Christian Foth	Hu et al. 2009
Arcovenator escotae	MHNA-PV.2011.12.20, 12.187, 12.297	Yes		
Angaturama limai	AMNH 30230 cast	Cast/publi		Kellner and Campos 1996
Aorun zhaoi	IVPP V15709	No/publi		Choiniere et al. 2014*b*
Atrociraptor marshalli	RTMP 95.166.1	No/publi		Currie and Varricchio 2004
Aucasaurus garridoi	MCF-PVPH 236	Yes	Matthew Lamanna	
Australovenator wintonensis	AODF 604	No/publi		Hocknull et al. 2009
Austroraptor cabazai	MML 195	No/photos	Martín Ezcurra	Novas et al. 2009
Bambiraptor feinbergi	AMNH 30556	Yes		
Baryonyx walker	NHM R.9951; ML 1190	Yes		
Berberosaurus liassicus	MNHN Pt339	Yes		
Bicentenaria argentina	MPCA 865, 866	Yes		
Buitreraptor gonzalezorum	MPCA 245	Yes	Martín Ezcurra	Gianechini et al. 2011*a*
Byronosaurus jaffei	IGM 100-983	Yes		
Carcharodontosaurus saharicus	MNN GAD8, IGU5; SGM Din-1; UC PV6; BSPG 1993 IX 328	Yes	Martín Ezcurra	
Carnotaurus sastrei	MACN-CH 894	Yes		
Ceratosaurus nasicornis	USNM 4735; UMNH VP 5278 = UUVP 155, 158, 674; MWC 1;	Yes	Matthew Carrano; Roger Benson	
Coelophysis bauri	AMNH 7223, 7224, 7227, 7228, 7229, 7231	Yes	Martín Ezcurra	Buckley 2009
Compsognathus longipes	MNHN CNJ 79	Yes	Karin Peyer	
Condorraptor currumili	MPEF-PV 1672	No/photos	Martín Ezcurra	Rauhut 2005*a*
Daspletosaurus torosus	NHM R.4863; FMNH PR308	Yes		
Deinonychus antirrhopus	YPM 5210, 5232	No/publi		Ostrom 1969
Dilong paradoxus	IVPP V14242, V14243	No/photos	Stephen Brusatte	Xu et al. 2004

Dilophosaurus wetherilli	UCMP 37302, 37303, 77270	No/photos	Martín Ezcurra	
Dromaeosauridae indet.	UC unnumbered	Yes		
Dromaeosaurus albertensis	AMNH 5356	Yes		Currie et al. 1990
Dryptosaurus aquilunguis	ANSP 9995	No/photos	Stephen Brusatte	Brusatte et al. 2011
Dubreuillosaurus valesdunensis	MNHN 1998-13	Yes		
Duriavenator hesperis	NHM R.332	Yes		
Ekrixinatosaurus novasi	MUCPv 294	Yes	Matthew Lamanna	
Eoabelisaurus mefi	MPEF PV 3990	No/photos	Christian Foth	Pol and Rauhut 2012
Eocarcharia dinops	MNN GAD7, GAD13, GAD14	Yes	Juan Canale	
Eodromaeus murphi	PVSJ 560, 561, 562	Yes	Martín Ezcurra	
Eoraptor lunensis	PVSJ 512	Yes	Martín Ezcurra	
Eotyrannus lengi	MIWG 1997.550	Yes		
Erectopus superbus	MNHN 2001-4	Yes		
Erlikosaurus andrewsi	PST 100/111	No/publi		Clark et al. 1994
Eustreptospondylus oxoniensis	OUMNH J.13558	Yes		
Frenguellisaurus ischigualastensis	PVSJ 053	Yes		
Fukuiraptor kitadaniensis	FPMN 9712203, 9712204, 9712205, 9712206 + many others	No/publi		Azuma and Currie 2000; Currie and Azuma 2006
Genyodectes serus	MLP 26-39	Yes		
Giganotosaurus carolinii	MUCPv-CH-1; MUCPv 95	Yes		
Gorgosaurus libratus	AMNH 5336, 5434, 5458, 5664; USMN 12814	Yes		
Guanlong wucaii	IVPP V14531, V14532	No/photos	Christian Foth	Xu et al. 2006
Herrerasaurus ischigualastensis	PVSJ 407	Yes	Martín Ezcurra	
Incisivosaurus gauthieri	IVPP V 13326	No/publi		Balanoff et al. 2009
Indosuchus raptorius	AMNH 1753, 1955, 1960	Yes		
Irritator challenger	SMNS 58022	Yes	Ricardo Araújo	
Ischisaurus cattoi	MACN 18.060	Yes		
Juravenator starki	JME Sch 200	No/publi		Chiappe and Göhlich 2010
Kryptops palaïos	MNN GAD1−1	Yes		
Liliensternus liliensterni	MB.R.2175	Cast/photos	Martín Ezcurra	Cillari 2010
Lourinhanosaurus antunesi	ML565 embryos	Yes		
Magnosaurus nethercombensis	OUMNH J.12143	Yes		
Majungasaurus crenatissimus	FMNH PR 114 2008, 2100, 2278; UA 8716	Yes		Fanti and Therrien 2007; Smith 2007
Mapusaurus roseae	MCF-PVPH 108	Yes		
Marshosaurus bicentesimus	AMNH 27638, 27640, 27641 cast	Cast/photos	Mathew Carrano	Madsen 1976*a*
Masiakasaurus knopfleri	FMNH PR 2182, 2183, 2201, 2221, 2453, 2471, 2476, 2696; UA 8680, 9091, 9128	Yes		
Megalosaurus bucklandii	OUMNH J.13505, J.13506; NHM R.8303, R.8305	Yes		

Megapnosaurus kayentakatae	MNA V2623	No/photos	Randal Irmis	
Megaraptora indet.	MUCPv unnumbered	Yes	Matthew Lamanna	
Microraptor zhaoianus	CAGS 20-7-004; BMNHC PH881	No/photos	Mick Ellison; Christian Foth	Xu et al. 2000; Hwang et al. 2002
Monolophosaurus jiangi	IVPP 84019	No/photos	Stephen Brusatte; Roger Benson	Brusatte et al. 2010*a*
Neovenator salerii	MIWG 6348; NHM R.10001	Yes	Stephen Brusatte	
Noasaurus leali	PVL 4061	Yes		
Nuthetes destructor	NHM R.48207, 48208	Yes		
Orkoraptor burkei	MPM-Pv 3457	No/photos	Martín Ezcurra	Novas et al. 2008
Ornitholestes hermanni	AMNH 619	Yes		
Piatnitzkysaurus floresi	PVL 4073; MACN-CH 895	Yes	Martín Ezcurra	
Proceratosaurus bradleyi	NHM R 4860	Yes		Rauhut et al. 2010
Pyroraptor olympius	MNHN BO014-015	Yes		
Rahiolisaurus gujaratensis	ISIR 401	No/photos	Fernando Novas	Novas et al. 2010
Raptorex kriegsteini	LH PV18	Yes		
Richardoestesia gilmorei	NMC 343	No/publi		Currie et al. 1990
Rugops primus	MNN IGU1	Yes		
Sanjuansaurus gordilloi	PVSJ 605	Yes		
Saurornithoides mongoliensis	AMNH 6516	Yes		
Saurornitholestes langstoni	DMNH 22870	Yes		Currie et al. 1990
Scipionyx samnicicus	SBA-SA 163760	No/photos	Cristiano Dal Sasso	Dal Sasso and Maganuco 2011
Sciurumimus albersdoerferi	BMMS BK 11	No/photos	Christian Foth	Rauhut et al. 2012
Shuvuuia deserti	IGM 100-977	Yes		
Siamosaurus suteethorni	DMR-TF 2043	No/publi		Buffetaut and Ingavat 1986; Bertin 2010
Sinornithosaurus millenii	IVPP V 12811	No/publi		Xu and Wu 2001
Sinosauropteryx prima	NIGP 127586, 127587	No/publi		Currie and Chen 2001
Sinosaurus triassicus	IVPP V34; ZLJ 0003; ZLJ T01; KMV 8701; LDM-LCA 10	No/photos	Philip Currie	Xing 2012
Sinraptor dongi	IVPP 10600	No/photos	Roger Benson	
Sinraptor hepigensis	ZDM T0024	No/photos	Philip Currie	
Skorpiovenator bustingorryi	MMCH-PV 48	Yes		
Spinosaurus aegyptiacus	MSNM V3976, V4047, V6422, V6424, V6865, V6896; NHM R.16420, R.16421	Yes	Andrea Cau	
Staurikosaurus gordilloi	MCZ 1669	No/photos	Randal Irmis	Bittencourt and Kellner 2009
Suchomimus tenerensis	MNN GDF501, GDF502, G2-2, G5-1, G6, G22-7, G26-5, G34-1, G34-7, G34-12, G35-9, G43-5, G54-4, G67-1, G67-8, G69-5, G73-3, G74-1, G100-4, G232	Yes		

Suchosaurus cultridens	NHM R36536	Yes		
Tarbosaurus bataar	ZPAL MgD-I/4	No/photos	Stephen Brusatte	Hurum and Sabath 2003
Torvosaurus tanneri	BYU-VP 2003, 4882, 9122 12817; ML 1100	Yes		
Troodon formosus	DMNH 22337, 22837	Yes		Currie 1987; Currie et al. 1990; Baszio 1997; Longrich 2008
Troodontidae indet.	IGM 100-1128	Yes		
Troodontidae indet.	IGM 100-1323	Yes		
Tsaagan mangas	IGM 100-1015	Yes		
Tyrannosaurus rex	CMNH 9380; AMNH 5027; FMNH PR2081; NHM R.7994	Yes		Smith 2005
Tyrannotitan chubutensis	MPEF-PV 1156	No/photos	Martín Ezcurra; Juan Canale	
Velociraptor mongoliensis	AMNH 6515	Yes		Sues 1977; Barsbold and Osmólska 1999
Yangchuanosaurus shangyuensis	CV 00215	No/photos	Philip Currie	
Zuolong sallei	IVPP V15912	No/publi		Choiniere et al. 2010*a*
Zupaysaurus rougieri	PULR 076	Yes	Martín Ezcurra	

Results and Discussion

The study of the dentition of more than one hundred theropod taxa allows us to propose a list of diagnostic features to help identifying isolated theropod teeth. These diagnostic features are not necessarily synapomorphies, but rather major guidelines for identifying teeth, and are a result of our previous phylogenetic work focused on theropod teeth (Hendrickx and Mateus 2014*b*) as well as new observations. The distribution of most dental features is illustrated in two phylogenetic trees (Figs. 3.1, 3.2) and one main table (Fig. 3.4). We also added some functional clues for dental features directly related to function in order to give some context whether they are synapomorphic or simply homoplastic features related to function and/or allometry. Although the dentition of theropods varies morphologically through ontogeny (e.g., Carr 1999; Carr and Williamson 2004; Rauhut et al. 2012; Araújo et al. 2013), the teeth of immature individuals (i.e., posthatchling individual) were also taken into consideration. However, identifying teeth of immature individuals is difficult, if not impossible, because their morphology can be remarkably similar to that of distantly related clades due to comparable diet or heterochronic processes (Rauhut et al. 2012). Dentition-based characters are common in cladistic analyses and are more and more often incorporated to help assessing the relationships of non-avian theropods. Here we also cite the prior use of dental characters, and discuss the scorings in the most recent phylogenetic analyses.

Dentition

Ziphodonty, i.e., a lateral dentition mostly composed of strongly labiolingually narrow crowns with a distal curvature, typically serrated carinae, and no constriction at the cervix (Hendrickx et al. in press*c*), is present in *Ornitholestes*, non-alvarezsaurid Alvarezsauroidea, Dromaeosauridae, and all non-maniraptoriform theropods other than Spinosauridae and Tyrannosauridae. Folidonty, i.e., a lateral dentition mostly composed of teeth with an important constriction at the level of the cervix, thus displaying a lanceolate leaf-shaped outline in lateral view (Hendrickx et al. in press*c*), is present in all maniraptoriform theropods other than Ornithomimosauria (with the exception of *Pelecanimimus*), Dromaeosauridae, *Ornitholestes*, and non-alvarezsaurid Alvarezsauroidea. Only mature tyrannosaurids display a pachydont dentition, i.e., lateral dentition mostly composed of labiolingually expanded and distally recurved crown in which the labiolingual width is greater than 60% of the mesiodistal length, from cervix to apex (Hendrickx et al. in press*c*). Finally, conidonty, i.e., lateral dentition mostly composed of conical crowns that have minute denticles or no denticles at all (Hendrickx et al. in press*c*), is present in all Spinosauridae as well as all toothed ornithomimosaurs excluding *Pelecanimimus*.

Most theropods are pseudoheterodont, i.e., they have a dentition in which the crown morphology gradually changes along the jaw so that mesial and lateral teeth differ significantly in

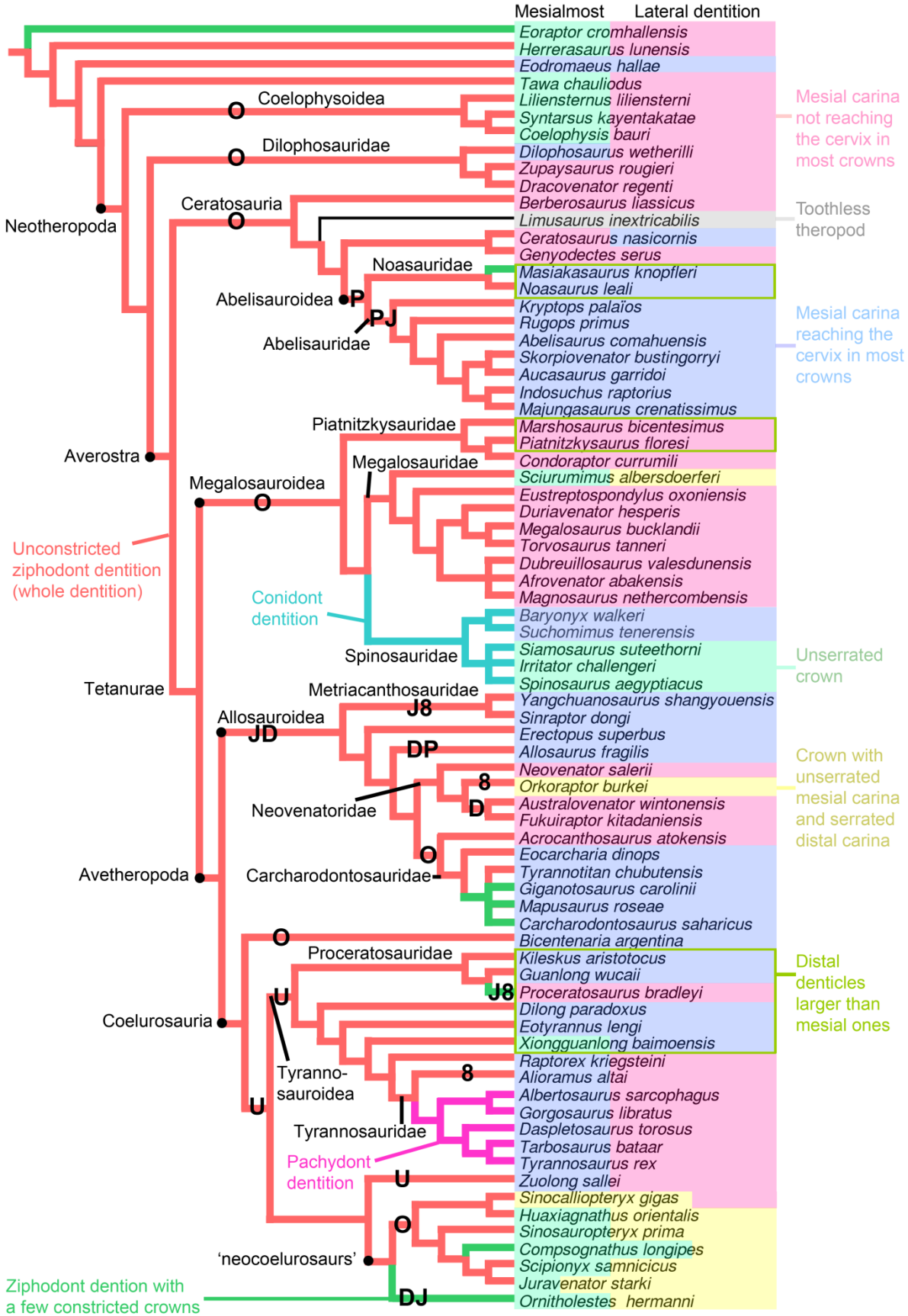

FIGURE 3.1. Distribution of dental features in non-coelurosaurian theropods. Phylogenetic tree based on the results obtained by Yates (2005), Smith et al. (2007), Brusatte et al. (2010b), Sues et al. (2011), Pol and Rauhut (2012), Carrano et al. (2012), Turner et al. (2012), and Tortosa et al. (2014). The branch colors represent the dentition types and the presence or absence of constricted crowns: ziphodont taxa with unconstricted crowns are

◄ in red, ziphodont taxa with a few constricted crowns are in green, conidont taxa are in turquoise, and pachydont taxa are in violet. The colors of taxa represent the presence or absence of serrations on the mesial and distal carinae for both mesial (left column) and lateral dentition (right column): toothless taxa are in grey, taxa with unserrated crown are in green, taxa with a serrated distal carina and a serrated mesial carina not reaching the cervix are in red, taxa with a serrated distal carina and a serrated mesial carina reaching the cervix are in blue, and taxa with a serrated distal carina and an unserrated mesial carina are in yellow. Taxa with distal denticles larger than mesial ones are boxed in green. Some compsognathid taxa possess a double condition in their mesial and lateral dentition: *Juravenator* bears mesial crowns with serrated and unserrated distal carina, *Compsognathus* shows lateral crowns with unserrated and serrated distal carina, and *Sinocalliopteryx* possesses serrated and unserrated mesial carinae in the lateral teeth. **Abbreviations**: **8**, eight-shaped cross-section of lateral teeth; **D**, D-shaped cross-section of mesial teeth; **J**, J-shaped cross-section of mesial teeth; **O**, subcircular/lanceolate cross-section of mesial teeth; **P**, parlinon-shaped cross-section of mesial teeth; **U**, U-shaped cross-section of mesial teeth.

their morphology. Interestingly, *Haplocheirus*, and the troodontids *Sinovenator*, *Xixiasaurus*, and *Byronosaurus* show a heterodont lateral dentition which encompasses both ziphodont and folidont teeth. *Haplocheirus* is a form of alvarezsauroid between non alvarezsauroid maniraptorans with ziphodont teeth and alvarezsaurids with a folidont dentition. On the other hand, *Sinovenator*, *Xixiasaurus*, and *Byronosaurus* are derived troodontids and such heterodont dentition is autapomorphic among Troodontidae.

A ziphodont dentition is well-suited to slashing, cutting through flesh and defleshing (Abler 1992; D'Amore 2009; D'Amore and Blumenschine 2009), whereas folidonty is related with herbivory (Zanno and Makovicky 2011; Pu et al. 2013) and omnivory (Holtz et al. 1998; Barrett 2000; Longrich 2008). If pachydont and conidont theropod dentition both possess thick crowns, the former have the ability of bone-crunching and bone-biting involving a high degree of torsion (e.g., Holtz 2003, 2008; Snively et al. 2006; Reichel 2010), whereas the latter are rather adapted to impaling and holding prey items (e.g., Charig and Milner 1997; Holtz 1998*b*; Sereno et al. 1998; Sues et al. 2002; Holtz et al. 2004; Xing et al. 2013*a*). Conidont teeth are often used to infer a piscivorous diet (Baszio 1997; Sankey 2001; Brinkman 2008), yet minute and simple conical teeth bore by basal ornithomimosaurs, which possessed gastrolithes, instead implied a herbivorous diet (Makovicky et al. 2004; Zanno and Makovicky 2011; Choiniere et al. 2012). It has also been suggested that the presence of minute conical teeth in ornithomimosaurs is likely a functional precursor of the theropod rhamphotheca existing in derived ornithomimosaurs (Zanno and Makovicky 2011). Likewise, the heterodont lateral dentition displayed by some coelurosaurs has also been interpreted as an indicator of a shift from a carnivorous to an herbivorous diet (Zanno and Makovicky 2011).

Characters distinguishing ziphodont, pachydont, conidont teeth, and folidont (lanceolate) teeth were first proposed by Pérez-Moreno et al. (1994, character 4), Forster et al. (1998, characters 3-4), and Holtz et al. (2004, character 263) based on shape, thickness, and curvature. Since then, many characters related to the crown morphology (unserrated, constricted, conical, incrassate, etc.) have been used that define each dentition type in non-avian theropods, and the codings of these features in previous cladistic analyses are discussed separately in the next sections.

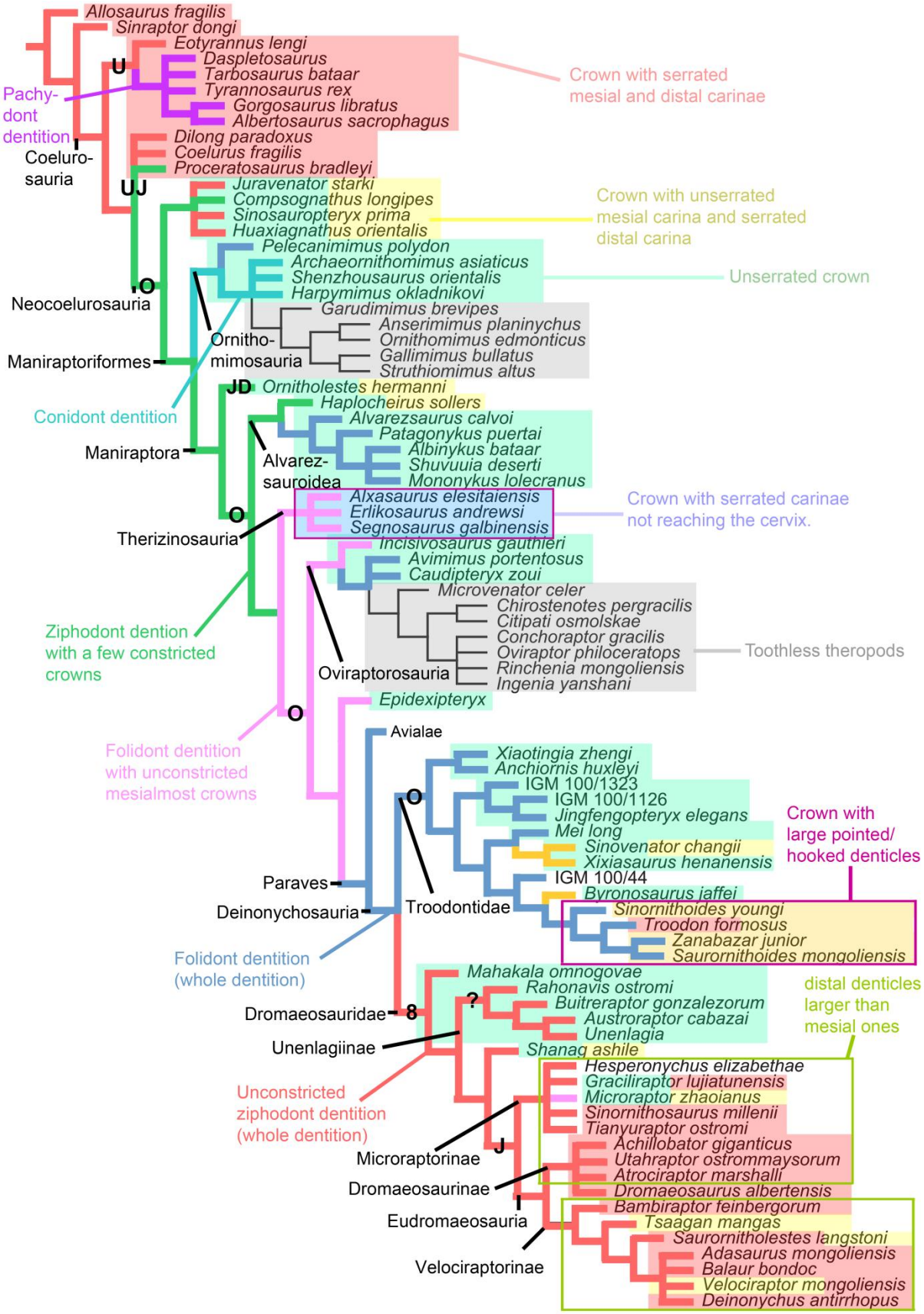

FIGURE 3.2. Distribution of dental features in Coelurosauria. Phylogenetic tree of Turner et al. (2012). The branch colors represent the dentition types: ziphodont taxa with unconstricted crowns are in red, ziphodont taxa with a few constricted crowns are in green, taxa with both folidont and ziphodont lateral dentition are in orange, folidont taxa with unconstricted mesial crowns are in pink, folidont taxa with constricted crowns only are in ◄

blue, conidont taxa are in turquoise, and pachydont taxa are in violet. Colors of taxa represent the presence or absence of serrations on the mesial and distal carinae for both mesial (left) and lateral dentition (right): toothless taxa are in grey, taxa with unserrated crowns are in green, taxa with a serrated distal carina and an unserrated mesial carina are in yellow, taxa with serrated mesial and distal carinae are in red, and taxa with both serrated mesial and distal carinae not reaching the cervix are in blue. Taxa showing both conditions (e.g., mesial dentition with unserrated teeth and lateral dentition with serrated teeth) are bicolored. Some deinonychosaurs such as *Troodon*, *Velociraptor* and *Saurornitholestes* possess a lateral dentition with serrated and unserrated carinae. Taxa with distal denticles larger than mesial ones are boxed in green, and taxa with large typically hooked denticles are boxed in purple. **Abbreviations**: **8**, eight-shaped cross-section of lateral teeth; **D**, D-shaped cross-section of mesial teeth; **J**, J-shaped cross-section of mesial teeth; **O**, subcircular/lanceolate cross-section of mesial teeth; **U**, U-shaped cross-section of mesial teeth.

Basal Constriction

A basal constriction at the cervix (Fig. 3.6) is present in *Eoraptor*, Noasauridae, Proceratosauridae and non-tyrannosauroid Coelurosauria for mesial teeth, *Eoraptor* and Carcharodontosaurinae for lateral teeth, and non-dromaeosaurid Maniraptoriformes other than *Microraptor* for the whole dentition (Figs. 3.1–3.2). In non-avian theropods, an important mesiodistal constriction at the cervix is present in some mesial and lateral teeth of *Eoraptor* (Sereno et al. 1993, 2013; Fig. 3.3A), some premaxillary teeth of the noasaurid *Masiakasaurus* (UA 8680, FMNH PR.2471), and in the whole dentition of the large majority of maniraptoriforms, including the basal ornithomimosaur *Pelecanimimus* (Pérez-Moreno et al. 1994), the derived alvarezsauroids *Shuvuuia* (IGM 100-977) and *Mononykus* (Perle et al. 1994), the oviraptorosaur *Caudipteryx* (Osmólska et al. 2004) and *Protarchaeopteryx* (Ji et al. 1998), the dromaeosaurid *Microraptor* (Xu et al. 2000; Turner et al. 2012), and all therizinosaurs (e.g., Russell and Dong 1993*a*; Zhao and Xu 1998; Xu et al. 2001*b*; Kirkland et al. 2005; Fig. 3.3C) and troodontids (e.g., Currie et al. 1990; Baszio 1997; Norell et al. 2000; Currie and Dong 2001*a*; Sankey et al. 2002; Averianov and Sues 2007; Fig. 3.3B). In ziphodont theropods, a weak constricted crown is also seen in some premaxillary teeth of the basal tyrannosauroid *Proceratosaurus* (Rauhut et al. 2010; Fig. 3.3D) and the basal coelurosaur *Ornitholestes* (AMNH 619), and some mesial dentary teeth in the compsognathid *Compsognathus* (Zinke and Rauhut 1994). Some crowns are also weakly constricted at the cervix in the lateral dentition of the basal alvarezsaurid *Haplocheirus* (Choiniere et al. 2010*b*: fig. S4), some dromaeosaurids such as *Atrociraptor* and *Richardoestesia* (Currie et al. 1990; Currie and Varricchio 2004; Agnolin and Novas 2011; Hendrickx and Mateus 2014*b*), and in some lateral teeth of the carcharodontosaurids *Carcharodontosaurus* (SGM Din 1) and *Giganotosaurus* (MUCPV-CH-1). With the exception of carcharodontosaurines, *Proceratosaurus*, *Compsognathus*, constricted teeth seem to be absent in all non-maniraptoriform theropods, and in the large majority of dromaeosaurids.

A constriction at the base of the crown appeared independently in noasaurids, carcharodontosaurids and coelurosaurs throughout the evolution of theropods. A constriction at the cervix and the lanceolate outline of the crown is typically correlated with diet involving a mixture of food, and primarily plant material (e.g., Galton 1984, 1985; Barrett 2000). Whilst the labiolingual compression of the tooth allows keeping a sharp edge that cuts food items, it is possible that a

mesiodistal expansion of the crown relative to the root increases the surface area of the enamel as well as strengthening the crown by dissipating the forces applied apically along the tooth width. This hypothesis, however, needs to be tested by using finite elements analysis, as already employed for tyrannosaurid teeth by Reichel (2010).

The presence of a weak constriction in some mesial teeth of the basal coelurosaurs *Proceratosaurus* and *Compsognathus* may represent an incipient development of folidont teeth in Maniraptora. However, *Proceratosaurus* and *Compsognathus* are considered to be derived members of Proceratosauridae and Compsognathidae, respectively, by some authors (Averianov et al. 2010; Brusatte et al. 2010*d*; Senter 2011), and a constricted crown may, therefore, be autapomorphic for both taxa. Likewise, *Pelecanimimus* is the only ornithomimosaur with folidont teeth, and this feature may be plesiomorphic if this taxon represents the basalmost member of Ornithomimosauria (e.g., Makovicky et al. 2010; Liyong et al. 2012; Turner et al. 2012), or autapomorphic to this taxon. The presence of a constriction in some mesial and lateral teeth occurs in all basal maniraptorans (*sensu* Senter 2011; Turner et al. 2012) such as *Ornitholestes*, *Haplocheirus* and *Falcarius*, and this feature is, therefore, synapomorphic for Maniraptora. Folidont teeth in the lateral dentition only is present in Therizinosauria, *Epidexipteryx* and the basal member of oviraptorosaurs *Incisivosaurus*, and this condition is synapomorphic for the clade Therizinosauria + Oviraptorosauria + Paraves. Finally, a folidont dentition that includes constricted crowns only appeared several times in theropods. Indeed, such dentition can be noticed in *Pelecanimimus* (Pérez-Moreno et al. 1994), Alvarezsauridae, Caenagnathoidea and Paraves, and 'pure' folidonty (i.e., folidont teeth in the whole dentition) is, therefore, the synapomorphic condition for these three clades.

The presence of a basal constriction is commonly used in previous cladistic analyses and was first proposed as a character by Pérez-Moreno et al. (1994, character 4). Among the most recent phylogenetic analyses on theropods, Senter (2011, character 153), Turner et al. (2012, character 88), Choiniere et al. (2014*b*, character 238), Godefroit et al. (2013*a*, character 160), this character was coded in *Pelecanimimus*, Alvarezsauroidea, Therizinosauria, Oviraptorosauria, Troodontidae and *Microraptor*. When applied to the whole dentition, this feature should be coded as a polymorphic character (01) in oviraptorids, scansoriopterygids, *Compsognathus*, *Proceratosaurus*, *Ornitholestes*, *Haplocheirus*, and the troodontids *Sinovenator*, *Xixiasaurus*, *Byronosaurus*. If applied to the lateral dentition, only the three troodontids should have the polymorphic character (01). As suggested by Hendrickx and Mateus (2014*b*), the degree of constriction should be quantified in order to differentiate the weak constriction occurring in basal averostrans teeth (e.g., carcharodontosaurids, *Proceratosaurus*, *Compsognathus*, and *Ornitholestes*), and the fully constricted tooth condition visible in alvarezsauroids, therizinosauroids, and troodontids. As proposed by Hendrickx and Mateus (2014*b*), the width of the crown at the cervix should be compared with the largest width of the crown. The teeth in which the crown has a base occupying 85% or less of the largest crown width is considered as strongly constricted. Indeed, alvarezsauroids, therizinosauroids, and troodontids have a greatly

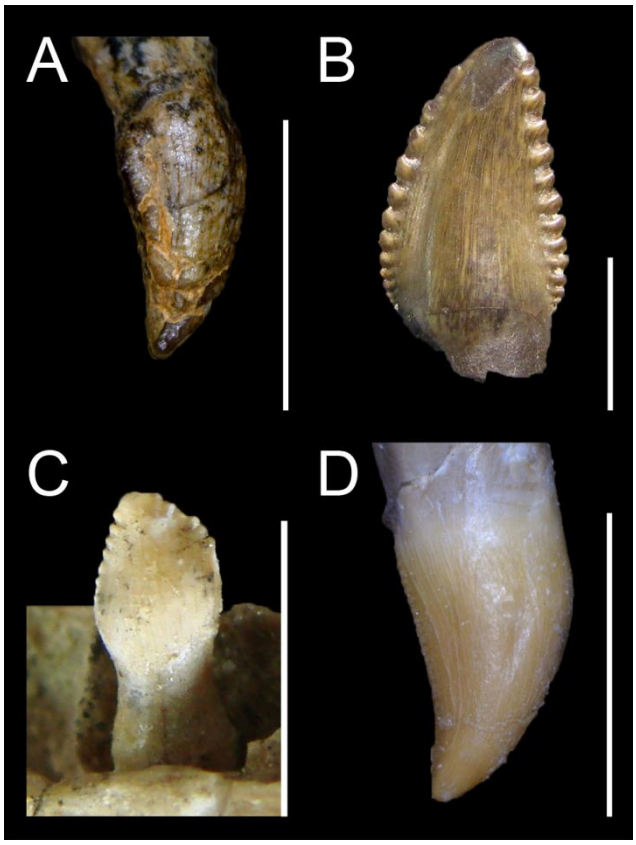

FIGURE 3.3. Basal constriction in non-avian Theropoda. **A**, Fourth right premaxillary tooth of the basal saurischian *Eoraptor lunensis* (PVSJ 512) in labial view; **B**, Isolated tooth of the troodontid *Troodon formosus* (DMNH 22837) in labial view; **C**, Isolated tooth of the therizinosaurid *Erlikosaurus andrewsi* (IGM 100-111) in lateral view (Clark et al. 1994); **D**, Fourth right premaxillary tooth of the proceratosaurid *Proceratosaurus bradleyi* (NHM R.4860) in labial view. Scale bars = 5 mm.

mesiodistally expanded crown just above the cervix, which is not the case in non-maniraptoriform theropods. Additional variation comes from the distribution within the tooth-bearing bones of the basal constriction. Thus, the presence of a constriction at the crown base should be coded for both mesial and lateral dentition. Basal coelurosaurs do not possess constricted teeth in the lateral dentition, whereas some therizinosaurids and dromaeosaurids only have constricted teeth in the lateral dentition.

Crown Base Ratio greater than 0.64

A crown base ratio (*sensu* Smith et al. 2005) is greater than 0.64 in most Theropoda for mesial teeth. Lateral teeth with a CBR higher than 0.64 is present Allosauridae, Spinosauridae, Tyrannosauridae, Ornithomimosauria, Alvarezsauroidea and Therizinosauria. A labiolingually broad crown is the typical condition of mesial teeth in non-avian theropods, and we have observed that a crown base ratio of more than 0.64 corresponds, in the majority of ziphodont theropods, to a mesial tooth. However, a weak labiolingually compression of the whole crown (and not only the base) is also seen in the dentition of Spinosauridae which bear subconical teeth (e.g., Charig and Milner 1997; Sereno et al. 1998; Sues et al. 2002) and large/mature Tyrannosauridae which possess incrassate teeth (e.g., Holtz 2003, 2008; pers. obs.), and these theropod have a crown-base ratio higher than this arbitrary value in both mesial and lateral teeth. The expansion of the crown labiolingually adds resistance and the ability to withstand bending loads applied from all directions (e.g., Therrien et al. 2005; Holtz 2008). Thick teeth are adapted to resist contact with hard items such as bones and

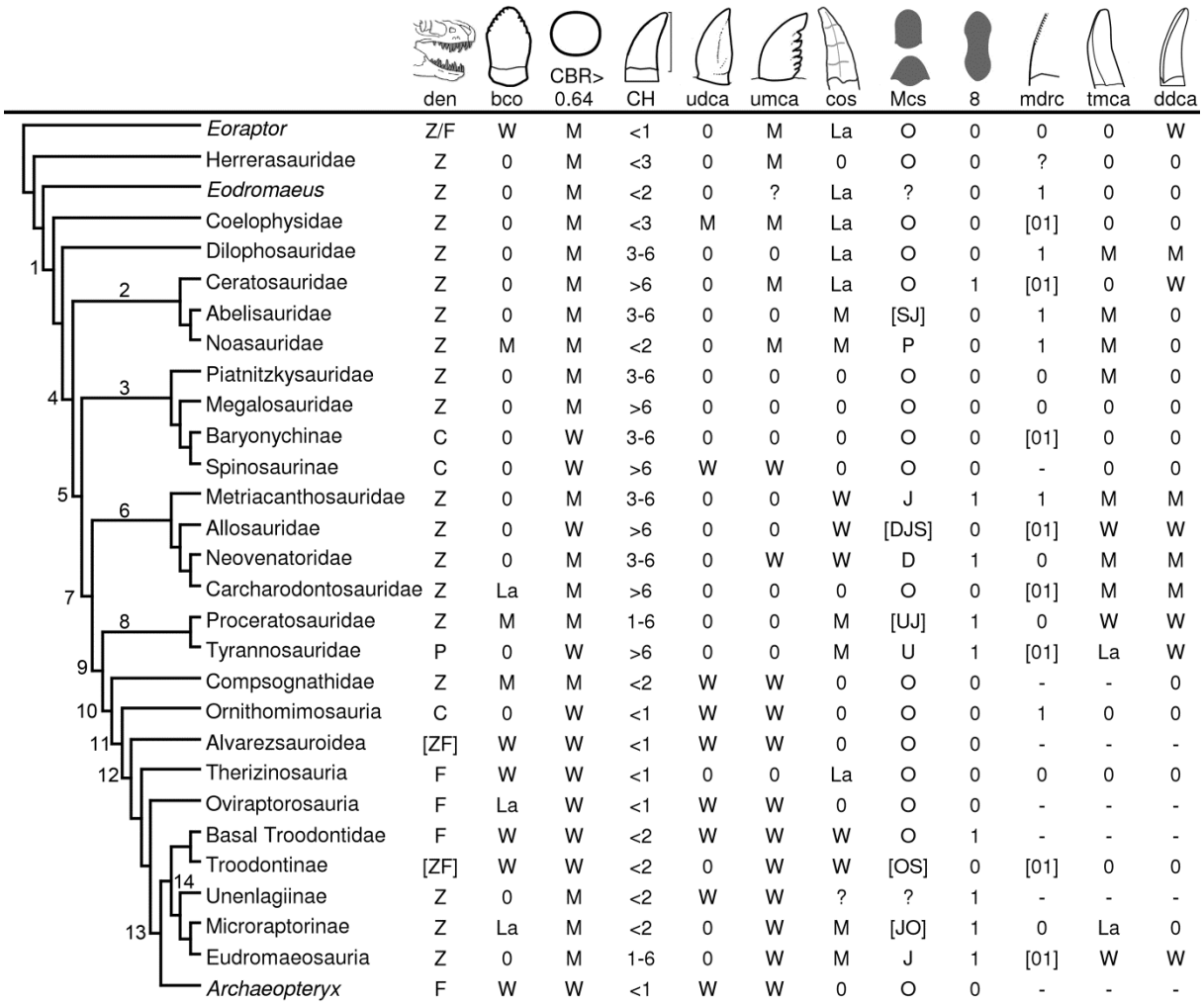

FIGURE 3.4A. Distribution of dental features in non-avian theropods. Phylogenetic tree based on Smith et al. (2007), Brusatte et al. (2010b), Sues et al. (2011), Carrano et al. (2012), Turner et al. (2012), and Tortosa et al. (2014). Letters and numbers between brackets represent polymorphic features. The asterisk refers to the basal ceratosaur *Limusaurus*. **Clade numbers**: **A**, Neotheropoda; **B**, Ceratosauria; **C**, Megalosauroidea; **D**, Averostra; **E**, Tetanurae; **F**, Allosauroidea; **G**, Avetheropoda; **H**, Tyrannosauroidea; **I**, Coelurosauria; **J**, Neotheropoda; K, Maniraptoriformes; **L**, Maniraptora; **M**, Paraves; **N**, Deinonychosauria. **Abbreviations**: **0**, absent; **1**, present at least in some teeth or some taxa; **8**, eight-shaped cross-section at the cervix; **?**, unknown; **-**, inapplicable; **~**, medium-sized denticles (i.e., between 15 and 250 denticles on the carina); **<<**, minute denticles (more than 250 denticles on the carina); **>>**, large denticles (less than 15 denticles on the carina); **A**, anastomosed oriented texture; **B**, braided oriented texture; **bco**, basal constriction at the cervix; **bst**, basal striations; **C**, conidonty (dentition with conical crowns); **CBR**, crown base ratio; **CH**, crown height in the largest teeth, in centimetres; **codm**, convex distal margin; **cos**, concave surface adjacent to carinae; **D**, D-shaped cross-section; **ddca**, displaced distal carina; **den**, dentition; **des**, denticle size; **ent**, enamel texture; **edg**, edentulous jaw; **F**, folidonty (dentition with lanceolate crowns); **flu**, fluted teeth; **hd**, hooked denticles; **I**, irregular, non-oriented, texture; **ids**, interdenticular sulci; **L**, present in lateral teeth; **lgr**, longitudinal groove; **lri**, longitudinal ridges; **M**, present in mesial teeth; **Mcs**, mesial teeth, cross-section at the cervix; **md<dd**, mesial denticles smaller than distal denticles (DSDI > 1.2); **mdrc**, mesial denticles reaching the cervix; **mun**, marginal undulations; **O**, subcircular/lanceolate cross-section; **P**, parlinon-shaped cross-section; **Pa**, pachydonty (dentition with banana-shaped crowns); **pct**, procumbent teeth; **tmca**, twisted mesial carina; **tun**, transverse undulations; **U**, U-shaped cross-section; **udca**, unserrated distal carina; **umca**, unserrated mesial carina; **V**, veined and anastomosed oriented texture; **W**, present in both mesial and lateral teeth; **Z**, ziphodonty (dentition with blade-shaped crowns).

scales during prey capture and feeding. The mesial dentition was most likely subject to higher stress and loads than lateral dentition during bites. In theropods, lateral crowns are as labiolingually wide as those of the mesial dentition in pachydont and conidont theropod teeth, used for bone crushing or to

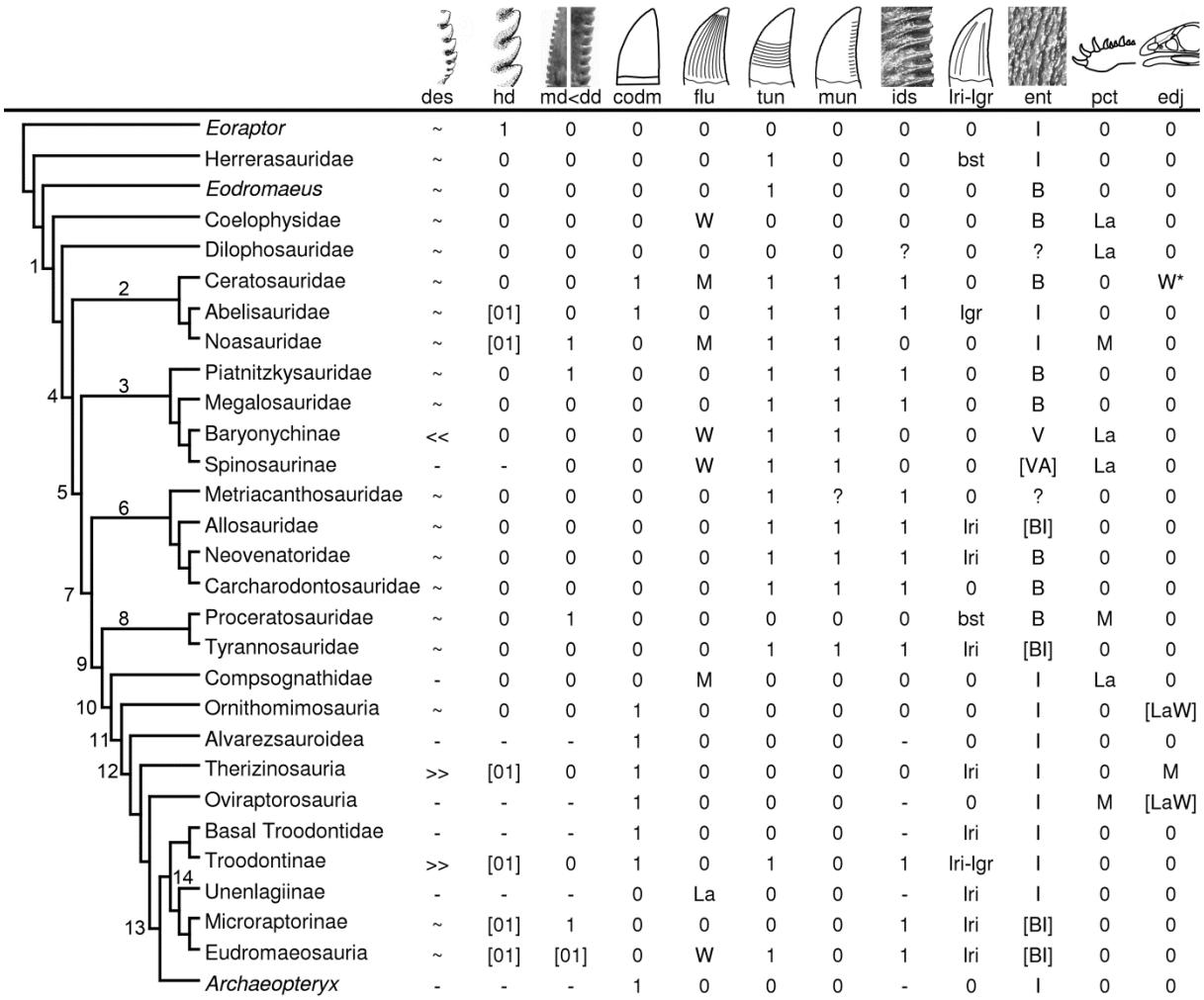

FIGURE 3.4B. (Continued)

impale and hold prey, respectively (e.g., Therrien et al. 2005; Holtz 2008). Interestingly, teeth with a CBR greater than 0.64 are also present in many maniraptoriforms such as ornithomimosaurs, therizinosauroids and alvarezsauroids in which the cross-section of the crown base is sub-circular (e.g., Clark et al. 1994; Xu et al. 2001*b*; Ji et al. 2003; Barrett 2009; Choiniere et al. 2012; pers. obs.). The allosauroid *Allosaurus* also shows incrassate teeth along most of the tooth row, and only the posteriormost lateral dentition (in many cases from the seventh maxillary crown) is moderately to strongly labiolingually narrow (pers. obs.). Pachydont teeth are also present in the transition between mesial and lateral teeth in *Acrocanthosaurus*. Present in the most basal spinosaurid *Ostafrikasaurus* (Buffetaut 2011) and ornithomimosaur *Nqwebasaurus* (Choiniere et al. 2012), the subcircular outline of the crown base is a synapomorphy of Spinosauridae (Sereno et al. 1998) and Ornithomimosauria. Likewise, incrassate teeth are absent in the non-tyrannosaurid tyrannosauroids *Xiongguanlong* (Li et al. 2010), *Raptorex* (Sereno et al. 2009), and *Dryptosaurus* (Brusatte et al. 2011) and present in the basal tyrannosaurids such as *Albertosaurus* and *Gorgosaurus* (pers. obs.) so that pachydont teeth is considered to be a synapomorphy of Tyrannosauridae.

The thickness of the crown was one of the first dental characters considered in cladistic analyses. Authors formulated a character to distinguish the conical teeth of Spinosauridae (Sereno et al. 1998, character 17) and Avialae (Forster et al. 1998, character 4) from the ziphodont teeth of other theropods. Later, Holtz et al. (2004, character 263) proposed a character to reflect the incrassate teeth of tyrannosaurids, which was then included in the cladistic analyses of Sereno et al. (2009, character 62), Brusatte et al. (2010*a*, character 201), and Loewen et al. (2013, character 303). Most conidont and folidont theropod teeth have a sub-circular cross-section at the cervix, therefore the thickness of the crown at mid-height, expressed by the ratio MCR proposed by Hendrickx et al. (in press*a*, *c*) should also be taken into consideration, as suggested by Carrano et al. (2012, character 144). Indeed, if conidont and pachydont teeth have a subcircular cross-section at mid-crown, this is rarely the case in folidont teeth (pers. obs.). Holtz et al. (2004) arbitrarily proposed a crown base ratio (CBR) of 0.6 or more to define incrassate teeth. Yet, Hendrickx and Mateus (2014*b*) preferred using 0.75, thus including the incrassate and subcircular crown cross-section. In fact, two characters states should be proposed: one for moderately narrow incrassate/conidont teeth with a crown base ratio from 0.64 to 0.75, and a second one for incrassate/conidont teeth with a subcircular cross section and a ratio higher than 0.75. Regarding Tyrannosauroidea, a multistate character was actually proposed by Brusatte et al. (2010*a*) and Loewen et al. (2013) to differentiate tyrannosaurids with slightly narrow incrassate teeth (i.e., width greater than 60% of length) from those bearing incrassate teeth with a sub-circular cross-sections. According to the data matrix of these authors, the derived tyrannosaurids *Lythronax*, *Tarbosaurus*, *Tyrannosaurus*, and *Zhuchengtyrannus* show lateral teeth with a labiolingual width nearly equal than the mesiodistal length, unlike other more basal tyrannosaurids such as *Gorgosaurus*, *Albertosaurus*, *Daspletosaurus*, and *Teratophoneus*. Based on our quantitative data, the CBR average value of the lateral dentition (i.e., dentition excluding premaxillary teeth, as well as first maxillary tooth and first three dentary teeth) is around 0.7 for *Gorgosaurus* and *Albertosaurus*, and 0.79 for *Tyrannosaurus*, yet the maxillary dentition of *Tyrannosaurus* has an average crown-base ratio of 0.65. To better reflect the difference in the dentition of primitive and derived tyrannosaurids, we propose that the average CBR should only be coded for the lateral dentary teeth, with a first character state proposing a CBR from 0.64 to 0.75, and a second character state with a CBR greater than 0.75.

Crown Height Higher than 70 mm

A crown height higher than 70 mm is present in ‘non-neocoelurosaur’ Averostrans. Absolute tooth size is a homoplastic feature which also varies allometrically, thus it must be treated with caution for classification purposes. Nonetheless, this feature has proven to be useful to discriminate teeth of different theropod taxa (Smith 2005; Smith et al. 2005; Han et al. 2011). Theropods bearing crowns larger than seven centimetres are indeed only known in ‘non-neocoelurosaur’ averostrans, as Ceratosauridae (e.g., *Ceratosaurus*, *Genyodectes*), Megalosauroidea (e.g., *Torvosaurus*, *Spinosaurus*), Allosauroidea (e.g., *Acrocanthosaurus*, *Carcharodontosaurus*, *Mapusaurus*, *Giganotosaurus*) and

Tyrannosauridae (e.g., *Daspletosaurus*, *Tyrannosaurus*, *Tarbosaurus*). Among 'non-neocoelurosaur' averostrans, abelisauroids, non-megalosaurine and non-spinosaurine megalosauroids, neovenatorids and non-tyrannosaurid tyrannosauroids have shorter teeth (pers. obs.). The presence of crowns higher than 70 mm in the dentition is a possible synapomorphy of Ceratosauridae, Carcharodontosauridae and Tyrannosauridae, and is an apomorphic condition in *Torvosaurus* and *Spinosaurus* among Megalosauroidea. Only Hendrickx and Mateus (2014*b*, character 65) included a character considering mature theropods with very large crowns (crown exceeding 60 centimetres) in a data matrix. Nevertheless, Pol and Rauhut (2012, character 95) incorporated a character differentiating the low crowns of Abelisauroidea from the long and elongated crowns born by their possible common ancestors the Ceratosauridae, a character also used by Tortosa et al. (2014, character 37). Ceratosauridae displays crowns exceeding the ventrodorsal height of the dentary, which is not the case in abelisauroids. Other theropods with crowns longer than the height of the dentary include non-neotheropod theropods (*Herrerasaurus*), coelophysoids (*Coelophysis*), dilophosaurids (*Dilophosaurus*), and basal tetanurans (*Sinosaurus*, *Monolophosaurus*). Megalosauroids and averostrans do not seem to have crowns exceeding the height of the dentary, and even *Dubreuillosaurus*, *Torvosaurus*, *Spinosaurus*, *Acrocanthosaurus*, *Tyrannosaurus*, and any dromaeosaurids with excessively elongated, sometimes very large crowns, do not display this condition.

Unserrated Teeth

Unserrated crowns (Fig. 3.5) are seen in Theropoda for mesial teeth, in 'neocoelurosaur' for lateral teeth, and in Spinosaurinae, and Maniraptoriformes other than Therizinosauria, derived Troodontidae and non-unenlagiine Dromaeosauridae for the whole dentition. The absence of serrations indicates less efficiency of slicing food (Xing et al. 2013*a*). Unserrated teeth are, therefore, used to either spear into flesh (Xing et al. 2013*a*) and deeply injure prey items, or for cropping and browsing vegetation. The absence of denticles seems also to result in the simplification of the crown in the theropod clades whose derived forms have lost their dentition (Gianechini et al. 2011*a*).

In embryo/juvenile individuals, unserrated mesial teeth have been recorded in *Coelophysis* (Colbert 1989), *Sciurumimus* (Rauhut et al. 2012), *Tyrannosaurus* (Carr and Williamson 2004), *Juravenator* (Chiappe and Göhlich 2010), *Scipionyx* (Dal Sasso and Maganuco 2011), *Aorun* (Choiniere et al. 2014*b*), and the whole dentition of *Torvosaurus* (Araújo et al. 2013), *Archaeornithoides* (Elzanowski and Wellnhofer 1993), and *Troodon* (Varricchio et al. 2002). In mature individuals, unserrated mesial teeth are present in some coelophysoids such as *Megapnosaurus rhodesiensis* and *kayentakatae* (Raath 1977; Rowe 1989), the basal tyrannosauroid *Xiongguanlong* (Li et al. 2010), and most compsognathids (*Compsognathus*, *Sinosauropteryx*; Currie and Chen 2001; Peyer 2006; Chiappe and Göhlich 2010), which may be juvenile specimens. Non-denticulate mesial most teeth have also been identified in *Ornitholestes* (AMNH 619), and some alvarezsauroids

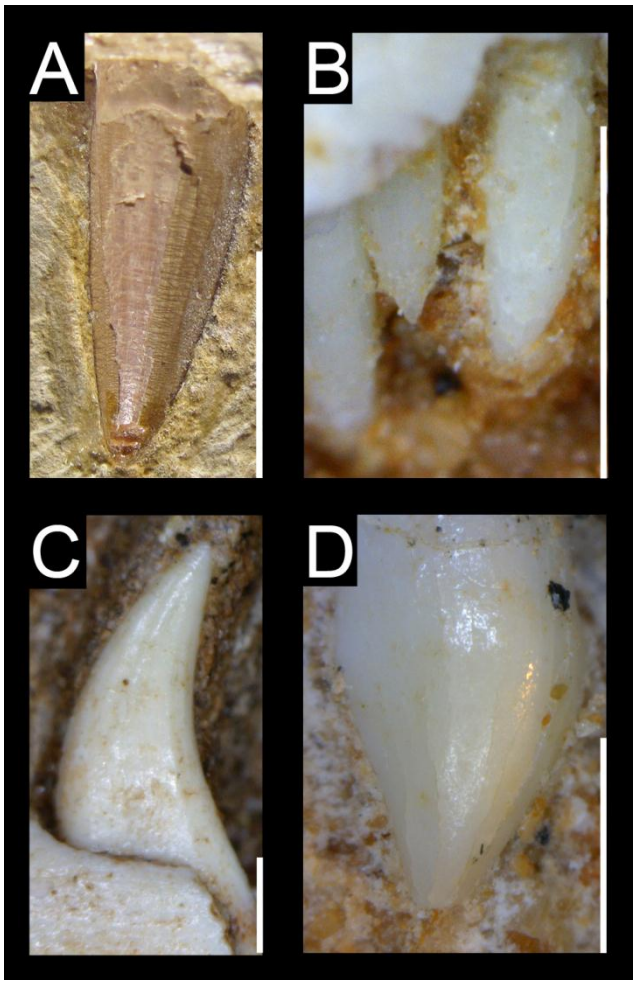

FIGURE 3.5. Unserrated teeth in non-avian Theropoda. **A**, Right maxillary tooth of the spinosaurid *Irritator challengeri* (SMNS 58022) in labial view; **B**, Right maxillary teeth of the alvarezsaurid *Shuvuuia deserti* (IGM 100-977) in labial view; **C**, Second left dentary tooth of the dromaeosaurid *Buitreraptor gonzalezorum* (MPCA 245) in labial view; **D**, Right maxillary tooth of an undescribed troodontid (IGM 100-1323) in labial view. Scale bars = 1 mm (B–D), 1 cm (A).

(*Haplocheirus*; Choiniere et al. 2010*b*, 2014*a*), troodontids (*Sinornithoides*, *Zanabazar*; Currie and Dong 2001*a*; Norell et al. 2009), and microraptorines (e.g., *Microraptor*, *Sinornithosaurus*, *Shanag*; Xu et al. 2000; Xu and Wu 2001; Turner et al. 2007*b*). Unserrated teeth are present in the whole dentition of Spinosaurinae such as *Irritator* (Sues et al. 2002; Fig. 3.5A), *Angaturama* (Kellner and Campos 1996) and *Spinosaurus* (Stromer 1915), basal Ornithomimosauria *Nqwebasaurus* (Choiniere et al. 2012), *Pelecanimimus* (Pérez-Moreno et al. 1994) and *Shenzhousaurus* (Ji et al. 2003), and all Alvarezsauridae such as *Shuvuuia* (Chiappe et al. 1998; Fig. 3.5B) and *Mononykus* (Perle et al. 1993). Unserrated crowns are also present in the basal Oviraptorosauria *Incisivosaurus* (Balanoff et al. 2009) and *Protarchaeopteryx* (Senter et al. 2004), all unenlagiine Dromaeosauridae such as *Buitreraptor* (Gianechini et al. 2011*a*; Fig. 3.5C), *Austroraptor* (Novas et al. 2009) and *Mahakala* (Turner et al. 2011), and, according to the data matrix of Turner et al. (2012, character 83.2), the microraptorine *Graciliraptor*. Many Troodontidae like *Mei* (Xu and Norell 2004), *Byronosaurus* (Makovicky et al. 2003), *Urbacodon* (Averianov and Sues 2007), *Xixiasaurus* (Lü et al. 2010) and two unnamed taxa (IGM 100-1128; IGM 100-1323; Fig. 3.5D) also bear non-denticulate crowns. Unserrated teeth are born by the scansoriopterygid *Epidexipteryx* (Zhang et al. 2008) as well, and the basal Paraves *Anchiornis* (Hu et al. 2009), *Eosinopteryx* (Godefroit et al. 2013*b*), *Aurornis* (Godefroit et al. 2013*a*),

and *Archaeopteryx* (e.g., Martin et al. 1980; Elzanowski and Wellnhofer 1996; Mayr et al. 2007). A combination of serrated and unserrated lateral teeth is present in a few theropods like *Compsognathus* (MNHN CNJ 79) and *Ornitholestes* (AMNH 619).

Unserrated lateral dentition is absent in mature individuals of non-neotheropod Theropoda, Coelophysoidea, Ceratosauria, non-spinosaurine Megalosauroidea, Allosauroidea, Tyrannosauroidea, Therizinosauria, and most derived Troodontidae and non-unenlagiine Dromaeosauridae. The loss of denticles in lateral teeth is a trend that happened several times in the evolution of theropods. The teeth of Spinosaurinae, Ornithomimosauria and Alvarezsauridae all lost denticles independently. With the presence of serrated teeth in the basal members of Alvarezsauroidea (*Haplocheirus*) and Therizinosauria (*Falcarius*), and the absence of serrations in basal taxa belonging to Oviraptorosauria (*Incisivosaurus*), Troodontidae, Dromaeosauridae and Avialae, unserrated teeth is the apomorphic condition of the clade Oviraptorosauria + Paraves ('Chuniaoae' of Ji et al. 1998). *Protarchaeopteryx*, interpreted as a basal oviraptorosaur and a senior synonym of *Incisivosaurus* (Senter et al. 2004), was described as possessing serrated teeth (Ji et al. 1998). However, Senter et al. (2004) revealed that no serrations could be observed in the holotype specimen of *Protarchaeopteryx*, and unserrated teeth are, therefore, considered to be the synapomorphy of Pennaraptora (Oviraptorosauria + Paraves). Likewise, the presence of unserrated teeth is synapomorphic in Spinosaurinae, Ornithomimosauria, Alvarezsauridae and Aves (*sensu* Choiniere et al. 2010*b*). On the other hand, serrations were independently reacquired by derived Troodontidae and the clade Microraptorinae + Eudromaeosauria (*sensu* Turner et al. 2012). The total absence of serration was thought to be a synapomorphy of the Unenlagiinae by Novas et al. (2009) and Gianechini et al. (2011*a*), yet their direct ancestors seem to share this feature as well, and unserrated teeth in Unenlagiinae is, therefore, considered to be the plesiomorphic condition.

The absence of crown denticles was included since the arise of computational cladistic analyses on theropods. (Chiappe et al. 1996) was the first author to incorporate this feature (char. 90) to describe the unserrated teeth of *Mononykus*. The presence of unserrated teeth is a character commonly used to investigate theropod relationships. However, this character is typically coded for both mesial and lateral dentition, which show distinct conditions. We agree with the codings of most recent cladistic analyses such as Turner et al. (2012, character 83.2), and Choiniere et al. (2014*b*, character 226.2), but a few taxa have been miscoded in Godefroit et al. (2013*a*, character 159.2). In fact, *Falcarius*, *Microraptor*, *Shanag*, *Sinovenator*, and *Sinusonasus* do not possess unserrated maxillary and dentary crowns. On the other hand, *Irritator* and *Shenzhousaurus*, should be coded as possessing unserrated crown in the data matrix of Choiniere et al. (2014*b*), and *Compsognathus* and *Ornitholestes* as having both serrated and unserrated crowns in Turner et al. (2012) and Choiniere et al. (2014*b*).

Unserrated Mesial Carina, Serrated Distal Carina

Crowns with unserrated mesial carina is seen in Theropoda for mesial teeth, and Megaraptora, Compsognathidae, basal Alvarezsauroidea, and a many derived Troodontidae and Dromaeosauridae for lateral teeth. Mesial teeth with unserrated mesial carina and serrated distal carina are present in most theropod clades as they can be observed in basalmost theropods such as *Eoraptor* (PVSJ 512), *Herrerasaurus* (PVSJ 407) and *Ischisaurus* (PVSJ 605), the coelophysoids *Coelophysis* (CMNH 81765, 82931), the ceratosaurid *Ceratosaurus* (Currie and Carpenter 2000; Bakker and Bir 2004), the basal coelurosaur *Ornitholestes* (AMNH 619), some compsognathids like *Huxiagnathus* (Ji et al. 2007*a*) and *Juravenator* (Chiappe and Göhlich 2010), the troodontids *Sinovenator* (Xu et al. 2002*b*) and the dromaeosaurids *Tsaagan* (Norell et al. 2006). In lateral teeth, this condition is visible in the juvenile megalosauroid *Sciurumimus* (Rauhut et al. 2012), some megaraptorans such as *Orkoraptor* (Novas et al. 2008), all compsognathids other than *Sinocalliopteryx* (e.g., Currie and Chen 2001; Peyer 2006; Ji et al. 2007*a*; Dal Sasso and Maganuco 2011), the basal coelurosaurs *Ornitholestes* (except perhaps the left dt6; AMNH 619), *Aorun* (Choiniere et al. 2014*b*) and possibly *Zuolong* (Choiniere et al. 2010*a*), the basal Alvarezsauroidea *Haplocheirus* (Choiniere et al. 2010*b*), a few dromaeosaurids such as *Velociraptor* (Godefroit et al. 2008), *Microraptor* (Xu et al. 2000; Hwang et al. 2002), *Shanag* (Turner et al. 2007*b*), *Saurornitholestes* (Currie et al. 1990) and *Tsaagan* (Norell et al. 2006; Xu et al. 2010*a*), and many derived troodontids, including *Troodon* (Currie 1987), *Sinornithoides* (Currie and Dong 2001*a*), *Saurornithoides* and *Zanabazar* (Norell et al. 2009). Similar to the loss of serrations for the whole dentition, the loss of mesial denticles happened several times convergently in the evolution of theropods. The presence of crowns with unserrated mesial carina and serrated distal carina seems indeed to be the derived condition in Megaraptora (*sensu* Benson et al. 2010) among Allosauroidea, and 'neocoelurosaurs' among Coelurosauria. The reacquisition of denticles in the mesial carina also occurred independently in derived troodontids like *Troodon* and *Pectinodon*, and in the members of the clade Microraptorinae + Eudromaeosauria.

The absence of denticles on the mesial margin of the crown was suggested as a character by Forster et al. (1998, character 50), and this feature is included in all recent phylogenetic analyses on coelurosaurs. A non-denticulate mesial carina should be coded separately for the mesial and lateral dentition to reflect the variability of this feature along the jaw. Among the most recent cladistic analyses on theropods, Turner et al. (2012, character 83.1), Novas et al. (2013, character 2.2), Choiniere et al. (2014*b*, character 226.1) and Godefroit et al. (2013*a*, character 159.1) all included this character and coded it as present in megaraptorans, compsognathids, *Haplocheirus*, dromaeosaurids, and troodontids. The lateral dentition of *Australovenator*, and *Suchomimus*, *Guanlong* and *Zuolong* were coded as displaying this condition in the data matrices of Novas et al. (2013) and Choiniere et al. (2014*b*), respectively. Yet, *Australovenator*, *Suchomimus* and *Guanlong* both possess serrated mesial and distal carinae (Xu et al. 2006; Hocknull et al. 2009; pers. obs.), and the absence of mesial denticles on the lateral teeth of *Zuolong* cannot be ruled out (Choiniere et al. 2010*a*).

Concave Surface Adjacent to Carinae

A concave surface marginal to the carinae is seen in Abelisauroidea, *Allosaurus*, Tyrannosauroidea and Deinonychosauria for mesial teeth, and non-neotheropod Theropoda, Ceratosauridae, Neovenatoridae and Metricanthosauridae for lateral teeth. Two concave surfaces adjacent to the mesial and distal carinae and separated by a longitudinal ridge on the lingual surface of the crown are characteristic of the mesial teeth of derived tyrannosauroids (see below). Concavities marginal to carinae and separated by a wide convexity also occur in the first mesial teeth (pm1–2, dt1) of abelisaurids such as *Abelisaurus* (MPCA 1, 5), *Indosuchus* (AMNH 1753) and *Majungasaurus* (Fanti and Therrien 2007: fig. 6C3; FMNH PR.2100; Fig. 3.7A), which show a salinon-shaped outline (salinon *sensu* Khelif 2010; Fig. 2.1K) of the crown base in cross-section. A similar morphology is present in the mesial dentary teeth of the noasaurids *Masiakasaurus* (e.g., UA 9128, FMNH PR.2182), the first premaxillary teeth of *Allosaurus* (AMNH 600, 851; CMNH 21703; UMNH VP 2151) and the mesial and lateral teeth of some troodontids such as *Troodon* (Currie 1987; Currie et al. 1990), *Urbacodon* (Averianov and Sues 2007) and *Zanabazar* (Norell et al. 2009: fig. 30). A concave surface adjacent to the mesial carina also occurs in more distal mesial teeth (pm3–4, mx1–2, dt2–3) of abelisaurids, which therefore have a rather J-shaped cross-section outline (Fig. 3.1M) of the crown base. Such morphology of the crown is also present in mesial teeth of the allosauroids *Allosaurus* (e.g., AMNH 851, CMNH 21703) and *Sinraptor* (Currie and Zhao 1993*a*: fig. 4D), the tyrannosauroid *Proceratosaurus* (NHM R.4860), and some deinonychosaurs like *Dromaeosaurus* (AMNH 5356; Fig. 3.8D), *Deinonychus* (Ostrom 1969: fig. 24D2), *Saurornitholestes* (Currie et al. 1990: fig. 8.6i) and *Linhevenator* (Xu et al. 2011*c*).

A slightly concave or planar surface adjacent to the distal and mesial carinae in lateral teeth was considered to be a ceratosaurian (neoceratosaurian *sensu* Rauhut 2004*b*) synapomorphy by Rauhut (2004*b*), yet the presence of this feature is widespread among non-coelurosaur theropods. Among basal theropods, a concave surface adjacent to the distal carina is also visible on the labial (and in some cases lingual) side of some lateral crowns in the primitive theropods *Eodromaeus* (PVSJ 560, 561), *Dilophosaurus* (UCMP 37303; Fig. 3.6A) and *Coelophysis* (CMNH 81765). As noted by Rauhut (2004*b*), this concave surface is indeed present in some Ceratosauridae such as *Ceratosaurus* (USNM 4735; UMNH VP 5278) and *Genyodectes* (MLP 26-39; Rauhut 2004*b*), but we could not identify this feature in the lateral teeth of any Abelisauridae or Noasauridae. A planar surface, however, is observable on the labial surface and adjacent to the distal carina in one lateral tooth of *Skorpiovenator* (MMCH-PV 48). The possible metriacanthosaurid *Erectopus* (MNHN 2001-4) also displays this planar surface, but on the lingual margin of the crown. A concave area adjacent to the distal carina, on the labiobasal part of the crown, is present in the megalosauroid *Piatnitzkysaurus* (MACN CH 895), *Afrovenator* (MNN TIG1; Fig. 3.6B), and the metriacanthosaurid *Sinraptor* (IVPP 10600; Fig. 3.6D). In Neovenatoridae, this concave surface is seen on one or both labial and lingual sides all along the

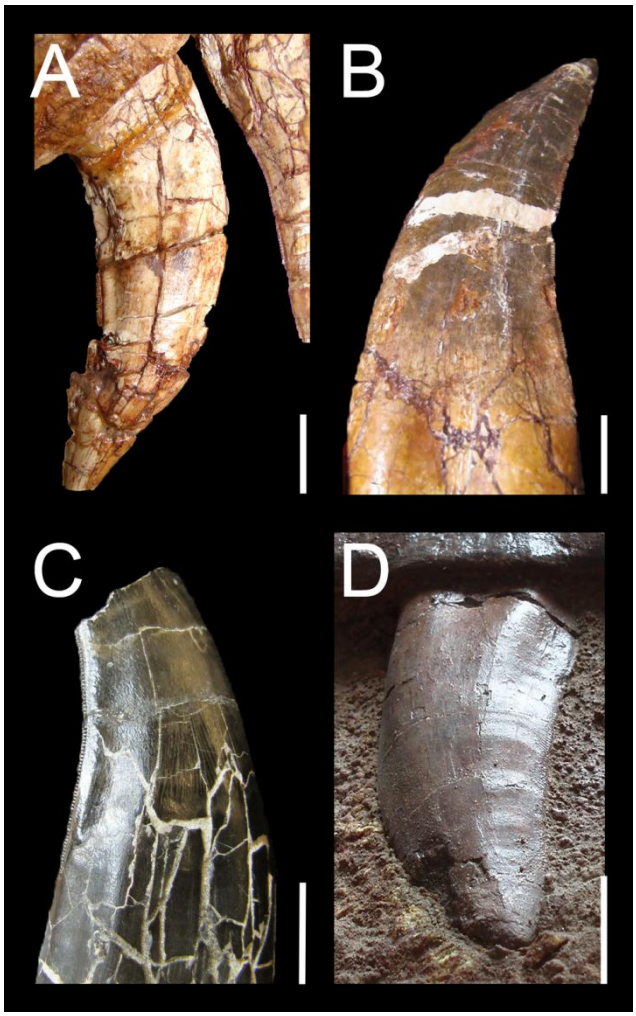

FIGURE 3.6. Concave surface adjacent to carinae in non-avian Theropoda. **A**, Third left maxillary tooth of the dilophosaurid *Dilophosaurus wetherilli* (UCMP 37303) in lingual view; **B**, Isolated tooth of the megalosaurid *Afrovenator abakensis* (MNN UBA1) in labial view; **C**, Isolated tooth of the neovenatorid *Neovenator salerii* (MIWG 6348) in labial view; **D**, Fifth left maxillary tooth of *Sinraptor dongi* (IVPP 10600) in labial view (courtesy of Roger Benson). Scale bars = 1 cm.

crown, as in *Neovenator* (MIWG 6348; Fig. 3.6C), *Fukuiraptor* (Azuma and Currie 2000: fig. 4; Molnar et al. 2009: fig. 3E) and *Australovenator* (Hocknull et al. 2009: fig. 20K, 21E). *Eoraptor* lateral teeth (PVSJ 512) are unique in having a strongly mesiodistally convex surface labio-mesially situated (‘rounded eminence’ of Sereno et al. 2013) and adjacent to a mesiodistally concave surface marginal to the distal carina. A similar concave surface is also present in the vicinity of the mesial carina in some lateral teeth of this taxon. A concave or planar surface adjacent to carinae in some lateral teeth is considered to be synapomorphic for Ceratosauridae, Neovenatoridae, and Metriacanthosauridae. The presence of concave surfaces marginal to carinae or mesially-situated on the tooth had several functional implications in theropods, namely to either enhance the structural strength and stability of the crown by increasing the surface area of the enamel (Folinsbee et al. 2007), or to allow rapid penetration and easier withdrawal during the bite (Freedman 1957). The presence of one or two concave surfaces marginal to carinae were coded for both mesial and lateral dentition in the cladistic analysis of Hendrickx and Mateus (2014*b*, characters 42, 71).

J-shaped and Salinon-Shaped Cross-section

A J-shaped cross-section (Fig. 2.5T) is present in mesial teeth of Abelisauridae, Allosauroidea, *Proceratosaurus*, *Ornitholestes* and Dromaeosauridae (Fig. 3.7D), whereas a salinon-shaped cross-section (Fig. 2.5R) is observable in mesial teeth of Abelisauroidea (Fig. 3.7A), and Allosauridae (*Allosaurus*), and lateral teeth of Troodontidae. The distribution of a concave surface adjacent to the mesial and/or distal carinae in mesial teeth, and resulting in a J-shaped or salinon-shaped outline of the cross-section at the crown base, has been discussed in the previous section. One or two concave surfaces marginal to the carinae appeared convergently in the mesial teeth of Abelisauroidea, non-carcharodontosaurid allosauroids, primitive coelurosaurs (*Proceratosaurus*, *Ornitholestes*) and Dromaeosauridae. A salinon-shaped outline in the mesial teeth in a possible synapomorphy of Abelisauroidea and a possible autapomorphy of *Allosaurus* or a synapomorphy of Allosauridae.

The presence of asymmetrical teeth in the mesial dentition was first included in a data matrix by Holtz (1994, character 126; based on Bakker et al. 1988). Since then, this feature is regularly used in cladistic analyses on the whole theropod clade, typically as a binary character (i.e., symmetrical/sub-circular *versus* asymmetrical/D-shaped premaxillary teeth). Some phylogenetic analyses (e.g., Holtz et al. 2004; Li et al. 2010; Godefroit et al. 2013*a*) have considered a multistate character defining a state for conical crown with symmetrical cross-section, another for slightly asymmetrical premaxillary crowns strongly convex labially, and flattened lingually, and finally a third state for a D-shaped or U-shaped cross-section with both carinae placed along the same plane perpendicular to the skull axis. In tyrannosauroids, a different multistate character was proposed by Brusatte et al. (2010*a*) to encompass variation along the tooth row. The mesial carina can either be coded as centrally-positioned on the mesial surface, rotated distally in the first and second premaxillary teeth, or rotated distally on all premaxillary teeth (e.g., Brusatte et al. 2010*d*; Novas et al. 2013). (Hendrickx and Mateus 2014*b*) proposed a character based on the cross-section outline of mesial teeth. Because morphological variation occurs along the tooth row in the mesial dentition, two multistate characters are proposed, one on the cross-section outline of the mesial teeth (first and second premaxillary teeth/first dentary tooth), and a second on more distal teeth of the mesial dentition (third and fourth premaxillary teeth/second and third dentary teeth). It is also proposed seven cross-section outlines character states for the mesial teeth at the cervix, namely 1. subcircular, ovoid or elliptical, 2. lanceolate, with acute distal carina, 3. salinon-shaped, 4. J-shaped, 5. D-shaped, 6. U-shaped, and 7. lenticular, with protuberant mesial and distal carinae.

D-shaped Cross-section

A D-shaped cross-section is present in mesial teeth of some Allosauroidea and *Ornitholestes*. A D-shaped cross-section (Fig. 2.5P) can be observed in mesial teeth of some allosauroids such as *Allosaurus* (CMNH 1254, 21703; SMA 005/02; Fig. 3.7C) and *Fukuiraptor* (Currie and Azuma 2006: fig. 1D). A similar cross-section seems to be present also in the mesial teeth of the neovenatorid *Australovenator* in which the mesial carina faces mesiolingually (and not ‘mesiolabially’ *sensu*

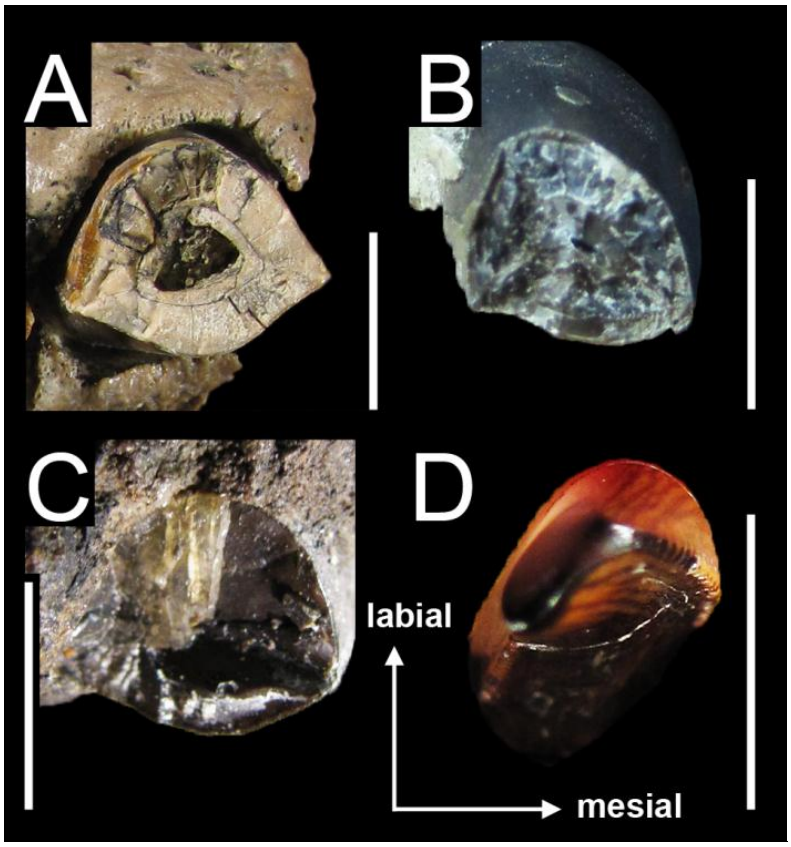

FIGURE 3.7. Cross-section of mesialmost teeth in non-avian Theropoda. **A**, First right premaxillary tooth of the abelisaurid *Majungasaurus crenatissimus* (FMNH PR.2008) in apical view; **B**, Isolated premaxillary tooth of the basal tyrannosauroid *Eotyrannus lengi* (MIWG 1997.550) in apical view; **C**, First right premaxillary tooth of the allosaurid *Allosaurus fragilis* (CMNH 1234) in apical view; **D**, Isolated right premaxillary tooth of the dromaeosaurid *Dromaeosaurus albertensis* (AMNH 5356) in apical view. Scale bars = 5 mm (B,D), 1 cm (A,C).

Hocknull et al. 2009) and extends to the cervix (Hocknull et al. 2009: fig. 20B). However, this morphology seems to have been lost in mesial teeth of Carcharodontosauridae, as in the mesial crowns of *Acrocanthosaurus* (NCSM 14345), *Giganotosaurus* (MUCPv-CH-1, dt1) and *Mapusaurus* (MCF-PVPH-108.166) display a mesial carina facing mesiolabially (pers. obs.), giving a wide lenticular/lanceolate outline of the crown in cross-section. Although deformed, *Ornitholestes* mesial teeth are asymmetrical and D-shaped in cross-section for the premaxillary ones, and J-shaped for the first maxillary one (pers. obs.). As seen with the mesial dentition of Abelisauridae, Allosauridae and *Ornitholestes* there is a *continuum* of morphological variation from a D-shaped/salinon-shaped cross-section outline of the first mesial crowns to a more J-shaped outline of the more distal crowns (Fanti and Therrien 2007). The differences in cross-section morphologies is then positional and can, therefore, be subtle so that a D-shaped, salinon-shaped, and J-shaped cross-section are not discrete conditions.

U-shaped Cross-section

Mesial teeth of both Tyrannosauroidea and *Zuolong* are U-shaped. An U-shaped cross-section of the crown at the cervix (Fig. 2.5H–I) is typically referred to a D-shaped outline by several authors (e.g., Hutt et al. 2001; Sereno et al. 2009; Choiniere et al. 2010*a*). However, D-shaped and U-shaped cross-sections cannot be confused because the carinae of the latter are positioned on the same side of the tooth and typically facing lingually, which is not the case in a crown with a D-shaped cross-section

in which the distal carina does not face lingually (pers. obs.). An U-shaped cross-section of the crown base is visible in the mesial teeth of the large majority of tyrannosauroids such as *Eotyrannus* (Hutt et al. 2001; Fig. 3.7B), *Dilong* (Xu et al. 2004), *Guanlong* (Xu et al. 2006), *Xiongguanlong* (Li et al. 2010), *Raptorex* (Sereno et al. 2009), *Daspletosaurus* (Lehman and Carpenter 1990), *Albertosaurus* (Currie 2003), *Tarbosaurus* (Hurum and Sabath 2003) and *Tyrannosaurus* (Smith 2005; pers. obs.). A similar morphology is seen in *Zuolong* premaxillary teeth (Choiniere et al. 2010*a*) which may be autapomorphic. In *Proceratosaurus*, the mesial carina of mesial teeth twists lingually and does not face entirely lingually so that the cross-section of mesial teeth is not U-shaped, but instead J-shaped. In many tyrannosauroids, the lingual surface of mesial teeth is concave, biconcave or planar, whereas in some tyrannosaurids like *Tyrannosaurus* and *Tarbosaurus*, the mesial margin is strongly convex, giving an oval-shaped of the crown base in cross-section (Smith 2005: fig. 8A). Due to the obvious lingual position of the carinae, the cross-section outline of these crowns is still referred as U-shaped. As *Proceratosaurus* is currently considered as a derived member of the Proceratosauridae (Brusatte et al. 2010*d*), mesial teeth with an U-shaped cross-section of the crown base is a synapomorphy of Tyrannosauroidea.

Eight-shaped Cross-section

An eight-shaped cross-section outline (Fig. 2.5L) is noticeable among Metriacanthosauridae, Megaraptora and Coelurosauria. The presence of an eight-shaped outline of the crown-base in cross-section, due to the presence of labial and lingual depressions on the crown base, is a common feature of dromaeosaurids such as *Saurornitholestes* (Currie et al. 1990; Sankey et al. 2002), *Tsaagan* (Norell et al. 2006), *Pyroraptor* (Allain and Taquet 2000; Gianechini et al. 2011*a*)b; pers. obs.) and *Buitreraptor* (Gianechini et al. 2011*a*) and the possible dromaeosaurid *Richardoestesia gilmorei* (Currie et al. 1990; Hendrickx and Mateus 2014*b*). This outline is also present in the neovenatorid *Orkoraptor* (Novas et al. 2008), the troodontids *Byronosaurus* (Lmx14) and *Xixiasaurus* (Lü et al. 2010: fig. 2), as well as the tyrannosauroids *Proceratosaurus* (Rauhut et al. 2010) and *Alioramus* (IGM 100-1844; Brusatte et al. 2012*a*). In tyrannosauroids, the presence of this feature may be due to the immaturity of the specimens as large and fully mature tyrannosauroids do not seem to share such feature (pers. obs.). A labial depression is also well-visible in many lateral teeth of *Sinraptor* (IVPP 10600) and the outline of the crown base in cross-section is likely to be an eight-shaped as well. Based on our observations, the crown base of coelophysoids, ceratosaurs, megalosauroids, allosaurids, neovenatorids, carcharodontosaurids, compsognathids, alvarezsaurids, therizinosaurs, oviraptorosaurs is never eight-shaped (pers. obs.). Such outline was also reported in the coelophysoid *Liliensternus* (Gianechini et al. 2011*a*: fig. 2c), yet based on the crown morphology of this taxon, it is likely that the eight-shaped outline corresponds to a cross-section in the root rather than at the base of the crown. An eight-shaped cross-section of the crown base is considered to be a possible synapomorphy of Dromaeosauridae.

The presence of medial depressions along the crown of *Sinornithosaurus*, and giving an 8-shaped outline of the cross-section, was interpreted as a venom delivery duct of a venomous animal by Gong et al. 2010, 2011), an hypothesis rejected by Gianechini et al. (2011*a*) which did not give an alternative morphological or functional interpretation. Both lingual and labial depressions may in fact result from the track of the erupting replacement tooth that grows lingually from the tooth root (e.g., *Torvosaurus*, *Acrocanthosaurus*) and sometimes within the root, beneath the crown of the erupted tooth (e.g., *Alioramus*). The labial and lingual depressions on the root and extending apically along the crown are then the remnant of the preceding tooth abutting against the labial surface, and the succeeding tooth in contact on the lingual surface of the root. Nevertheless, it must be noted that we did not observe a single erupted tooth growing labially in the examined theropods, which suggest that the preceding tooth always grows linguobasally from the erupted crown. As for the concave surface adjacent to carinae, the presence of a lingual and/or labial depression may also have some functional implications such as strengthening the crown, or allowing rapid penetration and withdrawal of the tooth from the substrate.

A figure eight-shaped cross-section in the lateral dentition was proposed as a character state by Gianechini et al. (2011*a*, character 253.2), and later by Hendrickx and Mateus (2014*b*, character 72.3). Gianechini et al. (2011*a*) coded the presence of this feature in *Saurornitholestes*, *Tsaagan* and *Buitreraptor* in their data matrix. Following our observations, this feature can also be coded in the sinraptorid *Sinraptor*, and the troodontid *Byronosaurus*.

Mesial Carina Reaching the Cervix

A mesial carina reaching the cervix is present in all theropod clades other than Megalosauridae and Therizinosauria. The mesial carina extends to the cervix (or even below it) in a large number of theropods, including the basal theropod *Eodromaeus* (PVSJ 560, 561), the coelophysoids *Coelophysis* (Buckley 2009) and *Liliensternus* (Cillari 2010), the dilophosaurid *Dilophosaurus* (UCMP 37303), the ceratosaurid *Ceratosaurus*, and in all abelisauroids and Spinosauridae (although not in all teeth of *Masiakasaurus* and Spinosauridae; pers. obs.). A similar feature also occurs in the basal megalosauroid *Piatnitzkysaurus* (PVL 4073) and many allosauroids such as *Allosaurus* (e.g., USNM 8335; SMA 0005/02), *Sinraptor* (ZDM T0024), *Fukuiraptor* (Currie and Azuma 2006). It is also present in the large majority of carcharodontosaurine teeth, although the mesial carina of some *Giganotosaurus* lateral teeth extends just above the cervix (pers. obs.). A mesial carina reaching the cervix also occurs in some mesial and lateral teeth in the tyrannosauroids *Raptorex* (LH PV18), *Alioramus* (IGM 100-1844), *Daspletosaurus* (Carr and Williamson 2004), *Gorgosaurus* (USNM 12814) and *Shanshanosaurus* (Currie and Dong 2001*b*). This is also the case in *Tyrannosaurus* in which some mesial and lateral teeth have a mesial carina reaching the crown base (*contra* Smith 2005; dt1 CMNH 9380; rdt12; ldt7 FMNH PR.2081). A similar feature is present in some teeth of several deinonychosaurs such as *Dromaeosaurus* (AMNH 5356), *Atrociraptor* (Currie

and Varricchio 2004), *Saurornitholestes* (Currie et al. 1990; Baszio 1997) and *Troodon* (Currie 1987; Currie et al. 1990). The mesial carina seems to never reach the cervix in *Eoraptor* (PVSJ 512), Megalosauridae, the neovenatorids *Neovenator* (MIWG 6348) and *Australovenator* (Hocknull et al. 2009), basal tyrannosauroids (e.g., *Proceratosaurus*, *Eotyrannus*), Therizinosauria, and Microraptorinae. On the other hand, the mesial carina does not reach the root in most lateral teeth of *Acrocanthosaurus*, *Dromaeosaurus, Alioramus, Tyrannosaurus,* and most other tyrannosaurids (Carr and Williamson 2004). A mesial carina terminating above the cervix is a possible synapomorphy of Megalosauridae and Therizinosauria.

It has been demonstrated that the extension of the denticulate mesial carina correlates with the distal curving of the crown in ziphodont theropods, the tooth curvature decreasing distally when approaching the mandibular articulation (D'Amore 2009). The crown area that may not contact the substrate, called the 'dead-space', tends to be unserrated, and the dead-space that is produced during the puncturing by the denticulate margins of the crown is what allows for the removal for flesh (D'Amore 2009). The extension of the serrated mesial carina in the different clade of ziphodont and pachydont theropods conforms to this model as, for instance, the mesial carina of the poorly curved crowns of Ceratosauridae, Abelisauridae and Baryonychinae almost always reaches the cervix. However, this model only applies to meat-eating dinosaurs with ziphodont, pachydont and conidont teeth, as herbivorous theropods with folidont dentition have denticles for tough and fibrous material that are subject to different selection pressure (D'Amore 2009).

The extension of the mesial carina along the theropod crown was first included in a data matrix by Benson (2010*a*, character 89), and subsequently incorporated in the data matrix of Hendrickx and Mateus (2014*b*, characters 50, 80). We mostly agree with the codings of Benson (2010*a*), yet some crowns of *Allosaurus* and *Acrocanthosaurus* display a mesial carina reaching the cervix, and these two taxa should be coded as having the polymorphic character (01). (Hendrickx and Mateus 2014*b*) proposed that the extension of the mesial carina should be coded separately for the mesial and lateral dentition. The extension of the distal carina also bears phylogenetic signal because a distal serrated carina extending to the cervix is present in all theropods other than therizinosauroids, and some compsognathids. Likewise, the distal serrated carina reaches or extends close to the crown apex in most theropods, yet a distal carina terminating well-beneath the tip of the crown is present in some compsognathids (*Compsognathus*, *Scipionyx*), and the basal megalosauroid *Sciurumimus* (pers. obs.). However, this character varies ontogenetically as it has been mostly recorded in juvenile specimens as well as in the embryo tentatively assigned to *Lourinhanosaurus* (ML 565.122).

Twisted and Split Mesial Carina

Twisted mesial carina occurs in Dilophosauridae, Abelisauroidea, Piatnitzkysauridae, Allosauroidea, Tyrannosauroidea, Dromaeosauridae for mesial teeth, and Allosauridae, Tyrannosauroidea and Dromaeosauridae for lateral teeth. Split mesial carina seems to be restricted to

'non-neocoelurosaur' Avetheropoda. A mesial carina spiraling from the mesial side apically to the mesiolingual or lingual side basally is seen in the mesial teeth of various theropods such as the coelophysoids *Dilophosaurus* (UCMP 37302), the abelisauroids *Masiakasaurus* (e.g., UA 8680; FMNH PR.2182, 2471), *Indosuchus* (AMNH 1753, pm4), the basal megalosauroids *Piatnitzkysaurus* (PVL 4073), the large majority of allosauroids like *Allosaurus* (e.g., AMNH 851; NHFO 455), *Sinraptor* (Currie and Zhao 1993*a*), *Fukuiraptor* (Currie and Azuma 2006: fig. 1D), *Australovenator* (Hocknull et al. 2009: fig. 20B) *Mapusaurus* (MCF-PVPH-108.166), and *Tyrannotitan* (MPEF-PV 1156). A twisted carina is also observable in basal tyrannosauroids like *Proceratosaurus* (BMBH R.4860; more derived tyrannosauroids having a straight mesial carina facing lingually), and many dromaeosaurids like *Deinonychus* (Ostrom 1969), *Dromaeosaurus* (Currie et al. 1990; pers. obs.), and *Saurornitholestes* (Currie et al. 1990). This condition appears in mesial teeth of the lateral dentition in *Allosaurus* (USNM 8335; UMNH VP 9168), tyrannosauroids such as *Proceratosaurus* (NHM R.4860), *Raptorex* (LH PV18), *Alioramus* (IGM 100-1844; Brusatte et al. 2012*a*), *Albertosaurus* (DMNH 22019) and *Tyrannosaurus* (FMNH PR.2081; Smith 2005), and the dromaeosaurids *Dromaeosaurus* (AMNH 5356; Currie et al. 1990; this was considered to be an autapomorphy of *Dromaeosaurus* by Turner et al. (2012) and perhaps *Saurornitholestes* (Currie et al. 1990: fig. 8.2V). In *Dromaeosaurus*, the mesial carina spirals along the crown even in more distal teeth of the lateral dentition (pers. obs.), a possible autapomorphy of this taxon among dromaeosaurids. A twisted mesial carina never occurs in lateral teeth of non-avetheropod theropods, Carcharodontosauridae, Metriacanthosauridae, Neovenatoridae, and non-eudromaeosaurid 'neocoelurosaurs'. A mesial carina twisting along the crown in the lateral dentition is synapomorphic for Avetheropoda.

According to Bakker (1998), a mesial carina passing inward from the crown tip, associated with a distal carina passing outward, would keep shallow wounds open during attack. In other words, lingually twisted mesial carina and a distal carina displaced labially would slice the flesh on a crown width when penetrating the prey item, resulting in wider wounds compared to those occasioned by strongly labiolingually narrow teeth with carinae positioned on a same plane. Although this hypothesis has never been tested, the presence of many crowns with twisted mesial carina in the lateral dentition of tyrannosauroids, *Allosaurus* and *Dromaeosaurus* seems to support the hypothesis of a predatory lifestyle rather than obligate scavenging in these theropods.

Split mesial carinae have been reported in several Tyrannosauridae including *Alectrosaurus*, *Albertosaurus*, *Daspletosaurus*, and *Tyrannosaurus* (Currie et al. 1990; Erickson 1995; Abler 1997; Smith 2005; Cillari 2010). This crown abnormality is not rare in the dentition of Tyrannosauridae, and among 993 tyrannosaurid teeth examined by Erickson (1995), 11% displayed such feature. Outside the clade of Tyrannosauridae, a split carina has only been identified in three allosauroids theropods, namely *Allosaurus* (Erickson 1995), an indeterminate carcharodontosaurid from Niger (Brusatte and Sereno 2007), and an indeterminate carcharodontosaurid from Brazil (Candeiro and Tanke 2008). Besides the isolated tooth MNN GAD15 illustrated by Brusatte and Sereno (2008), we did not observe

any split carina in the dentition of non-tyrannosaurid taxa examined first hand, suggesting that this condition is rare outside the clade of Tyrannosauridae. The development of split carinae in theropods has been exhaustively investigated by Erickson (1995) and seem to be caused by trauma, aberrant tooth replacement, and mostly by genetic factors. The split carinae condition still needs to be integrated in cladistic analyses on theropod teeth as this feature seem to bear phylogenetic signal. The presence of a twisted carina was first coded in a data matrix by Currie (1995, character 2) and this character was then incorporated in the data matrix of Hendrickx and Mateus (2014*b*). On the other hand, the presence of a split mesial carina has never been considered as a character in a phylogenetic analysis.

Distal Carina Strongly Deflected Labially

A distal carina is strongly deflected labially in *Dilophosaurus* and Allosauroidea for mesial teeth, and Ceratosauridae, *Allosaurus*, Tyrannosauroidea and *Dromaeosaurus* for the whole dentition. The distal carina of mesial and lateral teeth is strongly displaced labially (i.e., the distal carina is at the level of the labial margin of the crown in distal view) in the ceratosaurids *Genyodectes* (MLP 26-39), *Ceratosaurus* (USNM 4735) and *Berberosaurus* (MNHN To 339), the noasaurid *Masiakasaurus* (UA 8680; FMNH PR.2201, 2221, 2476), the allosaurid *Allosaurus* (USNM 8335; SMA 005/02), and the dromaeosaurids *Dromaeosaurus* (AMNH 5356). A strongly deflected distal carina towards the labial side of the crown also occurs in the mesial teeth in the neovenatorids *Fukuiraptor* (Currie and Azuma 2006: fig. 1SA–B), the carcharodontosaurids *Acrocanthosaurus* (NCSM 14345), *Giganotosaurus* (MUCPv-CH-1) and *Mapusaurus* (MCF-PVPH 108), and the deinonychosaurs *Deinonychus* (Ostrom 1969) and *Richardoestesia* (Currie et al. 1990). In the tyrannosauroids *Proceratosaurus* (NHM R.4860), *Raptorex* (LH PV18), *Alioramus* (IGM 100-1844), *Gorgosaurus* (USNM 12814; AMNH 5458) and *Tyrannosaurus* (CMNH 9380; NHM R.7994; FMNH PR.2081), the distal carina is strongly deflected labially in mesial teeth as well as in the mesial half of the lateral dentition, except in tyrannosaurids in which the carina is significantly displaced in most dentary teeth (pers. obs.). Interestingly, the distal carina of premaxillary teeth is displaced lingually and not labially in the coelophysoid *Dilophosaurus* (UCMP 37303). The same condition is present in the whole dentition of *Eoraptor* (PVSJ 512). Nevertheless, there is no displacement of the distal carina in mesial dentary teeth and in the lateral dentition of *Dilophosaurus*. The distal carina is centrally-positioned on the crown or only weakly displaced labially in the whole dentition of *Sanjuansaurus* (PVSJ 605), *Eodromaeus* (PVSJ 561), *Liliensternus* (MB R.2175), *Noasaurus* (PVL 4061), Abelisauridae and Megalosauroidea, in the lateral dentition of Metriacanthosauridae, Neovenatoridae, Carcharodontosauridae, Tyrannosauroidea, and possibly the whole dentition of ‘neocoelurosaurs’ with a few exceptions like *Dromaeosaurus* (pers. obs.). The strong labial displacement of the distal carina in lateral teeth is a possible synapomorphy of Ceratosauridae and Avetheropoda. A distal carina centrally positioned or only weakly displaced on the crown is a possible synapomorphy of

Abelisauridae and Megalosauroidea for the whole dentition, and Carcharodontosauria for lateral teeth. A strongly deflected carina has only been incorporated in a data matrix by Hendrickx and Mateus (2014*b*).

Hooked Denticles

Hooked denticles are seen in *Eoraptor*, Abelisauroidea, Therizinosauroidea, Troodontidae and Dromaeosauridae. The presence of distal denticles with an apex pointing towards the tip (Fig. 3.8) is a feature present in the teeth of the basal theropod *Eoraptor* (e.g., third right premaxillary tooth; PVSJ 512; Fig. 3.8A) and many abelisauroids such as *Masiakasaurus* (FMNH PR.2221, 2296; Fig. 3.8B), *Kryptops* (MNN GAD1-1), *Rugops* (MNN IGU1), *Majungasaurus* (FMNH PR.2008, 2100, 2278). Mesial and distal hooked denticles can also be observed in some therizinosaurids such as *Alxasaurus* (Russell and Dong 1993*a*) and *Nothronychus* (Kirkland and Wolfe 2001). Dromaeosaurids are well known to possess apically hooked denticles as they can be observed in the eudromaeosaurians *Deinonychus* (Ostrom 1969), *Saurornitholestes* (Currie et al. 1990; Fig. 3.8C), and *Atrociraptor* (Currie and Varricchio 2004). Finally, troodontids such as *Troodon* (e.g., Currie 1987; Currie et al. 1990; Holtz et al. 1998; Longrich 2008; Fig. 3.8D) and *Sinornithoides* (Currie and Dong 2001*a*) also display apically hooked denticles. In many theropod clades such as ceratosaurids, megalosauroids, allosauroids and tyrannosauroids, the denticles are symmetrically rounded or slightly asymmetrically convex in lateral view, but never pointed or hooked apically (*contra* Bakker and Bir 2004 for ceratosaurids and allosaurids, and Smith 2007 for tyrannosaurids; Currie et al. 1990; Abler 1992; pers. obs.). Likewise, some dromaeosaurids such as *Velociraptor* (AMNH 6515), *Bambiraptor* (AMNH 30556), *Tsaagan* (Norell et al. 2006), *Utahraptor* (Kirkland et al. 1993), *Microraptor* (CAGS 20-7-004) and *Sinornithosaurus* (Xu and Wu 2001) do not have apically hooked denticles, but rather symmetrically to asymmetrically convex serrations. The presence of hooked and/or pointed denticle is a possible synapomorphy of Abelisauroidea, Therizinosauridae, and Eudromaeosauria. The morphology of denticles with apically hooked external margin varies significantly among theropods displaying this feature. In some *Masiakasaurus* teeth, the hooked denticles are mesiodistally narrow, being different from the more subquadrangular denticles of abelisaurids, and dromaeosaurids. Likewise, denticles with hooked external margins are usually apically inclined in therizinosaurids, sometimes almost apicobasally oriented on the carinae. Nevertheless, many therizinosaurid taxa do not seem to have genuinely hooked denticles, but rather pointed denticles that are perpendicular to the crown margin, as in *Eshanosaurus* (Zhao and Xu 1998), and apically inclined and/or vertically oriented, as seen in *Jianchangosaurus* (Pu et al. 2013), *Beipiaosaurus* (Xu et al. 1999*a*), and *Erlikosaurus* (Clark et al. 1994). This is also the case in Troodontidae which tend to have particularly large, bulbous, and sometimes apically inclined denticles. Hooked denticles are clearly observed in *Troodon* (e.g., Currie 1987; Currie et al. 1990; Holtz et al. 1998; Ryan et al. 1998; Longrich 2008), *Sinornithoides* (Currie and Dong 2001*a*), *Pectinodon* (Longrich 2008) and some troodontid teeth from

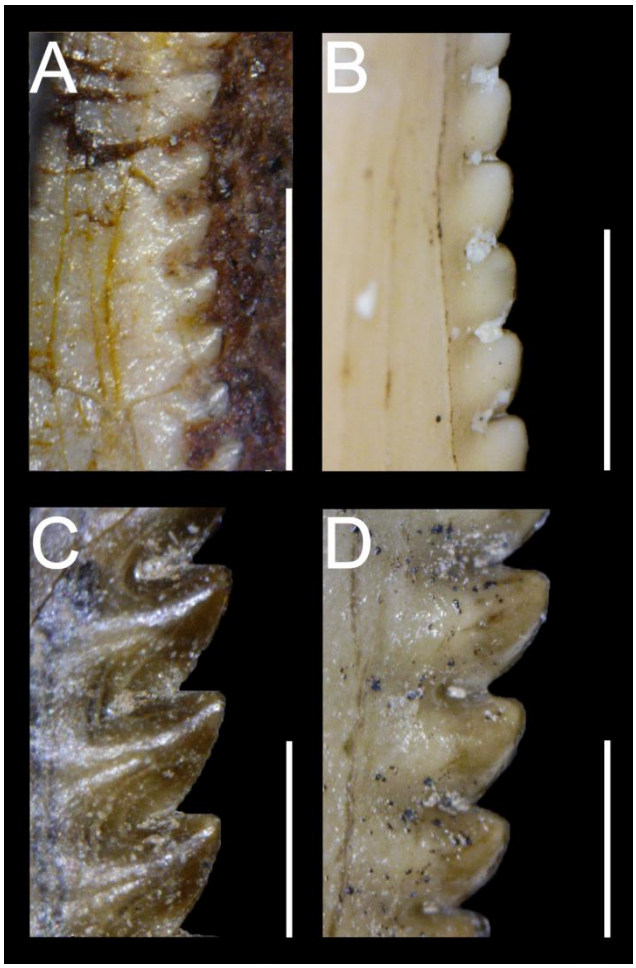

FIGURE 3.8. Hooked denticles in non-avian Theropoda. **A**, Distal carina of third right premaxillary tooth of the basal saurischian *Eoraptor lunensis* (PVSJ 512) in labial view; **B**, Distal carina of an isolated tooth of the noasaurid *Masiakasaurus knopfleri* (FMNH PR.2696) in lateral view; **C**, Distal carina of an isolated tooth of the dromaeosaurid *Saurornitholestes* sp. (DMNH 22870) in lateral view; **D**, Distal carina of an isolated tooth of the troodontid *Troodon formosus* (DMNH 22337) in lateral view. Scale bars = 1 mm.

Central Asia (Averianov and Sues 2007). Many troodontid taxa such as *Linhevenator* (Xu et al. 2011*c*), *Saurornithoides*, *Zanabazar* (Norell et al. 2009) and *Pectinodon* (Longrich 2008) show very large denticles either with a pointed or a parabolic and rounded external margin, as also seen in troodontid teeth from France (Vullo and Néraudeau 2010), Uzbekistan (Averianov and Sues 2007), and India (Goswami et al. 2013). Variation in denticle sizes and morphologies may however be positional, as proposed by Longrich (2008) for *Pectinodon bakkeri*.

Hooked denticles in the dromaeosaurid *Saurornitholestes* were interpreted as being adapted to slicing flesh off bones by Currie et al. (1990). According to Fowler et al. (2011), hooked denticles in dromaeosaurids are, however, not well-suited for tearing through flesh. They would instead enhance the effectiveness of the jaw's grip on prey, or helped removing feathers and fur from prey items (Fowler et al. 2011). Clearly, the origin of this structure is distinct from that of therizinosauroids and troodontids, being only superficially morphologically convergent. Although the morphology of the abelisauroid denticles is similar to those of dromaeosaurids, they are distantly related clades that could have converged morphologically as a result of selection to perform a similar function.

The presence of hooked denticles on the theropod crown was first included in Norell et al. (2001*b*, character 88) and this character is commonly considered in cladistic analyses on coelurosaurs.

Among the most recent cladistic analyses, Xu et al. (2009*a*, character 167), Turner et al. (2012, character 87) and Choiniere et al. (2014*b*, character 236) only consider large apically hooked and/or inclined denticles. Using the same character, Xu et al. (2009*a*) coded it in Dromaeosauridae, Turner et al. (2012) in Troodontidae, and Choiniere et al. (2014*b*) in Troodontidae, Therizinosauria and *Eoraptor*, suggesting some inconsistency in character coding among authors. On the other hand, Godefroit et al. (2013*a*, character 572) did not take into consideration the denticle size and coded hooked denticles apically in dromaeosaurids and troodontids. We follow Godefroit et al. (2013*a*) and Hendrickx and Mateus (2014*b*) codings, because the size of the denticle and the outline of its external margin should be considered as separated and independent features. Likewise, hooked denticles should not be confused with the baso-apically oriented denticles with rounded external margins, so that denticles with an apically hooked external margin should be coded in some dromaeosaurids, troodontids, and therizinosaurids, along with *Eoraptor*, *Masiakasaurus*, and some abelisaurids.

Small Number of Denticles on the Carina

The presence of fewer than 15 denticles along the carina has been noted in derived Therizinosauroidea and Troodontidae. A small number of denticles (< 15 denticles along a single carina) is well-known to characterize troodontids such as *Troodon* (Leidy 1856; Russell 1948; Currie 1987), *Sinornithoides* (Currie and Dong 2001*a*), *Linhevenator* (Xu et al. 2011*c*), *Pectinodon* (Carpenter 1982; Larson and Currie 2013), *Saurornithoides* and *Zanabazar* (Norell et al. 2009). They are also present in many therizinosauroids such as *Alxasaurus* (Russell and Dong 1993*a*), *Beipiaosaurus* (Xu et al. 1999*a*), *Nothronychus* (Kirkland and Wolfe 2001), *Eshanosaurus* (Xu et al. 2001*b*), *Erlikosaurus* (Clark et al. 1994), and *Jianchangosaurus* (Pu et al. 2013). A carina bearing few denticles can also be found in the dromaeosaurids *Microraptor* (CAGS 20-7-004) and *Paronychodon* (Currie et al. 1990) which is interpreted as a pathological specimen of already known dromaeosaurid and troodontid taxa (Hwang 2005). Some crowns of *Saurornitholestes* seems to have a low number of denticles on the carina (Currie et al. 1990; Baszio 1997; Larson and Currie 2013), but the quantitative data gathered by Larson and Currie (2013) indicates that the large majority of *Saurornitholestes* teeth have much more than 15 denticles along the crown. Finally, embryonic or juvenile theropods tend to bear few coarse denticles such as the theropod tentatively ascribed to *Lourinhanosaurus* (Araújo et al. 2013), the hatchling *Scipionyx* (Dal Sasso and Maganuco 2011), and the posthatchling *Sciurumimus* (Rauhut et al. 2012). The presence of a few denticles on the crown is a synapomorphy of Troodontidae and Therizinosauroidea among Therizinosauria (*sensu* Zanno 2010*a*).

In mature individual, a crown bearing relatively few large pointed denticles seems to be adapted to an omnivorous diet including plant material at least partially. Therizinosaur teeth are strongly convergent with those of basal sauropodomorphs and iguanas (Barrett 2000). Indeed, both possess relatively few and large pointed denticles on the carinae, mesial and distal carinae not reaching the cervix, and a convex margin of the crown, a tooth morphology that is correlated with omnivorous

diets (Barrett 2000). Troodontidae with very large apically hooked denticles on the distal carina have also been interpreted as omnivorous, as well as insectivorous based on the convergent dentition with iguanids and bat-eared fox, respectively (Varricchio 1997; Holtz et al. 1998; Zanno et al. 2009). However, predominantly carnivorous diet has been inferred by other authors due to sharp and hooked denticles and interdenticular sulci (Currie and Dong 2001*a*; Zanno and Makovicky 2011). Nevertheless, few troodontids actually possess sharply pointed and hooked serrations, and the denticles of *Linhevenator* (Xu et al. 2011*c*), *Pectinodon* (Carpenter 1982; Larson and Currie 2013), *Saurornithoides* and *Zanabazar* (Norell et al. 2009) rather display a rounded external margin. According to Currie et al. (Currie et al. 1990), the large denticles of troodontids would slice through soft material and bones. Another interpretation given by Holtz et al. (1998) is that large denticles of troodontids and therizinosaurs would instead sever larger-sized and/or more resistant structures such as plant fibers. Troodontid and therizinosaur denticles differ significantly from those of meat-eating dinosaurs with small chisel-shaped denticles, thus, an omnivorous diet combining plant material and meat seems likely in these theropods. Interestingly, large denticles are typically associated with constricted crown, as illustrated with *Microraptor*, the only established dromaeosaurid possessing a small number of denticles on the crown and a constriction at the crown base. This suggests that *Microraptor* had an atypical diet among dromaeosaurids which are typically considered as unquestionable carnivores (Norell and Makovicky 2004; Zanno and Makovicky 2011). The peculiar dentition of *Microraptor* seems indeed to support an omnivorous diet of this animal in which gut contents already revealed remains of mammals (Larsson et al. 2010), enantiornithine birds (O'Connor et al. 2011), and fish (Xing et al. 2013*a*).

Russell and Dong (1993*a*, character 20) were the first to propose a character distinguishing small and large denticles to acknowledge the presence of large denticles on the crowns of *Plateosaurus*, therizinosaurs, and troodontids. This character is still incorporated in most recent cladistic analyses as a binary character with the character states 'small' and 'large'. According to the character list of some authors (e.g., Norell et al. 2001*b*, character 87), Farlow et al. (1991) quantifies the difference between small and large denticles. However, Farlow et al. (1991) only offered some equations illustrating the relationship between tooth size and denticle size for a small tooth population (teeth less than 7 mm), and large tooth population (teeth greater than 7mm). Previous authors did not provide yet a quantifiable boundary between small and large denticles. Based on the examination of the dentition of more than 70 theropod taxa, it became apparent that denticle size correlates with a low number of denticles per crown. We, therefore, suggest a simple boundary of 15 denticles on the crown of mature individuals. Crowns with 15 or less denticles along the whole length of the distal carina have large denticles, and those with 15 to 250 denticles on the distal carina are considered as having small denticles. Crowns bearing more than 250 denticles along the whole length of the distal carina are coded as having minute denticles. The number of denticles on the crown can be extrapolated by using the formula DAVG/5 * CH (or DC/5 * CH if the number of denticles basally and apically are

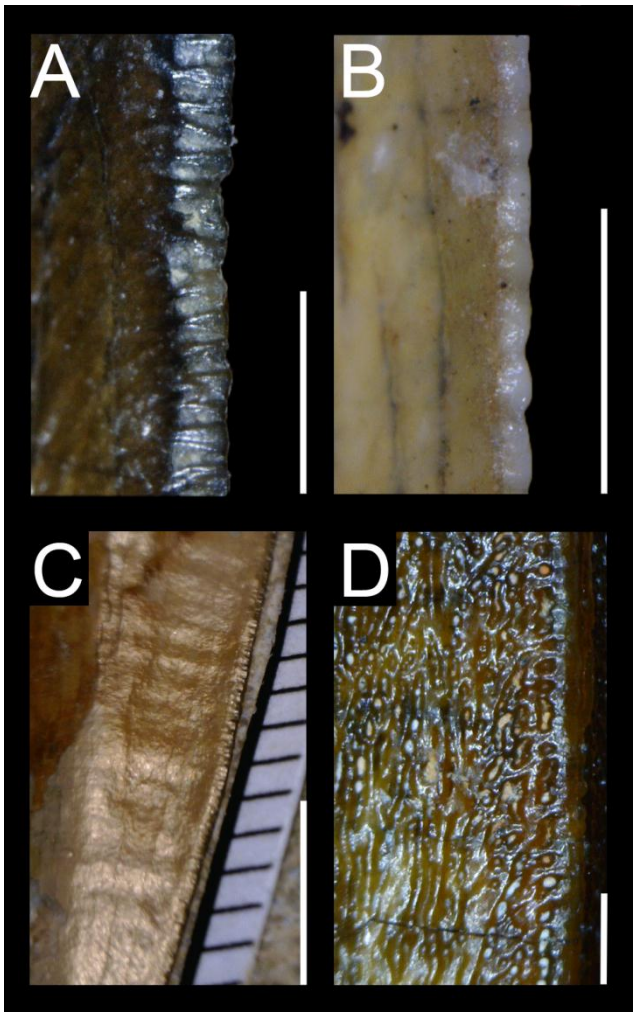

FIGURE 3.9. Denticles and carinae in Spinosauridae. **A**, Carina of an isolated tooth of *Baryonyx walkeri* (NHM R.9951 R.278) in lateral view; **B**, Carina of an isolated tooth of *Suchomimus tenerensis* (MNN G26-5b) in lateral view; **C**, Carina of a maxillary tooth of *Irritator challengeri* (SMNS 58022) in labial view; **D**, Carina of an isolated tooth of *Spinosaurus* cf. *aegyptiacus* (MSNM V6422) in lateral view. Scale bars = 5 mm (C), 1 mm (A–B, D).

unknown), giving an approximation of the total number of denticles on the distal carina. Senter (2011, character 150), Turner et al. (2012, character 86), Godefroit et al. (2013*a*, character 163), Choiniere et al. (2014*b*, character 237) all coded the presence of large denticles in derived therizinosaurs and troodontids, and *Microraptor* and *Gorgosaurus* were also coded as possessing large denticles in the data matrices of Turner et al. (2012) and Choiniere et al. (2014*b*), respectively. However, according to our definition only *Microraptor* also shares this condition.

Large Number of Denticles on the Carina

More than 250 denticles along the carinae are present in Baryonychinae and *Acrocanthosaurus*. However, more than 30 denticles per five millimeters are seen in non-tetanuran theropods, Baryonychinae and coelurosaurs. Minute denticles relative to the tooth size (i.e., more than 250 denticles along the distal carina) are found in the dentition of the baryonychines *Baryonyx* (~35 de/5mm; NHM R.9951; ML 1190; Fig. 3.9A) and *Suchomimus* (~35 de/5mm; e.g., UC G67-1, G22-7, G34-12; Fig. 3.9B) on both carinae, and, due to their large size, some lateral teeth of the carcharodontosaurid *Acrocanthosaurus* (~15 de/5mm; NCSM 14345; Smith et al. 2005). The presence

of minute denticles in large baryonychine teeth seems to be correlated with the increase in robustness of the crown (Charig and Milner 1997), and may also result from the simplification of the teeth, that were mostly used to impale prey rather than slicing their flesh, leading to unserrated crowns in Spinosaurinae (Charig and Milner 1997; Buffetaut 2011; Gianechini et al. 2011*a*). This dental simplification also occurs in other theropods such as *Compsognathus* in which many teeth have lost serrations. The reversal condition occurred in Therizinosauria and Troodontidae in which the primitive forms bear minute denticles that increase in size in more derived taxa. Minute denticles are not suitable for the 'rip and grip' cutting action of medium-sized serrations of most non-avian theropods, and might function in a similar way than unserrated teeth (Farlow et al. 1991; Charig and Milner 1997). A distal carina with more than 200 denticles is present in some very long lateral crowns of the ceratosaurid *Ceratosaurus* (~15 de/5mm; ML 865, 1151; Smith et al. 2005) and the tyrannosaurid *Tyrannosaurus* (~10 de/5mm; Smith 2005). Regardless of the tooth dimension, theropods with very small denticles, i.e., more than 30 denticles per five millimeters on the distal carina, include non-neotheropod Theropoda such as *Eoraptor*, *Eodromaeus*, *Liliensternus* and *Coelophysis*, Noasauridae, Baryonychinae, *Proceratosaurus*, Compsognathidae, *Aorun*, *Falcarius*, *Velociraptor*, Saurornitholestinae (including *Saurornitholestes*), and *Richardoestesia* (Smith et al. 2005; Zanno 2010*b*; Rauhut et al. 2012; Larson and Currie 2013; Choiniere et al. 2014*b*; pers. obs.). The presence of minute denticles along both carinae is a synapomorphy of Baryonychinae (Sereno et al. 1998).

Bilobate Denticles and Sporadic Variation of Denticle Size

Thought to be an autapomorphy of the carcharodontosaurid *Tyrannotitan chubutensis* (Novas et al. 2005*b*; Canale et al. 2014), denticles with a biconvex external margin (Fig. 3.10) have been observed in several theropod clades, typically on the mesial carina. Bilobate denticles have been identified in the abelisaurids *Aucasaurus* (MCF-PVPH 236; Fig. 3.10A) and possibly *Abelisaurus* (MPCA 5), the megalosaurids *Megalosaurus* (OUMNH J.13506; NHM R.234), *Duriavenator* (NHM R.332; Fig. 3.10B) and possibly *Torvosaurus* (ML 1100), the carcharodontosaurid *Acrocanthosaurus* (SMU 74646), and *Carcharodontosaurus* (UCRC PV6), the possible metriacanthosaurid *Erectopus* (MNHN 2001-4; Fig. 3.10C), and the tyrannosaurid *Tyrannosaurus* (FMNH PR.2081, mx10; Fig. 3.10D). Bilobate denticles seem to be malformations possibly resulting from trauma. Yet, they have not been observed in any non-averostran theropods and Maniraptoriformes, and may therefore correspond to a tooth trait change due to genetic factors influencing denticle morphology. As for the split carina (Erickson 1995), this however needs to be properly investigated in theropods in order to gain better understanding.

Random variation of denticle size along serrated carina has been observed in the baryonychines *Baryonyx walkeri* (NHM R.9951, ML 1190; Mateus et al. 2011; Fig. 3.9A), and *Suchomimus tenerensis* (MNN G26-5b; Fig. 3.9B) and seems to be restricted to Baryonychinae (Mateus et al. 2011). This feature is much more developed in *Baryonyx* and occurs along the whole

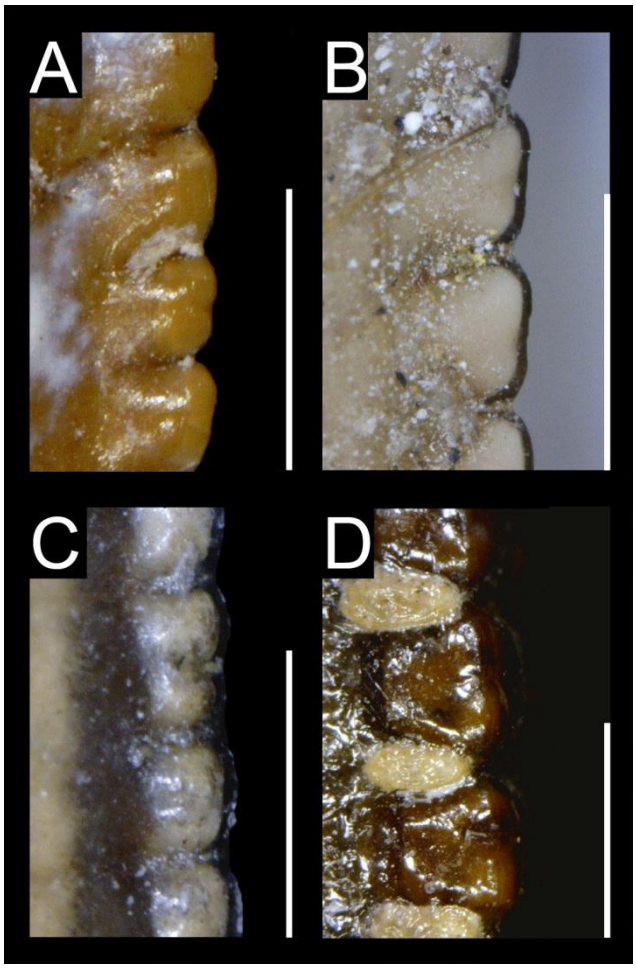

FIGURE 3.10. Bilobate denticles in non-avian Theropoda. **A**, Mesial carina of an isolated crown of the abelisaurid *Aucasaurus garridoi* (MCF-PVPH 236) in lateral view; **B**, Mesial carina of the sixth right maxillary tooth of the megalosaurid *Duriavenator hesperis* (NHM R.332) in lateral view; **C**, Mesial carina of the third left maxillary tooth of the possible metriacanthosaurid *Erectopus superbus* (MNHN 2001–4) in labial view; **D**, Mesial carina of the tenth maxillary tooth of the tyrannosaurid *Tyrannosaurus rex* (FMNH PR.2081) in labial view. Scale bars = 1 mm.

carinae in this taxon. In *Suchomimus*, most denticles gradually change in size along the carinae and the basal part of the carina only displays this sporadic change of denticle size. Such feature most likely results from the reduction of denticle dimension, which happened throughout the evolution of Spinosauridae. In Spinosaurinae, the carina is unserrated, yet it does not correspond to a smooth and regularly shape ridge. In lateral view, the carinae of *Irritator challengeri* and *Spinosaurus aegyptiacus* are indeed 'beaded' (*sensu* Sues et al. 2002; Fig. 3.10C) and sculptured (Fig. 3.10D), respectively (Sues et al. 2002; Hasegawa et al. 2010), thus indicating the vestigial presence of small denticles along the carinae. Characters on bilobate denticles and sporadic variation of denticle size along the carinae were only included in the data matrix of Hendrickx and Mateus (2014*b*, characters 93, 94). These characters should be considered in future cladistic analyses as they bear phylogenetic signal.

Distal Larger than Mesial Denticles

The distal denticles are significantly larger than the mesial ones in Noasauridae, Piatnitzkysauridae, non-tyrannosaurid Tyrannosauroidea and non-unenlagiine Dromaeosauridae. Long thought to characterize the dentition of Dromaeosauridae, and therefore used as a primary feature to identify dromaeosaurid teeth (e.g., Rauhut and Werner 1995; Sweetman 2004), the difference in size

between mesial and distal is widespread among other clades. Subtle differences in size may occur between mesial and distal denticles and we consider that a significant size variation between the mesial and distal carinae when the denticle size index (DSDI) is higher than 1.2. This arbitrary value was proposed by Rauhut et al. (2010) and corresponds to more than six mesial denticles for five distal serrations. A DSDI higher than 1.2 has been measured in the lateral dentition of the noasaurids *Noasaurus* (PVL 4061) and *Masiakasaurus* (e.g., UA 9091; FMNH PR.2201, 2211, 2696), the piatnitzkysaurids *Marshosaurus* (Madsen 1976*a*) and *Piatnitzkysaurus* (PVL 4043, MACN-CH 895), and many non-tyrannosaurid Tyrannosauroidea such as *Proceratosaurus* (Rauhut et al. 2010), *Dilong* (Xu et al. 2004), *Guanlong* (Xu et al. 2006), *Eotyrannus* (Hutt et al. 2001; MIWG 1997.550 mx1 with DSDI of 1.5, isolated lateral crown with DSDI of 1.35; *contra* Sweetman 2004) and *Xiongguanlong* (Li et al. 2010). Among dromaeosaurids, *Tianyuraptor* (Zheng et al. 2010), *Velociraptor* (Barsbold and Osmólska 1999), *Deinonychus* (Ostrom 1969), *Achillobator* (Perle et al. 1999), *Atrociraptor* (Currie and Varricchio 2004), *Pyroraptor* (Allain and Taquet 2000), *Bambiraptor* (Burnham 2004), *Saurornitholestes* (Currie et al. 1990), *Graciliraptor* (Xu and Wang 2004), *Acheroraptor* (Evans et al. 2013), and *Sinornithosaurus* (Xu and Wu 2001) also show this condition. Among Troodontidae, some isolated crowns assigned to *Troodon* also display a different in denticle size between the mesial and distal carina (Currie 1987: fig. 5k, m). Mesial denticles significantly smaller than distal denticles were also noted in the coelophysoid *Dilophosaurus* (Welles 1984) and *Liliensternus* (Smith et al. 2005), but both carinae bear denticles of relatively similar size in these two taxa (Cillari 2010; pers. obs.). A discrepancy in size between mesial and distal denticles was acquired independently in Noasauridae, Piatnitzkysauridae, Tyrannosauroidea and Dromaeosauridae, and teeth bearing distal denticles significantly bigger than the mesial ones are a possible synapomorphy of Noasauridae, Piatnitzkysauridae, Tyrannosauroidea and the clade Microraptorinae + Eudromaeosauria.

According to Fowler et al. (2011), the reduction of mesial denticles would enhance a piercing function of the tooth. However, this functional hypothesis has never been tested. What one can observe is that a difference in size between mesial and distal denticles is typically present in small sized meat-eating theropods (i.e., Noasauridae, basal Tyrannosauroidea, and Eudromaeosauria). Interestingly, in the only large sized dromaeosaurid *Utahraptor* the denticles are subequal in size in the distal and mesial carina (Kirkland et al. 1993). Nonetheless, Piatnitzkysauridae are the only medium-sized theropods showing a clear discrepancy in size between mesial and distal denticles. Thus, functional or developmental factors, or a combination of both, seems to come into play for the establishment of this condition in such disparate theropod clades.

A character encompassing the size difference between mesial and distal denticles was already included in a data matrix by Currie (1995, character 5) based on previous observations of Ostrom (1969) and Rauhut and Werner (1995). Since then, this dental feature is one of the most frequently used in phylogenetic analysis on coelurosaurs and maniraptoriforms. Among the most recent cladistic analysis incorporating this character, Rauhut et al. (2010, character 88), Senter (2011, character 151),

Turner et al. (2012, char. 247), Novas et al. (2013, character 2.1), and Godefroit et al. (2013*a*, character 884) correctly coded this feature among basal tyrannosauroids and dromaeosaurids, and only a few taxa were miscoded: *Piatnitzkysaurus* in Rauhut et al. (2010) and *Eotyrannus* in Turner et al. (2012) both possess mesial denticles significantly smaller than distal denticles. On the other hand, *Falcarius* and *Byronosaurus* from the data matrix of Senter (2011), and the derived tyrannosauroids *Appalachiosaurus*, *Albertosaurus*, and *Tyrannosaurus* from the data matrix of Novas et al. (2013), do not show this condition.

Straight to Convex Distal Profile

Although straight or convex distal margin of the crown is the most common condition in conidont and folidont teeth, most ziphodont and pachydont teeth are usually slightly to strongly concave distally (Ezcurra 2009; pers. obs.). Nevertheless, a straight or slightly curved distal profile in a ziphodont theropod was considered to be a synapomorphy for Abelisauridae by Smith (2007) as this feature is seen in the crowns of *Majungasaurus*, *Indosuchus*, *Rugops*, *Kryptops*, *Aucasaurus* (Smith and Dalla Vecchia 2006; Smith and Lamanna 2006; Candeiro 2007; Smith 2007; pers. obs.) and many indeterminate abelisaurids (e.g., UCPC 10; MNHN MRS1619, MRS1620). However, a straight or slightly concave curvature of the distal profile also occurs in the basalmost theropods *Eoraptor* (PVSJ 512), the ceratosaurids *Ceratosaurus* (USNM 4735) and *Genyodectes* (MLP 26-39), the noasaurids *Noasaurus* (PVL 4061), the allosaurid *Allosaurus* (NHFO 455), the metriacanthosaurids *Sinraptor* (IVPP 10600) and *Yangchuanosaurus* (CV 00215), the carcharodontosaurids *Carcharodontosaurus* (SGM Din1) and *Mapusaurus* (MCF-PVH 108.43), the tyrannosauroid *Eotyrannus* (MIWG 1997.550), and some coelurosaurs such as *Paronychodon* (Currie et al. 1990: fig. 8.5A) and *Zapsalis* (Sankey et al. 2002: fig. 4.10). A straight distal margin of the crown is also seen in pachydont teeth of some tyrannosaurids such as *Gorgosaurus* (USNM 12814) and *Tyrannosaurus* (FMNH PR.2081). A sigmoid outline of the distal margin of the crown, with the basal half slightly concave and the apical half weakly convex, is typical of carcharodontosaurid lateral teeth and can be observed in *Carcharodontosaurus* (SGM Din-1) and *Giganotosaurus* (MUCPv CH1). Given the wide distribution of a straight or convex distal profile, this feature cannot be used solely to identify teeth. However, a convex distal profile of the crown is a rare condition in ziphodont teeth and only is seen, to our knowledge, in Abelisauridae, and a few lateral teeth of *Ceratosaurus*.

A reduced crown curvature was first included in a data matrix by Sereno et al. (1998, character 35), and this feature is commonly used in phylogenetic analyses performed on the whole theropod clade. Among the most recent cladistic analyses on theropods, this character was coded in Spinosauridae and *Concavenator* by Carrano et al. (2012, character 141), in Abelisauridae by Pol and Rauhut (2012, character 89) and Tortosa et al. (2014, character 139), in *Ceratosaurus*, *Allosaurus*, *Neovenator*, *Kileskus*, *Albertosaurus*, Megalosauridae, Spinosauridae, and Carcharodontosauridae in Novas et al. (2013, character 8), and in Spinosauridae, Carcharodontosauridae, Alvarezsauroidea, and

Therizinosauria in Choiniere et al. (2014*b*, character 225). Throughout the literature there are inconsistencies on the definition of this character, thus the taxa it applies to. As suggested by Hendrickx and Mateus (2014*b*), the crown curvature of lateral teeth should be coded for both the mesial and distal surfaces of the crown. A straight crown lacking curvature is present in several theropod clades (e.g., Spinosauridae, Alvarezsauroidea, Therizinosauroidea), yet the curvature of both mesial and distal profiles is variable among them. The curvature of the mesial profile should then have two character states: strongly convex and slightly convex, almost straight, whereas the distal profile should be coded in four different ways, namely 1. strongly concave, 2. slightly concave, roughly straight, or straight, apex positioned at the same level as distal profile, 3. convex, apex positioned mesial to mesial profile, and 4. weakly sigmoid, basal half concave and apical half convex. A slightly convex and almost straight mesial profile is seen in Spinosaurinae and Ornithomimosauria, whereas all other theropods, including Alvarezsauroidea and Therizinosauria display a strongly convex mesial profile. As for the distal margin of the crown, a convex profile is visible in some Abelisauridae, *Ceratosaurus*, Spinosaurinae, Ornithomimosauria, Alvarezsauroidea, Therizinosauria, and Oviraptorosauria.

Flutes

Fluted crowns are seen in Theropoda for mesial teeth, and in *Coelophysis*, Spinosauridae and Dromaeosauridae in both mesial and lateral teeth. Flutes (Fig. 3.11) are well-known to characterize the dentition of spinosaurids, as they are present on the crowns in all of them (e.g., Charig and Milner 1997; Sereno et al. 1998; Taquet and Russell 1998; Dal Sasso et al. 2005; Fig. 3.11C). Nevertheless, flutes are also present on the lingual and/or labial surface of mesial teeth in many non-avian theropods such as *Coelophysis* (Buckley 2009), *Ceratosaurus* (e.g., Madsen and Welles 2000; Fig. 3.11A), *Masiakasaurus* (Carrano et al. 2002; Fig. 3.11B), *Scipionyx* (Dal Sasso and Maganuco 2011: fig. 45) or *Velociraptor* (AMNH 6515; Fig. 3.11D). Flutes are also visible in the lateral teeth of *Coelophysis* (Buckley 2009), the dromaeosaurids *Austroraptor* (Novas et al. 2008), *Richardoestesia*, *Zapsalis* (Cope 1876*a*; Larson and Currie 2013; n.b., *Zapsalis* corresponds to '*Dromaeosaurus*' Morphotype A of Longrich 2008, ?*Dromaeosaurus* morphotype A of Sankey et al. 2002 and Sankey 2008, and Dromaeosaurinae morphotype A of Larson 2008*a*), and the pathological? *Paronychodon* (e.g., Cope 1876*b*; Baszio 1997; Hwang 2005; Sankey 2008; *Paronychodon* is interpreted as being a tooth morphotype of *Richardoestesia* by Longrich 2008). Flutes have also been noted on the apical part of the crown in *Mononykus* (Perle et al. 1994), but they represent faint parallel grooves rather than genuine flutes. The presence of fluted lateral teeth is a synapomorphy of Spinosauridae (Sereno et al. 1998).

The presence of flutes, usually on conical teeth, is common in piscivorous tetrapods such as crocodiles (Longrich 2008), pterosaurs (e.g., Kellner and Tomida 2000; Andres et al. 2010), plesiosaurs and mosasaurs (Massare 1987). Yet, longitudinal ridges bounding flutes are present in a

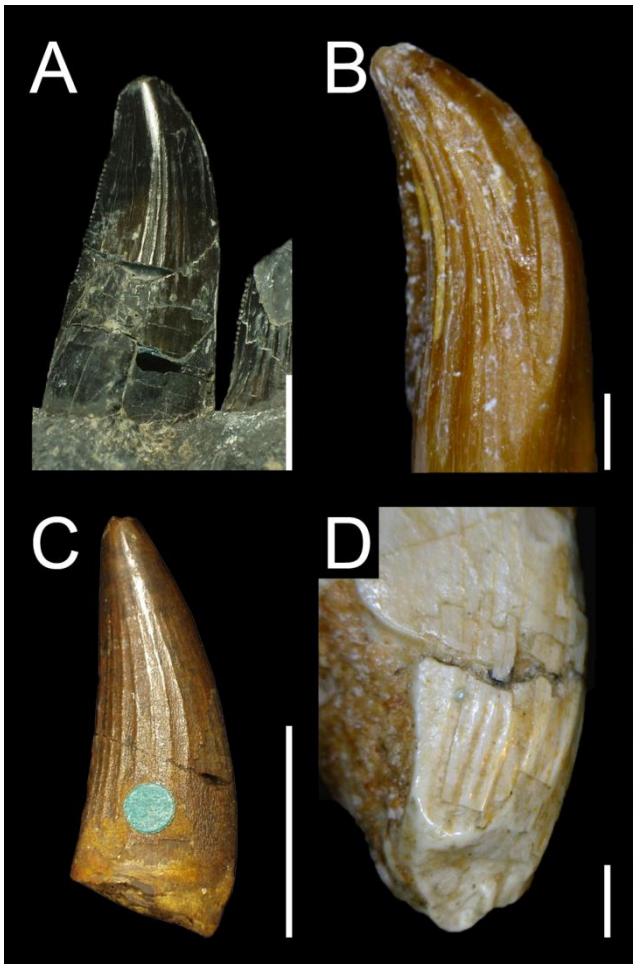

FIGURE 3.11. Fluted teeth in non-avian Theropoda. **A**, Second left dentary tooth of the ceratosaurid *Ceratosaurus nasicornis* (formerly *C. dentisulcatus*; UMNH VP 5278 = UUVP 158) in lingual view (courtesy of Roger Benson); **B**, Isolated mesialmost tooth of noasaurid *Masiakasaurus knopfleri* (FMNH PR.2696) in mesio-lingual view; **C**, Isolated tooth of the spinosaurid *Baryonyx* cf. *walkeri* (= *Suchosaurus cultridens*; NHM R.36536) in labial view; **D**, First right premaxillary tooth of the dromaeosaurid *Velociraptor mongoliensis* (AMNH 6515) in labial view. Scale bars = 1 cm (A, C), 1 mm (B, D).

large array of tooth morphologies associated with different diet in marine reptiles (Massare 1987). Plesiosauroids with very long slender cones and flutes delimited by low longitudinal ridges suggests that teeth were used to pierce soft prey, whereas the straight and robust cones with flutes delimited by prominent ridges were used for grasping prey with a hard exterior in ichthyosaurs. Likewise, the longitudinal and sharp ridge bounding each flutes of large pliosaurids are probably cutting edges used for tearing fleshy prey (Massare 1987). Therefore, the presence of flutes on the crown may have a broad and general function in animals with disparate tooth morphologies and teeth adapted to different diets. Flutes most likely have some piercing and gripping function, allowing the sharp ridges to pierce the skin and broadening the flesh as the tooth penetrates the prey body, and keeping slippery prey in the mouth (Sues et al. 2002). Fluted teeth seems to be an ontogenetic feature in *Coelophysis* as only juvenile-sized skulls display this feature (Buckley 2009). According to Buckley (2009), such ontogenetic variation may indicates different diets between juvenile and adult individuals, with young *Coelophysis* primarily eating arthropods and fish.

Sereno et al. (1998, character 18) were the first to include the presence of flutes (crown striations *sensu* Sereno et al. 1998) on phylogenetic data matrices, and this character was later incorporated in the cladistic analyses of Holtz et al. (2004, character 256.2), Benson (2010, character

93), and Carrano et al. (2012, character 142). As suggested by Hendrickx and Mateus (2014*b*, characters 59, 107, 108), flutes should be coded for both mesial and lateral dentition. Likewise, the number and distribution of flutes should be taken into consideration. Indeed, *Baryonyx*, *Ceratosaurus*, *Masiakasaurus*, and *Scipionyx* tend to have flutes restricted to one side of the crown, whereas *Suchomimus*, *Spinosaurus* and *Siamosaurus* shows flutes on both sides of the crown (pers. obs.). Likewise, the number of flutes on the crown does not exceed twelve in *Coelophysis* (1 to 8 flutes on the crown; Buckley 2009: figs. 4.3 and 4.4), *Ceratosaurus* (6 to 7 flutes in Ldt1-2 of UMNH VP 5278), *Masiakasaurus* (2 to 5), *Baryonyx* (4 to 8 in NHM R.9951, 10 in NHM R.36536 '*Suchosaurus cultridens*'), *Suchomimus* (2 to 10), *Irritator* (5-10), and *Scipionyx* (2 or 3; Dal Sasso and Maganuco 2011: fig. 45) whereas the number of flutes in some crowns of *Spinosaurus* and *Siamosaurus* can exceed 14 flutes, with up to 17 flutes in *Siamosaurus* (TF 2043), and 20 flutes in *Spinosaurus* (Lmx2 of MSNM V4047).

Transverse undulations

Transverse undulations are visible on the crown of all theropods, but transverse undulations that are numerous and cover most of the crown are present only in 'non-neocoelurosaur' Averostra. Although thought to be a possible tetanuran synapomorphy (Brusatte et al. 2007), transverse undulations (Fig. 3.12) are present in the crown of many non-avian theropods, from basal to derived forms. Indeed, they have been identified in basalmost theropods *Sanjuansaurus* (PVSJ 605; Fig. 3.12A) and *Eodromaeus* (PVSJ 561), ceratosaurids *Ceratosaurus* (USNM VP 4735), *Berberosaurus* (MNHN Pt369), *Genyodectes* (MLP 26-39), the noasaurids *Masiakasaurus* (FMNH PR.2221, 2476), and the abelisaurids *Aucasaurus* (MCF-PVPH 236) and *Majungasaurus* (FMNH PR.2278; Fig. 3.12B). As noted by Brusatte et al. (2007), transverse undulations are widespread among basal tetanurans and have been observed in the basal tetanurans *Monolophosaurus* (Brusatte et al. 2010*a*) and *Piatnitzkysaurus* (PVL 4073; MACN CH 895), the megalosaurids *Megalosaurus* (NHM R.8303; OUMNH J13505) and *Duriavenator* (NHM R.332), the spinosaurids *Baryonyx* (NHM R.9951; ML 1190) and *Irritator* (SMNS 58022), the allosauroids *Allosaurus* (AMNH 851; NHFO 455), *Neovenator* (MIWG 6348), *Sinraptor* (IVPP 10600), *Acrocanthosaurus* (NCSM 14345), and *Giganotosaurus* (MUCPv-CH-1), the tyrannosaurids *Alioramus* (IGM 100-1844; Brusatte et al. 2012*a*), *Gorgosaurus* (USNM 12814) and *Tyrannosaurus* (FMNH PR.2081), and the basal coelurosaur *Zuolong* (Choiniere et al. 2010*a*). Among 'neocoelurosaurs', they have only been identified in the deinonychosaurs *Dromaeosaurus* (Smith 2005; AMNH 5356; Appendices A4.3, Fig. A4.4F), an indeterminate velociraptorine dromaeosaurid (DMNH unknown; Fig. 3.12C) and *Troodon* (DMNH 22337; Fig. 3.12D), and may be genuinely absent in the teeth of Compsognathidae, Therizinosauria, Alvarezsauroidea, Ornithomimosauria, Oviraptorosauria, Unenlagiinae and Microraptorinae. Likewise, enamel undulations (i.e., transverse and marginal undulations) have not been observed in the teeth of any coelophysoids and basal tyrannosauroids, and these theropods may

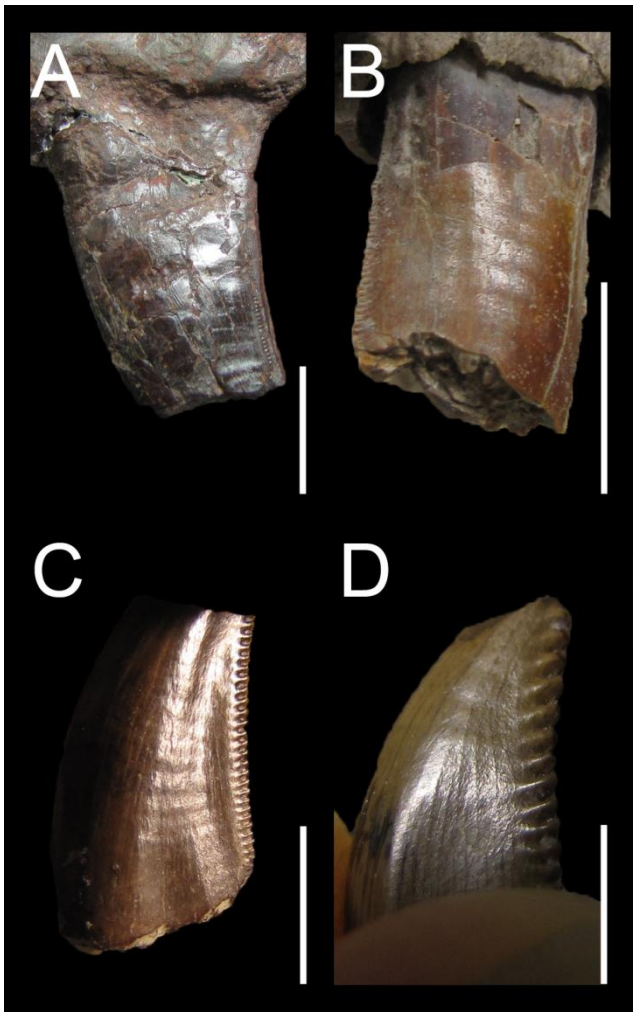

FIGURE 3.12. Transverse undulations in the teeth of most basal and most derived non-avian Theropoda. **A**, Fifth? left maxillary tooth of the herrerasaurid *Herrerasaurus ischigualastensis* (formerly *Sanjuansaurus gordilloi*, PVSJ 605) in labial view; **B**, Second left maxillary tooth of the abelisaurid *Majungasaurus crenatissimus* (FMNH PR.2278) in labiodistal view; **C**, Isolated tooth of a velociraptorine Dromaeosauridae (DMNH unknown) in labial view; **D**, Isolated tooth of the troodontid *Troodon formosus* (DMNH 22337) in labiobasal view. Scale bars = 1 cm (A–B), 5 mm (C–D).

also lack enamel undulations. Due to the wide distribution of these ornamentations in non-avian theropods, enamel undulations have to be used in conjunction with other dental features in order to assign teeth to more restricted theropod clades. Nevertheless, the presence of numerous and closely packed enamel undulations seems to be restricted to the crowns of large theropods such as Ceratosauridae, Megalosauridae, Allosauroidea and Tyrannosauroidea (pers. obs.).

Transverse undulations may have served to minimize suction when the tooth was pulled out of the flesh (Currie and Azuma 2006), to help strengthen the crown during feeding (Brusatte 2012), or may simply be a byproduct of growth (Brusatte et al. 2007). Transverse undulations in large meat-eating theropods are not necessarily homologous from those in taxa such as *Troodon* and *Dromaeosaurus*, and may differ in their development and origin. Transverse undulations are also present in many other tetrapods, including metriorhynchid crocodylomorphs (De Andrade et al. 2010) and rauisuchian crurotarsans (Brusatte et al. 2009*a*).

Marginal Undulations

Marginal undulations have been identified in 'non-neocoelurosaur' Averostra. Short and marginal undulations close to carinae are a well-known feature of carcharodontosaurid teeth (Sereno et al. 1996; Coria and Currie 2006) as they appear on the crown of *Carcharodontosaurus* (SGM Din-1; UC PV6), *Mapusaurus* (MCF-PVPH 108), *Giganotosaurus* (MUCPv-CH-1) and *Tyrannotitan* (Canale et al. 2014). However, marginal undulations (Fig. 3.13) have also been reported in the abelisaurid *Skorpiovenator* (Canale et al. 2009). In fact, they are present in a large range of non-coelurosaur avetheropods as they have been noticed in the ceratosaurs *Ceratosaurus* (USNM 4735; Fig. 3.13A), *Masiakasaurus* (FMNH PR.2182; Fig. 3.13B), *Aucasaurus* (MCF-PVPH 236), and *Majungasaurus* (FMNH 2100), but also in the megalosaurids *Afrovenator* (UC UBA1), *Megalosaurus* (NHM R.234; OUMNH J.23014) and *Torvosaurus* (ML 500; Hendrickx et al. 2014), the spinosaurids *Baryonyx* (NHM R.9951), *Suchomimus* (MNN G35-9), *Irritator* (Sues et al. 2002; Fig. 3.13C), the tyrannosaurids *Tyrannosaurus* (Brusatte et al. 2007), and many non-carcharodontosaurine allosauroids such as *Allosaurus* (USNM 8335), *Neovenator* (MIWG 6348; Fig. 3.13D) and *Acrocanthosaurus* (NCSM 14345). In most theropods, marginal undulations usually extend mesio-distally along the crown, and are typically elongated and parabolic, with the part adjacent to the carina curving apically. However, marginal undulations of some theropods can be short, broad, and mesio-distally straight, as seen adjacent to the mesial carina in *Ceratosaurus* (USNM 4735; Fig. 3.15A), *Masiakasaurus* (FMNH PR.2182; Fig. 3.13B), and *Afrovenator* (MNN UBA1). They can also be strongly diagonally-oriented, as observed in some teeth of *Masiakasaurus* (FMNH PR.2696), *Megalosaurus* (OUMNH J.23014), *Suchomimus* (MNN G51), *Irritator* (SMNS 58022; Fig. 3.13C), and an indeterminate Spinosauridae (Medeiros 2006). Numerous and extremely pronounced marginal undulation visible without orientating the tooth have only been identified in *Carcharodontosaurus saharicus* and seems indeed to be an autapomorphic feature among theropods (Brusatte and Sereno 2007). The marginal undulations of other carcharodontosaurids such as *Acrocanthosaurus*, *Mapusaurus*, *Giganotosaurus*, and *Tyrannotitan* are present, but not as pronounced and numerous as those visible in the teeth of the neotype of *Carcharodontosaurus saharicus* (Brusatte and Sereno 2007; pers. obs.). Marginal undulation is a more widespread feature than previously thought in non-avian theropods. The presence of marginal undulations is here considered to be a possible synapomorphy of Averostra. Yet, we cannot entirely dismiss the hypothesis that this feature is convergently present in several clades of theropods as it might have a particular functional role that converged after the split of the various theropod clades possessing it. Interestingly, marginal undulations are present only in large sized theropods with the exception of *Masiakasaurus.* Nevertheless, *Masiakasaurus* marginal undulations may only superficially resemble those of other clades, as they are not numerous and restricted to few mesial crowns.

The presence of marginal undulations was first included in a data matrix by Currie and Carpenter (2000, character 42) and Holtz (1998, character 131), and this character was latter adapted by Benson (2010, character 95) and Carrano et al. (2012, character 143) to distinguish marginal from

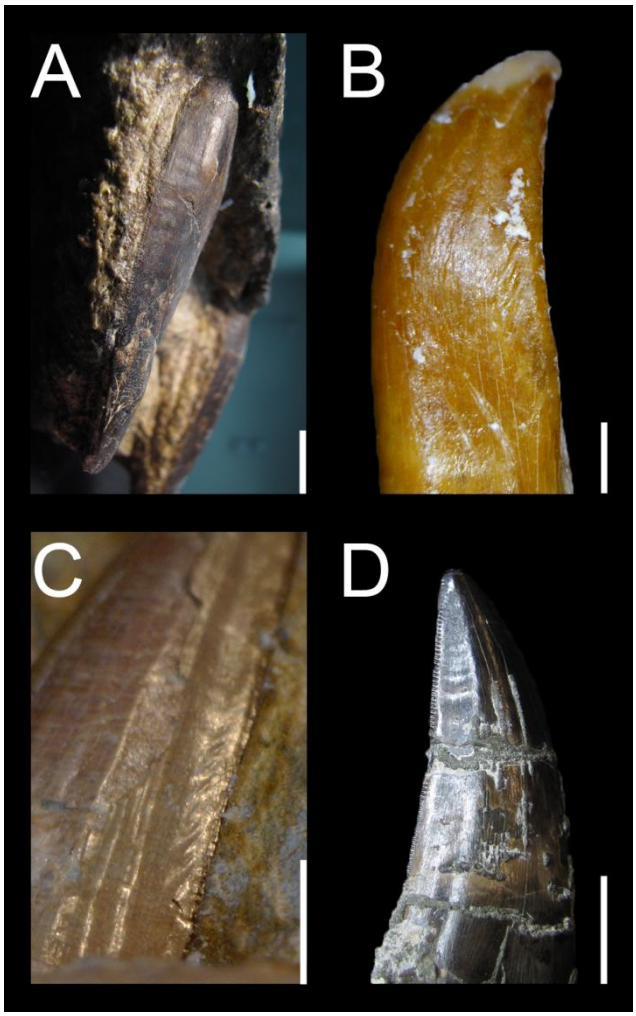

FIGURE 3.13. Marginal undulations in the teeth of non-avian Theropoda. **A**, Fourth left maxillary tooth of the ceratosaurid *Ceratosaurus nasicornis* (USNM 4735) in mesial view; **B**, Second left maxillary tooth of the abelisaurid *Majungasaurus crenatissimus* (FMNH PR.2278) in labiodistal view; **C**, Mesial carina of a left maxillary tooth of the spinosaurid *Irritator challengeri* (SMNS 58022) in mesiolabial view; **D**, Isolated crown of the neovenatorid *Neovenator salerii* (MIWG 6348) in lingual view. Scale bars = 1 cm (A, D), 5 mm (C), 1 mm (B).

transverse undulations. Hendrickx and Mateus (2014a, characters 109-114) proposed that transverse and marginal undulations should be considered separately as one single tooth can display both types of wrinkles (e.g., OUMNH J.23014; NCSM 14345). Likewise, characters on the distribution (present on the labial, lingual side, adjacent to the mesial, distal carina), orientation (mesio-distally elongated, diagonally oriented), abundance (few or numerous along the crown) and visibility (tenuous, very well-visible) for both transverse and marginal undulations should be provided. Carrano et al. (2012) identified pronounced marginal undulations (char. 143.2) only in carcharodontosaurid taxa, yet this feature should also be coded in ceratosaurs, megalosaurids, spinosaurids, allosaurids, and neovenatorids. Additionally, Carrano et al. (2012, character 143.1), Choiniere et al. (2014*b*, character 239), and Godefroit et al. (2013*a*, character 812) observed transverse undulations in *Zuolong*, tyrannosaurids and all non-coelurosaur tetanurans other than spinosaurids, but we also identified this type of enamel undulations in herrerasaurids, ceratosaurids, abelisaurids, and some deinonychosaurs. Carrano et al. (2012) did not code any carcharodontosaurine taxa with transverse undulations, yet they have been identified on the teeth of some Carcharodontosaurinae such as *Giganotosaurus* (MUCPv-CH1) and *Carcharodontosaurus* (BSPG 1993 IX 328; SMA 380).

Interdenticular Sulci

Interdenticular sulci are present in 'non-neocoelurosaur' Averostra and Dromaeosaurinae. Thought to be restricted to Tyrannosauroidea and Allosauroidea ('Carnosauria' of Gauthier 1986 and Rauhut and Kriwet 1994), interdenticular sulci (Fig. 3.14) occurs in many other clades. Strongly developed and elongated sulci have been observed in the abelisaurids *Kryptops palaios* (MNN GAD1−1) and *Majungasaurus crenatissimus* (FMNH PR.2100, 2278; Fig. 3.14A), the megalosauroids *Piatnitzkysaurus floresi* (PVL 4073), *Megalosaurus bucklandi* (OUMNH J13506; Fig. 3.14B) and *Torvosaurus gurneyi* (Hendrickx and Mateus 2014*a*), the allosauroids *Allosaurus* sp. (ML 1935), *Fukuiraptor kitadaniensis* (Azuma and Currie 2000), *Sinraptor dongi* (IVPP 10600), *Giganotosaurus carolinii* (MUCPv-CH-1; Fig. 3.14C) and *Mapusaurus roseae* (MCF-PVPH-108), and the tyrannosaurid *Tyrannosaurus rex* (FMNH PR.2081; Fig. 3.14D). Short interdenticular sulci are widespread among 'non-neocoelurosaur' Averostra as they have been noticed in almost all ceratosaurids, megalosaurids, allosauroids and tyrannosauroids (e.g., Hendrickx et al. in press*a;* Currie et al. 1990; Azuma and Currie 2000; Fanti and Therrien 2007; Hendrickx and Mateus 2014*b*). In 'neocoelurosaurs', they have also been observed in the dromaeosaurid *Saurornitholestes* (Currie et al. 1990) and *Dromaeosaurus* (AMNH 5356; Currie et al. 1990; Larson 2008*a*), as well as troodontids (Currie and Dong 2001b; Sankey 2008: fig. 3.13). Interdenticular sulci seem to be absent in noasaurids, spinosaurids, several abelisaurids such as *Rugops* (MNN IGU1), *Aucasaurus* (MCF-PVPH 236) and *Skorpiovenator* (MMCH-PV 48), the carcharodontosaurid *Acrocanthosaurus* (NCSM 14345; SMU 73417), and non-deinonychosaur 'neocoelurosaurs'. The presence of interdenticular sulci is considered to be the apomorphic character for Averostra.

Interdenticular sulci have been noticed in several theropods by many authors (Currie et al. 1990; Abler 1992; Buscalioni et al. 1997; Smith 2007; Benson 2009), but none provided functional implications of these structures. Interdenticular sulci may play several roles such as hosting septic bacteria for an infectious bite, helping the entry of venom in a possible venomous theropod, distributing stresses from the base of the denticle, or preventing suction when the crown was pulled out of the flesh. The first hypothesis was proposed by Abler (1997, 1999) for the deep interdenticular space ('cella' *sensu* Abler 1992, 1999) existing in between tyrannosaurids denticles. These interdenticular spaces would trap grease and food debris that functioned as receptacles for septic bacteria, becoming the source of a lethal infection when biting. The second hypothesis is here proposed because the venomous Komodo dragon possesses interdenticular sulci on the teeth (D'Amore and Blumenschine 2009), representing a rare example of an extant animal showing these sulci. The teeth of the Komodo dragon do not have any venom delivering system such as grooves along its crown or within a hollow tooth, like snakes and helodermatid lizards (Fry et al. 2009). On the other hand, the crown of this varanid is smooth and lacks any dental features besides short interdenticular sulci, so that the venom seems to enter via deep wounds when lacerating the prey items

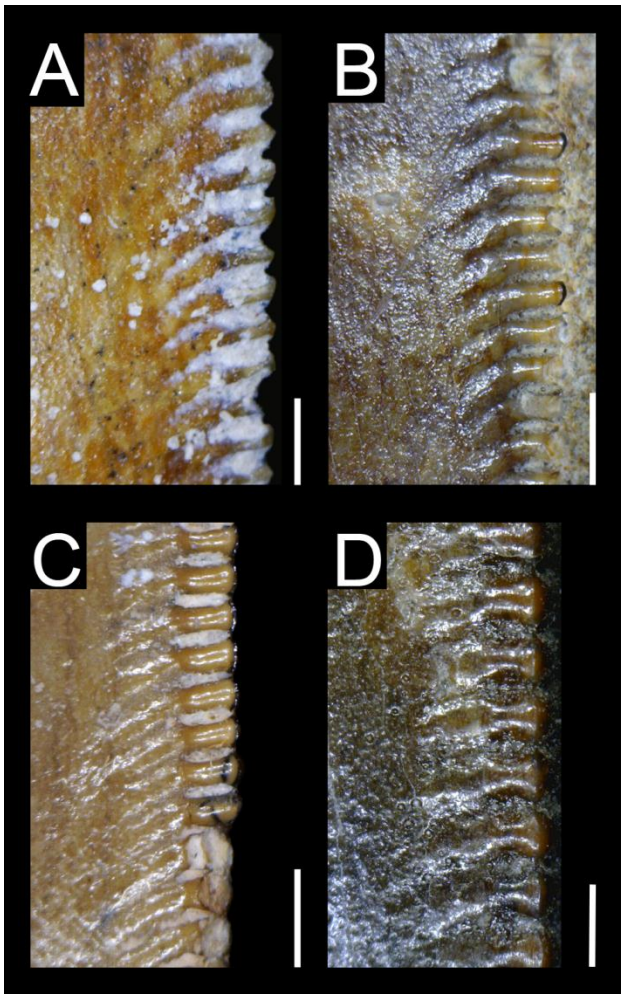

FIGURE 3.14. Well-developed interdenticular sulci in non-avian Theropoda. **A**, Distal carina of sixth right maxillary tooth of the abelisaurid *Majungasaurus crenatissimus* (FMNH PR.2278) in lateral view; **B**, Distal carina of an isolated tooth of the megalosaurid *Megalosaurus bucklandi* (NHM R.234) in labial view; **C**, Distal carina of an isolated tooth of the carcharodontosaurid *Giganotosaurus carolinii* (MUCPv CH1 L2) in lateral view; **D**, Distal carina of the fifth maxillary tooth of the tyrannosaurid *Tyrannosaurus rex* (FMNH PR.2081) in lateral view. Scale bars = 1 mm.

(Fry et al. 2009). Therefore, interdenticular sulci of *Varanus komodensis* and theropods may help venom to be administrated during biting. Nevertheless, the interdenticular sulci may also serve as stress-distributing structures as they re-orient the stresses at the base of the denticle towards the middle of the crown, thus preserving the integrity of the denticle under high stress regimes. Contrasting with the disparate distribution of hooked denticles among different theropod clades, interdenticular sulci are very similar, possibly homologous, in Ceratosauridae, Megalosauroidea, Allosauroidea, and Tyrannosauroidea. This condition favors the idea that interdenticular sulci are stress-dissipation or suction reduction structures, rather than specialized infectious or venomous delivery systems.

The presence of interdenticular sulci was first included in a character state by Makovicky and Sues (1998). Yet, it was used as a separate character by Benson (2010, character 90) and later incorporated in the data matrices of Godefroit et al. (2013*a*, character 720) and Hendrickx and Mateus (2014*b*, characters 104–106). Hendrickx and Mateus (2014*b*) proposed that interdenticular sulci should be coded for both mesial and distal carinae, as these structures are only present on the mesial carina for a few theropod taxa such as *Kryptops*, *Majungasaurus*, *Megalosaurus*, *Torvosaurus*, carcharodontosaurines, and *Tyrannosaurus*. Interdenticular sulci should also be coded as poorly or well-developed. Benson (2010*a*) identified the presence of interdenticular sulci in all non-coelurosaur

theropods other than *Dilophosaurus*, spinosaurids, some megalosaurids (*Magnosaurus*, *Eustreptospondylus*, *Duriavenator*), *Condorraptor*, and *Neovenator*. We, however, identified short interdenticular sulci in the teeth of all megalosaurids (Hendrickx et al. in press*a*) and *Neovenator*, and they are also possibly present in *Condorraptor*.

Longitudinal Ridges, Grooves and Basal Striations

Longitudinal ridges and/or grooves can be identified in Allosauroidea, Abelisauridae, and Tyrannosauroidea for mesial teeth, and Therizinosauria and Deinonychosauria for lateral teeth. A longitudinal ridge (Fig. 3.15) centrally-positioned on the lingual surface of the crowns and delimited by two concave surfaces is typical of mesial teeth of Tyrannosauroidea (Carr and Williamson 2004). Indeed, this feature has been observed in the tyrannosauroids *Xiongguanlong* (Li et al. 2010), *Raptorex* (Sereno et al. 2009; Fig. 3.15B), *Daspletosaurus* (Lehman and Carpenter 1990), *Albertosaurus* (Carr and Williamson 2004), *Gorgosaurus* (Cillari 2010) and *Tyrannosaurus* (Smith 2005). A discrete ridge is also seen on the lingual side of the first two premaxillary teeth in the basal tyrannosauroids *Dilong* and *Guanlong* (Sereno et al. 2009). This median ridge is absent in *Proceratosaurus* and *Eotyrannus* (pers. obs.). A prominent median ridge seems also to be present on the lingual surface of some maxillary crowns in the troodontid *Xixiasaurus* (Lü et al. 2010: fig. 3A1). Two longitudinal ridges delimiting the lingual depression are also observable on the lingual surface of some *Allosaurus* premaxillary teeth (UMNH VP 1251), and some lateral teeth of *Orkoraptor* (Novas et al. 2008; Fig. 3.15A). One, two or several longitudinal ridges delimiting grooves of irregular width and orientation are present on the crowns of the basal therizinosaur *Falcarius* (Zanno 2010*b*) and many deinonychosaurs. In dromaeosaurids, they have been noticed in *Buitreraptor* (Gianechini et al. 2011b; MPCA 245), *Velociraptor* (AMNH 6515), *Bambiraptor* (AMNH 30556; Fig. 3.15C), *Zapsalis* (Larson 2008*a*; Longrich 2008; Larson and Currie 2013), *Richardoestesia* (Longrich 2008; Sankey 2008), *Saurornitholestes* (Baszio 1997; Sankey 2008) and *Acheroraptor* (Evans et al. 2013; Fig. 3.15D). They are also present in some troodontids such as *Troodon* (Currie 1987: fig. 5S; Sankey 2008), cf. *Pectinodon* (Sankey 2008; Larson and Currie 2013), and the tooth-based taxa *Euronychodon* (Antunes and Sigogneau-Russell 1991) and *Paronychodon* (Currie et al. 1990; Zinke and Rauhut 1994; Baszio 1997; Larson 2008*a*; Sankey 2008). Faint longitudinal ridges delimiting shallow and narrow grooves are also present on the largest ziphodont crowns of the lateral dentition in *Byronosaurus* (Makovicky et al. 2003; pers. obs.).

Prominent ridges delimiting deep grooves are present on the crown of the possible venomous *Varanus* (*Megalania*) *priscus* (Fry et al. 2009: fig. 3) which also possesses a ziphodont dentition. These ridges are similar to those observed in *Velociraptor*, *Bambiraptor* and *Buitreraptor* which delimit the labial depression along the crown. These structures may have helped venom to enter in the prey flesh. Other authors have proposed that the labial and lingual depressions in the lateral dentition of *Sinornithosaurus* were related to venom delivering (Gong et al. 2010, 2011). The dentition of the

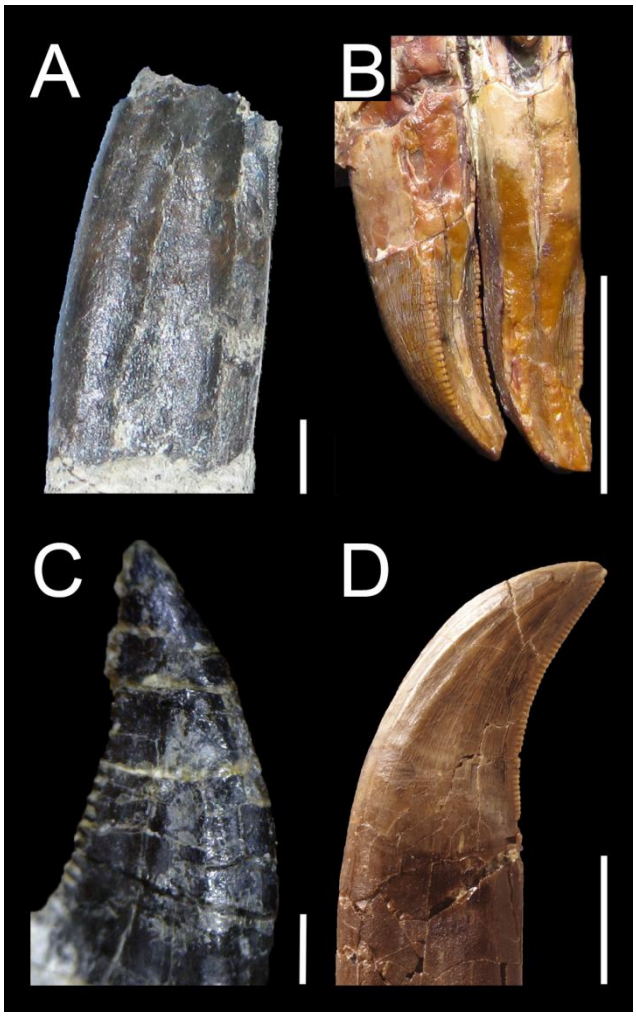

FIGURE 3.15. Longitudinal ridges in the teeth of non-avian Theropoda. **A**, Isolated tooth of the metriacanthosaurid *Orkoraptor* burkei (MPM-Pv 3458) in lateral view (courtesy of Martín Ezcurra); **B**, Third and fourth premaxillary teeth of the tyrannosaurid *Raptorex kriegsteini* (LH PV18) in labial view; **C**, Fifth left maxillary tooth of the dromaeosaurid *Bambiraptor feinbergi* (AMNH 30556) in labial view; **D**, Second? maxillary tooth of the dromaeosaurid *Acheroraptor temertyorum* (ROM 63777) in labial view (courtesy of Derek Larson). Scale bars = 1 cm (A–B, D), 1 mm (C).

possible venomous *Varanus priscus* is, to our knowledge, the closest analogue to the dromaeosaurid condition in terms of tooth type (i.e., ziphodont), denticle morphology and crown ornamentation (i.e., longitudinal ridges/grooves). Based solely on the fact that *Varanus* and some dromaeosaurids show some morphological convergence (and not any other anatomical features proposed by Gong et al. (2010, 2011) such as a 'subfenestral fossa' housing an ascinar venom gland), it is plausible that some theropods may had been venomous animals. For a different opinion, see Gianechini et al. (2011a). According to Gianechini et al. (2011b), the grooved teeth present in Unenlagiinae may indicate a fish-eating behavior among these dromaeosaurids that inhabited the proximity of fluvial deposits. However, the teeth of piscivorous tetrapods such as crocodiles, marine reptiles, pterosaurs, and spinosaurids are fluted and do not possess wide longitudinal grooves bounded by one or two poorly delimited ridges. Based on the tooth morphology, a piscivorous lifestyle of dromaeosaurid theropods, although evidenced in *Microraptor* (Xing et al. 2013*a*), is, therefore, poorly supported for Unenlagiinae. The longitudinal ridges in dromaeosaurids seem to be a genuine diagnostic feature (Evans et al. 2013) that is apomorphic for Dromaeosauridae.

The presence of longitudinal grooves on the crown, that differ from lingual/labial depressions, flutes, and concave surfaces, is poorly documented in theropods and may suggest the scarcity of this feature among these dinosaurs. A longitudinal groove on the mesiolingual surface of the crown has only been noted in the lateral tooth of an abelisaurid (Hendrickx and Mateus 2014*b*). A distinct groove in the vicinity of the mesial carina is also seen on the lingual surface of mesial teeth in the dromaeosaurid *Sinornithosaurus* (Xu and Wu 2001) and the lateral crowns of an indeterminate troodontid (Averianov and Sues 2007). Longitudinal grooves have been observed on the crowns of *Byronosaurus* (Makovicky et al. 2003), *Buitreraptor* and *Austroraptor* by Gianechini et al. (2011b), yet they result from the longitudinal ridges delimiting them, and we only consider the presence of ridges in these three deinonychosaurs. Although longitudinal grooves have not been observed in the 73 theropod taxa examined first hand, this feature should be present in many more clades, and a deeper investigation on the presence of longitudinal grooves in theropod teeth is necessary. Presence of longitudinal grooves (striations *sensu* Gianechini et al. 2011b) was first included in a data matrix by Gianechini et al. (2011b) who coded this feature in *Mononykus*, *Austroraptor*, and *Buitreraptor*. Nevertheless, the crown of *Austroraptor* and *Mononykus* have been described as fluted by Novas et al. (2009) and Perle et al. (1994), and the grooves and ridges are very subtle and only restricted to the crown apex in *Mononykus*. If the presence of one or several ridges are instead considered, then this feature should be coded in *Buitreraptor* along with other deinonychosaurs such as *Velociraptor*, *Bambiraptor*, *Acheroraptor*, *Byronosaurus* and *Troodon*.

Basal striations, forming short parallel grooves extending apicobasally on the crown base, have been noticed in some herrerasaurid mesial and lateral teeth as well as *Proceratosaurus* mesial dentition (Rauhut et al. 2010). In the herrerasaurids *Herrerasaurus* (PVSJ 407) and *Ischisaurus* (MACN 18.060), which may represent the same taxon (Novas 1992), they are numerous and closely packed, whereas in *Proceratosaurus*, they form wide longitudinal depressions (Rauhut et al. 2010). Apicobasally oriented striations at the base of the crown have also been noted for Spinosauridae by Mateus et al. (2011), but these basal striations could not be observed in any spinosaurid examined first hand.

A median ridge on the lingual surface of premaxillary teeth was first proposed as a character by Holtz et al. (2004, character 260), and later used by several authors (e.g., Sereno et al. 2009, character 60; Brusatte et al. 2010*d*, character 198; Godefroit al. 2013a, character 600). Brusatte et al. (2010*a*) identified this structure in all tyrannosauroids, coding this feature as subtle in proceratosaurids, and pronounced in other tyrannosauroids, including *Eotyrannus*. However, our observations do not follow some of these conclusions. The presence of one or several ridges extending diagonally or parallel to the crown margins on the labial and/or lingual surface of the crown is a possible synapomorphy of Deinonychosauria. Among Tyrannosauroidea, a median longitudinal ridge on the lingual surface of mesial teeth is a synapomorphy of a clade encompassing *Xiongguanlong* and

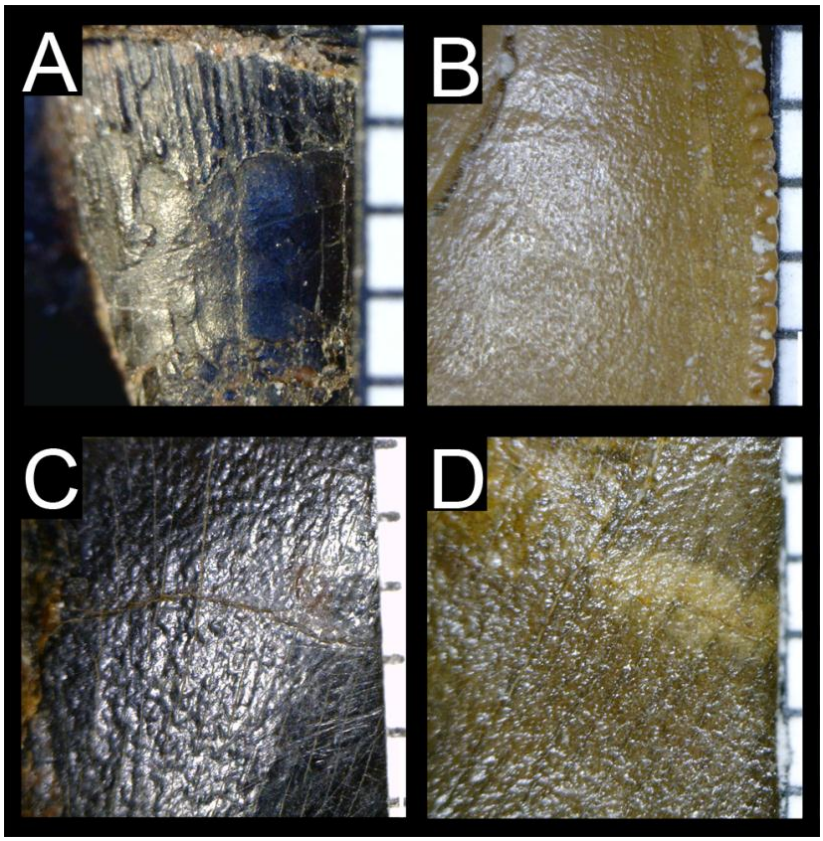

FIGURE 3.16. Irregular enamel texture of non-avian Theropoda. **A**, Tenth left maxillary tooth of the non-neotheropod theropod *Herrerasaurus ischigualastensis* (PVSJ 407) in labial view; **B**, Isolated tooth of the abelisaurid *Aucasaurus garridoi* (MCF-PVPH-236) in lateral view; **C**, Second premaxillary tooth of the allosaurid *Allosaurus* '*jimmadseni*' (NHFO 455) in labial view; **D**, Tenth maxillary tooth of the tyrannosaurid *Tyrannosaurus rex* (FMNH PR.2081) in labial view.

more derived tyrannosauroids. Indeed, this feature seem to be absent in more primitive tyrannosauroids such as *Proceratosaurus*, *Guanlong* and *Eotyrannus* (pers. obs.).

Irregular Texture

Except in Spinosauridae, the crown texture is rarely detailed in the theropod literature and we, therefore, rely on our own observations to investigate the distribution of this feature among non-avian theropods. An irregular non-oriented texture of the enamel (Fig. 3.16) is present in most non-tetanuran theropods, including *Eoraptor* (PVSJ 512), *Herrerasaurus* (PVSJ 407; Fig. 3.16A), *Ischisaurus* (MACN 18.060) and most abelisauroids (e.g., *Noasaurus*, *Abelisaurus*, *Kryptops*, *Majungasaurus*, *Aucasaurus*; Fig. 3.16B). An irregular texture has also been observed in most 'neocoelurosaurs' such as *Compsognathus* (MNHN CNJ 79), *Ornitholestes* (AMNH FARB 619), *Byronosaurus* (IGM 100-983), *Troodon* (DMNH 22337; 22837), *Buitreraptor* (MPCA 245), *Velociraptor* (AMNH 6515), *Tsaagan* (IGM 100-1015), *Saurornitholestes* (DMNH 22870) and the lateral dentition of *Dromaeosaurus* (AMNH 5356). Among 'non-neocoelurosaur' tetanurans, an irregular texture of the enamel is also seen in *Erectopus* (MNHN 2001-4) and *Irritator* (SMNS 58022), and based on our observation, the latter does not display the deeply veined texture of other spinosaurids (we could not identify the granular texture observed by Sues et al. 2002 in any maxillary tooth). The irregular texture is present in some Tyrannosauridae such as *Tyrannosaurus* (FMNH PR.2081; Fig. 3.16D), *Albertosaurus* (DMNH 22019) and *Daspletosaurus* (NHM R.4863). This pattern of the enamel texture

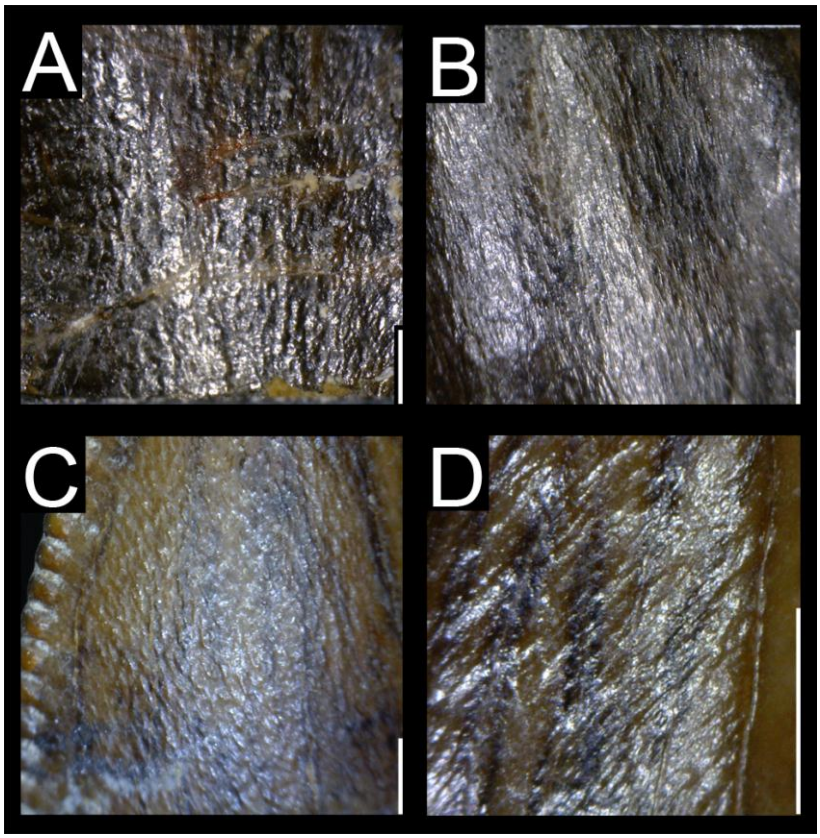

FIGURE 3.17. Braided enamel texture of non-avian Theropoda. **A**, Isolated tooth of the basal ceratosaur *Berberosaurus liassicus* (MNHN To 339) in lateral view; **B**, Isolated tooth of the neovenatorid *Neovenator salerii* (MIWG 6348) in lateral view; **C**, Fourteenth dentary tooth of the tyrannosaurid *Gorgosaurus libratus* (USNM 12814) in lateral view; **D**, Isolated premaxillary tooth of the dromaeosaurid *Dromaeosaurus albertensis* (AMNH 5356) in lingual view. Scale bars = 1 mm.

has also been identified in some *Allosaurus* teeth (NHFO 455; Fig. 3.16C), the other crowns displaying a more oriented texture. In fact, *Allosaurus* shows a transitional feature from non-averostran theropods with oriented texture and basal coelurosaurs with non-oriented texture. Enamel texture was first used as a dental character by Hendrickx and Mateus (2014*b*, characters 117, 118). Other features such as the differentiation between irregular, braided, and veined texture, as well as the orientation of the texture adjacent to carinae bear important phylogenetic signal and should be incorporated in phylogenetic analyses too (see below).

Braided Texture

Braided texture of the enamel, defined by alternating and interweaving grooves and sinuous ridges baso-apically oriented on the crown and never convergent (Hendrickx et al. in press*c*; Fig. 3.17), is present in 'non-neocoelurosaur' Neotheropoda, and can be observed in non- spinosaurid Megalosauroidea (e.g., *Piatnitzkysaurus*, *Eustreptospondylus*, *Afrovenator*, *Dubreuillosaurus*, *Duriavenator*, *Megalosaurus*, *Torvosaurus*), Allosauroidea (e.g., *Allosaurus*, *Acrocanthosaurus*, *Eocarcharia*, *Carcharodontosaurus*, *Giganotosaurus*, *Mapusaurus*, *Neovenator*; Fig. 3.17B), Tyrannosauroidea (e.g., *Proceratosaurus*, *Eotyrannus*, *Raptorex*, *Alioramus*, *Gorgosaurus*; Fig. 3.17C), and the basal coelurosaur *Bicentenaria* (MPCA 866). Such texture is also present, but less-pronounced, in the coelophysoid *Coelophysis* (CMNH 81765) and basal Ceratosauria (*Ceratosaurus*, *Genyodectes*, *Berberosaurus*; Fig. 3.17A). An oriented texture has also been identified in the basal

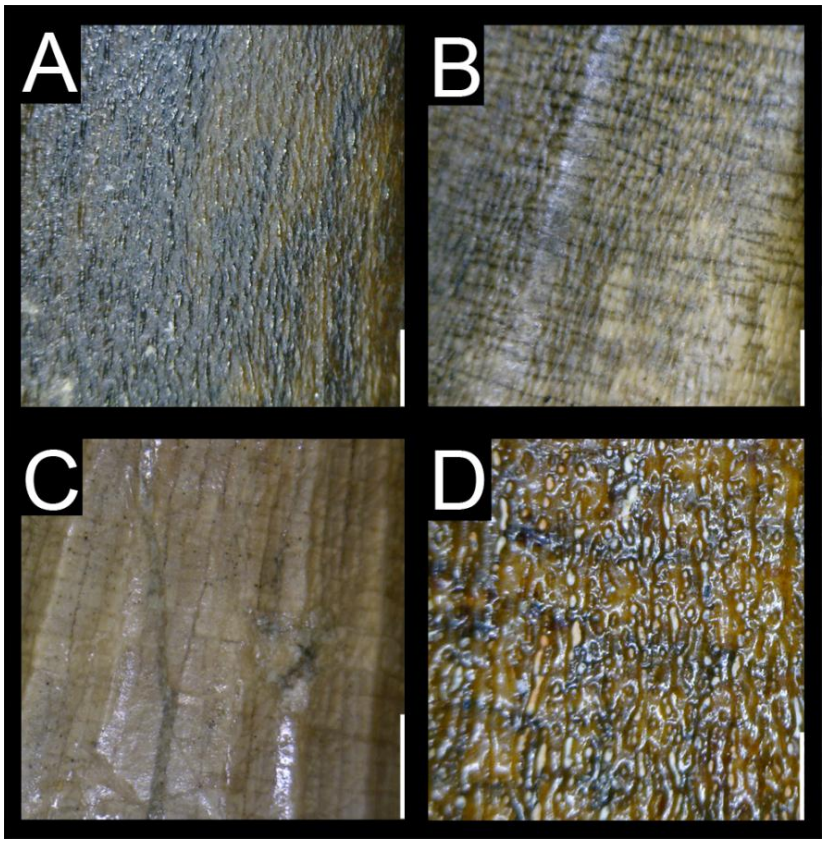

FIGURE 3.18. Enamel texture of spinosaurid teeth. **A**, Veined enamel texture of an isolated tooth of the baryonychine *Baryonyx walkeri* (NHM R.9951 278) in lateral view; **B**, Veined enamel texture of an isolated tooth of the baryonychine *Suchomimus tenerensis* (MNN G43–4) in lateral view; **C**, Smooth enamel texture of a maxillary tooth of the spinosaurine *Irritator challengeri* (SMNS 58022) in lateral view; **D**, Anastomosed enamel texture of an isolated tooth of the spinosaurine *Spinosaurus aegyptiacus* (MSNM V6422) in lateral view. Scale bars = 1 mm.

theropod *Eodromaeus* (PVSJ 561), the basal tetanuran *Sinosaurus* (the 'longitudinal striations in the enamel' of Xing 2012), the dromaeosaurid *Bambiraptor* (AMNH 30556), and some mesial teeth of *Masiakasaurus* (FMNH PR.2182, 2471) and *Dromaeosaurus* (AMNH 5356; Fig. 3.17D).

Veined and Anastomosed Texture

Veined and anastomosed texture characterize spinosaurid teeth. A veined texture of the enamel is made of oriented enamel texture made of deep alternating grooves and long sinuous and/or dichotomized ridges obliquely or baso-apically oriented and converging baso-mesially or baso-distally on the crown (Hendrickx et al. in press*c*), is present in the baryonychines *Baryonyx walkeri* (NHM R.9951; ML 1190; Fig. 3.18A**)** and *Suchomimus tenerensis* (e.g., MNN G35-9, G43-9, G73-73; Fig. 3.18B**)**, and the spinosaurine *Spinosaurus aegyptiacus* (Hasegawa et al. 2010; MNHN MRS 478). Although noted by Sues et al. (2002), the enamel texture of the spinosaurine *Irritator challengeri* is smooth or display an irregular pattern (Fig. 3.18C). An anastomosed enamel texture, which consists of multiple ridges dividing and reconnecting in an irregular way, is also present in *Spinosaurus aegyptiacus* (MSNM V4047, V6422; MNHN MRS 548; Fig. 3.18D). Such pattern of the enamel texture has only been observed in this taxon and may correspond to an autapomorphy of *Spinosaurus*. Veined and anastomosed enamel textures are characterized by their strong basal curvature adjacent to the carinae (Hasegawa et al. 2010; Mateus et al. 2011), a feature that is not present in theropods with a braided enamel texture of the crown (pers. obs.).

Procumbent Teeth

Procumbent teeth, especially for mesial dentary teeth, are widely distributed among theropods. Yet, procumbent mesial maxillary teeth seem to be restricted to Coelophysoidea, basal Tetanurae, Spinosauridae and Compsognathidae. Procumbent teeth are visible in the premaxilla of the basal theropod *Daemonosaurus* (Sues et al. 2011), the oviraptorosaur *Caudipteryx* (Ji et al. 1998; Zhou et al. 2000), and the scansoriopterygid *Epidexipteryx* (Zhang et al. 2008), and to a lesser degree in the coelophysoid *Dracovenator* (Yates 2005). Teeth facing anterolaterally are also seen in the mesial maxillary teeth of all Coelophysoidea such as *Coelophysis* (Colbert 1989), *Megapnosaurus* (Rowe 1989), *Zupaysaurus* (Ezcurra 2007) and *Dilophosaurus* (Welles 1984), the basal tetanuran *Sinosaurus* (ZLJ 0003), and all Spinosauridae (Charig and Milner 1997; Sereno et al. 1998; Taquet and Russell 1998; Dal Sasso et al. 2005) which possess a sigmoid alveolar margin of the upper jaw. A procumbent crown has also been noted in the first maxillary tooth in the compsognathid *Scipionyx* (Dal Sasso and Maganuco 2011), and *Masiakasaurus* (Tykoski 2005). However, the first maxillary alveolus is partially missing in *Masiakasaurus* so that it is not possible to determine whether the first maxillary tooth was procumbent or not (pers. obs.).

Lateral teeth facing anterolaterally have only been observed in the maxilla of the basal ornithomimosaur *Nqwebasaurus* (Choiniere et al. 2012) and *Epidexipteryx* (Zhang et al. 2008), although the anterior inclination of teeth in *Nqwebasaurus* may be due to diagnenetic factor (Choiniere et al. 2012). Procumbent teeth are seen in the anteriormost part of the dentary of the noasaurid *Masiakasaurus* (Carrano et al. 2002), the tyrannosauroid *Proceratosaurus* (Rauhut et al. 2010), the ornithomimosaur *Shenzhousaurus* (Ji et al. 2003) and the scansoriopterygid *Epidexipteryx* (Zhang et al. 2008). Procumbent dentary teeth also exist, yet to a lesser degree, in the basal theropod *Herrerasaurus* (Sereno and Novas 1994), the megalosaurid *Duriavenator* (Benson 2008*a*), the tyrannosaurids *Albertosaurus* and *Tyrannosaurus* (Carr and Williamson 2004), the basal maniraptoriform *Ornitholestes* (AMNH 619), the alvarezsauroid *Haplocheirus* (Choiniere et al. 2010*b*), the basal oviraptorosaur *Incisivosaurus* (Balanoff et al. 2009) and the dromaeosaurids *Sinornithosaurus* (Xu and Wu 2001) and *Microraptor* (Xing et al. 2013*a*).

Procumbent mesial teeth is common in piscivorous animals including crocodiles, fish, and pterosaurs (Xing et al. 2013*a*). Indeed, a forward-projecting mesial tooth arrangement seems to be adapted in the prehension of small prey such as invertebrates and small vertebrates as fish (Carrano et al. 2002). In coelophysoids and spinosaurids, procumbent maxillary teeth result from the sigmoid ventral margin of the maxilla and are suitable for gripping small to moderate-sized prey transversally through slashing bites (Charig and Milner 1997; Therrien et al. 2005). The sigmoid margin of the upper jaw, present in many crocodylomorphs, would also have enhanced the ability for holding prey and/or tearing their flesh (Russell and Wu 1997). In ornithomimosaurs with anteriorly inclined teeth like *Nqwebasaurus*, and *Shenzhousaurus*, in which a herbivorous diet has been inferred (Makovicky et

al. 2004; Zanno and Makovicky 2011; Choiniere et al. 2012), procumbency is most likely adapted in the prehension of vegetation, perhaps for branch raking/stripping as suggested for other saurischians like *Diplodocus* (e.g., Barrett and Upchurch 1994; Upchurch and Barrett 2000). The procumbency existing in ornithomimosaurs and other maniraptoriforms may also result from a trophic shift from carnivory to herbivory (Zanno and Makovicky 2011; Choiniere et al. 2012).

Procumbent teeth was first included in a data matrix by Tykoski and Rowe (2004, character 15; based on Rowe 1989). As proposed by Choiniere et al. (2014*b*, character 215, 221, 235), procumbent teeth should be coded separately for each tooth bearing bone. Among coelurosaurs, procumbent premaxillary teeth were coded in *Caudipteryx*, *Epidexipteryx* and *Ornitholestes* by Choiniere et al. (2014*b*), but we interpret the anteroventral inclination of premaxillary teeth in *Ornitholestes* as a taphonomic deformation. As for procumbent teeth that points anteriorly, posteroventrally inclined teeth is also seen in theropods. Firstly proposed as a character by Currie and Varricchio (2004, character 40), ventrally-inclined maxillary teeth have been recorded in the troodontid *Sinovenator*, the dromaeosaurids *Deinonychus*, *Bambiraptor*, *Atrociraptor* (Turner et al. 2012, character 248; and not *Epidexipteryx*, *contra* Turner et al. 2012, as the teeth are inclined anteroventrally), and an undescribed dromaeosaurid (UC uncatalogued) from the Ulansuhai Formation of Inner Mongolia (Varricchio et al. 2008*b*).

Edentulous Jaws

Edentulous portion of the jaws and toothless taxa are restricted to *Limusaurus* and Maniraptoriformes. Among toothed theropods, edentulous premaxillae are shared by Therizinosauroidea such as *Erlikosaurus* (Clark et al. 1994) and *Jianchangosaurus* (Pu et al. 2013). Edentulous premaxillae and maxillae combined with toothed dentaries are seen in the primitive ornithomimosaurs *Shenzhousaurus* (Ji et al. 2003), *Harpymimus* (Kobayashi and Barsbold 2005*a*) and *Hexing* (Liyong et al. 2012), which all bear teeth restricted to the anterior part of the dentary. Toothed premaxillae with edentulous maxillae and dentaries characterized the basal oviraptorosaurs *Caudipteryx* (Ji et al. 1998; Zhou et al. 2000) and *Avimimus* (Watabe et al. 2000; Tsuihiji et al. 2008), in which the teeth are present in the anterior part of the premaxilla. Absence of teeth in the anterior part of a dentulous dentary has been recorded in therizinosaurs (*Erlikosaurus*, *Jianchangosaurus*, *Neimongosaurus*) and primitive oviraptorosaurs (*Incisivosaurus*, *Protarchaeopteryx*). Toothless non-avian theropods are restricted to three clades, namely Ceratosauria with the basal form *Limusaurus* (Xu et al. 2009*a*), Ornithomimosauria with all members of the clade including *Garudimimus* and Ornithomimidae (Kobayashi and Barsbold 2005*a*; Makovicky et al. 2010), and Oviraptorosauria with all caenagnathoids (Caenagnathidae + Oviraptoridae, *sensu* Longrich et al. (Longrich et al. 2013) and Lamanna et al. 2014). Toothless jaws may result from heterochronic mechanisms as the timing of ossification of the dentary, premaxilla and maxilla is different from the formation of the teeth, as observed in crocodilians. The absence or presence of teeth was first proposed as a character by

Cracraft (1986, character 2) in one of the first cladistic analysis performed on dinosaurs. Since then, the absence of teeth in the premaxilla, maxilla, and dentary is commonly included in phylogenetic analysis performed on theropods. Presence or absence of teeth should be coded for the whole maxilla, as well as the anterior and posterior portions of the premaxilla and dentary. As for palatal teeth, this feature has only been retained by the possible theropod *Eoraptor* (Sereno et al. 2013) and the non-neotheropod theropod *Eodromaeus* (Martinez et al. 2011) among all whole clade of Dinosauria.

Chapter 4: Abelisauridae (Dinosauria: Theropoda) from the Late Jurassic of Portugal and dentition-based phylogeny as a contribution for the identification of isolated theropod teeth

Published in ***Zootaxa*** (IP 1.06):
Hendrickx, C. and Mateus, O. 2014. Abelisauridae (Dinosauria: Theropoda) from the Late Jurassic of Portugal and dentition-based phylogeny as a contribution for the identification of isolated theropod teeth. *Zootaxa* 3759 (1): 1–74.

Abstract

Theropod dinosaurs form a highly diversified clade, and their teeth are some of the most common components of the Mesozoic dinosaur fossil record. This is the case in the Lourinhã Formation (Late Jurassic, Kimmeridgian-Tithonian) of Portugal, where theropod teeth are particularly abundant and diverse. Four isolated theropod teeth are here described and identified based on morphometric and anatomical data. They are included in a cladistic analysis performed on a data matrix of 141 dentition-based characters coded in 60 taxa, as well as a supermatrix combining our dataset with six recent data matrices based on the whole theropod skeleton. The consensus tree resulting from the dentition-based data matrix reveals that theropod teeth provide reliable data for identification at approximately family level. Therefore, phylogenetic methods will help identifying theropod teeth with more confidence in the future. Although dental characters do not reliably indicate relationships among higher clades of theropods, they demonstrate interesting patterns of homoplasy suggesting dietary convergence in: 1) alvarezsauroids, therizinosaurs and troodontids; 2) coelophysoids and spinosaurids; 3) compsognathids and dromaeosaurids; and 4) ceratosaurids, allosauroids and megalosauroids.

Based on morphometric and cladistic analyses, the biggest tooth from Lourinhã is referred to a mesial crown of the megalosaurid *Torvosaurus tanneri*, due to the elliptical cross section of the crown base, the large size and elongation of the crown, medially positioned mesial and distal carinae, and the coarse denticles. The smallest tooth is identified as *Richardoestesia*, and as a close relative of *R. gilmorei* based on the weak constriction between crown and root, the eight-shaped outline of the crown base and, on the distal carina, the average of ten symmetrically rounded denticles per five mm, as well as a subequal number of denticles basally and at mid-crown. Finally, the two medium-sized teeth belong to the same taxon and exhibit pronounced interdenticular sulci between distal denticles, hooked distal denticles for one of them, an irregular enamel texture, and a straight distal margin, a combination of features only observed in abelisaurids. They provide the first record of Abelisauridae in the Jurassic of Laurasia and the one of the oldest records of this clade in the world, suggesting a possible radiation of Abelisauridae in Europe well before the Upper Cretaceous.

Introduction

The Upper Jurassic of Portugal has yielded an important fauna of dinosaurs, one of the richest of Europe. Dinosaur bones and teeth have been collected for more than 140 years, mainly from two important paleontological sites both situated in the center of Portugal (Rauhut 2000*a*; Antunes and Mateus 2003). The first, Guimarota Mine, is constituted by several layers of limestone, sandstone, mudstone, marl and coal belonging to the Alcobaça Formation (Kimmeridgian; Kullberg et al. in press; Helmdach 1971; Henkel and Krusat 1980; Schudack 2000). Exploration in the 1960s, and new excavations from 1972 to 1982, unearthed ornithischian and saurischian dinosaurs, mostly represented by isolated teeth (Zinke 1998; Rauhut 2000*b*, 2001). The second, the Lourinhã region, is the richest area for dinosaur fossils in Portugal (Antunes and Mateus 2003). Bones, teeth, tracks, eggs and embryos of dinosaurs have been uncovered in several localities of the Lourinhã Formation Kimmeridgian-Tithonian in age (Kullberg et al. in press; Antunes and Mateus 2003; see Introduction Fig. 1.15).

Most major clades of dinosaurs (ornithopods, thyreophorans, sauropodomorphs and theropods) are represented in the Upper Jurassic of Portugal, but theropods are the most diversified group of dinosaurs represented (Rauhut 2000*b*; Mateus 2006). Material from the Guimarota Mine and the Lourinhã region has been referred to at least seven theropod taxa, including *Ceratosaurus dentisulcatus* (Mateus and Antunes 2000*b*; Mateus et al. 2006; Malafaia et al. 2014), *Torvosaurus tanneri* (Mateus and Antunes 2000*a*; Mateus et al. 2006; Malafaia et al. 2008), *Allosaurus europaeus* (Mateus et al. 2006), *Allosaurus fragilis* (Pérez-Moreno et al. 1999; Malafaia et al. 2007), *Lourinhanosaurus autunesi* (Mateus 1998), *Aviatyrannis jurassica* (Rauhut 2003*b*), cf. *Compsognathus* sp. (Zinke 1998), and cf. *Archaeopteryx* sp. (Weigert 1995; Wiechmann and Gloy 2000). Also present are theropods belonging to Dromaeosauridae, Troodontidae and of uncertain affinities (cf. *Richardoestesia* sp. and cf. *Paronychodon* sp.; Zinke and Rauhut 1994; Zinke 1998; Mateus 2005). Moreover, theropod embryos and hatchlings, ascribed to *Lourinhanosaurus* (Mateus et al. 1998; de Ricqlès et al. 2001; Hendrickx and Mateus 2012), *Allosaurus* (Rauhut and Fechner 2005) and a megalosauroid (Araújo et al. 2013), were also collected in Portugal, and a diverse ichnological record is known (Mateus and Milàn 2010).

Theropod teeth are very common in the Lourinhã Formation, and some of them have been reported in the literature already. In the 1950s, several theropod teeth found at Porto das Barcas (Lourinhã Formation) near Lourinhã were briefly described by Lapparent and Zbyszewski (1957). The material was collected by Carlos Ribeiro during a geologic cross section on June 20, 1863, and those teeth seem to be the historically earliest dinosaur discovery in Portugal (Antunes and Mateus 2003). Identified by Lapparent and Zbyszewski (1957) as belonging to the species *Megalosaurus insignis* and the new taxon *Megalosaurus pombali*, these two taxa are however currently considered as invalid (Holtz 1994; Antunes and Mateus 2003; Carrano et al. 2012). Later, Antunes (1990) mentioned the

presence of a tooth fragment also attributed to the genus *Megalosaurus*. However, the first thorough study of theropod teeth from the Lourinhã area was made by Rauhut and Kriwet (1994), who described two large theropod teeth also found in Porto das Barcas, which they attributed cautiously to an indeterminate 'carnosaur'. Finally, Mateus (2005) and Mateus et al. (2006) mentioned and briefly described several theropod teeth from the Lourinhã Formation, recognizing the presence of *Ceratosaurus dentisulcatus* and the clades of Carcharodontosauridae and Troodontidae in this unit.

Although theropod teeth are rather simple structures, far less informative than mammal teeth (Longrich 2008; Han et al. 2011) or many other parts of the skeleton such as the quadrate (Hendrickx et al. 2012), a number of workers have successfully used theropod tooth morphology for taxonomic purposes (e.g., Currie et al. 1990; Fiorillo and Currie 1994; Rauhut and Werner 1995; Baszio 1997; Zinke 1998; Fiorillo and Gangloff 2001; Rauhut 2002; Sankey et al. 2002; Fanti and Therrien 2007; Longrich 2008; Sankey 2008; Soto and Perea 2008; Brinkman 2008; Larson 2008*a*; Ősi et al. 2010; Larson et al. 2010; Buckley et al. 2010; Han et al. 2011; Larson and Currie 2013). Tooth measurements were first utilized by Currie et al. (1990) and Farlow et al. (1991) for systematic identification of theropod teeth, and later authors followed or modified this method to document isolated theropod teeth (e.g., Torices et al. in press; Fiorillo and Currie 1994; Baszio 1997; Holtz et al. 1998; Sankey 2001, 2008; Sankey et al. 2002; Bakker and Bir 2004; Samman et al. 2005; Larson 2008*a*; Han et al. 2011). Smith (2005) and Smith et al. (2005) were the first to successfully discriminate theropod teeth to the genus level based on a quantitative methodology and discriminant analyses. Such methodology was later followed by Smith and Dalla Vecchia (2006), Smith and Lamanna (2006), Lubbe et al. (2009), Torres-Rodríguez et al. (2010) and Ősi et al. (2010) to identify isolated teeth of theropods, and used in a slightly different way by Fanti and Therrien (2007), Larson (2008*a*) and Larson and Currie (2013). The taxonomic utility of theropod teeth evaluated with cladistics tools has recently been investigated by Hwang (2007) who mostly focused on the enamel microstructure. Hwang (2007) performed a first cladistic analysis by using eight dental and 31 enamel characters coded in 52 dinosaur taxa, including 25 theropods, and combined their enamel based characters with the dataset of Makovicky et al. (2005). A same method was used by Cillari (2010) who performed a cladistic analysis using 19 dentition-based characters coded in 13 theropod taxa and 14 morphotypes of theropod teeth.

The present work aims to evaluate the systematic potential of theropod teeth and investigate the systematic palaeontology of four isolated theropod teeth chosen in the collection of the Museu of Lourinhã based on their completeness, particular shape and interesting features displayed (e.g., interdenticular sulci, transversal and marginal undulations, mesio-distal constriction of the crown). The systematic value of theropod teeth was assessed by following the methodology of Hwang (2007), i.e., performing a cladistic analysis on a data matrix including dentition-based characters only, and the taxonomic identification of the four teeth from Portugal was investigated by using the morphometric methodology of Smith et al. (2005). Our study is intended as a case study for identification of isolated

theropod teeth, which previous studies have often failed to identify with any certainty (e.g., Torices et al. in press; Maganuco et al. 2005; Ősi et al. 2010; Han et al. 2011).

Locality, Geological and Stratigraphical setting

The four teeth all come from the Lourinhã Formation near the town of Lourinhã. The Lourinhã Formation is 600 to 1100 meters thick and mostly appears along the cliffs bounding the Atlantic Ocean, 70 km North of Lisbon. The formation is delimited at its base by the Amaral Formation of Kimmeridgian age, comprising shallow marine sandstones and oolites, as well as a shallow marine carbonate shelf forming the contact with the Lourinhã Formation. The Cretaceous continental clastic Torres Vedras Formation (or Group) lies uncoformably above the Lourinhã Formation.

The Lourinhã Formation consists of continental deposits intercalated with some shallow marine deposits, corresponding to an alluvial fan and fluvio-deltaic environments punctuated by periodic marine transgressions (Kullberg et al. in press; Hill 1988, 1989). Theropod teeth can be found in both Porto Novo and Santa Rita members of the Lourinhã Formation. For more information regarding the sedimentology on those two members, see Hill (1988, 1989).

Several authors (e.g., Manuppella 1996, 1998; Manuppella et al. 1999) have considered the Alcobaça Formation as being similar to the Lourinhã Formation. However, the latter is dated Upper Kimmeridgian-Tithonian in age and is, therefore, slightly younger and also more continental than the Alcobaça Formation (Mateus 2006). Nevertheless, both the Lourinhã and Alcobaça Formation of Portugal are comparable with the Morrison Formation of North America and the Tendaguru Beds in Tanzania as the three regions are Kimmeridgian-Tithonian in age and show similar ecosystems, all dominated by dinosaurs (Mateus 2006).

Methodology

Morphometrics

The description of teeth follows the dental nomenclature proposed by Smith and Dodson (2003). Both descriptive morphological characters and quantitative morphometric techniques were used to analyse and identify the four theropod teeth. Observations were made with a binocular microscope Leica MZ6 as well as a digital microscope AM411T-Dino-Lite Pro. Photographs were taken with a digital camera for the biggest teeth and the digital microscope for the smaller tooth.

The quantitative methodology was based on numerical data developed by Smith (2005) and Smith et al. (2005), and updated by Smith and Dalla Vecchia (2006), Smith and Lamanna (2006), and Smith (2007). Additional morphometric data of theropod teeth were collected from Canudo et al. (2006), Soto and Perea (2008), Sereno and Brusatte (2008), Molnar et al. (2009), Lubbe et al. (2009), Torres-Rodríguez et al. (2010), Ősi et al. (2010), and Gianechini et al. (2011*a*). Morphometric

measurements were also taken on many theropod teeth belonging to the palaeontological collections of 24 museums from Argentina, Europe and the United States. The data file is available at DRYAD (http://doi.org/10.5061/dryad.33tb2). Anatomical and morphometric abbreviations follow Smith et al. (2005).

Measurements and ratios proposed by Smith et al. (2005) were taken with a digital caliper and the following measurements were done: **AL**, apical length (in mm); **CBL**, crown base length, measured at the base of the crown from its mesial to its distalmost extension (excluding the carinae; in mm); **CBR**, crown base ratio, numerical value derived from dividing CBW through CBL (= labiolingual compression); **CBW**, crown base width, labiolingual extension of the crown at its base (in mm); **CH**, crown height, measured from the basal-distal most point of the crown towards its tip (in mm); **CHR**, crown height ratio, numerical value derived from dividing CH through CBL; **DAVG**, average distal denticle density on 5 mm; **DA**, denticle density for distal apical serration, i.e., denticles per 5 mm at the most apical part of the distal carinae; **DB**, denticle density for distal basal serration, i.e., denticles per 5 mm at the most basal part of the distal carinae; **DC**, denticle density for distal mid-crown serration, i.e., denticles per 5 mm at the mid-crown part of the distal carinae; **DSDI**, denticle size difference index, ratio between the number of denticles per 5 mm of the mesial and distal carinae, at mid-crown; **MA**, denticle density for mesial apical serration, i.e., denticles per 5 mm at the most apical part of the mesial carinae; **MB**, denticle density for mesial basal serration, i.e., denticles per 5 mm at the most basal part of the mesial carinae; **MC**, denticle density for mesial mid-crown serration, i.e., denticles per 5 mm at the mid-crown part of the mesial carinae; **MAVG**, average mesial denticle density on 5 mm.

Cladistic Analysis

A character-taxon data matrix of dentition-based characters was created and scored in 60 non-avian theropod taxa (Table 4.1) in order to evaluate the taxonomic potential of theropod dentitions and assess the phylogenetic relationship of the four teeth from the Lourinhã Formation. Teeth pertaining to most clades of non-avian theropods were examined and coded from first-hand observations (54 taxa, 90% of the dataset), high-resolution photographs (*Dilophosaurus* and *Scipionyx*), and by using full descriptions and illustrations of the teeth in the literature for six taxa (*Fukuiraptor*, *Australovenator*, *Jianchangosaurus*, *Erlikosaurus* and *Zanabazar*; Table 4.1). *Eoraptor lunensis*, considered to be a basal saurischian (Langer and Benton 2006), a basal theropod (Nesbitt et al. 2009; Nesbitt 2011; Sues et al. 2011) or a basal sauropodomorph (Martinez et al. 2011; Sereno et al. 2013), was specified as the outgroup.

The data matrix encompasses 141 equally weighted morphological characters based on the morphology of the crown, root, mesial and distal carinae, denticles, interdenticular sulci (‘blood groove’ *sensu* Currie et al. 1990, and ‘caudae’ *sensu* Abler 1992), crown ornamentations (i.e., transverse and marginal undulations, flutes, longitudinal grooves and ridges, etc.), and enamel texture

and microstructure (Appendices A4.1–A4.3; Figs. A4.1-A4.4 for illustrations of dentition-based characters). Characters related to the shape, size and number of teeth/alveoli of the premaxilla, maxilla and dentary were also included in the data matrix. Seventy-four characters are derived from the literature, and 67 characters (47.5%) were revealed by descriptive work on the teeth and our personal observation. Due to the important variation of morphology between lateral and mesial dentition (i.e., the 'mesial dentition comprises the premaxillary teeth as well as mesial dentary teeth and, in some cases, maxillary teeth that share a morphology similar to those of premaxillary teeth), the dataset was divided into mesial and lateral teeth. Among the 141 morphological characters, 81 are multistate characters, ten are continuous (characters related to CH, CHR, CBR, MC and DC for both mesial and lateral teeth) and three are meristic and concern the number of premaxillary, maxillary and dentary teeth. All 13 continuous and meristic characters were transformed into discrete characters of no more than five character states by assigning a specific range or value, and ten multistate characters (characters 2, 4, 15, 17, 24, 25, 36, 53, 65 and 86) were ordered (Appendices A4.1).

The systematic potential of theropod teeth was first evaluated by performing a cladistic analysis on the data matrix of dentition-based characters without the isolated teeth from the Lourinhã Formation. In order to constrain all major theropod clades and visualize the dentition-based synapomorphies for each theropod clade. A second analysis was performed on a supermatrix combining our dentition-based data matrix with six recent datasets on non-avian theropods based on the whole skeleton (Xu et al. 2009*a*; Brusatte et al. 2010*d*; Martinez et al. 2011; Senter 2011; Carrano et al. 2012; Pol and Rauhut 2012), and from which all teeth-related characters were removed. The resulting supermatrix includes 1972 characters with 65 treated as ordered (the data file is available at Appendices A4.5). The four isolated teeth from the Lourinhã Formation were then incorporated in the matrix and supermatrix in order to assess their phylogenetic relationship.

TNT v1.1 (Goloboff et al. 2008) was employed to search for most-parsimonious trees (MPTs). The matrix and supermatrix were analysed under the 'New Technology Search' with the 'driven search' option (TreeDrift, Tree Fusing, Ratchet, and Sectorial Searches selected with default parameters), and stabilizing the consensus twice with a factor of 75. The consistency and retention indices as well as the Bremer supports (Bremer 1994) were calculated using the 'stats' and 'aquickie' commands, respectively, and a bootstrap analysis was performed with the standard options.

Results

Cladistic Analysis

The analysis of the data matrix of dentition-based characters including 60 theropod taxa yielded 10 most parsimonious trees (MPTs), in which the strict consensus trees (length = 681 steps; CI = 0.338, RI = 0.56) resulted in a few polytomies affecting clades of no more than three taxa (Appendices A4.6, Figs. A4.5-6). A similar topology was found when the four isolated teeth were

TABLE 4.1. Teeth and tooth bearing bones of non-avian theropod specimens examined and included in this study.

Taxon - author	Specimens	Examined	Other photo credits	Literature used
Eoraptor lunensis Sereno et al. 1993	PVSJ 512	Y	Martín Ezcurra	Sereno et al. 2013
Herrerasaurus ischigualastensis Reig 1963	PVSJ 053, 407, 605; MACN-CH 18.060	Y	Martín Ezcurra	Sereno and Novas 1994
Eodromaeus murphi Martinez et al. 2011	PVSJ 560, 561	Y		Martinez et al. 2011
Coelophysis bauri Cope 1887	CMNH 81765, 82931; AMNH 7223, 7224, 7227, 7228, 7229, 7231	Y		Rowe 1989; Buckley 2009
Dilophosaurus wetherilli Welles 1954	UCMP 37302, 37303, 77270	N	Martín Ezcurra; Steve Brusatte	Welles 1984
Ceratosaurus nasicornis Marsh 1884	USNM 4735; UMNH VP 5278 = UUVP 155, 158, 674; MWC 1;	Y	Matthew Carrano; Roger Benson	Gilmore 1920; Madsen and Welles 2000; Bakker and Bir 2004
Genyodectes serus Woodward 1901	MLP 26-39	Y		Rauhut 2004*b*
Berberosaurus liassicus Allain et al. 2007	MNHN Pt339	Y		
Noasaurus leali Bonaparte and Powell 1980	PVL 4061	Y		Bonaparte and Powell 1980; Candeiro 2007
Masiakasaurus knopfleri Sampson et al. 2001	FMNH PR 2182, 2183, 2201, 2221, 2453, 2471, 2476, 2696; UA 8680, 9091, 9128	Y	Matthew Carrano	Carrano et al. 2002, 2011
Kryptops palaios Sereno and Brusatte 2008	MNN GAD1−1	Y		Sereno and Brusatte 2008
Rugops primus Sereno et al. 2004	MNN IGU1	Y		Sereno et al. 2004
Abelisaurus comahuensis Bonaparte and Novas 1985	MPCA 1, 5, 229, 267, 687, 689, 709	Y		Bonaparte and Novas 1985; Candeiro 2007
Aucasaurus garridoi Coria et al. 2002	MCF-PVPH 236	Y	Matthew Lamanna	Candeiro 2007
Indosuchus raptorius Huene and Matley 1933	AMNH 1753, 1955, 1960	Y		Sampson et al. 1996
Skorpiovenator bustingorryi Canale et al. 2009	MMCH-PV 48	Y	Matthew Lamanna	Candeiro 2007; Canale et al. 2009
Majungasaurus crenatissimus Lavocat 1955	MNHN MAJ1; FMNH PR 114 2008, 2100, 2278; UA 8716	Y		Fanti and Therrien 2007; Smith 2007
Piatnitzkysaurus floresi Bonaparte 1979	PVL 4073; MACN-CH 895	Y	Matthew Carrano; Martín Ezcurra	Bonaparte 1986
Eustreptospondylus oxoniensis Walker 1964	OUMNH J.13558	Y		Sadleir et al. 2008Sadleir et al. 2008
Dubreuillosaurus valesdunensis Allain 2002	MNHN 1998-13	Y		Allain 2002

*Afrovenator abakensis** Sereno et al. 1994	UC UBA1	Y		Sereno et al. 1994
Duriavenator hesperis Waldman 1974	NHM R.332	Y		Benson 2008*a*
Megalosaurus bucklandii Mantell 1827	OUMNH J.13505, J.13506; NHM R.8303, R.8305	Y		Benson et al. 2008; Benson 2009, 2010*a*
Torvosaurus tanneri Galton and Jensen 1979	BYU-VP 2003, 4882, 9122 12817; ML 1100	Y	Matthew Carrano	Jensen 1985; Britt 1991; Bakker and Bir 2004
Baryonyx walkeri Charig and Milner 1986	NHM R.9951; ML 1190	Y		Charig and Milner 1997; Mateus et al. 2011
Suchomimus tenerensis Sereno et al. 1998	MNN GDF501, GDF502, G2-2, G5-1, G6, G22-7, G26-5, G34-1, G34-7, G34-12, G35-9, G43-5, G54-4, G67-1, G67-8, G69-5, G73-3, G74-1, G100-4, G232	Y	Roger Benson	Sereno et al. 1998
Irritator challengeri Martill et al. 1996/*Angaturama limai* Kellner and Campos 1996	SMNS 58022; AMNH 30230 cast	Y	Ricardo Araújo	Kellner and Campos 1996; Sues et al. 2002
Spinosaurus aegyptiacus Stromer 1915	MSNM V3976, V4047, V6422, V6424, V6865, V6896; NHM R.16420, R.16421	Y	Andrea Cau	Stromer 1915; Milner 2003; Dal Sasso et al. 2005; Hasegawa et al. 2010
Sinraptor sp. Currie and Zhao 1993*a*	IVPP 10600; ZDM T0024	N	Philip Currie	Currie and Zhao 1993*a*
Erectopus superbus Sauvage 1882	MNHN 2001-4	Y		Allain 2005
Allosaurus fragilis Marsh 1877	AMNH 600, 851; BYU-VP 2028; MWC 5440; USNM 8335; UMNH VP 5427 10.093, 40.585; CMNH 1254, 11844, 21703; SMA 0005/02	Y	Steve Brusatte	Osborn 1912; Gilmore 1920; Madsen 1976*b*; Chure 2000; Bakker and Bir 2004; Loewen 2010
Neovenator salerii Hutt et al. 1996	MIWG 6348; NHM R.10001	Y	Steve Brusatte; Roger Benson	Sereno and Brusatte 2008
Australovenator wintonensis Hocknull et al. 2009	AODF 604	N		Hocknull et al. 2009
Fukuiraptor kitadaniensis Azuma and Currie 2000	FPDM 9712203, 9712204 + many others	N		Azuma and Currie 2000; Currie and Azuma 2006; Molnar et al. 2009
Acrocanthosaurus atokensis Stovall and Langston Jr 1950	NCSM 14345; SMU 74646	Y	Drew Eddy; Vince Shneider; Ricardo Araújo	Harris 1998; Currie and Carpenter 2000; Eddy and Clarke 2011
Eocarcharia dinops Sereno and Brusatte 2008	MNN GAD7, GAD13, GAD14	Y	Juan Canale	Sereno and Brusatte 2008
Carcharodontosaurus saharicus Depéret and Savornin 1925	MNN GAD8, IGU5; SGM Din-1; UC PV6	Y		Stromer 1931; Sereno et al. 1996; Brusatte and Sereno 2007
Mapusaurus roseae Coria and Currie 2006	MCF-PVPH 108	Y	Matthew Lamanna	Coria and Currie 2006; Candeiro 2007
Giganotosaurus carolinii Coria and	MUCPv-CH-1; MUCPv 95	Y	Matthew Lamanna	Coria and Salgado 1995; Calvo and

Salgado 1995				Coria 1998; Candeiro 2007
Proceratosaurus bradleyi Huene 1926*b*	NHM R 4860	Y		Rauhut et al. 2010
Eotyrannus lengi Hutt et al. 2001	MIWG 1997.550	Y		Hutt et al. 2001
Raptorex kriegsteini Sereno et al. 2009	LH PV18	Y		Sereno et al. 2009
Alioramus altai Brusatte et al. 2009*b*	IGM 100-1844	Y	Steve Brusatte	Brusatte et al. 2009*b*, 2012*a*
Tyrannosaurus rex Osborn 1905	CMNH 9380; AMNH 5027; FMNH PR2081; NHM R.7994	Y	Mickey Mortimer	Osborn 1912; Molnar 1991; Brochu 2003; Smith 2005
Compsognathus longipes Wagner 1861	MNHN CNJ 79	Y	Karine Peyer	Stromer 1934; Ostrom 1978; Peyer 2006
Scipionyx samnicicus Dal Sasso and Signore 1998	SBA-SA 163760	N	Cristiano Dal Sasso	Dal Sasso and Maganuco 2011
Ornitholestes hermanni Osborn 1903	AMNH FARB 619	Y		Osborn 1903
Shuvuuia deserti Chiappe et al. 1998	IGM 100-977, 100-1001	Y		Chiappe et al. 1998; Dufeau 2003
Jianchangosaurus yixianensis Pu et al. 2013	41HIII-0308A	N		Pu et al. 2013
Erlikosaurus andrewsi Barsbold and Perle 1980	IGM 100-111	N		Clark et al. 1994
Buitreraptor gonzalezorum Makovicky et al. 2005	MPCA 245	Y		Makovicky et al. 2005; Gianechini et al. 2011*a*
Velociraptor mongoliensis Osborn 1924	AMNH 6515	Y		Osborn 1924; Sues 1977; Barsbold and Osmólska 1999
Bambiraptor feinbergi Burnham et al. 2000	AMNH 001	Y		Burnham 2004
Dromaeosaurus albertensis Matthew and Brown 1922	AMNH 5356	Y		Colbert and Russell 1969; Currie et al. 1990; Currie 1995; Baszio 1997
Saurornitholestes langstoni Sues 1978	DMNH 22870	Y		Sues 1978; Currie et al. 1990; Baszio 1997
Tsaagan mangas Norell et al. 2006	IGM 100-1015	Y		Norell et al. 2006
Byronosaurus jaffei Norell et al. 2000	IGM 100-983	Y		Norell et al. 2000; Makovicky et al. 2003
Zanabazar junior Barsbold 1974	IGM 100-1	N		Norell et al. 2009
Troodon formosus Leidy 1856	DMNH 22337, 22837	Y		Currie 1987; Currie et al. 1990; Baszio 1997; Longrich 2008
Richardoestesia gilmorei Currie et al. 1990	NMC 343	N		Currie et al. 1990; Baszio 1997; Sankey et al. 2002; Longrich 2008; Larson and Currie 2013

incorporated (Appendices A4.6, Fig. A4.7), and the cladistic analysis yielded 7 MPTs (length = 703 steps; CI = 0.331, RI = 0.564). Although the strict consensus trees did not recover the general topology of theropod classification with the usual major clades (e.g., Neotheropoda, Tetanurae, Avetheropoda, Coelurosauria), many theropod clades such as Ceratosauridae, Abelisauridae, Spinosauridae, Megalosauridae, Tyrannosauroidea and Therizinosauria were resolved, demonstrating some systematic potential of theropod teeth at approximately family level. As noted by Hwang (2007), dentition-based characters can be good at recovering individual clades, but not at resolving the relationship between those clades. This is obviously due to the large amount of convergence in theropod dentition, directly linked to diet, among a clade displaying the most variation of feeding strategies among dinosaurs (Rayfield 2005*a*; Therrien et al. 2005; Zanno and Makovicky 2011).

Similarly to Hwang (2007: fig. 38), the basalmost dinosaur *Eoraptor* and derived coelurosaurs such as troodontids and therizinosaurs appear closely related based on dental characters. They have similar dentitions in both their morphology (i.e., small crowns, constriction occurring between tooth and crown; distal denticles hooked and inclined apically from the distal margin), and microstructure (Hwang 2007), and might therefore have shared a similar diet, most likely omnivory (including partial herbivory) or herbivory (e.g., Russell and Dong 1993*a*; Holtz et al. 1998; Barrett 2000; Zanno and Makovicky 2011; Sereno et al. 2013). Coelophysoids and spinosaurids possess relatively similar dentitions to each other (i.e., premaxillary tooth-row posteriorly constricted, anterior maxillary teeth facing anterodorsally, fluted teeth in *Coelophysis* and spinosaurids, and terminal rosette of the dentary in *Dilophosaurus* and spinosaurids), suggesting they also had close diets involving grapping small prey such as small crocodylomorphs, juvenile dinosaurs and fishes (e.g., Paul 1988; Charig and Milner 1997; Farlow and Holtz 2002; Holtz 2003; Therrien et al. 2005; Nesbitt et al. 2006; Milner and Kirkland 2007). A similar morphological convergence occurs between the dentitions of noasaurids, compsognathids and dromaeosaurids which probably fed on small to medium-sized prey (e.g., Carpenter 1998; Carrano et al. 2002; Peyer 2006; Gignac et al. 2010; Dal Sasso and Maganuco 2011). These theropods all bear small ziphodont (i.e., labio-lingually compressed crown in which both mesial and distal margins possess serrated carinae) teeth with large sometimes apically inclined distal denticles and, when present, smaller mesial serrations (e.g., Currie et al. 1990; Currie and Chen 2001; Rauhut et al. 2012; pers. obs.). The mesial teeth of these theropods also tend to lack mesial and, in some cases, distal serrations (e.g., Stromer 1934; Dal Sasso and Maganuco 2011; Gianechini et al. 2011*a*).

Ceratosauridae, Megalosauridae, some basal allosauroids, Carcharodontosauridae and Tyrannosauroidea are nested in the same clade based on dental characters (Fig. 4.1), illustrating similar feeding strategies involving consumption of large prey (mostly dinosaurs) among these large, robust-skulled averostrans (e.g., Carpenter 1998; Farlow and Holtz 2002; Holtz 2003; Bakker and Bir 2004; Carpenter et al. 2005*b*; Hone and Rauhut 2010). Their lateral teeth are indeed sometimes very similar as members of these clades possess large, elongated and labio-lingually compressed teeth with

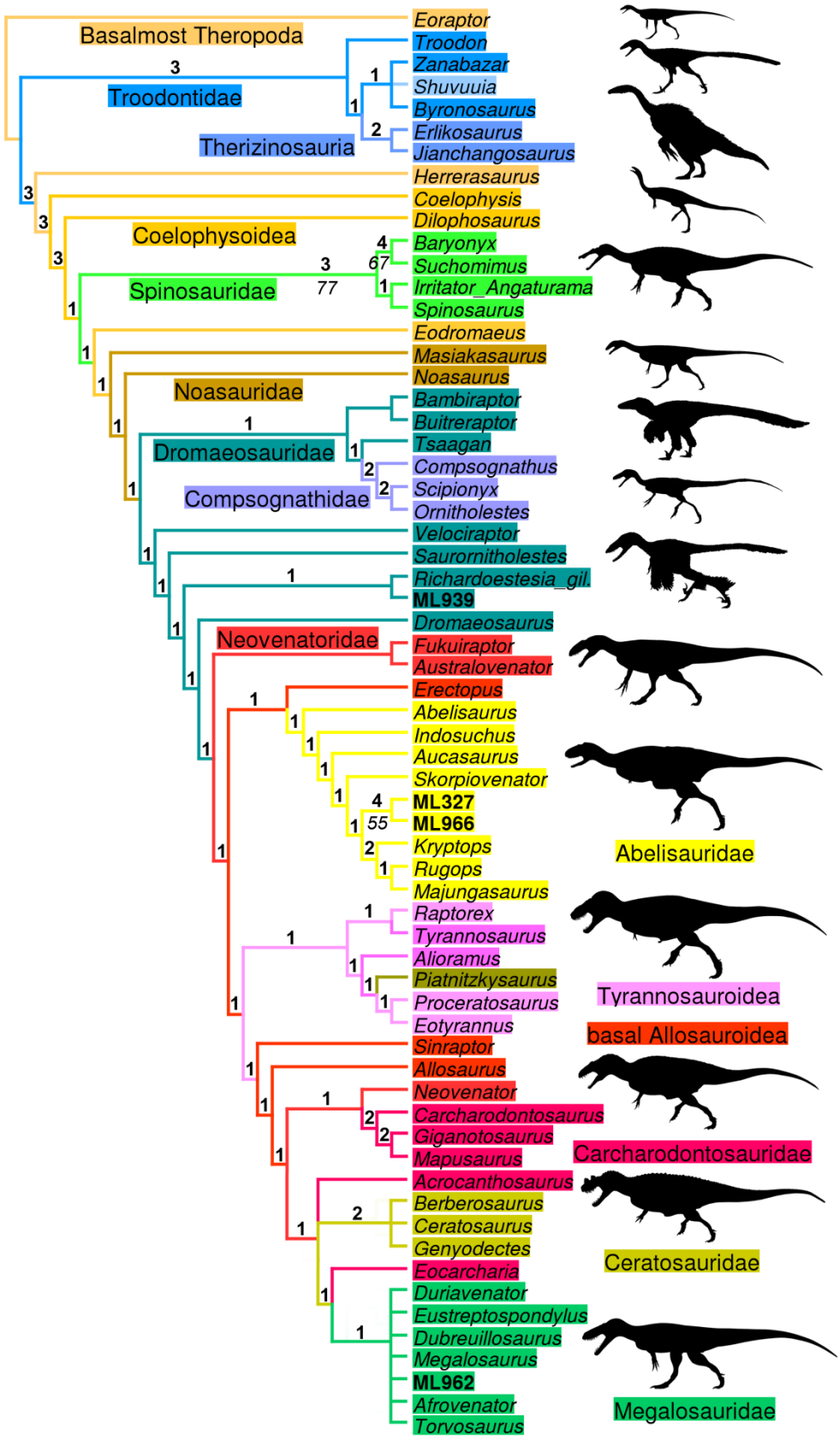

FIGURE 4.1. Strict consensus cladogram of seven most parsimonious trees recovered from analysis of dentition based characters. Initial analysis was a New Technology Search using TNT v.1.1 of a data matrix comprising 141 dentition-based characters for one outgroup (*Eoraptor*), 59 non-avian theropod taxa, as well as ML 327, ML 939, ML 962 and ML 966. Tree length = 703 steps; CI = 0.331; RI = 0.564. Bremer support values are in bold and bootstrap values are in italic. For silhouette attribution, see Appendices A1.1.

a distal carina bearing coarse symmetrical to asymmetrical chisel-like denticles with often deep and elongated interdenticular sulci (pers. obs.). The premaxillary and dentary teeth tend to be smaller than the maxillary dentition, and there is an overlap of the second and third premaxillary alveoli in these theropods. The lateral teeth of ceratosaurids, megalosaurids and allosauroids can also display the same crown structures: large transverse undulations (i.e., long mesio-distally oriented wrinkles on the crown; Brusatte et al. 2007) and short marginal undulations (i.e., pronounced mesio-distally oriented wrinkles adjacent to carinae) and a similar pattern of oriented texture of the enamel (pers. obs.; Appendices A4.3, Fig. A4.3F). Tyrannosaurid teeth also display similar structures on the crown, but their lateral teeth are much stouter and the mesial teeth have a mesial carina displaced lingually, rather than mesially or labially (e.g., Molnar 1998; Holtz 2003, 2004, 2008; Samman et al. 2005; Smith 2005).

Due to the variability of their dentitions, Dromaeosauridae and Allosauroidea were recovered as polyphyletic according to dental characters. Indeed, the lateral teeth of the dromaeosaurids *Buitreraptor*, *Dromaeosaurus* and *Saurornitholestes* are quite distinct from those of other dromaeosaurids. Regarding their serrations, for instance, *Buitreraptor* lacks mesial and distal denticles (Gianechini et al. 2011*a*), whereas *Dromaeosaurus* bears subquadrangular denticles with a convex margin (Currie et al. 1990; Currie 1995), and *Saurornitholestes* possesses large and apically hooked denticles, reminiscent of those of Troodontidae (Currie et al. 1990). The differences among allosauroid dentitions are more subtle. Most allosaurid teeth are incrassate, strongly recurved distally and bear a sharply twisted mesial carina in some teeth of the lateral dentition (Madsen 1976*b*; Bakker 1998; Holtz et al. 2004; pers. obs.). This contrasts with the strongly labio-lingually compressed crowns of Neovenatoridae (e.g., *Neovenator*, *Fukuiraptor* and *Australovenator*; Currie and Azuma 2006; Hocknull et al. 2009) and some Carcharodontosauridae (e.g., *Carcharodontosaurus*, *Mapusaurus*; Stromer 1931; Coria and Currie 2006; pers. obs.), and the weakly recurved teeth of Metriacanthosauridae and Carcharodontosauridae which possess a relatively straight mesial carina (e.g., Stromer 1931; Coria and Currie 2006; Brusatte and Sereno 2007; pers. obs.).

On the other hand, with their characteristic dentitions, ceratosaurids, abelisaurids, spinosaurids, megalosaurids, tyrannosauroids, compsognathids and therizinosaurs were found as monophyletic in this analysis (Fig. 4.1). Ceratosaurid teeth are characterized by larger mid-maxillary teeth when compared to anterior maxillary teeth and, in lateral teeth, a labial depression on the basal part of the crown, a distal carina extending to the cervix or just above it and a broad interdenticular space in between distal denticles (Bakker and Bir 2004; Rauhut 2004*b*; pers. obs.). Their lateral teeth also have a braided texture (i.e., oriented enamel texture made of alternating sinuous ridges and grooves: Appendices A4.3, Fig. A4.3K) of the enamel (unlike the irregular enamel texture of most abelisauroid teeth), and the crown tend to be strongly labiolingually compressed, sometimes bearing well-visible transverse undulations and a distal carina strongly labially deflected. In addition, the labial

surface adjacent to the distal and sometimes mesial carinae is often flat or concave in ceratosaurid lateral teeth (Rauhut 2004*b*; pers. obs.).

Likewise, abelisaurid teeth are weakly recurved distally, so that their distal profile is either straight or even convex in lateral view, and many abelisaurids tend to have low crowns (or 'brachydont' *sensu* Smith et al. 2005; Smith 2007; pers. obs.), although elongated crowns can be borne by some abelisaurid taxa such as *Aucasaurus garridoi* (MCF-PVPH 236) and *Skorpiovenator bustingorryi* (MMCH-PV 48). The enamel surface texture of abelisaurid crown is irregular (i.e., non-oriented enamel texture: Appendices A4.3, Fig. A4.3J), unlike the braided or veined (sculptured) enamel texture of most neotheropod (pers. obs.). Abelisaurid alveoli are always mesio-distally oriented, even the mesial ones, and subrectangular in outline (e.g., Sereno et al. 2004; Sampson and Witmer 2007; Sereno and Brusatte 2008; pers. obs.), and their lateral crowns also possess mesial and distal carinae centrally positioned on the crown in mesial and distal views, respectively (Smith 2007). Both carinae always reach the cervix of the crown and the denticles often show a deep interdenticular sulcus and/or apex pointing apically. Their mesial teeth are also typical, as they have a concave surface adjacent to the mesial carina and sometimes marginal to the distal carina in the mesial tooth (Fanti and Therrien 2007; Smith 2007; pers. obs.).

Due to their highly specialized skull and dentition, adapted for piscivory (e.g., Taquet 1984; Charig and Milner 1997; Sereno et al. 1998; Dal Sasso et al. 2005, 2009; Hendrickx and Buffetaut 2008), several features of spinosaurid teeth have already been used as synapomorphies by many authors (e.g., Sereno et al. 1998; Holtz et al. 2004; Benson 2010*a*; Mateus et al. 2011; Carrano et al. 2012). Their teeth are indeed highly diagnostic (in fact the most diagnostic among theropods; Table 4.2) as all spinosaurids possess subcircular mesial and lateral crowns displaying flutes (i.e., subparallel longitudinal grooves separated by acute ridges) on the lingual and/or labial margin, minute denticles or no serrations at all on both mesial and distal carinae, and the enamel texture of *Spinosaurus* and baryonychines is deeply veined (or 'sculptured' *sensu* Hasegawa et al. 2010) and curves basally close to the carinae. Their spatulated premaxillae bear a minimum of six teeth. The posterior premaxillary teeth are significantly smaller than the anterior ones and the premaxillary tooth row extends anterior to the external naris. Moreover, the dentaries also form a terminal rosette, in which the anteriormost teeth are significantly larger than mid- and posterior dentary teeth (e.g., Stromer 1915; Charig and Milner 1997; Sereno et al. 1998).

Megalosaurid dentitions are mostly characterized by the low-number of maxillary and dentary teeth (<15 alveoli: pers. obs.). The mesial and lateral teeth of Megalosauridae can be distinguished from those borne by their related cousins (i.e., Ceratosauria, Allosauroidea, Tyrannosauroidea) based on many features, which will be thoroughly described elsewhere. Tyrannosauroids can be differentiated from other theropods based mostly on the morphology of their mesial teeth. Indeed, the basal cross-section of the mesial crown is usually U-shaped (i.e., the mesial and distal carina are strongly displaced and face lingually or linguodistally), the third and

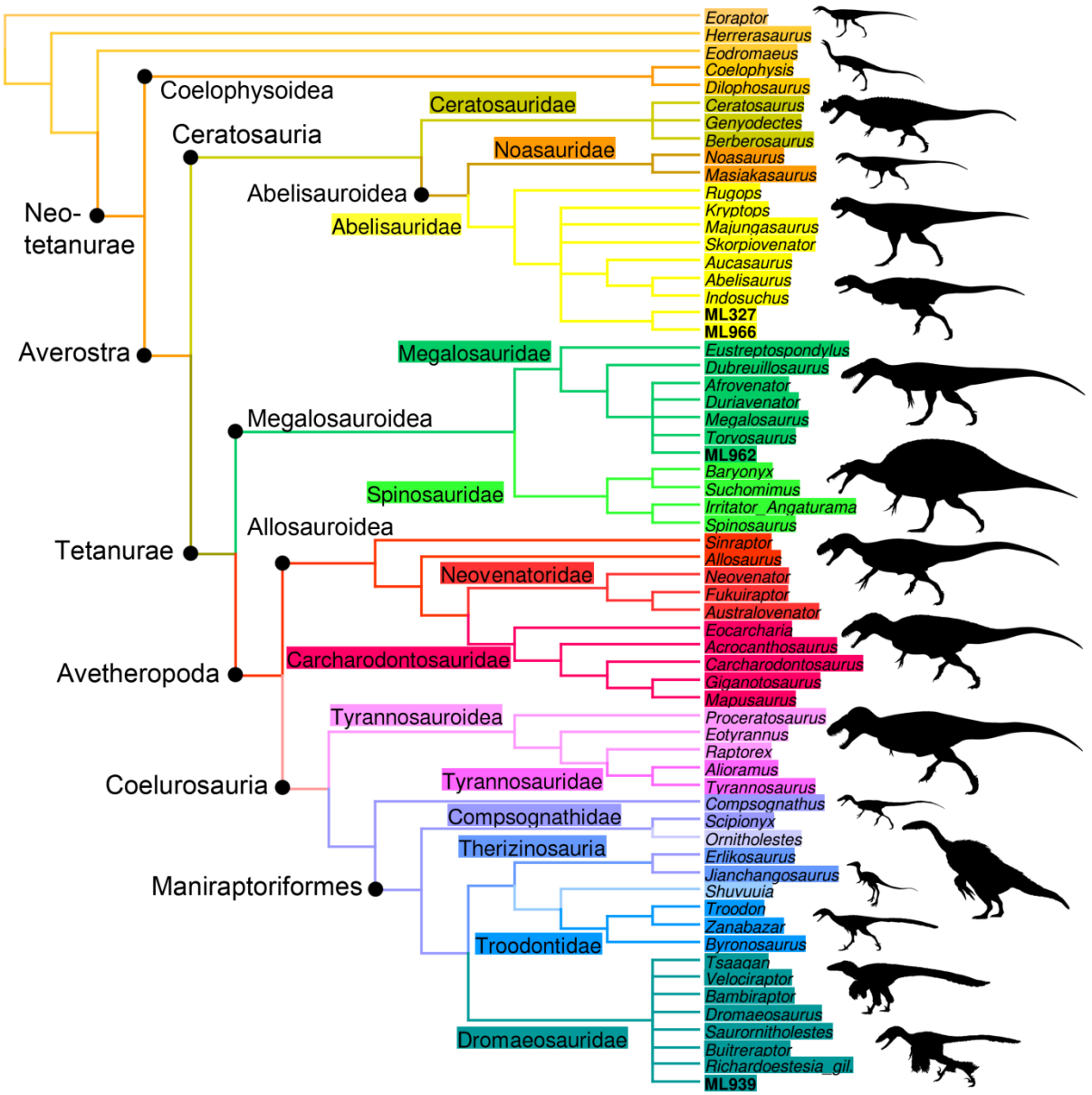

FIGURE 4.2. Strict consensus cladogram of 49 most parsimonious trees recovered from analysis of a supermatrix of 1972 discrete characters after the deletion of the two wildcard taxa Erectopus and Piatnitzkysaurus. The supermatrix includes a dentition-based data matrix of 141 discrete characters and six recent datasets based on whole theropod skeleton (Xu et al. 2009*b*; Brusatte et al. 2010*d*; Martinez et al. 2011; Senter 2011; Carrano et al. 2012; Pol and Rauhut 2012). Initial analysis was a New Technology Search using TNT v.1.1 for one outgroup (Eoraptor), 57 non-avian theropod taxa and ML 327, ML 966, ML 939 (coded as lateral teeth), and ML 962 (coded as a mesial tooth). Tree length = 3552 steps; CI = 0.563; RI = 0.628. For silhouette attribution, see Appendices A1.1.

fourth premaxillary teeth are distinctively overlapping, and the posterior premaxillary teeth are significantly smaller than the anterior maxillary teeth (e.g., Paul 1988; Molnar 1998; Holtz 2004; Samman et al. 2005; Smith 2005). The mesial maxillary and dentary teeth of tyrannosauroids are also significantly smaller than the mid-maxillary and dentary teeth, respectively, and the crowns display an oriented enamel texture (although not present in some tyrannosaurids), contrary to most other coelurosaurs. Like noasaurids and some dromaeosaurids, the distal denticles are larger than the

TABLE 4.2. List of ambiguous and unambiguous dentition-based synapomorphies by theropod clades for results of the cladistic analysis of the dentition-based dataset.

Clade	Synapomorphies
Coelophysoidea	**Unambiguous:** Premaxillary tooth row slightly constricted (15:1). **Ambiguous:** subnarial gap in the premaxilla (16:1); first maxillary alveoli open anteroventrally (21:1); enlarged fanglike anterior dentary tooth (30:1).
Averostra	**Unambiguous:** anterior premaxillary alveoli labio-lingually oriented, posterior premaxillary alveoli mesio-distally oriented (3:1); less than 14 denticles per 5mm on the mesial carina in mesial teeth (51:2); less than 16 denticles per 5mm on the mesial carina in lateral teeth (84:3).
Ceratosauridae	**Ambiguous:** Mid-maxillary teeth (or alveoli) significantly larger than anteriormost maxillary teeth (19:1); axis passing through both carinae at mid-crown sub-parallel to long axis of skull in mesial teeth (49:0); surface centrally positioned on the crown roughly flattened in lateral teeth (70:1); distal carina strongly labially deflected on the distal margin in lateral teeth, crown asymmetrical (83:1); mesial denticles inclined apically in lateral teeth (95:1); subequal or lower number of denticles apically than at the mid-crown on the mesial carina in lateral teeth (98:12); subequal number of denticles apically than at the mid-crown on the distal carina in lateral teeth (100:2); interdenticular space between distal denticles broad, more than one third of the denticle width, in lateral teeth (103:1); large and well-visible transverse undulations on the crown in some lateral teeth (109:2).
Noasauridae	**Ambiguous:** 30-44 denticles per 5mm on mesial carina in lateral teeth (84:1); 16-29 denticles per 5mm on distal carina in lateral teeth (85:2); distal denticles larger than mesial ones in lateral teeth (101:2).
Abelisauridae	**Ambiguous:** Premaxillary alveoli mesio-distally oriented (3:0); no overlap of the first and second premaxillary alveoli (4:0); subrectangular maxillary alveoli (23:1); hooked distal denticles in lateral teeth (88:2); distal denticles inclined apically in lateral teeth (96:1).
Tetanurae	**Ambiguous:** Maxillary tooth row anterior to the anterior rim of the orbit, posterior to the anteroventral rim of the antorbital fenestra (24:2).
Megalosauroidea	**Ambiguous:** Axis passing through both carinae at mid-crown sub-parallel to long axis of skull in mesial teeth (49:0); distal carina terminating well beneath the cervix in lateral teeth (81:1); resorption pit corresponding to a shallow concavity in the root of lateral teeth (140:1).
Spinosauridae	**Unambiguous:** More than five premaxillary teeth (2:34); premaxillary tooth row anterior to external naris (14:1); maxillary alveoli subcircular in outline (23:2); mesial carina terminates well beneath the cervix in mesial teeth (50:2); flutes present on both labial and lingual in lateral teeth (107:2); deeply veined enamel texture in lateral teeth (117:2). **Ambiguous:** Posterior premaxillary alveoli smaller than anterior premaxillary alveoli (7:1); anterior premaxillary teeth subequal in size than the first six anterior maxillary teeth (8:1); strongly constricted premaxillary tooth row (15:2); first maxillary alveolus significantly smaller than second alveolus (20:0); first maxillary alveolus opens anteroventrally (21:1); anteriormost dentary alveoli significantly larger than mid- and posterior dentary alveoli (27:1); enlarged fanglike anterior dentary tooth (30:1); four teeth within the terminal rosette of dentary (31:1); labiolingual compression of the crown weak, CBR > 0.75, tooth of the lateral dentition incrassate (66:2); subcircular outline of basal cross-section of the crown in lateral teeth (72:0).
Megalosauridae	**Ambiguous:** Less than 15 dentary teeth (25:3).
Avetheropoda	**Unambiguous:** Outline of basal cross-section D-shaped or J-shaped, with lingual margins strongly convex and labial margins convex or sigmoid, in the crown of mesial tooth (41:3). **Ambiguous:** Mesial carina twisted, curves onto the lingual surface in mesial teeth (46:1); mesial carina extends to the cervix or just above it in mesial teeth (50:1).
Allosauroidea	**Ambiguous:** Posterior premaxillary alveoli subequal in size than the first six anterior maxillary alveoli (9:1); outline of basal cross-section of the crown elliptical or bean-shaped in lateral teeth (72:2); mid-crown denticles on distal carina longer mediodistally than apicobasally and with horizontal subrectangular outline (92:1); interdenticular space between mid-crown denticles on the distal carina broad, more than one third of the denticle width (103:1); large transverse undulations well-visible on the crown in some lateral teeth (109:2).

Neovenatoridae	**Ambiguous:** Surface centrally positioned on the crown roughly flattened on the labial side of lateral teeth (70:1); concave surface adjacent to carinae all along the crown present on labial and lingual surfaces and adjacent to distal carina (71:12).
Carcharodontosauridae	**Ambiguous:** labiolingual compression of the crown important, CBR ≤ 0.5, lateral tooth strongly flattened (66:0); bilobate apical denticles present in lateral teeth (94:1).
Tyrannosauroidea	**Unambiguous:** Anteriormost dentary alveoli significantly smaller than mid- and posterior dentary alveoli (27:2); distal carina labially displaced and facing lingually or linguodistally in mesial teeth (48:2). **Ambiguous:** overlap of the third and fourth premaxillary alveoli (6:1); mid-maxillary alveoli significantly larger than anteriormost maxillary alveoli (48:2).
Therizinosauroidea	**Unambiguous:** Toothless premaxilla (1:1); constriction between root and crown present in some lateral teeth (64:0).
Troodontidae	**Unambiguous:** Anterior maxillary alveoli significantly smaller than posterior maxillary alveoli (18:2). **Ambiguous:** mid-maxillary teeth significantly larger than anteriormost maxillary teeth (19:1).
Dromaeosauridae	**Unambiguous:** labial depression extends along the basal half of the crown or more apically in lateral teeth (73:2). **Ambiguous:** outline of basal cross-section of the crown 8-shaped in lateral teeth (72:3).

mesial ones in the lateral teeth (DSDI < 1.2) of basal tyrannosauroids and juvenile tyrannosaurids (Carr and Williamson 2004; Xu et al. 2004, 2006; Li et al. 2010; Rauhut et al. 2012).

In Compsognathidae, and convergently with *Ornitholestes*, the mesial and distal carinae of mesial teeth are absent or unserrated, and the lateral teeth do not bear mesial denticles, whereas the distal denticles disappear well beneath the apex of the crown (e.g., Currie and Chen 2001; Hwang et al. 2004; Ji et al. 2007*a*; Chiappe and Göhlich 2010; Dal Sasso and Maganuco 2011; pers. obs.). Absence of mesial denticles in both mesial and lateral teeth and unserrated mesial teeth (in the first two mesial teeth at least) seem indeed to be a condition shared by all compsognathids other than *Sinocalliopteryx gigas* (Currie and Chen 2001; Hwang et al. 2004; Ji et al. 2007*a*; Chiappe and Göhlich 2010; Dal Sasso and Maganuco 2011). Therizinosaurs have a highly diagnostic dentition showing a superficial convergence with the teeth of basal sauropodomorphs and ornithischians (Zhao and Xu 1998; Barrett 2000, 2009; Pu et al. 2013). Therizinosaurs are indeed characterized by toothless premaxillae, an important constriction between root and crown, both mesial and distal carinae terminating well-above the cervix, pointed denticles oriented apically from the mesial and distal margins, and a subequal number of denticles at mid-crown and the apex (pers. obs.).

The cladistic analysis performed on the supermatrix of 60 taxa yielded nine most parsimonious trees (MPTs), the strict consensus of which (length = 3583 steps; CI = 0.546; RI = 0.604) displays a large polytomy affecting Avetheropoda (Appendices A4.6, Fig. A4.7a). A poorly resolved consensus tree (95 MPTs of length = 3607 steps; CI = 0.529; RI = 0.58) with an important polytomy was also found when incorporating the four isolated teeth to the supermatrix (Appendices A4.6, Fig. A4.7b). This is due to the wildcard taxa *Erectopus* (either found as a Ceratosauridae, a basal Tetanurae or a Megalosauroidea) and *Piatnitzkysaurus* (nested within the clade of Tetanurae or Megalosauroidea). The deletion of these two wildcard taxa in the first analysis allows constraining all major theropod clades, with the exception of Deinonychosauria (Appendices A4.6, Fig. A4.7a–b). Indeed, due to the obvious convergence of their dentition (i.e., dentition showing constricted tooth

with weak or no distal curvature, unserrated crown, carinae bearing large hooked/pointed denticles, and teeth sometimes set in an open groove; Russell and Dong 1993*a*; Holtz et al. 1998; pers. obs.), Troodontidae are more closely related to *Shuvuuia* and Therizinosauria than to Dromaeosauridae. The cladistic analysis performed on the supermatrix of 58 taxa (isolated teeth excluded), and yielding 4 MPTs (length = 3529 steps; CI = 0.575; RI = 0.642), shows that only a few unambiguous (i.e., unique or non-homoplasious) dentition-based synapomorphies define theropods clades (Table 4.2; Appendices A4.6, Fig. A4.8). The large majority of dentition-based characters are homoplastic, demonstrating of a high degree of convergence among theropod dentitions. Several clades of theropods such as Ceratosauridae, Abelisauroidea, Noasauridae, Abelisauridae, Megalosauroidea and Therizinosauria are characterized by a combination of ambiguous synapomorphies (i.e., homoplasious state changes), and only Coelophysoidea, Averostra, Spinosauridae, Avetheropoda, Tyrannosauroidea, non-tyrannosauroid Coelurosauria and Dromaeosauridae are defined by both ambiguous and unambiguous synapomorphic characters (Table 4.2). With six and three unambiguous synapomorphies, Spinosauridae and Averostra, respectively, are the best supported clades in terms of dental characters, and the clade of Tyrannosauroidea only includes two unambiguous synapomorphies (Table 4.2).

When integrating the fourth isolated teeth, the cladistic analyses resulted in a poorly resolved consensus tree (Appendices A4.6, Fig. A4.9). However, by excluding the wildcard taxa *Erectopus* and *Piatnitzkysaurus*, the cladistic analysis performed on the supermatrix of 62 taxa yielded 49 MPTs and a well-resolved consensus tree (length = 3552 steps; CI = 0.563; RI = 0.628) that mirrors to a large degree the general classification of theropods (Fig. 4.2). The phylogenetic position of the four isolated teeth from the Lourinhã Formation will be discussed in the following sections after describing each of them thoroughly.

Systematic Palaeontology

Dinosauria Owen, 1842

Saurischia Seeley, 1887

Theropoda Marsh, 1881

Ceratosauria Marsh, 1884

Abelisauroidea Bonaparte, 1991

Abelisauridae Bonaparte and Novas, 1985

Gen. and sp. indet.

Referred material. ML 327 and ML 966 (Figs. 4.3–4.4).

Locality and horizon. Cliffs of Lourinhã, Lourinhã, Portugal. Lourinhã Formation, Kimmeridgian-Tithonian, Upper Jurassic.

Description. ML 327 lacks the lowermost part of the crown, a small piece of the mesial carina on the lingual face and a few denticles on the distal carina. However, the crown is well preserved and most of the denticles are intact. The apical part of the distal carina of ML 966 is also missing; otherwise this tooth is relatively well-preserved, with some part of the enamel cracked and missing.

Crown. The teeth are slightly elongated baso-apically (CHR of 1.58 in ML 327 and 1.95 in ML 966) and ziphodont in shape. Both crowns are only weakly curved distally, and the apex has been worn.

In lateral view, the distal carina is slightly concave, almost straight. The axis passing through the basal part of distal carina is perpendicular to the transversal plane of the crown. The mesial margin of the crown is much more recurved than the distal margin and the curvature is more important apically than basally. The apex is not acute and pointed, but slightly rounded. In ML 327, it shows a small spalled surface on the labial face and a large wear facet (Fig. 4.3A) corresponding to an elongated tongue-shaped surface bearing diagonal striations and inclined mesio-basally on the two thirds of the lingual side. The spalled surface on the lingual side of the crown in ML 966 is rather subtriangular and only limited to the apex. Both mesial and distal carinae are serrated from the base to the tip of the crown. The lingual surface of ML 327 bears a prominent longitudinal depression on its mesial part, 4 mm from the mesial carina at the mid-crown. This narrow groove (Fig. 4.3H) of 1.5 mm width extends from around 8.5 mm above the cervix (or neck of the tooth, cervix *sensu* Smith and Dodson 2003) and ends at a distance of 8 mm from the apex. The longitudinal depression roughly follows the curvature of the crown, is closer to the mesial carina at its basal and apical endings and almost contacts the large wear facet apically. No longitudinal groove is present on the labial face of the crown in ML 327 and on both labial and lingual sides of the tooth in ML 966.

In mesial view, the mesial carina of both teeth is concave and inclined baso-lingually. The carina remains medially positioned on the tip of the crown and twists lingually towards the root more basally and extends mesio-lingually to the cervix (Figs. 4.3B and 4.4B). The crown apex remains straight and follows the general curvature of the crown. The lingual surface is slightly baso-apically sigmoid with the basal part of the crown concave and the apical one convex. On the other hand, the entire labial surface of the crown is strongly convex baso-apically. There is a flattened surface at the base of the mesial margin which is delimited lingually by the mesial carina in ML 327. This flattened surface, which appears above the cervix, extends on the first third of the crown. In ML 966 however, the surface at the base of the mesial margin is strongly convex.

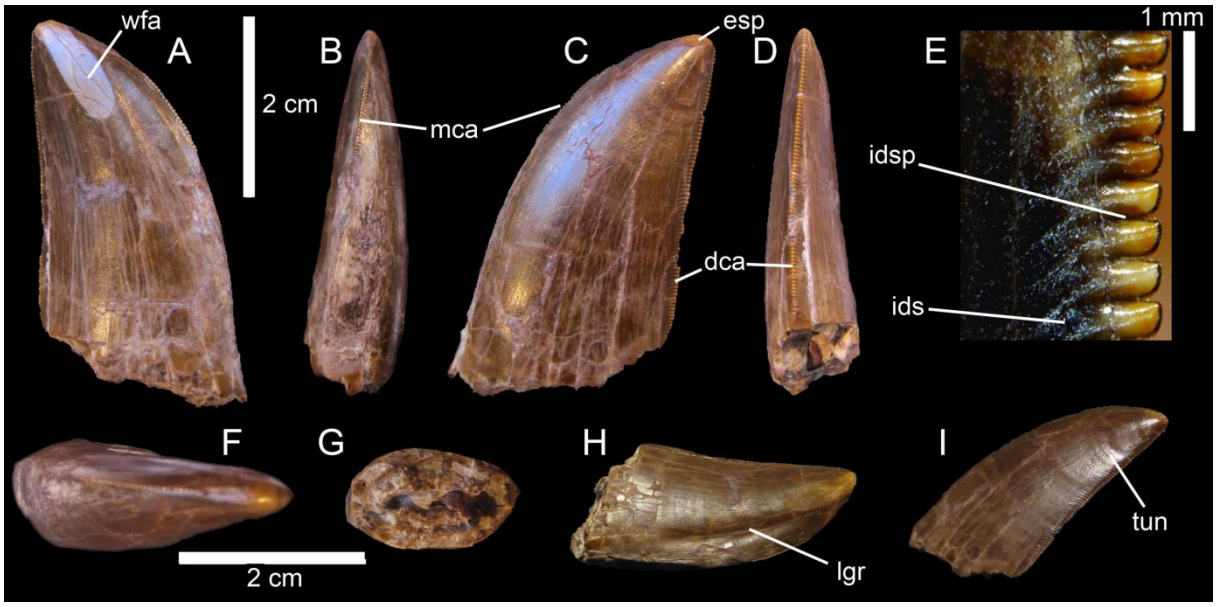

FIGURE 4.3. Isolated tooth (ML 327) of an Abelisauridae in **A**, lingual; **B**, mesial; **C**, labial; **D**, distal; **F**, apical; **G**, basal; **H**, mesio-lingual; and **E**, labio-distal views: **E**, apical denticles of the distal carina in labial view. **Abbreviations**: **dca**, distal carina; **esp**, enamel spalling; **ids**, interdenticular sulcus; **idsp**, interdenticular space; **lgr**, longitudinal groove; **mca**, mesial carina; **tun**, transverse undulation; **wfa**, wear facet.

In distal view, the distal carina is weakly sigmoid with a large bow oriented lingually along the basal two thirds of the crown while the apical part of the distal carina is straight. The carina is slightly lingually positioned on the distal margin of the crown, but moves medially at the tip.

In apical view, the tip of both crowns is distally positioned, with no curvature on the lingual or labial sides. The labial margin is globally convex, but the distal surface is rather flattened or weakly convex. On the contrary, the surface adjacent to the distal carina on the lingual margin is rather slightly concave. In ML 327, the mesial part of the labial face is strongly convex whereas the mesial part of the lingual surface has a double curvature due to the presence of the longitudinal depression. In both teeth, the distal carina is angular whereas the mesial carina forms a low, pointed ridge which strongly displaces lingually towards the root.

In basal view, the cross-section outline of the crown base is elliptical and slightly lanceolate (i.e., mesial margin convex and distal margin pointed) in ML 327 (Fig. 4.3G) whereas ML 966 has a well-marked lanceolate outline of the crown base (Fig. 4.4G). In ML 327, the mesial part is roughly triangular in shape with the tip of the triangle pointed lingua-mesially whereas the mesial part of ML 966 is strongly subtriangular with the tip of the triangle medially positioned. In both crowns, the distal margin of the crown forms a semicircle. The distal margin bears the superficial ridge of the distal carina which is mesio-lingually positioned. The labio-lingual width of the base of the crown is bigger mesially (CBW of 10.69 in ML 327 and 12.94 in ML 966). With their rather flattened bases, the middles of the lingual and labial faces are almost parallel. The middle of the labial surface remains roughly flat towards the tip while the lingual surface becomes strongly convex apically. In ML 327, the dentine layer is thin (1 mm on the labial margin) and becomes thicker in the distal part of the

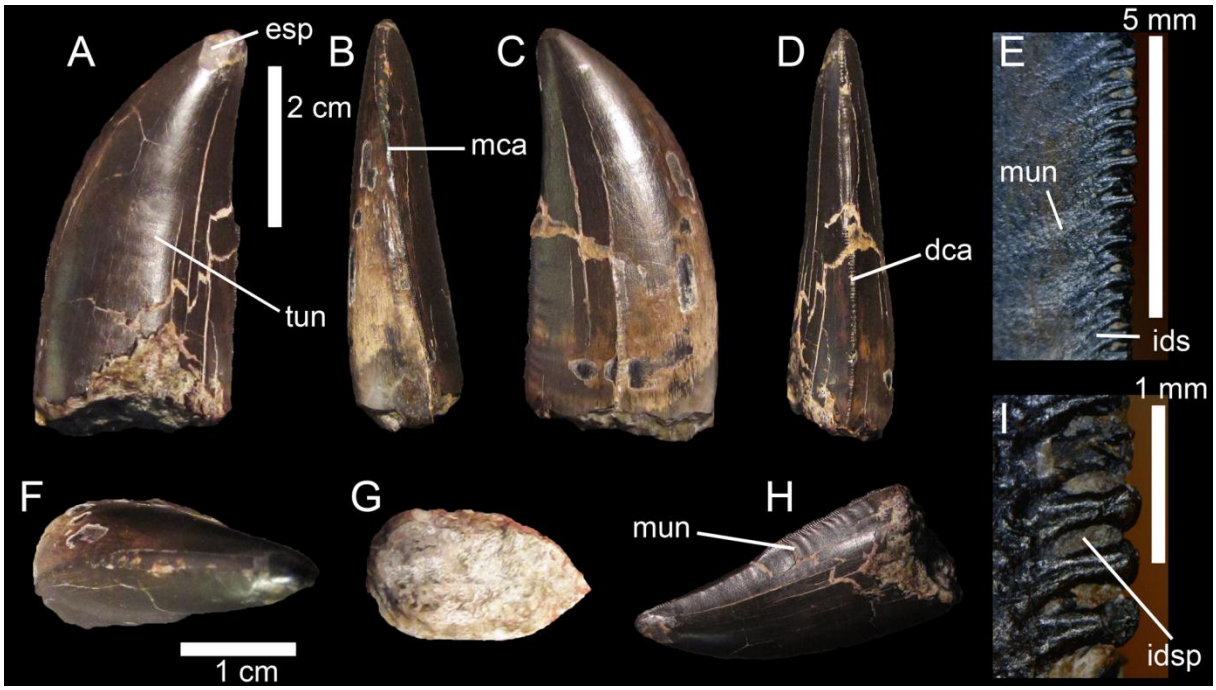

FIGURE 4.4. Isolated tooth (ML 966) of an Abelisauridae in **A**, lingual; **B**, mesial; **C**, labial; **D**, distal; **F**, apical; **G**, basal; and **H**, linguo-distal views; **E**, **I**, mid-crown denticles of the distal carina in lingual view. **Abbreviations**: **dca**, distal carina; **esp**, enamel spalling; **ids**, interdenticular sulcus; **idsp**, interdenticular space; **lgr**, longitudinal groove; **mca**, mesial carina; **mun**, marginal undulation; **tun**, transverse undulation.

crown (1.9 mm). Although the lingual margin has been damaged in this tooth, the pulp cavity seems to share the same lanceolate outline of the crown-base, but there is a weak labio-lingual constriction of the cavity 8 mm below the extremity of the distal carina.

Denticles. The mesial carina of ML 327 bears 11 denticles per 5 mm at the tip, 13 at the mid-crown and 20 near the cervix. In ML 966, the mesial carina shows the mesioapical denticles having been worn off, 15 at mid-crown, and 19 denticles at the base (Table 4.3). In both crowns, the denticles decrease in size towards the root at two thirds of the crown and the most basal denticles are minute. In lateral view, the mesial denticles are longer baso-apically than mesio-distally, which give them a subrectangular (or 'cartouche-like' *sensu* Harris 1998) outline. Since the denticles are inclined towards the tip of the crown and the main axis of the denticle is not perpendicular to the mesial margin of the crown, the shape of the denticle is rather parallelogram-shaped. The external margin of the mesial denticles is rounded and sometimes asymmetrically convex, with the concavity positioned slightly apically. In both teeth, the lingual and labial surfaces of the denticles are convex and the interdenticular space is shallow. In mesial view, the denticles are not labio-lingually large, they are roughly chisel-like in shape, but their external margin is rounded, and the main body of the denticles is almost cylindrical. There is no interdenticular sulcus between the mesial denticles in both teeth.

The distal carina of ML 327 has 12 denticles per 5 mm at the apex 13 at the mid-crown and around 15 at the crown base (but not near the cervix, this part being missing) so that they are similar in size to mesial denticles (DSDI of 1.14). In ML 966, 14, 12 and 14 denticles per 5 mm can be observed at the apex, mid-crown and base of the crown respectively and this tooth also share a DSDI close to

TABLE 4.3. Morphometric measurements of four isolated theropod teeth from the Lourinhã Formation of Portugal.

Specimen	ML 327	ML 966	ML 962	ML 939
Position	Isolated, lateral	Isolated, lateral	Isolated, mesial	Isolated, lateral
CBL	20.07	23.69	31.2	2.8
CBW	10.69	12.95	20.2	1
CH	31.76	46.41	85.8	5.1
AL	38.11	51.06	91.9	5.5
CBR	0.5326	0.5462	0.647	0.357
CHR	1.582	1.959	2.75	1.821
MA	11 (5mm)	?	?	?
MC	13 (5mm)	15 (5mm)	8 (5mm)	/
MB	20 (5mm)	19 (5mm)	/	/
DA	12 (5mm)	12 (5mm)	7 (5mm)	8 (1mm)
DC	11 (5mm)	14 (5mm)	8 (5mm)	9 (1mm)
DB	15 (5mm)	19 (5mm)	11 (5mm)	9 (1mm)
MAVG	14.66 (5mm)	16 (5mm)	8 (5mm)	?
DAVG	12.667 (5mm)	15 (5mm)	8.666 (5mm)	9.75 (1mm)
DSDI	1.14	1.06	0.931	?

one (Table 4.3). Unlike the mesial denticles, the distal denticles of both crowns are longer mesio-distally than baso-apically, except in the apical denticles which are squared-like in shape, and the main axis of the denticles is perpendicular to the distal margin. In lateral view, some distal denticles of ML 327 show an external margin pointing slightly towards the tip of the crown (Fig. 4.3E), so that the apical margin of the denticles is weakly concave whereas the basodistal margin is strongly convex. In all other distal denticles of ML 327 and all distal denticles of ML 966, the external margin is asymmetrically convex, with the denticle apex slightly apically positioned (Fig. 4.4I). In both teeth, the labial and lingual surfaces of the denticle body are convex. The distal denticles also have a deeper interdenticular space than the mesial ones and their external margin is more acute, giving them a real chisel-like shape in distal view. In ML 327, the enamel layer is thicker than in the mesial denticles and, in both teeth, most of denticles show an elongated interdenticular sulcus diagonally oriented basally away from the denticles (Figs. 4.3E and 4.4E). These shallow grooves are parallel to each other and extend from the base of the interdenticular space and run on both labial and lingual faces of the crown. They are shorter in the apical denticles, and completely absent in the most apical one, both on the labial and lingual surface. Their inclination also tends to be reduced towards the root with interdenticular sulci being almost perpendicular to the distal margin in the basal denticles.

Surface. The enamel surface of both crowns is very well preserved and shows perfectly a granular and irregular texture on both lingual and labial faces. Besides the large longitudinal depression present on the lingual face, transversal and shallow undulations are present on both lingual and distal surfaces in ML 327 (Fig. 4.3I). On the labial face of this tooth, they form large parabolic furrows curving apically near the distal carina, disappearing on the mesial part of the labial face due to the strong curvature of the crown. On the lingual face of this crown, they are visible distally, near the distal carina, and also in the middle of the crown, in the mid-crown surface. The undulations are

absent on both convex surface adjacent to the mesial carina and the longitudinal depression. Unlike the labial wrinkling, these undulations do not bent towards the tip of the crown near the carina. In ML 966, the transverse undulations are also clearly visible on both sides of the crown (Fig. 4.4A). They are particularly pronounced close to the distal carina on the labial margin where they also curve apically adjacent to the distal carina (Figs. 4.4E, H). As in ML 327, the transverse undulations are large, parabolic and shallow on the lingual side of the crown, and they do not curve towards the apex close to the carinae. In both teeth, these undulations are parallel and irregularly spaced and there are approximately 3 to 4 wrinkles per 5 mm on both faces of those crowns.

Discussion. Since the root is absent, ML 327 and ML 966 are most likely shed teeth. The labio-lingual compression of these moderately large teeth (CH > 30 mm), associated with serrated mesial and distal carinae and curvature of the tip distally, is a plesiomorphic condition seen in theropod dinosaurs. Amongst known large terrestrial Jurassic groups of vertebrates, this combination of characters is only seen in theropods.

Although ML 966 is slightly bigger than ML 327 (Table 4.3), both teeth can confidently be associated with the same taxon as they share the same outline, CBR, DSDI, and the following features: presence of well-developed interdenticular sulci pointing basally, transverse undulations on both labial and lingual faces, a mesial carina offset, strongly twisted lingually towards the root and reaching the cervix, a distal carina slightly sigmoid and lingually positioned, a lingual face baso-apically concave and a labial surface baso-apically sigmoid, and a lanceolate outline of the base-crown in cross-section. Nevertheless, some denticles of ML 327 differ from ML 966 as their external margin are pointing apically and are not asymmetrically convex on their entire distal margins. However, denticle curvature can vary in tooth row (Fanti and Therrien 2007; see below). The interdenticular space of the distal denticles is wider in ML 966, and the crown is also slightly more elongated than ML 327 (CHR of 1.95 and 1.58), but elongation of the crown also varies greatly along the tooth row in theropods (e.g., *Ceratosaurus*, *Allosaurus*, *Proceratosaurus*, *Tyrannosaurus*).

One of the most striking features in these two isolated teeth is the presence of tenuous to well-marked transverse undulations (‘enamel wrinckles’ *sensu* Brusatte et al. 2007) on the crown. Thought to be a possible tetanuran synapomorphy (Brusatte et al. 2007), transverse undulations are present on the crown of many theropods, from basal to derived forms, as well as metriorhynchid crocodylomorphs (De Andrade et al. 2010) and rauisuchian crurotarsans (Brusatte et al. 2009*a*), and this feature cannot therefore be considered as a reliable tool alone for identifying teeth. In theropods, they have indeed been observed in basalmost theropods such as *Sanjuansaurus gordilloi* (PVSJ 605) and *Eodromaeus murphi* (PVSJ 561), ceratosaurs such as *Ceratosaurus nasicornis* (USNM VP 4735), *Berberosaurus liassicus* (MNHN Pt369), *Genyodectes serus* (MLP 26-39), *Abelisaurus comahuensis* (MPCA 1, 229, 687), *Aucasaurus garridoi* (MCF-PVPH 236) and *Majungasaurus crenatissimus* (FMNH PR 2278), all non-Maniraptoriformes tetanurans (see Brusatte et al. 2007), and some

deinonychosaurs like *Troodon formosus* (DMNH 22337) and *Dromaeosaurus albertensis* (AMNH 5356).

ML 966 also displays pronounced undulations adjacent to the distal carina. Short and marginal undulations close to carinae are a well-known feature of carcharodontosaurids teeth (Sereno et al. 1996; Coria and Currie 2006) as they appear on the teeth of *Carcharodontosaurus saharicus* (SGM Din-1; UC PV6), *Mapusaurus roseae* (MCF-PVPH 108) and *Giganotosaurus carolinii* (MUCPv-CH-1). However, marginal undulations have also been reported among non-carcharodontosaurid theropods such as the abelisaurid *Skorpiovenator bustingorryi* (Canale et al. 2009). They actually seem to be present in a large range of non-coelurosaur averostrans as they have also been noticed in other ceratosaurs such as *Ceratosaurus nasicornis* (USNM 4735), *Abelisaurus comahuensis* (MPCA 5) and *Majungasaurus crenatissimus* (FMNH 2100), megalosaurids like *Afrovenator abakensis* (UC UBA1), *Megalosaurus bucklandii* (NHM R.234; OUMNH J.23014) and *Torvosaurus tanneri* (ML 1100), spinosaurids such as *Baryonyx walkeri* (NHM R.9951), *Suchomimus tenerensis* (MNN G35-9), and *Irritator challengeri* (SMNS 58022), and other allosauroids like *Allosaurus fragilis* (USNM 8335), *Neovenator salerii* (MIWG 6348) and *Acrocanthosaurus atokensis* (NCSM 14345).

Both teeth also possess a slightly curved distal profile of the crown, with the apex of the teeth located just apical to the most distal point of the crown at the cervix. This feature was considered to be a potential synapomorphy for Abelisauridae by Smith (2007) as a straight or slightly curved distal profile of the crown is seen in *Majungasaurus crenatissimus*, *Indosuchus raptorius*, *Rugops primus*, *Kryptops palaios*, *Aucasaurus garridoi* (Smith and Dalla Vecchia 2006; Smith and Lamanna 2006; Candeiro 2007; Smith 2007; pers. obs.) and many indeterminate abelisaurids (e.g., UCPC 10; MNHN MRS 1619, MRS 1620). Although the distal profile of the crown displays a strong curvature in most other theropods (Ezcurra 2009; pers. obs.), a weak curvature of the distal profile can also occur in some teeth of basalmost theropods (PVSJ 512), ceratosaurids (USNM 4735; MLP 26-39), noasaurids (PVL 4061), allosauroids (SGM Din1; MCF-PVH 108.43), tyrannosauroids (MIWG 1997.550; USNM 12814; FMNH PR2081) and some coelurosaurs (Currie et al. 1990: fig. 8.5A; Sankey et al. 2002: fig. 4.10); therefore, the systematic utility of this feature requires association with other characters.

Nevertheless, the presence of strongly developed and elongated interdenticular sulci between distal denticles seem to be a condition genuinely shared by non-maniraptoriform averostrans. This feature has been observed in the abelisaurids *Kryptops palaios* (MNN GAD1−1) and *Majungasaurus crenatissimus* (FMNH PR 2100, 2278), the megalosauroid *Piatnitzkysaurus floresi* (PVL 4073), the megalosaurids *Megalosaurus bucklandi* (OUMNH J13506) and *Torvosaurus tanneri* (ML 1100), the carcharodontosaurids *Giganotosaurus carolinii* (MUCPv-CH-1) and *Mapusaurus roseae* (MCF-PVPH-108), and the tyrannosaurid *Tyrannosaurus rex* (FMNH PR2081). However, an irregular texture of the enamel (i.e., no specific orientation of the enamel wrinkling texture) seems to be present in most non-tetanurans theropods such as Coelophysoidea and Abelisauroidea, some tyrannosaurids and many coelurosaurs, Compsognathidae and Deinonychosauria (pers. obs.). On the other hand, a

braided/veined oriented texture of the enamel has been observed in Ceratosauridae, Megalosauroidea, Allosauroidea and Tyrannosauroidea and it is therefore unlikely that ML 327 and ML 966 belong to one of those clades.

A peculiar anatomical feature of ML 327 is also the presence of distal denticles with an apex pointing towards the tip, a feature present in the teeth of some abelisauroids such as *Masiakasaurus knopfleri* (FMNH PR 2221, 2296), *Kryptops palaios* (MNN GAD1−1), *Rugops primus* (MNN IGU1), *Majungasaurus crenatissimus* (FMNH PR 2008, 2100, 2278) and other abelisaurid taxa (e.g., MUCPv 482; MUCPv 641). Among large theropods like ceratosaurids, megalosauroids, allosauroids and tyrannosauroids, the denticles are symmetrically rounded or slightly asymmetrically convex in lateral view and never hooked apically (*contra* Bakker and Bir 2004 for ceratosaurids and allosaurids, and Smith 2007 for tyrannosaurids; Currie et al. 1990; Abler 1992; pers. obs.). Slightly to strongly hooked distal denticles can also be observed in the basal saurischian *Eoraptor lunensis* (e.g., third right premaxillary tooth; PVSJ 512) and many Troodontidae (e.g., Currie 1987; Currie et al. 1990; Holtz et al. 1998; Longrich 2008; pers. obs.) and Dromaeosauridae (e.g., Currie et al. 1990; Baszio 1997; Currie and Varricchio 2004; Longrich 2008; pers. obs.). Deinonychosaurs, however, possess either very large and well-separated serrations, as in troodontids and *Saurornitholestes*, or a number of denticles per five millimeter larger than 14 on the distal carina (Smith et al. 2005). Likewise, both dromaeosaurids and *Masiakasaurus* tend to have distal denticles larger to mesial serrations (Currie et al. 1990; Currie and Varricchio 2004; Norell et al. 2006; Longrich 2008; pers. obs.). To our knowledge, neither noasaurids nor deinonychosaurs display a combination of pronounced and elongated interdenticular sulci and short marginal undulations on the crown.

Interestingly, ML 966 lacks hooked denticles on the distal carina as all denticles are either symmetrically or asymmetrically convex. This would therefore suggest that apically recurved denticles might not be present in all teeth along the tooth row. Denticle curvature seems indeed to vary in the dentition of *Majungasaurus crenatissimus* as strongly recurved denticles are present in lateral and mesial dentary teeth and slightly recurved to symmetrically rounded denticles are seen in some lateral and premaxilla teeth (Fanti and Therrien 2007; pers. obs.).

The presence of an elongated and deep groove adjacent to the mesial carina on the lingual side of the crown in ML 327 is another peculiar feature that, to our knowledge, has not been observed in any teeth belonging to a large theropod (crown with CH > 30 mm), and might therefore represent an autapomorphy. A concave surface adjacent to the mesial carina can be observed in the mesial teeth of many abelisaurids such as *Rugops primus* (MNN IGU1), *Indosuchus raptorius* (AMNH 1753) and *Majungasaurus crenatissimus* (FMNH PR 2100), but also in *Allosaurus fragilis* (AMNH 851), some tyrannosauroids such as *Proceratosaurus bradleyi* (NHM R 4860) and *Eotyrannus lengi* (MIWG 1997.550) and some dromaeosaurids like *Dromaeosaurus albertensis* (AMNH 5356). However, the surface adjacent of the mesial carina in ML 327 is convex and the concave area formed by the longitudinal groove is narrow. Longitudinal grooves running along the crown surface can also be

observed in several theropod taxa such as *Scipionyx samniticus* (Dal Sasso and Maganuco 2011), *Buitreraptor gonzalezorum* and *Austroraptor cabazai* (Gianechini et al. 2011*a*), in which there are two grooves separated by a large medial ridge (Gianechini et al. 2011*a*, *b*; pers. obs.). Likewise, the mesial groove present in ML 327 cannot be confused with the large medial concavity ('supradental groove' of Gong et al. 2010) present on the crown of many theropods like *Orkoraptor burkei* (Novas et al. 2008) and *Sinornithosaurus* (Gong et al. 2010), or the numerous flutes visible on the teeth of *Coelophysis bauri* (Buckley 2009), *Masiakasaurus knopfleri* (Carrano et al. 2002), *Ceratosaurus nasicornis* (Madsen and Welles 2000), spinosaurids (e.g., Charig and Milner 1997; Sereno et al. 1998; Sues et al. 2002), *Paronychodon lacustris* (e.g., Cope 1876*b*; Baszio 1997; Sankey et al. 2002; Sankey 2008) or *Velociraptor mongoliensis* (AMNH 6515).

On the basis of the combination of several important features in ML 966 and ML 327, a large crown (CH > 30 mm), an almost straight distal profile of the tooth, transverse and short marginal undulations on the crown, denticles with strongly developed interdenticular sulci, a DSDI close to one, an irregular enamel texture and the presence of apically pointed denticles on the distal carina in ML 327, these two teeth are assigned to a member of the Abelisauridae. Within this clade, ML327 and ML 966 only differ from other abelisaurids by having a strongly twisted mesial carina. However, this feature is also present in some basal abelisaurids such as *Abelisaurus* (MPCA 685). Also, ML 327 has a labially displaced distal carina which contrasts with the centrally positioned carina on the distal margin of the crown of abelisaurids (pers. obs.).

Bivariate plots of CBR and CHR reveal that ML 966 and ML 327 mainly occupy the same area of values as Abelisauridae (*Majungasaurus* + indeterminate abelisaurids), *Ceratosaurus*, *Allosaurus*, *Acrocanthosaurus* and *Gorgosaurus* teeth (Fig. 4.5). However, bivariate plots with MAVG or DAVG clearly show that the two teeth possess smaller mesial and distal denticles than any abelisaurids represented, with a number of denticles per five mm situated among the values of *Allosaurus*, *Acrocanthosaurus* and *Berberosaurus* (Figs. 4.6–4.8). The number of denticles per five mm of ML 966 and ML 327 are indeed situated between 13 to 16, a higher number than in *Majungasaurus*, *Indosuchus*, *Rugops* and UCPC 10 (Smith 2007; Sereno and Brusatte 2008; pers. obs.), but comparable to that of the most basal abelisaurid *Kryptops* (Sereno and Brusatte 2008) and *Abelisaurus* (pers. obs.).

Due to the relatively important labiolingual compression of the crown base (CBR close to 0.5), ML 966 and ML 327 are most likely lateral teeth and have therefore been coded as such in our datasets. When the two isolated teeth are included in the dentition-based data matrix, the resulting consensus tree of the cladistic analysis recovered both teeth together in a well-supported clade (Bremer support of 4) nested among abelisaurid theropods (Fig. 4.1). Both isolated teeth form the sister taxon of a clade encompassing the abelisaurids *Rugops*, *Kryptops* and *Majungasaurus*, and the monophyletic group formed by ML 966, ML 327 and these three abelisaurids is supported by two ambiguous synapomorphies: the long and well-developed interdenticular sulci of basal and mid-crown

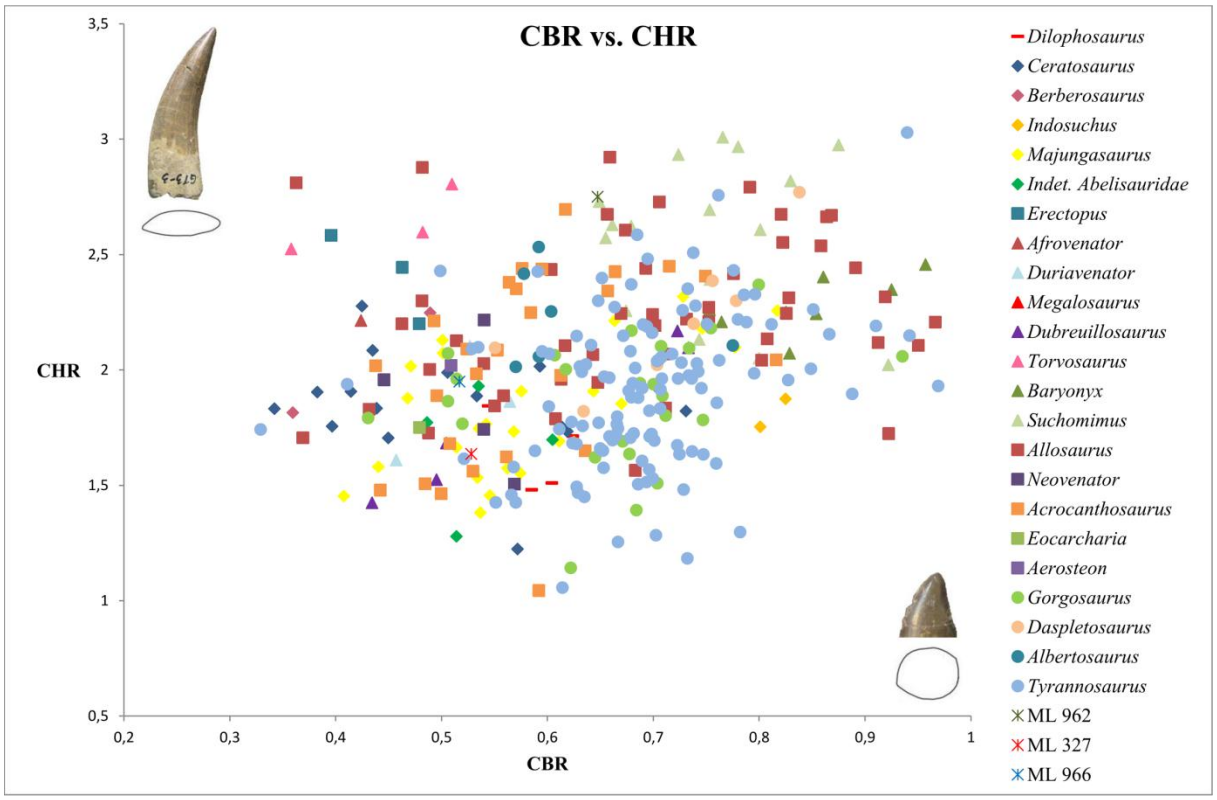

FIGURE 4.5. Plots of CBR versus CHR of ML 962, ML 327, ML 966 and 23 theropod taxa comprising the data set. For reasons of clarity, only taxa with CBR of less than 1 were considered.

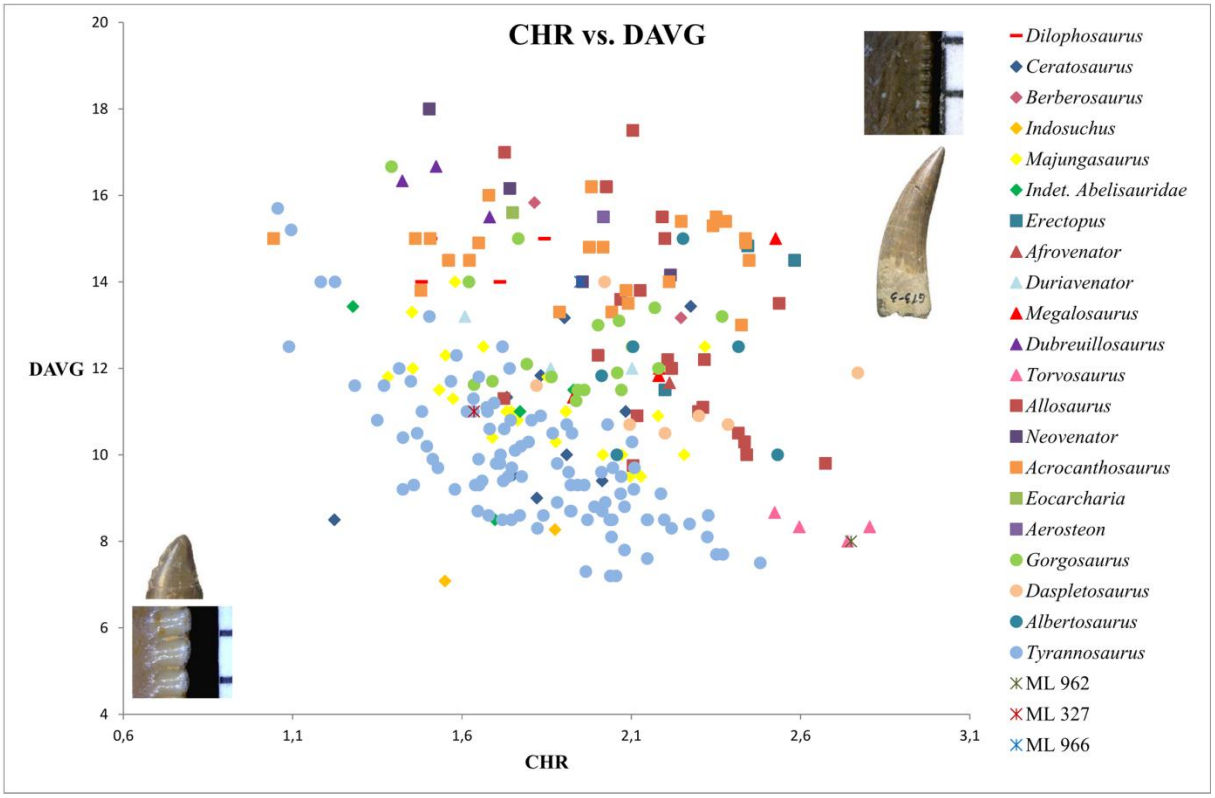

FIGURE 4.6. Plots of CHR versus DAVG of ML 962, ML 327, ML 966 and 21 theropod taxa comprising the data set. For reasons of clarity, only taxa with serration of less than 20 denticles were considered.

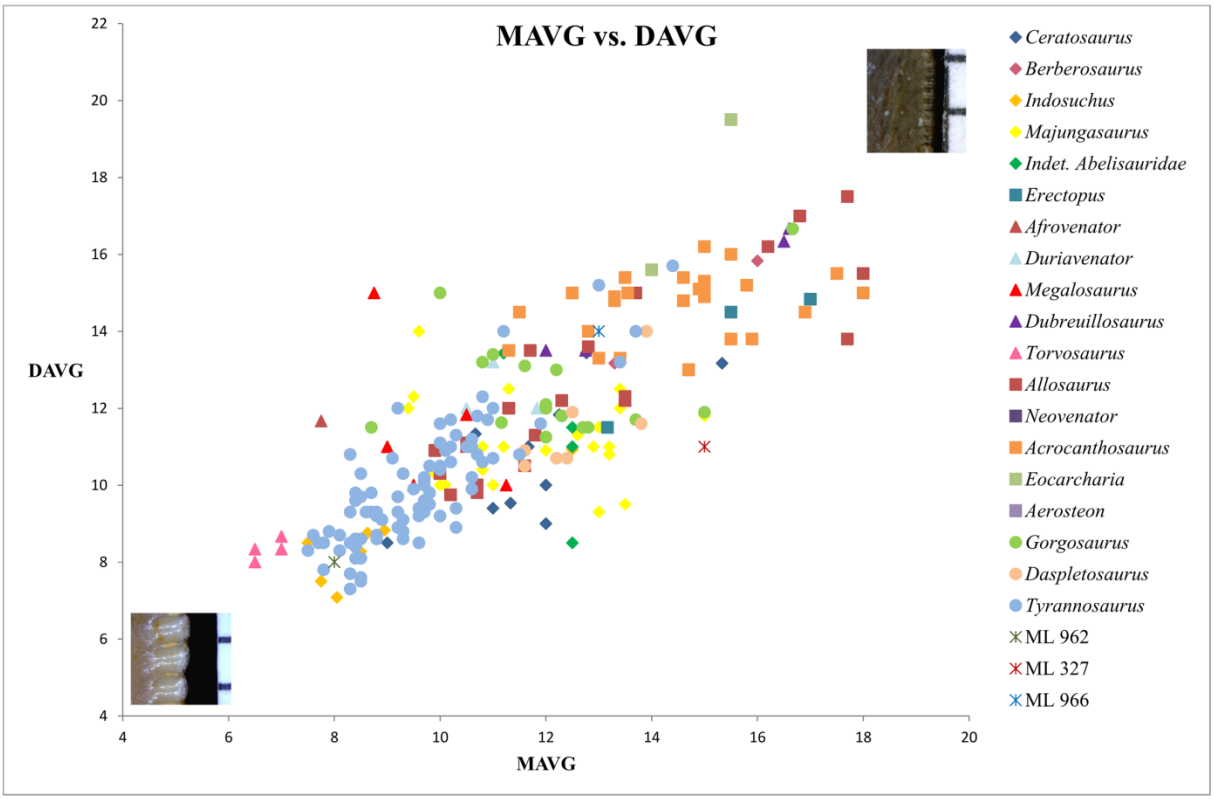

FIGURE 4.7. Plots of MAVG versus DAVG of ML 962, ML 327, ML 966 and 19 theropod taxa comprising the data set. For reasons of clarity, only taxa with serration of less than 20 denticles were considered.

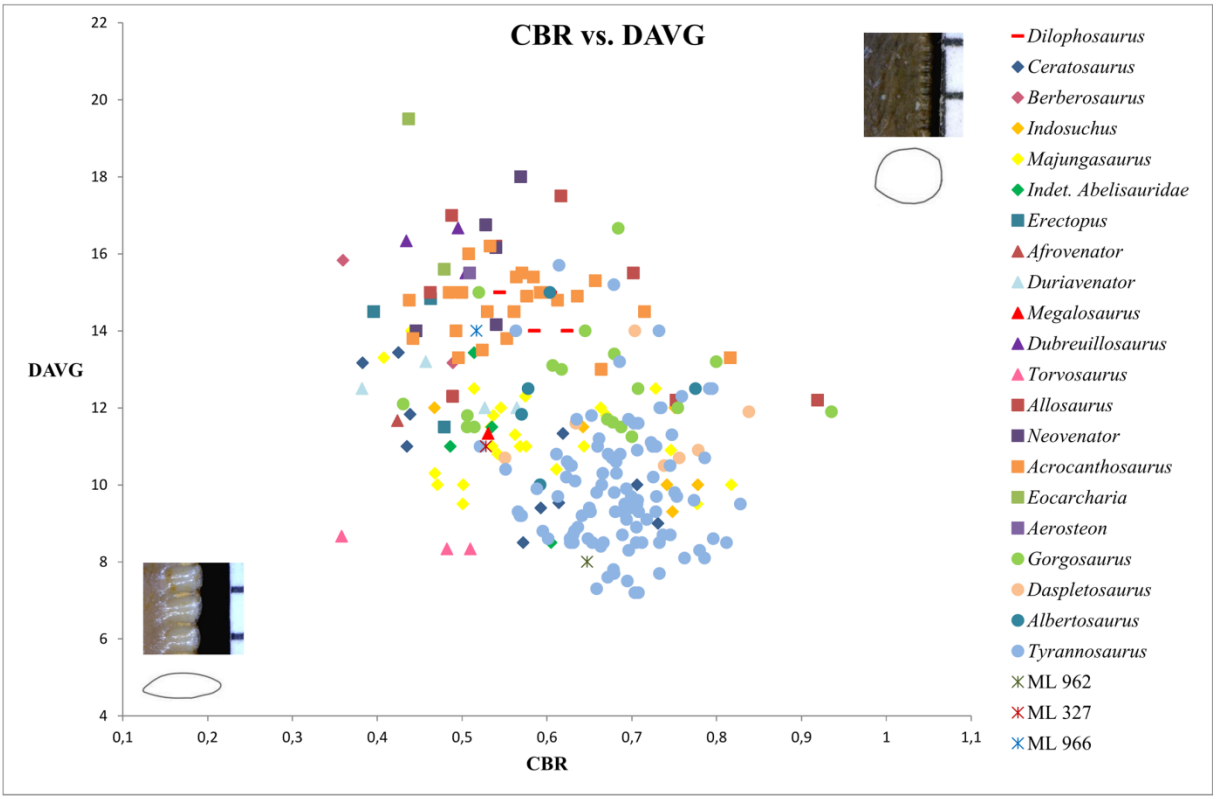

FIGURE 4.8. Plots of CBR versus DAVG of ML 962, ML 327, ML 966 and 21 theropod taxa comprising the data set. For reasons of clarity, only taxa with serration of less than 22 denticles were considered.

denticles on the distal carina (chars. 105 and 106). When incorporated into the supermatrix, the cladistic analyses resulted in a poorly resolved consensus tree in which ML 327 and ML 966 were found as a sister-taxa among the clade of Abelisauridae (Appendices A4.6, Fig. A4.9). The deletion of the wildcard taxa *Erectopus* and *Piatnitzkysaurus* resulted in a better resolved consensus tree in which ML 327 and ML 966 are still nested in the same clade within Abelisauridae (Fig. 4.2).

Tetanurae Gauthier, 1986

Megalosauroidea Fitzinger, 1843

Megalosauridae Fitzinger, 1843

Torvosaurus tanneri Galton and Jensen, 1979

Referred material. ML 962 (Fig. 4.9).

Locality and horizon. Cliffs of Praia da Area Branca North, Praia da Area Branca, Lourinhã, Portugal. Bombaral Member, Lourinhã Formation, Tithonian, Upper Jurassic.

Description. ML 962 is an elongated tooth lacking the mesial part of the tip. Although most of the mesial and distal denticles are damaged and missing, their bases are still present so that it was possible to count the number of denticles basally, apically and at the mid-crown.

Crown. The tooth is particularly large (CH of 85 mm) and the general shape of the tooth resembles the 'typical' blade-like theropod tooth by being labiolingually compressed, distally curved and having serrated carinae. However, the base is particularly narrow mesio-distally (CBL of 31.5 mm) and quite large labio-lingually (CBW of 20.2 mm) so that the crown-base has an ovoid cross-section (CBR of 0.64).

In lateral view, the mesial and distal margins of the root and basal half of the crown are roughly straight whereas the distal half of the crown is bent distally. The curvature of the crown is larger mesially than distally and the base of the crown is slightly larger than the mid-crown mesio-distally.

In distal view, the distal carina is medially positioned, slightly curved and bowed labially. The carina bears denticles all along the crown edge, from the preserved tip of the crown to the cervix.

In mesial view, the mesial carina, on the other hand, appears at the mid-crown, approximately 30 mm from the cervix, the basal part of the crown remaining smooth and rounded (Fig. 4.9D). The carina is labially positioned and weakly offset apically and slightly curves lingually towards the root, becoming medially positioned on the mesial margin of the crown. Both lingual and labial surfaces are baso-apically concave and the root surface remains almost straight.

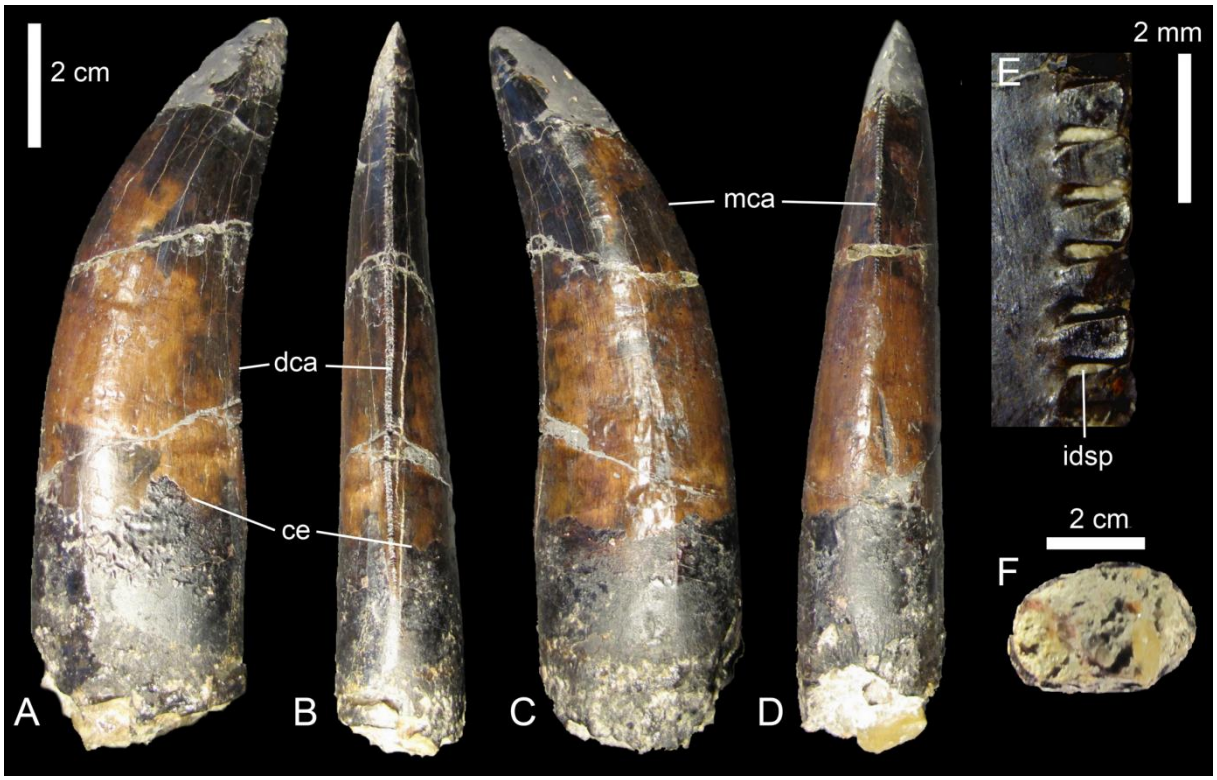

FIGURE 4.9. Isolated tooth of *Torvosaurus tanneri* (ML 962) in **A**, labial; **B**, distal; **C**, lingual; **D**, mesial; and **F**, basal views; **E**, apical denticles of the distal carina in labial view. **Abbreviations**: **ce**, cervix; **dca**, distal carina; **idsp**, interdenticular space; **mca**, mesial carina.

In apical view, the tip is weakly labio-lingually oriented and medially positioned on the crown. The mesial carina forms just a low ridge whereas the distal carina is more acute, and bends lingually towards the root.

In cross section, the basal crown is elliptical (Fig. 4.9F) with both mesial and distal parts rounded. The labial face shows a short flattened surface in its center whereas the lingual margin is weakly convex. Both labial and lingual surfaces are strongly mesio-distally convex all along the crown. The dentine layer is thin (0.6 mm in the lingual part) and its thickness is greater on the distal part of the crown (1.7 mm), the mesial part being absent. The length of the pulp cavity is 17.8 mm labio-lingually and around 28 mm mesio-distally.

Denticles. The mesial carina has 8 denticles at the mid-crown, and the number of denticles near the apex is unknown due to the missing part of tip of the crown (Table 4.3). The size of the denticles decreases towards the root from approximately the two thirds of the crown, a tendency also observable on the distal carina, but on a much longer distance.

The distal carina bears around 7 denticles per 5 mm at the apex, 8 at the mid-crown and 11 at the base of the crown, the latter being minute near the cervix. The biggest denticles can be found 20 mm below the apex of the crown and are the only denticles entirely preserved on the apical part of the distal carina. They are chisel-like in shape, mesio-distally longer than baso-apically and their main

axis is perpendicular to the distal margin (Fig. 4.9E). A transversal section of the denticles would reveal a triangular shape as their bases are labio-lingually large and their tips are angular.

The labial and lingual surfaces of both mesial and distal denticles are slightly convex or completely flattened baso-apically, and only their basal and apical borders are rounded and curved to form the limits of the interdenticular spaces. The latter are deep and narrow and often filled with sediments. Their width tends to decrease towards the tip of the denticles which is slightly wider baso-apically than the base.

The external margin of mesial and distal denticles is symmetrically and slightly convex and does not point towards the tip of the crown. The denticle surface is covered by enamel, but the layer of enamel has disappeared in the middle of several denticles surfaces. This might, however, be due to erosion rather than initial wear. A few other denticles are also preserved on the basal part of the distal carina. They are quite different from the apical denticles by having a much more rounded external margin. The denticles are symmetrically rounded in lateral view and their labial and lingual surfaces are strongly convex. The interdenticular space is shallower and also slightly wider than in the apical denticles.

The mesial and distal denticles differ in their elongation; the few preserved denticles on the mesial carina are longer baso-apically than mesio-distally. The interdenticular space of mesial denticle is narrow and deep and the external margin of the denticle is slightly convex, almost flat.

Short interdenticular sulci appear between the distal denticles, but not in the most apical and basal ones. These shallow grooves running on both labial and lingual surfaces of the crown are inclined towards the root and more pronounced on the lingual face. They are, however, totally absent between the mesial denticles.

Surface. The crown surface is rugged and show many irregularities. Possibly due to erosion and wear, the enamel texture of the crown is completely smooth and does not show any microscopic sculpturing. Two large transverse undulations appear on both labial and lingual surfaces of the basal part of the crown, but those deep structures do not correspond to the numerous and shallow transverse undulations illustrated by Brusatte et al. (2007) and might be due to deformation.

Discussion. Since most of the root is missing and the pulp cavity is excavated and filled with sediment, we interpret ML 962 as a shed tooth (Bakker and Bir 2004). A very large and fairly straight crown showing a labio-lingually compression, distinct serrations on mesial and distal carinae, and a slight curvature of the tip distally is a combination of characters observed in theropod dinosaurs only (Buffetaut and Ingavat 1986), especially in the Upper Jurassic of Portugal (pers. obs.).

With a crown height of more than eight centimeters (CH of 85.8 mm), ML 962 is a large crown belonging to a particularly large theropod. Although size is a plastic feature and must be used carefully for systematic purpose, this feature has already been demonstrated to be useful for discriminating teeth of different theropod taxa (Smith 2005; Smith et al. 2005; Han et al. 2011). Indeed, to our knowledge, crowns of more than eight centimeters are only borne by non-coelurosaur

averostrans and derived Tyrannosauroidea, as they can be found in Ceratosauridae (*Ceratosaurus*, *Genyodectes*), Megalosauroidea (e.g., *Torvosaurus* and *Spinosaurus*), Allosauroidea (e.g., *Carcharodontosaurus*, *Mapusaurus*, *Giganotosaurus*) and Tyrannosauridae (e.g., *Tyrannosaurus*, *Tarbosaurus*).

The denticles of ML 962 are also particularly coarse and an average of 8 denticles per 5 mm on both carinae is a condition present in particularly large basal tetanurans. Such feature can indeed be observed in Megalosauridae (Rauhut and Werner 1995; Smith 2007; pers. obs.), Carcharodontosaurinae (Rauhut and Werner 1995; Veralli and Calvo 2004; Coria and Currie 2006; pers. obs.) and Tyrannosauridae (Rauhut and Werner 1995; Smith 2005; pers. obs.). To our knowledge, less than 9 denticles on both mesial and distal carinae is a feature absent in basal Megalosauroidea (e.g., *Piatnitzkysaurus*), some Megalosauridae (e.g., *Eustreptospondylus*, *Dubreuillosaurus*), non-carcharodontosaurine Allosauroidea (e.g., *Allosaurus*, *Neovenator*, *Acrocanthosaurus*), and all Ceratosauridae and Spinosauridae (pers. obs.). *Indosuchus raptorius* (AMNH 1753, 1955, 1960) is the only abelisaurid possessing less than 8 denticles per 5 mm on both carinae, but the teeth are typical of abelisaurids as their crowns are low and weakly recurved distally. It is therefore unlikely that ML 962 belongs to one of these groups of theropods.

With an elliptical outline of the crown base in cross-section (CBR of 0.6) and a strong elongation, ML 962 is also very peculiar. In most carnivorous theropods, the lateral teeth are usually strongly mediolaterally flattened, giving a lenticular or lanceolate outline of the crown base in cross-section, and an elliptical outline of the crown base is usually present in mesial teeth, i.e., the premaxillary and mesial teeth of the dentary and maxilla (pers. obs.). Among basal tetanurans except Spinosauridae (which possess conical and fluted crowns along the tooth row), an ovoid subcircular outline of the crown base can clearly be observed in mesial teeth of megalosaurids such as *Duriavenator hesperis* (NHM R.332), *Dubreuillosaurus valesdunensis* (MNHN 1998-13) and *Torvosaurus tanneri* (Britt 1991) and allosauroids like *Acrocanthosaurus atokensis* (NCSM 14345) and *Giganotosaurus carolinii* (MUCPv-CH-1; Candeiro 2007). Some tetanurans like *Acrocanthosaurus*, *Giganotosaurus* and *Tyrannosaurus* can also have an ovoid cross-section of the crown base more distally in the jaws (Smith 2005; Candeiro 2007; pers. obs.). Nevertheless, the lateral teeth of those theropods are much more massive and incrassate, the labiolingual width of the crown base being sometimes equal or larger than its mesiodistal length in Tyrannosauridae, giving them the typical ‘banana’ shape (Smith 2005; pers. obs.). We therefore interpret ML 962 as a mesial tooth of a basal tetanuran.

This large crown also possesses a mesial carina medially positioned on the mesial margin of the crown, running slightly diagonally and terminating at the mid-crown, well above the cervix. Among mesial teeth of tetanurans, such a combination of features can be observed in Megalosauridae such as *Torvosaurus tanneri* (BYU-VP 2003), *Duriavenator hesperis* (NHM R.332) and *Dubreuillosaurus valesdunensis* (MNHN 1998-13) as well as the carcharodontosaurid

Acrocanthosaurus atokensis (NCSM 14345). In Allosauridae and Tyrannosauroidea, the mesial carina extends to the cervix of the crown, or very close to it, and either twists lingually like in *Allosaurus fragilis* (AMNH 851; CMNH 21703; SMA 0005/02) and *Proceratosaurus bradleyi* (Rauhut et al. 2010) or faces entirely lingually in more derived tyrannosauroids, giving the typical D-shaped cross-section of the base-crown (Smith 2005; Sereno et al. 2009; pers. obs.). The distal carina of ML 962 is also centrally positioned on the distal margin of the crown, a similar feature visible in the mesial teeth of megalosaurids such as *Eustreptospondylus oxoniensis* (OUMNH J.13558), *Dubreuillosaurus valesdunensis* (MNHN 1998-13) and *Duriavenator hesperis* (NHM R.332). On the other hand, the distal carina of mesial teeth of carcharodontosaurids such as *Acrocanthosaurus atokensis* (NCSM 14345) and *Giganotosaurus carolinii* (MUCPv-CH-1) is slightly to strongly displaced labially on the distal margin of the crown (a similar feature is found in *Genyodectes* and *Dromaeosaurus* for instance; Currie et al. 1990; Rauhut 2004*b*; pers. obs.), so that the mesial and distal carinae are not aligned on a same plan like in megalosaurid theropods (pers. obs.). It is, therefore, more likely that ML 962 belongs to Megalosauridae than Carcharodontosauridae.

Among Megalosauridae, a very large and strongly elongated crown (CHR > 2.5) with large chisel-like and symmetrically rounded denticles (less than 9 denticles on the distal carina) seems to be a combination of characters only seen in *Torvosaurus* (pers. obs.). The general shape and outline of ML 962 also resemble very much those of one probable *Torvosaurus tanneri* shed tooth illustrated by Jensen (1985: fig. 5e) and the first dentary tooth of *Torvosaurus* (BYU-VP 2003). These two teeth share with ML 962 same curvature and elongation as well as a lateral face that is particularly convex. In addition, the outline of the basal crown seems to fit with the alveoli of the mesial alveoli of the dentary of *Torvosaurus* (Britt 1991: fig. 3f), the premaxillary alveoli being more elongated mesio-distally (or labio-lingually for the first alveolus).

Both morphological and cladistic analyses support the identification of ML 962 to the taxon *Torvosaurus*. Bivariate plots of MAVG and DAVG (Fig.4.7) show that ML 962 possesses the same number of denticles per five mm as *Carcharodontosaurus*, *Tyrannosaurus* and *Indosuchus*, and close values of denticles as *Torvosaurus*. However, bivariate plots of CHR and DAVG clearly illustrates the same values of ML 962 and *Torvosaurus* teeth (Fig. 4.6), on the opposite of bivariate graphs with CBR, as CBR values of ML 962 and *Torvosaurus* teeth are significantly different (Figs. 4.5, 4.8). This can be explained by the absence of mesial teeth of *Torvosaurus* in our dataset. As it has already been mentioned previously, mesial teeth of many theropods are usually labiolingually thicker than lateral teeth, and this is clearly the case in *Torvosaurus* and Megalosauridae in which mesial teeth have an elliptical to rounded cross-section at the crown base instead of a lenticular outline typically present in the lateral teeth of these taxa. Following this observation, characters on mesial teeth were only coded in ML 962 in our data matrix.

The cladistic analysis performed on the data matrix of dentition-based characters recovered ML 962 as a megalosaurid theropod, forming a polytomy with all members of this clade (Fig. 4.1).

This lack of resolution can be explained by the absence of mesial teeth in *Afrovenator* and *Megalosaurus*, and the little information collected from mesial dentition of *Eustreptospondylus*, *Duriavenator* and *Torvosaurus* in our dataset. A similar position within the megalosaurid clade was found when the cladistic analysis was performed on the supermatrix, but ML 962 forms a polytomy with the megalosaurids *Torvosaurus*, *Megalosaurus*, *Afrovenator* and *Duriavenator* that bear large teeth (Fig. 4.2; Appendices A4.6, Fig. A4.9).

Following the results of both cladistic and morphological analyses, we identify ML 962 as a mesial tooth, perhaps a dentary tooth, belonging to the species *Torvosaurus tanneri*. Material of *Torvosaurus tanneri* are not rare in the Kimmeridgian – Tithonian of Europe and North America and have been reported several times in the Lourinhã Formation previously (Mateus and Antunes 2000*a*; Mateus 2005; Mateus et al. 2006). Therefore, this referral to *Torvosaurus* is consistent both stratigraphically and biogeographically.

Avetheropoda Paul, 1988

Coelurosauria Huene 1914*a*

Dromaeosauridae Matthew and Brown, 1922

Richardoestesia Currie et al., 1990

Richardoestesia aff. *Richardoestesia gilmorei* Currie et al., 1990

Referred material. ML 939 (Fig. 4.10).

Locality and horizon. Cliffs of Valmitão South, Lourinhã, Portugal. Amoreira-Porto Novo Member, Lourinhã Formation, Tithonian, Upper Jurassic.

Description. The crown is entirely preserved and shows an important spalled surface extending on the distal part of the mesial margin of the tooth. A small piece and some denticles of the distal carina are missing, yet most of them are intact and well-preserved. The tooth only preserved the basal part of the root.

Crown. The crown is small (CH of 5.1 mm), slightly elongated (CBH of 1.82) and strongly compressed labio-lingually (CBR of 0.5; Table 4.3). The tip is strongly recurved distally and the apex is pointed, mostly due to the wear facet. The mesial carina is missing and might have been worn on the tip of the crown. The distal carina is serrated and bears denticles from the cervix to the apex.

In lateral view, the crown has a straight crown along the basal part which then abruptly curves distally at two thirds of its height at an angle of 55° to the vertical, forming an acute backward tip. The most basal part of the crown is slightly constricted mesio-distally, but the constriction only occurs on the mesial margin of the crown, the distal margin being straight along the first fourth of the crown.

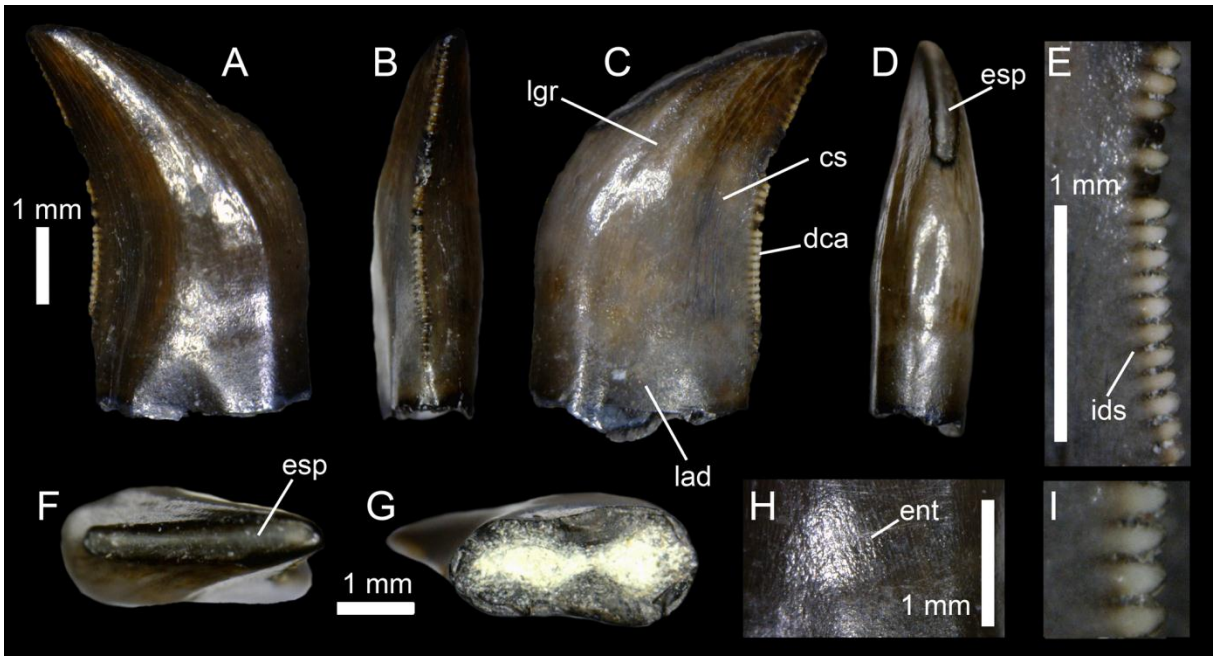

FIGURE 4.10. Isolated tooth (ML 939) of *Richardoestesia* aff. *gilmorei* in **A**, lingual; **B**, distal; **C**, labial; **D**, mesial; **F**, apical; and **G**, basal views; **E, I**, mid-crown denticles of the distal carina in labial views; and **H**, enamel texture in lingual view. **Abbreviations**: **cs**, concave surface; **dca**, distal carina; **ent**, enamel texture; **esp**, enamel spalling; **ids**, interdenticular sulcus; **idsp**, interdenticular space; **lad**, labial depression; **lgr**, longitudinal groove.

The distal carina is universally concave, but the carina is curved above the straight basal margin and the distal part of the carina is straight. The mesial margin is convex above the cervix only on the basal half of the crown, the other half remaining flat due to the wear facet. A convex surface delimited by a longitudinal groove mesially and a flattened or slightly concave surface distally appears on both lingual and labial faces. This large mesial ridge follows the same curvature of the crown and its mesio-distal width decreases towards the tip. It starts one-third of the way from the base of the crown on the labial face and from the apical part of the root on the lingual surface. Both lingual and labial grooves are narrow and reach the wear facet at the tip.

In mesial view the crown tip is straight and curves neither labially nor lingually. Both labial and lingual faces are weakly convex and the crown-base width is slightly narrower than the mid-crown width. The crown remains, however, strongly compressed labio-lingually all along its height, and the crown width slightly decreases from the mid-crown to the tip.

In distal view, the most basal part of the serrated carina is straight and vertical, but then curved all along the rest of the crown with the bow directed lingually. The distal carina is slightly oriented lingually (we regarded the lingual face of the crown as the face towards which the distal carina was displaced, at it is almost always the case in theropods; pers. obs.), and the lingual face adjacent to the carina is flat whereas the labial surface near the carina is concave.

In apical view, the basal part of the mesial margin is strongly convex and the wear facet situated on the distal part forms a narrow flat surface revealing the enamel and the dentine layers. In

basal view, the crown-base forms an eight-shaped in cross section (Fig. 4.10G) due to the basal concavity on both labial and lingual side of the crown. The concave surface on the lingual face is shallow, triangular in shape and extends on one-third of the crown whereas the one on the labial face is slightly deeper and ends at the cervix level. The mesial part of the crown is labio-lingually wider (1.2 mm) than the distal part (1 mm). The dentine layer is thicker in the center of both labial and lingual sides, giving an even well-pronounced eight-shaped to the pulp cavity, thinner distally.

Denticles. Only the distal carina is preserved and serrated, and the morphology of the denticles varies along the carina. With 10 denticles per 1 mm basally and at the mid-crown and 9 apically, the denticles slightly increase in size near the apex. The basal denticles are longer mesio-distally than baso-apically. In lateral view, they are tongue-shaped with their external margin strongly convex, parabolic and symmetrically rounded or slightly pointing towards the tip of the crown (Fig. 4.10I), giving them an asymmetrical outline. Although the basal denticles become mesio-distally shorter towards the root and the mid-crown, they share a same baso-apical width than denticles at mid-height of crown. On the other hand, the apical denticles are short and baso-apically larger than the basal ones. The most apical denticles are cartouche-shaped with their external margin symmetrically or asymmetrically convex. These denticles are also mesio-distally short and just form a small symmetrical bump at the apex in lateral view. In apical view, the lingual and dorsal surfaces of the body of the denticles are convex, and the denticle tip is chisel-like in shape.

The interdenticular sulci of basal denticles are absent or very short. When present, they are shallow and straight, extending perpendicular to the distal margin on the labial and lingual faces from between the denticles. The interdenticular sulci are totally absent in the apical denticles. The interdenticular space of distal denticles is narrow, slightly larger in the apical denticles, and usually filled with sediment.

Surface. The enamel texture of the crown surface is irregular and show finely wrinkled non-oriented structures on both sides (Fig. 4.10H). Except for the presence of those microscopic sculptures, there is no other ornamentations on the crown surface.

Discussion. ML 939 is interpreted as a shed tooth as it lacks most of the root and the pulp cavity is slightly excavated.

The presence of a basal constriction between the crown and root has been observed in basal most theropods like *Eoraptor lunensis* (Sereno et al. 1993, 2013) and many coelurosaurs such as the tyrannosauroid *Proceratosaurus* (Rauhut et al. 2010), the compsognathid *Compsognathus* (Zinke and Rauhut 1994), the ornithomimosaur *Pelecanimimus* (Pérez-Moreno et al. 1994), alvarezsaurids (Perle et al. 1993), basal oviraptorosaurs (Osmólska et al. 2004), therizinosaurs (e.g., Russell and Dong 1993*a*; Zhao and Xu 1998; Kirkland et al. 2005; Pu et al. 2013), troodontids (e.g., Currie et al. 1990; Baszio 1997; Norell et al. 2000; Currie and Dong 2001*a*; Sankey et al. 2002; Averianov and Sues 2007), the dromaeosaurids *Microraptor* (Xu et al. 2000; Hwang et al. 2002), and many basal avialans such as *Archaeopteryx* and *Cathayornis* (Hou 1997; Feduccia 2002).

Nevertheless, the presence of an eight-shaped outline of the crown-base in cross-section is a common feature of many deinonychosaurs such as *Saurornitholestes* (Currie et al. 1990; Sankey et al. 2002), *Tsaagan* (Norell et al. 2006), *Pyroraptor* (Allain and Taquet 2000; Gianechini et al. 2011*b*), *Buitreraptor* (Gianechini et al. 2011*b*) and the enigmatic theropod *Richardoestesia gilmorei* (Currie et al. 1990). With perhaps the exception of *Berberosaurus* (MNH Pt339), the crown base of non-maniraptoriform theropods like coelophysoids, ceratosaurs, megalosauroids, allosauroids and most of tyrannosauroids can be subcircular, ovoid, elliptical, lenticular or bean-shaped and not eight-shaped (pers. obs.). This also seems to be the case in more derived coelurosaurs such as Compsognathidae (e.g., Zinke 1998: fig. 2; Dal Sasso and Maganuco 2011: fig. 44 to 48), therizinosaurs (Clark et al. 1994: fig. 12; Zhao and Xu 1998: fig. 1), Oviraptorosaurs (Balanoff et al. 2009: fig. 2-7) and perhaps *Ornitholestes hermanni* (AMNH 619). The latter possesses a median concave surface on the labial surface of some crowns, but does not seem to have any on the lingual one, giving a bean-shaped outline of the crown base in cross section (pers. obs.). The tyrannosaurid *Alioramus altai* (IGM 100-1844) and the neovenatorid *Orkoraptor burkei* (Novas et al. 2008; Benson et al. 2010) are two exceptions; the latter possesses a particularly developed median depression on both labial and lingual sides of the crown. To our knowledge, it represents the second non-coelurosaurian theropods with an eight-shaped cross section of the crown (the other one being *Berberosaurus*), and other neovenatorids such as *Neovenator* (MIWG 6348), *Aerosteon* (Sereno et al. 2008; pers. obs.), *Fukuiraptor* (Azuma and Currie 2000; Currie and Azuma 2006; Molnar et al. 2009) and *Australovenator* (Hocknull et al. 2009) do not display this peculiarity. An eight-shaped outline of the crown base was also reported in the coelophysoid *Liliensternus* by Gianechini et al. (2011*b*: fig. 3c). Nevertheless, based on the crown morphology of this taxon, it is more likely that the eight-shaped outline corresponds to a cross section in the root rather than at the base-crown. ML 939 has a low crown with small denticles and a mesiodistal constriction at the base and therefore contrasts with the elongated teeth of Neovenatoridae and Tyrannosauridae which bear large denticles and never show a mesio-distal constriction at the crown base (pers. obs.). Therefore, it is unlikely that this shed tooth belongs to a non-maniraptoriform theropod.

ML 939 serrations are particularly minute and the distal carina bears nine to ten denticles per one millimeter. Among deinonychosaurs, such condition only is seen, to our knowledge, in the taxa *Richardoestesia gilmorei* and *Richardoestesia isosceles* (e.g., Currie et al. 1990; Baszio 1997; Sankey et al. 2002; Larson 2008*a*; Sankey 2008; Larson and Currie 2013), but the dental morphology of the latter (i.e., teeth with no constriction, straight to slightly recurved, crown subtriangular in outline) strongly differs from that of ML 939. The external margins of the denticles are symmetrically rounded or slightly curved towards the tip of the crown, and the basal and mid-crown denticles have similar size on the distal carina, two conditions shared by *Richardoestesia gilmorei* (Currie et al. 1990: fig. 8.4; Baszio 1997; Larson 2008*a*). Although the presence of a longitudinal groove mesially positioned on the crown has never been noticed in *Richardoestesia gilmorei*, this feature seems to be present in

some specimens assigned to this species (see Baszio 1997: Plate IV fig. 47; Sankey et al. 2002: fig. 5 n°6), and longitudinal grooves have already been observed in the genus *Richardoestesia* (Currie et al. 1990; Sankey 2001; Rauhut 2002). Nevertheless, several differences are seen between ML 939 and the teeth of the holotype of *Richardoestesia gilmorei*, namely, the presence of interdenticular sulci and mesio-distally elongated distal denticles, and the absence of a mesial carina reaching the cervix in ML 939. Although the mesial serration are usually restricted to the apicalmost part of the crown in *R. gilmorei*, the mesial carina always reaches the cervix in this taxon (Derek Larson pers. comm.).

With a strongly labiolingually compressed profile of the crown, ML 939 was coded as a lateral tooth. The cladistic analysis performed on the dentition-based dataset recovered ML 939 a close relative of *Richardoestesia gilmorei* (Fig. 4.1). The clade encompassing those two taxa is defined by two ambiguous synapomorphies: a weak constriction occurring at the crown base (characters 63) and subequal number of distal denticles basally and at the mid-crown (character 99). The analysis performed on the supermatrix recovered it as a Dromaeosauridae along with *Richardoestesia* (Fig. 4.2; Appendices A4.6, Figs. A4.9).

Richardoestesia gilmorei is a common species in the Late Cretaceous of North America and teeth belonging to this taxon, or referred to it, have been found in the Santonian Milk River Formation, the Campanian Belly River Group, the Campanian-Maastrichtian Horseshoe Canyon Formation, and the Maastrichtian Scollard Formation of Alberta, the Frenchman Formation of Saskatchewan (Canada), the Hell Creek Formation of Montana and the Lance Formation of Wyoming (e.g., Currie et al. 1990; Baszio 1997; Larson 2008*a*; Longrich 2008; Sankey 2008; Larson et al. 2010; Larson and Currie 2013). Given the results of the cladistic analysis, *R. gilmorei* is more likely to be a dromaeosaurid than any other theropod clade.

Small theropod teeth from the Upper Jurassic of Portugal have already been assigned with caution to the genus *Richardoestesia* by Zinke (1998). Nevertheless, they strongly differ from ML 939 by being extremely elongated and weakly recurved, resembling the elongated and subtriangular teeth assigned to *Richardoestesia* sp. by Baszio (1997), and *Richardoestesia isosceles* by Sankey (2001). Following the cladistic analysis and the diagnosis of teeth belonging to *Richardoestesia* sp. (and *R. gilmorei* in particular) given by Currie et al. (1990), Baszio (1997) and Longrich (2008), and since the presence of teeth similar to those of *Richardoestesia isosceles* has already been reported in the Late Jurassic of Portugal (Zinke 1998), ML 939 is ascribed to the possible dromaeosaurid *Richardoestesia*, which extends the stratigraphic range of the taxon back to the Jurassic. ML 939 is similar to *R. gilmorei* teeth in many aspects, but this taxon has only been recorded in the Late Cretaceous of North America, more than 90 million years after the Jurassic/Cretaceous boundary. We therefore consider that ML 939 belongs to a close relative of *Richardoestesia gilmorei*.

Discussion

Results of both cladistic and morphometric analyses indicate that ML 327 and ML 966 belong to a member of the Abelisauridae, representing the earliest record of this clade in Laurasia and the first record of abelisaurids in the Kimmeridgian-Tithonian. Abelisauridae have often been considered as one of the dominant terrestrial predators in most Gondwanian landmasses during the Cretaceous (Carrano and Sampson 2008). Their presence is now attested in the Jurassic of Gondwana as a newly described abelisaurid, *Eoabelisaurus mefi*, comes from the Middle Jurassic of Argentina, extending the lineage of this clade by more than 40 million years (Pol and Rauhut 2012). Abelisaurid teeth have also been reported in the Middle Jurassic of the Mahajanga basin of Madagascar by Maganuco et al. (2005).

With the exception of *Eoabelisaurus* and Middle Jurassic abelisaurids from Madagascar, the oldest records of Abelisauridae come from the Hauterivian-Barremian of Argentina (Rauhut et al. 2003) and the Aptian-Albian of Niger (Sereno and Brusatte 2008) as all potential abelisaurid remains from the Middle and Late Jurassic of Gondwana and Laurasia pertained to Abelisauroidea (e.g., Rauhut 2005*b*; Allain et al. 2007; Carrano and Sampson 2008; Ezcurra and Agnolín 2012). In the Morrison Formation, a humerus and a proximal tibia were assigned to the basal ceratosaur *Elaphrosaurus* (Galton 1982; Chure 2001), however the tibia resembles isolated abelisauroid tibiae from Tendaguru and may attest the presence of Abelisauroidea in the Western Hemisphere in the Upper Jurassic (Rauhut 2005*b*; Carrano and Sampson 2008). Abelisauroid taxa seems however to be particularly rare elements of the Morrison Formation fauna (Rauhut 2005*b*). In Europe, abelisauroid remains are scarce as well and Abelisauridae have only been collected from the Upper Cretaceous of France (Buffetaut et al. 1988; Le Loeuff and Buffetaut 1991; Carrano and Sampson 2008; Tortosa et al. 2012). The two abelisaurid teeth discovered in the Late Jurassic of Portugal therefore indicate a first radiation of this clade in the European archipelagos well before the Late Cretaceous. With Allosauridae, Ceratosauridae, Megalosauridae, Tyrannosauroidea, Compsognathidae, Dromaeosauridae and Archaeopterygidae previously documented, the theropod fauna of the Lourinhã Formation included elements specific to Europe (*Compsognathus* and *Archaeopteryx*) and also those known in North America (*Allosaurus*, *Ceratosaurus*, *Torvosaurus*, *Richardoestesia*), but the presence of Abelisauridae adds for the first time a typical Gondwanian element to the large diversity of the Laurasian theropods in the Late Jurassic of the Iberian Peninsula. As it was already suggested by Buffetaut (1989*a*) and Le Loeuff (1991) for Cretaceous theropods, the European Jurassic theropod fauna may have been a mixture of Gondwanian and Laurasian elements where the typical Gondwanian abelisaurids are in minority.

ML 939, assigned to *Richardoestesia* aff. *gilmorei*, supports the presence of the taxon *Richardoestesia* and the clade of Dromaeosauridae back to the Upper Jurassic in Europe, as it was previously suggested (e.g., Zinke 1998; Lubbe et al. 2009). Dromaeosaurids and the lineage leading to the genus *Richardoestesia* likely originated in Laurasia in the Middle to Late Jurassic while the

temporary regional uplift around the Callovian/Oxfordian transition created the temporary opportunity of land gateways between North America and the Iberian Meseta.

Conclusions

The description and identification of four theropod teeth from the Lourinhã Formation provide additional information on the Late Jurassic dinosaur fauna of the Iberian Peninsula and the biogeographical and stratigraphic distribution of Abelisauridae. Based on both morphological and cladistic analysis using a new data matrix of 141 characters on teeth, two isolated teeth have been successfully identified as belonging to an Abelisauridae, one to megalosaurid *Torvosaurus tanneri*, and one as a close relative of the enigmatic coelurosaur *Richardoestesia gilmorei*, spreading the already high diversity of predatory dinosaurs living in the Kimmeridgian–Tithonian of Southern Europe. If these referrals are correct, theropods from the Upper Jurassic of Europe are now represented by Ceratosauridae, Abelisauridae, Megalosauridae, Allosauridae, Tyrannosauroidea, Compsognathidae, Deinonychosauria and Avialae corresponding to a mixture of Laurasian and Gondwanan elements.

Although materials of *Torvosaurus tanneri* and a close relative of *Richardoestesia* have already been identified in the Upper Jurassic of Portugal, an abelisaurid is here reported for the first time in the Lourinhã Formation and therefore represents the first record of Abelisauridae in the Late Jurassic of Laurasia and one of the oldest records in the globe, revealing a first radiation of this clade in Europe back to the Jurassic.

As previously noted by Smith et al. (2005) and more recently by Han et al. (2011), this study also shows that morphometric data, combined with numerous anatomical characters on teeth, proves to be useful in order to clarify the phylogenetical position of isolated theropod teeth. Although many dentition-based characters are homoplastic, several theropod clades such as Ceratosauridae, Abelisauridae, Spinosauridae, Megalosauridae and Tyrannosauroidea have distinctive teeth, characterized by a combination of features that were not taken into consideration previously. This provides tools for the identification of isolated theropod teeth, often more common than bones, therefore allowing expanding our knowledge about the geography and chronology of theropod taxa, as demonstrated in this case for abelisaurids. This is particularly encouraging for future research on theropod dentition and, thereby, additional information regarding the size and shape of crown, carinae, denticles and enamel texture and microstructure remain to be collected on teeth of many theropod taxa. Moreover, the dentition of a large number of theropod dinosaurs is usually briefly described, sometimes even avoided, and detailed descriptions of premaxilla, maxilla and dentary teeth of many well-preserved theropods such as *Ceratosaurus*, *Torvosaurus*, *Allosaurus* and *Sinraptor* still need to be done and would greatly facilitate the assignment of isolated teeth to specific clades or taxa.

Chapter 5: The dentition of megalosaurid theropods

Published in ***Acta Palaeontologia Polonica*** (IP 1.722):
Hendrickx, C., Mateus, O. and Araújo, R. in press. The dentition of megalosaurid theropods. *Acta Palaeontologica Polonica*: DOI:10.4202/app.00056.2013.

Abstract

Theropod teeth are particularly abundant in the fossil record and frequently reported in the literature. Yet, the dentition of many theropods has not been described comprehensively, omitting details on the denticle shape, crown ornamentation and enamel texture. This paucity of information has been particularly striking in basal clades, thus making identification of isolated teeth difficult, and taxonomic assignments uncertain. We here provide a detailed description of the dentition of Megalosauridae, and a comparison to and distinction from superficially similar teeth of all major theropod clades. Megalosaurid dinosaurs are characterized by a mesial carina facing mesiolabially in mesial teeth, centrally positioned carinae on both mesial and lateral crowns, a mesial carina terminating above the cervix, and short to well-developed interdenticular sulci between distal denticles. A discriminant analysis performed on a dataset of numerical data collected on the teeth of 62 theropod taxa reveals that megalosaurid teeth are hardly distinguishable from other theropod clades with ziphodont dentition. This study highlights the importance of detailing anatomical descriptions and providing additional morphometric data on teeth with the purpose of helping to identify isolated theropod teeth in the future.

Introduction

Although dental morphology of several theropods such as *Majungasaurus* (Fanti and Therrien 2007; Smith 2007), *Tyrannosaurus* (Smith 2005), *Troodon* (Currie 1987) and *Buitreraptor* (Gianechini et al. 2011*a*) have been described in detail, the anatomy of the dentition of the vast majority of theropods is poorly documented and sometimes even lacks a description (Madsen 1976*b*; Currie and Zhao 1993*a*; Madsen and Welles 2000; Allain 2002; Benson 2010*b*; Brusatte et al. 2010*a*). As noted by Smith (2005), Smith et al. (2005), Brusatte et al. (2007), Buckley et al. (2010) and Han et al. (2011), morphology and size of denticles, length of the carinae, and crown ornamentation (i.e., interdenticular sulci, longitudinal ridges, flutes), are pivotal features to identify isolated teeth and should be explored further in many theropod taxa. Likewise, discriminant analysis based on dental measurements appeared to be a promising technique (yet to be used with caution, see Buckley et al. 2010) that facilitates the taxonomic identification of isolated teeth. Therefore, additional morphometric data on teeth still needs to be collected for a large number of theropods (Smith et al. 2005; Han et al. 2011).

Among theropods, the morphology and morphometry of megalosaurid teeth is particularly poorly known compared to other clades (e.g., Spinosauridae, Abelisauridae, Tyrannosauridae,

Troodontidae, Dromaeosauridae). Therefore, we comprehensively described the dentition of Megalosauridae, which was compared with and distinguished from other theropods based on qualitative features and quantitative data through morphological analyses.

Megalosauridae are medium to large-sized carnivorous tetanurans from the Middle to Late Jurassic of Africa, Asia, Europe, and North America (Carrano et al. 2012). These basal tetanurans include the first dinosaur to be formally described, *Megalosaurus bucklandii*, by William Buckland in 1824 (Naish 2012), and one of the largest Jurassic terrestrial predators, *Torvosaurus*, known from embryos and adult material from the United States and Portugal (Britt 1991; Mateus et al. 2006; Araújo et al. 2013; Hanson and Makovicky 2013; Hendrickx and Mateus 2014*a*). Megalosauridae is the sister-clade of Spinosauridae among megalosaurian Megalosauroidea, and includes two sub-families, Afrovenatorinae and Megalosaurinae (Carrano et al. 2012). Megalosaurid theropods have received considerable interest over the past years leading to a better understanding of their anatomy, and several taxa from the Middle Jurassic of England and the Late Jurassic of Portugal have been redescribed (i.e., *Eustreptospondylus*, *Magnosaurus*, *Duriavenator*, *Megalosaurus*, *Torvosaurus*; Benson 2008*a*, 2009, 2010*a*, *b*; Benson et al. 2008; Sadleir et al. 2008; Hendrickx and Mateus 2014*a*).

Material and methods

Material

We examined and collected morphometric data on the dentition of all representatives of each megalosaurid genus *sensu* Carrano et al. (2012) preserving teeth, i.e., *Eustreptospondylus oxoniensis* (Walker 1964), *Magnosaurus nethercombensis* (Huene 1923), *Afrovenator abakensis* (Sereno et al. 1994), *Dubreuillosaurus valesdunensis* (Allain 2002), *Duriavenator hesperis* (Waldman 1974), *Megalosaurus bucklandii* (Mantell 1827), *Torvosaurus tanneri* (Galton and Jensen 1979), and the newly named *Torvosaurus gurneyi* (Hendrickx and Mateus 2014*a*; Tables 5.1, 5.2). Only the teeth (QW200701) of the possible megalosaurid *Leshansaurus qianweiensis* (Li et al. 2009; Carrano et al. 2012) from the Late Jurassic of China could not be examined. The teeth of each of these megalosaurids have been briefly described in the scientific literature and the detailed description of the dentition of Megalosauridae here given is based on our personal observations of each specimen. The anatomical terminology used to described megalosaurid teeth follows the recommendations of Smith and Dodson (2003) and Hendrickx et al. (in press*c*). We also follow the topological definitions proposed by Smith and Dodson (2003), and the morphometric terms and abbreviations (Chapter 2, Fig. 2.5) of Smith et al. (2005) and Hendrickx et al. (in press*c*) nomenclatures.

Morphometric Analysis

We performed a morphometric analysis to understand whether megalosaurid teeth can be morphometrically identified and differentiated from other theropods based on quantitative data. We

followed the methodology developed by Smith (2005) and Smith et al. (2005) and performed a discriminant analysis (or canonical variate analysis, CVA) using PAST3 (Hammer et al. 2001) on numerical data collected by Smith (2005) and Smith et al. (2005), and updated by Smith and Lamanna (2006), Smith and Dalla Vecchia (2006) and Smith (2007). Additional morphometric data were collected from Sereno and Brusatte (2008), Molnar et al. (2009) and Hocknull et al. (2009) for Allosauroidea, and Larson and Currie (2013) for Deinonychosauria (see supplemental information of Larson and Currie (2013) for source of data collected from other authors). Original measurements were also taken on the teeth of 46 theropod taxa deposited in 24 museums from Europe, North America and South America (Appendices A5; SOM 5.1: Supplementary Online Material available on pages XXVI).

A first discriminant analysis was performed on the whole dataset, and theropod teeth were first grouped by clades, then by genera. Each clade was selected at the family and superfamily levels (Coelophysoidea, Noasauridae, Abelisauridae, Megalosauridae, Spinosauridae, Allosauridae, Neovenatoridae, Carcharodontosauridae, Tyrannosauridae, Dromaeosauridae, Troodontidae) following the phylogenies obtained by Pol and Rauhut (2012) for Ceratosauria, Carrano et al. (2012) for Coelophysoidea and non-coelurosaur Tetanurae, Brusatte et al. (2010*a*) for Tyrannosauroidea, and Turner et al. (2012) for Deinonychosauria (see SOM 5.1). Only a few groupings are paraphyletic (i.e., non-neotheropod Theropoda, non-abelisauroid Ceratosauria, and non-tyrannosaurid Tyrannosauroidea), but members of each paraphyletic group share similar dentition (CH personal observations). In this analysis, the theropods Erectopus, Nuthetes and *Richardoestesia*, with uncertain affinities, as well as *Dilophosaurus* and *Piatnitzkysaurus*, were analyzed at the genus level (see SOM 5.1).

In order to better discriminate teeth that are morphologically similar to those of megalosaurids, a second morphometric analysis was performed on a reduced dataset encompassing theropods with large ziphodont teeth (i.e., non-abelisaurid Ceratosauria, Abelisauridae, Megalosauridae, Allosauridae, Neovenatoridae, Carcharodontosauridae, and Tyrannosauridae; see SOM 5.2). Theropods have a pseudoheterodont dentition (i.e., dentition in which the crown morphology gradually changes along the jaw so that mesial and lateral teeth differ significantly in their morphology; Hendrickx and Mateus 2014*a*) and to visualize morphospace occupation of mesial and lateral dentitions, a third discriminant analysis was performed on a dataset including taxa with enough data on the dentition (i.e., *Ceratosaurus*, *Majungasaurus*, *Dubreuillosaurus*, *Allosaurus*, *Acrocanthosaurus*, *Gorgosaurus*, *Tyrannosaurus*; see SOM 5.3). In this analysis, we did not consider data collected on mesial teeth of *Tyrannosaurus* by Smith (2005), who mistook CBL (which should be measured between points A and B; Smith 2005: fig. 1C) for CBW (measured between points C and D; Smith 2005: fig. 1C), and only our own measurements were taken into consideration for the mesial dentition in this tyrannosaurid.

CBL, CBW, CH, AL, CBR, CHR, MCL, MCW, MCR, MC, and DC were used in the two analyses, as these variables best represent the amount of difference among theropod teeth and characterize crown size, width, elongation, thickness along the crown, and denticles size (Smith et al. 2005; CH personal observations). (Smith et al. 2005) methodology, which was followed by other authors (e.g., Smith and Dalla Vecchia 2006; Smith and Lamanna 2006; Kear et al. 2013; Richter et al. 2013), uses ratio variables such as CA, CBR, CHR, and DSDI. These non-independent variables weigh the variables used in the ratios, therefore each morphometric analysis was first performed without ratio variables. The latter were then included in a second analysis in order to visualize the influence of ratios and overemphasized variables on the results.

All values were log-transformed to better reflect a normally distributed multivariate dataset (Smith et al. 2005; Kear et al. 2013; Larson and Currie 2013; see rationalization in Samman et al. 2005, and references therein). Contrary to Smith et al. (2005), crown angle values (CA) *sensu* Smith et al. (2005) were not used in the morphometric analyses as this angle can be affected by the extent of the enamel layer both mesially and distally (Buckley et al. 2010) and only weakly reflects apical displacement (CH personal observations). Additionally, CA values obtained by Smith (2005) and Smith et al. (2005) differ from those calculated in this study using the same formula (i.e., the law of cosines on CBL, CH, and AL), and Smith (2005) and Smith et al. (2005) likely used another method to calculate CA. We also favored MC and DC instead of MAVG and DAVG because they are affected by the absence of data for both basal and apical denticles, typically smaller than mid-crown denticles and often unpreserved (CH personal observations). Likewise, we did not generate any size-corrected variables on MC and DC as denticle size, like tooth size, remains an important factor in the study of theropod teeth and can vary independently from tooth dimension (Smith et al. 2005; CH personal observations). Teeth with a great deal of missing data can blur the morphometric signal, and as the initial dataset included a large number of teeth (more than 2000 specimens initially), only complete teeth with data on crown height (CH), length (CBL), width (CBW) and number of distal denticles per 5 mm (DC) were selected. Unserrated teeth were also included, and MC and DC were treated as missing data. The final dataset comprised 995 teeth belonging to 62 theropod taxa and 19 groups, and the reduced dataset with large ziphodont theropods includes 393 teeth belonging to 33 taxa and 11 groupings.

The morphospace occupied by each megalosaurid was visualized in a fourth discriminant analysis performed on a dataset including Megalosauridae only (Table 5.1). In this analysis, all morphometric variables (i.e., CBL, CBW, CH, AL, CBR, CHR, MCL, MCW, MCR, MDE, MEC, TUD, DMT, DDT, DLAT, DLIT, MA, MC, MB, DA, DC, DB, MAVG, DAVG, DSDI, CA) were employed, and ratios (MAVG, DAVG, CBR, CHR, MCR, MEC, DSDI, CA) were first excluded, then taken into consideration in a second analysis. We selected teeth with two variables or more, and the measurements were not log-transformed, as the absence of mesiobasal denticles and transverse undulations was taken into consideration. In this analysis, missing data (coded with a question mark)

TABLE 5.1. Morphometric data of megalosaurid teeth.

Taxa	Specimen	Side	Position	CBL	CBW	CH	AL	CBR	CHR	MA	MC	MB	DA	DC	DB	DSDI
Eustreptospondylus	OUMNH J13558	Right	pm03	?	?	?	?	?	?	11.66	?	?	12	12.5	10.83	?
Eustreptospondylus	OUMNH J13560	Left	mx06	?	?	?	?	?	?	?	?	?	?	9.375	?	?
Eustreptospondylus	OUMNH J13562	Right	mx02	?	?	?	?	?	?	?	8.33	?	?	?	?	?
Eustreptospondylus	OUMNH J13561	Right	mx06	?	?	?	?	?	?	11.66	10	?	10.83	?	?	?
Eustreptospondylus	OUMNH J13563	Right	dt?	?	?	?	?	?	?	13.75	?	?	?	?	?	?
Eustreptospondylus	OUMNH J13563	Right	dt?	?	?	?	?	?	?	?	11.66	?	?	12.5	?	0.933
Eustreptospondylus	OUMNH J13564	Left	dt04	?	?	?	?	?	?	?	13.33	?	?	12.5	?	1.066
Magnosaurus	OUMNH J12143	Left	dt05	11.2	7.01	?	?	0.626	?	?	?	?	?	12	?	?
Magnosaurus	OUMNH J12143	Left	dt07	10.7	6.5	?	?	0.609	?	?	?	?	?	?	?	?
Magnosaurus	OUMNH J12143	Right	dt01	11.2	8.27	?	?	0.741	?	?	?	?	?	?	?	?
Magnosaurus	OUMNH J12143	Right	dt01	?	?	?	?	?	?	15	13.33	?	13.5	15	?	0.889
Magnosaurus	OUMNH J12143	Right	dt03	?	?	?	?	?	?	?	11.25	?	?	11.5	?	0.978
Magnosaurus	OUMNH J12143	Right	dt04	?	?	?	?	?	?	13.75	?	?	12.5	?	?	?
Magnosaurus	OUMNH J12143	Right	dt05	?	?	?	?	?	?	?	12.5	/	?	13	?	0.962
Magnosaurus	OUMNH J12143	Right	dt08	?	?	?	?	?	?	13.75	?	?	13.75	?	?	?
Magnosaurus	OUMNH J12143	Right	dt09	?	?	?	?	?	?	?	?	?	?	14	?	?
Magnosaurus	OUMNH J12143	Right	dt10	?	?	?	?	?	?	13.75	?	?	14	13.33	?	?
Dubreuillosaurus	MNHN 1998-13	Left	pm1	8.3	6	18	17	0.723	2.169	12	/	/	12	11.5	17	?
Dubreuillosaurus	MNHN 1998-13	Left	pm2	10.5	7.7	22	23.6	0.733	2.095	13	12.5	/	12	12.5	16	1
Dubreuillosaurus	MNHN 1998-13	Right	mx4	17.5	6.34	27.67	32.11	0.362	1.579	?	?	?	?	?	?	?
Dubreuillosaurus	MNHN 1998-13	Right	mx5	17.6	7.06	39.07	37.75	0.401	2.22	?	?	?	?	?	?	?
Dubreuillosaurus	MNHN 1998-13	Right	mx6	14.8	6.02	21.29	28.4	0.408	1.441	?	?	?	?	?	?	?
Dubreuillosaurus	MNHN 1998-13	Right	mx7	15.7	6.45	27.72	36.02	0.411	1.764	?	?	?	?	?	?	?
Dubreuillosaurus	MNHN 1998-13	Right	mx9	10.4	5.68	16.83	22.24	0.547	1.62	?	?	?	?	?	?	?
Dubreuillosaurus	MNHN 1998-13	Left	dt6	10.7	5.4	18	17.6	0.505	1.682	17.5	?	/	13.5	16	17	?
Dubreuillosaurus	MNHN 1998-13	Left	dt8	10.5	5.2	16	15.9	0.495	1.524	16.6	?	/	14	16	20	?
Dubreuillosaurus	MNHN 1998-13	/	Isolated	9.9	4.3	14.1	12.8	0.434	1.424	17	16	/	14	16	19	1
Afrovenator	UC UBA 1	/	Isolated	27.6	11.7	61.1	64.6	0.424	2.214	7.5	8	?	8	10	15	0.8
Duriavenator	NHMUK R332	Left	pm02	?	?	?	?	?	?	9	?	/	7.5	8.125	?	?
Duriavenator	NHMUK R332	Left	pm02	17.7	11.21	?	?	0.632	?	?	?	/	?	?	?	?
Duriavenator	NHMUK R332	Right	mx03	24.3	12.74	51.73	57.2	0.524	2.128	?	12	/	9	11	14	1.091
Duriavenator	NHMUK R332	Right	mx04	21.8	?	51.41	?	?	2.357	?	?	/	9.5	11	?	?
Duriavenator	NHMUK R332	Right	mx05	24.1	?	48.57	54.64	?	2.013	8.75	8	/	?	10.5	14	0.762
Duriavenator	NHMUK R332	Right	mx06	21	8.01	39.42	49.15	0.382	1.88	10	13	/	10	12.5	15	1.04
Megalosaurus	NHMUK R8305	Left	dt4	24.4	11.84	>50.69	>54.7	0.485	?	9.5	?	?	9	?	?	?
Megalosaurus	OUMNH J13505	Right	dt03	?	?	?	?	?	?	9.5	?	?	10	?	?	?
Megalosaurus	OUMNH J13505	Right	dt06	24.1	12.8	46.54	55.81	0.531	1.93	?	?	/	9	10	15	?

Taxa	Specimen	Side	Position	CBL	CBW	CH	AL	CBR	CHR	MA	MC	MB	DA	DC	DB	DSDI
Megalosaurus	OUMNH J13506	Left	mx01	24.8	14.85	62.72	68.02	0.598	2.527	8.75	?	/	?	?	15	?
Megalosaurus	OUMNH J13506	Left	mx04	29.3	?	63.92	67.76	?	2.182	10	11	/	10.5	10	15	1.1
Megalosaurus	OUMNH J13506	Left	mx05	?	?	?	?	?	?	10	12.5	/	9	11	?	1.136
Megalosaurus	OUMNH J13506	Left	mx06	25.1	?	54.73	52.1	?	2.183	?	?	/	?	?	12	?
Megalosaurus	OUMNH J13506	Left	mx07	25	?	50	52	?	2	?	?	/	?	?	11	?
Megalosaurus	OUMNH J13506	Left	mx08	?	?	?	?	?	?	9	?	?	11	?	?	?
Megalosaurus	OUMNH J13506	Left	mx09	18.8	?	33.33	41.13	?	1.769	?	?	/	12.5	13	14.16	?
Megalosaurus	NHMUK R234	/	Isolated	23.2	?	43.82	49.16	?	1.89	10	10.5	/	13.33	13.5	17.5	?
Megalosaurus	NHMUK R39476	/	Isolated	18.3	10.11	35.45	38.83	0.552	1.936	?	?	/	13.33	14.5	15	?
Megalosaurus	NHMUK R47152	/	Isolated	11.3	6.37	22.5	24.25	0.566	2	18.75	20.63	/	18	20	20	1.031
Megalosaurus	NHMUK R234	/	Isolated	24.3	13.14	52.33	54.19	0.541	2.155	10.65	9.5	/	10	12	15	0.792
Megalosaurus	NHMUK R31834	/	Isolated	17.7	6.84	28.64	33.38	0.386	1.618	12.5	12	/	12.5	14	16	0.857
Megalosaurus	NHMUK R47963	/	Isolated	23.9	12.06	51.74	48.85	0.504	2.163	10.83	11	/	12	13	17	0.846
Megalosaurus	NHMUK R28608	/	Isolated	21.4	13.66	47.37	44.93	0.639	2.216	6.5	8.5	/	7	8.75	10	0.971
Megalosaurus	NHMUK R2635	/	Isolated	26.5	13.93	54.42	59.29	0.527	2.057	11.25	11.25	/	10	11	12	?
Megalosaurus	NHMUK R2635	/	Isolated	11.4	7.72	26.63	29.75	0.68	2.344	?	?	/	10	13	16	?
Megalosaurus	OUMNH J23050	/	Isolated	20.8	?	30.39	33.3	?	1.458	10.5	12	/	11.88	12	14	?
Megalosaurus	OUMNH J29863	/	Isolated	26.3	?	61.11	67.78	?	2.324	9.375	10	/	10	9.5	10	1.053
Megalosaurus	OUMNH J29855	/	Isolated	23.7	?	45.1	51.26	?	1.904	9.16	11	/	9.5	10.5	16	1.048
Megalosaurus	OUMNH J29866	/	Isolated	27	14.84	?	?	0.55	?	10	10	/	10	11.5	15	0.87
Megalosaurus	OUMNH J23049	/	Isolated	25.5	13.89	?	?	0.545	?	?	/	/	11.5	13	16	?
Megalosaurus	OUMNH J29762	/	Isolated	21.6	?	45.76	41.09	?	2.115	10	9	/	11	11	12.5	0.818
Megalosaurus	OUMNH J23014	/	Isolated	29.4	?	59.02	63.78	?	2.007	9.5	9.5	/	9	9	11	1.056
Torvosaurus	BYU-VP 725 12817	Cast	Isolated	39.8	19.17	103.3	110.7	0.482	2.597	8	6	?	6	7	12	0.857
Torvosaurus	ML 1100	Left	mx02	45.5	16.4	106.4	118.6	0.36	2.337	6	8	/	7	8	11	1
Torvosaurus	ML 1100	Left	mx03	45.7	?	117	128.6	?	2.563	6	7	/	6	8	10	0.875
Torvosaurus	ML 1853	/	Isolated	24.8	13.74	43.53	46.39	0.554	1.755	7.5	9.5	/	7.5	9.5	?	1
Torvosaurus	ML 148	/	Isolated	35.2	17.66	>45.2	>43.7	0.501	?	?	7.5	/	?	8.125	11.5	0.923
Torvosaurus	ML 500	/	Isolated	41.3	19.94	>106.97	>114.33	0.483	~2.8	6	7	/	6	7	12	1
Torvosaurus	ML 962	/	Isolated	31.4	19.43	86.63	91.9	0.62	2.763	/	8	/	7	8	11	1
Torvosaurus	ML 857	/	Isolated	32.2	17.05	59.5	57.6	0.53	1.848	6.5	7	10	7.5	7	9	1

differ from those that are absent (like denticles and transverse undulations) and have zero as value.

The dentition of Megalosauridae

Tooth Count

Like the majority of non-avian theropods, all megalosaurids that have the premaxilla preserved (*Eustreptospondylus*, *Duriavenator*, *Dubreuillosaurus*, and *Torvosaurus*) bear four premaxillary teeth (Allain 2002; Benson 2008*a*; Table 5.2), even in *Torvosaurus*, which has often been considered to have only three premaxillary teeth (e.g., Galton and Jensen 1979; Holtz et al. 2004; see (Britt 1991; Benson 2008*a*). The maxilla of Megalosauridae shows ten to 14 maxillary alveoli (Table 5.2), and an exact tooth count is known in *Dubreuillosaurus* and *Megalosaurus* which both have 13 maxillary teeth (Allain 2002; Benson 2010*a*), and *Afrovenator* which bears 14 teeth (Sereno et al. 1994). In megalosaurid dentaries, the typical condition is 13 to 15 teeth (Table 5.2), and a complete dentary with 13 teeth is only known in *Dubreuillosaurus* (Allain 2002). Nevertheless, based on comparison of the preserved part of the left and right dentaries of *Eustreptospondylus* (OUMNH J.13558), we estimate a tooth count of 14 dentary teeth in this taxon.

On average, the premaxillary teeth of megalosaurids are smaller and more elongated than the lateral teeth. In all megalosaurids, the largest teeth erupt from the maxilla, at the level of the second to sixth maxillary alveoli. In fact, the maxillary alveoli are larger on average than the dentary alveoli in all megalosaurid specimens (i.e., *Eustreptospondylus*, *Dubreuillosaurus*, *Duriavenator*, and *Torvosaurus*). Yet, the maxillary teeth are much longer than those of the dentary in *Dubreuillosaurus*, whereas the difference in size between maxillary and dentary teeth is more subtle in *Duriavenator* (Table 5.1). As noticed in *Torvosaurus* (Britt 1991), megalosaurids display an overlap between the first and second, and second and third premaxillary alveoli, the second alveolus usually overlaps more than 75% of the first, and the third alveolus overlaps approximately 50% of the second one. The fourth premaxillary alveolus does not, however, overlap the third one in megalosaurids (*Eustreptospondylus*, *Dubreuillosaurus*, and *Torvosaurus*). There is an overlap of about 25% to 50% between the second and first dentary alveoli. There is no subnarial gap in megalosaurids and all alveoli are subequally separated and face ventrally, with all teeth pointing ventrally and slightly anteroventrally in the *Duriavenator* mesial dentary teeth (Benson 2008*a*). In the lateral alveoli, the long axis of the premaxillary alveoli orients anteroposteriorly; labiolingually for the mesial one and mesiodistally for the most distal ones. The lateral alveoli have approximately the same size as in the premaxilla. Yet, the first dentary alveolus is always much smaller than the more distal alveoli. The dentary alveoli are subcircular (for the mesial one) then lenticular for the distal ones, differing from the subrectangular alveoli of some other theropods such as abelisaurids (e.g., Hendrickx and Mateus 2014*a*). Additionally, the tooth row ends at the level of the lacrimal contact of the maxilla, well anterior from the posterior tip of the jugal ramus. Therefore, megalosaurid taxa possess the synapomorphic character

TABLE 5.2. Tooth-count and tooth-count estimation of the tooth bearing bones of Megalosauridae.

Taxa	Specimen	Premaxilla	Maxilla	Dentary	Source
Eustreptospondylus	OUMNH J.13558	4	>7	~14 (>8)	Sadleir et al. 2008
Magnosaurus	OUMNH J.12143	?	?	~14 (>11)	Benson 2010*b*
Leshansaurus	QW 200701	?	~11-12 (>9)	?	Pers. obs.
Dubreuillosaurus	MNHN 1998-13	4	13	13	Allain 2002
Afrovenator	MNN UBA1	?	14	?	Sereno et al. 1994
Duriavenator	NHMUK R.332	4	>11	~14-15 (>13)	Benson 2008*a*
Megalosaurus	NHMUK R.8303; OUMNH J13505, 13506, 13559	?	13	~13-14 (>11)	Benson 2010*a*
Torvosaurus	BYU-VP 2003, 4882, 9122; ML 1100	4	~11-12; ~10 (>10; >8)	~13	Britt 1991; Benson 2008*a*; Hendrickx and Mateus 2014*a*

of Tetanurae of having an antorbital tooth row (Gauthier 1986).

Mesial Teeth

As in most basal theropods, megalosaurid theropods bear ziphodont teeth and have a pseudoheterodont dentition with mesial and lateral teeth. In Megalosauridae, the mesial dentition includes the premaxillary teeth, the first maxillary tooth, and the first two dentary teeth. The premaxillary teeth and first dentary teeth are weakly labiolingually compressed, and are smaller as well as more elongated in average than the lateral teeth. Unfortunately, only *Dubreuillosaurus* and *Duriavenator* have preserved complete erupted mesial teeth. The first and second teeth of the left premaxilla of *Dubreuillosaurus* are the only erupted and complete premaxillary teeth present in all Megalosauridae (Fig. 5.1A–C). The second tooth of the *Duriavenator* right dentary is the only complete and erupted mesial dentary tooth in this clade (Benson 2008*a*). The bases of the second premaxillary tooth and the second dentary tooth have also been preserved in the left premaxilla of *Duriavenator* and the right dentary of *Magnosaurus*, respectively. The mesial unerupted teeth are partially visible in the second left and third right premaxillary alveoli of *Eustreptospondylus* (Fig. 5.2A), the second left premaxillary alveolus of *Duriavenator*, the first right dentary alveolus of *Magnosaurus*, and in the first left dentary alveolus of *Torvosaurus* (BYU-VP 2003) and *Megalosaurus* (NHMUK R.8305). Isolated mesial teeth were found for *Torvosaurus* (ML 962; Hendrickx and Mateus 2014*b*) and *Megalosaurus* (NHMUK R2635; NHMUK R3221; NHMUK R44806; CH personal observations). Among taxa with teeth, *Afrovenator* and *Leshansaurus* are the only megalosaurids in which the morphology of mesial teeth is unknown.

The crown base ratio of mesial teeth varies from 0.63 to 0.75 (0.72 and 0.73 in *Dubreuillosaurus* Lpm1 and Lpm2; 0.71 in *Magnosaurus* Rdt1; 0.63 in *Duriavenator* Lpm2 and

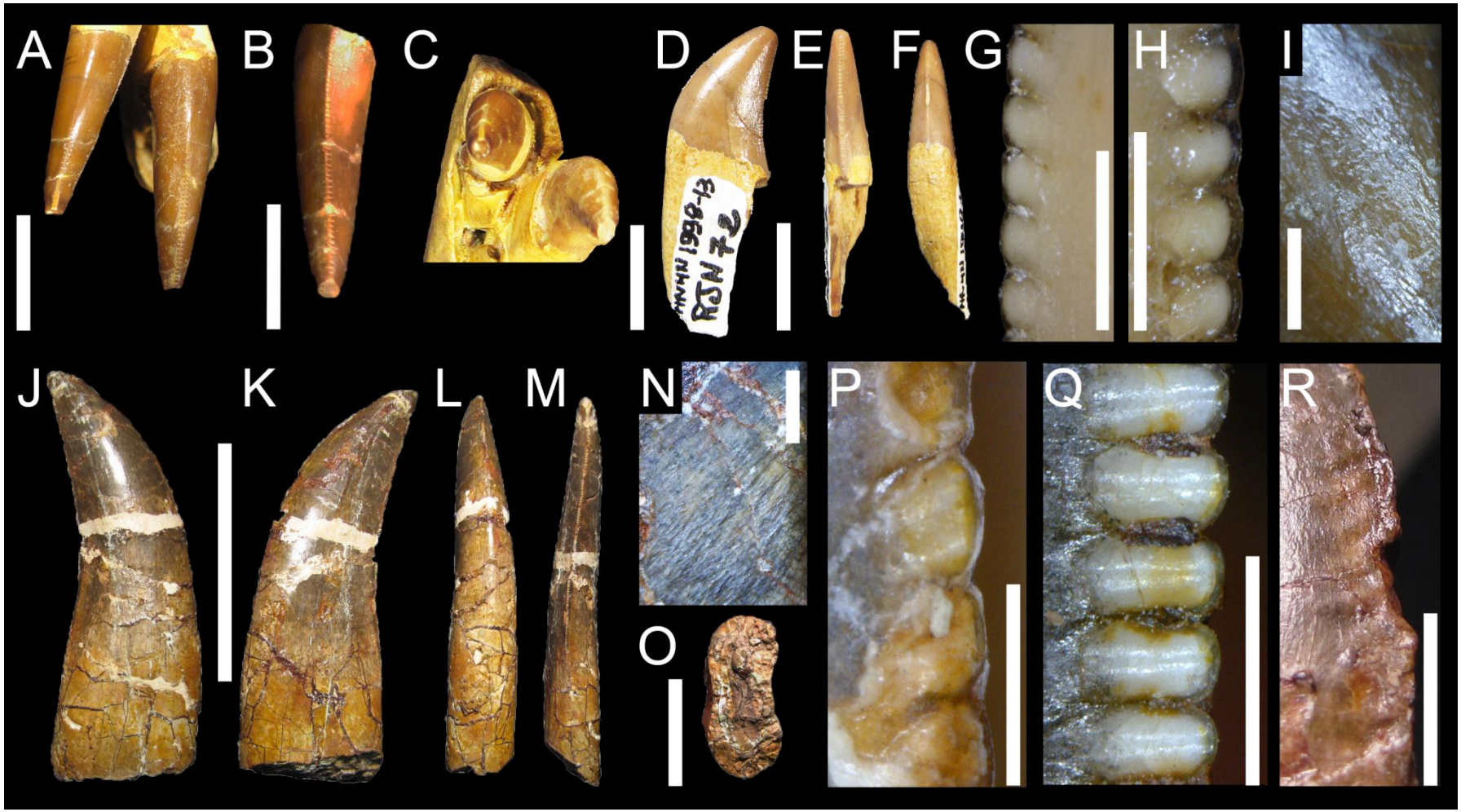

FIGURE 5.1. Dentition of Afrovenatorinae from the Middle Jurassic of France and Niger. **A–I**, Teeth and denticles of *Dubreuillosaurus valesdunensis* (Allain 2002; MNHN 1998-13); **A–C**, First and second left premaxillary teeth in **A**, anterior; and **C**, palatal views; and **B**, second left premaxillary tooth in distal view; **D–G**, Isolated lateral tooth in **D**, lingual; **E**, distal; and **F**, mesial views; **G**, detail of mesial denticles in lateral view; **H**, Distal denticles of sixth right dentary tooth in lateral view; **I**, Enamel texture of sixth right maxillary tooth; **J–R**, Isolated tooth of *Afrovenator abakensis* (Sereno et al. 1996; MNN UBA1) in **J**, lingual; **K**, labial; **L**, mesial; **M**, distal; and **O**, basal views; with **N**, details of enamel texture; **P**, mesial; and **Q**, distal denticles; and **R**, marginal undulations adjacent to the mesial carina. Scale bars = 5 cm (J–M); 2 cm (O); 1 cm (A–F); 5 mm (R); 2 mm (I, N); 1 mm (G–H, P-Q).

0.67for Ldt2; 0.65 in an isolated tooth of *Torvosaurus*; Table 5.1) giving a subcircular outline to the crown base in cross section (Benson 2008*a*). The crown height ratio fluctuates from 2 to 2.8 (2.1 in *Dubreuillosaurus* Lpm1 and Lpm2; 2 in *Duriavenator* Rdt2; 2.75 in an isolated tooth of *Torvosaurus*; Table 5.1), which corresponds to a moderately to strongly elongated crown. The mesial teeth are usually poorly to moderately curved distally and their distal margin is always concave. There is no concave area on the lingual surface of the crown, adjacent to the carinae. In fact, mesial crowns of megalosaurids have strongly convex labial and lingual margins, with no concavity on the lingual surface, as in lateral teeth.

An important feature of mesial teeth of megalosaurids is the central position of the mesial carina, serrated and not twisted lingually, which faces anteriorly and develops only on the apical half of the crown, extending basally well above the cervix. The distal carina is also serrated and centrally positioned to weakly offset labially, and faces posteriorly (Britt 1991; Allain 2002; Benson 2008*a*; CH personal observations). Therefore, both carinae are aligned on the same plane that passes through the apex of the tooth, and this plane is parallel to the true sagittal plane of the skull (i.e., parallel to the anteroposterior axis of the skull independent of the orientation of the tooth row) in all mesial teeth of Megalosauridae. The mesial serration occupies between 55 to 65% of the crown height. The distal carina, on the other hand, extends basally below the cervix, so that the crown base has a lanceolate shape in cross section and is not U-shaped, D-shaped or J-shaped as in allosauroids and tyrannosauroids (Hendrickx and Mateus 2014*b*). The mesial carina of the first two premaxillary teeth and the first dentary tooth face labially, whereas the distal carina faces labiodistally. The distal carina is straight or slightly sigmoid in distal view and the carina bears denticles that are similar in size than those of mesial carina (DSDI close to 1; Smith et al. 2005).

Mesial and distal denticles decrease in size towards the base of the crown and similarly towards the crown apex. When the crown apex is preserved, the denticles are clearly contiguous over the tip. Mesial and distal denticles differ significantly in their morphology, except in *Dubreuillosaurus*. Mesial denticles are subquadrangular to subrectangular in outline, with a basoapical axis of elongation, at two thirds of the crown (Fig. 5.2B). The distal denticles are always subquadrangular at mid-crown (Figs. 5.2C–D). The denticles project perpendicularly from the main axis of the carina and have symmetrically convex external margins, and apically hooked denticles have not been observed in any megalosaurids. The interdenticular space of all denticles is narrow and the interdenticular sulci are either totally absent (e.g., *Dubreuillosaurus*) or weakly developed in between the distal denticles at mid-length of the crown (e.g., *Magnosaurus*, *Eustreptospondylus*; Fig. 5.2C) or more basally (*Torvosaurus*). Mesial and apicodistal denticles do not possess interdenticular sulci (Fig. 5.2B). Due to tooth size disparity, the density of denticles is variable among megalosaurids. There are seven to eight denticles per 5 mm on mesial and distal carinae at mid-crown (or at two thirds of the crown) in *Torvosaurus* (Hendrickx and Mateus 2014*a*), eight to nine in *Duriavenator*, 11 to 12 in *Dubreuillosaurus* and *Eustreptospondylus*, and 13 to 15 in *Magnosaurus* (Table 5.1). mesial teeth

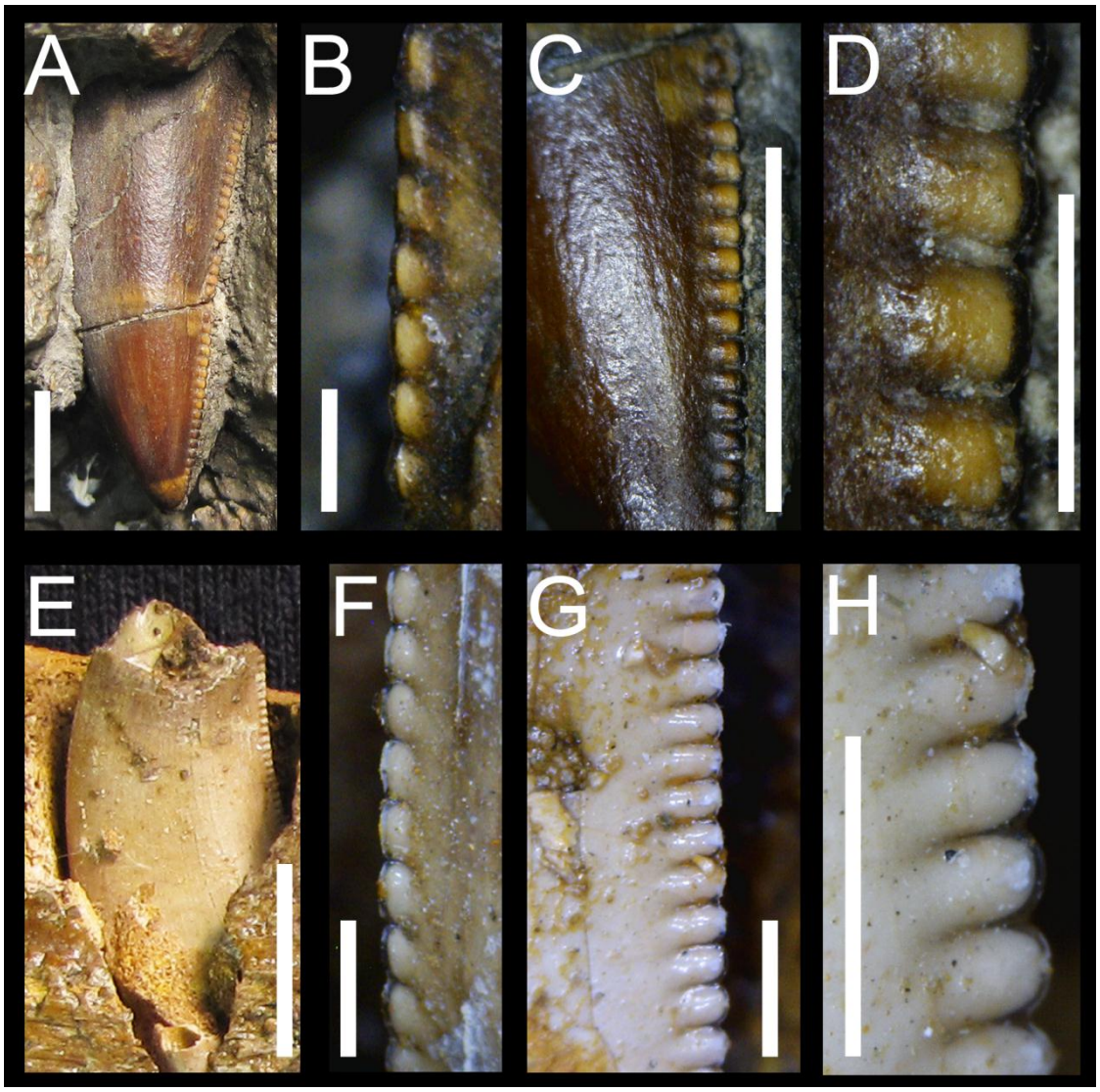

FIGURE 5.2. Dentition of *Eustreptospondylus* and *Magnosaurus* from the Middle Jurassic of England. **A–D**, crown and denticles of *Eustreptospondylus oxoniensis* (Walker 1964; OUMNH J.13558); **A, C–D**, Third right premaxillary tooth in lingual views; **A**, details of crown; **C**, distal serration and enamel texture; **D**, apicodistal denticles; **B**, Apicomesial denticles of the sixth left maxillary tooth in lingual view; **E–H**, Crown and denticles of *Magnosaurus nethercombensis* (Huene 1923; OUMNH J12143); **E**, Crown of fifth dentary tooth in lingual view; **F**, Mesial denticles of the third dentary tooth in lingual view; **G–H**, Distal denticles of the ninth right dentary tooth in lingual views. Scale bars = 1 cm (E); 5 mm (A, C); 1 mm (B, D, F–H).

do not display grooves, flutes or apparent wide transverse or short marginal undulations on the crown surface; only subtle to tenuous transverse undulations may be visible (Hendrickx and Mateus 2014*a*).

Lateral Teeth

Megalosaurid lateral teeth are an ideal example of ziphodont morphology in non-avian theropods, i.e., the teeth are blade-shaped, strongly laterally compressed, recurved distally, and serrated on both carinae. Complete lateral teeth are preserved in all members of megalosaurids but *Eustreptospondylus* and *Magnosaurus. Eustreptospondylus* only includes the base of one erupted maxillary tooth and several partially visible unerupted teeth, whereas *Magnosaurus* shows several

damaged and incomplete erupted and unerupted teeth. In *Afrovenator* there are three isolated teeth, and only one is complete and weakly damaged (Fig. 5.1J–M).

The crown base ratio of megalosaurid lateral teeth ranges between 0.35 (*Torvosaurus*, ML 1100, Lmx2) to 0.63 (*Magnosaurus*, Ldt5), with average values ranging from 0.45 to 0.55 (0.42 in *Afrovenator*; 0.44 in *Dubreuillosaurus*; 0.45 in *Duriavenator*; 0.47 in *Torvosaurus*; 0.53 in *Megalosaurus*, and 0.61 in *Magnosaurus*; Table 5.1; see SOM 5.3), thus moderately labiolingually compressed crowns. The crown height ratio varies considerably with tooth position, from 1.4 for very short crowns (*Dubreuillosaurus*, isolated tooth) to 2.8 for strongly elongated teeth (*Torvosaurus*, isolated tooth ML 500). In Megalosauridae, *Dubreuillosaurus* possesses shorter dentition, with an average of 1.65 for the lateral teeth, whereas *Torvosaurus* (ML 1100) has the most elongated and longest crowns, with a crown elongation of 2.3 on average and a length of 128 mm for the largest crown (*Torvosaurus*, ML 1100, Lmx3; Table 5.1; see SOM 5.3). Crown elongation cannot be properly measured in *Eustreptospondylus* and *Magnosaurus* as the teeth are unerupted, but the latter display short crowns (CHR < 2), as short as those of *Dubreuillosaurus*.

As in mesial teeth, the serrated mesial carina is not twisted and does not reach the cervix whereas the distal carina terminates well beneath the crown cervix. The basal extent of the mesial carina is variable; the most basal denticles appear only on the apical third of the crown (*Megalosaurus*, Lmx3) or at the basal one fifth of the crown (*Duriavenator*, Rmx6). The mesial carina extends along 40% to 80% of the crown height, from the apex to the basal half of the tooth (see SOM 5.3). As in mesial teeth, the mesial carina is straight or weakly diagonally oriented, but always centrally positioned on the lateral crowns, unlike the distal carina, which is usually weakly sigmoid or bowed lingually and centrally positioned to slightly offset labially on the crown in distal view, as in *Dubreuillosaurus* (Fig. 5.1E) and *Afrovenator* (Fig. 5.1M). The labial margin of the teeth is strongly convex and does not display any concave or flattened surface adjacent to the carinae. The lingual surface is weakly to strongly concave, but not flattened. There is, however, a large flattened surface or shallow concavity, centrally positioned on the basolingual part of the crown, representing the track of the erupting replacement crown. This concave area is clearly visible in *Torvosaurus*, *Megalosaurus*, *Duriavenator* and *Afrovenator* lateral teeth, whereas the basolingual surface of the lateral crowns is flat in *Dubreuillosaurus* (Fig. 5.1D) and *Magnosaurus*. In cross section, the crown base of megalosaurid lateral teeth is lenticular, with the lingual margin straight or slightly to strongly concave in its central part.

The mesial denticles are subrectangular, with an apicobasally long axis in most megalosaurids such as *Eustreptospondylus*, *Magnosaurus* (Fig. 5.2F), *Dubreuillosaurus* (Fig. 5.1G), *Afrovenator* (Fig. 5.1P), *Duriavenator* (Fig. 5.3B) and *Megalosaurus* (Fig. 5.3E). In *Torvosaurus* and *Megalosaurus*, the mesial denticles are also subquadrangular (Fig. 5.3L). The mesial denticles are usually perpendicular to the mesial margin of the crown. However, the mesial denticles tend to be apically inclined in some megalosaurids, such as *Afrovenator* (Fig. 5.1P), *Dubreuillosaurus* (Fig.

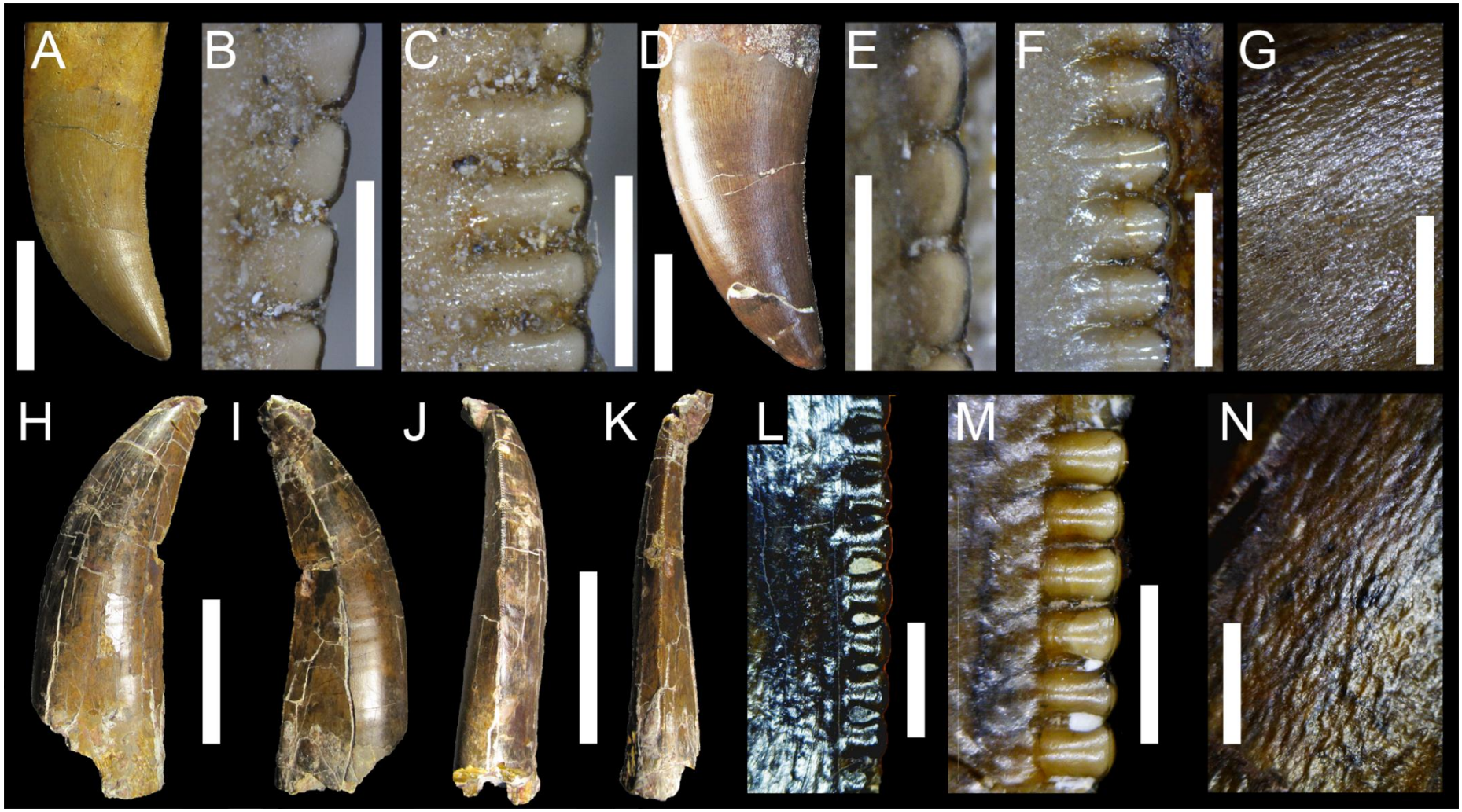

FIGURE 5.3. Dentition of Megalosaurinae from the Middle and Late Jurassic of Europe. **A–C**, Sixth right maxillary tooth of *Duriavenator hesperis* (Waldman 1974; NHMUK R.332); with details on **A**, crown; **B**, mesial; and **C**, distal denticles in lingual views; **D–G**, Sixth right dentary tooth of *Megalosaurus bucklandi* (Mantell 1827; OUMNH J13505); with details on **D**, crown; **E**, mesial; and **F**, distal denticles in labial views; and **G**, enamel texture; **H–K**, Isolated tooth of *Torvosaurus* cf. *gurneyi* (Hendrickx and Mateus 2014*a*; ML 500) in **H**, lingual; **I**, labial; **J**, mesial; **K**, and distal views; with details of **L**, mesial; and **M**, distal denticles; and **N**, enamel texture in lateral views. Scale bars = 5 cm (H–K); 2 cm (A, D); 3 mm (G); 2 mm (L–N); 1 mm (B–C, E–F).

5.1G), *Duriavenator* (Fig. 5.B) and resemble a parallelogram. The external margin of the denticles is symmetrically to asymmetrically convex, positioned apically when asymmetrical. The margin is usually parabolic, but it is also flat or even biconvex in some cases (Fig. 5.3B), as clearly seen in some mesial denticles of *Duriavenator* (Rmx6) and *Megalosaurus* (NHMUK R234, Lmx5). At the crown mid-height, the distal denticles are subquadrangular in *Dubreuillosaurus* (Fig. 5.1H) and *Magnosaurus* (Fig. 5.2H), and horizontally subrectangular in *Afrovenator* (Fig. 2Q), *Duriavenator* (Fig. 5.3C), *Megalosaurus* (Fig. 5.3F), and *Torvosaurus* (Fig. 5.3M). The external margin is symmetrically convex and parabolic as in *Dubreuillosaurus* (Fig. 5.1H) and *Torvosaurus* (Fig. 5.3M) to semi-circular in outline as in *Afrovenator* (Fig. 5.1Q) and some teeth of *Megalosaurus* (Fig. 5.3F). Both mesial and distal denticles are not hooked apically in Megalosauridae, and there is about the same number of denticles on both carinae (DSDI close to 1). There are 13-17 denticles per 5 mm on both carinae at mid-height of crown (or at two thirds) in *Dubreuillosaurus* (average of 16), 11-14 in *Magnosaurus* (average of 12.5), 8.5-13.5 in *Eustreptospondylus* (average of 11.5), 8-13 in *Duriavenator* and *Megalosaurus* (average of 11), 7.5-12 in *Afrovenator* (average of 9), and 6 to 9.5 in *Torvosaurus* (average of 7.5; Table 5.1).

Interdenticular sulci are present in the lateral dentition of megalosaurid taxa, but not in all crowns. Interdenticular sulci are absent in some lateral crowns of *Dubreuillosaurus* and *Megalosaurus*. Likewise, there is some variation in the length of the interdenticular sulci, as well as in their inclination along the tooth row, some being short and oriented perpendicular to the carinae, others being well-developed and strongly inclined basally (Benson 2009). Interdenticular sulci are rare in mesial denticles and occur in *Duriavenator*, *Megalosaurus* and *Torvosaurus.* In these taxa, the interdenticular sulci of the mesial denticles are always short and poorly developed. On the other hand, short to well-developed interdenticular sulci are very often seen on the distal carina of megalosaurid teeth. Short to medium interdenticular sulci (0.3 to 0.5 mm) are present between the distal denticles of *Magnosaurus* (*contra* Benson 2010*b*), *Afrovenator*, *Dubreuillosaurus*, *Duriavenator* (Benson 2008*a*) and *Megalosaurus* (Benson 2009), whereas there are strongly developed interdenticular sulci (~1 mm) in some crowns of *Megalosaurus* (Benson 2009) and most *Torvosaurus* teeth (Hendrickx and Mateus 2014*a*).

Megalosaurid teeth often display enamel structures such as large transverse undulations and short marginal undulations (Fig. 5.3I), but flutes, ridges, or wide longitudinal concavities extending along the crown have not been noticed hitherto. Wide transverse undulations covering most of the tooth are common in megalosaurine teeth, such as in *Duriavenator* (Benson 2008*a*), *Megalosaurus* (Benson 2009), and *Torvosaurus* (Hendrickx and Mateus 2014*a*). In *Duriavenator*, the transverse undulations are tenuous (Benson 2008*a*), while in *Megalosaurus* and *Torvosaurus*, they are visible, numerous and closely-packed in some cases (Benson 2009; CH personal observations). These large transverse bands are absent in *Dubreuillosaurus*, *Magnosaurus* and the only well-preserved crown of *Afrovenator*. Short undulations adjacent to the mesial and distal carinae are readily visible in

Afrovenator, especially marginal to the mesial carina where they are visibly developed (Fig. 5.1R). Some crowns of *Megalosaurus* and *Torvosaurus* also display these short undulations, either adjacent to both carinae (OUMNH J.29855, NHMUK R.234, ML 500) or in the vicinity of the distal carina only (NHMUK R47963). These marginal undulations are usually mesiodistally-oriented, but there is a diagonal orientation of these structures in some *Megalosaurus* teeth (OUMNH J.23014, NHMUK R.29855). The enamel of the crowns of megalosaurids has a braided texture with elongated intertwined ridges (Fig. 5.1I, N and Fig. 5.3G, N). This pattern differs from the deeply veined enamel texture visible in spinosaurids (e.g., *Baryonyx*, *Spinosaurus*, *Suchomimus*; e.g., Charig and Milner 1997; Hasegawa et al. 2010; Buffetaut 2011) and the irregular texture in Abelisauridae and most Maniraptoriformes (Hendrickx and Mateus 2014*b*).

Comparison to the dentition of other theropods

Morphological Comparison

Teeth of Megalosauridae are easily distinguishable from those of Coelophysidae, Abelisauridae, Noasauridae, Spinosauridae, Tyrannosauroidea, Compsognathidae, Dromaeosauridae, Therizinosauria, and Troodontidae, all of which have highly specialized dentition. Therizinosauria and Troodontidae have leaf-shaped crowns with constricted cervix, and the teeth are unserrated or bear very few serrations, and either minute denticles or large pointed denticles sometimes changing dramatically in shape along the carinae (e.g., Currie 1987; Currie et al. 1990; Clark et al. 1994; Zhao and Xu 1998; Barrett 2000; Norell et al. 2009; Zanno 2010*b*; Hendrickx and Mateus 2014*b*).

Coelophysids and compsognathids possess small crowns (CH < 15 mm) lacking in most cases a serrated mesial carina in mesial teeth, and the distal carina bears minute denticles (> 30 denticles per 5 mm; Buckley 2009; Hendrickx and Mateus 2014*b*). Teeth of abelisaurids are usually low and weakly recurved, and display a slightly concave, straight or convex distal profile, a mesial carina that always reaches the cervix, and an irregular and non-oriented enamel texture. They also possess hooked denticles in some taxa (e.g., *Rugops*, *Kryptops*, *Majungasaurus*), and the mesial mesial teeth show a concave area adjacent to the mesial and, in some cases, the distal carina on the lingual surface of the crown (e.g., Fanti and Therrien 2007; Smith 2007; Hendrickx and Mateus 2014*b*). Teeth of noasaurids are small (CH < 15 mm), the lateral teeth have a mesial carina reaching the cervix, the distal denticles are hooked apically in some taxa (e.g., *Masiakasaurus*), and are larger than mesial denticles. The mesial teeth are lanceolate and have a strongly twisted mesial carina and fluted lingual surface (Carrano et al. 2002; Hendrickx and Mateus 2014*b*). In spinosaurids, the mesial and distal serrations are minute or absent, the mesial carina always reaches the cervix, the enamel texture is deeply veined (except *Irritator*) and the crowns are subcircular in cross-section and fluted on one or both lingual and labial surfaces (e.g., Charig and Milner 1997; Sereno et al. 1998; Sues et al. 2002; Hendrickx and Mateus 2014*b*).

Among Tyrannosauroidea, tyrannosaurids have incrassate crowns, and the mesial carina of the teeth making the transition between the mesial (premaxillary and first two dentary teeth; Smith 2005) and lateral teeth is strongly twisted. Likewise, mesial teeth are U-shaped (*sensu* Hendrickx and Mateus 2014*b*) in cross section, with both mesial and distal carinae facing lingually (Holtz 2004). The mesial teeth of some primitive tyrannosauroids have a mesial carina twisting mesially, and the lateral teeth have distal denticles larger than the mesial ones (Xu et al. 2006; Rauhut et al. 2010; Hendrickx and Mateus 2014*b*).

The lateral teeth of some Dromaeosauridae are devoid of serrated carinae, as in *Buitreraptor* (Gianechini et al. 2011*a*) or lack a serrated mesial carina, as in *Tsaagan* (Norell et al. 2006) and some teeth of *Velociraptor* and *Bambiraptor* (CH personal observations). When present, the mesial carina of lateral teeth can be twisted, as in *Dromaeosaurus* (Currie et al. 1990; Currie 1995), or bear mesial denticles that are smaller than the distal ones, as in *Atrociraptor* (Currie and Varricchio 2004), *Deinonychus* (Ostrom 1969), *Velociraptor* (Sues 1977; Barsbold and Osmólska 1999), *Bambiraptor* (Burnham 2004), *Saurornitholestes* (Currie et al. 1990), and *Acheroraptor* (Evans et al. 2013). The distal denticles can also be hooked apically, as in *Deinonychus* (Ostrom 1969), *Saurornitholestes* (Currie et al. 1990) and *Atrociraptor* (Currie and Varricchio 2004). Moreover, the lateral teeth tend to have a wide apicobasally elongated concavity on the basolabial surface of the crown (Gianechini et al. 2011; CH personal observations), a depression which is also usually well-developed on the lingual surface of the crown. These lingual and labial concavities are particularly clear in some dromaeosaurids such as *Sinornithosaurus* (Xu and Wu 2001) and were interpreted as a venom delivery duct (Gong et al. 2010, 2011). Finally, the mesial teeth of dromaeosaurids are different from those of Megalosauridae; they either lack a mesial carina, as in *Tsaagan* (IGM 100-1015) and *Velociraptor* (AMNH 6515), or the mesial carina curves strongly lingually, as in *Deinonychus* (Ostrom 1969), *Dromaeosaurus* (Currie et al. 1990; Currie 1995) and *Saurornitholestes* (Currie et al. 1990).

Differentiating teeth of megalosaurids from those of Ceratosauridae, basal Megalosauroidea, and Allosauroidea is more difficult. These taxa have similar crown size (CH), thickness (CBR), and elongation (CHR), and a similar number of denticles along the carinae (DC and MC). Ceratosauridae have strongly labiolingually compressed lateral teeth (CBR < 0.5) with a flattened lingual margin and a concave surface adjacent to the distal carina on the labial and lingual sides of the crown, and a wide concave area centrally positioned on the labial side of the crown (CH personal observations). mesial teeth of *Ceratosaurus* are fluted lingually and the mesial carina of premaxillary crowns is absent (Currie and Carpenter 2000), whereas lateral teeth tend to have a mesial carina extending to the cervix. *Genyodectes* does not possess fluted teeth, but the premaxillary teeth are strongly elongated (CHR > 2.5) and the distal carina is offset labially (Rauhut 2004*b*).

Teeth of Megalosauridae are difficult to distinguish from those of Piatnitzkysauridae, but some differences exist. The mesial denticles of *Marshosaurus* and *Piatnitzkysaurus* are slightly smaller than the distal serrations (Madsen 1976b; CH personal observations), which is never the case

in megalosaurids. Likewise, *Piatnitzkysaurus* posterior maxillary teeth have a distal margin that is straight to slightly convex, a mesial carina reaching the cervix, and they are thick labiolingually (CBR of around 0.71 for Lmx13; PVL 4073). This is also the case in *Condorraptor* in which lateral teeth are thick labiolingually (CBR of around 0.6). The preserved crowns of this taxon are strongly elongated (CHR of almost 2.5), and do not display any interdenticular sulci between mesial and distal denticles (Rauhut 2005*a*). There are 14 denticles per 5 mm on the distal carina, at mid-crown, in *Condorraptor*, and 11 to 15 in *Piatnitzkysaurus* (CH personal observations).

Teeth of allosauroids are very similar to those of Megalosauridae. Allosaurid crowns are typically thicker to those of megalosaurids. The first eight maxillary teeth have a crown base ratio above 0.6-0.7 on average, and only the most posterior lateral teeth have a CBR within the same range (0.3 to 0.6) as megalosaurid crowns (CH personal observations). This is also the case with mesial teeth in which the CBR varies from 0.7 to 1.2. The mesial carinae of mesial teeth of *Allosaurus* reach or extend close to the cervix, and always twist lingually, giving a D-shaped cross-section (*sensu* Hendrickx and Mateus 2014*b*) at the base of the crown. This is also the case for teeth situated in the transition of mesial and lateral teeth (first, second maxillary teeth) in which the mesial carina also twists towards the lingual side of the crown. A concave surface adjacent to the mesial carina can also be observed on the lingual side of mesial teeth, and the distal margin is convex. A similar condition is present in metriacanthosaurid mesial teeth such as *Sinraptor*, in which the mesial carina curves lingually (Currie and Zhao 1993*a*) and the distal margin is convex. Allosaurid lateral teeth have a strongly displaced distal carina labially. The lateral dentition of metriacanthosaurids is weakly recurved distally and the distal profile of lateral crowns is either slightly concave or straight (CH personal observations). Furthermore, the lateral teeth of Metriacanthosauridae also have a mesiodistally-expanded concave or flattened surface centrally positioned on the labial margin of the crowns. Although not clearly observable in the lateral teeth of *Sinraptor dongi*, it seems that the mesial carina of lateral teeth extends to, or near to, the cervix. This feature is visible in *Sinraptor hepingensis* isolated teeth (ZDM 0024). Teeth of neovenatorids can be differentiated from those of megalosaurids by their relatively narrow lateral crowns typically displaying two concave surfaces adjacent to both mesial and distal carinae, and separated by a mesiodistally narrow planar surface. The mesial carina extends to the cervix in the lateral teeth of some neovenatorids (e.g., *Fukuiraptor*) and, in mesial teeth, the mesial carina is placed lingually whereas the distal carina is deflected labially.

The mesial teeth of carcharodontosaurids are similar to those of megalosaurids. The mesial carina faces mesially or mesiolabially and, in some cases, can terminate well above the cervix as in the premaxillary teeth of *Acrocanthosaurus* (NCSM 14345). Importantly, the distal carina is strongly displaced labially in mesial teeth of Carcharodontosauridae, which is not the case in Megalosauridae. Lateral teeth of *Acrocanthosaurus* are large (average of 70 mm for the whole dentition), but the denticles are relatively small, with an average of 14 per 5 mm on the distal carina at mid-height (Smith et al. 2005), giving a large number of denticles (>200) along the crown of the longest teeth.

Acrocanthosaurus teeth also display crown ornamentations such as marginal and transverse undulations as well as pronounced braided texture of the enamel. The lateral dentition of Carcharodontosaurinae possesses a mesial carina reaching the cervix or extending just above it, and typically displays pronounced arcuate marginal undulations on one side of the crown, or on both lingual and labial surfaces. The distal profile of the lateral crown is usually straight or weakly concave in lateral view. Often the distal profile of the lateral crowns of Carcharodontosaurinae display a diagnostic sigmoid outline, with the concavity covering the basal two thirds and a convexity on the resting apical third of the crown. A similar distal profile is also present in at least one isolated tooth of the non-carcharodontosaurine, *Eocarcharia* (MNN GAD14).

Morphometric Comparison

Smith et al. (2005) were the first to perform a multivariate analysis on teeth belonging to theropods from basal to derived taxa. Their analysis included 325 teeth from 20 taxa, but non-neotheropod Theropoda, Megalosauridae, Neovenatoridae, and non-tyrannosauroid Tyrannosauroidea were not represented. We use 995 teeth pertaining to 62 theropod taxa and 19 major groups of theropods. Our dataset includes three times more teeth and taxa, and the morphometric analysis shows the morphospace occupation of teeth belonging to all major theropod clades for the first time. The results of the discriminant analysis at the generic and familial levels (Fig. 5.4) are relatively similar to those obtained by Smith et al. (2005: fig. 14) as the morphospace occupation of each taxon is driven by the size of the teeth (CH, CBL, CBW) and the number of denticles on the carinae (MC, DC), so that Troodontidae, Noasauridae, Spinosauridae, and Tyrannosauridae are distributed in different zones of morphospace.

In our analysis, theropod teeth occupy four morphospace areas (Fig. 5.4; see SOM 5.4), one including taxa with small teeth and large denticles (Troodontidae), a second for taxa bearing relatively small teeth and small denticles (non-neotheropod Theropoda, Coelophysoidea, Noasauridae, and Dromaeosauridae), a third with taxa possessing large teeth and minute denticles (Spinosauridae), and a fourth with ziphodont taxa having relatively large teeth and large denticles (non-noasaurid Ceratosauria, Megalosauridae, Allosauroidea, and Tyrannosauridae). Overlap is seen between each of these areas, and clades bearing small teeth/denticles and large teeth/denticles show considerable overlap. This explains why only 66.5% and 71% of specimens were correctly classified to their genera and clades, respectively. Such results contrast with the 97% of correctly classified specimens obtained by Smith et al. (2005), a percentage that can be explained by the small sample size, and the restricted number of taxa with similar dentition in their dataset. In this morphometric analysis, Troodontidae, non-theropod Theropoda and Spinosauridae are the best classified theropods (>85% correctly classified; Table 5.3). The analysis had most difficulty classifying non-abelisaurid Ceratosauria (15%) and Megalosauridae (21%; Table 5.3) and, among the latter, 12% of megalosaurid teeth were classified as *Piatnitzkysaurus*, Allosauridae, Carcharodontosauridae and basal Tyrannosauroidea, 9%

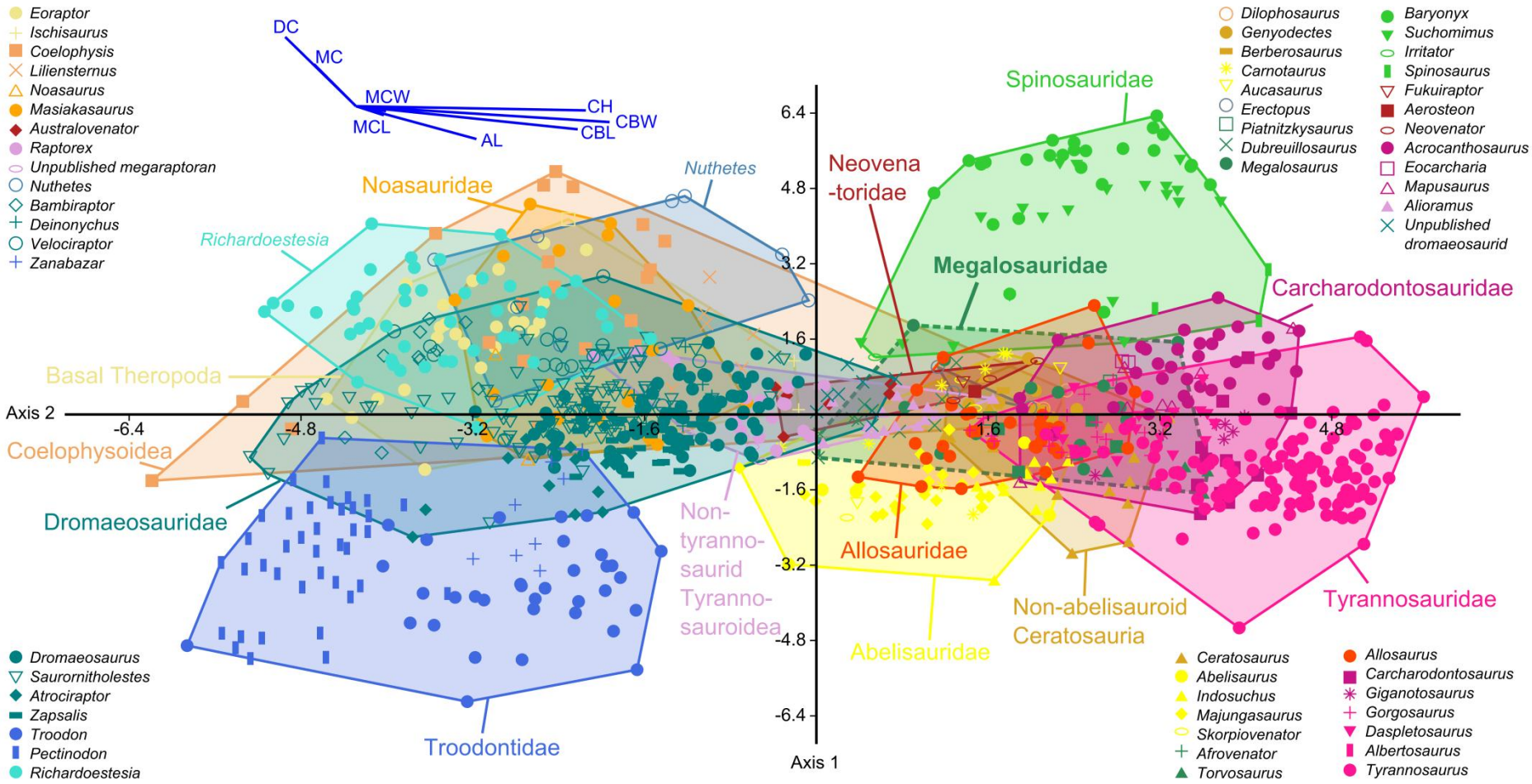

FIGURE 5.4. Graphical results of the discriminant analysis of 995 teeth belonging to 62 theropod taxa and 19 groupings along the first two canonical axes of maximum discrimination in the dataset (Eigenvalue of Axis 1 = 7.561, which accounted for 61.52% of the variation; Eigenvalue of Axis 2 = 2.62, which accounted for 21.38 % of the variation). Log-transformed CBL, CBW, CH, AL, MCL, MCW, MC, and DC were used in the analysis, and 70.97% of the specimens of non-avian theropods were correctly classified (see SOM 5.1 available at http://app.pan.pl/SOM/appXX-Hendrickx_etal_SOM.pdf). Morphospace occupation of megalosaurid teeth is delimited by a dashed line.

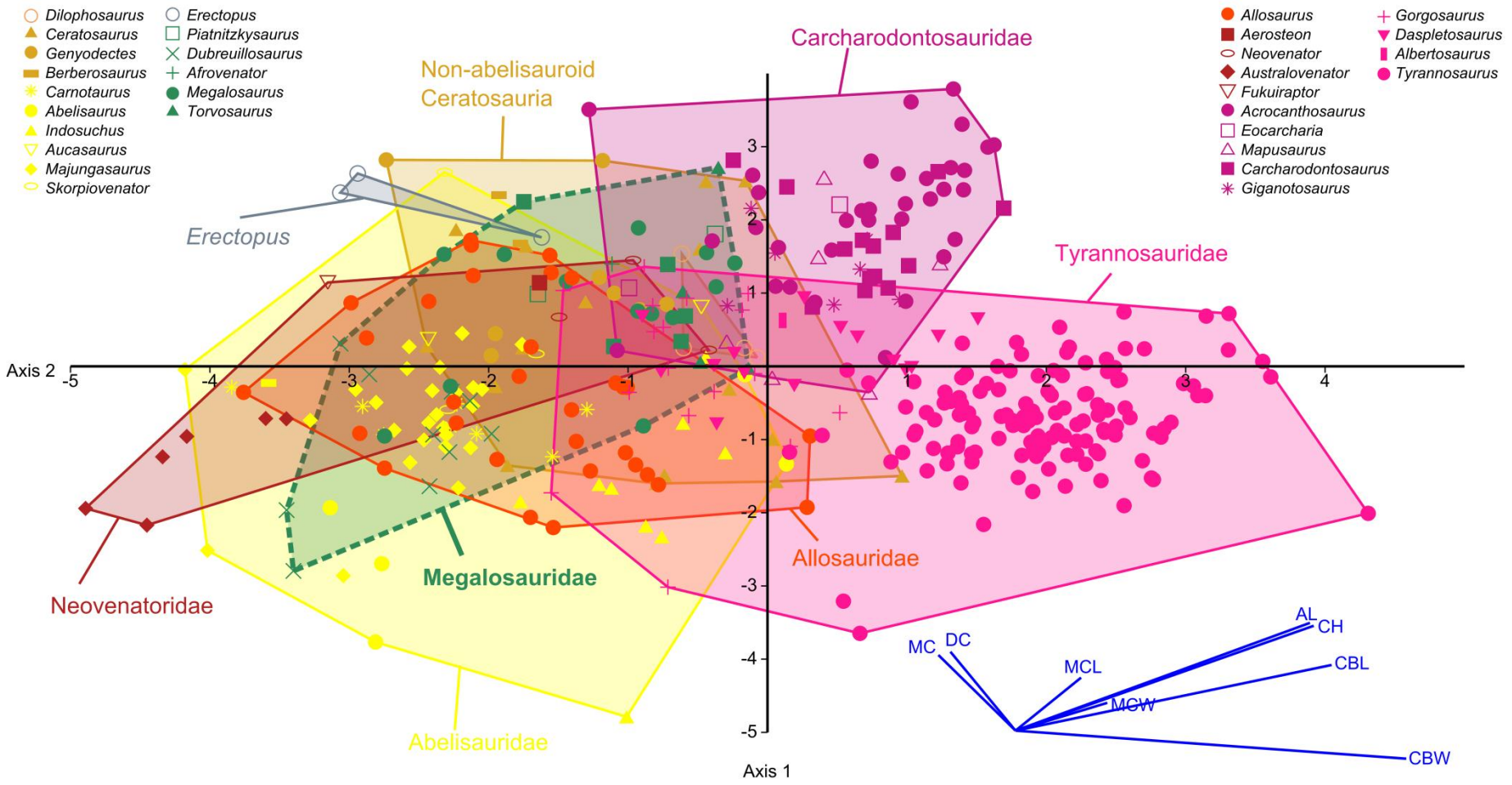

FIGURE 5.5. Graphical results of the discriminant analysis of 393 teeth belonging to 33 taxa and 11 groupings of large ziphodont theropods along the first two canonical axes of maximum discrimination in the dataset (Eigenvalue of Axis 1 = 2.52, which accounted for 65.75% of the variation; Eigenvalue of Axis 2 = 0.89, which accounted for 23.24% of the variation). Log-transformed CBL, CBW, CH, AL, MCL, MCW, MC, and DC were used in the analysis, and 68.19% of the specimens were correctly classified to their respective clades (see SOM 5.2). Morphospace occupation of megalosaurid teeth is delimited by a dashed line.

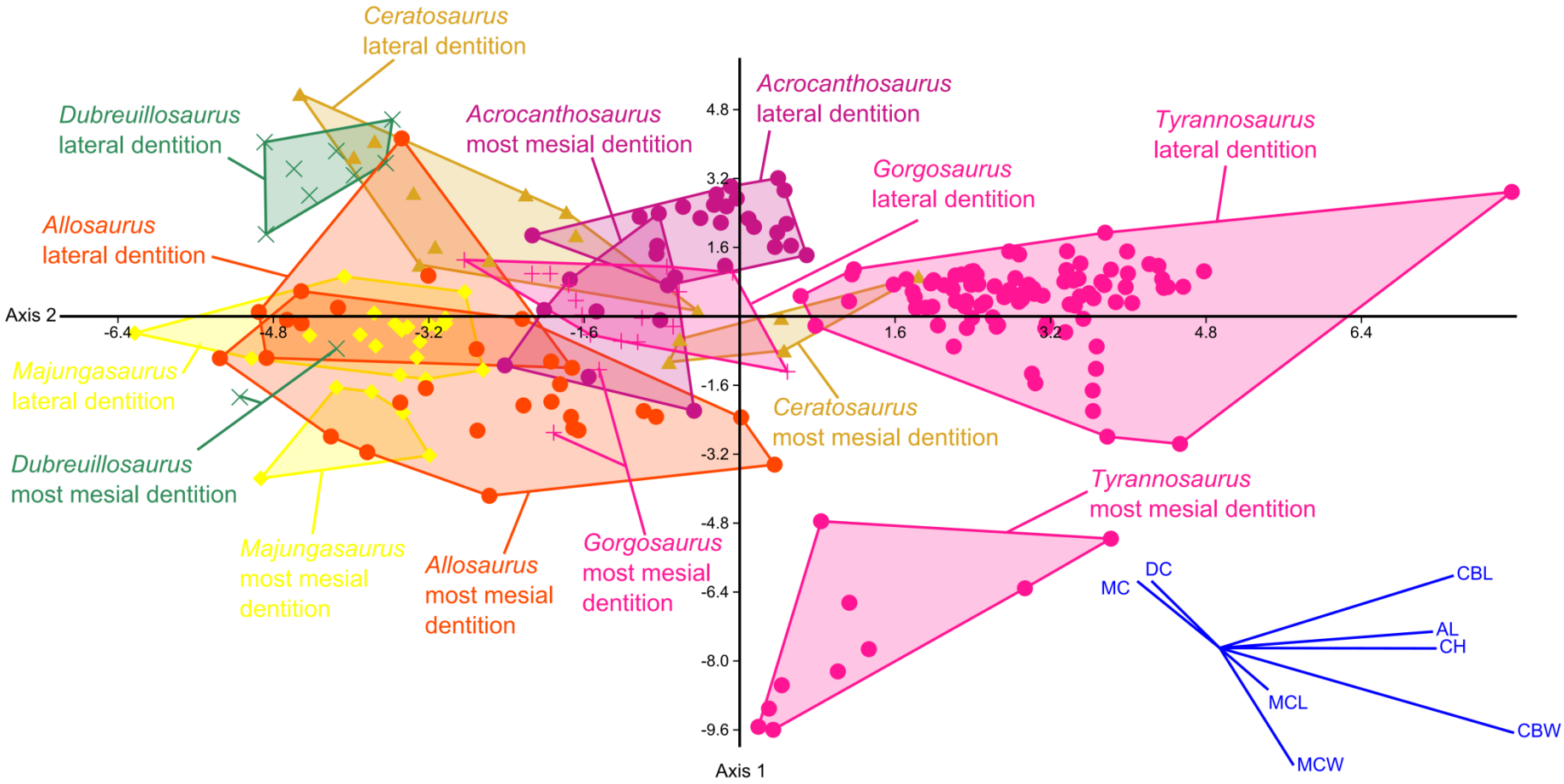

FIGURE 5.6. Graphical results of the discriminant analysis of 232 teeth belonging to 7 taxa whose dentition was separated into mesial and lateral teeth, along the first two canonical axes of maximum discrimination in the dataset (Eigenvalue of Axis 1 = 7.99, which accounted for 50.73% of the variation; Eigenvalue of Axis 2 = 4.52, which accounted for 28.73% of the variation). Log-transformed CBL, CBW, CH, AL, MCL, MCW, MC, and DC were used in the analysis, and 84.48% of the specimens were correctly classified to their respective taxa and dentition type (see SOM 5.3).

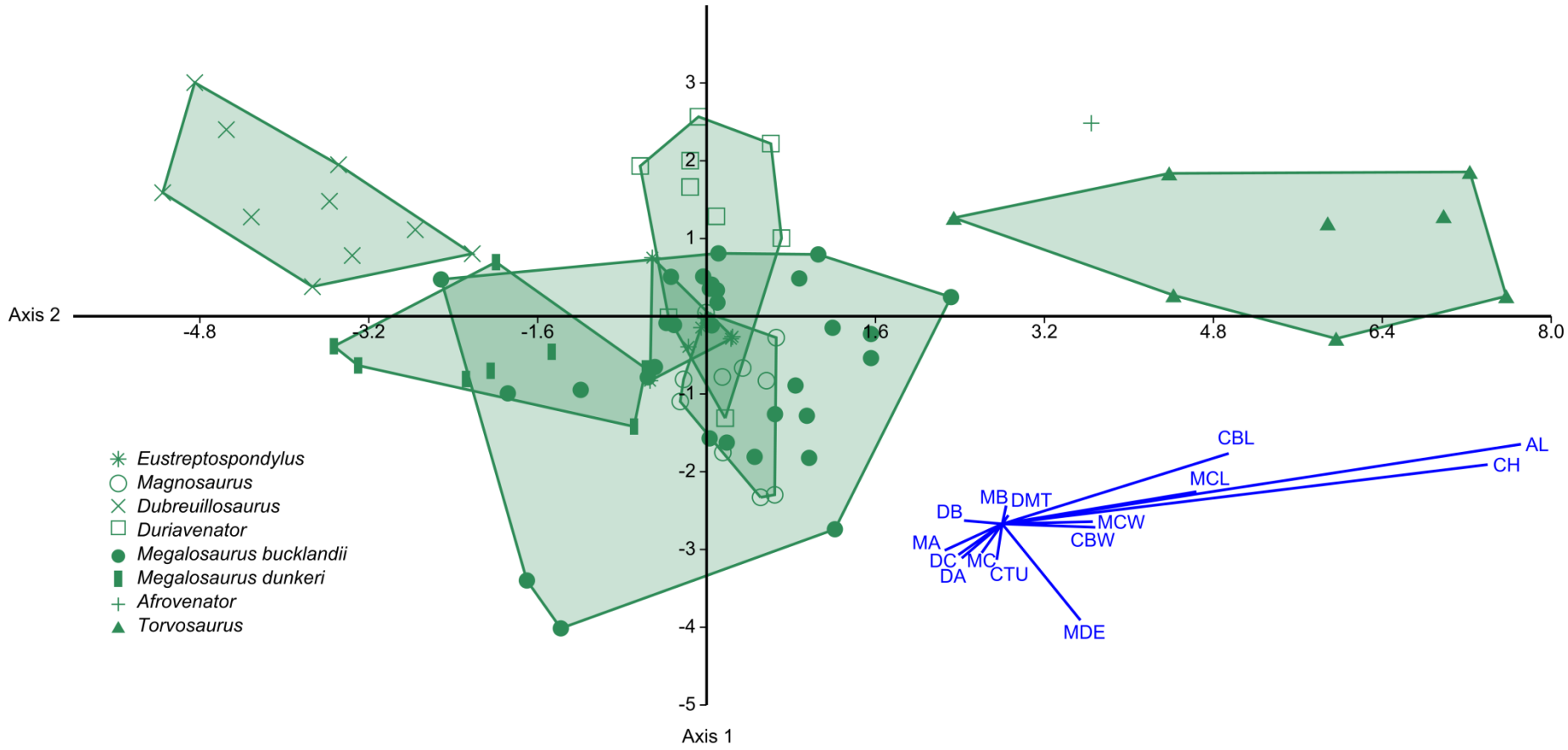

FIGURE 5.7. Graphical results of the discriminant analysis of 81 teeth belonging to 7 taxa of Megalosauridae, and one indeterminate tetanuran (‘*Megalosaurus dunkeri*’), along the first two canonical axes of maximum discrimination in the dataset (Eigenvalue of Axis 1 = 5.8, which accounted for 71% of the variation; Eigenvalue of Axis 2 = 1, which accounted for 12.36% of the variation). Raw data of CBL, CBW, CH, AL, MCL, MCW, MDE, TUD, DMT, DDT, DLAT, DLIT, MA, MC, MB, DA, DC, and DB were used in the analysis, and 65.48% of the specimens were correctly classified to their a priori genera (see SOM 5.4).

TABLE 5.3. Table of misclassification for the whole dataset grouped by clades (ratios excluded).

Clades	Number of teeth correctly assigned	Total	% correctly identified
Basal Theropoda	25	29	86.2%
Coelophysoidea	20	31	64.5%
Ceratosauridae	4	26	15.4%
Noasauridae	5	24	20.8%
Abelisauridae	39	55	70.9%
Erectopus	3	3	100%
Piatnitzkysaurus	2	2	100%
Megalosauridae	7	33	21.2%
Spinosauridae	43	49	87.8%
Allosauridae	18	31	58.1%
Neovenatoridae	8	11	72.7%
Carcharodontosauridae	47	64	73.4%
Basal Tyrannosauroidea	23	39	59%
Tyrannosauridae	129	164	78.7%
Nuthetes	8	9	88.9%
Dromaeosauridae	205	297	69%
Troodontidae	77	82	93.9%
Richardoestesia	42	45	93.3%
Total	705	994	70.9%

as Ceratosauridae, and 6 % as Abelisauridae, Neovenatoridae, and the enigmatic tetanuran *Erectopus*. In the same discriminant analysis performed at a generic level, megalosaurid taxa also show a low score, with 50% being successfully identified as those of *Torvosaurus*, 40% as *Duriavenator*, 30% as *Dubreuillosaurus*, and only 15% as *Megalosaurus* (see SOM 5.1).

The morphometric analyses performed on the reduced dataset, which includes large ziphodont teeth, reveals that megalosaurid teeth occupy the same morphospace as those of other ziphodont theropods (Figs. 5.4, 5.5; see SOM 5.1). Megalosauridae, Ceratosauridae, Abelisauridae, Allosauridae, and Neovenatoridae still show considerable overlap (Fig. 5.5), and significant overlap with Tyrannosauridae and Carcharodontosauridae, so that separating teeth of megalosaurids from the teeth of other similarly sized theropods is particularly difficult. Indeed, while 68% of all specimens were correctly classified to their clades, only 42% of megalosaurid specimens were successfully assigned to Megalosauridae (Table 5.4; see SOM 5.1), and 40% to their respective a priori genera (60% to *Duriavenator*, 50% to *Torvosaurus* and *Dubreuillosaurus*, and 15% to *Megalosaurus*). In the discriminant analysis performed at the generic level, taxa with the best data (*Tyrannosaurus*, *Allosaurus*, *Acrocanthosaurus*, *Ceratosaurus*, *Megalosaurus*) show the largest morphospace occupation. This is because quantitative data were collected in teeth from across the jaws, where there is important morphometric variation between mesial and lateral dentition. Indeed, morphometric analysis performed on taxa whose mesial and lateral dentition could be considered separately clearly shows that mesial and lateral teeth from individual taxa occupy different portions of morphospace (Fig. 5.6). This is particularly the case in Megalosauridae (*Dubreuillosaurus*) and Tyrannosauridae (*Tyrannosaurus*) in which mesial and lateral teeth strongly differ in their thickness and elongation.

TABLE 5.4. Table of misclassification for the reduced dataset (large ziphodont teeth) grouped by clades (ratios excluded).

Clades	Number of teeth correctly assigned	Total	% correctly identified
Dilophosaurus	4	4	100%
Ceratosauridae	7	26	26.9%
Abelisauridae	31	55	56.4%
Erectopus	3	3	100%
Piatnitzkysaurus	2	2	100%
Megalosauridae	14	33	42.4%
Allosauridae	20	31	64.5%
Neovenatoridae	7	11	63.6%
Carcharodontosauridae	46	64	71.9%
Tyrannosauridae	134	164	81.7%
Total	268	393	68.2%

Interestingly, overlap is seen only in the two included allosauroids, *Allosaurus*, and *Acrocanthosaurus*, confirming that the distinction between mesial and lateral teeth is not that clear in this clade.

In the morphometric analysis of megalosaurid teeth only, 65.38% of specimens were correctly assigned to their genera (Table 5.5). In this analysis, the teeth of *Dubreuillosaurus*, *Torvosaurus* and *Afrovenator* occupy different areas of morphospace and do not overlap with other taxa. However, *Megalosaurus bucklandi* shows limited overlap with the teeth of '*Megalosaurus dunkeri*' and the closely related taxon *Duriavenator*, and 100% overlap with those of *Magnosaurus* and *Eustreptospondylus* (Fig. 5.7; see SOM 5.10). This can be explained by the very similar dentition of *Duriavenator* and *Megalosaurus* (CH personal observations), and the limited data and sample size for *Eustreptospondylus* and *Magnosaurus*, which did not preserve a single complete erupted tooth. As for '*Megalosaurus dunkeri*' from the Lower Cretaceous of England, the teeth might pertain to one or several non-megalosaurid taxa from the Lower Cretaceous, such as *Neovenator*. The identification of isolated teeth referred to '*Megalosaurus dunkeri*' will however be discussed elsewhere.

The results of the discriminant analysis show that teeth of most clades of large ziphodont theropods, including Megalosauridae, are hardly distinguishable in terms of crown dimensions and number of denticles. Discriminant analysis should be used cautiously to identify large ziphodont teeth. Quantitative identification is only robust for the teeth of a few theropod clades such as Troodontidae, Spinosauridae, and Tyrannosauridae, which have typical morphometric features. Megalosauridae, along with Abelisauridae, Ceratosauridae, Allosauridae, and Neovenatoridae, possess teeth and denticles of similar dimensions, and only morphological qualitative characters, such as those proposed in the previous section, can really help differentiate them. In order to improve a quantitative analysis for differentiating the large ziphodont teeth, geometric morphometrics may be promising. For example, sections of the teeth may be digitized using quasi-homologous landmarks and superimposed using Procrustes analysis or a similar technique.

Although the large sample size of theropod teeth in this study provides opportunities for investigations of cladistic and taxonomic variability in non-avian theropods, the large number of taxa

TABLE 5.5. Table of misclassification for the reduced dataset (megalosaurid teeth only) grouped by taxa (ratios excluded).

Megalosaurid teeth	Number of teeth correctly assigned	Total	% correctly identified
Eustreptospondylus	3	7	42.9%
Magnosaurus	6	10	60%
Afrovenator	1	1	100%
Duriavenator	7	9	77.8%
Megalosaurus bucklandi	15	31	48.4%
'*Megalosaurus dunkeri*'	7	8	87.5%
Dubreuillosaurus	9	10	90%
Torvosaurus	7	8	87.5%
Total	55	84	65.5%

and teeth represented blurs the results of discriminant analysis. Nevertheless, the latter can be strengthened by improving the sample size for each taxon, but also by including additional morphometric variables, such as the elongation of mesial and distal denticles, the number of transverse undulations on the tooth, the extent of the mesial carina, the thickness of the dentine layer, and the curvature of the crown. Likewise, mesial and lateral dentitions, which have proven to be quantitatively distinct in theropods, should be considered separately for each taxon.

This study finally demonstrates that ratio variables have only weak influence on the results in most analyses. Discriminant analyses with and without ratio variables show nearly the same graphical results (see SOM 5.4–5.5, 5.8–5.10), and significant variations could only be noted in the analysis of megalosaurid teeth (see SOM 5.10), and of theropod teeth separated into mesial and lateral dentitions (see SOM 5.9). Likewise, the percentage of teeth correctly identified is rather similar in most analyses performed with and without ratio variables (see SOM 5.1–5.3). Nevertheless, important differences were noted in the discriminant analysis of the reduced dataset including large ziphodont theropod teeth at the generic level. In this analysis, 69.47% of specimens were correctly classified when excluding the ratios, whereas 34.61% were successfully identified when taking into account ratio variables. Given these results, it is recommended to avoid the use of ratio variables in discriminant analysis as they overemphasize some variables and do not help identify teeth.

Conclusions

The dentition of Megalosauridae, often considered to be similar to the dentition of other ziphodont theropods, can be distinguished by qualitative characters rather than quantitative data. Anatomically, megalosaurid teeth are characterized by a combination of features only visible in this clade, namely mesial teeth with a mesial carina facing mesiolabially, centrally-positioned carinae on both mesial and lateral crowns, a mesial carina terminating above the cervix, subquadrangular to subrectangular distal denticles with short to well-developed interdenticular sulci between them, symmetrically to asymmetrically convex external margin of the denticles, and braided and oriented

texture of the enamel. It is therefore clear that spinosaurid, abelisaurid, troodontid, dromaeosaurid or tyrannosaurid teeth are not the only theropods with diagnostic features, and a detailed study of the dentition of other important theropods such as *Dilophosaurus*, *Ceratosaurus*, *Allosaurus*, *Monolophosaurus*, *Sinraptor*, *Yangchuanosaurus*, *Dilong*, *Guanlong*, with additional quantitative data collected for each of them, is critically required in order to help to clarify the numerous variations existing between theropod clades (e.g., Ceratosauridae, Allosauridae, Metricanthosauridae, Neovenatoridae, and Proceratosauridae) with superficially similar dentitions.

III. EVOLUTION OF THE QUADRATE

Chapter 6: The non-avian theropod quadrate I: standardized terminology and overview of the anatomy, function and ontogeny

Published in ***PeerJ Preprints***, submitted to ***PeerJ*** (reviewed):
Hendrickx, C., Araújo, R. and Mateus, O. 2014. The non-avian theropod quadrate I: standardized terminology and overview of the anatomy, function and ontogeny. *PeerJ PrePrints*: 2:e379v1.

Hendrickx, C. and Mateus, O. 2012. Ontogenetical changes in the quadrate of basal tetanurans. In: Royo-Torres, R., Gascó, F. and Alcalá, L. (eds.), 10th Annual Meeting of the European Association of Vertebrate Palaeontologists. *¡Fundamental!*, Vol. 20, 101–104.

Abstract

By allowing the articulation of the mandible with the cranium, the quadrate of diapsids and most other tetrapods plays an important role morphofunctionally. In Theropoda, its morphology is particularly complex and varies importantly among different clades of non-avian theropods so that the quadrate possesses a strong taxonomic potential, making its morphology taxonomically useful. Inconsistencies in the notation and terminology used in discussions of the theropod quadrate anatomy have been noticed, a number of no less than eight different terms being sometimes given to a same structure. A standardized list of terms and notations for each quadrate anatomical entity is here proposed, with the goal of facilitating future descriptions of this important cranial bone.

An overview of the quadrate function, pneumaticity and ontogeny in non-avian theropods is also given. The quadrate of the large majority of non-avian theropods is akinetic, yet the diagonally oriented intercondylar sulcus of the mandibular articulation allowed both rami of the mandible to move laterally when opening the mouth in many of them. Pneumaticity of the quadrate is also present in most tetanuran clades and the pneumatic chamber, invaded by the quadrate diverticulum of the mandibular arch pneumatic system, was connected to one or several pneumatic foramina on the medial, lateral, posterior, anterior or ventral sides of the quadrate. Absence of a quadrate foramen and a poor delimitation of mandibular condyles seems to be ontogenetic features of some tetanurans.

Introduction

The quadrate (in Latin *quadratum*, meaning ‘square’) is a cranial bone of endochondral origin that articulates with the mandible in all gnathostomes except mammals, in which it evolved into the incus (Carroll 1988; Benton 2005; Brusatte 2012). In theropods, this bone plays many important functions such as a structural support for the basicranium, articulatory element with the lower jaws, attachment for several muscles, hearing and hosting important nerves and vascular passages (e.g., Witmer 1990, 1997*a*; Bakker 1998; Sedlmayr 2002; Kundrát and Janáček 2007; Holliday and Witmer 2008; Tahara and Larsson 2011; Appendices A6).

Although the outward morphology of the quadrate is simple, it varies significantly in the structure of its head, mandibular articulation, quadratojugal contact and the presence of pneumatic openings, quadrate foramen, and lateral processes among theropods with variable feeding strategies (e.g., Holtz 2003; Therrien et al. 2005; Hone and Rauhut 2010; Zanno and Makovicky 2011). Variation in the quadrate morphology in the derived theropod group Aves has long been used as a means of taxonomic distinction (e.g., Lowe 1926; Samejima and Otsuka 1987; Barbosa 1990; Elzanowski et al. 2001; Elzanowski and Stidham 2010). Likewise, but to a lesser degree, the systematic potential of the quadrate bone has also been noted for non-avian theropods (Maryańska and Osmólska 1997; Currie 2006), witnessing the particular importance that should be accorded to the description of this bone in the literature on non-avian theropod anatomy. Nevertheless, the terminology and abbreviations of the quadrate anatomy has been inconsistent in non-avian theropods, several different anatomical terms for the same quadrate sub-entity being often used (Table 6.1). Although a list of anatomical terms has been given by Baumel and Witmer (1993), Elzanowski et al. (2001) and Elzanowski and Stidham (2010) for the avian quadrate, the terminology proposed by these authors has never been followed in the description of the non-avian theropod quadrate hitherto. Indeed, the quadrate of birds has greatly changed in its morphology throughout the evolution of this clade and therefore displays many features absent in more primitive theropods, so that many anatomical terms coined by Elzanowski et al. (2001) and Elzanowski and Stidham (2010) cannot be applied for the non-avian theropod quadrate. Likewise, some quadrate entities such as the quadrate foramen and the lateral process observable in non-avian theropods are absent in their avian descendants and do not appear in the list of these authors.

The present paper has two major aims. The first is to propose a standardization of the anatomical terms for the quadrate sub-units, each associated with a two to four letters abbreviation and followed by a definition, in order to facilitate future description of this bone in the literature. The second is to review the function, pneumaticity and ontogeny of this important bone in non-avian theropods.

Proposed terminology of the quadrate anatomy

The anatomical terms of the theropod quadrate were grouped in five main sections, namely quadrate body, quadrate head, mandibular articulation, pterygoid flange, and pneumatic openings. The terms for each quadrate sub-units were selected by their relevance, significance and importance in the non-avian theropod literature. The non-standardized traditional Owenian/Romerian directional and anatomical terms (Harris 2004; Wilson 2006) were favoured over the terminology of the *Nomina Anatomica Veterinaria* (ICVGAN 2012) and the *Nomina Anatomica Avium* (Baumel 1993) because they are the most commonly used in the non-avian theropod literature (Eddy and Clarke 2011; pers. obs.). Consequently, ‘anterior’ and ‘posterior’ are used as directional terms rather than the veterinarian alternatives ‘cranial’ and ‘caudal’, respectively. The terminology of the avian theropod quadrate

TABLE 6.1. Terminology of non-avian theropod quadrate sub-unit by authors.

Source	Referred taxa	Quadrate shaft	Quadrate ridge	Pterygoid flange	Lateral process	Quadrate foramen	Quadrate head	Ento-/Ectocondyles
Sereno and Novas 1994	*Herrerasaurus*	Shaft	/	Pterygoid ramus	/	Quadrate foramen	Head	Distal condyles
Colbert 1989	*Coelophysis*	Ascending process	/	Quadrate flange	Smaller surface/wing	/	Upper extremity	Quadrate condyle
Welles 1984	*Dilophosaurus*	Shaft	Column	Pterygoid wing	Dorsal wing	Quadrate foramen	Head	Ento/Ectocondyles
Smith et al. 2007	*Cryolophosaurus*	Body	Rounded ridge	/	/	Paraquadrate fenestra	Dorsal head	Medial/Lateral condyles
Gilmore 1920	*Ceratosaurus/ Allosaurus*	/	/	Sheet/projection	/	Quadrate foramen	/	articular surfaces
Madsen and Welles 2000	*Ceratosaurus*	Pillar	/	Pterygoid wing	Anterolateral wing	Quadrate foramen	Head	Ento/Ectocondyles
Carrano et al. 2011	*Masiakasaurus*	Shaft/body	/	Pterygoid articular flange	/	Foramen	/	Medial/Lateral condyles
Coria and Salgado 1998	*Ilokelesia*	/	/	Medial process	Lateral lamina/process	/	Squamosal condyle	Medial/Lateral condyles
Bonaparte et al. 1990	*Carnotaurus*	/	/	Anteromedial projection	/	/	/	Lower condyles
Sampson and Witmer 2007	*Majungasaurus*	Shaft	/	Pterygoid ramus	Lateral/quadratojugal ramus	Paraquadrate foramen	Head	Medial/Lateral condyles
Sadleir et al. 2008	*Eustreptospondylus*	Shaft	/	Pterygoid ala	/	/	Head	Medial/Lateral condyles
Britt 1991	*Torvosaurus*	Shaft	/	Pterygoid blade	/	Quadrate foramen	Head	Medial/Lateral condyles
Charig and Milner 1997	*Baryonyx*	Shaft	/	Pterygoid flange	/	Quadrate foramen	Head	Quadrate condyle
Madsen 1976*b*	*Allosaurus*	Shaft/body	/	Contact with the pterygoid	/	Quadrate foramen	Head	Condyles
Sereno et al. 2008	*Aerosteon*	Shaft	/	Pterygoid process	/	Quadrate foramen	Head	Distal condyles
Currie 2006	*Sinraptor*	Column	/	Pterygoid flange/ala	Wing-like process	Quadratic foramen	Quadrate cotyle	Medial/Lateral condyles
Currie and Carpenter 2000	*Acrocanthosaurus*	/	/	/	/	Quadrate foramen	Head	Condyles
Eddy and Clarke 2011	*Acrocanthosaurus*	/	/	Pterygoid wing/contact	/	Quadrate foramen/fenestra	Quadrate cotylus	Medial/Lateral condyles
Brusatte et al. 2010*b*	*Shaochilong*	Shaft	/	Quadrate flange	/	Quadrate foramen	Quadrate cotylus/head	Medial/Lateral condyles
Coria and Currie 2006	*Mapusaurus*	/	/	Pterygoid flange	/	Quadratic foramen	Quadrate cotyle	Mandibular articulation
Rauhut et al.	*Proceratosaurus*	/	Columnar	Pterygoid flange	/	Quadrate foramen	Head	Medial/Lateral

2010			ridge					condyles
Li et al. 2010	*Xiongguanlong*	Shaft	/	Quadrate wing	/	Quadrate foramen	/	Medial/Lateral condyles
Brusatte et al. 2012*a*	*Alioramus*	Shaft	Robust ridge	Quadrate flange	/	Quadrate foramen	Head	Medial/Lateral condyles
Carr 1996	*Albertosaurus*	Quadrate body	Ridge	Pterygoid flange/process	/	Quadrate fenestra	Quadrate cotyle	Medial/Lateral condyles
Currie 2003	*Albertosaurus*/ *Daspletosaurus*	/	/	Pterygoid ala	/	Quadrate fenestra	Quadrate cotylus	Mandibular condyles
Molnar 1991	*Tyrannosaurus*	Vertical bar	/	Pterygoid process	/	Quadrate foramen	Hemispherical surface	Quadrate condyle
Brochu 2003	*Tyrannosaurus*	/	/	Pterygoidal flange	/	Quadrate foramen	Head	Medial/Lateral hemicondyles
Dal Sasso and Maganuco 2011	*Scipionyx samniticus*	/	/	Pterygoid ala	/	Paraquadrate foramen	Quadrate head	Medial/Lateral condyles
Kobayashi and Lü 2003	*Sinornithomimus*	/	/	Pterygoid wing	/	Paraquadratic foramen	/	Medial/Lateral condyles
Kobayashi and Barsbold 2005*a*	*Garudimimus*	/	/	Pterygoid wing	/	Paraquadratic foramen	/	Mandibular condyles
Zanno 2010*b*	*Falcarius*	/	/	Pterygoid process/flange/wing	/	Quadrate foramen	Head/Squamosal capitulum	Medial/Lateral condyles
Clark et al. 1994	*Erlikosaurus*	Body	/	Orbital process	/	Quadrate foramen	Dorsal process	Mandibular process
Maryańska and Osmólska 1997	Oviraptoridae	Shaft	/	Pterygoid ramus	/	Quadrate foramen	Otic process	Medial/Lateral condyles
Choiniere et al. 2010*a*	*Zuolong*	Shaft	Ridge	Pterygoid ramus	/	Quadrate foramen	Dorsal condyle	Medial/Lateral condyles
Burnham 2004	*Bambiraptor*	/	/	/	/	/	Otic process	Medial/Lateral condyles
Norell et al. 2006	*Tsaagan*	Shaft	/	Anterior/pterygoid flange	Squamosal ramus	Quadrate foramen	Dorsal articulation	Articular ramus
Colbert and Russell 1969	*Dromaeosaurus*	Shaft	/	Pterygoid flange/wing	/	Quadrate foramen	Head	Medial/Lateral condyles
Currie 1995	*Dromaeosaurus*	/	/	Anterodorsal lamina	/	Quadrate fenestra	Head	/
Norell and Hwang 2004	*Saurornithoides*	Shaft	/	Pterygoid flange	/	/	/	Medial/Lateral condyles
Norell et al. 2009	*Zanabazar*	Shaft	/	/	/	/	Head	/

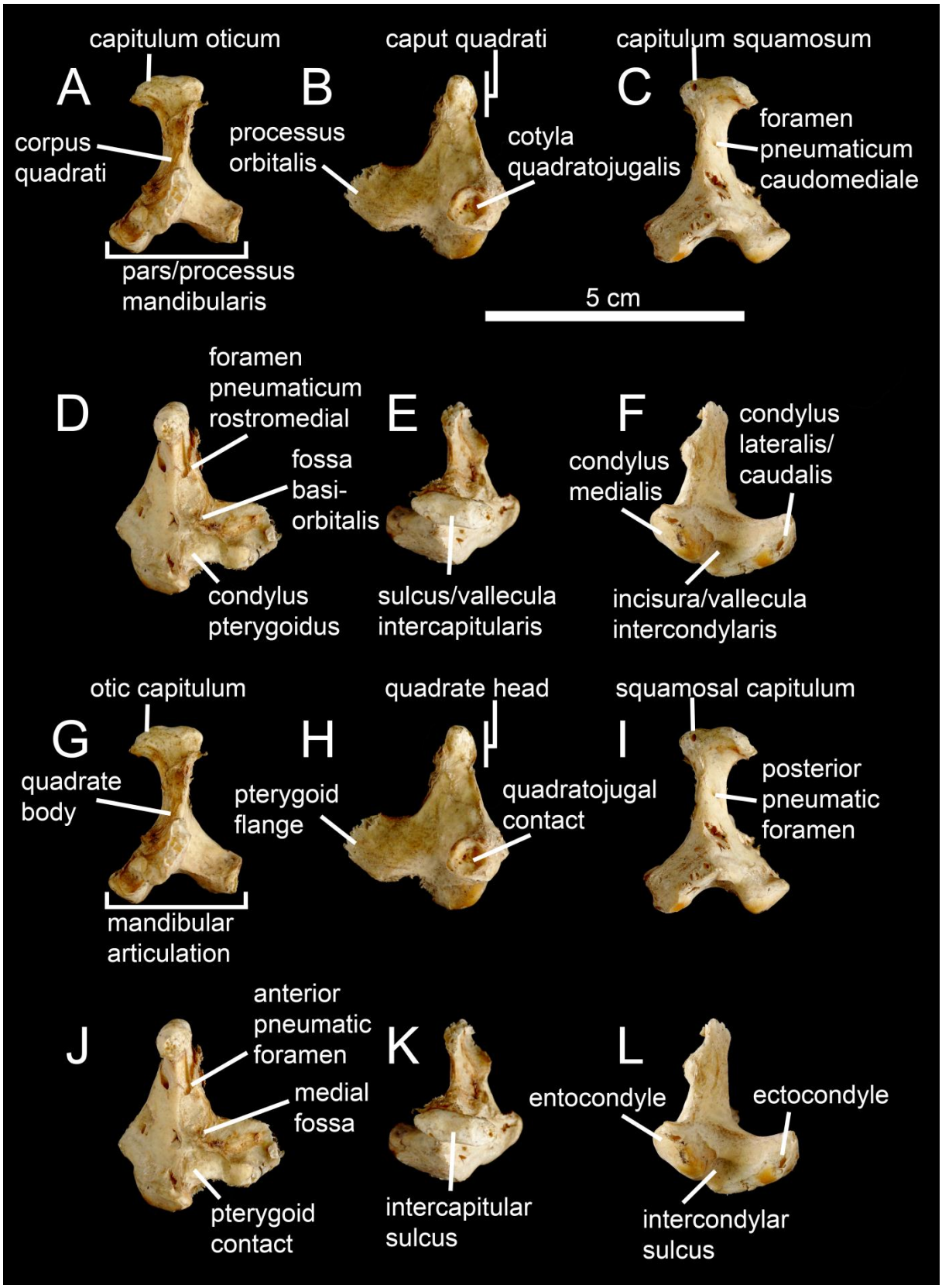

FIGURE 6.1. Avian and non-avian theropod terminology of the quadrate bone. Left quadrate of the common ostrich *Struthio camelus* (NH.11.75; courtesy of Paolo Viscardi, Horniman Museum & Gardens) annotated with **A-F**, Baumel and Witmer (1993), Elzanowski et al. (2001) and Elzanowski and Stidham (2010) terminologies; and **G-L**, the here proposed terminology for the non-avian theropod quadrate. Quadrate in **A, G**, anterior; **B, H**, lateral; **C, I**, posterior; **D, J**, medial; **E, K**, dorsal; and **F, L**, ventral views.

adopted by the *Nomina Anatomica Avium* (Baumel 1993) and updated by Elzanowski et al. (2001) and Elzanowski and Stidham (2010) is also compared with the here proposed terminology of the non-avian theropod quadrate (Fig. 6.1; Table 6.2).

Quadrate Body

Quadrate body (qb)—Part of the quadrate that includes the quadrate shaft, the quadrate ridge, the lateral contact (quadratojugal and/or squamosal contact), and the lateral process, and excludes the quadrate head, mandibular articulation, and pterygoid flange (Figs. 6.1G, 6.2C). In posterior view, the quadrate body is delimited by the lateral margin of the lateral contact and sometimes by the medial margin of the quadrate foramen, the dorsal margin of the mandibular articulation, the ventral margin of the quadrate head, and a medial margin mostly formed by the quadrate shaft and the medial fossa of the pterygoid flange. The quadrate body is equivalent to the 'Corpus ossis quadrati' of Baumel and Witmer (1993), and the 'Corpus quadrati' of Elzanowski et al. (2001) and Elzanowski and Stidham (2010) for avian theropods.

Quadrate shaft (qs)—Part of the quadrate body that excludes the lateral process and all articulating surfaces (i.e., quadrate head, quadratojugal/squamosal/pterygoid contacts, and mandibular articulation; Fig. 6.2C–D). The quadrate shaft, as called by Welles (1984), Sereno and Novas (1994), Norell et al. (2006), Sampson and Witmer (2007), Sereno et al. (2008), Carrano et al. (2011), and Brusatte et al. (2012*a*), is also referred as the 'quadrate pillar' by Madsen and Welles (2000), and the 'ascending process' by Colbert (1989).

Quadrate ridge (qr)—Dorsoventrally elongated column, ridge or crest located on the quadrate body and visible in posterior view (Fig. 6.2C–D). Although the quadrate ridge is present in the large majority of non-avian theropods, a description of the structure is often omitted in the literature. The quadrate ridge is referred as 'a column' by Welles (1984), a 'ridge-like mediodorsal edge' by Carr (1996), 'a prominent rounded ridge' by Smith et al. (2007), a 'columnar ridge' by Rauhut et al. (2010) and a 'robust ridge' by Brusatte et al. (2012*a*).

Quadrate ridge groove (qrg)—Groove dividing the quadrate ridge in two different units at two thirds, or more dorsally, of the quadrate body height. A quadrate ridge groove is seen in some allosauroid theropods (Fig. 6.2G).

Quadrate foramen (qf)—Aperture in the quadrate body or concavity on the lateral margin of the quadrate body and delimited ventrally by the ventral quadratojugal contact and dorsally by the dorsal quadratojugal contact and its ventral projection in some theropod taxa (Fig. 6.2). Most authors usually refer to this perforation as the quadrate foramen (e.g., Welles 1984; Sereno and Novas 1994; Charig and Milner 1997; Maryańska and Osmólska 1997; Currie and Carpenter 2000; Coria and Currie 2006; Norell et al. 2006; Zanno 2010*b*; Choiniere et al. 2010*a*; Brusatte et al. 2012*a*; Rauhut et al. 2012), but it can be also called the 'paraquadratic foramen' (e.g., Barsbold and Osmólska 1999; Kobayashi and Lü 2003; Kobayashi and Barsbold 2005*a*), the 'paraquadrate foramen' (Sampson and

Witmer 2007; Dal Sasso and Maganuco 2011), the ‘paraquadrate fenestra’ (Smith et al. 2007) or the ‘quadrate fenestra’ (e.g., Carr 1996; Sereno et al. 1998; Currie 2003; Eddy and Clarke 2011). A quadrate foramen is seen in all non-avian theropods other than Ceratosauria and Megalosauridae.

Lateral process (lpq)—Lateral or anterolateral projection of the lateral margin of the quadrate body (Fig. 6.2A–B, E). Also known as the ‘dorsal wing’ (Welles 1984; Currie 2006), the ‘anterolateral wing’ (Madsen and Welles 2000), the ‘lateral lamina’ (Coria and Salgado 1998) and the ‘lateral ramus’ (Sampson and Witmer 2007), this process can contact the quadratojugal and/or the squamosal and therefore either be referred to the quadratojugal ramus by Sampson and Witmer (2007) or the squamosal ramus Norell et al. (2006).

Quadratojugal contact (qjc)—Contact of the quadrate with the quadratojugal on the lateral, anterolateral or, posterolateral margin of the quadrate body (Fig. 6.2G). The quadratojugal contact, which is similar to the ‘cotyla quadratojugalis’ of Baumel and Witmer (1993), Elzanowski et al. (2001) and Elzanowski and Stidham (2010) for avian theropods (Fig. 6.1B), can be divided into a ventral and a dorsal quadratojugal contact when the quadrate foramen is present and delimited by both quadrate and quadratojugal.

Ventral quadratojugal contact (vqjc)—ventral contact of the quadrate with the quadratojugal. The ventral quadratojugal contact of the quadrate always receives the quadratojugal bone (Fig. 6.2).

Dorsal quadratojugal contact (dqjc)—dorsal contact of the quadrate with the quadratojugal (Fig. 6.2). The ventral quadratojugal contact of the quadrate can either receive the quadratojugal or both quadratojugal and squamosal in some theropod taxa.

Ventral projection of the dorsal quadratojugal contact (vpdq)—Ventrodorsally short projection of the dorsal quadratojugal contact extending ventrally, and delimiting the dorsolateral margin of the quadrate foramen (Fig. 6.2F, I).

Dorsal projection of the ventral quadratojugal contact (dpvq)—Ventrodorsally short projection of the ventral quadratojugal contact extanding dorsally, and delimiting the ventrolateral margin of the quadrate foramen.

Quadratojugal process (qjp)—Anterior projection of the ventral quadratojugal contact of the quadrate (Fig. 6.2B).

Lateroventral process (lvp)—Lateromedially oriented ventral projection of the ventral quadratojugal contact of the quadrate that bounds the quadratojugal ventrally (Fig. 6.2H). The lateroventral process is similar to the ‘lateral process’ of Maryańska and Osmólska (1997).

Squamosal contact (sqc)—Contact on the lateral margin of the quadrate with the squamosal (Fig. 6.2A–B).

Posterior fossa (pfq)—Depression or concavity situated on the posterior side of the quadrate body and dorsal to the mandibular articulation, ventral to the quadrate head and lateral to the quadrate ridge. The posterior fossa can include or exclude the quadrate foramen (Fig. 6.2B–C).

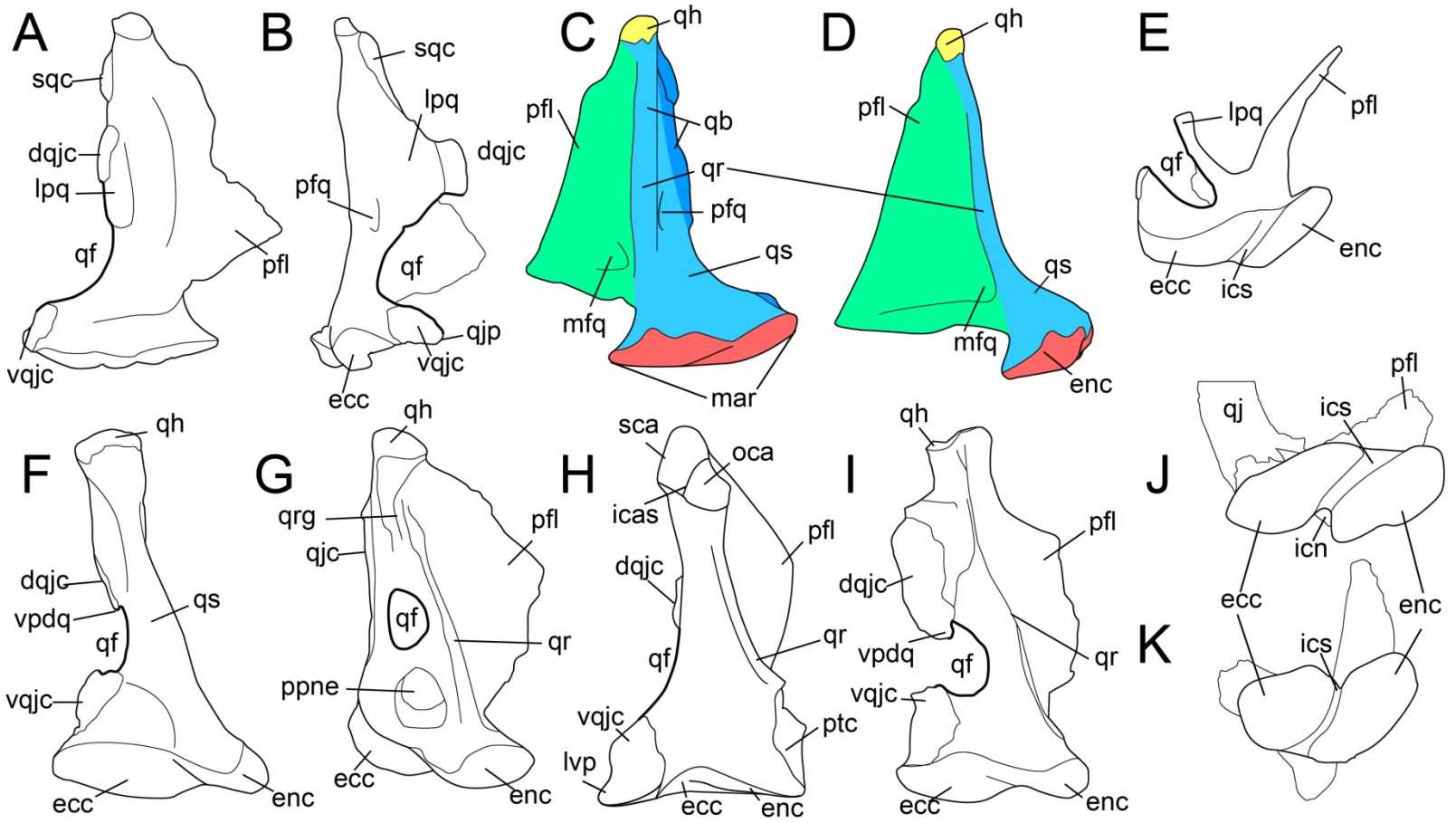

FIGURE 6.2. Anatomy of non-avian theropod quadrates. **A–E**, Line drawings of the right quadrate of *Tsaagan mangas* (IGM 100-1015) in **A**, anterior; **B**, lateral; **C**, posterior; **D**, medial; and **E**, ventral views; **F–I**, left and **J–K**, right quadrates of **F**, *Baryonyx walkeri* (NHM R9951); **G**, *Aerosteon riocoloradensis* (MCNA-PV-3137); **H**, an indeterminate Oviraptoridae (IGM A; Maryańska and Osmólska 1997); **I**, *Tyrannosaurus rex* (BHI 3333; Larson 2008*b*); **J**, *Allosaurus* sp. (SMA 005/02); and **K**, *Majungasaurus crenatissimus* (FMNH PR 2100) in **F–I**, posterior; and **J–K**, ventral views. **Abbreviations**: **dqjc**, dorsal quadratojugal contact; **ecc**, ectocondyle; **enc**, entocondyle; **icn**, intercondylar notch; **ics**, intercondylar sulcus; **lpq**, lateral process of the quadrate; **lvp**, lateroventral process; **mar**, mandibular articulation (in red); **mfq**, medial fossa of the quadrate; **oca**, otic capitulum; **pfl**, pterygoid flange (in green); **pfq**, posterior fossa of the quadrate; **ppne**, posterior pneumatic foramen; **qb**, quadrate body (in light and dark blue); **qf**, quadrate foramen (delimited by a broader line); **qh**, quadrate head (in yellow); **qj**, quadratojugal; **qjp**, quadratojugal process; **qr**, quadrate ridge; **qrg**, quadrate ridge groove; **qs**, quadrate shaft (in light blue); **sqc**, squamosal contact; **sca**, squamosal capitulum; **vqjc**, ventral quadratojugal contact; **vpdq**, ventral projection of the dorsal quadratojugal contact; **vsh**, ventral shelf.

TABLE 6.2. Standardized terminology and abbreviation of the non-avian theropod quadrate and comparison with the terminology of the avian quadrate based on Baumel and Witmer (1993), Elzanowski et al. (2001) and Elzanowski and Stidham (2010).

Non-avian theropod quadrate	q	Avian theropod quadrate
Quadrate body	qb	Corpus quadrati
Quadrate shaft	qs	/
Quadrate ridge	qr	/
Quadrate ridge groove	qrg	/
Quadrate head	qh	Processus oticus/Pars otica/Caput quadrati
Otic capitulum	oca	Capitulum oticum
Squamosal capitulum	sca	Capitulum squamosum
Intercapitular sulcus	icas	Incisura/Vallecula intercapitularis
Quadrate foramen	qf	/
Mandibular articulation	mar	Pars/Processus mandibularis
Ectocondyle	ecc	Condylus (mandibularis) lateralis
Entocondyle	enc	Condylus (mandibularis) medialis
Mediocondyle	mec	Condylus caudalis
Intercondylar sulcus	ics	Vallecula intercondylaris
Intercondylar notch	icn	Depressio praecondylaris
Lateral process	lpq	/
Quadratojugal contact	qjc	Cotyla quadratojugalis
Ventral quadratojugal contact	vqjc	/
Dorsal quadratojugal contact	dqjc	/
Quadratojugal process	qjp	/
Ventral projection of the dorsal quadratojugal contact	vpdq	/
Squamosal contact	sqc	/
Posterior fossa	pfq	/
Quadrate diverticulum	qdi	/
Dorsal pneumatic foramen	dpne	Foramen pneumaticum caudomediale
Medial pneumatic foramen	mpne	Foramen pneumaticum basiorbitale
Posterior pneumatic foramen	ppne	Foramen pneumaticum rostromediale
Ventral pneumatic foramen	vpne	Foramen pneumaticum adventitium
Pterygoid flange	pfl	Processus orbitalis
Pterygoid contact	ptc	Condylus pterygoideus/Facies articularis pterygoidea
Medial fossa	mfq	Fossa basiorbitalis
Ventral shelf	vsh	/

Quadrate Head

Quadrate head (qh)—Dorsal articulation of the quadrate abutting to the cotyle of the squamosal and touching other bones of the braincase in some theropod taxa (Fig. 6.2). The quadrate head, as it is called by Britt (1991), Charig and Milner (1997), Madsen and Welles (2000), Sampson and Witmer (2007), Sereno et al. (2008), Norell et al. (2009) and Brusatte et al. (2012*a*) among others, has also been termed ‘quadrate cotylus’ (Currie 2003; Coria and Currie 2006), ‘quadrate cotyle’ (Currie 2003; Coria and Currie 2006), ‘squamosal condyle’ (Coria and Salgado 1998), ‘squamosal articulation’ (Turner et al. 2011), and ‘otic process’ (Maryańska and Osmólska 1997; Burnham 2004; Holliday and Witmer 2008). In avian theropods, the quadrate head is homologous to the ‘Caput quadrati’ of Elzanowski et al. (2001) and Elzanowski and Stidham (2010; Fig. 6.1B), and roughly equivalent to the ‘Processus oticus’ of Baumel and Witmer (1993). In birds, the ‘Processus oticus’ of Baumel and Witmer (1993), and the ‘Pars oticus’ of Elzanowski et al. (2001) and Elzanowski and

Stidham (2010) also includes several sub-units that are either absent in non-avian theropods (e.g., Crista Tympanica, Tuberculum subcapitulare), or here included in the quadrate body (e.g., Sulcus pneumaticus, Foramen pneumaticum rostromediale). The bistylic quadrate head present in alvarezsauroids, oviraptorids and avian theropods is divides into otic and squamosal capitula.

Otic capitulum (oca)—Medial capitulum of the quadrate head articulating with the braincase (Fig. 6.2H). The otic capitulum is referred as the 'capitulum (condylus) oticum' by Baumel and Witmer (1993), Elzanowski et al. (2001) and Elzanowski and Stidham (2010) for avian theropods.

Squamosal capitulum (sca)—Lateral capitulum of the quadrate head articulating with the squamosal (Fig. 6.2H). The squamosal capitulum is similar to the 'capitulum (condylus) squamosum' of Baumel and Witmer (1993), Elzanowski et al. (2001) and Elzanowski and Stidham (2010) for avian theropods.

Intercapitular sulcus (icas)—Groove separating the ootic capitulum from the squamosal capitulum on the dorsal surface of the quadrate head (Fig. 6.2H). The intercapitular sulcus (*sensu* Witmer 1990) is equivalent to the 'incisura intercapitularis' of Baumel and Witmer (1993), and the 'vallecula intercapitularis' of Elzanowski et al. (2001) and Elzanowski and Stidham (2010) for avian theropods.

Mandibular Articulation

Mandibular articulation (mar)—Ventral surface of the quadrate, articulating with the mandible and fitting in the glenoid fossa of the lower jaw. It includes the ectocondyle, entocondyles, sometimes a mediocondyle, and an intercondylar sulcus (Fig. 6.2C). The mandibular articulation is equivalent to the 'Processus mandibularis' of Baumel and Witmer (1993; Fig. 6.1A), and 'Pars mandibularis' of Elzanowski et al. (2001) and Elzanowski and Stidham (2010) for avian theropods. Although most authors (e.g., Currie 2006; Sampson and Witmer 2007; Rauhut et al. 2010; Brusatte et al. 2012*a*) referred the ectocondyle and entocondyles as the lateral and medial condyles (or hemicondyles) respectively, the terms ectocondyle and entocondyle have been used by Welles (1984), and Madsen and Welles (2000). The condyle present in between the ecto- and entocondyles in some theropods is here coined mediocondyle.

Ectocondyle (ecc)—Lateral condyle of the mandibular articulation (Fig. 6.2). The ectocondyle is equivalent to the 'condylus (mandibularis) lateralis' of Baumel and Witmer (1993; Fig. 6.1F), Elzanowski et al. (2001) and Elzanowski and Stidham (2010) for avian theropods.

Entocondyle (enc)—Medial condyle of the mandibular articulation. The entocondyle has been referred as the 'condylus (mandibularis) medialis' by Baumel and Witmer (1993; Fig. 6.1F), Elzanowski et al. (2001) and Elzanowski and Stidham (2010) for avian theropods.

Mediocondyle (mdc)—Median condyle of the mandibular articulation. The mediocondyle is referred as the third condyle by Clark et al. (1994) and Xu and Wu (2001), the 'accessory condyle' by

Kobayashi and Lü (2003), and the ‘condylus caudalis’ of Baumel and Witmer (1993) and Elzanowski et al. (2001) for avian theropods.

Intercondylar sulcus (ics)—Groove separating the ectocondyle from the entocondyle and articulated with the interglenoid ridge of the articular (Fig. 6.2E, J, K). The intercondylar sulcus, a term also used by Carrano et al. (2011), can be referred as a ‘groove’ (e.g., Madsen 1976*b*; Britt 1991; Madsen and Welles 2000; Currie 2006), ‘swelling’ (Charig and Milner 1997), ‘sulcus’ (e.g., Kobayashi and Lü 2003; Norell et al. 2006; Sadleir et al. 2008), ‘trochlea’ (Brochu 2003; Brusatte et al. 2010*b*), trochlear surface (Brusatte et al. 2010*b*, 2012*a*), and ‘intercondylar bridge’ (Zanno 2010*b*). The intercondylar sulcus is similar to the ‘sulcus intercondylaris’ (Baumel and Witmer 1993) and the ‘vallecula intercondylaris’ (Elzanowski et al. 2001; Elzanowski and Stidham 2010) of the quadrate of avian theropods (Fig. 6.1L).

Intercondylar notch (icn)—Notch located in between the ectocondyle and entocondyle, either on the anterior or posterior margin of the mandibular articulation, and being referred as the ‘pit’ of Bakker (1998; Fig. 6.2J).

Pterygoid Flange

Pterygoid flange (pfl)—Sheet-like projection anteriorly or anteromedially from the anterior surface of the quadrate body to contact the pterygoid bone (Fig. 6.2). The pterygoid flange, a term also used by Charig and Milner (1997), Brochu (2003), Currie (2006), Coria and Currie (2006) and Rauhut et al. (2010), is also known as the ‘quadrate/anterior flange’ (e.g., Colbert 1989; Norell et al. 2006; Brusatte et al. 2010*b*, 2012*a*), the ‘pterygoid ramus’ (e.g., Sereno and Novas 1994; Sampson and Witmer 2007; Choiniere et al. 2010*a*), the ‘pterygoid wing’ (e.g., Welles 1984; Madsen and Welles 2000; Eddy and Clarke 2011), the ‘pterygoid ala’ (e.g., Currie 2003, 2006; Sadleir et al. 2008; Dal Sasso and Maganuco 2011), the ‘pterygoid process’ (Molnar 1991; Carr 1996; Sereno et al. 2008), the ‘optic wing’ (Balanoff and Norell 2012), the ‘orbital process’ (Clark et al. 1994; Chiappe et al. 2002), and the ‘processus orbitalis’ (Baumel and Witmer 1993; Elzanowski et al. 2001; Elzanowski and Stidham 2010; Fig. 6.1B) for avian theropods.

Pterygoid contact (ptc)—Contact on the medial margin of the pterygoid flange, or the quadrate body, with the pterygoid. In avian theropods, the pterygoid contact is homologous, to the ‘facies pterygoidea’ in Elzanowski et al. (2001) and the ‘facies articularis pterygoidea’ in Elzanowski and Stidham (2010), as well as the ‘condylus pterygoideus’, located on the quadrate body in Baumel and Witmer (1993; Fig. 6.1D), Elzanowski et al. (2001), and Elzanowski and Stidham (2010).

Medial fossa (mfq)—Depression or concavity located on the medial surface of the pterygoid flange, typically in the posteroventral end of the pterygoid flange (Fig. 6.2C–D). The medial fossa is delimited by the quadrate shaft and the ventral shelf in some theropod taxa. The medial fossa is similar to the ‘fossa corporis quadrati’ of Fuchs (1954) and the ‘fossa basiorbitalis’ of Elzanowski et al. (2001) and Elzanowski and Stidham (2010) for avian theropods (Fig. 6.1D).

Ventral shelf (vsh)—A medial or medioposterior fold of the ventral margin of the pterygoid flange. The term 'shelf' was employed by Sereno and Novas (1994) and ventral shelf was used by Sampson and Witmer (2007), Eddy and Clarke (2011) and Carrano et al. (2011).

Pneumatic Openings

Quadrate diverticulum (qdi)—Air sac invading the pneumatic chamber inside the quadrate body and communicating with other diverticula by the quadrate pneumatic foramina.

Dorsal pneumatic foramen (dpne)—Pneumatic foramen located on the anterodorsal surface of the quadrate, just ventral to the quadrate head.

Medial pneumatic foramen (mpne)—Pneumatic foramen or recess situated on the medial side of the quadrate, typically in the ventromedial part of the pterygoid flange. The medial pneumatic foramen is homologuous to the 'foramen pneumaticum' of Baumel and Witmer (1993), and the 'foramen pneumaticum basiorbitale' of Elzanowski et al. (2001) and Elzanowski and Stidham (2010) for avian theropods.

Posterior pneumatic foramen (ppne)—Pneumatic foramen or recess on the posterior surface of the quadrate body, typically at mid-height of the quadrate (Fig. 6.2G). The posterior pneumatic foramen is similar to the 'foramen pneumaticum caudomediale' of Elzanowski and Stidham (2010) for avian theropods (Fig. 6.1C).

Anterior pneumatic foramen (apne)—Pneumatic foramen or recess on the anterior surface of the quadrate body, typically at mid-height of the quadrate. The anterior pneumatic foramen is likely homologous to the 'foramen pneumaticum medial' of Elzanowski et al. (2001), and the 'foramen pneumaticum rostromediale' of Elzanowski and Stidham (2010; Fig. 6.1D).

Ventral pneumatic foramen (vpne)—Pneumatic foramen or recess on the ventral surface of the quadrate. The ventral pneumatic foramen is equivalent to the 'foramen pneumaticum adventitium' (ectopic pneumatic foramen) of Elzanowski and Stidham (2010) for avian theropods.

Lateral pneumatic foramen (lpne)—Pneumatic foramen or recess on the lateral surface of the quadrate.

Inter-taxic Topological Homologies

To establish comparisons between taxa with widely disparate quadrate morphology, a homology concept of the feature in question is required. Here, we give a general account of the variability within different anatomical sub-units of the quadrate and by following the criteria summarized in Rieppel (2006).

The quadrate ridge is easily distinguishable in many theropod taxa such as *Dilophosaurus whetherilli* (Welles 1984; Fig. 6.3C), *Aerosteon riocoloradensis* (MCNA-PV 3137; Fig. 6.4C) and *Proceratosaurus bradleyi* (NHM R.4860), but the demarcation of this structure may be only subtly

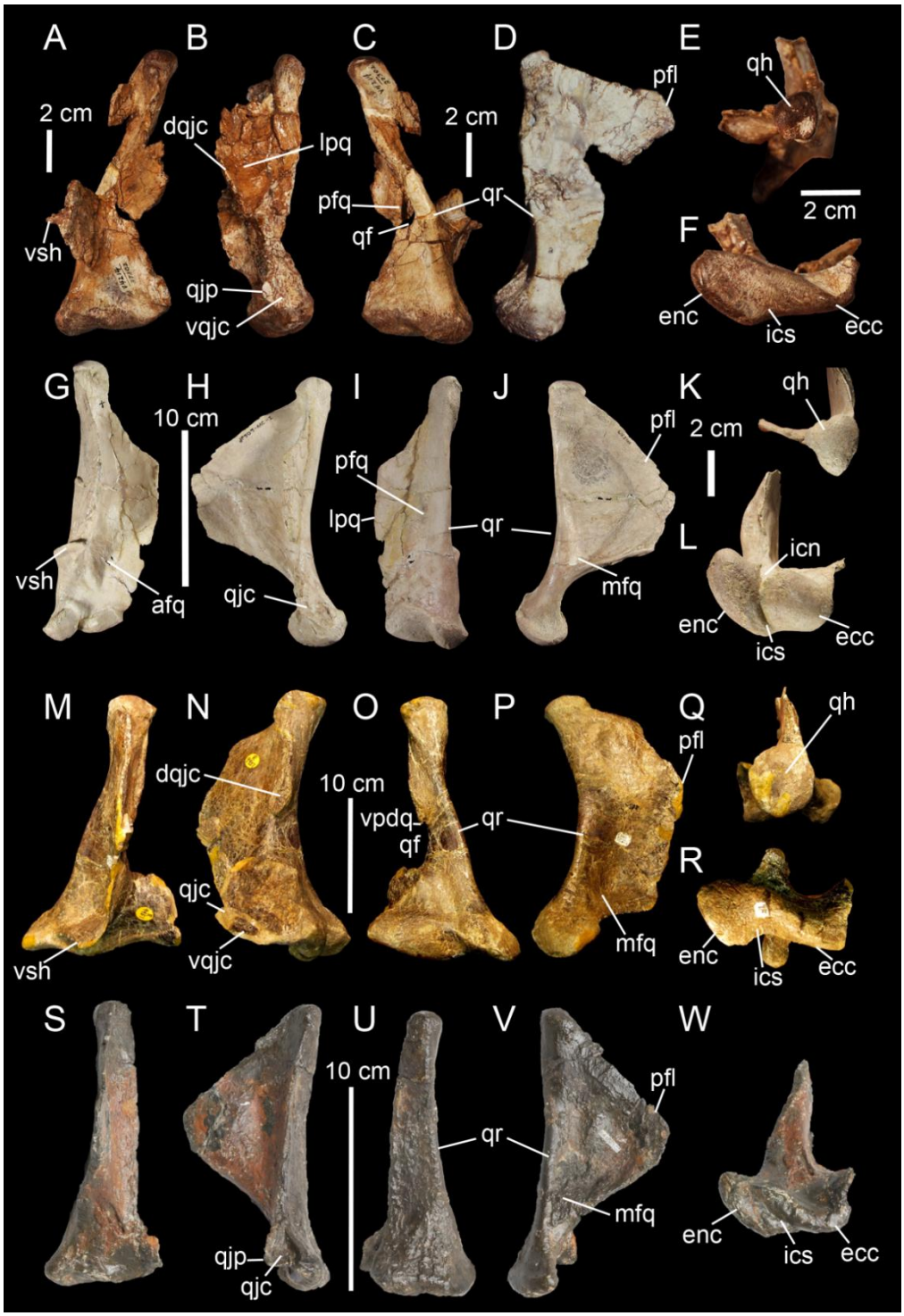

FIGURE 6.3. Topological homologies in the non-averostran theropod quadrate. **A, C, F**, Left; and **B, D, E**, right (reversed) quadrates of *Dilophosaurus wetherilli* (UCMP 37302) in **A**, anterior; **B**, lateral; **C**, posterior; **D**, medial; **E**, dorsal; and **F**, ventral views (courtesy of Randall Irmis and Matthew Carrano); **G–L**, Right quadrate (reversed) of *Majungasaurus crenatissimus* (FMNH PR 2100) in **G** anterior; **H**, lateral; **I**, posterior; **J**, medial; **K**, dorsal; and **L**, ventral views; **M–R**, Left quadrate of *Baryonyx walkeri* (NHM R9951) in **M**, anterior; **N**, lateral; **O**, posterior; **P**, medial; **Q**, dorsal; and **R**, ventral views. **S–W**, Right quadrate of *Eustreptospondylus oxoniensis* (OUMNH J.13558; reversed) in **S**, anterior; **T**, lateral; **U**, posterior; **V**, medial; and **W**, ventral views (courtesy of Paul Barrett). **Abbreviations**: **afq**, anterior fossa; **dqjc**, dorsal quadratojugal contact; **ecc**, ectocondyle; **enc**, entocondyle; **icn**, intercondylar notch; **ics**, intercondylar sulcus; **lpq**, lateral process; **mfq**, medial fossa; **pfq**, posterior fossa; **pfl**, pterygoid flange; **qf**, quadrate foramen; **qh**, quadrate head; **qjp**, quadratojugal process; **qr**, quadrate ridge; **vpdq**, ventral projection of the dorsal quadratojugal contact; **vqjc**, ventral quadratojugal contact; **vsh**, ventral shelf of the pterygoid flange.

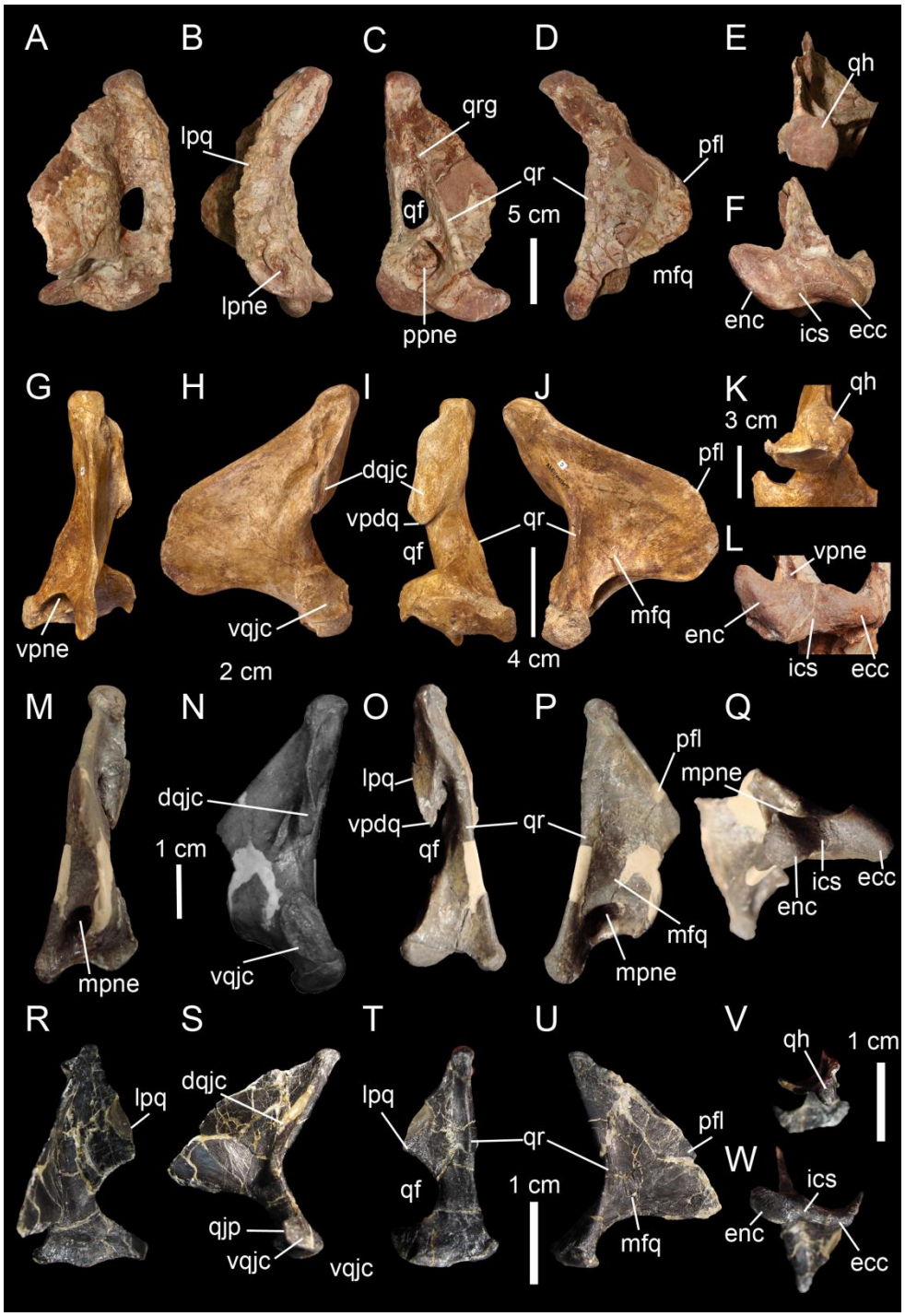

FIGURE 6.4. Topological homologies in the non-avian averostran quadrate. **A–F**, Left quadrate of *Aerosteon riocoloradensis* (MCNA-PV-3137) in **A**, anterior; **B**, lateral; **C**, posterior; **D**, medial; **E**, dorsal; and **F**, ventral views (courtesy of Martin Ezcurra); **G–K**, Left quadrate of *Alioramus altai* (IGM 100-1844) in **G**, anterior; **H**, lateral; **I**, posterior; **J**, medial; and **K**, dorsal views (courtesy of Mick Ellison © AMNH). **L**, Right quadrate of *Qianzhousaurus sinensis* (GM F10004-1; reversed) in ventral views (courtesy of Stephen Brusatte); **M–Q**, Right quadrate of *Falcarius utahensis* (UMNH VP 14559; reversed) in **M**, anterior; **N**, lateral; **O**, posterior; **P**, medial; and **Q**, ventral views (courtesy of Lindsay Zanno); **R–W**, Left quadrate of *Bambiraptor feinbergi* (AMNH 30556) in **R**, anterior; **S**, lateral; **T**, posterior; **U**, medial; **V**, dorsal; and **W**, ventral views. **Abbreviations**: **afq**, anterior fossa; **dqjc**, dorsal quadratojugal contact; **ecc**, ectocondyle; **enc**, entocondyle; **icn**, intercondylar notch; **ics**, intercondylar sulcus; **lpq**, lateral process; **mfq**, medial fossa; **mpne**, medial pneumatic foramen; **pfq**, posterior fossa; **ppne**, posterior pneumatic foramen; **pfl**, pterygoid flange; **qf**, quadrate foramen; **qh**, quadrate head; **qjp**, quadratojugal process; **qr**, quadrate ridge; **vpdq**, ventral projection of the dorsal quadratojugal contact; **vpne**, ventral pneumatic foramen; **vqjc**, ventral quadratojugal contact; **vsh**, ventral shelf of the pterygoid flange.

developed, as in *Noasaurus leali* (PVL 4061), *Majungasaurus crenatissimus* (FMNH PR 2100; Fig. 6.3I), and *Eustreptospondylus oxoniensis* (OUMNH J.13558; Fig. 6.3U). The quadrate ridge is developed as a 'columnar ridge' in many theropod clades like in *Dilophosaurus wetherilli* (Welles 1984), *Allosaurus* (SMA 005/02) and *Eotyrannus lengi* (MIWG 1997.550), and also forms to a thin crest as in Tyrannosauridae (AMNH 5027; Carr 1996; Brusatte et al. 2012*a*). Although the ventral portion of the quadrate ridge is usually demarcated just above the entocondyle of the mandibular articulation, its dorsal termination is more variable. The dorsal termination can reach the quadrate head like in *Acrocanthosaurus atokensis* (NCSM 14345) or flatten at the mid-height of the quadrate such as in *Albertosaurus sarcophagus* (Currie 2003: fig. 10B). The quadrate ridge can be divided into two ridges by a deep groove as in *Allosaurus fragilis* (AMNH 600) and *Allosaurus europaeus* (ML 415).

The quadrate ridge can also flare at the second dorsal third of the quadrate, and reappears slightly more dorsally, as observed in some derived Spinosauridae (Hendrickx et al. 2014*a*). Likewise, the ventral portion can also dichotomize in two ridges separated by a concavity such as in the tyrannosaurids *Albertosaurus sarcophagus*, *Daspletosaurus* sp. (Currie 2003: fig. 10 and 28) and *Tyrannosaurus rex* (AMNH 5027).

The pterygoid flange contacts the quadrate process of the pterygoid anteriorly or anteromedially, and sometimes other bones such as the epipterygoid in *Herrerasaurus ischigualastensis* (PVSJ 407), the basipshenoid and prootic in *Erlikosaurus andrewsi* (Clark et al. 1994), and the squamosal in *Khaan mckennai* (Balanoff and Norell 2012). Although the pterygoid flange can be easily homologized between taxa, it may acquire subtrapezoidal, subtriangular, subrectangular and M-shaped outlines or form a large semi-oval structure. The ventral limit of the flange can reach the mandibular condyles (e.g., *Tyrannosaurus rex*, *Baryonyx walkeri*; Fig. 6.3P) or get attached to the quadrate body well-above the mandibular articulation (e.g., *Majungasaurus crenatissimus*; Fig. 6.3J). This structure can in some instances be divided into two ridges delimited by a deep pneumatic fossa facing ventrally (e.g., *Alioramus altai*; Fig. 6.4J; *Tyrannosaurus rex* FMNH PR2081). In anterior view, the pterygoid flange can be straight and only projected anteriorly, as in the carcharodontosaurid *Shaochilong maortuensis* (Brusatte et al. 2010*b*: fig. 7a), or anteromedially recurved. The anteroventral margin of the pterygoid flange can either be straight, or medially and/or dorsally deflected, forming an horizontally oriented or dorsally inclined shelf-like structure here referred as the ventral shelf, as in *Majungasaurus crenatissimus* (FMNH PR 2100; Fig. 6.3G), *Carnotaurus sastrei* (MACN-CH 894) and *Allosaurus fragilis* (Madsen 1976*b*: plate 3d).

The medial fossa of the quadrate is easily homologized between taxa as it is always situated on the pterygoid flange, typically on its dorsoventral surface. This fossa is posteriorly delimited by the quadrate body in non-avian theropods and sometimes by the ventral shelf of the pterygoid flange. The medial fossa can be of variable depth (deep in *Cryolophosaurus* and shallow in *Eustreptospondylus*), pneumatized (e.g., *Falcarius*; Fig. 6.4P), and situated in the ventralmost part of the pterygoid flange

(e.g., *Tsaagan*) or at mid-height of it and just above a large pneumatic recess like in *Mapusaurus roseae* (MCF PVPH-106.102).

The posterior fossa of the quadrate can be located either in between the quadrate and the quadratojugal, being confluent with the quadrate foramen (e.g., *Mapusaurus*), or in the middle of the quadrate shaft and between the quadrate ridge and the lateral limit of the quadrate shaft (e.g., *Megapnosaurus*, *Tsaagan*, *Majungasaurus*; Fig. 6.3I). The posterior fossa can either be strongly ventrodorsally elongated like in the carcharodontosaurid *Acrocanthosaurus*, or form an oval concavity lateromedially wide (e.g., *Majungasaurus*). Similarly to the medial fossa, the posterior fossa can have a large pneumatic recess positioned dorsally (e.g., *Sinornithomimus*) or ventrally (e.g., *Garudimimus*) inside the fossa.

Due to the highly variable morphology of the quadrate foramen, this structure deserves special attention. It can be completely absent (e.g., *Carnotaurus*, *Torvosaurus*, *Eustreptospondylus*; Fig. 6.3U), or form a very small aperture (e.g., *Megapnosaurus*) to a large opening (e.g., *Bambiraptor*; Fig. 6.4T). In most non-avian theropods, the quadrate foramen is mostly delimited by the quadrate and only its lateral margin is bounded by the quadratojugal (e.g., *Sinraptor*). In some non-avian theropods, however, the medial margin of the quadrate foramen and part of the ventral and dorsal margins are formed by the quadrate, the other lateral half being delimited by the quadratojugal (e.g., *Dromaeosaurus*). Finally, in a few theropods, the foramen can be completely enclosed in the quadrate (e.g., *Aerosteon*; Fig. 6.4C).

The quadratojugal contact of the quadrate can either be a unique extensive contact or made of two contacts separated by the quadrate foramen. In the latter case, the ventral quadratojugal contact and the dorsal quadratojugal contact of the quadrate are not always clearly separated and their dorsal and ventral margins, respectively, can overlap like in the sinraptorid *Sinraptor dongi* (IVPP 10600). If the quadrate foramen is absent or located inside the quadrate, the lateral quadratojugal contact typically corresponds to an elongated line of variable width along the lateral margin of the quadrate. When separated by the quadrate foramen, the ventral and dorsal contacts can display a wide variety of surface and outlines. Both quadratojugal contacts may face laterally, anteriorly or posteriorly, and their articulating surface can be smooth, irregular or deeply grooved by several radiating ridges, as in *Allosaurus fragilis* (Madsen 1976*b*). The ventral quadratojugal contact is typically D-shaped or ovoid in lateral view. Its anterior margin can extend far anteriorly, forming the quadratojugal process (Norell et al. 2006), and its ventral margin can project far laterally, as in Oviraptoridae (Maryańska and Osmólska 1997). The dorsal quadratojugal contact can vary from a very thin line to a broad surface in lateral or posterior views and its dorsal extension can reach the dorsal condyle or terminate well beneath it. A ventral projection of this contact may be present, and such projection delimiting part of the lateral border of the quadrate can either be short, like in *Daspletosaurus* sp. (Currie 2003: fig. 28A) and *Baryonyx walkeri* (Fig. 6.3O), or form an elongated ramus, like in the therizinosaurid *Falcarius*

utahensis (Zanno 2010*b*; Fig. 6.4O) and the coelurosaur *Zuolong salleei* (Choiniere et al. 2010*a*: fig. 3B).

In some basal theropods, ceratosaurs and dromaeosaurids, the lateral process of the quadrate forms a wing-like projection similar to the pterygoid flange. This process is an extension of the quadrate body laterally so that it can be difficult to delimitate and one can see the presence of such process in *Allosaurus* sp. (undescribed specimen SMA 005/02), *Sinraptor dongi* (Currie 2006: fig. 1D), and *Erlikosaurus andrewsi* (Clark et al. 1994: fig. 7). The lateral process can also vary in shape and size, as it can be lateromedially short and parabolic in posterior view (e.g., *Carnotaurus*), or lateromedially elongated and subtriangular in posterolateral view (e.g., *Dilophosaurus*; Fig. 6.3B). Its ventral border can also extend to the quadrate foramen (e.g., *Bambiraptor*; Fig. 6.4T) or more ventrally, sometimes reaching the medial condyle of the mandibular articulation (e.g., *Ilokelesia*, *Majungasaurus*; Fig. 6.3I).

The quadrate head always articulates with the deep cotylus of the squamosal and contacts more rarely other bones of the braincase such as the opisthotic in oviraptorids (Maryańska and Osmólska 1997), the prootic in *Mononykus olecranus* (Perle et al. 1994; Chiappe et al. 2002) and the postorbital in *Shuvuuia deserti* (Chiappe et al. 1998, 2002; see next section). The contact of the braincase between the dorsal part of the quadrate and the opistothic-exoccipital or the paroccipital process is also present in *Herrerasaurus ischigualastensis* (Sereno and Novas 1994), *Dilophosaurus wetherilli* (Welles 1984), *Ceratosaurus magnicornis* (Madsen and Welles 2000; Sanders and Smith 2005), tyrannosaurids (Currie 2003), *Heyuannia huangi* (Lü 2005), and perhaps *Erlikosaurus andrewsi* (Clark et al. 1994), but this contact occurs on a small medial surface just below the quadrate head and not with the quadrate head itself. The large majority of non-avian theropods have a monostylic quadrate head (Rauhut 2003*a*; pers. obs.); however, oviraptorids (Maryańska and Osmólska 1997: fig. 3B) and the alvarezsaurid *Shuvuuia deserti* (Chiappe et al. 1998) have the apomorphic condition of possessing a bistylic quadrate head. This condition has also been observed in the dromaeosaurid *Mahakala omnogovae* (Turner et al. 2007*b*), but Turner et al. (2011: fig. 4) later reconsidered the head of the quadrate as not being bistylic. The morphology of the quadrate head is variable; it may be subtriangular in most basal theropods (Sereno and Novas 1994) like *Dilophosaurus* (UCMP 37302; Fig. 6.3E) and *Bambiraptor* (AMNH 30556; Fig. 6.4V), oval or subcircular in megalosaurids like *Afrovenator* (UC OBA1) and *Torvosaurus* (BYUVP 9246), and allosauroids such as *Aeroston* (MCNA-PV-3137; Fig. 6.4E), *Sinraptor* (IVPP 10600) and *Shaochilong* (IVPP V2885.3), subquadrangular in Spinosaurinae like *Irritator* (SMNS 58022), or conical in Oviraptoridae (Maryańska and Osmólska 1997: fig. 1B). Whilst most non-avian theropods have either a convex or a flattened quadrate head, the quadrate of some allosaurids (Bakker 1998: fig. 5C) and derived tyrannosaurids (FMNH PR208) can also possess a well-marked concavity on the dorsal margin of the quadrate head. Despite this variability, the quadrate head can be easily homologized inter-taxically due to the obvious location of this structure.

With the exception of the therizinosaur *Erlikosaurus andrewsi* and the ornithomimosaur *Sinornithomimus dongi* which both seem to have a unique tricondylar condition on the mandibular articulation (Clark et al. 1994; Kobayashi and Lü 2003), all other non-avian theropods have two mandibular condyles. The presence of three mandibular condyles was also noted in the alvarezsaurid *Avimimus portentosus* (Chatterjee 1995) and the dromaeosaurid *Sinornithosaurus millenii* (Xu and Wu 2001). However, Vickers-Rich et al. (2002) only found two condyles in the former and our observations confirm that the third condyle of *Sinornithosaurus* seems to be part of the much broader lateral condyle (Xu and Wu 2001: fig. 4D).

The shape of the mandibular articulation in posterior view can vary from the biconvex condition known in most theropods, to the W-shaped articulation typical of *Citipati osmolskae* (Clark et al. 2002: fig. 6) or a unique convex articulation seen in some dromaeosaurids such as *Tsaagan mangas* (IGM 100-1015). The intercondylar sulcus varies in orientation, size and depth. It can be large, shallow and sub-perpendicular to the long axis passing through the mandibular articulation as in *Falcarius* (UMNH VP 14559; Fig. 6.4Q), or narrow, deep and strongly lateromedially-oriented as in *Eustreptospondylus* (Fig. 6.3W) and some derived spinosaurids (pers. obs.). The intercondylar notch is present in *Allosaurus* sp. (Bakker 1998: fig. 5B, C; SMA 005/02) and *Suchomimus tenerensis* (MNN GAD 502) on the posterior side of the mandibular articulation, and in *Majungasaurus crenatissimus* (FMNH PR 2100; Fig. 6.3L) and *Carnotaurus sastrei* (MACN-CH 894) on its anterior margin. The ectocondyle (Fig. 6.2) and entocondyle (Fig. 6.2) are highly variable among each clade of non-avian theropods in terms of shape, size and orientation.

Pneumaticity of the quadrate can either be internal or, externally expressed by pneumatic foramina. The establishment of inter-taxic homologies is difficult to assess because these structures have very diverse interspecific variability. Nevertheless, as in other saurischian taxa (Schwarz et al. 2007), these pneumatic structures have phylogenetic signal. These openings can appear on different views and portions of the quadrate. The medial and posterior pneumatic foramina usually occur in the medial and posterior fossa respectively, and their position inside the fossae is again quite variable. Pneumatic foramina can also be located in a pneumatic recess outside the medial fossa and just beneath it such as in the carcharodontosaurids *Mapusaurus roseae* (Coria and Currie 2006) and *Acrocanthosaurus atokensis* (Eddy and Clarke 2011). In the latter, the pneumatic aperture is divided by a septum.

Overview of the function, pneumaticity and ontogeny

Function of the Quadrate

In all archosaurs, and all amniotes except Mammaliaformes, the main function of the quadrate is the articulation of the cranium with the mandible, yet this bone also play an important role in the mobility of the skull in many extant theropods. Streptostyly is a fundamental property of all avian

theropods, and quadrate kinesis in birds, known already in the beginning of the 19th century (Nitzsch 1816), has been extensively studied over the past sixty years (e.g., Fisher 1955; Bock 1964, 1999; Bühler 1981; Zusi 1984, 1993; Bühler et al. 1985, 1988; Chatterjee 1991, 1997; Hoese and Westneat 1996; Zweers et al. 1997; Zweers and Vanden Berge 1998; Bout and Zweers 2001; Gussekloo and Bout 2005; Meekangvan et al. 2006). Streptostyly consists of the rotation of the quadrate at its dorsal articulation against the squamosal which typically lead to a transverse movement, although a lateral movement of the quadrate around an anteroposteriorly directed axis occurs in some lepidosaur taxa (Metzger 2002). Cranial kinesis in avian theropods with a streptostylic quadrate includes upward (protraction) and downward (retraction) rotation of the upper jaw relative to the braincase and three main types of kinesis are recognized relative to the position of the dorsal flexion zone of the cranium and the nature of the nasal opening in modern theropods (Bock 1964; Bühler 1981; Zusi 1984; Meekangvan et al. 2006). In prokinesis, flexion occurs at the nasofrontal joint and the upper jaw thereby moves as one unit; in amphikinesis, flexion occurs in two zones of flexibility and the upper jaw and its tip are bent upward;in rhynchokinesis, flexion occurs forward from the nasofrontal joint, allowing its anterior part to be moved (Zusi 1984).

Inference of the cranial kinesis and quadrate mobility in non-avian theropods has been recently investigated by Holliday and Witmer (2008) which regard the cranium of this group of dinosaurs as partially kinetically competent, since synovial joints and protractor muscles are present, but not fully kinetic like in birds. The strong suture of the quadrate to the quadratojugal and the immobile contact of the quadrate and the pterygoid on the medial side of the pterygoid flange in most non-avian theropods seem to indicate a very limited movement, and perhaps even the total absence of movement of this bone within the cranium. Although the synovial quadrate head joint existing in theropods, and all other archosaurs, is necessary to infer cranial kinesis, its presence in akinetic taxa such as crocodiles demonstrates that the synovial joint cannot be considerate alone as an argument for cranial kinesis. Synovial joints have actually been interpreted as growth zones rather than articular surfaces of mobile joints based on the presence of very thin articular cartilage covering the end of this joint (Holliday and Witmer 2008). According to Holliday and Witmer (2008: p.1085) "articular cartilage persists in loading environments that exert hydrostatic pressures (which result in a change in volume but not shape) but exert low shear stresses". Indeed, one of the key centres of deformation during normal biting is the quadrate-squamosal contact, which would have experienced large shear stresses associated with torque and asymmetrical loading during biting (Rayfield 2005*b*), and the presence of a minimal amount of cartilage between the quadrate and squamosal would therefore suggest that the synovial zone was rather a growth zone than a mobile one. A streptostylic quadrate in *Tyrannosaurus rex* (Molnar 1991, 1998), *Oviraptor philoceratops* (Smith 1992), *Heyuannia huangi* (Lü 2005) and *Dromiceiomimus brevitertius* (Russell 1972) based on the saddle joint between the quadrate and squamosal only is thereby unlikely.

Nevertheless, and more convincingly, a streptostylic quadrate has also been proposed in the alvarezsaurid *Shuvuuia deserti* (Chiappe et al. 1998). In this taxon, the jugal it has been suggested that the quadratojugal is absent in *Shuvuuia deserti*; Dufeau 2003), rather than being firmly sutured to the quadrate asin other non-avian theropods, would have contacted the lateral surface of the quadrate though a movable joint (Chiappe et al. 1998, 2002; Fig. 6.9A). According to Chiappe et al. (1998), the absence of a laterodorsal contact of the quadrate with the quadratojugal/jugal, as well as a ventrolateral process of the squamosal, would have permitted to the quadrate of this mononykine to pivot anteroposteriorly, and the upper jaw to rotate ventrodorsally thanks to this transversal movement. Although these authors have implied the existence of a bending zone between the frontals and the nasal–preorbital bones in *S. deserti*, allowing the flexion of the snout as a single unit when the quadrate displaced forward, like in prokinetic birds, the complex contacts between the nasal, frontal and prefrontal illustrated by Sereno (2001: fig. 12B) makes assessment of Chiappe et al. (1998) hypothesis quite dubious (Holliday and Witmer 2008). In addition, Holliday and Witmer (2008) noted that a maxillojugal and palatal flexion zones allowing a true prokinesis to be present in alvarezsaurids is still not clear. Likewise, the contact between the pterygoid flange of the quadrate and the pterygoid needs also to be better documented in order to imply any specific movement of the quadrate inside the cranium of *S. deserti*.

A movable articulation between the quadrate and quadratojugal may have also been present in the oviraptorids *Heyuannia huangi* (Lü 2003) and *Nemegtia huangi* (Lü et al. 2004). In *Heyannia*, the quadrate and quadratojugal articulation corresponds to a trochlea-like structure (Lü 2003, 2005), while the quadratojugal contact of *Nemegtia* is convex and fit into a quadratojugal cotyle (Lü et al. 2004).

Quadrate articulation with the mandible and orientation of the intercondylar sulcus are highly variable among non-avian theropods, therefore suggesting some variation in the movement of the rami when the jaw opened. The helical intercondylar sulcus present in many non-avian theropods, but not all of them (pers. obs.), was noticed by Bakker (1998) in primitive theropod dinosaurs, Hendrickx and Buffetaut (2008) in spinosaurids, and Molnar (1991) and Larson (2008*b*) in *Tyrannosaurus rex*. These authors suggested that such spiral groove of the mandibular articulation constrained the diagonal ridge of the articular glenoid fossa, which fitted into the intercondylar sulcus, to slide laterally. This would force the rami of the mandible to displace laterally when the lower jaw was depressed, enlarging the width of the larynx in order to swallow food of large size (Hendrickx and Buffetaut 2008).

In *Allosaurus*, the enlargement of the mandibular condyles associated with the posteroventral inclination of the ventral part of the quadrate, and the intercondylar notch, were interpreted by Bakker (1998) as joint-stabilization zones. According to Bakker (1998), the anteroposterior enlargement of the articulating surface would improve the stability of the mandibular articulation when the mouth was widely opened, whereas the intercondylar notch, morphologically convergent to the depression of the knee joints in crocodiles and birds, would be hosting one or several ligaments within the quadrate-mandibular articulation (Bakker 1998). An intercondylar notch has also been noticed in the

abelisaurids *Carnotaurus sastrei* (MACN-CH 894) and *Majungasaurus crenatissimus* (FMNH PR 2100), and the spinosaurid *Suchomimus tenerensis* (MNN GAD 502), perhaps implying a similar jaw mechanic of the mandibular articulation than *Allosaurus*. Yet, Bakker (1998) hypotheses of the jaw mechanic based on the shape of the mandibular articulation and the presence of an intercondylar notch need to be further investigated with modern methods of functional analysis such as FEA.

Pneumaticity in the Quadrate

Pneumatization of the quadrate bone has long been recognized for its phylogenetic value (e.g., Gauthier 1986; Holtz 1998*a*; Chiappe 2001; Rauhut 2003*a*; Holtz et al. 2004; Smith et al. 2007; Benson 2010*a*; Carrano et al. 2012; Turner et al. 2012; Novas et al. 2013; Choiniere et al. 2014*b*). Pneumatic foramina within the quadrate are widespread among avetheropod clades (Gold et al. 2013; Fig. 6.5). The presence of one or several pneumatic foramina has indeed been recorded in carcharodontosaurids (e.g., Coria and Currie 2006; Eddy and Clarke 2011), megaraptorans (Sereno et al. 2008), tyrannosauroids (e.g., Molnar 1991; Brochu 2003; Currie 2003; Xu et al. 2004; Brusatte et al. 2012*a*; Gold et al. 2013), compsognathids (Currie and Chen 2001), alvarezsauroids (Choiniere pers. comm.), therizinosauroids (Clark et al. 1994; Zanno 2010*b*), oviraptorids (e.g., Maryańska and Osmólska 1997; Lü 2003; Kundrát and Janáček 2007; Balanoff and Norell 2012), ornithomimosaurs (Witmer 1997*a*; Tahara and Larsson 2011), dromaeosaurids (Makovicky et al. 2005) and troodontids (Barsbold et al. 1987; Currie and Zhao 1993*b*; Varricchio 1997; Xu et al. 2002*b*; Xu and Norell 2004). An incipient development of a pneumatic recess is also seen in the basal allosauroid *Sinraptor dongi* (Currie 2006), and quadrate pneumaticity therefore seems to be an avetheropod synapomorphy (Fig. 6.5).

The pneumatic opening is particularly large in some allosauroids such as *Aerosteon riocoloradensis* (Sereno et al. 2008; Fig. 6.6F) and *Acrocanthosaurus atokensis* (Eddy and Clarke 2011; Fig. 6.6A), and the therizinosaur *Falcarius utahensis* (Zanno 2010*b*; Fig. 6.6D). It however corresponds to a small rounded or oval aperture lodged in the posterior fossa of the quadrate body in most avetheropods (Fig. 6.6). Indeed, a posterior pneumatic foramen is seen in the tyrannosauroid *Dilong paradoxus* (Xu et al. 2004), the compsognathid *Sinosauropteryx prima* (Currie and Chen 2001: fig. 3f), the ornithomimids *Garudimimus brevipes* (the 'foramen' of Kobayashi and Barsbold 2005*a* ; Fig. 6.6G), *Sinornithomimus dongi* (the 'quadratic foramen' of Kobayashi and Lü 2003) and *Ornithomimus edmontonicus* (Tahara and Larsson 2011), the dromaeosaurid *Buitreraptor gonzalezorum* (Makovicky et al. 2005; Fig. 6.6H), and the troodontids *Mei long* (Xu and Norell 2004), and *Sinovenator changii* (Xu et al. 2002*b*). A pneumatic foramen can also be located in the ventral corner of the pterygoid flange, as observed in the carcharodontosaurids *Acrocanthosaurus atokensis* (Eddy and Clarke 2011; Fig. 6.6A), *Mapusaurus roseae* (Coria and Currie 2006; Fig. 6.6B), *Giganotosaurus carolinii* (MUCPv-CH-1; Fig. 6.6C), and the tyrannosaurid *Albertosaurus sarcophagus* (Currie 2003: fig. 10B).

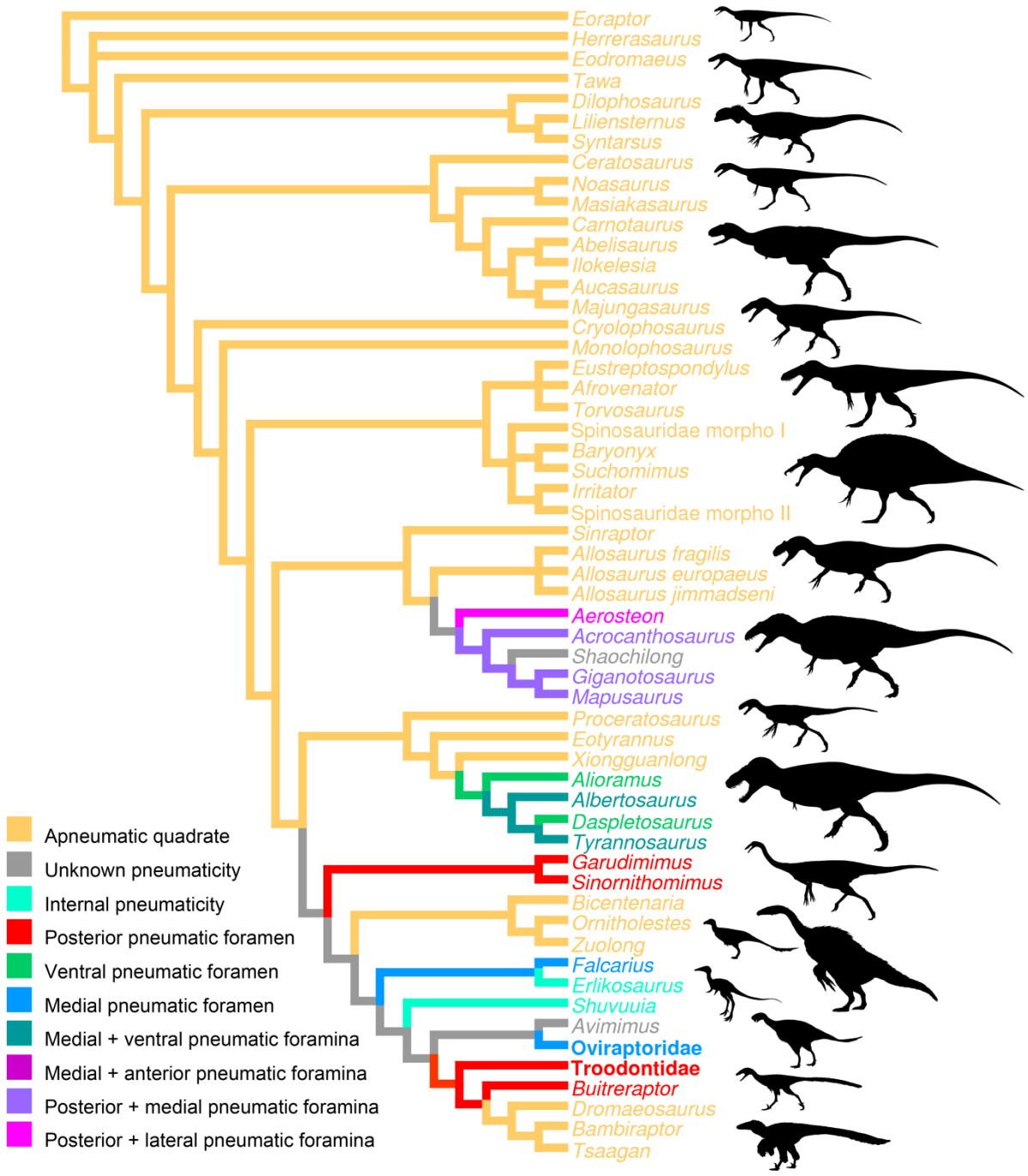

FIGURE 6.5. Distribution of quadrate pneumaticity in Theropoda. Cladogram of non-avian theropods based on the most recent cladistic analyses on theropods (see Chapter 1) and showing the phylogenetic distribution of quadrate pneumatic foramina in non-avian theropods. For silhouette attribution, see Appendices A1.1.

A pneumatic opening is also present anteroventrally, within a recess on the posteroventral part of the pterygoid flange ('funnellike external opening on the rostral surface of the quadrate, above the condyles' of Gold et al. 2013: p. 37) like in the therizinosauroid *Falcarius utahensis* (Zanno 2010*b*; Fig. 6.6D) and the tyrannosaurids *Alioramus altai* (Brusatte et al. 2012*a*; Gold et al. 2013; Fig. 6.6I), *Daspletosaurus* sp. (Currie 2003: fig. 28C) and *Tyrannosaurus rex* (Brochu 2003; Fig. 6.6J). This ventral pneumatic foramen has also been reported in the basal tyrannosauroid *Dilong paradoxus*

FIGURE 6.6. Morphology and position of pneumatic openings in the quadrate of non-avian Theropoda. Right quadrate (**A**) of the carcharodontosaurid *Acrocanthosaurus atokensis* (NCSM 14345; reversed) in medial view. Left quadrate (**B**) of the carcharodontosaurid *Mapusaurus roseae* (MCF-PVPH-108) in medial view. Left quadrate (**C**) of the carcharodontosaurid *Giganotosaurus carolinii* (MUCPv CH 1) in medial view. Right quadrate (**D**) of the therizinosauroid *Falcarius utahensis* (UMNH VP 14559; reversed) in medial view (courtesy of Lindsay Zanno). Right quadrate (**E**) of the metriacanthosaurid *Sinraptor dongi* (IVPP 10600; reversed) in posterior view (courtesy of Philip Currie). Left quadrate (**F**) of the neovenatorid *Aerosteon riocoloradensis* (MCNA PV 3137) in posterior view (courtesy of Martín Ezcurra). Left quadrate (**G**) of the ornithomimid *Garudimimus brevipes* (IGM 100–13) in posterior view (courtesy of Yoshitsugu Kobayashi). Right quadrate (**H**) of the dromaeosaurid *Buitreraptor gonzalezorum* (MPCA 245; reversed) in posterior view. Right quadrate (**I**) of the tyrannosaurid *Alioramus altai* (IGM 100–844) in ventral view (courtesy of Mick Ellison). Left quadrate (**J**) of the tyrannosaurid *Tyrannosaurus rex* (FMNH PR2081; cast, reversed) in ventral view. Left quadrate (**K**) of the carcharodontosaurid *Mapusaurus roseae* (MCF-PVPH-108) in anterior view. Left quadrate (**L**) of the neovenatorid *Aerosteon riocoloradensis* (MCNA PV 3137) in lateral view (courtesy of Martín Ezcurra). **Abbreviations**: **apne**, anterior pneumatic foramen; **lpq**, lateral process; **lpne**, lateral pneumatic foramen; **mpne**, medial pneumatic foramen; **ppne**, posterior pneumatic foramen; **qf**, quadrate foramen; **vpne**, ventral pneumatic foramen. Scale bars = 10 cm (A–C, J, K), 5 cm (E–G,L), 1 cm (D,H, I).

(Gold et al. 2013), but was not observed in the closely related taxa *Guanlong wucaii*, *Proceratosaurus lengi*, and *Xiongguanlong baimoensis* (Gold et al. 2013), and its presence cannot be established in *Eotyrannus lengi* (*contra* Gold et al. 2013; pers. obs.). More rarely, a pneumatic opening can be situated on the lateral surface of the quadrate body, as in *Aerosteon riocoloradensis* (MCNA-PV 3137; Fig. 6.6L), and in the anterior part of the quadrate, as in *Mapusaurus roseae* (Coria and Currie 2006; Fig. 6.6K), *Troodon formosus* (Currie and Zhao 1993*b*), *Heyuannia huangi* (Lü 2005), and perhaps *Tyrannosaurus rex* (Molnar 1991).

Carcharodontosauridae (Coria and Currie 2006; Eddy and Clarke 2011) and Tyrannosauridae (Molnar 1991; Brochu 2003) possess several pneumatic openings which perforate different sides of the quadrate and sometimes intercommunicate (Brochu 2003). The pneumatic foramina usually enter a large pneumatic chamber within the quadrate bone such as in *Tyrannosaurus rex* (Molnar 1991; Brochu 2003), *Alioramus altai* (Gold et al. 2013; Fig. 6.6I), *Conchoraptor gracilis* (Kundrát and Janáček 2007) or *Ornithomimus edmontonicus* (Tahara and Larsson 2011). The neovenatorid *Aerosteon riocoloradensis* also possess a large posterior pneumatic foramen leading to a pneumatic chamber, as well as a shallow pneumatic recess on the lateral surface of the quadrate shaft (Fig. 6.6F, L).

These pneumatic foramina and the pneumatic chamber associated with them are invaded by the quadrate diverticulum of the mandibular arch pneumatic system which, together with the periotic pneumatic system, forms the tympanic sinus of archosaurs (Dufeau 2011; Tahara and Larsson 2011). The mandibular arch pneumatic system includes the quadrate and/or the articular diverticulum which both have their embryological origins as parts of the first pharyngeal (= mandibular) arch, like the middle ear sac itself (Witmer 1997*a*). As in non-avian theropods, the quadrate diverticulum of modern birds exhibits a large variety of morphologies, and can either pneumatize the quadrate by entering through a single medial or anteromedial foramen or not (Witmer 1990; Tahara and Larsson 2011). In the basal theropods that do not have a pneumatic quadrate, both medial and posterior fossae of the quadrate correspond to the osteological trace of the quadrate diverticulum. In non-avian theropods with a pneumatic quadrate, the position of the quadrate diverticulum is variable such as in ornithomimids (Tahara and Larsson 2011), carcharodontosaurids and oviraptorids (pers. obs.). The quadrate diverticulum of non-avian theropods may also have communicated with other diverticula such as the squamosal diverticulum as in *Conchoraptor gracilis* (Kundrát and Janáček 2007), and the siphoneal diverticulum of the articular as in *Dilong paradoxus*, *Aerosteon riocoloradensis* and perhaps other non-avian maniraptorans (Sereno et al. 2008; Tahara and Larsson 2011). In *Tyrannosaurus rex*, however, the siphoneal diverticulum does not pass through the quadrate and the quadrate diverticulum only enters the ventral opening of the pterygoid flange, and then passes with or without the siphoneal diverticulum along the medial fossa of the pterygoid flange. Likewise, the quadrate diverticulum only pneumatizes two distinct regions of the quadrate in *Acrocanthosaurus atokensis* and *Mapusaurus roseae* (Tahara and Larsson 2011).

Quadrate Ontogeny

Skull ontogeny has been generally poorly studied in non-avian theropod, especially in their early stage of development (Rauhut and Fechner 2005), but the ontogeny of the quadrate bone has particularly received very little attention when compared to other cranial bones (see Carr 1999; Loewen 2010). Although the quadrate of embryonic and juvenile specimens has been reported in many non-avian theropod clades such as basal Megalosauroidea (Rauhut et al. 2012), Spinosauridae (Hendrickx and Mateus 2012), basal Avetheropoda (Hendrickx and Mateus 2012), Tyrannosauridae (e.g. Bakker et al. 1988; Carr and Williamson 2010; Tsuihiji et al. 2011), Compsognathidae (Dal Sasso and Maganuco 2011), Alvarezsauroidea (Dufeau 2003), Oviraptoridae (Norell et al. 1994, 2001*b*; Weishampel et al. 2008) and Troodontidae (Varricchio et al. 2002), the ontogenic variations of the non-avian theropod quadrate has only been investigated by Hendrickx and Mateus (2012) hitherto.

Quadrate pneumaticity appears early in ontogeny as it has been reported in the embryo of *Troodon formosus* (Varricchio et al. 2002) and the juvenile *Tarbosaurus baatar* (Tsuihiji et al. 2011). Although absent in the embryonic specimen of *Lourinhanosaurus autunesi*, a quadrate foramen is seen in many juvenile specimens of theropods such as the hatchling *Scipionyx samniticus* (Dal Sasso and Maganuco 2011) and the early posthatchling *Sciurumimus albersdoerferi* (Rauhut et al. 2012). Although the quadrate and quadratojugal are weakly articulated to each other in immature tetanurans (Hendrickx and Mateus 2012), a fusion between the quadrate and pterygoid was already present in oviraptorid embryos (Norell et al. 2001*b*).

The case of *Lourihanosaurus antunesi*

Two isolated quadrates (ML565-10; ML565-150; Figs. 6.7–6.8) were discovered among the skeletal remains of several embryos ascribed to the basal avetheropod *Lourinhanosaurus antunesi* (Mateus et al. 1998; Ricqlès et al. 2001; Mateus 2005) from the Lourinhã Formation (Kimmeridgian–Tithonian, Upper Jurassic) of Portugal. Formerly regarded as a basal allosauroid (Mateus 1998) and a eustreptospondylid (Mateus 2005; Mateus et al. 2006), *Lourinhanosaurus antunesi* is currently considered as a mecriacanthosaurids by Benson (2010*a*) and Benson et al. (2010), and as a basal coelurosaur by Carrano et al. (2012). Absence of cranial material in the mature specimen of *Lourinhanosaurus autunesi* does not allow direct comparison between embryos and adult specimens, thereby the two quadrates were compared to the quadrates of the most closely related taxa *Sinraptor dongi* (Currie 2006), *Bicentenaria argentina* (MPCA 865), *Zuolong sallei* (IVPP V15912), and *Proceratosaurus sallei* (NHM R.4860).

ML565-150 (Fig. 6.7) and ML565-10 (Fig. 6.8) are two incomplete left quadrates missing the dorsal part of the quadrate body, the quadrate head, and part of the pterygoid flange. ML565-10 is the best preserved one but the specimen was lost in the 1990s and only one photograph and two drawings of it remain (Fig. 6.8). The bone surface of the second remaining quadrate ML565-150 (Fig. 6.7) has been damaged during preparation but the general morphology is still preserved.

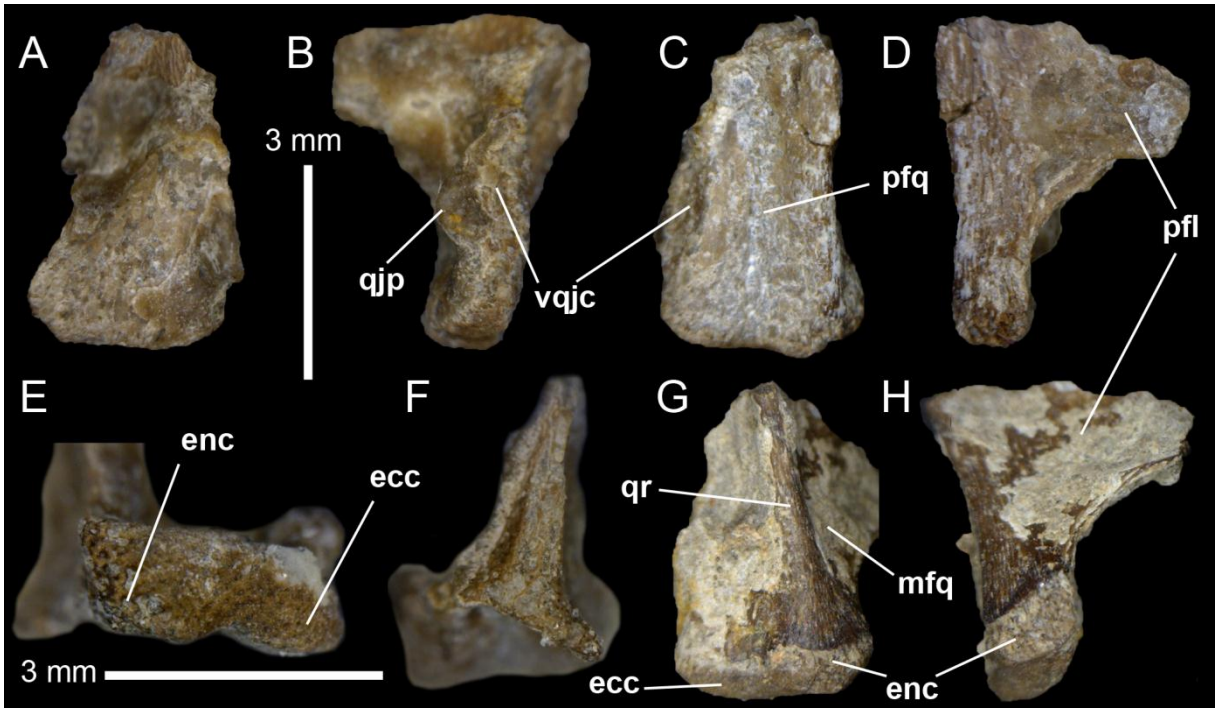

FIGURE 6.7. Quadrate of embryonic specimen of *Lourinhanosaurus antunesi* (ML565-150). **A–H**, Incomplete left quadrate in **A**, anterior; **B**, lateral; **C**, posterior; **D**, medial; **E**, ventral; **F**, dorsal; **G**, posteromedial; and **H**, ventromedial views (the quadrate in **G** and **H** was photographed before preparation). **Abbreviations**: **dqjc**, dorsal quadratojugal contact; **ecc**, ectocondyle; **enc**, entocondyle; **mfq**, medial fossa; **pfl**, pterygoid flange; **pfq**, posterior fossa; **qjp**, quadratojugal process; **qr**, quadrate ridge; **vqjc**, ventral quadratojugal contact.

Although incomplete, the two quadrates share a mixture of features observed in the quadrates of allosauroids and basal coelurosaurs, particularly with *Sinraptor* and *Zuolong*. Similar to allosauroids and unlike basal coelurosaurs, the pterygoid flange reaches the quadrate body well-above the mandibular articulation. In the basal coelurosaurs *Zuolong*, *Bicentenaria*, and *Proceratosaurus*, the pterygoid flange attaches the quadrate body slightly above the mandibular articulation. As in allosauroids and basal coelurosaurs, the pterygoid flange is straight and projects only anteriorly, yet the pterygoid flange of *Lourinhanosaurus* embryos does not show the ventral shelf present in many allosauroids and basal coelurosaurs such as *Sinraptor*, *Allosaurus*, *Acrocanthosaurus*, *Bicentenaria*, and *Proceratosaurus*. A ventral shelf is also absent in *Zuolong*, megalosaurids, and some allosauroids such as *Aerosteon* and *Shaochilong*. The ventral quadratojugal contact possesses a well-developed quadratojugal process projecting anteriorly, a feature shared with allosauroids and at least *Zuolong*. A ventrodorsally elongated depression is present on the posterior surface of the quadrate body, between the quadrate shaft and the quadratojugal contact (Fig. 6.7C). This depression seems to be homologuous to the posterior fossa present in *Zuolong*, and some allosauroids such as *Sinraptor* and carcharodontosaurids. The quadrate ridge of *Lourinhanosaurus* embryos is rod-shaped, well-delimited at one half of the quadrate body, and gets flared dorsal to the entocondyle without reaching the later. A similar condition occurs in some allosauroids and basal coelurosaurs like *Allosaurus*, *Bicentenaria* and *Zuolong*. A well-delimited quadrate ridge contrasts with the poorly delimited ridge of ceratosaurs (i.e.,

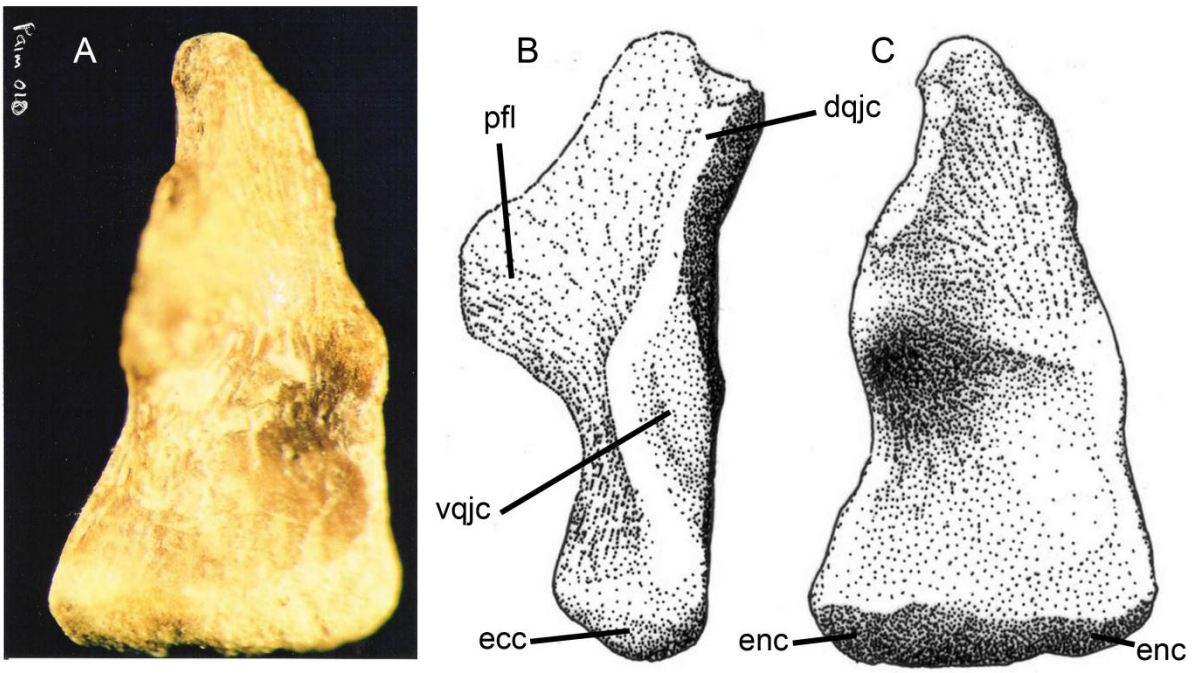

FIGURE 6.8. Incomplete left quadrate of *Lourinhanosaurus antunesi* embryo (ML565-10; lost) in **A, C**, anterior; and **B**, lateral views. **Abbreviations**: **dqjc**, dorsal quadratojugal contact; **ecc**, ectocondyle; **enc**, entocondyle; **pfl**, pterygoid flange; **vqjc**, ventral quadratojugal contact (drawings by and courtesy from Simão Mateus).

ceratosaurids, abelisaurids, and noasaurids) and megalosaurids. ML565-10 and ML565-150 share with *Sinraptor*, and possibly with *Zuolong*, a lanceolate ventral quadratojugal contact facing posterolaterally, a laterally positioned dorsal quadratojugal contact forming an elongated line, and a very shallow medial fossa (Fig. 6.7). The ventral quadratojugal of the basal coelurosaur *Bicentenaria* is not piriform in lateral view, nor it faces posterolateraly, and the medial fossa of this theropod is particularly deep.

The two quadrates show some important differences with the quadrate of closely related taxa that most likely come from the embryonic stage of the individuals. Unlike all allosauroids and basal coelurosaurs, the quadrate foramen is absent in both ML565-10 and ML565-150 so that the ventral and dorsal quadratojugal contacts are united to form a single quadratojugal contact (Fig. 6.8B). The quadrate foramen is also absent in more basal averostrans like ceratosaurs and megalosaurids (Currie 2006; Benson 2010*a*), yet the absence of a quadrate foramen is here interpreted as an ontogenetic feature in *Lourinhanosaurus* embryos, and possibly basal avetheropods. Likewise, the mandibular articulation of the two embryonic quadrates shows two shallow and poorly-delimited ento- and ectocondyle barely separated by a broad and very shallow intercondylar sulcus (Fig. 6.7E). This strongly differs from the typical avetheropod mandibular articulation formed by two elliptical, globular and prominent condyles separated by a deep intercondylar sulcus. The latter seems to run perpendicular to the long axis passing through the mandibular articulation in *Lourinhanosaurus* embryos and differ from the diagonally oriented intercondylar sulcus of mature individuals in Allosauroidea and basal Coelurosauria. A similar condition occurs in juvenile specimens of

spinosaurids (see last chapter) and the poorly delimited mandibular condyles is obviously an ontogenetic features of basal tetanurans (Hendrickx and Mateus 2012)

The case of *Shuvuuia deserti*

Well-preserved quadrates are present in a small and large specimens of the alvarezsaurid *Shuvuuia deserti* (Chiappe et al. 1998; Dufeau 2003). Dufeau (2003) interprets the small skull (IGM 100-1001) and the larger one (IGM 100-977) as belonging to a juvenile and adult specimens of *Shuvuuia deserti*, respectively, and comprehensively described the quadrate bone. Yet, he did not investigate the ontogenetic variation occurring in the skull of *Shuvuuia deserti*. Personal examination of the two specimens allowed to observe major differences in the quadrate morphology (Fig. 3.3-3.6) that could be interpreted as ontogenetic variations. The quadrate body of IGM 100-1001 is extremely ventrodorsally elongated, with a prominent and narrow quadrate ridge along the dorsal half of the quadrate bone. On the other hand, the quadrate body of the larger specimen IGM 100-977 is shorter, with a relatively shallow quadrate ridge. The mandibular articulation of IGM 100-1001 is lateromedially expanded and the lateral part of the articulation is subtriangular in outline and strongly projects laterally. The mandibular articulation of IGM 100-977 is particularly short, subrectangular in outline in posterior view, and lacks a lateral projection (Fig. 6.9D). This projection may however be broken and present as an isolated piece of bone displaced on the ventrolateral surface of the pterygoid flange (pers. obs.). In IGM 100-1001, the lateral process is ventrodorsally long, subtriangular in lateral view, almost subrectangular in posterior view, and reaches the quadrate head dorsally. The most lateral corner projects anteriorly to contact the postorbital, and the postorbital contact of the quadrate extends along the anterodorsal surface of the lateral process. The ventral most part of the lateral process forms a small corner dorsal to the parabolic outline of the ventral part of the quadrate body. On the contrary, the lateral process of IGM 100-977 only projects laterally and does not extend to the quadrate head dorsally. The lateral margin of the lateral process is parabolic in outline, and neither includes a small corner ventrally, nor an important projection anteriorly. The quadrate foramen of IGM 100-1001, forms a large fenestra delimited by the quadrate, jugal and, postorbital. If an articulation between the postorbital and the lateral corner of the lateral process was present in IGM 100-977 as well, the quadrate foramen of this specimen would have been much smaller, and delimited by the ventral half of the quadrate only. The quadrate head of the small specimen (IGM 100-1001) is incipiently bistylic and oriented posteromedially to contact the squamosal dorsally, and the braincase posteromedially (Fig. 6.9B). The quadrate head of IGM 100-977 is strongly inclined laterally and seems to include a single condyle only, although Dufeau (2003) noted that the quadrate head was also divided by a very weak intercondylar sulcus in the adult specimen.

Dufeau (2003) interpreted these differences in the two specimens of *Shuvuuia deserti* as ontogenetic and taphonomic variations (Dufeau pers. comm.). According to Dufeau (2003), the contact between the quadrate head and the junction of the squamosal and postorbital, which is unique

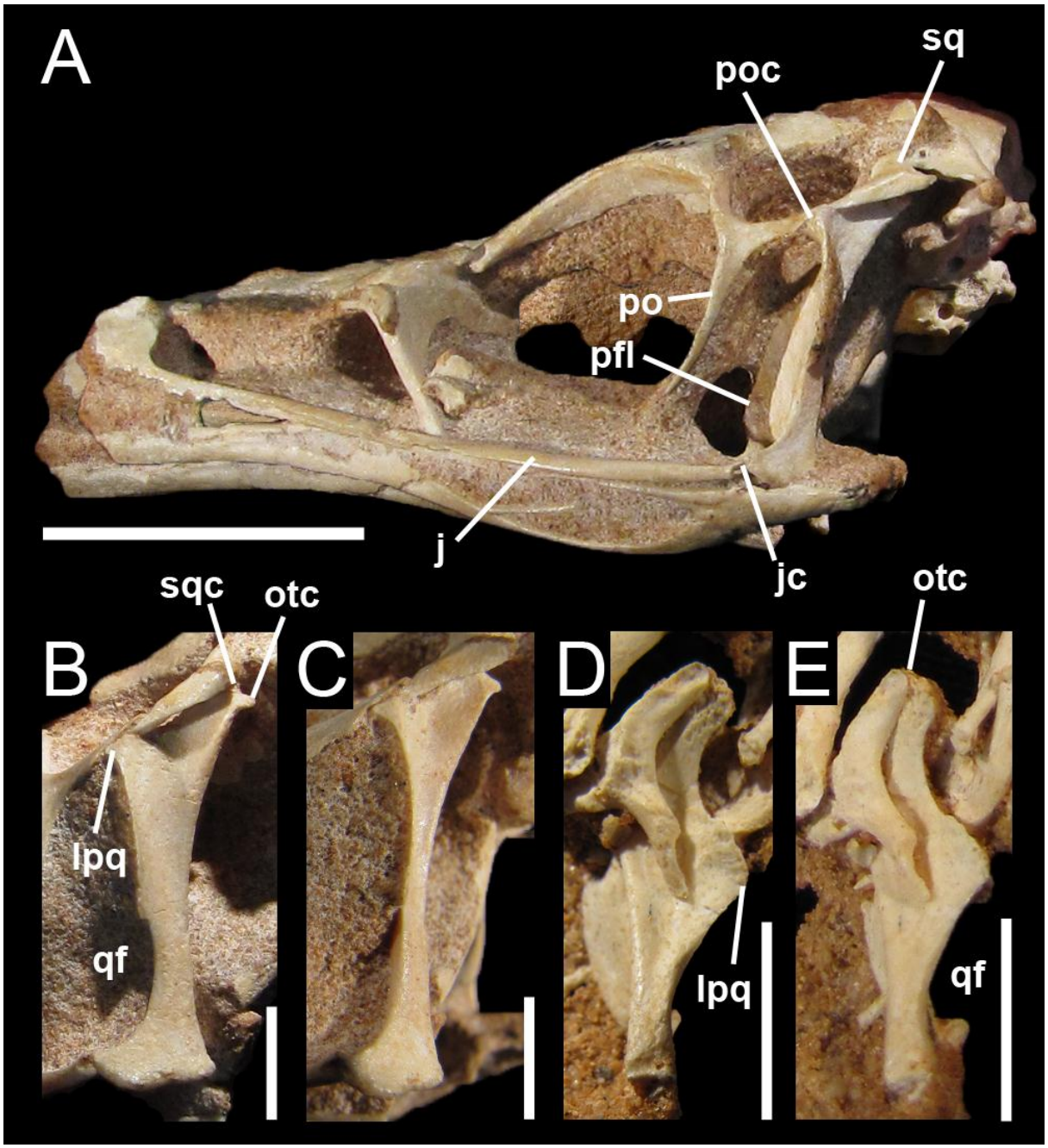

FIGURE 6.9. Quadrates of juvenile and adult specimens of *Shuvuuia deserti*. **A**, Skull of the juvenile *Shuvuuia deserti* (IGM 100-1001; reversed) in lateral view; **B–C**, comparison between the left quadrate of the juvenile specimen of *Shuvuuia deserti* (IGM 100-1001) in **B**, posterior; and **C**, lateral view; and **D–E**, the right quadrate of the adult specimen of *Shuvuuia deserti* (IGM 100-977) in **D**, posterior; and **E**, posterolateral views. **Abbreviations**: **j**, jugal; **jc**, jugal contact; **lpq**, lateral process; **oca**, otic capitulum; **pfl**, pterygoid flange; **po**, postorbital; **poc**, postorbital contact; **qf**, quadrate foramen; **sq**, squamosal; **sca**, squamosal capitulum. Scale bars = 2 cm (1-2), 1 cm (5-6), and 5 mm (3-4).

in IGM 100-1001 among non-avian theropods, is, for instance, interpreted as a taphonomic condition where the quadrate head would be taphonomically displaced laterally. Nevertheless, both left and rightquadrates of IGM 100-1001 occupy the same position and share similar contact with the postorbital and squamosal, and the skull suffered neither compressional nor shear distortions (Dufeau 2003; pers. obs.). A taphonomic displacement of the quadrate of IGM 100-1001 seems therefore

unlikely, and the postorbital contact of the quadrate is an autapomorphy of *Shuvuuia deserti*. Despite the fact that the right quadrate of the larger specimen IGM 100-977 may have been subject to important postmortem compression (as the rest of the skull which is ventrodorsally flattened), the numerous differences existing between IGM 100-1001 and IGM 100-977 suggest that these variations may be taphonomic, ontogenetic, but also perhaps taxonomic. The ontogenetic variations occurring in the spinosaurid quadrates are subtle and only concern the delimitation of the condyles and quadrate head, and the reinforcement of the quadrate and quadratojugal suture, so that the general morphology of the quadrate bone does not change at all. If the features differentiating IGM 100-1001 and IGM 100-977 are mostly ontogenetic, the quadrate of *Shuvuuia deserti* would therefore undergo a major metamorphosis during its development, including a dorsoventral shortening of the quadrate bone, rotation of the quadrate head from a medial to a lateral orientation, posterior displacement of the lateral process, and morphological transformation of the lateral process from a subtriangular to a parabolic process. Although plausible, these ontogenetic transformations seem a bit extreme, and it is reasonable to suggest that IGM 100-977 and IGM 100-977 may belong to two taxa, perhaps two species of *Shuvuuia*.

Conclusions

A revised nomenclature of the quadrate bone, along with a corresponding set of abbreviations, is here proposed and provides a standard set of terms for describing this cranial bone in non-avian theropod dinosaurs. The quadrate can be divided into two regional categories, the quadrate body and the pterygoid flange, and twelve anatomical sub-units, the quadrate shaft, quadrate head, quadrate ridge, quadrate foramen, lateral process, quadratojugal contact, squamosal contact, pterygoid contact, mandibular articulation, medial fossa, and posterior fossa. Although being highly variable in shape, all of these quadrate entities, with perhaps the exception of the posterior fossa, are easy to homologize across taxa and a description of their morphology should be provided in the literature.

A summary of the current knowledge on the quadrate function, pneumaticity and ontogeny in non-avian theropods allows some evidence about this bone to be highlighted. The quadrate of large majority of non-avian theropods is akinetic and a streptostylic quadrate may have been present in some derived coelurosaurs such as the alvarezsaurid *Shuvuuia deserti* and the oviraptorid *Nemegtia huangi*. A lateral movement of the rami while the mandible was depressed was permitted in many theropods such as spinosaurids thanks to a helicoidal and diagonally oriented intercondylar sulcus of the mandibular articulation. The presence of an intercondylar notch in allosaurids was interpreted to be a joint-stabilization zone that would improve the stability of the mandibular articulation when the mouth was widely opened. Yet, this assumption needs further investigation from modern techniques dealing with functional morphology to support it.

A pneumatic quadrate was present in members of most non-avian avetheropod clades such as allosauroids, tyrannosaurids, compsognathids, therizinosauroids, ornithomimoids, oviraptorids,

troodontids and dromaeosaurids, in which pneumatic foramina typically open in the ventral part of the pterygoid flange and in the medial and lateral fossae. Although the pneumatic recess invaded by the quadrate diverticulum of the mandibular arch pneumatic system was linked to only one pneumatic foramen in most avetheropods, the presence of several pneumatic openings perforating different sides of the quadrate have been recorded in Neovenatoridae, Carcharodontosauridae and Tyrannosauridae.

A poorly delimited mandibular condyles, intercondylar sulcus and quadrate head, and a quadratojugal contact with a smooth surface have been interpreted as ontogenetic features in the quadrate of embryonic and juvenile basal tetanurans. The development of a quadrate foramen and a ventral projection of the dorsal quadratojugal contact seem also to happen during ontogeny in allosauroids and spinosaurids, respectively. On the other hand, pneumaticity and a strong suture between the quadrate and quadratojugal appear early in ontogeny, in the embryonic stage of coelurosaurs.

Chapter 7: The non-avian theropod quadrate II: systematic usefulness, major trends and cladistic and phylogenetic morphometrics analyses

Published in ***PeerJ Preprints***, submitted to ***PeerJ*** (reviewed):
Hendrickx, C., Araújo, R. and Mateus, O. 2014. The non-avian theropod quadrate II: systematic usefulness, major trends and cladistic and phylogenetic morphometrics analyses. *PeerJ PrePrints*: 2:e380v1.

Abstract

The skull-bone quadrate in non-avian theropods is very diverse morphologically alongside the disparity of the group as a whole. However, this disparity has been underestimated for taxonomic purposes. In order to evaluate the phylogenetic potential and investigate the evolutionary transformations of the quadrate, we conducted a phylogenetic morphometric analysis as well as a cladistic analysis using 98 discrete quadrate related characters. The cladistic analysis provides a fully resolved tree mirroring to some degree the classification of non-avian theropods.

The quadrate morphology by its own provides a wealth of data with strong phylogenetic signal and allows inference of major trends in the evolution of this bone. Important synapomorphies include: for Abelisauroidea, a lateral process extending to the ectocondyle; for Tetanurae, the absence of the lateral process; for Spinosauridae, a medial curvature of the ventral part of the pterygoid flange occurring directly above the mandibular articulation; for Avetheropoda, an anterior margin of the pterygoid flange formed by a roughly parabolic margin; and for Tyrannosauroidea, a semi-oval pterygoid flange shape in medial view. The phylogenetic morphometric analysis reveals two main morphotypes of the mandibular articulation of the quadrate linked to function. The first morphotype, characterized by an anteroposteriorly long mandibular articulation with two ovoid/subcircular condyles roughly subequal in size, is found in Ceratosauria, Tyrannosauroidea and Oviraptorosauria. This morphotype allows a very weak displacement of the mandible laterally. The second morphotype is characterized by an elongate and anteroposteriorly short mandibular articulation and a wide and parabolic/sigmoid ectocondyle. Present in Megalosauroidea, Carcharodontosauridae and Dromaeosauridae, this morphotype permits the lower jaw rami to be displaced laterally when the mouth opened.

Introduction

In theropods and non-mammalian tetrapods in general, the quadrate is a paired bone located in the posterior part of the skull, allowing the lower jaw to articulate with the cranium (Brusatte 2012). The non-avian theropod quadrate always displays a common anatomical architecture: a ventrodorsally tall body, an anteriorly-oriented pterygoid flange, a mandibular articulation with two condyles separated by a furrow, a lateral articulation with the quadratojugal, and a dorsal condyle, or quadrate head, articulated with the cotylus of the squamosal. Nevertheless, the quadrate morphology and each

quadrate sub-units change conspicuously among different clades of theropods (Maryańska and Osmólska 1997; Sereno et al. 2008) so that this cranial bone shows great taxonomic potential (Elzanowski et al. 2001; Currie 2006). However, no thorough study has tried to evaluate the phylogenetic value of the quadrate bone in non-avian theropods. Quadrate-related cladistic characters are minimal in most cladistic analyses performed in non-avian theropods, with a maximum of eight characters in Choiniere et al. (2014*b*) data matrices. Maryańska and Osmólska (1997) and Currie (2006) were the first quadrate-driven articles that investigated the morphological differences among non-avian theropod quadrates; however, the latter considered only five characters in order to determine theropod relationships. In essence, the paucity of characters that have been used underestimates the morphological diversity among the various clades of non-avian theropods. Here, we conduct a cladistic analysis based on a data matrix of 98 quadrate-related characters coded for 56 taxa belonging to the majority of clades of non-avian theropods. We also performed a phylogenetic morphometric analysis (Catalano et al. 2010; Goloboff and Catalano 2011) based on quasi homologous landmark configurations of a sub-sample of 23 taxa out of the 56 taxa above. If geometric morphometrics is a common method that has recently been used several times on theropod dinosaurs (e.g., Marugán-Lobón et al. 2004; Bhullar et al. 2012; Brusatte et al. 2012*b*; Foth and Rauhut 2013*a*, *b*), phylogenetic morphometric analysis is here applied on dinosaurs for the first time.

Materials and methods

Cladistic Analysis

In order to assess the evolution and taxonomic value of the quadrate bone in non-avian theropods, a data matrix including quadrate-related characters only was created and scored in 55 non-avian theropod taxa and one outgroup taxon (Table 7.1). Quadrates pertaining to most clades of non-avian Theropoda have been examined and coded from 1) first-hand observations (35 taxa equivalent to 62.5% of the dataset) 2) high-resolution photographs (16 taxa equivalent to 28.5%), and 3) by using full descriptions and illustrations of the bone in the literature for 5 taxa (Table 7.1). Most non-avian theropods with well-preserved and well-visible quadrates were included in the analysis and coded at the species level. Due to the weak variation of quadrate morphology among oviraptorid taxa and the exhaustive description of their anatomy in a single paper (Maryańska and Osmólska 1997), Oviraptoridae was coded at the 'family' level as operational taxonomic units (OTU). Likewise, troodontid quadrates were also coded at the 'family' level due to the scarcity of information on their morphology, gleaned from several published and unpublished specimens, and the absence of a single complete and well-illustrated troodontid in the literature.

Compsognathidae were not included in the cladistic analysis due to lack of information of the quadrate morphology and bad preservations of this bone. Indeed, the quadrates of taxa recovered by some authors among Compsognathidae such as *Compsognathus corallestris*

TABLE 7.1. Non-avian theropod specimens and clades examined and scored in the cladistic analysis. Taxa and clades with an asterisk were used in the phylogenetic morphometric analysis. **Abbreviations**: **Y**, Yes; **N**, No.

Taxon	Specimens	Examined	Photo credits	Literature
Eoraptor lunensis Sereno et al. 1993	PVSJ 512	Y	Martín Ezcurra	Sereno et al. 2013
Herrerasaurus ischigualastensis Reig 1963	PVSJ 53, 407	Y	Martín Ezcurra	
Eodromaeus murphi Martinez et al. 2011	PVSJ 562	Y	Carol Abraczinskas	
*Tawa hallae** Nesbitt et al. 2009	GR 241	N	Sterling Nesbitt	Nesbitt et al. 2009
Megapnosaurus kayentakatae Rowe 1989	MNA V2623	N	Ronald Tykoski; Randall Irmis	Rowe 1989
Liliensternus liliensterni Huene 1934	MB R.2175	N	Martín Ezcurra	Huene 1934
*Dilophosaurus wetherilli** Welles 1954	UCMP 37302	N	Randall Irmis; Martín Ezcurra; Mathew Carrano	Welles 1984
*Ceratosaurus nasicornis** Marsh 1884	USNM 4735; MWC 1	Y	Mathew Carrano	Madsen and Welles 2000
Noasaurus leali Bonaparte and Powell 1980	PVL 4061	Y		
*Masiakasaurus knopfleri** Sampson et al. 2001	FMNH PR 2496	Y	Mathew Carrano	
Abelisaurus comahuensis Bonaparte and Novas 1985	MPCA 11098	Y		
Ilokelesia aguadagrandensis Coria and Salgado 1998	MCF PVPH 35	Y	Matthew Lamanna	
Carnotaurus sastrei Bonaparte 1985	MACN CH 894	Y	Pablo Asaroff	
Aucasaurus garridoi Coria et al. 2002	MCF-PVPH-236	Y		
*Majungasaurus crenatissimus** Lavocat 1955	FMNH PR 2100	Y	Lawrence Witmer	
Cryolophosaurus ellioti Hammer and Hickerson 1994	FMNH PR1821	N	Nathan Smith	Smith et al. 2007
Monolophosaurus jiangi Zhao and Currie 1993	IVPP 84019	N		Zhao and Currie 1993; Brusatte et al. 2010*a*
*Eustreptospondylus oxoniensis** Walker 1964	OUMNH J.13558	N	Paul Barrett	
*Afrovenator abakensis** Sereno et al. 1994	UC OBA1	N	Roger Benson; Juan Canale; Mathew Carrano	
Torvosaurus tanneri Galton and Jensen 1979	BYU-VP 9246	Y	Matthew Lamanna	
*Baryonyx walkeri** Charig and Milner 1986	NHM R9951	Y	Eric Buffetaut	
Suchomimus tenerensis Sereno et al. 1998	MNN GAD 502	Y	Steve Brusatte	
Irritator challengeri Martill et al. 1996	SMNS 58022	Y		
Spinosaurinae morphotype I*	MSNM V6896; WDC-CSG Q1, Q2, Q4,Q5	Y		
Spinosaurinae morphotype II	WDC-CSG Q3	Y		
*Allosaurus fragilis** Marsh 1877	BYU VP8901	Y		Osborn 1912; Gilmore 1920; Madsen 1976*b*; Chure 2000
Allosaurus europaeus Mateus et al. 2006	ML 415	Y		
Allosaurus '*jimmadseni*'* Chure 2000	SMA 005/02	Y		
*Aerosteon riocoloradensis** Sereno et al. 2008	MCNA-PV-3137	N	Carol Abraczinskas; Martin Ezcurra	
*Sinraptor dongi** Currie and Zhao 1993*a*	IVPP 10600	N	Philip Currie	Currie 2006
*Acrocanthosaurus atokensis** Stovall and Langston Jr	NCSM 14345	Y	Drew Eddy; Vince Shneider	

1950				
*Shaochilong maortuensis** Brusatte et al. 2009*c*	IVPP V2885.3	N	Steve Brusatte	Brusatte et al. 2009*c*, 2010*b*
Mapusaurus roseae Coria and Currie 2006	MCF PVPH 108.102	Y	Matthew Lamanna	
*Giganotosaurus carolinii** Coria and Salgado 1995	MUCPv-CH-1	Y	Matthew Lamanna	
Ornitholestes hermanni Osborn 1903	AMNH FARB 619	Y	Mickey Mortimer	
Bicentenaria argentina Novas et al. 2012	MPCA 865	Y		
Zuolong salleei Choiniere et al. 2010*a*	IVPP V15912	N		Choiniere et al. 2010*a*
Proceratosaurus bradleyi Huene 1926*b*	NHM R 4860	Y		Rauhut et al. 2010
Eotyrannus lengi Hutt et al. 2001	MIWG 1997.550	Y	Darren Naish	
Xionggualong baimoensis Li et al. 2010	FRDC-GS JB16-2-1	N		Li et al. 2010
Alioramus altai Brusatte et al. 2009*b*	IGM 100-1844	N	Mick Ellison	Brusatte et al. 2012*a*; Gold et al. 2013
Albertosaurus sarcophagus Osborn 1905	RTMP 81.10.1; FMNH PR308; CMN 12; CMN 2120	N		Carr 1996; Currie 2003
Daspletosaurus sp. Russell 1970	RTMP 94.143.1	N		Currie 2003
*Tyrannosaurus rex** Osborn 1905	AMNH 5027; FMNH PR2081	Y	Mickey Mortimer	Molnar 1991; Brochu 2003; Larson 2008*b*
Garudimimus brevipes Barsbold 1981	IGM 100-13	N	Yoshitsugu Kobayashi	Kobayashi and Barsbold 2005*a*
Sinornithomimus dongi Kobayashi and Lü 2003	IVPP−V11797−10	N	Yoshitsugu Kobayashi	Kobayashi and Lü 2003
Shuvuuia deserti (Chiappe et al. 1998)	IGM 100-977, 100-1001	Y		Dufeau 2003
*Falcarius utahensis** Kirkland et al. 2005	UMNH VP 14559	N	Lindsay Zanno	Zanno 2010*b*
Erlikosaurus andrewsi Barsbold and Perle 1980	PST 100-111	N	Stephan Lautenschlager	Clark et al. 1994
Avimimus portentosus Kurzanov 1981	PIN 3907/1	N	Lawrence Witmer	Kurzanov 1985; Vickers-Rich et al. 2002
Oviraptoridae* Barsbold 1986	AMNH FARB 6517; IGM 100-1002; IGM 100-1127; IGM 100-978	Y		Maryańska and Osmólska 1997; Clark et al. 2002; Kundrát and Janáček 2007; Balanoff and Norell 2012
Buitreraptor gonzalezorum Makovicky et al. 2005	MPCA 245	Y	Martín Ezcurra	
*Bambiraptor feinbergi** Burnham et al. 2000	FIN 001	Y	David Burnham	
*Tsaagan mangas** Norell et al. 2006	IGM 100-1015	Y	Mick Ellison	
Dromaeosaurus albertensis Matthew and Brown 1922	AMNH 5356	Y		
Troodontidae Gilmore 1924	IGM 100-1083; IGM 100-1128; IGM 100-1323	Y	Rui Pei	Barsbold et al. 1987; Norell and Hwang 2004; Xu and Norell 2004; Hu et al. 2009; Xu et al. 2011*b*; Gao et al. 2012

(Ostrom 1978; Peyer 2006), *Juravenator starki* (Chiappe and Göhlich 2010; n.b., *Juravenator* is found as a non-compsognathid coelurosaur in the cladistic analyses of Butler and Upchurch 2007 and Rauhut et al. 2012), *Scipionyx samniticus* (Dal Sasso and Signore 1998; Dal Sasso and Maganuco 2011), *Huxiagnathus orientalis* (Hwang et al. 2004), *Sinocalliopteryx gigas* (Ji et al. 2007*a*) and *Sinosauropteryx prima* (Currie and Chen 2001) have been flattened by post mortem deformation and are either poorly preserved or obscured by other bones.

The data matrix encompasses 98 equally weighted discrete morphological characters related to the quadrate (Appendices A7.1–A7.2) and allowing to test and propose several quadrate synapomorphies for the 56 taxa coded. A combination of 18 characters are taken from the literature and 80 characters (81%) are new. Among the 54 multistate characters, twelve were treated as ordered (Appendices A7.1), and most quadrate related characters are illustrated in the appendices (Figs. 7.S1-S3). *Eoraptor lunensis*, considered to be either a basal sauropodomorph (Martinez et al. 2011; Sereno et al. 2013) or a basal theropod (e.g., Nesbitt et al. 2009; Nesbitt 2011; Sues et al. 2011) in the most recent cladistic studies, was treated as the outgroup. In order to constrain all major theropod clades and visualize the quadrate-based synapomorphies for each clade, a second analysis was performed on a supermatrix combining our quadrate-based data matrix to six recent datasets on non-avian theropods based on the whole skeleton (Brusatte et al. 2010*d*; Choiniere et al. 2010*b*; Martinez et al. 2011; Carrano et al. 2012; Pol and Rauhut 2012), and from which all quadrate-related characters were removed. The resulting supermatrix includes 1889 characters and only twelve quadrate related characters were treated as ordered (Appendices A7.3).

TNT v1.1 (Goloboff et al. 2008) was employed to search for most-parsimonious trees (MPTs). The matrix and supermatrix were analyzed under the ‘New Technology Search’ with the ‘driven search’ option (TreeDrift, Tree Fusing, Ratchet, and Sectorial Searches selected with default parameters), and stabilizing the consensus twice with a factor of 75. The consistency and retention indices as well as the Bremer supports (Bremer 1994) were calculated using the ‘stats’ and ‘aquickie’ commands, respectively, and a bootstrap analysis was performed with the standard options. The dataset was also analyzed with WinClada 1.00.08 (Nixon 2002) after making characters non-additive (*fitch*) and trees were searched for using the Ratchet (Island Hopper) option with default settings.

Phylogenetic Morphometrics Analysis

The phylogenetic morphometrics (hereinafter phylo-morpho) analysis approach is based on Catalano et al. (2010) and Goloboff and Catalano (2011) method. This method extends the parsimony criteria for characters like landmark data that change in more than one dimension. The method calculates the score of landmark configurations on a tree as the sum of the difference (weighted or not) in landmark position of each of its landmarks along all the branches of the tree. A different landmark configuration (i.e., set of quasi-homologous points that describes the structure under analysis) is therefore regarded as a different character. For example, the same set of landmarks of the anterior

view of the quadrate is considered a character. Several configurations can be included in a single phylogenetic analysis and landmark data can also be analyzed in combination with alternative sources of evidence like traditional morphological characters or molecules. In that case the tree score is the sum of the scores for each landmark configuration plus the score for each traditional character. We ran two different sets of analyses: 1) each individual phylo-morpho character alone; and 2) a combination of all phylo-morpho characters. This array of analysis allowed us to understand the influence of the phylo-morpho characters on resolving the phylogeny of non-avian theropod quadrates and, to provide a substantial basis for discretization of morphotypes that can be seen with the naked eye, but are hard to define verbally (e.g., outline of the posterior view of the non-avian theropod quadrate).

The phylo-morpho analysis comprised a sample of 23 taxa out of the 56 used in the traditional cladistic analysis (Table 7.1). The selection of a smaller sample of non-avian theropod quadrates was based on the following criteria, the quadrate 1) had to be complete, 2) could not be post-mortem deformed, 3) had to be isolated from the cranium, and 4) all views had to be well-preserved. Two quadrate morphotypes were included for *Allosaurus* (*A. fragilis* and *A.* '*jimmadseni*') and *Ceratosaurus* (*C.* '*magnicornis*' and *C.* '*dentisulcatus*' *sensu* Madsen and Welles, 2000). In our analysis we used three different phylo-morpho characters of the quadrate: outline of the medial view (character 1; 8 landmarks), outline of the ventral view (character 2; 8 landmarks) and outline of the posterior view (character 3; 12 landmarks). The rationale for the position of the landmarks is summarized in Appendices A7.5, Fig. A7.6 and detailed below. The outline of the anterior and dorsal views was not used. Some of the landmarks visible anteriorly are also visible posteriorly (i.e., it would imply overweighting certain landmarks) and dorsally, because it was hard to find homologous landmarks through taxa due to the lack of reference points of the quadrate head in non-avian theropods. Pictures from different taxa were sorted and compiled for each character individually using tpsUtil (Tps geometric morphometrics software is available for free download at http://life.bio.sunysb.edu/morph/soft-utility.html). The digitization of the landmarks on the pictures was done with tpsDig2. The resulting file was taken to tpsRelw where only the alignment was saved by using 'Save aligned specimens' option. The resulting *.tps file had to be parsed in order to run in TNT v1.1 (Goloboff et al. 2008; Appendices A7.6). A pre-requisite for the analysis of landmark data is the superimposition of the configurations (= alignment). This is accomplished by superimposition methods, i.e., rotation, translation and sizing. Because different alignments can produce different phylogenetic results, we generated two different datasets, the first aligned using RFTRA (Rho-Theta Resistant-fit Analysis, see Siegel and Benson 1982; Rohlf and Slice 1990) and the second performing an ordinary superimposition by minimizing the sum of linear distances of each configuration against a reference configuration (Catalano and Goloboff 2012).

In order to reconstruct a phylogeny from landmark data alone, we used the LandschW.run TNT script. To run the combined search we used the TNT script landcombsch.run. The latter allows running a combined analysis of traditional and phylo-morpho characters in an analogous way as two

(or more) different gene sequences can be analyzed together where each one contributes to the resolution of a phylogeny. Both scripts are available at http://tnt.insectmuseum.org/index.php/Scripts. The phylogenetic searches were re-run considering four different levels of search thoroughness (the scripts pre-defined levels 0, 1, 2 and 3). The parameters that define a 'level of thoroughness' are: number of replicates, termpoints (i.e., inclusion of the geometric medians as a possible point for an ancestral landmark position), number of cells in the grid (i.e., the higher number of cells the more points available for reconstruction of the ancestral positions), nesting level (i.e., a grid can be nested within another grid in order to allow a more precise, and computationally-efficient, reconstruction of the landmark ancestral positions), and neighbors level (i.e., number of neighboring cells included in the nesting level). The score of each configuration were rescaled in all the analysis is such a way that the contribution of one landmark configuration character is similar to a traditional character (TNT default option). For analysis 3 the driven search option of TNT was used considering Sectorial search, tree drifting, tree fusing, and ratchet algorithms, and finishing the search upon consensus stabilization. The exact same characters used in analysis 4 were used in analysis 3. For the analysis of the traditional characters TBR (tree bisection and reconnection) and 116 non-additive characters were employed. The resulting tree score is the sum of the tree length and the scaled weighted score for the phylo-morpho characters (see Goloboff and Catalano, 2011: p. 47).

In this analysis both the tree scores of ordinary superimposition minimization and RFTRA converged to an asymptote at the level 2 of thoroughness. This implies that the optimality of the trees can be correctly established with a thoroughness level 2. Thus, we selected the tree that would mirror more accurately present day knowledge on non-avian theropod phylogeny. A more accurate tree is the one that recovers a higher number of known clades in the analysis. In our analysis that was the case for level 2, re-aligned using RFTRA. The criterion used for picking between different trees was based on the tree score; the lowest the tree scores the more parsimonious the tree topology (see Catalano et al. 2010 for an explanation of the tree score calculation).

Landmark configurations.

The landmark configuration schemes chosen (Appendices 7.5; Fig. A7.6) attempt to capture as much information possible that can depict accurately the evolutionary processes on the non-avian theropod quadrate (Zelditch et al. 2009). The landmarks chosen were selected manually and are all of Bookstein's type 2, i.e., tip of a bony process or local curvature minima or maxima (Bookstein 1997).

Medial view (Character 1; Fig. A7.6A)—Landmark 1 is the apex of the curvature of the mandibular articulation. Landmark 2 is the apex of the curvature of the dorsal quadrate head. Landmark 3 is the mid-distance between the apices of the dorsal quadrate head and the mandibular articulation. Landmark 4 is the dorsal intersection between the quadrate ridge and the pterygoid flange. Landmark 5 is the dorsal kink of the pterygoid flange. Landmark 6 is the ventral kink of the pterygoid

flange. Landmark 7 is the apex of the curvature of the ventral portion of the pterygoid flange. Landmark 8 is the ventral intersection of the quadrate ridge and the pterygoid flange.

Ventral view (Character 2; Fig. A7.6B)—Landmark 1 is the anterior point on the semi-major axis of the ellipse formed by the entocondyle. Landmark 2 is the posterior point on the semi-major axis of the ellipse formed by the entocondyle. Landmark 3 is the medial point on the semi-minor axis of the ellipse formed by the entocondyle. Landmark 4 is the lateral point on the semi-minor axis of the ellipse formed by the entocondyle. Landmark 5 is the medial point on the semi-major axis of the ellipse formed by the ectocondyle. Landmark 6 is the lateral point on the semi-major axis of the ellipse formed by the ectocondyle. Landmark 7 is the anterior point on the semi-minor axis of the ellipse formed by the ectocondyle. Landmark 8 is the posterior point on the semi-minor axis of the ellipse formed by the ectocondyle.

Posterior view (Character 3; Fig. A7.6C)—Landmark 1 is the ectocondyle curvature apex and landmark 2 is the curvature apex of the entocondyle, while landmark 3 is the dorsal quadrate head curvature apex. Landmark 4 is on the lateral margin of the photographic plane at the level of the mid-height of the quadrate, and the landmark 5 is on the medial margin. Landmark 6 is the dorsalmost point of the ventral quadratojugal contact. Landmark 7 is the ventralmost point of the ventral quadratojugal contact. Landmark 8 is the apex of the concavity formed by the quadrate foramen. Landmark 9 is the dorsalmost point of the quadrate foramen. Landmark 10 is the ventralmost point of the quadrate foramen. Landmark 11 is located on the lateral-most point of the posterodorsal margin of the ectocondyle. Landmark 12 is located on the medial-most point of the posterodorsal margin of the entocondyle.

Results

Cladistic Analysis

The cladistic analysis of the data matrix of quadrate-based characters and including 56 theropod taxa yielded 40 most parsimonious trees (MPTs), in which the strict consensus trees (Length = 592 steps; CI = 0.271, RI = 0.536) resulted in a few polytomies affecting clades of no more than three taxa (see Appendices A7.4; Fig. A7.4). Although the consensus tree poorly mirrors the current classification of non-avian theropods, many theropod clades such as Noasauridae, Megalosauridae, Spinosauridae, Allosauridae, Carcharodontosauridae, Tyrannosauridae, Ornithomimosauria, Therizinosauroidea, Oviraptorosauria and Dromaeosauridae were found resolved. As it was noted for teeth (Hwang 2007; Hendrickx and Mateus 2014*b*), quadrate-related characters are good at recovering individual clades, but not at resolving the relationship between those clades. Nevertheless, the deletion of *Eoraptor*, *Abelisaurus* and *Irritator*, from which little information on the quadrate can be extracted (55%, 46% and 64% of missing data, respectively), gave a different tree topology. The cladistic analysis performed on the data matrix of 53 taxa yielded, this time, 19 MPTs in which the consensus

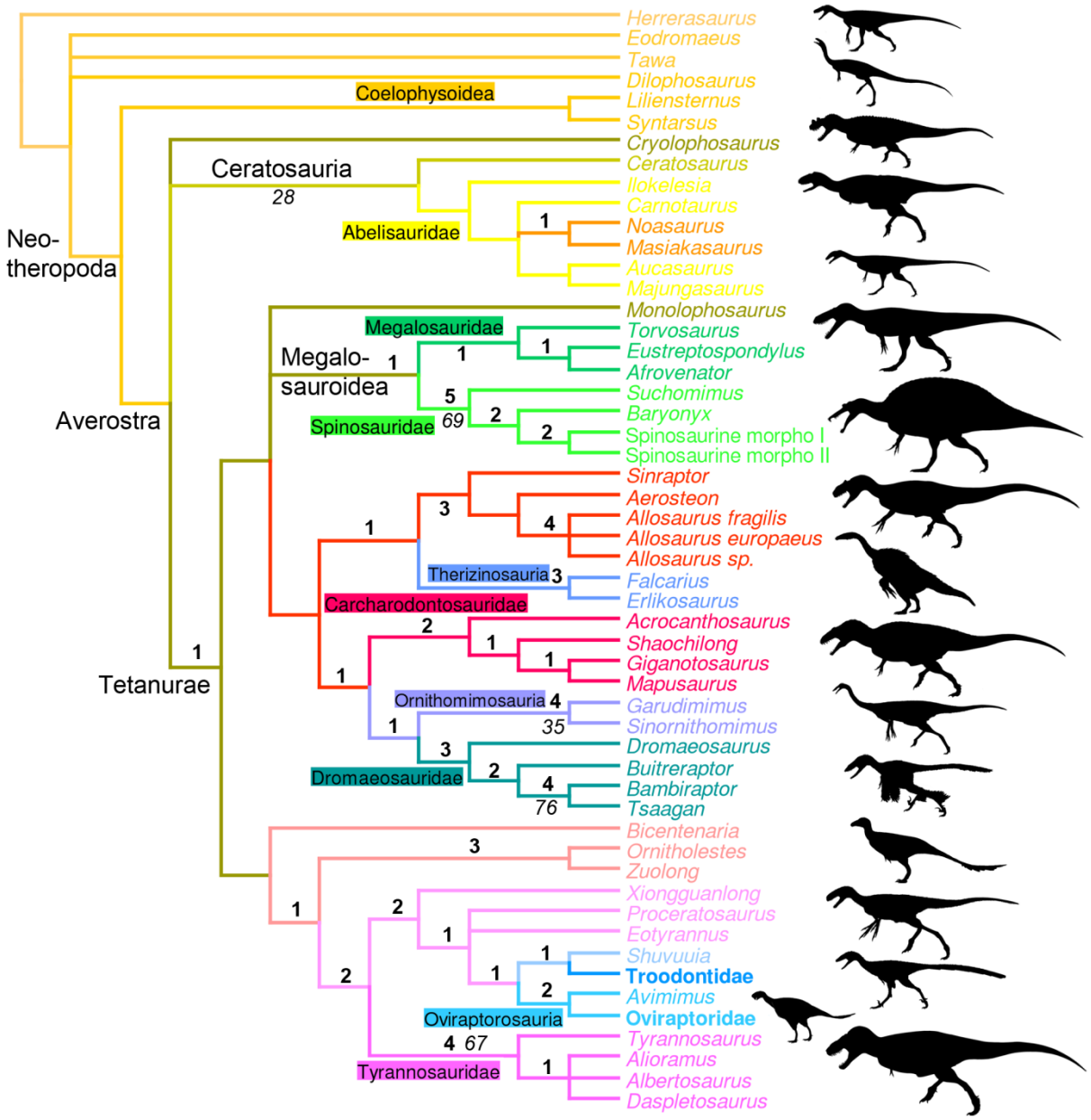

FIGURE 7.1. Strict consensus cladogram from 13 most parsimonious trees. Initial analysis was a New Technology Search using TNT v.1.1 of a data matrix comprising 98 quadrate based characters for one outgroup (*Herrerasaurus ischigualastensis*) and 54 non-avian theropod taxa. Tree length = 589 steps; CI = 0.282; RI = 0.556. Bremer support values are in bold and bootstrap values are in italic. For silhouette attribution, see Appendices A1.1.

tree (Length = 580 steps; CI = 0.285, RI = 0.554; Fig. 7.1) recovered to a much better degree the general topology of theropod classification with the usual major clades (e.g., Neotheropoda, Averostra, Ceratosauria, Tetanurae, Megalosauroidea). Indeed, when rooting *Herrerasaurus* as the outgroup, *Eodromaeus*, *Tawa*, *Dilophosaurus* and coelophysoids (*Liliensternus* + *Megapnosaurus*) were correctly recovered as the most-basal theropods, Neotheropoda and Averostra were found monophyletic and the latter includes both Ceratosauria and Tetanurae. Likewise, Megalosauroidea was recovered as a clade closely related to the basal tetanuran *Monolophosaurus* (Carrano et al. 2012) and correctly includes Megalosauridae and Spinosauridae.

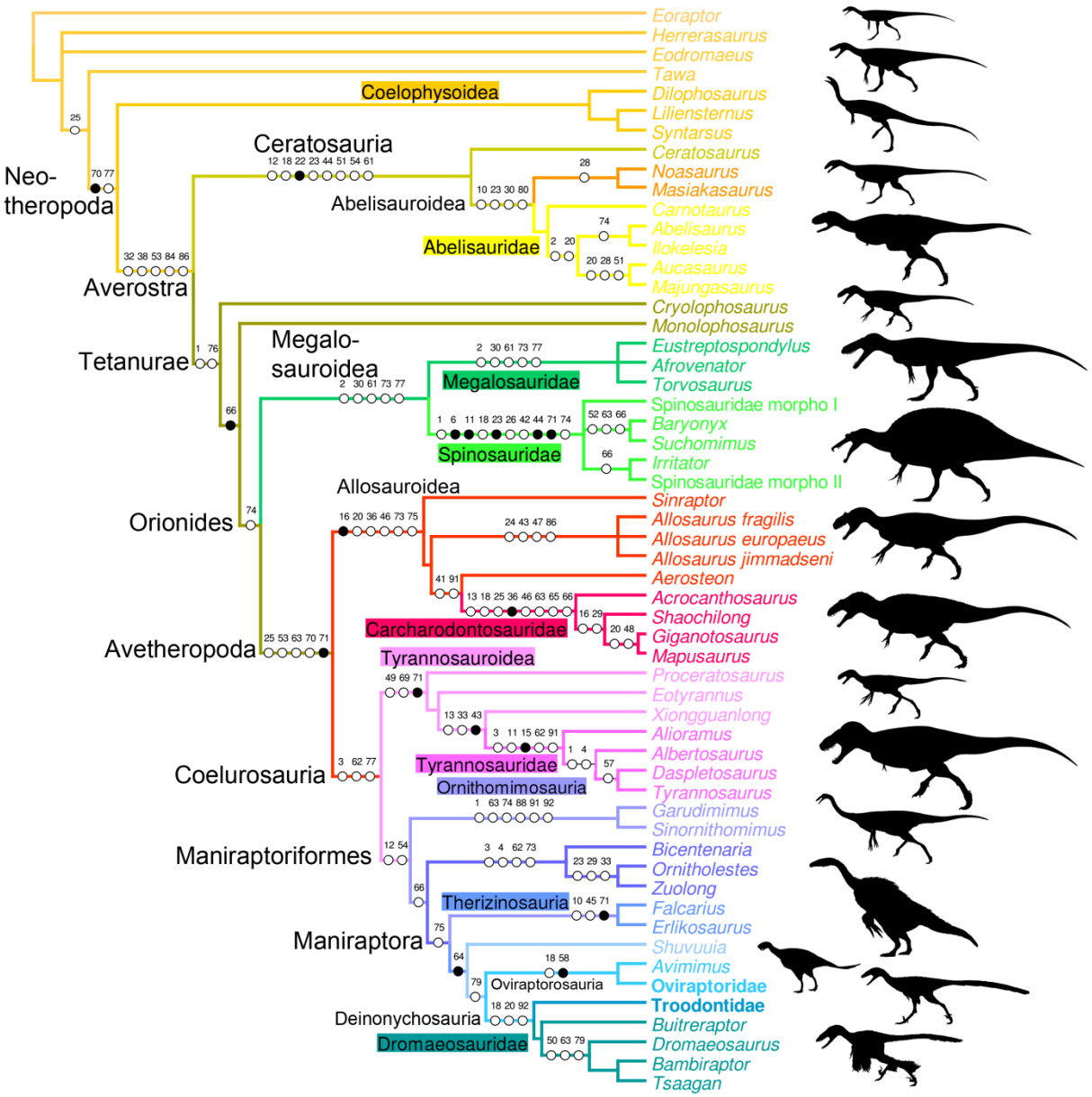

FIGURE 7.2. Strict consensus cladogram from 34 most parsimonious trees. Initial analysis was a New Technology Search using TNT v.1.1 of a supermatrix comprising 98 quadrate based characters combined with six recent datasets based on the whole skeleton (Brusatte et al. 2010*a*; Choiniere et al. 2010*b*; Martinez et al. 2011; Carrano et al. 2012; Pol and Rauhut 2012) for one outgroup (*Eoraptor lunensis*) and 54 non-avian theropod taxa. Tree length = 3616 steps; CI = 0.562; RI = 0.63113. Bremer support values are in bold and bootstrap values are in italic.

Nevertheless, the Tetanurae clade does not correspond to the general idea of the classification of these derived averostrans (Fig. 7.1) as the common clades of Allosauroidea, Avetheropoda, Coelurosauria and Maniraptora were not resolved. For instance, non-carcharodontosaurids allosauroids were found closely related to Therizinosauria, Carcharodontosauridae forms the sister clade of Ornithomimosauria + Dromaeosauridae, and non-tyrannosaurid Tyrannosauroidea, Oviraptorosauria and Troodontidae are gathered in a same clade. In fact, the classification of basal theropods (i.e., non-tetanuran Theropoda) is much better resolved than Tetanurae. This can be

explained by the large sample of non-coelurosaur theropods in the dataset (60% of the data matrix), whereas coelurosaurs are under-represented (21 taxa representing 36.5%) and includes one or two taxa of several coelurosaur clades such as Ornithomimosauria, Alvarezsauroidea and Therizinosauria. Furthermore, the clades of Oviraptoridae and Troodontidae have both been coded as a single OTU and no compsognathid taxa were included in the data matrix. It is therefore likely that the inclusion of more coelurosaur taxa into the data matrix of quadrate-based characters in the future will allow mirroring to a better degree the current classification of Tetanurae and Coelurosauria. Interestingly, the quadrate of megalosauroids and allosauroids are relatively similar as members of those two clades were found closely related, giving some support to a monophyletic Carnosauria (Megalosauroidea + Allosauroidea) as it was previously suggested (e.g., Rauhut 2003*a*).

With a high decay index, Spinosauridae (Bremer support of 5), Allosauridae (Bremer support of 4), Tyrannosauridae (Bremer support of 4) and Ornithomimosauria (Bremer support of 4) are the best supported clades and all possess a highly diagnostic quadrate. The quadrate of non-carcharodontosaurid Allosauroidea (here gathered in a monophyletic group), Therizinosauria and Dromaeosauridae, all with a Bremer support of 3, is also easily recognizable in these theropods. In fact, the cladistic analysis performed on the supermatrix of 56 taxa, and yielding 34 MPTs (Length = 3616 steps; CI = 0.562; RI = 0.631; Fig. 7.2), has shown that many theropod clades can be defined by using a combination of ambiguous and unambiguous quadrate-based synapomorphies (Fig. 7.2; Appendices 7.4, Fig. A7.5A-B). Among the best resolved clades, Spinosauridae are supported by 10 synapomorphies (with five unambiguous), and eight synapomorphies defined the clades of Ceratosauria and Carcharodontosauridae. Clades of more than three quadrate synapomorphies include Abelisauroidea (4), Averostra (5), Megalosauridae (5), Avetheropoda (5), Allosauroidea (6), Allosauridae (4), Tyrannosauridae (5) and Ornithomimosauria (6). Coelophysoidea, Abelisauridae and Dromaeosauridae are the only clade of theropods that are not defined by a single quadrate synapomorphy.

Phylogenetic Morphometrics Analysis

The two most interesting results concerning the phylogenetic morphometric analysis performed character by character is the dichotomy recovered when character 2 and 3 are run independently (Fig. 7.3; Appendices A7.7). For the posterior view (character 3; Fig. 7.3A; Appendices A7.7, Fig. A7.8), this consists essentially on a ‘coelurosaurian’ (Morphotype A) *versus* a ‘non-coelurosaurian’ type (Morphotype B). The distinction of these two morphotypes lies essentially on the clear differences of the morphology of the quadrate foramen (landmarks 6-10) and the robustness of the quadrate body (landmarks 1,2 and 3). In morphotype A, the quadrate is low and stout comparatively to the tall and slender bone in morphotype B. Also the quadrate foramen of morphotype A is well-delimited and relatively lateromedially wide, but it is lateromedially narrow or completely absent in morphotype B. The latter morphotype can be found in ceratosaurian taxa, as well as in

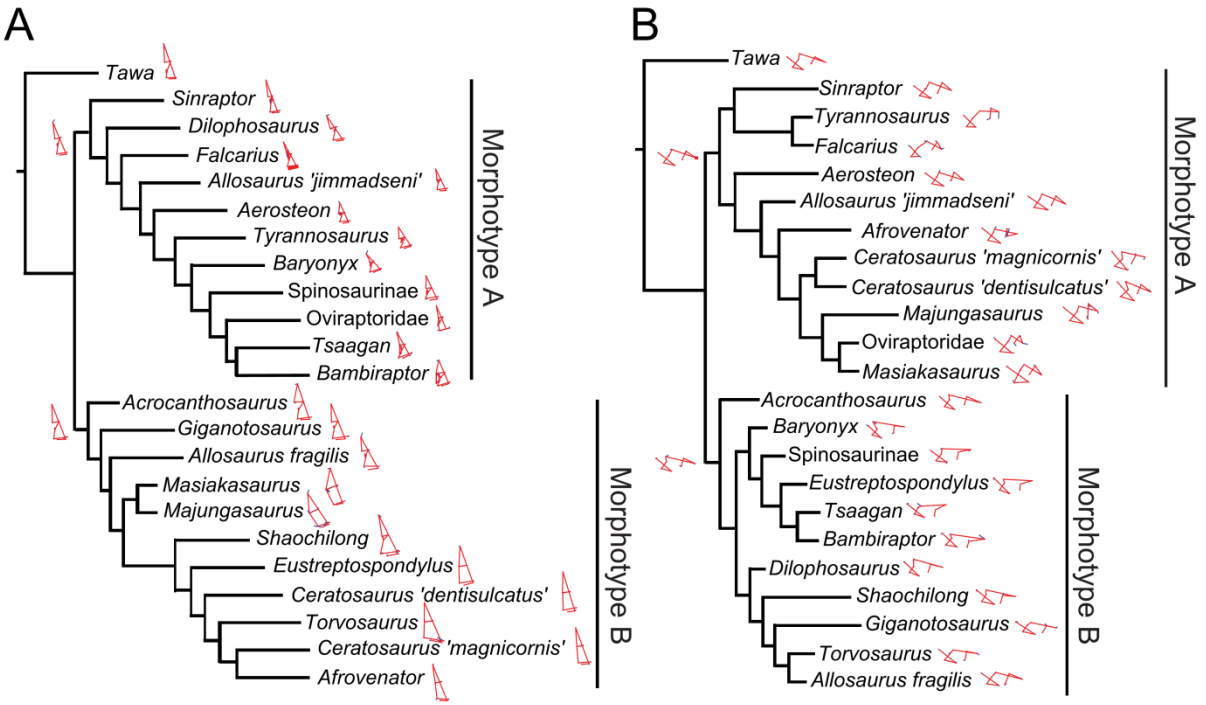

FIGURE 7.3. **A**, Cladogram resulting from the phylogenetic morphometrics analysis of the quadrate body shape in posterior view using 12 landmarks (tree score: 3.25, by using RFTRA) and revealing two morphotypes: low and stout quadrate with well-delimited and relatively broad lateromedially quadrate foramen (morphotype A; Spinosauridae and Coelurosauria) versus tall and slender quadrate with a lateromedially narrow or completely absent quadrate foramen (morphotype B; Ceratosauria and Megalosauridae); **B**, Cladogram resulting from the phylogenetic morphometrics analysis of the mandibular articulation in ventral view using 8 landmarks (tree score: 2.92; by using RFTRA) and revealing two morphotypes: anteroposteriorly broad mandibular articulation with two ovoid/subcircular condyles roughly subequal in size (Morphotype A; Ceratosauria, Tyrannosauroidea and Oviraptorosauria) versus elongate and anteroposteriorly narrow mandibular articulation with a long and parabolic/sigmoid ectocondyle (Morphotype B; Megalosauroidea, Carcharodontosauridae and Dromaeosauridae).

megalosaurids and carcharodontosaurids theropods (Appendices A7.7, Fig. A7.8). On the other hand, morphotype A is present in all coelurosaurians and *Dilophosaurus*, Metricanthosauridae and Spinosauridae. The basal placement of *Sinraptor* and *Acrocanthosaurus* in each 'morphoclade' reveals the transition from one morphotype to the other during the evolution of Allosauroidea.

For the ventral view (character 2; Fig. 7.3B; Appendices A7.7, Fig.A7.9), the dichotomy divides a ceratosaurian (Morphotype A) *versus* a megalosauroid type (Morphotype B), although this result is more blurred due to the recovery of *Afrovenator* among the ceratosaurian-dominated clade. Tyrannosauroids, metriacanthosaurids, therizinosauroids, and oviraptosaurids are recovered among the ceratosaurian type, whereas dilophosaurids, carcharodontosaurids, and dromaeosaurids belong to the megalosauroid type.

In both phylogenetic morphometric analyses of the quadrate in posterior and ventral views, the two species of *Allosaurus*, *A. 'jimmadseni'* and *A. fragilis* are recovered among the ceratosaurian/non-coelurosaurian and megalosauroid-dominated clade, respectively.

Anatomy of the non-avian theropod quadrate

The quadrate morphology of each non-avian theropod clade typically at a 'family' or 'super-family' level is here thoroughly illustrated and investigated. Given the topological changes occurring for several taxa in the results of different recent cladistic analyses performed on non-avian theropods, the theropod classification is here based on the largest scale phylogenetic analyses of Sues et al. (2011) for non-neotheropod Theropoda (*Cryolophosaurus* excluded), Ezcurra and Brusatte (2011) for non-averostran Neotheropoda (*Cryolophosaurus* excluded), Pol and Rauhut (2012) for Ceratosauria, Carrano et al. (2012) for non-coelurosaur Tetanurae, Lü et al. (2014) for Tyrannosauroidea, and Choiniere et al. (2014*b*) for non-tyrannosauroid Coelurosauria.

Non-neotheropod Theropoda

Eoraptor lunensis (PVSJ 512; Sereno et al. 2013; Fig. 7.4E), *Herrerasaurus ischigualastensis* (PVSJ 53 = *Frenguellisaurus ischigualastensis*; PVSJ 407; Fig. 7.4B–4D), *Eodromaeus murphi* (PVSJ 562; Fig. 7.4E–J); *Daemonosaurus chauliodus* (Sues et al. 2011); *Tawa hallae* (Nesbitt et al. 2009; Fig. 7.4K–P).

Although recent discoveries of new basal theropods have increased dramatically in the last five years, information regarding the quadrate anatomy can be improved. The quadrates of many basalmost theropods are still articulated in the cranium and therefore not visible in anterior, ventral and dorsal views. This is the case for *Eoraptor lunensis*, where most of the right quadrate is covered by matrix, and *Herrerasaurus ischigualastensis* (PVSJ 407) in which the mandibular condyles are still in articulation with the lower jaw (Sereno and Novas 1994). Likewise, the right quadrate bone of *Daemonosaurus chauliodus* is not only badly preserved, but also shows the lateral part of the bone only. Fortunately, the left quadrate of *Eodromaeus murphi* and both left and right quadrates of *Frenguellisaurus ischigualastensis* (PVSJ 53), now considered to be a junior synonym of *Herrerasaurus ischigualastensis* (Novas 1992), and *Tawa hallae*, the most derived form of non-neotheropod Theropoda (*sensu* Nesbitt et al. 2009), are relatively well preserved and allow a better understanding of the quadrate anatomy in non-neotheropod Theropoda.

The quadrate of these basalmost theropods is tall (strongly ventrodorsally tall relative to the lateromedial width of the mandibular articulation; ratio corresponding to the lateromedial width of mandibular articulation divided by the ventrodorsal length from entocondyle to quadrate head of less than 0.35), lateromedially narrow, and possesses a small quadrate foramen (Fig. 7.4A, E) at the lower one-third of the quadrate body in *E. lunensis* and *H. ischigualastensis* (presence of a quadrate foramen in *E. murphi*, *D. chauliodus* and *T. hallae* is unknown). The quadrate foramen of these two taxa is mostly delimited by the quadrate and only the lateral border is formed by the quadratojugal. In *H. ischigualastensis*, the quadrate foramen is adjacent to the quadrate ridge (PVSJ 53, 407; Fig. 7.4A), whereas the foramen is well-separated from the ridge in *E. lunensis* (*contra* Martinez and Alcober

2009; Fig. 7.4E) as in the basal sauropodomorph *Panphagia protos* (PVSJ 874, Martinez and Alcober 2009).

The quadrate ridge in *H. ischigualastensis* and *E. murphi* is prominent (i.e., well-delimited), rod-shaped, laterodorsally inclined (angle between the main axis of the quadrate ridge and the main axis of the mandibular articulation of 75°, in posterior view), and fades away dorsal to the entocondyle, at one third of the height of the quadrate body (Fig. 7.4A, H). In *E. lunensis*, the quadrate

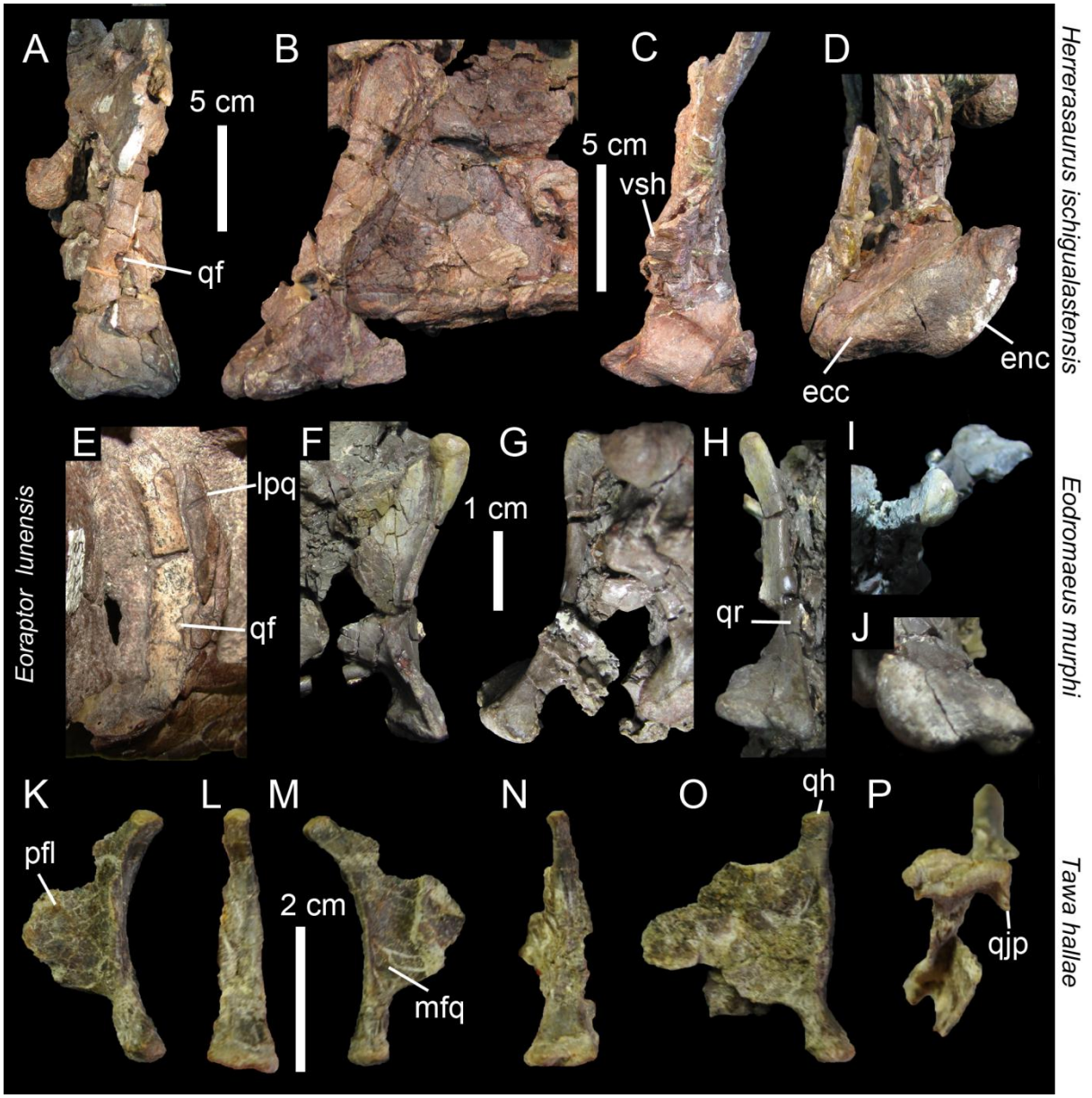

FIGURE 7.4. Quadrate diversity in non-neotheropod Theropoda. **A–D**, Right quadrate of *Herrerasaurus ischigualastensis* (PVSJ 53, formerly *Frenguellisaurus ischigualastensis*) in **A**, posterior; **B**, medial; **C**, anterior; and **D**, ventral views; **E**, Right quadrate of *Eoraptor lunensis* (PVSJ 512) in posterolateral view; **F–J**, Left quadrate of *Eodromaeus murphi* (PVSJ 562) in **F**, lateral; **G**, medial; **H**, posterior; **I**, dorsal; and **J**, ventral views; **K–M**, Left and **N–P**, right quadrates of *Tawa hallae* (GR 241) in **K**, lateral; **L, N**, posterior; **M, O**, medial; and **P**, ventral views (courtesy of Sterling Nesbitt). **Abbreviations**: **ecc**, ectocondyle; **enc**, entocondyle; **lpq**, lateral process; **mfq**, medial fossa; **pfl**, pterygoid flange; **pfq**, posterior fossa; **qf**, quadrate foramen; **qjp**, quadratojugal process; **qr** quadrate ridge; **vsh**, ventral shelf of the pterygoid flange.

ridge is only visible on the dorsal part of the quadrate body, directly below the quadrate head. Like in *H. ischigualastensis* and *E. murphi*, the ridge reaches the quadrate head, but similar to *T. hallae* it is vertical and not inclined laterally. In lateral view, the posterior margin of the quadrate ridge is concave in *E. lunensis* (Sereno et al. 2013), *E. murphi* and *T. hallae*, whereas it is straight in *H. ischigualastensis*.

In *E. murphi* and *T. hallae*, the ventral quadratojugal contact is ovoid to D-shaped, with an irregular articulating surface. It faces posterolaterally in *E. murphi* (Fig. 4.8), and laterally in *T. hallae*. The ventral quadratojugal contact is anteroposteriorly longer than the dorsal one in all non-neotheropod theropods, as the dorsal quadratojugal contact corresponds to a the rim of the lateral process in *E. lunensis* and *H. ischigualastensis*. The ventral quadratojugal contact projects slightly anteriorly in *T. hallae* (Fig. 7.4P), unlike the condition seen in *H. ischigualastensis* and *E. murphi* where the quadratojugal process is absent (Fig. 7.4D, J).

As seen in non-tetanuran theropods, the quadrate of *H. ischigualastensis* possesses a subtriangular lateral process projecting anterolaterally that joins the quadrate body at the level of the foramen ventrally and the quadrate head dorsally. A lateral process reaching the quadrate head is also present in *E. lunensis* (Sereno et al. 2013), but its lateral margin is rather parabolic (i.e., two-dimensional symmetrical curve similar to a widely spread parabola), and the process is relatively short and only projects laterally (Fig. 7.4E) in contrast to *H. ischigualastensis*. A parabolic lateral process is also seen in *D. chauliodus*, but its dorsal extent terminates far-beneath the quadrate head. The lateral process of all non-neotheropod theropods contacts the quadratojugal and the squamosal along its lateroventral and laterodorsal rims, respectively. The presence of a lateral process in *E. murphi* and *T. hallae* cannot be determined as this part of the quadrate body is missing.

The pterygoid flange of basalmost theropods is subtrapezoidal in outline (i.e., the anterior margin of the flange is roughly formed by three sides where the most anterior one is straight and short ventrodorsally), and the most anterior point of the flange occurs at the level of the mid-height of the quadrate. The pterygoid flange joins the quadrate body at one sixth or one fifth of the height of the quadrate and far above the mandibular condyles in *H. ischigualastensis*, *E. murphi* and *D. chauliodus*, a condition shared by most other non-tetanuran theropods (e.g., MB R.2175; MWC 1; FMNH PR 2100; MCNA-PV-3137; IVPP 10600; UCMP 37302). The angle formed by the ventral margin of the pterygoid flange and the main axis of the quadrate ridge varies between 60° and 70°. The flange only projects anteriorly and its anterior part does not curve medially. Nevertheless, there is a weak medial curvature of the ventral margin of the flange (‘horizontal shelf’ *sensu* Sereno et al. 2013), and a shallow medial fossa occurs in the posteroventral part of the pterygoid flange.

In *D. chauliodus*, the quadrate head is situated upon a cylindrical projection of the quadrate shaft. It is single headed, anteroposteriorly short (Sues et al. 2011), and the posterior margin is convex. The pterygoid flange reaches the quadrate body directly ventral to the anteroventral limit of the quadrate head. The same condition occurs in *E. murphi* where the quadrate head is globular in lateral

view, and in dorsal view it is roughly subtriangular in shape with rounded corner (Fig. 7.4I). In lateral view, the quadrate head and the dorsalmost part of the quadrate body is slightly posterodorsaly-oriented in *E. lunensis* whereas it is sub-horizontal in *H. ischigualastensis*, *D. chauliodus* and *E. murphi* (*contra* Martinez et al. 2011: fig. 1B). In *H. ischigualastensis*, the quadrate head is convex, subtriangular in outline in posterior view and exposed in lateral view, and a flattened medial surface below the quadrate head contacts the paroccipital process (Sereno and Novas 1994).

Although little information is known about the morphology of the mandibular articulation in the holotypes of *E. lunensis* and *H. ischigualastensis*, this part of the quadrate is well-preserved in a specimen referred to *H. ischigualastensis* (PVSJ 53; Fig. 7.4E), and almost complete in *E. murphi* and *T. hallae* in which the anterior part of the ectocondyle and entocondyle, respectively, is missing. Both ecto- and entocondyle are subequal in size in *H. ischigualastensis*, but the ectocondyle is lateromedially wider in *E. murphi* and *T. hallae*. The ectocondyle is elliptical of *H. ischigualastensis* and *E. murphi* whereas it is slightly sigmoid in *T. hallae*. The entocondyle is elliptical, anteroposteriorly long, and does not protrude anteriorly in both *H. ischigualastensis* (Fig. 7.4D) and *E. murphi* (Fig. 7.4J). The mandibular condyles are separated by a shallow and diagonally-oriented intercondylar sulcus in these two taxa, whereas the sulcus is deep and well-delimited in *T. hallae* (Fig. 7.4P). Likewise, the angle between the main axes passing through the intercondylar sulcus and mandibular articulation is lower than 135° in *H. ischigualastensis* and *E. murphi*, but much higher than this value in *T. hallae*.

Although the quadrate height of all basal theropods is subequal or less than 80% of the orbital fenestra height, the quadrate inclination may have been variable among primitive theropods. Indeed, the mandibular articulation lies anterior to the quadrate head in *E. lunensis* (Sereno et al. 1993, 2013), at the same level in *D. chauliodus* (Sues et al. 2011), and posterior to the quadrate head in *H. ischigualastensis* (Sereno and Novas 1994).

Non-averostran neotheropods (Coelophysoidea + Dilophosauridae)

Liliensternus liliensterni (Huene 1934; Fig. 7.5A–F); *Megapnosaurus* (‘*Syntarsus*’) *kayentakatae* (Rowe, 1989; Fig. 7.5G–I); *Megapnosaurus* (‘*Syntarsus*’) *rhodesiensis* (Raath 1977); *Coelophysis bauri* (CMNH 81765; AMNH FARB 7223, 7224,7225, 7227, 7237, 7238); *Zupaysaurus rougieri* (PULR 076) *Dilophosaurus wetherilli* (Welles, 1984; Fig. 7.5J–O).

As in basalmost theropods, little information regarding the quadrate anatomy of non-averostran neotheropods can be extracted from the literature, as the cranial material of these taxa are still in articulation with the skull, and cannot be observed in all views. This is the case of both quadrates of *Megapnosaurus kayentakatae*, *Zupaysaurus rougieri* (in which the quadrates are mostly covered by the matrix; Arcucci and Coria, 2003; Ezcurra, 2007) and all specimens of *Coelophysis bauri* examined in this study (CMNH 81765; AMNH FARB 7223, 7224,7225, 7227, 7237, 7238). However, the right quadrate of *M. kayentakatae* is particularly well-exposed (Tykoski 2005) in

posterior view (Fig. 7.5G–H), although the pterygoid flange is hidden by matrix and the mandibular articulation is still articulated to the lower jaw. An incomplete isolated right quadrate of *Liliensternus liliensterni* (Fig. 7.5A–F) also gives us the opportunity to have a better understanding of the quadrate anatomy of non-averostran neotheropods.

As seen in the earliest forms of theropods, the quadrate of non-averostran neotheropods is ventrodorsally tall and relatively narrow lateromedially, and the posterior margin of the quadrate body is lateromedially concave. A quadrate foramen seems to be present and situated at mid-height of the bone in all non-averostran neotheropods. However, The size and limits of this foramen are highly variable in this clade, being relatively large, oval and inside the quadrate body in *Z. rougieri* (Arcucci and Coria 2003; Ezcurra 2007), small, deeply recessed and equally surrounded by the quadrate and quadratojugal in *M. rhodesiensis* (Raath, 1977: fig. 3D, 4J; Yates, 2005; Tykoski, 2005), and minute and largely encircled by the quadrate in *M. kayentakatae* (Tykoski, 2005; Fig. 7.5G). A quadrate foramen has also been reported in *Liliensternus liliensterni* (Huene 1934), but not in *C. bauri* (Colbert 1989); however, according to Tykoski (2005), poor preservation renders its absence uncertain in *Coelophysis*, an opinion that we also follow for *L. liliensterni* as some part of the quadrate body are missing in this specimen (Fig. 7.5C).

The quadrate ridge is subvertical, prominent and particularly lateromedially narrow, forming a low crest in *M. kayentakatae* (Fig. 7.5G). In *L. liliensterni*, the quadrate ridge is rod-shaped and laterodorsally inclined (angle between the main axis of the quadrate ridge and the main axis of the mandibular articulation of 65°, in posterior view; Fig. 7.5C). Nevertheless, the ridge extends directly dorsal to the entocondyle in both taxa, and reaches the quadrate head in *M. kayentakatae*. As some basal forms like *H. ischigualastensis*, the quadrate of non-averostran neotheropods possesses a subtriangular lateral process (Colbert 1989) that extends anterolaterally from above the quadrate foramen. This process is seen in *M. kayentakatae*, *M. rhodesiensis* (Raath, 1977: fig. 4j), *Z. rougieri* and *L. liliensterni* (Fig. 7.5B) and contacts the quadrate body directly ventral to the quadrate head at least in *M. kayentakatae*.

Although the dorsal and ventral quadratojugal contacts are not visible or not preserved in most basal neotheropods, the ventral quadratojugal contact of *L. liliensterni* is anteroposteriorly long, and much longer than the dorsal quadratojugal contact as the latter corresponds to the rim of the lateral process (Fig. 7.5B). A posterior fossa is well-visible in *M. kayentakatae* (Fig. 7.5G–H) and *L. liliensterni*. This fossa is relatively small, oval and centered on the quadrate body in both taxa. It does not surround the quadrate foramen at least in *M. kayentakatae*, but it may have bordered the quadrate foramen in *L. liliensterni*.

The mandibular articulation is ventrally visible in *M. kayentakatae* and shows a diagonal intercondylar sulcus separating a lateromedially wide ectocondyle and a narrow entocondyle. The

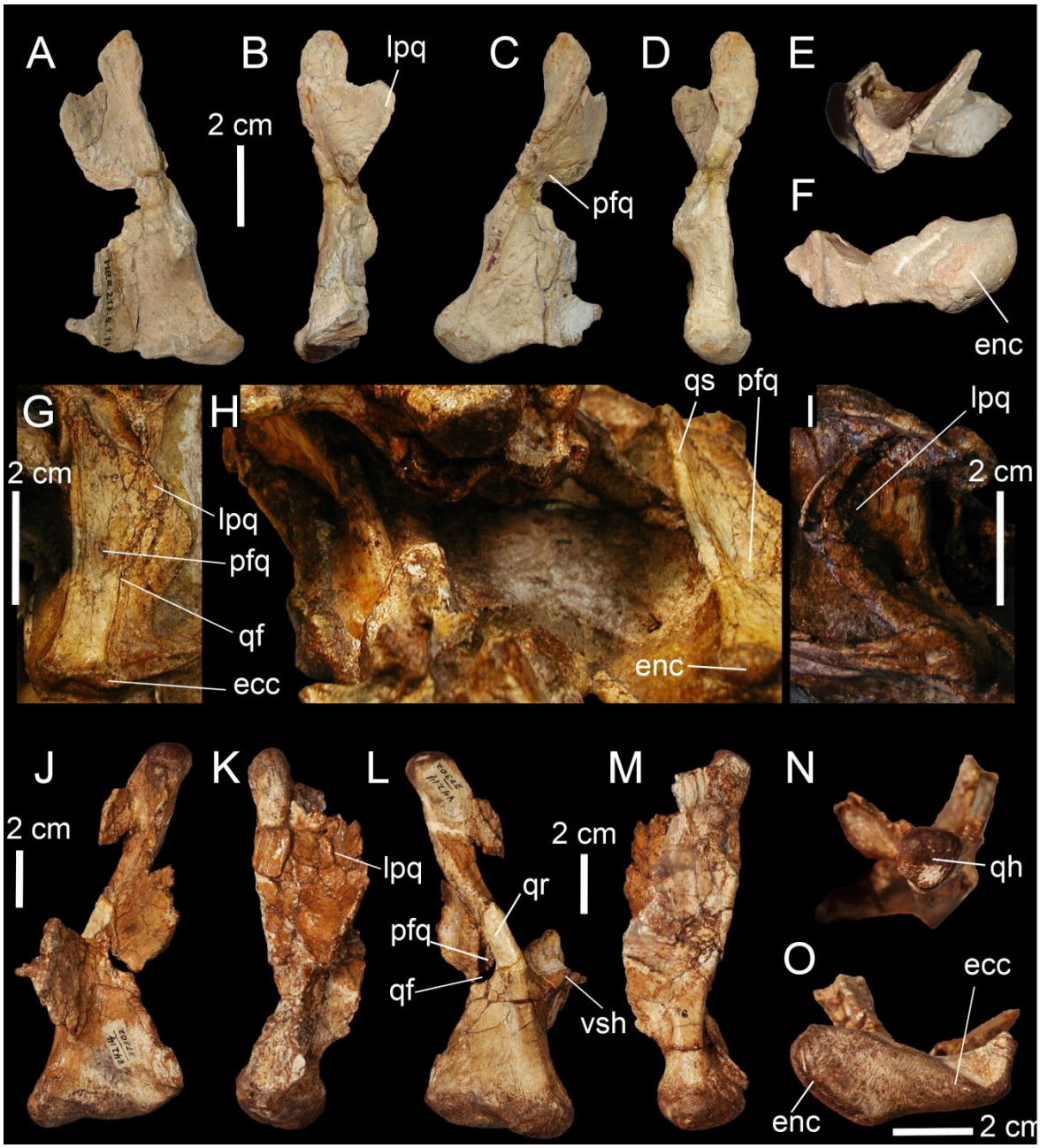

FIGURE 7.5. Quadrate diversity in Coelophysoidea. **A–F**, Right quadrate of *Liliensternus liliensterni* (MB R.2175) in **A**, anterior; **B**, lateral; **C**, posterior; **D**, medial; **E**, dorsal; and **F**, ventral views (courtesy of Martín Ezcurra). **G–H**, Right and **H–I**, left quadrates of *Megapnosaurus kayentakatae* (MNA V2623) in **I**, lateral; and **G, H**, posterior views (courtesy of Ronald Tykoski); **J, L, O**, Left and **K, M–N**, right quadrates of *Dilophosaurus wetherilli* (UCMP 37302) in **J**, anterior; **K**, lateral; **L**, posterior; **M**, medial; **N**, dorsal; and **O**, ventral views (courtesy of Randall Irmis). **Abbreviations**: **ecc**, ectocondyle; **enc**, entocondyle; **lpq**, lateral process; **mfq**, medial fossa; **pfl**, pterygoid flange; **pfq**, posterior fossa; **qf**, quadrate foramen; **qh**, quadrate head; **qjp**, quadratojugal process; **qr** quadrate ridge; **vsh**, ventral shelf of the pterygoid flange.

ectocondyle of *M. kayentakatae* seems to project ventral to the quadratojugal, below the ventral edge of that bone. Such lateroventral process of the quadrate is only seen in this taxon and in oviraptorids (Maryańska and Osmólska 1997). In *L. liliensterni*, the entocondyle is ovoid to elliptical in outline and does not protrude anteriorly (Fig. 7.5F).

The quadrate inclination is quite variable in non-averostran neotheropods in lateral view, as the quadrate is strongly inclined anteriorly in *M. kayentakatae* (Fig. 7.5I), subvertical in some specimens *C. bauri* (AMNH 7224; MCZ 4326) and posteriorly inclined in *Z. rougieri* (PULR 076; Ezcurra 2007) and other *C. bauri* specimens (AMNH 7228).

Dilophosaurus

The morphology of the *Dilophosaurus* quadrate differs significantly from this of other coelophysoids and ceratosaurians and will therefore be described separately from other non-averostran neotheropods. Two disarticulated quadrates are available in *Dilophosaurus wetherilli* and Welles (1984) provided a relatively detailed description of them. However, they are here figured for the first time (Fig. 7.5.10–5.15) so that comparison with the quadrate of other theropods can be given.

Unlike other very basal theropods and coelophysoids, the quadrate of *D. wetherilli* are moderately tall (ratio of 0.39) ventrodorsally, with a relatively lateromedially wide mandibular articulation. In addition, the quadrate ridge is particularly prominent and well-defined, rod-shaped, laterodorsally-inclined (angle between the main axis of the quadrate ridge and the main axis of the mandibular articulation of 55-60°, in posterior view), and slightly twisted so that both ventromedial and laterodorsal margins of the ridge are convex (Fig. 7.5L). Nevertheless, the ridge is prominent above the entocondyle and terminates beneath the quadrate head without reaching the entocondyle. However, the quadrate ridge of *D. wetherilli* is convex in medial view (Fig. 7.5M), a condition also shared with the megalosaurid *Dubreuillosaurus valesdunensis* (Allain 2002).

The pterygoid flange of *D. wetherilli* projects anteriorly, is anteroposteriorly straight (i.e., not medially bent in its anterior part), subtrapezoidal with the anteriormost margin inclined posteriorly in lateral view, and does not seem to possess a ventral shelf extending all along the ventral margin of the flange as seen in other taxa such as *Ceratosaurus* (Fig. 7.6D) and *Allosaurus* (SMA 005/02; Fig. 7.10D). The flange also reaches the quadrate head at its anteroventral margin dorsally, and the quadrate body well above the mandibular condyles ventrally (Fig. 7.5M). The anteriormost point of the pterygoid flange in *D. wetherilli* is situated at two thirds of the height of the bone relative to its ventral end and the ventroposterior margin is slightly medially folded (UCMP 37302).

Like more basal theropods, *D. wetherilli* possesses a subtriangular lateral process that reaches the quadrate body beneath the quadrate head (Fig. 7.5K). This lateral process projects mostly anteriorly and is particularly well-developed in this taxon.

Unlike ceratosaurs and megalosaurids, a quadrate foramen is present in *D. wetherilli* and its shape and position are autapomorphic to this taxon (Fig. 7.5L). The main axis of the foramen, rather than being subparallel to the long axis of the quadrate, is sub-perpendicular to the quadrate axis and the foramen has an atypical ‘keyhole’ shape, an autapomorphic character of *D. wetherilli*. The foramen is mostly delimited by the quadrate and it is surrounded by a deep posterior fossa (Fig. 7.5L). This fossa is atypical in *D. wetherilli* as it is subtriangular in shape and deep inside the ventral part of

the lateral process, delimited by the prominent quadrate ridge medially and a prominent and ventrodorsally oriented ridge on the posterior surface of the lateral process laterally (Fig. 7.5L).

Like most basal theropods, the ventral quadratojugal contact is ovoid, almost D-shaped, and anteroposteriorly longer than the dorsal quadratojugal suture, which corresponds to the edge of the lateral process (Fig. 7.5K). The anterior margin of the ventral quadratojugal contact slightly projects anteriorly.

The mandibular articulation is well-preserved in the left quadrate of *D. wetherilli*. It clearly shows a sigmoid and lateromedially wide ectocondyle delimited from an elliptical, and non-protuberant entocondyle by a wide and shallow intercondylar sulcus (Fig. 7.5O). Like megalosauroids, the ectocondyle is lateromedially wider than the entocondyle, and the angle made by the intercondylar sulcus with the long axis passing through the mandibular articulation is around 130°. These conditions are not seen in any ceratosaurs.

An unnamed clade encompassing *D. wetherilli*, *Dracovenator regenti* and *Z. rougieri* was recovered in Yates (2005) and later by Smith et al. (2007) which also includes *Sinosaurus triassicus* (Hu 1993; Xing 2012; Xing et al. 2013*b*) and *Cryolophosaurus ellioti* (Hammer and Hickerson 1994), but without *Z. rougieri*. The quadrates of the two latter are indeed quite as in those of *D. wetherilli* in many aspects such as the shape and inclination of the quadrate ridge and the size and position of the quadrate foramen. However, *C. ellioti* does not have a lateral process and the quadrate foramen of both *C. ellioti* and *Z. rougieri* has a ventrodorsally extending long axis, and no subtriangular posterior fossa surrounds it. While there is little doubt that *Z. rougieri* is a non-averostran neotheropod, *C. ellioti* has also been considered to be a basal tetanuran (Sereno et al. 1994, 1996; Carrano et al. 2012).

Ceratosaurus

Ceratosaurus nasicornis (USNM 4735; MWC 1; Madsen and Welles 2000; Fig. 7.6A–E).

Both quadrates of the holotype of *Ceratosaurus nasicornis* USNM 4735 are in articulation within the cranium and strongly distorted (Gilmore 1920), yet the disarticulated quadrates of MWC 1 (formerly known as *Ceratosaurus* '*magnicornis*') and UUVP 1646 (formerly known as *Ceratosaurus* '*dentisulcatus*') are relatively complete and slightly deformed (Madsen and Welles 2000), allowing a full picture of their anatomy. The quadrates of MWC 1 and UUVP 1646 have been briefly described by Madsen and Welles (2000) and a full description of their anatomy is here given for the first time.

As in more basal theropods, the quadrate bone of *Ceratosaurus* is ventrodorsally tall, the mandibular articulation is lateromedially narrow (Fig. 7.6C), and the pterygoid flange is anteroposteriorly straight, subtrapezoidal (i.e., the anterior margin of the pterygoid flange is formed by three well defined dorsal, anterior, and ventral borders), and reaches the quadrate body at one fourth of the bone, well dorsal to the mandibular condyles (Fig. 7.6D). In addition, the quadrate also possesses a subtriangular lateral process attached to the quadrate body roughly at mid-height of the bone ventrally and far beneath the quadrate head dorsally (Fig. 7.6C). The latter is prominent, lateromedially narrow

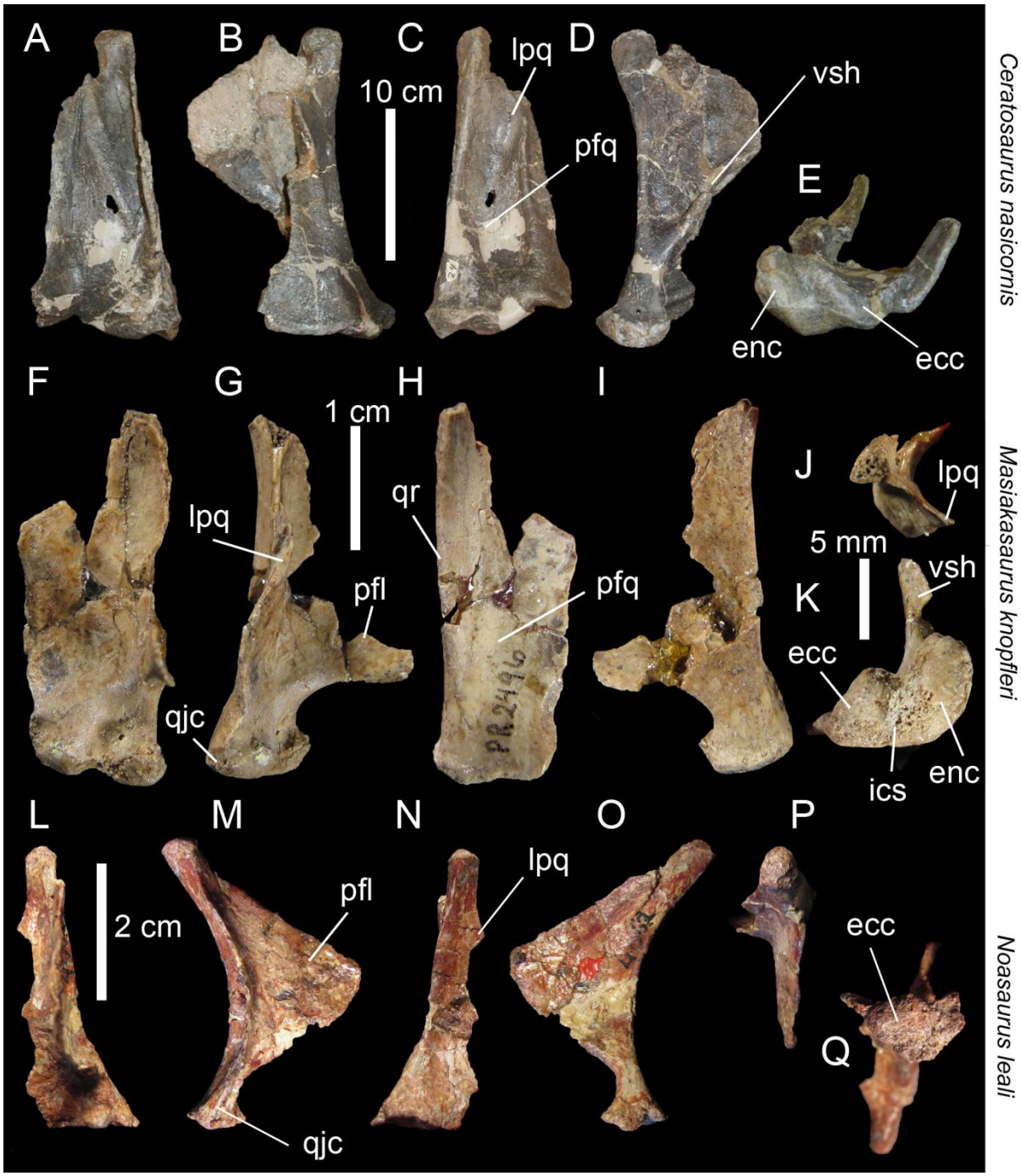

FIGURE 7.6. Quadrate diversity in Ceratosauridae and Noasauridae. **A, C**, Coosified right and **B, D–E**, left quadrates and quadratojugals of *Ceratosaurus nasicornis* (MWC 1; formerly known as *C.* '*magnicornis*') in **A**, anterior; **B**, lateral; **C**, posterior; **D**, medial; and **E**, ventral views; **F–I**, Right quadrate of *Masiakasaurus knopfleri* (FMNH PR 2496) in **F**, lateral; **G**, posterior; **H**, medial; and **I**, ventral views (courtesy of Matthew Carrano); **J**–**O**, Right quadrate of *Noasaurus leali* (PVL 4061) in **J**, anterior; **K**, lateral; **L**, posterior; **M**, medial, dorsal; and **N, O**, ventral views. **Abbreviations**: **ecc**, ectocondyle; **enc**, entocondyle; **ics**, intercondylar sulcus; **lpq**, lateral process; **mfq**, medial fossa; **pfl**, pterygoid flange; **qh**, quadrate head; **qjc**, quadratojugal contact; **qr** quadrate ridge; **vsh**, ventral shelf of the pterygoid flange; **pfq**, posterior fossa.

in posterior view, and subtriangular in outline in dorsal view. The quadrate is fused to the quadratojugal (Fig. 7.6A, C), a condition seen in some derived abelisaurids such as *Carnotaurus* (Fig. 7.7N).

The ventral part of the quadratojugal contact is anteroposteriorly longer than the dorsal one. As in *D. wetherilli*, the ventral margin of the pterygoid flange curves medially and there is a well-defined and thick ventral shelf extending all along the ventral rim of the pterygoid flange. The most anterior point of the pterygoid flange is situated at two thirds of the quadrate height relative to its ventral end (Fig. 7.6D).

The quadrates of the different specimens of *Ceratosaurus* share also together a combination of characters only observed in this genus: the absence of a quadrate foramen, making the quadratojugal contact of the quadrate continuous; a relatively thick, subvertical, and not-well delimited quadrate ridge, becoming visible at one-third of the quadrate, well-above the entocondyle, but reaching the quadrate head; a deep medial fossa and a lateromedially wide fossa formed by both quadrate and quadratojugal and centered on the suture of these two bones; a lateral process that is laterally extended; and both ecto- and entocondyle are parabolic, subparallel and similar in size in ventral and posterior views. The two mandibular condyles are also separated by a shallow intercondylar sulcus as wide as the condyles (Fig. 7.6E). The ventral quadratojugal contact is lanceolate (i.e., tear-drop shaped), and does not possess any anterior projection, whereas the dorsal contact extends along the rim of the lateral process.

Noasauridae

Masiakasaurus knopfleri (FMNH PR 2496; Fig. 7.6F–K); *Noasaurus leali* (PVL 4061; Fig. 7.6L–6Q).

In noasaurids, only the right quadrates are known in *Noasaurus leali* and *Masiakasaurus knopfleri*. The quadrate of the latter is incomplete (most of the dorsal part of the pterygoid flange and quadrate body are missing) and has recently been extensively described by Carrano et al. (2011). The quadrate of *N. leali* has been only figured in medial view and very briefly described by Bonaparte and Powell (1980: fig. 7C).

M. knopfleri and *N. leali* quadrate morphology are similar in many aspects and clearly reflects their ceratosaurian affinity. They are indeed quite similar to the quadrate of *Ceratosaurus* and only differ from those of Abelisauridae in its derived features. As in *Ceratosaurus*, the quadrate of *M. knopfleri* and *N. leali* possesses a sub-vertical and poorly delimited quadrate ridge emerging dorsal to the entocondyle and terminating at the quadrate head (Fig. 7.6H, N). Although incomplete, the lateral process of both noasaurids is present, mostly laterally-oriented and the dorsal margin of the process reaches the quadrate body well-ventral to the quadrate head, at three-fourth of the quadrate height relative to its ventral end. Similar to Abelisauridae, the ventral margin of the process joins the quadrate body at the level of the mandibular articulation (Fig. 7.6H, N).

The pterygoid flange is anteroposteriorly straight (i.e., not curved medially) and the posteroventral margin is medially folded in *M. knopfleri* (Fig. 7.6K). A ventral shelf is absent in *N. leali* and its presence cannot be determined in *M. knopfleri*. The dorsal margin of the flange reaches

the quadrate head, and the ventral margin attaches the quadrate body at around one fourth of the quadrate height relative to its ventral end, well-dorsal to the mandibular articulation (Fig. 7.6G, M). Although figured as a subtriangular flange by Bonaparte and Powell (1980: fig. 7C), the pterygoid flange of *N. leali* is subtrapezoidal in medial view, with a ventrodorsally short anterior border (Fig. 7.6O). The medial fossa of the pterygoid flange is shallow, and, due to preservation, the existence of a posterior fossa cannot be determined in both noasaurids.

In agreement with Carrano et al. (2011), the presence of the quadrate foramen in *M. knopfleri* cannot be ruled out due to damage of the lateral margin of the quadrate body. Likewise, the presence of a quadrate foramen in *N. leali* cannot be determined as the lateral margin of the bone is badly preserved, and both ventral and dorsal parts are missing (PVL 4061). Bonaparte and Powell (1980) noted the presence of the quadrate foramen in this taxon and Carrano and Sampson (2008) coded it as absent in their data matrix, therefore our interpretation contradicts these observations.

The ventral part of the quadratojugal contact of *M. knopfleri* and *N. leali* is similar in shape, and forms a ventrodorsally tall and lanceolate shape facing laterally. Although partly damaged in *M. knopfleri* and completely absent in *N. leali*, the dorsal part of the quadratojugal contact was most likely formed by the rim of the lateral process, as observed in more basal theropods.

The quadrate head of *M. knopfleri* is strongly damaged, but the head is well-preserved in *N. leali* and corresponds to a semi-spherical condyle with a convex dorsal margin in posterior view (Fig. 7.6P). The mandibular articulation of *M. knopfleri* is very similar to those of Abelisauridae in possessing a subcircular ectocondyle smaller than the ovoid entocondyle, and a lateromedially narrow and deep intercondylar sulcus (Fig. 7.6K), two derived features absent in non-abelisauroids Ceratosauria. In *N. leali*, although incomplete, the entocondyle was obviously wider than the ectocondyle. The latter corresponds to a subcircular condyle separated from the entocondyle by a shallow and poorly delimited intercondylar sulcus (Fig. 7.6Q).

Abelisauridae

Abelisaurus comahuensis (MPCA 11098); *Ilokelesia aguadagrandensis* (MCF PVPH 35; Fig. 7.7A–F); *Aucasaurus garridoi* (MCF-PVPH 236); *Majungasaurus crenatissimus* (FMNH PR 2100; Fig. 7.7G–7L); *Carnotaurus sastrei* (MACN CH 894; Fig. 7.7M–Q).

The quadrates of *Abelisaurus comahuensis* and *Carnotaurus sastrei* have only been briefly described in the literature (e.g., Bonaparte and Novas, 1985; Bonaparte, 1991). The quadrate anatomy of *Ilokelesia aguadagrandensis*, which includes the two portion of a right quadrate, and *Majungasaurus crenatissimus*, from which the two quadrates are well-preserved, are well-known as they have been described in detail and are illustrated by Coria and Salgado (1998) and Sampson and Witmer (2007), respectively. The quadrate of other abelisaurids such as *A. comahuensis*, *Aucasaurus garridoi*, and *Carnotaurus sastrei* is however poorly described or even lack of a description.

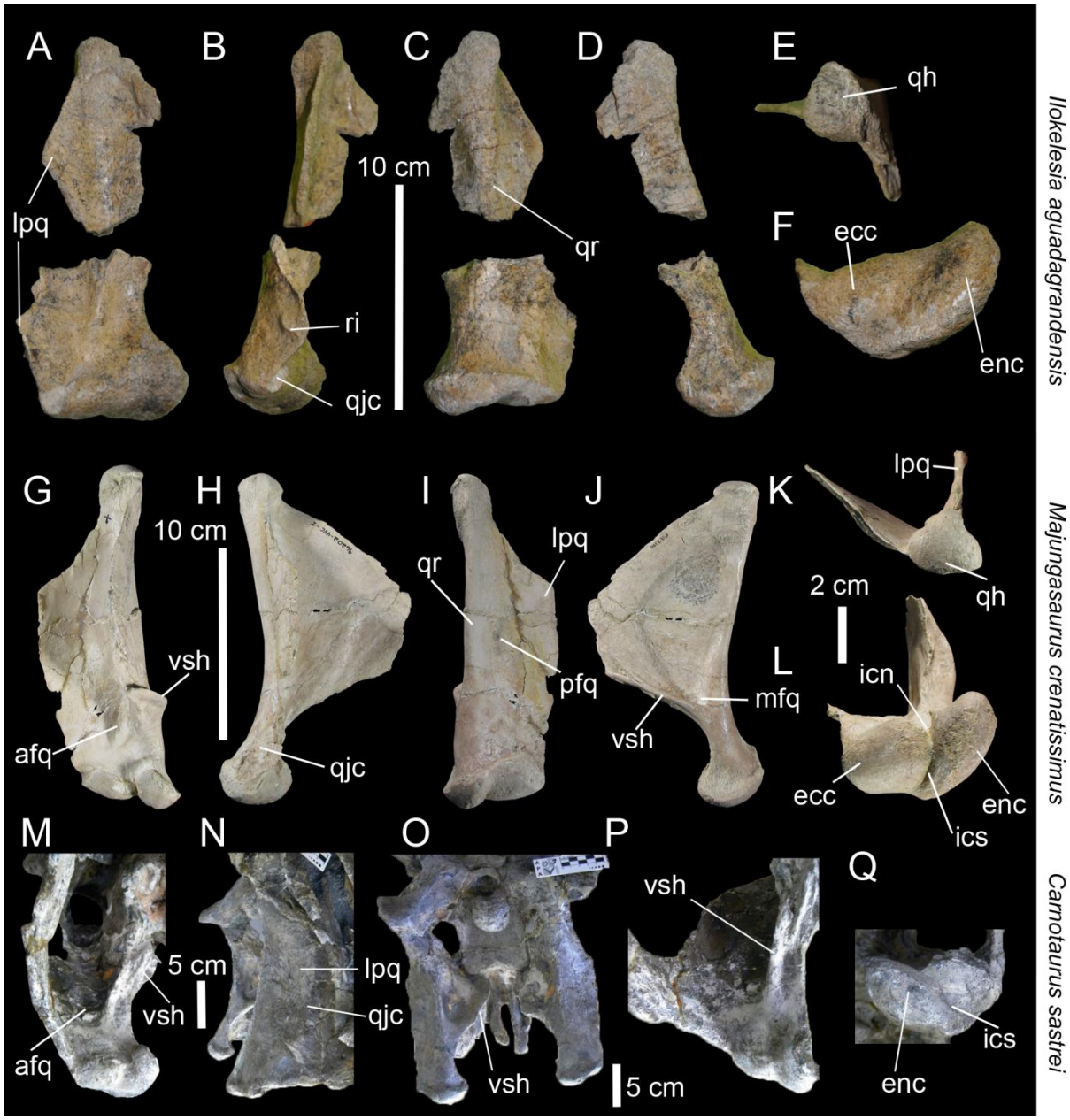

FIGURE 7.7. Quadrate diversity in Abelisauridae. **A–F**, Right quadrate of *Ilokelesia aguadagrandensis* (PVPH 35) in **A**, anterior; **B**, lateral; **C**, posterior; **D**, medial; **E**, dorsal; and **F**, ventral views (courtesy of Matthew Lamanna); **G–L**, Right quadrate of *Majungasaurus crenatissimus* (FMNH PR 2100) in **G**, anterior; **H**, lateral; **I**, posterior; **J**, medial; **K**, dorsal; and **L**, ventral views (courtesy of Lawrence Witmer); **M, N, O, P**, Right; and **O, Q**, left quadrates of *Carnotaurus sastrei* (MACN CH 894) in **M**, anteroventral; **N**, lateral; **O**, posterior; **P**, anteromedial; and **Q**, ventral views (courtesy of Pablo Asaroff). **Abbreviations**: **ecc**, ectocondyle; **enc**, entocondyle; **icn**, intercondylar notch; **ics**, intercondylar sulcus; **lpq**, lateral process; **mfq**, medial fossa; **pfq**, posterior fossa; **qh**, quadrate head; **qjc**, quadratojugal contact; **qr** quadrate ridge; **ri**, ridge on the ventrolateral surface of the quadrate body; **vsh**, ventral shelf of the pterygoid flange.

Abelisaurid quadrates are easily recognizable by a few features present in these derived ceratosaurians, namely a lateral process extending below the mid-height of the quadrate body; directly dorsal to the ectocondyle or reaching the latter, and, in some of them; anterior and posterior fossae. The quadrate is strongly ventrodorsally-tall with a relatively narrow mandibular articulation. However, the quadrate body is lateromedially wider than basal ceratosaurians as they possess a lateral process

attaching well beneath the quadrate head, and almost joining the ectocondyle ventrally, forming a tall and laterally-oriented or lateromedially-oriented subtriangular flange (*I. aguadagrandensis*; Fig. 7.7C; *M. crenatissimus*; Fig. 7.7I; *C. sastrei*; Fig. 7.7N). Like basal ceratosaurs, there is no quadrate foramen piercing the quadrate body in Abelisauridae.

The quadrate ridge is sub-vertical and only well-delimited at mid-height and two thirds of the height of the quadrate bone (relative to its ventral end) in posterior view (Fig. 7.7C, I, O). The ridge becomes noticeable at one-third of the quadrate body, well above the mandibular condyles, and fades away below the quadrate head.

As seen in *Ceratosaurus*, the pterygoid flange of abelisaurids is subtrapezoidal and displays a ventral shelf extending all along the ventral margin of the flange (Fig. 7.7J, O). The anteriormost point of this flange is situated at about two thirds of the quadrate height relative to its ventral end, and its ventral margin connects the quadrate body well-dorsal to the ectocondyle, around one fourth of the quadrate height relative to its ventral end, while the dorsal margin gets attached to the quadrate body directly ventral to the ventral margin of the quadrate head. The latter is subtriangular in outline in dorsal view and subvertical (not bent medially in its anterior part) in lateral view.

When present, the posterior fossa is small, ovoid and situated at mid-height of the quadrate body, as seen in *A. garridoi* (MCF-PVPH 236) and *M. crenatissimus* (Fig. 7.7I) in posterior view. In some abelisaurids, a second fossa occurs on the anterior surface of the quadrate body, lateral to the ventralmost part of the pterygoid flange in anterior view. This anterior fossa is deep and well-visible in *A. comahuensis*, *M. crenatissimus* (Fig. 7.7G), and *C. sastrei* (Fig. 7.7M).

As observed in other ceratosaurians, the ventral quadratojugal contact of *M. crenatissimus* is lanceolate and the dorsal quadratojugal contact follows the lateral edge of the lateral process, in lateral view (Fig. 7.7H). On the other hand, the ventral quadratojugal contact of *I. aguadagrandensis* is hemicircular and placed on the anterolateral part of the ectocondyle (Fig. 7.7A).

Abelisaurids and noasaurids share a very similar mandibular articulation in which both ecto- and entocondyle are ovoid or subcircular, and the entocondyle is wider than the ectocondyle (Fig. 7.7F, L, Q). The intercondylar sulcus is very narrow in *M. crenatissimus* and *C. sastrei*, whereas it is wide and shallow in *A. comahuensis* and *I. aguadagrandensis*. The first two taxa also possess a deep quadrate notch on the anterior margin of the mandibular articulation (Fig. 7.7L, Q).

Basal Tetanurae

Cryolophosaurus ellioti (Smith et al. 2007); *Monolophosaurus jiangi* (Zhao and Currie 1993; Brusatte et al. 2010*a*); *Marshosaurus bicentissimus* (Madsen 1976*a*); *Sinosaurus triassicus* (Hu 1993; Xing 2012).

Recent cladistic analyses performed on tetanurans by Benson (2010*a*) and Carrano et al. (2012) found several theropod taxa placed basally among Tetanurae, but outside the clades of Megalosauria and Allosauroidea. Among those basal tetanurans, *Cryolophosaurus ellioti*,

Marshosaurus bicentissimus, *Sinosaurus triassicus* and *Monolophosaurus jiangi* have a quadrate preserved, but this bone has only been well-described in *M. jiangi* (Brusatte et al. 2010*a*). *M. jiangi* was recovered at the base of a clade encompassing Megalosauroidea, Allosauroidea, and Dromaeosauridae in the quadrate-based analysis (Fig. 7.1). *Cryolophosaurus ellioti*, on the other hand, was found outside Tetanurae, along with Ceratosauria. As noted before, *C. ellioti* was considered to be closely related to *D. wetherilli* by Smith et al. (2007), but Carrano et al. (2012) analysis found it as a basalmost tetanuran. Both quadrates of *C. ellioti* (Hammer and Hickerson 1994) are preserved, and only the right quadrate is well-visible (Smith et al. 2007), but the mandibular condyles are still in connection with the mandible and only the posterior and the lateral views of the bone can be seen. As for *S. triassicus*, both quadrate are in articulation within the skull of two specimens (KMV 8701; LDM-LCA 10), but the bone has been poorly described by Hu (1993) and a full picture of the cranial anatomy of this taxon is still unavailable.

The quadrate body of basal tetanurans is moderately tall (ratio of 0.44 for *M. jiangi* and around 0.36 for *C. ellioti*) and the mandibular articulation is positioned posterior to the quadrate head. A ventrodorsally tall quadrate foramen is present in all basal tetanurans (e.g., Hu 1993; Carrano et al. 2012). In *C. ellioti*, it is small (around 3% of the ventrodorsal depth of the quadrate body) and elliptical, whereas the quadrate bone of *M. jiangi* possesses a wider and tall lanceolate quadrate foramen. However, both taxa have their quadrate foramen almost equally delimited by the quadrate and quadratojugal, with the quadrate contributing slightly more to the margin of the foramen than the quadratojugal (FMNH PR1821; Zhao and Currie 1993; Brusatte et al. 2010*a*: fig. 1D).

In posterior view, the quadrate ridge of basal tetanurans is rod-shaped, well-delimited, strongly laterodorsally inclined (angle between the main axis of the quadrate ridge and the main axis of the mandibular articulation of 60-65°, in posterior view), and slightly ventrodorsally twisted in *C. ellioti*. The ridge seems to reach the entocondyle in *M. jiangi* and fades away directly dorsal to the medial condyle in *C. ellioti*. The quadrate head of *M. jiangi* only contacts the squamosal and is clearly exposed in lateral view rather than being obscured by the squamosal (Zhao and Currie 1993). The same condition is seen in *S. triassicus* (LDM-LCA 10).

Contrarily to most basal theropods and ceratosaurians, there is no lateral process projecting from the quadrate body in *S. triassicus*, *C. ellioti* and *M. jiangi*. The pterygoid flange of *M. jiangi* is moderately expanded anteroposteriorly (ratio of the pterygoid flange, corresponding to the anteroposterior length of the flange divided by the ventrodorsal elongation of the quadrate body, of 0.43), while the pterygoid flange is surprisingly long in *C. ellioti* (ratio of 0.7). In lateral view, as in megalosaurids and spinosaurids, the anteriormost point of the flange of the articulated quadrate is located at the two thirds of the height of the quadrate body relative to its ventral end in basal tetanurans. In lateral view, the most anterior border of the flange is weakly inclined anterodorsally in *M. jiangi* and strongly inclined posterodorsally in *C. ellioti*. In both taxa, a posterior fossa is absent and the medial fossa is deep and located in the posteroventral corner of the pterygoid flange. The

posteroventral margin of the pterygoid flange projects medially, and this ventral fold extends all along the ventral margin of the pterygoid flange in *M. jiangi*. In *M. jiangi*, a small concavity directly dorsal to the boundary between the ento- and ectocondyles appears on the posterior face of the quadrate body (Zhao and Currie 1993: fig. 1D). A concave area seems to be also present at this place in *C. ellioti*, but it is shallower than in *M. jiangi*. Similar to the non-averostran condition, the quadrate of *M. jiangi* and *C. ellioti* is apneumatic (Smith et al. 2007; Benson 2010*a* data matrix).

According to Benson (2010*a*) data matrix, the quadrate of the basal megalosauroid *M. bicentissimus* is also apneumatic, lacking a quadrate foramen and possessing "a small circular depression adjacent to the mandibular condyle" (Benson 2010*a*: p. 35) on the medioventral side of the quadrate and dorsal to the entocondyle. As stated by this author, it "may represent incipient development" (Benson 2010*a*: p. 35) of the medial foramen above the entocondyle and adjacent to the ventral margin of the pterygoid flange in some derived Megalosauridae.

Megalosauridae

Eustreptospondylus oxoniensis (OUMNH J.13558; Fig. 7.8A–E); *Dubreuillosaurus valesdunensis* (Allain 2002); *Torvosaurus tanneri* (Britt, 1991; BYU-VP 9246; Fig. 7.8F–K); *Afrovenator abakensis* (UC OBA1; Fig. 7.8L–Q).

The quadrate of *Eustreptospondylus oxoniensis* and *Afrovenator abakensis* are complete (Sereno et al. 1994; Sadleir et al. 2008), but the right quadrate of *Torvosaurus tanneri* is missing the pterygoid flange (Britt 1991). Only a fossil imprint of pterygoid flange of the left quadrate has been recovered in *Dubreuillosaurus valesdunensis* (Allain 2002).

The quadrate is moderately tall in comparison to the lateromedial width of the mandibular articulation (ratio between 0.35-0.45). In posterior view, the quadrate body is significantly laterally-inclined from the horizontal axis passing through the mandibular articulation (angle between the main axis of the quadrate ridge and the main axis of the mandibular articulation of 65-75°, in posterior view; Fig. 7.8C, H, N). It has lateral and medial margins subparallel in posterior view, and the posterior margin is concave except in *D. valesdunensis* in which this margin seems to be convex (Allain 2002). Like ceratosaurians, the quadrate of megalosaurid taxa lacks a quadrate foramen, therefore the quadratojugal contact extends all the way ventrodorsally. The ventral part of the quadratojugal contact is subtriangular in shape and shows an anterior projection, whereas the dorsal part is a ventrodorsally tall and anteroposteriorly short suture with subparallel anterior and posterior margins (Fig. 7.8C, H, 8N). The quadrate ridge is rod-shaped as in ceratosaurians, and can be either low and not well-marked (*E. oxoniensis*; Fig. 7.8C) or, well-delimited at mid-height of the quadrate body (*T. tanneri*; Fig. 7.8H; *A. abakensis*; Fig. 7.8N). Nevertheless, the ridge always becomes visible well above the entocondyle, at one third of the height of the bone relative to its ventral end, and reaches the quadrate head. As all megalosauroids, there is no lateral process of the quadrate body.

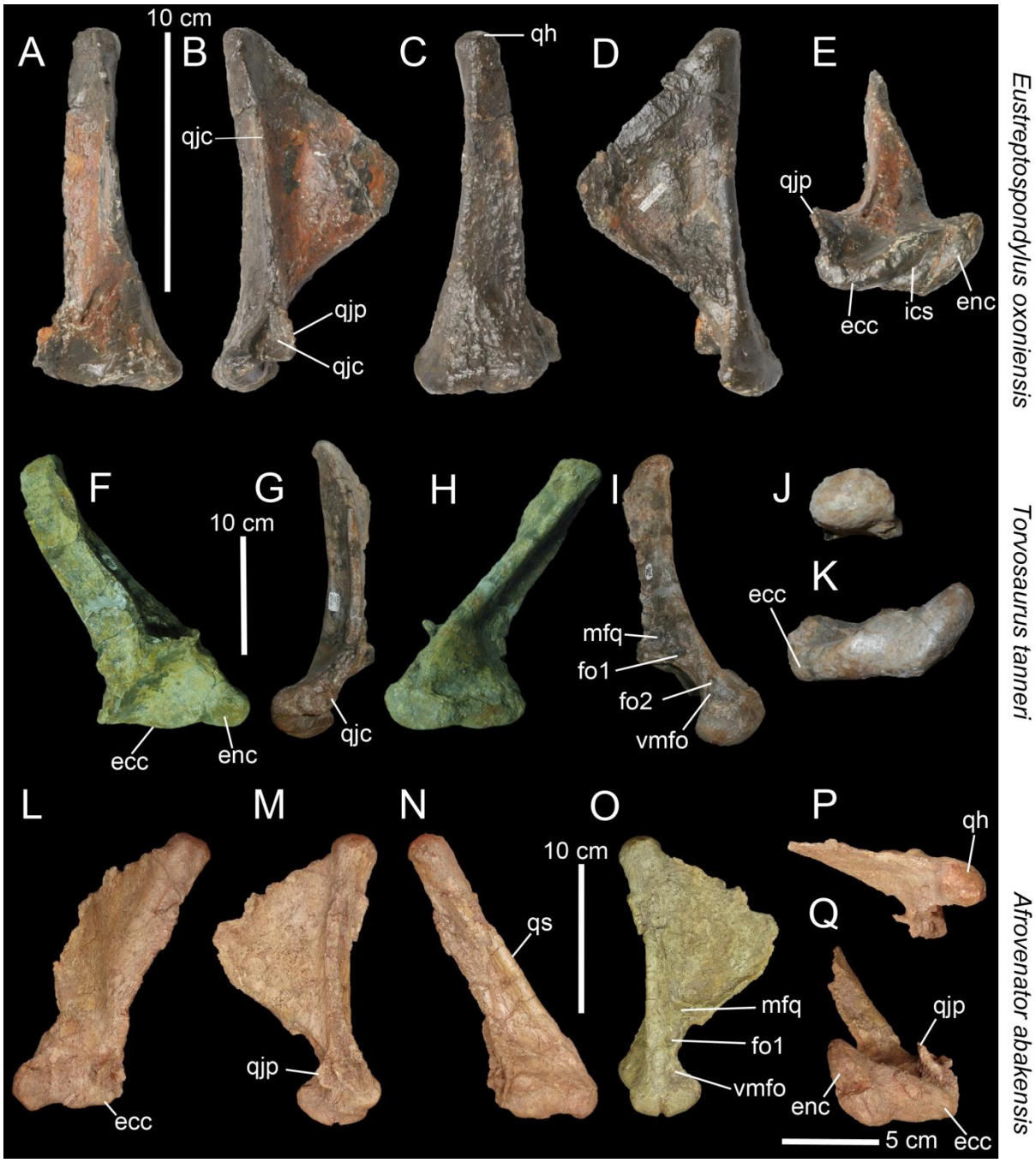

FIGURE 7.8. Quadrate diversity in Megalosauridae. **A–E**, Right quadrate of *Eustreptospondylus oxoniensis* (OUMNH J.13558) in **A**, anterior; **B**, lateral; **C**, posterior; **D**, medial and **E**, ventral views (courtesy of Paul Barrett), **F–K**; Right quadrate of *Torvosaurus tanneri* (BYU-VP 9246) in **F**, anterior; **G**, lateral; **H**, posterior; **I**, medial; **J**, dorsal; and **K**, ventral views (courtesy of Matthew Lamanna); **L–Q**, Left quadrates of *Afrovenator abakensis* (UC OBA1) in **L**, anterior; **M**, lateral; **N**, posterior; **O**, medial; **P**, dorsal; and **Q**, ventral views (courtesy of Roger Benson). **Abbreviations**: **ecc**, ectocondyle; **enc**, entocondyle; **fo1**, medial foramen 1; **fo2**, medial foramen 2; **ics**, intercondylar sulcus; **mfq**, medial fossa; **pfq**, posterior fossa; **qh**, quadrate head; **qjc**, quadratojugal contact; **qjp**, quadratojugal process; **vmfo**, ventromedial foramen.

In medial view, the pterygoid flange is straight (no medial curvature of the anterior part), subtrapezoidal and reaches the dorsal margin of the quadrate head dorsally and, not far above from the entocondyle ventrally (Fig. 7.8B, G, O). The posteroventral margin of the flange is medially-folded, but there is no ventral shelf in the anteroventral part of the flange. The medial fossa of the quadrate is

shallow and there is no distinct posterior fossa, but a ventrodorsally tall depression along the quadrate body, lateral to the quadrate ridge. The quadrate head projects vertically and its shape is ovoid rather than subtriangular in posterior view as in other non-tetanuran theropods (Fig. 7.8I, P).

The mandibular articulation is also lateromedially wider than in more basal theropods. In both posterior and ventral views, the ectocondyle is longer than the entocondyle and its ventral margin is slightly sigmoid in *T. tanneri* in anterior view (Fig. 7.8F). The ectocondyle is parabolic in *T. tanneri* (Fig. 7.8K) and *E. oxoniensis* (Fig. 7.8E), but it is rather elliptical in *A. abakensis* (Fig. 7.8Q). Likewise, the anterior margin of the ectocondyle is concave both in *T. tanneri* and *E. abakensis.* The entocondyle is elliptical to oblong in outline, and strongly protrudes anteriorly. The intercondylar sulcus is deep and well-marked in *E. oxoniensis* (Fig. 7.8E), and wide and shallow in *T. tanneri* (Fig. 7.8K) and *A. abakensis* (Fig. 7.8Q).

In *T. tanneri*, the ventral margin of the ventral quadratojugal contact and the posteroventral margin of the pterygoid flange are joined together to form a convex arc on the anteroventral side of the quadrate (Fig. 7.8F). This taxon can also be distinguished from the two other megalosaurids by having a concavity on the anteroventral margin of the quadrate, ventral to the pterygoid flange and anterior to the entocondyle. A similar yet wider and deeper concavity has also been noted in some derived Spinosauridae (WDC-CSG Q3).

A subtriangular depression with a small foramen inside is present in *T. tanneri* on the ventromedial part of the quadrate directly dorsal to the entocondyle (Fig. 7.8I; Britt, 1991; Benson, 2010). A shallow concavity with no foramen is also seen at the same position in *A. abakensis*, but nothing comparable is present in *E. oxoniensis* (OUMNH J.13558; Benson 2010*a*). In *T. tanneri* and *A. abakensis*, a second and longer ovoid foramen also occurs at the ventralmost part of the pterygoid flange, beneath the medial fossa and above the shallow fossa dorsal to the entocondyle (Fig. 7.8I, O; Benson, 2010: fig. 19A). Although a medial pneumatic foramen was noted by Sadleir et al. (2008) at the base of the pterygoid flange in *E. oxoniensis*, no pneumatic foramen was observed at this place in this taxon. Instead, there is a groove leading to a small foramen on the anteroventral part of the quadrate, lateral to the ventral part of the pterygoid flange (Fig. 7.8A), but this structure might be an artifact of preservation. The quadrate of megalosaurids seems therefore to be apneumatic.

Spinosauridae

Baryonyx walkeri (NHM R9951; Fig. 7.9A–F); *Suchomimus tenerensis* (MNN GAD 502; Fig. 7.9G–L); *Irritator challengeri* (SMNS 58022); Undescribed Spinosaurinae (MSNM V6896; WDC-CSG Q1–Q5; Hendrickx and Mateus 2012; Fig. 7.9M–L).

Both quadrates of *Baryonyx walkeri* provide a good basis to understand the anatomy of this derived clade of Megalosauroidea. An incomplete left quadrate of *Suchomimus tenerensis*, a small portion of the lateral part of the right quadrate and the quadrate head of the left quadrate in *Irritator*

challengeri (Sues et al. 2002), and six indeterminate spinosaurid quadrates from the Cenomanian of the Kem Kem beds (Morocco) offer further details.

The quadrates of *B. walkeri* have been described in detail by Charig and Milner (1997), but the anatomy of the quadrate of *I. challengeri* has been very briefly given by Sues et al. (2002) and that of *S. tenerensis* has not yet been described. A detailed description of the six spinosaurid quadrates from Morocco and comparison with other spinosaurid quadrates will be given elsewhere.

The spinosaurid quadrate is highly diagnostic and differ significantly from this of megalosaurids. The mandibular articulation is wide lateromedially and the quadrate body is short (ratio more than 0.5). It also seems that the quadrate bone was posteriorly-inclined in the cranium as this configuration appears in *I. challengeri*, the only reported spinosaurid taxon with an articulated quadrate.

In Baryonychinae, the quadrate foramen is large (thereby called the 'quadrate fenestra' by Sereno et al. (1998), ventrodorsally tall and predominantly formed by the quadrate (Fig. 7.9C, I). Indeed, the dorsal quadratojugal contact possesses a short ventral projection making the laterodorsal margin of the quadrate foramen. Such feature can also be seen in the quadrates of spinosaurid taxa from Morocco (Fig. 7.9O), but its presence is uncertain in *I. challengeri* (SMNS 58022). However, the quadrate foramen of Spinosaurinae is slightly to much smaller and also subcircular to bean-shaped when compared to this of Baryonychinae. As in Megalosauridae, there is no lateral process in all spinosaurid other than in *I. challengeri* (SMNS 58022). In the latter, the lateral process is lateromedially narrow, projects only laterally, and is parabolic in outline.

In posterior view, the quadrate ridge of spinosaurids is lateromedially wide, the widest among non-avian theropods, as the lateromedial width of the quadrate ridge corresponds to the lateromedial width of the quadrate body at the level of the quadrate foramen (Fig. 7.9C, I, O). The ridge is also strongly laterodorsally inclined (angle between the main axis of the quadrate ridge and the main axis of the mandibular articulation of 60-75°, in posterior view), becomes marked directly dorsal to the entocondyle, and fades away at two thirds of the quadrate body in posterior view where, in some derived spinosaurids, it can reappear more dorsally, directly beneath the quadrate head (WDC-CSG Q5).

By having a ventrodorsally tall anteriormost margin in medial view, the pterygoid flange of the quadrate is sub-rectangular in outline and such morphology is typical of spinosaurid theropods (Fig. 7.9D, P). The flange attaches dorsally at the level of the quadrate head and descends the quadrate body to join the entocondyle. A shallow notch occurs at one-fifth of the pterygoid flange and the dorsal margin of the flange is slightly medially-folded from that point (Fig. 7.9A, G). Unlike Baryonychinae, the flange is strongly medially curved in Spinosaurinae. The medial fossa, located ventrally and delimited by the prominent ridge, is particularly deep in contrast to other theropods (Fig. 7.9D, P).

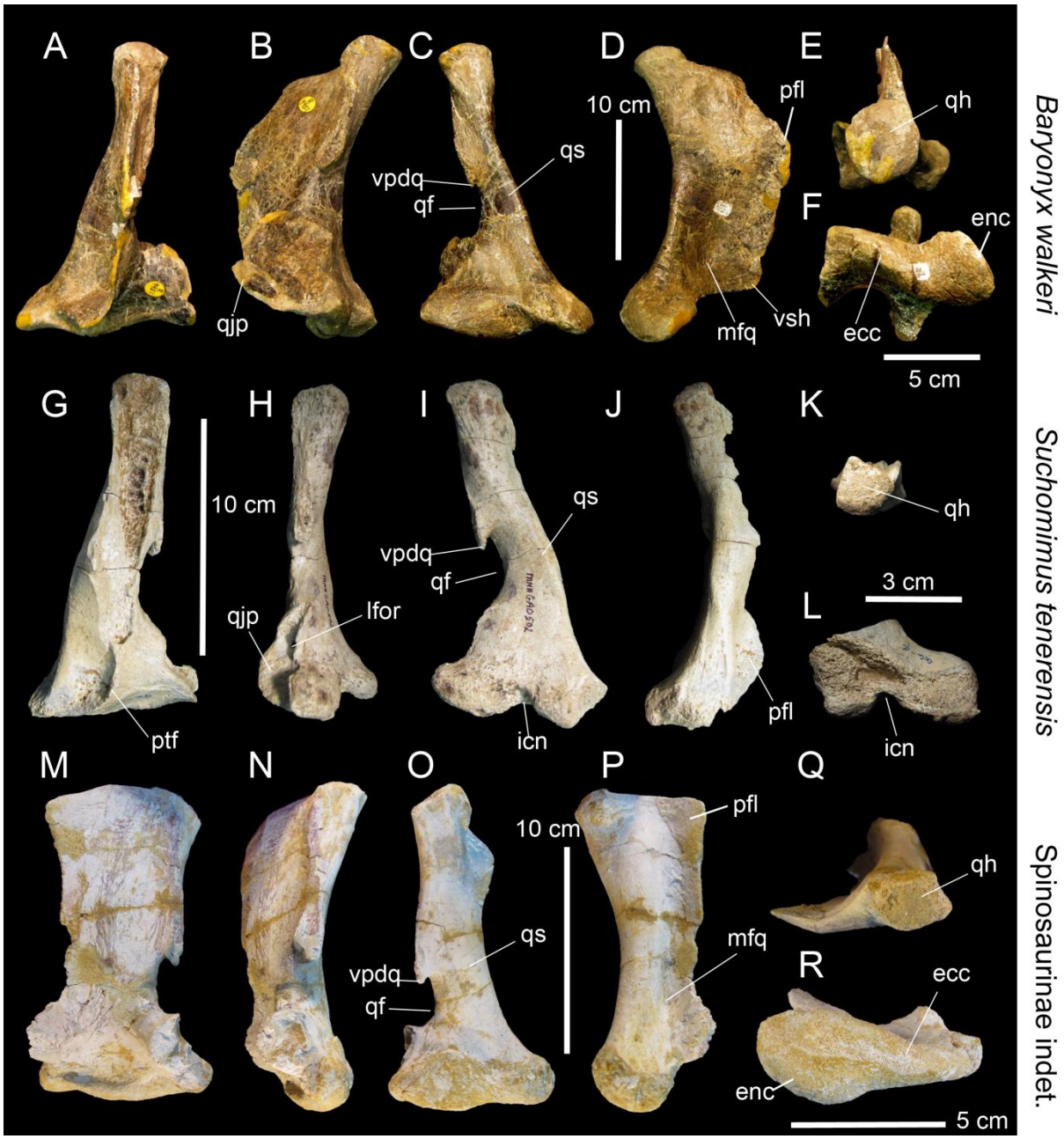

FIGURE 7.9. Quadrate diversity in Spinosauridae. **A–F**, Left quadrate of *Baryonyx walkeri* (NHM R9951) in **A**, anterior; **B**, lateral; **C**, posterior; **D**, medial; **E**, dorsal; and **F**, ventral views; **G–L**, Left quadrate of *Suchomimus tenerensis* (MNN GAD 502) in **G**, anterior; **H**, lateral; **I**, posterior; **J**, medial; **K**, dorsal; and **L**, ventral views; **M–R**, Left quadrate of and indeterminate Spinosaurinae from the Kem Kem beds (MSNM V6896) in **M**, anterior; **N**, lateral; **O**, posterior; **P**, medial; **Q**, dorsal; and **R**, ventral views. **Abbreviations**: **ecc**, ectocondyle; **enc**, entocondyle; **icp**, intercondylar pit; **lfo**, lateral foramen; **mfq**, medial fossa; **pfl**, pterygoid flange; **qf**, quadrate foramen; **qh**, quadrate head; **qjp**, quadratojugal process; **qr**, quadrate ridge; **vpdq**, ventral projection of the dorsal quadratojugal contact; **vsh**, ventral shelf of the pterygoid flange.

In ventral view, the shape of the quadrate head is highly variable among spinosaurid theropods: subcircular in *B. walkeri* (Fig. 7.9I), subtriangular in *S. tenerensis* (Fig. 7.9K), and diamond shaped in *I. challengeri* and an indeterminate spinosaurine (MSNM V6896; Fig. 7.9Q). There is a small concavity situated on the posterior side of the quadrate body, directly ventral to the quadrate head, a feature shared among all Spinosauridae (e.g., WDC-CSG Q3).

The ventral quadratojugal contact is anteroposteriorly long, reniform to D-shaped, and much longer than the dorsal quadratojugal contact, which is lanceolate, anteroposteriorly short, and ventrodorsally tall (Fig. 7.9B, H, N). The suture between the quadrate and quadratojugal must have been rigid as the ventral contact is deeply excavated by one or several cavities, and the surface of the dorsal contact is irregular and sometimes shows a central ridge delimited by two parallel grooves. The ventral quadratojugal contact has an anterior projection and the contacts extends on to the ectocondyle (Fig. 7.9B, H, N). On the posterior side of the quadrate, a shallow and recurved groove running from above the ventral quadratojugal to the junction between the ecto- and entocondyles is seen in *B. walkeri* and other spinosaurines (e.g., NHM R9951; WDC-CSG Q3).

With a strongly lateromedially wide and sigmoid ectocondyle and a lateromedially narrow entocondyle, both being delimited by a diagonally-oriented intercondylar sulcus, the mandibular articulation of the quadrate is also diagnostic to Spinosauridae (Fig. 7.9F, L, R). The entocondyle is subtriangular and not well-marked and the intercondylar sulcus is shallow in *B. walkeri*, possibly due to the immaturity of the specimen (Charig and Milner 1997). In more derived spinosaurids, the entocondyle is elliptical in shape and does not protrude anteriorly. The ectocondyle is much wider than the entocondyle in both posterior and anterior views. In anterior view, the ventral margin of the condyle is sigmoid. The intercondylar sulcus is deep and well-delimited in mature individuals of Spinosaurine (Hendrickx and Mateus 2012).

Non-carcharodontosaurid Allosauroidea

Allosaurus fragilis (Madsen 1976*b*; Bakker 1998); *Allosaurus europaeus* (ML 415); *Allosaurus* '*jimmadseni*' (SMA 005/02; Fig. 7.10A–F); *Aerosteon riocoloradensis* (Sereno et al. 2008; Fig. 7.10G–L); *Sinraptor dongi* (Currie 2006; Fig. 7.10M–Q).

The quadrate of non-carcharodontosaurid allosauroids is known in *Allosaurus fragilis* (Madsen 1976*b*), *Allosaurus* '*jimmadseni*' (Chure 2000), *Allosaurus europaeus* (Mateus et al. 2006), *Sinraptor dongi* (Currie 2006), and *Aerosteon riocoloradensis* (Sereno et al. 2008). However, the quadrate has only been relatively well-described in *A.* '*jimmadseni*' and *S. dongi*. Although *Allosaurus*, *Sinraptor* and *Aerosteon* pertain to different clades of allosauroids (*sensu* Benson et al. 2010; Carrano et al. 2012), they share many features that are not seen in other theropods and Carcharodontosauridae. Thus, the quadrate of Carcharodontosauridae will thereby be described and compared to other theropod taxa in the next chapter.

The quadrate of allosaurids and *A. riocoloradensis* is moderately tall (ratio between 0.35 and 0.5; Fig. 7.10C), but that of *S. dongi* is notably tall (ratio is approximately 0.3; Fig. 7.10O) and similar to non-tetanuran theropods. This can be explained by the relatively narrow mandibular articulation in *S. dongi*, whereas the mandibular articulation of other allosauroids is much wider lateromedially.

The quadrate foramen of allosaurids and *S. dongi* is mostly delimited by the quadrate (Currie 2006; Fig. 7.10C), but it is completely enclosed in *A. riocoloradensis* (Fig. 7.10G), a feature also

present in the coelophysoid *Z. rougieri* (Ezcurra 2007). In *A. riocoloradensis*, the quadrate foramen is particularly large (18% of quadrate height), ovoid and situated at mid-height of the bone, while in allosaurids and sinraptorids, the quadrate foramen is more elliptical, smaller (3.5-10% of the quadrate height), slightly to strongly ventrodorsally tall, and positioned slightly ventral from the mid-height of the quadrate body.

The quadrate ridge is prominent (well-delimited), laterodorsally inclined (angle between the main axis of the quadrate ridge and the main axis of the mandibular articulation of 60-75°, in posterior view), and rod-shaped in allosaurids (Fig. 7.10C, O), and forming almost a lateromedially wide crest in *A. riocoloradensis* (Fig. 7.10I). Interestingly, the ridge is divided in two portions by a groove at one-third or one-fourth of the height of the quadrate body (relative to its ventral end), instead of forming a single structure as in other non-avian theropods. This groove is deep and slightly dorsomedially inclined in *A. fragilis*, *A. europaeus* and *Allosaurus* '*jimmadseni*' (ML 415; SMA 0005/02; Fig. 7.10C) and well-marked and subvertical in *A. riocoloradensis* (Fig. 7.10I). In fact, in *A. riocoloradensis* the ventral part of the ridge extends to the quadrate head while the remaining dorsal portion appears well beneath the quadrate head laterally, and is parallel to the squamosal contact, as interpreted by Sereno et al. (2008). In *S. dongi*, however, this feature is not clear, but it seems that the dorsal part of the quadrate ridge extends laterodorsally beneath the quadrate head (Fig. 7.10O). A second and much narrower ridge of *S. dongi* becomes distinct more medially at one fourth of the height of the quadrate body relative to its ventral end, and remains parallel to the other (Fig. 7.10O). In allosaurids, the ridges forms a convex protuberance at one-third of the height of the quadrate body and well-visible in lateral view (Fig. 7.10B). This bump on the posterodorsal margin in the quadrate body is not unique to these theropods as it has also been observed in the *C. ellioti* (Smith et al. 2007: fig. 4A–B).

A short lateral process projects laterally from the quadrate foramen to the quadrate head in allosaurids (Fig. 7.10C) and *S. dongi* (Fig. 7.10O). In posterior view, the process extends well ventral to the quadrate head in these taxa, and its lateral margin is parabolic in outline. In the other hand, the lateral process projects completely anteriorly in *A. riocoloradensis*, and extends entirely on the quadrate body, from the mandibular articulation ventrally to the quadrate head dorsally (Fig. 7.10G-H).

In posterior view, the pterygoid flange is very slightly medially-recurved in allosaurids (Fig. 7.10A) and *S. dongi* (Fig. 7.10M), and curves strongly anteromedially in *A. riocoloradensis* (Fig. 7.10G). However, the shape of the flange is quite similar between them, as the flange is parabolic in shape with a rounded anteriormost margin instead of a straight margin present in more basal theropods. The flange joins the quadrate body well-ventral to the mandibular condyles, at almost one fourth of the height of the quadrate body relative to its ventral end, while it reaches the quadrate head directly ventral to its ventral margin dorsally. In dorsal view, the quadrate head is subcircular in allosauroids and, in lateral view, it follows the curvature of the quadrate body in allosaurids and *S.*

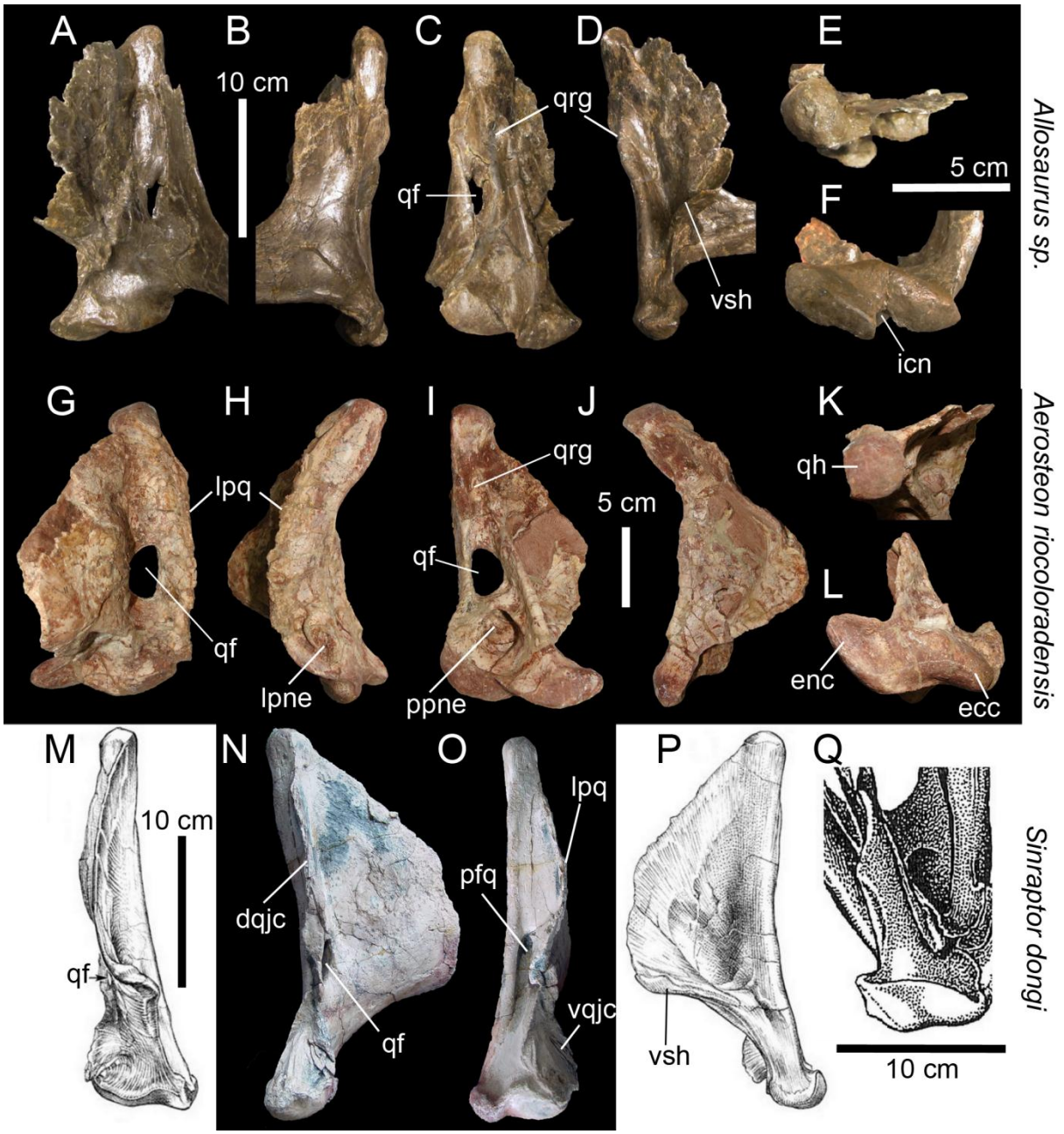

FIGURE 7.10. Quadrate diversity in non-carcharodontosaurid Allosauroidea. **A–F**, Left coosified quadrate and quadratojugal of *Allosaurus* '*jimmadseni*'. (SMA 005/02) in **A**, anterior; **B**, lateral; **C**, posterior; **D**, medial; **E**, dorsal; and **F**, ventral views; **G–L**, Left quadrate of *Aerosteon riocoloradensis* (MCNA-PV-3137) in G, anterior; **H**, lateral; **I**, posterior; **J**, medial; **K**, dorsal, and **L**, ventral views (courtesy of Martin Ezcurra); **M–Q**, Right quadrate of *Sinraptor dongi* (IVPP 10600) in **M**, anterior; **N**, lateral; **O**, posterior; **P**, medial; and **Q**, ventral views (Currie 2006 for M, P–Q; courtesy of Philip Currie for N–O). **Abbreviations**: **ecc**, ectocondyle; **enc**, entocondyle; **dqjc**, dorsal quadratojugal contact; **icp**, intercondylar pit; **lpq**, lateral process; **pfq,** posterior fossa; **ppne**, posterior pneumatic foramen; **qf**, quadrate foramen; **qr**, quadrate ridge; **qrg**, quadrate ridge groove; **vqjc**, ventral quadratojugal contact; **vsh**, ventral shelf of the pterygoid flange.

dongi, whereas the dorsal fourth of the quadrate strongly bends posteriorly in *A. riocoloradensis* (Fig. 7.10J).

In medial view, the medial fossa is shallow and roughly centrally positioned on the ventral surface of the pterygoid flange in *A. riocoloradensis* and *S. dongi*. This fossa is deeper and more

ventral in *Allosaurus* '*jimmadseni*', in the posteroventral corner of the pterygoid flange,due to a well-developed ventral shelf in this taxon (Fig. 7.10D). Such a shelf is also present in *S. dongi*, but instead of being projected dorsomedially like in *Allosaurus* '*jimmadseni*', the shelf projects medially (Fig. 7.10P). *A. riocoloradensis* does not have such a feature. The posterior fossa of *S. dongi*, considered to be a pneumatic fossa by Currie (2009), is deep, ventrodorsally tall and does not include the quadrate foramen. No similar fossa is seen in allosaurids and *A. riocoloradensis*, yet there is a ventrodorsally-tall depression surrounding the quadrate foramen in these allosauroids. This concavity is bounded medially by the quadrate ridge and laterally by the quadratojugal contact in allosaurids, and a ridge delimiting posteriorly the lateral process in *A. riocoloradensis*.

The ventral quadratojugal contact of *A. fragilis* is D-shaped and faces laterally whereas it is lanceolate and faces posterolaterally in *S. dongi* (Fig. 7.10N). Nevertheless, both ventral quadratojugal contacts share a short quadratojugal process that projects anteriorly. The dorsal quadratojugal contact is ventrodorsally tall and faces anterolaterally or completely anteriorly in these taxa. Although we agree with (Sereno et al. 2008) that the lateral contact of *A. riocoloradensis* extends from the ectocondyle to the dorsal margin of the quadrate head along the lateral process (Fig. 7.10H), we are giving a different interpretation of the morphology of this contact. According to Sereno et al. (2008: fig. 4A), the quadratojugal/squamosal contact is anteroposteriorly long, its anterior and posterior margins are subparallel, its surface is flat, and the dorsal part of the lateral contact of *A. riocoloradensis* quadrate would have been connected to the squamosal (Sereno et al. 2008: fig. 4). Our observation of the quadrate of *A. riocoloradensis* suggests that only the anterior rim of the lateral process contacts the quadratojugal anteriorly. The presence of a deep depression on the lateroventral part of the lateral process, here interpreted as an additional pneumatic fossa, seems to support this interpretation. Nevertheless, it is indeed likely that the squamosal joined the quadrate on the dorsal surface of the lateral process, as suggested by Sereno et al. (2008: fig. 4A).

The mandibular articulation of the allosauroids *S. dongi* (Fig. 7.10Q) and *A. riocoloradensis* (Fig. 7.10L) is very similar in shape as both condyles are elliptical, globular and prominent, with a relatively deep intercondylar sulcus separating them. The main axis of both the ecto- and entocondyles is medially-oriented, and the ectocondyle axis is slightly more inclined medially than the entocondyle one, although both axes can be subparallel is some allosaurids (SMA 0005/02; Fig. 7.10F). All *Allosaurus* specimens, however, show a diagnostic quadrate notch on the posterior side of the mandibular articulation.

Quadrate pneumaticity is seen in some non-carcharodontosaurid allosauroids such as *A. riocoloradensis* (Sereno et al. 2008; Fig. 7.10I) where a wide and deep pneumatic recess is located on the posterior side of the quadrate body. (Currie 2006) estimates that the deep posterior fossa posteromedial to the quadrate foramen in *S. dongi* (Fig. 7.10O) was presumably pneumatic in origin, an interpretation followed here. A depression also occurs on the lateroventral surface of the lateral process in *A. riocoloradensis* (Fig. 7.10H) and was originally pneumatic as well in this taxon.

Carcharodontosauridae

Acrocanthosaurus atokensis (NCSM 14345; Fig. 7.11A–11E); *Shaochilong maortuensis* (Brusatte et al. 2009*c*); *Giganotosaurus carolinii* (MUCPv-CH-1; Fig. 7.11F–K); *Mapusaurus roseae* (MCF PVPH-1011.102; Fig. 7.11L–Q).

The quadrate of Carcharodontosauridae is relatively well-known due to its detailed description for *Acrocanthosaurus atokensis* (Eddy and Clarke 2011), *Shaochilong maortuensis* (Brusatte et al. 2010*b*) and *Mapusaurus roseae* (Coria and Currie 2006). In posterior view, the bone is moderately tall ventrodorsally, and it has a lateral process along the dorsal half of the body and a relatively lateromedially wide mandibular articulation ventrally. The quadrate ridge is well-delimited, laterodorsally-inclined (angle between the main axis of the quadrate ridge and the main axis of the mandibular articulation of 75-80°, in posterior view), becomes noticeable at one-third of the height of the quadrate (relative to its ventral end) and more dorsally, then disappears at one third of the height of the quadrate body (Fig. 7.11C, H, N). The ridge varies in width, being lateromedially wide at mid-height of the quadrate and reducing in width to form a narrow crest below the quadrate head in *A. atokensis* (Fig. 7.11C).

The quadrate of the carcharodontosaurids retains many plesiomorphic features with basal allosauroids, such as a small quadrate foramen (less than 7% of the ventrodorsal height of the quadrate body; Fig. 7.11C, H, N) mostly delimited by the quadrate, a short lateral process between the quadrate foramen and quadrate head, and a lateromedially narrow quadrate ridge relatively at two thirds of the height of the quadrate body relative to its ventral end, and divided into ventral and dorsal portions.

The quadrate body has a wide posterior fossa that extends to the quadrate foramen ventrally. This depression is elliptical in shape, poorly-delimited, ventrodorsally tall, and dorsomedially inclined at an angle of 75° from the horizontal in carcharodontosaurids (Fig. 7.11C, H, N). The quadrate body of *S. maortuensis* (Brusatte et al. 2010*b*: fig. 7b) does not show a similar posterior fossa, yet the lateral part of the quadrate body seems to be missing (*contra* Brusatte et al. 2010*b*) and therefore the posterior fossa is lost to damage.

Unlike more basal allosauroid taxa, the pterygoid flange is straight, with no medial curvature, and the medial fossa is sub-circular, centrally positioned on the flange, and very shallow. Furthermore, the flange joins the quadrate body directly dorsal to the entocondyle and well-ventral from the ventral margin of the quadrate head. Nevertheless, as other allosauroids, the pterygoid flange is roughly parabolic in medial view, with a large and rounded anterior margin (Fig. 7.11D). The quadrate head is subcircular in outline in dorsal view in carcharodontosaurids (Fig. 7.11J), and subvertical rather than flexing posteriorly as in *A. riocoloradensis* in lateral view.

Both ventral and dorsal quadratojugal contacts of carcharodontosaurids are morphologically similar to allosaurids and *S. dongi* (Fig. 7.11G, M). The dorsal quadratojugal contact is a narrow, ventrodorsally tall and anteroposteriorly short, and extends along the lateral surface of the rim of the

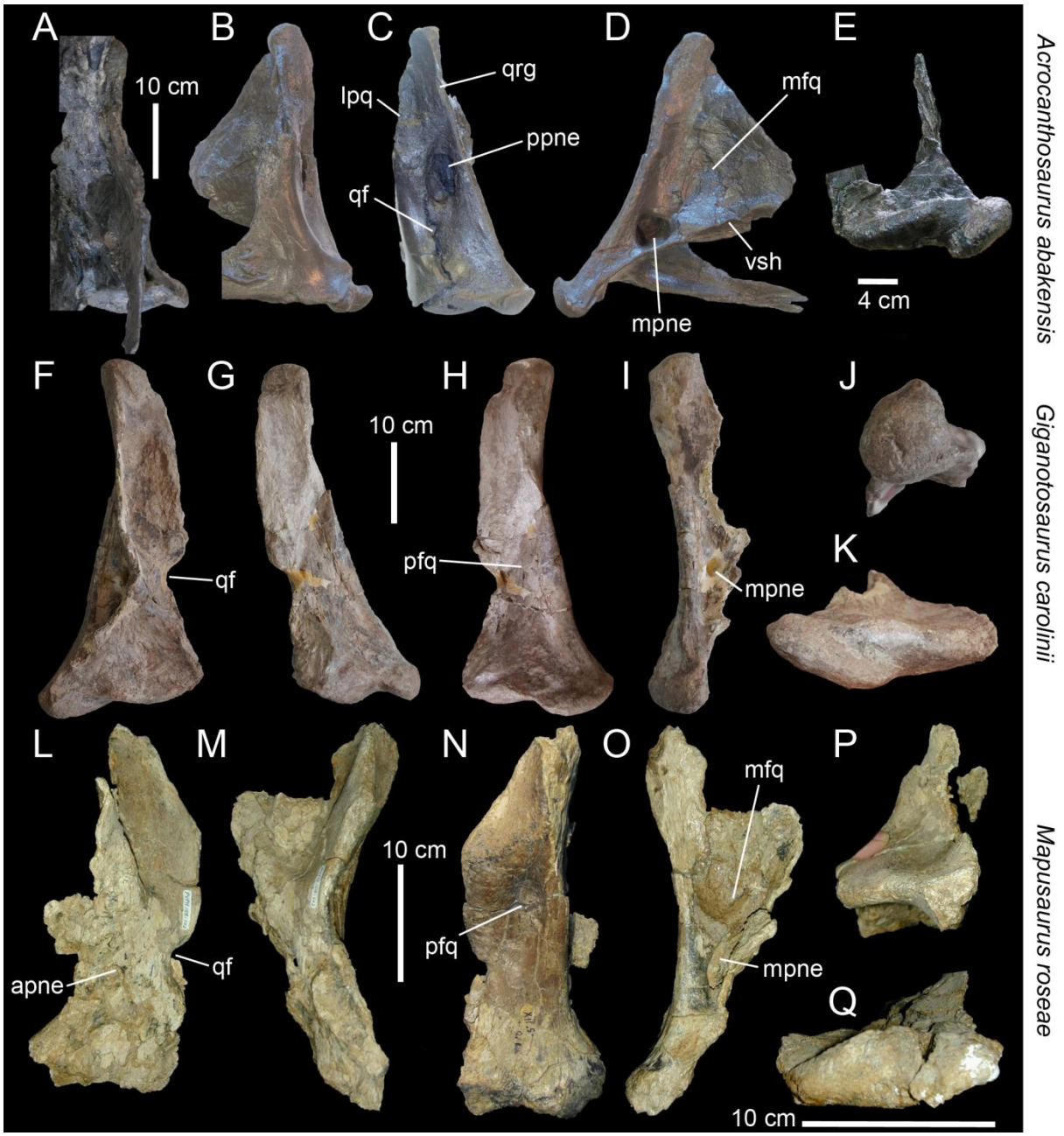

FIGURE 7.11. Quadrate diversity in Carcharodontosauridae. **A, E**, Right and **B–D**, left coosified quadrate and quadratojugal of *Acrocanthosaurus atokensis* (NCSM 14345) in **A**, anterior; **B**, lateral; **C**, posterior; **D**, medial; and **E**, ventral views (courtesy of Drew Eddy and Vince Shneider); **F–K**, Right quadrate of *Shaochilong moartuensis* (IVPP V2885.3) in **F**, anterior; **G**, lateral; **H**, posterior; **I**, medial; **J**, dorsal; and **K**, ventral views (courtesy of Steve Brusatte); **L–Q**, Left quadrate of *Mapusaurus rosea* (MCFPVPH-108.102) in **L**, anterior; **M**, lateral; **N**, posterior; **O**, medial; **P**, dorsal; and **Q**, ventral views (courtesy of Matthew Lamanna). **Abbreviations**: **apne**, anterior pneumatic foramen; **lpq**, lateral process; **mfq**, medial fossa; **mpne**, medial pneumatic foramen; **pfq**, posterior fossa; **ppne**, posterior pneumatic foramen; **qf**, quadrate foramen; **qrg**, quadrate ridge groove; **vsh**, ventral shelf of the pterygoid flange.

lateral process. Unlike *A. atokensis* and non-carcharodontosaurid allosauroids, the ventral quadratojugal contact does not show any anterior projection.

In posterior view, the mandibular articulation is lateromedially wide, with an ectocondyle always lateromedially wider than the entocondyle in both anterior and posterior views (Fig. 7.11E, K,

Q). It is constituted of an elliptical to oblong bulged entocondyle and an lateromedially wide parabolic to sigmoid ectocondyle, usually separated by a lateromedially narrow yet deep intercondylar sulcus (Fig. 7.11E, K). Although the entocondyle is prominent on both anterior and posterior sides in most carcharodontosaurids, its margins are rather poorly defined in *S. maortuensis*, which also displays a very shallow intercondylar sulcus.

All carcharodontosaurids other than *S. maortuensis* have a pneumatic quadrate. However, the latter does not preserved the laterodorsal part of the quadrate which may have hosted a pneumatic fossa. The pneumatic quadrate of carcharodontosaurids is penetrated by a pneumatic foramen at the base of the pterygoid flange, ventral to the medial fossa (Fig. 7.11D, I, O). This medial pneumatic recess is large, subcircular and divided by a septum in *A. atokensis*. In *M. roseae*, the medial pneumatic foramen is also relatively large yet it is elliptical and does not possess a septum, as seen in *G. carolinii*. The pneumatic opening of the latter is relatively small, subcircular and further dorsally from the posteroventral corner of the pterygoid flange. Unlike *A. atokensis*, Giganotosaurinae taxa do not have a posterior pneumatic foramen inside the posterior fossa of the quadrate body. However, an anterior pneumatic aperture is present at one third of the height of the quadrate relative to its ventral end in *M. roseae*, lateral to the ventralmost part of the pterygoid flange (Fig. 7.11L).

Basal Coelurosauria

Bicentenaria argentina (MPCA 865; Fig. 7.14A–14F); *Zuolong salleei* (Choiniere et al. 2010*a*); *Lourinhanosaurus antunesi* (ML 565-10, 565-150; Hendrickx and Mateus 2012); *Aorun zhaoi* (Choiniere et al. 2014*b*).

The quadrate of the basal coelurosaurs of *Zuolong salleei* (Choiniere et al. 2010*a*), *Lourinhanosaurus antunesi* (Hendrickx and Mateus 2012), and *Aorun zhaoi* (Choiniere et al. 2014*b*) are relatively well-known as a thorough description has been provided for these taxa. Nevertheless, additional information is added for *Bicentenaria argentina* (Novas et al. 2012) as the quadrate of this coelurosaur shows some interesting features not seen in other theropod clades.

Only the ventral half of the left and right quadrates of *B. argentina* are preserved (Fig. 7.14A–F). The quadrate of this taxon displays a prominent and well-defined rod-shaped quadrate ridge extending ventrodorsally, perpendicular to the long axis of the mandibular articulation. The quadrate ridge does not reach the mandibular articulation posteriorly, but it extends to the entocondyle in its medial part (Fig. 7.14D). The quadrate foramen is vertically oriented and ventrolaterally bounded by a short and pointed projection of the basal quadratojugal contact so that the foramen is mostly delimited by the quadrate (Fig. 7.14C).

As seen in some tyrannosauroids, the pterygoid flange of *B. argentina* extends far anteriorly, its anterior margin is semi-oval in outline in medial view, and the ventral margin of the flange forms a right angle with the long axis of the quadrate ridge (Fig. 7.14D). The pterygoid flange projects anteriorly and does not curve medially. It also reaches the quadrate body directly dorsal to the

mandibular articulation, at the level of the entocondyle, and displays a rod-like ventral shelf oriented dorsomedially in its posteroventral margin, so that the medial fossa is relatively deep. In lateral view, the ventral quadratojugal contact is elliptical in shape and slightly anteriorly inclined (Fig. 7.14B). The contact is concave is posterior view and does not extend on the ectocondyle laterally. The articulating surface of the ventral quadratojugal contact is smooth and slightly excavated in its central part, and its posterodorsal margin is bounded by an anteroposteriorly thick yet short lateral projection.

The mandibular articulation is unique in possessing two well-delimited and lateroposteriorly oriented condyles in which the ectocondyle is one-third longer than the entocondyle and markedly protrudes laterally in ventral view (Fig. 7.14F). The mandibular condyles share a same width and both condyles are separated by a lateromedially wide and deep intercondylar sulcus. The long axis of the ento-, ectocondyles and intercondylar sulcus is parallel.

The most interesting features in the quadrate of the embryonic specimens of *L. antunesi* are the absence of a quadrate foramen and the poor delimitation of the mandibular articulation, both interpreted as embryonic features (see the chapters on the quadrate ontogeny in Hendrickx et al. 2014: the non-avian theropod quadrate I). The quadrate shows some similarities with this of *B. argentina* such as a well-defined rod-shaped quadrate ridge (‘quadrate shaft’ *sensu* Hendrickx and Mateus 2012) almost reaching the entocondyle medially, a ventral quadratojugal not extending on the ectocondyle, and a pterygoid flange projecting mostly anteriorly whose the ventral margin is perpendicular to the long axis passing through the quadrate ridge.

The quadrate of *Z. salleei* shows a combination of features only seen in this taxon, namely a deep posterior fossa bounded medially by a well-delimited and rod-shaped quadrate ridge, and laterally by an ventrodorsally tall ventral projection of the dorsal quadratojugal contact; a large dorsomedially inclined quadrate foramen showing a lenticular outline in posterior view; a ventral quadratojugal contact extending along almost the ventral half of the quadrate body; a dorsal quadratojugal contact facing anteriorly; and two relatively small mandibular condyles separated by a lateromedially wide intercondylar sulcus. The pterygoid flange projects only anteriorly and possesses a shallow medial fossa and no ventral shelf on its ventral margin. As seen in the two other basal coelurosaurs, the ventral margin of the pterygoid flange extends perpendicular to the long axis of the quadrate shaft, but the anterior margin of the flange is parabolic rather that semi-oval.

The quadrate of the basal coelurosaur *A. zhaoi* significantly differs from those of *B. argentina* and *Z. sallei*. The pterygoid flange is autapomorphically triangular and convergently similar to of the condition seen in dromaeosaurids. A vertically oriented ventral shelf (‘sliver of bone’ *sensu* Choiniere et al. 2014*b*) seems to be present on the medial surface of the pterygoid flange, along the posteroventral margin of the flange. The quadrate foramen is large, subcircular, and entirely developed within the quadrate body at one half of the bone (Choiniere et al. 2014*b*). A quadrate foramen with similar size, shape and occupation only occurs in the neovenatorid *Aerosteon*. Similar to basal

coelurosaurs, the lateral process is absent in *A. zhaoi*, yet no pronounced and well-delimited posterior fossa surrounding the quadrate foramen is present in this taxon (Choiniere et al. 2014*b*).

Tyrannosauroidea

Proceratosaurus bradleyi (NHM R 4860; Rauhut et al. 2010; Fig. 7.12A–C); *Eotyrannus lengi* (MIWG 1997.550; Fig. 7.12D–I); *Xiongguanlong baimoensis* (Li et al. 2010); *Alioramus altai* (Brusatte et al. 2012*a*; Fig. 7.12J–L); *Albertosaurus sarcophagus* (Currie 2003); *Gorgosaurus libratus* (AMNH 5336, 5664); *Daspletosaurus* sp. (Currie 2003); *Tyrannosaurus rex* (FMNH PR2081, AMNH 5027; Molnar 1991; Brochu 2003).

Although a significant amount of work has recently been published on tyrannosauroid paleobiology and anatomy due to recent discoveries (e.g., Xu et al. 2004, 2006; Brusatte et al. 2009*b*; Ji et al. 2009; Sereno et al. 2009; Carr and Williamson 2010; Averianov and Sues 2011; Hone et al. 2011; Loewen et al. 2013), the quadrate anatomy in this important clade of theropods is not particularly well-known. Detailed descriptions are available only for four tyrannosauroid taxa: *Proceratosaurus bradleyi* (Rauhut et al. 2010), *Alioramus altai* (Brusatte et al. 2012*a*; Gold et al. 2013), *Albertosaurus sarcophagus* (Carr 1996) and *Tyrannosaurus rex* (Molnar 1991; Brochu 2003).

In posterior view, the tyrannosaurid quadrate is particularly short (ratio of more than 0.5) while in the basal forms like *P. bradleyi* and *X. baimoensis* it is moderately ventrodorsally-tall (ratio between 0.45 and 0.5) like in basal tetanurans (Fig. 7.12A). In Tyrannosauridae and some basal tyrannosauroids such as *X. baimoensis*, the mandibular articulation and the quadrate body at the level of the ventral quadratojugal contact are particularly lateromedially wide (Fig. 7.12L). However, the quadrate body is lateromedially constricted at the level of the quadrate foramen, giving the typical axe shape to the quadrate in posterior view (Fig. 7.12L).

The quadrate ridge is laterally-inclined (angle between the main axis of the quadrate ridge and the main axis of the mandibular articulation of 55-65°, in posterior view) and usually distinct, and rod-shaped in basal forms like *P. bradleyi* (Fig. 7.12A), but forming a typical crest delimiting the medial margin of the quadrate body in some derived tyrannosauroids like *T. rex* (AMNH 5027; Larson 2008*b*). This crest is prominent directly dorsal to the entocondyle at the posteromedial portion of the quadrate, and reaches the second thirds of the height of the quadrate body relative to its ventral end in *A. sarcophagus* and *Daspletosaurus* sp. (Currie 2003: figs. 10, 28) while it extends to the quadrate head in *T. rex* as a narrow crest. The quadrate ridge is straight in posterior view in most tyrannosauroids, yet the ridge is biconvex in posterior view, and strongly posteriorly-inclined in the dorsal half of the quadrate body in medial view in *A. altai* (Fig. 7.12M) and *T. rex*. The quadrate ridge of tyrannosaurids is also divided into two ridges separated by a small concavity at the ventral part of the ridge, directly dorsal to the entocondyle, although the two ridges are rather low in *A. altai* (Fig. 7.12M) and *Daspletosaurus* (Currie 2003: fig. 10). The concavity bordered by those two ridges is deep

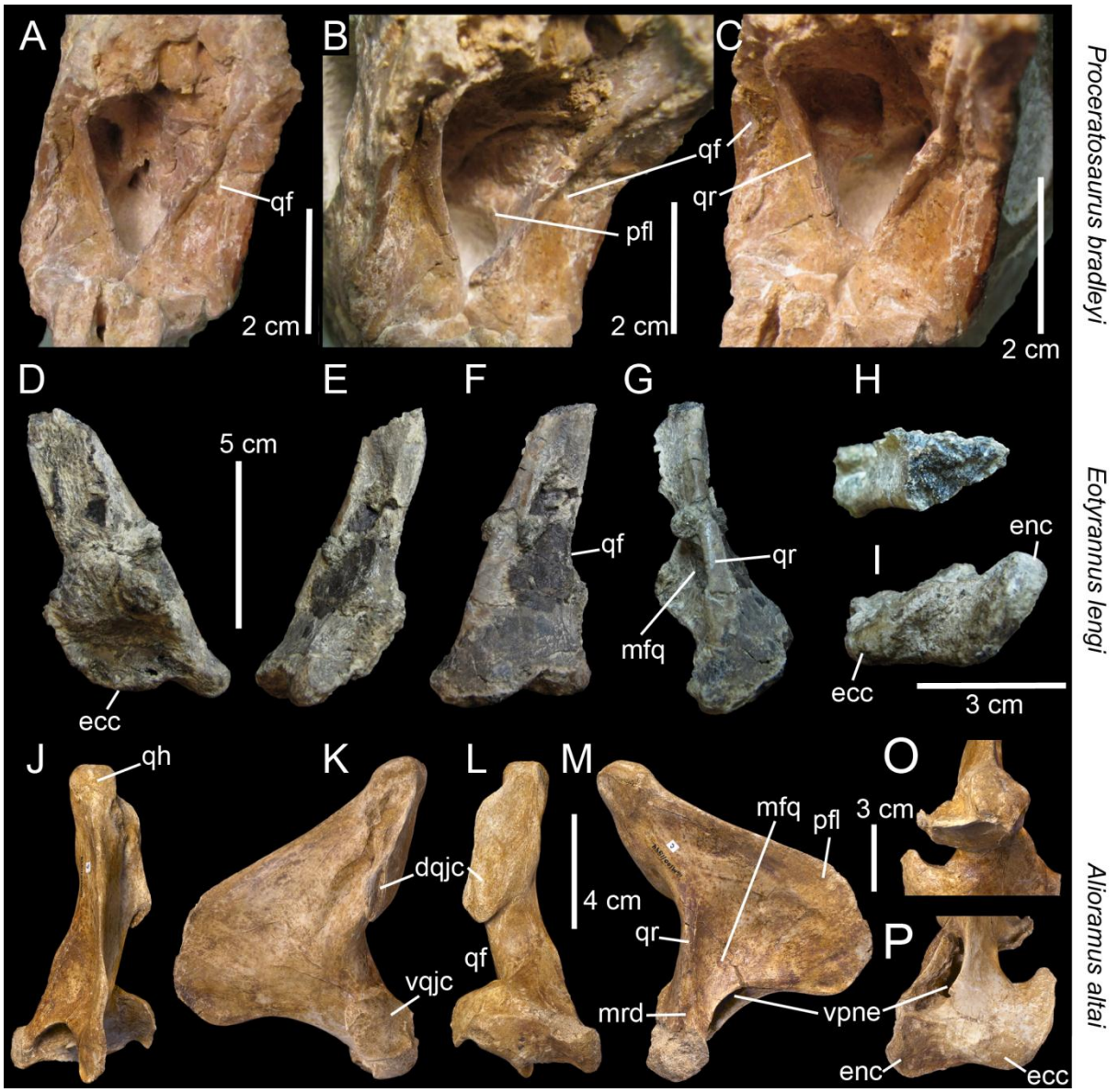

FIGURE 7.12. Quadrate diversity in Tyrannosauroidea. **A–C**, Left and right quadrates of *Proceratosaurus bradleyi* (NHM R 4860) in A, posterior; and **B–C**, posteromedial views; **D–I**, Ventral part of the right quadrate of *Eotyrannus lengi* (MIWG 1997.550) in **D**, anterior; **E**, lateral; **F**, posterior; **G**, medial; **H**, dorsal; and **I**, ventral views; **J–O**, Left quadrate of *Alioramus altai* (IGM 100-1844) in **J**, anterior; **K**, lateral; **L**, posterior; **M**, medial; **N**, dorsal; and **O**, ventral views (courtesy of Mick Ellison © AMNH). **Abbreviations**: **dqjc**, dorsal quadratojugal contact; **ecc**, ectocondyle; **enc**, entocondyle; **mfq**, medial fossa; **pfl**, pterygoid flange; **pfq**, posterior fossa; **qf**, quadrate foramen; **qh**, quadrate head; **qr**, quadrate ridge; **vqjc**, ventral quadratojugal contact; **vpne**, ventral pneumatic foramen.

and well-visible in *A. sarcophagus* (Currie 2003: fig. 10) and *T. rex* (AMNH 5027), and strongly ventrodorsally tall, covering the basal half of the quadrate ridge, in the latter.

The quadrate foramen is mostly delimited by the quadrate bone in Tyrannosauroidea (Fig. 7.12A, L). In basal forms such as *P. bradleyi*, the quadrate foramen is small, elliptical and strongly ventrodorsally-tall. It becomes larger in more derived tyrannosauroids like *X. baimoensis*, *G. libratus* and *T. rex*, in which it is lenticular or lanceolate. In tyrannosaurids, a short ventral projection of the dorsal quadratojugal contact delimits the dorsal margin of the quadrate foramen laterally.

Another condition uniting most tyrannosauroid taxa is the semi-oval outline of the pterygoid flange, particularly anteroposteriorly-long relative to the height of the quadrate body relative to its ventral end (ratio of more than 0.8). The pterygoid flange forms an elongated subtrapezoidal shape in derived tyrannosaurids like *A. altai* (Fig. 7.12M), where both ventral and dorsal margins are concave and the anterior margin is rugged. In tyrannosaurids, the ventral margin of the flange is divided into two crests in which the lateral one terminates at the midwidth of the quadrate body, directly dorsal to the intercondylar sulcus of the mandibular condyle, or reaching it. The medial crest, on the other hand, joins the quadrate body at its medial margin either directly dorsal to the entocondyle, or more dorsally. A ventral pneumatic recess is found between these two ridges of the pterygoid flange in *A. altai* (Fig. 7.12O), *A. sarcophagus* (Carr 1996), *Daspletosaurus* sp. (Currie 2003: fig. 28C) and *T. rex* (Brochu 2003200). The lateral process of the quadrate body is absent from all tyrannosauroids.

In lateral view, the quadrate head of some tyrannosaurids like *Daspletosaurus* sp. and *A. altai* is convex (Currie 2003: fig. 28D; Brusatte et al. 2012*a*), but it is biconvex and double-headed in *T. rex* (BHI 3033) and *A. sarcophagus* (Currie 2003: fig. 10B), which possess a narrow concavity centrally-positioned on the quadrate head. The posterior fossa of tyrannosauroids is absent. Nonetheless, the quadrate foramen of some derived tyrannosaurids is bounded by a large depression on the quadrate shaft which is delimited dorsally by the dorsal quadratojugal contact, and laterally by the quadrate ridge. This depression is, however, not considered homologous to the posterior fossa of other theropod taxa.

Most tyrannosauroids have a dorsal quadratojugal contact facing lateroposteriorly (Fig. 7.12L) or completely posteriorly as in *T. rex* (Larson 2008*b*). This feature is difficult to assess in the basal taxon *P. bradleyi* because the descending process of the squamosal covers the posterodorsal side of the quadrate. However, a dorsal quadratojugal contact on the lateroposterior margin of the quadrate body seems to be present in *X. baimoensis*. Unlike other tyrannosaurids, the ventral quadratojugal contact of the quadrate is lateromedially wide and lanceolate in *T. rex*, whereas it is more ventrodorsally tall and irregularly-shaped in more basal tyrannosaurids. The ventral quadratojugal contact of some Tyrannosauridae such as *Eotyrannus lengi* (Fig. 7.12E), *A. altai*, *A. sarcophagus*, and *T. baatar* is also lateroposteriorly-positioned and D-shaped or subquadrangular (Fig. 7.12K).

The mandibular articulation in Tyrannosauroidea is composed of two ovoid and subparallel condyles obliquely-oriented, roughly similar in size, and delimited by a lateromedially wide and shallow intercondylar sulcus which is parallel to the main axis passing through the mandibular condyles (Fig. 7.12I, O). Although the ectocondyle of *P. bradleyi* is lateromedially wider than the entocondyle in posterior view (Rauhut et al. 2010), they are usually subequal in other tyrannosauroids taxa like *E. lengi* and *T. rex*.

Pneumaticity is a common feature among tyrannosaurids and, besides the ventral pneumatic foramen present in most of them (e.g., *A. altai*; Fig. 7.12O), pneumatic foramina can also appear in a pneumatic recess in the medial fossa of the pterygoid flange such as in *A. sarcophagus* (Currie 2003:

fig. 10B) and *T. rex* (Molnar 1991: fig. 7). Also, *T. rex* and *A. sarcophagus* possess a pneumatic foramen on the anterodorsal side of the quadrate, beneath the quadrate head (Molnar 1991; Brochu 2003: fig. 7).

Compsognathidae

Compsognathus longipes (MNHN CNJ 79; Ostrom 1978; Peyer 2006); *Scipionyx samnicicus* (Dal Sasso and Maganuco 2011); *Juravenator starki* (Chiappe and Göhlich 2010); *Sinosauropteryx prima* (Currie and Chen 2001).

The quadrate anatomy of compsognathids is one of poorest known among non-avian theropods. A thorough description of the bone was only given by Dal Sasso and Maganuco (2011) for *Scipionyx samnicicus*, and the quadrate of other Compsognathidae was either briefly described, as in *Compsognathus longipes* (Ostrom 1978; Peyer 2006), *Juravenator starki* (Chiappe and Göhlich 2010), and *Sinosauropteryx prima* (Currie and Chen 2001), or not described at all, as in *Huxiagnathus orientalis* (Hwang et al. 2004) and *Sinocalliopteryx gigas* (Ji et al. 2007*a*). Although most of compsognathid specimens with cranial material tend to be extremely well preserved and almost complete, their remains are found in two dimensions on slabs of fine grained limestone, usually in articulation with other cranial bones, or associated with them. Therefore, due to crushing, missing bones and hidden parts, little information on the compsognathid quadrate can be extracted. This is particularly the case in *J. starki* and *H. orientalis* in which only a small portion of the quadrate is visible.

The quadrate of Compsognathidae is a tall and slender bone in which the mandibular articulation is relatively lateromedially narrow and anteroposteriorly short, so that the quadrate body is ventrodorsally tall both in lateral and posterior views. When articulated, the quadrate lies perpendicular to the ventral margin of the cranium, then gently curves posteriorly such that the quadrate head is positioned posteriorly relative to the mandibular articulation. An anterior inclination of the quadrate was proposed by Dal Sasso and Maganuco (2011) for *S. samniticus*, but the quadrate seems to be slightly posteriorly inclined even in articulation, as represented by these authors in the cranial reconstruction of this taxon (Dal Sasso and Maganuco 2011: fig. 175b). The posterior margin of the quadrate body is widely concave and the lateral margin is sigmoid in *S. prima* (Currie and Chen 2001: fig. 3f).

A small quadrate foramen is seen at the ventral third of the height of the quadrate body relative to its ventral end in *S. samniticus*, but its presence cannot be determined in other compsognathids. Nevertheless, the quadrate and quadratojugal tend to be disarticulated instead of fused together, so that the presence of a quadrate foramen between the quadrate and quadratojugal seems to be likely. No quadrate ridge has been illustrated in *S. prima*, but if present, the ridge was ventrodorsally oriented rather than medially inclined. The ventral quadratojugal contact corresponds to

a lanceolate surface extending on the ectocondyle in *S. samniticus*, and the shape of the dorsal quadratojugal contact is unknown in this taxon and other compsognathids.

The quadrate head is single headed and is a spherical or semi-spherical structure separated from the quadrate shaft by a narrow constriction. The ventral margin of the pterygoid flange attaches to the quadrate body directly dorsal to the mandibular articulation, as in *S. samniticus* (Dal Sasso and Maganuco 2011: fig. 41) and possibly in *C. longipes* (MNHN CNJ 79), or at the same level than the mandibular condyles, as it seems to be the case in *S. prima* (Currie and Chen 2001: fig. 3f). The shape of the pterygoid flange cannot be determined with precision, but it seems to be roughly parabolic in *C. longipes* and sub-trapezoidal in *S. samniticus*. It is unknown whether the dorsal margin of the flange reached the quadrate head or not dorsally.

The mandibular articulation includes two condyles in which the ectocondyle is smaller than the entocondyle in posterior view in *S. prima* (Currie and Chen 2001: fig. 3f). According to Peyer (2006), the reverse condition occurs in *C. longipes*, but the mandibular articulation is not well-preserved enough to support this observation. A pneumatic quadrate is present at least in *S. prima* which shows a posterior pneumatic foramen at midwidth of the quadrate body, at mid-height of the quadrate, and within the ventral part of a large posterior fossa (Currie and Chen 2001).

Ornithomimosauria

Ornithomimus edmontonicus (Tahara and Larsson 2011; Fig. 7.13A–D); *Sinornithomimus dongi* (Kobayashi and Lü 2003; Fig. 7.13E); *Garudimimus brevipes* (Kobayashi and Barsbold 2005*a*; Fig. 7.13F–G); *Gallimimus bullatus* (IGM 100-1133); *Struthiomimus altus* (AMNH 5339); Ornithomimosauria gen. et sp. indet. (Makovicky and Norell 1998).

The quadrate has been described usually briefly for some ornithomimosaurs taxa such as *Gallimimus bullatus* (Osmólska et al. 1972), *Sinornithomimus dongi* (Kobayashi and Lü 2003), *Garudimimus brevipes* (Kobayashi and Barsbold 2005*a*), and an indeterminate ornithomimosaur from Mongolia (Makovicky and Norell 1998).

The quadrate is slender (ratio of less than 0.35) in posterior view with a lateromedially wide mandibular articulation, the dorsal portion is particularly lateromedially narrow and ventrodorsally tall (Fig. 7.13E–G), and both lateral and medial margins converge dorsally to the quadrate head. The quadrate of ornithomimosaurs is inclined posteriorly in the cranium so that the mandibular articulation is always anterior relative to the quadrate head.

The quadrate foramen is present in *S. dongi* (Fig. 7.13E), *G. brevipes* (the ‘paraquadrate foramen’ of Kobayashi and Lü 2003 and the ‘paraquadrate foramen’ or ‘paraquadratic foramen’ of Kobayashi and Barsbold 2005*a* respectively; Fig. 7.13F–G), *O. edmontonicus* (Makovicky et al. 2004: fig. 6.2A; Fig. 7.13C–D) and *S. altus* (AMNH 5339) and corresponds to a narrow and lenticular aperture positioned at the ventral two-fifths of the height of the quadrate body relative to its ventral

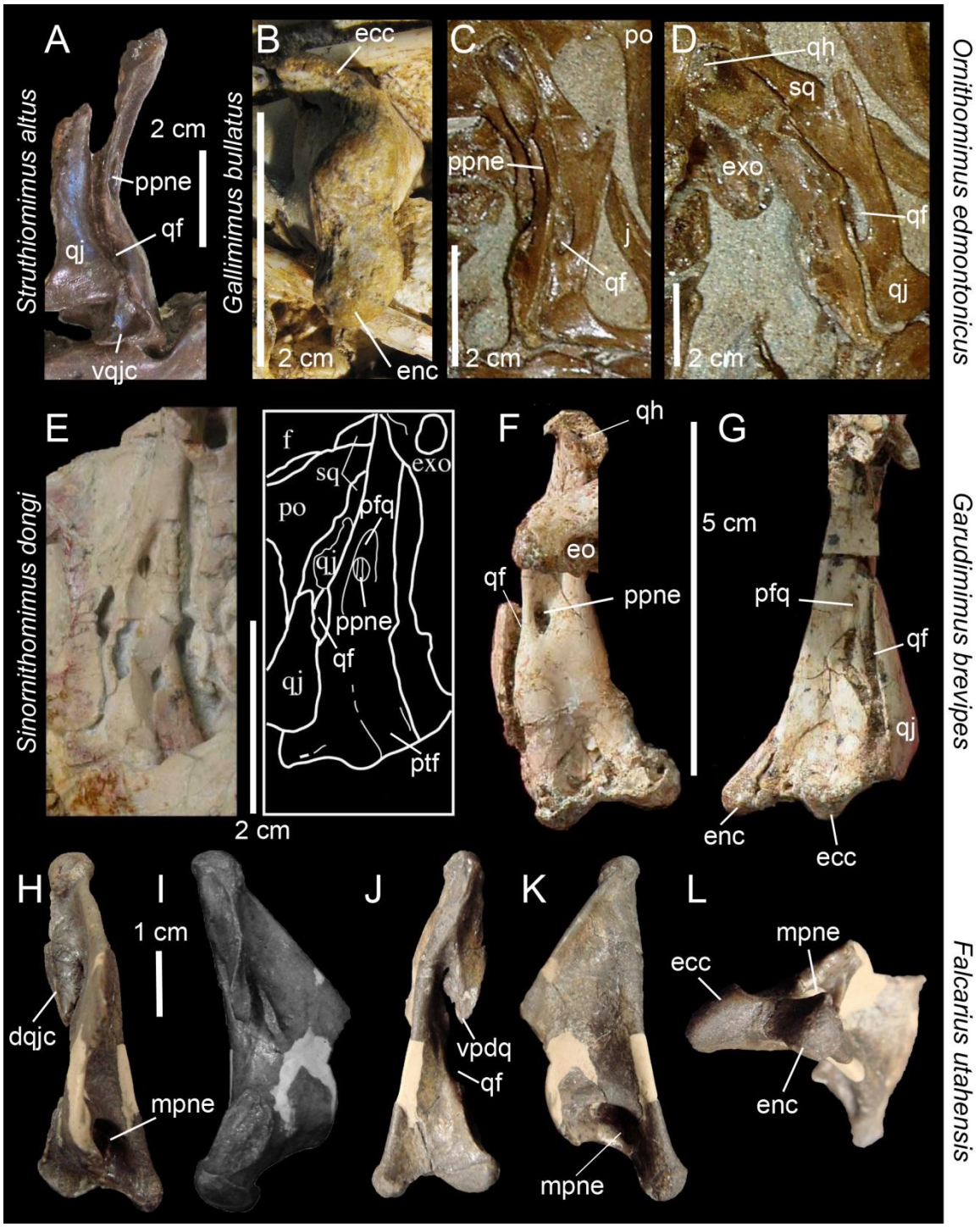

FIGURE 7.13. Quadrate diversity in Ornithomimosauria and Therizinosauria. **A**, Left quadrate of *Struthiomimus altus* (AMNH 5339) in lateral view; **B**, Left quadrate of *Gallimimus bullatus* (IGM 100-1133) in ventral view; **C–D**, Right coosified quadrates and quadratojugal of *Ornithomimus edmontonicus* (RTMP 95.110.1) in **A, C**, lateral; and **B, D**, lateroposterior views (courtesy of Rui Tahara and Yoshitsugu Kobayashi); **E**, Left coosified quadrate and quadratojugal of *Sinornithomimus dongi* (IVPP−V11797−10) in posterior view (courtesy of Yoshitsugu Kobayashi, modified); **F**, Left and **G**, right coosified quadrates and quadratojugals of *Garudimimus brevipes* (IGM 100-13) in posterior view (courtesy of Yoshitsugu Kobayashi, modified); **H–L**, Right quadrate of *Falcarius utahensis* (UMNH VP 14559) in **H**, anterior; **I**, lateral; **J**, posterior; **K**, medial; and **L**, ventral views (courtesy of Lindsay Zanno). **Abbreviations**: **dqjc**, dorsal quadratojugal contact; **ecc**, ectocondyle; **enc**, entocondyle; **exo**, exoccipital; **j**, jugal; **la**, lacrimal; **mpne**, medial pneumatic foramen; **pfq**, posterior fossa; **po**, postorbital; **ppne**, posterior pneumatic foramen; **qf**, quadrate foramen; **qh**, quadrate head; **qj**, quadratojugal; **pfq**, posterior fossa; **ppne**, posterior pneumatic foramen; **sq**, squamosal; **vqjc**, ventral quadratojugal contact.

end. The quadrate foramen is equally delimited by the quadrate and quadratojugal in basal forms, and mostly bounded by the quadratojugal in derived forms like *O. edmontonicus*.

The quadrate ridge of ornithomimosaurs is not well-defined except when delimited by the deep posterior fossa which forms a narrow rod-shaped structure subparallel to the long axis passing through the quadrate body (Fig. 7.13E–G). The pterygoid flange is well-visible in *G. brevipes* in lateral view (Kobayashi and Barsbold 2005*a*: fig. 4A). The flange is parabolic in shape, with a rounded anterior margin in which the most anterior point occurs at mid-height of the quadrate body relative to its ventral end. The flange is moderately anteroposteriorly long (ratio of 0.58), but seems to be much longer than the pterygoid flange of *S. dongi* with a ratio of approximately 0.4 (Kobayashi and Lü 2003). As is seen in *S. dongi*, the ventral margin of the pterygoid flange of *G. brevipes* seems to join the quadrate body just above the mandibular condyles, and the dorsal margin reaches the quadrate head at its base. In *G. brevipes*, the quadrate head is single headed and fits in the quadrate head of the squamosal (Makovicky et al. 2004). The articulation with the squamosal is not exposed in lateral view in *Shenzhousaurus orientalis*, unlike the condition seen in *G. bullatus* and *O. edmontonicus* (Ji et al. 2003).

One of the most diagnostic features of most ornithomimosaur quadrate is the deep, lanceolate and well-defined posterior fossa at midwidth on the quadrate body and including a small pneumatic foramen, in posterior view (Makovicky et al. 2004; Fig. 7.13A, C–G). Such fossa is present in *S. dongi* (the 'quadrate foramen' of Kobayashi and Lü 2003) and includes an ovoid pneumatic foramen divided by a vertical septum and located within the dorsal part of the fossa. It is also seen in *G. brevipes* (the 'quadrate foramen' of Kobayashi and Barsbold 2005*a*) whose the elliptical foramen is present ventrally in the depression, and an indeterminate ornithomimosaur (IGM 100-987) in which the deep and strongly ventrodorsally tall posterior fossa includes a tiny subcircular foramen at the most dorsal part of the fossa (Makovicky and Norell 1998). A deep lanceolate posterior fossa is also present in *G. bullatus* and *S. altus* at the ventral two thirds of the height of the quadrate body relative to its ventral end (IGM 100-1133; AMNH 5339), yet it is unknown whether this depression was pneumatic or not. According to Makovicky and Norell (1998), a pneumatic and well-defined posterior fossa is not present in some ornithomimids such as *O. edmontonicus* (ROM 851, ROM 840). Yet, the specimen RTMP 95.110.1 of *O. edmontonicus* does possess a pneumatic foramen on the posteromedial surface of the quadrate and leading to a vast pneumatic chamber inside the quadrate bone (Tahara and Larsson 2011; Fig. 7.13C).

The ventral quadratojugal contact of the quadrate has a unique morphology among ornithomimids. In *S. altus*, the ventral part of this contact corresponds to a ear-shaped depression facing laterally and bounded by a prominent ridge along its ventral and posterior margin (Fig. 7.13A). The dorsal part of the ventral quadratojugal contact corresponds, on the other hand, to a ventrodorsally tall and lateromedially narrow surface diminishing in width dorsally to join the quadrate head. In *O. edmontonicus*, the quadratojugal displays a dorsal projection, which articulates along this articular

surface, and delimits the quadrate foramen posteroventrally. The dorsal quadratojugal contact is located on the lateral surface of the quadrate body in *G. brevipes*, and on the anterior margin of the quadrate body in more derived ornithomimids like *S. altus* and *O. edmontonicus*. The quadrate of ornithomimids does not have a lateral process.

In ventral view, the typical mandibular articulation structure of two condyles separated by an intercondylar sulcus is different in derived ornithomimosaurs. According to Kobayashi and Lü (2003) and Kobayashi and Barsbold (2005*a*), the ecto- and entocondyles of *S. dongi* and *G. brevipes* are subequal in size and well-separated by an anteroposterior intercondylar sulcus. Yet the entocondyle is protuberant and projected medially in *S. dongi*, whereas there is an accessory condyle lateral to the ectocondyle and dorsally-positioned relative to the two mandibular condyles (Kobayashi and Lü 2003). The examination of the quadrate of an undescribed skull of *Gallimimus bullatus* (IGM 100-1133) supports this morphology of the mandibular articulation of ornithomimids. The accessory condyle of Kobayashi and Lü (2003) corresponds in fact to a lateral extension of the ectocondyle, and the ecto- and entocondyle therefore differ significantly in their morphology (Fig. 7.13B). Indeed, the ectocondyle is parabolic and comma shaped, with an anteroposteriorly short and diagonally oriented lateral part and an anteroposteriorly long and ovoid medial part, whereas the entocondyle is elliptical, almost spherical. This lateral extension of the ectocondyle articulates with a laterodorsal flange of the surangular, just anterior to the mandibular glenoid (Makovicky et al. 2004). Both mandibular condyles are separated by a lateromedially wide, shallow and poorly delimited intercondylar sulcus that extends anteroposteriorly (Fig. 7.13B). In basal ornithomimids like *Nqwebasaurus thwazi*, the quadrate articulation is not as complex, and consists of a lateromedially wide hemi-cylindrical ectocondyle and a hemispherical entocondyle (Choiniere et al. 2012).

Basal Maniraptora

Ornitholestes hermanni (AMNH FARB 619; Fig. 7.14G–K); *Mononykus olecranus* (Chiappe et al. 2002); *Shuvuuia deserti* (IGM 100-977, Fig. 7.14L–M; IGM 100-1001, Fig. 7.14N–P; Dufeau 2003).

The quadrate was comprehensively described in the alvarezsaurids *Shuvuuia deserti* and *Mononykus olecranus* (Chiappe et al. 2002), yet the cranial bone has not received any detailed description in *Ornitholestes hermanni*. Although all three taxa are basal members of the Maniraptora, *O. hermanni* is the most primitive maniraptoran (*sensu* Senter 2011; Turner et al. 2012) whereas the two alvarezsaurids are derived forms of Alvarezsauroidea (Nesbitt et al. 2011; Xu et al. 2011*b*; Choiniere et al. 2014*b*), so that their quadrates significantly differ in their morphology.

The left quadrate of *O. hermanni* is crushed and fragmented, and only the right quadrate provides data on the anatomy of this bone. The right quadrate is complete, slightly damaged but strongly deformed in its midheight. It is preserved in articulation with the cranium, which is crushed and filled with sediment in its internal part so that little information can be extracted in anterior and

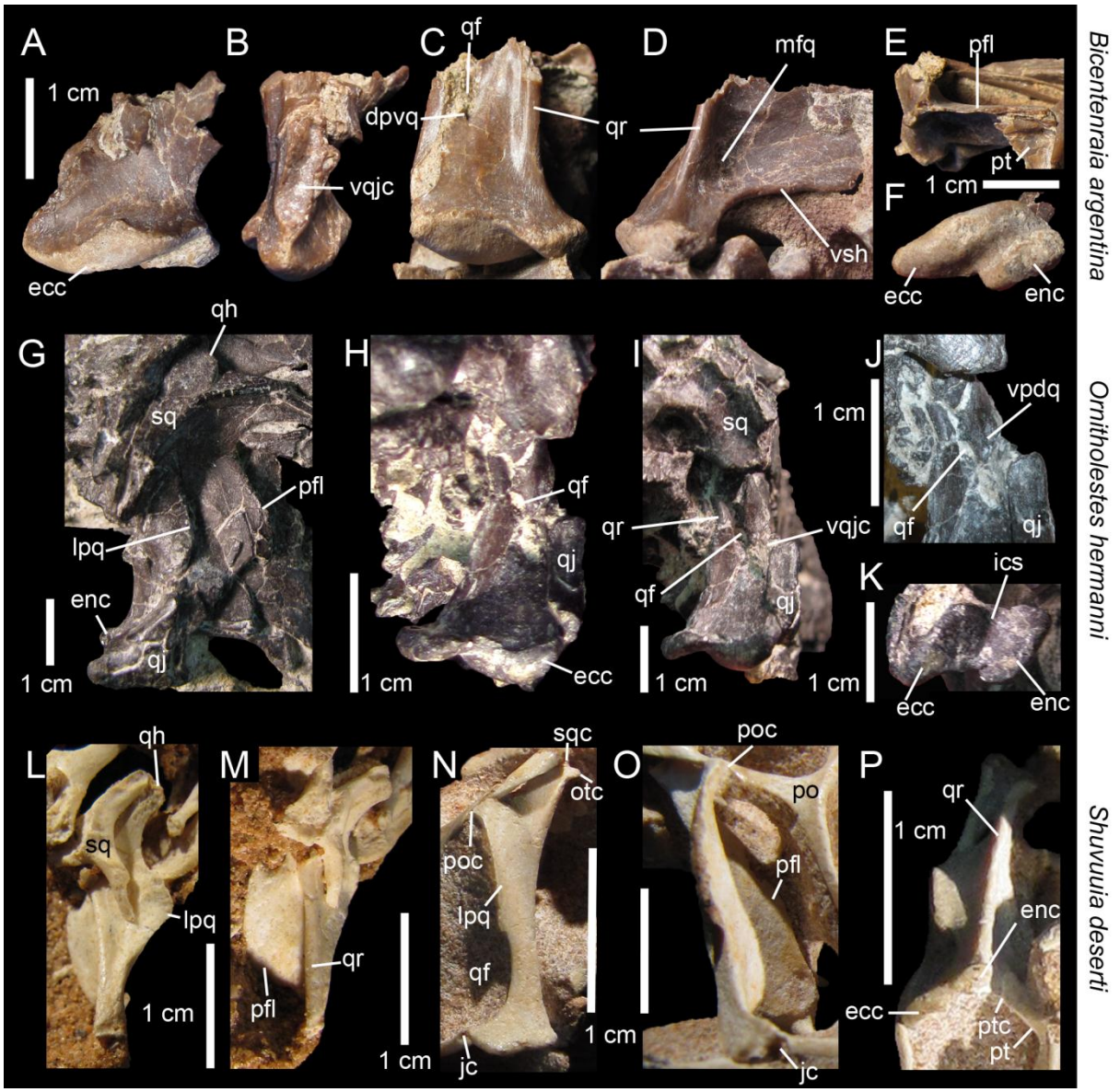

FIGURE 7.14. Quadrate diversity in basal Coelurosauria and Alvarezsauroidea. **A**–**B**, **F**, Right; and **C**–**E**, left quadrates of *Bicentenaria argentina* (MPCA 865) in **A**, anterior; **B**, lateral; **C**, posterior; **D**, medial; **E**, dorsal; and **F**, ventral views; **G**–**H**, Right quadrate of *Ornitholestes hermanni* (AMNH FARB 619) in **G**, lateral; **H, J**, posterior; **I**, posterolateral; and **K**, ventral views; **J**, details of the central part of the quadrate body (photo courtesy shared by Mickey Mortimer); **L**–**M**, Right and **N**–**P**, left quadrates of *Shuvuuia deserti* (L–M: IGM 100-977; N–P: IGM 100-1001) in **L**, **N**, posterior; **M**, posteromedial; **O**, lateral; and **P**, ventral views. **Abbreviations**: **dpvq**, dorsal projection of the ventral quadratojugal contact; **ecc**, ectocondyle; **enc**, entocondyle; **ics**, intercondylar sulcus; **lpq**, lateral process; **mfq**, medial fossa; **oca**, ootic capitulum; **pfl**, pterygoid flange; **pfq**, posterior fossa; **po**, postorbital; **poc**, postorbital contact; **pt**, pterygoid; **ptc**, pterygoid contact; **qf**, quadrate foramen; **qh**, quadrate head; **qj**, quadratojugal; **qjc**, quadratojugal contact; **qr**, quadrate ridge; **sca**, squamosal capitulum; **sq**, squamosal; **vpdq**, ventral projection of the dorsal quadratojugal contact; **vpne**, ventral pneumatic foramen; **vqjc**, ventral quadratojugal contact; **vsh**, ventral shelf.

medial views. Besides, only the ventral part of the bone is visible, the dorsal part other than the quadrate head being obscured by the squamosal (Fig. 7.14G).

The quadrate of *O. hermanni* is tall (0.28). Despite some deformation in the central part of the quadrate body, the quadrate has a quadrate foramen at the ventral one-third of the height of the bone

relative to its ventral end, lateral to the prominent quadrate ridge, and open laterally (Fig. 7.14H–J). The quadrate foramen was mostly bordered by the quadrate as a well-developed ventral projection of the dorsal quadratojugal contact seems to have delimited part of the lateral margin of the quadrate foramen (Fig. 7.14J). A lateral process with a parabolic outline is visible in lateral view. This process projects anteriorly, yet it is unknown whether it was extending mostly laterally or anteriorly before taphonomic deformation. The ventral quadratojugal contact extends along the ventral half of the quadrate body and was most likely anteriorly inclined. There is no quadratojugal process extending from the ventral quadratojugal contact. The quadrate head, only visible in lateral view, is single headed and has a rounded dorsal margin. It is weakly oriented anteriorly and the pterygoid flange is not attached to its dorsal margin. The quadrate ridge is prominent, rod-shaped, laterally inclined and reaches the ectocondyle in its medial section.

In *O. hermanni*, the pterygoid flange only projects anteriorly and its anteroposterior extension is relatively short compared to other basal coelurosaurs. The anterior margin of the pterygoid flange is parabolic and almost subtriangular, and the anteriormost point of the flange is situated at mid-height of the quadrate body relative to its ventral end. A deep posterior fossa occupies most of the quadrate body in posterior view, and extends from the mandibular articulation ventrally to at least the quadrate foramen. The mandibular articulation encompasses two condyles subequal in shape, size and orientation, and separated by a lateromedially wide and shallow intercondylar sulcus (Fig. 7.14K). Both ecto- and entocondyles are elliptical and the angle between the long axis of the mandibular articulation and the main axis passing through the condyles and the intercondylar sulcus is approximately 120°.

S. deserti is the only alvarezsauroid preserving a complete quadrate that has been well-described in the literature. Both quadrates of the primitive alvarezsauroid *Haplocheirus sollers* (Choiniere et al. 2010*b*) seems to be preserved as well, but neither illustrations nor a description have been provided for the quadrate in this taxon. As for *M. olecranus*, only the quadrate head, which is double headed and contacts both the squamosal and prootic (Perle et al. 1994; Chiappe et al. 2002), is preserved. Access to both articulated skulls of *S. deserti* (IGM 100-977; IGM 100-1001) allows us to provide a list of unique features in this taxon.

The quadrate is remarkably different from that of other theropods in many aspects. Both specimens have been interpreted as belonging to different ontogenetic stages (Dufeau 2003), yet the quadrate of each specimens strongly differ in their morphology so much so that the assignation of both specimens to a same species is questionable. The right quadrate of the largest specimen (IGM 100-977) is complete and well-preserved, but only its posterior side is well-visible (Fig. 7.14L–M). The most striking features of this bone is the lateral orientation of the quadrate head, the short and parabolic pterygoid flange, and the notch on the dorsal margin of this flange. In this specimen, the quadrate head seems to be single headed and lateromedially wider than the mandibular articulation. There is a faint quadrate ridge in posterior view, but the ridge is well-demarcated in medial view. The

dorsal margin of the pterygoid flange is unique in possessing a deep notch, which does not seem to result from the loss of a fragment. The mandibular articulation is just a prolongation of the quadrate shaft. It is subrectangular, flat and seems to be unicondylar in posterior view. Nonetheless, a fragment of bone lying on the ventrolateral surface of the pterygoid flange may correspond to the lateral part of the mandibular articulation.

The mandibular articulation of IGM 100-1001 is lateromedially much wider than the quadrate shaft, and the ventral part of the quadrate body is boot-shaped in posterior view, i.e., the lateroventral margin is convex, almost pointed, and projects far anteriorly. The lateral process is subtriangular and anterolaterally directed. Its anterior corner contacts both the postorbital and the squamosal, a quadrate autapomorphy of *S. deserti* (Chiappe et al. 1998). A small corner marks the ventral limit of the lateral process. The dorsal quadratojugal contact typically extends to that level in many other theropods, but the quadratojugal only articulates at the ventrolateral corner of the quadrate body. As a result, the quadrate foramen is merged with the infratemporal fenestra, which is a second quadrate autapomorphy of *S. deserti*. The quadrate head of IGM 100-1001 clearly displays two condyles, the squamosal capitulum, directed dorsally to contact the squamosal, and the otic capitulum, oriented medially towards the braincase (Chiappe et al. 1998, 2002).

The pterygoid flange of IGM 100-1001 extends anteromedially and forms a short subtrapezoidal ala in which the anterior margin is anteroposteriorly long and posteriorly inclined at an angle of 65° with the horizontal plane of the skull (Fig. 7.14O). The anteriormost point of the pterygoid flange is located at the ventral one fifth of the height of the quadrate body relative to its ventral end, and the ventral margin of the flange attaches the quadrate flange just above the mandibular articulation. The pterygoid articulates with the medioventral part of the pterygoid flange close to the quadrate body (Fig. 7.14P). The mandibular articulation clearly shows two condyles in posterior view, and the ectocondyle is lateromedially wider than the entocondyle. In ventral view, the distinction between the two condyles is subtle, and both ecto- and entocondyles are elliptical and follows the same orientation than the long axis of the mandibular articulation (Fig. 7.14P), which is also an autapomorphical feature of *S. deserti.*

Therizinosauria

Falcarius utahensis (Zanno 2010*b*; Fig. 7.13H–L); *Erlikosaurus andrewsi* (Clark et al. 1994); *Jianchangosaurus yixianensis* (Pu et al. 2013)

The quadrate of therizinosaurs has been well-described and illustrated in only two taxa: *Erlikosaurus andrewsi* (Clark et al. 1994) and *Falcarius utahensis* (Zanno 2010*b*). The quadrate morphology in these two specialized theropods is significantly different from other closely related coelurosaurs, and both taxa share a combination of apomorphic characters. The articulated quadrate is vertically oriented within the cranium in *Jianchangosaurus yixianensis* and *E. andrewsi*, so that the quadrate head lies at the same level than the mandibular articulation. In lateral view, the posterior

margin of basal therizinosaurs is distinctly concave and strongly arched, yet the posterior margin of *E. andrewsi* is strongly sigmoid, with an apomorphically convex posterior margin of the ventral third of the quadrate in lateral view.

Due to the large quadrate foramen almost adjacent to the quadrate ridge, the quadrate body is constricted at mid-height in posterior view (Fig. 7.13J). Both ventral and dorsal parts are lateromedially wide, roughly making an hourglass shape of the quadrate body in posterior view. The quadrate is a moderately tall bone (ratio between 0.38-0.4) whose quadrate ridge is poorly defined in posterior view. It is better delimited in medial view in *F. utahensis*, but almost unnoticeable in *E. andrewsi*. As in many tetanurans, the quadrate ridge of *F. utahensis* is laterally-inclined (angle between the main axis of the quadrate ridge and the main axis of the mandibular articulation of 70°, in posterior view) and becomes distinctly visible directly dorsal to the entocondyle and reaches the quadrate head (Fig. 7.13J). In posterior view, the medial margin of the quadrate body of these two therizinosaurs is biconcave, and the convexity separating the two concavities is situated at the ventral one third of the height of the quadrate body relative to its ventral end in *E. andrewsi* and at the ventral two thirds in *F. utahensis*.

The quadrate foramen is mostly delimited by the quadrate in therizinosaurs, and the ventral projection of the dorsal quadratojugal contacts may have delimited an important part of the foramen laterodorsally in *F. utahensis* (Fig. 7.13J). It is, however, unknown whether the quadrate foramen of *F. utahensis* was extending dorsally within the quadrate body, between the quadrate ridge and the ventral projection of the dorsal quadratojugal contact, or whether this part of the quadrate body is damaged, with missing bones. The shape of the quadrate foramen is lenticular in *E. andrewsi* and possibly in *F. utahensis*.

The lateral process is here considered present in *F. utahensis* (Fig. 7.13I), J. *yixianensis*, and *E. andrewsi* because there is a short lateral projection of the quadrate body from above the quadrate foramen to the quadrate head in these taxa. The lateral process projects completely laterally in *F. utahensis*, whereas it extends anterolaterally in *E. andrewsi*, and the lateral margin of this process is parabolic in outline in these two therizinosaurs.

In medial view, the pterygoid flange is anteroposteriorly short in therizinosaurs, particularly in *F. utahensis* (Fig. 7.13K) whose ratio between the anteroposterior length and the ventrodorsal width of the quadrate body is low (0.33). The anterior margin of the flange is M-shaped in *F. utahensis* (Fig. 7.13K) while the pterygoid flange of *E. andrewsi* is parabolic, with a small concavity at its anteroventral margin (Clark et al. 1994: fig. 2). In both therizinosaurs, the pterygoid flange projects anteromedially and does not curve medially in posterior view. In addition, the ventral margin of the pterygoid flange joins the quadrate body well- dorsal to the entocondyle, at around one sixth of the quadrate height relative to its ventral end in *F. utahensis*, and one fourth in *E. andrewsi*. The dorsal margin reaches the ventral limit of the quadrate head in both taxa in medial view. Interestingly, the prootic and basipshenoid contact the pterygoid flange posterodorsally in *E. andrewsi* (Clark et al.

1994). Although the cranium of this taxon has been strongly deformed and this part of the skull has been badly preserved, a contact between the pterygoid flange and the braincase seems to be genuine. A contact between the quadrate and braincase is also seen in the oviraptorosaur *Avimimus portentosus* (PIN 3907/1).

In therizinosaurs, the dorsal quadratojugal contact is positioned on the anterior side of the short lateral process (Fig. 7.13H). This contact also possesses a well-developed ventral projection in *F. utahensis*, whereas such projection is absent in *E. andrewsi*. The dorsal quadratojugal contact is anteroposterioly short and ventrodorsally tall, and extends along the anterior surface of the in *F. utahensis* (Fig. 7.13H) and possibly *E. andrewsi*. The ventral quadratojugal contact is elliptical and situated directly dorsal to the ectocondyle in *F. utahensis* (Fig. 7.13I) and *E. andrewsi*, but this suture with the quadratojugal is much longer anteroposteriorly in the former, and it is anteroposteriorly short and oblong in outline in the latter.

The mandibular articulation is formed by two condyles in *F. utahensis* (Fig. 7.13L) and by three condyles in *E. andrewsi* (Clark et al. 1994). The mandibular condyles are ovoid to subcircular in both therizinosaurs. In *F. utahensis*, the ectocondyle is ovoid and the long axis passing through it is inclined laterally by an angle of 130° relative to the long axis of the mandibular articulation (Fig. 7.13L). The entocondyle is protuberant and separated from the ectocondyle by a wide yet shallow intercondylar sulcus, which is parallel to the long axis of the lateral condyle. The three mandibular condyles of *E. andrewsi* are well developed, with a larger ectocondyle, a medium entocondyle (two thirds of the size of the ectocondyle) and a third much smaller condyle (half of the size of the entocondyle) positionned posteriorly between the two (Clark et al. 1994).

A large pneumatic recess appears in the ventromedial part of the flange in *F. utahensis* (Fig. 7.13K). This recess penetrates deeply inside the pterygoid flange and quadrate body, and is strongly displaced laterally relative to the lateromedial midline of the bone, contrarily to the medial pneumatic foramen of other theropods (Fig. 7.13H). It is unknown whether this pneumatic opening is homologous to the medial pneumatic opening of carcharodontosaurids, or to the ventral pneumatic foramen of tyrannosaurids. Because the pneumatic foramen of *F. utahensis* covers a larger surface medially, it is assumed that this homologous to the medial pneumatic opening of other theropods. Due to the lateral position of the medial pneumatic foramen, the ventralmost margin of the pterygoid flange joins the quadrate body at the level of the intercondylar sulcus instead of the entocondyle. Although pneumaticity might have been present in the quadrate of *E. andrewsi*, it is not conspicuously expressed like in *F. utahensis*. (Clark et al. 1994) inferred the possible existence of a pneumatic foramen in a posteromedial depression near the dorsal margin of the bone, which is not observable due to crushing. Nevertheless, a large medial pneumatic recess is not present in *E. andrewsi*.

Oviraptorosauria

Incisivosaurus gauthieri (Balanoff et al. 2009); *Avimimus portentosus* (Kurzanov 1985; Vickers-Rich et al. 2002; Fig. 7.15A–D); *Citipati osmolskae* (IGM 100-978; Fig. 7.15E–H); *Khaan mckennai* (IGM 100-1002; IGM 100-1127; Balanoff and Norell 2012; Fig. 7.15I–L); *Heyuannia huangi* (Lü 2003); *Conchoraptor gracilis* (Kundrát and Janáček 2007); Oviraptoridae gen. et sp. indet. (Maryańska and Osmólska 1997).

The anatomy of the quadrates of some derived oviraptorids (*Oviraptor*? sp. ZPAL MgD-I 95; *Ingenia yanshini* or *Conchoraptor gracilis*; IGM 100-30A, IGM A&B) has been comprehensively investigated by Maryańska and Osmólska (1997), and the quadrate anatomy of other oviraptorosaurs is well-documented in the literature with good descriptions of the bone in *Incisivosaurus gauthieri* (Balanoff et al. 2009), *Avimimus portentosus* (Kurzanov 1985; Vickers-Rich et al. 2002), *Citipati osmolskae* (Chiappe et al. 2002) and *Khaan mckennai* (Balanoff and Norell 2012). The quadrate of oviraptorids, and to some extent oviraptorosaur theropods, is atypical because of the shape of its mandibular articulation, its contact with the pterygoid and, especially, its quadrate head (Maryańska and Osmólska 1997). In this paper, the quadrate of the basal oviraptorosaur *A. portentosus* (PIN 3907/1) will be described before summarizing the synapomorphic characters found in Oviraptoridae.

In *A. portentosus*, the quadrate is fused to the braincase and the pterygoid flange (Fig. 7.15A–C). In lateral view, the quadrate body is vertically oriented so that the mandibular articulation and the quadrate head lies on a same plane. In posterior view, the posterior surface of the quadrate body is slightly lateromedially concave all along the ventrodorsal height of the bone. In posterior view, the quadrate body has subparallel lateral and medial margins in its ventral part. Dorsally, the quadrate body enlarges at about two-fifths of the bone height, where the pterygoid flange joins the quadrate body at its medial margin. The ventral part of the pterygoid flange, instead of projecting anteriorly or anteromedially as in all non-avian theropods, curves medially to contact the braincase on its posterior side. In ventral view, the dorsal part of the pterygoid flange is oriented anteromedially and fuses to the pterygoid flange anteriorly and the endocranium anterodorsally (Fig. 7.15D). In lateral view, the anterior margin of the pterygoid flange is parabolic in outline, and the most anterior point is situated at one third of the height of the quadrate relative to its ventral end (Fig. 7.15A–C).

What is here interpreted as being a ventral projection of the pterygoid bone contacts the quadrate body on its anteroventral side just above the mandibular articulation (Fig. 7.15D). If our interpretation is correct, this would be an autapomorphic character for *A. portentosus*. This long bone was interpreted by Kurzanov (1985) as being intergrown jugal and quadratojugal bones. However, the presence of a ventral quadratojugal contact on the lateral side of the left quadrate as well as a pterygoid contact on the anteroventral margin of the right quadrate makes this interpretation doubtful.

Due to the absence of both quadratojugals in PIN 3907/1, it is hard to detect the presence of a quadrate foramen. However, the quadratojugal contact of the quadrate seems to form a unique suture along the entire lateral surface of the quadrate body. The ventral portion of the contact is anteroposteriorly longer and lanceolate, whereas the dorsal part is anteroposteriorly short,

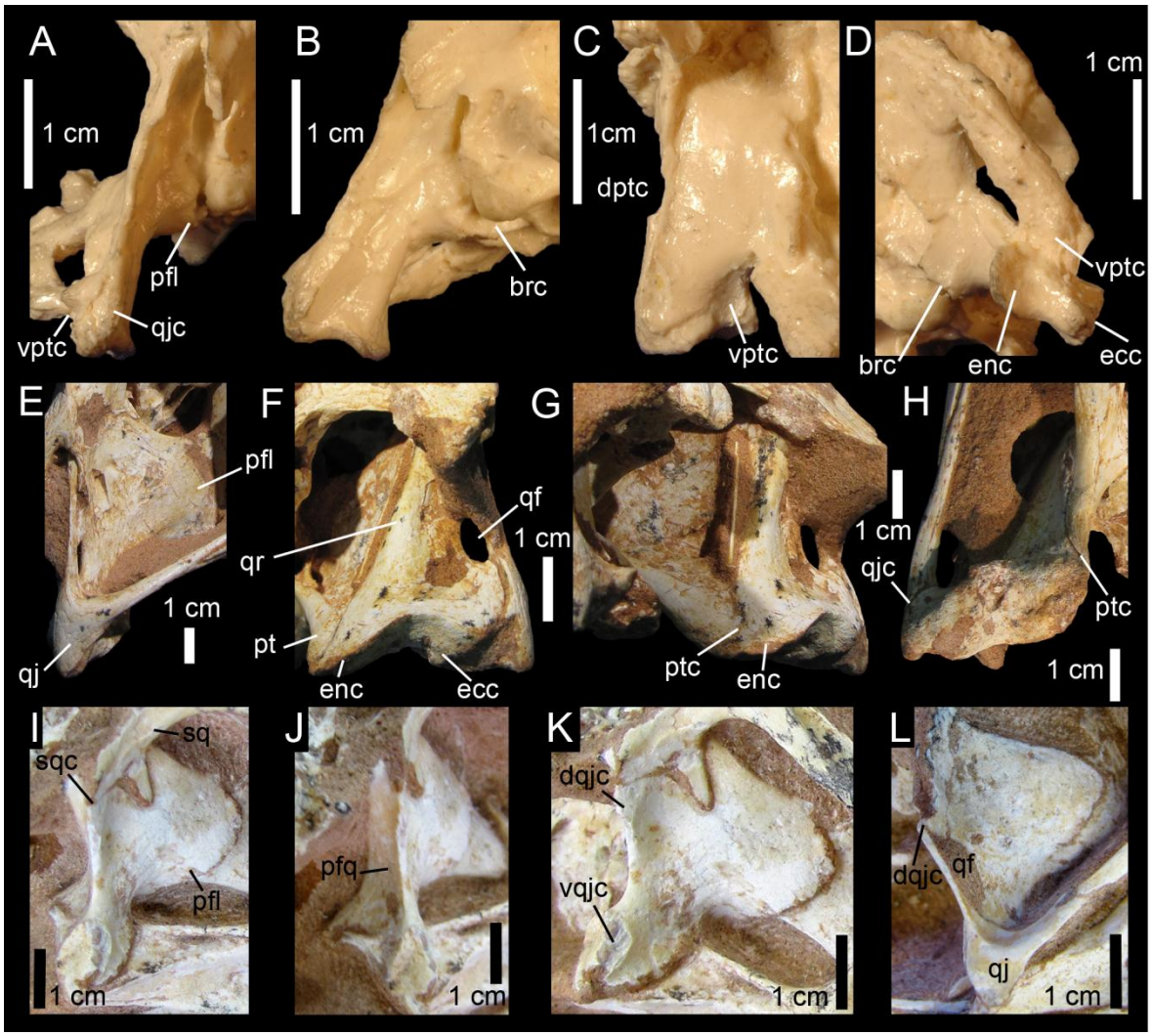

FIGURE 7.15. Quadrate diversity in Oviraptorosauria. **A–D**, Occipital part of the cranium of *Avimimus portentosus* (cast of PIN 3907/1) in **A**, lateral; **B**, posterior; **C**, anterolateral, and **D**, ventral views (courtesy of Lawrence Witmer); **E–H**, Right quadrate of *Citipati osmolskae* (IGM 100-978) in **E**, lateral; **F**, posterior; **G**, medioposterior; and **H**, ventral views; **I–L**, Right quadrate of *Khaan mckennai* (IGM 100-1127 for I–J, IGM 100-1002 for L) in **I**, **L**, lateral; **J**, posterolateral; and **K**, anterolateral views. **Abbreviations**: **brc**, braincase contact; **dptc**, dorsal pterygoid contact; **dqjc**, dorsal quadratojugal contact; **ecc**, ectocondyle; **enc**, entocondyle; **pfl**, pterygoid flange; **pfq**, posterior fossa; **pt**, pterygoid; **ptc**, pterygoid contact; **qf**, quadrate foramen; **qj**, quadratojugal; **qjc**, quadratojugal contact; **qr**, quadrate ridge; **sq**, squamosal; **sqc**, squamosal contact; **vptc**, ventral pterygoid contact; **vqjc**, ventral quadratojugal contact.

ventrodorsally tall contact receiving both the quadratojugal and the squamosal. A short anterior projection occurs on the anteroventral part of the quadrate body, at the level of the ectocondyle and directly dorsal to it. The quadrate head is not completely visible in PIN 3907/1, yet close observation suggests that the quadrate head does contact the squamosal and the braincase (Fig. 7.15A). The mandibular articulation of *A. portentosus* is formed by two elliptical and subparallel condyles of the same size (Fig. 7.15D). These two condyles are separated by a wide and shallow intercondylar sulcus parallel to the anteroposterior axis passing through the two condyles. There is no pneumatic foramen in *A. portentosus* and the quadrate is possibly apneumatic in this taxon.

The quadrate of oviraptorid theropods is highly diagnostic given the combination of the following features, namely an 'Eiffel-tower' shape of the quadrate body in posterior view, terminating dorsally as a conical double-headed quadrate head formed by the squamosal and otic capitula; a pterygoid contact on the medial side of the quadrate body and joining the entocondyle (this might not however be the case in *C. gracili*s, see Kundrát and Janáček 2007: fig. 2D), and a W-shaped mandibular articulation with a pointed ventromedial margin of the quadrate body in posterior view (Fig. 7.15F).

The quadrate foramen is medium-sized (7% to 20% of the quadrate height), lenticular, and equally formed by the quadrate and quadratojugal. It is ventrodorsally tall, and the foramen is partially visible in lateral view (Fig. 7.15F). The quadrate ridge of oviraptorids is poorly-delimited in posterior view, and almost absent. When present, it is inclined laterally (65° in *C. osmolskae*) and has a biconcave medial margin. As most tetanurans, there is no lateral process projecting from the quadrate body (Fig. 7.15J). The double-headed quadrate head is tall and conical, with a rounded tip pointing dorsally, and a small constriction separates the head from the rest of the quadrate body.

The pterygoid flange mostly projects anteriorly and slightly curves medially, and in *C. osmolskae* and *K. mckennai* the flange is subtrapezoidal in shape with a straight (and short in *K. mckennai*) anteriormost margin inclined posteriorly (Fig. 7.15I) like in most basal theropods. In lateral view, the ventral quadratojugal contact is ventrodorsally elongated yet relatively anteroposteriorly long and typically lanceolate (i.e., tear-drop shaped) in outline. The ventral quadratojugal contact faces posterolaterally, and in some oviraptorids such as *C. osmolskae*, a ventral process projects laterally from the ventral part of this articulation to contact the quadratojugal dorsally (= lateral process *sensu* Maryańska and Osmólska 1997). Among non-avian theropods, such the ventral process is only seen in oviraptorids. The dorsal quadratojugal contact forms a ventrodorsally tall anteroposteriorly short surface for receiving the dorsal quadratojugal process. The ventral margin of the pterygoid flange joins the quadrate body close to the mandibular articulation, at the level of the entocondyle and just dorsal to the latter (Fig. 7.15G).

A pneumatic quadrate has been reported in several oviraptorosaurs, including *K. mckennai* (Balanoff and Norell 2012), *Heyuannia huangi* (Lü 2003), and *C. gracili*s (Kundrát and Janáček 2007). No pneumatic foramen is visible in the posterior surface of *K. mckennai* and *C. gracilis*, however, there is indication that the dorsal tympanic recess of *C. gracilis* invades the multichambered quadrate pneumatic sinus through an opening on the medial side of the otic capitulum (Kundrát and Janáček 2007). In *H. huangi*, a pneumatic foramen is autapomorphically located on the ventrolateral surface of the pterygoid flange. On the other hand, an elliptical pneumatic foramen is present on the ventromedial surface of the pterygoid flange in some oviraptorid specimens of Mongolia (Maryańska and Osmólska 1997). This large and ventrodorsally elongated pneumatic opening is subdivided into numerous hollow compartments and leads into a pneumatic chamber invading the quadrate shaft, mandibular articulation, and ventral part of the pterygoid flange (Maryańska and Osmólska 1997).

Dromaeosauridae

Buitreraptor gonzalezorum (MPCA 245); *Bambiraptor feinbergi* (AMNH FARB 30556; Fig. 7.16A–F); *Tsaagan mangas* (IGM 100-1015; Fig. 7.16G–K); *Dromaeosaurus albertensis* (AMNH FARB 5356; Fig. 7.16L–Q); *Velociraptor mongoliensis* (AMNH 6415; Sues 1977; Barsbold and Osmólska 1999); *Sinornithosaurus millenii* (Xu and Wu 2001).

Isolated quadrates of dromaeosaurid theropods have been well-illustrated for *Tsaagan mangas* (Norell et al. 2006) and *Bambiraptor feinbergi* (Burnham 2004), and a detailed description of the bone is given for *T. mangas* (Norell et al. 2006), *Dromaeosaurus albertensis* (Colbert and Russell 1969; Currie 1995), *Velociraptor mongoliensis* (Sues 1977; Barsbold and Osmólska 1999), and *Sinornithosaurus millenii* (Xu and Wu 2001).

As many other theropod clades, the quadrate of Dromaeosauridae is highly diagnostic. The quadrate is particularly short (ratio of the elongation of the quadrate body higher than 0.5) due to an the lateromedially expanded mandibular articulation (Fig. 7.16C–G). The quadrate body has a well-defined quadrate ridge being visible from or directly dorsal to the entocondyle to reach the quadrate head, as in *T. mangas*, *V. mongoliensis*, and *D. albertensis*. The ridge is weakly laterodorsally inclined or extends perpendicular to the main axis of the mandibular articulation (angle between the main axis of the quadrate ridge and the main axis of the mandibular articulation of 80-90°, in posterior view). The quadrate head of derived dromaeosaurid such as *V. mongoliensis* (Barsbold and Osmólska 1999), *D. albertensis* (Currie 1995), *B. feinbergi* (Burnham 2004) and *T. mangas* (Norell et al. 2006) is single-headed and articulates exclusively with the squamosal. A ‘bistylic quadrate head’ (*sensu* Turner et al. 2007*b*) is present in the basal dromaeosaurid *Mahakala omnogovae* and may have been articulated with the squamosal and the prootic of the braincase (Turner et al. 2007*b*, 2011). However, the quadrate head is not double-headed “but the compressed rectangular profile coupled with the abrupt change to a triangular cross section gives the articular portion of the quadrate a medially directed ‘head’” (Turner et al. 2011: p.8).

The quadrate foramen is well-visible in lateral view and typically large (long axis greater than 15% of the ventrodorsal depth of the quadrate; Paul 1988; Barsbold and Osmólska 1999), forming a lanceolate fenestra equally delimited by the quadrate and quadratojugal. In some dromaeosaurids like *T. mangas* and *B. feinbergis*, the quadrate foramen is delimited ventrally by an elongated quadratojugal process; i.e., a well-developed projection of the ventral quadratojugal contact of the quadrate (Fig. 7.16B–H). This quadratojugal process is present in many theropods such as Spinosauridae and Allosauridae, yet the process does not extend much anteriorly, unlike the condition seen in dromaeosaurids. The quadratojugal process is short in the basal dromaeosaurid *Buitreraptor gonzalezorum*.

The dorsomedial margin of the quadrate foramen is formed by a subtriangular or parabolic lateral process. This process is particularly well-developed in *B. gonzalezorum* (MPCA 245), *B.*

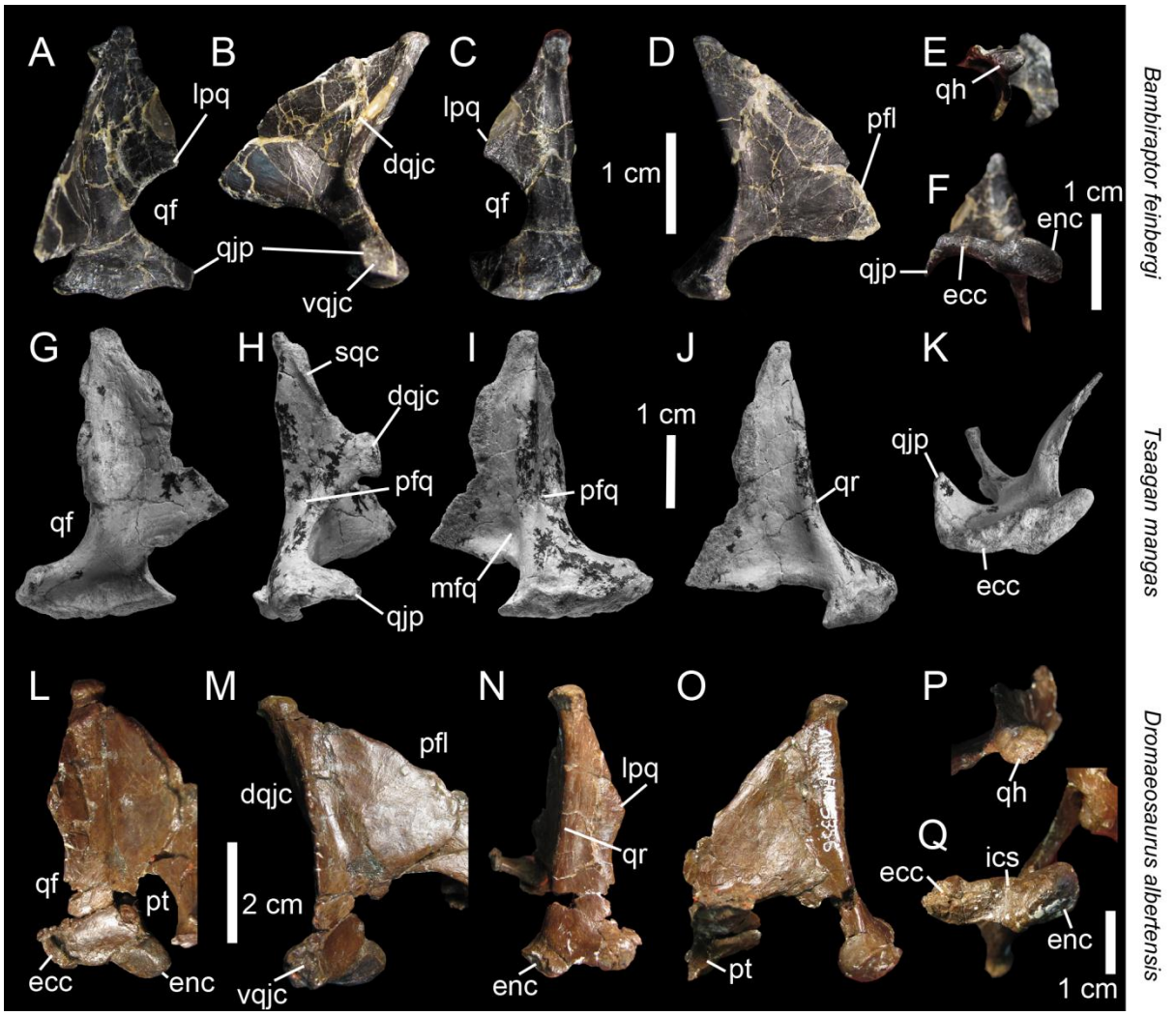

FIGURE 7.16. Quadrate diversity in Dromaeosauridae. **A–F**, Left quadrate of *Bambiraptor feinbergi* (AMNH 30556) in **A**, anterior; **B**, lateral; **C**, posterior; **D**, medial; **E**, dorsal; and **F**, ventral views; **G–K**, Right quadrate of *Tsaagan mangas* (IGM 100-1015) in **G**, anterior; **H**, lateral; **I**, posterior; **J**, medial; and **K**, ventral views (courtesy of Mick Ellison); **L–Q**, Right quadrate of *Dromaeosaurus albertensis* (AMNH 5356) in **L**, anterior; **M**, lateral; **N**, posterior; **O**, medial; **P**, dorsal; and **Q**, ventral views. **Abbreviations**: **dqjc**, dorsal quadratojugal contact; **ecc**, ectocondyle; **enc**, entocondyle; **ics**, intercondylar sulcus; **lpq**, lateral process; **mfq**, medial fossa; **pfl**, pterygoid flange; **pfq**, posterior fossa; **pt**, pterygoid; **qf**, quadrate foramen; **qh**, quadrate head; **qjp**, quadratojugal process; **qr**, quadrate ridge; **sqc**, squamosal contact; **vqjc**, ventral quadratojugal contact; **vptc**, ventral pterygoid contact.

feinbergi (FIP 001; Fig. 7.16C), *T. mangas* (IGM 100-1015; Fig. 7.16H), and *V. mongoliensis* (Barsbold and Osmólska 1999), whereas it is much shorter in *D. albertensis* (AMNH 5356; Fig. 7.16N) and *S. millenii* (Xu and Wu 2001). The orientation of the lateral process is variable among dromaeosaurids, projecting laterally in *D. albertensis*, and *B. gonzalezorum*, and being anterolaterally oriented in *T. mangas* and *Adasaurus mongoliensis*. The lateral process of the latter is apomorphically displaced dorsally, with the anteriormost point of the process being situated at fourth fifth of the quadrate body, slightly below the quadrate head (Turner et al. 2012). A subtriangular lateral process was previously thought to be unique among Dromaeosauridae but, as noted by Agnolin and Novas (2011), this feature is also seen in many basal theropods and basal Avialae such as *Archaeopteryx*

lithographica (Walker 1985). Nevertheless, the morphology of the lateral process of some dromaeosaurids can be apomorphic in possessing a subrectangular projection that receives the dorsal process of the quadratojugal, as in *T. mangas* (Fig. 7.16H).

The atypical pterygoid flange in dromaeosaurid theropods corresponds to a subtriangular flange formed by two elongated sides meeting ventrally in the quadrate body, at one-third or one-fourth of the height of the quadrate bone relative to its ventral end (Xu and Wu 2001; Figs. 7.15D, J, M). The ventral margin of the pterygoid flange joins the quadrate body well-above the entocondyle, whilst the dorsal margin attaches to the quadrate body just beneath the articulating surface of the quadrate head. The dorsal margin of the pterygoid flange is apomorphically columnar in *S. millenii* (Xu and Wu 2001), the margin being thickened and round along most of the flange, contrasting with the thin dorsal margin of the pterygoid flange of other theropods. However, a columnar posterior margin of the pterygoid flange is also seen in an undescribed troodontid (IGM 100-1128). The flange can either be straight and projecting anteromedially like in *B. feinbergi* and *D. albertensis* (Colbert and Russell 1969: fig. 9), or slightly curved anteromedially as in *T. mangas*.

The medial fossa, posteroventrally situated on the pterygoid flange, is shallow and is not excavated by a pneumatic recess. A posterior fossa lies on the posterior side of the quadrate body at mid-height of the quadrate body relative to its ventral end in *T. mangas* (Norell et al. 2006) and *B. feinbergi* (FIP 001). In ventral view, the mandibular articulation consists of an ovoid to oblong entocondyle delimited from the lateromedially wide, anteroposteriorly short and sigmoid/parabolic ectocondyle by a deep intercondylar sulcus (Fig. 7.16F, K, Q). The intercondylar sulcus is anteromedially-oriented and its main axis is sometimes parallel to the main axis passing through the entocondyle. In posterior view, both ecto- and entocondyles are strongly lateromedially-widened and shortly ventrodorsally-expanded. They are delimited by the shallow intercondylar sulcus that gives the mandibular articulation a convex form, rather than a well-marked biconvex shape like in most other non-avian theropods.

A pneumatic quadrate is absent from *T. mangas* (Norell et al. 2006), *B. feinbergi* (Burnham 2004), *V. mongoliensis* (Barsbold and Osmólska 1999) and *D. albertensis* (Currie 1995) but present in the basal dromaeosaurid *B. gonzalezorum* (Makovicky et al. 2005) suggesting that the quadrate may have been pleisiomorphically pneumatic in dromaeosaurids. The pneumatic foramen of *B. gonzalezorum* is deep and subcircular, and the pneumatic opening is located on the posterolateral side of the quadrate body, at the level of the ventral part of the lateral process (Makovicky et al. 2005: fig. 2E).

Troodontidae

Anchiornis huxleyi (Hu et al. 2009); *Xiaotingia zhengi* (Xu et al. 2011*b*); *Mei long* (Xu and Norell 2004; Gao et al. 2012); *Sinovenator changii* (Xu et al. 2002*b*); *Troodon formosus* (Currie and

Zhao 1993*b*); *Saurornithoides mongoliensis* (Norell and Hwang 2004); Troodontidae gen. et sp. indet. (Barsbold et al. 1987); undescribed Troodontidae (IGM 100-1128; IGM 100-1323).

Information regarding quadrate anatomy of Troodontidae (*sensu* Turner et al. 2012 and Godefroit et al. 2013*b*) is very scarce in the literature because most troodontid taxa such as *Saurornithoides mongoliensis* (Russell 1969; Barsbold 1974; Norell et al. 2009), *Zanabazar junior* (Norell et al. 2009), *Byronosaurus jaffei* (Makovicky et al. 2003; Bever and Norell 2009), *Sinovenator changii* (Xu et al. 2002*b*), *Xixiasaurus henanensis* (Lü et al. 2010), and *Troodon formosus* (Currie 1985; Currie and Zhao 1993*b*) either preserved just a small portion of the quadrate or did not have preserved the bone at all. Nevertheless, the quadrates of *Mei long*, *Anchiornis huxleyi* and *Xiaotingia zhengi* are visible in lateral view; the left quadrate of an indeterminate troodontid lacking the pterygoid flange (IGM 100-44) was briefly described and illustrated in posterior view by Barsbold et al. (1987), and a well-preserved ventral portion of a right quadrate probably belonging to *Saurornithoides mongoliensis* has been described by Norell and Hwang (2004). Likewise, the quadrate bone of two undescribed troodontid skulls (IGM 100-1128; IGM 100-1323) from the Upper Cretaceous of Mongolia are also preserved, yet only IGM 100-1128 shows undistorted and relatively complete left and right quadrates.

The troodontid quadrate is moderately, almost very tall (ratio of 0.353 in IGM 100-1128 and 0.4 in IGM 100-44). Both quadrates of IGM 100-1128 are found in articulation within an undistorted skull and their mandibular articulation lies at the same level as the alveolar margin of the upper jaw. This is, however, not the case in *M. long* and *A. huxleyi* in which the mandibular articulation projects well ventral from the ventral margin of the upper jaw. In IGM 100-1128, the ventral half of the quadrate body extends horizontally, perpendicular to the ventral margin of the cranium, whereas the dorsal half is strongly inclined posteriorly so that the quadrate is inclined posteriorly in the cranium and the mandibular articulation is always anterior relative to the quadrate head. A similar condition occurs in *A. huxleyi* (Hu et al. 2009: fig. S2d). The dorsal margin of the quadrate body is parabolic in outline in lateral view in IGM 100-1128, and the medial margin is biconcave. The quadrate ridge is rod-shaped and prominent at one third of the quadrate height relative to its ventral end, and along the second third of the quadrate body. The quadrate ridge does not extend to the entocondyle but reaches the quadrate head.

The quadrate head of IGM 100-1128 is clearly monostylic and contacts the braincase medially. This is the case of the quadrate heads of other troodontid taxa which are also single headed (Currie 1985; Barsbold et al. 1987198) and mostly contacts the squamosal (Currie and Zhao 1993*b*) and other bones of the braincase (exoccipital/opisthotic and prootic), as noted in *T. formosus* (Currie and Zhao 1993*b*), *S. mongoliensis* (Norell et al. 2009), the perinate *Byronosaurus* sp. (Bever and Norell 2009) and *Sinornithoides youngi* (Russell and Dong 1993*b*).

The ventral quadratojugal contact of troodontids is ventrodorsally long, lanceolate, and inclined medially at an angle of 55-65° with the horizontal in posterior view. The ventral

quadratojugal contact faces posterolaterally in IGM 100-1083, and laterally in IGM 100-1128 and IGM 100-44 (Barsbold et al. 1987: plate 49 figure 4). There is no contact with the quadratojugal along the dorsal part of the quadrate body in *M. long* as the quadratojugal of this taxon only gets attached to the lower part of the quadrate body, at the level of the mandibular articulation. Both the quadratojugal and the lateral margin of the quadrate are incomplete in IGM 100-1128 and the presence of a quadrate foramen and a dorsal quadratojugal contact cannot be ruled out in this specimen. A large quadrate foramen similar to that of dromaeosaurids has been noted in *X. zhengi* (Xu et al. 2011*b*). Likewise, the notched lateral margin of the quadrate has been interpreted as contributing to a large quadrate foramen in *A. huxleyi* (Hu et al. 2009: fig. S2d). The quadrate foramen seems to be equally delimited by the quadrate and quadratojugal in these two taxa. However, there is no evidence of a quadrate foramen, nor a dorsal quadratojugal contact on the quadrate of more derived troodontids.

In lateral view, the anterior margin of the pterygoid flange of *M. long* (Xu and Norell 2004: fig. 1B) and IGM 100-1128 is convex and almost subrectangular. The most anterior point is situated at one third of the height of the quadrate body (relative to its ventral end) in both specimens. Similar to the condition seen in Dromaeosauridae, the ventral margin of the pterygoid flange contacts the quadrate body well-dorsal to the entocondyle, at one fifth of the quadrate height (f relative to its ventral end), and the dorsal margin of the flange is strongly inclined anteroventrally at an angle of 40° with the long axis of the skull. The dorsal margin of the flange meets the quadrate head beneath the articular surface of the head, and the flange is straight and projects only anteriorly. Nevertheless, the pterygoid flange of Troodontidae is particularly short anteroposteriorly (ratio of 0.25-0.3; Xu et al. 2011*b*), which is not the case in dromaeosaurids. Some troodontids such as *A. huxleyi* and *X. zhengi* possess a well-developed lateral process (Hu et al. 2009; Xu et al. 2011*b*). It is unknown whether this process is present in more derived troodontid taxa.

The mandibular articulation of troodontid quadrates has only been well-illustrated and well-described by Norell and Hwang (2004) in IGM 100-1083. As in some oviraptorids and dromaeosaurids, the medial margin of the mandibular articulation of IGM 100-1083 is pointed in posterior view, but the medial corner is oriented medially. On the other hand, the medial margin of the entocondyle is rounded and does not show this medial corner in IGM 100-44 and IGM 100-1128, yet the ventral margin of the ectocondyle is pointed in posterior view in both specimens. In ventral view, the mandibular articulation of IGM 100-1083 is composed of two condyles separated by a shallow and poorly delimited intercondylar sulcus. The condyles are roughly oval and the entocondyle is lateromedially wider than the ectocondyle, as observed in IGM 100-44 (Barsbold et al. 1987: plate 49, fig. 4) and IGM 100-1128 in posterior view. There is no quadratojugal process in IGM 100-1083 and IGM 100-1128.

Quadrate pneumaticity in Troodontidae is well-known (Varricchio 1997) and has been reported in a Jurassic troodontid (Hartman et al. 2005), *T. formosus* (Currie and Zhao 1993*b*), *S. changii* (Xu et al. 2002*b*), *M. long* (Xu and Norell 2004; Gao et al. 2012) and *X. zhengi* (Xu et al.

2011*b*) where a posterior pneumatic foramen has been observed on the quadrate body in the two latter taxa. This is also the case of the quadrate described by Barsbold et al. (1987) which has a small pneumatic foramen positioned medially on the posterior surface of the quadrate body, at mid-height of the bone, and leading to a canal (Barsbold et al. 1987). Because a pneumatic chamber is absent in the broken quadrate of IGM 100-1083 (Norell and Hwang 2004), it is possible that some troodontid quadrate did not possess a pneumatic quadrate.

Discussion

Cladistic Analysis

This cladistic analysis performed based on a character data matrix related to one single bone gives strikingly similar results to those from analyses using characters from the entire skeleton (Figs. 7.1 & 2). The well-resolved tree follows the topology of the classification of non-avian theropods, thus demonstrating the phylogenetic value of the quadrate and offering more quadrate-related characters to be used in future cladistic analyses.

Expectedly, when analyzed in a phylogenetic context, the morphology of the quadrate recovers all major non-avian theropod clades (Neotheropoda, Ceratosauria, Tetanurae and Avetheropoda) as well as more restricted clades (e.g., Abelisauroidea, Abelisauridae, Megalosauridae, Spinosauridae, Carcharodontosauridae, Tyrannosauridae, Dromaeosauridae) supporting the idea that many quadrate synapomorphies contribute to clarifying non-avian theropod relationships.

Although the major clades of non-avian theropods have been found resolved by this analysis, some important discrepancies with the current classification of theropods are apparent. The disparate position of basal and derived Allosauroidea is the most striking and can be explained by the following characters: the shape of the ventral part above the mandibular articulation on the posterior surface of the quadrate body (char. 8) and the morphology of the mandibular articulation (chars. 20, 28, 19) and the quadrate foramen (chars. 73, 76). In basal allosauroids (Allosauridae, Sinraptoridae and Neovenatoridae), the posterior surface of the quadrate body dorsal to the mandibular articulation is deeply concave whereas it is strongly convex in Carcharodontosauridae. In addition, the mandibular articulation of carcharodontosaurids is lateromedially wider than those of basal allosauroids: the ectocondyle is lateromedially wide, parabolic and with a sigmoid anterior margin, convergent with the ectocondyle morphology of dromaeosaurids, whereas in other allosauroids, the ectocondyle is shorter, ovoid and with a convex anterior margin in ventral view. As in dromaeosaurids, the quadrate foramen of carcharodontosaurids is also equally delimited by the quadrate and quadratojugal and situated well ventral to the mid-height of the quadrate body. In basal allosauroids, and by convergence with therizinosaurs, the quadrate foramen is roughly positioned at mid-height of the quadrate, mostly delimited by the quadrate and elliptical or bean-shaped.

Major Trends in the Evolution of the Quadrate in Non-avian Theropods

The results of the phylogenetic analysis allow the identification of evolutionary trends of the quadrate across Theropoda. Our intention is to propose simple hypotheses as a result of our phylogenetic results and anatomical overview, the understanding of the functional reasons and interdependence of anatomical sub-units will be reserved for another study. The major trends can be summarized as follows:

Quadrate body—Shortening of the height of the quadrate body and widening of the mandibular articulation across the evolution of Tyrannosauroidea, Megalosauroidea towards Spinosauridae, and Maniraptoriformes towards Dromaeosauridae. Tall quadrates with lateromedially narrow mandibular articulation can be seen in ceratosaurs and ornithomimosaurs while ventrodorsally short quadrates with lateromedially wide mandibular articulation are present in spinosaurids, tyrannosaurids and dromaeosaurids.

Quadrate ridge—Widening of the ridge across the evolution of Megalosauroidea leading to Spinosauridae, and narrowing of it in Tyrannosauroidea and Coelophysoidea. Most of non-avian theropods have rod-shaped ridges, but the Coelophysoidea, Tyrannosauridae and the neovenatorid *Aerosteon* have a lateromedially narrow crest-like ridge, whereas the Spinosauridae possess a very lateromedially wide shaft-like ridge. The quadrate ridge is usually well-delimited in non-avian theropods but a very poorly defined ridge can be observed in abelisauroids, *Eustreptospondylus*, ornithomimosaurs, therizinosaurs and oviraptorosaurs.

Quadrate foramen—1) Loss of the quadrate foramen independently in Ceratosauria and Megalosauridae. 2) Reduction of the size of the foramen during the evolution of the Spinosauridae and increase of the foramen size in Tyrannosauroidea. A small quadrate foramen is seen in non-tetanuran theropods, spinosaurines and basal Tyrannosauroidea while a large quadrate foramen (or quadrate fenestra) can be seen in some Baryonychinae, Tyrannosauroidea, Alvarezsauroidea and Dromaeosauridae. 3) Increase of the contribution of the quadratojugal to the quadrate foramen during the evolution of Coelurosauria. The quadrate foramen is mostly delimited by the quadrate in all non-avian theropods other than Maniraptoriformes (*Falcarius* excluded) where the contribution of the quadrate and quadratojugal in the foramen is roughly equal.

Lateral process—1) Loss of the lateral process in Tetanurae. A lateral process is absent in basal tetanurans, megalosauroids (*Irritator* excluded), and some basal averostrans. A very well-developed subtriangular lateral process anterolaterally oriented is seen in basal theropods and ceratosaurs, and also in alvarezsaurids, therizinosauroids, and dromaeosaurids where this structure reappears. 2) Ventral extension of the lateral process during the evolution of Ceratosauria. In basal-most theropods, coelophysoids (Dilophosauridae + Coelophysidae), some ceratosaurs (Ceratosauridae + Noasauridae), derived therizinosauroids, alvarezsauroids, and dromaeosaurids, the lateral process extends ventrally at mid-height of the quadrate body, from the quadrate foramen when present.

However, in Abelisauroidea the lateral process extends ventrally at the level of the mandibular articulation or directly dorsal to it.

Pterygoid flange—1) Dorsal displacement of the anteriormost point of the pterygoid flange in Ceratosauria and Megalosauroidea, and 2) ventral displacement of this point during the evolution of Dromaeosauridae and Therizinosauria. The anteriormost point of the pterygoid flange of most non-avian theropods is situated at mid-height of the quadrate in lateral/medial views. On the other hand, this point is situated at two thirds of the quadrate height relative to its ventral end in ceratosaurs and megalosauroids, and at one-third of the quadrate in *Erlikosaurus*, *Zuolong* and some dromaeosaurids. 3) Appearance of a medial fold of the ventral margin of the pterygoid flange in Ceratosauria and disappearance of it in Megalosauridae, derived Carcharodontosauridae, and Coelurosauria. A straight ventral margin of the pterygoid flange is present in basal theropods, megalosaurids, derived carcharodontosaurids and coelurosaurs. The ventral margin of this flange is folded medially in ceratosaurs, basal tetanurans, spinosaurids, sinraptorids and neovenatorids, and mediodorsally or dorsally folded in allosaurids and basal carcharodontosaurids.

Quadrate head—1) Dorsal displacement of the quadrate head to or close to the level of the dorsal margin of the orbit in Ceratosauria and Megalosauridae. A quadrate head at the level or slightly ventral to the dorsal margin of the orbit can be seen in most ceratosaurs and megalosaurids whereas all other non-avian theropods show a quadrate head well ventral to the dorsal margin of the orbit. 2) Decrease of the lateromedial width of the quadrate head (relative to the width of the mandibular articulation) across the evolution of Allosauroidea and Dromaeosauridae. 3) Development of two capitula in the quadrate head during the evolution of Tyrannosauridae, Oviraptorosauria and Alvarezsauridae (and convergently in Avialae). The quadrate head is single headed in most non-avian theropods other than oviraptosaurids and the derived alvarezsaurid *Shuvuuia* which possess two well-distinguished heads contacting the squamosal and the braincase.

Mandibular articulation—1) Ventral displacement of the mandibular articulation in Spinosauridae and Avetheropoda, and dorsal displacement of the mandibular articulation to be situated at the level of the alveolar margin of the maxilla in Tyrannosauridae. A mandibular articulation at the level of the alveolar margin of the maxilla can be seen in most basal Theropoda, most Ceratosauria, basal Tetanurae, Megalosauridae and Tyrannosauridae. On the other hand, a mandibular articulation projecting well-ventral to the alveolar margin of the cranium is seen in *Irritator*, the coelophysoid *Zupaysaurus* and most avetheropods. 2) Lateromedial widening of the mandibular articulation during the evolution of Megalosauroidea, Allosauroidea and Maniraptoriformes, and increase of its anteroposterior length during the evolution of Ceratosauria. A very lateromedially wide mandibular articulation (ratio > 3) is seen in Spinosauridae, Carcharodontosauridae and Deinonychosauria, whereas a particularly anteroposteriorly long mandibular articulation (ratio < 2) appears in Ceratosauria.

Entocondyle—Increase of the lateromedial width of the entocondyle during the evolution of Ceratosauria, Oviraptorosauria and some Megalosauridae. Among non-avian theropods, an entocondyle wider than the ectocondyle is seen in Abelisauroidea, Oviraptoridae and the megalosaurid *Afrovenator*.

Ectocondyle—Development of a sigmoid ectocondyle in Dilophosauridae and Spinosauridae, and an ovoid ectocondyle in Abelisauroidea, Oviraptorosauria, basal Allosauroidea, Tyrannosauroidea, and Therizinosauria.

Pneumaticity—1) Pneumatization of the quadrate independently in Carcharodontosauridae, Megaraptora, Tyrannosauridae and Maniraptoriformes. 2) Reduction of the size of the medial pneumatic foramen in derived Carcharodontosauridae.

Phylogenetic Morphometrics Analysis

Phylogenetic morphometrics characters are here proposed for the first time for Dinosauria. By exclusively analyzing the ventral view of the mandibular articulation of non-avian theropods (analysis 2, character 2; Fig. 7.2.2) two distinct 'morphoclades' emerged from the analysis. This presents evidence of two fundamentally distinct morphotypes that might be congruent with two differently adapted functional systems.

The first morphotype of the mandibular articulation (morphotype A) is characterized by an anteroposteriorly long mandibular articulation, two ovoid/subcircular ecto- and entocondyles roughly subequal in size, and an intercondylar sulcus in which the angle formed by the main axis of the sulcus and the long axis of mandibular articulation is relatively low (< 135°). This morphotype is present in all ceratosaurs and also in oviraptorosaurs, therizinosaurs, megaraptorans, tyrannosaurids and *Allosaurus* '*jimmadseni*'. Morphotype A is present in a large variety of non-avian theropods, from the small and slender oviraptorosaurs to the large and robust tyrannosaurids. However, all of these taxa share a roughly similar articulation with the lower jaw. In these theropods, the two rami of the mandibles are slightly displaced laterally when the mouth opened, due to the lateromedially narrow ectocondyle and mandibular articulation, and an angle of the intercondylar sulcus of less than 135°, lower than in the second morphotype.

On the other hand, the second morphotype (morphotype B) corresponds to an elongate and anteroposteriorly short mandibular articulation, a lateromedially wide and parabolic/sigmoid ectocondyle much wider than the entocondyle, and an intercondylar sulcus in which the angle between the main axis passing through the sulcus also the long axis of the mandibular articulation is high (more than 135°). This combination of features allows the lower jaw rami to be slightly to strongly displaced laterally when sliding along the intercondylar sulcus of the quadrate. Morphotype B can be seen in a large variety of theropods as they include all megalosauroids other than *Afrovenator*, *Dilophosaurus*, *Allosaurus fragilis*, the dromaeosaurids and the carcharodontosaurids. Once again, although these theropods with morphotype B show some important morphological disparity in their skull and body, it

seems that their mandibular articulation was morphofunctionally convergent. These theropods were able to enlarge the pharynx by opening the mouth like some ornithocheiroid pterosaurs and living pelecanid birds (Wellnhofer 1980; Bennett 2001; Ibrahim 2008).

The presence of *Sinraptor* and *Acrocanthosaurus* at the base of each 'morphotypes' clearly demonstrates the transition from one morphotype to the other during the evolution of Allosauroidea. Likewise, the presence of *Allosaurus* in both morphotypes implies some important variability of the mandibular articulation among this particular taxon.

Although their skull seem to be very disparate, morphotype A includes theropods with either relatively short and broad skulls resisting torsional bending like ceratosaurs, some allosauroids and tyrannosaurids (Rayfield 2005*a*; Sampson and Witmer 2007), or beaked skulls like in the herbivorous oviraptorosaurs and therizinosaurs (Zanno et al. 2009). In both cases, an anteroposteriorly long and lateromedially narrow articulation of the quadrate was advantageous for either feeding on large prey or on hard plants thanks to a powerful and high efficiency biting (Therrien et al. 2005; Sakamoto 2010). On the other hand, theropods with a lateromedially widened mandibular articulation displaying a strongly diagonally oriented intercondylar sulcus where those favoring the deglutition of whole prey, or large chunk of food. They include weak and fast biter theropods with elongated skulls like Dilophosauridae, Spinosauridae and Dromaeosauridae (Sakamoto 2010). Those theropods were feeding on relatively small prey they were swallowing in one piece such as fishes (Charig and Milner 1997; Ibrahim 2008) and perhaps insects (Senter 2009). Morphotype B also includes massive theropods with extremely powerful skulls like Carcharodontosauridae and *Torvosaurus* that must have swallowed large chunk of meat from prey they would easily disarticulate owing their strong bite force (Therrien et al. 2005; Sakamoto 2010).

Conclusion

The present study goes along the lines of other research efforts that recognize that a single bone can bear a wealth of phylogenetic information that cannot be dismissed, such as the quadrate of mosasaurs (Polcyn and Bell 2005), the ilium of anura (Gardner et al. 2010), the coracoid of eosauropterygian (White 1940) or the teeth of ornithopods (Araújo et al. 2008). To the eight characters on the quadrate bones used in one of the most recent publication on a phylogenetic context for non-avian theropod (Choiniere et al. 2014*b*), we added 80 quadrate related characters to obtain 94 characters that help to describe the disparity and evolutionary transformations of the bone. Many quadrate-related characters are synapomorphic to several major theropod clades such as Neotheropoda, Averostra, Ceratosauria, Tetanurae, Megalosauroidea and Avetheropoda and almost all subclades of non-avian theropods (e.g., Abelisauridae, Megalosauridae, Spinosauridae, Carcharodontosauridae, Tyrannosauridae, Oviraptoridae and Dromaeosauridae) are recovered based on the combination of homologous and non-homologous quadrate related synapomorphies.

The cladistic analysis performed on the data matrix of 98 quadrate related characters allowed many evolutionary trends for this bone to be drawn such as 1) a shortening of the ventrodorsal height of the quadrate body and lateromedial widening of the mandibular articulation across the evolution of Theropoda, 2) the loss of the quadrate foramen independently in Ceratosauria and Megalosauridae, 3) the loss of the lateral process in Tetanurae and 4) a lateromedial narrowing of the quadrate ridge in Tyrannosauridae.

Phylogenetic morphometrics analysis on the quadrate bone in non-avian theropods also recovered the existence of two different morphotypes in the mandibular articulation. These morphotypes almost certainly reflect the functional aspect of the articulation between the lower jaw and the cranium. In morphotype A, characterized by an anteroposteriorly long mandibular articulation with two ovoid/subcircular condyles roughly subequal in size, the lateral displacement of the mandible was weak or even inexistent. On the other hand, in morphotype B characterized by an elongate and anteroposteriorly short mandibular articulation and a lateromedially wide and parabolic/sigmoid ectocondyle, the lower jaw rami was displaced laterally when the mouth opened.

Chapter 8: Morphofunctional analysis of the quadrate of Spinosauridae (Dinosauria: Theropoda) and the first definitive evidence of two cohabiting *Spinosaurus* in the Upper Cretaceous of North Africa.

Submitted to ***PLoS ONE*** (IP 3.534):
Hendrickx, C., Mateus, O and Buffetaut, E. in review. Morphofunctional analysis of the quadrate of Spinosauridae (Dinosauria: Theropoda) and the first definitive evidence of two cohabiting spinosaurids in the Upper Cretaceous of North Africa. *PLoS ONE*.

Abstract

Six quadrate bones from the Kem Kem beds (Cenomanian, Upper Cretaceous) of South-eastern Morocco are determined to be from juvenile and adult individuals of Spinosaurinae based on phylogenetic, morphometric, and phylogenetic morphometric analyses. Their morphology indicates two morphotypes evidencing the presence of two coexisting spinosaurine taxa ascribed to two species of *Spinosaurus*, increasing the already large diversity of theropod dinosaurs in the Kem Kem beds and casting doubt on the accuracy of some recent skeletal reconstructions which may be based on elements from several distinct species. Morphofunctional analysis of the mandibular articulation of the quadrate has shown that the jaw mechanics was peculiar in Spinosauridae. In mature spinosaurids, the posterior parts of the two mandibular rami displaced laterally when the jaw was depressed due to a mediolaterally oriented intercondylar sulcus of the quadrate. Such lateral movement of the mandibular ramus was possible due to a movable mandibular symphysis in spinosaurids, allowing the pharynx to be widened. Similar jaw mechanics also occur in some pterosaurs and living pelecanids which are both adapted to capture and swallow large prey items. Spinosauridae, which were engaged, at least partially, in a piscivorous lifestyle, were able to consume large fish and may have occasionally fed on other prey such as pterosaurs and juvenile dinosaurs.

Introduction

The Kem Kem region of South-eastern Morocco (Fig. 8.1A) is very well known for its rich vertebrate assemblage of Cenomanian in age, which is characterized by a particularly high diversity of predatory dinosaurs (Russell 1996; Sereno et al. 1996; Ibrahim 2008; Cavin et al. 2010; Cau et al. 2013; Läng et al. 2013; McFeeters et al. 2013; Richter et al. 2013; Evans et al. 2014). The presence of at least five non-avian theropod clades has been documented in the Kem Kem beds hitherto including non-abelisaurid Ceratosauria (Noasauridae?), Abelisauridae, Spinosauridae, Carcharodontosauridae, and Dromaeosauridae.

Ceratosaurs are represented by abelisaurids (Russell 1996; Sereno et al. 2004; Mahler 2005; Porchetti et al. 2011; Richter et al. 2013), and *Deltadromeus agilis* (Sereno et al. 1996) interpreted

either as a basal form (Carrano and Sampson 2008; Pol and Rauhut 2012) or a noasaurid (Sereno et al. 2004; Tortosa et al. 2014). Material resembling the primitive ceratosaurs *Elaphrosaurus* was already reported by Lavocat (1954*b*), and additional remains of noasaurids have been recently described and may belong to a juvenile individual of *Deltadromeus* (Evans et al. 2014). Among tetanurans, spinosaurids are documented by material assigned to two species of *Spinosaurus*, namely *Spinosaurus aegyptiacus* (Buffetaut 1989*b*, *c*, 1992; Milner 2003; Dal Sasso et al. 2005; Ibrahim et al. 2014*b*) and *Spinosaurus maroccanus* (Russell 1996; Taquet and Russell 1998). Likewise, carcharodontosaurid allosauroids are represented by at least two taxa: the very large form *Carcharodontosaurus saharicus* (Lavocat 1954*b*; Sereno et al. 1996; Brusatte and Sereno 2007), and the thick-skulled *Sauroniops pachytholus* (Cau et al. 2012, 2013). *Sigilmassasaurus brevicolis*, coined by Russell (1996) and initially classified to the new clade Sigilmassasauridae, was interpreted as belonging to *Carcharodontosaurus saharicus* (Sereno et al. 1998; Brusatte and Sereno 2007; Cavin et al. 2010), *Spinosaurus maroccanus* (Mahler 2005), and recently to *Spinosaurus aegyptiacus* (Ibrahim et al. 2014*b*). This hypothesis was rejected by Novas et al. (2005), and recent investigations on the anatomy of *Sigilmassasaurus* retained it as a valid taxon, and a tetanuran other than a carcharodontosaurid (McFeeters et al. 2013). Yet, the recent discovery of additional material of *Spinosaurus aegyptiacus* and *Ichthyovenator laosensis* supports the fact that all material ascribed to the taxon *Sigilmassasaurus* belong to the species *S. aegyptiacus* (Allain 2014; Ibrahim et al. 2014*b*). Finally, Dromaeosauridae, the only known non-avian coelurosaurs from the Kem Kem beds, have so far been documented by isolated teeth (Amiot et al. 2004*a*; Richter et al. 2013). *Kemkemia*, an additional theropod of uncertain affinities known from a single caudal vertebra (Cau and Maganuco 2009), was reinterpreted as belonging to a Crocodyliformes *incertea sedis* (Lio et al. 2012). Likewise, an isolated vertebra of avian origin was reported by Riff et al. (2004) but does not seem to preserve any avian synapomorphies (Cavin et al. 2010). Birds seem, however, to be present in the Kem Kem beds alongside non-avian dinosaurs (Cavin et al. 2010).

Various scenarios have been suggested to explain such large diversity of theropods while herbivorous dinosaurs seem to be rare. The latter are indeed documented by a few ornithopod tracks (Ibrahim et al. 2014*a*) and sauropods (Ibrahim 2008; Cavin et al. 2010), known from two clades only, i.e., Rebbachisauridae and Lithostrothia (e.g., Lavocat 1951, 1952, 1954*b*, 1955; Russell 1996; Sereno et al. 1996; Cavin et al. 2010; Mannion and Calvo 2011; Mannion and Barrett 2013; Lamanna and Hasegawa 2014). The dominant theropod assemblage in the Kem Kem was first interpreted by Russell (1996) as resulting from an attraction of the predators to the margin of streams which were a major source of prey, or from a food chain linked to large bodies of water. Yet, the apparent scarcity of herbivorous taxa may indicate biased collecting in the Kem Kem area (McGowan and Dyke 2009). This overabundance of carnivorous dinosaurs may also be caused by the effect of ‘time-averaging’ in which fossils of different ages are mixed into a single rock layer, therefore altering the interpretation of the ecosystems based on fossil collections (Dyke 2010). Nonetheless, an unbalanced ratio between

herbivorous and carnivorous dinosaurs was clearly observed by Läng et al. (2013) based on field data. These authors suggest that such an abundance of predators is linked to a widespread deltaic paleoenvironment with unstable climatic and hydric features. Such an heterogeneous environment would have indeed favoured the existence of many ecological niches, and the very abundant aquatic life could have formed the base of an aquatic or semi-aquatic food chain which could have directly fed top predators (Läng et al. 2013).

Spinosaurid material seems to be particularly abundant in the Kem Kem beds (spinosaurid teeth represent 60% of the dinosaurian fauna in all considered samples collected in the Ifezouane Formation; Amiot et al. 2004*a*; Läng et al. 2013), and isolated teeth and cranial and postcranial bones of Spinosauridae have been regularly reported in the literature over the past 30 years (Cavin et al. 2010). Although a probable spinosaurid tooth from the Kem Kem beds was illustrated and misinterpreted as belonging to *Crocodilus* sp. by Choubert et al. in 1952 (Cavin et al. 2010), spinosaurid material from Morocco was first reported by Taquet (1984). This author was the first to mention the presence of this family in the Kem Kem region, and Buffetaut (1989*b*, 1992) was the first to describe and refer to an incomplete maxilla from the continental red beds to *Spinosaurus* cf. *aegyptiacus*. An American expedition in the Sahara desert in 1995 led to the discovery of additional remains of *Spinosaurus* from the Kem Kem region, including isolated teeth, fused nasals and vertebrae (Sereno et al. 1996; Dal Sasso et al. 2005; Ibrahim and Sereno 2011). Dentary fragments, a cervical vertebra and a dorsal neural arch collected in the Tafilalt plain (northern part of the Kem Kem region) by locals, allowed Russell (1996) to erect a second species of *Spinosaurus*, *S. maroccanus*. Isolated teeth from the Kem Kem beds were also reported by Kellner (1996) and Sadleir (2008) who identified the material as belonging to a spinosaurid and the genus *Spinosaurus*, respectively. In the beginning of the 21st century, more complete and better preserved skull remains were assigned to the species *S. aegyptiacus*. Milner (2003) briefly described an incomplete snout and a left dentary deposited in the Natural History Museum of London. Two years later, Dal Sasso et al. (2005) reported a well-preserved snout of very large size collected by locals in 1975, and ascribed the materiel to *Spinosaurus aegyptiacus*. More recently, the enamel texture of *Spinosaurus* teeth from the Kem Kem was investigated by Hasegawa et al. (2010) whereas three morphotypes of isolated teeth assigned to *Spinosaurus* were described by Richter et al. (2013) and may attest the presence of more than one species of *Spinosaurus* in the Kem Kem. Finally, the discovery of the first associated cranial and postcranial material of *Spinosaurus aegyptiacus* by an international team of paleontologists in the Zrigat locality (northern part of the Tafilalt) in 2013 allowed an accurate reconstruction of this animal's anatomy to be given for the first time (Ibrahim et al. 2014*b*).

Functional morphology of the spinosaurid mandible and cranium were investigated by Therrien et al. (2005), and Rayfield et al. (2007), Rayfield (2011) and Cuff and Rayfield (2013) respectively. Therrien et al. (2005) study on the biomechanical properties of the jaws of *Suchomimus* (n.b., given the paleogeographic and stratigraphic distribution of the two taxa, *Suchomimus tenerensis*

Sereno et al. 1998 is most likely a junior synonym of *Cristatusaurus lapparenti*) based on beam theory indicates that spinosaurid theropods were specialized in capturing small prey thanks to their upturned chin with the terminal rosette, large mandibular symphysis allowing to resist the important stresses induced by struggling prey, and conical teeth designed to impale and hold prey and withstand bending loads applied in all directions. Rayfield et al.'s (2007) study based on finite element analysis (FEA) on the rostrum of *Baryonyx* reveals that the snout of *Baryonyx* and *Gavialis* are morphologically and functionally homologous in terms of resistance to bending and torsional feeding loads, thereby supporting the hypothesis of a partially piscivorous lifestyle in this theropod as well. Using FEA on 2D models of skulls, Rayfield (2011) found that *Suchomimus* and *Spinosaurus*' skulls experience cranial stresses in different ways. Whereas *Suchomimus* is scaling in a similar manner to most non-spinosaurid tetanurans, *Spinosaurus* experiences a much higher magnitude of cranial stress than what would be predicted, suggesting it may have fed on smaller prey. This hypothesis was later confirmed by Cuff and Rayfield (2013) whose results of FEA on 3D models of the *Baryonyx* and *Spinosaurus* snout suggest that the crania of both taxa resist well to dorsoventral bending but are poorly equipped to resist mediolateral and torsional loads.

Here we report additional cranial material of spinosaurids from the Kem Kem beds consisting of six isolated quadrates. The quadrate is a cranial bone of endochondral origin that articulates with the mandible in all gnathostomes other than mammals (Carroll 1988; Benton 2005; Brusatte 2012). In theropods, the quadrate had many important functions such as a structural support for the basicranium, an articulatory element with the lower jaw, insertion area for several muscles, and in hosting important nerves, pneumatic sinuses, and vascular passages (e.g., Witmer 1990, 1997; Bakker 1998; Sedlmayr 2002; Kundrát and Janáček 2007; Holliday and Witmer 2008; Tahara and Larsson 2011). This work aims to investigate the phylogenetic position of the isolated quadrates and the morphofunctional aspects of their mandibular articulations based on cladistic, morphometric, and phylogenetic morphometric analyses.

Material and methods

Material and geological settings

Six isolated quadrates of different sizes were collected in the Kem Kem beds of southern Morocco (Fig. 8.1A) by locals and acquired commercially. Five bones (MHNM.KK374 to .KK378; Figs. 8.2–8.4; see Appendices A8 Fig. A8.1) were provided by François Escuillié and are deposited in the collections of the Muséum d'Histoire Naturelle of Marrakech (MHNM). A sixth quadrate (MSNM V6896; Fig. 8.3M–R) was donated to the Museo di Storia Naturale di Milano by an Italian fossil dealer who purchased it from locals (Dal Sasso pers. comm.). Two specimens, MHNM.KK376 and .KK378, were uncovered in reddish to violet sandstones with peddles near the town of Jorf (Tafilalt) northwest of Erfoud (Fig. 8.1A; Escuillié pers. comm.). Unfortunately, the exact horizon and locality

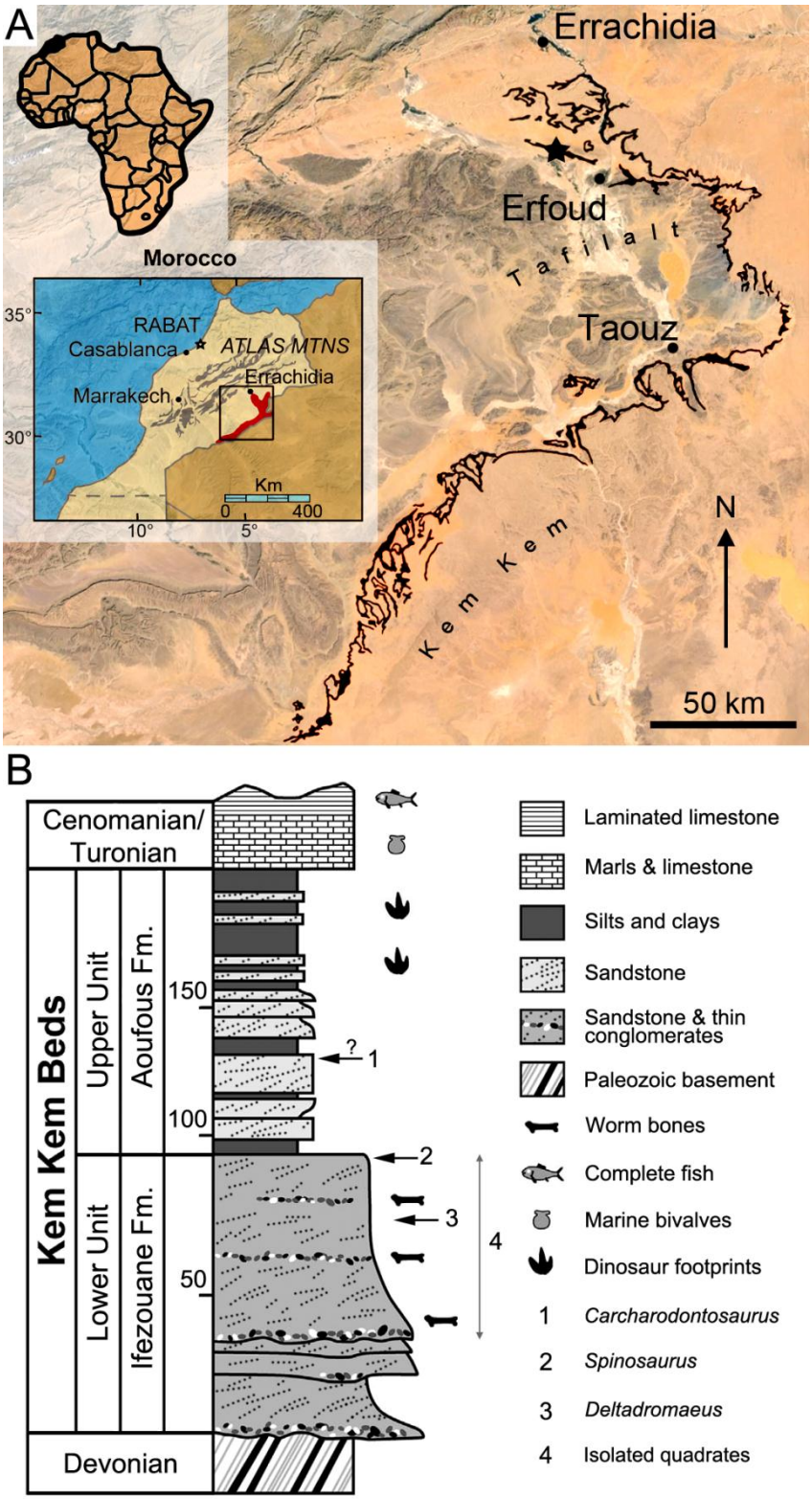

FIGURE 8.1. Geographical location and stratigraphy of the Kem Kem beds. **A**, Location of Morocco (in black) in Africa (left corner), the Kem Kem and Tafilalt regions (in red) in Morocco (middle left), and the Kem Kem beds (in black) in the Kem Kem plateau (right). The black star indicates the site in which two quadrates were found; **B**, Stratigraphic column of the Kem Kem beds of South-Eastern Morocco. Stratigraphic position of the type remains of **1**, *Carcharodontosaurus saharicus* (neotype; Sereno et al. 1996; Brusatte and Sereno 2007); **2**, *Spinosaurus aegyptiacus* (neotype; Ibrahim et al. 2014*b*); and **3**, *Deltadromeus agilis* (holotype; Sereno et al. 1996); and **4**, probable stratigraphic position of the here studied material. The presence of *Carcharodontosaurus* material in the 'upper unit' is here questioned. Modified from Sereno et al. (1996) and Ibrahim et al. (2014*a*).

of the other specimens are unknown, yet the three other bones housed at the MHNM were bought in local markets in Erfoud (Escuillié pers. comm.). Based on the general color of the bone, MHNM.KK374 was found in reddish iron-rich sandstones, whereas MHNM.KK375, .KK377 and MSNM V6896 come from ironless layers of white to yellow sandstones.

Sediment adhering to the six quadrates is consistent with the lithology of the Kem Kem beds in color, composition, and texture, and the material most certainly comes from this lithostratigraphic unit. The Kem Kem beds are dated to the Cenomanian (and likely to the early Cenomanian; Cavin et al. 2010; Benyoucef et al. 2015) and divided into the Ifezouane and Aoufous formations, which correspond to the lower and upper units of Sereno et al. (1996), respectively (Fig. 8.1B; for the geology, stratigraphy, and paleoenvironment of the Kem Kem beds, see Introduction section Case of study and Figs. 1.17–1.18, as well as Cavin et al. (2010) and references therein). Given the fact that the large majority of fossil vertebrates come from the upper part of the Ifezouane Formation (even in the northern Kem Kem area, see Chapter 1 section Case of study), all specimens most probably come from this unit (Cavin et al. 2010; Läng et al. 2013; Ibrahim et al. 2014*b*; Cavin pers. comm.; Fig. 8.1B). The Aoufous Formation has indeed yielded a very few amount of vertebrate fossils (Cavin et al. 2010; Ibrahim et al. 2014*b*), and large vertebrate remains seem to always come from the Ifezouane Formation (Cavin pers. comm.). In addition, the Aoufous Formation essentially includes marls and mudstones (Cavin et al. 2010; Ibrahim et al. 2014*b*), and the sandstone matrix visible on the quadrates supports the fact that they were uncovered in the Ifezouane Formation.

Anatomical Nomenclature

The description of the quadrates follows the anatomical terminology proposed by Hendrickx et al. (2014a; see Chapter 6, Fig. 6.2) which can be summarized as follow: The quadrate is comprised of two main parts: the quadrate body posteriorly, and the pterygoid flange anteriorly. The latter projects anteriorly from the quadrate body to contact the pterygoid. The quadrate body includes the quadrate shaft, which links the quadrate head dorsally to the mandibular articulation ventrally. The quadrate foramen, which typically lies at mid-height of the quadrate body, separates the ventral quadratojugal contact from the dorsal quadratojugal contact, which faces laterally, and sometimes anteriorly or posteriorly. Two processes project laterally or anterolaterally from the lateral margin of the quadrate body, namely the lateral process and the quadratojugal process. The lateral process either extends from the laterodorsal part of the quadrate body, dorsal to the quadrate foramen, or from the whole lateral margin of the quadrate shaft, whereas the quadratojugal process always projects anteriorly from the anterior margin of the ventral quadratojugal contact. The quadrate shaft corresponds to the part of the quadrate body excluding the quadrate head, mandibular articulation, quadratojugal contacts, lateral process, and quadratojugal process. The quadrate shaft typically includes a ventrodorsally oriented ridge, or quadrate ridge, on its posteromedial side. In some cases, the quadrate shaft also encompasses a ventrodorsally elongated depression, or fossa, on the posterior

side of the quadrate and known as the posterior fossa. A second depression, the medial fossa, is located in the ventromedial surface of the pterygoid flange and is bounded by the quadrate shaft posteriorly. The quadrate head can be single headed, or double headed and divided by an intercapitular sulcus into the squamosal and otic capitula. The mandibular articulation includes, in the large majority of theropods, two condyles. The lateral condyle of the mandibular articulation, called ectocondyle, is separated from the medial condyle, or entocondyle, by the intercondylar sulcus. An intercondylar notch can sometimes be seen either on the anterior or posterior surface of the intercondylar sulcus, between the mandibular condyles. When pneumatic, the quadrate includes one or several pneumatic openings, i.e., the anterior, posterior, medial, ventral and dorsal pneumatic opening, pending on their position on the quadrate.

Cladistic Analysis

A phylogenetic analysis was performed to assess the phylogenetic relationships of the quadrate bones from the Kem Kem beds and the bones were coded in an updated version of the supermatrix of Hendrickx and Mateus (2014*b*). The supermatrix encompasses 98 quadrate related characters originally associated with six recent datasets (i.e., Brusatte et al. 2010*d*; Choiniere et al. 2010; Martinez et al. 2011; Carrano et al. 2012; Pol and Rauhut 2012) on the whole theropod skeleton. All quadrate based characters were removed from the six datasets. The main changes are the inclusion, in the supermatrix, of the data matrix of Novas et al. (2012) as well as four additional taxa (i.e., *Spinosaurus*, *Guanlong*, *Sinosauropteryx*, and *Ornithomimus*), and the replacement of the dataset of Choiniere et al. (2010) by an updated version of Choiniere et al. (2014). The final supermatrix includes 2377 characters and 59 taxa for one outgroup (*Eoraptor*; Appendices A8.1). TNT v1.1 (Goloboff et al. 2008) was employed to search for most-parsimonious trees (MPTs). The supermatrix was analyzed under the ‘New Technology Search’ with the ‘driven search’ option (TreeDrift, Tree Fusing, Ratchet, and Sectorial Searches selected with default parameters), and stabilizing the consensus twice with a factor of 75. The consistency and retention indices as well as the Bremer supports (Bremer 1994) were calculated using the ‘stats’ and ‘aquickie’ commands, respectively, and a bootstrap analysis was performed with the standard options.

Morphometric and Phylogenetic Morphometric Analyses

The morphological diversity of the mandibular articulation was investigated through geometric morphometric and phylogenetic morphometric analyses based on landmark configuration defined by Hendrickx et al. (2014*b*) for the quadrate in ventral view (character 2). Both morpho- and phylo-morpho analyses comprise a sample of 37 theropod taxa selected for their completeness and preservation (Appendices A8.2). Two additional landmarks were added to the eight initial landmarks proposed by Hendrickx et al. (2014*b*) to account for the orientation of the intercondylar sulcus (Fig.

8.5E). As a result, ten landmarks defining the outline of the mandibular articulation and the ecto- and entocondyles provide a comprehensive coverage of the ventral view of the quadrate. Pictures from each taxon were sorted alphabetically and compiled using tpsUtil (Tps geometric morphometrics software is available for free download at http://life.bio.sunysb.edu/morph/soft-utility.html) and the digitization of the landmarks on the pictures was done with tpsDig2. The morphometric analysis was performed with MorphoJ (Klingenberg 2011) in which the landmarks were first aligned by a procrustes fit. A principal component analysis (PCA) was then conducted after generating a covariance matrix, and the morphospace occupation for each taxon was mapped onto phylogeny and along the two principal axes of the PCA (a link towards the file is available at Appendices A8.2).

In order to reconstruct a phylogeny departing from landmark data alone, we performed a phylogenetic morphometric analysis using the same landmark position of the 37 theropod taxa (Appendices A8.3). The file created from the digitization of the landmarks using tpsUtil was first taken to tpsRelw where the alignment was saved by using the 'Save aligned specimens' option, after computing Consensus, Partial warps and Relative warps. In order to run in TNT v1.1 (Goloboff et al. 2008), the *.tps file was transformed into a *.tnt file using the tps2tnt software. A phylogenetic morphometric analysis was then performed on the newly created file by using the TNT script LandschW.run. To reconstruct a phylogeny using a combination of landmark data and the 2377 discrete characters of the supermatrix, we used the Landcombsch.run TNT script. This method allows to constrain all major theropod clades and see the ancestral landmark configuration of the mandibular articulation for each node. The phylogenetic searches were run considering three different levels of search thoroughness (the scripts pre-defined levels 0, 1 and 2; see Hendrickx et al. 2014*b* for more explanation). The scores of each configuration were rescaled in all analyses is such a way that the contribution of one landmark configuration character is similar to a traditional character (Appendices A8.3).

Systematic Paleontology

Dinosauria Owen, 1842

Saurischia Seeley, 1887

Theropoda Marsh, 1881

Tetanurae Gauthier, 1986

Megalosauroidea Fitzinger, 1843

Spinosauridae Stromer, 1915

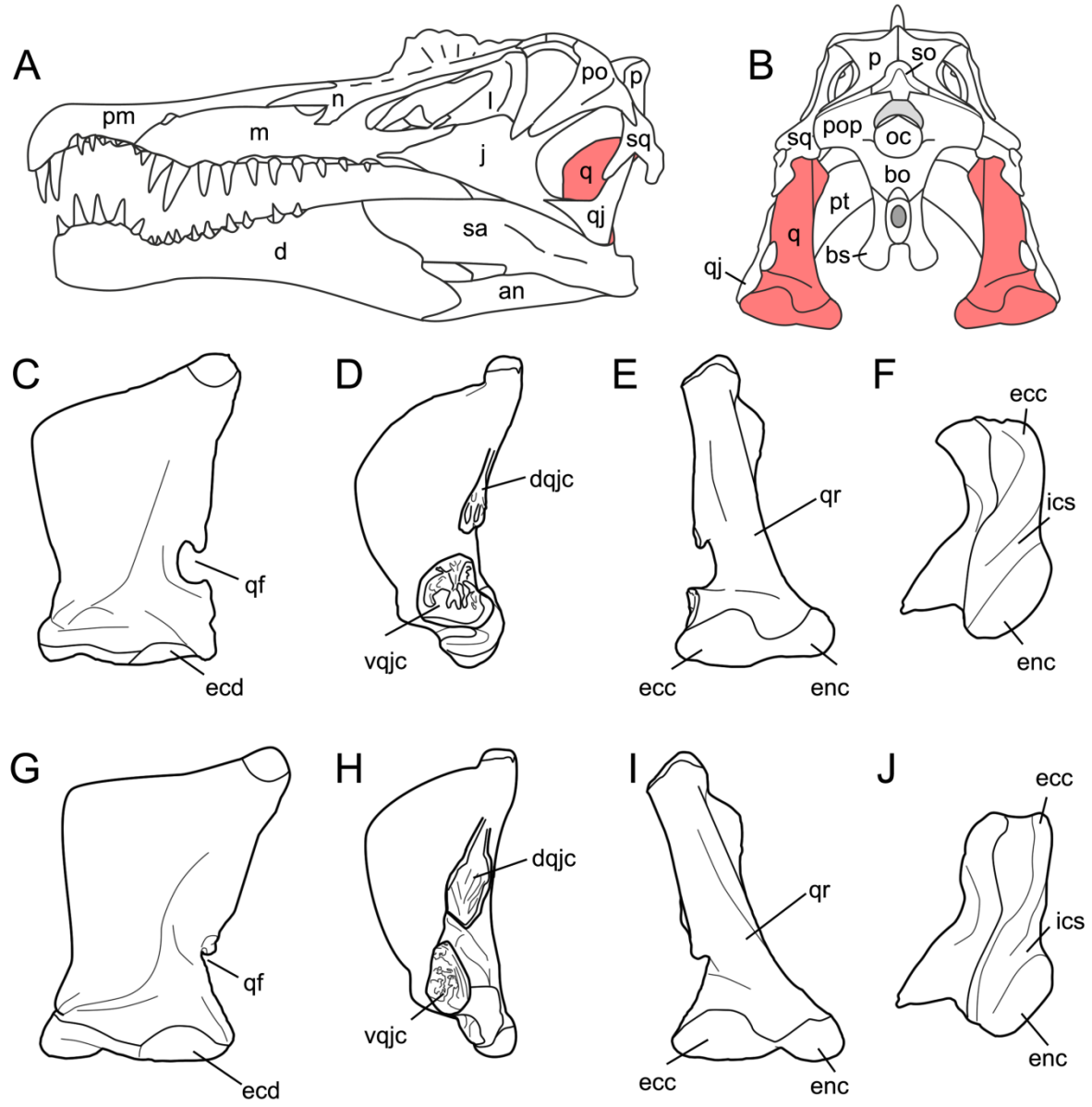

FIGURE 8.2. Quadrate position and quadrate morphotypes in Spinosaurinae from the Kem Kem beds. **A–B**, Position of the quadrate bone in the *Spinosaurus* skull in **A**, left lateral; and **B**, occipital views; **C–F**, Morphotype 1; and **G–J**, reconstructed morphotype 2 of an idealized left quadrate of *Spinosaurus* in **C,G**, anterior; **D, H**, lateral; **E, I**, posterior; and **F, J**, ventral views. **Abbreviations**: **an**, angular; **bo**, basioccipital; **bs**, basisphenoid; **d**, dentary; **dqjc**, dorsal quadratojugal contact; **ecc**, ectocondyle; **ecd**, ectocondyle depression; **enc**, entocondyle; **ics**, intercondylar sulcus; **j**, jugal; **l**, lacrimal; **m**, maxilla; **n**, nasal; **oc**, occipital condyle; **p**, parietal; **pm**, premaxilla; **pop**, paroccipital process; **pt**, pterygoid; **q**, quadrate; **qf**, quadrate foramen; **qj**, quadratojugal; **qr**, quadrate ridge; **sa**, surangular; **so**, supraoccipital; **sq**, squamosal; **vqjc**, ventral quadratojugal contact.

Spinosaurinae Sereno et al., 1998

Spinosaurus Stromer, 1915

Gen. et sp. indet.

The six isolated quadrates from the Kem Kem beds of Morocco clearly belong to two morphotypes (Figs. 8.2–8.4) based on the size and outline of the quadrate foramen, shape of the

mandibular articulation, and outline, surface, and orientation of the quadratojugal contacts. Measurements taken on each quadrate (Fig. 8.5A–D) are provided in Table 8.1.

Spinosaurus aegyptiacus Stromer, 1915

Morphotype 1

Five quadrates (MHNM.KK374 to .KK375 and .KK377 to .KK378; MSNM V6896) belonging to individuals of different ontogenetic stages are referred to a first morphotype (Fig. 8.2C–F). MHNM.KK374 (Fig. 8.3A–F) is a left quadrate of small size displaying ontogenetic features typical of immature theropods so that the bone can confidently be ascribed to a juvenile individual (a justification for the ontogenetic stages will be given below). MHNM.KK375 (Fig. 8.3G–L), MHNM.KK377, and MSNM V6896 (Fig. 8.3M–R) are mid-size left quadrates of roughly similar dimensions (Table 8.1). Based on the excavation of the quadratojugal contacts and the morphology of the quadrate ridge, MHNM.KK375 likely belongs to a subadult individual whereas MHNM.KK377 and MSNM V6896 belong to relatively immature specimens (see below). The largest bone is MHNM.KK378, a right quadrate is referred to a fully mature individual due to its particularly large size and the morphology of its mandibular condyles, quadrate head and quadrate ridge. Three of these quadrates (MHNM.KK374, .KK375; MSNM V6896) are relatively well-preserved as the anterior margin of the pterygoid flange is only missing some pieces of bones in these specimens (Fig. 8.3). Among the two poorly preserved quadrates, MHNM.KK377 shows several anteroposteriorly oriented fractures and the ventral and dorsal halves of the bone were inaccurately glued, as the dorsal part should be rotated around 10 degrees clockwise (see Appendices Fig. A8A–F). This quadrate is particularly damaged as part of the quadrate shaft, the ectocondyle and the pterygoid flange are missing. MHNM.KK378 is not deformed, yet the anterior surface is strongly damaged and the whole ectocondyle, the ventral quadratojugal contact and most of the pterygoid flange are missing (see Appendices Fig. A8.1G–L). The quadrate shaft, the entocondyle and the dorsal quadratojugal contact are, however, well-preserved in this specimen.

In posterior view, the quadrate body of this first quadrate morphotype has a rough Eiffel tower outline as the quadrate tapers dorsally, from a lateromedially wide mandibular articulation ventrally to a lateromedially narrow quadrate head dorsally (Fig. 8.3C, O). The medial margin of the quadrate body is concave in posterior view, and straight to weakly convex at mid-height of the quadrate shaft. The lateral margin of the quadrate is straight to slightly concave along the ventral quadratojugal contact, and straight to sigmoid from the quadrate foramen to the quadrate head. The quadrate body displays a prominent and lateromedially wide, yet poorly delimited, quadrate ridge extending from the dorsal end of the entocondyle to two thirds of the bone, well beneath the quadrate head. The main axis of the quadrate ridge is inclined laterally at an angle of 110-120° from the main axis passing through the mandibular articulation. In the largest specimen (MHNM.KK378), a ventrodorsally long

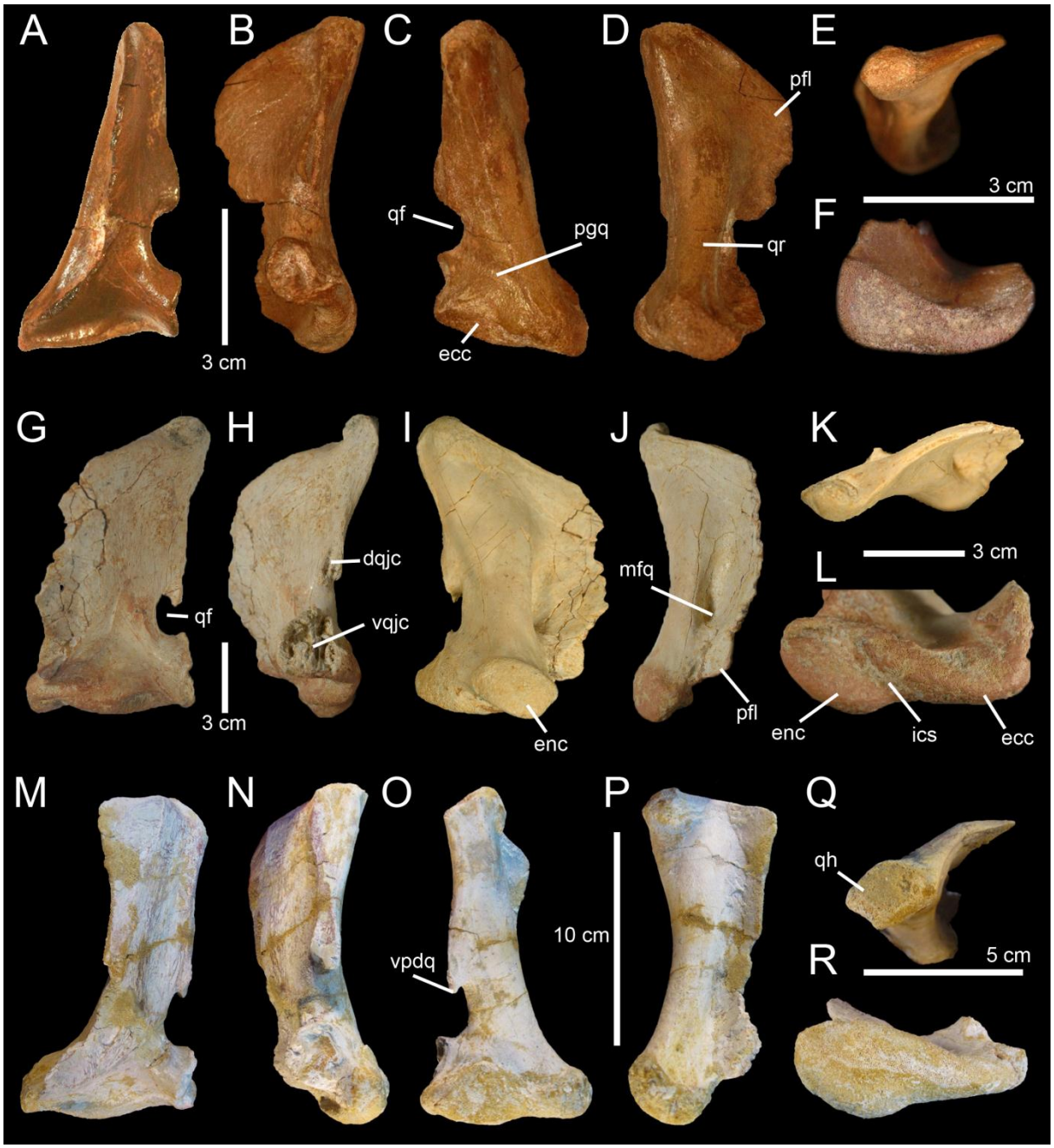

FIGURE 8.3. Quadrates of Morphotype 1 referred to *Spinosaurus aegyptiacus*. **A–N**, Left quadrates of specimens **A–F**, MHNM.KK374; **G–L**, MHNM.KK375; and **M–N**, MSNM V6896, in **A, G, M**, anterior; **B, H, N**, lateral; **C, O**, posterior; **I**, posteromedial; **D**, posterolateral; **J, P**, lateral; **E, K, P**, dorsal; and **F, L, R**, ventral views. **Abbreviations**: **dqjc**, dorsal quadratojugal contact; **ecc**, ectocondyle; **enc**, entocondyle, **ics**, intercondylar sulcus; **mfq**, medial fossa; **pfl**, pterygoid flange; **pgq**, posterior groove; **qf**, quadrate foramen; **qh**, quadrate head; **qr**, quadrate ridge; **vpdq**, ventral projection of the dorsal quadratojugal contact; **vqjc**, ventral quadratojugal contact.

prominence can be seen on the dorsal third of the quadrate, ventral to the quadrate head and strongly deflected laterally (see Appendices Fig. A8I-J). This prominence, which is here interpreted as a second quadrate ridge, reaches the quadrate head dorsally and may have contacted the medial surface of the squamosal laterally. This anteroposterioly narrow convexity is also present in the smaller quadrates but not so well-delimited. The squamosal capitulum is convex and sometimes semi-circular in

posterior view. A small concavity is visible directly ventral to the quadrate and was most likely in contact with the squamosal. A well-defined quadrate foramen, delimited by the ventral quadratojugal contact ventrally and the dorsal quadratojugal contact dorsally appears on the lateral side of the quadrate, at one third of the bone (Fig. 8.3C, I, O). The foramen is parabolic in outline in MHNM.KK374, .KK377 and .KK378 and reniform in MHNM.KK375 and MSNM V6896 due to the presence of a well-developed ventral projection of the dorsal quadratojugal contact in these two specimens (Fig. 8.3O). This ventral projection is absent in MHNM.KK374 (Fig. 8.3C) and missing in MHNM.KK377 and .KK378. A shallow and lateromedially oriented groove runs from the ventral margin of the quadrate foramen to the laterodorsal margin of the ectocondyle in the smallest quadrate (MHNM.KK374; Fig. 8.3C). This groove is poorly visible in the largest quadrate and absent in the others. The articulating surface of the two mandibular condyles is well-delimited, and delimited from the rest of the quadrate surface by a small step in mature specimens. The surface outline of the mandibular condyles is roughly oval to subtriangular. Both mandibular condyles are separated by a diagonally oriented groove so that the ventral margin of the mandibular articulation is biconvex in posterior view. The ecto- and entocondyle extend at the same level dorsally, yet the posterior surface of the ectocondyle is always more important than the entocondyle. The posterior surface of MHNM.KK375 is well-preserved and shows some pits where tendons of muscles were attached: one ventral to the quadrate foramen and medial to the ventral quadratojugal contact, a second beneath the ventral margin of the quadrate head and a third one on the dorsal surface of the pterygoid, directly medial to the quadrate head.

In medial view, the pterygoid flange expands from the dorsal margin of the quadrate head dorsally to the anterior extremity of the entocondyle ventrally (Fig. 8.3D, J, P). The flange is subtrapezoidal in outline, with an anteroposteriorly long and anteroventrally inclined dorsal margin and an anteroposteriorly short and anterodorsally inclined ventral margin. The dorsal margin is inclined ventrally at an angle of 10° to 50° from the main axis of the quadrate shaft. The anterior margin is ventrodorsally biconvex in MHNM.KK375, which preserved most of the pterygoid flange (Fig. 8.3J), as the flange makes an angle to extends only ventrally at one fifth. A deep medial fossa lays at two fifth of the bones between the quadrate shaft and the pterygoid flange. This fossa is not pneumatic as it does not lead to any internal pneumatic chamber within the quadrate (Fig. 8.3J). The depression formed by the medial fossa extends adjacently to the quadrate ridge along two thirds of the flange. The posterior margin of the shaft is strongly concave and almost straight in the largest specimen. The entocondyle is globular, D-shaped and posteroventrally oriented.

In anterior view, the pterygoid flange covers $5/6^{th}$ of the bone and its anterior surface curves medially (Fig. 8.3A, G, M). The flange terminates dorsally by a small subtriangular concavity anterior to the quadrate head in MHNM.KK375 (Fig. 8.3G). The dorsal two-thirds of the flange are ventrodorsally oriented, whereas the ventral third curves postero-medially to reach the entocondyle. The medial margin of the pterygoid flange was most likely biconvex in anterior view, with a short

subtriangular convexity at one-third of the bone. The ventral margin of the mandibular articulation is biconcave and the ectocondyle covers three fourths of the mandibular articulation in anterior view. This lateral condyle is strongly mediolaterally elongated and its ventral margin is sigmoid. A deep yet poorly delimited concavity is seen on the anterior surface of the ectocondyle, medial to the ventral quadratojugal contact (Fig. 8.3A, G, M). The articulating surface of the entocondyle only forms a small subtriangular surface in anterior view. A mediolaterally oriented groove is visible dorsal to the entocondyle and ventral to the pterygoid flange in MHNM.KK374 (Fig. 8.3A). This groove, which is not present in other specimens, extends to the anterior depression of the ectocondyle in this specimen.

In lateral view, the two quadratojugal contacts are well-delimited and separated by the quadrate foramen (Fig. 8.3B, H, N). The ventral quadratojugal contact is always anteroposteriorly longer than the dorsal contact in this quadrate morphotype. It has an oval and a reversed D-shaped outline in MHNM.KK374 and MHNM.KK375, respectively (Fig. 8.3B, H). In mature specimens, the ventral quadratojugal contact is deeply excavated by several grooves and deep depressions, suggesting a strong and immovable contact between the quadrate and quadratojugal (Fig. 8.3H). The ventral quadratojugal contact is incomplete in MHNM.KK377 and totally missing in MHNM.KK378. The dorsal quadratojugal contact of the quadrate is ventrodorsally elongated and has a lanceolate outline in lateral view. The lateral surface of the dorsal quadratojugal contact is flattened and faces posteriorly in the smallest specimen MHNM.KK374 (Fig. 8.3B). It is dug by two longitudinal grooves in MHNM.KK375 and MHNM.KK377, which seems to be the condition in the quadrate of mature specimens belonging to morphotype 1 (Fig. 8.3H). A flattened surface with a reverse tear-drop outline extends from the dorsal extremity of the dorsal quadratojugal contact ventrally, to the quadrate head dorsally. This surface is bounded by the dorsal quadrate ridge in MHNM.KK378, and was most likely receiving the squamosal. Both anterior and posterior surface of the ectocondyle are convex in lateral view, and the lateral mandibular condyle bows anteriorly from the ventral quadratojugal contact to the ventral extremity of the pterygoid flange. The quadrate head is prominent in mature specimens MHNM.KK375 and MHNM.KK378 (Fig. 8.3H). The anteroposterior length of the quadrate head varies in quadrate of morphotype 1, being short in MHNM.KK375 and long in MHNM.KK378 and MSNM V6896. This is also the case with the outline of the quadrate head, the latter being weakly convex in the immature specimens MHNM.KK374, .KK376, and MSNM V6896, and subconical in the largest quadrate MHNM.KK378.

In dorsal view, the quadrate head is diamond shaped in MSNM V6896 and oval to subcircular in all other specimens (Fig. 8.3E, K, Q). In MHNM.KK375 and MSNM V6896, the pterygoid flange extends anteriorly and bends anteromedially in its anteriormost part (Fig. 8.3Q). In MHNM.KK374, .KK377, and .KK378, the pterygoid flange remains straight and only projects anteriorly in its dorsal part (Fig. 8.3E). The pterygoid flange tapers anteriorly so that it has the same thickness than the quadrate head posteriorly and gets thinner to form a sheet-like structure more anteriorly (Fig. 8.3Q).

The pterygoid flange is, however, relatively thick anteriorly in the largest specimen. The quadrate ridge is an anteroposteriorly compressed cylinder at the level of the medial depression.

In ventral view, the mandibular condyles are strongly asymmetrical (Fig. 8.3L, R). The entocondyle is oval to oblong in outline and its main axis is anteromedially oriented. The ectocondyle, on the other hand, is helicoidal and strongly lateromedially elongated, so that the lateral condyle covers most of the anterior surface of the mandibular articulation, from the ventral quadratojugal contact to the anterior extremity of the entocondyle (Fig. 8.3L). The thickness of the ectocondyle diminishes laterally, and a weak concavity is visible on the anterior surface of the condyle. The intercondylar sulcus separating the two mandibular condyles is straight and poorly delimited in immature specimens, and well-visible and sigmoid in more mature individuals. It is particularly deep in the subadult specimens MHNM.KK375 and .KK378 where the entocondyle is well-demarcated. The main axis of the intercondylar sulcus is lateromedially oriented in all specimens, and forms an angle of 130-140° with the main axis of the mandibular articulation. In MHNM.KK374, the two condyles are not easily distinguishable as the intercondylar sulcus separating them is almost absent (Fig. 8.3F). In this juvenile specimen, the mandibular condyles are not prominent and the posterior margin of the mandibular articulation is roughly convex. On the other hand, the posterior margin of the mandibular articulation is biconvex in more mature specimens. The ventral quadratojugal contact projects anteriorly in the best preserved specimen (MHNM.KK375), and this anterior projection is absent in MHNM.KK374 and most likely missing in MHNM.KK377 and MSNM V6896.

Spinosaurus maroccanus

Revised diagnosis

Megalosauroid theropod with a minute quadrate foramen (long axis less than 15% of the lateromedial width of the mandibular condyle), a trapezoidal ventral quadratojugal contact of the quadrate with a flattened surface showing punctuations, a deep and well-delimited depression on the anterior surface of the ectocondyle, and a sigmoid, strongly lateromedially elongated and anteroposteriorly short ectocondyle in ventral view.

Morphotype 2

The ventral portion of a right quadrate (MHNM.KK376) shows some important morphological variations in comparison to the five other quadrates, namely a minute quadrate foramen, both ventral and dorsal quadratojugal contacts of similar anteroposterior length, a dorsal quadratojugal contact excavated by a deep depression, a trapezoidal ventral quadratojugal contact with a flat lateral margin strongly inclined medially, a deep and well-defined depression on the anterior surface of the ectocondyle, and a lateromedially wider and anteroposteriorly shorter ectocondyle (Fig. 8.2G–J). The dorsal part of MHNM.KK376 is missing above the dorsal end of the dorsal

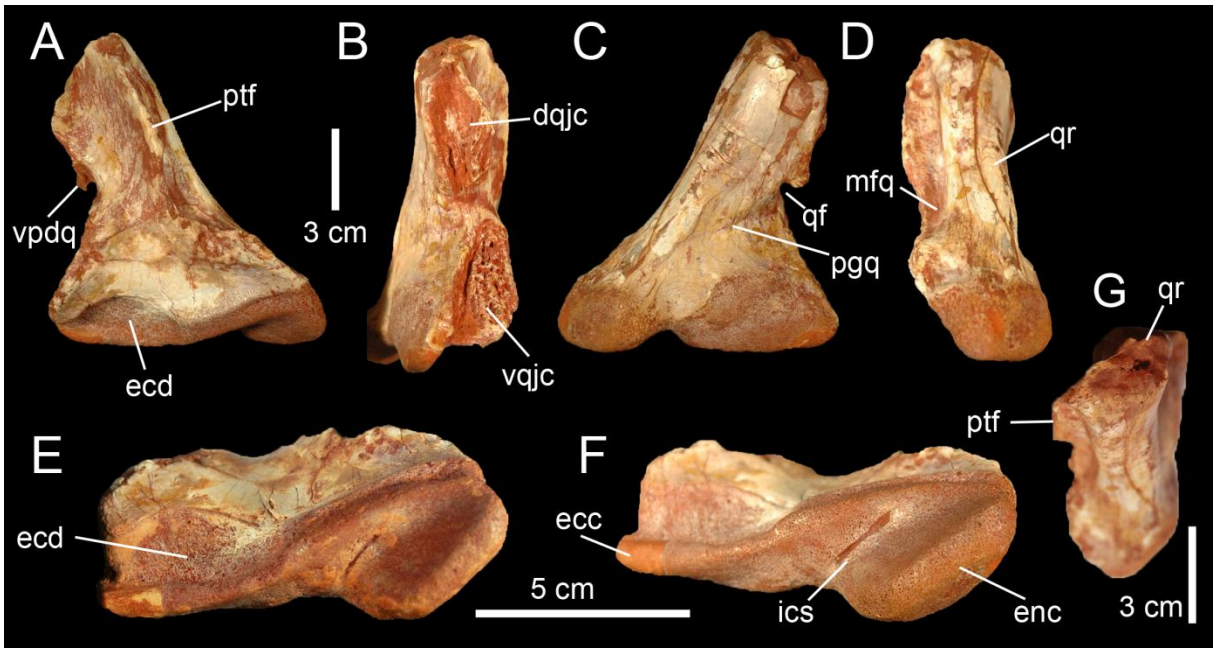

FIGURE 8.4. Quadrate of Morphotype 2 referred to *Spinosaurus maroccanus*. **A–F**, Right quadrate MHNM.KK376 in **A**, anterior; **B**, lateral; **C**, posterior; **D**, medial; **E**, ventral; **F**, ventromedial; and **G**, dorsal views. **Abbreviations**: **dqjc**, dorsal quadratojugal contact; **ecc**, ectocondyle; **ecd**, depression of the ectocondyle; **enc**, entocondyle, **ics**, intercondylar sulcus; **mfq**, medial fossa; **pfl**, pterygoid flange; **qf**, quadrate foramen; **qr**, quadrate ridge; **vpdq**, ventral projection of the dorsal quadratojugal contact; **vqjc**, ventral quadratojugal contact.

quadratojugal contact, and the preserved portion corresponds to half of the bone in the quadrates of morphotype 1. The pterygoid flange is also almost entirely missing, yet its posteriormost part is visible (Fig. 8.4A). Both quadratojugal contacts and mandibular condyles are well-preserved although a small portion of the ectocondyle, on the latero-ventral margin of the condyle, was restored.

In posterior view, the quadrate shaft is inclined laterally at an angle of around 30° with the main axis passing through the mandibular articulation (Fig. 8.4C). The ridge is massive and its medial margin is concave ventrally and weakly convex at mid-height of the quadrate. The quadrate ridge is slightly constricted at the level of the quadrate foramen, and its thickness gently increases more dorsally. Unlike quadrates of morphotype 1, the lateral margins of the quadratojugal contacts are not aligned on the same vertical plane. The lateral surface of the ventral quadratojugal contact is dorsomedially inclined whereas the dorsal quadratojugal contact is weakly laterodorsally inclined (Fig. 8.4C). The surface of the ventral and dorsal quadratojugal contacts is roughly straight and the dorsal quadratojugal contact shows a short ventral projection as in morphotype 1. The quadrate foramen is significantly ventrodorsally shorter and lateromedially narrower than that of morphotype 1. When the quadrate was in articulation with the quadratojugal, the outline of the quadrate foramen was most likely a reverse tear-drop shape . The ento- and the ectocondyle are separated ventrally by an intercondylar sulcus formed by a lateromedially narrow and ventrodorsally tall concavity. The articulating surface of ectocondyle is elliptical in outline, lateromedially wider than the entocondyle and extends slightly more dorsally than the medial condyle (Fig. 8.4C). The articulating surface of the latter is oval to D-shaped in outline in posterior view. There is no step delimiting the articulating

surface of the mandibular condyles with the rest of the quadrate body. A diagonally oriented groove extends from the ventral margin of the quadrate foramen laterally to the level of the intercondylar sulcus (Fig. 8.4C). This groove is homologous with that seen in MHNM.KK374.

In medial view, the anteroposterior length of the quadrate ridge remains relatively constant along its ventrodorsal height (Fig. 8.4D). The preserved portion of the pterygoid flange projects anteriorly and its ventralmost part reaches the entocondyle ventrally. There is a medial fossa situated between the quadrate shaft and the pterygoid flange. This depression is deep, yet it does not lead to a pneumatic chamber. The entocondyle protrudes ventrally and the articulating surface of the entocondyle is roughly D-shaped in outline in medial view.

In lateral view, the two quadratojugal contacts of MHNM.KK376 are well-delimited and their morphology strongly differs from that of morphotype 1. Both ventral and dorsal quadratojugal contacts share the same anteroposterior length in their longest part (Fig. 8.4B). The dorsal quadratojugal contact is incomplete and its remaining portion is excavated by a deep depression dorsally and two ventrodorsally oriented grooves converging ventrally in its ventral part (Fig. 8.4B). The ventral quadratojugal contact, on the other hand, is fully preserved and its general outline is subtrapezoidal instead of D-shaped as in morphotype 1 (Fig. 8.2). It is slightly anteriorly deflected from the dorsal quadratojugal contact. The ventral quadratojugal contact gently tapers dorsally and its lateral surface is irregular and excavated by several foramina and irregular furrows. A deeper groove is also visible adjacent to the posterior margin of the ventral quadratojugal contact. The ectocondyle is anteroposteriorly short and weakly oriented posteroventrally. The ventral quadratojugal contact does not extend on the whole surface of the ectocondyle.

In anterior view, the preserved portion of the pterygoid flange is centrally positioned on the quadrate body and follows the orientation of the quadrate ridge dorsal to the ventral quadratojugal contact (Fig. 8.4A). The pterygoid flange curves ventromedially at the level of the dorsalmost part of the ventral quadratojugal contact to reach the entocondyle ventrally. The anteromedial orientation of the posteriormost part of the pterygoid flange suggests that the latter mostly extended anteromedially. The ectocondyle is much wider lateromedially than the entocondyle as it occupies more than three fourths of the mandibular articulation. A deep and well-delimited depression is seen on the anterolateral surface of the ectocondyle (Fig. 8.4A). The dorsal margin of this depression, which marks the dorsal limit of the ectocondyle, is convex and extends laterally directly ventral to the ventral quadratojugal contact. The medial part of the ectocondyle corresponds to a lateromedially elongated surface with parallel dorsal and ventral margins. The entocondyle, which is separated by the ectocondyle by the intercondylar sulcus in its ventral part, is roughly D-shaped. A shallow furrow parallel and adjacent to the dorsal margin of the ectocondyle runs along the dorsomedial part of the ectocondyle.

In dorsal view, the cross-section outline of the quadrate shaft is D-shaped, with the convexity oriented posteromedially (Fig. 8.4G). This transverse section reveals the presence of a small hole

TABLE 8.1. Measurements of five quadrates of Spinosaurinae from the Kem Kem beds of Morocco. Values are given in millimeters. [1]Distance taken from the posterior margin of the squamosal capitulum to the ventral margin of the entocondyle. [2]Distance taken from the dorsalmost point of the dorsal quadratojugal contact to the anterior surface of the pterygoid flange. [3]Distance taken from the apex of the anterodorsal curvature of the pterygoid flange to the apex of the anteroventral curvature. * Distance taken from the base of the mandibular condyles to the dorsal extremity of the broken shaft.

	WDC-CSG Q1	WDC-CSG Q2	WDC-CSG Q3	WDC-CSG Q4	WDC-CSG Q5	MSNM V6896
1. Ventrodorsal length of the quadrate[1]	78	145	113*	130	220	145
2. Anteroposterior width of the quadrate[2]	30	75	?	45	?	>50
3. Anteroposterior length of the dorsal margin of the pterygoid flange[3]	27	56	?	?	115	55
4. Ventrodorsal length of the anterior margin of the pterygoid flange	57	93	?	60	164	104
5. Anteroposterior width of the pterygoid flange at the level of the medial depression[4]	?	30	?	?	?	?
6. Anteroposterior thickness of the quadrate shaft at the level of the quadrate foramen	10	25	25	20	30	19
7. Lateromedial width of the mandibular articulation	36	77	108	70	?	76
8. Lateromedial length of ectocondyle	28	40	57	?	?	60
9. Ventrodorsal width of ectocondyle	8	24	30	17	?	14
10. Lateromedial length of entocondyle	26	50	50	47	80	31
11. Ventrodorsal width of entocondyle	10	21	24	17	33	22
12. Anteroposterior length of squamosal capitulum	13	25	?	25	33	28
13. Ventrodorsal width of quadrate head	9	16	?	18	22	20
14. Ventrodorsal length of quadrate foramen	14	18	15	25	30	20
15. Lateromedial width of quadrate foramen	7	11	10	10	13	11
16. Ventrodorsal length of the quadratojugal contacts	46	75	90	?	?	73
17. Ventrodorsal length of the dorsal quadratojugal contact	18	33	43	23	40	33
18. Anteroposterior width of the dorsal quadratojugal contact	6	11	21	11	15	11
19. Ventrodorsal length of the ventral quadratojugal contact	14	33	43	?	?	22
20. Anteroposterior width of the ventral quadratojugal contact	12	28	24	?	?	18
21. Lateromedial length of the ectocondyle fossa	/	/	48	/	/	/
22. Ventrodorsal width of the ectocondyle fossa	/	/	27	/	/	/

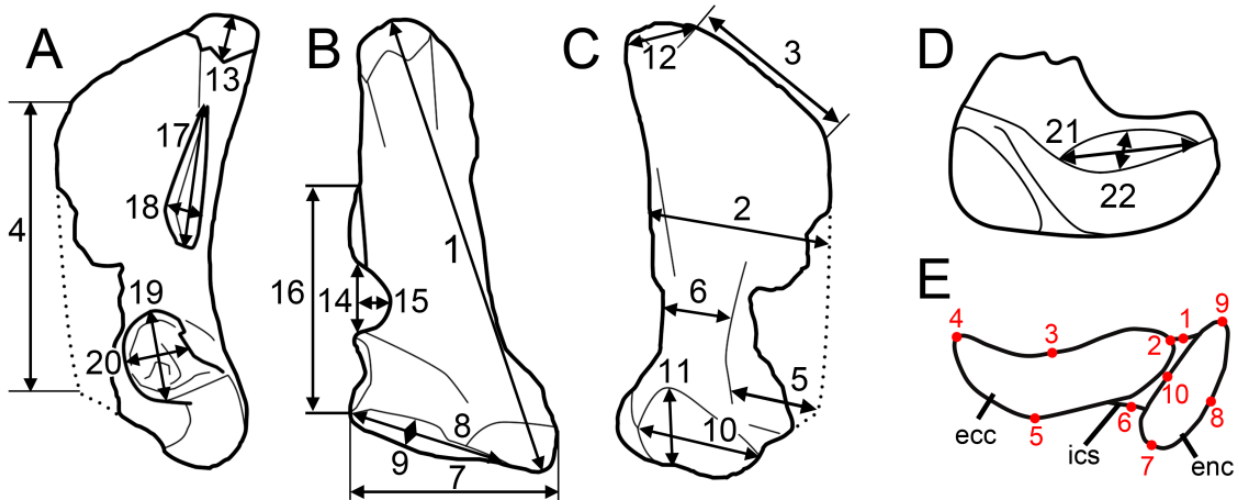

◄FIGURE 8.5. **A–D**, Measurements taken on the six spinosaurine quadrates from the Kem Kem beds of Morocco in **A**, lateral; **B**, posterior, **C**, medial; and **D**, ventral views; **E**, location of the ten landmarks used in the morphometric analyses in an idealized mandibular articulation of a non-avian theropod in ventral view. **Abbreviations**: **ecc**, ectocondyle; **enc**, entocondyle, **ics**, intercondylar sulcus.

within the quadrate, suggesting that at least a portion of the quadrate was hollow and may have included a small pneumatic chamber. The pterygoid flange projects anteromedially from the anterior surface of the quadrate body, which faces anterolaterally.

In ventral view, the mandibular condyles are strongly asymmetrical, with a much wider ectocondyle (Fig. 8.4E). The entocondyle is oblong in outline and its main axis is lateroposteriorly oriented. The anterior surface of the entocondyle is flat whereas its posterior margin is convex. The ectocondyle is antero-posteriorly narrow, strongly lateromedially elongated, and less prominent than the entocondyle. It is helicoidal in shape and covers the whole surface of the mandibular articulation, from the ventral quadratojugal contact to the anteromedial extremity of the entocondyle. The main axis of the ectocondyle is lateromedially oriented and the ectocondyle corresponds to a low ridge in the medial half of the mandibular articulation. The anterior margin of the ectocondyle is biconvex, with the lateral convexity marking the limit of the anterior depression of the ectocondyle (Fig. 8.4E). This deep fossa excavates the anterolateral surface of the ectocondyle so that the posterolateral part of the ectocondyle corresponds to a prominent ridge. The intercondylar sulcus is lateromedially wide in its posterior part, shallow, and tapers anteromedially. Its main axis is lateromedially oriented and inclined at an angle of 148° from the main axis of the mandibular articulation (Fig. 8.4F).

Results

Cladistic Analysis

The full phylogenetic analysis produced 43 most parsimonious trees (MPTs) of length 5049, consistency index (CI) 0.485 and retention index (RI) 0.548 (Fig. 8.6). The strict consensus tree is relatively unresolved as an important polytomy occurs among Neotheropoda. Yet, Ceratosauria, Megalosauroidea, and Coelurosauria are resolved clades, and the two quadrate morphotypes are recovered among spinosaurine Spinosauridae. This lack of resolution is due to the instability of *Monolophosaurus*, and a reduced consensus approach (Wilkinson 1994) was used to calculate a consensus tree excluding this taxon. The new cladistic analysis yielded 49 MPTs (length 4994, CI of 0.522 and RI of 0.61) and produced a much better resolved consensus tree mirroring to a large degree the current consensus classification of non-avian theropods (Fig. 8.6). This clearly demonstrates the utility of the quadrate to solve theropod relationships, like in mosasaurs (Polcyn and Bell 2005). Both morphotypes are still recovered among Spinosaurinae which is supported by two ambiguous synapomorphies: the straight margin of the ventral quadratojugal contact (char. 48.1) and the ventral position of the quadrate foramen, beneath the mid-height of the quadrate body, on the lateral surface of the quadrate (char. 63.1). Yet, the clade of Spinosaurinae is unresolved due to missing data for the

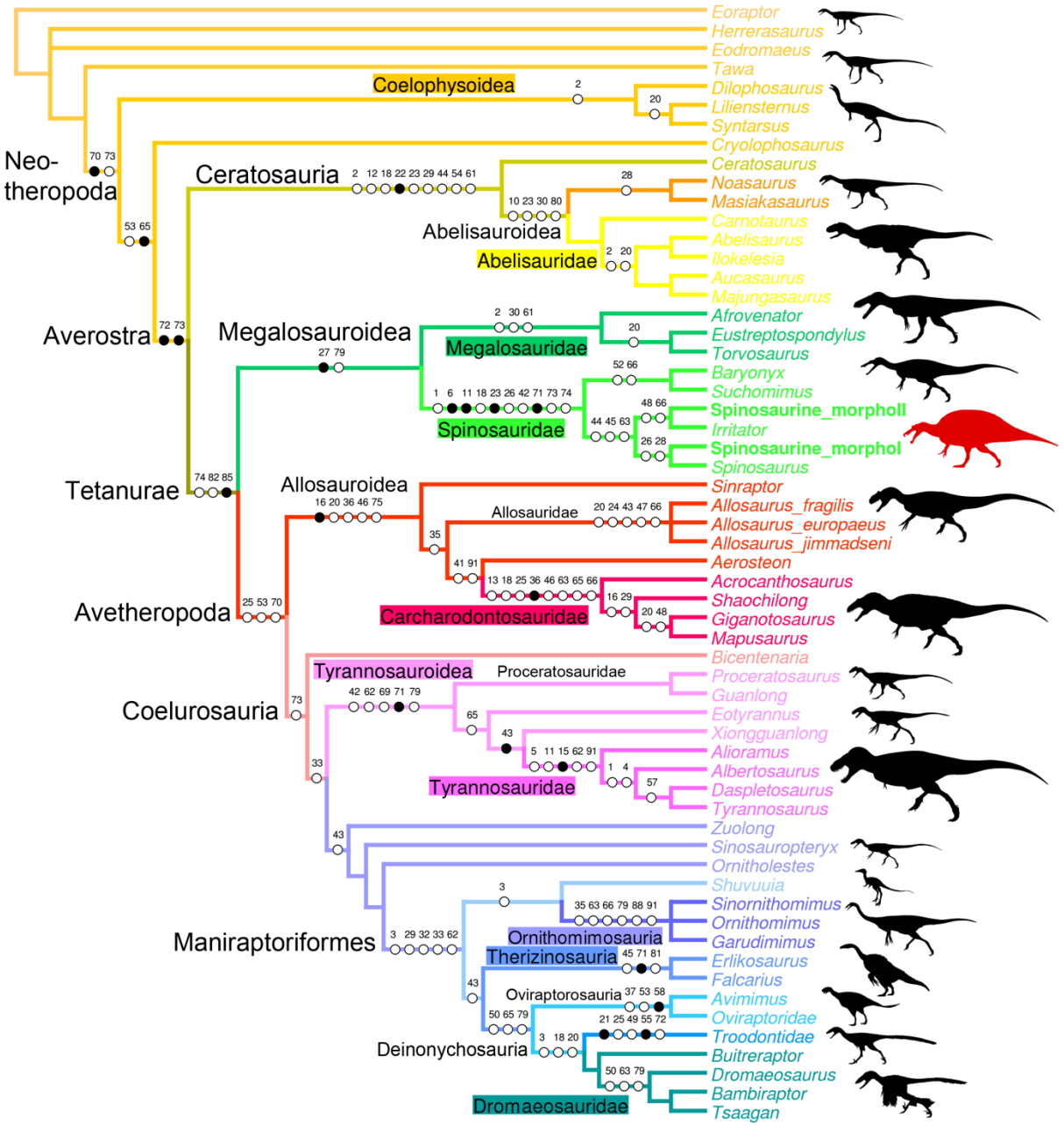

FIGURE 8.6. Quadrate based phylogeny of non-avian theropods. Strict consensus cladogram from most parsimonious trees after the a posteriori deletion of *Monolophosaurus*. Initial analysis was a New Technology Search using TNT v.1.1 of a supermatrix comprising 98 quadrate based characters combined with seven recent datasets (i.e., Brusatte et al. 2010*d*; Martinez et al. 2011; Carrano et al. 2012; Pol and Rauhut 2012; Novas et al. 2013; Choiniere et al. 2014*b*) based on the whole skeleton, for one outgroup (*Eoraptor lunensis*) and 58 non-avian theropod taxa. Tree length = 4994; CI = 0.522, RI = 0.61. For silhouette attribution, see Appendices A1.1.

quadrate of *Spinosaurus*. Among non-avian theropods, the clade of Spinosauridae is the best resolved in terms of quadrate related characters, with four unambiguous and six ambiguous synapomorphies constraining it. With seven quadrate related synapomorphies, Carcharodontosauridae and Ornithomimosauria are also very well-resolved. These clades are followed by the Ceratosauria (6 synapomorphies), and Tyrannosauroidea, Tyrannosauridae, and Troodontidae (5 synapomorphies) clades. In this analysis, no quadrate related synapomorphies define Maniraptoriformes, Maniraptora, and Dromaeosauridae.

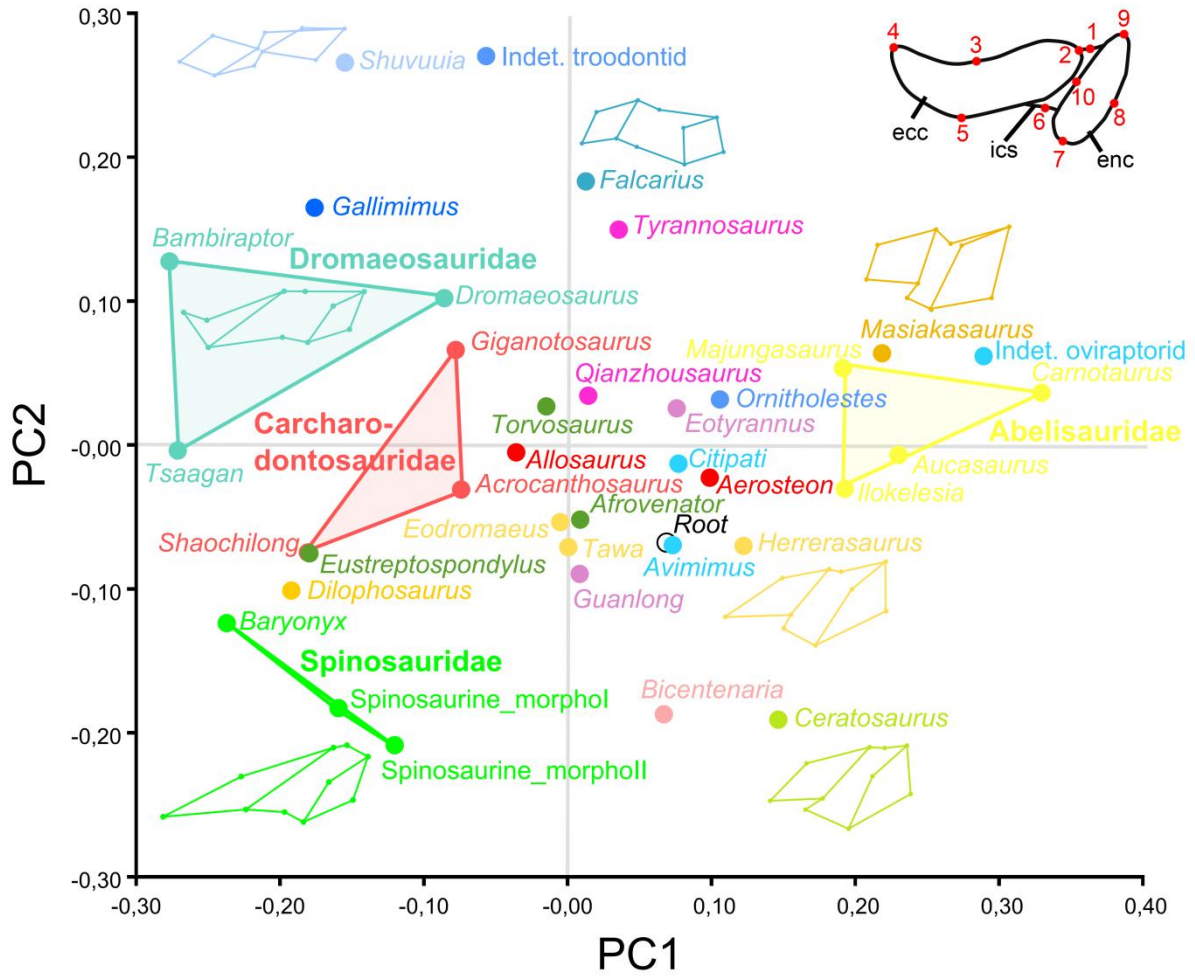

FIGURE 8.7. Results of the geometric morphometric analysis performed on the mandibular articulation of non-avian theropods. PCA plot of the principal component analysis performed on 37 theropod taxa and 10 landmarks along the first two principal axes explaining 35.8% and 20.04% of the variation in the sample. Colors refer to theropod clades and correspond to those in Figure 8.6. Major groupings at family level are delimited and outline images are associated with taxa of hypothetical extremes.

Morphometric Analysis

The first two main axes of the principal component analysis (PCA) performed on 37 theropod taxa and 10 landmarks, explained 35.8% and 20.04% of the variation in the sample, respectively (Fig. 8.7). The first principal axis PC1 accounts for the lateromedial elongation of the mandibular articulation whereas the second one PC2 captures the anteroposterior thickness of this articulation. With their typical and relatively similar mandibular articulations, abelisaurid, carcharodontosaurid, and dromaeosaurid taxa are relatively closely distributed and occupy a unique region of the morphospace (Fig. 8.7). On the other hand, the morphospace occupation of tyrannosauroid and oviraptorid taxa is particularly important as the morphology of the mandibular articulation of the most basal taxon significantly differs from that of the derived members, in both clades. With their strongly elongated, yet anteroposteriorly broad ectocondyle associated with their oblong entocondyle, the two morphotypes are closely distributed and cluster away from other theropods, with *Baryonyx* as the closest taxon in the morphospace. Likewise, with a lateromedially short mandibular articulation

including two subcircular ecto- and entocondyles, noasaurids, abelisaurids, and some derived oviraptorids cluster together. The most primitive theropods *Herrerasaurus*, *Eodromaeus* and *Tawa* also occupy very close positions, near the root of the morphospace (Fig. 8.7). Other distantly related taxa, such as the megalosaurid *Afrovenator*, the tyrannosauroid *Guanlong*, and the basal oviraptorid *Avimimus*, also cluster with basalmost theropods.

Phylogenetic Morphometric Analysis

The phylogenetic morphometric analysis departing from landmark data alone yielded a single tree which, for each different degree of thoroughness, poorly mirrors the current classification of non-avian theropods. Yet, several closely related taxa such as ceratosaurs were recovered in the same grouping (or morphoclade as the grouping results from a cladistic analysis solely based on landmark data) in the analysis performed with a degree of thoroughness of one and above (Fig. 8.8A). The two morphotypes are closely related to *Baryonyx* in the analyses performed with a degree of thoroughness of zero and one (Fig. 8.8A). In the trees obtained with a level of thoroughness of one and two, three morphoclades, associated with three morphotypes of the mandibular articulation, emerged. A first morphoclade consists essentially of ceratosaurs, and includes the oviraptorid *Ingenia* (Gin A; Maryańska and Osmólska 1997). This first morphotype is defined by a mandibular articulation with two anteroposteriorly wide condyles in which the entocondyle is larger than the ectocondyle. A second morphotype encompasses theropods with an lateromedially elongated and parabolic to sigmoid ectocondyle, and a smaller and anteromedially oriented entocondyle. This morphoclade includes Spinosauridae, and a mixture of dilophosaurid, basal tyrannosauroid, carcharodontosaurid and dromaeosaurid taxa. Finally, a third morphoclade gathers some megalosaurid, tyrannosaurid, alvarezsaurid, therizinosaurid, and troodontid taxa. This grouping is characterized by two mandibular condyles of equal sizes and relatively similar orientation, and by ecto- and ento- condyles either anteromedially inclined, or extending parallel to the long axis of the mandibular articulation.

The phylogenetic analysis combining discrete characters and landmarks resulted in a single tree mirroring to a much better degree the current classification of theropods. Once again, the two morphotypes were placed among the clade of Spinosauridae (n.b., we here refer to clade and not morphoclade as the cladistic analysis is now based on both discrete characters and landmark data), along with *Baryonyx* (Fig. 8.8B). Most theropod clades were found resolved, yet a ‘carnosaur’ clade (sensu Rauhut 2003*a*) including Megalosauroidea and Allosauroidea was recovered, and the alvarezsaurid *Shuvuuia* and the troodontid *Saurornithoides* together form the sister clade of Oviraptorosauria. Likewise, *Afrovenator* is excluded from the clade of Megalosauridae formed by *Torvosaurus* and *Eustreptospondylus*. The most important landmark migrations from an ancestral landmark configuration of the mandibular articulation occur in the dilophosaurid *Dilophosaurus*, the spinosaurid *Baryonyx*, the ornithomimid *Gallimimus*, the basal coelurosaur *Bicentenaria*, the therizinosauroid *Falcarius*, and the indeterminate oviraptorid. This is, however, due to the absence, in

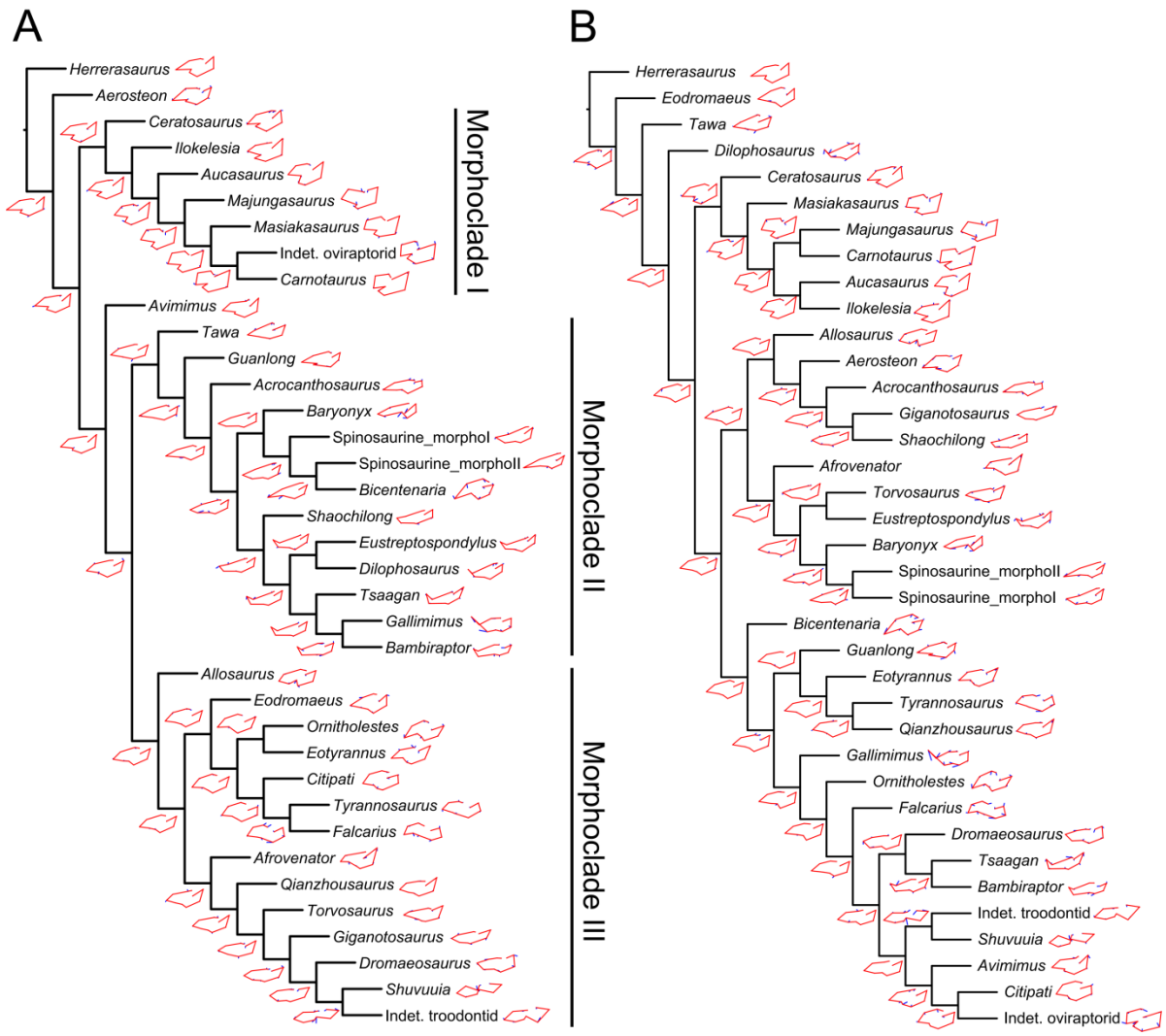

FIGURE 8.8. Results of the phylogenetic morphometric analysis. **A–B**, Phylogenetic morphometric analysis of the mandibular articulation of 36 non-avian taxa performed with a degree of thoroughness of one, and using **A**, 10 landmarks on the quadrate in ventral view (Tree score = 5.18); and **B**, a combination of the phylogenetic morphometric character based on 10 landmarks of the mandibular articulation in ventral view and 2377 discrete characters from the supermatrix (Tree score = 6.61).

our dataset, of closely related taxa for *Dilophosaurus* (no coelophysoids), *Baryonyx* (no basal spinosaurid), and *Gallimimus* (no basal ornithomimosaur), and the peculiar morphology of the mandibular articulation in the basal coelurosaur *Bicentenaria* and the basal therizinosaur *Falcarius*.

Discussion

Systematics

Based on the cladistic, geometric morphometric, and phylogenetic morphometric analyses, the six isolated quadrates can confidently be assigned to Spinosauridae. Both morphotypes clearly share a combination of features only seen in this clade. The quadrate is short (ambiguous synapomorphy of Spinosauridae; char. 1:2) and show a quadrate ridge that is thick, cylindrical, and forms a prominent

shaft (unambiguous syn.; char. 11:2). The quadrate ridge bounds a deep medial fossa on the ventromedial part of the pterygoid flange (char. 86:1). The dorsal quadratojugal contact is lanceolate in outline (ambiguous syn.; char. 42:1) and shows a ventral projection (char. 18:3), and the quadrate foramen is ventrodorsally elongated (char. 65:1) and mostly delimited by the quadrate (char. 62:1). The pterygoid flange is subrectangular in outline (unambiguous syn.; char. 71:1) and mostly projects anteriorly. Its ventral portion curves ventromedially, slightly above the mandibular articulation, and reaches the entocondyle ventrally (ambiguous syn.; char. 74:2). The mandibular articulation is lateromedially broad and anteroposteriorly narrow (ambiguous syn.; char. 18:3), and the ectocondyle is sigmoid, much longer than the entocondyle (unambiguous syn.; char. 23:3), and shows a concavity on its anterior surface (ambiguous syn.; char. 26:3). This combination of features is observed in the quadrate of Baryonychinae and absent in all other dinosaur clades (Hendrickx et al. 2014*a*; pers. obs.).

Similar to megalosauroids (other than *Irritator*), tyrannosaurids, some allosauroids, oviraptorids, and troodontids, the quadrate of both morphotypes lacks a lateral process. Such a process is present in non-neotheropod theropods, coelophysoids, ceratosaurs, basal Maniraptora, alvarezsauroids, therizinosauroids, and dromaeosaurids (Hendrickx et al. 2014*a*). Likewise, a quadrate foramen is developed as a distinct opening between the quadrate and quadratojugal, and is mostly delimited by the quadrate. This condition contrasts with the absence of quadrate foramen in megalosaurids and ceratosaurs (Ceratosauridae + Abelisauroidea), and with the equally delimited foramen of carcharodontosaurids and dromaeosaurids. It also differs from the very large quadrate fenestra of alvarezsauroids and deinonychosaurs. A mandibular articulation with a sigmoid and strongly elongated ectocondyle much longer than the entocondyle differs from that of ceratosaurids, tyrannosaurids, oviraptorids, alvarezsauroids, therizinosauroids, and troodontids in which the mandibular condyles are subequal in size, and that of abelisauroids in which the ectocondyle is ovoid (Hendrickx et al. 2014*a*). Finally, given the absence of externally expressed pneumatic openings, these six quadrates differ from the pneumatic quadrate of carcharodontosaurids, tyrannosaurids, ornithomimosaurs, therizinosauroids, and some compsognathids, oviraptorids, dromaeosaurids, and troodontids (Hendrickx et al. 2014*b*).

A subrectangular pterygoid flange with a ventral part curving medially and reaching the entocondyle, associated with a prominent and thick quadrate ridge has in fact only been identified in *Baryonyx* and *Suchomimus* (Hendrickx et al. 2014*a*). Nevertheless, quadrates belonging to morphotype 1 and 2 differ from those of Baryonychinae by a relatively small quadrate foramen situated at one third of the quadrate body (ambiguous syn. of Spinosaurinae; char. 63:0), as well as a cylindrical quadrate ridge and an oblong entocondyle. Baryonychine quadrates possess a large and strongly ventrodorsally elongated quadrate foramen (ambiguous syn. of Baryonychinae; char. 66) at one half of the quadrate body. Likewise, the posteromedial surface of the quadrate ridge is slightly acute rather than rounded, and the entocondyle is subtriangular and shallowly delimited at least in *Baryonyx*. Quadrates of both morphotypes also differ from *Baryonyx* quadrates by a smaller ventral

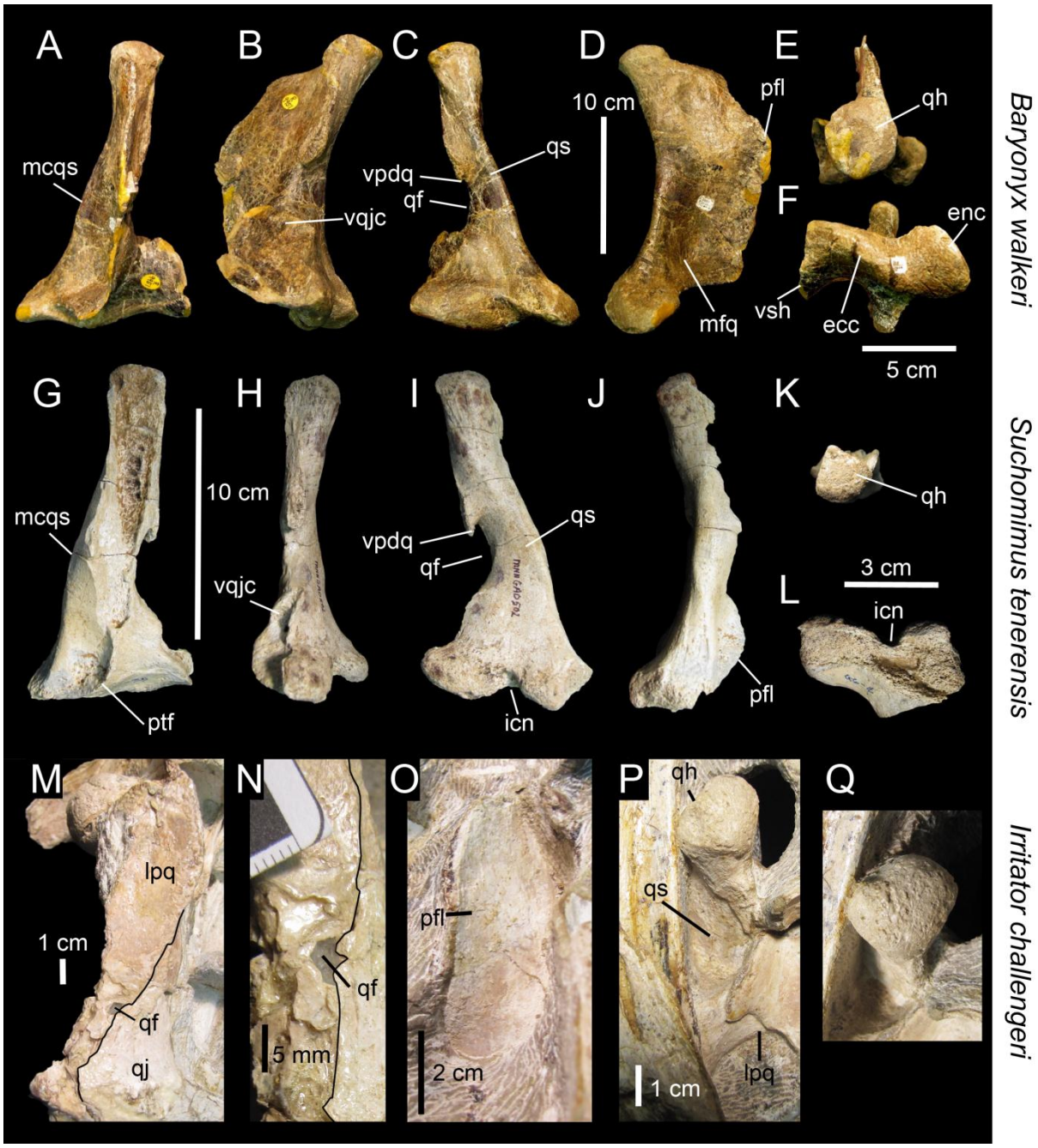

FIGURE 8.9. Quadrate morphology in Baryonychinae and *Irritator*. **A–L**, Left quadrates of **A–F**, *Baryonyx walkeri* (NHM R9951); and **G–L**, *Suchomimus tenerensis* (MNN GAD 502) in **A, G**, anterior; **B, H**, lateral; **C, I**, posterior; **D, J**, medial; **E, K**, dorsal; and **F, L**, ventral views. **M–N**, Right and **O–Q**, left quadrates of *Irritator challengeri* (SMNS 58022) with **M**, close up on the lateral portion of the quadrate body; **N**, quadrate foramen; **O**, anteromedial surface of the pterygoid flange; and **P–Q**, quadrate head in **M–N, P**, posterolateral, **O**, anterior; **Q**, and dorsal views. **Abbreviations**: **ecc**, ectocondyle; **enc**, entocondyle; **icp**, intercondylar pit; **lfo**, lateral foramen; **lpq**, lateral process; **mfq**, medial fossa; **pfl**, pterygoid flange; **qf**, quadrate foramen; **qh**, quadrate head; **qjp**, quadratojugal process; **qr**, quadrate ridge; **qs**, quadrate shaft; **vpdq**, ventral projection of the dorsal quadratojugal contact; **vsh**, ventral shelf of the pterygoid flange.

quadratojugal contact in which the posterodorsal part only faces laterally and not lateroposteriorly (Fig. 8.9A–F). They can also be distinguished from the *Suchomimus* quadrate by the absence of a posteriorly located intercondylar notch (Fig. 8.9G–L), a subtriangular projection of the ventral

quadratojugal contact towards the quadrate foramen, and an elevated rim along the dorsal and posterior margin of the ventral quadratojugal contact.

Quadrates of Spinosaurinae are known in *Irritator* (Sues et al. 2002) and *Spinosaurus* (Ibrahim et al. 2014*b*), yet little information on the quadrate can be extracted from the single specimen of *Irritator* (SMNS 58022; Fig. 8.9M-Q). The left quadrate is partially visible, with most of the quadrate body and pterygoid flange obscured by matrix (Sues et al. 2002), and only the quadrate head and the anterodorsal extremity of the pterygoid flange of this quadrate are visible (Fig. 8.9O-Q). The posterior part of the dorsal process of the right quadratojugal, which faces posterolaterally and is separated by the rest of the quadratojugal by an acute lateral ridge (Sues et al. 2002), is here interpreted as the lateral portion of the quadrate body of the right quadrate (Fig. 8.9M). If this interpretation is correct, the right quadrate of *Irritator* shows a short laterally projected lateral process lateral to the quadrate ridge and quadrate head, a feature visible in the left quadrate as well in posterodorsal view (Fig. 8.9P). This condition is, however, absent in both morphotypes in which the prominent and cylindrical quadrate shaft is adjacent to the quadratojugal contacts. A minute quadrate foramen seems also to be present in *Irritator* (Fig. 8.9N) and contrasts with the much larger quadrate foramen of morphotype 1. The quadrate head of *Irritator* has a rounded triangular to subrectangular outline in dorsal view (Sues et al. 2002; Fig. 8.9Q) and differs from the subcircular squamosal capitulum of MHNM.KK374, .KK375, .KK377, and .KK378 (Fig. 8.3E, K; see Appendices Fig. A8.1E, K), and the diamond-shaped quadrate head of MSNM V6896 (Fig. 8.3Q). Morphotype 2 also differs from *Irritator* by a medially inclined ventral quadratojugal contact in posterior view. Yet, due to the very small quadrate foramen and the straight surface of the ventral quadratojugal contact in posterior view, the second spinosaurine morphotype is morphologically closer to *Irritator*.

The holotype specimen of *S. aegyptiacus* did not preserve any quadrate (Stromer 1915), and we were just informed about the erection of a neotype for this species (FSAC-KK 11888) based on newly discovered material from the Kem Kem beds which includes the left and right quadrates (Ibrahim et al. 2014*b*). The latter were only mentioned by Ibrahim et al. (2014*b*) in the supplemental material, along with the quadrate MSNM V6896 here described and referred to a subadult individual of *S. aegyptiacus* by Ibrahim et al. (2014*b*). Photos of the two quadrate specimens FSAC-KK 11888 were kindly provided by Nizar Ibrahim shortly before the final submission of this study, allowing us to compare the isolated quadrates from the Kem Kem beds with those of *S. aegyptiacus*, and to include this taxon in our cladistic analysis. Given the fact that the quadrates of the *Spinosaurus* neotype will be illustrated and thoroughly described in a future publication (Ibrahim, pers. comm.), this study will only focus on the main anatomical similarities and differences observed between FSAC-KK 11888 and the here-studied quadrates. Although incomplete, the two quadrates of *Spinosaurus* share a large amount of features with the six isolated quadrates from the Kem Kem beds, confirming their spinosaurine status. Indeed, similar to the six quadrates, the two quadrate specimens FSAC-KK 11888 display a large cylindrical quadrate ridge and a small quadrate foramen situated at one third of the quadrate

body. This contrasts with the more lateromedially angular quadrate ridge and the large quadrate foramen located at mid-height of the quadrates of baryonychines. Unlike *Irritator*, the quadrates of *Spinosaurus* and morphotypes I and II share a subcircular squamosal capitulum in dorsal view, the absence of a lateral process, and the presence of a ventral projection of the dorsal quadratojugal contact. Quadrates of *Spinosaurus* and morphotype 1 are almost identical and only differ by subtle morphological features. Unlike Morphotype 2, these quadrates show a small yet not minute quadrate foramen as well as a D-shaped ventral quadratojugal contact in which the anteroposterior length is significantly longer than that of the dorsal quadratojugal contact. The lateral surface of the ventral quadratojugal contact is concave in posterior view and extends on the whole surface of the ectocondyle in lateral view. Likewise, similar to morphotype 1, the ectocondyle of FSAC-KK 11888 is not anterodorsally short in ventral view, as in MHNM.KK376, and the concavity on the anterior surface of the ectocondyle is shallow and poorly delimited, contrasting with the deep and well-defined anterior concavity on the ectocondyle in morphotype 2. The main differences between the *Spinosaurus* quadrates and two quadrate morphotypes mostly lie in the morphology of the dorsal quadratojugal contact. In *Spinosaurus*, the dorsal quadratojugal contact protrudes laterally in anterior view and faces posterolaterally in posterior view. This is due to the lateromedially wide anterior margin of the dorsal quadratojugal contact, a feature absent in all isolated quadrates from the Kem Kem beds. The deep intercondylar sulcus of *Spinosaurus* also extends far dorsally along the posterior surface of the quadrate, forming an intercondylar notch absent in both quadrate morphotypes (but present in *Suchomimus*). This feature may, however, results from ontogeny as a small intercondylar notch was probably present on the posterior surface of the largest quadrate MHNM.KK378.

Morphotypes 1 and 2 were recovered in two separate spinosaurine clades in the phylogenetic analysis, the former being closely related to *Spinosaurus* whereas the latter forms a sister-taxon pair with *Irritator* (Fig. 8.6). Nevertheless, the two ambiguous synapomorphies uniting Morphotype 2 and *Irritator* (i.e., a minute quadrate foramen and a straight lateral margin of the ventral quadratojugal contact in posterior view) result from our tentative interpretation of the morphology of the lateral part of the right *Irritator* quadrate, interpreted by Sues et al. (2002) as being the posterior part of the quadratojugal. Consequently, based on the phylogenetic analysis and given the fact that fossils of Spinosauridae, which are not rare in the Kem Kem beds, have so far only been assigned to the spinosaurine *Spinosaurus*, morphotype 1 is referred with confidence to *Spinosaurus*, and morphotype 2 most likely belongs to this taxon. Likewise, given the almost identical morphology of quadrates of morphotype 1 and FSAC-KK 11888, morphotype 1 is confidently assigned to *Spinosaurus aegyptiacus*, an opinion followed by Ibrahim et al. (2014*b*) for MSNM V6896.

Ontogeny

Ontogenetic variation occurring in the spinosaurid quadrate was briefly investigated by Hendrickx and Mateus (2012). Based on Morphotype 1, which includes quadrates belonging to

juvenile, immature, sub-adult and adult individuals, a sequence list of ontogenetic character transformations (maturity dependent characters) can be provided for the quadrate of *Spinosaurus aegyptiacus*:

State 1—At a juvenile stage represented by MHNM.KK374, the quadrate lacks several deep grooves on the lateral side of the ventral quadratojugal contact, and two grooves on the dorsal quadratojugal contact (Fig. 8.10A–C). This suggests a weak and loose articulation between the quadrate and quadratojugal. The ectocondyle is also poorly developed and the dorsal quadratojugal contact lacks a ventral projection.

State 2—Both quadrates MHNM.KK377 and MSNM V6896 show some signs of immaturity based on the fact that the mandibular condyles are not globular (Fig. 8.10A–C) and prominent and the squamosal capitulum is poorly delimited. The two condyles of the mandibular articulation are also weakly separated by a shallow intercondylar sulcus, indicating a loose articulation between the cranium and mandibles. Yet, the ventral projection of the dorsal quadratojugal contact is present in MSNM V6896, and was most likely lost in MHNM.KK377 due to taphonomical processes (Fig. 8.10E). This indicates that mid-sized specimens MHNM.KK377 and MSNM V6896 belonged to immature yet not juvenile individuals and not to subadult animals, as suggested by Ibrahim et al. (2014*b*) for MSNM V6896.

State 3—At a slightly more advanced stage of maturity reached by the immature specimen MHNM.KK377, the mandibular condyles and intercondylar sulcus are still weakly delimited but the dorsal quadratojugal contact displays a low ridge separating two shallow grooves (Fig. 8.10D). This indicates a stronger articulation between the quadrate and quadratojugal at that stage.

State 4—In the first stages of maturity (here referred as a subadult stage), the quadratojugal contacts of MHNM.KK375 (and fully mature MHNM.KK378) are deeply excavated by ridges and fossae, evidencing a strong and immobile suture between the quadrate and quadratojugal (Fig. 8.10G–I). Both ento- and ectocondyles are also well-delimited and the intercondylar sulcus is deep. This indicates that the quadrate was tightly articulated with the lower jaw.

State 5—MHNM.KK378 is the largest quadrate and most likely belongs to a fully mature individual. The quadrate is much larger than the other ones, and the entocondyle is strongly prominent, suggesting that the intercondylar sulcus of the mandibular articulation was particularly deep (Fig. 8.10J-L). The squamosal capitulum is also globular and an additional quadrate ridge appears ventral to it (Fig. 8.10K).

These ontogenetic transformations result from the fusion between the quadrate and quadratojugal, the reinforcement of the quadrate shaft, and the stabilization and tightening of the articulation of the squamosal capitulum and mandibular condyles with the squamosal and lower jaw, respectively. Given the fact that both quadratojugal contacts are deeply excavated or have an irregular surface, that the mandibular condyles are well-developed and well-delimited by an intercondylar

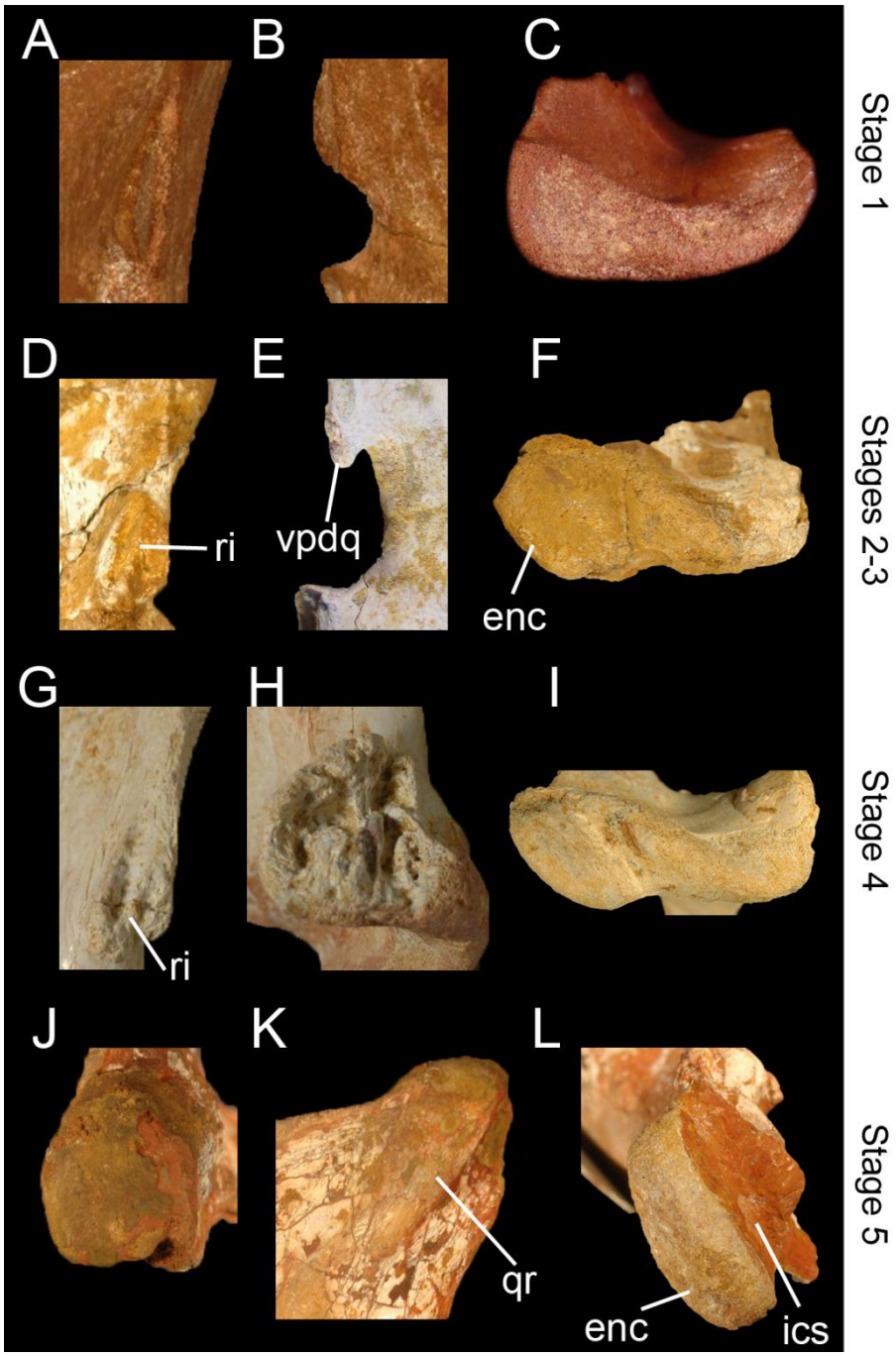

FIGURE 8.10. Ontogenetical changes in the quadrates of *Spinosaurus aegyptiacus* (Morphotype 1). **A–C**, Left quadrate MHNM.KK374 representing ontogenetic stage 1 (juvenile) with **A**, close up on the smooth lateral surface of the dorsal quadratojugal contact in lateral view; **B**, quadrate foramen and absence of a ventral projection of the dorsal quadratojugal contact in posterior view; **C**, and non-delimited mandibular condyles in ventral view. **D–E**, Left quadrates of specimens **D, F**, MHNM.KK377; and **E**, MSNM V6896 representing ontogenetic stage 2 and 3 (immature to subadult) with **D**, close up on the ridged dorsal quadratojugal contact in lateral view; **E**, quadrate foramen and a ventral projection of the dorsal quadratojugal contact in posterior view; and **F**, poorly delimited mandibular condyles in ventral view. **G–I**, Left quadrate MHNM.KK375 representing ontogenetic stage 4 (adult) with **G**, close up on the irregular and ridged lateral surface of the dorsal quadratojugal contact in lateral view; **H**, deeply excavated ventral quadratojugal contact in lateral view; and **I**, well-delimited mandibular condyles in ventral view. **J–L**, Left quadrate MHNM.KK378 representing ontogenetic stage 4 (large fully mature) with **J**, close up on the protuberant squamosal capitulum in ventral view; **K**, second dorsal quadrate ridge extending to the quadrate head in posterior view; and **L**, well-delimited entocondyle with deep intercondylar sulcus in ventral view. **Abbreviations**: **enc**, entocondyle; **ics**, intercondylar sulcus; **qr**, quadrate ridge; **ri**, ridge of the dorsal quadratojugal contact; **vpdq**, ventral projection of the dorsal quadratojugal contact. Quadrates not to scale.

sulcus, and that the ectocondyle is excavated by a deep depression, MHNM.KK376 (Morphotype 2) clearly belongs to a mature individual (Stage 4 to 5). Likewise, the poorly delimited mandibular condyles, associated with an irregular surface of the dorsal quadratojugal contacts, suggest that the quadrates of *Baryonyx* (and possibly *Suchomimus*) belong to an immature individual (Stage 3). Based on the deep intercondylar sulcus, the globular squamosal capitulum, the deeply excavated quadratojugal contacts and the absence of a second quadrate ridge ventral to the quadrate head, we interpret the quadrates of *Spinosaurus* neotype as belonging to a subadult individual, an opinion followed by Ibrahim et al. (2014*b*) based on the coossification between vertebral centra and neural arch and between the ilium and sacral.

Size

Spinosauridae encompasses large tetanurans and some of the largest terrestrial predators on Earth. A complete snout from the Kem Kem beds assigned to *Spinosaurus aegyptiacus* belongs to an animal with an estimated skull length of 175 cm (Dal Sasso et al. 2005; n.b., the estimated skull length by Ibrahim et al. (2014*b*) seems to be closer to 160 cm as it is 32% larger than the neotype subadult skull estimated as 112 cm; Ibrahim pers. comm.) and a body length estimated to reach 15 meters (Ibrahim et al. 2014*b*). Based on comparison with the quadrates of *Baryonyx* and the estimated length of its skull, an estimation of the skull size for each quadrate can be proposed. The proportion of the quadrate relative to the skull length is significantly different in the baryonychines *Baryonyx* and *Suchomimus*, yet this difference can be explained by the fact that the isolated quadrate of *Suchomimus* likely pertains to a smaller individual than the holotype MNN GDF500 and the paratype MNN GDF501. Indeed, the premaxillae and humerus of *Baryonyx* are 17-20% smaller than those of *Suchomimus* (Charig and Milner 1997; Sereno et al. 1998; pers. obs.) whereas the best preserved quadrate is 20% larger than that of *Suchomimus* (Table 8.2; pers. obs.). With a quadrate of 145 mm long from entocondyle to squamosal capitulum, and an estimated skull of 1190 mm (Therrien and Henderson 2007), the quadrate to skull ratio is only 0.12 in *Suchomimus*, which seems to be particularly low (Table 8.2).

Based on the reconstruction of the *Suchomimus* skull, and given the fact that *Baryonyx* cranial material is 20% smaller than that of *Suchomimus*, the skull length of *Baryonyx* can be estimated to reach around 950 mm (910 for Therrien and Henderson 2007). Given a quadrate length of 220 mm and a quadrate-skull ratio of 0.19, the largest quadrate WDC-CSG Q5 belongs to an animal with an estimated skull length of approximately 1160 mm. This estimate is much lower than the estimated length of the skull of the largest specimen of *Spinosaurus* (i.e., 175 cm in MSNM V4047; Dal Sasso et al. 2005). Likewise, WDC-CSG Q5 is 48% and 37% smaller than the quadrates of the largest carcharodontosaurids *Giganotosaurus* (43 cm for the quadrate height; pers. obs.), and *Acrocanthosaurus* (35 cm; Eddy and Clarke 2011) and *Mapusaurus* (35 cm; Coria and Currie 2006), respectively. This can be explained by the fact that the spinosaurid skull is particularly ventrodorsally

TABLE 8.2. Quadrate size and estimated skull length. *Estimations. **Considering that MNN GAD 502 (quadrate) and MNN GAD 501 (articulated premaxillae and maxillae) pertain to the same individual of *Suchomimus*.

Taxa	Specimen	Quadrate subunit	Size (mm)	Width-Length Ratio	% skull	Skull (mm)
Baryonyx walkeri	NHM R.9951 (left quadrate)	Quadrate length Mandibular articulation width	181 100	0.55	19% 10.5%	950*
Suchomimus tenerensis	MNN GAD 502	Quadrate length Mandibular articulation width	145 70	0.48	12.1%** 5.9%**	1190*
Spinosaurus morphotype 1	WDC-CSG Q1	Quadrate length Mandibular articulation width	78 36	0.46	? ?	340-410*
	WDC-CSG Q2	Quadrate length Mandibular articulation width	145 77	0.53	? ?	730-760*
	WDC-CSG Q4	Quadrate length Mandibular articulation width	130 70	0.54	? ?	665-685*
	WDC-CSG Q5	Quadrate length	220	?	?	~1160*
	MSNM V6896	Quadrate length Mandibular articulation width	145 76	0.52	? ?	730-760*
Spinosaurus morphotype 2	WDC-CSG Q3	Quadrate length Mandibular articulation width	200* 108	?	? ?	1030-1050*

low compared to that of other basal tetanurans, and the cranium, along with the quadrate ventrodorsal length, was subject to a reduction throughout the evolution of Megalosauroidea leading to Spinosauridae. Interestingly, five out of six of the spinosaurine quadrates collected from the Kem Kem beds and belonging to non-juvenile individuals (WDC-CSG Q2-Q4; MSNM V6896; Cabot private collection) are 20% smaller to 10% larger than that of *Baryonyx* and pertain to animals with estimated skulls varying from 65 to 105 cm (Table 8.2). This either suggests that very large forms of *Spinosaurus* with skulls of more than 150 centimeters in length may have been rare in the Kem Kem assemblage compound, or that the quadrate bone is proportionally smaller relative to the skull length in Spinosaurinae than in Baryonychinae.

Diversity

Based on our investigation on the ontogenetic variations in the quadrates of morphotype 1, and given the fact that morphotype 2 and two quadrates of morphotype 1 (MHNM.KK375 and MHNM.KK378) belong to mature individuals, the morphological differences observed between morphotypes 1 and 2 cannot be explained by ontogeny. Likewise, all isolated quadrates from the Kem Kem beds do not show any sign of taphonomic distortion, and it is clear that the morphological variations seen in morphotype 2 do not result from postmortem deformation. There is also no evidence supporting the fact that the morphological differences observed in MHNM.KK376 are pathological

and we, therefore, exclude morphotype 2 as belonging to a pathological animal. It is finally highly unlikely that these differences are due to sexual dimorphism or interindividual variation among a single species. Indeed, the amount of differences observed in the quadrates of the two baryonychine taxa *Baryonyx walkeri* (NHM R.9951) and *Suchomimus tenerensis* (MNN GAD 502) are as important as those displayed by the two spinosaurine morphotypes. *Baryonyx* and *Suchomimus* quadrates only differ in the morphology of the ventral quadratojugal contact and the quadrate head, the degree of curvature of the medial margin of the quadrate shaft and the presence of an intercondylar notch (Fig. 8.9A–L). Unlike *Baryonyx*, the quadrate of *Suchomimus* shows a dorsal projection of the ventral quadratojugal contact (Fig. 8.9H), a longer ventral projection of the dorsal quadratojugal contact, and an intercondylar notch (Fig. 8.9I, K). The quadrate head is also subtriangular rather than subcircular and the convexity of the medial margin of the quadrate shaft is more pronounced in anterior view (Fig. 8.9G). Contrary to the two spinosaurine morphotypes, the quadrate foramen and the dorsal quadratojugal contact of the two baryonychine taxa are almost identical in shape and outline, and the anterior surface of the ectocondyle shows the same concavity. The ventral quadratojugal contact of the two Baryonychinae and the two spinosaurine morphotypes also display the same level of differences. Each morphotype can, therefore, be confidently referred to different spinosaurine taxa, evidencing the presence of two species of Spinosaurinae, likely two species of *Spinosaurus*, in the Cenomanian of North Africa.

Given the fact that the first morphotype clearly belongs to the neotype of *Spinosaurus aegyptiacus* proposed by Ibrahim et al. (2014*b*), we assign the quadrate of morphotype 2 to the second species of *Spinosaurus*, *S. maroccanus*. This taxon was erected by Russell (1996) in 1996 based on dentary fragments, cervical vertebrae and a dorsal neural arch uncovered in the Kem Kem beds of the Tafilalt, north to the Kem Kem region (Fig. 8.1A). An incomplete snout and additional vertebral material from the Tademaït of Algeria (Adrar Province, center of Algeria; Albian) were later ascribed to this species by Taquet and Russell (1998). The validity of *S. maroccanus* was, however, questioned by Sereno et al. (1998), Buffetaut and Ouaja (2002), Rauhut (2003*a*), Dal Sasso et al. (2005) and Ibrahim et al. (2014*b*) who regard this species as a *nomen dubium*. Russell (1996) distinguished *S. maroccanus* from *S. aegyptiacus* by the proportion of the mid-cervical vertebrae based on one isolated cervical vertebra. According to Russell (1996), the "ratio between length of centrum (excluding anterior articular condyle) and height of posterior articular facet of centrum [is] approximately 1.5 in mid-cervical vertebrae" (Russell 1996, p. 356) versus 1.1 in the Egyptian species (Taquet and Russell 1998). Rauhut (2000) interpreted this difference to a more posterior position of the cervical vertebra, noticing that "the posterior cervicals are relatively shorter than the mid-cervicals" in theropods, therefore "the difference in ratio is thus insufficient to diagnose a separate species" (Rauhut 2000, p. 100). Similarly, Buffetaut and Ouaja (2002) doubt of the exact position of the isolated vertebra described by Russell (1996), arguing that Stromer's original material of *Spinosaurus aegyptiacus* is no longer available for direct comparison and that the material illustrated by Stromer was damaged. In

addition, Mortimer (2014) notes that ratios in *Baryonyx walkeri* cervical series range from 1.25 to 1.81, which is the same amount of variation supposedly separating the *Spinosaurus* species. Recently, Ibrahim et al. (2014*b*) regarded the difference in proportion "as an artifact of differing ways to measure opisthocoelous vertebrae" (Ibrahim et al. 2014*b*, supplemental information p.10).

As to the cranial material assigned to the Moroccan species of *Spinosaurus*, Russell (Russell 1996) mentioned the fact that the dentary fragments referred to the holotype of *S. maroccanus* are "essentially indistinguishable" from the type *S. aegyptiacus* (Russell 1996, p. 356). A similar observation can be done for the premaxillae, maxillae and dentary later ascribed to *S. maroccanus* by Taquet and Russell (1998). Indeed, the differential diagnosis proposed by these authors for this species corresponds exactly to the description of the material identified as belonging to *S. aegyptiacus* by Milner (2003) and Dal Sasso et al. (2005). The morphology of the fused premaxillae and maxillae referred to *S. maroccanus* are extremely similar to those ascribed to *S. aegyptiacus*, and the main difference lies in the premaxillary tooth count (Fig. 8.11). In *S. maroccanus*, each premaxilla bears seven alveoli whereas the premaxilla of the specimen MSNM V4047 referred to belong to *S. aegyptiacus*, only has 6 teeth. This difference is, however, negligible given the fact that tooth count can vary during ontogeny in some basal tetanurans (e.g., Carr 1999; Rauhut and Fechner 2005), between individuals of the same species (e.g., Madsen 1976; Colbert 1990; Currie 2003; Sampson and Witmer 2007), and even between left and right premaxillae of a same specimen (e.g., Charig and Milner 1997; Hendrickx and Mateus 2014*a*). In addition, a second specimen with fused premaxillae referred to *Spinosaurus* cf. *aegyptiacus* (NHM R.16420; Milner 2003) also possesses seven premaxillary alveoli. Consequently, such a difference in premaxillary tooth count between the two species of *Spinosaurus* is here considered as ontogenetic or intraspecific, and not taxonomically significant, and cranial and postcranial material ascribed to *Spinosaurus maroccanus* are here tentatively considered to belong to *Spinosaurus aegyptiacus*, pending on a comprehensive description of this material.

More recently, Richter et al. (2013) reported three types of crown ornamentation and enamel texture in isolated teeth assigned to *Spinosaurus*. In a first morphotype, flutes are distinct, numerous, and strongly developed on the lingual surface and only weakly developed on the labial surface. A second morphotype is defined by well-developed flutes on both lingual and labial sides, yet this fluting is more distinct, numerous and narrower lingually. Finally, the absence of flutes and a smooth enamel surface texture on the crown characterize a third morphotype of *Spinosaurus* teeth. According to Richter et al. (2013), there is no gradational transition between each crown ornamentation which may suggest that more than one species of *Spinosaurus* were present in the Cenomanian of Morocco. However, Richter et al. (2013) suggested that different ornamentations may also be related to a strong variation in the dentition of *Spinosaurus*, although they noted that such heterodonty has never been observed in any articulated specimen of *Spinosaurus*. Nonetheless, no *Spinosaurus* tooth-bearing bones reported in the literature so far preserves complete in-situ teeth, and the morphological variation

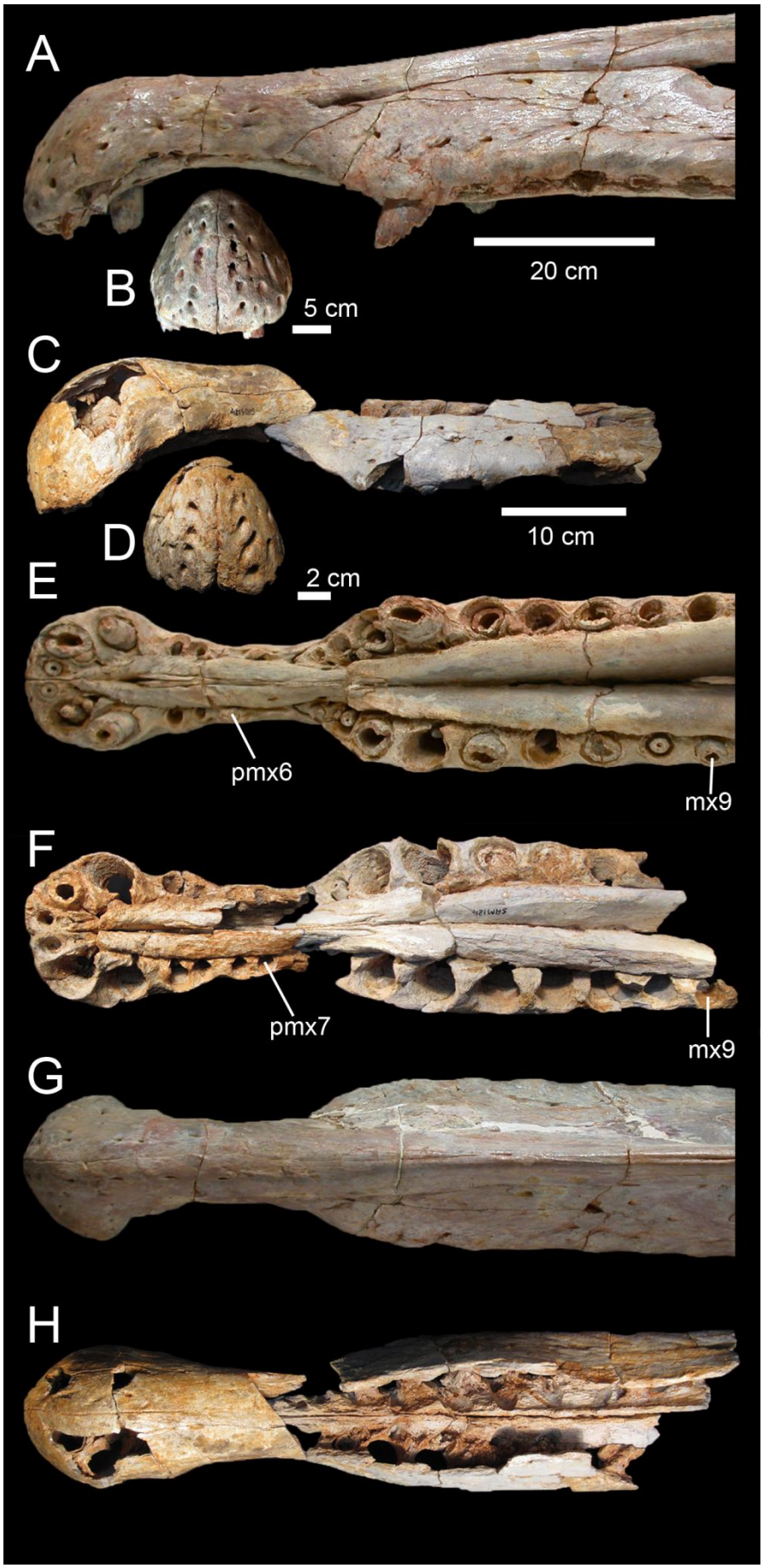

FIGURE 8.11. Comparison of the snout of two specimens of *Spinosaurus* from the 'Continental intercalaire' of Northwestern Africa. **A–H**, Fused maxillae and premaxillae of **A–B, E, G**, MSNM V4047 referred to *Spinosaurus aegyptiacus* by Dal Sasso et al. (2005) (courtesy of Simone Maganuco); and **C–D, F, H**, MNHM SAM 124 referred to *Spinosaurus maroccanus* by Taquet and Russell (1998) in **A, C**, lateral; **B, D**, anterior; **E, F**, ventral; and **G, H**, dorsal views. Abbreviation: **mx9**, ninth maxillary alveolus; **pmx6**, sixth premaxillary alveolus, **pmx7**, seventh premaxillary alveolus. Scale = 20 cm (A, E, G), 10 cm (C, F, H), 5 cm (B), 2 cm (D).

of *Spinosaurus* teeth along the dentition remains unknown (pers. obs.). Furthermore, due to the straight and centrally positioned carinae and the absence of lingual and/or labial depressions mediobasally situated on the crown, the labial and lingual sides are excessively difficult to distinguish in isolated teeth of Spinosauridae (pers. obs.). In addition, variations in crown ornamentation may be due to ontogenetic factors, as in the case with denticle size and density, and crown thickness in the dentition of basal tetanurans (e.g., Carr 1999; Araújo et al. 2013). Finally, teeth of *Baryonyx* and *Suchomimus* display a similar variation in the number and development of flutes (pers. obs.). In *Baryonyx*, in which all isolated teeth with the specimen number NHM R.9951 belong to same individual (Charig and Milner 1997), some crowns do not possess any flutes whereas others show more than eight distinctly developed flutes on the lingual side (pers. obs.). Variation in the development of the veined enamel texture of the crowns have also been noted. It is, therefore, likely that variation in crown ornamentation in Spinosauridae is positional and possibly ontogenetic rather than taxonomic, and the hypothesis that more than one species of *Spinosaurus* coexisted based on different tooth morphotypes is, therefore, poorly supported.

As recently formulated by Ibrahim and Sereno (2011), we agree that there was hitherto "no basis to distinguish spinosaurid remains at generic or specific levels from eastern and western localities in coeval Cenomanian-age rocks on Africa" (Ibrahim and Sereno 2011, p. 130). Following the opinion of Sereno et al. (1998), Buffetaut and Ouaja (2002), Rauhut (2003*a*), Dal Sasso et al. (2005), and Ibrahim et al. (2014*b*), we consider that the material hitherto reported in the literature did not convincingly support the existence in the Kem Kem beds of a species of *Spinosaurus* distinct from *S. aegyptiacus*. However, the occurrence of two morphotypes of spinosaurid quadrates in the Kem Kem beds indicates, for the first time, that a second unquestionable spinosaurine taxon represented by the isolated quadrate MHNM.KK376, here referred to *S. maroccanus*, was living in the Early Late Cretaceous of what is now Morocco, increasing the already high diversity of predatory dinosaurs in the Kem Kem beds. The presence of specimens belonging to two morphotypes in the same site (MHNM.KK378 of morphotype 1 and MHNM.KK376 of morphotype 2) also suggests that the two species of *Spinosaurus*, *S. aegyptiacus* and *S. maroccanus*, were cohabiting in the same environment (n.b., given the fact that the large majority, if not all, of theropod material comes from the upper part of the Ifezouane Formation, it is very likely that all theropod taxa recovered from the Kem Kem beds were coeval). Caution should, therefore, be exercised when referring spinosaurid material from the Kem Kem beds to the single species *Spinosaurus aegyptiacus* based on paleogeographical and stratigraphical data. Ibrahim et al.'s (2014*b*) recent reconstruction of *Spinosaurus aegyptiacus* based on the association of cranial and postcranial elements belonging to different individuals of *Spinosaurus* should, therefore, be regarded as only tentative as it is highly possible that the reconstructed morphology is based on artificially associated bones from two different species of *Spinosaurus*.

Several scenarios have tried to explain the high diversity of theropod dinosaurs in the Kem Kem beds, and the unbalanced ratio between predatory and herbivorous dinosaurs. Up to seven theropod clades have been recorded in the Kem Kem beds (i.e., Basal Ceratosauria, Noasauridae, Abelisauridae, Spinosauridae, Carcharodontosauridae, Sigilmassasauridae, and Dromaeosauridae), and the overabundance of theropod material, explained by collecting bias (McGowan and Dyke 2009) and a 'time-averaging' effect (Dyke 2010), but supported by field data (Läng et al. 2013), strongly suggests some niche partitioning in a very widespread heterogeneous deltaic paleoenvironment (Russell and Paesler 2003; Läng et al. 2013). This taxonomic abundance of theropods might, however, be due to an overestimation of the number of coexisting clades in the Kem Kem compound assemblage. A better understanding of spinosaurine postcranial anatomy supports the fact that the material ascribed to the indeterminate tetanuran *Sigilmassasaurus* in fact belongs to *Spinosaurus* (Allain 2014; Ibrahim et al. 2014*b*). In addition, a recently reported femur of a juvenile noasaurid may belong to the basal ceratosaur *Deltadromeus*, and isolated teeth referred to dromaeosaurids may in fact belong to a noasaurid (Evans et al. 2014). Given the important morphological similarities noted by Fanti and Therrien (2007), Hendrickx and Mateus (2014*b*), and Evans et al. (2014) between the dentition of Noasauridae and Dromaeosauridae, it is indeed likely that the dromaeosaurid teeth reported by Amiot et al. (2004*a*) and Richter et al. (2013) from the Kem Kem beds belong to *Deltadromeus*. Consequently, only four non-avian theropod clades (Noasauridae, Abelisauridae, Spinosauridae, and Carcharodontosauridae) and six taxa (*Deltadromeus*, an indeterminate abelisaurid, *Spinosaurus aegyptiacus*, *Spinosaurus maroccanus*, *Carcharodontosaurus*, and *Sauroniops*) may have coexisted in the Cenomanian of Northern Africa, a diversity equal to that of the Late Jurassic Lourinhã Formation of Portugal, which yielded remains of at least five definitive coexisting non-avian theropod clades and possibly nine taxa (i.e., the ceratosaurid *Ceratosaurus*, an indeterminate abelisaurid, the megalosaurid *Torvosaurus*, the allosaurid *Allosaurus*, the tyrannosauroid *Aviatyrannis*, the basal coelurosaur *Lourinhanosaurus*, the compsognathid cf. *Compsognathus*, and the paravians *Richardoestesia* and cf. *Paronychodon*; see Hendrickx and Mateus (2014*b*) and reference therein). Likewise, the abundance of spinosaurid remains in the Ifezouane Formation (Läng et al. 2013) and 'Grès rouges' Formation of the Guir basin (Benyoucef et al. 2015; which is contemporaneous to the Kem Kem beds; see Benyoucef et al. 2015), in Western Algeria, may also be explained by the presence of two coeval species of *Spinosaurus* in the fluvial system of the 'Continental intercalaire' of North Africa, and by the particularly high replacement and low formation rates of teeth in this taxon (Heckeberg 2009).

Morphofunctional analysis

Spinosauridae form a highly specialized clade of tetanurans characterized by an elongated and narrow snout with spatulate jaws (or 'terminal rosette' *sensu* Charig and Milner 1997), sigmoid alveolar margin of the rostrum, posteriorly retracted external nares, a secondary bony palate, and

subconical fluted teeth bearing minute or no denticles (Charig and Milner 1997; Sereno et al. 1998; Sues et al. 2002; Dal Sasso et al. 2005; Benson 2010*a*; Bertin 2010; Ibrahim et al. 2014*b*). Such combination of cranial features, associated with the development of robust anterior limbs bearing a huge claw in digit I, was interpreted as indicating piscivorous (Taquet 1984; Charig and Milner 1986, 1997; Buffetaut 1989*c*; Martill et al. 1996; Sereno et al. 1998; Sues et al. 2002; Milner 2003; Dal Sasso et al. 2005; Rayfield et al. 2007; Ibrahim et al. 2014*b*) or scavenging lifestyles (Kitchener 1987; Charig and Milner 1997). Postcranial bones of a juvenile *Iguanodon* and *Lepidotes* scales found in the ribcage of the holotype of *Baryonyx* (Charig and Milner 1997), as well a tooth of a spinosaurid embedded within a pterosaur cervical vertebra (Buffetaut et al. 2004) and the association of *Baryonyx* material with isolated *Iguanodon* teeth from Portugal (O.M. pers. obs.), support the fact that these derived tetanurans were opportunistic animals feeding on fish, ornithopods, and pterosaurs. Likewise, on the basis on the isotopic ratios of oxygen in their remains, spinosaurids have been interpreted as semi-aquatic (Amiot et al. 2010*b*), a conclusion subsequently supported by the peculiar morphology of their hind limbs and feet, and the high density of their bones in *Spinosaurus* (Ibrahim et al. 2014*b*).

The peculiar morphology of the mandibular articulation of *Baryonyx* and Morphotype 1 and 2 of Spinosaurinae provides additional information on the jaw mechanics of Spinosauridae. In mature spinosaurid individuals, the shape of the articulation significantly differs from that of other theropods (Fig. 8.12P). Whereas the ectocondyle typically forms a broad subcircular, elliptical or parabolic protuberance in many theropods, the ectocondyle of Spinosauridae is particularly elongated, much longer than the entocondyle, and corresponds to a narrow and sigmoid ridge that extends behind the entocondyle anteromedially. Although the ectocondyle is anteroposterioly large in its lateral part, a concavity is present on the anterolateral surface of the condyle so that the apical ridge of the ectocondyle is posteriorly displaced in its lateral part in Spinosauridae. In addition, the intercondylar sulcus is narrow and strongly diagonally oriented so that its posterior orientation follows the posterior surface of the ectocondyle, which becomes entirely lateromedially oriented along its lateral part. This condition is exacerbated in WDC-CSG Q3 in which the ectocondyle forms a particularly narrow and sigmoid ridge extending well behind the entocondyle. The ectocondyle is, therefore, much longer than the entocondyle which is oblong in outline and much more protuberant than the ectocondyle. In this second spinosaurine morphotype, the anterior surface of the ectocondyle is deeply excavated by a large depression whereas the diagonal intercondylar sulcus is narrow and very well-defined.

The morphology of the mandibular articulation strongly differs from that of the first and third morphoclades obtained in the phylogenetic morphometric analysis (Fig. 8.6A). Both morphotypes of the mandibular articulation are characterized by a weakly lateromedially elongated mandibular articulation showing a wide and poorly lateromedially oriented mandibular sulcus and an ectocondyle subequal to or smaller than the entocondyle. Theropods recovered in these two morphoclades encompass ceratosaurs, allosaurids, non-proceratosaurid tyrannosauroids, therizinosaurs, alvarezsauroids, oviraptorosaurs, and troodontids. As already noted by Hendrickx et al. (2014*b*), these

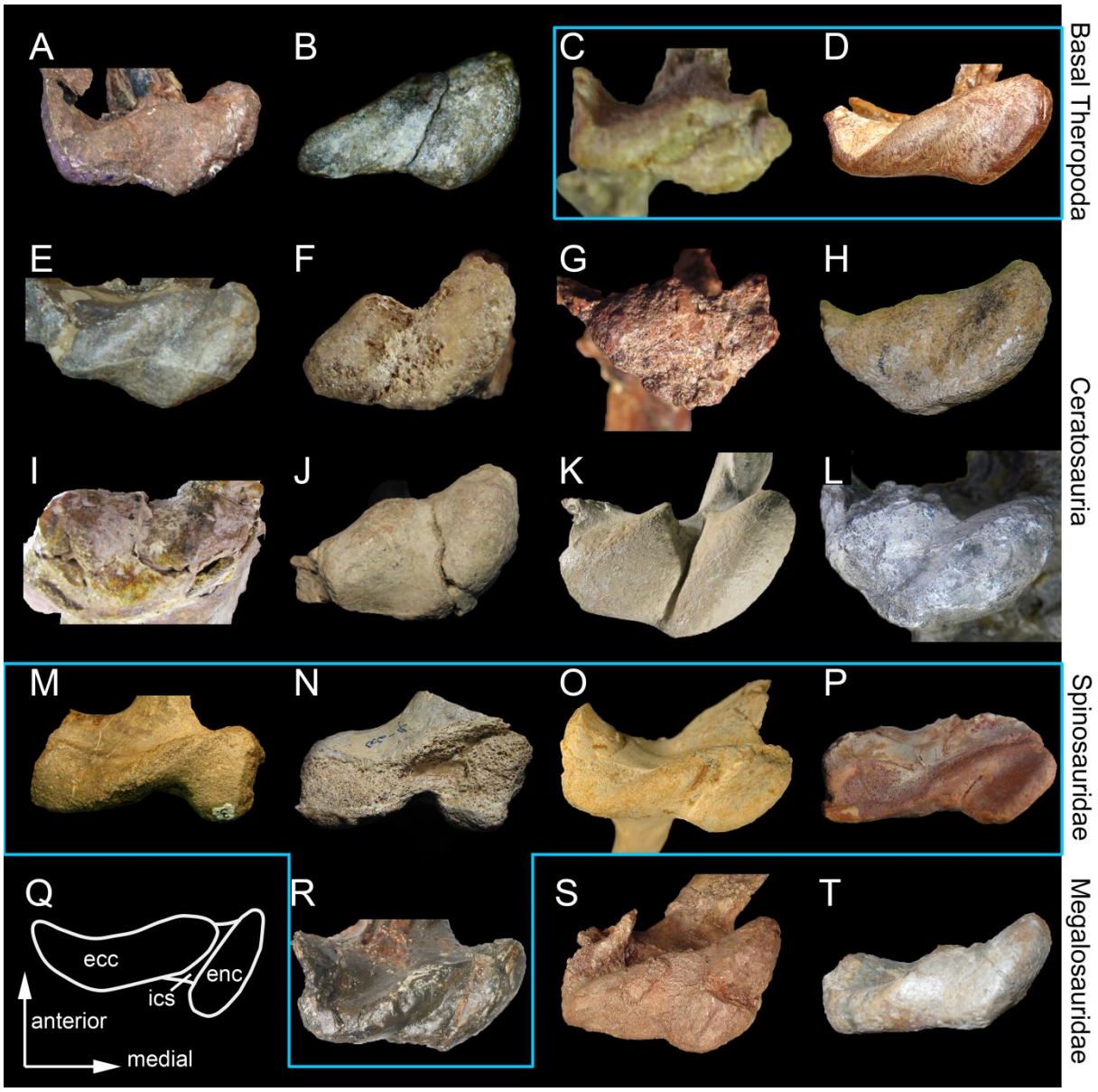

FIGURE 8.12. Morphological diversity of the mandibular articulation in non-avetheropod theropods. **A**–**P**, **R**–**T**, right quadrate (unless indicated) in ventral view in; **A**, *Herrerasaurus ischigualastensis* (formerly '*Frenguellisaurus*' *ischigualastensis*; PVSJ 053; left reversed); **B**, *Eodromaeus murphi* (PVSJ 562); **C**, *Tawa hallae* (GR 241; courtesy of Sterling Nesbitt); **D**, *Dilophosaurus wetherilli* (UCMP 37302; left reversed; courtesy of Juan Canale); **E**, *Ceratosaurus nasicornis* (MWC 1; left reversed); **F**, *Masiakasaurus knopfleri* (FMNH PR 2496); **G**, *Noasaurus leali* (PVL 4061); **H**, *Ilokelesia aguadagrandensis* (MCF-PVPH 35); **I**, *Abelisaurus comahuensis* (MPCA 11098; left reversed; in posteroventral view); **J**, *Aucasaurus garridoi* (MCF-PVPH 236); **K**, *Majungasaurus crenatissimus* (FMNH PR 2100; left reversed); **L**, *Carnotaurus sastrei* (MACN-CH 894; left reversed; courtesy of Pablo Asaroff); **M**, *Baryonyx walkeri* (NHM R.9951; left reversed); **N**, *Suchomimus tenerensis* (MNN GAD502; left reversed); **O**, *Spinosaurus aegyptiacus* Morphotype 1 (MHNM.KK375; left reversed); **P**, *Spinosaurus maroccanus* Morphotype 2 (MHNM.KK376; left reversed); **Q**, anatomy and orientation of an idealized right quadrate in ventral view; **R**, *Eustreptospondylus oxoniensis* (OUMNH J.13558; courtesy of Paul Barrett); **S**, *Afrovenator abakensis* (MNN UBA1; left reversed; courtesy of Roger Benson); **T**, *Torvosaurus tanneri* (BYU-VP 5110). **Abbreviations**: **ecc**, ectocondyle; **enc**, entocondyle; **ics**, intercondylar sulcus. Taxa framed in blue are those belonging to morphoclade 2 retrieved in the phylogenetic morphometric analysis. Quadrates not to scale.

clades encompass two types of theropods: the large predators with relatively short and broad skulls resisting torsional bending such as ceratosaurs, some megalosaurids and allosauroids, and

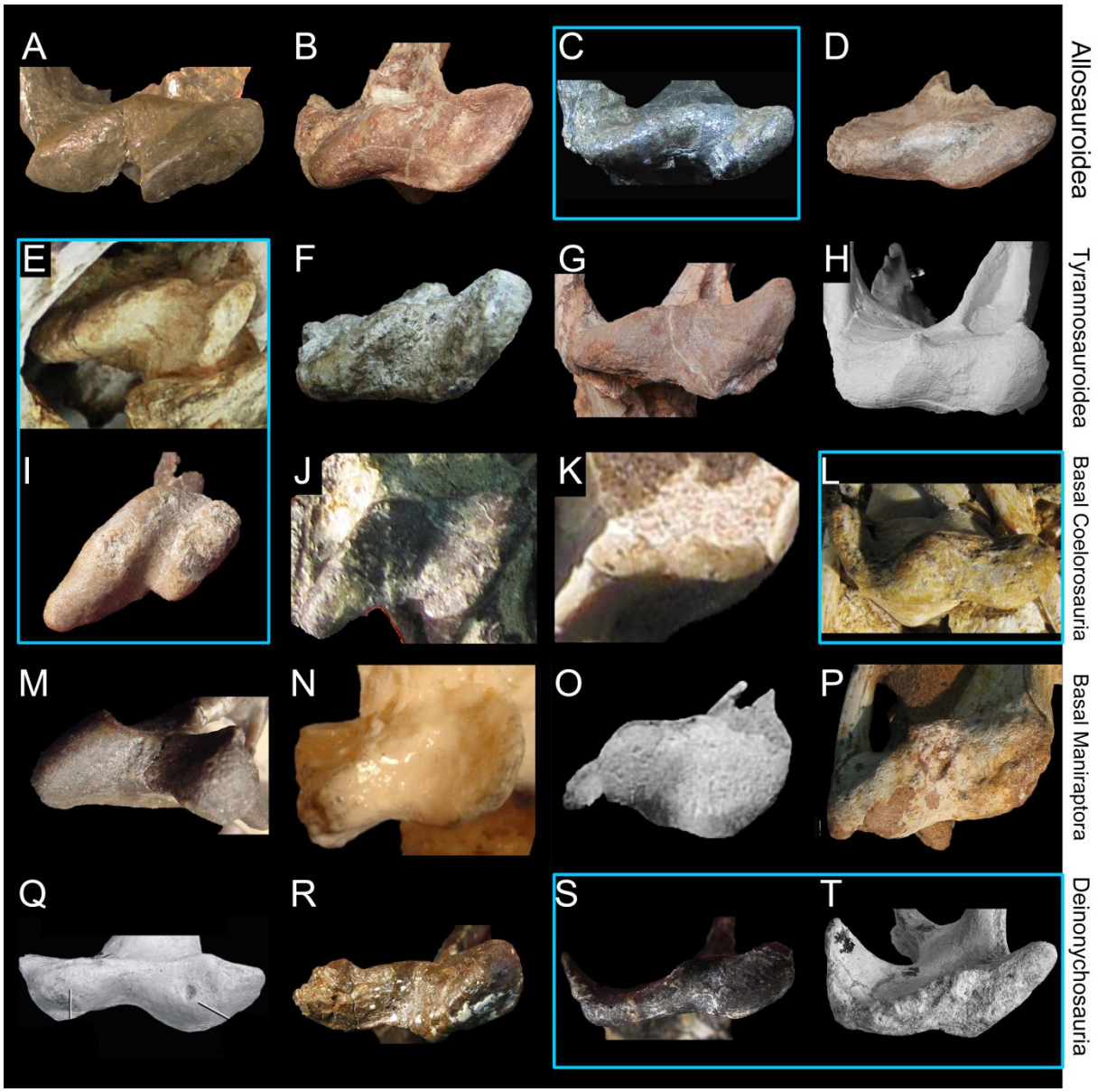

FIGURE 8.13. Morphological diversity of the mandibular articulation in non-avian Avetheropoda. **A–T**, Right quadrate (unless indicates) in ventral view in; **A**, *Allosaurus* '*jimmadseni*' (SMA 05/002); **B**, *Aerosteon riocoloradensis* (MCNA-PV-3137; left reversed; courtesy of Martin Ezcurra); **C**, *Acrocanthosaurus atokensis* (NCSM 14345); **D**, *Giganotosaurus carolinii* (MUCPv-CH-1; left reversed); **E**, *Guanlong wucaii* (IVPP V14531; left reversed; courtesy of Oliver Rauhut); **F**, *Eotyrannus lengi* (MIWG 1997.550); **G**, *Qianzhousaurus sinensis* (GM F10004-1; left reversed; courtesy of Stephen Brusatte); **H**, *Tyrannosaurus rex* (BHI l013; from Larson 2008*b*, modified); **I**, *Bicentenaria argentina* (MPCA 865; left reversed); **J**, *Ornitholestes hermanni* (AMNH FARB 619); **K**, *Shuvuuia deserti* (IGM 100-1001; left reversed); **L**, *Gallimimus bullatus* (IGM 100-1133; left reversed); **M**, *Falcarius utahensis* (UMNH VP 14559; left reversed; courtesy of Lindsay Zanno); **N**, *Avimimus portentosus* (cast of PIN 3907-3; left reversed; courtesy of Lawrence Witmer); **O**, Indeterminate Oviraptoridae (?*Ingenia yanshini* or ?*Conchoraptor gracilis*; IGM A; left reversed; Maryańska and Osmólska 1997); **P**, *Citipati osmolskae* (IGM 100-978); **Q**, Indeterminate Oviraptoridae (?*Saurornithoides mongoliensis*; IGM 100-1083; Norell and Hwang 2004, modified); **R**, *Dromaeosaurus albertensis* (AMNH FARB 5356); **S**, *Bambiraptor feinbergi* (AMNH FARB 30556; left reversed); **T**, *Tsaagan mangas* (IGM 100-1015; Norell et al. 2006; courtesy of Mick Ellison). Quadrates not to scale. Taxa framed in blue are those belonging to morphoclade 2 retrieved in the phylogenetic morphometric analysis. Quadrates not to scale.

tyrannosaurids, and the herbivorous theropods with beaks, edentulous jaws or leaf-shaped crowns such as alvarezsauroids, therizinosauroids, oviraptorosaurs, and troodontids. In these two types of

theropods, a broad and/or lateromedially short articulation of the quadrate was advantageous for either feeding on large prey or on hard plants thanks to a powerful and highly efficient bite that could resist high degrees of stresses and torsional bending (Rayfield 2005*b*; Therrien et al. 2005; Sakamoto 2010).

On the other hand, spinosaurid taxa were recovered among the second morphoclade obtained in the phylogenetic morphometric analysis (Fig. 8.6A). This morphotype of the mandibular articulation is characterized by a diagonally oriented intercondylar sulcus combined with an elongatedand lateromedially oriented ectocondyle much longer than the entocondyle. Such a morphology of the mandibular articulation is also present in the primitive theropod *Tawa*, the dilophosaurid *Dilophosaurus*, the megalosaurid *Eustreptospondylus*, the basal carcharodontosaurids *Acrocanthosaurus* and *Shaochilong*, the proceratosaurid *Guanlong*, and the dromaeosaurids *Bambiraptor* and *Tsaagan* (Figs. 8.10–8.11; blue frames). These taxa are roughly distributed in the same morphospace in the geometric morphometric analysis (Fig. 8.7). They have also been recovered in a same morphoclade in the phylogenetic morphometric analysis performed by Hendrickx et al. (2014*b*). Based on similar results, Hendrickx et al. (2014*b*) have suggested that these distantly related theropods shared the same jaw mechanics where the two mandibular rami were laterally displaced when the mandible was depressed. Two types of theropods show this morphology of the mandibular articulation, namely the weakly and fast biting carnivores with an elongated skull, and sometimes a sigmoid alveolar margin of the upper jaw (i.e., *Tawa*, *Dilophosaurus*, *Eustreptospondylus*, *Guanlong*, *Tsaagan*, *Bambiraptor*), and the massive predators with powerful and robust skulls that were able to swallow large chunks of meat (*Acrocanthosaurus*, *Shaochilong*). Spinosauridae pertain to the first type of theropods, yet they differ from dilophosaurids, *Eustreptospondylus*, proceratosaurids and dromaeosaurids by having a much larger body size and a strongly elongated crocodile-like skull. Such a transformation of the skull also affected the mandibular articulation which shows a derived morphology among theropods.

The presence of a narrow and posteriorly displaced ectocondyle displaying a large concave surface on the anterior face first implies a very strong and particularly stable articulation between the mandibular condyles of the quadrate and the glenoid fossa of the articular. In *Baryonyx* and *Irritator*, the dorsal margin of the articular bone shows a deep glenoid fossa formed by two depressions separated by a faint interglenoid ridge (Fig. 8.14B; Sues et al. 2002; n.b., the left articular of *Baryonyx* was identified as the right atlantal neural arch by Charig and Milner (1997) and the central body of the left pterygoid by Sereno et al. (1998), whereas the right articular was interpreted as the left postorbital by Charig and Milner (1997) and the posterior portion of the right surangular by Sereno et al. (1998); Carrano pers. comm.). A similar morphology most likely existed in *Spinosaurus*, and Morphotype 2 probably had one of the most stable mandibular articulations among all theropods. Indeed, based on the morphology of the mandibular articulation, the articular of WDC-CSG Q3 was deeply excavated by a narrow glenoid fossa, and had two well-defined lateral and medial glenoid depressions divided by an acute interglenoid ridge. The articulation must also have been stabilized by a smooth and prominent

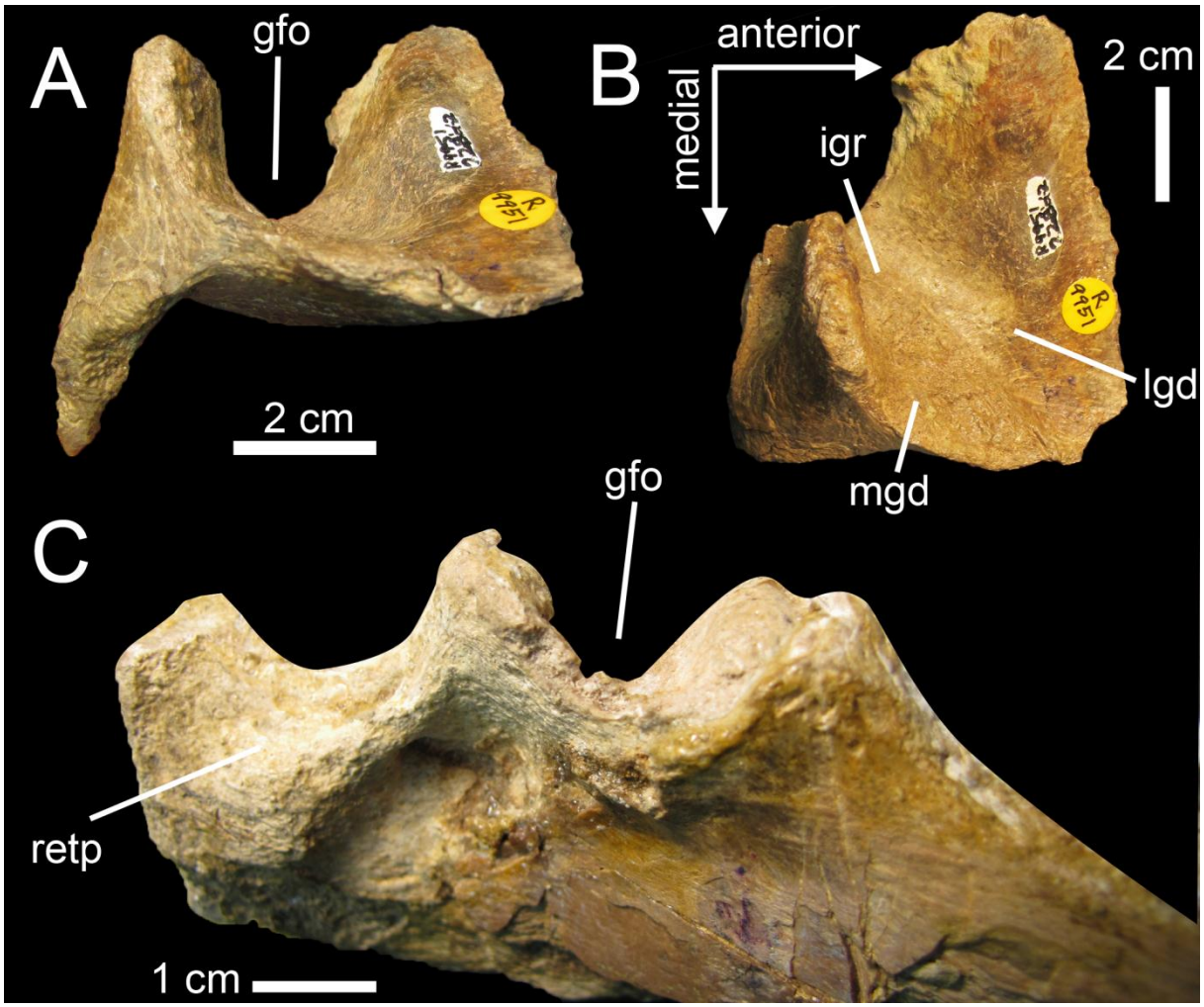

FIGURE 8.14. Left articular morphology in Spinosauridae. **A–B**, *Baryonyx walkeri* (NHM R.9951); and **C**, *Irritator challengeri* (SMNS 58022) in **A, C**, medial; and **B**, dorsal views. **Abbreviations**: **igr**, interglenoid ridge; **gfo**, glenoid fossa; **lgd**, lateral glenoid depression; **mgd**, medial glenoid depression; **retp**, retroarticular process.

convexity delimiting the anterior surface of the lateral glenoid depression. Evolution towards a particularly stable mandibular articulation in Spinosauridae was probably the result of two independent factors: an important lateral displacement of the two rami of the mandible, and the swift movement of the jaw opening. As soon as the mandible was depressed, the interglenoid ridge of the articular sliced along the obliquely oriented intercondylar sulcus of the quadrate, forcing the articular, and consequently the two mandibular rami, to be displaced laterally (Fig. 8.15). This lateral displacement was increased by the fact that the interglenoid fossa could carry on its way further from the intercondylar sulcus, along the lateromedially oriented anterior surface of the ectocondyle. A strong lateral displacement of the two rami allowed the pharynx of Spinosauridae to be significantly enlarged, therefore favouring the deglutition of whole prey or large chunks of food.

A similar lateral displacement of the lower jaw was also observed in pterosaurs and living pelecanids, which share an elongated and narrow skull and a piscivorous diet with spinosaurids. Eaton (1910) was one of the first to describe a spiral groove in the quadrate of *Pteranodon*. This obliquely

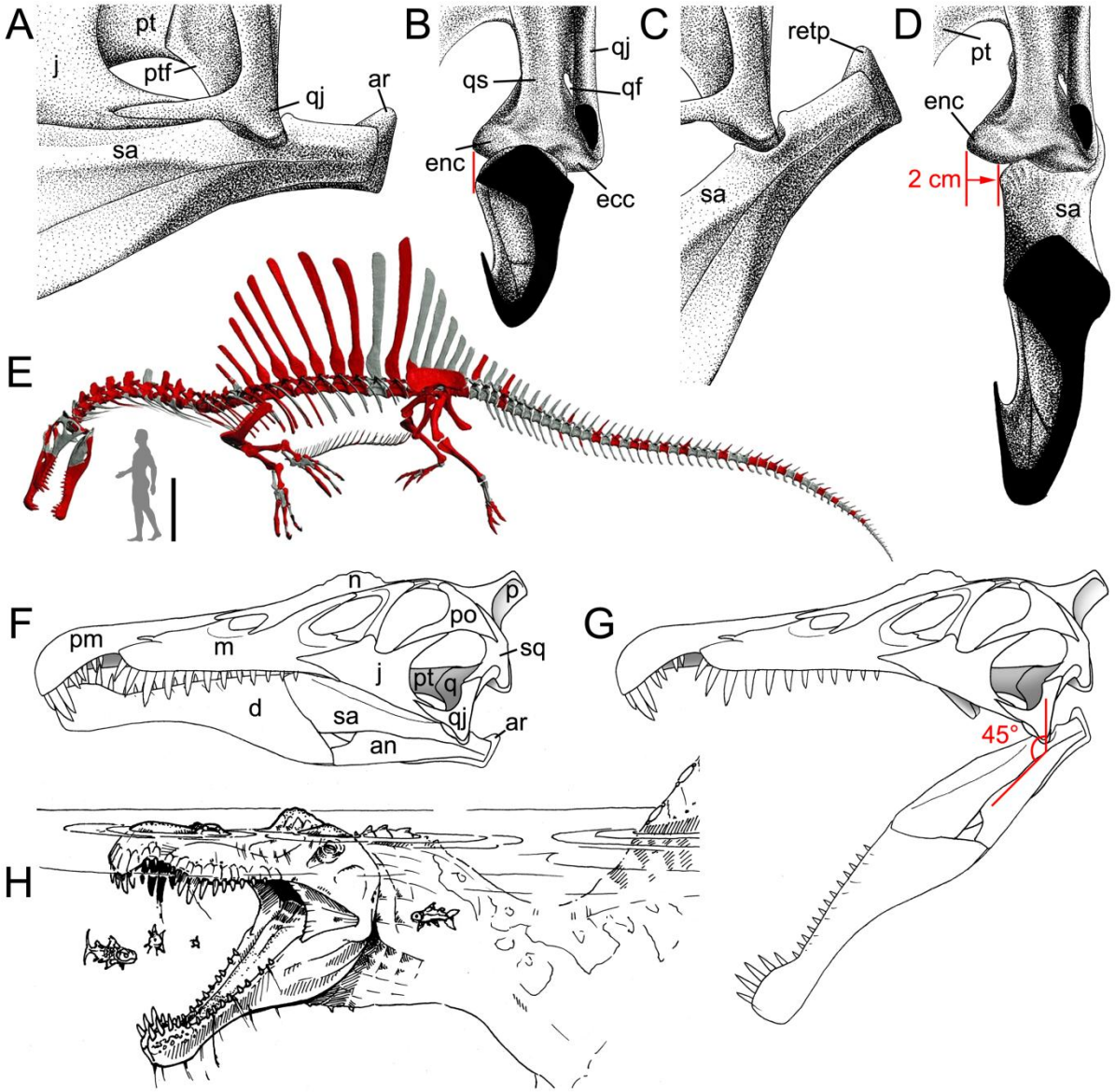

FIGURE 8.15. Jaw mechanic in the spinosaurid *Spinosaurus*. **A–D**, Mandibular articulation; and **F, G**, skull in **A, C, F–G**, lateral; and **B, D**, anterior views; when **A–B, F**, the mouth is closed; and **C–D, G**, fully open, illustrating the lateral movement (in red) of the mandibular ramus for a 45° rotation of the lower jaw (courtesy of © Jaime A. Headden); **E**, skeletal reconstruction of *Spinosaurus aegyptiacus* by Ibrahim et al. (2014*b*) in swimming position in lateral view with a human (1.8 m) as a scale (modified from Ibrahim et al. 2014*b*). This model is based on all spinosaurid cranial and postcranial material (in red color) known from the Cenomanian of North Africa, and which likely belong to two spinosaurine taxa; **H**, reconstruction of a semi-aquatic *Spinosaurus* in fishing position (i.e., jaws wide open) in anterolateral view (courtesy of © Jason Poole). **Abbreviations**: **an**, angular; **ar**, articular; **d**, dentary; **ecc**, ectocondyle; **enc**, entocondyle; **j**, jugal; **m**, maxilla; **n**, nasal; **p**, parietal; **pm**, premaxilla; **po**, postorbital; **pt**, pterygoid; **ptf**, pterygoid flange; **q**, quadrate; **qf**, quadrate foramen; **qj**, quadratojugal; **retp**, retroarticular process of the articular; **sa**, surangular; **sq**, squamosal.

oriented intercondylar sulcus was interpreted as forming "an effective screw that thrust apart the mandibular rami when the mouth is opened" and as being "directly concerned in the widening of the mouth" (Eaton 1910, p. 5). Eaton (1910) and Wellnhofer (1980) compared this peculiar jaw mechanism with that of the pelican. The lateral displacement of the rami when the jaw was depressed was illustrated and exhaustively described by Wellnhofer (1980) in *Ornithocheirus* and *Pteranodon*

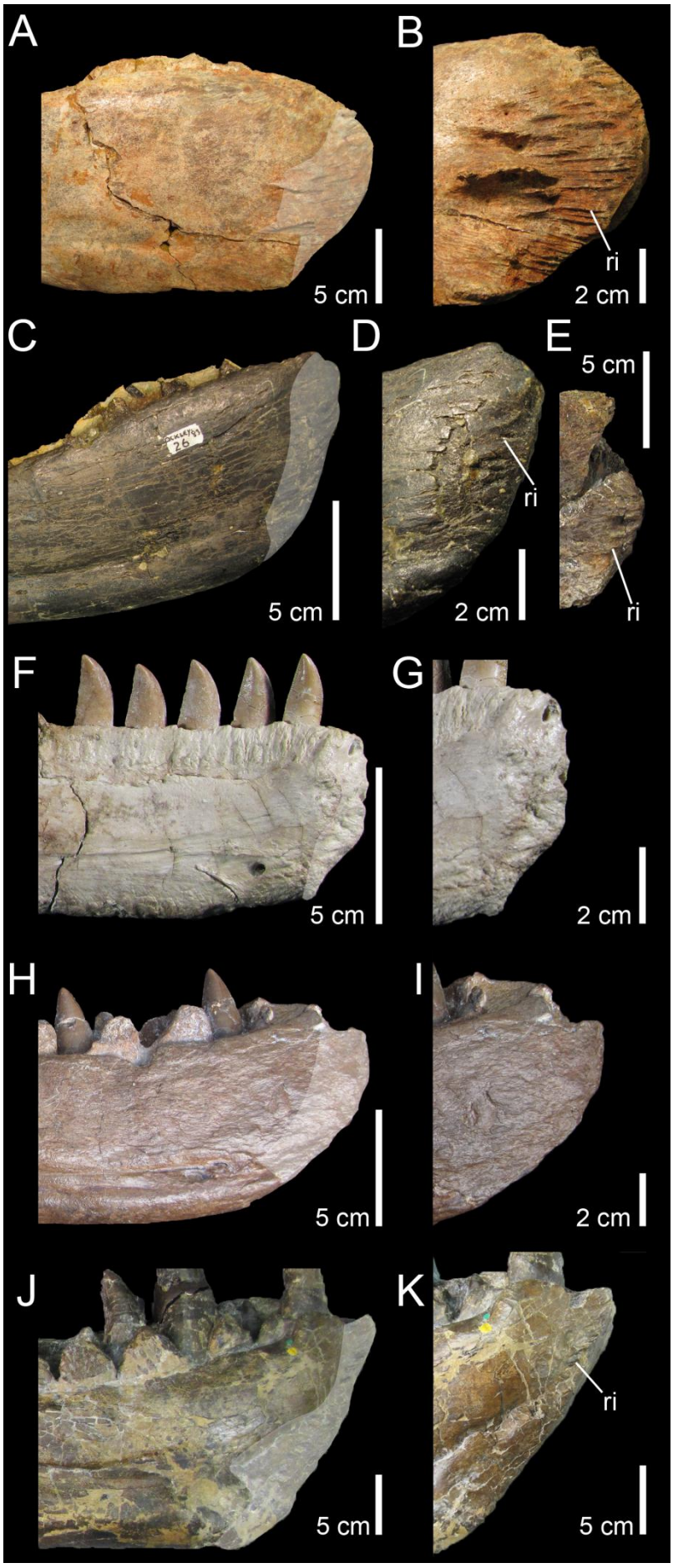

FIGURE 8.16. Morphological diversity of the mandibular symphysis in non-avian theropods in medial view. **A–B**, left dentary of *Spinosaurus* cf. *aegyptiacus* (NHM R.16421); **A**, Anterior portion; and **B**, close up on the well-developed anterior ridges of the mandibular symphysis. **C–E**, left dentary of *Baryonyx walkeri* (NHM R.9951 and ML 1190); **C**, anterior portion; and **D–E**, close up on the weakly developed anterior ridges of the mandibular symphysis in **D**, NHM R.9951; and **E**, ML 1190. **F–G**, right dentary of *Majungasaurus crenatissimus* (FMNH PR 2100; reversed); **F**, anterior portion; and **G**, close up on the irregular surface of the mandibular symphysis. **H–I**, right dentary of *Megalosaurus bucklandii* (OUMNH J13505; reversed); **H**, anterior portion; and **I**, close up on the smooth surface of the mandibular symphysis. **J–K**, right dentary of *Tyrannosaurus rex* (NHM R.7994); **J**, anterior portion; and **K**, close up on the poorly developed anterodorsal ridges of the mandibular symphysis. The symphyseal surface is colored in light grey. **Abbreviation**: **ri**, anteroposterior ridges of the mandibular symphysis.

Wellnhofer (1980) and Bennett (2001) measured a lateral displacement of one centimeter for a 90° depression of the mandible in the pelican and *Pteranodon*, respectively. According to Wellnhofer (1980), this corresponds to a widening of 25% of the mouth in *Pelecanus*. By using a cast in clay, we could measure, in WDC-CSG Q3, a displacement of two centimeters of the rami for a 45° depression (Fig. 8.15). This corresponds to 18% of the lateromedial length of the mandibular articulation of this specimen. As noted by Bennett (2001) for *Pteranodon*, the depression of the mandible only spreads the rami slightly, but may have helped in swallowing large items.

Wellnhofer (1980) noted that the lateral displacement of the ramus prevents the retroarticular process of the articular from contacting the quadrate, allowing extreme depression of the mandible (Wellnhofer 1980: fig. 7). Spinosaurids did not have such extreme movement of the lower jaw as the glenoid fossa is deep, and a process posterior to this fossa and visible in the *Baryonyx* and *Irritator* articular (Fig. 8.14), was most likely abutting against the quadrate body before the mandible was depressed at an angle of 90°. Yet, based on a reconstruction of the *Irritator* skull (Sues et al. 2002), in which the long axis of the mandibular articulation of the quadrate is ventrodorsally inclined, a 70° depression of the mandible seems possible. Similar to what has been noted for *Pteranodon*, the helical joint of spinosaurids also provided better resistance to medial displacement of the mandibular rami, and was important in maintaining accurate alignment between the jaws (Bennett 2001).

Unlike pterosaurs and similar to pelecanids, lateral displacement of the mandibular rami was possible due to a movable mandibular symphysis of the dentaries in Spinosauridae (Charig and Milner 1997; Buffetaut and Ouaja 2002). A short mandibular symphysis has been noticed in *Baryonyx walkeri* (Charig and Milner 1997; pers. obs.) and *Spinosaurus aegyptiacus* (Stromer 1915; Buffetaut and Ouaja 2002), yet the anteroposterior width of the mandibular symphysis of *Spinosaurus* is not shorter, but actually longer than in other theropods (Fig. 8.16). Likewise, the symphyseal surface of the spinosaurid dentaries bears anteroposteriorly oriented striations suggesting that the mandibular rami were articulated by connective tissue (Fig. 8.16; Charig and Milner 1997; Buffetaut and Ouaja 2002). These ridges are short and only restricted to the anteriormost part of the dentary in *Baryonyx walkeri* (NHM R.9951; ML1190). Nevertheless, a dentary ascribed to *Spinosaurus* cf. *aegyptiacus* (NHM R.16421) shows strongly developed ridges covering the whole symphyseal surface of the dentary. Symphyseal ridges in spinosaurids suggest the presence of connective tissues linking the two dentaries, allowing some lateromedial mobility of the mandibular rami (Charig and Milner 1997; Buffetaut and Ouaja 2002). This condition is once again exacerbated in *Spinosaurus aegyptiacus* in which the ridges are particularly numerous and prominent (Fig. 8.16). Such peculiar morphology of the symphyseal surface is, to our knowledge, unique among theropods as non-spinosaurid theropods typically have a smooth or irregular symphyseal surface (Fig. 8.16).

Conclusion

The description and identification of six isolated quadrates from the Kem Kem beds of Morocco provide additional information on the Cenomanian dinosaur fauna of North Africa. Based on cladistic, morphometric, and phylogenetic morphometric analyses, two morphotypes have been successfully identified as belonging to two taxa of Spinosaurinae, and ascribed to two cohabiting species of *Spinosaurus*, *S. aegyptiacus* and *S. maroccanus*. Given the fact that all previous evidence of the presence of more than one spinosaurid taxon in the Kem Kem beds is poorly supported, this is the first definitive evidence of two spinosaurine taxa in the Cenomanian of North Africa, increasing the already high diversity of predatory dinosaurs living in the Kem Kem environment around 100 million years ago.

Ontogenetic changes occurring in the spinosaurid quadrates include the suture of the quadrate and quadratojugal, delimitation of the mandibular condyles and squamosal capitulum, and development of a ventral projection of the dorsal quadratojugal contact and a second quadrate ridge ventral to the quadrate head. Based on the quadrate proportions and estimated skull length of *Baryonyx*, quadrates of mature individuals from Morocco belong to animals with a skull length of no more than 130 centimeters. This suggests that very large forms of *Spinosaurus* may have been rare in the Kem Kem assemblages.

Morphofunctional analysis of the spinosaurid quadrates has revealed peculiar jaw mechanics in these specialized theropods. An helicoidal and strongly lateromedially oriented joint of the jaw articulation allowed to displace the mandibular ramus laterally when the lower jaw was depressed. This lateral movement of the ramus was possible due to a movable mandibular symphysis as the dentaries were joined by connective tissues, and allowed the pharynx to be widened. A similar jaw articulation was convergently present in pterosaurs and particularly pelecanids which also have a mandibular articulation restricted to the anterior extremity of the mandible. Spinosauridae, which are considered to be semi-aquatic and partially piscivorous animals, were able to swallow large prey such as fish in the same way as pelecanids.

IV. *TORVOSAURUS* REMAINS FROM PORTUGAL

Chapter 9: *Torvosaurus gurneyi* n. sp., the largest terrestrial predator from Europe, and a proposed terminology of the maxilla anatomy in non-avian theropods

Published in ***PLoS ONE*** (IP 3.534):
Hendrickx, C. and Mateus, O. 2014. *Torvosaurus gurneyi* n. sp., the largest terrestrial predator from Europe, and a proposed terminology of the maxilla anatomy in non-avian theropods. *PLoS ONE* 9 (3): e88905.

Abstract

The Lourinhã Formation (Kimmeridgian-Tithonian) of Central West Portugal is well known for its diversified dinosaur fauna similar to that of the Morrison Formation of North America; both areas share dinosaur taxa including the top predator *Torvosaurus*, reported in Portugal. The material assigned to the Portuguese *T. tanneri*, consisting of a right maxilla and an incomplete caudal centrum, was briefly described in the literature and a thorough description of these bones is here given for the first time. A comparison with material referred to *Torvosaurus tanneri* allows us to highlight some important differences justifying the creation of a distinct Eastern species. *Torvosaurus gurneyi* n. sp. displays two autapomorphies among Megalosauroidea, a maxilla possessing fewer than eleven teeth and an interdental wall nearly coincidental with the lateral wall of the maxillary body. In addition, it differs from *T. tanneri* by a reduced number of maxillary teeth, the absence of interdental plates terminating ventrally by broad V-shaped points and falling short relative to the lateral maxillary wall, and the absence of a protuberant ridge on the anterior part of the medial shelf, posterior to the anteromedial process. *T. gurneyi* is the largest theropod from the Lourinhã Formation of Portugal and the largest land predator discovered in Europe hitherto. This taxon supports the mechanism of vicariance that occurred in the Iberian Meseta during the Late Jurassic when the proto-Atlantic was already well formed. A fragment of maxilla from the Lourinhã Formation referred to *Torvosaurus* sp. is ascribed to this new species, and several other bones, including a femur, a tibia and embryonic material all from the Kimmeridgian-Tithonian of Portugal, are tentatively assigned to *T. gurneyi*. A standard terminology and notation of the theropod maxilla is also proposed and a record of the *Torvosaurus* material from Portugal is given.

Introduction

The Upper Jurassic beds of central Portugal have yielded numerous dinosaur taxa representing one of the richest European faunas of dinosaurs from the Mesozoic, and certainly the most diverse one from the Late Jurassic of Europe. Members of all major clades of dinosaurs other than marginocephalians are represented, and theropods are by far the most diversified group of the clade

Dinosauria (Rauhut 2000*b*; Antunes and Mateus 2003; Mateus 2006). Hitherto, tracks, eggs, teeth and bone material (including embryos and hatchlings) discovered in the Alcobaça Formation (Kimmeridgian) of the Guimarota mine (Rauhut 2000*b*) and Lourinhã Formation (Kimmeridgian-Tithonian) of the Lourinhã region (Mateus 2006; Mateus et al. 2006; see Introduction, Fig. 1.15) have been assigned to at least ten theropod taxa belonging to the clade of Ceratosauridae (Mateus and Antunes 2000*b*; Mateus et al. 2006), Abelisauridae (Hendrickx and Mateus 2014*b*), Megalosauridae (Mateus and Antunes 2000*a*; Mateus et al. 2006; Malafaia et al. 2008; Araújo et al. 2013; Hendrickx and Mateus 2014*b*), Allosauroidea (Mateus et al. 2006; Mateus 1998; Mateus et al. 1998; Pérez-Moreno et al. 1999; Rauhut and Fechner 2005; Malafaia et al. 2007, 2009), Tyrannosauroidea (Rauhut 2003*b*), Compsognathidae (Zinke 1998), Avialae (Weigert 1995; Wiechmann and Gloy 2000), and some uncertain systematic theropod clades (Zinke and Rauhut 1994; Zinke 1998; Hendrickx and Mateus 2014*b*).

The Alcobaça and Lourinhã Formation are comparable to the contemporaneous Morrison Formation of North America both paleoenvironmentally and sedimentologically (Mateus 2006). Most of non-coelurosaurian taxa (i.e., *Allosaurus*, *Ceratosaurus* and *Torvosaurus*) were present on both continents, indicating some faunal exchanges between the Iberian Meseta and North America in the Late Jurassic, although an intercontinental sea was already separating them (Mateus 2006; Mateus et al. 2014). Mateus et al. (2014) proposed that during the Callovian/Oxfordian transition, there were temporary land bridges that allowed terrestrial faunal exchange between North America and the Iberian Meseta. The high diversity of theropods in the Late Jurassic of Laurasia, represented by small, medium-sized and large individuals, indicates important niche partitioning between these carnivorous dinosaurs. The top predators at the acme of the food chain were represented by three large theropods, *Lourinhanosaurus*, *Ceratosaurus* and *Allosaurus*, and a very large form, *Torvosaurus*, which was functionally and ecologically similar to the super-predators *Carcharodontosaurus* and *Tyrannosaurus* from the Late Cretaceous of Africa and North America, respectively.

Torvosaurus has been reported several times in the Upper Jurassic of central Portugal in the locality of Casal do Bicho (Alcobaça), Quinta do Gradil (Cadaval), Praia da Corva (Porto Novo) and Praia da Vermelha (Lourinhã). This taxon is represented by a large tibia (ML 430) and a left maxilla (ML 1100) briefly described by Mateus and Antunes (2000*a*) and Mateus et al. (2006), respectively, as well as a distal end of a femur (ML 632), a caudal vertebra (ML 1100) and a fragment of an unidentified limb bone (ML 1100) reported by Mateus et al. (2006). Malafaia et al. (2008) published a fragment of right maxilla (ALT–SHN.116) whereas a mesial tooth (ML 962) was described by Hendrickx and Mateus (2014*b*). Finally, embryonic remains (ML1188) discovered among a clutch of eggs have recently been reported by Araújo et al. (2013). These elements were all ascribed to the genus *Torvosaurus* or the species *Torvosaurus tanneri* although differences have been noted between the material from Portugal and the United States (Mateus et al. 2006).

The present work aims to propose a standard terminology of the maxilla for non-avian theropods as well as to provide a thorough description of the material ML 1100 assigned to the species *Torvosaurus tanneri* (Mateus et al. 2006). Attribution to this taxon will be discussed after a detailed comparison with other megalosaurid material. A review of the *Torvosaurus* material from Portugal will finally be given.

Proposed terminology of the maxilla anatomy in non-avian theropods

The maxilla is a cranial bone displaying an important morphological variability among non-avian theropods (e.g., Araújo et al. 2013: note 3; Lamanna et al. 2002: fig. 3; Currie and Varricchio 2004: fig. 4.5). Such morphological variation shows the great taxonomical utility and systematic potential of the maxilla in this clade of dinosaurs. As this bone provides for more information than many other parts of the skeleton, and the diagnostic value of the maxilla is significant, particular attention should be accorded to the description of this bone in the literature on non-avian theropod anatomy. Nevertheless, the terminology and abbreviations of the maxilla anatomy have been inconsistent in non-avian theropods. Several different anatomical terms for the same maxilla sub-entity have been often used, as in some examples given below. An attempt of a standard terminology for the maxilla was already proposed by Witmer (1997*a*) who, however, mostly concentrated on the maxillary sinuses and did not provide a terminology for the maxillary rami, processes and articulations. The present paper aims to propose a standardization of the anatomical terms for each of the maxilla sub-units (Figs. 9.1–9.3), mostly selected by their relevance, significance and importance in the theropod literature, in order to facilitate future descriptions of this bone. The anatomical terms were grouped into nine sections, and each term is associated with a three to four letters abbreviation and followed by a definition. The nomenclature for pneumatic recesses and openings mostly follows the terminology given by Witmer (1997*a*) and only differs for a few terms. For clarity reasons, the internal antorbital fenestra, caudal fenestra of the maxillary antrum, and fenestra communicans of Witmer (1997*a*) are here referred to as the antorbital fenestra, posteromedial maxillary fenestra, and anteromedial maxillary fenestra, respectively. Gold et al. (2013) noticed some confusion with the term ‘recess’ in the literature and preferred using ‘promaxillary sinus’ instead of ‘promaxillary recess’. Nevertheless, only one maxillary sinus may have invaded both maxillary antrum and promaxillary recess (Witmer 1997*b*) and we therefore favored Witmer’s terminology. The presence of unnamed fossae/fenestrae within the antorbital fossa in some allosauroids (Fig. 9.1), tyrannosaurids (Figs. 9.2–9.3) and oviraptorosaurs have led us to propose additional terms for several maxillary sub-units, namely pneumatic fenestra, ventral maxillary fenestra, medial maxillary fenestra, dorsomedial maxillary fenestra, postmaxillary fenestra, anteromedial and posteromedial maxillary recesses, postmaxillary and preantral struts. Likewise, we are proposing the terms ‘interdental wall’ for the

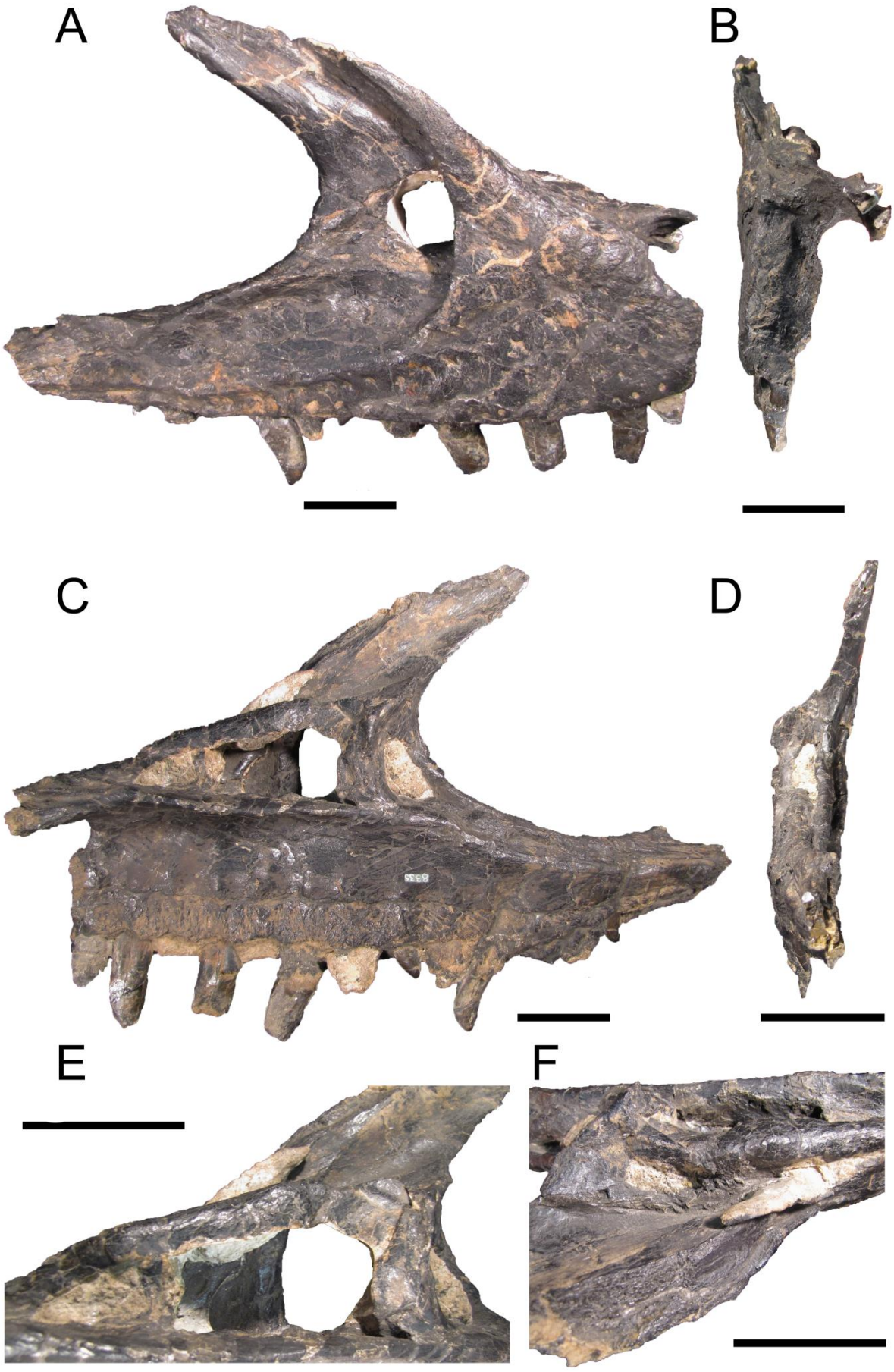
A
B
C
D
E
F

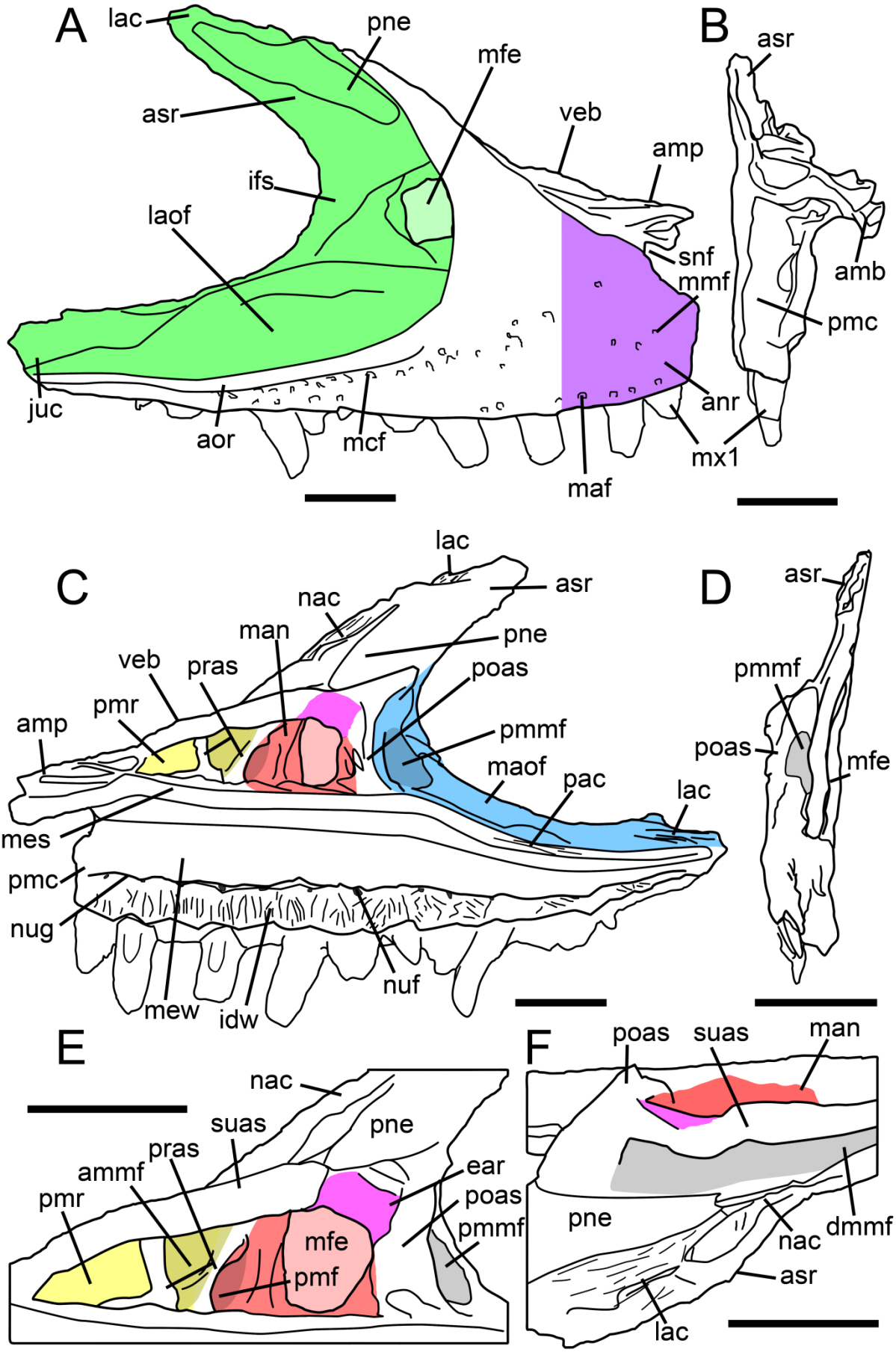
A
lac
pne
mfe
asr
veb
amp
ifs
laof
snf
mmf
juc
aor
mcf
maf
anr
mx1
B
asr
amb
pmc
C
lac
asr
nac
man
pne
veb
pras
poas
pmr
amp
pmmf
maof
pac
lac
mes
pmc
nug
nuf
mew
idw
D
asr
pmmf
poas
mfe
E
nac
suas
pne
pras
ammf
ear
pmr
poas
pmmf
mfe
pmf
F
poas
suas
man
pne
dmmf
nac
asr
lac

◄FIGURE 9.1. Proposed terminology and annotation of the non-avian theropod maxilla. Right maxilla of *Allosaurus fragilis* (USNM 8335) in **A**, lateral; **B**, anterior; **C**, medial and **D**, posterior views, with details of **E**, promaxillary recess and maxillary antrum in medial view; and **F**, ascending ramus and dorsal margin of vestibular bulla in dorsal view. **Abbreviations**: **ammf**, anteromedial maxillary fenestra; **amp**, anteromedial process; **anr**, anterior ramus; **aor**, antorbital ridge; **asr**, ascending ramus; **idw**, interdental wall; **ifs**, interfenestral strut; **juc**, jugal contact; **lac**, lacrimal contact; **laof**, lateral antorbital fossa; **law**, lateral wall; **maf**, maxillary alveolar foramina; **man**, maxillary antrum; **maof**, medial antorbital fossa; **mbo**, maxillary body; **mcf**, maxillary circumfenestra foramina; **mes**, medial shelf; **mew**, medial wall; **mfe**, maxillary fenestra; **mfo**, maxillary fossa; **mmf**, medial maxillary foramina; **mx1**, first maxillary tooth; **nac**, nasal contact; **nuf**, nutrient foramina; **nug**, nutrient groove; **pac**, palatine contact; **pmc**, premaxillary contact; **pmmf**, posteromedial maxillary fenestra; **pmr**, promaxillary recess; **pne**, pneumatic excavation; **poas**, postantral strut; **pras**, preantral strut; **snf**, subnarial foramen; **suas**, suprantral strut; **veb**, vestibular bulla. Scale bars = 5 cm.

continuous lamina formed by the fusion of interdental plates.

Bodies, Rami and Processes

The anatomical term ‘ramus’ was favored over ‘process’ for the large projecting parts of the maxilla (e.g., ascending ramus, jugal ramus, anterior ramus), the term ‘process’ being referred to a smaller projection of bone (e.g., anteromedial process).

Maxillary body (mbo)—Ventral part of the maxilla that excludes the ascending ramus (Fig. 9.2A). The delimitation of the maxillary body from the ascending ramus is somewhat subjective. Usually, these two units are virtually delimited by a constriction formed by the antorbital fenestra and a concave step on the anterodorsal margin of the maxilla. However, the anterior margin of the maxillary body and the ascending ramus can be confluent. In that case, the maxillary body and the ascending ramus should be delimited by a virtual line starting from the apex of the curvature of the antorbital fenestra (which is not always the anteriormost point of the antorbital fenestra) and extending in parallel to the main axis of the ventral margin of the maxilla. The maxillary body, as used by several authors (e.g., Britt 1991; Currie and Carpenter 2000; Mateus et al. 2006; Brusatte et al. 2010*a*; Rauhut et al. 2010, 2012), is also termed the ‘main body’ (e.g., Hurum and Sabath 2003; Dal Sasso et al. 2005; Coria and Currie 2006; Brusatte and Sereno 2007; Brusatte et al. 2010*b*, 2012*a*). It includes two main anatomical units: the anterior body and the jugal ramus.

Anterior body (anb)—Anterior part of the maxillary body that extends from the premaxilla contact to the anteriormost point of the antorbital fenestra (Fig. 9.2A). The anterior body, corresponding to the ‘ventral ramus of the nasal process’ of Turner et al. (2007*b*), includes both the preantorbital body and anterior ramus.

Preantorbital body (pab)—Anterior part of the maxillary body that extends from the premaxilla contact to the anteriormost point of the antorbital fossa (Fig. 9.2B). The preantorbital body, also known as the ‘preantorbital process’ (Rauhut et al. 2010), is part of the anterior body.

Anterior ramus (anr)—Anterior projection of the maxillary body that extends from the premaxilla contact to a concave step on the anterodorsal margin of the maxilla that corresponds to the boundary between the maxillary body and the ascending ramus (Fig. 9.1A). The anterior ramus is

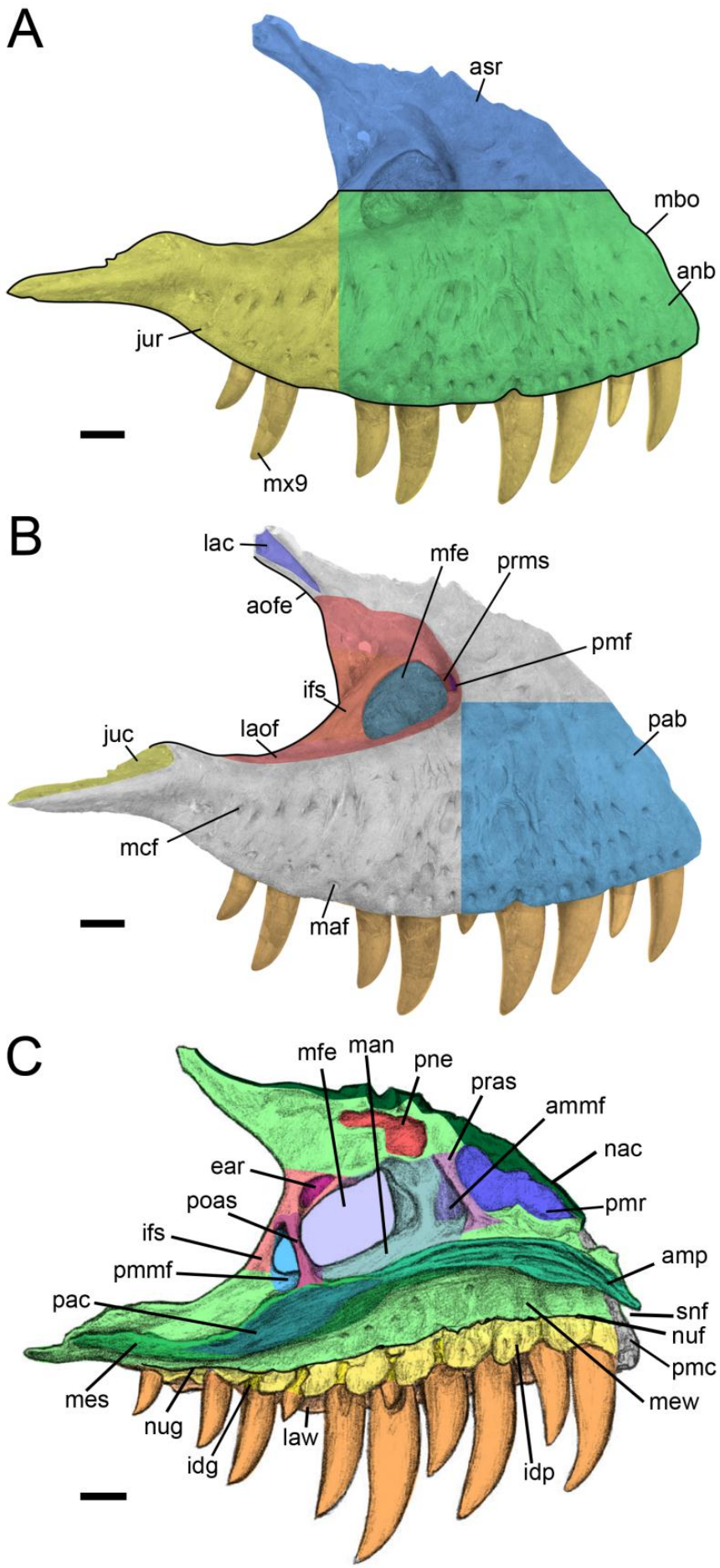

FIGURE 9.2. Proposed terminology and annotation of the non-avian theropod maxilla. Left maxillae of *Tyrannosaurus rex* in **A-B**, lateral view (CMNH 9380, reversed); and **C**, medial view (BHI 3033; modified from Hurum and Sabath 2003). **Abbreviations**: **ammf**, anteromedial maxillary fenestra; **amp**, anteromedial process; **anb**, anterior body; **aofe**, antorbital fenestra; **asr**, ascending ramus; **ear**, epiantral recess; **idg**, interdental gap; **idp**, interdental plate; **ifs**, interfenestral strut; **juc**, jugal contact; **jur**, jugal ramus; **lac**, lacrimal contact; **laof**, lateral antorbital fossa; **law**, lateral wall; **maf**, maxillary alveolar foramina; **man**, maxillary antrum; **mbo**, maxillary body; **mcf**, maxillary circumfenestra foramina; **mes**, medial shelf; **mew**, medial wall; **mfe**, maxillary fenestra; **mx9**, ninth maxillary tooth; **nac**, nasal contact; **nuf**, nutrient foramina; **nug**, nutrient groove; **pab**, preantorbital body; **pac**, palatine contact; **pmc**, premaxillary contact; **pmf**, promaxillary fenestra; **pmmf**, posteromedial maxillary fenestra; **pmr**, promaxillary recess; **pne**, pneumatic excavation; **poas**, postantral strut; **pras**, preantral strut; **prms**, promaxillary strut; **snf**, subnarial foramen. Scale bars = 5 cm.

considered to be absent when the anterodorsal margin of the maxillary body and the anterior margin of the ascending ramus are confluent. The anterior ramus, also called the 'rostral ramus' (Holtz et al. 2004) or 'anterior process' (e.g., Holtz et al. 2004; Tykoski 2005; Turner et al. 2007*b*; Benson 2008*a*, 2010*a*; Brusatte et al. 2012*a*) is part of the anterior body. It can also be part of the preantorbital body, or confluent with it when the concave step on the anterodorsal margin of the maxilla and the anteriormost point of the antorbital fossa are at the same level.

Ascending ramus (asr)—Dorsal part of the maxilla that excludes the maxillary body and contacts the nasal anteriorly and the lacrimal dorsally (Fig. 9.2A). Also known as the 'ascending process' (e.g., Sadleir et al. 2008; Brusatte et al. 2010*b*; Rauhut et al. 2010), 'posterodorsal process' (e.g., Currie and Zhao 1993*a*; Sereno and Novas 1994; Currie and Carpenter 2000), 'nasal process' (e.g., Madsen 1976*b*; Britt 1991; Madsen and Welles 2000), 'lacrimal process' (e.g., Coria and Currie 2006) and 'dorsal/ascending ramus of the nasal process' (Turner et al. 2007*b*).

Jugal ramus (jur)—Posterior part of the maxillary body situated below the antorbital fenestra (Fig. 9.2A). The jugal ramus, as used by several authors (e.g., Dal Sasso et al. 2005; Coria and Currie 2006), is also referred as the 'jugal process' (e.g., Carr 1999; Benson 2008*a*, 2010*a*), 'posterior process' (e.g., Brusatte et al. 2010*a*), 'posterior ramus' (e.g., Sereno and Brusatte 2008; Eddy and Clarke 2011; Sereno et al. 2013), 'subantorbital ramus' (e.g., Rauhut et al. 2010), and 'subantorbital process' (e.g., Turner et al. 2007*b*).

Anteromedial process (amp)—Projection of bone on the medial surface of the maxillary body, on the anterodorsal corner of the anterior maxillary body, protruding anteriorly or anteroventrally to contact the premaxilla anteriorly, and the vomer and the opposite maxilla medially (Figs. 9.1C, 9.2C). The anteromedial process is also known as the 'rostromedial process' (e.g., Dal Sasso et al. 2005; Gold et al. 2013) and 'palatal process' (e.g., Carr 1999; Carrano et al. 2002; Sampson and Witmer 2007; Choiniere et al. 2010*a*).

Walls, Shelves and Ridges

Lateral wall (law)—Bone surface laterally situated, covering the whole surface of the maxilla, from the ventral margin ventrally to the posterior tip of the ascending ramus dorsally, and bounding laterally the maxillary alveoli and different diverticula located within the maxilla (Fig. 9.2C). The lateral wall (lamina lateralis *sensu* Witmer 1997*a*), as used by Brusatte et al. (2010*b*) and Benson (2010*a*), is also known as the 'labial wall' (e.g., Norell and Hwang 2004; Brusatte et al. 2010*a*) and 'lateral lamina' (e.g., Turner et al. 2007*b*; Benson 2010*a*; Brusatte et al. 2010*a*).

Antorbital ridge (aor)—Low crest on the lateral surface of the maxilla, extending from the maxillary body to the ascending ramus, and bordering the lateral antorbital fossa anteriorly and ventrally (Fig. 9.1A).

Vestibular bulla (veb)—Convexity located on the anterodorsal margin of the maxillary body and the floor of the nasal vestibule, and corresponding to an inflated, thin-walled bony bubble of the

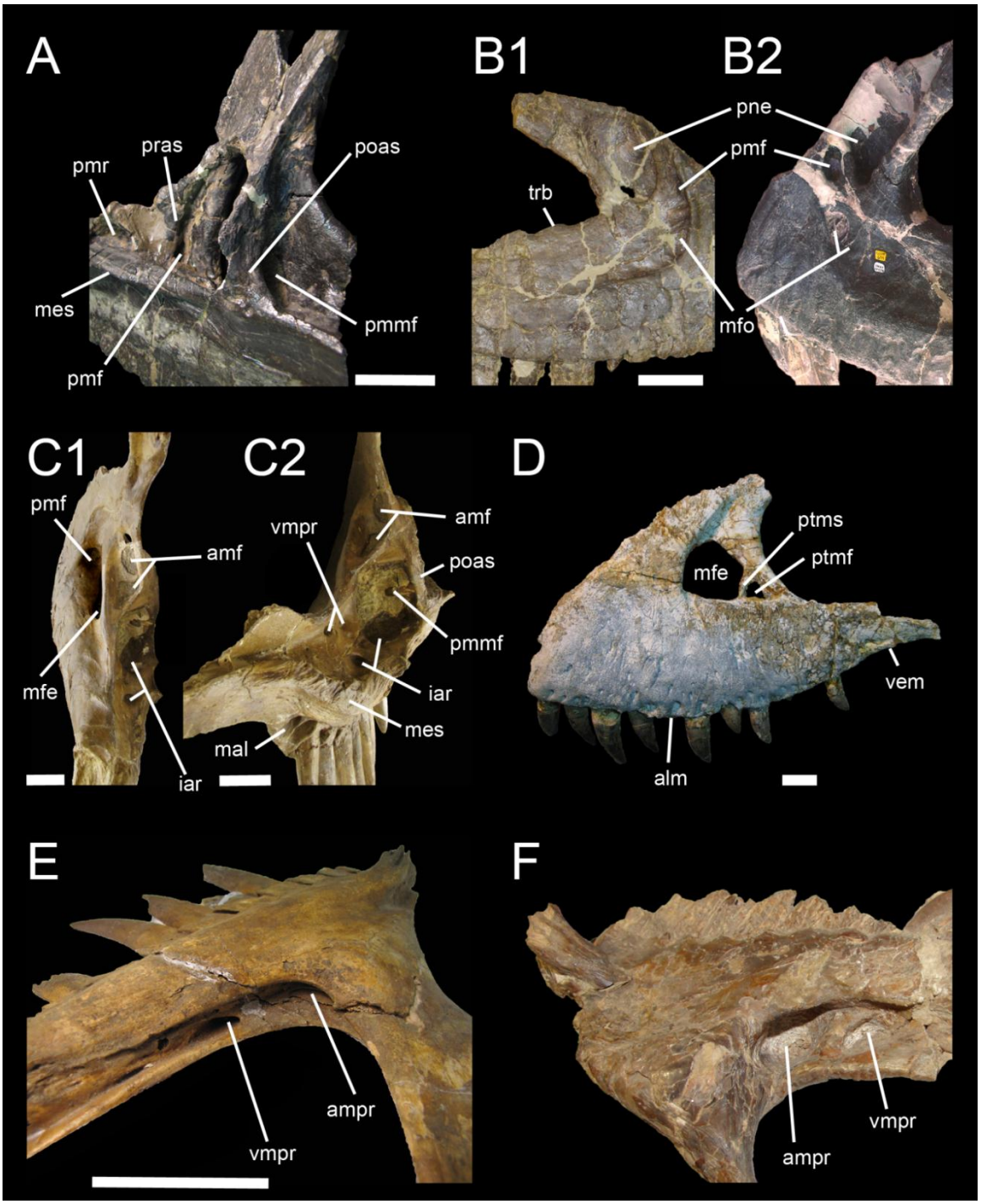

FIGURE 9.3. Proposed terminology and annotation of the non-avian theropod maxilla. **A**, Right maxilla of *Allosaurus fragilis* (AMNH 600) in posteromedial view; **B**, lateral antorbital fossae of *Ceratosaurus* in lateral view; **B1**, right maxilla of *Ceratosaurus magnicornis* (MWC 1) and; **B2**, left maxilla of *Ceratosaurus dentisulcatus* (UMNH VP 5278; courtesy of Roger Benson); **C**, left maxilla of *Tyrannosaurus rex* (CMNH 9380) in posterodorsal (**C1**) and dorsal (**C2**) views; **D**, left maxilla of *Tarbosaurus baatar* (ZPAL MgD-I/4; courtesy of Stephen Brusatte) in lateral view; **E**, right maxilla of *Duriavenator hesperis* (NHM R332) in dorsomedial view; and **F**, left maxilla of *Piatnitzkysaurus floresi* (PVL 4073) in dorsomedial view (courtesy of Martin Ezcurra). **Abbreviations**: **amf**, accessory maxillary fenestra; **ammf**, anteromedial maxillary fenestra; **ampr** anteromedial pneumatic recess; **iar**, interalveolar recess; **mal**, maxillary alveoli; **mes**, medial shelf; **mfe**, maxillary fenestra; **mfo**, maxillary fossa; **pmf**, promaxillary fenestra; **pmmf**, posteromedial maxillary fenestra; **pmr**, promaxillary recess; **pne**, pneumatic excavation; **poas**, postantral strut; **pras**, preantral strut; **ptmf**, postmaxillary fenestra; **ptms**, postmaxillary strut; **trb**, tooth root bulge; **vmpr**, ventromedial pneumatic recess. Scale bars = 5 cm.

anterodorsal portion of the promaxillary recess (Witmer 1997*a*; Sampson and Witmer 2007; Fig. 9.1A–C). The vestibular bulla (‘bulla vestibularis’ *sensu* Witmer 1997*a*) can be perforated and opened to the external naris through a small foramen (the anterodorsal foramen). A vestibular bulla is noticeable in many non-avian theropods such as *Marshosaurus*, *Allosaurus*, *Sinraptor* (Witmer 1997*a*), *Acrocanthosaurus* (Eddy and Clarke 2011), *Proceratosaurus* (Rauhut et al. 2010), *Albertosaurus* (Carr 1999), *Appalachiosaurus* (Carr et al. 2005: fig. 6A), *Byronosaurus* (Bever and Norell 2009) and *Troodon* (Currie 1985: fig. 2.1).

Medial wall (mew)—Bone surface medially situated, covering the surface of the maxilla dorsal to the nutrient groove (i.e., medial surface of the maxilla excluding the interdental plates), and bounding medially the different diverticula situated within the maxilla (Figs. 9.1C, 9.2C). The surface of the medial wall can be fenestrated at the level of the ascending ramus, and the maxillary antrum and promaxillary recess. Likewise, the medial wall ventral to the medial shelf can be undulated for receiving the dentary teeth if they are abutting against this surface when the jaws are closed (e.g., *Torvosaurus*, *Carcharodontosaurus*, *Tyrannosaurus*). The medial wall is also known as the ‘medial lamina’ for some authors (e.g., Ezcurra 2007; Turner et al. 2007*b*; Sereno and Brusatte 2008).

Medial shelf (mes)—Anterodorsally elongated ridge on the medial surface of the maxillary body, extending from the anteromedial process to the jugal ramus (and in some cases the jugal contact), and protruding medially to contact the opposite maxilla, palatine and, in some cases, vomer (Figs. 9.1C, 9.2C). Also known as the ‘lingual bar’ (e.g., Madsen and Welles 2000; Benson 2010*a*) or ‘palatal shelf’ (e.g., Hurum and Sabath 2003; Makovicky et al. 2003; Coria and Currie 2006).

Lingual wall (liw)—Bone surface medially situated, covering the surface of the maxilla ventral to the nutrient groove and bounding each maxillary interdental plates medially, anteriorly and posteriorly **(**Figs. 9.1C, 9.2C**).** The lingual wall, as used by Brusatte et al. (2010*c*) and Brusatte et al. (2010*b*), is either formed by a row of separated interdental plates or a continuous interdental wall.

Interdental plate (idp)—Flat bony structure medial to the dental tooth row and attached to the lateral wall of the maxilla by a perpendicular and mediolaterally oriented lamina that separates each individual tooth socket (Fig. 9.2C). The interdental plates, also known as ‘paradental plates’ (Carrano et al. 2002, 2012; Carrano and Sampson 2008), vary in size and morphologies and can either be separated by an interdental gap, or completely fused.

Interdental wall (idw)—Continuous medial wall ventral to the nutrient groove and formed by the fusion of interdental plates (Fig. 9.1C). The interdental wall is also known as the ‘paradental lamina’ (Rauhut et al. 2010) or ‘paradental shelf’ (Rauhut 2004*b*), and the array of unfused interdental plates present in many theropods does not constitute an interdental wall.

Alveoli, Teeth and Margins

Maxillary alveoli (mal)—Tooth sockets located on the ventral margin of the maxilla (Fig. 9.3C2). They can be well-separated by the interdental plates, or merged to form an open groove like in troodontids.

Maxillary teeth (mx)—Teeth of the maxilla located within the alveoli (Figs. 9.1A–B, 9.2A). Due to the multiple generations of replacement teeth in the alveoli at one time, maxillary teeth, like those of the premaxilla and dentary, can be unerupted, semi-erupted and fully erupted.

Tooth root bulge (trb)—Crenulated margin of the anterodorsal rim of the jugal ramus resulting from the protrusion of the tooth roots into the antorbital fenestra (Fig. 9.3B1). A tooth root bulge (eminentia radices dentis *sensu* Witmer 1997*a*) is seen in some basal averostrans such as *Ceratosaurus* (USNM 4735; UMNH VP 5278; MWC 1.1) and *Marshosaurus* (UMNH VP 7824, 7825).

Alveolar margin (alm)—Ventral border of the maxilla along the maxillary tooth row (i.e., distance from the anterior point of the anteriormost maxillary alveolus to the posterior point of the posteriormost maxillary alveolus; Fig. 9.3D).

Ventral margin (vem)—Ventral border of the lateral wall of the maxilla, from the anteroventral corner of the anterior body, to the posteroventral extremity of the jugal ramus (Fig. 9.3D). The ventral margins of the lateral and medial walls do not always coincide, but the lateral margin extends more ventrally in the large majority of theropods (pers. obs.).

Maxillary Contacts

Premaxillary contact (pmc)—Articular surface on the anterior margin of the maxillary body and receiving the premaxilla (Figs. 9.1B, 9.2C).

Jugal contact (juc)—Articular surface on the posterolateral or ventral surface of the jugal ramus of the maxilla and receiving the jugal bone (Figs. 9.1A, 9.2B).

Palatine contact (pac)—Articular surface along the medial shelf or the medial wall of the maxilla and receiving the palatine (Figs. 9.1C, 9.2C).

Nasal contact (nac)—Articular surface on the dorsal surface of the maxillary body and the anterior, dorsal, lateral and medial surface of the ascending ramus and receiving the nasal (Figs. 9.1C, E, 9.2C).

Lacrimal contact (lac)—Articular surface on the laterodorsal or dorsomedial surface of the ascending ramus and receiving the lacrimal (Figs. 9.1A, 9.2B).

Fossae and Pneumatic Openings

Antorbital fossa (aofo)—Large depression surrounding and including the antorbital fenestra on the lateral and, in some cases, the medial surface of the maxilla. Its anterior, ventral and dorsal extensions are highly variable among theropods, covering most of the maxillary body in some basal

tetanurans or reduced to a very short depression adjacent to the antorbital fenestra in some abelisaurids.

Lateral antorbital fossa (laof)—Depression surrounding the antorbital fenestra on the lateral surface of the maxilla (Figs. 9.1A, 9.2B). A peripheral rim and, in some case, a raised antorbital ridge along the lateral wall of the maxilla delimit the lateral antorbital fossa. The lateral antorbital fossa, corresponding to the 'external antorbital fenestra' of Witmer (1997*a*), typically hosts the accessory antorbital fossae and fenestrae of the maxilla (e.g., promaxillary, maxillary, postmaxillary and pneumatic fenestrae and fossae) and pneumatic excavations. The lateral antorbital fossa is continuous with the antorbital fossa of the nasal, lacrimal and jugal in most of theropods.

Medial antorbital fossa (maof)—Depression surrounding the antorbital fenestra on the medial surface of the maxilla (Fig. 9.1C). The medial antorbital fossa is usually bordered by a peripheral step running from the maxillary body to the ascending ramus. It typically hosts some opening such as the posteromedial maxillary fenestra, several ventral pneumatic foramina and neurovascular openings. The medial antorbital fossa, which corresponds to the 'pneumatic fossa' of Benson (2010*a*), is continuous with the antorbital fossa of the palatine in most of theropods.

Maxillary fossa (mfo)—Depression variable in size and shape, homologous to the maxillary fenestra but bounded medially by a thick medial wall (Fig. 9.3B1–B2). The maxillary fossa, also known as the 'preantorbital fossa' (Sadleir et al. 2008) and 'maxillary fenestra' (e.g., Madsen 1976*b*; Benson 2008*a*, 2010*a*; Carrano and Sampson 2008), differs from the maxillary fenestra by being a shallow or deep and well-delimited depression that does not lead to a maxillary antrum. A maxillary fossa is present in coelophysoids (e.g., *Dracovenator*, *Zupaysaurus*, *Megapnosaurus*), *Ceratosaurus*, and non-spinosaurid megalosauroids (e.g., *Marshosaurus*, *Afrovenator*, *Dubreuillosaurus*, *Eustreptospondylus*, *Megalosaurus*, *Torvosaurus*). Given its size, shape and comparable location to this of coelophysoids and megalosauroids, the large depression located in the anterior corner of the lateral antorbital fossa is interpreted as the maxillary fossa in *Ceratosaurus*, *Limusaurus*, *Noasaurus*, *Masiakasaurus* and *Monolophosaurus*.

Promaxillary fossa (pmfo)—Depression variable in size and shape, homologous to the promaxillary fenestra but bounded medially by a thick medial wall. As for the maxillary fossa, the promaxillary fossa differs from the promaxillary fenestra in not leading to a promaxillary recess. A promaxillary fossa occurs in coelophysoids such as *Coelophysis*, *Dracovenator* and *Zupaysaurus*.

Pneumatic excavation (pne)—Fossa variable in size and shape but usually being a large ovoid or lanceolate depression located within the lateral or medial surface of the ascending ramus and bounded by the medial wall medially or lateral wall laterally (Figs. 9.1A, C, 9.2C, 9.3B1–B2). The pneumatic excavation ('excavation pneumatica' *sensu* Witmer 1997*a*) can be fenestrated, as in *Eocarcharia* (Sereno and Brusatte 2008), and is generally located at mid-height of the ascending ramus, within the antorbital fossa. In some cases, it also communicates with other maxillary recesses situated more ventrally (Witmer 1997*a*). A pneumatic excavation exits in many theropods such as

Coelophysis (Tykoski 2005), *Ceratosaurus* (USNM 4735; MWC 1.1; UMNH VP 5278; Fig. 9.3B), *Sinosaurus* (KMV 8701), *Sinraptor* (IVPP 10600), *Yangchuanosaurus* (CV 00215, 00216), *Allosaurus* (UMNH VP 5393, 9168; USNM 8335), *Alioramus* (IGM 100-1844) and *Bambiraptor* (AMNH 30556).

Medial pneumatic complex (mpc)—Set of pneumatic excavations located within the anterior corner and dorsomedial surface of the medial antorbital fossa, and penetrating the ascending and jugal rami (Benson 2010*a*). The medial pneumatic complex includes both anteromedial and posteromedial pneumatic recesses.

Anteromedial pneumatic recess (ampr)—Pneumatic excavation located within the anterior corner of the medial antorbital fossa and penetrating the ascending ramus of the maxilla (Fig. 9.3E–F). The anteromedial pneumatic recess, also known as the 'pneumatic excavation' (Benson 2008*a*, 2010*a*), is homologous to the posteromedial maxillary fenestra but differs from the latter by not leading to a maxillary antrum. An anteromedial pneumatic recess can be observed in many megalosauroids such as *Piatnitzkysaurus* (PVL 4073), *Marshosaurus* (UMNH 7825), *Eustreptospondylus* (OUMNH J.13558), *Afrovenator* (MNN UBA1), *Megalosaurus* (OUMNH J.13506) and *Duriavenator* (NHM R.332).

Ventromedial pneumatic recess (vmpr)—Pneumatic excavation located within the anteroventral corner or ventral part of the medial antorbital fossa, on the dorsomedial surface of the jugal ramus, and penetrating the jugal ramus of the maxilla (Fig. 9.3E–F; Fig. 9.3C2). The ventromedial pneumatic recess, also known as the 'pneumatic excavation' (Benson et al. 2008; Benson 2010*a*), is usually associated with an anteromedial pneumatic recess situated anterodorsally to it. A ventromedial pneumatic recess can be observed in several megalosauroids such as *Piatnitzkysaurus* (PVL 4073) and *Duriavenator* (NHM R.332), and the tyrannosaurid *Tyrannosaurus* (CMNH 9380).

Fenestrae

Antorbital fenestra (aofe)—Large opening posterior to the external naris and anterior to the orbital fenestra, and mostly delimited by the maxilla, jugal and lacrimal (Fig. 9.2B). Also known as the 'internal antorbital fenestra' ('fenestra antorbitalis interna' *sensu* Witmer 1997*a*), the external antorbital fenestra (fenestra antorbitalis externa *sensu* Witmer 1997*a*) being delimited by the peripheral rim of the antorbital fossa (Witmer 1997*a*).

Accessory antorbital fenestra (aafe)—Opening anterior to the antorbital fenestra within the anterior corner of the lateral antorbital fossa. Accessory antorbital fenestrae encompasses the promaxillary, maxillary, postmaxillary and pneumatic fenestrae. The accessory antorbital fenestra, also known as the 'accessory antorbital opening' (e.g., Brusatte et al. 2010*a*), is usually employed when it cannot be referred with certainty to the promaxillary or maxillary fenestra (e.g., Clark et al.

2002; Makovicky et al. 2003; Turner et al. 2007*b*; Sereno and Brusatte 2008). It also refers to the maxillary fenestra (Turner et al. 2012).

Maxillary fenestra (mfe)—Aperture variable in size and shape, but usually being a large, sub-circular opening, leading medially to the maxillary antrum or perforating the medial wall of the maxilla (Witmer 1997*a*; Figs. 9.1A, E, 9.2B, C, 9.3D). The maxillary fenestra (Madsen 1976*b*; Gauthier 1986; fenestra maxillaris *sensu* Witmer 1997*a*), also known as the 'accessory foramen', 'second antorbital fenestra' (Osborn 1912), 'second antiorbital fenestra' (Gilmore 1920), 'subsidiary antorbital fenestra' (Ostrom 1969, 1978), and 'accessory antorbital fenestra' (e.g., Turner et al. 2012), is situated within the anterior corner of the lateral antorbital fossa, at the base of the ascending ramus, posterior (and sometimes dorsal) to the promaxillary fenestra and anterior to the antorbital fenestra and the postmaxillary fenestra. Its presence has been noted in most non-avian neotetanurans (e.g., allosauroids, tyrannosauroids, compsognathids, ornithomimosaurs, therizinosauroids, oviraptorosaurs, deinonychosaurs), with perhaps the exception of *Erlikosaurus* (Clark et al. 1994).

Promaxillary fenestra (pmf)—Aperture variable in size and shape, but usually being a small slit-like opening, leading medially to the promaxillary recess, or in some cases, perforating the medial wall of the maxilla (Witmer 1997*a*; Figs. 9.1C, E, 9.2B, 9.3B1–C1). The promaxillary fenestra (Carpenter 1992; fenestra promaxillaris *sensu* Witmer 1997*a*), also known as the 'promaxillary foramen' (e.g., Ezcurra 2007; Rauhut et al. 2010; Eddy and Clarke 2011), 'premaxillary fenestra' (e.g., Kundrát et al. 2008; Rauhut et al. 2012; Godefroit et al. 2013*a*) and 'tertiary antorbital fenestra' (e.g., Turner et al. 2007*b*, 2012), is situated within the anterior corner of the lateral antorbital fossa, at the base of the ascending ramus and anterior to the maxillary fenestra. It is not always visible in lateral view, being concealed by the lateral wall of the maxilla and stuck up in the anterior corner of the lateral antorbital fossa. A slit-shaped promaxillary fenestra is seen in many theropods such as *Herrerasaurus*, *Eodromaeus*, *Dilophosaurus*, Abelisauroidea, Megalosauroidea, Allosauroidea (e.g., *Allosaurus*, *Neovenator*), Tyrannosauroidea and most Maniraptoriformes, whereas a large discrete promaxillary fenestra can be observed in basal averostrans (e.g., *Ceratosaurus*, *Sinosaurus*), some allosauroids (e.g., *Sinraptor*, *Yangchuanosaurus*, *Acrocanthosaurus*, *Eocarcharia*), compsognathids (e.g., *Compsognathus*, *Scipionyx*) and possibly in oviraptorosaurs (e.g., *Incisivosaurus*, *Citipati*, *Khaan*, see Balanoff and Norell 2012) for discussion on the accessory antorbital openings in Oviraptorosauria). Carcharodontosaurinae, some dromaeosaurids, and most derived Troodontidae seem to be devoid of a promaxillary fenestra (Turner et al. 2007*b*, pers. obs.), the maxillary and promaxillary fenestrae having most likely merged in Carcharodontosaurinae.

Pneumatic fenestra (pnf)— Aperture variable in size and shape, situated within the pneumatic excavation, and leading medially to a deep pneumatic recess within the ascending ramus, or in some cases, perforating the medial wall of the maxilla. The pneumatic fenestra, also known as the 'accessory fenestra' (Sereno and Brusatte 2008), is present in the sinraptorid *Sinraptor* (Currie and Zhao 1993*a*; Witmer 1997*a*), the basal carcharodontosaurids *Acrocanthosaurus* (right maxilla, Eddy

and Clarke 2011) and *Eocarcharia* (Sereno and Brusatte 2008), and the dromaeosaurid *Bambiraptor* (AMNH 30556).

Postmaxillary fenestra (ptmf)—Small sub-circular aperture situated within the antorbital fossa, between the maxillary fenestra and the antorbital fenestra (Fig. 9.3D). According to Larson (Larson 2008*b*), the postmaxillary fenestra, also known as the 'accessory maxillary fenestra' (Hone et al. 2011; 'small foramen along the ventral margin of the antorbital fossa' of Molnar 1991), may result from depositional weathering or breakage. Its presence in many specimens of Tyrannosaurinae such as *Tyrannosaurus* (e.g., BHI 3033; LACM 23844; UCMP 118742), *Tarbosaurus* (ZPAL MgD-I/4) and *Zhuchengtyrannus* (Hone et al. 2011: fig. 2C–D) however makes this hypothesis unlikely. One or two small openings is also seen within the antorbital fossa, between a large promaxillary fenestra (interpreted as such by Balanoff and Norell 2012) and the antorbital fenestra, in the maxilla of the oviraptorid *Khaan* (Balanoff and Norell 2012, pers. obs.). Although the postmaxillary fenestra and these 'postmaxillary' foramina occupy the same location within the antorbital fossa, they are not homologous.

Ventral maxillary fenestra (vmf)—Anteroposterioly elongated aperture situated on the antorbital body, beneath the lateral antorbital fossa. One or several ventral maxillary fenestrae have been noticed in several Oviraptoridae such as *Citipati* (IGM 100-978), *Khaan* (IGM 100-1127), *Conchoraptor* (Osmólska et al. 2004: fig. 8.1G) and an unpublished oviraptorid (MPC-D 100/4; Osmólska et al. 2004: fig. 8.1GE). These openings, referred to as the 'additional accessory foramen' by Balanoff and Norell (2012), may not be pneumatic in nature, and may represent maxillary neurovascular foramina that are greatly enlarged, feeding the rhamphotheca and soft tissues of the jaw margin in oviraptorids (J. Headden pers. comm.). The ventral maxillary fenestrae may therefore be homologous to the row of maxillary circumfenestra foramina existing in other theropods. These large apertures do not seem to be present in any other non-avian theropod clade.

Posteromedial maxillary fenestra (pmmf)—Ventrodorsally elongated aperture delimited by the lateral wall of the maxilla laterally and the medial wall medially (Figs. 9.1C–D, 9.2C, 9.3A, C1–C2). The posteromedial maxillary fenestra, corresponding to the 'caudal fenestra of the maxillary antrum' of Witmer (1997*a*) and used as such by several authors (e.g., Norell and Hwang 2004; Carr et al. 2005; Bever and Norell 2009), is situated within the anterior corner of the medial antorbital fenestra and leads to the maxillary antrum. A posteromedial maxillary fenestra is seen in spinosaurids (e.g., *Suchomimus*, *Spinosaurus*), allosauroids (*Sinraptor*, *Allosaurus*) and tyrannosauroids (e.g., *Alioramus*, *Tyrannosaurus*).

Dorsomedial maxillary fenestra (dmmf)—Elongated aperture located on the medial surface of the maxilla and perforating the dorsal wall of the maxillary antrum and, in some cases, promaxillary recess (Fig. 9.1F). The dorsomedial maxillary fenestra, corresponding to the 'subnarial fenestra' of Madsen (1976*b*), is present in some Allosauroidea such as *Sinraptor* (IVPP 10600; Currie and Zhao

1993*a*: fig. 4.12) and *Allosaurus* (Madsen 1976*b*; Witmer 1997*a*; USNM 8335), the troodontid *Troodon* (Currie 1985) and possibly some tyrannosaurids such as *Alioramus* (Gold et al. 2013).

Anteromedial maxillary fenestra (ammf)—Aperture within the anterior wall of the maxillary antrum (preantral strut) and leading to the promaxillary recess (Fig. 9.1E, 2C). An anteromedial maxillary fenestra, corresponding to the 'fenestra communicans' *sensu* Witmer 1997*a*), is seen in the majority of allosauroid and tyrannosauroid theropods.

Accessory maxillary fenestra (amf)—Aperture located within a fossa dorsomedial to the maxillary fenestra, dorsal to the posteromedial maxillary fenestra, and leading to the maxillary antrum (Fig. 9.3C2). Several accessory maxillary fenestrae have been noticed in one maxilla (CMNH 9380) of *Tyrannosaurus*.

Medial maxillary fenestra (mmf)—Subtriangular aperture perforating the medial wall of the maxilla and leading laterally to the maxillary antrum and promaxillary recess. The medial maxillary fenestra is delimited by the postantral strut posteriorly, the suprantral strut dorsally, the medial shelf ventrally and the anterior corner of the promaxillary recess anteriorly. Its presence has only been noticed in some basal allosauroids such as *Sinraptor* and *Allosaurus*.

Antrum and Recesses

Maxillary antrum (man)—Large cavity located between the lateral and medial walls, anterior to the medial antorbital fossa, and communicating laterally with the maxillary fenestra (Witmer 1997*a*; Figs. 9.1C, E, 9.2C). The maxillary antrum (Witmer 1997*a*) can also lead to the promaxillary recess via the anteromedial maxillary fenestra. The walls of the maxillary antrum can be reinforced by several struts (see below) that can be fenestrated. The maxillary antrum is also known as the 'maxillary sinus' (e.g., Madsen 1976*b*; Currie and Zhao 1993*a*) but the latter may refer to the sinus invading both maxillary antrum and promaxillary recess (Witmer 1997*a*).

Promaxillary recess (pmr)—Cavity variable in volume within the medial wall, anterior to the maxillary antrum, and communicating laterally with the promaxillary fenestra (Figs. 9.1C, E, 9.2C). The promaxillary recess (Witmer 1997*a*) is also known as the 'promaxillary sinus' (e.g., Barsbold and Osmólska 1999; Brusatte et al. 2012*a*; Gold et al. 2013).

Epiantral recess (ear)—Small depression situated on the medial surface of the maxilla, posterodorsal to the maxillary fenestra, and excavating the anterodorsal surface of the interfenestral strut (Figs. 9.1C, E, 9.2C). An epiantral recess (Witmer 1997*a*) is present in Allosauroidea (e.g., *Sinraptor*, *Allosaurus*) and Tyrannosauroidea (e.g., *Alioramus*, *Raptorex*, *Tyrannosaurus*, *Tarbosaurus*).

Interalveolar recess (iar)—Diverticula within the medial wall and the medial shelf and directed ventrally from the maxillary antrum and promaxillary recess, between the maxillary teeth (Fig. 9.3C1–2). An interalveolar recess, also known as the 'interalveolar pneumatic recess' ('recessus

pneumatici interalveolares' *sensu* Witmer 1997*a*) is only present in Tyrannosauridae like *Alioramus*, *Albertosaurus* and *Tyrannosaurus* (Witmer 1997*a*; Gold et al. 2013; pers. obs.).

Foramina and Grooves

Subnarial foramen (snf)—Small opening variable in outline and located between the premaxilla and maxilla, below the external naris (Fig. 9.1A). The subnarial foramen corresponds to the 'maxilla-premaxillary fenestra' of Osborn (1912) and Gilmore (1920), and the 'subnarial fenestra' of Coria et al. (2002).

Anterodorsal foramen (adf)—Small opening located on the anterodorsal margin of the maxilla and perforating the dorsomedial wall of the promaxillary recess. The anterodorsal foramen is present in some troodontids such as *Troodon* (Currie 1985).

Nutrient groove (nug)—Furrow running anterodorsally on the medial surface of the maxillary body and hosting the nutrient foramina (Figs. 9.1C, 9.2C). The nutrient groove, also known as the 'groove for the dental lamina' (e.g., Brusatte and Sereno 2007; Sereno and Brusatte 2008; Brusatte et al. 2012*a*) and the 'paradental groove' (e.g., Brusatte et al. 2009*c*, 2010*b*; Rauhut et al. 2010), corresponds to the junction between the interdental plates and the medial wall. Due to the fact that the medial wall slightly overlaps the interdental plates medially, the nutrient groove is delimited by the interdental plates laterally and the medial wall medially, and by both interdental plates and medial wall dorsally and ventrally. A similar groove, the paradental groove, is seen on the medial surface of the dentary, ventral to the interdental plates.

Nutrient foramina (nuf)—Small openings on the interdental plates, at the level of the nutrient groove, permitting the unerupted teeth to be innervated by blood vessels inside their alveoli (Eddy and Clarke 2011; Figs. 9.1C, 9.2C). Also known as 'nutrient notches' (e.g., Welles 1984; Madsen and Welles 2000), 'suprainterdental plate foramina' (Britt 1991), or 'dental foramina' (e.g., Gilmore 1920; Mahler 2005; Sampson and Witmer 2007).

Interdental gap (idg)—Ventrodorsally elongated groove separating each interdental plate whereas they are unfused (Fig. 9.2C).

Maxillary neurovascular foramina (mnf)—Small openings located on the lateral surface of the maxillary body and permitting the passage of blood vessels to innervate the lips and cheeks.

Maxillary alveolar foramina (maf)—Row of neurovascular foramina parallel with and adjacent to the ventral margin of the maxilla (Figs. 9.1A, 9.2B).

Maxillary median foramina (mmf)—Neurovascular foramina randomly distributed and located between the rows of maxillary alveolar and circumfenestra foramina (Fig. 9.1A).

Maxillary circumfenestra foramina (mcf)—Row of neurovascular foramina parallel with and adjacent to the ventral rim of the antorbital fossa (Figs. 9.1A, 9.2B).

Maxillary Struts

Promaxillary strut (prms)—Lamina or column separating the promaxillary fenestra from the maxillary fenestra (Fig. 9.2B). The promaxillary strut (‘pila promaxillaris’ *sensu* Witmer 1997*a*), as called by several authors (e.g., Hurum and Sabath 2003; Ezcurra 2007; Eddy and Clarke 2011), is also known as the ‘promaxillary pila’ (e.g., Norell et al. 2006; Godefroit et al. 2008).

Interfenestral strut (ifs)—Bone wall separating the maxillary fenestra from the antorbital fenestra (Figs. 9.1A, 9.2B, C). The interfenestral strut (pila interfenestralis *sensu* Witmer 1997*a*), is also known as the ‘interfenestral bar’ (e.g., Welles 1984; Rauhut 2004*b*; Carr et al. 2005; Norell et al. 2006; Ezcurra 2007).

Postmaxillary strut (ptms)—Bone surface separating the maxillary fenestra from the postmaxillary fenestra (Fig. 9.3D). Only present in Tyrannosauridae (e.g., BHI 3033, LACM 23844, ZPAL MgD-I/4).

Postantral strut (poas)—Pillar of bone delimiting the posteromedial maxillary fenestra medially, and the maxillary antrum posteromedially (Figs. 9.1C–F, 9.2C, 9.3A, C2). The postantral strut (pila postantralis *sensu* Witmer 1997*a*) can be fenestrated by the posteromedial maxillary fenestra, allowing communication of the antorbital cavity and the maxillary antrum (Witmer 1997*a*).

Suprantral strut (suas)—Ridge reinforcing the dorsal wall of the maxillary antrum dorsomedially (Fig. 9.1E). The suprantral strut can be perforated by the dorsomedial maxillary fenestra (Witmer 1997*a*).

Preantral strut (pras)—Pillar of bone separating the maxillary antrum from the promaxillary recess (Figs. 9.1C, E, 9.2C). The preantral strut, corresponding to the ‘maxillary septum’ *sensu* Madsen (1976*b*), can be doubled (i.e., presence of lateral and medial preantral struts) when the promaxillary fenestra is internal (i.e., within the maxilla and the maxillary antrum) as in *Allosaurus* (Fig. 9.1E).

Results

Systematic Paleontology

Dinosauria Owen, 1842

Saurischia Seeley, 1887

Theropoda Marsh, 1881

Tetanurae Gauthier, 1986

Megalosauroidea Fitzinger, 1843

Megalosauridae Fitzinger, 1843

Torvosaurus Galton and Jensen, 1979

Revised diagnosis—Megalosauroid theropod with very shallow maxillary fossa (i.e., maxillary fossa forming a poorly delimited concavity in the anterior corner of the lateral antorbital fossa; Carrano et al. 2012), protuberant ridge below the maxillary fossa, in the ventral part of the anterior corner of the lateral antorbital fossa, interdental wall making up one-half the medial surface of the maxillary body (modified from Britt 1991), expanded fossae in posterior dorsal and anterior caudal centra forming enlarged and deep pneumatic openings (Carrano et al. 2012), highly ossified puboischiadic plate (Carrano et al. 2012), and distal expansion of ischium with prominent lateral midline crest and oval outline in lateral view (Carrano et al. 2012).

Torvosaurus tanneri Galton and Jensen 1979

Galton and Jensen (1979: figs. 1, 2, 3A, G, L, 4A–F, 4I–N; 6–7, 8H); Jensen (1985: figs. 1–4A–D, E–F, 5A–F, H); Britt (1991: figs. 2–24)

1988 *Megalosaurus tanneri*; Galton and Jensen 1979; Paul 1988: p. 282.

1992 *Edmarka rex* gen. nov.; Bakker et al. 1992: figs. 1, 3, 7, 10, 12–15.

1997 ‘*Brontoraptor*’ sp. gen. nov.; Siegwarth et al. 1997: figs. 1–9, 10A–E, 11A–E, 12–13A, 14–15A, 16A–H, 17 (*nomen nudum*).

Lectotype—BYU-VP 2002, left humerus (Britt 1991).

Paralectotype—BYU-VP 2002, the rest of left and right forelimbs (Britt 1991).

Referred material—(from Carrano et al. 2012) BYU-VP 2003, 2004, 2005, 2006, 2007, 2008, 2016, 2017, 4838, 4853, 4860, 4882, 4883, 4884, 4890, 4908, 4951, 4952, 4976, 4998, 5004, 5005, 5008, 5009, 5010, 5020, 5029, 5077, 5086, 5092, 5110, 5129, 5136, 5147, 5242, 5254, 5276, 5277, 5278, 5279, 5280, 5281, 5286, 8907, 8910, 8937, 8938, 8966, 8982, 9013, 9090, 9108, 9120, 9121, 9135, 9136, 9141, 9142, 9143, 9144, 9152, 9161, 9162, 9163, 9249, 9620, 9621, 9622, cranial and postcranial elements (Britt 1991; TATE 401, 1002–1005 (*Edmarka rex*), jugal, scapulocoracoid, and ribs (Bakker et al. 1992; TATE 0012, with 0012-11 formally 1003 (‘*Brontoraptor*’), atlas, axis, sacrum, caudal vertebrae, chevrons, scapula, coracoids, ilium, pubis, ischium, femur, tibia, fibula (Siegwarth et al. 1997; FMNH PR 3060, three midline fragments of gastralia, right metacarpal III, right manual phalanx III-2, left metatarsals II–IV, left pedal phalanx I-1 (Hanson and Makovicky 2013).

Locality and horizon—Dry Mesa Quarry, Montrose County, Calico Gulch Quarry, Uncompahgre Plateau, Moffit County, and Meyer site, Garden Park, north of Cañon City, Fremont County, Colorado; Carnegie Quarry, Dinosaur National Monument, Uintah County, Utah; Gilmore Quarry N and Quarry 6, Freezeout Hills, Carbon County, and Nail and Louise Quarries, Como Bluff,

Albany County, Wyoming, USA; Salt Wash and Brushy Basin Members, Morrison Formation; Kimmeridgian-Tithonian, Late Jurassic (Carrano et al. 2012; Hanson and Makovicky 2013).

Diagnosis—Megalosauroid theropod with a protuberant ridge on the anterior part of the medial shelf, posterior to the anteromedial process, and an interdental wall falling short relative to the lateral wall (i.e., ventral margin of the interdental wall much more dorsal than the ventral margin of the lateral wall) and formed by the fusion of interdental plates with broad V-shaped ventral margin.

Torvosaurus gurneyi Hendrickx & Mateus 2014 sp. nov.

urn:lsid:zoobank.org:act:189C1060-7887-4837-9E30-870079E2B2B9 (Fig. 9.4).

Torvosaurus tanneri Mateus et al. (2006: fig. 6).

Holotype—ML 1100, an incomplete left maxilla (Figs. 9.4B, 9.5–9.6) bearing one erupted tooth and one unerupted tooth (Fig. 9.7), and the posterior portion of a proximal caudal vertebra (Fig. 9.8).

Referred material—ALT-SHN.116, a portion of a right maxilla (Malafaia et al. 2008; Fig. 9.11). ML 962, a mesial shed tooth (Hendrickx and Mateus 2014*b*: fig. 9), FUB PB Ther 1, a lateral tooth, ML 430, an incomplete tibia (Mateus and Antunes 2000*a*; Fig. 9.12), ML 632, a partial femur (Mateus et al. 2006; Fig. 9.12), and ML 1186, cranial and postcranial material of embryos (Araújo et al. 2013), are tentatively referred to *T. gurneyi*.

Type—Cliffs of Praia da Vermelha, Lourinhã, Portugal. Porto Novo-Amoreira Members, Lourinhã Formation, Upper Kimmeridgian, Upper Jurassic (Mateus et al. 2014).

Etymology—In honor of the paleoartist James Gurney, creator of the utopic world of *Dinotopia*.

Diagnosis—Megalosauroid theropod with maxillae bearing fewer than eleven teeth and possessing fused interdental plates with straight ventral margin forming an interdental wall nearly coincidental with the lateral wall of the maxillary body. Differs from *Torvosaurus tanneri* by fewer than eleven maxillary alveoli, the absence of interdental plates terminating ventrally by broad V-shaped points and falling short relative to the lateral wall, the absence of a protuberant ridge on the anterior part of the medial shelf, posterior to the anteromedial process, and the coincidental posterior extension of the dorsal and medial ridges of the anteromedial process.

Taphonomy—The specimen was found in beach eroded boulders that fell from the sea cliff. The bones did not show any signs of articulation, except the maxilla preserving the teeth in situ. The elements are not visibly compressed or deformed. The caudal centrum, directly associated with the maxilla and showing some *Torvosaurus* characters, has three patches of pyrite encrustations and is attached to charcoal. This suggests taphonomical or depositional anoxic conditions.

Description

Maxilla—A fairly complete and undistorted left maxilla (Fig. 9.5) was collected in Praia da Vermelha in June 2003 (Mateus et al. 2006). Some bone surfaces on the lateroposterior side of the anterior ramus and on the anterodorsal corner of the lateral antorbital fossa are missing. Likewise, some bone fragments on the medial surface of the jugal ramus, including the posteriormost alveoli, are

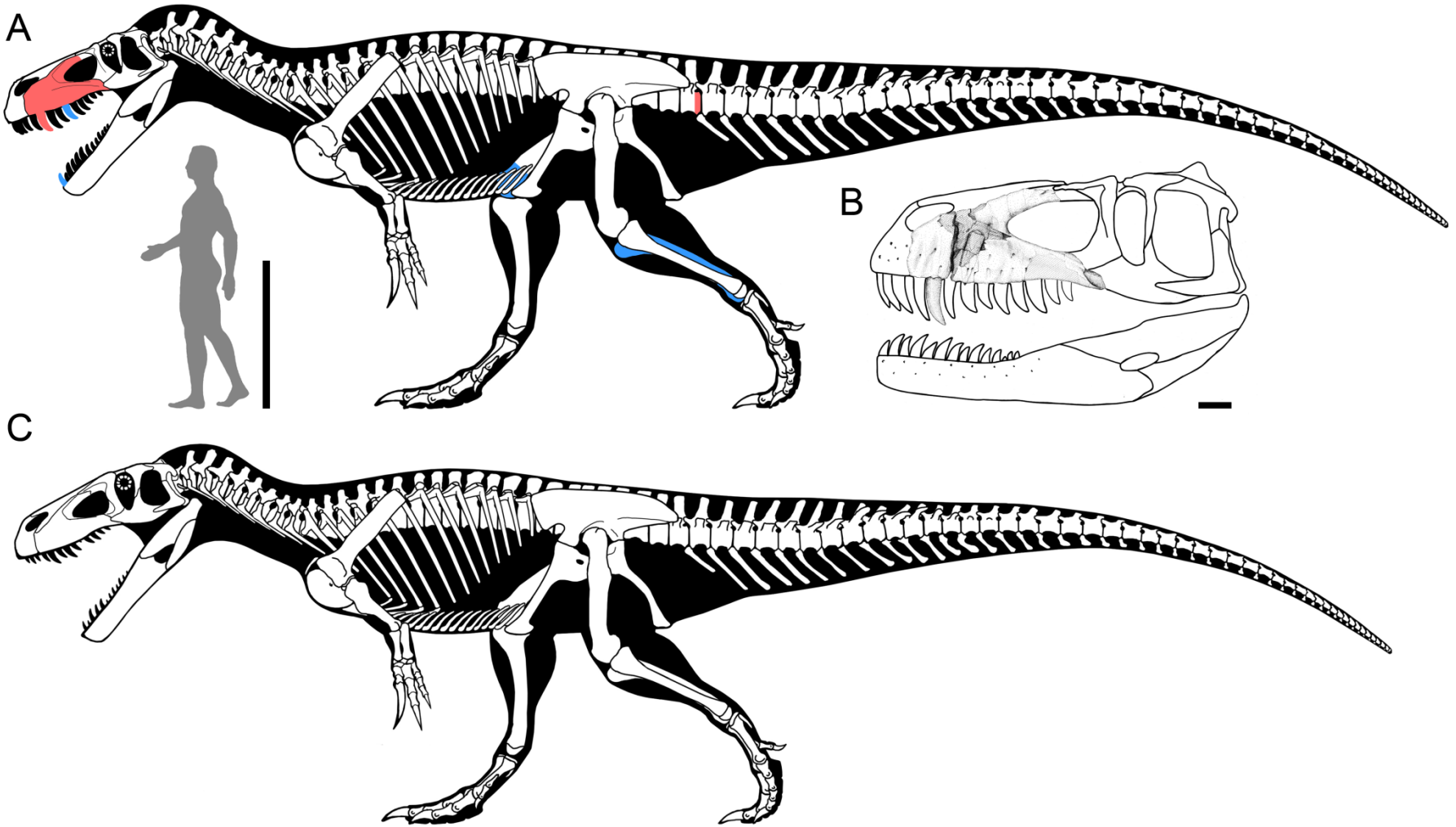

FIGURE 9.4. Reconstruction of *Torvosaurus gurneyi* in lateral view. **A**, Skeletal reconstruction of *Torvosaurus gurneyi* in lateral view illustrating, in red, the elements present in the holotype specimen (ML 1100) and, in blue, the elements tentatively assigned to this species (artwork by Scott Hartman, used with permission and modified; drawing of man by Carol Abraczinskas, University of Chicago, used with permission); **B**, Skull reconstruction of *Torvosaurus gurneyi* in lateral view illustrating the incomplete left maxilla (ML 1100) of the holotype specimen (artwork by Simão Mateus, used with permission and modified); **C**, Skeletal reconstruction of *Torvosaurus gurneyi* in lateral view by Scott Hartman (courtesy of Scott Hartman). Scale bars = 1 m (A, C) and 10 cm (B).

absent. The maxilla is also broken in two pieces at the level of the third alveolus, and a fragment of the lateral surface of the maxilla can be removed at the level of alveolus 4, allowing examination of a complete unerupted tooth (Figs. 9.5–9.6A). Only a fully-erupted tooth, the second maxillary tooth, is preserved, and the crown tips of the third and six alveoli are visible. The maxilla is thick and massive, with a short posterodorsally angled ascending ramus and a high anteroposteriorly elongated maxillary body (Fig. 9.5–6A; Table 1). The ventral margin of the maxillary body is weakly sigmoid, with a convex, almost straight, ventral margin of the anterior body, and a concave ventral margin of the jugal ramus.

The anterior body of the maxilla is longer than the jugal ramus (Table 9.1), yet the posterior extremity of the jugal ramus is broken and the posterior part may have extended further posteriorly. Nevertheless, the anterior body is high and about one third higher than the jugal ramus at its anteriormost part (Figs. 9.5–9.6A). The dorsal rim of the anterior body is convex and anteroventrally inclined. It includes an anterior ramus which is demarcated by a concave step on the anterodorsal margin of the maxilla. Both anterior ramus and preantorbital body have similar anteroposterior extensions along the maxillary body. The anterior ramus is particularly high and elongated, and its posterior rim is concave whereas its ventral margin is straight. The anterior rim of the anterior ramus is high (about two thirds of the anterior ramus height in its highest part), subvertical, and perpendicular to the ventral margin of the maxillary body. The outline of the anterior margin is irregular and roughly sigmoid in lateral view, the ventral half is convex whereas the dorsal half is concave due to the presence of a ventrodorsally wide subnarial foramen. The dorsal margin of the anterior ramus bears a thin crest, the anterodorsal crest (Figs. 9.5–9.6D–E), running from alveoli 1 to 3 and adjacent to the anteromedial process. This narrow crest is slightly medially inclined and taller in its anterior part. It also shows an undulating dorsal rim. The anteromedial process and the anterodorsal crest both delimit a deep anteroposteriorly extended groove that received the ventral articular surface of the nasal. The nasal contact of the anterior ramus is narrow and shallow in its posterior part, anterior to the ascending ramus, and gets wider and deeper at the level of the anteromedial process.

The premaxillary contact is located on the anterior rim of the anterior ramus. It is a rather simple articulation that corresponds to a roughly flat but uneven surface. The premaxillary articulation bears two large foramina on its dorsalmost part, the smaller one being situated dorsolateral to the larger one, in the dorsolateral corner of the premaxillary contact. These two anterior foramina (Fig. 9.5–9.6E) lead to the subnarial foramen, an aperture that is posteriorly delimited by the maxillary body and the maxillary contact of the premaxilla anteriorly. The subnarial foramen is not clearly visible but corresponds to a wide concavity on the anterolateral margin of the maxillary body, at the dorsalmost third of the premaxilla contact. Additional foramina are visible medial to the anterior foramina, and along the ventral half of the premaxillary contact. These additional foramina are minute in size, and smaller than the two anterior foramina (Figs. 9.5–9.6E). Two pits also occur on the dorsalmost part of

FIGURE 9.5. Maxilla of *Torvosaurus gurneyi* (ML 1100) and comparison with *T. tanneri*. Incomplete left maxilla of the holotype specimen of *Torvosaurus gurneyi* (ML 1100) in **A**, lateral; **B**, medial; **C**, ventral; **D**, dorsal; **E**, anterior; **F**, posterior views with details of **G**, Anterodorsal margin of jugal ramus in dorsomedial view; and **H**, Posterior part of jugal ramus in dorsal view. **I-J**, Anterior part of interdental wall of **I**, *T. gurneyi*; and **J**, *T. tanneri* (BYU-VP 9122) in medial view. **K-L**, Anteromedial process of **K**, *T. gurneyi*; and **L**, *T. tanneri* (BYU-VP 9122) in medial views. Scale bars = 10 cm (A-H), 5 cm (G-L).

the premaxillary contact, between the lateral wall of the anterior ramus and the medial wall attached to the anteromedial process. These two pits accommodated the bifurcated maxillary process of the premaxilla. In anterior view, the medial margin of the premaxillary articulation is straight whereas the lateral margin is convex. In medial view, the lateral wall of the anterior ramus extends slightly further anteriorly than the medial wall.

The jugal ramus is sub-triangular in outline and tapers gently ventroposteriorly. The surface of the jugal ramus bears a small and shallow concavity on its anterolateral margin, at the level of the sixth alveolus. This concavity is bounded ventrally by the antorbital ridge. A wide furrow is visible on the dorsomedial surface of the jugal ramus, ventral to the antorbital fenestra. This groove most likely corresponds to a neurovascular opening serving for the passage of the maxillary branch of the trigeminal nerve (O. Rauhut, pers. comm.). The neurovascular opening (Fig. 9.6B–G) runs from the lacrimal contact of the maxilla to the level of the eighth alveolus, just below the antorbital fenestra. The groove is shallow anterior to the lacrimal contact but penetrates deeply inside the medial wall of

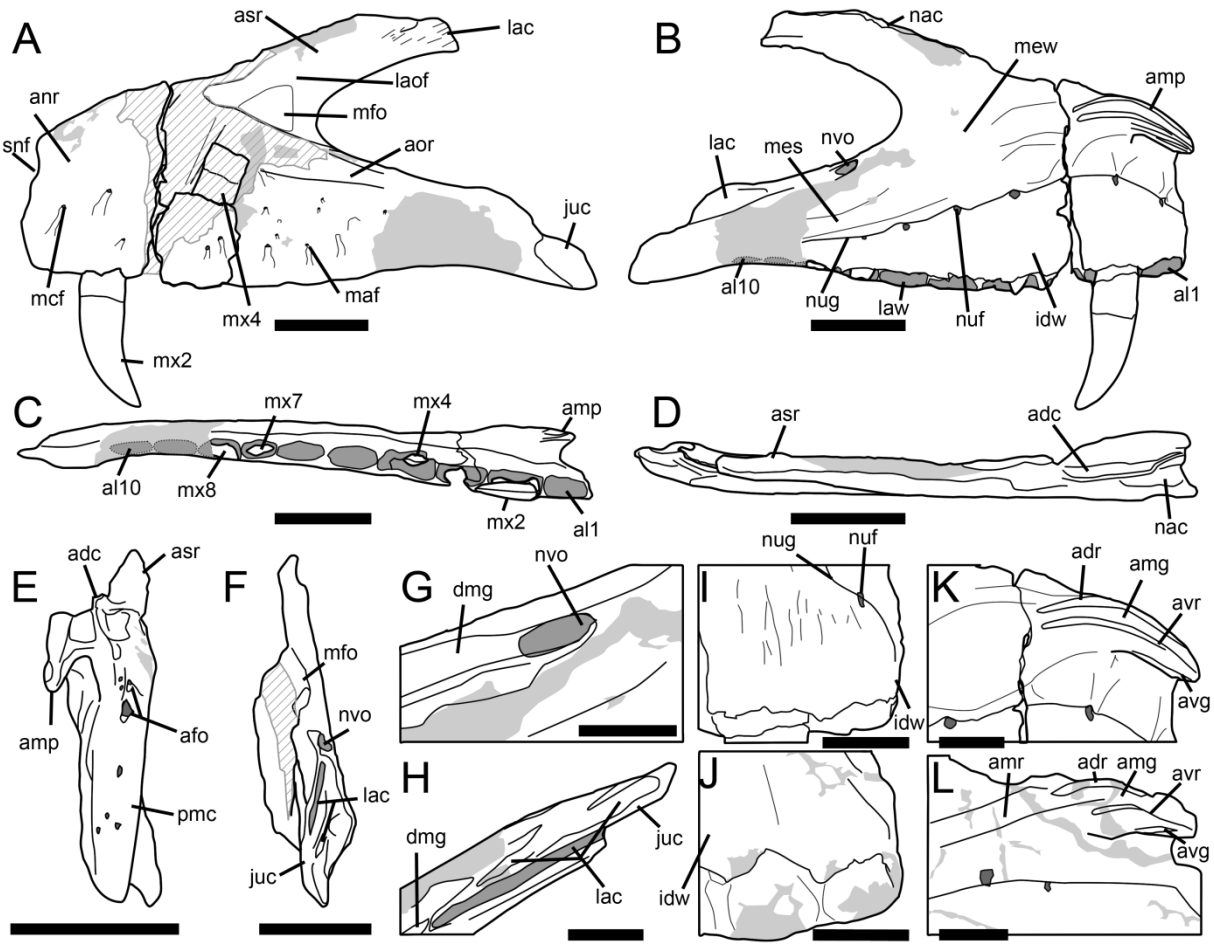

FIGURE 9.6. Maxilla of *Torvosaurus gurneyi* (ML 1100) and comparison with *T. tanneri*. Interpretive line drawing of the left maxilla of the holotype specimen of *Torvosaurus gurneyi* (ML 1100) in **A**, lateral; **B**, medial; **C**, ventral; **D**, dorsal; **E**, anterior; **F**, posterior views with details of **G**, anterodorsal margin of jugal ramus in dorsomedial view; and **H**, posterior part of jugal ramus in dorsal view. **I-J**, Interpretive line drawing of the anterior part of interdental wall of **I**, *T. gurneyi*; and **J**, *T. tanneri* (BYU-VP 9122) in medial view. **K-L**, Interpretive line drawing of the anteromedial process of **K**, *T. gurneyi*; and **L**, *T. tanneri* (BYU-VP 9122) in medial views. Hatched areas represents missing parts, light grey tone indicates reconstructed part, and dark grey tone corresponds to the foramina, and alveoli, with alveoli 9 and 10 being reconstructed. **Abbreviations**: **adc**, anterodorsal crest; **adr**, anterodorsal ridge of the anteromedial process; **afo**, anterior foramina; **al**, alveolus; **amg**, anteromedial groove of the anteromedial process; **amp**, anteromedial process; **amr**, anteromedial ridge; **anr**, anterior ramus; **aor**, antorbital ridge; **asr**, ascending ramus; **avg**, anteroventral groove of the anteromedial process; **avr**, anteroventral ridge on the anteromedial process; **dmg**, dorsomedial groove; **idw**, interdental wall; **juc**, jugal contact; **lac**, lacrimal contact; **laof**, lateral antorbital fossa; **law**, lateral wall; **maf**, maxillary alveolar foramina; **mcf**, maxillary circumfenestra foramina; **mes**, medial shelf; **mew**, medial wall; **mfo**, maxillary fossa; **mx**, maxillary teeth; **nac**, nasal contact; **nuf**, nutrient foramina; **nug**, nutrient groove; **nvo**, neurovascular opening; **pmc**, premaxillary contact; **snf**, subnarial foramen. Scale bars = 10 cm (A-H), 5 cm (G-L).

the jugal ramus in its anterior part. The jugal articulates with the posterior extremity of the jugal ramus, along a smooth articular surface on the lateroventral margin of the jugal ramus. The anterior rim of the jugal contact is parabolic in outline, and the main axis of the articulation is inclined ventroposteriorly. Its ventral rim corresponds to a narrow groove penetrating the lateral wall of the jugal ramus.

A second articulating surface, the lacrimal contact, appears on the posteromedial margin of the jugal ramus, posterior to the neurovascular opening, and at two thirds of the jugal ramus (Fig. 9.6B). The lacrimal contact extends along the posterior extremity of the jugal ramus, posterior to the eighth alveolus. The lacrimal contact covers around one half of the jugal ramus. The dorsal rim of the lacrimal contact forms a convexity on the dorsal margin of the jugal ramus, and the ventral part consists of a very deep slit inside the jugal ramus, so that the maxillary contact of the jugal corresponds to a very thin articular structure (Fig. 9.6F–H). The lacrimal contact also includes a second furrow running along the dorsomedial rim of the jugal ramus, medial to the deep split and dorsal to the lateral part of the lacrimal articulation(Fig. 9.6H). The latter is bounded laterally by the lateral wall of the maxillary body on its anterior part, its posterior part being adjacent to the jugal contact on the lateroposterior surface of the jugal ramus. The main axis of the lacrimal contact is directed posteroventrally, parallel to the ventral rim of the antorbital fenestra. Similar to the jugal contact, the lacrimal contact of the jugal ramus is a simple suture i.e., it is not reinforced by a series of grooves and rugosities.

TABLE 9.1. Measurements of left maxilla of the holotype of *Torvosaurus gurneyi* (ML 1100).

	Measurements (mm)
Anteroposterior length of maxilla:	612
Dorsoventral depth of maxilla at the posteriormost point of the ascending ramus:	274
Dorsoventral depth of maxillary body at the level of the step delimiting the anterior ramus and ascending ramus:	226
Anteroposterior length of antorbital body:	310
Anteroposterior length of jugal ramus:	299
Dorsoventral depth of jugal ramus at the anterior margin of antorbital fenestra:	170
Dorsoventral depth of ascending ramus along its main axis:	237
Dorsoventral depth of anterior margin of maxillary body:	122
Anteroposterior length of anteromedial process	115
Anteroposterior length of jugal contact:	83
Dorsoventral depth of interdental wall at the level of the third alveolus:	106
Basoapical length of second maxillary tooth, root included:	138
Basoapical length of third non-erupted maxillary tooth, root included:	165

The ascending ramus forms a wing-like structure diverging from the maxillary body to an angle of around 30° with the ventral margin (Figs. 9.5–9.6A). The ascending ramus is short compared to the anteroposterior extension of the maxillary body (Table 9.1), but its posterior extremity is broken and must also have extended further posteriorly (Fig. 9.4). Although some parts of the anterior margin of the ascending ramus are missing, the anterior and posterior rims are sub-parallel along the anterior part of the ramus but the anterodorsal rim abruptly changes orientation at two thirds of the process so that the jugal ramus tapers posteriorly. The medial surface of the ascending ramus is slightly concave, and a small depression appears on the posteromedial surface of the ascending ramus, on the center of the process. Unlike other articular surfaces on the maxilla, the lacrimal contact of the ascending ramus is not clearly delimited. A few parallel ridges are visible on the lateroposterior surface of the ascending ramus, and the lacrimal contact is bounded by a sharp ridge parallel to the rim of the

antorbital fenestra on its ventromedial surface. A furrow is also present on the posterolateral margin of the ascending ramus and was bordering the anterior rim of the lacrimal. This wide groove runs diagonally on the posterior extremity of the ascending ramus and is bounded by a short crest anteriorly. Two shallow concavities appear anterior to this ridge and their main axis is sub-parallel to the diagonal furrow.

The anteromedial process of the maxilla is complete, protuberant and clearly-visible on the anterodorsal corner of the anterior body, immediately ventral to its dorsal rim, and to a certain distance dorsal to the nutrient groove (Figs. 9.5, 9.6B, K). This process sweeps gradually and tapers ventrally at the level of the first alveolus. It bears two large and parallel ridges separated by a wide groove on its medial surface, and a shallow and straight groove on its ventromedial surface (Fig. 9.6K). Both ventral and dorsal ridges get flared at the level of the third alveolus posteriorly, and the wide groove they delimit gets deeper anteriorly. The anteromedial process does not extend further than the third alveolus posteriorly, and only expands slightly further than the anterior rim of the maxillary body anteriorly.

The medial shelf is poorly delimited. It corresponds to a wide but shallow ridge running on the medial wall of the maxillary body, from the anteromedial process to the posterior part of the jugal ramus (Figs. 9.5–9.6B). The medial shelf is clearly sigmoid i.e., it is convex along the jugal ramus and concave along the anterior ramus. A subtle flattened surface is visible at the level of the fourth alveolus, posteroventral to the anteromedial process. There is no trace of articulating surface for the palatine on the preserved medial shelf. The palatine may have been in contact with the medial margin of the maxillary body posterior to the eighth alveolus, yet the palatine articulation may have just been eroded more anteriorly.

The surface of the medial wall is smooth all along the maxilla. It bears two concavities just ventral to the anteromedial process, at the level of the first and second alveoli (Fig. 9.6K). The anterior concavity is significantly wider than the posterior one and subcircular in outline. The posterior depression is weakly ventrodorsally elongated and subrectangular in outline. These two deep pits accommodated two large crowns of the dentary whereas the jaws of the animal were closed. A deep depression occurs on the anterodorsal surface of the anterior body, beneath the anterior part of the anteromedial process. This depression is bounded dorsally by a thin convex lamina linking the anteromedial process to the anterior ramus. The medial wall is neither fenestrated nor perforated at the base of the ascending ramus, and there is no trace of medial antorbital fossa and medial pneumatic complex.

The nutrient groove is distinct and forms a strong step between the medial wall and the interdental plates (Figs. 9.5–9.6B). The groove is sigmoid and subparallel to the medial wall, and strongly curves ventrally at the level of the second alveolus. It bears seven clearly-visible nutrient foramina at the level of each alveolus, exactly aligned with their centra (Figs. 9.5–9.6B). The nutrient foramen of the third, eighth and more posterior alveoli are not preserved. These dental foramina increase in size with the fourth alveoli and then decrease in dimension more posteriorly. They are

lanceolate to elliptical in outline, the largest one being almost subcircular at the level of the fourth alveolus. The nutrient foramina weakly penetrates the medial wall dorsally.

The interdental plates are completely fused to form a continuous lamina along the medial surface of the maxillary body (Figs. 9.5–9.6B, I). Their height increases along the two first alveoli, then their ventrodorsal extension decreases posterior to alveolus 3. They are particularly high at the level of the second and third alveolus, being two times higher than wide, and the ventral extent of the interdental wall is as far ventral as the lateral wall of the maxillary body. The medial surface of the interdental plates is irregular and rugose, and the presence of faint grooves running ventrodorsally on the ventral margin can be noticed (Fig. 9.6I).

The antorbital fenestra is almost perfectly parabolic in outline i.e., the curvatures of the ventral and dorsal rims of the antorbital fenestra are subsymmetrical, the ventral margin being only slightly wider ventrally. The medial antorbital fossa is absent but the lateral antorbital fossa extends far anterior on the maxilla. The extension of the lateral antorbital fossa is important on the ascending ramus but limited to the dorsalmost part of the maxillary body. The lateral antorbital fossa is bounded ventrally by a wide and poorly delimited antorbital ridge on the dorsal part of the jugal ramus (Figs. 9.5–9.6A). The antorbital ridge is missing in the dorsal part of the anterior body and all along the ascending ramus so that it is not possible to know the exact extension of the antorbital fossa in its anteriormost corner.

No promaxillary or maxillary fenestrae are present within the lateral antorbital fossa. Nevertheless, a subtriangular depression is visible on the anterior corner of the antorbital fossa, just anterior to the anteriormost point of the antorbital fenestra and dorsal to the antorbital ridge of the anterior body. Due to its large size, shape and location, the subtriangular depression is here interpreted as homologous to the maxillary fossa (or imperforated maxillary ‘fenestra’ of Benson 2010*a*). A single accessory antorbital fossa occupying most of the anterior corner of the lateral antorbital fossa has usually been interpreted as being a maxillary fossa/fenestra rather than a promaxillary fossa/fenestra, and the latter is only large when associated with the maxillary fenestra (pers. obs.). It is very likely that the antorbital ridge was forming a lateral rim on the anteroventral part of the ascending ramus, delimiting a deep recess within the anterior corner of the lateral antorbital fossa. The posteriormost part of a poorly defined ridge is visible dorsal to the antorbital ridge, on the anterodorsal part of the jugal ramus, at the level of the fourth alveolus. Although this ridge is strongly damaged more anteriorly, its posterior rim can be followed from the antorbital fenestra to the anteriormost part of the maxillary recess.

The texture of the lateral surface of the maxilla is not rugose or sculptured, but the lateral surface of the maxillary body is pierced by a series of large, deep and well-delimited neurovascular foramina. A wide groove, parabolic in outline in some cases, extends ventrally from each neurovascular foramina which penetrate the lateral wall of the maxilla dorsally. Although many neurovascular foramina are missing due to damage of the lateral bone surface, two rows of

neurovascular foramina are clearly visible and both run anteroposteriorly on the maxillary body, parallel to the ventral margin. The ventral row, which includes the maxillary alveolar foramina, is adjacent and slightly dorsal to the ventral margin of the maxillary body, whereas the dorsal row, that encompasses the circumfenestra foramina, is centrally positioned on the maxillary body and runs shortly dorsally to the row of alveolar foramina.

Eight maxillary alveoli are distinctly visible along the maxillary body, and the preserved posterior part of the jugal ramus does not preserve any alveolus (Figs. 9.5–9.6C). The tooth row extends anterior to the jugal contact, and the largest tooth-sockets are located at mid-length of the maxillary body, the largest alveolus being the sixth one. The alveoli are well-separated and elliptical in outline all along the tooth row.

Dentition—The second fully erupted maxillary tooth and the third unerupted tooth (Figs. 9.5, 9.7) are well preserved and allow the crown and denticles morphology to be investigated comprehensively. The second erupted tooth is complete and undistorted whereas the unerupted one has been crushed inside its alveolus and the labial and lingual surfaces are damaged. The apical part of a third unerupted tooth appears on the basolingual surface of the unerupted tooth, inside the fourth alveolus (Fig. 9.7D). This second unerupted crown correspond to the third generation of teeth in the maxilla.

TABLE 9.2. Measurements of maxillary teeth of the holotype of *Torvosaurus gurneyi* (ML 1100).

	Measurements (mm)
Second erupted maxillary tooth	
Crown base length (CBL)	45.52
Crown base width (CBW)	16.4
Crown height (CH)	109.4
Apical length (AL)	118.57
Mid-crown length (MCL)	33.1
Mid-crown width (MCW)	16.8
Extension of mesial denticles from cervix (MDE)	55.51
Third unerupted maxillary tooth	
Crown base length (CBL)	45.65
Crown base width (CBW)	?
Crown height (CH)	116.98
Apical length (AL)	128.59
Mid-crown length (MCL)	39.54
Mid-crown width (MCW)	?
Extension of mesial denticles from cervix (MDE)	46.38

The crowns are ziphodont (i.e., blade shaped, labiolingually compressed, distally curved and having serrated carinae), large (crown height > 100 mm; Table 9.2) and strongly elongated (crown height ratio > 2.5; Hendrickx and Mateus 2014*b*). They are significantly recurved distally and bear prominent carinae mesially and distally. In distal view, the crown and the distal carina of the erupted tooth are gently sigmoid in outline, with the root curving lingually from the crown (Fig. 9.7F). The basolabial surface of the erupted crown is mesiodistally concave and this depression allows the accommodation of an unerupted crown lingually. The distal carina extends to the cervix whereas the

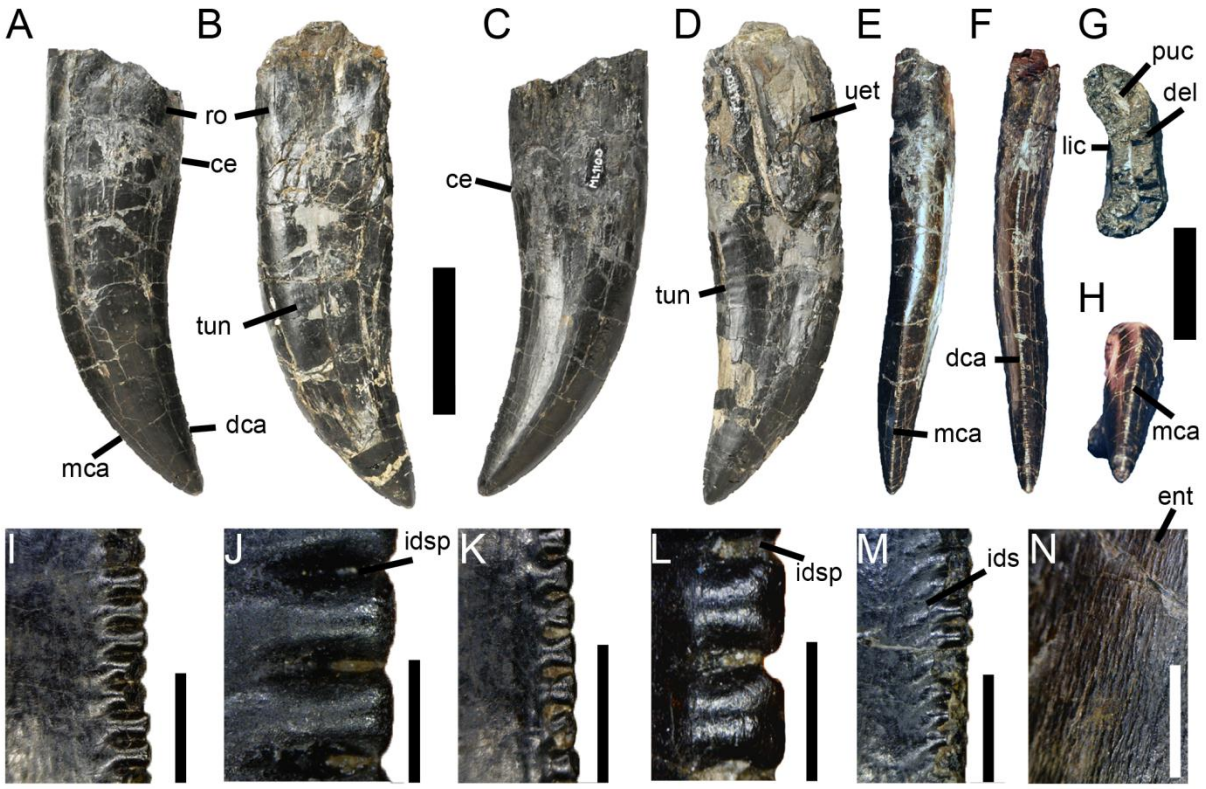

FIGURE 9.7. Dentition of *Torvosaurus gurneyi* (ML 1100). **A, C, E-H**, Second maxillary tooth; and **B, D**, third non-erupted maxillary tooth of the holotype specimen of *Torvosaurus gurneyi* in **A-B**, labial; **C-D**, lingual; **E**, mesial; **F**, distal; **G**, basal; and **H**, apical views. **I-J**, Distal; and **K-M**, mesial denticles of the second maxillary tooth in lateral view. **M**, Distal serrations showing the interdenticular sulci; and **N**, enamel texture of the third non-erupted tooth in labial view. **Abbreviations**: **ce**, cervix; **dca**, distal carina; **del**, dentine layer; **ent**, enamel texture; **ids**, interdenticular sulci; **idsp**, interdenticular space; **mca**, mesial carina; **lic**, lingual concavity for the erupting tooth; **puc**, pulp cavity; **ro**, root; **uet**, unerupted tooth; **tun**, transverse undulation. Scale bars = 5 cm (A-F), 3 cm (G-H), 3 mm (I, K, M-N), 1 mm (J, L).

mesial carina does not reach the root and gets flared at one third of the crown (Fig. 9.7E). Both carinae are centrally positioned on the crown although the basal part of the mesial carina tends to get slightly offset at mid-height of the crown. The cross section outline of the crown is reniform at the cervix, lanceolate at one third of the crown and elliptical more apically. The external surface is particularly well-preserved and shows a clear braided and apicobasally oriented texture of the enamel (Fig. 9.7N). Although not present on the erupted crown, subtle transverse undulations (‘enamel wrinckles’ *sensu* Brusatte et al. 2007) are observable on the basal half of the unerupted crown, on both labial and lingual sides (Fig. 9.7B, D). The undulations are more pronounced adjacent to the distal carina on the lingual surface of the crown. Only the basal part of the root of the second maxillary tooth is preserved. The root clearly shows a deep concavity on its lingual surface for receiving the unerupted crown. Such lingual concavity is also present on the other teeth of the maxilla as the cross section outline in the root of these teeth is clearly reniform.

The denticles are large and coarse, with an average of eight denticles per five millimeters on both carinae (Fig. 9.7I–M; Table 9.3). The crown apex is damaged in the erupted crown, but the

TABLE 9.3. Number of denticles in maxillary teeth of the holotype of *Torvosaurus gurneyi* (ML 1100).

	Denticles (per 5 mm)
Second erupted maxillary tooth	
Mesioapical denticles (MA)	6
Mesial denticles at mid-height (MC)	8
Mesiobasal denticles (MB)	/
Distoapical denticles (DA)	7
Denticles at mid-height (DC)	8
Distobasal denticles (DB)	11
Third unerupted maxillary tooth	
Mesioapical denticles (MA)	6
Mesial denticles at mid-height (MC)	7
Mesiobasal denticles (MB)	/
Distoapical denticles (DA)	6
Denticles at mid-height (DC)	8
Distobasal denticles (DB)	10

serrations are clearly crossing the apex of the unerupted tooth. In the second maxillary crown, there is a density of ten to eleven denticles per five millimeters basodistally, eight denticles at mid-crown and six to seven serrations per five millimeters apically for both carinae, so that the denticle size increases from the base to the apex (Table 9.3). Mesial and distal denticles of both erupted and unerupted crown differ in their morphology and elongation. The distal denticles are chisel-like in shape (i.e., denticles with a sharp edge) in mesial and distal views and finger-like in shape (i.e., horizontal subrectangular denticles with convex labial and lingual surfaces) in lateral view (Fig. 9.7I–J). They extend perpendicularly from the distal margin of the crown and possess narrow but deep interdenticular space. The external margin of each denticle is symmetrically to asymmetrically convex but never hooked apically. Pronounced and clearly-visible interdenticular sulci are present all along the distal carina (Fig. 9.7M). These grooves curve basally from each interdenticular space and are particularly long at mid-crown. They are shorter more basally and apically, being very short to absent near to the cervix and the apex. Unlike the distal serrations, the mesial denticles have subquadrangular to vertical subrectangular profile in lateral view (Fig. 9.7K–L). They are either perpendicular to or weakly apically inclined from the mesial margin of the crown, and their external margin is symmetrically to asymmetrically convex. The interdenticular space is deep and tends to be apicobasally wider at mid-height and narrower at the level of the apex in some denticles, creating an elliptical to lanceolate outline of the interdenticular space. The interdenticular sulci are short or totally absent from mesial serrations. On the unerupted tooth where they are clearly visible, they are short to absent on the lingual side but totally absent on the labial surface of the crown.

Several isolated bone fragments, including the proximal portion of a rib, a strongly damaged fragment of a long bone and a caudal vertebra, have been uncovered from the same area of the maxilla. Nevertheless, only the caudal vertebra comes from the same spot and was directly associated with the maxilla. Likewise, its size, preservation and taxonomic identification allows assigning the caudal vertebra to the same specimen with confidence.

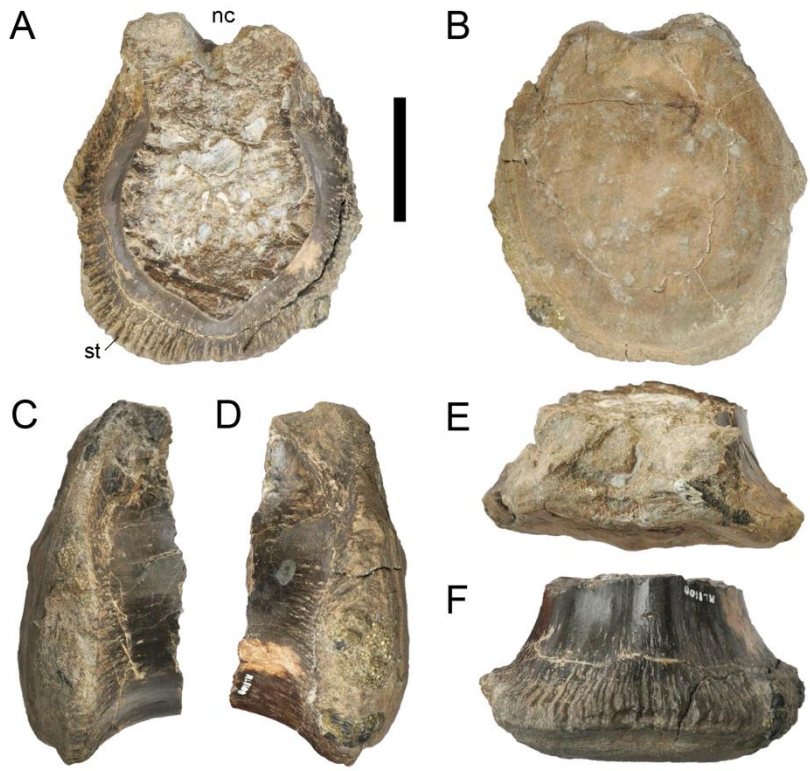

FIGURE 9.8. Caudal vertebra of *Torvosaurus gurneyi* (ML 1100). **A**-**F**, Posterior part of an anterior caudal centrum of the holotype specimen of *Torvosaurus gurneyi* (ML 1100) in **A**, anterior; **B**, posterior; **C**, right lateral; **D**, left lateral; **E**, dorsal; and **F**, ventral views. **Abbreviations**: **nc**, neural canal; **st**, striation. Scale bar = 5 cm.

Caudal vertebra—The posterior third of a caudal centrum (Fig. 9.8) with about 57 mm is preserved. We interpret this bone as a proximal caudal vertebra based on comparisons with the *T. tanneri* holotype (BYU-VP 13745), in particular based on the lack of an elongated pneumatic foramen extending along most of the centrum length, shallow chevron facets and the flattened to sub-convex articular surface. The general outline of the posterior view forms a large ellipse about 131 mm tall and 120 mm wide (Table 9.4). The articular facet is moderately flat; however, in the middle of the surface there is a tuberosity projecting posteriorly, and shallow depressions below and above it are also visible (Fig. 9.8E). The lateral and ventral margin of the centrum have well-defined striations that run anteroposteriorly on the centrum, being deeper and pronounced in the ventral half the centrum (Fig. 9.8A, F). These sulci are up to 20 mm long, 2 mm wide, and 1.2 mm deep, but the dimensions vary. These dimensions provide a density of 3.5 ridges per centimeter. The ventroposterior corner of the centrum is expanded but with no clear individual facet for the chevrons. The posterior rim if the centrum possesses circular striations. There is a horizontal transversal groove on the posteroventral corner of the centrum between the ventralmost rim of the centrum and the platform of the articular facet. This gives a salient aspect to the posterior region of the centrum, but this can also be interpreted as a sub-convexity of this facet. The anterior broken transversal section has an amphora-like outline.

This outline is produced ventrally by a rounded ridge-like midline crest, and dorsally by the posterodorsal corner of the centrum that is slightly narrower transversely, giving a constriction of the amphora-like outline (Fig. 9.8A). The bone is compact towards the periost, and camellate in the anterior part of the centrum. The neural canal is narrow ventrally which gives a V-shaped at the cross-

TABLE 9.4. Measurements of proximal caudal vertebra of the holotype of *Torvosaurus gurneyi* (ML 1100).

	Measurements (mm)
Dorsoventral height of centrum at the level of the neural canal:	129
Dorsoventral height of centrum at its maximum height:	145
Transverse width of centrum:	121
Anteroposterior length of centrum:	52

section in anterior view but broader and U-shaped in posterior view (Fig. 9.8A–B). The pedicel width is equivalent to the neural canal at mid-level of the neural canal, where it is broken dorsally. The pedicels reach the posteriormost facet of the centrum. The general surface of the bone is lustrous in the lateral and ventral surface of the centrum, but matt on the posterior facet. If complete, the centrum would be moderately excavated, giving a hourglass outline in ventral view.

Phylogenetic Analysis

ML 1100 was previously assigned to *Torvosaurus tanneri* by Mateus et al. (2006) based on an antorbital tooth row, the absence of a maxillary fenestra (antorbital foramen of Mateus et al. 2006) and pneumatization on the ascending ramus, and the posterior orientation of the ascending ramus of the maxilla. In order to confirm the phylogenetic affinities of this specimen, a cladistic analysis was performed using the data matrix of Carrano et al. (2012), the most recent and exhaustive analysis focusing on relationships of basal Tetanurae. The data matrix includes 60 ingroup taxa and two outgroups (*Eoraptor* and *Herrerasaurus*) coded in 353 unordered and equally weighted characters (Carrano et al. 2012). Following personal observation of the maxilla in basal tetanurans, one character was modified from Carrano et al. (Carrano et al. 2012) and two additional characters were created (Appendices A9.1). A total of 36 characters were coded for the maxilla, two for the interdental plates, nine for the dentition and one for the caudal vertebra (Appendices A9.2). TNT v1.1 (Goloboff et al. 2008) was employed to search for most-parsimonious trees (MPTs). As a first step, the matrix was analysed under the ‘New Technology search’ with the ‘driven search’ option, TreeDrift, Tree Fusing, Ratchet, and Sectorial Searches selected with default parameters, and stabilizing the consensus twice with a factor of 75. The generated trees were then analysed under traditional TBR (tree bisection and reconnection) branch (Goloboff et al. 2008). Bremer support (Bremer 1994) and Reduced Cladistic Consensus Support Trees (Wilkinson 1994) were calculated with TNT by saving 10,000 suboptimal trees up to 10 steps longer than the MPTs. The consistency and retention indexes as well as the Bremer and relative Bremer supports were calculated using the ‘stats’ and the ‘aquickie’ commands, respectively.

The cladistic analysis yielded 93 MPTs, 1033 length, with a consistency index of 0.404 and a retention index of 0.677 for the strict consensus tree. The tree mirrors to a large degree the topology obtained by Carrano et al. (2012) and recovered ML 1100 and *Torvosaurus tanneri* as sister taxa. The clade of Megalosauria (*sensu* Carrano et al. 2012) was however badly resolved and a reduced consensus approach (Wilkinson 1994, 1995, 1996) was used by excluding a posteriori four wildcard

taxa with a lot of missing data (*Magnosaurus*, *Poekilopleuron*, *Streptospondylus* and *Xuanhanosaurus*). The topology of the resulting consensus tree is similar to the consensus tree obtained when excluding a priori the four taxa (Fig. 9.9), and the tree displays a few polytomies, mostly in the clade of Megalosauridae and Carcharodontosaurinae. Nevertheless, all major clades of Tetanurae were found resolved and the *Torvosaurus* taxa are still closely related, forming the sister clade of the taxon *Megalosaurus* (Fig. 9.9). Following the result of the cladistic analysis, ML 1100 can confidently be assigned to the taxon *Torvosaurus*. The maxilla ML 1100 indeed belongs to a theropod based on the combination of a subnarial foramen and very large ziphodont teeth bearing coarse denticles, a tetanuran due to its anteroposteriorly long anterior ramus, the presence of a maxillary recess (i.e., either a maxillary fenestra or a maxillary fossa) within the lateral antorbital fossa, and a tooth row extending anterior to the orbit. In also pertain to a megalosaurid by the presence of a maxillary fossa, to the clade encompassing *Megalosaurus* and *Torvosaurus* by the tall interdental plates (ventrodorsal depth relative to the anteroposterior width > 1.8; Carrano et al. 2012), and to the *Torvosaurus* by the shallow maxillary fossa, limited ventral extension of the lateral antorbital fossa on the maxillary body, and fused interdental plates forming an interdental wall (Carrano et al. 2012).

Discussion

The maxillae of ML 1100 and the referred specimen of *T. tanneri* BYU-VP 9122 share striking similarities (Fig. 9.10). Not only their anatomy is very close but they also share similar size and angles of rami. Many other features are common between ML 1100 and BYU-VP 9122, namely, large and elongated teeth with coarse denticles (a maximum of 8 denticles per 5 mm), a shallow subtriangular maxillary fossa at the base of the ascending ramus, an ascending ramus angled at 30° from the ventral margin, an anteroposteriorly oriented ridge ventral to the shallow maxillary fossa within the lateral antorbital fossa, and very tall fused interdental plates that are perforated by large nutrient foramina at the level of the nutrient groove. Therefore, the Portuguese specimen clearly belongs to the taxon *Torvosaurus* first described from the Kimmeridgian-Tithonian of North America (Galton and Jensen 1979). The two taxa also share similar stratigraphical range as the Portuguese specimen is late Kimmeridgian in age, and its American counterpart has been recorded in late Kimmeridgian to late Tithonian deposits (Carrano et al. 2012). Nevertheless, they were geographically separated by thousands of kilometers and the proto Atlantic epicontinental sea was restraining the European *Torvosaurus* to the Iberian Meseta (Mateus et al. 2014). Even though the assignation of ML 1100 to *Torvosaurus* is hardly doubtable, it is legitimate to assess its affiliation to the species *T. tanneri* given the paleogeographical context.

A detailed comparison of ML 1100 with BYU-VP 9122 (and ML 1186, a cast of BYU-VP 9122 deposited at the Museu of Lourinhã) allows highlighting some differences between the two maxillae (Figs. 9.6, 9.7I–L, 9.10). One of the most notable was observed by Mateus et al. (2006) and concerns the maxillary tooth count. Eleven alveoli have been noticed by Britt (1991) for BYU-VP

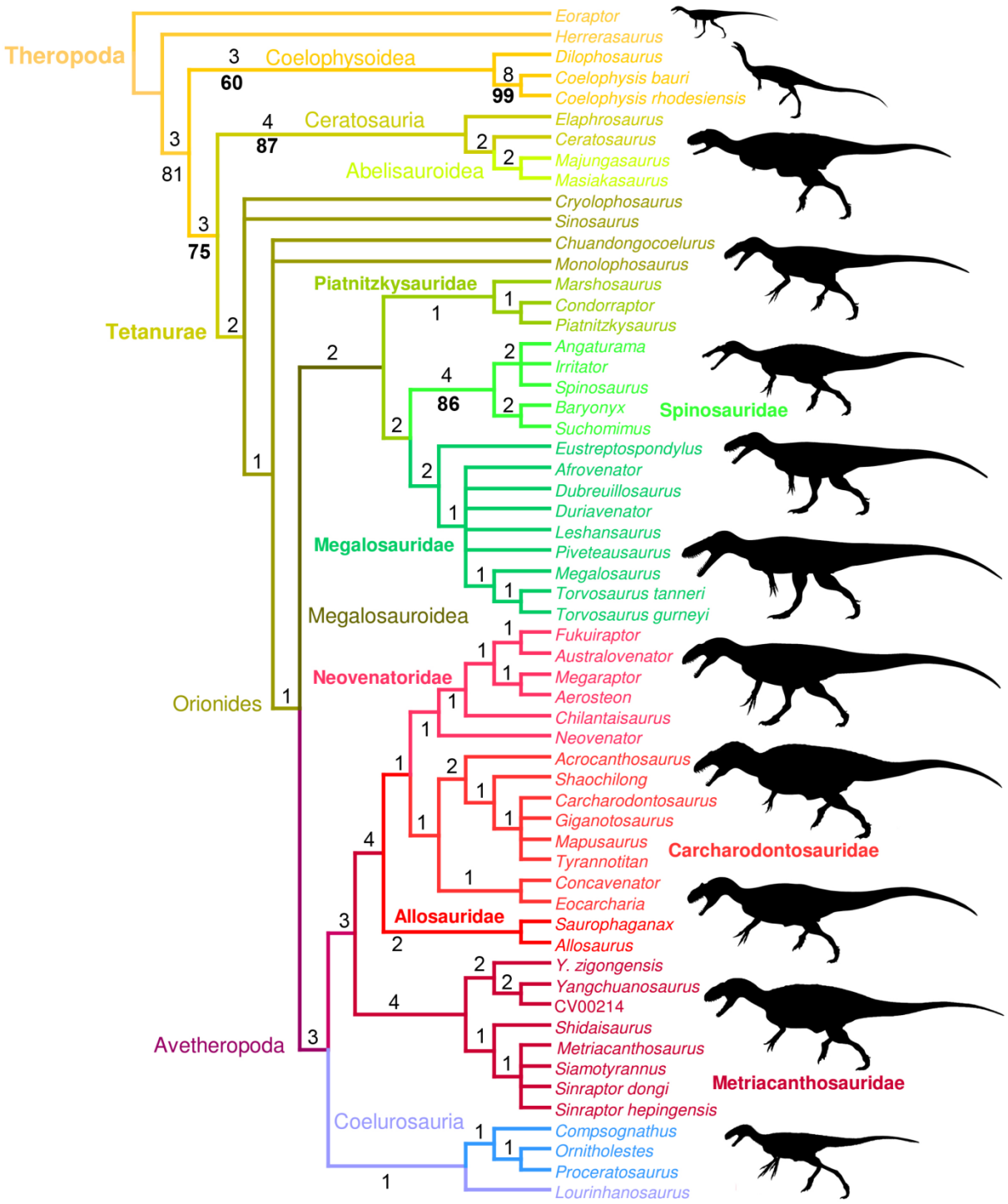

FIGURE 9.9. Cladogram of basal Theropoda and phylogenetic position of *Torvosaurus gurneyi*. Strict consensus cladogram from 71 most parsimonious trees after pruning *Magnosaurus*, *Poekilopleuron*, *Streptospondylus* and *Xuanhanosaurus* from the full set of most parsimonious trees. Initial analysis used New Technology Search using TNT v.1.1 of a data matrix comprising 353 characters for two outgroup (*Eoraptor* and *Herrerasaurus*) and 60 non-avian theropod taxa. Tree length = 1022 steps; CI = 0.414, RI = 0.685. Bremer support values are in regular and bootstrap values are in bold. For silhouette attribution, see Appendices A1.1.

9122 and, according to this author, there were up to 12 or 13 maxillary teeth based on the intersection of the medial wall and ventral margin. On the other hand, the Portuguese specimen possesses eight maxillary alveoli, with a maximum number of ten teeth (Mateus et al. 2006). Although maxillary

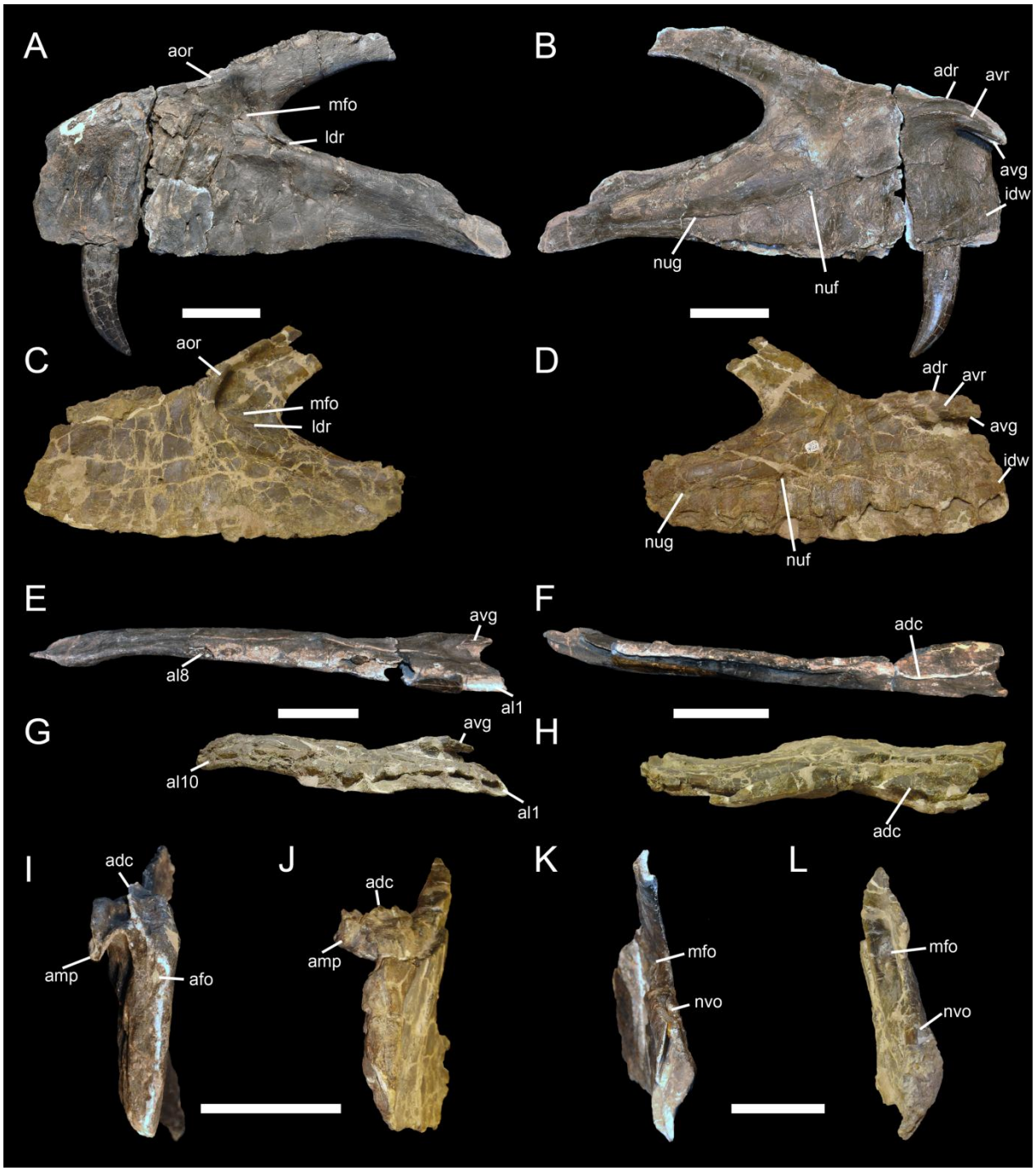

FIGURE 9.10. Comparison of the maxillae of *Torvosaurus gurneyi* and *Torvosaurus tanneri*. Left maxillae of the holotype specimen of *Torvosaurus gurneyi* (ML 1100) in **A**, lateral; **B**, medial; **E**, ventral; **F**, dorsal; **I**, anterior; and **K**, posterior views. Left maxillae of a specimen referred to *Torvosaurus tanneri* (BYU-VP 9122) in **C**, lateral; **D**, medial; **G**, ventral; **H**, dorsal; **J**, anterior; and **L**, posterior views. **Abbreviations**: **adc**, anterodorsal crest; **adr**, anterodorsal ridge of the anteromedial process; **afo**, anterior foramina; **al1**, first alveolus; **al8**, eighth alveolus; **al10**, tenth alveolus; **amp**, anteromedial process; **aor**, antorbital ridge; **avg**, anteroventral groove of the anteromedial process; **avr**, anteroventral ridge on the anteromedial process; **idw**, interdental wall; **ldr**, laterodorsal ridge within the anterior corner of the lateral antorbital fossa; **mfo**, maxillary fossa; **nuf**, nutrient foramina; **nug**, nutrient groove; **nvo**, neurovascular opening. Scale bars = 5 cm.

alveoli gradually decrease in size in theropods, the spacing between them remains the same (pers. obs.). In megalosauroids, the last alveoli never occupy less than 50% of the size of the largest alveoli (pers. obs.), so that the presence of more than two alveoli in the missing section of the jugal ramus is

very unlikely, and there were almost certainly no more than ten teeth in ML 1100. Examination of ML 1186 does not clearly reveal the presence of an eleventh alveoli, and only ten alveoli, with nine complete and the posteriormost one incomplete, could only be observed. Based on the posterior intersection of the boundary between the interdental wall and the ventral margin, we evaluate the total number of alveoli to eleven or twelve in *T. tanneri*. This therefore corresponds to a slightly closer tooth count of BYU-VP 9122 from ML 1100. Although tooth count is commonly used for taxonomic purpose by many authors in non-avian theropods (e.g., Holtz et al. 2004; Carrano and Sampson 2008; Benson 2010*a*; Carrano et al. 2012; Hendrickx and Mateus 2014*b*), variation in the number of maxillary alveoli occurs through ontogeny (e.g., Carr 1999; Rauhut and Fechner 2005), between individuals of the same species (e.g., Madsen 1976*b*; Colbert 1990; Currie 2003; Sampson and Witmer 2007), and even between left and right maxillae of a same specimen (e.g., Currie 2003; Hurum and Sabath 2003; Castanhinha and Mateus 2006). Tooth count should therefore be cautiously employed for synapomorphic purpose. Nevertheless, it is interesting to highlight that ML 1100 is the only megalosauroid possessing fewer than eleven teeth on the maxilla and, with the exception of the toothless ceratosaur *Limusaurus* (Xu et al. 2009*a*) and the primitive theropod *Daemonosaurus* (Sues et al. 2011), the only non-coelurosaurian theropod with such a low number of maxillary teeth (pers. obs.). The maxilla of *Noasaurus*, reported to have 10 to 11 maxillary teeth (Bonaparte and Powell 1980), in fact possesses 12 to 13 alveoli (pers. obs.).

Another difference between the American and European specimens is the ventral extension of the interdental plates relative to the lateral wall as well as the morphology of the ventral terminations of the interdental plates (Fig. 9.5–6I–J). In ML 1100, the interdental plates extend almost as far ventral as the lateral wall, whereas the interdental plates of *T. tanneri* fall short and end well dorsal of the lateral wall of the maxillary body. This later feature is considered to be a synapomorphical character of the clade encompassing *Torvosaurus* and *Megalosaurus* by Benson (2010*a*) and Carrano et al. (Carrano et al. 2012). It can also be observed in other theropods such as the tyrannosauroids *Guanlong*, *Daspletosaurus* and *Tyrannosaurus* and the allosauroids *Allosaurus* and *Neovenator* (see Table S1; pers. obs.). Britt (Britt 1991) remarked that this character may be due to crushing but examination of ML 1186 seems to reveal that the interdental plates genuinely end well dorsal to the lateral wall of the maxilla. Nonetheless, it is difficult to know whether this feature can variate ontogenetically, intraspecifically or can genuinely distinguish two taxa. Based on very large and similar size of their maxillae, ML 1100 and BYU-VP 9122 clearly belong to animals of the same size and ontogenetic stage, and most likely fully adult individuals of more than nine meters (see below), so that ontogenetic variation cannot be taken into consideration. The maxillae of the different specimens of *Dilophosaurus wetherilli* (UCMP 37303, TMM 43646-1; Appendices Fig. A9.1), *Ceratosaurus nasicornis* (UMNH VP 5278; MWC 1), *Majungasaurus crenatissimus* (FMNH PR 2100, 2278), *Marshosaurus bicentesimus* (UMNH VP 7824, 7825; CMNH 21704), *Megalosaurus bucklandii* (NHM R.8303; OUMNH J13506, 13559), *Allosaurus fragilis* (AMNH 600, 851; BYU-VP 2008;

UMNH VP 5393, 9168, USNM 8335) and *Tyrannosaurus rex* (CMNH 9380; FMNH PR 2081; BHI 3033) all show similar ventral extension of the interdental plates. On the other hand, the two species of *Carcharodontosaurus*, *C. saharicus* (SGM Din–1) and *C. iguidensis* (MNN IGU2) can be differentiated on this aspect as the interdental plates of the former extend more ventral than the latter (pers. obs.). Based on this observation, the ventral extension of the interdental plate relative to the lateral wall may genuinely variate interspecifically and this feature is therefore considered to be a synapomorphical character differentiating the two species of *Torvosaurus*. To our knowledge, the presence of an interdental wall coincidental with the lateral wall of the maxillary body is an autapomorphical feature of *T. gurneyi* among Megalosauroidea.

As noted by Britt (1991:17), the interdental plates of the maxilla also "terminate ventrally in broad, V-shaped points" in BYU-VP 9122 (Fig. 9.5J). On the contrary, the ventral rim of the interdental plates are straight and continuous all along the interdental wall in ML 1100 (Fig. 9.5I). A V-shaped margin of the interdental plates is common among theropods and can be observed in the noasaurid *Masiakasaurus*, the abelisaurids *Rugops* and *Indosuchus*, the megalosauroids *Marshosaurus*, *Piatnitzkysaurus*, *Eustreptospondylus*, *Duriavenator* and *Afrovenator*, the allosauroids *Allosaurus*, *Neovenator*, *Sinraptor* and *Mapusaurus*, and the tyrannosaurids *Alioramus*, *Tarbosaurus* and *Tyrannosaurus* (Appendices A9.3; Table A9.3). Subrectangular interdental plates can however be seen in the ceratosaurs *Ceratosaurus*, *Noasaurus*, *Aucasaurus* and *Majungasaurus*, the megalosaurid *Megalosaurus*, the allosauroid *Shaochilong*, and the tyrannosauroid *Eotyrannus* (pers. obs.; Table A9.1). Variation in the ventral margin of the interdental plates does not seem to occur among mature individuals of the same species, with perhaps the exception of *Mapusaurus* in which the V-shaped of the interdental plates seems to be much more pronounced in MCF-PVPH-108.169 than in MCF-PVPH-108.115 (Coria and Currie 2006: fig. 2B–D). However, anterior interdental plates are badly preserved in MCF-PVPH-108.115 and the posterior ones show the distinct V-shaped condition (pers. obs.). A similar variation is also seen in the two species of *Carcharodontosaurus* (pers. obs.). In *C. iguidensis*, the ventral margin of the fused interdental plates are clearly V-shaped whereas in *C. saharicus*, although many of them are not intact, the plates tend to have a much straighter ventral margin. Surprisingly, in *Dilophosaurus wetherilli* the morphology of the interdental plates differ significantly between the youngest juvenile TMM 43646-1, the adult specimen UCMP 77270 and the immature individuals UCMP 37302 (holotype) and 37303 (paratype; Tykoski 2005: fig. 36; Appendices A9.3). In TMM 43646-1 and UCMP 77270, the plates are separated, subquadrangular to vertical subrectangular and the ventral margin is clearly V-shaped whereas the type specimens possess fused interdental plates that are horizontally rectangular with a straight ventral margin (Fig. A9.1). Whether fusion and variation in the interdental plates morphology may occur throughout ontogeny, such intraspecific variability of the interdental plates seems very unlikely and we therefore estimates that TMM 43646-1 and UCMP 77270 may represent a different taxon of *Dilophosaurus wetherilli*, as already suggested (Welles 1984; Appendices A9.3). We therefore consider the straight ventral margin

of the interdental plates as a potential synapomorphical character of the clade encompassing *Megalosaurus* + *Torvosaurus* (under ACCTRAN optimization), and interdental plates with V-shaped ventral margin are therefore the plesiomorphic condition in tetanurans and megalosauroids.

The morphology of the medial wall and the anteromedial process also differ between the American and European *Torvosaurus* (Figs. 9.5, 9.6K–L). BYU-VP 9122 displays a protruding ridge corresponding to the anterior part of the medial shelf (Fig. 9.5L). It extends from the posterodorsal part of the anteromedial process and gets flared to the level of alveolus 4. This ridge is absent from ML 1100 where only a low and wide anteroposteriorly oriented convexity corresponding to the anterior part of the medial shelf is observable (Fig. 9.5K). The medial shelf of the jugal ramus is more prominent in *T. tanneri* than in ML 1100 but the latter displays a low crest centrally positioned on the medial shelf, a feature absent in BYU-VP 9122. The ventral ridge of the anteromedial process also extends more anterior than the dorsal one, and only to the level of the second alveolus in BYU-VP 9122. On the other hand, the two main ridges of the anteromedial process of ML 1100 get flared at the same level posteriorly. In Megalosauroidea, this condition is shared with *Marshosaurus*, *Piatnitzkysaurus*, *Eustreptospondylus*, *Afrovenator* and *Megalosaurus* whereas in *Duriavenator* and *Dubreuillosaurus* the dorsal ridge of the anteromedial process extends further posteriorly than the ventral one (pers. obs.). Likewise, the groove delimited by the two ridges of the anteromedial process is notably wider in BYU-VP 9122 than in ML 1100. Furthermore, the posterior nutrient foramina are conspicuously larger in BYU-VP 9122 and, in this specimen, the anterior rim of the maxillary body is more inclined posteriorly, the anterior part of the ventral margin smoothly curves dorsally, and the parabolic outline of the antorbital fenestra is ventrodorsally wider. Again, it is difficult to know whether these differences between the American and European specimens exist inter- or intraspecifically, but some of them can certainly be considered as intraspecific variations.

As noted, some anatomical differences can be observed between ML 1100 and BYU-VP 9122, mostly in the morphology of the medial shelf and interdental plates. The presence of fused interdental plates forming a wall coinciding with the lateral wall of the maxilla is an autapomorphical character of ML 1100 among megalosauroids and, to our knowledge, this feature does not vary intraspecifically. Likewise, the protruding ridge posterior to the anteromedial process of BYU-VP 9122 seems to be an autapomorphy of *Torvosaurus tanneri* among non-coelurosaurs theropods, and the absence of this feature in ML 1100 supports its affiliation to a different taxon. Finally, the geographical context of the European specimen of *Torvosaurus*, which seems to have been isolated on the Iberian Meseta in the Kimmeridgian (Mateus et al. 2014), favors this option, and we therefore refer the Portuguese specimen to a new species of *Torvosaurus*, *Torvosaurus gurneyi*.

Torvosaurus gurneyi provides additional information on the maxilla anatomy of *Torvosaurus*. The dorsal margin of the ascending ramus is smoothly convex and the anterodorsal rim of the ascending ramus makes a step at two thirds of the process so that the ventral part of the ascending ramus tapers posteriorly. There is a small convexity on the dorsal margin of the jugal ramus, at two

thirds of it, where the lacrimal articulates with the maxilla medially. Likewise, the lacrimal articulation of the maxilla corresponds to a deep slit within the jugal ramus. The presence of a neurovascular opening penetrating the maxilla on the dorsomedial margin of the jugal ramus, at the level of the eighth alveolus, can also be noted and represents an autapomorphy for the taxon *Torvosaurus*. This opening is also present in BYU-VP 9122 but not well visible due to crushing so that Britt (Britt 1991) did not mention it.

Size and Paleogeographical Implications

With a minimum length of 612 mm, the maxilla of *Torvosaurus gurneyi* pertains to a very large individual positioned at the apex of the food chain in the Late Jurassic ecosystem of Iberia. The maxilla occupies 52% (*Allosaurus*) to 61% (*Yangchuanosaurus*) of the skull length in the largest avetheropods belonging to the clades of Ceratosauria, Megalosauroidea, Allosauroidea and Tyrannosauroidea, 53% being the proportion of the maxilla in the closely related basal tetanurans *Sciurumimus* and *Monolophosaurus*. Following this tendency, we can estimate the skull length of *Torvosaurus gurneyi* (ML 1100) to approximately 115 cm (Fig. 9.4B), lower than what was proposed by Mateus et al. (Mateus et al. 2006). *Torvosaurus* was therefore not competing in size with the largest theropod *Tyrannosaurus* (maxilla length of ~750 mm in CMNH 9380), *Carcharodontosaurus* (> 710 mm in SGM Din-1) or *Giganotosaurus* (> 680 mm in MUCPv-CH-1) but likely had a similar size than the tyrannosaurids *Daspletosaurus*, *Gorgosaurus* and *Tarbosaurus* (Therrien and Henderson 2007) from the Cretaceous. Nonetheless, with a body length of around 10 meters (Fig. 9.4A) and a weight of approximately 4 to 5 tons (estimations based on Therrien and Henderson 2007), *Torvosaurus gurneyi* represents the largest theropod from the Lourinhã Formation of Portugal, one of the largest land predators of the Jurassic, and the largest terrestrial predator discovered in Europe hitherto.

Torvosaurus occurrences are restricted to the Late Jurassic of Morrison and Lourinhã Formations, in United States and Portugal, respectively. The Portuguese form, *T. gurneyi*, is Late Kimmeridgian in age based on strontium and biostratigraphy (Ribeiro and Mateus 2012). The holotype specimen of *T. tanneri* is from Dry Mesa (Brushy Basin Member) which has been placed in the Late Kimmeridgian (Smith et al. 2010: p. 1466), but the isotopic dates are still within the Early Tithonian according to the new chronostratigraphic dates of ICS International Commission on Stratigraphy (http://www.stratigraphy.org) for the Late Jurassic.

The closest relative of the genus *Torvosaurus* is likely to be the European Bathonian *Megalosaurus* (Benson 2010*a*; Carrano et al. 2012), therefore the lineage leading to the genus likely originated during or around the Bathonian. At this time, the proto-Atlantic sea was well formed as demonstrated by ammonites and other sea fauna in the Portuguese west margin since the Early Jurassic. Therefore, the North American/European passage was already limited for terrestrial vertebrates well before the cladogenesis of *Megalosaurus*/*Torvosaurus* or *T. tanneri*/*T. gurneyi*. However, as suggested by Mateus et al. (2014), the passage of *Torvosaurus* and other genera between

North America and the Iberian Meseta may have happened during the temporary short-duration regional uplift around the Callovian/Oxfordian transition (ca. 163.5 Ma) that created the temporary opportunity of land gateways in the proto-Atlantic. The isolation of the Iberian block after that temporary uplift led to an important vicariance during nearly 10 My until the occurrence of many Laurasian taxa such as *Torvosaurus* in the Late Kimmeridgian. This pattern of occurrences shared by Morrison and Lourinhã Formations is also corroborated with the presence of other common genera, *Allosaurus*, *Ceratosaurus*, *Stegosaurus*, *Dryosaurus*, and related sister-taxa. This timing of vicariance also explains why the two regions have vertebrate faunas that are generically similar but specifically different. Finally, the true oceanization, with oceanic crust, of that section of North-Atlantic started during the Early Cretaceous.

Other Occurrences of *Torvosaurus* in Portugal

Cranial bones—The anterior part of a right maxilla (ALT-SHN.116; Fig. 9.11) discovered in the Lourinhã Formation of Praia da Corva (Torres Vedras) was described and referred to the taxon *Torvosaurus* sp. by Malafaia et al. (2008). The fragment of maxilla consists of an incomplete portion of the antorbital body and the anteroventral part of the ascending ramus (Malafaia et al. 2008). The anterior part of the anterior ramus as well as the posterior portion of the antorbital body are missing, and both alveolar and dorsal margins of the antorbital body are strongly damaged. In lateral view, the anteriormost part of the lateral antorbital fossa has been preserved and is delimited by the antorbital ridge that bounds a depression filled with sediment laterally (Malafaia et al. 2008). Two large maxillary alveolar foramina and one medium alveolar foramen are present at the level of what we interpret to be the fourth alveolus, just dorsal to the ventral margin of the maxilla (Fig. 9.11A). Only one small maxillary circumfenestra foramen seems to be preserved dorsal to the posteriormost alveolar foramen. As noted by Malafaia et al. (2008), the lateral surface of the maxilla is smooth rather than rugose. In medial view, only the posterior part of the anteromedial process is preserved and displays two parallel ridges running longitudinally on the medial side of the process (Fig. 9.11B). The groove delimited by these two ridges is broad and shallow. The interdental plates are not well-preserved but are tall and clearly fused, and their surface seems to be striated by parallel grooves running ventrodorsally. The medial shelf is ventrodorsally broad but poorly protuberant, and its main axis is oriented posteroventrally. The nutrient groove is visible but not clearly marked, and two large nutrient foramina, likely of the second and fourth alveoli, are present at the level of this groove. Dorsomedially, the nasal contact is broad and not visible laterally (Malafaia et al. 2008). An unerupted tooth can be seen throughout a small fracture and its mesial carina bears around 10 denticles per 5 mm (Malafaia et al. 2008).

This fragment of maxilla was assigned to *Torvosaurus* sp. by Malafaia et al. (2008) based on the absence of a maxillary fenestra between the antorbital fenestra and the nasal contact, and the shape and position of the antorbital ridge bounding the antorbital fenestra anteroventrally

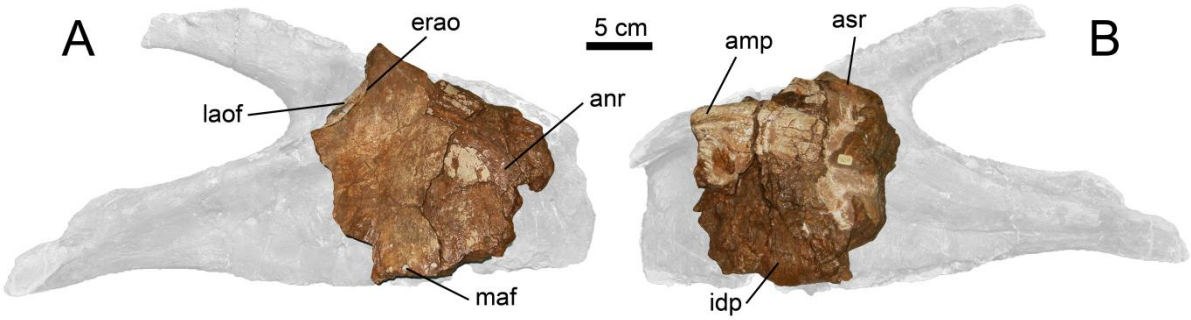

FIGURE 9.11. Incomplete maxilla of *Torvosaurus gurneyi* (ALT-SHN.116; courtesy of Elisabete Malafaia). **A–B**, Anterior portion of a right maxilla in **A**, lateral; and **B**, medial view. **Abbreviations**: **amp**, anteromedial process; **anr**, anterior ramus; **asr**, ascending ramus; **erao**, external rim of antorbital fossa; **idp**, interdental plates; **laof**, lateral antorbital fossa; **maf**, maxillary alveolar foramina.

(Malafaia et al. 2008). We agree with the assignment of this fragment to *Torvosaurus* but for different reasons. The presence (or absence) of a maxillary fenestra/fossa cannot be determined due to the fact that most of the anterior corner of the lateral antorbital fossa and the posteroventral portion of the ascending ramus are not preserved. The maxillary sinus are always located in this area in all basal theropods, including *Torvosaurus*, and the presence of a maxillary fenestra cannot therefore be ruled out. In fact, the shallow maxillary fossa diagnostic of *Torvosaurus tanneri* (Britt 1991) is not preserved in ALT-SHN.116, and what has been interpreted as the anteriormost rim of the antorbital fenestra by Malafaia et al. (2008: fig. 2B1) is, in fact, a diagnostic ridge located on the anteriormost corner of the lateral antorbital fossa (pers. obs.). Likewise, an antorbital ridge forming a lateral rim that bounds a recess within the anteriormost corner of the lateral antorbital fossa is a feature shared by a few basal theropods such as *Ceratosaurus*, *Torvosaurus*, *Afrovenator* and *Dubreuillosaurus* (pers. obs.). As correctly noticed by Malafaia et al. (2008), an antorbital ridge located just below the antorbital fenestra in the anteroventral part of the lateral antorbital fossa is indeed present in *Torvosaurus*, but equally shared by abelisaurids, *Monolophosaurus* and *Eustreptospondylus* (pers. obs.). However, the rim of the antorbital fenestra is not preserved in ALT-SHN.116, and the position of the antorbital ridge relative to the antorbital fenestra cannot therefore be used as a diagnostic feature.

Nonetheless, this fragment of maxilla includes several important features that support affinities with the genus *Torvosaurus*. ALT-SHN.116 belongs to tetanurans given the presence of a moderately (or strongly) elongated anterior ramus, to Megalosauria or Allosauria (as proposed by Carrano et al. 2012) due to the position of the anteromedial process, immediately ventral to the dorsal surface of the anterior ramus (Carrano et al. 2012), to the clade including *Torvosaurus* and *Megalosaurus* because of the tall interdental plates, and to *Torvosaurus* by the presence of fully fused interdental plates (Carrano et al. 2012) and a prominent anteroposteriorly oriented ridge (different from the antorbital ridge) in the anteriormost corner of the lateral antorbital fossa, an autapomorphy of *Torvosaurus* (pers. obs.). ALT-SHN.116 can furthermore be assigned to the new taxon *Torvosaurus*

gurneyi by the presence of interdental plates extending to the same level than the lateral wall, the straight ventral margin of interdental plates (absence of V-shaped interdental plates), two longitudinal ridges of the anteromedial process that get flared at the same level posteriorly, and the absence of a prominent ridge posterior to the anteromedial process. ALT-SHN.116 can therefore be referred to *Torvosaurus gurneyi* with confidence.

A mesial tooth (ML 962; Chapter 4, Fig. 4.9) from the Early Tithonian of the Lourinhã Formation in Praia da Area Branca (Lourinhã) was recently identify to belong to *Torvosaurus tanneri* (Hendrickx and Mateus 2014*b*) based on size (CH >80 mm), crown elongation (CHR of 2.7), large denticles (~8 denticles per 5 mm on both carinae), outline of the cross-section (CBR of 0.64) and position and basal extension of the mesial carina (Hendrickx and Mateus 2014*b*: fig.9). Given the fact that ML 962 and *T. gurneyi* have close paleogeographical and stratigraphical distributions, we tentatively assign the tooth to the Portuguese species of *Torvosaurus*.

A large tooth (FUB PB Ther 1) discovered in the Late Kimmeridgian of the Lourinhã Formation (Sobral Member = Praia Azul Member *sensu* Hill 1989) in Porto das Barcas was ascribed to an indeterminate Carnosauria by Rauhut & Kriwet (Rauhut and Kriwet 1994) based on large size and interdenticular sulci. A discriminant analysis used by Smith et al. (2005) classified it as *Ceratosaurus* although the authors admitted that this analysis "cannot provide a genus-level classification for a tooth that came from a taxon for which there are no data in the standard" (Smith et al. 2005: p. 715). A better understanding of theropod dentition, as well as morphometric data collected in the dentition of *Torvosaurus*, allows us to confidently refer this lateral tooth to this taxon, and tentatively to *T. gurneyi* given the stratigraphic and geographic contexts. Indeed, FUB PB Ther 1 shares a combination of features only seen in *Torvosaurus* lateral teeth such as a large (CH = 80 mm) moderately labiolingually compressed (CBR of 0.53) crown bearing large and coarse denticles (6.5 denticles/5 mm on both carinae), well-developed interdenticular sulci, a clearly-visible braided enamel texture, and a mesial carina centrally positioned on the crown (not offset or twisted) and extending on the apical half of the crown. Large teeth of eight centimeters or more are only borne by ceratosaurids, non-coelurosaur tetanurans and tyrannosauroids, and lateral teeth with very large denticles (<8 denticles/5 mm) by Megalosauridae, Carcharodontosaurinae, and Tyrannosauridae (pers. obs.). Tyrannosaurid teeth are distinctly incrassate (CBR > 0.55), and the mesial carina of carcharodontosaurine and *Ceratosaurus* teeth either reaches the cervix or extend just above it (pers. obs.). Among Megalosauridae, large crowns with very well-developed interdenticular sulci and marked enamel texture are, to our knowledge, a combination of features only existing in *Torvosaurus*. Furthermore, the latter is the only megalosaurid theropod from the Late Jurassic of Portugal.

Postcranial bones—The distal portion of a right femur (ML 632; Fig. 9.12A–G) from Cadaval (Quinta do Gradil) has been briefly reported by Mateus et al. (2006) and tentatively assigned to *Torvosaurus* based on its large size. The femur preserves the distal diaphysis, which includes two partially damaged condyles, and a portion of the shaft is preserved to the proximal extension of the

mesiodistal crest. The bone is massive, the proximo-distal length of the distal portion measuring more than 370 mm (Table 9.5), and one can estimate the total length of the whole bone to around 1110 mm based on the length and proportion of the femur of *Megalosaurus bucklandii* (NHM 31806; Benson 2010*a*). The minimum circumference of the shaft is 370 mm at the level of the break and its transversal ratio (lateromedial width/anteroposterior width) is 1.44.

The shaft expands mediolaterally towards the distal diaphysis and gives rise to two condyles separated by the extensor groove anteriorly (Fig. 9.12A) and the flexor groove posteriorly (Fig. 9.12D). The medial condyle is anteroposteriorly longer than the lateral one and elliptical in outline in distal view (160 mm long by 80 mm wide at its midpoint; Table 9.5) with its long axis directed posterolaterally (Fig. 9.12G). Fragments of the laterodistal, mesiodistal and posterior surface of the medial condyle are missing so that it is not possible to know the proximal extension of the articulating surface posteriorly. This surface is, however, well-preserved anteriorly and extends further proximally than in the lateral condyle. The medial margin of the medial condyle corresponds to a planar surface bearing a shallow concavity centrally positioned on its distal most part. The medial margin of the diaphysis displays many shallow striations extending along 190 mm of the medial side of the femur posteriorly (Fig. 9.12E). The posterior margin of the medial condyle is strongly convex, forming a large protuberance delimiting the flexor groove medially. The latter is lateromedially large (40 mm width) and extends along 120 mm of the bone surface, keeping the same width proximo-distally. The floor of the flexor groove is flat and grooved on its medial part, and the larger sulcus penetrates the bone on the proximomedial corner of the flexor groove.

The lateral condyle is roughly D-shaped (100 mm anteroposterioly by 105 mm posteromedially to form the crista tibiofibularis in which most of the posterior portion is missing (Fig. 9.12B). The crista tibiofibularis corresponds to a large crest of 55 mm in width in its posteriormost part, and extends proximo-distally along 130 mm of the lateral surface of the femur. The crest tapers proximally and curves proximo-laterally so that the medial margin of the crista tibiofibularis is convex whereas the lateral surface is weakly concave. This surface is also deeply striated by radiating grooves converging proximally. The posterior margin of the lateral condyle is shallowly concave and weakly grooved, in contrast to its lateral and anterior surfaces which, together, form a wide convexity. The latter is covered by large, deep and well-developed parallel striations in which the longest extend along 65 mm of the bone. The largest and deepest grooves are located on the anterolateral margins of the lateral condyles and show a strong attachment of the disto-femoral muscles (Fig. 9.12B).

The anterodistal surface of the femur is deeply excavated by the extensor groove which is narrower and deeper than the flexor groove (Fig. 9.12A). The extensor groove corresponds to a shallow depression in its proximal part and a deep fossa more distally, having a width of 20 mm in its distalmost part. The anterior surface of the femur displays a massive medial distal crest with a can-shaped outline (or a reversed J) and extending from above the medial condyle along 190 mm of the shaft (Fig. 9.12A). The medial distal crest is poorly delimited laterally and bounded by a short

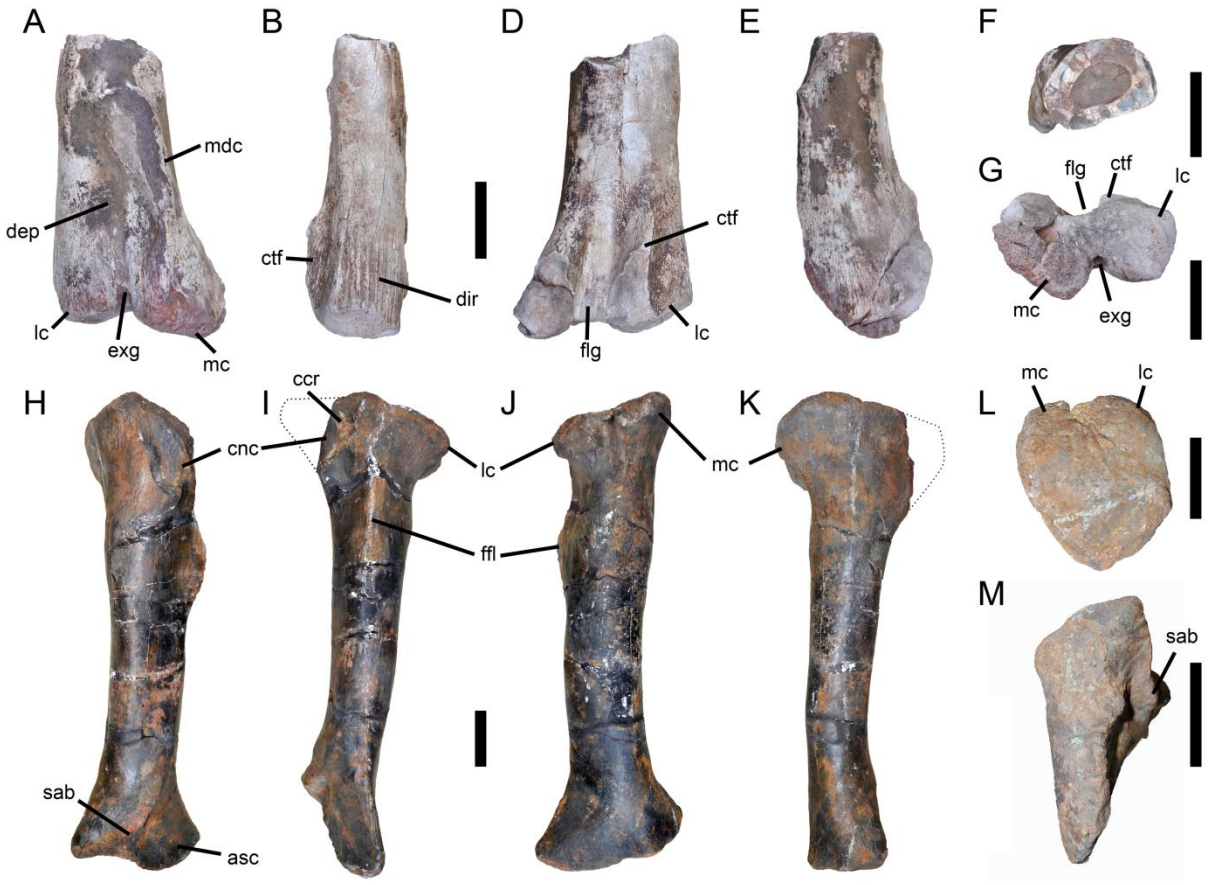

FIGURE 9.12. Femur and tibia of Megalosauridae from the Late Jurassic of Portugal. Distal portion of a left femur (ML 632) of a megalosaurid tentatively referred to *Torvosaurus gurneyi* in **A**, anterior; **B**, lateral; **C**, posterior; **D**, medial; **E**, proximal; and **F**, distal views. Incomplete left tibia (ML 430) of *Torvosaurus* sp. (and tentatively referred to *Torvosaurus gurneyi*), with reconstruction of missing part of cnemial crest, in **A**, anterior; **B**, lateral; **C**, posterior; **D**, medial; **E**, proximal; and **F**, distal views. **Abbreviations**: **asc**, contact with astragalus; **ccr**, cnemial crest ridge; **cnc**, basal part of cnemial crest; **ctf**, crista tibiofibularis; **dep**, anterodistal depression; **dir**, distal ridges; **exg**, extensor groove; **ffl**, fibular flange; **flg**, flexor groove; **lc**, lateral condyle; **mc**, medial condyle; **mdc**, mediodistal crest; **sab**, supracetabular buttress. Scale bars = 10 cm.

elevation of the shaft proximally. A wide depression, bounded by the medial distal crest laterally, occupies the central part of the anterodistal surface of the femur. This large concavity has a rugose surface proximo-laterally, just medial to the mediodistal crest, and merges with the extensor groove distally (Fig. 9.12A).

The femur is tentatively referred to *Torvosaurus gurneyi* based on its size, paleogeographic and stratigraphic distributions, and a combination of features only seen in derived megalosaurids. ML 632 belongs to Orionides based on the presence of an extensor groove anteriorly, to Megalosauroidea due to the absence of a large depression on the anterodistal surface of the mesial condyle of the distal diaphysis (the rugose depression that is seen on the anterior surface of the medial condyle in coelophysoids, ceratosaurs and allosauroids cannot be confused with the centrally positioned depression on the anterodistal surface of ML 632), and to Megalosauria based on the longitudinal and narrow tibiofibularis crest (Carrano et al. 2012). Among Megalosauria, the protuberant medial distal crest running on the anterodistal surface of the femur is absent in Spinosauridae and some

TABLE 9.5. Measurements of limb bones tentatively referred to *Torvosaurus gurneyi*.

	Measurements (mm)
Femur (ML 632)	
Maximal length of distal portion	370
Minimal circumference	390
Maximal circumference	600
Anteroposterior diameter of distal diaphysis	110
Lateromedial diameter of distal diaphysis	235
Tibia (ML 430)	
Maximum length	820
Minimum circumference	385
Circumference at the level of the fibular crest	470
Fibular crest length	140
Anteroposterior diameter of proximal diaphysis	110
Lateromedial diameter of proximal diaphysis	290
Anteroposterior diameter of distal diaphysis	240
Lateromedial diameter of distal diaphysis	180

megalosaurids such as *Eustreptospondylus* and *Leshansaurus*. It is poorly developed in *Megalosaurus* (Benson 2010*a*), and only well-developed and protuberant in the femur TATE 0012 (Siegwarth et al. 1997: fig. 16B), a specimen of large megalosaurid of the Morrison Formation (Siegwarth et al. 1997) referred to *Torvosaurus tanneri* (Carrano et al. 2012). Furthermore, the distal diaphysis bears large and deep striations on its anterior, lateral and medial surface, a condition shared with TATE 0012 (Jensen 1985: fig. 16). As for TATE 0012, ML 632 is tentatively assigned to *Torvosaurus*. It however differs from TATE 0012 by a long axis of the medial condyle directed posterolateral in distal view (a condition shared with Baryonychinae; Carrano et al. 2012), a much deeper extensor groove, and a long axis of the medial distal crest directed proximo-distally (like in *Megalosaurus*) rather than proximo-laterally (Siegwarth et al. 1997: fig. 16B). In fact, a posterolateral orientation of the mediodistal condyle as well as a prominent medial distal crest curving proximo-laterally and delimiting a large concavity medially, seem to be two autapomorphies of ML 632 among Megalosauridae (pers. obs.). The femur comes from a different site than the type specimen of *T. gurneyi* and cannot be assigned to this taxon as the latter did not preserve any limb bones. Nevertheless, given the geographic and stratigraphic position of ML 632 and the numerous features shared with TATE 0012, it is likely that the bone belongs to *Torvosaurus gurneyi*. However, this referral has to be regarded as tentative, pending detailed description and analysis of TATE 0012.

With a lateromedial width of 235 mm for the distal diaphysis and an approximate length of 1100 mm for the femur (Table 9.5), ML 632 pertains to an animal of around 3 to 4 tons, for a body length of around 10 meters (estimations based on Therrien and Henderson 2007 and Christiansen and Fariña 2004).

A large sized left tibia (ML 430; Fig. 9.12H–M) from Casal do Bicho was the first bone unequivocally ascribed to *Torvosaurus* in Portugal (Mateus and Antunes 2000*a*). The tibia has a unique character combination that allows a generic identification, as recognized since Britt (Britt 1991), including the high diaphyseal perimeter/length ratio, low astragalar contact surface and short

and round cnemial crest. With a total length of 820 mm and a minimum circumference of 385 mm (Table 9.5), ML 430 pertained to a slightly bigger animal than BYU VP 2016 (length of 725 mm, min. circ. of 327 Britt 1991) that should have had a body mass of around 1.6 to 1.7 tons for a body length of around 7 meters (estimation based on Therrien and Henderson 2007 and Christiansen and Fariña 2004). Given its paleogeographic and stratigraphic distributions and a combination of features only existing in *Torvosaurus* tibiae, ML 430 is tentatively referred to *Torvosaurus gurneyi*.

Tracks—Only in rare cases in vertebrate paleontology, one can establish a connection between a track and a genus of species of trackmaker. However, in Portugal there is no other theropod that could rival *Torvosaurus* in size, and produce such large tracks as the ones from the beds of Porto Dinheiro (ML 2035; Mateus and Milàn 2010: fig. 9). Being 79 cm long and 60 cm wide, ML 2035 is one of the largest theropod tracks known from the Jurassic. These tracks found at the base of Sobral Member of Lourinhã Formation are dated as Late Kimmeridgian, just as the *Torvosaurus* bones from Portugal. Nevertheless, due to the absence of clear pedal autapomorphies that are recognizable in *Torvosaurus* tracks, the trackmaker of ML 2035 is tentatively referred to *Torvosaurus*.

Embryos—Araújo et al. (2013) recently reported an incomplete right maxilla and dentary and three centra of a single or several *Torvosaurus* embryos (ML 1188; see next chapter Fig. 10.3) from the Late Kimmeridgian Lourinhã Formation (Sobral Member that overlies Porto Novo-Amoreira Member from which *T. gurneyi* type comes from) of Porto das Barcas. The cranial and postcranial elements are referred to *Torvosaurus* sp. based on the absence of both medial antorbital fossa and medial pneumatic complex on the maxilla, tall interdental plates and blunt anterior margin of the dentary, low angle of the ascending ramus and the tongue-shaped posterior extremity of the jugal ramus (Araújo et al. 2013). As highlighted by these authors, some notable difference can however be observed in the maxilla of the embryonic and adult specimens of *Torvosaurus*, the most important being a short anterior ramus, unserrated crowns and unfused interdental plates, all interpreted as ontogenetic features. There are four preserved interdental plates for the maxilla (*contra* Araújo et al. 2013), a first one situated between the first and second maxillary teeth, a second incomplete one between teeth 2 and 3 (Araújo et al. 2013: fig. 9D), a badly preserved one between teeth 3 and 5 and an isolated one below the maxilla (pers. obs.). As observed in the interdental plates of the dentary, and similar to the condition seen in the adult *Torvosaurus gurneyi* and *Megalosaurus bucklandi*, the maxillary interdental plates are tall and all have a vertical rectangular outline. The lateral wall of the maxilla is not visible in the embryos ML 1188 and it is unknown whether the interdental plates were extending at the same level than the ventral margin of the lateral wall like in *T. gurneyi*. Nonetheless, the ventral margins of the plates are straight and do not display the 'V-shaped' condition shared by the American taxon. Likewise, there is no apparent ridge posterior to the anteromedial process, as seen in *T. tanneri*. Nevertheless, these features may all vary ontogenetically in theropods so that ML 1188 is tentatively assign to the species *T. gurneyi* based on paleogeographical and stratigraphical contexts only.

Chapter 10: Late Jurassic *Torvosaurus* clutch with embryos from Portugal and the ontogeny of the maxilla in non-avian theropods.

Published in ***Scientific Reports*** (IP 5.078):
Araújo, R., Castanhinha, R., Martins, R. M. S., Mateus, O., Hendrickx, C., Beckmann, F., Schell, N. and Alves, L. C. 2013. Filling the gaps of dinosaur eggshell phylogeny: Late Jurassic theropod clutch with embryos from Portugal. *Scientific Reports* 3 (1924): 1–8.

Abstract

Theropod embryos are rare in the fossil record and are only represented by avetheropods, thus missing the basal theropod representatives. A theropod clutch containing several crushed eggs and embryonic material from the Lourinhã Formation (early Tithonian) of Portugal is here reported. The skeletal material, which includes an incomplete maxilla, the anterior portion of a dentary, and several vertebrae, are assigned to the megalosaurid *Torvosaurus* based on a moderately elongated anterior ramus bearing six maxillary teeth, tong-shaped posterior extremity of the jugal ramus, elongated maxillary crowns, and the absence of an internal antorbital fenestra. This clutch represents the first associated eggshells and embryos of megalosauroids, and the basalmost theropod embryos found to date. Investigation on the maxilla ontogeny in basal tetanurans based on the maxilla of *Torvosaurus* and *Lourinhanosaurus* embryos, as well as an isolated maxilla assigned to an *Allosaurus* hatchling, suggests that crown denticles, elongation of the anterior ramus, and fusion of interdental plates appear at a posthatchling stage. On the other hand, maxillary pneumaticity, including maxillary and promaxillary fenestrae, are already present at an embryonic stage in non-avian theropods.

Introduction

Embryonic material has been reported in all three major dinosaur clades: theropods, sauropodomorphs, and ornithischians (Brusatte 2012). Nevertheless, the discovery of fossilized eggs containing embryos is rare (e.g., Carpenter et al. 1996; Grellet-Tinner et al. 2006, 2011), and embryonic material remains to be found for several dinosaur clades such as pachycephalosaurs, stegosaurs, and ankylosaurs. Theropod embryos are the best represented among dinosaurs hitherto, yet all embryos have been assigned to avetheropods, and most of them belong to relatively derived non-avian theropod lineages. Skeletal material of non-avian theropod embryos have been reported in the basal avetheropod (metriacanthosaurid/coelurosaur?; see Benson 2010*a*; Carrano et al. 2012) *Lourinhanosaurus antunesi* from the Upper Jurassic of Portugal (Mateus et al. 1998, 2001), a therizinosauroid from the Upper Cretaceous of China (Kundrát et al. 2008), two indeterminate oviraptorids from the Upper Cretaceous of Mongolia (Norell et al. 1994, 2001*b*; Weishampel et al. 2008), and two troodontids, namely *Byronosaurus* (Bever and Norell 2009) and *Troodon* (Varricchio et al. 2002) from the Upper Cretaceous of Mongolia and Montana, respectively (Fig. 10.1). Three theropod eggs containing embryos from the Lower Cretaceous of Thailand have also been described

and likely belong to a small derived theropod of unknown affinities (Buffetaut et al. 2005*a*; Fernandez et al. 2012).

Although cranial material including a maxilla has been preserved in most theropod embryos (i.e., *Lourinhanosaurus*, therizinosauroid, oviraptorid, *Byronosaurus*, *Troodon*), the development of the maxilla at an early stage is still poorly known in basal theropods, and investigation on the maxilla ontogeny mostly relied on cranial material belonging to hatchling and immature specimens. Rauhut and Fechner (2005) were the first to comprehensively discussed the early development of the craniofacial region of an allosauroid based on an isolated maxilla referred to an hatchling *Allosaurus*. The maxilla ontogeny has also been investigated in compsognathids and troodontids based on well-preserved skulls belonging to a *Scipionyx* hatchling (Dal Sasso and Maganuco 2011) and a *Byronosaurus* embryo (Bever and Norell 2009), respectively. Nonetheless, a full picture of the maxilla ontogeny in non-avian theropods based on several specimens remains to be done.

This paper aims to provide a thorough description of recently discovered cranial and postcranial material of theropod embryos (ML 1188) from the Lourinhã Formation of Portugal. Given the presence of a maxilla among the embryonic material, and based on the examination of the maxilla of several embryonic, hatchling and juvenile specimens of theropods, the early stage of the development of the maxillary region was also examined in non-avian theropods.

Material

ML 1188 is a non-delimited, strongly crushed nest containing a large number (>500) of eggshell fragments associated with randomly distributed and generally poorly preserved embryonic bones (Fig. 10.2). The clutch is 65 cm in diameter and was discovered in August 2005 by Dutch collector and amateur paleontologist Aart Walen at the beach of Porto das Barcas (Lourinhã). Excavation using specific techniques (see Araújo et al. 2009) and preparation of the specimen was carried on from 2005 to 2009 by a team of professionals and amateurs from the Museu of Lourinhã. The nest was found in a grey mudstone layer of the Praia Azul Member (see Introduction, Fig. 1.15). The latter is situated in the middle of the Lourinhã Formation and dated to the latest Kimmeridgian–early Tithonian (Mateus et al. 2014). The Lourinhã Formation is well-known for its rich Mesozoic vertebrate fauna, one of the richest in Europe (Mateus 2006). The region has already provided material of theropods (*Ceratosaurus*, *Torvosaurus*, *Allosaurus*, *Lourinhanosaurus*), sauropods (*Lusotitan*, *Zby*, *Lourinhasaurus*), ornithischians (*Dracopelta*, *Miragaia*, *Draconyx*), crocodiles, turtles, and dinosaur and pterosaur tracks (e.g., Lapparent and Zbyszewski 1957; Dantas et al. 1998; Mateus and Telles Antunes 2001; Antunes and Mateus 2003; Mateus 2006; Mateus et al. 2006, 2009; Mannion et al. 2013). It is, however, particularly famous for its dinosaur eggs with embryos (Antunes and Mateus 2003). In 1993, several nests preserving a large number of embryonic bones were discovered less than ten kilometres away from the area where ML 1188 was collected (Mateus et al. 1997, 1998). The clutches, referred to as the Paimogo nest, was found in a penecontemporaneous iron-rich mudstone

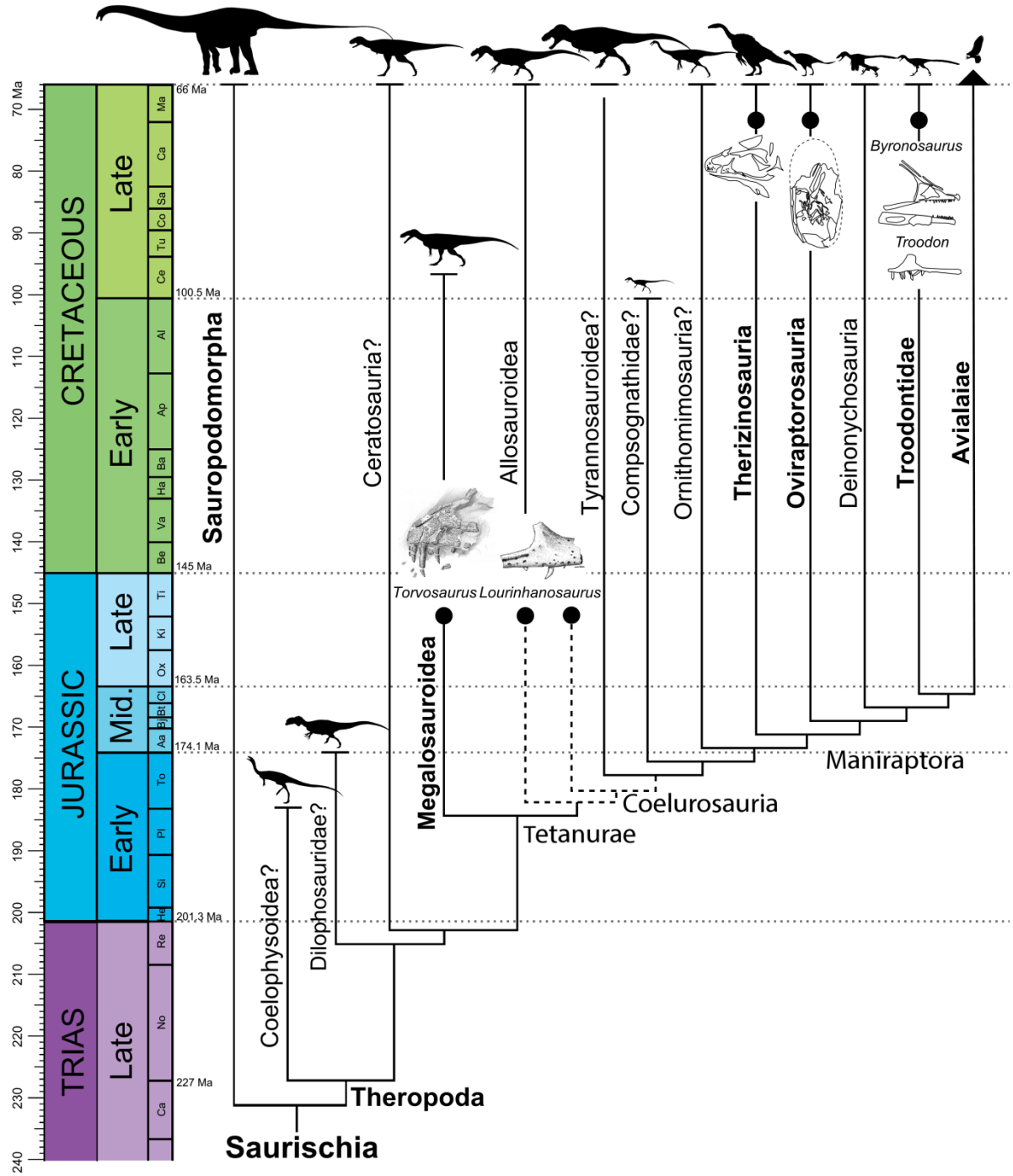

FIGURE 10.1. The known record of embryos and associated eggshell structure explicit the phylogenetic position of the *Torvosaurus* embryos (ML1188), which occupies a gap at the base of the Theropoda cladogram. Dashed lines indicate the dubious position of *Lourinhanosaurus* as an Allosauroidea or as a basal Coelurosauria in the light of the most recent analysis (see Chapter 1). Major clades in bold indicate the presence of associated embryo-eggshell fossils. For silhouette attribution, see Appendices A1.1.

layer, and the embryos were assigned to the basal avetheropod *Lourinhanosaurus antunesi* (Mateus et al. 2001).

Although individual boundaries between the eggs are difficult to distinguish (Fig. 10.2A), the clutch (ML 1188) contains more than three eggs. The latter were crushed by post-burial compression and were ovideposited *en masse* given that all eggshells are accumulated in one single layer. Cranial

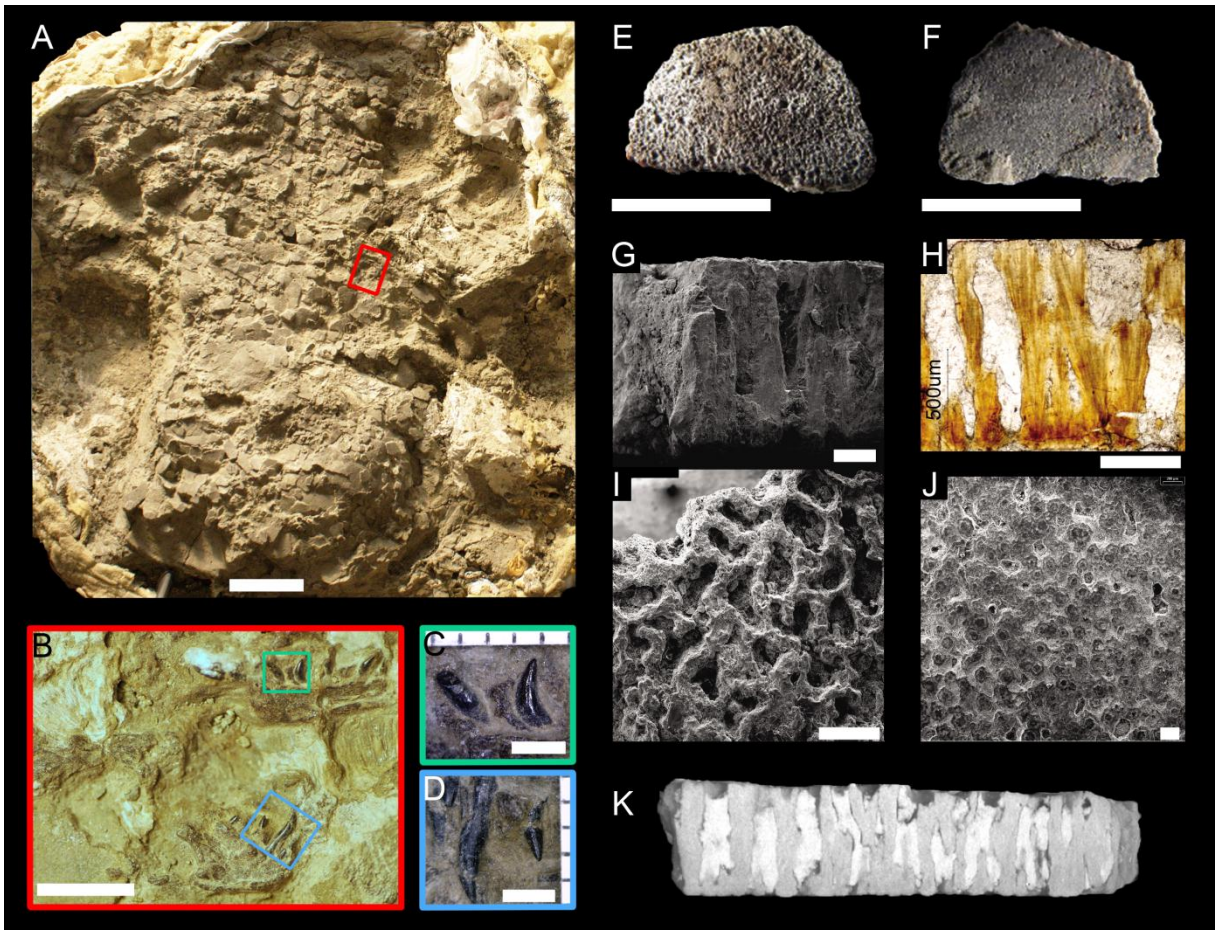

FIGURE 10.2. *Torvosaurus* eggs, eggshells, and embryos from the Lourinhã Formation (early Tithonian) of Portugal. **A**, Clutch of *Torvosaurus* eggs (ML1188); **B**, Dentary and maxilla in medial view of *Torvosaurus* sp.; **C**, Second and third dentary teeth, separated by interdental plate in medial view; **D**, Second and third maxillary teeth, separated by interdental plate in medial view; **E**, Eggshell external morphology in lateral view; **F**, Eggshell internal morphology in medial view; **G**, SEM micrograph of the eggshell radial section showing acicular crystals and a single layer; **H**, Eggshell radial section; **I**, Eggshell external morphology SEM photograph; **J**, Eggshell internal morphology SEM photograph; **K**, SR-µCT image of an eggshell radial section. Scale bars 10 cm (A), 5 mm (B), 2 mm (C, D), 500 µm (E, F, H, I), 200 µm (G, J).

and postcranial material associated with the clutch (Fig. 10.2B–D) were found mixed with and often beneath eggshells so that they unquestionably pertain to embryos belonging to a single individual that laid the eggs. Embryonic material consists of several isolated teeth, a partial maxilla preserving four teeth, a dentary bearing four teeth and one disarticulated tooth near by the bone, three articulated vertebrae, and many unidentifiable bones (Fig. 10.3).

Description

Maxilla—The medial side of the incomplete right maxilla is on the surface of the clutch (Fig. 10.4). The partial maxilla comprises the anterior ramus, an incomplete ascending ramus, and the jugal ramus whose the posterior part is separated from the rest of the maxillary bone. The main body has a Subtriangular anterior ramus projecting moderately anteriorly from the antorbital fenestra (Fig. 10.4C). The anterior margin of the anterior ramus is convex and forms a right angle with the ventral

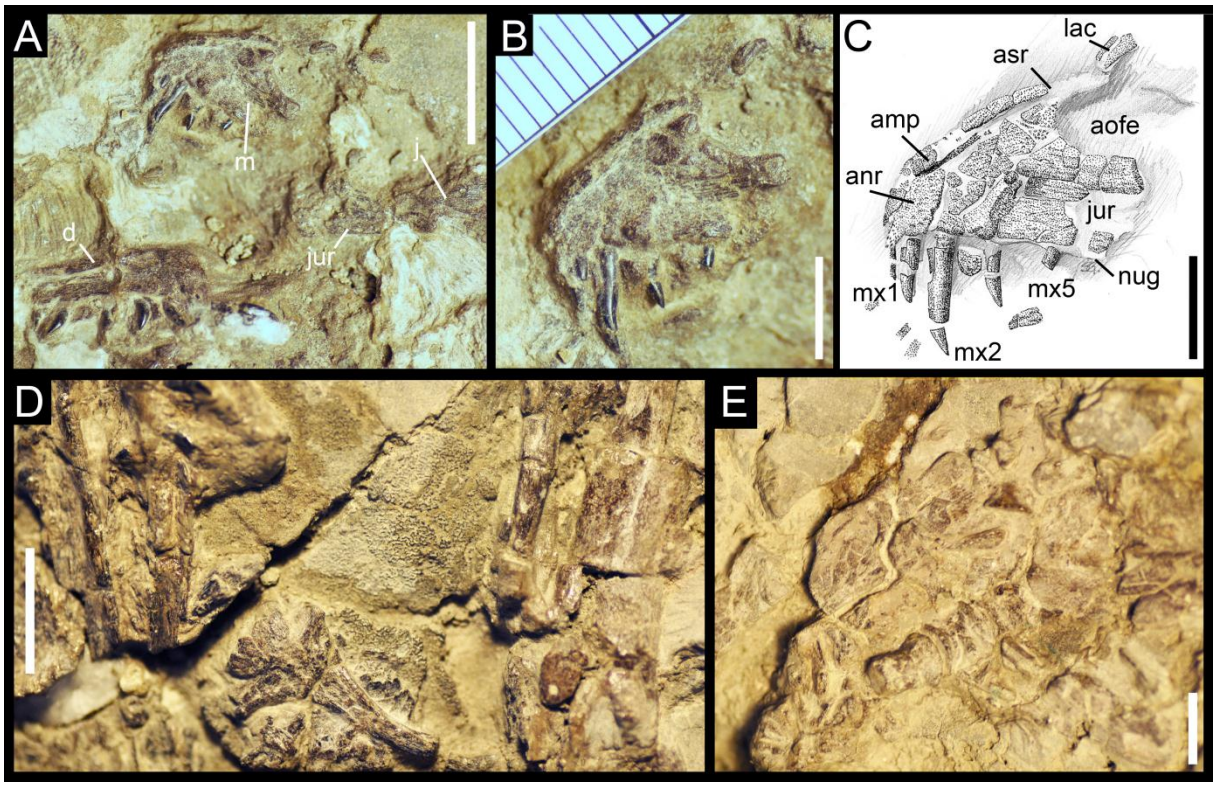

FIGURE 10.3. Embryonic material of *Torvosaurus* sp. (ML 1188). **A**, Right maxilla, dentary and jugal in medial view; **B-C**, Close up on the anterior part of the right maxilla in medial view; **D**, Indeterminate postcranial bones; and **E**, Articulated vertebrae. **Abbreviations**: **amp**, anteromedial process; **anr**, anterior ramus; **aofe,** antorbital fenestra; **j**, jugal; **jur**, jugal ramus; **lac**, lacrimal contact of the maxilla; **m**, maxilla; **mx1**, first maxillary tooth; **mx2**, second maxillary tooth; **mx5**, fifth maxillary tooth; **nug**, nutrient groove. Scale: 10 mm (A, D, E), 5 mm (B–D).

margin of the maxilla. The anterodorsal margin of the anterior ramus is slightly concave and confluent with the ascending ramus, thus, there is no step delimiting the two structures. The jugal ramus is broken in two pieces, the posterior part lying one centimetre below the maxilla. Once digitally restored, the jugal ramus is elongated with some parts in the middle of the ramus missing. The dorsal margin of the horizontal ramus, corresponding to the ventral rim of the antorbital fenestra, is straight and subparallel

to the tooth row in its anterior part whereas the posterior part of the ramus has a sigmoid outline and slopes ventroposteriorly towards the jugal contact of the ramus.

The posteriormost part of the jugal ramus corresponds to a tongue-like process delimited by a small concavity on its dorsal margin and the main axis passing through this posterior process is oriented ventroposteriorly (Fig. 10.4A). The ventral margin of the jugal ramus is straight and parallel to the anteroposterior axis of the jugal ramus. Little information can be extracted from the jugal but the contact between the jugal and maxilla extends one third on the lateral side of the jugal ramus. The articular surface for the lacrimal is visible on the anteromedial part of the jugal, at the level of the posterior process of the jugal ramus. The lacrimal was also contacting the maxilla along one third of the jugal ramus. The ascending ramus is thick at its base and tapers dorsally. The anteroventral margin

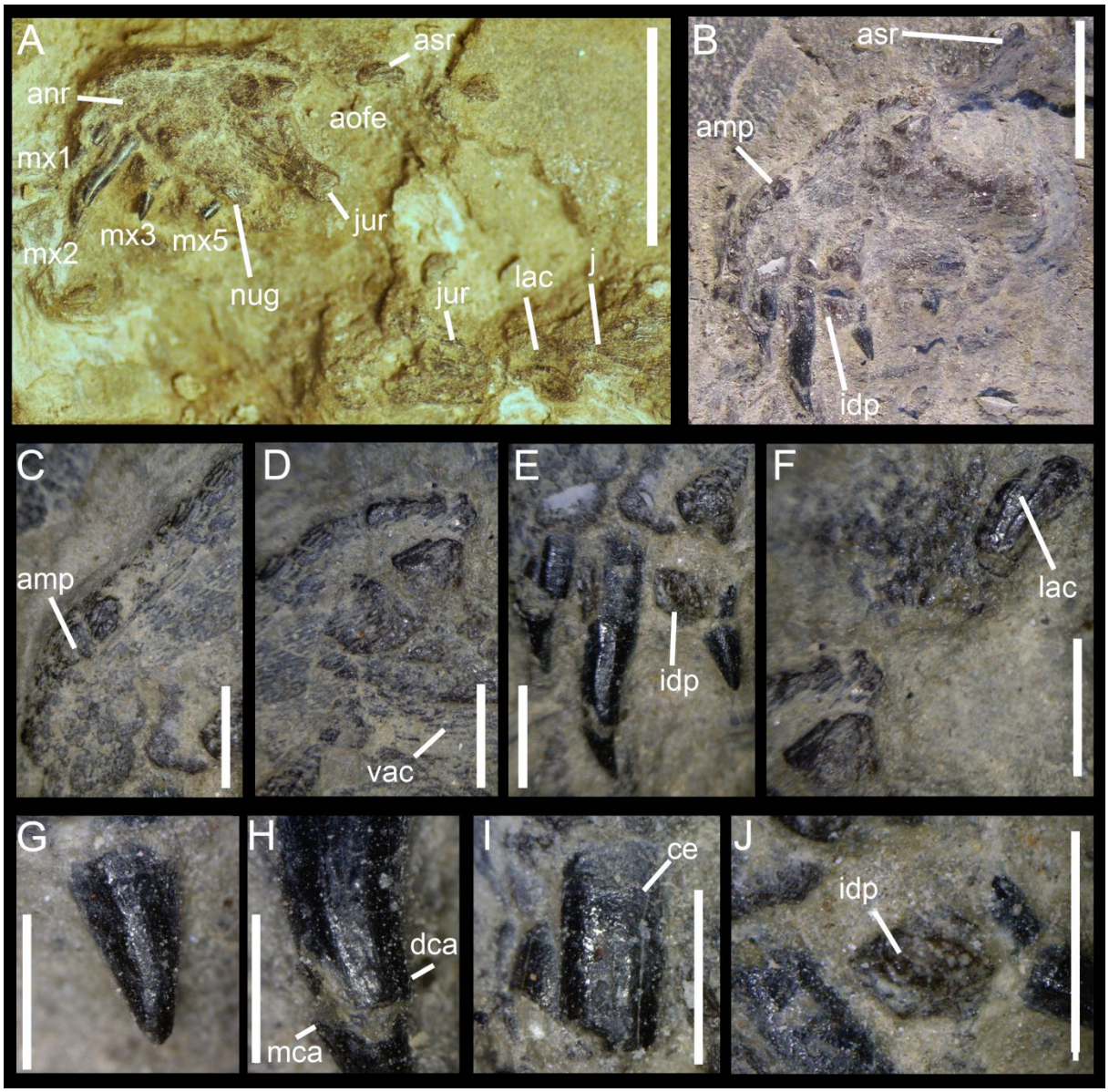

FIGURE 10.4. **A**, Incomplete right maxilla of *Torvosaurus* sp. embryo (ML 1188) in articulation with the jugal in medial view; **B**, Anterior part of maxilla (jugal ramus not included); **C**, Anterior part of anterior ramus; **D**, Ventral part of ascending ramus; **E**, Anteriormost maxillary teeth; **F**, Dorsal part of ascending ramus; **G.** Apex of the crown of first maxillary tooth; **H**, Medial part of the crown of second maxillary tooth; **I**, Roots of first and second maxillary teeth; **J**, Interdental plate in between second and fourth maxillary tooth. **Abbreviations**: **amp**, anteromedial process; **anr**, anterior ramus; **aofe,** antorbital fenestra; **asr**, ascending ramus; **ce**, cervix; **dca**, distal carina; **idp**, interdental plate; **j**, jugal; **jur**, jugal ramus; **lac**, lacrimal contact of the maxilla; **mca**, mesial carina; **mx1**,first maxillary tooth; **mx2**, second maxillary tooth; **mx4**, fourth maxillary tooth; **nug**, nutrient groove; **vac**, vascular canals. Scale: 10 mm (A); 5 mm (B and C); 2 mm (D to G, K); 1 mm (H to J).

of the ascending ramus is convex, almost forming an obtuse angle, and the main axis passing through this process angles 28° with the ventral margin of the maxilla. Two elongated and subparallel ridges are present at the dorsal tip of the ascending ramus and delimit the lacrimal contact of the maxilla (Fig. 10.4F). The antorbital fenestra is parabolic in outline. There is no medial antorbital fossa. The medial surface of the maxilla bears parallel stripes corresponding to vascular canals (Fig. 10.4D). On the main body of the maxilla, these canals are anteroposterioly aligned but, on the ascending ramus they are

parallel to its main axis. However, the canals are more irregularly placed on the anterior part of the ascending ramus. Although the anteromedial surface of the maxilla is damaged, the surface is composed of solid bone, thus no maxillary and promaxillary fenestrae, maxillary antrum and pneumatic excavations are present. At the level of the teeth roots, only one isolated interdental plate has been preserved in between the second and fourth maxillary teeth. This suggests that the interdental plates of the maxilla were unfused (Fig. 10.4E, J). The plate is subrectangular, and its surface is punctuated. The anteromedial process has been crushed at the level of the anterior margin of the maxilla. The anteromedial process is located on the anterodorsal border of the anterior ramus, being a long finger-like projection parallel to the anterodorsal rim of the anterior ramus.

Four maxillary teeth are preserved on the anterior part of the maxillary body and there is an isolated tooth near the maxilla and two more loose teeth located some distance away from this bone. The maxillary tooth count is difficult to estimate because the posterior part of the main body bears no teeth. However, on the anterior ramus of the maxilla there were probably five teeth. All teeth are strongly elongated (Crown Height Ratio > 2.5), their apices are sharply acute and both mesial and distal carinae lack denticles (Fig. 10.4G–I). The mesial and distal profiles are recurved distally and the crowns are subconical. Nevertheless, the lingual surface of the crowns is mostly flattened except the basal surface which is concave. This concave area on the medial surface of the crown received the erupting tooth of the maxilla. The enamel surface of the teeth is smooth and does not bear transverse undulations, enamel wrinkling, longitudinal grooves, or wear facets.

Dentary—A right dentary is lying on its lateral side just below the anterior part of the maxilla (Fig. 10.5). The bone is almost complete and only part of the bone posterior to the opening of the Meckelian fossa is missing. It is fractured in the middle by a transversal fissure. The dentary is massive, with a ventrodorsally large medial wall remaining the same width along the bone. Four fully erupted teeth are present on the dentary, but only two of them, the third and seventh dentary teeth, are complete. A fifth isolated tooth, most likely the first dentary tooth, is lying beside the anteroventral corner of the dentary. Based on the positions of the remaining teeth, we estimate a total of eight alveoli on this portion of the dentary. The interdental plates are unfused (Fig. 10.5E–F). Three interdental plates are preserved in between the first and second dentary teeth, the second and third, and the fifth and seventh teeth. Variation occurs in the shape of the interdental plates along the tooth row as the two anteriormost plates form a vertical rectangle whereas the third one, more posteriorly located, has a horizontal rectangular outline. The mandibular symphysis is short, smooth and forms an elongated triangle on the anteriormost part of the dentary. The paradental groove separating the medial wall of the dentary with the interdental plates is large, gently concave and seems to have been open in between those two structures. The Meckelian groove is well visible on the dentary, running along the bone just above the dorsal margin of the dentary (Fig. 10.5C–D). This longitudinal groove is filled with sediment and seems to extend anteriorly until the third dentary teeth. The step between the Meckelian groove and Meckelian fossa occurs at the level of the seventh dentary tooth. Only the

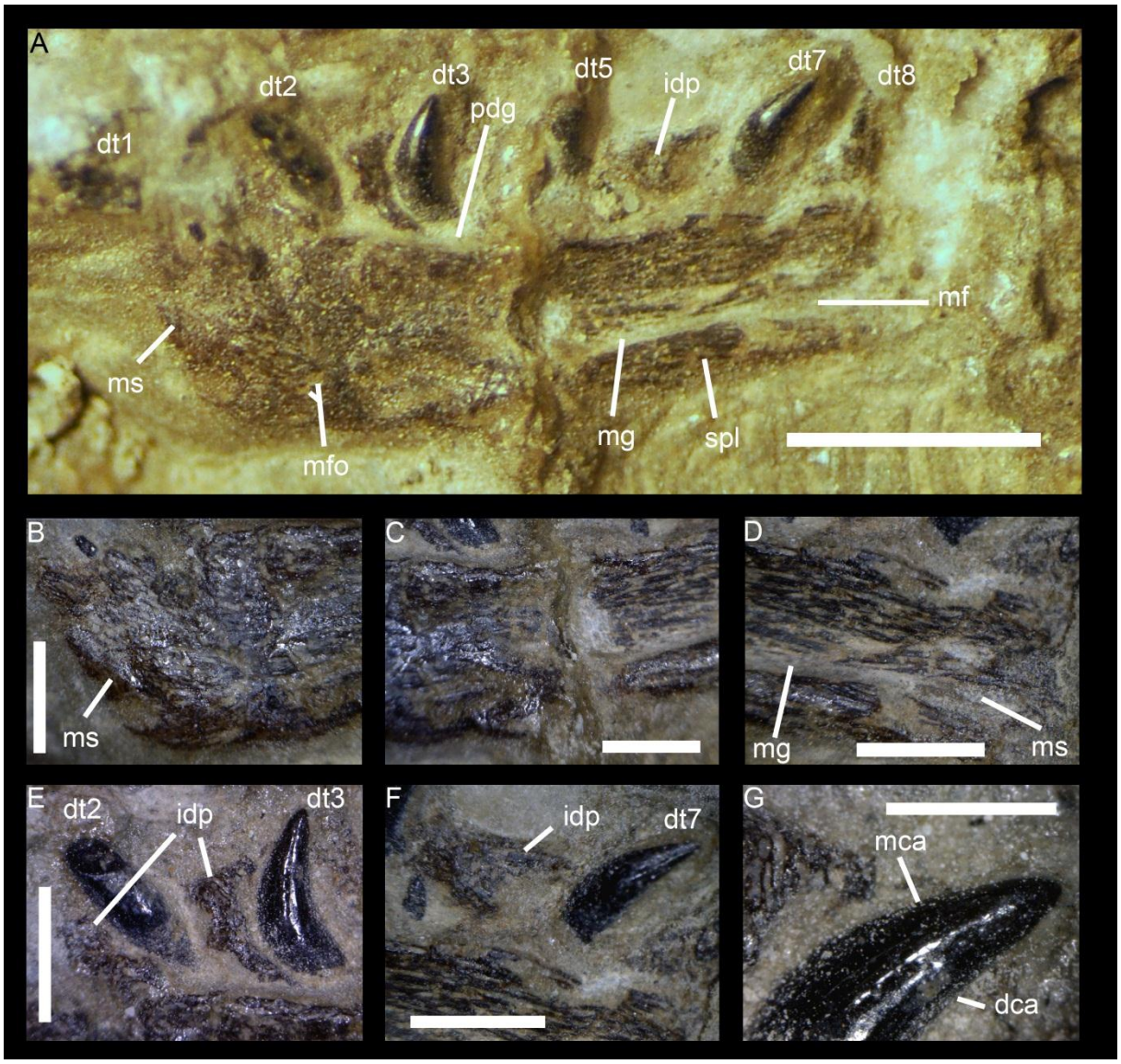

FIGURE 10.5. **A**, Incomplete right dentary of *Torvosaurus* sp. embryo (ML 1188) in medial view; **B**, Anterior part of medial wall of dentary; **C**, Mesial part of medial wall of dentary; **D**, Posterior part of medial wall of dentary; **E**, Anteriormost interdental plates and dentary teeth; **F**, Mesial interdental plate and tooth; **G**, Apex of the crown of seventh dentary tooth. **Abbreviations**: **dca**, distal carina; **dt1**, first dentary tooth; **dt2**, second dentary tooth; **dt3**, third dentary tooth; **dt5**, fifth dentary tooth; **dt7**, seventh dentary tooth; **dt8**, height dentary tooth; **idp**, interdental plate; mca, mesial carina; **mf**, Meckelian fossa; **mef**, Meckelian foramina; **mg**, Meckelian groove; **ms**, mandibular symphysis; **pdg**, paradental groove; **spl**, splenial contact. Scale: 5 mm (A); 2 mm (B to F), 1 mm (G).

anterior part of the Meckelian fossa is preserved. A large concavity at the level of the third dentary tooth is present just above the ventral margin of the dentary and includes a short anteroposterioly oriented ridge. Two small grooves located in between this concavity and the mandibular symphysis are interpreted to be Meckelian foramina (Fig. 10.5A). The anteroventral margin of the dentary is rounded and almost subrectangular, with the inflexion point close to the level of the anteriormost point of the dentary. The anteroventral margin is unexpanded with no articular brace forming a chin, and the ventral margin appears to have been fairly straight. The teeth of the dentary are unserrated and the crowns are pointed, strongly apicobasally elongated and recurved posteriorly, and devoid of enamel

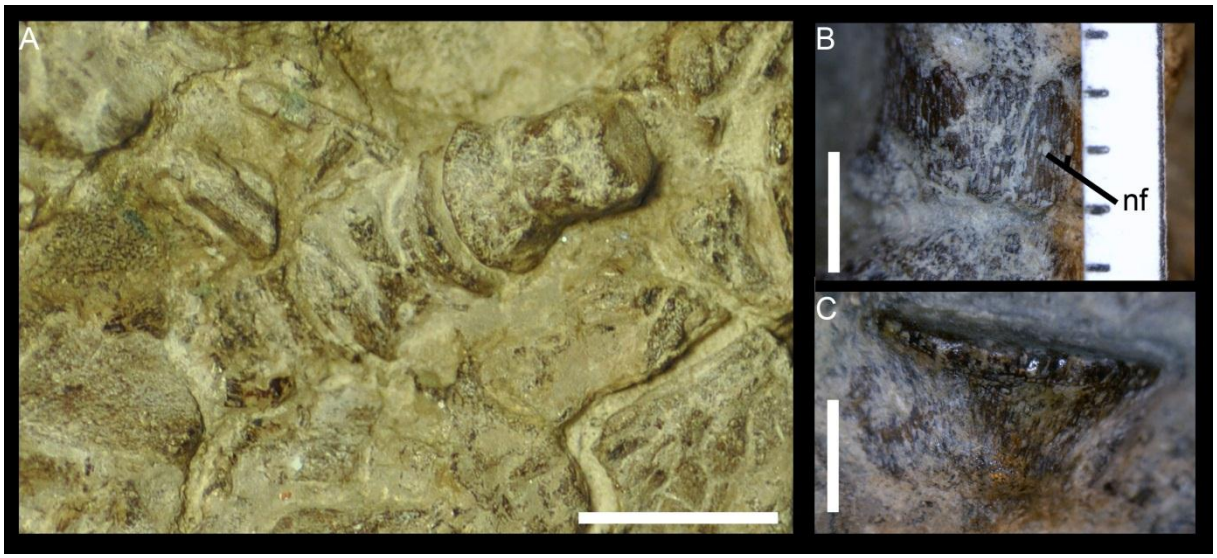

FIGURE 10.6. **A**, Set of three amphiplatyan centra in articulation in dorsal view; **B**, Mesial part of the first centrum in dorsal view; **C**, Fourth isolated centrum in dorsal view. **Abbreviation**: **nf**, neurovascular foramina. Scale: 10 mm (A), 2 mm (B, C).

structure (Fig. 10.5E–G).

Vertebrae—Three articulated amphiplatyan vertebrae were fully prepared (Fig. 10.6). The ventral part of the centrum bears two paired pits identified as neurovascular foramina (Fig. 10.6B). The anterior and posterior faces of the vertebrae show evenly distributed small pits, consistent with an early developmental stage (Salgado et al. 2005). The centrum faces are expanded (~38% relative to the mid-centrum) and bear confluent striations, whereas in the median part of the centrum, the striations are parallel. Although other fragmentary bones are present and scattered within the clutch none are identifiable, thus, no further information could be obtained.

Method and Results

In order to assess the phylogenetic affinities of ML 1188, we performed a cladistic analysis by using a recently published data matrix focusing on the relationships of basal tetanurans (Carrano et al. 2012). This data matrix includes 351 characters coded in 59 operational taxonomic units and two outgroup taxa (*Eoraptor* and *Herrerasaurus*). We coded ML 1188, as well as the maxilla of the embryonic specimens of *Lourinhanosaurus* (ML 565 122 & ML 565 125; Mateus et al. 1998, 2001) and *Allosaurus* (MG 27804 = IPFUB Gui Th 4 of Rauhut and Fechner 2005). Two characters were modified and twelve additional characters were created in order to take into consideration the morphological variations of the medial view of the maxilla (Appendices A10.1–A10.2).

TNT v1.1 (Goloboff et al. 2008) was employed to search for most-parsimonious trees (MPTs). As a first step, the matrix was analysed under the ‘New Technology search’ with the ‘driven search’ option, TreeDrift, Tree Fusing, Ratchet, and Sectorial Searches selected with default parameters, and stabilizing the consensus twice with a factor of 75. The generated trees were then analysed under traditional TBR (tree bisection and reconnection) branch (Goloboff et al. 2008). Bremer support

(Bremer 1994) and Reduced Cladistic Consensus Support Trees (Wilkinson 1994) were calculated with TNT by saving 10,000 suboptimal trees up to 10 steps longer than the MPTs. The consistency and retention indexes as well as the Bremer and relative Bremer supports were calculated using the 'stats' and the 'aquickie' commands, respectively.

Cladistic analysis of the data matrix using TNT v1.1 yielded 95 MPTs, length 1099, with a consistency index of 0.371 and a retention index of 0.632 for the resulting consensus tree (Fig. 10.7). The strict consensus tree did not resolve completely the clade of Tetanurae. However, the combinable components of the 96 MPTs recovered the clades of Spinosauridae, Megalosauridae, Piatnitzkysauridae and Allosauria (Fig. 10.7). Nevertheless, by using the 50% Majority rule consensus tree the Tetanurae phylogeny is fully resolved, retrieving the major clades of Megalosauroidea, Avetheropoda, Allosauroidea and Coelurosauria (Fig. 10.8). Most clades have low Bremer support except for Averostra, Neotheropoda, Coelophysoidea and Ceratosauria. Likewise, high Bootstrap values (>65) are found for Averostra, Neotheropoda, Coelophysoidea, Ceratosauria and Spinosauridae.

The majority rule consensus mirror to a large degree the topology obtained by Carrano et al. (2012). However, a major difference occurs in the topology of the Megalosauridae where *Duriavenator* is recovered among the Afrovenatorinae, and the sister-clade of Megalosaurinae encompasses six taxa such as *Dubreuillosaurus* and *Eustreptospondylus*. This change can be explained by the inclusion of additional maxillary and dentary characters. Indeed, among five synapomorphies, the clade of Megalosaurinae is defined by one synapomorphic characters of the maxilla, and one of the dentary: absence of a medial antorbital fossa in the maxilla (char. 352) and dentary tooth count, from the anteriormost part of the dentary, to the step between the Meckelian groove and the Meckelian fossa (char. 363). The absence of a medial antorbital fossa, as well as less than ten dentary teeth along the tooth row from the mandibular symphysis to the Meckelian fossa can indeed be observed in *Torvosaurus*, *Eustreptospondylus* and *Dubreuillosaurus*, but not in *Afrovenator* and *Duriavenator*.

In both analyses, ML 1188 was recovered with *Torvosaurus* among megalosaurine Megalosauroidea (Figs. 10.7–10.8). Although the comparison of the embryonic maxilla with the maxilla of *Torvosaurus* is not straightforward, the two bones, as well as the dentaries of both ML 1188 and *Torvosaurus*, share many features: anterior end of the junction between medial maxillary wall and paradental plates is inclined anteroventrally (Megalosauridae); strongly convergent ventral and dorsal margins of the jugal ramus of the maxilla (Megalosauridae); dentary, from the anteriormost point of the mandibular symphysis to the anteriormost point of the Meckelian fossa, bearing less than 10 teeth (Megalosaurinae); blunt anteroventral margin of the dentary (*Megalosaurus* + *Torvosaurus*); elongated (CHR > 2.5) maxillary teeth (*Megalosaurus* + *Torvosaurus*); unfused and tall (vertical subrectangular outline) anteriormost interdental plates of the dentary (*Megalosaurus* + *Torvosaurus*); maxilla lacking of promaxillary and maxillary fenestrae, as well as any pneumatic complex in medial view (*Torvosaurus*); broad tongue-like process of the posterior extremity of the jugal ramus (*Torvosaurus*); angle of the base of the ascending ramus with the ventral margin of the maxilla of less than 35°

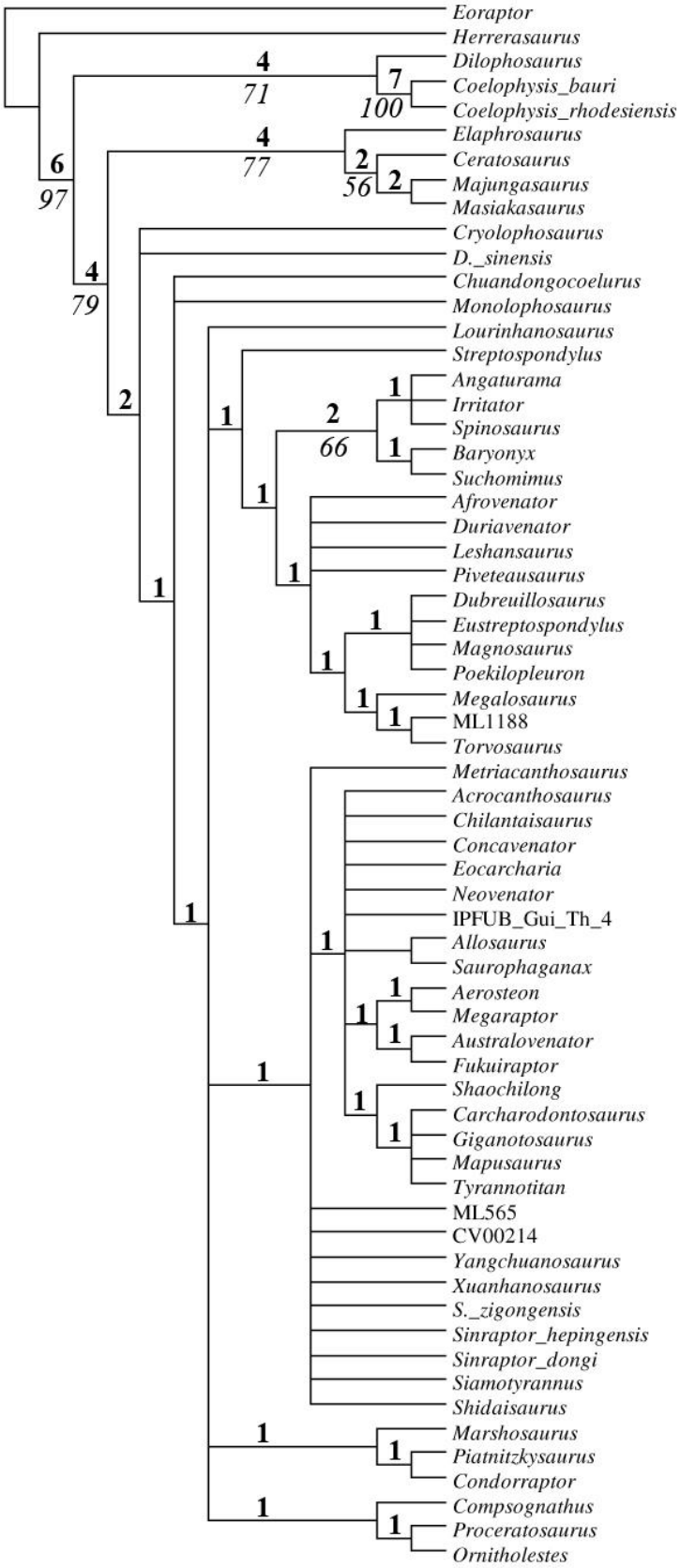

FIGURE 10.7. Strict consensus cladogram from 96 most parsimonious trees. Initial analysis used New Technology Search using TNT v.1.1 of a data matrix comprising 361 characters for two outgroup (*Eoraptor* and *Herrerasaurus*) and 62 non-avian theropod taxa. Tree length = 1094 steps; CI = 0.371; RI = 0.632. Bremer support values are in bold and above the stem. Bootstrap values, in italic, and unambiguous character support are below the stem of each clade.

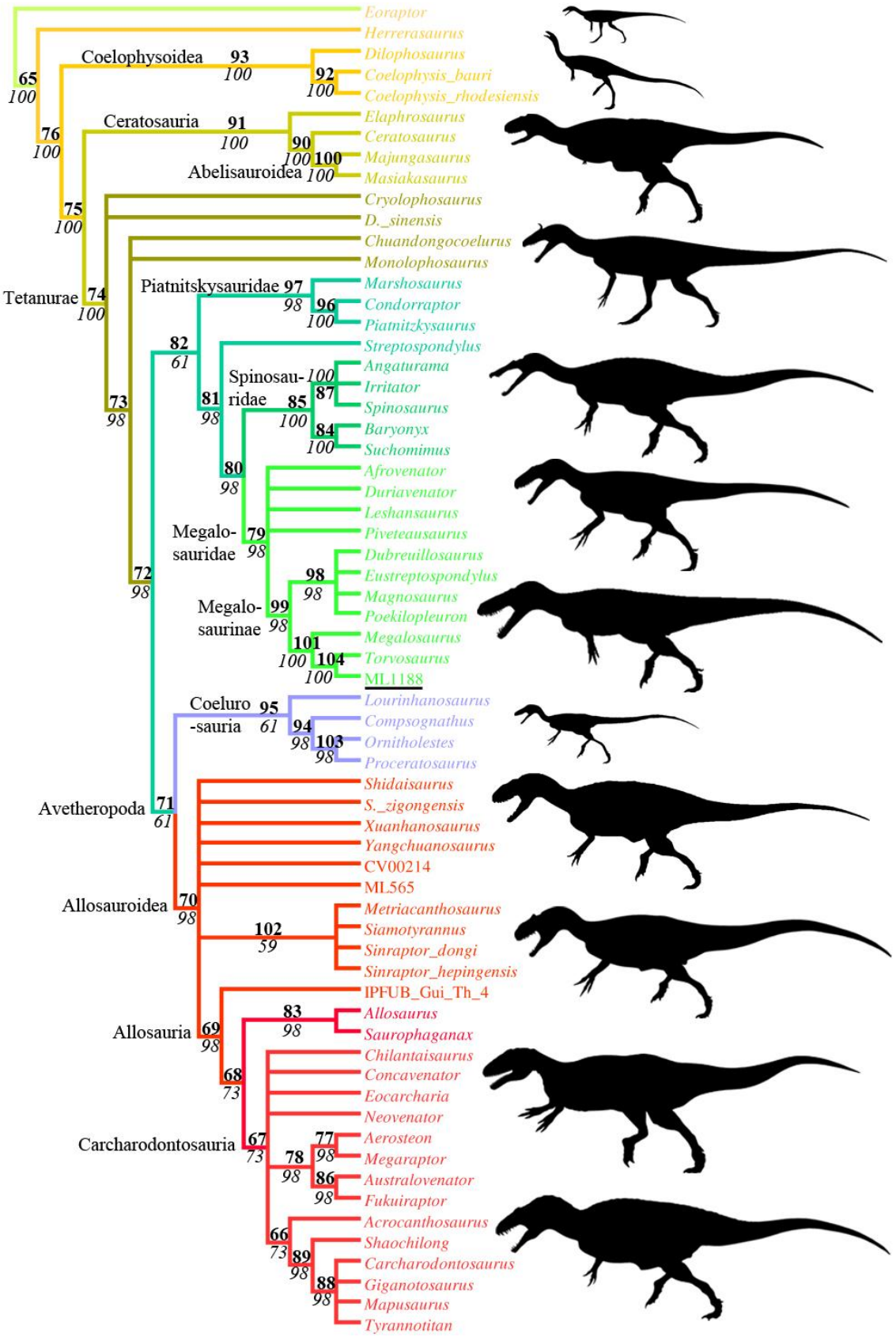

FIGURE 10.8. 50% Majority Rule cladogram from 96 most parsimonious trees. Initial analysis was a New Technology Search using TNT v.1.1 of a data matrix comprising 363 characters for two outgroup (*Eoraptor* and *Herrerasaurus*) and 62 non-avian theropod taxa. Tree length = 1094 steps; CI = 0.394; RI = 0.665. Clade number, in bold, and above the stem of each clade, is used in the synapomorphy list below. The percentage of clade occurrence is below each clade and in italic. For silhouette attribution, see Appendices A1.1.

(*Torvosaurus*). There are three main differences between the ML 1188 and *Torvosaurus* maxillae. (1) A short anterior ramus bearing less than 6 teeth. These may be ontogenetic and plesiomorphic features of *Torvosaurus* embryos that are present in the closely related taxon *Megalosaurus*. (2) Unfused maxillary interdental plates. Once again an ontogenetic and plesiomorphic feature present in the *Torvosaurus* embryo and the closely related taxon *Megalosaurus*. (3) Unserrated teeth which is an ontogenetic character visible in *Troodon* embryos as well.

The cranial material (maxilla and dentary) of *Lourinhanosaurus* embryo ML 565 was recovered among Allosauroidea in the strict consensus tree, and as a non allosaurian Allosauroidea in the 50% majority rule consensus (Figs. 10.7–10.8). The taxon *Lourinhanosaurus* and ML 565 were not recovered in the same clade. In some trees, *Lourinhanosaurus* and ML 565 are closely related when the embryo is recovered as the most basal member of the Allosauroidea and *Lourinhanosaurus* as the most basal member of the Coelurosauria. In some trees, *Lourinhanosaurus* is also found recovered as a basal allosauroid, whereas ML 565 is a member of Metriacanthosauridae. In fact, *Lourinhanosaurus* was recently found among coelurosaur theropod (Carrano et al. 2012), yet it was also formerly assigned to the metriacanthosaurid Allosauroidea (Benson 2010*a*; Benson et al. 2010). According to Carrano et al. (2012), only two steps are required to recover *Lourinhanosaurus* as a basal Allosauroidea or a basal Avetheropoda in their analysis. Since *Lourinhanosaurus* skull material is missing and does not allow any comparison with the skull material of the embryo, the position of ML 565 among basal Allosauroidea, or Sinraptoridae, is therefore not surprising. A single autapomorphy of *Lourinhanosaurus* holotype was used to assign ML 565 to this taxon: the medial condyle of the tibia is half the transverse width of the fibular condyle. However, the variation of this trait has not yet been studied through ontogeny.

The maxilla MG 27804 (= IPFUB Gui Th 4) described as an *Allosaurus* embryo (Rauhut and Fechner 2005) was recovered as the most basal taxon of Allosauria, and closely related to Allosauridae, in the Majority rule consensus tree (Figs. 10.7–10.8). In the strict consensus tree, it was recovered among the clade of Allosauria, sometimes being also found at the base of the clade of Carcharodontosauridae in some trees. MG 27804 was identified as belonging to Allosauridae by the presence of an excavation pneumatica in the ascending ramus and the lack of a greatly enlarged promaxillary fenestra (a condition present in Metriacanthosauridae), and to the genus *Allosaurus* by the apomorphically large maxillary fenestra and the presence of this taxon in the Late Jurassic of Portugal (Rauhut and Fechner 2005; Mateus et al. 2006; Malafaia et al. 2007, 2009). Nonetheless, a pneumatic fossa is also present in the basal carcharodontosaurids *Acrocanthosaurus atokensis* and *Eocarcharia dinops* (Carrano et al. 2012), yet the fossa is perforated by an accessory fenestra in these taxa (Sereno and Brusatte 2008; Eddy and Clarke 2011). In MG 27804, the ascending ramus of the maxilla is damaged and the perforation in the large pneumatic fossa is missing bone, therefore an accessory fenestra inside the pneumatic fossa of the ascending ramus cannot be excluded. Among Allosauroidea, a large maxillary fenestra is also present in the carcharodontosaurids *Eocarcharia*

dinops (Sereno and Brusatte 2008), *Acrocanthosaurus atokensis* (Eddy and Clarke 2011) and *Giganotosaurus carolinii* (MUCPv CH1). Moreover, MG 27804 shares several anatomical features with basal carcharodontosaurids that are absent in *Allosaurus* such as a promaxillary fenestra clearly visible in lateral view (char. 354) and an anteromedial process in which the most posterior point is situated on the anterior part of the anterior ramus (char. 356). Nevertheless, these features might be changing through ontogeny and the referral to *Allosaurus*, which is present in the Late Jurassic of Portugal, remains highly plausible.

Discussion

ML 1188 can be assigned to Theropoda due to the presence of strongly elongated, sharply pointed crowns with a distal curvature. Among non-theropod dinosaurs, this condition is only present in the basalmost sauropodomorph *Eoraptor* (Sereno et al. 2013). Nonetheless, some *Eoraptor* crowns are lanceolate and the maxillary teeth are not so elongated, contrarily to ML 1188. Among Theropoda, the antorbital tooth row indicates tetanuran relationships (Carrano et al. 2012) for ML 1188. An anteriorly inclined nutrient groove between the medial wall of the maxillary body and the interdental plate, as well as strongly convergent ventral and dorsal margins of the jugal ramus are also two synapomorphies for Megalosauridae (Appendices A10.3). We ascribe ML 1188 to Megalosaurinae based on the presence of fewer than ten dentary teeth, from the anteriormost point of the mandibular symphysis to the anteriormost point of the Meckelian fossa, as well as the absence of the internal antorbital fossa on the medial side of the maxilla.

The maxillary fenestra, promaxillary fenestra and pneumatic recesses appear early in ontogeny in the maxilla of Tetanurae embryos (Varricchio et al. 2002; Rauhut and Fechner 2005). The maxillary fenestra pierces the maxilla in most tetanurans (Witmer 1997*a*; Rauhut and Fechner 2005), but corresponds to a small opening located within the internal antorbital fossa in some basal tetanurans (Witmer 1997*a*; Benson 2010*a*), for example, *Duriavenator* and *Megalosaurus* (Fig. 10.9). However, as in ML 1188, an unfenestrated and unpneumatized maxilla lacking a medial-antorbital fossa is only present in a few megalosaurids (e.g., *Torvosaurus*, *Dubreuillosaurus*, see Appendices A10.1, Table A10.1). The embryonic remains of ML 1188 share three synapomorphies with both Megalosaurinae *Megalosaurus* and *Torvosaurus*: a blunt and unexpanded anteroventral margin of the dentary, very elongated maxillary crowns (Crown Height Ratio > 2.5) and tall and unfused anteriormost interdental plates of the dentary (Fig. 10.10). This embryo can be referred to the genus *Torvosaurus* due to the lack of pneumaticity posterior to the base of the ascending ramus, an angle of less than 35° in between the base of the ascending ramus and the ventral margin of the maxilla, and the tongue-shaped extremity of the jugal ramus of the maxilla. The maxilla of *Megalosaurus* displays two pneumatic excavations on the medial surface of the maxillary body, dorsal to the lingual bar and posterior to the ascending ramus in medial view (Benson 2010*a*). In addition, the angle in between the base of the ascending ramus and the alveolar margin of the maxilla exceeds 35° and the posterior extremity of the

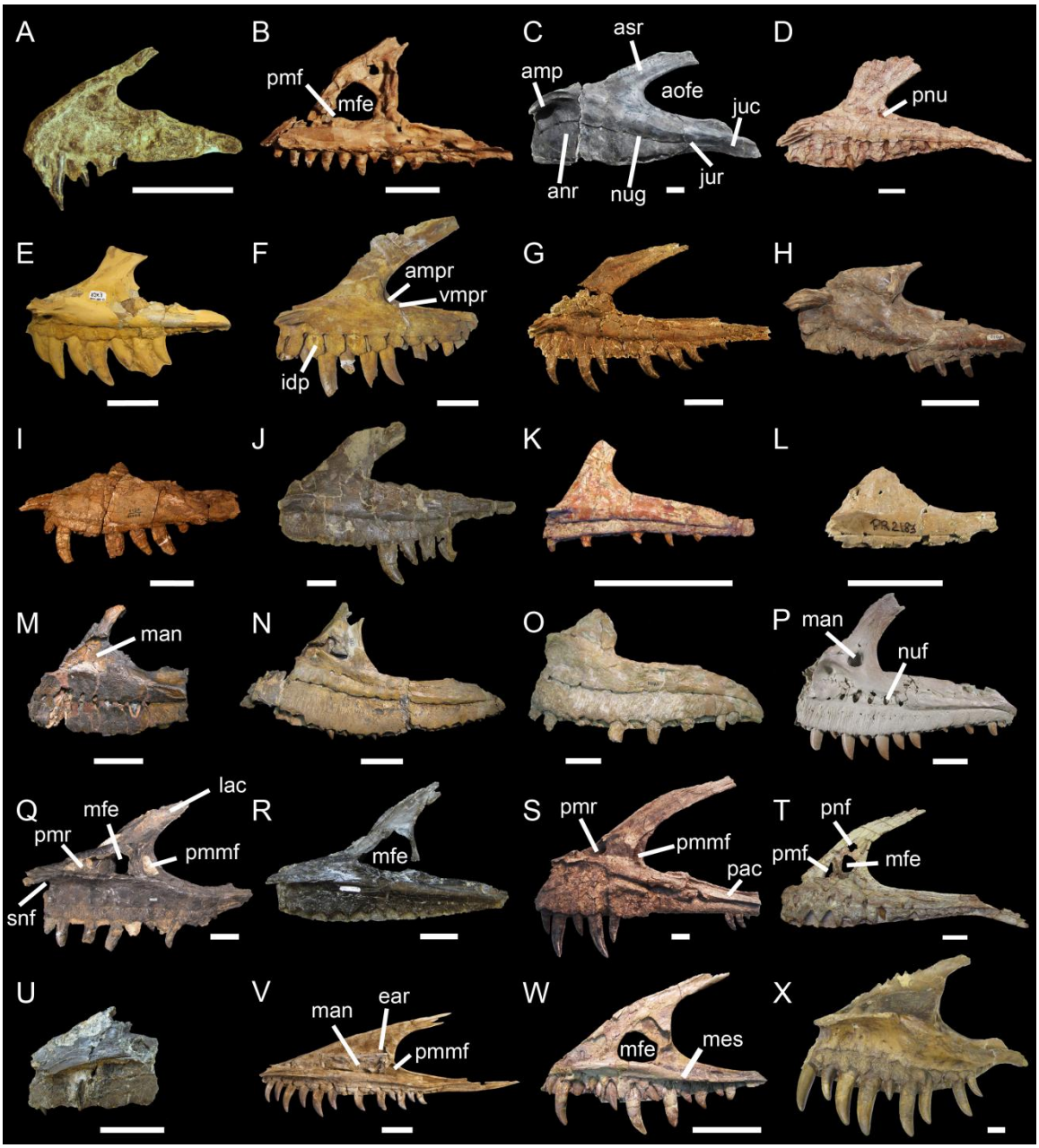

FIGURE 10.9. Maxillae of non-avian theropods in medial view. **A**, Embryo of *Torvosaurus* sp. **(**ML 1188, reconstructed); **B**, Hatchling of *Allosaurus* (MG 27804); **C**, *Torvosaurus tanneri* (ML1100); **D**, *Afrovenator abakensis* (MNN UBA1; courtesy of Juan Canale); **E**, *Dubreuillosaurus valesdunensis* (MNHN 1998-13); **F**, *Duriavenator hesperis* (NHM R.332); **G**, *Marshosaurus bicentesimus* (DINO 16455; courtesy of Matt Carrano); **H**, *Piatnitzkysaurus floresi* (PVL 4073; courtesy of Martín Ezcurra); **I**, *Dilophosaurus wetherilli* (UCMP 37303; courtesy of Martín Ezcurra); **J**, *Ceratosaurus magnicornis* (USNM 4735); **K**, *Noasaurus leali* (PVL 4061); **L**, *Masiakasaurus knopfleri* (FMNH PR 2183); **M**, *Kryptops palaios* (MNN GAD1−1); **N**, *Rugops primus* (MNN IGU1); **O**, *Indosuchus raptorius* (AMNH 1955); **P**, *Majungasaurus crenatissimus* (FMNH PR 2100); **Q**, *Allosaurus fragilis* (USNM 8335); **R**, *Neovenator salerii* (MIWG 6348); **S**, *Acrocanthosaurus atokensis* (NCSM 14345; courtesy of Drew Eddy); **T**, *Eocarcharia dinops* (MNN GAD2); **U**, *Eotyrannus lengi* (MIWG 1997.550); **V**, *Alioramus altai* (IGM 100-1844; courtesy of Mick Ellison ©AMNH); **W**, *Raptorex kriegsteini* (LH PV18); **X**, *Tyrannosaurus rex* (CMNH 9380). **Abbreviations**: **amp**, anteromedial process; **ampr**, anteromedial pneumatic recess; **anr**, anterior ramus; **aofe,** antorbital fenestra; **asr**, ascending ramus; **ear**, epiantral recess; **idp**, interdental plate; **juc**, jugal contact; **jur**, jugal ramus; **lac**, lacrimal contact; **mes**, medial shelf; **mfe**, maxillary fenestra; **man**, maxillary antrum; **nuf**, nutrient foramen; **nug**, nutrient groove; **pac**, palatal contact; **pmmf**, posteromedial maxillary fenestra; **pmf**, promaxillary fenestra; **pnf**, pneumatic fenestra; **snf**, subnarial foramen; **vmpr**, ventromedial pneumatic recess. Scale: 5 mm (A, B), 2 cm (L), 5 cm (C to K; M to X).

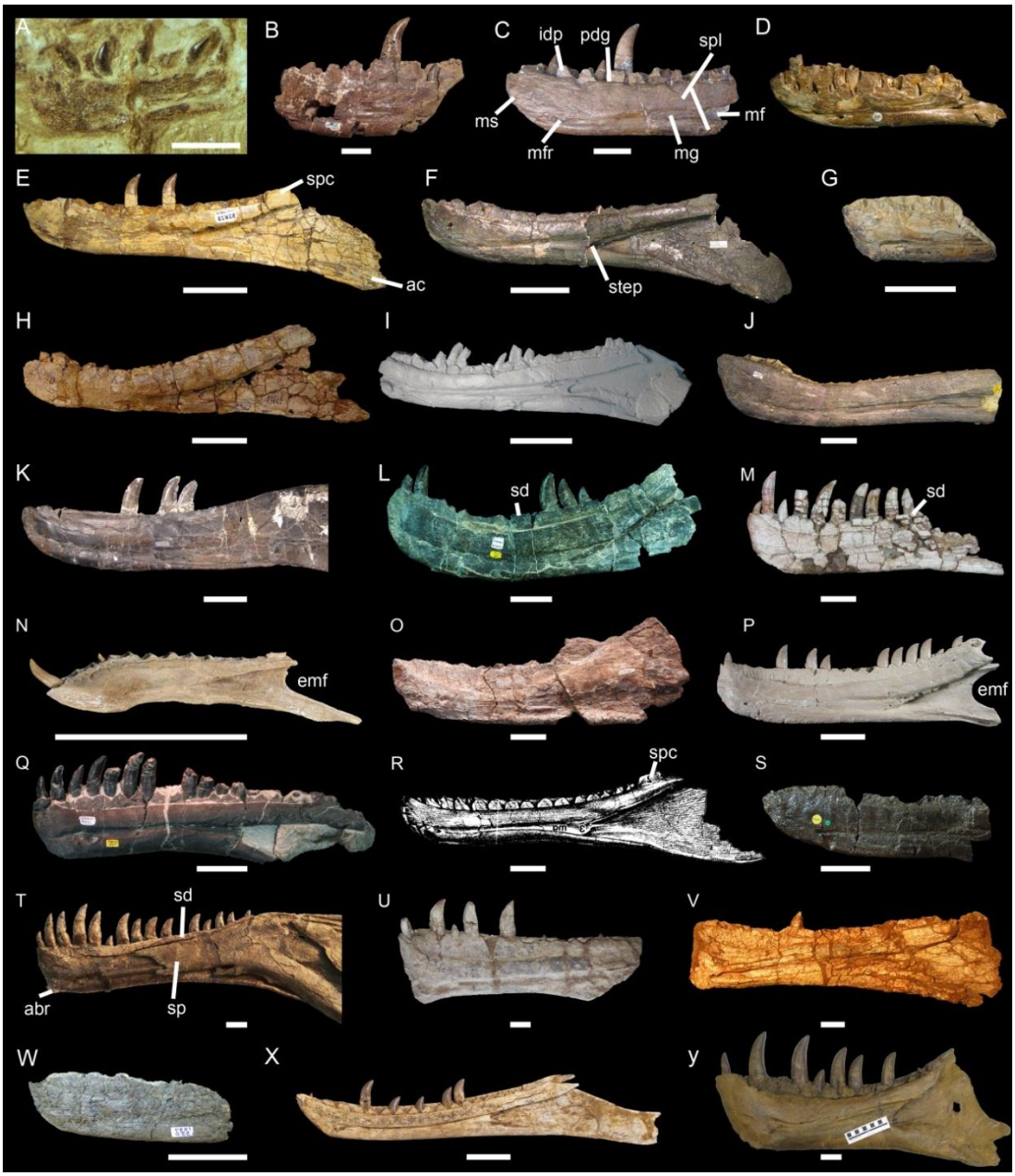

FIGURE 10.10. Dentaries of non-avian theropods in medial view. **A**, Embryo of *Torvosaurus* sp. (ML 1188, reconstructed); **B**, *Torvosaurus tanneri* (BYU-VP 2003); **C**, *Megalosaurus bucklandii* (OUMNH J13505); **D**, *Magnosaurus nethercombensis* (OUMNH J.12143); **E**, *Dubreuillosaurus valesdunensis* (MNHN 1998-13); **F**, *Eustreptospondylus oxoniensis* (OUMNH J.13558); **G**, *Piatnitzkysaurus floresi* (PVL 4073); **H**, *Dilophosaurus wetherilli* (UCMP 37303; courtesy of Martín Ezcurra); **I**, *Marshosaurus bicentesimus* (AMNH 27641); **J**, *Baryonyx walkeri* (NHM R.9951); **K**, *Ceratosaurus nasicornis* (USNM 4735); **L**, *Ceratosaurus dentisulcatus* (UUVP 158); **M**, *Genyodectes serus* (MLP 26-39); **N**, *Masiakasaurus knopfleri* (FMNH PR 2471); **O**, *Ekrixinatosaurus novasi* (MUCPv 294; courtesy of Matthew Lamanna); **P**, *Majungasaurus crenatissimus* (FMNH PR 2100); **Q**, *Allosaurus fragilis* (UUVP 10.093; courtesy of Stephen Brusatte); **R**, *Sinraptor dongi* (Currie and Zhao 1993*a*; fig. 11B); **S**, *Neovenator salerii* (NHM R10001; courtesy of Roger Benson); **T**, *Acrocanthosaurus atokensis* (NCSM 14345; courtesy of Drew Eddy); **U**, *Giganotosaurus carolinii* (MUCPv-CH-1; courtesy of Matthew Lamanna); **V**, *Tyrannotitan chubutensis* (MPEF-PV 1157; courtesy of Juan Canale); **W**, *Eotyrannus lengi* (MIWG 1997.550); **X**, *Alioramus altai* (IGM 100-1844; courtesy of Mick Ellison © AMNH); **Y**, *Tyrannosaurus rex* (CMNH 9380). **Abbreviations**: **abr**, articular brace; **ac**, angular contact; **emf**, external mandibular fenestra; **idp**, interdental plate; **mf**, Meckelian fossa; **mfr**, Meckelian foramen; **mg**, Meckelian groove; **ms**, mandibular symphysis; **pdg**, paradental groove; **sd**, supradentary; **sdc**, supradentary contact; **sp**, splenial; **spl**, splenial contact; **step**, step between Meckelian fossa and Meckelian groove. Scale: 5 mm (A), 5 cm (B to Y).

jugal ramus tapers as a very long pointing process. Importantly, *Torvosaurus* has been previously reported from the same Formation in Portugal (Mateus and Antunes 2000*a*; Mateus et al. 2006).

Four features differentiate ML 1188 from the maxilla of adult *Torvosaurus*: 1) absence of denticles on the mesial and distal carinae, 2) absence of fusion of the interdental plates in the maxilla, and 3) an anteroposteriorly short anterior ramus 4) bearing less than six maxillary teeth (Fig. 10.9). These features are most likely related to morphological variation through ontogeny. The lack of tooth denticles among non-coelurosaur theropods is rare, being only observed in teeth of Spinosaurinae (Sues et al. 2002). However, the lack of denticles in portions of the maxillary teeth has been observed in the embryo of the basal avetheropod *Lourinhanosaurus* ML 565-122, namely in the mesial and apical portion of the distal carinae. Likewise, the embryonic specimen of *Troodon* also bears unserrated crowns, in contrast to the condition found in adults (Varricchio et al. 2002). ML 1188 is the only case of complete absence of denticles known to date in non-coelurosaur theropod embryos. In coelurosaurs, besides *Troodon*, the *Byronosaurus* embryo also lacks denticles as in the adult (Varricchio et al. 2002; Bever and Norell 2009). Separated interdental plates occur in the maxilla in several adult specimens of megalosaurids (e.g., *Megalosaurus*, *Duriavenator*). In the *Torvosaurus* holotype (BYU-VP 9122, BYU-VP - Brigham Young University Vertebrate Paleontology, Provo, Utah, USA), and a larger maxilla (ML 1100) discovered in the Lourinhã Formation, the maxillary interdental plates are completely fused unlike part of the dentary in the holotype of *Torvosaurus* (BYU-VP 2003). Unpreserved interdental plates in the hatchling *Allosaurus* may suggest that these elements were unfused in juveniles, contrary to the condition seen in adult *Allosaurus*. Thus, fusion of interdental plates in the maxilla of basal tetanurans seems to occur at post-hatchling stages. Likewise, the proportion of the anterior ramus and the maxillary tooth count have also been previously described as traits that may vary ontogenetically at post-embryonic stages (Rauhut and Fechner 2005). These four conditions, the absence of denticles, fusion of the maxillary interdental plates, elongation of the anterior ramus and the differences in maxillary tooth counts, are traits that vary trough theropod ontogeny after hatchling.

Ontogeny of the maxilla in basal tetanurans

Personal examination of the maxillae of embryo and hatchling specimens of *Allosaurus* (MG 27804), *Torvosaurus* (ML 1188), *Lourinhanosaurus* (ML 565-122) and *Byronosaurus* (IGM 100-972), associated with high-resolution photos of the maxilla provided for the juvenile specimens of *Sciurumimus* (BMMS BK 11) and *Scipionyx* (SBA–SA 163760), allows a detailed investigation of the early development of the maxilla in non-avian theropods.

Anterior ramus—A major differences between the maxillae of juvenile and adult individuals of *Allosaurus* and *Torvosaurus* is the anterodorsally short anterior ramus seen in immature specimens (Rauhut and Fechner 2005). Postnatal elongation of the snout is common in dinosaurs and represents

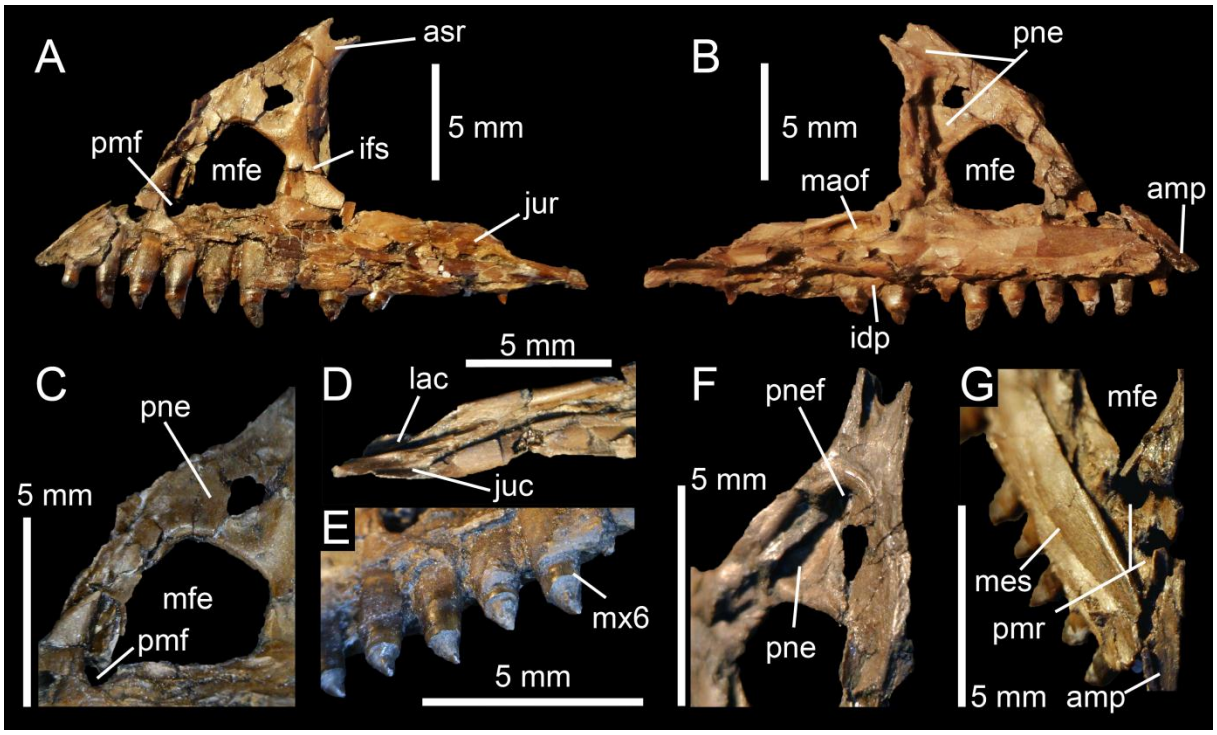

FIGURE 10.11. Isolated maxilla of an hatchling specimen of *Allosaurus* sp. (MG 27804). Left maxilla in **A**, lateral; and **B**, medial views; with close up on **C**, the anterolateral pneumatic complex of the maxilla in lateral view; **D**, the jugal ramus in dorsal view; **E**, the maxillary teeth in anteroventral view; **F**, the ascending ramus in posteromedial view; and **G**, the promaxillary recess in posteromedial view. **Abbreviations**: **amp**, anteromedial process; **asr**, ascending ramus; **idp**, interdental plates; **ifs**, interfenestral strut; **juc**, jugal contact; **jur**, jugal ramus; **lac**, lacrimal contact; **maof**, medial antorbital fossa; **mes**, medial shelf; **mfe**, marillary fenestra; **mx6**, sixth maxillary tooth; **pmf**, promaxillary fenestra; **pmr**, promaxillary recess; **pne**, pneumatic excavation; **pnef**, pneumatic foramen.

the plesiomorphic condition in this clade (Coombs Jr 1982; Horner and Currie 1994; Varricchio 1997; Carr 1999; Rauhut and Fechner 2005; Bever and Norell 2009; Dal Sasso and Maganuco 2011). It is, however, interesting to note that the anterior ramus of juvenile basal tetanurans tend to be shorter than maniraptoriforms (Rauhut and Fechner 2005; Bever and Norell 2009; pers. obs.). Embryonic and juvenile specimens of Maniraptora such as therizinosauroid (Kundrát et al. 2008: fig. 2B) and the troodontids *Troodon* (Varricchio et al. 2002: fig. 2C) and *Byronosaurus* (Bever and Norell 2009) indeed possess an anteroposterioly elongated anterior ramus whereas the latter is short in *Sciurumimus* and totally absent in *Allosaurus* hatchlings (Fig. 10.11) and *Scipionyx*. The embryonic maxilla of *Torvosaurus* and *Lourinhanosaurus* also follows this tendency. In *Torvosaurus*, the anterior ramus of the embryo is roughly subtriangular and poorly developed whereas the anterior ramus is slightly more expanded (Fig. 10.12A–B) in the embryo of the basal avetheropod *Lourinhanosaurus* (Carrano et al. 2012), and corresponds to the elongation seen in the immature megalosauroid *Sciurumimus*. A reverse condition seems however to occur in Tyrannosauroidea in which juveniles tend to have a rather long snout (Carr 1999; Rauhut and Fechner 2005; Tsuihiji et al. 2011).

Denticles—The absence of denticles in the embryos of *Torvosaurus* is also considered to be an ontogenetic feature, as witnesses by the crowns of the embryos of *Troodon* embryos that lack of

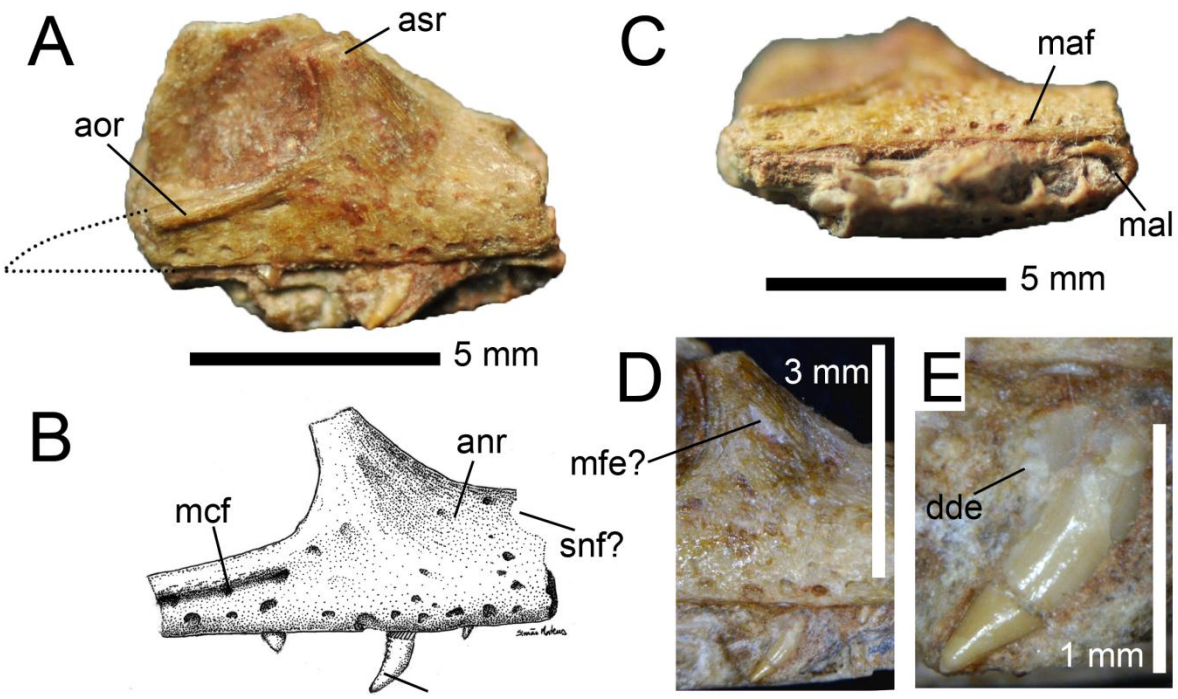

FIGURE 10.12. Isolated maxillae of an embryonic specimen of *Lourinhanosaurus antunesi* (ML 565-122). Left and right maxilla in **A–B**, right lateral; and **C**, ventral views; with close up on **D**, the ascending ramus and the anterior portion of the lateral antorbital fossa, and **E**, the fifth? maxillary crown of the right maxilla in lateral view. **Abbreviations**: **anr**, anterior ramus; **aor**, antorbital ridge; **asr**, ascending ramus; **dde**, distal denticles; **mal**, first maxillary alveolus; **mcf**, maxillary circumfenestra foramina; **mfe**, marillary fenestra; **snf**, subnarial foramen. Artwork in B courtesy of Simão Mateus.

denticles (Varricchio et al. 2002) and unlike the condition seen in adults (e.g., Currie 1987). Contrarily to *Torvosaurus* teeth that are all unserrated, the only in-situ tooth of *Lourinhanosaurus* embryo bears large denticles on the basodistal carina, and the apical two thirds of the distal carina and the mesial carina are both unserrated (Fig. 10.12E). A similar condition occurs in some crowns of the juvenile individuals *Sciurumimus* and *Scipionyx* in which the teeth significantly differ from those with serrated mesial and distal carinae belonging to mature basal tetanurans, with the only exception of some megaraptorans (Novas et al. 2008; pers. obs.). Their morphology corresponds however to the teeth borne by some basal and derived coelurosaurs such as compsognathids and dromaeosaurids (Rauhut et al. 2012; pers. obs.). As noted by Rauhut et al. (2012), this implies different diet among juvenile and adult theropods of the same taxon, perhaps heterochronies and most likely similar feeding ecologies among juvenile basal tetanurans and some adult megaraptorans and coelurosaurs. The denticles of *Lourinhanosaurus* embryo differ from those of *Sciurumimus* and *Scipionyx* by their size and density. Only three denticles appear in the distal carina, whereas the denticles of the two juvenile tetanurans are much more numerous and extend more apically on the distal carina. This suggests some ontogenetic pattern in the development of the denticles in the lateral dentition of basal tetanurans, with an embryonic stage bearing large basodistal denticles or no denticles on the crowns, a

hatchling/juvenile stage with coarse denticles on the distal carina, and a mature stage with both serrated mesial and distal carinae.

Interdental plates—According to Rauhut et al. (2010), interdental plates fuse very early in ontogeny in theropods that exhibit fusion. Nevertheless, their absence in a large portion of the maxilla in the *Allosaurus* hatchling suggest that interdental plates were separated and lost in this taxa while fully fused plates are seen in more mature individuals. Since fused interdental plates occur in a few juvenile theropods such as *Dilophosaurus* (Tykoski 2005), fusion of interdental plates, like most of other cranial and postcranial bones, is therefore considered to occur at a post-hatchling state, and much later than the embryonic stage in theropods.

Maxillary pneumatic openings—The maxillary sinus, situated in the anterior corner of the lateral antorbital fossa, appears early in ontogeny in basal tetanurans, and seems to be a plastic anatomical feature among juvenile individuals (e.g., Witmer 1995, 1997*a*; Rauhut and Fechner 2005). In *Scipionyx*, it is present as a large and well-delimited subrectangular fossa bounded by a medial wall and located dorsal to the small promaxillary fenestra (Dal Sasso and Maganuco 2011). In the *Allosaurus* hatchling, it, however, corresponds to a large subcircular fenestra dorsal to a minute promaxillary fenestra (Rauhut and Fechner 2005). A large maxillary fenestra is also present in the embryo of derived coelurosaurs such as *Troodon*, and *Byronosaurus*, yet the latter do not display any promaxillary fenestra (Varricchio 1997; Bever and Norell 2009). In *Lourinhanosaurus*, the maxillary fenestra is a small piriform opening that may or may not perforate the maxilla, and no apparent promaxillary fenestra can be seen (pers. obs.). On the other hand, the maxilla of the *Torvosaurus* embryo does not display any promaxillary recess, maxillary antrum and maxillary and promaxillary fenestrae on its medial side. This suggests that the paranasal pneumatic system was not well-developed in basal tetanuran embryos, and the opportunistic invasion and resorption of non-functional tissues by the epithelia (Witmer 1997*a*) only existed in some theropod embryos such as *Allosaurus* (Rauhut and Fechner 2005). Likewise, the poor development of the maxillary sinus in *Lourinhanosaurus* embryo may imply that the enlargement of the maxillary fenestra was happening throughout ontogeny in this basal avetheropod. Indeed, adult avetheropods display rather large maxillary fenestra and an increase in size of the maxillary fenestra has been already noticed throughout craniofacial ontogeny in Tyrannosauridae (Carr 1999). Nevertheless, it has been demonstrated that there is no correlation between the size of the maxillary fenestral and this of an individual in other basal tetanurans such as *Allosaurus* (Loewen 2010), and the development of the paranasal pneumatic system may therefore variate significantly in different individuals sharing similar ontogenetic stage.

Medial shelf—Other ontogenetic features are absent in the maxilla of juveniles and present in the adults of the same taxon in basal tetanurans, but not in coelurosaurs. This is the case of the medial shelf which seem to be absent along the medial wall of the maxilla in the *Torvosaurus* embryo and

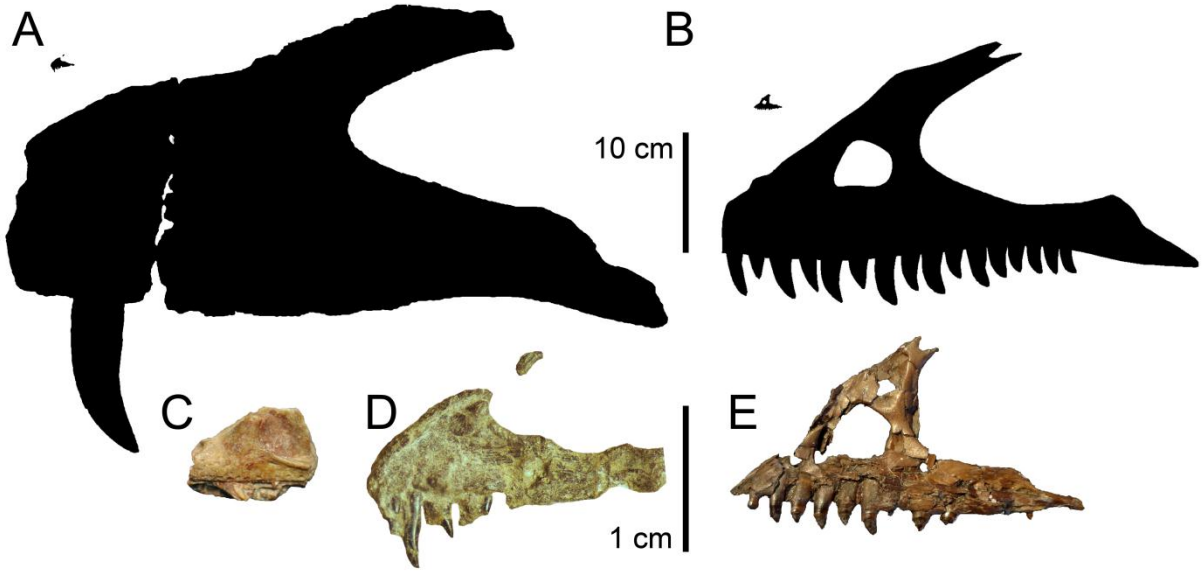

FIGURE 10.13. Size comparison of the maxilla of embryonic, hatchling and adult specimens of basal tetanurans in lateral view. **A**, Size comparison of embryonic and adult maxilla of *Torvosaurus gurneyi*; **B**, size comparison of hatchling and adult maxilla of *Allosaurus* sp.; **C**-**E**, size comparison of embryonic maxillae of **C**, *Lourinhanosaurus antunesi*; **D**, *Torvosaurus gurneyi*; and **E**, hatchling maxilla of *Allosaurus* sp. Scale: 10 cm (A–B), and 1 cm (C–E).

lateromedially low in the *Allosaurus* hatchling, whereas the medial shelf is low and poorly delimited in the adults of *Torvosaurus* and protuberant, forming a broad crest, in the adults of *Allosaurus*. In coelurosaurs, the medial shelf of *Lourinhanosaurus* embryos is broad and well-delimited (pers. obs.) and thin and extensive in *Byronosaurus* embryos, contributing to the formation of a secondary palate like in the adults (Bever and Norell 2009). Likewise, there is no palatal contact in the juvenile specimens of non-coelurosaurian tetanurans, which also seems to be the case in the adult maxillae of *Torvosaurus* and not in *Allosaurus*, and one can wonder whether the maxilla and palate were articulating in embryos and hatchlings of these basal tetanurans. There are two longitudinal grooves for the articulation of the palate in the posterior part of the medial shelf in *Lourinhanosaurus*. In the adult *Torvosaurus*, the lacrimal contact of the jugal ramus is complex and corresponds to a flat surface on the medial side of the ramus, at the level of a convexity on the dorsal rim of the jugal ramus, as well as a deep slit inside the ramus and medial to the jugal contact. Although details of the lacrimal contact are hardly visible in ML 1188, a similar articulation is absent in the *Torvosaurus* embryo and the development of such complex lacrimal contact was likely developed throughout ontogeny.

Size—Based on a digital restoration of the maxilla (Fig. 10.13), the embryonic specimen of *Torvosaurus* has a total length of approximately 20 millimetres which corresponds to 3.2 % the size of the fully adult specimen ML 1100 (total length of 612 mm; Table 10.1). This is a lower value than the proportion of 6 to 8% between MG 27804 and adult maxillae of *Allosaurus* (Rauhut and Fechner 2005; pers. obs.; Fig. 10.13; Table 10.1), suggesting that MG 27804 was most likely a hatchling individual rather than an embryo. Indeed, the maxilla of the *Torvosaurus* embryo is slightly smaller than the *Allosaurus* hatchling (23 mm), although *Torvosaurus* was a bigger animal than *Allosaurus* (10

TABLE 10.1. Maxilla, skull and body lengths of juvenile and adult individuals in non-avian tetanurans. Values are given in millimeters for the maxilla, the skull and the body lengths of juvenile individuals, and in metres for the body lengths of adult individuals. *Estimated values. § In adults. **Abbreviations**: **Juv**., juvenile; **max**, maxilla.

Taxa	Stage	Juv. maxilla	Adult maxilla	Juv. skull	Adult skull	Juv. body	Adult body	Proportion maxilla	Proportion max/skull
Torvosaurus	Embryo	20	612	37*	1580*	350*	10-12*	3.2%	?
Sciurumimus	Juvenile	42	?	79	?	719	>5*	?	53%
Lourinhanosaurus	Embryo	11*	?	22*	?	220*	4-5*	?	?
Allosaurus	Hatchling	23	370	48*	682	460*	7-8*	6.2%	54%§
Scipionyx	Neonate	23.2	?	48.9	?	461*	~2*	?	47%
Therizinosauroid	Embryo	13	?	26	?	?	2-3*	?	50%
Oviraptorid	Embryo	5	31-65	35	118-172	?	1.5-3*	7-16%	26-37%§
Archaeornithoides	Juvenile	24.5	?	50*	?	?	?	?	?
Troodon	Embryo	18	?	50*	?	?	2-3*	?	?
Byronosaurus	Embryo	19	97	50*	134	?	1-2*	19%	72%§

and 8 meters respectively; Mateus et al. 2006; Therrien and Henderson 2007; Table 10.1). Likewise, the maxilla of *Lourinhanosaurus* embryo, estimated to be 11 mm in length, is significantly smaller than this of *Torvosaurus* (Fig. 10.13), and compares well with the estimated size of the adult specimens of *Lourinhanosaurus* (Mateus 1998: fig. 1). Based on the ratio between the maxilla, the skull and the body length in the juvenile tetanurans *Sciurumimus* and *Scipionyx*, the skull and body size of juvenile tetanurans can also be evaluated. In immature individuals of basal tetanurans, the maxilla represents around one half of the skull length (53% in *Sciurumimus*, 47% in *Scipionyx* and 50% in therizinosauroid embryo; Table 10.1), and the skulls of *Lourinhanosaurus* and *Torvosaurus* embryos may have reached a length of around 2 to 2.5 cm and 3.5 to 4 cm respectively, while the skull of the *Allosaurus* hatchling can be estimated to have a length of around 5 cm. In *Sciurumimus* and *Scipionyx*, the maxilla occupies 5 to 6 % of the body length (pers. obs.), therefore the length of *Lourinhanosaurus* and *Torvosaurus* embryos can be evaluated to around 18 to 22 cm and 33 to 40 cm respectively, and around 38 to 46 cm for the *Allosaurus* hatchling. Interestingly, the maxillae of *Torvosaurus* and derived coelurosaur embryos like *Troodon* and *Byronosaurus*, as well as *Allosaurus* and *Archaeornithoides* hatchlings, are very similar in size although the adult of derived coelurosaurs tend to be considerably smaller than those of basal tetanurans (Rauhut and Fechner 2005). Very large basal tetanurans and derived coelurosaurs, therefore, had close size in early ontogenetic stages, but the formers grew longer and faster than the latters in order to achieve such large size.

V. CONCLUSIONS

Theropods are the most diversified group of dinosaurs both taxonomically and morphologically. Thorough investigation on the dentition and quadrate morphology in this successful group of dinosaurs, associated with the description of embryonic and adult specimens of *Torvosaurus* from Portugal, allowed to provide tools to better study, describe, and identify theropod cranial and dental material, and to draw several conclusions regarding the ontogeny, paleoecology, paleostratigraphy, and paleobiogeography of non-avian theropods.

Theropod Teeth

Isolated theropod teeth are one of the most abundant dinosaur material in the Mesozoic fossil record and are constantly reported in the literature. In order to facilitate the description and measurements of theropod teeth, a standardized list of 122 positional, anatomical, morphological, and morphometric terms was provided, and a methodology to thoroughly describe the tooth state, crown, denticles, tooth ornamentations, and root was also given.

Isolated theropod teeth are often assigned to diagnose taxa on the basis of qualitative characters with questionable phylogenetic potential, so that the distribution of thirty dental characters among 113 theropod taxa was investigated. Ziphodonty occurs in all non-alvarezsaurid Alvarezsauroidea, Dromaeosauridae, and non-maniraptoriform theropods other than Spinosauridae and Tyrannosauridae. Pachydonty, corresponding to a lateral dentition with incrassate and coarsely serrated teeth, is synapomorphic to Tyrannosauridae. Conidonty, defined by a lateral dentition with conical teeth, is seen in spinosaurids and ornithomimids whereas a folidont dentition, corresponding to a lateral dentition with strongly constricted crown at the cervix, is synapomorphic to Alvarezsauridae, Caenagnathoidea, and Paraves. Unserrated crowns are seen in ‘neocoelurosaur’ for lateral teeth, and in Spinosaurinae, and Maniraptoriformes other than Therizinosauria, derived Troodontidae and non-unenlagiine Dromaeosauridae for the whole dentition. A U-shaped cross-section in mesial teeth is synapomorphic to Tyrannosauridae, whereas an eight-shaped cross-section outline is noticeable among the clades of Metriacanthosauridae, Megaraptora and Coelurosauria. The presence of more than 250 denticles is synapomorphic to Baryonychinae, and crowns bearing distal denticles significantly bigger than the mesial ones is a possible synapomorphy of Noasauridae, Piatnitzkysauridae, Tyrannosauroidea and the clade Microraptorinae + Eudromaeosauria. Hooked and/or pointed denticles is a possible synapomorphy of Abelisauroidea, Therizinosauridae, and Eudromaeosauria, and flutes on both sides of the crown in mesial and lateral teeth is a synapomorphy of Spinosauridae. Transversal undulations are seen in almost all non-avian theropod clades whereas marginal undulations have been identified in ‘non-neocoelurosaur’ Averostra, and their presence is a possible synapomorphy of averostran theropods.

As a case of study on theropod teeth, the phylogenetic position of four isolated theropod teeth from the Lourinhã Formation (Kimmeridgian–Tithonian) of Portugal was investigated based on a cladistic analysis performed on a data matrix of 141 dentition-based characters coded in 60 taxa, and a supermatrix combining the dentition related dataset with six recent data matrices based on the whole theropod skeleton. The largest and smallest teeth were referred to a mesial crown of *Torvosaurus* and a lateral crown of *Richardoestesia*, respectively, and *Richardoestesia* was recovered as a dromaeosaurid in the cladistic analysis on teeth. Two medium-sized teeth were ascribed to an abelisaurid theropod, providing the first record of Abelisauridae in the Jurassic of Laurasia and suggesting a possible radiation of Abelisauridae in Europe well before the Upper Cretaceous.

A thorough investigation on the morphology of megalosaurid teeth revealed that the dentition of Megalosauridae, often considered to be similar to the dentition of other ziphodont theropods, can be distinguished by qualitative characters rather than quantitative data. Megalosaurid teeth are characterized by a mesial carina facing mesiolabially in mesial teeth, centrally positioned carinae on both mesial and lateral crowns, a mesial carina terminating above the cervix, and short to well-developed interdenticular sulci between distal denticles. A discriminant analysis performed on a dataset of measurements variables collected on the teeth of 62 theropod taxa indicates that, unlike Spinosauridae, Troodontidae, Tyrannosauridae, megalosaurid teeth are hardly distinguishable from other ziphodont theropod clades. This study also demonstrated that ratio variables have only weak influence on the results in most analyses, and it is recommended to avoid the use of ratio variables in discriminant analysis as they overemphasize some variables.

All this shows that carefull analysis of isolated bones and teeth can provide an accurate classication often down to the genus level. This is particularly important to correlate teeth of theropods that are commonly found in strata around the world and may be useful to correlate stratigraphic units.

Theropod Quadrate

In order to facilitate the description of the quadrate in the literature on non-avian theropod anatomy, a standardized list of 36 terms and notations for each quadrate anatomical entity was proposed. The quadrate can be divided into two regional categories, the quadrate body and the pterygoid flange, and twelve anatomical sub-units (i.e., quadrate shaft, quadrate head, quadrate ridge, quadrate foramen, lateral process, quadratojugal contact, squamosal contact, pterygoid contact, mandibular articulation, medial fossa, and posterior fossa). The quadrate of the large majority of non-avian theropods is akinetic, and a streptostylic quadrate suggested in some coelurosaurs is unlikely. Internal or external pneumaticity of the quadrate has been recorded in all avetheropod clades other than Allosauridae, and a pneumatic quadrate is a possible synapomorphy of Averostra. Quadrate pneumaticity and a strong suture between the quadrate and quadratojugal appear early in ontogeny in coelurosaurs. In basal tetanurans, however, a poorly delimited mandibular condyles, intercondylar

sulcus and quadrate head, and a quadratojugal contact with a smooth surface have been interpreted as ontogenetic features present in embryonic/juvenile individuals.

The phylogenetic potential and evolutionary transformations of the quadrate were both investigated based on a phylogenetic morphometric analysis and a cladistic analysis using 98 discrete quadrate related characters. The cladistic analysis provides a fully resolved tree mirroring to some degree the classification of non-avian theropods and allowing several important evolutionary trends to be drawn for this bone, namely: a shortening of the height of the quadrate body and widening of the mandibular articulation across the evolution of Tyrannosauroidea, Megalosauroidea towards Spinosauridae, and Maniraptoriformes towards Dromaeosauridae; a pneumatization of the quadrate independently in Carcharodontosauridae, Megaraptora, Tyrannosauridae and Maniraptoriformes; a loss of the quadrate foramen independently in Ceratosauria and Megalosauridae; a loss of the lateral process in Tetanurae; a lateromedial widening of the mandibular articulation during the evolution of Megalosauroidea, Allosauroidea and Maniraptoriformes and an increase of its anteroposterior length during the evolution of Ceratosauria.

The phylogenetic morphometrics analysis performed on the non-avian theropod quadrate recovered two morphotypes of the mandibular articulation linked to two differently adapted functional systems. In a first morphotype characterized by an anteroposteriorly long mandibular articulation with two ovoid condyles, the lateral displacement of the mandible was weak or inexistent. This morphotype includes either carnivorous theropods with relatively short and broad skulls resisting torsional bending or herbivorous theropods with beaked skulls. On the other hand, a second morphotype is characterized by an elongate and anteroposteriorly short mandibular articulation, and a lateromedially wide and parabolic/sigmoid ectocondyle. Theropods with such mandibular articulation where those favoring the deglutition of whole prey, or large chunk of food and include weak and fast biter theropods with elongated skulls, and massive theropods with extremely powerful skulls.

As a case of study on the theropod quadrate, the phylogenetic distribution, ontogeny, and morphofunctional aspect of six isolated quadrates from the Kem Kem beds (Cenomanian) of Morocco were investigated based on cladistic, morphometric, and phylogenetic morphometric approaches. The quadrates are determined to be from juvenile and adult individuals and to two morphotypes of Spinosaurinae tentatively assigned to *Spinosaurus*. Ontogenetic changes occurring in the spinosaurid quadrates include the suture of the quadrate and quadratojugal, delimitation of the mandibular condyles and squamosal capitulum, and development of a ventral projection of the dorsal quadratojugal contact and a second quadrate ridge directly ventral to the quadrate head. Morphofunctional analysis of the spinosaurid quadrates has revealed a peculiar jaw mechanic in which an helicoidal and strongly lateromedially oriented joint of the jaw articulation allowed to displace the mandibular ramus laterally when the lower jaw was depressed. This lateral movement of the spinosaurid ramus was possible due to a movable mandibular symphysis that allowed the pharynx to

be widened. Spinosauridae, which are considered to be semi-aquatic and partially piscivorous animals, were able to swallow large prey such as fish the same ways as pelecanids.

Torvosaurus Material from Portugal

A thorough description of the Portuguese material referred to *Torvosaurus tanneri*, combined with a detailed comparison with the material referred to *T. tanneri* from North America, allowed to highlight some differences justifying the creation of a distinct Eastern species. The new taxon, *Torvosaurus gurneyi*, is defined based on two autapomorphies among Megalosauroidea, namely a maxilla possessing fewer than eleven teeth and an interdental wall nearly coincidental with the lateral wall of the maxillary body. The European *Torvosaurus* also differs from the American species by the absence of interdental plates terminating ventrally by broad V-shaped points and the absence of a protuberant ridge posterior to the anteromedial process. *T. gurneyi* is the largest land predator discovered in Europe hitherto and supports the mechanism of vicariance that occurred in the Iberian Meseta during the Late Jurassic when the proto-Atlantic was already well formed. The anterior portion of a right maxilla referred to *Torvosaurus* sp. is ascribed to this new species, and postcranial material including a tibia and the distal portion of a femur are tentatively assigned to *T. gurneyi* based on their paleogeographic and stratigraphic distribution. A standardized list of 65 terms and notations on the theropod maxilla is proposed to describe this important cranial bone with more ease in the future.

A theropod clutch containing several crushed eggs and embryonic material from the Lourinhã Formation of Portugal is also referred to *Torvosaurus gurneyi*. The clutch represents the first associated eggshells and embryos of megalosauroids, and the basalmost theropod embryos found to date. Investigation on the maxilla ontogeny in basal tetanurans reveals that mesial and sometimes distal denticles, elongation of the anterior ramus, and fusion of interdental plates appear at a posthatchling stage whereas maxillary pneumatic openings are already present at an embryonic stage in non-avian theropods.

FUTURE DEVELOPMENTS

By proposing a standard terminology for teeth, quadrate, and maxilla, describing the dentition of megalosaurids, detailing the functionality of several dental features and the mandibular articulation of the quadrate, and investigating the phylogenetic potential and ontogenetic changes in teeth and quadrates, the present work serves as the basis for similar studies applied on other bones in other theropod and dinosaur clades.

- As for the teeth, quadrate and maxilla, the terminology and abbreviations used to describe the anatomy of other cranial and postcranial bones is inconsistent in non-avian theropods and dinosaurs in general, with several anatomical terms for the same sub-entity being often employed. It is therefore crucial to provide a standard terminology for other cranial and postcranial bones with the aim of facilitating the osteological description of theropod specimens and taxa.

- This study has revealed the phylogenetic potential of theropod teeth based on dental features such as the carina extension, crown ornamentations, denticle morphology, and enamel texture. The description of these features is currently limited to some theropods, and the dentition of the large majority of theropod clades such as Coelophysidae, Dilophosauridae, Noasauridae, Sinraptoridae, Allosauridae, Neovenatoridae, and Megaraptora is still poorly known. This work, therefore, demonstrates the need for more thorough descriptions of the dentition of these clades with the goal of identifying isolated theropod teeth with more ease in the future.

- Cladistic and discriminant analyses on theropod teeth based on the data matrix of dentition-related characters and the dataset including a large number of measurement variables, respectively, have proven to be successful for identifying theropod teeth to the genus level. Consequently, incorporation of more theropod taxa into our data matrix and morphometric dataset will broaden the utility of both cladistic and DFA approaches.

- A large number of theropod taxa erected in the early history of theropod discoveries are based on one or several isolated teeth (e.g., *Megalosaurus chubutensis*, *Massospondylus rawesi*, *Suchosaurus cultridens*, *Szechuanosaurus campi*, *Wakinosaurus satoi*; see Holtz et al. 2004 and Carrano et al. 2012 for more examples) and are, therefore, typically considered as *nomen dubium*. Investigation on the phylogenetic position of these dental-based taxa using the dentition-based cladistic and discriminant analyses developped in this study is needed to solve the validity of these taxa.

- Functional clues were given for several dental features and the mandibular articulation of the quadrate. These hypotheses need, however, to be tested with modern methods such as FEA. The latter technique could, for instance, be performed on 3D models of digitalized ziphodont, folidont, conidont, and pachydont teeth, and on a ceratosaurian versus a megalosauroid-type of mandibular articulation.

- As for the quadrate, a thorough description of other bones of the skeleton should be provided in theropods. The evolution of each of these cranial and postcranial bones should be thoroughly investigated based on cladistic, morphometric, and phylogenetic morphometric analyses performed on large scaled data matrices, and landmarks.

REFERENCES

Abler, W. L. 1992. The serrated teeth of tyrannosaurid dinosaurs, and biting structures in other animals. *Paleobiology* 18 (2): 161–183.

Abler, W. L. 1997. Tooth serrations in carnivorous dinosaurs. *In*: Currie, P. J. and Padian, K. (eds.), *Encyclopedia of Dinosaurs*, 740–741. Academic Press, San Diego, California.

Abler, W. L. 1999. The teeth of the tyrannosaurs. *Scientific American* 281 (3): 50–51.

Abler, W. L. 2013. Internal structure of tooth serrations. *In*: Parrish, J. M., Molnar, R. E., Currie, P. J. and Koppelhus, E. B. (eds.), *Tyrannosaurid Paleobiology*, 81–88. Indiana University Press, Bloomington, Indiana.

Abramovich, S., Keller, G., Adatte, T., Stinnesbeck, W., Hottinger, L., Stueben, D., Berner, Z., Ramanivosoa, B. and Randriamanantenasoa, A. 2003. Age and paleoenvironment of the Maastrichtian to Paleocene of the Mahajanga Basin, Madagascar: a multidisciplinary approach. *Marine Micropaleontology* 47 (1–2): 17–70.

Agnolín, F. L. and Martinelli, A. G. 2007. Did oviraptorosaurs (Dinosauria; Theropoda) inhabit Argentina? *Cretaceous Research* 28 (5): 785–790.

Agnolín, F. L. and Chiarelli, P. 2010. The position of the claws in Noasauridae (Dinosauria: Abelisauroidea) and its implications for abelisauroid manus evolution. *Paläontologische Zeitschrift* 84 (2): 293–300.

Agnolín, F. L. and Novas, F. E. 2011. Unenlagiid theropods: are they members of the Dromaeosauridae (Theropoda, Maniraptora)? *Anais da Academia Brasileira de Ciências* 83 (1): 117–162.

Agnolín, F. L. and Novas, F. E. 2013. *Avian Ancestors - A Review of the Phylogenetic Relationships of the Theropods Unenlagiidae, Microraptoria,* Anchiornis *and Scansoriopterygidae*. *In* Lohmann, G., Mysak, L. A., Notholt, J., Rabassa, J. and Unnithan (eds.) SpringerBriefs South America and the Southern Hemisphere, Springer Verlag, Dordrecht, Heidelberg, New York, London, 96pp.

Agnolín, F. L., Ezcurra, M. D., Pais, D. F. and Salisbury, S. W. 2010. A reappraisal of the Cretaceous non-avian dinosaur faunas from Australia and New Zealand: evidence for their Gondwanan affinities. *Journal of Systematic Palaeontology* 8 (2): 257–300.

Agnolín, F. L., Powell, J. E., Novas, F. E. and Kundrát, M. 2012. New alvarezsaurid (Dinosauria, Theropoda) from uppermost Cretaceous of north-western Patagonia with associated eggs. *Cretaceous Research* 35: 33–56.

Alcober, O. A. and Martinez, R. N. 2010. A new herrerasaurid (Dinosauria, Saurischia) from the Upper Triassic Ischigualasto Formation of northwestern Argentina. *ZooKeys* (63): 55–81.

Alifanov, V. R. and Barsbold, R. 2009. *Ceratonykus oculatus* gen. et sp. nov., a new dinosaur (?Theropoda, Alvarezsauria) from the Late Cretaceous of Mongolia. *Paleontological Journal* 43 (1): 94–106.

Allain, R. 2002. Discovery of megalosaur (Dinosauria, Theropoda) in the middle Bathonian of Normandy (France) and its implications for the phylogeny of basal Tetanurae. *Journal of Vertebrate Paleontology* 22 (3): 548–563.

Allain, R. 2005. The enigmatic theropod dinosaur *Erectopus superbus* (Sauvage 1882) from the Lower Albian of Louppy-le-Chateau. *In*: Carpenter, K. (ed.), *The Carnivorous Dinosaurs*, 72–86. Indiana University Press, Bloomington, Indiana.

Allain, R. 2014. New material of the theropod *Ichtyovenator* from Ban Kalum type locality (Laos): implications for the synonymy of *Spinosaurus* and *Sigilmassasaurus* and the phylogeny of Spinosauridae. *74th Annual Meeting Society of Vertebrate Paleontology, Berlin, Germany. (November 5-8, 2014), Program and Abstracts*: 78.

Allain, R. and Taquet, P. 2000. A new genus of Dromaeosauridae (Dinosauria, Theropoda) from the Upper Cretaceous of France. *Journal of Vertebrate Paleontology* 20 (2): 404–407.

Allain, R. and Chure, D. J. 2002. *Poekilopleuron bucklandii*, the theropod dinosaur from the Middle Jurassic (Bathonian) of Normandy. *Palaeontology* 45 (6): 1107–1121.

Allain, R., Xaisanavong, T., Richir, P. and Khentavong, B. 2012. The first definitive Asian spinosaurid (Dinosauria: Theropoda) from the early cretaceous of Laos. *Naturwissenschaften* 99 (5): 369–377.

Allain, R., Tykoski, R., Aquesbi, N., Jalil, N.-E., Monbaron, M., Russell, D. and Taquet, P. 2007. An abelisauroid (Dinosauria: Theropoda) from the Early Jurassic of the High Atlas Mountains, Morocco, and the radiation of ceratosaurs. *Journal of Vertebrate Paleontology* 27 (3): 610–624.

Ameghino, F. 1899. Nota preliminar sobre el *Loncosaurus argentinus*, un representante de la familia de los Megalosauridae en la República Argentina. *Anales de la Sociedad Científica Argentina* 47: 61–62.

Ameghino, F. 1900. L'âge des formations sédimentaires de Patagonie. *Anales de la Sociedad Científica Argentina* 50: 145–165.

Ameghino, F. 1906. Les formations sédimentaires du Crétacé supérieur et du Tertiaire de Patagonie. *Anales del Museo Nacional de Buenos Aires* 3 (8): 1–568.

Amiot, R., Kusuhashi, N., Xu, X. and Wang, Y. 2010a. Isolated dinosaur teeth from the Lower Cretaceous Shahai and Fuxin formations of northeastern China. *Journal of Asian Earth Sciences* 39 (5): 347–358.

Amiot, R., Buffetaut, E., Tong, H., Boudad, L. and Kabiri, L. 2004a. Isolated theropod teeth from the Cenomanian of Morocco and their palaeobiogeographical significance. *Revue de Paléobiologie* 9: 143–149.

Amiot, R., Lécuyer, C., Buffetaut, E., Fluteau, F., Legendre, S. and Martineau, F. 2004b. Latitudinal temperature gradient during the Cretaceous Upper Campanian–Middle Maastrichtian: δ18O record of continental vertebrates. *Earth and Planetary Science Letters* 226 (1–2): 255–272.

Amiot, R., Lécuyer, C., Buffetaut, E., Escarguel, G., Fluteau, F. and Martineau, F. 2006. Oxygen isotopes from biogenic apatites suggest widespread endothermy in Cretaceous dinosaurs. *Earth and Planetary Science Letters* 246 (1–2): 41–54.

Amiot, R., Buffetaut, E., Lécuyer, C., Fernandez, V., Fourel, F., Martineau, F. and Suteethorn, V. 2009. Oxygen isotope composition of continental vertebrate apatites from Mesozoic formations of Thailand; environmental and ecological significance. *Geological Society, London, Special Publications* 315 (1): 271–283.

Amiot, R., Wang, X., Zhou, Z., Wang, X., Buffetaut, E., Lécuyer, C., Ding, Z., Fluteau, F., Hibino, T., Kusuhashi, N., Mo, J., Suteethorn, V., Wang, Y., Xu, X. and Zhang, F. 2011. Oxygen isotopes of East Asian dinosaurs reveal exceptionally cold Early Cretaceous climates. *Proceedings of the National Academy of Sciences* 108 (13): 5179–5183.

Amiot, R., Buffetaut, E., Lécuyer, C., Wang, X., Boudad, L., Ding, Z., Fourel, F., Hutt, S., Martineau, F., Medeiros, M. A., Mo, J., Simon, L., Suteethorn, V., Sweetman, S., Tong, H., Zhang, F. and Zhou, Z. 2010b. Oxygen isotope evidence for semi-aquatic habits among spinosaurid theropods. *Geology* 38 (2): 139–142.

De Andrade, M., Young, M. T., Desojo, J. B. and Brusatte, S. L. 2010. The evolution of extreme hypercarnivory in Metriorhynchidae (Mesoeucrocodylia: Thalattosuchia) based on evidence from microscopic denticle morphology. *Journal of Vertebrate Paleontology* 30 (5): 1451–1465.

Andres, B., Clark, J. M. and Xing, X. 2010. A new rhamphorhynchid pterosaur from the Upper Jurassic of Xinjiang, China, and the phylogenetic relationships of basal pterosaurs. *Journal of Vertebrate Paleontology* 30 (1): 163–187.

Antunes, M. T. 1990. Dinossauros de Sesimbra e Zambujal-Episódios de há cerca de 140 milhões de anos. *Sesimbra Cultural* 0: 12–14.

Antunes, M. T. and Sigogneau-Russell, D. 1991. Nouvelles données sur les dinosaures du Crétacé supérieur du Portugal. *Comptes rendus de l'Académie des sciences. Série 2, Mécanique, Physique, Chimie, Sciences de l'univers, Sciences de la Terre* 313 (1): 113–119.

Antunes, M. T. and Mateus, O. 2003. Dinosaurs of Portugal. *Comptes Rendus Palevol* 2 (1): 77–95.

Araújo, R., Castahinha, R. and Mateus, O. 2008. Major trends in the evolution of teeth and mandibles in ornithopod dinosaurs. *Tercer Congreso Latinoamericano de Paleontología de Vertebrados, Neuquén, Argentina*: 18.

Araújo, R., Castanhinha, R. and Mateus, O. 2011. Evolutionary major trends of ornithopod dinosaurs teeth. *In*: Calvo, J. O., Porfiri, J. D., González Riga, B. J. and Dos Santos, D. (eds.), *Dinosaurios Y Paleontología Desde América Latina*, 25–31. EDIUNC, Editorial de la Universidad Nacional de Cuyo.

Araújo, R., Mateus, O., Walen, A. and Christiansen, N. 2009. Preparation techniques applied to a stegosaurian dinosaur from Portugal. *Journal of Paleontological Techniques* 5: 1–23.

Araújo, R., Castanhinha, R., Martins, R. M. S., Mateus, O., Hendrickx, C., Beckmann, F., Schell, N. and Alves, L. C. 2013. Filling the gaps of dinosaur eggshell phylogeny: Late Jurassic theropod clutch with embryos from Portugal. *Scientific Reports* 3 (1924): 1–8.

Arcucci, A. B. and Coria, R. A. 2003. A new Triassic carnivorous dinosaur from Argentina. *Ameghiniana* 40 (2): 217–228.

Auffenberg, W. 1981. *The Behavioral Ecology of the Komodo Monitor*. University Press of Florida, Gainesville, 406pp.

Averianov, A. and Sues, H. D. 2011. Skeletal remains of Tyrannosauroidea (Dinosauria: Theropoda) from the Bissekty Formation (Upper Cretaceous: Turonian) of Uzbekistan. *Cretaceous Research*.

Averianov, A. O. and Sues, H.-D. 2007. A new troodontid (Dinosauria: Theropoda) from the Cenomanian of Uzbekistan, with a review of troodontid records from the territories of the former Soviet Union. *Journal of Vertebrate Paleontology* 27 (1): 87–98.

Averianov, A. O. and Skutschas, P. P. 2009. Additions to the Early Cretaceous dinosaur fauna of Transbaikalia, eastern Russia. *Proceedings of the Zoological Institute RAS* 313: 363–378.

Averianov, A. O., Krasnolutskii, S. A. and Ivantsov, S. V. 2010. A new basal coelurosaur (Dinosauria: Theropoda) from the Middle Jurassic of Siberia. *Proceedings of the Zoological Institute RAS* 314 (1): 42–57.

Avery, J. K. 2001. *Oral Development and Histology*. Thieme, Stuttgart ; New York, 480pp.

Azevedo, R. P. F. de, Simbras, F. M., Furtado, M. R., Candeiro, C. R. A. and Bergqvist, L. P. 2013. First Brazilian carcharodontosaurid and other new theropod dinosaur fossils from the Campanian–Maastrichtian Presidente Prudente Formation, São Paulo State, southeastern Brazil. *Cretaceous Research* 40: 131–142.

Azuma, Y. and Currie, P. J. 2000. A new carnosaur (Dinosauria: Theropoda) from the Lower Cretaceous of Japan. *Canadian Journal of Earth Sciences* 37 (12): 1735–1753.

Bailey, J. B. 1997. Neural spine elongation in dinosaurs: Sailbacks or buffalo-backs? *Journal of Paleontology*: 1124–1146.

Bakker, R. T. 1986. *The Dinosaur Heresies: New Theories Unlocking the Mystery of the Dinosaurs and Their Extinction*. William Morrow, New York, 481pp.

Bakker, R. T. 1998. Brontosaur killers: late Jurassic allosaurids as sabre-tooth cat analogues. *Gaia* 15: 145–158.

Bakker, R. T. and Bir, G. 2004. Dinosaur crime scene investigations: theropod behavior at Como Bluff, Wyoming, and the evolution of birdness. *In*: Currie, P. J., Koppelhus, E. B., Shugar, M. A. and Wright, J. L. (eds.), *Feathered Dragons: Studies on the Transition from Dinosaurs to Birds.*, 301–342. Indiana University Press, Bloomington, Indiana.

Bakker, R. T., Williams, M. and Currie, P. J. 1988. *Nanotyrannus*, a new genus of pygmy tyrannosaur, from the latest Cretaceous of Montana. *Hunteria* 1 (5): 1–30.

Bakker, R. T., Siegwarth, J. D., Kralis, D. and Filla, J. 1992. *Edmarka Rex*: A new, gigantic theropod dinosaur from the Middle Morrison Formation, Late Jurassic of the Como Bluff outcrop region. *Hunteria* 2 (9): 1–24.

Balanoff, A. M. and Norell, M. A. 2012. Osteology of *Khaan mckennai* (Oviraptorosauria: Theropoda). *Bulletin of the American Museum of Natural History*: 1–77.

Balanoff, A. M., Xu, X., Kobayashi, Y., Matsufune, Y. and Norell, M. A. 2009. Cranial osteology of the theropod dinosaur *Incisivosaurus gauthieri* (Theropoda: Oviraptorosauria). *American Museum Novitates* 3651: 1–35.

Barbosa, A. 1990. Identification key of Iberian waders (Charadriiformes) based on the os quadratum. *Miscellània Zoològica* 14: 181–185.

Barrett, P. M. 2000. Prosauropod dinosaurs and iguanas: speculations on the diets of extinct reptiles. *In*: Sues, H.-D. (ed.), *Evolution of Herbivory in Terrestrial Vertebrates*, 42–78. Cambridge University Press, Cambridge, U.K.; New York.

Barrett, P. M. 2005. The diet of ostrich dinosaurs (Theropoda: Ornithomimosauria). *Palaeontology* 48 (2): 347–358.

Barrett, P. M. 2009. The affinities of the enigmatic dinosaur *Eshanosaurus deguchiianus* from the Early Jurassic of Yunnan Province, People's Republic of China. *Palaeontology* 52 (4): 681–688.

Barrett, P. M. and Upchurch, P. 1994. Feeding mechanisms of *Diplodocus*. *Gaia* 10: 195–204.

Barrett, P. M., Butler, R. J. and Nesbitt, S. J. 2010. The roles of herbivory and omnivory in early dinosaur evolution. *Earth and Environmental Science Transactions of the Royal Society of Edinburgh* 101 (Special Issue 3-4): 383–396.

Barsbold, R. 1974. Saurornithoididae, a new family of small theropod dinosaurs from central Asia and North America. *Palaeontologia Polonica* 30: 5–22.

Barsbold, R. 1976a. K evolyutsii i sistematike pozdnemezozoyskikh khishchnykh dinozavrov (The evolution and systematics of late Mesozoic carnivorous dinosaurs) (Russian). *The Joint Soviet-Mongolian Paleontological Expedition, Transactions* 3: 68–75.

Barsbold, R. 1976b. On a new Late Cretaceous family of small theropods (Oviraptoridae fam. n.) of Mongolia. *Doklady Akademia Nauk SSSR* 226: 685–688.

Barsbold, R. 1977. On the evolution of carnivorous dinosaurs (in rushian). *Transactions of the Joint Soviet Mongolian Paleontological Expedition* 4: 48–56.

Barsbold, R. 1981. Toothless carnivorous dinosaurs of Mongolia. *Trudy Sovmestnoi Sovetsko-Mongol'skoi Paleontologicheskoi Ekspeditsii* 15: 28–39.

Barsbold, R. 1983. Carnivorous dinosaurs from the Cretaceous of Mongolia. *Transactions of the Joint Soviet-Mongolian Paleontological Expedition* 19: 1–120.

Barsbold, R. 1986. Raubdinosaurier Oviraptoren. *In*: Vorobyeva, E. I. (ed.), *Gerpetologičeskie Issledovaniâ v Mongol'skoi Narodnoj Respublike*, 210–223. Moscow.

Barsbold, R. 1997. Oviraptorosauria. *In*: Currie, P. J. and Padian, K. (eds.), *Encyclopedia of Dinosaurs*, 505–509. Academic Press, San Diego, California.

Barsbold, R. and Perle, A. 1980. Segnosauria, a new infraorder of carnivorous dinosaurs. *Acta Palaeontologica Polonica* 25 (2): 187–195.

Barsbold, R. and Osmólska, H. 1999. The skull of *Velociraptor* (Theropoda) from the Late Cretaceous of Mongolia. *Acta Palaeontologica Polonica* 44 (2): 189–219.

Barsbold, R., Osmólska, H. and Kurzanov, S. M. 1987. On a new troodontid (Dinosauria, Theropoda) from the Early Cretaceous of Mongolia. *Acta Palaeontologica Polonica* 32 (1-2): 121–132.

Baszio, S. 1997. Systematic palaeontology of isolated dinosaur teeth from the latest Cretaceous of south Alberta, Canada. *Courier Forschungsinstitut Senckenberg* 196: 33–77.

Bates, K. T. and Falkingham, P. L. 2012. Estimating maximum bite performance in *Tyrannosaurus rex* using multi-body dynamics. *Biology Letters* 8 (4): 660–664.

Baumel, J. J. 1993. Handbook of Avian Anatomy: Nomina Anatomica Avium. 2nd ed. *Publications of the Nuttall Ornithological Club* 23.

Baumel, J. J. and Witmer, L. M. 1993. Osteologia. *In*: Baumel, J. J. (ed.), *Handbook of Avian Anatomy : Nomina Anatomica Avium*, 45–132. Nuttall Ornithological Club, Cambridge.

Becerra, M. G., Pol, D., Marsicano, C. A. and Rauhut, O. W. M. 2013. The dentition of *Manidens condorensis* (Ornithischia; Heterodontosauridae) from the Jurassic Cañadón Asfalto Formation of Patagonia: morphology, heterodonty and the use of statistical methods for identifying isolated teeth. *Historical Biology* 0 (0): 1–13.

Belvedere, M., Jalil, N.-E., Breda, A., Gattolin, G., Bourget, H., Khaldoune, F. and Dyke, G. J. 2013. Vertebrate footprints from the Kem Kem beds (Morocco): A novel ichnological approach to faunal reconstruction. *Palaeogeography, Palaeoclimatology, Palaeoecology* 383–384: 52–58.

Benedetto, J. L. 1973. Herrerasauridae, nueva familia de saurisquios triásicos. *Ameghiniana* 10 (1): 89–102.

Bennett, S. C. 2001. The osteology and functional morphology of the Late Cretaceous pterosaur *Pteranodon* Part I. General description of osteology. *Palaeontographica Abteilung A* 260 (1-6): 1–112.

Benson, R., Carrano, M. and Brusatte, S. 2010. A new clade of archaic large-bodied predatory dinosaurs (Theropoda: Allosauroidea) that survived to the latest Mesozoic. *Naturwissenschaften* 97 (1): 71–78.

Benson, R. B. J. 2008a. A redescription of '*Megalosaurus*' *hesperis* (Dinosauria, Theropoda) from the Inferior Oolite (Bajocian, Middle Jurassic) of Dorset, United Kingdom. *Zootaxa* 1931: 57–67.

Benson, R. B. J. 2008b. New information on *Stokesosaurus*, a tyrannosauroid (Dinosauria: Theropoda) from North America and the United Kingdom. *Journal of Vertebrate Paleontology* 28 (3): 732–750.

Benson, R. B. J. 2009. An assessment of variability in dinosaur remains from the Bathonian (Middle Jurassic) of Stonesfield and New Park Quarry, UK and taxonomic implications for *Megalosaurus bucklandii* and *Iliosuchus incognitus*. *Palaeontology* 52 (4): 857–877.

Benson, R. B. J. 2010a. A description of *Megalosaurus bucklandii* (Dinosauria: Theropoda) from the Bathonian of the UK and the relationships of Middle Jurassic theropods. *Zoological Journal of the Linnean Society* 158 (4): 882–935.

Benson, R. B. J. 2010b. The osteology of *Magnosaurus nethercombensis* (Dinosauria, Theropoda) from the Bajocian (Middle Jurassic) of the United Kingdom and a re-examination of the oldest records of tetanurans. *Journal of Systematic Palaeontology* 8 (1): 131–146.

Benson, R. B. J., Barrett, P. M., Powell, H. P. and Norman, D. B. 2008. The taxonomic status of *Megalosaurus bucklandii* (Dinosauria, Theropoda) from the Middle Jurassic of Oxfordshire, UK. *Palaeontology* 51 (2): 419–424.

Benton, M. J. 1986. The late Triassic reptile *Teratosaurus*—a rauisuchian, not a dinosaur. *Palaeontology* 29 (2): 293–301.

Benton, M. J. 2005. *Vertebrate Palaeontology (Third edition)*. Wiley-Blackwell, 472pp.

Bertin, T. 2010. A catalogue of material and review of the Spinosauridae. *PalArch's Journal of Vertebrate Palaeontology* 7 (4): 1–39.

Bever, G. S. and Norell, M. A. 2009. The perinate skull of *Byronosaurus* (Troodontidae) with observations on the cranial ontogeny of paravian theropods. *American Museum Novitates* 3657: 1–52.

Bhullar, B.-A. S., Marugán-Lobón, J., Racimo, F., Bever, G. S., Rowe, T. B., Norell, M. A. and Abzhanov, A. 2012. Birds have paedomorphic dinosaur skulls. *Nature* 487 (7406): 223–226.

Bidar, A., Demay, L. and Thomel, G. 1972. *Compsognathus corallestris*: nouvelle espèce de dinosaurien théropode du Portlandien de Canjuers (sud-est de la France). *Annales du Muséum d'Histoire Naturelle de Nice* 1: 9–40.

Bittencourt, J. S. and Kellner, A. W. A. 2009. The anatomy and phylogenetic position of the Triassic dinosaur *Staurikosaurus pricei* Colbert, 1970. *Zootaxa* 2079: 1–56.

Blob, R. W. and Badgley, C. 2007. Numerical methods for bonebed analysis. *In*: Rogers, R. R., Eberth, D. A. and Fiorillo, A. R. (eds.), *Bonebeds: Genesis, Analysis, and Paleobiological Significance*, 333–396. University of Chicago Press, Chicago.

Bock, W. J. 1964. Kinetics of the avian skull. *Journal of Morphology* 114 (1): 1–41.

Bock, W. J. 1999. Avian cranial kinesis revisited. *Acta Ornitologica* 34 (2): 115–122.
Bonaparte, C. L. J. L. 1850. *Conspectus systematum herpetologiae et amphibiologiae*. Editio Altera Reformata [Survey of the systems of reptiles and amphibians. Second revised edition], E. J. Brill, Leyden 1, pp.
Bonaparte, J. F. 1979. Dinosaurs: A Jurassic Assemblage from Patagonia. *Science* 205 (4413): 1377–1379.
Bonaparte, J. F. 1985. A horned Cretaceous carnosaur from Patagonia. *National Geographic Research* 1: 149–151.
Bonaparte, J. F. 1986. Les dinosaures (Carnosaures, Allosauridés, Sauropodes, Cétiosauridés) du Jurassique Moyen de Cerro Cóndor (Chubut, Argentina). *Annales de Paléontologie (Vert.-Invert.)* 72 (3): 247–289.
Bonaparte, J. F. 1991a. Los vertebrados fósiles de la Formación Río Colorado, de la ciudad de Neuquén y cercanías, Cretácico Superior, Argentina. *Revista del Museo Argentino de Ciencias naturales 'Bernardino Rivadavia' e Instituto Nacional de Investigacion de las Ciencias Naturales*. 4 (3): 17–123.
Bonaparte, J. F. 1991b. The Gondwanian theropod families Abelisauridae and Noasauridae. *Historical Biology* 5 (1): 1–25.
Bonaparte, J. F. 1996. Cretaceous tetrapods of Argentina. *Münchener Geowissenschaftliche Abhandlungen, A* 30: 73–130.
Bonaparte, J. F. 1999. Tetrapod faunas from South America and India: a palaeobiogeographic interpretation. *Proceedings of the Indian National Science Association* 65A (3): 427–437.
Bonaparte, J. F. and Powell, J. E. 1980. A continental assemblage of tetrapods from the Upper Cretaceous beds of El Brete, northwestern Argentina (Sauropoda-Coelurosauria-Carnosauria-Aves). *Mémoires de la Société Géologique de France, Nouvelle Série* 139: 19–28.
Bonaparte, J. F. and Novas, F. E. 1985. *Abelisaurus comahuensis*, n.g., Carnosauria del Crétacico Tardio de Patagonia. *Ameghiniana* 21 (2-4): 259–265.
Bonaparte, J. F., Novas, F. E. and Coria, R. A. 1990. *Carnotaurus sastrei* Bonaparte, the horned, lightly built carnosaur from the Middle Cretaceous of Patagonia. *Natural History Museum of Los Angeles County Contributions in Science* 416 (416): 1–42.
Bookstein, F. L. 1997. *Morphometric Tools for Landmark Data: Geometry and Biology*. Cambridge University Press, 459pp.
Bout, R. G. and Zweers, G. A. 2001. The role of cranial kinesis in birds. *Comparative Biochemistry and Physiology Part A: Molecular & Integrative Physiology* 131 (1): 197–205.
Breithaupt, B. H. 1999. The first discoveries of dinosaurs in the American West. *Vertebrate Paleontology in Utah*: 59–65.
Breithaupt, B. H. and Elizabeth, H. 2008. Wyoming's *Dynamosaurus imperiosus* and other early discoveries of *Tyrannosaurus rex* in the rocky mountain West. *In*: Larson, P. L. and Carpenter, K. (eds.), *Tyrannosaurus Rex, the Tyrant King*, 57–61. Indiana University Press, Bloomington, Indiana.
Bremer, K. 1994. Branch support and tree stability. *Cladistics* 10 (3): 295–304.
Briggs, D. E. G. and Crowther, P. R. 2001. *Palaeobiology II*. Blackwell Science, Osney Mead, Oxford; Malden, MA, 583pp.
Brink, K. S. and Reisz, R. R. 2014. Hidden dental diversity in the oldest terrestrial apex predator *Dimetrodon*. *Nature Communications* 5.
Brinkman, D. B. 2008. The structure of Late Cretaceous (late Campanian) nonmarine aquatic communities: a guild analysis of two vertebrate microfossil localities in Dinosaur Provincial Park, Alberta, Canada. *In*: Sankey, J. T. and Baszio, S. (eds.), *Vertebrate Microfossil Assemblages: Their Role in Paleoecology and Paleobiogeography*, 33–60. Bloomington, Indiana.
Bristowe, A. and Raath, M. A. 2004. A juvenile coelophysoid skull from the Early Jurassic of Zimbabwe, and the synonymy of *Coelophysis* and *Syntarsus*. *Palaeontologia Africana* 40: 31–41.
Britt, B. B. 1991. Theropods of Dry Mesa Quarry (Morrison Formation, Late Jurassic), Colorado, with emphasis on the osteology of *Torvosaurus tanneri*. *Brigham Young University Geology Studies* 37: 1–72.
Brochu, C. A. 2003. Osteology of *Tyrannosaurus rex*: Insights from a nearly complete skeleton and high-resolution computed tomographic analysis of the skull. *Journal of Vertebrate Paleontology* 22 (sup4): 1–138.
Brookes, R. 1763. *The Natural History of Waters, Earths, Stones, Fossils, and Minerals, with their Virtues, Properties, and Medicinal Uses: To Which is added, The Method in which LINNAEUS has treated these Subjects*. Vol. 5. J. Newbery, London, pp.
Brusatte, S. and Benson, R. B. J. 2013. The systematics of Late Jurassic tyrannosauroids (Dinosauria: Theropoda) from Europe and North America. *Acta Palaeontologica Polonica* 58 (1): 47–54.
Brusatte, S. L. 2012. *Dinosaur Paleobiology*. Wiley-Blackwell, 336pp.
Brusatte, S. L. and Sereno, P. C. 2007. A new species of *Carcharodontosaurus* (Dinosauria: Theropoda) from the Cenomanian of Niger and a revision of the genus. *Journal of Vertebrate Paleontology* 27 (4): 902–916.

Brusatte, S. L. and Sereno, P. C. 2008. Phylogeny of Allosauroidea (Dinosauria: Theropoda): comparative analysis and resolution. *Journal of Systematic Palaeontology* 6 (2): 155–182.

Brusatte, S. L., Benson, R. B. J. and Hutt, S. 2008. The osteology of *Neovenator salerii* (Dinosauria: Theropoda) from the Wealden Group (Barremian) of the Isle of Wight. *Palaeontographical Society* 162 (631): 1–75.

Brusatte, S. L., Benson, R. B. J. and Norell, M. A. 2011. The anatomy of *Dryptosaurus aquilunguis* (Dinosauria: Theropoda) and a review of its tyrannosauroid affinities. *American Museum Novitates* 3717: 1–53.

Brusatte, S. L., Carr, T. D. and Norell, M. A. 2012a. The osteology of *Alioramus*, a gracile and long-snouted tyrannosaurid (Dinosauria: Theropoda) from the Late Cretaceous of Mongolia. *Bulletin of the American Museum of Natural History* 366: 1–197.

Brusatte, S. L., Butler, R. J., Sulej, T. and Niedźwiedzki, G. 2009a. The taxonomy and anatomy of rauisuchian archosaurs from the Late Triassic of Germany and Poland. *Acta Palaeontologica Polonica* 54 (2): 221–230.

Brusatte, S. L., Benson, R. B. J., Currie, P. J. and Xijin, Z. 2010a. The skull of *Monolophosaurus jiangi* (Dinosauria: Theropoda) and its implications for early theropod phylogeny and evolution. *Zoological Journal of the Linnean Society* 158 (3): 573–607.

Brusatte, S. L., Chure, D. J., Benson, R. B. J. and Xu, X. 2010b. The osteology of *Shaochilong maortuensis*, a carcharodontosaurid (Dinosauria: Theropoda) from the Late Cretaceous of Asia. *Zootaxa* 2334: 1–46.

Brusatte, S. L., Butler, R. J., Prieto-Márquez, A. and Norell, M. A. 2012b. Dinosaur morphological diversity and the end-Cretaceous extinction. *Nature Communications* 3: 804.

Brusatte, S. L., Sakamoto, M., Montanari, S. and Harcourt Smith, W. E. H. 2012c. The evolution of cranial form and function in theropod dinosaurs: insights from geometric morphometrics. *Journal of Evolutionary Biology* 25 (2): 365–377.

Brusatte, S. L., Lloyd, G. T., Wang, S. C. and Norell, M. A. 2014a. Gradual assembly of avian body plan culminated in rapid rates of evolution across the dinosaur-bird transition. *Current Biology* 24 (20): 2386–2392.

Brusatte, S. L., Benson, R. B. J., Carr, T. D., Williamson, T. E. and Sereno, P. C. 2007. The systematic utility of theropod enamel wrinkles. *Journal of Vertebrate Paleontology* 27 (4): 1052–1056.

Brusatte, S. L., Carr, T. D., Erickson, G. M., Bever, G. S. and Norell, M. A. 2009b. A long-snouted, multihorned tyrannosaurid from the Late Cretaceous of Mongolia. *Proceedings of the National Academy of Sciences* 106 (41): 17261–17266.

Brusatte, S. L., Benson, R. B. J., Chure, D. J., Xu, X., Sullivan, C. and Hone, D. W. E. 2009c. The first definitive carcharodontosaurid (Dinosauria: Theropoda) from Asia and the delayed ascent of tyrannosaurids. *Naturwissenschaften* 96 (9): 1051–1058.

Brusatte, S. L., Nesbitt, S. J., Irmis, R. B., Butler, R. J., Benton, M. J. and Norell, M. A. 2010c. The origin and early radiation of dinosaurs. *Earth-Science Reviews* 101 (1–2): 68–100.

Brusatte, S. L., Vremir, M., Csiki-Sava, Z., Turner, A. H., Watanabe, A., Erickson, G. M. and Norell, M. A. 2013. The Osteology of *Balaur bondoc*, an Island-Dwelling Dromaeosaurid (Dinosauria: Theropoda) from the Late Cretaceous of Romania. *Bulletin of the American Museum of Natural History*: 1–100.

Brusatte, S. L., Norell, M. A., Carr, T. D., Erickson, G. M., Hutchinson, J. R., Balanoff, A. M., Bever, G. S., Choiniere, J. N., Makovicky, P. J. and Xu, X. 2010d. Tyrannosaur paleobiology: new research on ancient exemplar organisms. *Science* 329 (5998): 1481–1485.

Brusatte, S. L., Butler, R. J., Barrett, P. M., Carrano, M. T., Evans, D. C., Lloyd, G. T., Mannion, P. D., Norell, M. A., Peppe, D. J., Upchurch, P. and Williamson, T. E. 2014b. The extinction of the dinosaurs. *Biological Reviews*: n/a – n/a.

Buckland, W. 1824. Notice on the *Megalosaurus* or great fossil lizard of Stonesfield. *Transactions of the Geological Society* 21: 390–397.

Buckley, L. G. 2009. Individual and ontogenetic variation in theropod dinosaur teeth: a case study of *Coelophysis bauri* (Theropoda: Coelophysoidea) and implications for identifying isolated theropod teeth. MSc. Dissertation, University of Alberta, Edmonton, Alberta, Canada, 109pp.

Buckley, L. G., Larson, D. W., Reichel, M. and Samman, T. 2010. Quantifying tooth variation within a single population of *Albertosaurus sarcophagus* (Theropoda: Tyrannosauridae) and implications for identifying isolated teeth of tyrannosaurids. *Canadian Journal of Earth Sciences* 47 (9): 1227–1251.

Buffetaut, E. 1989a. Archosaurian reptiles with Gondwanan affinities in the Upper Cretaceous of Europe. *Terra nova* 1 (1): 69–74.

Buffetaut, E. 1989b. New remains of *Spinosaurus* from the Cretaceous of Morocco. *Archosaurian Articulation* 1 (9): 65–68.

Buffetaut, E. 1989c. New remains of the enigmatic dinosaur *Spinosaurus* from the Cretaceous of Morocco and the affinities between *Spinosaurus* and *Baryonyx*. *Neues Jahrbuch für Geologie und Paläontologie, Monatshefte* 2: 79–87.

Buffetaut, E. 1992. Remarks on the Cretaceous theropod dinosaurs *Spinosaurus* and *Baryonyx*. *Neues Jahrbuch für Geologie und Paläontologie, Monatshefte* 2: 88–96.
Buffetaut, E. 1994. *Les Dinosaures*. Presses Universitaires de France - PUF, Paris, 127pp.
Buffetaut, E. 2005. Les premiers dinosaures sahariens. *Pour la Science* (331): 8–11.
Buffetaut, E. 2007. The spinosaurid dinosaur *Baryonyx* (Saurischia, Theropoda) in the Early Cretaceous of Portugal. *Geological Magazine* 144 (6): 1021–1025.
Buffetaut, E. 2010. *Spinosaurs* before Stromer: early finds of spinosaurid dinosaurs and their interpretations. *Geological Society, London, Special Publications* 343 (1): 175–188.
Buffetaut, E. 2011. An early spinosaurid dinosaur from the Late Jurassic of Tendaguru (Tanzania) and the evolution of the spinosaurid dentition. *Oryctos* 10: 1–8.
Buffetaut, E. and Ingavat, R. 1986. Unusual theropod dinosaur teeth from the Upper Jurassic of Phu Wiang, northeastern Thailand. *Revue de Paléobiologie* 5 (2): 217–220.
Buffetaut, E. and Ouaja, M. 2002. A new specimen of *Spinosaurus* (Dinosauria, Theropoda) from the Lower Cretaceous of Tunisia, with remarks on the evolutionary history of the Spinosauridae. *Bulletin de la Societe Geologique de France* 173 (5): 415–421.
Buffetaut, E., Mechin, P. and Mechin-Salessy, A. 1988. Un dinosaure théropode d'affinités gondwaniennes dans le Crétacé supérieur de Provence. *Comptes rendus de l'Académie des sciences. Série 2, Mécanique, Physique, Chimie, Sciences de l'univers, Sciences de la Terre* 306 (2): 153–158.
Buffetaut, E., Suteethorn, V. and Tong, H. 1996. The earliest known tyrannosaur from the Lower Cretaceous of Thailand. *Nature* 381 (6584): 689–691.
Buffetaut, E., Martill, D. and Escuillié, F. 2004. Pterosaurs as part of a spinosaur diet. *Nature* 430 (6995): 33–33.
Buffetaut, E., Escuillié, F. and Pohl, B. 2005a. First theropod dinosaur from the Maastrichtian phosphates of Morocco. *Kaupia* 14: 3–8.
Buffetaut, E., Escuillié, F. and Pohl, B. 2005b. First theropod dinosaur from the Maastrichtian phosphates of Morocco. *Kaupia* 14: 3–8.
Buffetaut, E., Suteethorn, V., Tong, H. and Amiot, R. 2008. An Early Cretaceous spinosaurid theropod from southern China. *Geological Magazine* 145 (5): 745–748.
Buffetaut, E., Grellet-Tinner, G., Suteethorn, V., Cuny, G., Tong, H., Košir, A., Cavin, L., Chitsing, S., Griffiths, P. J., Tabouelle, J. and Loeuff, J. L. 2005c. Minute theropod eggs and embryo from the Lower Cretaceous of Thailand and the dinosaur-bird transition. *Naturwissenschaften* 92 (10): 477–482.
Bühler, P. 1981. Functional anatomy of the avian jaw apparatus. *Form and function in birds* 2: 439–468.
Bühler, P., Martin, L. D. and Witmer, L. M. 1988. Cranial kinesis in the Late Cretaceous birds Hesperornis and Parahesperornis. *The Auk* 105 (1): 111–122.
Bühler, P., Hecht, M. K., Ostrom, J. H., Viohl, G. and Wellnhofer, P. 1985. On the morphology of the skull of *Archaeopteryx*. *The Beginnings of Birds*: 135–140.
Burch, S. H. and Carrano, M. T. 2012. An articulated pectoral girdle and forelimb of the abelisaurid theropod *Majungasaurus crenatissimus* from the Late Cretaceous of Madagascar. *Journal of Vertebrate Paleontology* 32 (1): 1–16.
Burnham, D. A. 2004. New Information on *Bambiraptor feinbergi* (Theropoda: Dromaeosauridae) from the Late Cretaceous of Montana. *In*: Currie, P. J., Koppelhus, E. B., Shugar, M. A. and Wright, J. L. (eds.), *Feathered Dragons: Studies on the Transition from Dinosaurs to Birds*, 67–111. Indiana University Press, Bloomington, Indiana.
Burnham, D. A., Derstler, K. L., Currie, P. J., Bakker, R. T., Zhou, Z. and Ostrom, J. H. 2000. Remarkable new birdlike dinosaur (Theropoda: Maniraptora) from the Upper Cretaceous of Montana. *The Paleontological Institute, The University of Kansas* 13: 1–14.
Buscalioni, A. D., Gasparini, Z., Pérez-Moreno, B. P. and Sanz, J. L. 1997. Argentinean theropods: first morphological analysis on isolated teeth. *Proceedings from the First European Workshop on Vertebrate Palaeontology. Geological Museum, Copenhagen University, 1– 4 May 1996*.
Butler, R. J. and Upchurch, P. 2007. Highly incomplete taxa and the phylogenetic relationships of the theropod dinosaur *Juravenator starki*. *Journal of Vertebrate Paleontology* 27 (1): 253–256.
Calvo, J. O. and Coria, R. 1998. New specimen of *Giganotosaurus carolinii* (Coria & Salgado, 1995), supports it as the largest theropod ever found. *Gaia* 15: 117–122.
Canale, J. I., Novas, F. E. and Pol, D. 2014. Osteology and phylogenetic relationships of *Tyrannotitan chubutensis* Novas, de Valais, Vickers-Rich and Rich, 2005 (Theropoda: Carcharodontosauridae) from the Lower Cretaceous of Patagonia, Argentina. *Historical Biology* 0 (0): 1–32.
Canale, J. I., Scanferla, C. A., Agnolín, F. L. and Novas, F. E. 2009. New carnivorous dinosaur from the Late Cretaceous of NW Patagonia and the evolution of abelisaurid theropods. *Naturwissenschaften* 96 (3): 409–414.

Candeiro, C. R., Currie, P. J. and Bergqvist, L. P. 2012. Theropod teeth from the Marília Formation (late Maastrichtian) at the paleontological site of Peirópolis in Minas Gerais State, Brazil. *Brazilian Journal of Geology* 42 (2): 323–330.

Candeiro, C. R. A. 2007. Padrões morfológicos dos dentes de Abelisauroidea y Carcharodontosauridae (Therópoda, Dinosauria) do Cretáceo da América do Sul. Ph.D. Dissertation, Universidade Federal do Rio de Janeiro, Departamento de Geología, Rio de Janeiro, Brazil, 180pp.

Candeiro, C. R. A. and Martinelli, A. G. 2005. Abelisauroidea and Carcharodontosauridae (Theropoda, Dinosauria) in the Cretaceous of South America. Paleogeographical and geocronological implications. *Sociedade e Natureza, Uberlândia* 17 (33): 5–19.

Candeiro, C. R. A. and Tanke, D. H. 2008. A pathological Late Cretaceous carcharodontosaurid tooth from Minas Gerais, Brazil. *Bulletin of Geosciences* 83 (3): 351–354.

Canudo, J. I., Ruiz-Omeñaca, J. I., Aurell, M., Barco, J. L. and Cuenca-Bescos, G. 2006. A megatheropod tooth from the late Tithonian-middle Berriasian (Jurassic Cretaceous transition) of Galve (Aragon, NE Spain). *Neues Jahrbuch für Geologie und Paläontologie, Abhandlungen* 239 (3): 77.

Canudo, J. I., Filippi, L., Salgado, L., Garrido, A., Cerda, I., García, R. and Otero, A. 2009. Dientes de terópodos asociados con una carcasa de saurópodo en el Cretácico Superior (Formación Plottier) de Rincón de los Sauces (Patagonia, Argentina). *Colectivo Arqueológico-Paleontológico Salense (CAS)(ed.). Burgos, Actas de las IV Jornadas Internacionales sobre Paleontología de Dinosaurios y su entorno, Sala de los infantes*: 321–330.

Carabajal, A. P. 2011. The braincase anatomy of *Carnotaurus sastrei* (Theropoda: Abelisauridae) from the Upper Cretaceous of Patagonia. *Journal of Vertebrate Paleontology* 31 (2): 378–386.

Carpenter, K. 1982. Baby dinosaurs from the Late Cretaceous Lance and Hell Creek formations and a description of a new species of theropod. *Contributions to Geology, University of Wyoming* 20 (2): 123–134.

Carpenter, K. 1992. Tyrannosaurids (Dinosauria) of Asia and North America. *Aspects of Nonmarine Cretaceous Geology. China Ocean Press, Beijing*: 250–268.

Carpenter, K. 1998. Evidence of predatory behavior by carnivorous dinosaurs. *Gaia* 15: 135–144.

Carpenter, K., Hirsch, K. F. and Horner, J. R. 1996. *Dinosaur Eggs and Babies*. Cambridge University Press, 394pp.

Carpenter, K., Miles, C., Ostrom, J. H. and Cloward, K. 2005a. Redescription of the small maniraptoran theropods *Ornitholestes* and *Coelurus* from the Upper Jurassic Morrison Formation of Wyoming. *In*: Carpenter, K. (ed.), *The Carnivorous Dinosaurs*, 49–71. Indiana University Press, Bloomington, Indiana.

Carpenter, K., Sanders, F., McWhinney, L. A. and Wood, L. 2005b. Evidence for Predator-Prey Relationships. *In*: Carpenter, K. (ed.), *The Carnivorous Dinosaurs*, 325–350. Bloomington, Indiana.

Carrano, M. T. and Sampson, S. D. 2004. A review of coelophysoids (Dinosauria: Theropoda) from the Lower Jurassic of Europe, with Comments on the Late History of the Coelophysoidea. *Neues Jahrbuch für Geologie und Paläontologie Monatshefte* 2004 (9): 537–558.

Carrano, M. T. and Sampson, S. D. 2008. The phylogeny of Ceratosauria (Dinosauria: Theropoda). *Journal of Systematic Palaeontology* 6 (2): 183–236.

Carrano, M. T., Sampson, S. D. and Forster, C. A. 2002. The osteology of *Masiakasaurus knopfleri*, a small abelisauroid (Dinosauria: Theropoda) from the Late Cretaceous of Madagascar. *Journal of Vertebrate Paleontology* 22 (3): 510–534.

Carrano, M. T., Hutchinson, J. R. and Sampson, S. D. 2005. New information on *Segisaurus halli*, a small theropod dinosaur from the Early Jurassic of Arizona. *Journal of Vertebrate Paleontology* 25 (4): 835–849.

Carrano, M. T., Wilson, J. A. and Barrett, P. M. 2010. The history of dinosaur collecting in central India, 1828–1947. *Geological Society, London, Special Publications* 343 (1): 161–173.

Carrano, M. T., Loewen, M. A. and Sertich, J. J. W. 2011. New materials of *Masiakasaurus knopfleri* Sampson, Carrano, and Forster, 2001, and implications for the morphology of the Noasauridae (Theropoda: Ceratosauria). *Smithsonian Contributions to Paleobiology* 95: 1–53.

Carrano, M. T., Benson, R. B. J. and Sampson, S. D. 2012. The phylogeny of Tetanurae (Dinosauria: Theropoda). *Journal of Systematic Palaeontology* 10 (2): 211–300.

Carroll, R. L. 1988. *Vertebrate Paleontology and Evolution*. W. H. Freeman and Company, 698pp.

Carr, T. D. 1996. Cranial osteology and craniofacial ontogeny of Tyrannosauridae (Dinosauria: Theropoda) from the Dinosaur Park Formation (Judith River Group, Upper Cretaceous, Campanian) of Alberta. MSc. Dissertation, University of Toronto, Toronto, Ontario, Canada, 358pp.

Carr, T. D. 1999. Craniofacial ontogeny in Tyrannosauridae (Dinosauria, Coelurosauria). *Journal of Vertebrate Paleontology* 19 (3): 497–520.

Carr, T. D. and Williamson, T. E. 2004. Diversity of late Maastrichtian Tyrannosauridae (Dinosauria: Theropoda) from western North America. *Zoological Journal of the Linnean Society* 142 (4): 479–523.
Carr, T. D. and Williamson, T. E. 2010. *Bistahieversor sealeyi*, gen. et sp. nov., a new tyrannosauroid from New Mexico and the origin of deep snouts in Tyrannosauroidea. *Journal of vertebrate Paleontology* 30 (1): 1–16.
Carr, T. D., Williamson, T. E. and Schwimmer, D. R. 2005. A new genus and species of tyrannosauroid from the Late Cretaceous (Middle Campanian) Demopolis Formation of Alabama. *Journal of Vertebrate Paleontology* 25 (1): 119–143.
Casal, G., Candeiro, C. R. A., Martínez, R., Ivany, E. and Ibiricu, L. 2009. Dientes de Theropoda (Dinosauria: Saurischia) de la Formación Bajo Barreal, Cretácico Superior, Provincia del Chubut, Argentina. *Geobios* 42 (5): 553–560.
Castanhinha, R. and Mateus, O. 2006. On the left-right asymmetry in dinosaurs. *Journal of Vertebrate Paleontology* 26: 48A.
Catalano, S. A. and Goloboff, P. A. 2012. Simultaneously Mapping and Superimposing Landmark Configurations with Parsimony as Optimality Criterion. *Systematic Biology* 61 (3): 392–400.
Catalano, S. A., Goloboff, P. A. and Giannini, N. P. 2010. Phylogenetic morphometrics (I): the use of landmark data in a phylogenetic framework. *Cladistics* 26 (5): 539–549.
Cau, A. and Maganuco, S. 2009. A new theropod dinosaur, represented by a single unusual caudal vertebra, from the Kem Kem Beds (Cretaceous) of Morocco. *Atti della Società italiana di scienze naturali e del museo civico di storia naturale di Milano* 150 (2): 239–257.
Cau, A., Vecchia, F. M. D. and Fabbri, M. 2012. Evidence of a new carcharodontosaurid from the Upper Cretaceous of Morocco. *Acta Palaeontologica Polonica* 57 (3): 661–665.
Cau, A., Dalla Vecchia, F. M. and Fabbri, M. 2013. A thick-skulled theropod (Dinosauria, Saurischia) from the Upper Cretaceous of Morocco with implications for carcharodontosaurid cranial evolution. *Cretaceous Research* 40: 251–260.
Cavin, L., Tong, H., Boudad, L., Meister, C., Piuz, A., Tabouelle, J., Aarab, M., Amiot, R., Buffetaut, E., Dyke, G. and others. 2010. Vertebrate assemblages from the early Late Cretaceous of southeastern Morocco: an overview. *Journal of African Earth Sciences* 57 (5): 391–412.
Chabou, M. C., Laghouag, M. Y. and Bendaoud, A. 2015. Dinosaur track sites in Algeria: A significant national geological heritage in danger. *In*: Errami, E., Brocx, M. and Semeniuk, V. (eds.), *From Geoheritage to Geoparks*, 157–166. Springer International Publishing.
Charig, A. J. and Milner, A. C. 1986. *Baryonyx*, a remarkable new theropod dinosaur. *Nature* 324 (6095): 359–361.
Charig, A. J. and Milner, A. C. 1990. The systematic position of *Baryonyx walkeri*, in the light of Gauthier's reclassification of the Theropoda. *In*: Carpenter, K. and Currie, P. J. (eds.), *Dinosaur Systematics: Approaches and Perspectives*, 127–140. Cambridge University Press, New York, New York.
Charig, A. J. and Milner, A. C. 1997. *Baryonyx walkeri*, a fish-eating dinosaur from the Wealden of Surrey. *Bulletin of the Natural History Museum* 53 (1): 11–70.
Chatterjee, S. 1991. Cranial anatomy and relationships of a new Triassic bird from Texas. *Philosophical Transactions: Biological Sciences* 332 (1265): 277–342.
Chatterjee, S. 1995. The Triassic bird Protoavis. *Archaeopteryx* 13: 15–31.
Chatterjee, S. 1997. *The Rise of Birds: 225 Million Years of Evolution*. Johns Hopkins University Press, Baltimore, Maryland, 312pp.
Chiappe, L. M. 2001. Phylogenetic relationships among basal birds. *In*: Gauthier, J. and Gall, L. F. (eds.), *New Perspectives on the Origin and Early Evolution of Birds: Proceedings of the International Symposium in Honor of John H. Ostrom*, 125–139. Yale Univ Peabody Museum.
Chiappe, L. M. and Witmer, L. M. 2002. *Mesozoic Birds: Above the Heads of Dinosaurs*. University of California Press, 548pp.
Chiappe, L. M. and Göhlich, U. B. 2010. Anatomy of *Juravenator starki* (Theropoda: Coelurosauria) from the Late Jurassic of Germany. *Neues Jahrbuch für Geologie und Paläontologie Abhandlungen* 258 (3): 257–296.
Chiappe, L. M., Norell, M. A. and Clark, J. M. 1996. Phylogenetic position of *Mononykus* (Aves: Alvarezsauridae) from the Late Cretaceous of the Gobi Desert. *Memoirs of the Queensland Museum* 39: 557–582.
Chiappe, L. M., Norell, M. A. and Clark, J. M. 1998. The skull of a relative of the stem-group bird *Mononykus*. *Nature* 392 (6673): 275–278.
Chiappe, L. M., Norell, M. A. and Clark, J. M. 2002. The Cretaceous, short-armed Alvarezsauridae: *Mononykus* and its kin. *In*: Chiappe, L. M. and Witmer, L. M. (eds.), *Mesozoic Birds: Above the Heads of Dinosaurs*, 87–120. University of California Press.

Choiniere, J. N., Forster, C. A. and de Klerk, W. J. 2012. New information on *Nqwebasaurus thwazi*, a coelurosaurian theropod from the Early Cretaceous Kirkwood Formation in South Africa. *Journal of African Earth Sciences* 71–72: 1–17.

Choiniere, J. N., Clark, J. M., Forster, C. A. and Xu, X. 2010a. A basal coelurosaur (Dinosauria: Theropoda) from the Late Jurassic (Oxfordian) of the Shishugou Formation in Wucaiwan, People's Republic of China. *Journal of Vertebrate Paleontology* 30 (6): 1773–1796.

Choiniere, J. N., Clark, J. M., Norell, M. and Xu, X. 2014a. Cranial osteology of *Haplocheirus sollers* Choiniere et al., 2010 (Theropoda, Alvarezsauroidea). *American Museum Novitates* 3816.

Choiniere, J. N., Xu, X., Clark, J. M., Forster, C. A., Guo, Y. and Han, F. 2010b. A basal alvarezsauroid theropod from the Early Late Jurassic of Xinjiang, China. *Science* 327 (5965): 571–574.

Choiniere, J. N., Clark, J. M., Forster, C. A., Norell, M. A., Eberth, D. A., Erickson, G. M., Chu, H. and Xu, X. 2014b. A juvenile specimen of a new coelurosaur (Dinosauria: Theropoda) from the Middle–Late Jurassic Shishugou Formation of Xinjiang, People's Republic of China. *Journal of Systematic Palaeontology* 12 (2): 177–215.

Choubert, G. 1948. Essai sur la paléogéographie du Mésocrétacé marocain. *Volume Jubilaire de la Société des Sciences Naturelles du Maroc*: 307–329.

Christiansen, P. and Fariña, R. A. 2004. Mass prediction in theropod dinosaurs. *Historical Biology* 16 (2-4): 85–92.

Chure, D. J. 1994. *Koparion douglassi*, a new dinosaur from the Morrison Formation (Upper Jurassic) of Dinosaur National Monument; the oldest troodontid (Theropoda: Maniraptora). *Brigham Young University Geology Studies* 40 (1): 11–15.

Chure, D. J. 1995. A reassessment of the gigantic theropod *Saurophagus maximus* from the Morrison Formation (Upper Jurassic) of Oklahoma, USA. *Sixth Symposium on Mesozoic Terrestrial Ecosystems and Biota, Short Papers*: 103–106.

Chure, D. J. 2000. A new species of *Allosaurus* from the Morrison Formation of Dinosaur National Monument (Utah-Colorado) and a revision of the theropod family Allosauridae. Ph.D. Dissertation, Columbia University, New York, New York., 909pp.

Chure, D. J. 2001. The second record of the African theropod *Elaphrosaurus* (Dinosauria, Ceratosauria) from the Western Hemisphere. *Neues Jahrbuch fur Geologie und Palaontologie-Monatshefte* 2001 (9): 565–576.

Chure, D. J., Litwin, R., Hasiotis, S. T., Evanoff, E. and Carpenter, K. 2006. The fauna and flora of the Morrison Formation: 2006. *New Mexico Museum of Natural History and Science Bulletin* 36: 233–249.

Cillari, A. 2010. Teeth of Theropoda (Dinosauria, Saurischia): morphology, function and classification. Ph.D. Dissertation, Scienze della Terra, Sapienza Universitá di Roma, Rome, 193pp.

Clark, J. M., Perle, A. and Norell, M. 1994. The skull of *Erlicosaurus andrewsi*, a late Cretaceous 'Segnosaur' (Theropoda, Therizinosauridae) from Mongolia. *American Museum Novitates* 3115: 1–39.

Clark, J. M., Norell, M. and Chiappe, L. M. 1999. An oviraptorid skeleton from the late Cretaceous of Ukhaa Tolgod, Mongolia, preserved in an avianlike brooding position over an oviraptorid nest. *American Museum Novitates* 3265: 1–36.

Clark, J. M., Norell, M. A. and Barsbold, R. 2001. Two new oviraptorids (Theropoda: Oviraptorosauria), Upper Cretaceous Djadokhta Formation, Ukhaa Tolgod, Mongolia. *Journal of Vertebrate Paleontology* 21 (2): 209–213.

Clark, J. M., Norell, M. A. and Rowe, T. 2002. Cranial anatomy of *Citipati osmolskae* (Theropoda, Oviraptorosauria), and a reinterpretation of the holotype of *Oviraptor philoceratops*. *American Museum Novitates* 3364: 1–24.

Clark, J. M., Maryańska, T. and Barsbold, R. 2004. Therizinosauroidea. *In*: Weishampel, D. B., Dodson, P. and Osmólska, H. (eds.), *The Dinosauria, Second Edition*, 151–164. University of California Press, Berkeley, California.

Cobos, A., Lockley, M. G., Gascó, F., Royo–Torres, R. and Alcalá, L. 2014. Megatheropods as apex predators in the typically Jurassic ecosystems of the Villar del Arzobispo Formation (Iberian Range, Spain). *Palaeogeography, Palaeoclimatology, Palaeoecology* 399: 31–41.

Colbert, E. H. 1964. Relationships of the saurischian dinosaurs. *American Museum Novitates* 2181.

Colbert, E. H. 1989. The Triassic dinosaur *Coelophysis*. *Museum of Northern Arizona Bulletin* 57: 1–174.

Colbert, E. H. 1990. Variation in *Coelophysis bauri*. *In*: Carpenter, K. and Currie, P. J. (eds.), *Dinosaur Systematics: Approaches and Perspectives*, 81–90. Cambridge University Press, New York, New York.

Colbert, E. H. and Russell, D. A. 1969. The small Cretaceous dinosaur *Dromaeosaurus*. *American Museum Novitates* 2380: 1–49.

Coombs Jr, W. P. 1982. Juvenile specimens of the ornithischian dinosaur *Psittacosaurus*. *Palaeontology* 25 (1): 89–107.

Cope, E. D. 1866. [On the anomalous relations existing between the tibia and fibula in certain of the Dinosauria]. *Proceedings of the Academy of Natural Sciences of Philadelphia* 18: 316–317.

Cope, E. D. 1871. On the homologies of some of the cranial bones of the Reptilia, and on the systematic arrangement of the class. *Proceedings of the American Association for the Advancement of Science* 1870: 194–247.
Cope, E. D. 1876a. On some extinct reptiles and Batrachia from the Judith River and Fox Hills Beds of Montana. *Proceedings of the Academy of Natural Sciences of Philadelphia* 28: 340–359.
Cope, E. D. 1876b. Descriptions of some vertebrate remains from the Fort Union beds of Montana. *Proceedings of the Academy of Natural Sciences of Philadelphia* 28: 248–261.
Cope, E. D. 1877. Descriptions of extinct vertebrata from the Permian and Triassic Formamations of the United States. *Proceedings of the American Philosophical Society* 17 (100): 182–193.
Cope, E. D. 1887. The dinosaur genus *Coelurus*. *American Naturalist* 21: 367–369.
Cope, E. D. 1889. On a new genus of Triassic Dinosauria. *American Naturalist* 23: 626.
Coria, R. A. and Salgado, L. 1995. A new giant carnivorous dinosaur from the Cretaceous of Patagonia. *Nature* 377 (6546): 224–226.
Coria, R. A. and Salgado, L. 1996. '*Loncosaurus argentinus*' Ameghino, 1899 (Ornithischia, Ornithopoda): a revised description with comments on its phylogenetic relationships. *Ameghiniana* 33 (4): 373–376.
Coria, R. A. and Salgado, L. 1998. A basal Abelisauria Novas, 1992 (Theropoda-Ceratosauria) from the Cretaceous of Patagonia, Argentina. *Gaia* 15: 89–102.
Coria, R. A. and Currie, P. J. 2006. A new carcharodontosaurid (Dinosauria, Theropoda) from the Upper Cretaceous of Argentina. *Geodiversitas* 28 (1): 71–118.
Coria, R. A., Chiappe, L. M. and Dingus, L. 2002. A new close relative of *Carnotaurus sastrei* Bonaparte 1985 (Theropoda: Abelisauridae) from the Late Cretaceous of Patagonia. *Journal of Vertebrate Paleontology* 22 (2): 460–465.
Cracraft, J. 1986. The origin and early diversification of birds. *Paleobiology* 12 (4): 383–399.
Csiki-Sava, Z., Buffetaut, E., Ősi, A., Pereda-Suberbiola, X. and Brusatte, S. L. 2015. Island life in the Cretaceous - faunal composition, biogeography, evolution, and extinction of land-living vertebrates on the Late Cretaceous European archipelago. *ZooKeys* 469: 1–161.
Csiki, Z., Vremir, M., Brusatte, S. L. and Norell, M. A. 2010. An aberrant island-dwelling theropod dinosaur from the Late Cretaceous of Romania. *Proceedings of the National Academy of Sciences* 107 (35): 15357–15361.
Cuff, A. R. and Rayfield, E. J. 2013. Feeding mechanics in spinosaurid theropods and extant crocodilians. *PLoS ONE* 8 (5): e65295.
Cúneo, R., Ramezani, J., Scasso, R., Pol, D., Escapa, I., Zavattieri, A. M. and Bowring, S. A. 2013. High-precision U–Pb geochronology and a new chronostratigraphy for the Cañadón Asfalto Basin, Chubut, central Patagonia: Implications for terrestrial faunal and floral evolution in Jurassic. *Gondwana Research* 24 (3–4): 1267–1275.
Currie, P. J. 1985. Cranial anatomy of *Stenonychosaurus inequalis* (Saurischia, Theropoda) and its bearing on the origin of birds. *Canadian Journal of Earth Sciences* 22 (11): 1643–1658.
Currie, P. J. 1987. Bird-like characteristics of the jaws and teeth of troodontid theropods (Dinosauria, Saurischia). *Journal of Vertebrate Paleontology* 7 (1): 72–81.
Currie, P. J. 1995. New information on the anatomy and relationships of *Dromaeosaurus albertensis* (Dinosauria: Theropoda). *Journal of Vertebrate Paleontology* 15 (3): 576–591.
Currie, P. J. 2003. Cranial anatomy of tyrannosaurid dinosaurs from the Late Cretaceous of Alberta, Canada. *Acta Palaeontologica Polonica* 48 (2): 191–226.
Currie, P. J. 2004. *Feathered Dragons: Studies on the Transition from Dinosaurs to Birds*. Indiana University Press, Bloomington, Indiana, 400pp.
Currie, P. J. 2006. On the quadrate of *Sinraptor dongi* (Theropoda: Allosauroidea) from the Late Jurassic of China. *Mesozoic and Cenozoic Vertebrates and Paleoenvironments. Tributes to the career of Prof. Dan Grigorescu*: 111–115.
Currie, P. J. and Zhao, X.-J. 1993a. A new carnosaur (Dinosauria, Theropoda) from the Jurassic of Xinjiang, People's Republic of China. *Canadian Journal of Earth Sciences* 30 (10): 2037–2081.
Currie, P. J. and Zhao, X.-J. 1993b. A new troodontid (Dinosauria, Theropoda) braincase from the Dinosaur Park Formation (Campanian) of Alberta. *Canadian Journal of Earth Sciences* 30 (10): 2231–2247.
Currie, P. J. and Padian, K. 1997. *Encyclopedia of Dinosaurs*. Academic Press, San Diego, California, 869pp.
Currie, P. J. and Carpenter, K. 2000. A new specimen of *Acrocanthosaurus atokensis* (Theropoda, Dinosauria) from the Lower Cretaceous Antlers Formation (Lower Cretaceous, Aptian) of Oklahoma, USA. *Geodiversitas* 22 (2): 207–246.
Currie, P. J. and Chen, P. 2001. Anatomy of *Sinosauropteryx prima* from Liaoning, northeastern China. *Canadian Journal of Earth Sciences* 38 (12): 1705–1727.
Currie, P. J. and Dong, Z. 2001a. New information on Cretaceous troodontids (Dinosauria, Theropoda) from the People's Republic of China. *Canadian Journal of Earth Sciences* 38 (12): 1753–1766.

Currie, P. J. and Dong, Z. 2001b. New information on *Shanshanosaurus huoyanshanensis*, a juvenile tyrannosaurid (Theropoda, Dinosauria) from the Late Cretaceous of China. *Canadian Journal of Earth Sciences* 38 (12): 1729–1737.

Currie, P. J. and Varricchio, D. J. 2004. A new dromaeosaurid from the Horseshoe Canyon Formation (upper Cretaceous) of Alberta, Canada. *In*: Currie, P. J., Koppelhus, E. B., Shugar, M. A. and Wright, J. L. (eds.), *Feathered Dragons: Studies on the Transition from Dinosaurs to Birds.*, 112–132. Bloomington, Indiana.

Currie, P. J. and Azuma, Y. 2006. New specimens, including a growth series, of *Fukuiraptor* (Dinosauria, Theropoda) from the Lower Cretaceous Kitadani Quarry of Japan. *Journal of the Paleontological Society of Korea* 22 (1): 173–193.

Currie, P. J., Rigby, J. K. J. and Sloan, R. E. 1990. Theropod teeth from the Judith River Formation of southern Alberta, Canada. *In*: Carpenter, K. and Currie, P. J. (eds.), *Dinosaur Systematics: Approaches and Perspectives*, 107–125. Cambridge University Press, New York, New York.

Cuvier, G. 1805. *Leçons d'Anatomie Comparée: La Première Partie des Organes de la Digestion*. Crochard, 600pp.

Cuvier, G. 1808. Sur les ossements fossiles de crocodiles: et particulièrement sur ceux des environs du Havre et de Honfleur, avec des remarques sur les squelettes des Sauriens de la Thuringe. *Annales du Muséum d'Histoire naturelle de Paris* XII: 73–110.

Cuvier, G. 1812. *Recherches sur les ossemens fossiles de quadrupèdes, où l'on rétablit les caractères de plusieurs espèces d'animaux que les révolutions du globe paroissent avoir détruites.* Chez Deterville, 486pp.

Cuvier, G. 1824. *Recherches sur les ossemens fossiles, où l'on rétablit les caractères de plusieurs animaux dont les révolutions du globe ont détruit les espèces*. chez G. Dufour et E. D'Ocagne, libraires, quai Voltaire, 630pp.

Czerkas, S. A. and Yuan, C. 2002. An arboreal maniraptoran from northeast China. *Feathered Dinosaurs and the Origin of Flight. The Dinosaur Museum Journal 1. The Dinosaur Museum, Blanding, UT* 1: 63–95.

D'Amore, D. C. 2009. A functional explanation for denticulation in theropod dinosaur teeth. *The Anatomical Record: Advances in Integrative Anatomy and Evolutionary Biology* 292 (9): 1297–1314.

D'Amore, D. C. and Blumenschine, R. J. 2009. Komodo monitor (*Varanus komodoensis*) feeding behavior and dental function reflected through tooth marks on bone surfaces, and the application to ziphodont paleobiology. *Paleobiology* 35 (4): 525–552.

Dantas, P., Sanz, J., Marques da Silva, C., Ortega, F., Santos, V. and Cachão, M. 1998. *Lourinhasaurus* n. gen. novo dinossáurio saurópode do Jurássico superior (Kimeridgiano superior-Titoniano inferior) de Portugal. *Actas do V Congresso Nacional de Geologia.-Com. Inst. Geol. Mineiro* 84: 91–94.

Delair, J. B. and Sarjeant, W. A. 1975. The earliest discoveries of dinosaurs. *Isis*: 5–25.

Delair, J. B. and Sarjeant, W. A. S. 2002. The earliest discoveries of dinosaurs: the records re-examined. *Proceedings of the Geologists' Association* 113 (3): 185–197.

Depéret, C. 1896a. Note sur les dinosauriens sauropodes et théropodes du Crétacé supérieur de Madagascar. *Bulletin de la Société Géologique de France* 21: 176–194.

Depéret, C. 1896b. Sur l'existence de dinosauriens, sauropodes et théropodes dans le Crétacé supérieur de Madagascar. *Comptes Rendus de l'Académie des Sciences (Paris), Série II* 122: 483–485.

Depéret, C. and Savornin, J. 1925. Sur la découverte d'une faune de vertébrés albiens à Timimoun (Sahara occidental). *Comptes Rendus Hebdomadaires des Séances de l'Académie des Sciences à Paris* 181: 1108–1111.

Depéret, C. and Savornin, J. 1927. La faune de reptiles et de poissons albiens de Timimoun (Sahara algérien). *Bulletin de la Société Géologique de France, 4e Série* 27 (4e série): 257–265.

Dong, Z., Zhou, S. W. and Zhang, Y. 1983. Dinosaurs from the Jurassic of Sichuan. *Palaeontologica Sinica, New Series C* 162 (23): 1–136.

Dong, Z.-M. 2003. Contributions of new dinosaur materials from China to dinosaurology. *Memoir of the Fukui Prefectural Dinosaur Museum* 2: 123–131.

Downs, A. 2000. *Coelophysis bauri* and *Syntarsus rhodesiensis* compared, with comments on the preparation and preservation of fossils from the Ghost Ranch *Coelophysis* Quarry. *New Mexico Museum of Natural History and Science Bulletin* 17: 33–38.

Dufeau, D. L. 2003. The cranial anatomy of the theropod dinosaur *Shuvuuia deserti* (Coelurosauria: Alvarezsauridae), and its bearing upon coelurosaurian phylogeny. MSc. Dissertation, University of Texas, Austin, Texas, 275pp.

Dufeau, D. L. 2011. The Evolution of Cranial Pneumaticity in Archosauria: Patterns of Paratympanic Sinus Development. Ph.D. Dissertation, Ohio University, Athens, Ohio, USA, 175pp.

Dutheil, D. B. 1999. An overview of the freshwater fish fauna from the Kem Kem beds (Late Cretaceous: Cenomanian) of southeastern Morocco. *Mesozoic fishes* 2: 553–563.

Dyke, G. J. 2010. Palaeoecology: different dinosaur ecologies in deep time? *Current Biology* 20 (22): R983–R985.
Eastman, C. R. 1899. Descriptions of new species of *Diplodus* teeth from the Devonian of Northeastern Illinois. *The Journal of Geology* 7 (5): 489–493.
Eaton, G. F. 1910. Osteology of *Pteranodon*. *Memoirs of the Connecticut Academy of Arts and Sciences* 2: 1–38.
Eddy, D. R. and Clarke, J. A. 2011. New information on the cranial anatomy of *Acrocanthosaurus atokensis* and its implications for the phylogeny of Allosauroidea (Dinosauria: Theropoda). *PLoS ONE* 6 (3): e17932.
Elzanowski, A. and Wellnhofer, P. 1993. Skull of *Archaeornithoides* from the Upper Cretaceous of Mongolia. *American Journal of Science* 293 (A): 235–252.
Elzanowski, A. and Wellnhofer, P. 1996. Cranial morphology of *Archaeopteryx*: evidence from the seventh skeleton. *Journal of Vertebrate Paleontology* 16 (1): 81–94.
Elzanowski, A. and Stidham, T. A. 2010. Morphology of the quadrate in the Eocene anseriform *Presbyornis* and extant galloanserine birds. *Journal of Morphology* 271 (3): 305–323.
Elzanowski, A., Paul, G. S. and Stidham, T. A. 2001. An avian quadrate from the Late Cretaceous Lance formation of Wyoming. *Journal of Vertebrate Paleontology* 20 (4): 712–719.
Erickson, G. M. 1995. Split carinae on tyrannosaurid teeth and implications of their development. *Journal of Vertebrate Paleontology* 15 (2): 268–274.
Erickson, G. M. 1996. Incremental lines of von Ebner in dinosaurs and the assessment of tooth replacement rates using growth line counts. *Proceedings of the National Academy of Sciences of the United States of America* 93 (25): 14623–14627.
Erickson, G. M., Kirk, S. D. V., Su, J., Levenston, M. E., Caler, W. E. and Carter, D. R. 1996. Bite-force estimation for *Tyrannosaurus rex* from tooth-marked bones. *Nature* 382 (6593): 706–708.
Erickson, G. M., Makovicky, P. J., Currie, P. J., Norell, M. A., Yerby, S. A. and Brochu, C. A. 2004. Gigantism and comparative life-history parameters of tyrannosaurid dinosaurs. *Nature* 430 (7001): 772–775.
Estes, R. 1969. Studies on fossil phyllodont fishes: interrelationships and evolution in the Phyllodontidae (Albuloidei). *Copeia* 1969 (2): 317.
Ettachfini, E. M. and Andreu, B. 2004. Le Cénomanien et le Turonien de la Plate-forme Préafricaine du Maroc. *Cretaceous Research* 25 (2): 277–302.
Eudes-Deslongchamps, J. A. 1837. *Mémoire sur le* Poekilopleuron bucklandii, *grand saurien fossile, intermédiaire entre les crocodiles et les lézards, découvert dans les carrières de la Maladrerie, près Caen, au mois de juillet 1835*. impr. A. Hardel, 144pp.
Evans, D. C., Larson, D. W. and Currie, P. J. 2013. A new dromaeosaurid (Dinosauria: Theropoda) with Asian affinities from the latest Cretaceous of North America. *Naturwissenschaften* 100 (11): 1041–1049.
Evans, D. C., Barrett, P. M., Brink, K. S. and Carrano, M. T. 2014. Osteology and bone microstructure of new, small theropod dinosaur material from the early Late Cretaceous of Morocco. *Gondwana Research*.
Evans, M. 2010. The roles played by museums, collections and collectors in the early history of reptile palaeontology. *Geological Society, London, Special Publications* 343 (1): 5–29.
Evans, S. E. 1994. The Solnhofen (Jurassic: Tithonian) genus *Bavarisaurus*: new material and a new interpretation. *Neues Jahrbuch fur Geologie und Palaontologie Abhandlungen* 192: 37–52.
Ezcurra, M. D. 2006. A review of the systematic position of the dinosauriform archosaur *Eucoelophysis baldwini* Sullivan & Lucas, 1999 from the Upper Triassic of New Mexico, USA. *Geodiversitas* 28 (4): 649–684.
Ezcurra, M. D. 2007. The cranial anatomy of the coelophysoid theropod *Zupaysaurus rougieri* from the Upper Triassic of Argentina. *Historical Biology* 19 (2): 185–202.
Ezcurra, M. D. 2009. Theropod remains from the uppermost Cretaceous of Colombia and their implications for the palaeozoogeography of western Gondwana. *Cretaceous Research* 30 (5): 1339–1344.
Ezcurra, M. D. 2010. A new early dinosaur (Saurischia: Sauropodomorpha) from the Late Triassic of Argentina: a reassessment of dinosaur origin and phylogeny. *Journal of Systematic Palaeontology* 8 (3): 371–425.
Ezcurra, M. D. 2012. Phylogenetic analysis of Late Triassic - Early Jurassic neotheropod dinosaurs. *72nd Annual Meeting Society of Vertebrate Paleontology, Raleigh, USA. (October 17-20, 2012), Program and Abstracts*: 91.
Ezcurra, M. D. and Cuny, G. 2007. The coelophysoid *Lophostropheus airelensis*, gen. nov.: a review of the systematics of '*Liliensternus*' *airelensis* from the Triassic–Jurassic outcrops of Normandy (France). *Journal of Vertebrate Paleontology* 27 (1): 73–86.
Ezcurra, M. D. and Novas, F. E. 2007. Phylogenetic relationships of the Triassic theropod *Zupaysaurus rougieri* from NW Argentina. *Historical Biology* 19 (1): 35–72.
Ezcurra, M. D. and Brusatte, S. L. 2011. Taxonomic and phylogenetic reassessment of the early neotheropod dinosaur *Camposaurus arizonensis* from the Late Triassic of North America. *Palaeontology* 54 (4): 763–772.

Ezcurra, M. D. and Agnolín, F. L. 2012. An abelisauroid dinosaur from the Middle Jurassic of Laurasia and its implications on theropod palaeobiogeography and evolution. *Proceedings of the Geologists' Association* 123 (3): 500–507.

Fanti, F. and Therrien, F. 2007. Theropod tooth assemblages from the Late Cretaceous Maevarano Formation and the possible presence of dromaeosaurids in Madagascar. *Acta Palaeontologica Polonica* 52 (1): 155–166.

Fanti, F., Cau, A., Martinelli, A. and Contessi, M. 2014. Integrating palaeoecology and morphology in theropod diversity estimation: A case from the Aptian-Albian of Tunisia. *Palaeogeography, Palaeoclimatology, Palaeoecology* 410: 39–57.

Farke, A. A. and Sertich, J. J. W. 2013. An abelisauroid theropod dinosaur from the Turonian of Madagascar. *PLoS ONE* 8 (4): e62047.

Farlow, J. O. and Holtz, T. R. J. 2002. The fossil record of predation in dinosaurs. *Paleontological Society Papers* 8: 251–266.

Farlow, J. O., Brinkman, D. L., Abler, W. L. and Currie, P. J. 1991. Size, shape, and serration density of theropod dinosaur lateral teeth. *Modern Geology* 16 (1-2): 161–198.

Fauchard, P. 1728. *Le Chirurgien Dentiste, ou Traité des Dents*. Chez Jean Mariette, 564pp.

Feduccia, A. 2002. Birds are dinosaurs: simple answer to a complex problem. *The Auk* 119 (4): 1187–1201.

Fernandez, V., Buffetaut, E., Maire, E., Adrien, J., Suteethorn, V. and Tafforeau, P. 2012. Phase contrast synchrotron microtomography: improving noninvasive investigations of fossil embryos In ovo. *Microscopy and Microanalysis* 18 (01): 179–185.

Fiorillo, A. R. and Currie, P. J. 1994. Theropod teeth from the Judith River Formation (Upper Cretaceous) of south-central Montana. *Journal of Vertebrate Paleontology* 14 (1): 74–80.

Fiorillo, A. R. and Gangloff, R. A. 2001. Theropod teeth from the Prince Creek Formation (Cretaceous) of northern Alaska, with speculations on Arctic dinosaur paleoecology. *Journal of Vertebrate Paleontology* 20 (4): 675–682.

FIPAT. 2011. *Terminologia Anatomica: International Anatomical Terminology*. Thieme, Stuttgart u.a., 304pp.

Fisher, H. I. 1955. Some aspects of the kinetics in the jaws of birds. *The Wilson Bulletin*: 175–188.

Fitzinger, L. 1843. *Systema reptilium. Fasciculus primus: Amblyglossae*. Vienna, 106pp.

Folinsbee, K. E., Müller, J. and Reisz, R. R. 2007. Canine grooves: morphology, function, and relevance to venom. *Journal of Vertebrate Paleontology* 27 (2): 547–551.

Forster, C. A., Sampson, S. D., Chiappe, L. M. and Krause, D. W. 1998. The theropod ancestry of birds: new evidence from the Late Cretaceous of Madagascar. *Science* 279 (5358): 1915–1919.

Foth, C. and Rauhut, O. W. M. 2013a. Macroevolutionary and Morphofunctional Patterns in Theropod Skulls: A Morphometric Approach. *Acta Palaeontologica Polonica* 58 (1): 1–16.

Foth, C. and Rauhut, O. W. M. 2013b. The good, the bad, and the ugly: the influence of skull reconstructions and intraspecific variability in studies of cranial morphometrics in theropods and basal saurischians. *PLoS ONE* 8 (8): e72007.

Foth, C., Tischlinger, H. and Rauhut, O. W. M. 2014. New specimen of *Archaeopteryx* provides insights into the evolution of pennaceous feathers. *Nature* 511 (7507): 79–82.

Fowler, D. W., Freedman, E. A., Scannella, J. B. and Kambic, R. E. 2011. The predatory ecology of *Deinonychus* and the origin of flapping in birds. *PLoS ONE* 6 (12): e28964.

Frankfurt, N. G. and Chiappe, L. M. 1999. A possible oviraptorosaur from the Late Cretaceous of northwestern Argentina. *Journal of Vertebrate Paleontology* 19 (1): 101–105.

Freedman, L. 1957. The fossil Cercopithecoidea of South Africa. *Annals of the Transvaal Museum* 23: 121–262.

Frey, E. and Martill, D. M. 1995. A possible oviraptorosaurid theropod from the Santana Formation (Lower Cretaceous,? Albian) of Brazil. *Neues Jahrbuch fur Geologie und Palaontologie-Monatshefte* (7): 397–412.

Fry, B. G., Wroe, S., Teeuwisse, W., Osch, M. J. P. van, Moreno, K., Ingle, J., McHenry, C., Ferrara, T., Clausen, P., Scheib, H., Winter, K. L., Greisman, L., Roelants, K., Weerd, L. van der, Clemente, C. J., Giannakis, E., Hodgson, W. C., Luz, S., Martelli, P., Krishnasamy, K., Kochva, E., Kwok, H. F., Scanlon, D., Karas, J., Citron, D. M., Goldstein, E. J. C., Mcnaughtan, J. E. and Norman, J. A. 2009. A central role for venom in predation by *Varanus komodoensis* (Komodo Dragon) and the extinct giant *Varanus* (*Megalania*) *priscus*. *Proceedings of the National Academy of Sciences* 106 (22): 8969–8974.

Fuchs, A. 1954. On the correlation between the skull structure and the muscles in the male *Phasianus colchicus* L. IV. The attachment of the musculus protractor quadrati et pterygoidei and of the musculus depressor mandibulae. *Koninklige Nederlandse Akademie van Wetenschappen, Proceedings, C* 57: 666–672.

Galton, P. M. 1982. *Elaphrosaurus*, an ornithomimid dinosaur from the upper jurassic of north America and Africa. *Paläontologische Zeitschrift* 56 (3-4): 265–275.

Galton, P. M. 1984. Cranial anatomy of the prosauropod dinosaur *Plateosaurus* from the Knollenmergel (Middle Keuper, Upper Triassic) of Germany. I. Two complete skulls from Trossingen/Württ. with comments on the diet. *Geologica et Palaeontologica* 18: 139–171.

Galton, P. M. 1985. Diet of prosauropod dinosaurs from the late Triassic and early Jurassic. *Lethaia* 18 (2): 105–123.

Galton, P. M. and Jensen, J. A. 1979. A new large theropod dinosaur from the Upper Jurassic of Colorado. *Brigham Young University Geology Studies* 26 (2): 1–12.

Gao, C., Morschhauser, E. M., Varricchio, D. J., Liu, J. and Zhao, B. 2012. A second soundly sleeping dragon: new anatomical details of the Chinese troodontid *Mei long* with implications for phylogeny and taphonomy. *PLoS ONE* 7 (9): e45203.

Gardner, J. L., Trueman, J. W. H., Ebert, D., Joseph, L. and Magrath, R. D. 2010. Phylogeny and evolution of the Meliphagoidea, the largest radiation of Australasian songbirds. *Molecular Phylogenetics and Evolution* 55 (3): 1087–1102.

Gates, T., Zanno, L. E. and Makovicky, P. J. in press. Theropod teeth from the upper Maastrichtian Hell Creek Formation 'Sue' Quarry: new morphotypes and faunal comparisons. *Acta Palaeontologica Polonica*: DOI:10.4202/app.2012.0145.

Gauthier, J. 1986. Saurischian monophyly and the origin of birds. *In*: Padian, K. (ed.), *The Origin of Birds and the Evolution of Flight*, Vol. 8, 1–55. Memoirs of the California Academy of Sciences, San Francisco, California.

Gauthier, J. and Gall, L. F. 2002. *New Perspectives on the Origin and Early Evolution of Birds: Proceedings of the International Symposium in Honor of John H. Ostrom*. Yale Univ Peabody Museum, 613pp.

Gay, R. 2005. Sexual dimorphism in the Early Jurassic theropod dinosaur *Dilophosaurus* and a comparison with other relataed forms. *In*: Carpenter, K. (ed.), *The Carnivorous Dinosaurs*, 277–283. Indiana University Press, Bloomington, Indiana.

Gianechini, F. A. and Apesteguía, S. 2011. Unenlagiinae revisited: dromaeosaurid theropods from South América. *Anais da Academia Brasileira de Ciências* 83 (1): 163–195.

Gianechini, F. A., Makovicky, P. J. and Apesteguía, S. 2011a. The teeth of the unenlagiine theropod *Buitreraptor* from the Cretaceous of Patagonia, Argentina, and the unusual dentition of the Gondwanan dromaeosaurids. *Acta Palaeontologica Polonica* 56 (2): 279–290.

Gianechini, F. A., Agnolín, F. L. and Ezcurra, M. D. 2011b. A reassessment of the purported venom delivery system of the bird-like raptor *Sinornithosaurus*. *Paläontologische Zeitschrift* 85 (1): 103–107.

Gignac, P. M., Makovicky, P. J., Erickson, G. M. and Walsh, R. P. 2010. A description of *Deinonychus antirrhopus* bite marks and estimates of bite force using tooth indentation simulations. *Journal of Vertebrate Paleontology* 30 (4): 1169–1177.

Gilmore, C. W. 1920. Osteology of the carnivorous Dinosauria in the United State National museum: with special reference to the genera *Antrodemus* (*Allosaurus*) and *Ceratosaurus*. *Bulletin of the United States National Museum* 110: 1–159.

Gilmore, C. W. 1924. On *Troodon validus*, an ornithopodus dinosaur from the Belly River Cretaceous of Alberta, Canada. *Bulletin of the Department of Geology, University of Alberta* 1: 1–143.

Gilmore, C. W. 1942. Paleocene Faunas of the Polecat Bench Formation, Park County, Wyoming Part II. Lizards. *Proceedings of the American Philosophical Society*: 159–167.

Godefroit, P., Currie, P. J., Hong, L., Yong, S. C. and Zhi-Ming, D. 2008. A new species of *Velociraptor* (Dinosauria: Dromaeosauridae) from the Upper Cretaceous of northern China. *Journal of Vertebrate Paleontology* 28 (2): 432–438.

Godefroit, P., Cau, A., Dong-Yu, H., Escuillié, F., Wenhao, W. and Dyke, G. 2013a. A Jurassic avialan dinosaur from China resolves the early phylogenetic history of birds. *Nature* 498: 359–362.

Godefroit, P., Demuynck, H., Dyke, G., Hu, D., Escuillié, F. and Claeys, P. 2013b. Reduced plumage and flight ability of a new Jurassic paravian theropod from China. *Nature Communications* 4: 1394.

Gold, M. E. L., Brusatte, S. and Norell, M. 2013. The cranial pneumatic sinuses of the tyrannosaurid *Alioramus* (Dinosauria, Theropoda) and the evolution of cranial pneumaticity in theropod dinosaurs. *American Museum Novitates* 3790: 1–46.

Goloboff, P. A. and Catalano, S. A. 2011. Phylogenetic morphometrics (II): algorithms for landmark optimization. *Cladistics* 27 (1): 42–51.

Goloboff, P. A., Farris, J. S. and Nixon, K. C. 2008. TNT, a free program for phylogenetic analysis. *Cladistics* 24 (5): 774–786.

Gong, E., Martin, L. D., Burnham, D. A. and Falk, A. R. 2010. The birdlike raptor *Sinornithosaurus* was venomous. *Proceedings of the National Academy of Sciences* 107 (2): 766–768.

Gong, E., Martin, L. D., Burnham, D. A. and Falk, A. R. 2011. Evidence for a venomous *Sinornithosaurus*. *Paläontologische Zeitschrift* 85 (1): 109–111.

Goswami, A., Prasad, G. V. R., Verma, O., Flynn, J. J. and Benson, R. B. J. 2013. A troodontid dinosaur from the latest Cretaceous of India. *Nature Communications* 4: 1703.

Grellet-Tinner, G., Chiappe, L., Norell, M. and Bottjer, D. 2006. Dinosaur eggs and nesting behaviors: A paleobiological investigation. *Palaeogeography, Palaeoclimatology, Palaeoecology* 232 (2–4): 294–321.

Grellet-Tinner, G., Sim, C. M., Kim, D. H., Trimby, P., Higa, A., An, S. L., Oh, H. S., Kim, T. J. and Kardjilov, N. 2011. Description of the first lithostrotian titanosaur embryo in ovo with Neutron characterization and implications for lithostrotian Aptian migration and dispersion. *Gondwana Research*.

Gussekloo, S. W. S. and Bout, R. G. 2005. Cranial kinesis in palaeognathous birds. *Journal of Experimental Biology* 208 (17): 3409–3419.

Halstead, L. B. 1970. *Scrotum humanum* Brookes 1763—the first named dinosaur. *Journal of Insignificant Research* 5: 14–15.

Halstead, L. B. and Sarjeant, W. A. S. 1993. Scrotum humanum Brookes—the earliest name for a dinosaur? *Modern Geology* 18: 221–224.

Hammer, Ø., Harper, D. A. T. and Ryan, P. D. 2001. Past: Paleontological Statistics Software Package for education and data analysis. *Palaeontologia Electronica* 4 (1): 1–9.

Hammer, W. R. and Hickerson, W. J. 1994. A crested theropod dinosaur from Antarctica. *Science* 264 (5160): 828–830.

Han, F., Clark, J. M., Xu, X., Sullivan, C., Choiniere, J. and Hone, D. W. E. 2011. Theropod teeth from the Middle-Upper Jurassic Shishugou Formation of northwest Xinjiang, China. *Journal of Vertebrate Paleontology* 31 (1): 111–126.

Han, G., Chiappe, L. M., Ji, S.-A., Habib, M., Turner, A. H., Chinsamy, A., Liu, X. and Han, L. 2014. A new raptorial dinosaur with exceptionally long feathering provides insights into dromaeosaurid flight performance. *Nature Communications* 5.

Hanson, M. and Makovicky, P. J. 2013. A new specimen of *Torvosaurus tanneri* originally collected by Elmer Riggs. *Historical Biology*: 1–10.

Harris, J. D. 1998. A reanalysis of *Acrocanthosaurus atokensis*, its phylogenetic status, and paleobiogeographic implications, based on a new specimen from Texas. *New Mexico Museum of Natural History and Science Bulletin* 13: 1–75.

Harris, J. D. 2004. Confusing dinosaurs with mammals: Tetrapod phylogenetics and anatomical terminology in the world of homology. *The Anatomical Record Part A: Discoveries in Molecular, Cellular, and Evolutionary Biology* 281A (2): 1240–1246.

Hartman, S., Lovelace, D. and Wahl, W. 2005. Phylogenetic assessment of a maniraptoran from the Morrison Formation. *Journal of Vertebrate Paleontology* 25 (3): 67A – 68A.

Hasegawa, Y., Tanaka, G., Takakuwa, Y. and Koike, S. 2010. Fine sculptures on a tooth of *Spinosaurus* (Dinosauria, Theropoda) from Morocco. *Bulletin of Gunma Museum of Natural History* 14: 11–20.

Haug, E. 1904. Sur la faune des couches à *Ceratodus* crétacées du Djoua, Près de Timassanine (Sahara). *Comptes Rendus de l'Académie des Sciences* 138: 1529–1531.

Haug, E. 1905. Documents scientifiques de la mission saharienne, mission Foureau-Lamy. « D'Alger au Congo par le Tchad ». *Publication de la Société de Géographie: Paris*: 751–832.

Heckeberg, N. 2009. About the lifetime of a spinosaur tooth-new histologic investigation of tooth formation rates. *69th Annual Meeting Society of Vertebrate Paleontology, Bristol, UK. (September 23-26, 2009), Program and Abstracts* 29 (supp. 3): 112A.

Hellman, M. 1928. Racial characters in human dentition Part I. A racial distribution of the *Dryopithecus* pattern and its modifications in the lower molar teeth of man. *Proceedings of the American Philosophical Society*: 157–174.

Helmdach, F. F. 1971. Stratigraphy and ostracod-fauna from the Coalmine Guimarota (Upper Jurassic). *Mémoires des Services Géologiques du Portugal* 17: 43–48.

Henderson, D. M. 1998. Skull and tooth morphology as indicators of niche partitioning in sympatric Morrison Formation theropods. *Gaia* 15: 219–226.

Hendrickx, C. and Buffetaut, E. 2008. Functional interpretation of spinosaurid quadrates (Dinosauria: Theropoda) from the Mid-Cretaceous of Morocco. *56th Annual Symposium of Vertebrate Palaeontology and Comparative Anatomy. Dublin (September 2nd-6th 2008)*: 25–26.

Hendrickx, C. and Mateus, O. 2012. Ontogenetical changes in the quadrate of basal tetanurans. *In*: Royo-Torres, R., Gascó, F. and Alcalá, L. (eds.), *10th Annual Meeting of the European Association of Vertebrate Palaeontologists. ¡Fundamental!*, Vol. 20, 101–104. Fundación Conjunto Paleontológico de Teruel – Dinópolis.

Hendrickx, C. and Mateus, O. 2014a. *Torvosaurus gurneyi* n. sp., the largest terrestrial predator from Europe, and a proposed terminology of the maxilla anatomy in nonavian theropods. *PLoS ONE* 9 (3): e88905.

Hendrickx, C. and Mateus, O. 2014b. Abelisauridae (Dinosauria: Theropoda) from the Late Jurassic of Portugal and dentition-based phylogeny as a contribution for the identification of isolated theropod teeth. *Zootaxa* 3759 (1): 1–74.

Hendrickx, C., Mateus, O. and Araújo, R. in pressa. The dentition of megalosaurid theropods. *Acta Palaeontologica Polonica*: DOI:10.4202/app.00056.2013.

Hendrickx, C., Mateus, O. and Buffetaut, E. in pressb. Morphofunctional analysis of the quadrate of Spinosauridae (Dinosauria: Theropoda) and the first definitive evidence of two cohabiting *Spinosaurus* in the Cenomanian of North Africa. *PLoS ONE*.

Hendrickx, C., Mateus, O. and Araújo, R. in pressc. A proposed terminology of theropod teeth (Saurischia: Dinosauria). *Journal of Vertebrate Paleontology*.

Hendrickx, C., Araújo, R. and Mateus, O. 2012. The nonavian theropod quadrate: systematic usefulness, major trends and phylogenetic morphometrics analysis. *72nd Annual Meeting Society of Vertebrate Paleontology, Raleigh, USA. (October 17-20, 2012), Program and Abstracts*: 110.

Hendrickx, C., Araújo, R. and Mateus, O. 2014a. The nonavian theropod quadrate II: systematic usefulness, major trends and cladistic and phylogenetic morphometrics analyses. *PeerJ PrePrints*: 2:e380v1.

Hendrickx, C., Araújo, R. and Mateus, O. 2014b. The nonavian theropod quadrate I: standardized terminology and overview of the anatomy, function and ontogeny. *PeerJ PrePrints*: 2:e379v1.

Henkel, S. and Krusat, G. 1980. Die Fossil-Lagerstätte in der Kohlengrube Guimarota (Portugal) und der erste Fund eines Docodontiden-Skelettes. *Berliner geowissenschaftliche Abhandlungen A* 20: 209–214.

Hennig, W. 1950. *Grundzüge einer Theorie der phylogenetischen Systematik*. Berlin, 370pp.

He, T., Wang, X.-L. and Zhou, Z.-H. 2008. A new genus and species of caudipterid dinosaur from the Lower Cretaceous Jiufotang Formation of western Liaoning, China. *Vertebrata PalAsiatica* 46 (3): 178–189.

Hill, G. 1988. The sedimentology and lithostratigraphy of the Upper Jurassic Lourinhã Formation, Lusitanian Basin, Portugal. Ph.D. Dissertation, The Open University, Milton Keynes, UK, Milton Keynes, UK, 292pp.

Hill, G. 1989. Distal alluvial fan sediments from the Upper Jurassic of Portugal: controls on their cyclicity and channel formation. *Journal of the Geological Society* 146 (3): 539–555.

Hillson, S. 2005. *Teeth: Second Edition*. Cambridge University Press, New York, 373pp.

Hislop, S. 1861. Remarks on the geology of Nágpur. *Journal of the Bombay Branch of the Royal Asiatic Society* 6: 194–206.

Hislop, S. 1864. Extracts from letters relating to the further discovery of fossil teeth and bones of reptiles in Central India. *Quarterly Journal of the Geological Society* 20 (1-2): 280–282.

Hocknull, S. A., White, M. A., Tischler, T. R., Cook, A. G., Calleja, N. D., Sloan, T. and Elliott, D. A. 2009. New mid-Cretaceous (Latest Albian) dinosaurs from Winton, Queensland, Australia. *PLoS ONE* 4 (7): e6190.

Hoese, W. J. and Westneat, M. W. 1996. Biomechanics of cranial kinesis in birds: testing linkage models in the white-throated sparrow (*Zonotrichia albicollis*). *Journal of Morphology* 227 (3): 305–320.

Holliday, C. M. 2009. New insights into dinosaur jaw muscle anatomy. *The Anatomical Record: Advances in Integrative Anatomy and Evolutionary Biology* 292 (9): 1246–1265.

Holliday, C. M. and Witmer, L. M. 2008. Cranial kinesis in dinosaurs: intracranial joints, protractor muscles, and their significance for cranial evolution and function in diapsids. *Journal of Vertebrate Paleontology* 28 (4): 1073–1088.

Holtz, T. R. 1994. The phylogenetic position of the Tyrannosauridae: implications for theropod systematics. *Journal of Paleontology* 68 (5): 1100–1117.

Holtz, T. R. 1996. Phylogenetic taxonomy of the Coelurosauria (Dinosauria: Theropoda). *Journal of Paleontology* 70: 536–538.

Holtz, T. R. J. 1995. A new phylogeny of the Theropoda. *Journal of Vertebrate Paleontology* 15 (suppl 3): 35A.

Holtz, T. R. J. 1998a. A new phylogeny of the carnivorous dinosaurs. *Gaia* 15: 5–61.

Holtz, T. R. J. 1998b. Spinosaurs as crocodile mimics. *Science* 282 (5392): 1276–1277.

Holtz, T. R. J. 2001. The phylogeny and taxonomy of the Tyrannosauridae. *In*: Tanke, D. H., Carpenter, K. and Skrepnick, M. W. (eds.), *Mesozoic Vertebrate Life*, 64–83. Indiana University Press, Bloomington, Indiana.

Holtz, T. R. J. 2003. Dinosaur predation: evidence and ecomorphology. *In*: Kelley, P. H., Kowalewski, M. and Hansen, T. A. (eds.), *Predator—Prey Interactions in the Fossil Record*, 325–340. Springer US.

Holtz, T. R. J. 2004. Tyrannosauroidea. *In*: Weishampel, D. B., Dodson, P. and Osmólska, H. (eds.), *The Dinosauria. Second Edition*, 111–136. University of California Press, Berkeley, California.

Holtz, T. R. J. 2008. A critical reappraisal of the obligate scavenging hypothesis for *Tyrannosaurus rex* and other tyrant dinosaurs. *In*: Larson, P. L. and Kenneth, C. (eds.), Tyrannosaurus Rex, *the Tyrant King*, 371–396. Indiana University Press, Bloomington, Indiana.

Holtz, T. R. J. 2012. Theropods. *In*: Brett-Surman, M. K., Holtz, T. R. J. and Farlow, J. O. (eds.), *The Complete Dinosaur, Second Edition*, 347–378. Indiana University Press, Bloomington, Indiana.
Holtz, T. R. J. and Padian, K. 1995. Definition and diagnosis of Theropoda and related taxa. *Journal of Vertebrate Paleontology* 15 (suppl 3): 35A.
Holtz, T. R. J. and Osmólska, H. 2004. Saurischia. *In*: Weishampel, D. B., Dodson, P. and Osmólska, H. (eds.), *The Dinosauria. Second Edition*, 21–24. University of California Press, Berkeley, California.
Holtz, T. R. J., Brinkman, D. L. and Chandler, C. L. 1998. Denticle morphometrics and a possibly omnivorous feeding habit for the theropod dinosaur *Troodon*. *Gaia* 15: 159–166.
Holtz, T. R. J., Molnar, R. E. and Currie, P. J. 2004. Basal Tetanurae. *In*: Weishampel, D. B., Dodson, P. and Osmólska, H. (eds.), *The Dinosauria. Second Edition*, 71–110. University of California Press, Berkeley, California.
Hone, D. W. E. and Rauhut, O. W. M. 2010. Feeding behaviour and bone utilization by theropod dinosaurs. *Lethaia* 43 (2): 232–244.
Hone, D. W. E., Xu, X. and Wang, D. Y. 2010. A probable baryonychine (Theropoda: Spinosauridae) tooth from the Upper Cretaceous of Henan Province, China. *Vertebrata PalAsiatica* 48 (1): 19–26.
Hone, D. W. E., Wang, K., Sullivan, C., Zhao, X., Chen, S., Li, D., Ji, S., Ji, Q. and Xu, X. 2011. A new, large tyrannosaurine theropod from the Upper Cretaceous of China. *Cretaceous Research* 32 (4): 495.
Hopson, B. J. A. 1964. Tooth replacement in cynodont, dicynodont and therocephalian Reptiles. *Proceedings of the Zoological Society of London* 142 (4): 625–654.
Horner, J. R. and Currie, P. J. 1994. Embryonic and neonatal morphology and ontogeny of a new species of *Hypacrosaurus* (Ornithischia, Lambeosauridae) from Montana and Alberta. *In*: Carpenter, K., Hirsch, K. F. and Horner, J. R. (eds.), *Dinosaur Eggs and Babies*, 312–337. Cambridge, UK.
Horner, J. R. and Padian, K. 2004. Age and growth dynamics of *Tyrannosaurus rex*. *Proceedings of the Royal Society of London. Series B: Biological Sciences* 271 (1551): 1875–1880.
Hou, L. 1997. Mesozoic birds of China. *Taiwan Provincial Feng Huang Ku Bird Park, Nan Tou, Taiwan*.
Hu, D., Hou, L., Zhang, L. and Xu, X. 2009. A pre-*Archaeopteryx* troodontid theropod from China with long feathers on the metatarsus. *Nature* 461 (7264): 640–643.
Huene, F. 1929a. Los Saurisquios y Ornithisquios de Cretaceo Argentine. *Annales de Museo de La Plata* 3 (Series 2): 1–196.
Huene, F. R. von. 1909. Skizze zu einer systematik und stammesgeschichte der dinosaurier. *Centralblatt für Mineralogie, Geologie und Paläontologie* 1909: 12–22.
Huene, F. R. von. 1914a. Das natürliche System der Saurischia. *Zentralblatt für Mineralogie, Geologie, und Paläontologie B* 1914: 154–158.
Huene, F. R. von. 1914b. Saurischia and Ornithischia. *Geological Magazine* 1 (10): 444–445.
Huene, F. R. von. 1914c. Beiträge zur Geschichte der Archosaurier. *Geologie und Paläontologie Abhandlungen* 13 (7): 1–56.
Huene, F. R. von. 1923. Carnivorous Saurischia in Europe since the Triassic. *Bulletin of the Geological Society of America* 34: 449–458.
Huene, F. R. von. 1926a. The carnivorous Saurischia in the Jura and Cretaceous formations, principally in Europe. *Revista del Museo de La Plata* 29: 35–167.
Huene, F. R. von. 1926b. On several known and unknown reptiles of the order Saurischia from England and France. *Journal of Natural History Series 9* 17 (101): 473–489.
Huene, F. R. von. 1929b. Kurze Übersicht über die Saurischia und ihre natürlichen Zusammenhänge. *Palaeontologische Zeitschrift* 11 (3): 269–273.
Huene, F. R. von. 1932. Die fossile Reptil-Ordnung Saurischia, ihre Entwicklung und Geschichte. *Monographien zur Geologie und Palaontologie, Series 1*, 4: 1–361.
Huene, F. R. von. 1934. Ein neuer Coelurosaurier in der thüringischen Trias. *Paläontologische Zeitschrift* 16 (3): 145–170.
Huene, F. R. von and Matley, C. A. 1933. The Cretaceous Saurischia and Ornithischia of the Central Provinces. *Memoirs of the Geological Survey of India, New Series* 21: 1–74.
Hurum, J. H. and Sabath, K. 2003. Giant theropod dinosaurs from Asia and North America: Skulls of *Tarbosaurus bataar* and *Tyrannosaurus rex* compared. *Acta Palaeontologica Polonica* 48 (2): 161–190.
Hu, S. 1993. A new Theropoda (*Dilophosaurus sinensis* sp. nov.) from Yunnan, China. *Vertebrata PalAsiatica* 31 (1): 65–69.
Hutt, S., Martill, D. M. and Barker, M. J. 1996. The first European allosaurid dinosaur (Lower Cretaceous, Wealden Group, England). *Neues Jahrbuch für Geologie und Paläontologie Monatshefte* 1996: 635–644.
Hutt, S., Naish, D., Martill, D. M., Barker, M. J. and Newbery, P. 2001. A preliminary account of a new tyrannosauroid theropod from the Wessex Formation (Early Cretaceous) of southern England. *Cretaceous Research* 22 (2): 227–242.

Hwang, S. H. 2005. Phylogenetic patterns of enamel microstructure in dinosaur teeth. *Journal of Morphology* 266 (2): 208–240.
Hwang, S. H. 2007. Phylogenetic patterns of enamel microstructure in dinosaur teeth. Ph.D. Dissertation, Columbia University, New York, New York., 274pp.
Hwang, S. H., Norell, M. A., Ji, Q. and Keqin, G. 2002. New specimens of *Microraptor zhaoianus* (Theropoda: Dromaeosauridae) from Northeastern China. *American Museum Novitates* 3381: 1–44.
Hwang, S. H., Norell, M. A., Qiang, J. and Keqin, G. 2004. A large compsognathid from the Early Cretaceous Yixian Formation of China. *Journal of Systematic Palaeontology* 2 (1): 13–30.
Ibrahim, N. 2008. Too many theropods? The diversity of predatory dinosaurs in the mid-Cretaceous of Morocco. *56th Annual Symposium of Vertebrate Palaeontology and Comparative Anatomy. Dublin (September 2nd-6th 2008)*: 29.
Ibrahim, N. and Sereno, P. C. 2011. New data on spinosaurids (Dinosauria: Theropoda) from Africa. *Journal of Vertebrate Paleontology* 31 (supp. 2): 130.
Ibrahim, N., Varricchio, D. J., Sereno, P. C., Wilson, J. A., Dutheil, D. B., Martill, D. M., Baidder, L. and Zouhri, S. 2014a. Dinosaur footprints and other ichnofauna from the Cretaceous Kem Kem Beds of Morocco. *PLoS ONE* 9 (3): e90751.
Ibrahim, N., Sereno, P. C., Sasso, C. D., Maganuco, S., Fabbri, M., Martill, D. M., Zouhri, S., Myhrvold, N. and Iurino, D. A. 2014b. Semiaquatic adaptations in a giant predatory dinosaur. *Science* 345 (6204): 1613–1616.
ICVGAN. 2012. *Nomina Anatomica Veterinaria*. International Committee on Veterinary Gross Anatomical Nomenclature (ICVGAN), 160pp.
Illiger, J. K. W. 1811. *Prodromus Systematis Mammalium et Avium: Additis Terminis Zoographicis Utriusque Classis, Eorumque Versione Germanica*. Salfeld, 328pp.
Irmis, R. B. 2007. Axial skeleton ontogeny in the Parasuchia (Archosauria: Pseudosuchia) and its implications for ontogenetic determination in archosaurs. *Journal of Vertebrate Paleontology* 27 (2): 350–361.
Ivie, M. A., Slipinski, S. A. and Wegrzynowicz, P. 2001. Generic Homonyms in the Colydiinae (Coleoptera: Zopheridae). *Insecta Mundi* 15 (1): 63–64.
Jensen, J. A. 1985. Uncompahgre dinosaur fauna: a preliminary report. *The Great Basin Naturalist* 45 (4): 710–720.
Ji, Q., Ji, S. A. and Zhang, L. J. 2009. First large tyrannosauroid theropod from the Early Cretaceous Jehol Biota in northeastern China. *Geological Bulletin of China* 28 (10): 1369–1374.
Ji, Q., Currie, P. J., Norell, M. A. and Shu-An, J. 1998. Two feathered dinosaurs from northeastern China. *Nature* 393 (6687): 753–761.
Ji, Q., Ji, S., Lü, J. and Yuan, C. 2007a. A new giant compsognathid dinosaur with long filamentous integuments from lower Cretaceous of Northeastern China. *Acta Geologica Sinica* 81: 8–15.
Ji, Q., Norell, M. A., Gao, K.-Q., Ji, S.-A. and Ren, D. 2001. The distribution of integumentary structures in a feathered dinosaur. *Nature* 410 (6832): 1084–1088.
Ji, Q., Norell, M. A., Makovicky, P. J., Gao, K.-Q., Ji, S. and Yuan, C. 2003. An early ostrich dinosaur and implications for ornithomimosaur phylogeny. *American Museum Novitates* 3420: 1–19.
Ji, S., Gao, C., Liu, J., Meng, Q. and Qiang, J. 2007b. New Material of *Sinosauropteryx* (Theropoda: Compsognathidae) from Western Liaoning, China. *Acta Geologica Sinica - English Edition* 81 (2): 177–182.
Joly, F. 1962. Études sur le relief du Sud-Est marocain. *Travaux de l'Institut Scientifique Chérien. Série géologie et géographie physique* 10: 1–578.
Karhu, A. A. and Rautian, A. S. 1996. A new family of Maniraptora (Dinosauria: Saurischia) from the Late Cretaceous of Mongolia. *Paleontological Journal* 30 (5): 583–592.
Kear, B. P., Rich, T. H., Vickers-Rich, P., Ali, M. A., Al-Mufarreh, Y. A., Matari, A. H., Al-Massari, A. M., Nasser, A. H., Attia, Y. and Halawani, M. A. 2013. First dinosaurs from Saudi Arabia. *PLoS ONE* 8 (12): e84041.
Kellner, A. W. A. 1996. Remarks on Brazilian dinosaurs. *Memoirs of the Queensland Museum* 39 (3): 611–626.
Kellner, A. W. A. and Campos, D. A. 1996. First Early Cretaceous theropod dinosaur from Brazil with comments on Spinosauridae. *Neues Jahrbuch für Geologie und Paläontologie - Abhandlungen* 199 (2): 151–166.
Kellner, A. W. A. and Tomida, Y. 2000. Description of a new species of Anhangueridae (Pterodactyloidea) with comments on the pterosaur fauna from the Santana Formation (Aptian-Albian), Northeastern Brazil. *National Science Museum Monographs* 17: 1–137.
Khelif, H. 2010. *Le Jardin des Courbes - Dictionnaire Raisonné des Courbes Planes Célèbres et Remarquables*. Ellipses Marketing, Paris, 527pp.
Kilian, C. 1931. Des principaux complexes continentaux du Sahara. *Comptes Rendus sommaires de la Société géologique de France* 9: 109–111.

Kirkland, J. I. and Wolfe, D. G. 2001. First definitive therizinosaurid (Dinosauria; Theropoda) from North America. *Journal of Vertebrate Paleontology* 21 (3): 410–414.

Kirkland, J. I., Gaston, R. and Burge, D. 1993. A large dromaeosaur (Theropoda) from the Lower Cretaceous of eastern Utah. *Hunteria* 2 (10): 1–16.

Kirkland, J. I., Zanno, L. E., Sampson, S. D., Clark, J. M. and DeBlieux, D. D. 2005. A primitive therizinosauroid dinosaur from the Early Cretaceous of Utah. *Nature* 435 (7038): 84–87.

Kitchener, A. 1987. Function of Claws' claws. *Nature* 325: 114.

Klingenberg, C. P. 2011. MorphoJ: an integrated software package for geometric morphometrics. *Molecular Ecology Resources* 11 (2): 353–357.

Kobayashi, Y. and Lü, J.-C. 2003. A new ornithomimid dinosaur with gregarious habits from the Late Cretaceous of China. *Acta Palaeontologica Polonica* 48 (2): 235–259.

Kobayashi, Y. and Barsbold, R. 2005a. Reexamination of a primitive ornithomimosaur, *Garudimimus brevipes* Barsbold, 1981 (Dinosauria: Theropoda), from the Late Cretaceous of Mongolia. *Canadian Journal of Earth Sciences* 42 (9): 1501–1521.

Kobayashi, Y. and Barsbold, R. 2005b. Anatomy of *Harpymimus okladnikovi* Barsbold and Perle 1984 (Dinosauria; Theropoda) of Mongolia. *In*: Carpenter, K. (ed.), *The Carnivorous Dinosaurs*, 97–126. Indiana University Press, Bloomington, Indiana.

Kobayashi, Y., Lu, J.-C., Dong, Z.-M., Barsbold, R., Azuma, Y. and Tomida, Y. 1999. Palaeobiology: Herbivorous diet in an ornithomimid dinosaur. *Nature* 402 (6761): 480–481.

Kocsis, G., Marcsik, A., Kokai, E. and Kocsis, K. S. 2002. Supernumerary occlusal cusps on permanent human teeth. *Acta Biol Szeged* 46 (1/2): 71–82.

Kohn, S. I. 1942. Treatment of temporomandibular dysfunction accompanied by severe pain syndrome. *American Journal of Orthodontics and Oral Surgery* 28 (5): 302–310.

Krause, D. W., Sampson, S. D., Carrano, M. T. and O'Connor, P. M. 2007. Overview of the history of fiscovery, taxonomy, phylogeny, and biogeography of *Majungasaurus crenatissimus* (Theropoda: Abelisauridae) from the Late Cretaceous of Madagascar. *Journal of Vertebrate Paleontology* 27 (sup2): 1–20.

Kullberg, J. C., Rocha, R. B., Soares, A. F., Rey, J., Terrinha, P., Azerêdo, A. C., Callapez, P., Duarte, L. V., Kullberg, M. C., Martins, L., Miranda, J. R., Alvez, C., Mata, J., Madeira, J., Mateus, O., Moreira, M. and Nogueira, C. R. in press. A Bacia Lusitaniana: estratigrafia, paleogeografia e tectónica. *In*: Dias, R., Araújo, A., Terrinha, P. and Kullberg, J. C. (eds.), *Geologia de Portugal No Contexto Da Ibéria (2nd Edition)*, 989–1141. Escolar Editora.

Kundrát, M. and Janáček, J. 2007. Cranial pneumatization and auditory perceptions of the oviraptorid dinosaur *Conchoraptor gracilis* (Theropoda, Maniraptora) from the Late Cretaceous of Mongolia. *Naturwissenschaften* 94 (9): 769–778.

Kundrát, M., Cruickshank, A. R. I., Manning, T. W. and Nudds, J. 2008. Embryos of therizinosauroid theropods from the Upper Cretaceous of China: diagnosis and analysis of ossification patterns. *Acta Zoologica* 89 (3): 231–251.

Kurzanov, S. M. 1981. An unusual theropod from the Upper Cretaceous of Mongolia. *Joint Soviet-Mongolian Paleontological Expedition* 15: 39–49.

Kurzanov, S. M. 1985. The skull structure of the dinosaur *Avimimus*. *Paleontological Journal* 1985: 92–99.

Lamanna, M. C. and Hasegawa, Y. 2014. New titanosauriform sauropod dinosaur material from the Cenomanian of Morocco: implications for paleoecology and sauropod diversity in the Late Cretaceous of north Africa. *Bulletin of Gunma Museum of Natural History* 18: 1–9.

Lamanna, M. C., Martínez, R. D. and Smith, J. B. 2002. A definitive abelisaurid theropod dinosaur from the early Late Cretaceous of Patagonia. *Journal of Vertebrate Paleontology* 22 (1): 58–69.

Lamanna, M. C., Sues, H.-D., Schachner, E. R. and Lyson, T. R. 2014. A new large-bodied oviraptorosaurian theropod dinosaur from the Latest Cretaceous of Western North America. *PLoS ONE* 9 (3): e92022.

Läng, E., Boudad, L., Maio, L., Samankassou, E., Tabouelle, J., Tong, H. and Cavin, L. 2013. Unbalanced food web in a Late Cretaceous dinosaur assemblage. *Palaeogeography, Palaeoclimatology, Palaeoecology* 381–382: 26–32.

Langer, M. C. 2014. The origins of Dinosauria: much ado about nothing. *Palaeontology* 57 (3): 469–478.

Langer, M. C. and Benton, M. J. 2006. Early dinosaurs: a phylogenetic study. *Journal of Systematic Palaeontology* 4 (04): 309–358.

Langer, M. C. and Ferigolo, J. 2013. The Late Triassic dinosauromorph *Sacisaurus agudoensis* (Caturrita Formation; Rio Grande do Sul, Brazil): anatomy and affinities. *Geological Society, London, Special Publications* 379: 353–392.

Langer, M. C., Ezcurra, M. D., Bittencourt, J. S. and Novas, F. E. 2010. The origin and early evolution of dinosaurs. *Biological Reviews* 85 (1): 55–110.

Langer, M. C., Rincón, A. D., Ramezani, J., Solórzano, A. and Rauhut, O. W. M. 2014. New dinosaur (Theropoda, *stem*-Averostra) from the earliest Jurassic of the La Quinta formation, Venezuelan Andes. *Royal Society Open Science* 1 (2): 140184.

Langston, W. 1975. Ziphodont crocodiles, *Pristichampsus vorax* (Troxell), new combination, from the Eocene of North America. *Fieldiana, Geology* 33: 291–314.

De Lapparent, A. F. 1960. Les dinosauriens du 'Continental Intercalaire' du Sahara Central. *Mémoire de la Société Géologique de France* 88A: l – 57.

Lapparent, A. F. de and Zbyszewski, G. 1957. Les dinosauriens du Portugal. *Mémoires du Service géologique du Portugal* 2: 1–63.

Larson, D. W. 2008a. Diversity and variation of theropod dinosaur teeth from the uppermost Santonian Milk River Formation (Upper Cretaceous), Alberta: a quantitative method supporting identification of the oldest dinosaur tooth assemblage in Canada. *Canadian Journal of Earth Sciences* 45 (12): 1455–1468.

Larson, D. W. and Currie, P. J. 2013. Multivariate analyses of small theropod dinosaur teeth and implications for paleoecological turnover through time. *PLoS ONE* 8 (1): e54329.

Larson, D. W., Brinkman, D. B. and Bell, P. R. 2010. Faunal assemblages from the upper Horseshoe Canyon Formation, an early Maastrichtian cool-climate assemblage from Alberta, with special reference to the *Albertosaurus sarcophagus* bonebed. *Canadian Journal of Earth Sciences* 47 (9): 1159–1181.

Larson, P. L. 2008b. Atlas of the skull bones of *Tyrannosaurus rex*. *In*: Larson, P. L. and Carpenter, K. (eds.), *Tyrannosaurus Rex, the Tyrant King*, 233–243. Indiana University Press, Bloomington, Indiana.

Larsson, H. C. E., Hone, D. W., Dececchi, T. A., Sullivan, C. and Xu, X. 2010. The winged non-avian dinosaur *Microraptor* fed on mammals: Implications for the Jehol Biota ecosystem. *J Vert Paleont* 30: 114A.

Lautenschlager, S., Witmer, L. M., Altangerel, P., Zanno, L. E. and Rayfield, E. J. 2014. Cranial anatomy of *Erlikosaurus andrewsi* (Dinosauria, Therizinosauria): new insights based on digital reconstruction. *Journal of Vertebrate Paleontology* 34 (6): 1263–1291.

Lavocat, R. 1951. Découverte de restes d'un grand dinosaurien sauropode dans le Crétacé du sud marocain. *Compte Rendus de l'Académie des Sciences Paris Série 2* 232: 169–170.

Lavocat, R. 1952. Les gisements de dinosauriens du Crétacé du Sud Marocain. *Compte rendu sommaire des séances de la Société géologique de France* 1952 (2): 12–13.

Lavocat, R. 1954a. Reconnaissance géologique dans les Hammadas des confins algéro-marocains du Sud. *Notes et Mémoires du Service Géologique du Maroc* 116: 1–147.

Lavocat, R. 1954b. Sur les dinosauriens du Continental Intercalaire des Kem-Kem de la Daoura. *19th International Geological Congress* 15: 65–68.

Lavocat, R. 1955. Sur une portion de mandibule de théropode provenant du Crétacé supérieur de Madagascar. *Bulletin du Muséum National d'Histoire Naturelle* 27: 256–259.

Lebrun, P. 2004. *Dinosaures carnivores: une histoire naturelle des théropodes non aviaires. Tome 1: histoire des découvertes, anatomie et physiologie, phylogenèse, théropodes basaux et carnosauriens*. Minéraux & Fossiles Hors-série n°18. CEDIM, 128pp.

Lecuona, A. and Pol, D. 2008. Tooth morphology of *Notosuchus terrestris* (Notosuchia: Mesoeucrocodylia): New evidence and implications. *Comptes Rendus Palevol* 7 (7): 407–417.

Lee, Y.-N., Barsbold, R., Currie, P. J., Kobayashi, Y., Lee, H.-J., Godefroit, P., Escuillié, F. and Chinzorig, T. 2014. Resolving the long-standing enigmas of a giant ornithomimosaur *Deinocheirus mirificus*. *Nature* advance online publication.

Lehman, T. M. and Carpenter, K. 1990. A partial skeleton of the tyrannosaurid dinosaur *Aublysodon* from the Upper Cretaceous of New Mexico. *Journal of Paleontology* 64 (6): 1026–1032.

Leidy, J. 1856. Notice of remains of extinct reptiles and fishes, discovered by Dr. F.V. Hayden in the Bad Lands of the Judith River, Nebraska Territory. *Proceedings of the Academy of Natural Sciences of Philadelphia* 8: 72–73.

Leidy, J. 1860. Extinct Vertebrata from the Judith River and Great Lignite Formations of Nebraska. *Transactions of the American Philosophical Society* 11: 139–154.

Leonardi, G. 1984. Le impronte fossili di dinosauri. *In*: Ligabue, G. (ed.), *Sulle Orme Dei Dinosauri*, Vol. 9, 165–186. Erizzo for Le Societá del Gruppo ENI.

Lhota, S., Jůnek, T., Bartoš, L. and Kuběna, A. A. 2008. Specialized use of two fingers in free-ranging aye-ayes (*Daubentonia madagascariensis*). *American Journal of Primatology* 70 (8): 786–795.

Lhuyd, E. 1699. *Lithophylacii Britannici ichnographia*. E Typographeo Clarendoniano, 284pp.

Licker, D. M. 2003. *Dictionary of Bioscience*. McGraw-Hill Professional Publishing, McGraw-Hill Companies, The Distributor, 674pp.

Li, D., Norell, M. A., Gao, K. Q., Smith, N. D. and Makovicky, P. J. 2010. A longirostrine tyrannosauroid from the Early Cretaceous of China. *Proceedings of the Royal Society B: Biological Sciences* 277 (1679): 183–190.

Li, F., Peng, G., Ye, Y., Jiang, S. and Huang, D. 2009. A new carnosaur from the Late Jurassic of Qianwei, Sichuan, China. *Acta Geologica Sinica* 83: 1203–1213.

Linnaeus, C. 1758. Systema Naturae per regna tria naturae, secundum classes, ordines, genera, species, cum characteribus, differentiis, synonymis, locis. *Editio decima, reformata. Laurentius Salvius: Holmiae* 1 (7): 1–824.

Lio, G., Agnolín, F., Cau, A. and Maganuco, S. 2012. Crocodyliform affinities for *Kemkemia auditorei* Cau & Maganuco, 2009 from the Late Cretaceous of Morocco. *Atti della Società italiana di scienze naturali e del museo civico di storia naturale di Milano* 153 (1): 119–126.

Livezey, B. C. and Zusi, R. L. 2007. Higher-order phylogeny of modern birds (Theropoda, Aves: Neornithes) based on comparative anatomy. II. Analysis and discussion. *Zoological Journal of the Linnean Society* 149 (1): 1–95.

Liyong, J., Jun, C. and Godefroit, P. 2012. A new basal ornithomimosaur (Dinosauria: Theropoda) from the Early Cretaceous Yixian Formation, Northeast China. *In*: Godefroit, P. (ed.), *Bernissart Dinosaurs and Early Cretaceous Terrestrial Ecosystems*, 466–487. Indiana University Press, Bloomington, Indiana.

Le Loeuff, J. 1991. The Campano-Maastrichtian vertebrate faunas from southern Europe and their relationships with other faunas in the world; palaeobiogeographical implications. *Cretaceous Research* 12 (2): 93–114.

Le Loeuff, J. and Buffetaut, E. 1991. *Tarascosaurus salluvicus* nov. gen., nov. sp.,dinosaure théropode du Crétacé supérieur du Sud de la France. *Geobios* 24 (5): 585–594.

Loewen, M. A. 2010. Variation in the Late Jurassic theropod dinosaur *Allosaurus*: Ontogenetic, functional, and taxonomic implications. Ph.D. Dissertation, The University of Utah, Texas, Utah, USA, 326pp.

Loewen, M. A., Irmis, R. B., Sertich, J. J. W., Currie, P. J. and Sampson, S. D. 2013. Tyrant dinosaur evolution tracks the rise and fall of Late Cretaceous oceans. *PLoS ONE* 8 (11): e79420.

Longrich, N. 2008. Small theropod teeth from the Lance Formation of Wyoming, USA. *In*: Sankey, J. T. and Baszio, S. (eds.), *Vertebrate Microfossil Assemblages: Their Role in Paleoecology and Paleobiogeography*, 135–158. Bloomington, Indiana.

Longrich, N. R. and Currie, P. J. 2009a. *Albertonykus borealis*, a new alvarezsaur (Dinosauria: Theropoda) from the Early Maastrichtian of Alberta, Canada: implications for the systematics and ecology of the Alvarezsauridae. *Cretaceous Research* 30 (1): 239–252.

Longrich, N. R. and Currie, P. J. 2009b. A microraptorine (Dinosauria–Dromaeosauridae) from the Late Cretaceous of North America. *Proceedings of the National Academy of Sciences* 106 (13): 5002–5007.

Longrich, N. R., Currie, P. J. and Zhi-Ming, D. 2010. A new oviraptorid (Dinosauria: Theropoda) from the Upper Cretaceous of Bayan Mandahu, Inner Mongolia. *Palaeontology* 53 (5): 945–960.

Longrich, N. R., Barnes, K., Clark, S. and Millar, L. 2013. Caenagnathidae from the Upper Campanian Aguja Formation of West Texas, and a Revision of the Caenagnathinae. *Bulletin of the Peabody Museum of Natural History* 54 (1): 23–49.

Lowe, P. R. 1926. More notes on the quadrate as a factor in avian classification. *Ibis* 68 (1): 152–188.

Lubbe, T. van der, Richter, U. and Knötschke, N. 2009. Velociraptorine dromaeosaurid teeth from the Kimmeridgian (Late Jurassic) of Germany. *Acta Palaeontologica Polonica* 54 (3): 401–408.

Lü, J. 2003. A new oviraptorosaurid (Theropoda: Oviraptorosauria) from the Late Cretaceous of southern China. *Journal of Vertebrate Paleontology* 22 (4): 871–875.

Lü, J. 2005. Oviraptorid dinosaurs from southern China. Ph.D. Dissertation, Southern Methodist University, Dallas, Texas, USA, 200pp.

Lü, J., Tomida, Y., Azunia, Y., Dong, Z. and Lee, Y. N. 2004. New oviraptorid dinosaur (Dinosauria: Oviraptorosauria) from the Nemegt Formation of Southwestern Mongolia. *Bulletin of the National Science Museum: Geology & paleontology* 30: 95–130.

Lü, J., Xu, L., Liu, Y., Zhang, X., Jia, S. and Ji, Q. 2010. A new troodontid theropod from the Late Cretaceous of central China, and the radiation of Asian troodontids. *Acta Palaeontologica Polonica* 55 (3): 381–388.

Lü, J., Yi, L., Brusatte, S. L., Yang, L., Li, H. and Chen, L. 2014. A new clade of Asian Late Cretaceous long-snouted tyrannosaurids. *Nature Communications* 5.

Lydekker, R. 1879. Indian Pretertiary Vertebrata. 3. Fossil Reptilia and Batrachia. *Memoirs of the Geological Survey of India: Palaeontologia Indica* 4 (1): 1–35.

Lydekker, R. 1885. Indian Pretertiary Vertebrata. Vol I. Part 5. The Reptilia & Amphibia of the Maleri and Denwa Groups. *Memoirs of the Geological Survey of India: Palaeontologia Indica*: 1–38.

Lydekker, R. 1890. Note on certain vertebrate remains from the Nagpur district. *Records of the Geological Survey of India* 23 (1): 20–24.

Mader, B. J. and Bradley, R. L. 1989. A redescription and revised diagnosis of the syntypes of the Mongolian tyrannosaur *Alectrosaurus olseni*. *Journal of Vertebrate Paleontology* 9 (1): 41–55.

Madsen, J. H. 1976a. A second new theropod dinosaur from the Late Jurassic of east central Utah. *Utah geology* 3 (1): 51–60.

Madsen, J. H. 1976b. *Allosaurus fragilis*: A revised osteology. *Utah Geological Survey Bulletin* 109: 1–177.
Madsen, J. H. and Welles, S. P. 2000. *Ceratosaurus* (Dinosauria, Theropoda): a revised osteology. *Utah Geological Survey, Miscellaneous Publication* 00-2: 1–89.
Madzia, D. in press. The first non-avian theropod from the Czech Republic. *Acta Palaeontologica Polonica*: DOI:10.4202/app.2012.0111.
Maganuco, S., Cau, A. and Pasini, G. 2005. First description of theropod remains from the Middle Jurassic (Bathonian) of Madagascar. *Atti della Società italiana di scienze naturali e del museo civico di storia naturale di Milano* 146 (2): 165–202.
Maganuco, S., Cau, A., Dal Sasso, C. and Pasini, G. 2007. Evidence of large theropods from the Middle Jurassic of the Mahajanga Basin, NW Madagascar, with implications for ceratosaurian pedal ungual evolution. *Atti della Società italiana di scienze naturali e del museo civico di storia naturale di Milano* 148 (2): 261–271.
Mahler, L. 2005. Record of Abelisauridae (Dinosauria: Theropoda) from the Cenomanian of Morocco. *Journal of Vertebrate Paleontology* 25 (1): 236–239.
Maisch, M. W. and Matzke, A. T. 2003. Theropods (dinosauria, saurischia) from the middle Jurassic Toutunhe Formation of the Southern Junggar Basin, NW China. *Paläontologische Zeitschrift* 77 (2): 281–292.
Makovicky, P. J. and Sues, H. D. 1998. Anatomy and phylogenetic relationships of the theropod dinosaur *Microvenator celer* from the Lower Cretaceous of Montana. *American Museum novitates* 3240: 1–27.
Makovicky, P. J. and Norell, M. 1998. A partial ornithomimid braincase from Ukhaa Tolgod (Upper Cretaceous, Mongolia). *American Museum Novitates* 3247: 1–16.
Makovicky, P. J. and Norell, M. A. 2004. Troodontidae. *In*: Weishampel, D. B., Dodson, P. and Osmólska, H. (eds.), *The Dinosauria. Second Edition*, 184–195. University of California Press, Berkeley, California.
Makovicky, P. J., Kobayashi, Y. and Currie, P. J. 2004. Ornithomimosauria. *In*: Weishampel, D. B., Dodson, P. and Osmólska, H. (eds.), *The Dinosauria. Second Edition*, 137–150. University of California Press, Berkeley, California.
Makovicky, P. J., Apesteguía, S. and Agnolín, F. L. 2005. The earliest dromaeosaurid theropod from South America. *Nature* 437 (7061): 1007–1011.
Makovicky, P. J., Norell, M. A., Clark, J. M. and Rowe, T. 2003. Osteology and relationships of *Byronosaurus jaffei* (Theropoda: Troodontidae). *American Museum Novitates* 3402: 1–32.
Makovicky, P. J., Li, D., Gao, K.-Q., Lewin, M., Erickson, G. M. and Norell, M. A. 2010. A giant ornithomimosaur from the Early Cretaceous of China. *Proceedings of the Royal Society B: Biological Sciences* 277 (1679): 191–198.
Malafaia, E., Dantas, P., Ortega, F. and Escaso, F. 2007. Nuevos restos de *Allosaurus fragilis* (Theropoda: Carnosauria) del yacimiento de Andrés (Jurásico Superior; centro-oeste de Portugal). *Cantera Paleontológica* 1: 255–271.
Malafaia, E., Ortega, F., Silva, B. and Escaso, F. 2008. Fragmento de un maxilar de terópodo de Praia da Corva (Jurásico Superior. Torres Vedras, Portugal). *Palaeontologica Nova. SEPAZ* 8: 273–279.
Malafaia, E., Ortega, F., Escaso, F. and Silva, B. 2014. New evidence of *Ceratosaurus* (Dinosauria: Theropoda) from the Late Jurassic of the Lusitanian Basin, Portugal. *Historical Biology* 0 (0): 1–9.
Malafaia, E., Ortega, F., Escaso, F., Silva, B., Ramalheiro, G., Dantas, P., Moniz, C. and Barriga, F. 2009. Análisis preliminar de un nuevo ejemplar de *Allosaurus* del Grupo Lourinhã (Jurásico Superior de Torres Vedras, Portugal). *Actas de las IV Jornadas Internacionales sobre Paleontología de Dinosaurios y su Entorno. Ed. Colectivo Arqueológico y Paleontológico de Salas*: 243–251.
Maleev, E. A. 1954. Noviy cherepachoobrazhniy yashcher v Mongolii [New tortoise-like saurian from Mongolia]. *Priroda* 1954 (3): 106–108.
Mannion, P. D. and Calvo, J. O. 2011. Anatomy of the basal titanosaur (Dinosauria, Sauropoda) *Andesaurus delgadoi* from the mid-Cretaceous (Albian–early Cenomanian) Río Limay Formation, Neuquén Province, Argentina: implications for titanosaur systematics. *Zoological Journal of the Linnean Society* 163 (1): 155–181.
Mannion, P. D. and Barrett, P. M. 2013. Additions to the sauropod dinosaur fauna of the Cenomanian (early Late Cretaceous) Kem Kem beds of Morocco: Palaeobiogeographical implications of the mid-Cretaceous African sauropod fossil record. *Cretaceous Research* 45: 49–59.
Mannion, P. D., Upchurch, P., Barnes, R. N. and Mateus, O. 2013. Osteology of the Late Jurassic Portuguese sauropod dinosaur *Lusotitan atalaiensis* (Macronaria) and the evolutionary history of basal titanosauriforms. *Zoological Journal of the Linnean Society* 168 (1): 98–206.
Mantell, G. A. 1822. *The fossils of the South Downs, or, Illustrations of the geology of Sussex*. London, 446pp.
Mantell, G. A. 1827. *Illustrations of the Geology of Sussex: A General Viewof the Geological Relations of the South-Eastern Part of England, with Figures and Descriptions of the Fossils of Tilgate Forest*. Lupton Relfe, London, 92pp.
Mantell, G. A. 1833. *The Geology of the South-East of England*. Green and Longman, London, 415pp.

Manuppella, G. 1996. Carta geológica de Portugal 1/50 000. Folha 30-A, Lourinhã. *Instituto Geológico e Mineiro*.
Manuppella, G. 1998. Geologic data about the 'Camadas de Alcobaça'(Upper Jurassic) North of Lourinhã, and facies variation. *Memórias da Academia de Ciências de Lisboa* 37: 17–24.
Manuppella, G., Antunes, M. T., Pais, J., Ramalho, M. M. and Rey, J. 1999. Notícia Explicativa da Folha 30-A Lourinhã. *Instituto Geológico e Mineiro*: 1–83.
Marsh, O. C. 1871a. Notice of some new fossil reptiles from the Cretaceous and Tertiary formations. *American Journal of Science* 6 (1): 447–459.
Marsh, O. C. 1871b. A communication on some new reptiles and fishes from the Cretaceous and Tertiary formations. *Proceedings of the Academy of Natural Sciences of Philadelphia* 1871: 103–105.
Marsh, O. C. 1877. Notice of new dinosaurian reptiles from the Jurassic Formation. *American Journal of Science* 14 (5): 14–516.
Marsh, O. C. 1878. Notice of new dinosaurian reptiles. *American Journal of Science* (87): 241–244.
Marsh, O. C. 1881. Principal characters of American Jurassic dinosaurs. Part V. *American Journal of Science (Series 3)* 21: 417–423.
Marsh, O. C. 1882. Classification of the Dinosauria. *American Journal of Science (Series 3)* 23: 81–86.
Marsh, O. C. 1884a. The classification and affinities of dinosaurian reptiles. *Nature* 31: 68–69.
Marsh, O. C. 1884b. Principal characters of the American Jurassic dinosaurs. Part VIII. The order Theropoda. *American Journal of Science, Series 3* 27: 329–340.
Marsh, O. C. 1890. Description of new dinosaurian reptiles. *American Journal of Science* (229): 81–86.
Marsh, O. C. 1895. On the affinities and classification of the dinosaurian reptiles. *American Journal of Science* (300): 483–498.
Marsh, O. C. 1896. *The dinosaurs of North America*. Washington, 462pp.
Martill, D. M., Cruickshank, A. R. I., Frey, E., Small, P. G. and Clarke, M. 1996. A new crested maniraptoran dinosaur from the Santana Formation (Lower Cretaceous) of Brazil. *Journal of the Geological Society* 153 (1): 5–8.
Martinez, R. N. and Alcober, O. A. 2009. A basal sauropodomorph (Dinosauria: Saurischia) from the Ischigualasto Formation (Triassic, Carnian) and the early evolution of Sauropodomorpha. *PLoS ONE* 4 (2): e4397.
Martinez, R. N., Sereno, P. C., Alcober, O. A., Colombi, C. E., Renne, P. R., Montañez, I. P. and Currie, B. S. 2011. A basal dinosaur from the dawn of the dinosaur era in southwestern Pangaea. *Science* 331 (6014): 206–210.
Martin, L. D., Stewart, J. D. and Whetstone, K. N. 1980. The origin of birds: structure of the tarsus and teeth. *The Auk* 97: 86–93.
Martin, R. E. 1999. *Taphonomy: a process approach*. Cambridge University Press, Cambridge, England; New York, 526pp.
Martin, T. and Krebs, B. 2000. *Guimarota – A Jurassic Ecosystem*. Friedrich Pfeil, München, 156pp.
Marugán-Lobón, J., Buscalioni, A. D. and Elewa, A. M. T. 2004. Geometric morphometrics in macroevolution: morphological diversity of the skull in modern avian forms in contrast to some theropod dinosaurs. *In*: *Morphometrics: Applications in Biology and Paleontology*, 157–173. Springer−Verlag, Berlin.
Maryańska, T. and Osmólska, H. 1997. The quadrate of oviraptorid dinosaurs. *Acta Palaeontologica Polonica* 42 (3): 361–371.
Maryańska, T., Osmólska, H. and Wolsan, M. 2002. Avialan status for Oviraptorosauria. *Acta Palaeontologica Polonica* 47 (1): 97–116.
Massare, J. A. 1987. Tooth morphology and prey preference of Mesozoic marine reptiles. *Journal of Vertebrate Paleontology* 7 (2): 121–137.
Mateus, I., Mateus, H., Antunes, M. T., Mateus, O., Taquet, P., Ribeiro, V. and Manuppella, G. 1997. Couvée, œufs et embryons d'un dinosaure théropode du Jurassique supérieur de Lourinha (Portugal). *Comptes Rendus de l'Académie des Sciences - Series IIA - Earth and Planetary Science* 325 (1): 71–78.
Mateus, I., Mateus, H., Antunes, M. T., Mateus, O., Taquet, P., Ribeiro, V. and Manuppella, G. 1998. Upper Jurassic theropod dinosaur embryos from Lourinhã (Portugal). *Memórias da Academia das Ciências de Lisboa* 37: 101–110.
Mateus, O. 1998. *Lourinhanosaurus antunesi*, a new upper Jurassic allosauroid (Dinosauria: Theropoda) from Lourinhã, Portugal. *Memórias da Academia de Ciências de Lisboa* 37: 111–124.
Mateus, O. 2005. Dinossauros do Jurássico Superior de Portugal, com destaque para os saurísquios. Ph.D. Dissertation, Universidade Nova de Lisboa, Lisbon, Portugal, 375pp.
Mateus, O. 2006. Late Jurassic dinosaurs from the Morrison Formation (USA), the Lourinhã and Alcobaça Formations (Portugal), and the Tendaguru beds (Tanzania): a comparison. *New Mexico Museum of Natural History and Science Bulletin* 36: 223–232.

Mateus, O. and Antunes, M. T. 2000a. *Torvosaurus* sp. (Dinosauria: Theropoda) in the Late Jurassic of Portugal. *Libro de resúmenes, I Congresso Ibérico de Paleontología-XVI Jornadas de la Sociedad Española de Paleontología*: 115–117.

Mateus, O. and Antunes, M. T. 2000b. *Ceratosaurus* sp. (Dinosauria: Theropoda) in the Late Jurassic of Portugal. *Abstracts, 31st International Geological Congress*.

Mateus, O. and Telles Antunes, M. 2001. *Draconyx loureiroi*, a new camptosauridae (Dinosauria, Ornithopoda) from the Late Jurassic of Lourinhã, Portugal. *Annales de paléontologie* 87: 61–73.

Mateus, O. and Milàn, J. 2010. A diverse Upper Jurassic dinosaur ichnofauna from central-west Portugal. *Lethaia* 43 (2): 245–257.

Mateus, O., Antunes, M. T. and Taquet, P. 2001. Dinosaur ontogeny: the case of *Lourinhanosaurus* (Late Jurassic, Portugal). *Journal of Vertebrate Paleontology* 21 (Suppl 3): 78A.

Mateus, O., Walen, A. and Antunes, M. T. 2006. The large theropod fauna of the Lourinhã Formation (Portugal) and its similarity to the Morrison Formation, with a description of a new species of *Allosaurus*. *New Mexico Museum of Natural History and Science Bulletin* 36: 123–129.

Mateus, O., Maidment, S. C. R. and Christiansen, N. A. 2009. A new long-necked 'sauropod-mimic' stegosaur and the evolution of the plated dinosaurs. *Proceedings of the Royal Society B: Biological Sciences* 276 (1663): 1815–1821.

Mateus, O., Dinis, J. and Cunha, P. P. 2014. Upper Jurassic to Lowermost Cretaceous of the Lusitanian Basin, Portugal - landscapes where dinosaurs walked. *Ciências da Terra. special no. VIII*: 1–37.

Mateus, O., Araújo, R., Natário, C. and Castanhinha, R. 2011. A new specimen of the theropod dinosaur *Baryonyx* from the early Cretaceous of Portugal and taxonomic validity of *Suchosaurus*. *Zootaxa* 2827: 54–68.

Matthew, W. D. and Brown, B. 1922. The family Deinodontidae, with notice of a new genus from the Cretaceous of Alberta. *Bulletin of the American Museum of Natural History* 46 (6): 367–385.

Mayor, A. and Sarjeant, W. A. S. 2001. The folklore of footprints in stone: from classical antiquity to the present. *Ichnos* 8 (2): 143–163.

Mayr, G., Pohl, B. and Peters, D. S. 2005. A well-preserved *Archaeopteryx* specimen with theropod features. *Science* 310 (5753): 1483–1486.

Mayr, G., Pohl, B., Hartman, S. and Peters, D. S. 2007. The tenth skeletal specimen of *Archaeopteryx*. *Zoological Journal of the Linnean Society* 149 (1): 97–116.

McFeeters, B., Ryan, M. J., Hinic-Frlog, S. and Schröder-Adams, C. 2013. A reevaluation of *Sigilmassasaurus brevicollis* (Dinosauria) from the Cretaceous of Morocco. *Canadian Journal of Earth Sciences* 50 (6): 636–649.

McGowan, A. J. and Dyke, G. J. 2009. A surfeit of theropods in the Moroccan Late Cretaceous? Comparing diversity estimates from field data and fossil shops. *Geology* 37 (9): 843–846.

Medeiros, M. A. 2006. Large theropod teeth from the Eocenomanian of northeastern Brazil and the occurrence of Spinosauridae. *Revista brasileira de Paleontologia* 9 (3): 333–338.

Meekangvan, P., Barhorst, A., Burton, T. D., Chatterjee, S. and Schovanec, L. 2006. Nonlinear dynamical model and response of avian cranial kinesis. *Journal of Theoretical Biology* 240 (1): 32–47.

Le Mesle, G. and Peron, P. A. 1880. Sur des empreintes de pas d'oiseaux observées par M. le Mesle dans le Sud de l'Algérie. *Association Française pour l'Avancement des Sciences. Congrès de Reims*: 1–6.

Metzger, K. 2002. Cranial kinesis in lepidosaurs: skulls in motion. *Topics in functional and ecological vertebrate morphology. Maastricht: Shaker Publishing. p*: 15–46.

Meyer, H. von. 1832. *Paleologica zur Geschichte der Erde*. Frankfurt am Main, 560pp.

Milner, A. C. 2002. Theropod dinosaurs of the Purbeck limestone group, Southern England. *Special Papers in Palaeontology* 68: 191–202.

Milner, A. C. 2003. Fish-eating theropods: a short review of the systematics, biology and palaeobiogeography of spinosaurs. *Journadas Internacionales sobre paleontologiá de Dinosaurios y su Entoro* 2: 129–138.

Milner, A. R. and Kirkland, J. I. 2007. The case for fishing dinosaurs at the St. George Dinosaur Discovery site at Johnson Farm. *Utah Geological Survey Notes* 39: 1–3.

Miyashita, T., Tanke, D. H. and Currie, P. J. 2010. Variation in premaxillary tooth count and a developmental abnormality in a tyrannosaurid dinosaur. *Acta Palaeontologica Polonica* 55 (4): 635–643.

Molnar, R. E. 1991. The cranial morphology of *Tyrannosaurus rex*. *Palaeontographica Abteilung A* 217 (4-6): 137–176.

Molnar, R. E. 1998. Mechanical factors in the design of the skull of *Tyrannosaurus rex* (Osborn, 1905). *Gaia* 15: 193–218.

Molnar, R. E., Lopez Angriman, A. and Gasparini, Z. 1996. An Antarctic Cretaceous theropod. *Memoirs of the Queensland Museum* 39: 669–674.

Molnar, R. E., Obata, I., Tanimoto, M. and Matsukawa, M. 2009. A tooth of *Fukuiraptor* aff. *F. kitadaniensis* from the Lower Cretaceous Sebayashi Formation, Sanchu Cretaceous, Japan. *Bulletin of Tokyo Gakugei University, Division of Natural Sciences* 61: 105–117.

Mortimer, M. 2014. Spinosaurus *Stromer, 1915*. The Theropod Database. Downloaded from http://archosaur.us/theropoddatabase/Megalosauroidea.htm#Spinosaurusaegyptiacus on 19 May 2014.

Naish, D. 2002. The historical taxonomy of the Lower Cretaceous theropods (Dinosauria) *Calamospondylus* and *Aristosuchus* from the Isle of Wight. *Proceedings of the Geologists' Association* 113 (2): 153–163.

Naish, D. 2011. Theropod dinosaurs. *In*: Batten, D. J. (ed.), *English Wealden Fossils*, Vol. 10, 526–559. London, U.K.

Naish, D. 2012. Birds. *In*: Brett-Surman, M. K., Holtz, T. R. J. and Farlow, J. O. (eds.), *The Complete Dinosaur, Second Edition*, 379–423. Indiana University Press, Bloomington, Indiana.

Naish, D. and Dyke, G. J. 2004. *Heptasteornis* was no ornithomimid, troodontid, dromaeosaurid or owl: the first alvarezsaurid (Dinosauria: Theropoda) from Europe. *Neues Jahrbuch für Geologie und Paläontologie* 7: 385–401.

Naish, D., Martill, D. M. and Frey, E. 2004. Ecology, systematics and biogeographical relationships of dinosaurs, including a new theropod, from the Santana Formation (?Albian, Early Cretaceous) of Brazil. *Historical Biology* 16 (2-4): 57–70.

Nelson, S. J. and Ash, M. M. J. 2009. *Wheeler's Dental Anatomy, Physiology and Occlusion*. Saunders, St. Louis, Mo, 368pp.

Nesbitt, S. J. 2011. The early evolution of archosaurs: relationships and the origin of major clades. *Bulletin of the American Museum of Natural History*: 1–292.

Nesbitt, S. J., Turner, A. H., Erickson, G. M. and Norell, M. A. 2006. Prey choice and cannibalistic behaviour in the theropod *Coelophysis*. *Biology Letters* 2 (4): 611–614.

Nesbitt, S. J., Clarke, J. A., Turner, A. H. and Norell, M. A. 2011. A small alvarezsaurid from the eastern Gobi Desert offers insight into evolutionary patterns in the Alvarezsauroidea. *Journal of Vertebrate Paleontology* 31 (1): 144–153.

Nesbitt, S. J., Smith, N. D., Irmis, R. B., Turner, A. H., Downs, A. and Norell, M. A. 2009. A complete skeleton of a Late Triassic saurischian and the early evolution of dinosaurs. *Science* 326 (5959): 1530–1533.

Nicholls, E. L. and Russell, A. P. 1981. A new specimen of *Struthiomimus altus* from Alberta, with comments on the classificatory characters of Upper Cretaceous ornithomimids. *Canadian Journal of Earth Sciences* 18 (3): 518–526.

Nitzsch, C. L. 1816. Über die bewegung des oberkiefers der vögel. *Deutsches Archiv für die Physiologie* 2: 361–380.

Nixon, K. C. 2002. WinClada, version 1.00.08. *Published by the author, Ithaca, New York.*

Nopcsa, F. von. 1928. The genera of reptiles. *Palaeobiologica* 1: 163–188.

Norell, M. and Makovicky, P. J. 1997. Important features of the dromaeosaur skeleton : information from a new specimen. *American Museum Novitates* 3215: 1–28.

Norell, M. and Makovicky, P. J. 1999. Important features of the dromaeosaurid skeleton. 2, Information from newly collected specimens of *Velociraptor mongoliensis*. *American Museum Novitates* 3282: 1–45.

Norell, M. A. and Hwang, S. H. 2004. A troodontid dinosaur from Ukhaa Tolgod (Late Cretaceous Mongolia). *American Museum Novitates* 3446: 1–9.

Norell, M. A. and Makovicky, P. J. 2004. Dromaeosauridae. *In*: Weishampel, D., Dodson, P. and Osmólska, H. (eds.), *The Dinosauria. Second Edition*, 196–209. University of California Press, Berkeley, California.

Norell, M. A., Makovicky, P. J. and Clark, J. M. 2000. A new troodontid theropod from Ukhaa Tolgod, Mongolia. *Journal of Vertebrate Paleontology* 20 (1): 7–11.

Norell, M. A., Makovicky, P. J. and Currie, P. J. 2001a. Palaeontology: the beaks of ostrich dinosaurs. *Nature* 412 (6850): 873–874.

Norell, M. A., Clark, J. M. and Chiappe, L. M. 2001b. An embryonic oviraptorid (Dinosauria: Theropoda) from the Upper Cretaceous of Mongolia. *American Museum Novitates* 3315: 1–20.

Norell, M. A., Clark, J. M., Turner, A. H., Makovicky, P. J., Barsbold, R. and Rowe, T. 2006. A new dromaeosaurid theropod from Ukhaa Tolgod (Ömnögov, Mongolia). *American Museum Novitates* 3545: 1–51.

Norell, M. A., Makovicky, P. J., Bever, G. S., Balanoff, A. M., Clark, J. M., Barsbold, R. and Rowe, T. 2009. A review of the Mongolian Cretaceous dinosaur *Saurornithoides* (Troodontidae: Theropoda). *American Museum Novitates* 3654: 1–63.

Norell, M. A., Clark, J. M., Demberelyin, D., Rhinchen, B., Chiappe, L. M., Davidson, A. R., McKenna, M. C., Altangerel, P. and Novacek, M. J. 1994. A theropod dinosaur embryo and the affinities of the Flaming Cliffs dinosaur eggs. *Science* 266 (5186): 779–782.

Nothdurft, W. 2003. *The Lost Dinosaurs of Egypt: The Astonishing and Unlikely True Story of One of the Twentieth Century's Greatest Paleontological Discoveries*. Random House Trade Paperbacks, New York, 272pp.

Novas, F. E. 1991. Relaciones filogeneticas de los dinosaurios teropodos ceratosaurios. *Ameghiniana* 28 (3-4): 410.

Novas, F. E. 1992. La evolución de los dinosaurios carnivoros. *In*: Sanz, J. L. and Buscalioni, A. D. (eds.), *Los Dinosaurios Y Su Entorno Biotico: Actas Del Segundo Curso de Paleontología En Cuenca*, 126–163. Instituto 'Juan Valdez,' Cuenca, Spain.

Novas, F. E. 1997a. Abelisauridae. *In*: Currie, P. J. and Padian, K. (eds.), *Encyclopedia of Dinosaurs*, 1–2. Academic Press, San Diego, California.

Novas, F. E. 1997b. Anatomy of *Patagonykus puertai* (Theropoda, Avialae, Alvarezsauridae), from the Late Cretaceous of Patagonia. *Journal of Vertebrate Paleontology* 17 (1): 137–166.

Novas, F. E. and Puerta, P. F. 1997. New evidence concerning avian origins from the Late Cretaceous of Patagonia. *Nature* 387 (6631): 390–392.

Novas, F. E., Dalla Vecchia, F. and Pais, D. F. 2005a. Theropod pedal unguals from the Late Cretaceous (Cenomanian) of Morocco, Africa. *Revista del Museo Argentino de Ciencias Naturales* 7 (2): 167–175.

Novas, F. E., Ezcurra, M. D. and Lecuona, A. 2008. *Orkoraptor burkei* nov. gen. et sp., a large theropod from the Maastrichtian Pari Aike Formation, Southern Patagonia, Argentina. *Cretaceous Research* 29 (3): 468–480.

Novas, F. E., Valais, S., Vickers-Rich, P. and Rich, T. 2005b. A large Cretaceous theropod from Patagonia, Argentina, and the evolution of carcharodontosaurids. *Naturwissenschaften* 92 (5): 226–230.

Novas, F. E., Chatterjee, S., Rudra, D. K. and Datta, P. M. 2010. *Rahiolisaurus gujaratensis*, n. gen. n. sp., A New Abelisaurid Theropod from the Late Cretaceous of India. *In*: Bandyopadhyay, S. (ed.), *New Aspects of Mesozoic Biodiversity*, 45–62. Springer Berlin Heidelberg.

Novas, F. E., Pol, D., Canale, J. I., Porfiri, J. D. and Calvo, J. O. 2009. A bizarre Cretaceous theropod dinosaur from Patagonia and the evolution of Gondwanan dromaeosaurids. *Proceedings of the Royal Society B: Biological Sciences* 276 (1659): 1101–1107.

Novas, F. E., Ezcurra, M. D., Agnolín, F. L., Pol, D. and Ortíz, R. 2012. New Patagonian Cretaceous theropod sheds light about the early radiation of Coelurosauria. *Revista del Museo Argentino de Ciencias Naturales* 14 (1): 57–81.

Novas, F. E., Agnolín, F. L., Ezcurra, M. D., Porfiri, J. and Canale, J. I. 2013. Evolution of the carnivorous dinosaurs during the Cretaceous: The evidence from Patagonia. *Cretaceous Research* 45: 174–215.

O'Connor, J., Zhou, Z. and Xu, X. 2011. Additional specimen of *Microraptor* provides unique evidence of dinosaurs preying on birds. *Proceedings of the National Academy of Sciences* 108 (49): 19662–19665.

Ortega, F., Escaso, F. and Sanz, J. L. 2010. A bizarre, humped Carcharodontosauria (Theropoda) from the Lower Cretaceous of Spain. *Nature* 467 (7312): 203–206.

Osborn, H. F. 1903. *Ornitholestes hermanni*, a new compsognathoid dinosaur from the Upper Jurassic. *Bulletin of the American Museum of Natural History* 19: 459–464.

Osborn, H. F. 1905. *Tyrannosaurus* and other Cretaceous carnivorous dinosaurs. *Bulletin of the American Museum of Natural History* 21: 259–265.

Osborn, H. F. 1906. *Tyrannosaurus*, Upper Cretaceous Carnivorous Dinosaur:(second Communication). *Bulletin of the American Museum of Natural History* 22 (16): 281–296.

Osborn, H. F. 1912. Crania of *Tyrannosaurus* and *Allosaurus*. *Memoirs of the American Museum of Natural History. New Series* 1 (1): 1–30.

Osborn, H. F. 1924. Three New Theropoda, *Protoceratops* Zone, Central Mongolia. *American Museum Novitates* 144 (7): 1–12.

Ősi, A., Apesteguía, S. and Kowalewski, M. 2010. Non-avian theropod dinosaurs from the early Late Cretaceous of central Europe. *Cretaceous Research* 31 (3): 304–320.

Osmólska, H. 1997. Ornithomimosauria. *In*: Currie, P. J. and Padian, K. (eds.), *Encyclopedia of Dinosaurs*, 499–503. Academic Press, San Diego, California.

Osmólska, H. and Roniewicz, E. 1970. Deinocheiridae, a new family of theropod dinosaurs. *Palaeontologica Polonica* 21: 5–19.

Osmólska, H., Roniewicz, E. and Barsbold, R. 1972. A new dinosaur, *Gallimimus bullatus* n. gen., n. sp.(Ornithomimidae) from the Upper Cretaceous of Mongolia. *Palaeontologia Polonica* 27: 103–143.

Osmólska, H., Currie, P. J. and Barsbold, R. 2004. Oviraptorosauria. *In*: Weishampel, D. B., Dodson, P. and Osmólska, H. (eds.), *The Dinosauria. Second Edition*, 165–183. University of California Press, Berkeley, California.

Ostrom, J. H. 1969. Osteology of *Deinonychus antirrhopus*, an unusual theropod from the Lower Cretaceous of Montana. *Bulletin Peabody Museum of Natural History* 30: 1–165.

Ostrom, J. H. 1972. Carnivorous dinosaurs. *McGraw-Hill Yearbook of Science and Technology for 1971* 1971: 176–179.
Ostrom, J. H. 1976a. *Archaeopteryx* and the origin of birds. *Biological Journal of the Linnean Society* 8 (2): 91–182.
Ostrom, J. H. 1976b. On a new specimen of the Lower Cretaceous theropod dinosaur *Deinonychus antirrhopus*. *Breviora* 439: 1–21.
Ostrom, J. H. 1978. The osteology of *Compsognathus longipes* Wagner. *Zitteliana* 4: 73–118.
Ostrom, J. H. and Wellnhofer, P. 1986. The Munich specimen of *Triceratops* with a revision of the genus. *Zitteliana* 14: 111–158.
Owen, R. 1840. *Odontography; or, A treatise on the comparative anatomy of the teeth; their physiological relations, mode of development, and microscopic structure, in the vertebrate animals*. London, H. Baillière, 766pp.
Owen, R. 1842. Report on British fossil reptiles. *Report of the British Association for the Advancement of Science* 11 (1841): 60–294.
Owen, R. 1849. *A History of British Fossil Reptiles*. Cassell & company limited, 690pp.
Owen, S. R. 1854. On some fossil reptilian and mammalian remains from the Purbecks. *Quarterly Journal of the Geological Society of London* 10: 420–433.
Padian, K. 1997. Deinonychosauria. *In*: Currie, P. J. and Padian, K. (eds.), *Encyclopedia of Dinosaurs*, 166–167. Academic Press, San Diego, California.
Padian, K. 2004. Basal Avialae. *In*: Weishampel, D. B., Dodson, P. and Osmólska, H. (eds.), *The Dinosauria. Second Edition*, 210–231. University of California Press, Berkeley, California.
Padian, K. and Hutchinson, J. R. 1997. Allosauroidea. *In*: Currie, P. J. and Padian, K. (eds.), *Encyclopedia of Dinosaurs*, 6–9. Academic Press, San Diego, California.
Padian, K. and Chiappe, L. M. 1998. The origin and early evolution of birds. *Biological Reviews* 73 (1): 1–42.
Padian, K., Hutchinson, J. R. and Holtz, T. R. 1999. Phylogenetic definitions and nomenclature of the major taxonomic categories of the carnivorous Dinosauria (Theropoda). *Journal of Vertebrate Paleontology* 19 (1): 69–80.
Park, E.-J., Yang, S.-Y. and Currie, P. J. 2000. Early Cretaceous dinosaur teeth of Korea. *Paleontological Society of Korea Special Publication* 4: 85–98.
Paul, G. S. 1988. *Predatory Dinosaurs of the World: A Complete Illustrated Guide*. Simon & Schuster, 464pp.
Paul, G. S. 2002. *Dinosaurs of the Air: The Evolution and Loss of Flight in Dinosaurs and Birds*. Johns Hopkins University Press, Baltimore, 472pp.
Pérez-Moreno, B. P., Sanz, J. L., Buscalioni, A. D., Moratalla, J. J., Ortega, F. and Rasskin-Gutman, D. 1994. A unique multitoothed ornithomimosaur dinosaur from the Lower Cretaceous of Spain. *Nature* 370 (6488): 363–367.
Pérez-Moreno, B. P., Chure, D. J., Pires, C., Silva, C. M. D., Santos, V. D., Dantas, P., Póvoas, L., Cachão, M., Sanz, J. L. and Carvalho, A. M. G. D. 1999. On the presence of *Allosaurus fragilis* (Theropoda: Carnosauria) in the Upper Jurassic of Portugal: first evidence of an intercontinental dinosaur species. *Journal of the Geological Society* 156 (3): 449–452.
Perle, A., Chiappe, L. M. and Barsbold, R. 1994. Skeletal morphology of *Mononykus olecranus* (Theropoda: Avialae) from the Late Cretaceous of Mongolia. *American Museum Novitates* 3105: 1–29.
Perle, A., Norell, M. and Clark, J. M. 1999. A new maniraptoran theropod, *Achillobator giganticus* (Dromaeosauridae), from the Upper Cretaceous of Burkhant, Mongolia. *Contributions from the Geology and Mineralogy Chair, National Museum of Mongolia* 101: 1–105.
Perle, A., Norell, M. A., Chiappe, L. M. and Clark, J. M. 1993. Flightless bird from the Cretaceous of Mongolia. *Nature* 362 (6421): 623–626.
Peyer, B. 1968. *Comparative Odontology*. University of Chicago Press, 458pp.
Peyer, K. 2006. A reconsideration of *Compsognathus* from the upper Tithonian of Canjuers, southeastern France. *Journal of Vertebrate Paleontology* 26 (4): 879–896.
Platt, J. 1758. An account of the fossile thigh-bone of a large animal, dug up at Stonesfield, near Woodstock. *Philosophical Transactions of the Royal Society of London* 50: 524–527.
Plot, R. 1677. *The Natural History of Oxfordshire, Being an Essay Toward the Natural History of England*. Printed at the Theater, Oxford, 378pp.
Polcyn, M. J. and Bell, G. L. 2005. *Russellosaurus coheni* n. gen., n. sp., a 92 million-year-old mosasaur from Texas (USA), and the definition of the parafamily Russellosaurina. *Netherlands Journal of Geosciences* 84 (3): 321–333.
Pol, D. and Rauhut, O. W. M. 2012. A Middle Jurassic abelisaurid from Patagonia and the early diversification of theropod dinosaurs. *Proceedings of the Royal Society B: Biological Sciences* 279 (1741): 3170–3175.

Porchetti, S. D., Nicosia, U., Biava, A. and Maganuco, S. 2011. New abelisaurid material from the Upper Cretaceous (Cenomanian) of Morocco. *Rivista Italiana di Paleontologia e Stratigrafia* 117 (3): 463–472.

Porfiri, J. D., Novas, F. E., Calvo, J. O., Agnolín, F. L., Ezcurra, M. D. and Cerda, I. A. 2014. Juvenile specimen of *Megaraptor* (Dinosauria, Theropoda) sheds light about tyrannosauroid radiation. *Cretaceous Research* 51: 35–55.

Prasad, G. V. and de Lapparent de Broin, F. 2002. Late Cretaceous crocodile remains from Naskal (India): comparisons and biogeographic affinities. *Annales de Paléontologie* 88: 19–71.

Pu, H., Kobayashi, Y., Lü, J., Xu, L., Wu, Y., Chang, H., Zhang, J. and Jia, S. 2013. An unusual basal therizinosaur dinosaur with an ornithischian dental arrangement from Northeastern China. *PLoS ONE* 8 (5): e63423.

Raath, M. A. 1969. A new coelurosaurian dinosaur from the Forest Sandstone of Rhodesia. *National Museums of Southern Rhodesia. Arnoldia* 4: 1–25.

Raath, M. A. 1977. The anatomy of the Triassic theropod *Syntarsus rhodesiensis* (Saurischia: Podokesauridae) and a consideration of its biology. Ph.D. Dissertation, Department of Zoology and Entomology, Rhodes University, Salisbury, Rhodesia, 233pp.

Rauhut, O. W. 2004a. Braincase structure of the Middle Jurassic theropod dinosaur *Piatnitzkysaurus*. *Canadian Journal of Earth Sciences* 41 (9): 1109–1122.

Rauhut, O. W. 2011. Theropod dinosaurs from the Late Jurassic of Tendaguru (Tanzania). *Special Papers in Palaeontology* 86: 195–239.

Rauhut, O. W. and Hungerbühler, A. 1998. A review of European Triassic theropods. *Gaia* 15: 75–88.

Rauhut, O. W. M. 1995. Zur systematischen Stellung der afrikanischen Theropoden *Carcharodontosaurus* Stromer 1931 und *Bahariasaurus*Stromer 1934. *Berliner Geowissenschaften Abhlandlungen E* 16: 357–375.

Rauhut, O. W. M. 2000a. The interrelationships and evolution of basal theropods (Dinosauria, Saurischia). Ph.D. Dissertation, University of Bristol, Bristol, UK, Bristol, UK, 583pp.

Rauhut, O. W. M. 2000b. The dinosaur fauna from the Guimarota mine. *In*: Martin, T. and Krebs, B. (eds.), *Guimarota - A Jurassic Ecosystem*, 75–82. München.

Rauhut, O. W. M. 2001. Herbivorous dinosaurs from the Late Jurassic (Kimmeridgian) of Guimarota, Portugal. *Proceedings of the Geologists' Association* 112 (3): 275–283.

Rauhut, O. W. M. 2002. Dinosaur teeth from the Barremian of Uña, Province of Cuenca, Spain. *Cretaceous Research* 23 (2): 255–263.

Rauhut, O. W. M. 2003a. The interrelationships and evolution of basal theropod dinosaurs. *Special Papers in Palaeontology* 69: 1–213.

Rauhut, O. W. M. 2003b. A tyrannosauroid dinosaur from the Upper Jurassic of Portugal. *Palaeontology* 46 (5): 903–910.

Rauhut, O. W. M. 2004b. Provenance and anatomy of *Genyodectes serus*, a large-toothed ceratosaur (Dinosauria: Theropoda) from Patagonia. *Journal of Vertebrate Paleontology* 24 (4): 894–902.

Rauhut, O. W. M. 2005a. Osteology and relationships of a new theropod dinosaur from the Middle Jurassic of Patagonia. *Palaeontology* 48 (1): 87–110.

Rauhut, O. W. M. 2005b. Post-cranial remains of 'coelurosaurs' (Dinosauria, Theropoda) from the Late Jurassic of Tanzania. *Geological Magazine* 142 (1): 97–107.

Rauhut, O. W. M. and Kriwet, J. 1994. Teeth of a big theropod dinosaur from Porto das Barcas (Portugal). *Berliner Geowissenschaftliche Abhandlungen, E* 13: 179–185.

Rauhut, O. W. M. and Werner, C. 1995. First record of the family Dromaeosauridae (Dinosauria: Theropoda) in the Cretaceous of Gondwana (Wadi Milk Formation, northern Sudan). *Paläontologische Zeitschrift* 69 (3): 475–489.

Rauhut, O. W. M. and Xu, X. 2005. The small theropod dinosaurs *Tugulusaurus* and *Phaedrolosaurus* from the early Cretaceous of Xinjiang, China. *Journal of Vertebrate Paleontology* 25 (1): 107–118.

Rauhut, O. W. M. and Fechner, R. 2005. Early development of the facial region in a non-avian theropod dinosaur. *Proceedings of the Royal Society B: Biological Sciences* 272 (1568): 1179–1183.

Rauhut, O. W. M. and López-Arbarello, A. 2009. Considerations on the age of the Tiouaren Formation (Iullemmeden Basin, Niger, Africa): implications for Gondwanan Mesozoic terrestrial vertebrate faunas. *Palaeogeography, Palaeoclimatology, Palaeoecology* 271 (3-4): 259–267.

Rauhut, O. W. M., Milner, A. C. and Moore-Fay, S. 2010. Cranial osteology and phylogenetic position of the theropod dinosaur *Proceratosaurus bradleyi* (Woodward, 1910) from the Middle Jurassic of England. *Zoological Journal of the Linnean Society* 158 (1): 155–195.

Rauhut, O. W. M., Cladera, G., Vickers-Rich, P. and Rich, T. H. 2003. Dinosaur remains from the Lower Cretaceous of the Chubut Group, Argentina. *Cretaceous Research* 24 (5): 487–497.

Rauhut, O. W. M., Foth, C., Tischlinger, H. and Norell, M. A. 2012. Exceptionally preserved juvenile megalosauroid theropod dinosaur with filamentous integument from the Late Jurassic of Germany. *Proceedings of the National Academy of Sciences* 109 (29): 11746–11751.

Rauhut, O. W. M., Remes, K., Fechner, R., Cladera, G. and Puerta, P. 2005. Discovery of a short-necked sauropod dinosaur from the Late Jurassic period of Patagonia. *Nature* 435 (7042): 670–672.

Rayfield, E. J. 2005a. Aspects of comparative cranial mechanics in the theropod dinosaurs *Coelophysis*, *Allosaurus* and *Tyrannosaurus*. *Zoological Journal of the Linnean Society* 144 (3): 309–316.

Rayfield, E. J. 2005b. Using finite-element analysis to investigate suture morphology: A case study using large carnivorous dinosaurs. *The Anatomical Record Part A: Discoveries in Molecular, Cellular, and Evolutionary Biology* 283A (2): 349–365.

Rayfield, E. J. 2011. Structural performance of tetanuran theropod skulls, with emphasis on the Megalosauridae, Spinosauridae and Carcharodontosauridae. *Special Papers in Palaeontology* 86: 241–253.

Rayfield, E. J., Milner, A. C., Xuan, V. B. and Young, P. G. 2007. Functional morphology of spinosaur 'crocodile-mimic' dinosaurs. *Journal of Vertebrate Paleontology* 27 (4): 892–901.

Reichel, M. 2010. The heterodonty of *Albertosaurus sarcophagus* and *Tyrannosaurus rex*: biomechanical implications inferred through 3-D models. *Canadian Journal of Earth Sciences* 47 (9): 1253–1261.

Reid, R. E. H. 1997. Histology of bones and teeth. *In*: Currie, P. J. and Padian, K. (eds.), *Encyclopedia of Dinosaurs*, 329–339. Academic Press, San Diego, California.

Reig, O. A. 1963. La presencia de dinosaurios saurisquios en los 'Estratos de Ischigualasto' (Mesotriásico Superior) de las provincias de San Juan y La Rioja (República Argentina). *Ameghiniana* 3 (1): 3–20.

Remes, K., Ortega, F., Fierro, I., Joger, U., Kosma, R., Ferrer, J. M. M., Ide, O. A. and Maga, A. 2009. A new basal sauropod dinosaur from the Middle Jurassic of Niger and the early evolution of Sauropoda. *PLoS One* 4 (9): e6924.

Ribeiro, V. and Mateus, O. 2012. Chronology of the Late Jurassic dinosaur faunas, and other reptilian faunas, from Portugal. *72nd Annual Meeting Society of Vertebrate Paleontology, Raleigh, USA. (October 17-20, 2012), Program and Abstracts*: 161.

Richter, U., Mudroch, A. and Buckley, L. G. 2013. Isolated theropod teeth from the Kem Kem Beds (Early Cenomanian) near Taouz, Morocco. *Paläontologische Zeitschrift* 87 (2): 291–309.

De Ricqlès, A., Mateus, O., Antunes, M. T. and Taquet, P. 2001. Histomorphogenesis of embryos of Upper Jurassic theropods from Lourinhã (Portugal). *Comptes Rendus de l'Académie des Sciences-Series IIA-Earth and Planetary Science* 332 (10): 647–656.

Rieppel, O. 2006. The merits of similarity reconsidered. *Systematics and Biodiversity* 4 (2): 137–147.

Riff, D., Mader, B., Kellner, A. W. A. and Russell, D. 2004. An avian vertebra from the continental Cretaceous of Morocco, Africa. *Arquivos do Museu Nacional Rio de Janeiro* 62 (2): 217–223.

Von Ritgen, F. A. 1826. Versuchte Herstellung einiger Becken urweltlichter Thiere. *Nova Acta Academiae Caesarea LeopoldinoCarolinae Germanicae Naturae Curiosorum* 13: 331–358.

Rogers, R. R., Eberth, D. A. and Fiorillo, A. R. 2007. *Bonebeds: Genesis, Analysis, and Paleobiological Significance*. University of Chicago Press, Chicago, 499pp.

Rohlf, F. J. and Slice, D. 1990. Extensions of the procrustes method for the optimal superimposition of landmarks. *Systematic Biology* 39 (1): 40–59.

Romer, A. 1956. *Osteology of the Reptiles*. University of Chicago Press, Chicago, 772pp.

Rowe, T. 1989. A new species of the theropod dinosaur *Syntarsus* from the Early Jurassic Kayenta Formation of Arizona. *Journal of Vertebrate Paleontology* 9 (2): 125–136.

Rowe, T. and Gauthier, J. 1990. Ceratosauria. *In*: Weishampel, D., Dodson, P. and Osmólska, H. (eds.), *The Dinosauria. First Edition*, 151–168. University of California Press, Berkeley, California.

Ruiz, J., Torices, A., Serrano, H. and López, V. 2011. The hand structure of *Carnotaurus sastrei* (Theropoda, Abelisauridae): implications for hand diversity and evolution in abelisaurids. *Palaeontology* 54 (6): 1271–1277.

Ruiz-Omeñaca, J. I., Piñuela, L. and García-Ramos, J. C. 2012. Primera descripción de dientes de dinosaurios terópodos en la Formación Tereñes (Kimmeridgiense), Asturias. *Geogaceta* 52: 177–180.

Russell, A. P. 1997. Therizinosauria. *In*: Currie, P. J. and Padian, K. (eds.), *Encyclopedia of Dinosaurs*, 729–730. Academic Press, San Diego, California.

Russell, D. A. 1969. A new specimen of *Stenonychosaurus* from the Oldman Formation (Cretaceous) of Alberta. *Canadian Journal of Earth Sciences* 6 (4): 595–612.

Russell, D. A. 1970. Tyrannosaurs from the Late Cretaceous of western Canada. *National Museum of Natural Sciences Publications in Paleontology* 1: 1–34.

Russell, D. A. 1972. Ostrich dinosaurs from the Late Cretaceous of Western Canada. *Canadian Journal of Earth Sciences* 9 (4): 375–402.

Russell, D. A. 1984. A check list of the families and genera of North American dinosaurs. *Syllogeus* 53: 1–35.

Russell, D. A. 1996. Isolated dinosaur bones from the Middle Cretaceous of the Tafilalt, Morocco. *Bulletin du Muséum National d'Histoire Naturelle* 4 (18): 349–402.
Russell, D. A. and Dong, Z. 1993a. The affinities of a new theropod from the Alxa Desert, Inner Mongolia, People's Republic of China. *Canadian Journal of Earth Sciences* 30 (10): 2107–2127.
Russell, D. A. and Dong, Z.-M. 1993b. A nearly complete skeleton of a new troodontid dinosaur from the Early Cretaceous of the Ordos Basin, Inner Mongolia, People's Republic of China. *Canadian Journal of Earth Sciences* 30 (10): 2163–2173.
Russell, D. A. and Wu, X.-C. 1997. The Crocodylomorpha at and between geological boundaries: the Baden-Powell approach to change? *Zoology* 100 (3): 164–182.
Russell, D. A. and Paesler, M. A. 2003. Environments of Mid-Cretaceous Saharan dinosaurs. *Cretaceous Research* 24 (5): 569–588.
Russell, L. S. 1948. The dentary of *Troödon*, a genus of theropod dinosaurs. *Journal of Paleontology* 22 (5): 625–629.
Ryan, M. J., Currie, P. J., Gardner, J. D., Vickaryous, M. K. and Lavigne, J. M. 1998. Baby hadrosaurid material associated with an unusually high abundance of *Troodon* teeth from the Horseshoe Canyon Formation, Upper Cretaceous, Alberta, Canada. *Gaia* 15: 123–133.
Sadleir, R., Barrett, P. M. and Powell, H. P. 2008. The anatomy and systematics of *Eustreptospondylus oxoniensis*, a theropod dinosaur from the Middle Jurassic of Oxfordshire, England. *Monograph of the Palaeontographical Society, London* 160: 1–82.
Sadleir, R. W. 2008. Theropod teeth from the Cretaceous of Morocco. *Journal of Vertebrate Paleontology* 18 (3): 74A.
Sakamoto, M. 2008. Bite force and the evolution of feeding function in birds, dinosaurs and cats. Ph.D. Dissertation, University of Bristol, Brisol, U.K., 254pp.
Sakamoto, M. 2010. Jaw biomechanics and the evolution of biting performance in theropod dinosaurs. *Proceedings of the Royal Society B: Biological Sciences* 277 (1698): 3327–3333.
Salgado, L., Coria, R. A. and Chiappe, L. M. 2005. Osteology of the sauropod embryos from the Upper Cretaceous of Patagonia. *Acta Palaeontologica Polonica* 50 (1): 79–92.
Salgado, L., Canudo, J. I., Garrido, A. C., Ruiz-Omeñaca, J. I., García, R. A., de la Fuente, M. S., Barco, J. L. and Bollati, R. 2009. Upper Cretaceous vertebrates from El Anfiteatro area, Río Negro, Patagonia, Argentina. *Cretaceous Research* 30 (3): 767–784.
Samejima, M. and Otsuka, J. 1987. Observations on the Quadrate of Birds. *Japanese Journal of Ornithology* 35 (4): 129–144.
Samman, T., Powell, G. L., Currie, P. J. and Hills, L. V. 2005. Morphometry of the teeth of western North American tyrannosaurids and its applicability to quantitative classification. *Acta Palaeontologica Polonica* 50 (4): 757–776.
Sampson, S. D. and Witmer, L. M. 2007. Craniofacial anatomy of *Majungasaurus crenatissimus* (Theropoda: Abelisauridae) from the Late Cretaceous of Madagascar. *Journal of Vertebrate Paleontology* 27 (sup2): 32–104.
Sampson, S. D., Carrano, M. T. and Forster, C. A. 2001. A bizarre predatory dinosaur from the Late Cretaceous of Madagascar. *Nature* 409 (6819): 504–506.
Sampson, S. D., Krause, D. W., Dodson, P. and Forster, C. A. 1996. The premaxilla of *Majungasaurus* (Dinosauria: Theropoda), with implications for Gondwanan paleobiogeography. *Journal of Vertebrate Paleontology* 16 (4): 601–605.
Sampson, S. D., Witmer, L. M., Forster, C. A., Krause, D. W., O'Connor, P. M., Dodson, P. and Ravoavy, F. 1998. Predatory dinosaur remains from Madagascar: implications for the Cretaceous biogeography of Gondwana. *Science* 280 (5366): 1048–1051.
Sander, P. M. 1997. Teeth and jaws. *In*: Currie, P. J. and Padian, K. (eds.), *Encyclopedia of Dinosaurs*, 717–725. Academic Press, San Diego, California.
Sander, P. M. 1999. The microstructure of reptilian tooth enamel: terminology, function, and phylogeny. *Münchner Geowissenschaftliche Abhandlungen, Reihe A* 38: 1–102.
Sander, P. M., Gee, C. T., Hummel, J. and Clauss, M. 2010. Mesozoic plants and dinosaur herbivory. *In*: Gee, C. T. (ed.), *Plants in Mesozoic Time: Morphological Innovations, Phylogeny, Ecosystems*, 331–359. Bloomington.
Sanders, R. K. and Smith, D. K. 2005. The endocranium of the theropod dinosaur *Ceratosaurus* studied with computed tomography. *Acta Palaeontologica Polonica* 50 (3): 601.
Sankey, J. T. 2001. Late Campanian Southern Dinosaurs, Aguja Formation, Big Bend, Texas. *Journal of Paleontology* 75 (1): 208–215.
Sankey, J. T. 2008. Diversity of Latest Cretaceous (Late Maastrichtian) small theropods and birds: teeth from the Lance and Hell Creek Formations, USA. *In*: Sankey, J. T. and Baszio, S. (eds.), *Vertebrate Microfossil Assemblages: Their Role in Paleoecology and Paleobiogeography*, 117–134. Bloomington, Indiana.

Sankey, J. T., Brinkman, D. B., Guenther, M. and Currie, P. J. 2002. Small theropod and bird teeth from the Late Cretaceous (Late Campanian) Judith River Group, Alberta. *Journal of Paleontology* 76 (4): 751–763.

Dal Sasso, C. 2003. Dinosaurs of Italy. *Comptes Rendus Palevol* 2 (1): 46–66.

Dal Sasso, C. and Signore, M. 1998. Exceptional soft-tissue preservation in a theropod dinosaur from Italy. *Nature* 392 (6674): 383–387.

Dal Sasso, C. and Maganuco, S. 2011. *Scipionyx samniticus* (Theropoda: Compsognathidae) from the Lower Cretaceous of Italy: osteology, ontogenetic assessment, phylogeny, soft tissue anatomy, taphonomy and palaeobiology. *Memorie della Società Italiana di Scienze Naturali e del Museo Civico di Storia Naturale di Milano* 37 (1): 1–281.

Dal Sasso, C., Maganuco, S. and Cioffi, A. 2009. A neurovascular cavity within the snout of the predatory dinosaur *Spinosaurus*. *First International Congress on North African Vertebrate Palaeontology, 25-27 May 2009 Marrakech (Morocco)*: 22–23.

Dal Sasso, C., Maganuco, S., Buffetaut, E. and Mendez, M. A. 2005. New information on the skull of the enigmatic theropod *Spinosaurus*, with remarks on its size and affinities. *Journal of Vertebrate Paleontology* 25 (4): 888–896.

Sauvage, H. E. 1882. Recherches sur les reptiles trouvés dans le Gault de l'Est du bassin de Paris. *Mémoire de la Société Géologique de France* 2: 1–41.

Schubert, B. W. and Ungar, P. S. 2005. Wear facets and enamel spalling in tyrannosaurid dinosaurs. *Acta Palaeontologica Polonica* 50 (1): 93–99.

Schudack, M. E. 2000. Ostracodes and charophytes from the Guimarota beds. *In*: Martin, T. and Krebs, B. (eds.), *Guimarota–a Jurassic Ecosystem.*, 33–36. München.

Schwarz, D., Frey, E. and Meyer, C. A. 2007. Pneumaticity and soft-tissue reconstructions in the neck of diplodocid and dicraeosaurid sauropods. *Acta Palaeontologica Polonica* 52 (1): 167.

Schweitzer, M. h., Watt, J. a., Avci, R., Knapp, L., Chiappe, L., Norell, M. and Marshall, M. 1999. Beta-keratin specific immunological reactivity in feather-like structures of the Cretaceous Alvarezsaurid, Shuvuuia deserti. *Journal of Experimental Zoology* 285 (2): 146–157.

Schwenk, K. 2000. *Feeding: Form, Function and Evolution in Tetrapod Vertebrates*. Academic Press, 556pp.

Sedlmayr, J. C. 2002. Anatomy, evolution, and functional significance of cephalic vasculature in Archosauria. Ph.D. dissertation, Ohio University, Athens, Ohio, USA, 398pp.

Seeley, H. G. 1887. On the classification of the fossil animals commonly named Dinosauria. *Proceedings of the Royal Society of London* 43 (258-265): 165–171.

Senter, P. 2003. New information on cranial and dental features of the Triassic archosauriform reptile *Euparkeria capensis*. *Palaeontology* 46 (3): 613–621.

Senter, P. 2005. Function in the stunted forelimbs of *Mononykus olecranus* (Theropoda), a dinosaurian anteater. *Paleobiology* 31 (3): 373–381.

Senter, P. 2007. A new look at the phylogeny of Coelurosauria (Dinosauria: Theropoda). *Journal of Systematic Palaeontology* 5 (4): 429–463.

Senter, P. 2009. Pedal function in deinonychosaurs (Dinosauria: Theropoda): a comparative study. *Bulletin of the Gunma Museum of Natural History* 13: 1–14.

Senter, P. 2011. Using creation science to demonstrate evolution 2: morphological continuity within Dinosauria. *Journal of Evolutionary Biology* 24 (10): 2197–2216.

Senter, P., Kirkland, J. I. and DeBlieux, D. D. 2012a. *Martharaptor greenriverensis*, a New Theropod Dinosaur from the Lower Cretaceous of Utah. *PLoS ONE* 7 (8): e43911.

Senter, P., Barsbold, R., Britt, B. B. and Burnham, D. A. 2004. Systematics and evolution of Dromaeosauridae (Dinosauria, Theropoda). *Bulletin of Gunma Museum of Natural History* 8: 1–20.

Senter, P., Kirkland, J. I., DeBlieux, D. D., Madsen, S. and Toth, N. 2012b. New dromaeosaurids (Dinosauria: Theropoda) from the Lower Cretaceous of Utah, and the evolution of the dromaeosaurid tail. *PLoS ONE* 7 (5): e36790.

Sereno, P. C. 1997. The origin and evolution of dinosaurs. *Annual Review of Earth and Planetary Sciences* 25 (1): 435–489.

Sereno, P. C. 1998. A rationale for phylogenetic definitions, with application to the higher-level taxonomy of Dinosauria. *Neues Jahrbuch fur Geologie und Palaontologie Abhandlungen* 210: 41–83.

Sereno, P. C. 1999. The Evolution of Dinosaurs. *Science* 284 (5423): 2137–2147.

Sereno, P. C. 2001. Alvarezsaurids: birds or ornithomimosaurs. *In*: Gauthier, J. and Gall, L. F. (eds.), *New Perspectives on the Origin and Early Evolution of Birds: Proceedings of the International Symposium in Honor of John H. Ostrom*, 69–98. Yale Univ Peabody Museum.

Sereno, P. C. 2005. *Stem Archosauria – TaxonSearch*. TaxonSearch Database for Suprageneric Taxa & Phylogenetic Definitions. Downloaded from http://www.taxonsearch.org/dev/filehome.php [version 1.0, 7 November 2005] .

Sereno, P. C. and Novas, F. E. 1992. The Complete Skull and Skeleton of an Early Dinosaur. *Science* 258 (5085): 1137–1140.
Sereno, P. C. and Wild, R. 1992. *Procompsognathus*: theropod, 'thecodont' or both? *Journal of Vertebrate Paleontology* 12 (4): 435–458.
Sereno, P. C. and Novas, F. E. 1994. The skull and neck of the basal theropod *Herrerasaurus ischigualastensis*. *Journal of Vertebrate Paleontology* 13 (4): 451–476.
Sereno, P. C. and Brusatte, S. L. 2008. Basal abelisaurid and carcharodontosaurid theropods from the Lower Cretaceous Elrhaz Formation of Niger. *Acta Palaeontologica Polonica* 53 (1): 15–46.
Sereno, P. C., Wilson, J. A. and Conrad, J. L. 2004. New dinosaurs link southern landmasses in the Mid–Cretaceous. *Proceedings of the Royal Society of London. Series B: Biological Sciences* 271 (1546): 1325–1330.
Sereno, P. C., Martínez, R. N. and Alcober, O. A. 2013. Osteology of *Eoraptor lunensis* (Dinosauria, Sauropodomorpha). *Journal of Vertebrate Paleontology* 32 (sup1): 83–179.
Sereno, P. C., Forster, C. A., Rogers, R. R. and Monetta, A. M. 1993. Primitive dinosaur skeleton from Argentina and the early evolution of Dinosauria. *Nature* 361 (6407): 64–66.
Sereno, P. C., Wilson, J. A., Larsson, H. C. E., Dutheil, D. B. and Sues, H.-D. 1994. Early Cretaceous dinosaurs from the Sahara. *Science* 266 (5183): 267–271.
Sereno, P. C., Martinez, R. N., Wilson, J. A., Varricchio, D. J., Alcober, O. A. and Larsson, H. C. E. 2008. Evidence for avian intrathoracic air sacs in a new predatory dinosaur from Argentina. *PLoS ONE* 3 (9): e3303.
Sereno, P. C., Tan, L., Brusatte, S. L., Kriegstein, H. J., Zhao, X. and Cloward, K. 2009. Tyrannosaurid skeletal design first evolved at small body size. *Science* 326 (5951): 418–422.
Sereno, P. C., Dutheil, D. B., Larochene, M., Larsson, H. C. E., Lyon, G. H., Magwene, P. M., Sidor, C. A., Varricchio, D. J. and Wilson, J. A. 1996. Predatory dinosaurs from the Sahara and Late Cretaceous faunal differentiation. *Science* 272 (5264): 986–991.
Sereno, P. C., Beck, A. L., Dutheil, D. B., Gado, B., Larsson, H. C. E., Lyon, G. H., Marcot, J. D., Rauhut, O. W. M., Sadleir, R. W., Sidor, C. A., Varricchio, D. D., Wilson, G. P. and Wilson, J. A. 1998. A long-snouted predatory dinosaur from Africa and the evolution of spinosaurids. *Science* 282 (5392): 1298–1302.
Serrano-Brañas, C. I., Torres-Rodríguez, E., Reyes Luna, P. C., González, I. and González-León, C. 2014. Tyrannosaurid teeth from the Lomas Coloradas Formation, Cabullona Group (Upper Cretaceous) Sonora, México. *Cretaceous Research* 49: 163–171.
Siegel, A. F. and Benson, R. H. 1982. A Robust Comparison of Biological Shapes. *Biometrics* 38 (2): 341.
Siegwarth, J. D., Lindbeck, R. A., Redman, P. D., Southwell, E. H. and Bakker, R. T. 1997. Giant carnivorous dinosaurs of the family Megalosauridae from the Late Jurassic Morrison Formation of eastern Wyoming. *Contributions from the Tate Museum Collections, Casper, Wyoming* 2: 1–33.
Smith, D. 1992. The type specimen of *Oviraptor philoceratops*, a theropod dinosaur from the Upper Cretaceous of Mongolia. *Neues Jahrbuch für Geologie und Paläontologie, Abhandlungen* 186: 365–388.
Smith, D. K., Allen, E. R., Sanders, R. K. and Stadtman, K. L. 2010. A new specimen of *Eutretauranosuchus* (Crocodyliformes; Goniopholididae) from Dry Mesa, Colorado. *Journal of Vertebrate Paleontology* 30 (5): 1466–1477.
Smith, J. B. 2005. Heterodonty in *Tyrannosaurus rex*: implications for the taxonomic and systematic utility of theropod dentitions. *Journal of Vertebrate Paleontology* 25 (4): 865–887.
Smith, J. B. 2007. Dental morphology and variation in *Majungasaurus crenatissimus* (Theropoda: Abelisauridae) from the Late Cretaceous of Madagascar. *Journal of Vertebrate Paleontology* 27 (sup2): 103–126.
Smith, J. B. and Dodson, P. 2003. A proposal for a standard terminology of anatomical notation and orientation in fossil vertebrate dentitions. *Journal of Vertebrate Paleontology* 23 (1): 1–12.
Smith, J. B. and Lamanna, M. C. 2006. An abelisaurid from the Late Cretaceous of Egypt: implications for theropod biogeography. *Naturwissenschaften* 93 (5): 242–245.
Smith, J. B. and Dalla Vecchia, F. M. 2006. An abelisaurid (Dinosauria: Theropoda) tooth from the Lower Cretaceous Chicla formation of Libya. *Journal of African Earth Sciences* 46 (3): 240–244.
Smith, J. B., Vann, D. R. and Dodson, P. 2005. Dental morphology and variation in theropod dinosaurs: implications for the taxonomic identification of isolated teeth. *The Anatomical Record Part A: Discoveries in Molecular, Cellular, and Evolutionary Biology* 285 (2): 699–736.
Smith, J. B., Lamanna, M. C., Mayr, H. and Lacovara, K. J. 2006. New information regarding the holotype of *Spinosaurus aegyptiacus* Stromer, 1915. *Journal of Paleontology* 80 (2): 400–406.
Smith, N. D., Makovicky, P. J., Hammer, W. R. and Currie, P. J. 2007. Osteology of *Cryolophosaurus ellioti* (Dinosauria: Theropoda) from the Early Jurassic of Antarctica and implications for early theropod evolution. *Zoological Journal of the Linnean Society* 151 (2): 377–421.

Snively, E., Henderson, D. M. and Phillips, D. S. 2006. Fused and vaulted nasals of tyrannosaurid dinosaurs: implications for cranial strength and feeding mechanics. *Acta Palaeontologica Polonica* 51 (3): 435.

Soto, M. and Perea, D. 2008. A ceratosaurid (Dinosauria, Theropoda) from the Late jurassic–Early Cretaceous of Uruguay. *Journal of Vertebrate Paleontology* 28 (2): 439–444.

Spalding, D. E. A. and Sarjeant, W. A. S. 2012. Dinosaurs: The Earliest Discoveries. *In*: Brett-Surman, M. K., Holtz, T. R. J. and Farlow, J. O. (eds.), *The Complete Dinosaur, Second Edition*, 3–24. Indiana University Press, Bloomington, Indiana.

Sternberg, R. M. 1940. A toothless bird from the Cretaceous of Alberta. *Journal of Paleontology* 14 (1): 81–85.

Stevens, K. A. 2006. Binocular vision in theropod dinosaurs. *Journal of Vertebrate Paleontology* 26 (2): 321–330.

Stiegler, J., Wang, S., Xu, X. and Clark, J. M. 2014. New anatomical details on the basal ceratosaur *Limusaurus* and implications for the Jurassic radiation of Theropoda. *74th Annual Meeting Society of Vertebrate Paleontology, Berlin, Germany. (November 5-8, 2014), Program and Abstracts*: 235.

Stokosa, K. 2005. Enamel microstructure variation within the Theropoda. *In*: Carpenter, K. (ed.), *The Carnivorous Dinosaurs*, 163–178. Indiana University Press, Bloomington, Indiana.

Stovall, J. W. and Langston Jr, W. 1950. *Acrocanthosaurus atokensis*, a new genus and species of Lower Cretaceous Theropoda from Oklahoma. *American Midland Naturalist*: 696–728.

Stromer, E. 1915. Ergebnisse der Forschungsreisen Prof. E. Stromers in den Wüsten Ägyptens. II. Wirbeltier-Reste der Baharîje-Stufe (unterstes Cenoman). 3. Das Original des Theropoden *Spinosaurus aegyptiacus* nov. gen., nov. spec. *Abhandlungen der Königlichen Bayerischen Akademie der Wissenschaften, Mathematisch- Physikalische Klasse* 28: 1–32.

Stromer, E. 1931. Wirbeltier-Reste der Baharije-Stufe (unterstes Cenoman). 10. Ein Skelett-Rest von *Carcharodontosaurus* nov. gen. *Abhandlungen der Bayerischen Akademie der Wissenschaften Mathematisch-naturwissenschaftliche Abteilung* 9: 1–31.

Stromer, E. 1934. Die Zähne des *Compsognathus* und Bemerkungen über das Gebiss der Theropoda. *Centralblatt für Mineralogie, Geologie und Paläontologie, Abteilung B* 4: 74–85.

Sues, H.-D. 1977. The skull of *Velociraptor mongoliensis*, a small Cretaceous theropod dinosaur from Mongolia. *Paläontologische Zeitschrift* 51 (3-4): 173–184.

Sues, H.-D. 1978. A new small theropod dinosaur from the Judith River Formation (Campanian) of Alberta Canada. *Zoological Journal of the Linnean Society* 62 (4): 381–400.

Sues, H.-D. 1997. On Chirostenotes, a Late Cretaceous oviraptorosaur (Dinosauria: Theropoda) from western North America. *Journal of Vertebrate Paleontology* 17 (4): 698–716.

Sues, H.-D. and Averianov, A. 2013. Enigmatic teeth of small theropod dinosaurs from the Upper Cretaceous (Cenomanian-Turonian) of Uzbekistan. *Canadian Journal of Earth Sciences* 50 (3): 306–314.

Sues, H.-D., Frey, E., Martill, D. M. and Scott, D. M. 2002. *Irritator challengeri*, a spinosaurid (Dinosauria: Theropoda) from the Lower Cretaceous of Brazil. *Journal of Vertebrate Paleontology* 22 (3): 535–547.

Sues, H.-D., Nesbitt, S. J., Berman, D. S. and Henrici, A. C. 2011. A late-surviving basal theropod dinosaur from the latest Triassic of North America. *Proceedings of the Royal Society B: Biological Sciences* 278 (1723): 3459–3464.

Suzuki, S., Chiappe, L. M. and Dyke, G. J. 2002. A new specimen of *Shuvuuia deserti* Chiappe *et al.*, 1998, from the Mongolian late Cretaceous with a discussion of the relationships of alvarezsaurids to other theropod dinosaurs. *Contributions in Science* 194: 1–18.

Sweetman, S. C. 2004. The first record of velociraptorine dinosaurs (Saurischia, Theropoda) from the Wealden (Early Cretaceous, Barremian) of southern England. *Cretaceous Research* 25 (3): 353–364.

Tahara, R. and Larsson, H. C. E. 2011. Cranial pneumatic anatomy of *Ornithomimus edmontonicus* (Ornithomimidae: Theropoda). *Journal of Vertebrate Paleontology* 31 (1): 127–143.

Taquet, P. 1984. Une curieuse spécialisation du crâne de certains dinosaures carnivores du Crétacé: le museau long et étroit des spinosauridés. *Comptes-rendus des séances de l'Académie des sciences. Série 2, Mécanique-physique, chimie, sciences de l'univers, sciences de la terre* 299 (5): 217–222.

Taquet, P. 2010. The dinosaurs of Maghreb: the history of their discovery. *Historical Biology* 22 (1-3): 88–99.

Taquet, P. and Russell, D. A. 1998. New data on spinosaurid dinosaurs from the Early Cretaceous of the Sahara. *Comptes Rendus de l'Académie des Sciences-Series IIA-Earth and Planetary Science* 327 (5): 347–353.

Tavares, S. A. S., Ricardi Branco, F. and Santucci, R. M. 2014. Theropod teeth from the Adamantina Formation (Bauru Group, Upper Cretaceous), Monte Alto, São Paulo, Brazil. *Cretaceous Research* 50: 59–71.

Taylor, A. M., Gowland, S., Leary, S., Keogh, K. J. and Martinius, A. W. 2014. Stratigraphical correlation of the Late Jurassic Lourinhã Formation in the Consolação Sub-basin (Lusitanian Basin), Portugal. *Geological Journal* 49 (2): 143–162.

Therrien, F. and Henderson, D. M. 2007. My theropod is bigger than yours … or not: estimating body size from skull length in theropods. *Journal of Vertebrate Paleontology* 27 (1): 108–115.

Therrien, F., Henderson, D. M. and Ruff, C. B. 2005. Bite me: biomechanical models of theropod mandibles and implications for feeding behavior. *In*: Carpenter, K. (ed.), *The Carnivorous Dinosaurs*, 179–237. Indiana University Press, Bloomington, Indiana.

Thulborn, R. A. 1984. The avian relationships of *Archaeopteryx*, and the origin of birds. *Zoological Journal of the Linnean Society* 82 (1-2): 119–158.

Thulborn, T. 1990. *Dinosaur Tracks*. Chapman and Hall, London ; New York, 410pp.

Torices, A., Currie, P. J., Canudo, J. I. and Pereda-Suberbiola, X. in press. Theropod dinosaurs from the Upper Cretaceous of the South Pyrenees Basin of Spain. *Acta Palaeontologica Polonica*: DOI:10.4202/app.2012.0121.

Torres-Rodríguez, E., Montellano-Ballesteros, M., Hernández-Rivera, R. and Benammi, M. 2010. Dientes de terópodos del Cretácico Superior del Estado de Coahuila, México. *Revista mexicana de ciencias geológicas* 27 (1): 72–83.

Tortosa, T., Buffetaut, E., Dutour, Y. and Cheylan, G. 2012. Abelisaur remains from Provence (Southeastern France): phylogenetic and paleobiogeographic implications. Mésogée (66): 55.

Tortosa, T., Buffetaut, E., Vialle, N., Dutour, Y., Turini, E. and Cheylan, G. 2014. A new abelisaurid dinosaur from the Late Cretaceous of southern France: Palaeobiogeographical implications. *Annales de Paléontologie* 100 (1): 63–86.

Tsuihiji, T., Witmer, L. M., Watabe, M., Barsbold, R. and Tsogtbaatar, K. 2008. New information on the cranial anatomy of *Avimimus portentosus* (Dinosauria: Theropoda) including virtual endocasts of the brain and inner ear. *Journal of Vertebrate Paleontology* 3: 153A.

Tsuihiji, T., Barsbold, R., Watabe, M., Tsogtbaatar, K., Chinzorig, T., Fujiyama, Y. and Suzuki, S. 2014. An exquisitely preserved troodontid theropod with new information on the palatal structure from the Upper Cretaceous of Mongolia. *Naturwissenschaften* 101 (2): 131–142.

Tsuihiji, T., Watabe, M., Tsogtbaatar, K., Tsubamoto, T., Barsbold, R., Suzuki, S., Lee, A. H., Ridgely, R. C., Kawahara, Y. and Witmer, L. M. 2011. Cranial osteology of a juvenile specimen of *Tarbosaurus bataar* (Theropoda, Tyrannosauridae) from the Nemegt Formation (Upper Cretaceous) of Bugin Tsav, Mongolia. *Journal of Vertebrate Paleontology* 31 (3): 497–517.

Turner, A. H., Makovicky, P. J. and Norell, M. A. 2007a. Feather quill knobs in the dinosaur *Velociraptor*. *Science* 317 (5845): 1721–1721.

Turner, A. H., Hwang, S. H. and Norell, M. A. 2007b. A small derived theropod from Öösh, Early Cretaceous, Baykhangor Mongolia. *American Museum Novitates* 3557: 1–27.

Turner, A. H., Pol, D. and Norell, M. A. 2011. Anatomy of *Mahakala omnogovae* (Theropoda: Dromaeosauridae), Tögrögiin Shiree, Mongolia. *American Museum Novitates* 3722: 1–66.

Turner, A. H., Makovicky, P. J. and Norell, M. 2012. A review of dromaeosaurid systematics and paravian phylogeny. *Bulletin of the American Museum of Natural History* 371: 1–206.

Tykoski, R. S. 2005. Anatomy, ontogeny, and phylogeny of coelophysoid theropods. Ph.D. Dissertation, The University of Texas, Austin, Texas, 553pp.

Tykoski, R. S. and Rowe, T. 2004. Ceratosauria. *In*: Weishampel, D., Dodson, P. and Osmólska, H. (eds.), *The Dinosauria. Second Edition*, 47–70. University of California Press, Berkeley, California.

Upchurch, P. and Barrett, P. M. 2000. The evolution of sauropod feeding mechanisms. *In*: Sues, H.-D. (ed.), *Evolution of Herbivory in Terrestrial Vertebrates*, 79–122. Cambridge University Press, Cambridge, U.K.; New York.

Upchurch, P., Mannion, P. D., Benson, R. B. J., Butler, R. J. and Carrano, M. T. 2011. Geological and anthropogenic controls on the sampling of the terrestrial fossil record: a case study from the Dinosauria. *Geological Society, London, Special Publications* 358 (1): 209–240.

Varricchio, D. J. 1997. Troodontidae. *In*: Currie, P. J. and Padian, K. (eds.), *Encyclopedia of Dinosaurs*, 749–754. Academic Press, San Diego, California.

Varricchio, D. J., Horner, J. R. and Jackson, F. D. 2002. Embryos and eggs for the Cretaceous theropod dinosaur *Troodon formosus*. *Journal of Vertebrate Paleontology* 22 (3): 564–576.

Varricchio, D. J., Moore, J. R., Erickson, G. M., Norell, M. A., Jackson, F. D. and Borkowski, J. J. 2008a. Avian paternal care had dinosaur origin. *Science* 322 (5909): 1826–1828.

Varricchio, D. J., Sereno, P. C., Xijin, Z., Lin, T., Wilson, J. A. and Lyon, G. H. 2008b. Mud-trapped herd captures evidence of distinctive dinosaur sociality. *Acta Palaeontologica Polonica* 53 (4): 567–578.

Veralli, C. and Calvo, J. O. 2004. Dientes de terópodos carcharodontosáuridos del Turoniano superior-Coniaciano inferior del Neuquén, Patagonia, Argentina. *Ameghiniana* 41 (4): 587–590.

Vianey-Liaud, M., Jain, S. L. and Sahni, A. 1988. Dinosaur eggshells (Saurischia) from the Late Cretaceous Intertrappean and Lameta formations (Deccan, India). *Journal of Vertebrate Paleontology* 7 (4): 408–424.

Vickers-Rich, P., Chiappe, L. M. and Kurzanov, S. 2002. The enigmatic birdlike dinosaur *Avimimus portentosus*. *In*: Chiappe, L. M. and Witmer, L. M. (eds.), *Mesozoic Birds: Above the Heads of Dinosaurs*, 65–86. University of California Press, Berkeley/Los Angeles/London.

Vullo, R. and Néraudeau, D. 2010. Additional dinosaur teeth from the Cenomanian (Late Cretaceous) of Charentes, southwestern France. *Comptes Rendus Palevol* 9 (3): 121–126.

Vullo, R., Néraudeau, D. and Lenglet, T. 2007. Dinosaur teeth from the Cenomanian of Charentes, Western France: Evidence for a mixed Laurasian-Gondwanan assemblages. *Journal of Vertebrate Paleontology* 27 (4): 931–943.

Wagner, A. 1859. Über einige, im lithographischen Schiefer neu aufgefundene Schildkröten und Saurier. *Gelehrte Anzeigen der königlich-bayerischen Akademie der Wissenschaften* 22 (69): 553.

Wagner, A. 1861. Neue Beiträge zur Kenntnis der urweltlichen Fauna des lithographischen Schiefers; V. *Compsognathus longipes* Wagner. *Abhandlungen der Bayerischen Akademie der Wissenschaften* 9: 30–38.

Waldman, M. 1974. Megalosaurids from the Bajocian (Middle Jurassic) of Dorset. *Palaeontology* 17 (2): 325–339.

Walker, A. D. 1964. Triassic reptiles from the Elgin Area: *Ornithosuchus* and the origin of carnosaurs. *Philosophical Transactions of the Royal Society of London. Series B, Biological Sciences* 248 (744): 53–134.

Walker, A. D. 1985. The braincase of *Archaeopteryx*. *In*: Hecht, M. K., Ostrom, J. H., Viohl, G. and Wellnhofer, P. (eds.), *The Beginnings of Birds*, 123–134. Freunde des Jura-Museums Eichstätt, Germany.

Watabe, M., Weishampel, D. B., Barsbold, R. and Tsogtbaatar, K. 2000. New nearly complete skeleton of the bird−like theropod, *Avimimus*, from the Upper Cretaceous of the Gobi Desert, Mongolia. *Journal of Vertebrate Paleontology* 20 (3): 77A.

Weigert, A. 1995. Isolated teeth of cf. *Archaeopteryx* sp. from the Upper Jurassic of the coalmine Guimarota (Portugal). *Neues Jahrbuch für Geologie und Paläontologie Monatshefte H* 9: 562–576.

Weishampel, D. B., Fastovsky, D. E., Watabe, M., Varricchio, D., Jackson, F., Tsogtbaatar, K. and Barsbold, R. 2008. New oviraptorid embryos from Bugin-Tsav, Nemegt Formation (Upper Cretaceous), Mongolia, with insights into their habitat and growth. *Journal of Vertebrate Paleontology* 28 (4): 1110–1119.

Welles, S. P. 1954. New Jurassic Dinosaur from the Kayenta Formation of Arizona. *Geological Society of America Bulletin* 65 (6): 591–598.

Welles, S. P. 1970. *Dilophosaurus* (Reptilia, Saurischia), a new name for a dinosaur. *Journal of Paleontology* 44 (5): 989.

Welles, S. P. 1984. *Dilophosaurus wetherilli* (Dinosauria, Theropoda). Osteology and comparisons. *Palaeontographica Abteilung A* 185 (4-6): 85–180.

Welles, S. P. and Pickering, D. 1995. Dilophosaurus breedorum*: An extract from: Archosauromorpha: cladistics & osteologies*. A Fractal Scaling in Dinosaurology Project, Capitola, California, 70pp.

Wellnhofer, P. 1980. Flugsaurierreste aus der Gosau-Kreide von Muthmannsdorf (Niederösterreich)–ein Beitrag zur Kiefermechanik der Pterosaurier. *Mitteilungen der Bayerischen Statssammlung fur Paleontologie und historische Geologie* 20: 95–112.

Wellnhofer, P. 2008. Archaeopteryx*: Der Urvogel von Solnhofen*. Pfeil, F, München, 256pp.

White, T. E. 1940. Holotype of *Plesiosaurus longirostris* Blake and classification of the plesiosaurs. *Journal of Paleontology*: 451–467.

Wiechmann, M. F. and Gloy, U. 2000. Pterosaurs and urvogels from the Guimarota mine. *In*: Martin, T. and Krebs, B. (eds.), *Guimarota–a Jurassic Ecosystem*, 83–86. München.

Wilkinson, M. 1994. Common cladistic information and its consensus representation: reduced Adams and reduced cladistic consensus trees and profiles. *Systematic Biology* 43 (3): 343–368.

Wilkinson, M. 1995. More on reduced consensus methods. *Systematic Biology* 44 (3): 435–439.

Wilkinson, M. 1996. Majority-rule reduced consensus trees and their use in bootstrapping. *Molecular Biology and Evolution* 13 (3): 437–444.

Williamson, T. E. and Brusatte, S. L. 2014. Small theropod teeth from the Late Cretaceous of the San Juan Basin, Northwestern New Mexico and their implications for understanding Latest Cretaceous dinosaur evolution. *PLoS ONE* 9 (4): e93190.

Wilson, J. A. 1999. A nomenclature for vertebral laminae in sauropods and other saurischian dinosaurs. *Journal of Vertebrate Paleontology* 19 (4): 639–653.

Wilson, J. A. 2006. Anatomical nomenclature of fossil vertebrates: standardized terms or 'lingua franca'? *Journal of Vertebrate Paleontology* 26 (3): 511–518.

Wilson, J. A., D'Emic, M. D., Ikejiri, T., Moacdieh, E. M. and Whitlock, J. A. 2011. A nomenclature for vertebral fossae in sauropods and other saurischian dinosaurs. *PLoS ONE* 6 (2): e17114.

Wilson, J. A., Sereno, P. C., Srivastava, S., Bhatt, D. K., Khosla, A. and Sahni, A. 2003. A new abelisaurid (Dinosauria, Theropoda) from the Lameta Formation (Cretaceous, Maastrichtian) of India. *Contributions from the Museum of Paleontology, University of Michigan* 31 (1): 1–42.

Wilson, R. C. L. 1988. Mesozoic development of the Lusitanian basin, Portugal. *Revista de la Sociedad Geológica de España* 1 (3-4): 393–407.

Witmer, L. M. 1990. The craniofacial air sac system of Mesozoic birds (Aves). *Zoological Journal of the Linnean Society* 100 (4): 327–378.

Witmer, L. M. 1995. Homology of facial structures in extant archosaurs (birds and crocodilians), with special reference to paranasal pneumaticity and nasal conchae. *Journal of Morphology* 225 (3): 269–327.

Witmer, L. M. 1997a. The evolution of the antorbital cavity of archosaurs: a study in soft-tissue reconstruction in the fossil record with an analysis of the function of pneumaticity. *Journal of Vertebrate Paleontology* 17 (sup001): 1–76.

Witmer, L. M. 1997b. Craniofacial air sinus systems. *In*: Currie, P. J. and Padian, K. (eds.), *Encyclopedia of Dinosaurs*, 151–159. Academic Press, San Diego, California.

Witmer, L. M. and Ridgely, R. C. 2009. New insights into the brain, braincase, and ear region of tyrannosaurs (Dinosauria, Theropoda), with implications for sensory organization and behavior. *The Anatomical Record: Advances in Integrative Anatomy and Evolutionary Biology* 292 (9): 1266–1296.

Woodward, A. S. 1901. On some extinct reptiles from Patagonia, of the genera *Miolania*, *Dinilysia*, and *Genyodectes*. *Proceedings of the Zoological Society of London* 70 (2): 169–184.

Woodward, A. S. 1906. On a tooth of *Ceratodus* and a Dinosaurian claw from the Lower Jurassic of Victoria, Australia. *Journal of Natural History Series 7* 18 (103): 1–3.

Woodward, A. S. 1910. On remains of a megalosaurian dinosaur from New South Wales. *Report of the British Association for the Advancement of Science* 79: 482–483.

Woodward, J. M. D. 1729. *An attempt towards a natural history of the fossils of England in a catalogue of the English fossils in the collection of J. Woodward, M.D.* Printed for F. Fayram, J. Senex, and J. Osborn and T. Longman, 656pp.

Xing, L. 2012. *Sinosaurus* from southwestern China. MSc. Dissertation, University of Alberta, Edmonton, Alberta, Canada, 267pp.

Xing, L., Bell, P. R., Persons, W. S., Ji, S., Miyashita, T., Burns, M. E., Ji, Q. and Currie, P. J. 2012. Abdominal contents from two Large Early Cretaceous compsognathids (Dinosauria: Theropoda) demonstrate feeding on confuciusornithids and dromaeosaurids. *PLoS ONE* 7 (8): e44012.

Xing, L., Bell, P. R., Rothschild, B. M., Ran, H., Zhang, J., Dong, Z., Zhang, W. and Currie, P. J. 2013a. Tooth loss and alveolar remodeling in *Sinosaurus triassicus* (Dinosauria: Theropoda) from the Lower Jurassic strata of the Lufeng Basin, China. *Chinese Science Bulletin* 58 (16): 1931–1935.

Xing, L., Persons, W. S., Bell, P. R., Xu, X., Zhang, J., Miyashita, T., Wang, F. and Currie, P. J. 2013b. Piscivory in the feathered dinosaur *Microraptor*. *Evolution* 67 (8): 2441–2445.

Xing, L., Paulina-Carabajal, A., Currie, P. J., Xu, X., Zhang, J., Wang, T., Burns, M. E. and Dong, Z. 2014. Braincase anatomy of the basal theropod *Sinosaurus* from the Early Jurassic of China. *Acta Geologica Sinica - English Edition* 88 (6): 1653–1664.

Xu, X. and Wu, X.-C. 2001. Cranial morphology of *Sinornithosaurus millenii* Xu et al. 1999 (Dinosauria: Theropoda: Dromaeosauridae) from the Yixian Formation of Liaoning, China. *Canadian Journal of Earth Sciences* 38 (12): 1739–1752.

Xu, X. and Wang, X.-L. 2004. A new troodontid (Theropoda: Troodontidae) from the lower Cretaceous Yixian Formation of western Liaoning, China. *Acta Geologica Sinica* 78 (1): 22–26.

Xu, X. and Norell, M. A. 2004. A new troodontid dinosaur from China with avian-like sleeping posture. *Nature* 431 (7010): 838–841.

Xu, X. and Zhang, F. 2005. A new maniraptoran dinosaur from China with long feathers on the metatarsus. *Naturwissenschaften* 92 (4): 173–177.

Xu, X. and Han, F. L. 2010. A new oviraptorid dinosaur (Theropoda: Oviraptorosauria) from the Upper Cretaceous of China. *Vertebrata PalAsiatica* 48: 11–18.

Xu, X. and Pol, D. 2014. *Archaeopteryx*, paravian phylogenetic analyses, and the use of probability-based methods for palaeontological datasets. *Journal of Systematic Palaeontology* 12 (3): 323–334.

Xu, X., Tang, Z. and Wang, X. 1999a. A therizinosauroid dinosaur with integumentary structures from China. *Nature* 399 (6734): 350–354.

Xu, X., Wang, X.-L. and Wu, X.-C. 1999b. A dromaeosaurid dinosaur with a filamentous integument from the Yixian Formation of China. *Nature* 401 (6750): 262–266.

Xu, X., Zhou, Z. and Wang, X. 2000. The smallest known non-avian theropod dinosaur. *Nature* 408 (6813): 705–708.

Xu, X., Zhao, X. and Clark, J. M. 2001a. A new therizinosaur from the Lower Jurassic lower Lufeng Formation of Yunnan, China. *Journal of Vertebrate Paleontology* 21 (3): 477–483.

Xu, X., Zhou, Z. and Prum, R. O. 2001b. Branched integumental structures in *Sinornithosaurus* and the origin of feathers. *Nature* 410 (6825): 200–204.
Xu, X., Zheng, X. and You, H. 2009a. A new feather type in a nonavian theropod and the early evolution of feathers. *Proceedings of the National Academy of Sciences* 106 (3): 832–834.
Xu, X., Zheng, X. and You, H. 2010a. Exceptional dinosaur fossils show ontogenetic development of early feathers. *Nature* 464 (7293): 1338–1341.
Xu, X., Cheng, Y.-N., Wang, X.-L. and Chang, C.-H. 2002a. An unusual oviraptorosaurian dinosaur from China. *Nature* 419 (6904): 291–293.
Xu, X., You, H., Du, K. and Han, F. 2011a. An *Archaeopteryx*-like theropod from China and the origin of Avialae. *Nature* 475 (7357): 465–470.
Xu, X., Norell, M. A., Wang, X., Makovicky, P. J. and Wu, X. 2002b. A basal troodontid from the Early Cretaceous of China. *Nature* 415 (6873): 780–784.
Xu, X., Tan, Q., Sullivan, C., Han, F. and Xiao, D. 2011b. A short-armed troodontid dinosaur from the Upper Cretaceous of Inner Mongolia and its implications for troodontid evolution. *PLoS ONE* 6 (9): e22916.
Xu, X., Zhou, Z., Wang, X., Kuang, X., Zhang, F. and Du, X. 2003. Four-winged dinosaurs from China. *Nature* 421 (6921): 335–340.
Xu, X., Norell, M. A., Kuang, X., Wang, X., Zhao, Q. and Jia, C. 2004. Basal tyrannosauroids from China and evidence for protofeathers in tyrannosauroids. *Nature* 431 (7009): 680–684.
Xu, X., Clark, J. M., Forster, C. A., Norell, M. A., Erickson, G. M., Eberth, D. A., Jia, C. and Zhao, Q. 2006. A basal tyrannosauroid dinosaur from the Late Jurassic of China. *Nature* 439 (7077): 715–718.
Xu, X., Wang, K., Zhang, K., Ma, Q., Xing, L., Sullivan, C., Hu, D., Cheng, S. and Wang, S. 2012. A gigantic feathered dinosaur from the Lower Cretaceous of China. *Nature* 484 (7392): 92–95.
Xu, X., Choiniere, J. N., Pittman, M. D., Tan, Q., Xiao, D., Li, Z., Tan, L., Clark, J. M., Norell, M. A. and Hone, D. W. 2010b. A new dromaeosaurid (Dinosauria: Theropoda) from the Upper Cretaceous Wulansuhai Formation of Inner Mongolia, China. *Zootaxa* 2403: 1–9.
Xu, X., Sullivan, C., Pittman, M., Choiniere, J. N., Hone, D., Upchurch, P., Tan, Q., Xiao, D., Tan, L. and Han, F. 2011c. A monodactyl nonavian dinosaur and the complex evolution of the alvarezsauroid hand. *Proceedings of the National Academy of Sciences* 108 (6): 2338–2342.
Xu, X., Upchurch, P., Ma, Q., Pittman, M., Choiniere, J., Sullivan, C., Hone, D. W., Tan, Q., Tan, L., Xiao, D. and others. 2013. Osteology of the Late Cretaceous alvarezsauroid *Linhenykus monodactylus* from China and comments on alvarezsauroid biogeography. *Acta Palaeontologica Polonica* 58 (1): 25–46.
Xu, X., Clark, J. M., Mo, J., Choiniere, J., Forster, C. A., Erickson, G. M., Hone, D. W. E., Sullivan, C., Eberth, D. A., Nesbitt, S., Zhao, Q., Hernandez, R., Jia, C., Han, F. and Guo, Y. 2009b. A Jurassic ceratosaur from China helps clarify avian digital homologies. *Nature* 459 (7249): 940–944.
Yates, A. M. 2005. A new theropod dinosaur from the Early Jurassic of South Africa and its implications for the early evolution of theropods. *Palaeontologia Africana* 41: 105–122.
You, H.-L., Azuma, Y., Wang, T., Wang, Y.-M. and Dong, Z.-M. 2014. The first well-preserved coelophysoid theropod dinosaur from Asia. *Zootaxa* 3873 (3): 233.
Young, M. T., Brusatte, S. L., Ruta, M. and De Andrade, M. B. 2010. The evolution of Metriorhynchoidea (mesoeucrocodylia, thalattosuchia): an integrated approach using geometric morphometrics, analysis of disparity, and biomechanics. *Zoological Journal of the Linnean Society* 158 (4): 801–859.
Zanno, L. E. 2006. The pectoral girdle and forelimb of the primitive therizinosauroid *Falcarius utahensis* (Theropoda, Maniraptora): analyzing evolutionary trends within Therizinosauroidea. *Journal of Vertebrate Paleontology* 26 (3): 636–650.
Zanno, L. E. 2010a. A taxonomic and phylogenetic re-evaluation of Therizinosauria (Dinosauria: Maniraptora). *Journal of Systematic Palaeontology* 8 (4): 503–543.
Zanno, L. E. 2010b. Osteology of *Falcarius utahensis* (Dinosauria: Theropoda): characterizing the anatomy of basal therizinosaurs. *Zoological Journal of the Linnean Society* 158 (1): 196–230.
Zanno, L. E. and Makovicky, P. J. 2011. Herbivorous ecomorphology and specialization patterns in theropod dinosaur evolution. *Proceedings of the National Academy of Sciences* 108 (1): 232–237.
Zanno, L. E. and Makovicky, P. J. 2013. Neovenatorid theropods are apex predators in the Late Cretaceous of North America. *Nature Communications* 4.
Zanno, L. E., Gillette, D. D., Albright, L. B. and Titus, A. L. 2009. A new North American therizinosaurid and the role of herbivory in 'predatory' dinosaur evolution. *Proceedings of the Royal Society B: Biological Sciences* 276 (1672): 3505–3511.
Zanno, L. E., Varricchio, D. J., O'Connor, P. M., Titus, A. L. and Knell, M. J. 2011. A New Troodontid Theropod, *Talos sampsoni* gen. et sp. nov., from the Upper Cretaceous Western Interior Basin of North America. *PLoS ONE* 6 (9): e24487.
Zelditch, M. L., Wood, A. R. and Swiderski, D. L. 2009. Building Developmental Integration into Functional Systems: Function-Induced Integration of Mandibular Shape. *Evolutionary Biology* 36 (1): 71–87.

Zelenitsky, D. K., Therrien, F. and Kobayashi, Y. 2009. Olfactory acuity in theropods: palaeobiological and evolutionary implications. *Proceedings of the Royal Society B: Biological Sciences* 276 (1657): 667–673.

Zelenitsky, D. K., Therrien, F., Erickson, G. M., DeBuhr, C. L., Kobayashi, Y., Eberth, D. A. and Hadfield, F. 2012. Feathered non-avian dinosaurs from North America provide insight into wing origins. *Science* 338 (6106): 510–514.

Zhang, F., Zhou, Z., Xu, X. and Wang, X. 2002. A juvenile coelurosaurian theropod from China indicates arboreal habits. *Naturwissenschaften* 89 (9): 394–398.

Zhang, F., Zhou, Z., Xu, X., Wang, X. and Sullivan, C. 2008. A bizarre Jurassic maniraptoran from China with elongate ribbon-like feathers. *Nature* 455 (7216): 1105–1108.

Zhang, F., Kearns, S. L., Orr, P. J., Benton, M. J., Zhou, Z., Johnson, D., Xu, X. and Wang, X. 2010. Fossilized melanosomes and the colour of Cretaceous dinosaurs and birds. *Nature* 463 (7284): 1075–1078.

Zhang, S. and Barnes, C. R. 2000. *Anticostiodus*, a new multielement conodont genus from the Lower Silurian, Anticosti Island, Québec. *Journal Information* 74 (4).

Zhang, X.-H., Xu, X., Zhao, X.-J., Sereno, P., Kuang, X.-W. and Tan, L. 2001. A long-necked therizinosauroid dinosaur from the Upper Cretaceous Iren Dabasu Formation of nei Mongol, People's Republic of China. *Vertebrata PalAsiatica* 39 (4): 283–294.

Zhao, X. and Xu, X. 1998. The oldest coelurosaurian. *Nature* 394 (6690): 234–235.

Zhao, X.-J. and Currie, P. J. 1993. A large crested theropod from the Jurassic of Xinjiang, People's Republic of China. *Canadian Journal of Earth Sciences* 30 (10): 2027–2036.

Zheng, X., Xu, X., You, H., Zhao, Q. and Dong, Z. 2010. A short-armed dromaeosaurid from the Jehol Group of China with implications for early dromaeosaurid evolution. *Proceedings of the Royal Society B: Biological Sciences* 277 (1679): 211–217.

Zhou, C.-F., Wu, S., Martin, T. and Luo, Z.-X. 2013. A Jurassic mammaliaform and the earliest mammalian evolutionary adaptations. *Nature* 500 (7461): 163–167.

Zhou, Z.-H. and Wang, X. L. 2000. A new species of *Caudipteryx* from the Yixian Formation of Liaoning, northeast China. *Vertebrata PalAsiatica* 38 (2): 113–130.

Zhou, Z.-H., Wang, X.-L., Zhang, F.-C. and Xu, X. 2000. Important features of *Caudipteryx*-evidence from two nearly complete new specimens. *Vertebrata PalAsiatica* 38 (4): 243–265.

Zinke, J. 1998. Small theropod teeth from the Upper Jurassic coal mine of Guimarota (Portugal). *Paläontologische Zeitschrift* 72 (1): 179–189.

Zinke, J. and Rauhut, O. W. M. 1994. Small theropods (Dinosauria, Saurischia) from the Upper Jurassic and Lower Cretaceous of the Iberian Peninsula. *Berliner Geowissenschaftliche Abhandlugen (E)* 13: 163–177.

Zusi, R. L. 1984. A functional and evolutionary analysis of rhynchokinesis in birds. *Smithsonian Contributions to Zoology* 395: 1–40.

Zusi, R. L. 1993. Patterns of diversity in the avian skull. *The skull* 2: 391–437.

Zweers, G. A. and Vanden Berge, J. C. 1998. Birds at geological boundaries. *Zoology* 100: 183–202.

Zweers, G. A., Vanden Berge, J. C. and Berkhoudt, H. 1997. Evolutionary patterns of avian trophic diversification. *Zoology* 100: 25–57.

APPENDICES

A1. Silhouette attribution and examined taxa

A1.1. Attribution of silhouettes

All the theropod silhouettes have been downloaded from Phylopic.org. All images are under a Creative Commons Attribution-NonCommercial-ShareAlike 3.0 Unported License unless stated otherwise.

- Basalmost Theropoda (*Eoraptor*, *Herrerasaurus*, *Tawa*): Scott Hartman
- *Eodromaeus*: Fonty
- Coelophysoidea/Coelophysidae (*Elaphrosaurus*): Funkmonk (Public Domain)
- Dilophosauridae (*Dilophosaurus*): Funkmonk (Public Domain)
- Ceratosauridae: Scott Hartman
- Noasauridae: Scott Hartman
- Abelisauridae: Scott Hartman
- Basal Megalosauroidea/Piatnitzkysauridae: Scott Hartman
- Megalosauridae: Scott Hartman
- Spinosaurinae: Scott Hartman
- Baryonychinae: Scott Hartman
- Avetheropoda/Allosauridae: Scott Hartman
- Metriacanthosauridae (*Yangchuanosaurus*): Gregory S. Paul
- *Neovenator*: Scott Hartman
- Carcharodontosauridae: Scott Hartman
- Proceratosauridae (*Kileskus*): Fonty
- Basal Tyrannosauroidea (*Eotyrannus*): Scott Hartman
- Megaraptora (*Australovenator*): Travis R. Tischler
- Tyrannosauridae: Scott Hartman
- Ornithomimosauria: Scott Hartman
- Compsognathidae: Scott Hartman
- Therizinosauria (*Suzhousaurus*): Funkmonk (Public Domain)
- Alvarezsauroidea (*Shuvuuia*): Funkmonk (Public Domain)
- Oviraptorosauria: Scott Hartman
- Troodontidae: Scott Hartman
- Dromaeosauridae: Scott Hartman (*Sinornithosaurus*) & Funkmonk (*Dromaeosauroid*; Public Domain)
- Avialae (*Pandion*): Traver

A1.2. Examined taxa

	Taxa	Type	Material	Institutions
1	*Abelisaurus comahuensis*	Holotype	pmx, mx, teeth, q	MPCA 1, 5, 229, 267, 687, 689, 709, 11098
2	*Acrocanthosaurus atokensis*	Other	pmx, mx, dt, teeth, q	NCSM 14345; SMU 73417, 74646
3	*Aerosteon riocoloradensis*	Cast	tooth	UC uncatalogued (cast of MCNA-PV-3137)
4	*Afrovenator abakensis*	Holotype	mx, teeth, q	MNN UBA1
5	*Albertosaurus sarcophagus*	Other	pmx, mx, dt, teeth, q	AMNH 5218; DMNH 22019
6	*Alioramus altai*	Holotype	mx, dt, teeth	IGM 100-1844
7	*Allosaurus europaeus*	Holotype, hatchling	mx, tooth, q	ML 415; MG 27804
8	*Allosaurus fragilis*	Other	pmx, mx, dt, teeth, q	AMNH 600, 851; CMNH 1254, 11844, 21703; USNM 8335
9	*Allosaurus* '*jimmadseni*'	Other	pmx, mx, dt, teeth, q	SMA 005/02; NHFO 455
10	*Angaturama limai*	Cast	cast: pmx, mx, teeth	AMNH 30230
11	*Arcovenator escotae*	Holotype	teeth	MHNA.PV 2011.12
12	*Aucasaurus garridoi*	Holotype	pmx, mx, teeth, q	MCF-PVPH 236
13	*Bambiraptor feinbergi*	Holotype	pmx, mx, dt, teeth, q	AMNH 30554
14	*Baryonyx walkeri*	Holotype	pmx, mx, dt, teeth, q	NHM R.9951; ML 1190
15	*Berberosaurus liassicus*	Holotype	teeth	MNHN To 339

16	*Bicentenaria argentina*	Holotype	pmx, mx, teeth, q	MPCA 865, 866
17	*Buitreraptor gonralezorum*	Holotype	mx, dt, teeth, q	MPCA 245
18	*Byronosaurus jaffei*	Holotype	pmx, mx, dt, teeth, q	IGM 100-972, IGM 100-983
19	*Carcharodontosaurus saharicus*	Holotype	mx, dt, teeth	SGM Din-1, MNN GAD8, UCRC PV6; MNN GAD15?
20	*Carcharodontosaurus iguidensis*	Holotype	mx, teeth	MNN IGU5, MNN IGU6
21	*Carnotaurus sastrei*	Holotype	pmx, mx, dt, teeth, q	MACN 894
22	*Ceratosaurus nasicornis*	Holotype	pmx, mx, dt, teeth, q	USNM 4735
23	*Citipati osmolskae*	Holotype	pmx, mx, dt, q	IGM 100-978
24	*Coelophysis bauri*	Holotype	pmx, mx, dt, teeth, q	AMNH 7223, 7224, 7227, 7228, 7229, 7231; CMNH 81765, 82931
25	*Compsognathus longipes*	Other	pmx, mx, dt, teeth, q	MNHN CNJ79
26	*Cristatusaurus lapparenti*	Holotype	pmx, dt	MNHN GDF 365-366
27	*Daspletosaurus torosus*	Cast, other	pmx, mx, dt, teeth	FMNH PR308; NHM R.4863
28	*Dromaeosaurus albertensis*	Holotype	pmx, mx, dt, teeth, q	AMNH 5356
29	*Dubreuillosaurus valesdunensis*	Holotype	pmx, mx, dt, teeth	MNHN 1998-13
30	*Duriavenator hesperis*	Holotype	pmx, mx, dt, teeth	NHM R.332
31	*Ekrixinatosaurus novasi*	Holotype	mx, dt, teeth	MUCPv 294
32	*Eocarcharia dinops*	Holotype	mx, teeth	MNN GAD7, MNN GAD13, MNN GAD14
33	*Eodromaeus murphi*	Holotype	mx, dt, teeth	PVSJ 560
34	*Eoraptor lunensis*	Holotype	pmx, mx, dt, teeth, q	PVSJ 512
35	*Eotyrannus lengi*	Holotype	pmx, mx, dt, teeth, q	MIWG 1997.550
36	*Erectopus superbus*	Holotype	mx, teeth	MNHN 2001-4
37	*Eustreptospondylus oxoniensis*	Holotype	pmx, mx, dt, q	OUMNH J.13558
38	*Frenguellisaurus ischigualastensis*	Holotype	mx, dt, teeth	PVSJ 407
39	*Gallimimus bullatus*	Other	pmx, mx, dt, q	IGM 100-1133
40	*Genyodectes serus*	Holotype	pmx, mx, dt, teeth	MLP 26-39
41	*Giganotosaurus carolinii*	Holotype	pmx, mx, dt, teeth, q	MUCPv- CH 1; MUCPv 95
42	*Gorgosaurus libratus*	Other	dt, teeth	AMNH 5336, 5432, 5458, 5664; USNM 12814
43	*Herrerasaurus ischigualastensis*	Holotype	pmx, mx, dt, teeth, q	PVSJ 053
44	*Ilokelesia aguadagrandensis*	Holotype	q	MCF-PVPH 35
45	*Indosuchus raptorius*	Holotype	pmx, mx, dt, teeth	AMNH 1753, 1955, 1960
46	*Irritator challengeri*	Holotype	mx, dt, teeth, q	SMNS 58022
47	*Ischisaurus cattoi*	Holotype	pmx, mx, dt, teeth	MACN 18.060
48	*Khaan mckennai*	Holotype	pmx, mx, dt, q	IGM 100-1002, IGM 100-1127
49	*Kryptops palaïos*	Holotype	mx, teeth	MNN GAD1−1
50	*Labrosaurus ferox*	Holotype	dt	USNM 2315
51	*Liliensternus liliensterni*	Cast	cast: mx, dt	SMNS unknown = cast of MBR 21751
52	*Lourinhanosaurus antunesi*	Holotype	embryos	ML 565
53	*Magnosaurus nethercombensis*	Holotype	dt, teeth	NHM J.12143
54	*Majungasaurus crenatissimus*	Holotype, other	mx, dt, teeth, q	MNHN MAJ 1; FMNH PR 114, 2008, 2100, 2278, UA 8716
55	*Mapusaurus roseae*	Holotype	mx, dt, teeth, q	MCF-PVPH 108
56	*Marshosaurus bicentesimus*	Cast	cast: mx, dt, teeth	AMNH 27638, 27640, 27641)
57	*Masiakasaurus knopfleri*	Holotype	pmx, mx, dt, teeth	FMNH PR 2177, 2178, 2179, 2182, 2183, 2201, 2221, 2222, 2453, 2476, 2496, 2471; UA 8680, 9091, 9128
58	*Megalosaurus bucklandii*	Holotype	mx, dt, teeth	OUMNH J.13505, J.13506, J.13559, J.23014, J.23049, J.23050, J.29762, J.29809, J.29855, J.29856, J.29866, J.48171; NHM R.8303
59	*Megaraptor namunhuaiquii*	Other	pmx, mx, teeth	MUCPv 595
60	*Neovenator salerii*	Holotype	pmx, mx, dt, teeth	MIWG 6348; NHM R.10001
61	*Noasaurus leali*	Holotype	mx, teeth, q	PVL 4061
62	*Nuthetes destructor*	Holotype	dt, teeth	NHM R.48207, R.48208, R.15870, R.15871, R.15872, R.15873, R.15874, R.15876, R.15878, R.48208

63	*Ornitholestes hermanni*	Holotype	pmx, mx, dt, teeth, q	AMNH 619
64	*Oviraptor philoceratops*	Holotype	pmx, mx, dt, q	AMNH 6517
65	*Oxalaia quilombensis*	Cast	cast: pmx	AMNH unknown = cast of MN61A-V
66	*Paronychodon* sp.	Other	dt, teeth	MG 27799
67	*Piatnitzkysaurus floresi*	Holotype	mx, dt, teeth	MACN 895; PVL 4073
68	*Proceratosaurus bradleyi*	Holotype	pmx, mx, dt, teeth, q	NHM R.4860
69	*Pyroraptor olympius*	Holotype	teeth	MNHN BO014-015
70	*Raptorex kriegsteini*	Holotype	pmx, mx, dt, teeth	LH PV18
71	*Rugops primus*	Holotype	pmx, mx, teeth	MNN IGU1
72	*Sanjuansaurus gordilloi*	Holotype	mx, teeth	PVL 605
73	*Saurornithoides mongoliensis*	Holotype	pmx, mx, dt, teeth, q	AMNH 6516
74	*Saurornitholestes* sp.	Other	tooth	DMNH 22870
75	*Shuvuuia deserti*	Holotype	pmx, mx, dt, teeth, q	IGM 100-977; IGM 100-1001
76	*Skorpiovenator bustingorryi*	Holotype	pmx, mx, dt, teeth, q	MMCN-PV 48
77	*Spinosaurus aegyptiacus*	Other	pmx, mx, dt, teeth, q	MSNM V3976, V4047, V6422, V6424, V6865, V6896; NHM R.16420, R.16421
78	*Spinosaurus maroccanus*	Holotype	mx, dt	MNHN SAM 124
79	*Suchomimus tenerensis*	Holotype	pmx, mx, dt, teeth, q	MNN GDF501, 502, G2-2, G5-1, G34-1, G74-1, G232,
80	*Struthiomimus altus*	Holotype	pmx, mx, dt, q	AMNH 5339
81	*Torvosaurus gurneyi*	Holotype, embryos	mx, teeth; embryos	ML 148, 632, 962, 1100
82	*Torvosaurus tanneri*	Cast	mx, teeth	ML 1188
83	*Troodon formosus*	Other	teeth	DMNH 22337, 22837
84	*Tsaagan mangas*	Holotype	pmx, mx, dt, teeth, q	IGM 100-1015
85	*Tyrannosaurus rex*	Holotype	pmx, mx, dt, teeth, q	AMNH 5027, 21542; CMNH 9380; NHM R.7994 = AMNH 5866; FMNH PR2081
86	Unnamed dromaeosaurid	Holotype	pmx, mx, teeth	UC uncatalogued
87	Unnamed troodontid	Holotype	pmx, mx, dt, teeth	IGM 100-1128
88	Unnamed troodontid	Holotype	pmx, mx, dt, teeth	IGM 100-1128
89	*Velociraptor mongoliensis*	Holotype	pmx, mx, dt, teeth, q	AMNH 6515
90	*Zanclodon cambriensis*	Cast	cast: dt, teeth	R.2912
91	*Zupaysaurus rougieri*	Holotype	mx, dt, teeth, q	PULR 076

A2. Visited institutions

	Acronym	Institution	Date of visit	People in charge	Examined taxa
1	AMNH	American Museum of Natural History, collection of fossil reptiles, amphibians and birds, New York, New York, USA	02-11/10/2012	Carl Mehling (AMNH), Mark Norell (AMNH)	*Albertosaurus* (5218); *Alioramus* (IGM 100-1844); *Allosaurus* (600, 851); *Angaturama* (cast: 30230); *Bambiraptor* (30554); *Byronosaurus* (IGM 100-972, IGM 100-983); *Citipati* (IGM 100-978); *Coelophysis* (7223, 7224, 7227, 7228, 7229, 7231); *Dromaeosaurus* (5356); *Gallimimus* (IGM 100-1133); *Gorgosaurus libratus* (5336, 5432, 5458, 5664); *Khaan* (IGM 100-1002, IGM 100-1127); *Marshosaurus* (cast: 27638, 27640, 27641); *Ornitholestes* (619); *Oviraptor* (6517); *Saurornithoides* (6516); *Shuvuuia* (IGM 100-977, IGM 100-1001); *Struthiomimus* (5339); *Tsaagan* (IGM 100-1015); *Tyrannosaurus* (5027, 21542); *Velociraptor* (6515); Unnamed Troodontidae (IGM 100-1128, IGM 100-1128)
2	CMNH	Carnegie Museum, Pittsburgh, Pennsylvania, USA	10-12/11/2010	Matthew Lamanna (CMNH), Amy Henrici (CMNH)	*Allosaurus* (1254, 11844, 21703); *Coelophysis* (81765, 82931); *Tyrannosaurus* (9380)
3	DMNH	Dallas Museum of Natural History, Dallas, Texas, USA	28/10/2010	Anthony Fiorillo DMNH), Ronald Tykoski (DMNH)	*Albertosaurus* (22019); *Troodon* (22337, 22837); *Saurornitholestes* (22870); Indeterminate Tyrannosauridae (21030, 21184, 22019)
4	FMNH	Field Museum of Natural History, Chicago, Illinois, USA	05/11/2010; 08/11/2010	Peter Makovicky (FMNH), William Simpson (FMNH)	*Daspletosaurus torosus* (PR308); *Tyrannosaurus* (PR2081)
5	MACN-CH	Museo Argentino de Ciencias Naturales 'Bernardino Rivadavia', Buenos Aires, Argentina	29/02/2012; 20-22/03/2012	Alejandro Kramarz (MACN), Fernando Novas (MACN)	*Abelisaurus* (MPCA 1, 5, 229, 267, 687, 689, 709); *Bicentenaria* (MPCA 865, 866); *Carnotaurus* (894); *Ischisaurus* (18.060); '*Megalosaurus inexpetatus*' (18.189); *Noasaurus* (PVL 4061); *Piatnitzkysaurus* (895; PVL 4073); *Megaraptor* (MUCPv 595); *Zupaysaurus* (PULR 076); isolated carcharodontosaurid? teeth (MPCA 685, 694)
6	MCF-PVPH	Museo Municipal Carmen Funes, Paleontologia de Vertebrados, Plaza Huincul, Argentina	08-09/03/2012; 13-14/03/2012	Rodolfo Coria (MCF-PVPH), Cecilia Succar (MCF-PVPH)	*Aucasaurus* (236); *Ilokelesia* (35); *Mapusaurus* (108)
7	MG	Museu Geológico, Lisbon, Portugal	24/07/2013	Jorge Sequeira (LNEG)	*Allosaurus* (27804); *Paronychodon* (27799); *Aviatyrannis* (27763, 27803, 27812)
8	MHNA.PV	Muséum d'Histoire Naturelle d'Aix-en-Provence, France	17/01/2014	Yves Dutour (MHNA), Thierry Tortosa (MHNA)	*Arcovenator* (2011.12); isolated abelisaurid and dromaeosaurid teeth

9	MIWG	Dinosaur Isle, Isle of Wight Museum Services, Sandown, United Kingdom	04/03/2011	Stephen Hutt (MIW)	*Eotyrannus* (1997.550); *Neovenator* (6348)
10	ML	Museu da Lourinhã, Lourinhã, Portugal	01/01/2010-2014	Octávio Mateus (ML), Simão Mateus (ML)	*Allosaurus* (415); *Torvosaurus* (148, 632, 962, 1100, 1188); *Lourinhanosaurus* (565); *Baryonyx* (1190); many isolated theropod teeth (e.g., 148, 324, 327, 500, 857, 865, 935, 939, 962, 966, 1151, 1853)
11	MLP	Museo de La Plata, La Plata, Argentina	02/03/2012	Marcello Reguero (MLP)	*Genyodectes* (26-39)
12	MNHN	Muséum national d'Histoire naturelle, Paris, France	23/11/2010; 25-26/11/2010; 25/10/2012	Ronan Allain (MNHN)	Abelisauridae (MRS 1919-1920); *Berberosaurus* (To 339); *Compsognathus* (CNJ79); *Cristatusaurus* (GDF 365-366); *Dubreuillosaurus* (1998-13); *Erectopus* (2001-4); *Genusaurus* (Bev.1); *Majungasaurus* (MAJ 1); *Pyroraptor* (BO014-015); *Spinosaurus* (SAM 124); *Spinosaurus* indet. (MRS 478); Carcharodontosauridae indet. (INA, MRS 1802)
13	MPCA	Museo Provincial Carlos Ameghino, Cipolletti, Río Negro, Argentina	07/03/2012	Ruben Barbieri (MPCA)	*Abelisaurus* (11098); *Buitreraptor* (245)
14	MSNM	Museo di Storia Naturale di Milano, Milan, Italy	15/04/2011	Christiano Dal Sasso (MSNM)	*Spinosaurus* (V3976, V4047, V6422, V6424, V6865, V6896)
15	MUCPv	Museo de Ciencias Naturales de la Universidad Nacional de Comahue, Lago Barreales, Argentina	12/03/2012	Jorge Calvo (CePaLB), Juan D. Porfiri (UNDC)	*Ekrixinatosaurus* (294); *Giganotosaurus* (95); abelisaurid teeth (e.g., 482, 641)
16	MUCPv-CH	Museo de Ciencias Naturales de la Universidad Nacional de Comahue, El Chocón collection, Villa El Chocón, Argentina	05-06/03/2012	Juan Ignacio Canale (MUCPv-CH)	*Giganotosaurus* (1); *Skorpiovenator* (MMCH-PV 48)
17	NCSM	North Carolina Museum of Natural Sciences, Raleigh, North Carolina, USA	16/10/2012; 19/10/2012; 21/10/2012	Paul Brinkman (NCSM), Lindsay Zanno (NCSM)	*Acrocanthosaurus* (14345)
18	NHFO	Paleontological collections, Natural History Museum of Qatar	08-15/11/2013	Fareed Krupp (QMA), Khalid Hassan Al-Jaber (QMA), Sanker S.B (QMA)	*Allosaurus* (455)
19	NHM	The Natural History Museum, London, United Kingdom	23-28/02/2011; 01/03/2011	Sandra Chapman (NHM), Paul Barrett (NHM)	*Baryonyx* (R.9951); *Daspletosaurus* sp. (R.4863); *Duriavenator* (R.332); *Megalosaurus* (R.234, R.2637, R.8303, R.8305, R.8307, R.28608, R.31834, R.39476, R.47152; R.47963); '*Megalosaurus*

					dunkeri' (R.210, R.1997, R.3221, R.3333, R.36522, R.36523, R.44806); *Neovenator* (R.10001); *Nuthetes* (R.48207, R.48208, + many other isolated teeth); *Proceratosaurus* (R.4860); *Spinosaurus* (R.16420, R.16421); *Tyrannosaurus* (R.7994 = AMNH 5866); *Zanclodon* (R.2912)
20	OUMNH	Oxford University Museum, Oxford, UK	02-03/03/2011	Paul Jeffery (OUMNH)	*Eustreptospondylus* (J.13558); *Magnosaurus* (J.12143); *Megalosaurus* (J.13505, J.13506, J.13559 + many isolated teeth, e.g., J.23014, J.23049, J.23050, J.29762, J.29809, J.29855, J.29856, J.29866, J.48171)
21	PVL	Fundación 'Miguel Lillo', San Miguel de Tucumán, Argentina	20/02/2014	Jaime Powell (PVL)	*Piatnitzkysaurus* (4073)
22	PVSJ	Museo de Ciencias Naturales, Universidad Nacional de San Juan, San Juan, Argentina	15-17/03/2012	Ricardo Martínez (PVSJ)	*Eodromaeus* (560); *Eoraptor* (512); *Herrerasaurus* (053) = *Frenguellisaurus* 407) = *Sanjuansaurus* (605)
23	SBU	Stony Brook University	13/10/2012	David Krauze (SBU), Joseph Groenke (SBU)	*Majungasaurus* (FMNH PR 114, 2008, 2100, 2278, UA 8716); *Masiakasaurus* (FMNH PR 2177, 2178, 2179, 2182, 2183, 2201, 2221, 2222, 2453, 2476, 2496, 2471, UA 8680, 9091, 9128)
24	SMA	Sauriermuseum Aathal, Aathal, Switzerland	16-17/03/2010; 17-21/05/2010; 12-14/04/2011	Hans-Jacob Siber (SMA)	*Allosaurus* 'Big Al 2' (005/02); many isolated theropod teeth
25	SMNS	Staatliches Museum für Naturkunde, Stuttgart, Germany	11/04/2011	Rainer Schoch (SMNS)	*Irritator* (58022); *Liliensternus* (cast of MBR 21751)
26	SMU	Southern Methodist, University, Dallas, Texas, USA	26-27/10/2010	Louis Jacobs (SMU), Dale Winkler (SMU)	*Acrocanthosaurus* (73417, 74646); many isolated theropod teeth (e.g., 20BF1, 2, 5, 8, 18, 20, 46, 53, 100, 118, 119, 126)
27	UC	University of Chicago Paleontological Collection, Chicago, Illinois, USA	02-05/11/2010	Paul Sereno (Uni. Chicago)	Abelisauridae indet. (PC 10); *Aerosteon* (cast of MCNA-PV-3137); *Afrovenator* (MNN UBA1); *Carcharodontosaurus iguidensis* (MNN IGU5, MNN IGU6); *Carcharodontosaurus saharicus* (SGM Din-1, MNN GAD8, UCRC PV6); cfr. *Carcharodontosaurus* (MNN GAD15); *Eocarcharia* (MNN GAD7, MNN GAD13, MNN GAD14); *Eoraptor* (cast of PVSJ 512); *Herrerasaurus* (cast of PVSJ 407); *Indosuchus* (AMNH 1753, 1955, 1960); *Kryptops* (MNN GAD1−1); *Oxalaia* (cast of MN61A-V); *Raptorex* (LH PV18); *Rugops* (MNN IGU1); *Suchomimus* (MNN GDF501, 502, G2-2, G5-1, G34-1, G74-1, G232, etc.).
28	USNM	United State National Museum Vertebrate Paleontology, Washington, District of Columbia, USA	15/11/2010	Matthew Carrano (NMNH), Michael Brett-Surman (NMNH)	*Allosaurus* (8335); *Ceratosaurus* (4735); *Gorgosaurus* (12814); *Labrosaurus* (2315); Tyrannosauridae indet. (8346)

A3. Non-avian theropod taxa included in this study

Abbreviations: **c**, photos of cast provided; **C/**, cast examined; **E**, original material examined; **f**, photos of original material provided; **p**, publication(s).

		Genus	species		Locality, horizon and age	Collection number
Non-neotheropod Theropoda		*Eoraptor*	*lunensis*	**E**	Valley of the Moon, Ischigualasto Provincial Park, San Juan, Argentina; Ischigualasto Formation; mid-Carnian	PVSJ 512
		Herrerasaurus	*ischigualastensis*	**E**		PVSJ 407
		Frenguellisaurus	*ischigualastensis*	**E**		PVSJ 053
		Ischisaurus	*cattoi*	**E**		MACN 18.060
		Sanjuansaurus	*gordilloi*	**E**		PVSJ 605
		Staurikosaurus	*gordilloi*	f	Locality of Sanga Grande, city of Santa Maria, Rio Grande do Sul, Brazil; outcrop of the Alemoa Member, Santa Maria Formation; Carnian	MCZ 1669
		Daemonosaurus	*chauliodus*	f	*Coelophysis* Quarry, Ghost Ranch, New Mexico, USA; 'Siltstone member', Chinle Formation; ?Rhaetian	CMNH 76821
		Tawa	*hallae*	f	Site 2, Ghost Ranch, New Mexico, USA; Petrified Forest Member, Chinle Formation; Norian	GR 241
		Eodromaeus	*murphi*	**E**	Valley of the Moon, Ischigualasto Provincial Park, San Juan, Argentina; Ischigualasto Formation; mid-Carnian	PVSJ 560, 561, 562
Non-averostran Neotheropoda	Coelophysidae	*Megapnosaurus* (= *'Syntarsus'*)	*kayentakatae*	f	MNA locality No 555-3, 'Rock Head North', Sand Mesa, Little Colorado River Valley, Arizona, USA; Silty Facies Member, Kayenta Formation; Hettangian	MNA V2623
			rhodesiensis	f	Maura River, Southcote farm and Spring Grange farm, Nyamandhlovu, Matabeleland North and Chitake River, Mashonaland North, Zimbabwe; area between farms Edelweiss and Welbedacht, Ladybrand District, Free State, South Africa; Forest Sandstone and Upper Elliot Formations; ?Hettangian–Sinemurian	QG 165
		Coelophysis	*bauri*	**E**	Ghost Ranch, Abiquiu, Rio Arriba County, New Mexico; Petrified Forest National Park, Arizona; Petrified Forest Member, Chinle Formation; Norian	CMNH 81765, 82931; AMNH FARB 7223, 7224,7225, 7227, 7237, 7238
	Basal averostrans	*Liliensternus*	*liliensterni*	**C/** f	Knollenmergel, Thüringen and Württemberg; Germany; Trossingen Formation; Norian	MB.R.2175 = HMN R1291-R1292
		Zupaysaurus	*rougieri*	**E**	Quebrada de los Jachaleros, La Rioja Province, Argentina; Upper levels of the Los Colorados Formation, Agua de la Peña Group; Norian	PULR 076
		Dilophosaurus	*wetherilli*	f	Little Colorado Valley, Near Tuba City and Rock Head, Coconino County, Navajo Indian Reservation, Arizona, USA; Silty Facies, Kayenta Formation; Hettangian	UCMP 37302, 37303, 77270

Ceratosauria	Ceratosauridae	*Ceratosaurus*	*nasicornis*	**E**	Canyon City, Garden Park, Quarry I, Colorado, USA; Brushy Basin Member, Morrison Formation; Kimmeridgian-Tithonian; Cleveland-Lloyd Dinosaur Quarry, Emery Co., Utah, USA; Fruita Paleontological Area, Fruita, Colorado, USA; Brushy Basin Member, Morrison Formation; Kimmeridgian-Tithonian	USNM 4735; UUVP 674 = UMNH VP 5278; MWC 1
		Genyodectes	*serus*	**E**	Cañadón Grande, Departamento Paso de Indios, Chubut Province, Argentina; ?Cerro Castaño Member, Cerro Barcino Formation; Aptian–Albian	MLP 26-39
	Basal Abelisauroidea	*Berberosaurus*	*liassicus*	**E**	Douar of Tazouda, Toundoute, Province of Ouarzazate, High Atlas, Morocco; Upper bone-bed of the Toundoute continental series; Pliensbachian–Toarcian	MNHN To 339
		Eoabelisaurus	*mefi*	f	Jugo Loco locality, village of Cerro Cóndor, Chubut, Argentina; series of finely bedded mud-, marl- and limestones of the Cañadón, Asfalto Formation; Aalenian–Bajocian	MPEF-PV 3990
	Noasauridae	*Masiakasaurus*	*knopfleri*	**E**	Near the village of Berivotra, Mahajanga Province, Madagascar; Anembalemba and Masorobe members, Maevarano Formation; Maastrichtian	FMNH PR 2177, 2178, 2179, 2183, 2222, 2453, 2496, 2471
		Noasaurus	*leali*	**E**	El Brete, southern Salta Province, Argentina; Lecho Formation; ?upper Campanian–Maastrichtian	PVL 4061
	Abelisauridae	*Kryptops*	*palaïos*	**E**	'Gadoufaoua', western edge of the Ténéré Desert, Niger; Elrhaz Formation; Aptian–Albian	MNN GAD1−1
		Rugops	*primus*	**E**	Near In Abangharit, Niger Republic; Echkar Formation, Tegama Group; Cenomanian	MNN IGU1
		Ilokelesia	*aguadagrandensis*	**E**	Aguada Grande, 15 km south of Plaza Huincul City, Neuquén Province, Argentina; Huincul Formation, Río Limay Subgroup, Neuquén Group; Turonian–Santonian	MCF-PVPH 35
		Indosuchus	*raptorius*	**E**	Bara Simla Hill, Jabalpur, Madhya Pradesh, India; 'Carnosaur Bed', Lameta Formation; Maastrichtian	AMNH FARB 1753, 1955, 1960
		Arcovenator	*escotae*	**E**	Jas Neuf Sud locality, along the A8 motorway near the village of Pourrières, Var, France; Lower Argiles Rutilantes Formation, upper part of the Lower Rognacian; Late Campanian	MHNA-PV.2011.12.20, 12.187, 12.297
		Skorpiovenator	*bustingorryi*	**E**	Bustingorry's farm, Villa El Chocón, Neuquén Province, Patagonia, Argentina; lower levels of the Huincul Formation; Late Cenomanian–Early Turonian	MMCN-PV 48
		Ekrixinatosaurus	*novasi*	**E**	Approximately 34 km northwest of Añelo, Neuquén Province, Argentina; Candeleros Formation, Río Limay Subgroup, Neuquén Group; late? Cenomanian	MUCPv 294

		Rahiolisaurus	*gujaratensis*	f	Rahioli village, Kheda District, Gujarat, western India; Mudstone unit of the Lameta Formation; Maastrichtian	ISIR 401
		Abelisaurus	*comahuensis*	**E**	Lago Pellegrini stone quarries, General Roca department, Río Negro Province, Argentina; Anacleto Formation, Río Colorado Subgroup, Neuquén Group; early–middle Campanian	MPCA 11.098, 689 (+ others?)
		Aucasaurus	*garridoi*	**E**	Auca Maheuvo, near La Escondida Mine, northeastern Neuquén Province, Argentina; Anacleto Formation, Río Colorado Subgroup, Neuquén Group; early–middle Campanian	MCF-PVPH 236
		Carnotaurus	*sastrei*	**E**	Estancio Pocho Sastre, near Bajada Moreno, Telsen department, Chubut Province, Argentina; Lower section, La Colonia Formation; Maastrichtian	MACN-CH 894
		Majungasaurus	*crenatissimus*	**E**	Meravana and Berivotra, Mahajanga Basin, Mahajanga, Madagascar; Anembalemba Member, Maevarano Formation; Maastrichtian	MNHN MAJ 1; FMNH PR 2008, 2100, 2278
Basal Tetaurae		*Sinosaurus*	*triassicus*	f	Qinglongshan near Muchulang Village, Xiyangyi Rural Tribal District, Jinning County, Yunnan, China; lower Lufeng Formation; Hettangian–Sinemurian	IVPP V34; ZLJ 0003; ZLJ T01; KMV 8701; LDM-LCA 10
		Cryolophosaurus	*ellioti*	f	Mt. Kirkpatrick, near Beardmore Glacier, central Transantarctic Mountains, Antarctica; Hanson Formation; Sinemurian–Pliensbachian	FMNH PR1821
		Monolophosaurus	*jiangi*	f	34 km north-east of Jianjungmiao, Junggar Basin, Xinjiang Uygur Zizhiqu, China; lower Shishugou (= Wucaiwan) Formation; middle Bathonian–late Callovian	IVPP 84019
Megalosauroidea		*Sciurumimus*	*albersdoerferi*	f	Rygol quarry, Painten, Bavaria, Germany; Thin-bedded to laminated micritic limestones equivalent to the upper part of the Rögling Formation; Upper Kimmeridgian	(BMMS) BK 11
	Piatnitzkysauridae	*Marshosaurus*	*bicentesimus*	**C/**	Cleveland-Lloyd Dinosaur Quarry, Emery County and Dinosaur National Monument, Uintah County, Utah; DMNH loc. 882, Moffat County and Dry Mesa Quarry, Montrose County, Colorado, USA; Brushy Basin Member, Morrison Formation; Kimmeridgian	UMNH 7820 (= UUVP 3266), 7824 (= UUVP 1846, 1864), 7825 (= UUVP 4695), 6364 (= UUVP 40-555), 6367 (= UUVP 3454), 6368 (= UUVP 3502); CMNH 021704 (= DINO 16455); DNMH 3718
		Piatnitzkysaurus	*floresi*	**E**	Cerro Cóndor, 1.5 km west of the former Farias store, Cerro Cóndor village, right bank of the river, Chubut, Argentina; Cañadon Asfalto Formation, Sierra de Olte Group; Bajocian–Callovian	PVL 4073; MACN CH 895
		Condoraptor	*currumili*	f	Las Chacritas, 2.3 km west of Cerro Cóndor, Chubut, Argentina; Cañadón Asfalto Formation, Sierra de Olte Group; Bajocian–Callovian	MPEF-PV 1694, 1695

Megalosauridae	*Eustreptospondylus*	*oxoniensis*	**E**	Summertown brick pit, Wolvercot and Little-more, Oxfordshire, England; Peltoceras athleta Zone, Stewart Member, Oxford Clay Formation and Corallian Formation; late Callovian	OUMNH J.13558
	Magnosaurus	*nethercombensis*	**E**	Nethercomb, 1.6 km north of Sherbourne, Dorset, England; Stephanoceras humphriesianum Zone and Subzone, middle part of Inferior Oolite; early Bajocian	OUMNH J.12143
	Dubreuillosaurus	*valesdunensis*	**E**	Near Conteville, Calvados, Basse-Normandie, France; Procerites progracilis Zone, Pierre de Caen, Calcaires de Caen; middle Bathonian	MNHN 1998-13
	Afrovenator	*abakensis*	**E**	In Abaka, Agadez, Niger; Tiourarén Formation, Irhazer Group; Middle–Late Jurassic or Neocomian	MNN UBA1
	Duriavenator	*hesperis*	**E**	Greenhill, Sherborne, Dorset, England; Garantiana garantiana Subzone, Parkinsonia parkinsoni Zone, upper part of Inferior Oolite Group; late Bajocian	NHM R.332
	Megalosaurus	*bucklandii*	**E**	Stonesfield, near Woodstock, 19 km north-west of Oxford, and Sarsgrove and Workhouse Quarry, Chipping Norton, Oxfordshire; New Park Quarry and Oakham Quarry, Gloucestershire, England; Stonesfield Slate, Taynton Limestone Formation, Chipping Norton Limestone Formation and Sharp's Hill Formation; lowest middle Bathonian	NHM R.8303; OUMNH J13505, 13506, 13559 + many other teeth
	Torvosaurus	*gurneyi*	**E**	Cliffs of Praia da Vermelha, Praia do Porto das Barcas, Praia da Area Branca, region of Lourinhã, Lisbon district, Portugal; Lourinhã Formation; Kimmeridgian–Tithonian	ML 148, 962, 1100, 1403
		tanneri	**C/**	Dry Mesa Quarry, Montrose County, Colorado; Salt Wash and Brushy Basin Members, Morrison Formation; Kimmeridgian–Tithonian	BYUVP 2003, 4882, 5110, 9122, 9246;
Spinosauridae	*Baryonyx*	*walkeri*	**E**	Smokejacks Brickworks (Ockley brick pit), Walliswood, Ockley, near Dorking and Ewhurst Brick-works, Surrey, England; Cypridea clavata zone, Upper Weald Clay; Barremian–early Aptian. Praia das Aguncheiras, Sesimbra Municipality, Portugal; Papo Seco Formation; early Barremian	NHM R.9951; ML 1190
	Suchosaurus	*cultridens*	f	A quarry at Whiteman's Green (Tilgate forest site), Cuckfield, Sussex, England; Grinstead Clay Member, Tunbridge Wells Sand Formation, Wealden Group; middle–upper Valanginian	NHM R36536
	Suchomimus	*tenerensis*	**E**	Gadoufaoua outcrop, Agadez, Niger; Elrhaz Formation, Tegama Group; Aptian–Albian?	MNN GDF501, GDF502, G2-2, G5-1, G34-1, G74-1, G232, G6-?
	Cristatusaurus	*lapparenti*	**E**	Gadoufaoua outcrop, Agadez, Niger; Elrhaz Formation, Tegama Group; Aptian–Albian?	MNHN GDF 366

		Siamosaurus	*suteethorni*	p	Phu Pratu Teema, Phu Wiang, Changwat Khon Kaen, Thailand; Sao Khua Formation, Khorat Group; Barremian–Aptian	DMR TF 2043a - i; IVPP V4793; GMNH-PV-999
		Irritator	*challengeri*	**E**	Near Buxéxé, 5 km south of Santana do Cariri, Araripe Basin, southern Ceará, Brazil; Romualdo Member, Santana Formation; Albian	SMNS 58022
		Angaturama	*limai*	**C/**	Unspecified locality in the Araripe Basin, southern Ceará, Brazil; Romualdo Member, Santana Formation; Albian	GP/2T5
		Spinosaurus	*aegyptiacus*	**E**	Bahariya Oasis, Marsa Matruh, Egypt; Bahariya Formation; Albian?–early Cenomanian. Tafilalt and Kem Kem region, South-eastern Morocco; Kem Kem beds; early Cenomanian	MSNM V3976, V4047, V6422, V6424, V6865, V6896; MNHN SAM 124; NMC 50832
Allosauroidea	Allosauridae	*Allosaurus*	*fragilis*	**E**	Bone Cabin Quarry (BCQ), Albany County, Wyoming; Como Bluff (CBQ), Reed's Quarries 1, 4, and 9, Alban County, Wyoming; Marsh's Felch Quarry 1 (FQ1), Garden Park, Colorado; Cleveland-Lloyd Dinosaur Quarry (CLDQ), Cleveland, Utah; Carnegie Quarry (DNMCQ) Dinosaur National Monument, Brushy Basin Member, Uinta County, Utah; Moffit County Quarry (MC), Moffit County, Colorado; Brushy Basin Members, Morrison Formation; Kimmeridgian–Tithonian	AMNH FARB 600, 851; BYUVP 2028, 8901; CMNH 1254, 11844, 21703; USNM 8335; UMNH VP 1251, 5393, 6475, 9168, 9351; MWC 5440
			europaeus	**E**	Praia de Vale Frades, 5 km North of Lourinhã, Portugal; Porto Novo Member, Lourinhã Formation; Kimmeridgian	ML 415
			jimmadseni	**E**	Big Al Quarry (BAQ), Big Horn County, Wyoming; Dry Mesa Quarry (DMQ), Colorado; DNM-116 at Dinosaur National Monument (DNMSW), Salt Wash Member, Uinta County, Utah; Hinkle Quarry (HKQ), Mesa County, Colorado; Howe Quarry (HQ), Big Horn County, Wyoming; Moffit County Quarry (MC), Moffit County, Colorado; Little Houston Quarry (LHQ), Crook County, Wyoming; Meilyn Quarry (MQ), Carbon County, Wyoming, USA; Salt Wash Member and lower part of the Brushy Basin Member, Morrison Formation; Kimmeridgian–Tithonian	DINO 11541; SMA 005/02; MOR 693; NHFO 455
	Metriacanthosauridae	*Sinraptor*	*dongi*	f	Jianjungmiao, Junggar Basin, Xinjiang Uygur Zizhiqu, China; upper part, Shishugou Formation; Oxfordian	IVPP 10600
			hepigensis	f	Dashanpu Dinosaur Quarry, Zigong, Sichuan, China; Shangshaximiao Formation; Oxfordian–early Kimmeridgian, Late Jurassic	ZDM T0024
		Yangchuanosaurus	*shangyouensis*	f	Shangyou Reservoir and Hongjiang Machine Factory, near Yongchuan, Yongchuan County, Sichuan, China; Shangshaximiao Formation; Oxfordian–early Kimmeridgian	CV 00215, CV 00216
		Erectopus	*superbus*	**E**	Louppy-le-Château, Meuse, France; phosphatic 'La Penthi` eve Beds', Douvilleiceras mammilatum Zone; lower Albian	MNHN 2001-4

		Neovenator	*salerii*	**E**	Cliffs near Grange Chine, south-west coast of Isle of Wight, England; Wessex Formation; late Hauterivian–early Barremian	MIWG 6348; NHM R.10001
	Neovenatoridae	*Aerosteon*	*riocoloradensis*	C/f	Cañadon Amarillo, Mendoza, Argentina; Anacleto Formation, Río Colorado Subgroup, Neuquén Group; early Campanian	MCNA-PV 3137
	Megaraptora	*Megaraptor*	*namunhuaiquii*	**E**	North of Lago Barreales, Añelo region, Neuquén Province, Argentina; Candeleros Formation, Río Limay Subgroup, Neuquén Group; late? Cenomanian	MUCPv 595
		Australovenator	*wintonensis*	p	ODF 85, 'Matilda Site,' Elderslie Station, 60 km north-west of Winton, Queensland, Australia; Winton Formation; late Albian	AODF 604
		Fukuiraptor	*kitadaniensis*	p	Kitadani locality, along Sugiyama River, northern part of Katsuyama city, Fukui Prefecture, Japan; Kitadani Formation, Akaiwa Subgroup, Tetori Group; Barremian	FPMN 9712203, 9712204, 9712205, 9712206 + many others
		Orkoraptor	*burkei*	F	Los Hornos Hill, southern coast of Viedma Lake, SW Santa Cruz Province, Argentina; Pari Aike Formation; Early Maastrichtian	MPM-Pv 3457
	Carcharodontosauridae	*Acrocanthosaurus*	*atokensis*	**E**	McLeod Prison, Arnold Farm and Cochran Farm, Atoka and McCurtain Counties, Oklahoma, and Hobson Ranch, Parker County, Texas, USA; Antlers and Twin Mountains Formations; late Aptian–early Albian	NCSM 14345
		Shaochilong	*maortuensis*	f	Maortu, 60 km north of Chilantai (Jilantai), eastern Alashan Desert, Nei Mongol Zizhiqu, China; Ulan-suhai Formation; Turonian?	IVPP V.2885
		Eocarcharia	*dinops*	**E**	G88 and other sites along the Gadoufaoua outcrop, Agadez, Niger; Elrhaz Formation, Tegama Group; Aptian–Albian?	MNN GAD7, GAD13, GAD14
		Kelmayisaurus	*petrolicus*	f	Near Wuerho (Urdo), Junggar Basin, Xinjiang, China; Lianmugin Formation, Tugulu Group; ?Valanginian–Albian	IVPP V4022
		Tyrannotitan	*chubutensis*	f	Stancia 'La Juanita', 28 km north-east of Paso de Indios, Chubut, Argentina; Cerro Castaño Member, Cerro Barcino Formation; Aptian–Albian	MPEF-PV 1156
		Carcharodontosaurus	*saharicus*	**E**	Timimoun, Algeria, the Bahariya Oasis, Egypt and the Kem Kem region, Morocco; 'Continental Intercalaire,' Bahariya, and Kem Kem beds, respectively; Albian?–Cenomanian	SGM Din-1, MNN GAD8, UCRC PV6
			iguidensis	**E**	Iguidi, west of In Abangarit, Agadez, Niger; Echkar Formation, Tegama Group; Cenomanian	MNN IGU5, IGU6
		Giganotosaurus	*carolinii*	**E**	South and west of El Chocón, Lake Esquiel Ramos Mexia, Neuquén, Argentina; Candeleros Formation, Río Limay Subgroup, Neuquén Group; ?late Cenomanian	MUCPv CH1; MUCPv 95
		Mapusaurus	*roseae*	**E**	Caénadón del Gato, Cortaderas area, 20 km south-west of Plaza Huincul, Neuquén, Argentina; Huincul Formation, Río Limay Subgroup, Neuquén Group; Turonian–Santonian	MCF-PVPH 108

Basal Coelurosauria		*Zuolong*	*sallei*	p	Wucaiwan, Xinjiang, People's Republic of China; Upper part of the Shishugou Formation; Oxfordian	IVPP V15912
		Ornitholestes	*hermanni*	**E**	Bone Cabin Quarry, near Medicine Bow, Albany County, Wyoming, USA; Morrison Formation; Kimmeridgian–Tithonian	AMNH FARB 619
		Bicentenaria	*argentina*	**E**	East shore of Ezequiel Ramos Mexía Reservoir, Río Negro Province, Northern Patagonia, Argentina; Upper levels of the Candeleros Formation, Río Limay Subgroup, Neuquén Group; Cenomanian	MPCA 865, 866
		Lourinhanosaurus	*antunesi*	**E**	Peralta, near Lourinhã, Estremadura, Portugal; Sobral Formation; late Kimmeridgian–early Tithonian	ML565
		Aorun	*zhaoi*	p	Mower half of the Shishugou Formation, Wucaiwan locality, Xinjiang, China; Callovian	IVPP V15709
Tyrannosauroidea	Basal Tyrannosauroidea	*Guanlong*	*wucaii*	f	Wucaiwan area, Junggar Basin, Xinjiang; upper part of the Shishugou Formation; Oxfordian	IVPP V14531, V14532
		Dilong	*paradoxus*	f	Lujiatun, Beipiao, western Liaoning; fine sand beds of the lower part of the Yixian Formation; Barremian	IVPP V14242, V14243, ?V11579
		Proceratosaurus	*bradleyi*	**E**	Minchinhampton Reservoir, Gloucester-shire, England; White Limestone Formation, Great Oolite Group; middle–late Bathonian	NHM R.4860
		Eotyrannus	*lengi*	**E**	Between Atherfield Point and Hanover Point, Southwest coast of the Isle of Wight; Wessex Formation, Wealden Group; probably Barremian	MIWG 1997.550
		Xiongguanlong	*baimoensis*	p	White Ghost Castle field area, Yujingzi Basin, Gansu, China; grey mudstone near the bottom of the Early Cretaceous sedimentary series, Xinminpu Group; Albian	FRDC-GS JB16-2-1
		Dryptosaurus	*aquilunguis*	f	West Jersey Marl Company Pit, near Barnsboro, Gloucester County, New Jersey; New Egypt Formation; Maastrichtian	ANSP 9995
		Raptorex	*kriegsteini*	**E**	Border area between Liaoning Province and the Nei Mongol Autonomous Region, Northeast China; Lujiatun Beds, Yixian Formation; Barremian-Aptian	LH PV18
	Tyrannosauridae	*Alioramus*	*altai*	**E**		IGM 100-1844
		Albertosaurus	*sarcophagus*	**E**		AMNH FARB 5218, 5222; MOR 657; NMC 5600, 5601, 11315; ROM 807; RTMP 81.10.1; 85.98.1; 86.64.1; 86.205.1; 97.58.1

	Gorgosaurus	*libratus*	**E**	(Tyrannosauridae) Judith River Formation, Montana, USA; Lance Formation, Wyoming, USA; Horseshoe Canyon Formation, Alberta, Canada; Iren Dabasu Formation, Nei Mongol Zizhiqu, China; Baynshiren Svita, Omnogov, Mongolia; Beds of Nogon Tsav, Bayankhongor, Mongolia; Two Medicine and Hell Creek formations, Montana; Denver Formation, Colorado; Kirtland Shale, New Mexico, USA; Judith River Formation, Alberta, Canada; Fruitland Formation, New Mexico, USA; Nemegt Formation, Omnogov, Mongolia; Subashi Formation, Xinjiang, China; Nemegt Svita, White beds of Khermeen Tsav, Bayankhongor, Mongolia; ?unnamed unit, Heilongjiang, China; Scollard and Willow Creek formations, Alberta, Canada; Frenchman Formation, Saskatchewan, Canada; Hell Creek Formation, South Dakota, USA; Livingston Formation, Montana, USA; Lance Formation, Wyoming, USA; Laramie Formation, Colorado, USA; McRae Formation, New Mexico, USA; Campanian-Maastrichtian	AMNH FARB 3963, 5423, 5336?, 5428, 5432, 5434, 5458; 5664; NMC 2120, 8782, 11593; ROM 1247, 1422; RTMP 86.144.1, 91.36.500, 91.163.1, 94.12.602, 95.5.1, 99.33.1, 2000.12.11
	Daspletosaurus	*torosus*	**E**		AMNH FARB 5336?, 5346, 535; FHM PR (308); MOR 395, 590; NHM R.4863; NMC 8506; RTMP 2001.36.1
	Tarbosaurus	*bataar*	f		ZPAL MgD−I/3, MgD−I/4, MgD−I/5, MgD−I/26, M gD−I/29, MgD−I/31, MgD−I/34, MgD−I/38, MgD−I/44, MgD−I/45, MgD−I/46, MgD−I/109, MgD−I/178; IGM 100-60, 100/61, 100/62, 100/65, 100/67, 107/3; PIN 551−1, 551−91, 552−2, 553−1
	Tyrannosaurus	*rex*	**E**		AMNH FARB 973= CMNH 9380, 5027, 5866 cfr. NHM; BHI 3033; CMNH 9380; FMNH PR 2081; MOR 008, 009, 125, 555, 980, 1125, 1128, 1626; NHM R.7994 = AMNH FARB 5866; RTMP 81.6.1, 81.12.1; CMNH 7541; BMRP 2002.4.1
Compsognathidae	*Scipionyx*	*samnicicus*	f	Le Cavere quarry, Pietraroja, Benevento Province, Italy; upper Plattenkalk horizon ‘Calcari selciferi e ittiolitiferi di Pietraroja’ Formation; Lower Albian	SBA-SA 163760
	Compsognathus	*longipes*	**E**	Reidenburg-Kelheimarea, Bayern, Germany; Petit Plan de Canjuers, Var, Provence-Alpes-Côte d’Azur, France; Ober Solnhofen Plattenkalk; Lithographic Portlandian Limestone of the’Petit Plan’; Lower Tithonian.	BSP ASI 563; MNHN CNJ 79

	Sinosauropteryx	*prima*	p	Sihetun-Jianshangou region, near Beipiao and Dawangzhangzi of Lingyuan, Liaoning, China; Jianshangou intercalated bed in the lower part of the Yixian Formation; Neocomian	NIGP 127586, 127587
	Juravenator	*starki*	f	Stark Quarry, west of Schamhaupten, district of Eichstätt, Southern Franconian, Bavaria, Germany; Silicified, laminated limestone, Beckeri Zone, Ulmense Subzone; Late Kimmeridgian	JME Sch 200
Ornithomimosauria	*Nqwebasaurus*	*thwazi*	p	17 km west of Kirkwood Village, South Africa; Kirkwood Formation; Berriasian–Valanginian	AM 6040
	Pelecanimimus	*polyodon*	p	Las Hoyas fossil site, Cuenca Province, Spain; Calizas de La Huérguina Formation; Late Barremian	LH 7777
	Shenzhousaurus	*orientalis*	f	Sihetun fossil site, Beipiao, Western Liaoning, China; Yixian Formation; Barremian–Aptian	NGMC 97-4-002
	Garudimimus	*brevipes*	f	Baishin Tsav, Ömnögov', Mongolia; Bayanshiree Formation; Cenomanian to Turonian.	IGM 100-13
	Sinornithomimus	*dongi*	f	Ulan Suhai, Alashanzuo Banner, Nei Mongol Autonomous Region of China; Ulansuhai Formation; Late Cretaceous	IVPP V11797−10, V11797−11
	Gallimimus	*bullatus*	**E**	Tsagan Khushu, Nemegt Basin, Gobi Desert, Mongolia; Upper Nemegt Beds; Maastrichtian.	IGM DPS 100/10, 100/11; ZPAL MgD-I/1, MgD-I/94
	Ornithomimus	*edmontonicus*	f	Dinosaur Provincial Park, Alberta, Canada; Dinosaur Park Formation; Late Campanian–early Maastrichtian.	RTMP 95.110.1; ROM 851
	Struthiomimus	*altus*	**E**	South side of Red Deer River, Jenner Ferry Crossing, Dinosaur Provincial Park, Alberta, Canada; Dinosaur Park Formation; Late Campanian–early Maastrichtian.	AMNH FARB 5339; ROM 1790
Alvarezsau-roidea	*Haplocheirus*	*sollers*	p	Wucaiwan area, Junggar Basin, Xinjiang, China; orange mudstone beds, upper part of the Shishugou formation; Oxfordian	IVPP V15988
	Mononykus	*olecranus*	p	Bugin Tsav, South Gobi Aimak, southwest Mongolia; Nemegt formation; mid-Maastrichtian.	IGM 107/6
	Shuvuuia	*deserti*	**E**	UkhaaTolgod and Tugrugeen Shireh, South Gobi Aimak, Mongolia. Djadokhta formation; Campanian?	IGM 100-977, 100/1001; MPD 100/120?
Therizinosauria	*Falcarius*	*utahensis*	f	The Crystal Geyser Quarry, Grand County, Utah, USA; Yellow Cat Member, base of the Cedar Mountain Formation; Barremian	UMNH VP 14526, 14565, 14558, 14559, 14527, 14528, 14529
	Jianchangosaurus	*yixianensis*	p	Niujiaogou of Jianchang, Liaoning Province, China; Yixian Formation; Early Cretaceous	41HIII-0308A
	Eshanosaurus	*deguchiianus*	f	Eshan County, Yunnan, southeastern China; Lower part of Lower Lufeng Formation; Hettangian?	IVPP V11579
	Erlikosaurus	*andrewsi*	f	Baynshin Tsav, South Gobi (Omnogov) Aimak, Mongolia; upper part of the Bayan Shire Formation; Cenonmanian-Turonian	IGM (=PST) 100/111

Oviraptorosauria		*Incisivosaurus*	*gauthieri*	p	Lujiatun, Shangyuan, Beipiao City, Liaoning, China; Lujiatun Beds, lower part of the Yixian Formation; Barremian?	IVPP V 13326
		Avimimus	*portentosus*	c	Udan-Sayr Locality, 75 km south of Hovd-somon Ubur-Hangayskaymak, Mongolia; Barun Goyot (‘Burungoyotskaya’ Svita) and Djadohkta (‘Djadochtinskaya’ Svita) Formations; Campanian	PIN 3907/1
		Khaan	*mckennai*	**E**	Mark’s Second Egg locality, Ukhaa Tolgod, Gurvan Tes Somon, Omnogov Aimak, Gobi Desert, Mongolia; Campanian	IGM 100-1127; IGM 100-1002; IGM 100-973
		Citipati	*osmolskae*	**E**	Djadokhta Formation at Ankylosaur Flats, Ukhaa Tolgod, Gurvan Tes Somon, Omnogov Aimak, Mongolia; Campanian	IGM 100-978
		Oviraptor	*philoceratops*	**E**	Sabarakh Usu, Bayn Dzak, Mongolian People’s Republic; Djadochta Formation; ?middle Campanian	AMNH 6517
		Oviraptoridae	indet.	p	Khermeen Tsav, Omnogov aimak, southern Gobi province, Mongolia; red beds of Khermeen Tsav; ?middle–late Campanian	IGM A, B, 100/30A; ZPAL MgD-I/95; ZPAL MgD-I/96
Dromaeosauridae	Unenlagiinae	*Buitreraptor*	*gonzalezorum*	**E**	‘La Buitrera’, 80 km southwest from Cipolletti, south shore of the Ezequiel Ramos−Mexía Lake, northwestern Río Negro Province, Argentina; Candeleros Formation; Cenomanian–Turonian	MPCA 245
		Australovenator	*wintonensis*	f	Bajo de Santa Rosa; 90 km southwest of Lamarque town, Río Negro Province, Patagonia, Argentina; Allen Formation; Campanian–Maastrichtian	AODF 604
	Unclassified eudromaeosaurs	*Nuthetes*	*destructor*	**E**	Swanage, Durdleston Bay, Dorset, England; Cherty Freshwater Member, Lulworth Formation, Purbeck Limestone Group; Berriasian	NHM R.48207, R.48208, R.15870, R.15871, R.15872, R.15873, R.15874, R.15876, R.15878, R.48208
		Richardoestesia	*gilmorei*	p	Section 30, Twp. 20, Rge 11, W4M, Dinosaur Provincial Park, Alberta, Canada; Judith River (Oldman Formation); Late Campanian	NMC 343
		Pyroraptor	*olympius*	**E**	La Boucharde, two kilometres to the south-east of Trets, Bouches-du-Rhône, France; Fluvio-lacustrine sandstones, Begudian; Upper Campanian–Lower Maastrichtian	MNHN BO014-015
	Microraptor-inae	*Microraptor*	*zhaoianus*	f	Qianyang village, 10 km southwest of the city of Yixian in Liaoning Province, China; Yixian and Jiufotang Formations; Aptian-Albian	CAGS 20-7-004; BMNHC PH881
		Sinornithosaurus	*millenii*	p	Sihetun site, Beipiao City, Liaoning Province, northeastern China; lower part of the Lower Cretaceous Yixian Formation; Early Cretaceous	IVPP V 12811
	Dromaeosaur-inae	*Dromaeosaurus*	*albertensis*	**E**	‘Sand Creek’, on the south bank of the Red Deer River, several miles below Steveville, Alberta, Canada; Oldman Formation; Campanian	AMNH 5356
		Atrociraptor	*marshalli*	p	5 km west of the Royal Tyrell Museum of Paleontology, Drumheller, Alberta, Canada; Horeshoe Canyon Formation; Late Campanian or Early Maastrichtian	RTMP 95.166.1

	Velociraptorinae	*Bambiraptor*	*feinbergi*	**E**	Northern edge of Blackleaf Creek, 11 miles north of Bynum, Montana on the Jones Ranch, Teton County, Montana; Two Medicine Formation; Mid to late Campanian	AMNH 30556
		Velociraptor	*mongoliensis*	**E**	Sabarakh Usu (Bayn Dzak), Tugrikin-Shire, Ömnögov Aimag, Gobi desert, Mongolia; Djadokhta Formation; Campanian	AMNH 6515; IGM 100-24;
		Tsaagan	*mangas*	**E**	Xanadu sublocality, Ukhaa Tolgod, Ömnögov Aimag, Mongolia; Djadokhta Formation, Campanian	IGM 100-1015
		Acheroraptor	*temertyorum*	f	45 km southwest of the town of Jordan, Garfield County, Montana, USA; Hell Creek Formation; Upper Maastrichtian	ROM 63777, 63778
		Deinonychus	*antirrhopus*	p	Carbon County, Big Horn County, south central Montana, USA; Cloverly Formation; Late Aptian or Early Albian	YPM 5210, 5232
		Saurornitholestes	*langstoni*	**E** p	sd. 13, section 27, township 21, range 12 west of the Fourth Meridian Dinosaur Provincial Park, south-central Alberta, Canada; Liscomb Quarry, Alaska, USA; Judith River Formation, Prince Creek Formation; Campanian	TMP 74.10.5; DMNH 22870
Troodontidae		*Anchiornis*	*huxleyi*	f	Daxishan locality, Jianchang County, western Liaoning Province, Liaoning, China; Tiaojishan Formation; ?Oxfordian	LPM B00169
		Byronosaurus	*jaffei*	**E**	‘‘Ankylosaur Flats’’ and Xanadu sublocalities, Ukhaa Tolgod, Gobi desert, Mongolia; Djadokhta Formation; Campanian	IGM 100-983; IGM 100-972
		Saurornithoides	*mongoliensis*	**E**	Bayan Zag, Tugrikin-Shire, Ömnögov Aimag, Gobi desert, Mongolia; Djadokhta Formation; Campanian	AMNH 6516
		Zanabazar	*junior*	p	Bugiin Tsav, Ömnögov Aimag, Gobi desert, Mongolia; Nemegt Formation; Maastrichtian	IGM 100-1
		Troodon	*formosus*	**E** p	Dinosaur Provincial Park, Midland Provincial Park, Alberta, Canada; Liscomb Quarry, Alaska, USA; Judith River and Horseshoe Canyon Formations; Prince Creek Formation; Campanian	ANSP 9259; TMP 8.12.11; ROM 1445; DMNH 22337, 22837
		Troodontidae	indet.	p	Barunbayaskaya Svita, Khamareen Us locality, Dornogov, south-eastern Gobi Desert, Mongolia; ?Aptian–Albian	IGM 100-44
		Undescribed Troodontidae		**E**	Gobi desert, Mongolia; Djadokhta formation; Campanian	IGM 100-1128
		Undescribed Troodontidae		**E**	Gobi desert, Mongolia; Djadokhta formation; Campanian	IGM 100-1323

A4. Phylogenetic analysis on dentition-based characters

A4.1. Character list

The full set of 141 dentition-based characters is listed here. 74 characters are derived from the literature and the original and sometimes previous usages of the character are indicated by citations (with the corresponding character number) in parentheses. 67 characters (47.5%) were revealed by our personal observation of the dentition of more than hundred theropod taxa. Among the 81 multistate characters, 71 were left unordered such as the elongation and thickness of the tooth, the extension of the carinae along the crown, and the development of interdenticular sulci, due to the variability of these features along the tooth row. Therefore, only characters with obvious evolutionary continuity were ordered and concern the overlap of the first and second premaxillary alveoli (char. 4), the constriction of the premaxillary tooth rows (char. 15), the posterior extension of the tooth row relative to the orbit (char. 24), and the size of the crown (chars. 36 and 65) and denticles (chars. 53 and 86), i.e., there must be a theropod bearing moderately large teeth/denticles between two closely related taxa with one having very small crowns (CH < 10 mm)/denticles (> 250 denticles on the carinae), and another possessing very large teeth (CH > 60 mm)/denticles (< 15 denticles on the carinae).

Characters related to the number of teeth borne by the premaxilla (char. 2), the maxilla (char. 17) and the dentary (char. 25) were also ordered. According to Miyashita et al. (2010), characters based on tooth count do not accurately reflect true phylogenetic signal as tooth count varies ontogenetically, intraspecifically and even between the left and right jaws of a same individual. Yet, the number of premaxillary teeth is for instance remarkably stable among theropods (Miyashita et al. 2010; pers. obs.), and a large number of closely related theropod taxa share the same number of teeth borne by the maxilla (e.g., non-carcharodontosaurid allosauroids) and dentary (e.g., megalosaurids). Likewise, the ontogenetical variation of the number of maxillary and dentary teeth, and suggested by Carr (1999) for tyrannosaurids, was questioned by Currie (2003) and refuted by Tsuihiji et al. (2011). Furthermore, the tooth counts typically varies of one or two teeth between the left and right jaws of a same individual (Currie 2003). Although the tooth count variation seems to exceed two teeth for the maxilla or the dentary in some taxa (e.g., *Ceratosaurus nasicornis*, *Tyrannosaurus rex*; Carrano and Sampson 2008; Brusatte et al. 2012*a*), the character states of our data matrix regarding the maxillary and dentary tooth count corresponds, in most cases, to a range of two teeth or more, and we therefore assume that there must be a theropod with an intermediate tooth count between a more primitive one with two teeth less and a more derived with two teeth more. Given the results of the cladistic analysis, this assumption is coherent with the evolution of maxillary and dentary tooth count for most theropod clades, except perhaps for baryonychine and spinosaurine Spinosauridae that may have followed two different path in the evolution of their dentition.

Some characters concern the curvature of the labial and lingual sides of the crown, and the presence of ornamentations on their surface. The labial and lingual sides of a theropod tooth can be identified thanks to the position and orientation of the mesial and distal carinae. The mesial carina, when curving towards the base of the crown, always twists towards the lingual side, whereas the distal carina, when deflected from the center of the distal margin, is displaced labially in the large majority of theropods. Furthermore, there is typically a centrally positioned depression on the lingual side of the root which can extends on the basal part of the crown in many taxa. If this depression appears on both labial and distal sides of the crown, the lingual depression is usually deeper than the labial one (pers. obs.).

Two characters are related to the outline of the crown base in cross-section. This feature is particularly important in mesial teeth which have a typical cross-section outline in many theropod clades. The following figure illustrates the different outlines and the associated terms used in this paper. Because theropod teeth morphology varies through ontogeny (Araújo et al. 2013), some dentition-based characters are only coded in mature (i.e., sub-adults and adults) individuals. They concern the crown size (CH), the average number of denticles (per 5 mm) on the mesial and distal carinae, and the size of the denticles along the carinae for both mesial and distal dentition. Indeed embryo and hatchling individuals have logically smaller crowns with smaller denticles, as well as larger denticles at the base of the crown (pers. obs.).

I. PREMAXILLA ALVEOLI/TEETH

1. Premaxillary teeth (Russell and Dong 1993 #2): (0) present; (1) absent.
2. Number of premaxillary teeth (or alveoli; Modified from Harris 1998 #47; Sereno et al. 1998 #19; **Ordered**): (0) 3; (1) 4; (2) 5; (3) 6; (4) 7.
3. Premaxillary alveoli, direction of main axis of elongation in palatal view (**New**; Unordered): (0) all alveoli mesio-distally oriented; (1) anterior alveoli labio-lingually oriented, posterior alveoli mesio-distally oriented; (2) all alveoli labio-lingually oriented.
4. Premaxillary alveoli, overlap of the first and second alveoli in palatal view (**New**; **Ordered**): (0) absent; (1) present, partial; (2) present, complete.
5. Premaxillary alveoli, overlap of the second and third alveoli in palatal view (**New**): (0) absent; (1) present.

6. Premaxillary alveoli, overlap of the third and fourth alveoli in palatal view (**New**): (0) absent; (1) present.
7. Premaxillary teeth (or alveoli), size (Modified from Holtz et al. 2004 #261; Unordered): (0) all approximately equal in size; (1) posterior teeth (or alveoli) smaller than anterior teeth (or alveoli); (2) anterior teeth (or alveoli) smaller than posterior teeth (or alveoli).
8. Anterior premaxillary teeth (or alveoli), size (**New**; Unordered): (0) significantly smaller than the first six anterior maxillary teeth (or alveoli); (1) subequal in size than the first six anterior maxillary teeth (or alveoli); (2) significantly larger than the first six anterior maxillary teeth (or alveoli).
9. Posterior premaxillary teeth (or alveoli), size (Modified from Holtz 2001 #15; Unordered): (0) significantly smaller than the first six anterior maxillary teeth (or alveoli); (1) subequal in size than the first six anterior maxillary teeth (or alveoli).
10. First premaxillary tooth (or alveolus), size (Modified from Sereno et al. 1998 #38; Unordered): (0) subequal in size than second tooth (or alveolus); (1) significantly smaller than second tooth (or alveolus); (2) significantly bigger than second tooth (or alveolus).
11. Second premaxillary tooth (or alveolus), size (Modified from Currie 1995 #4; Unordered): (0) subequal in size than third (and fourth) premaxillary tooth (or alveolus); (1) significantly smaller than third (and fourth) tooth (or alveolus); (2) significantly larger than third (and fourth) tooth (or alveolus).
12. Posteriormost premaxillary tooth (or alveolus), size (**New**; Unordered): (0) subequal in size than more anterior teeth (or alveoli); (1) significantly smaller than more anterior teeth (or alveoli); (2) significantly larger than more anterior teeth (or alveoli).
13. Distal premaxillary alveoli, shape in palatal view (**New**): (0) oval to subcircular; (1) subrectangular.
14. Premaxillary tooth row, posterior extension (position of posteriormost premaxillary tooth; Modified from Sereno 1999 #36): (0) aligned (ventral) to external naris; (1) anterior to external naris.
15. Premaxillary tooth row, posterior part in palatal view (**New**; **Ordered**): (0) unconstricted; (1) slightly constricted; (2) strongly constricted, terminal rosette of premaxilla.
16. Subnarial gap (i.e., posterior part of premaxillary alveolar margin unedentelous, resulting in an interruption of the upper tooth row; Modified from Gauthier 1986; Welles 1984; Rowe 1989; Rowe and Gauthier 1990; Sereno 1999 #34): (0) absent; (1) present.

II. MAXILLA ALVEOLI/TEETH

17. Number of maxillary teeth (or alveoli; Modified from Perle et al. 1993; **Ordered**): (0) >19; (1) 18-19; (2) 16-17; (3) 15; (4) 10-14; (5) 1-9.
18. Anterior maxillary teeth (or alveoli), size (Modified from Zanno et al. 2009 #340; Unordered): (0) subequal in size than posterior teeth (or alveoli); (1) significantly larger than posterior maxillary teeth (or alveoli); (2) significantly smaller than posterior maxillary teeth (or alveoli).
19. Mid-maxillary teeth (or alveoli), mesiodistal length: (**New**): (0) subequal in size than anteriormost maxillary teeth (or alveoli); (1) significantly larger than anteriormost maxillary teeth (or alveoli).
20. First maxillary alveolus, size (Modified from Sereno et al. 1998 #38): (0) significantly smaller than second tooth (or alveolus); (1) subequal in size than second tooth (or alveolus).
21. First maxillary alveolus opens (Rowe 1989): (0) ventrally; (1) anteroventrally.
22. Maxillary teeth, inclination (**New**): (0) pointing ventrally; (1) pointing ventrolaterally.
23. Maxillary alveoli, shape in palatal view (**New**; Unordered): (0) oval to lenticular; (1) subrectangular; (2) circular.
24. Maxillary tooth row, posterior extension (i.e., position of posteriormost tooth; Modified from Gauthier 1986; Harris 1998 #3; Holtz 1998 #133; Rauhut 2003 #70; **Ordered**): (0) posterior to the anterior rim of orbit; (1) aligned (ventral) to the anterior rim of orbit; (2) anterior to the anterior rim of the orbit, posterior to the anteroventral rim of the antorbital fenestra; (3) aligned to the anteroventral rim of the antorbital fenestra; (4) anterior to the anteroventral rim of the antorbital fenestra.

III. DENTARY ALVEOLI/TEETH

25. Number of dentary teeth (or alveoli; Modified from Senter 2002 #22; Carrano et al. 2002 #59; **Ordered**): (0) > 25; (1) 18-25; (2) 15-17; (3) < 15.
26. Dentary alveoli in dorsal view (Currie 1987 #24): (0) well-separated; (1) merged to form a paradental groove.
27. Anteriormost dentary teeth (or alveoli), size (Modified from Russell and Dong 1993; Unordered): (0) subequal in size than mid- and posterior dentary teeth (or alveoli); (1) significantly larger than mid- and posterior dentary teeth (or alveoli); (2) significantly smaller than mid- and posterior dentary teeth (or alveoli).
28. First dentary tooth (or alveolus), size in comparison to second and third dentary alveoli (Modified from Gauthier 1986 #36 and Harris 1998 #48. Based on Holtz et al. 2004 #213 and Sereno et al. 2004 #71): (0) subequal in size; (1) first tooth (or alveolus) substantially smaller.

29. Mid-dentary teeth (or alveoli), size (Modified from Pérez-Moreno et al. 1994): (0) subequal in size than anterior maxillary teeth (or alveoli); (1) significantly smaller than anterior maxillary teeth (or alveoli).
30. Enlarged fanglike anterior dentary tooth (that inserts into a notch between the premaxilla and maxilla; Clark et al. 1994): (0) absent; (1) present.
31. Terminal rosette of dentary, number of teeth (or alveoli; **New**; Unordered): (0) terminal rosette absent; (1) four teeth (or alveoli); (2) five teeth (or alveoli).
32. Anterior dentary teeth (**New**): (0) facing dorsally; (1) procumbent, facing anterodorsally.

VI. PALATAL TEETH

33. Palatal teeth on the pterygoid (Sereno 1999 #107): (0) present; (1) absent.

V. MESIAL TEETH

Crown

34. Mesial teeth, constriction between root and crown (Modified from Martin et al. 1980; Hou et al. 1996; Currie 1987; Unordered): (0) absent; (1) constriction important, base of crown occupying 85% or less of largest crown width; (2) constriction weak, base of crown occupying more than 85% of largest crown width.
35. Mesial teeth, constriction between root and crown along the tooth row (**New**): (0) present in some teeth; (1) present in all teeth.
36. Mesial teeth, crown height (CH in centimeters) in subadult/adult (**New**; **Ordered**): (0) CH ≤ 1; (1) 1 < CH ≤ 6; (2) CH > 6.
37. Mesial teeth, labiolingual compression of the crown (CBR = CBW/CBL; Modified from Sereno et al. 1998 #17; Charig and Milner 1997; Unordered): (0) CBR ≤ 0.75, oval to lenticular; (1) weak, 0.75 < CBR < 1.2, tooth subcircular; (2) teeth labiolingually elongated, CBR > 1.2.
38. Mesial teeth, baso-apical elongation of the crown (CHR = CH/CBL; **New**; Unordered): (0) strongly elongated, CHR > 3; (1) important, 2.5 < CHR ≤ 3; (2) normal, 2 < CHR ≤ 2.5; (3) weak, CHR ≤ 2.
39. Mesial teeth, crown curvature (lingually or distally; Modified from Sereno et al. 1998 #35; Unordered): (0) present, strongly recurved; (1) present, slightly recurved; (2) absent, tooth crown straight and apex centrally positioned or almost centrally positioned.
40. Mesial teeth, distal margin of the crown in lateral view (Modified from Canale et al. 2009 #5 (Smith 2007; Unordered): (0) mainly concave; (1) straight; (2) mainly convex.
41. Mesial teeth, outline of basal cross-section of the crown in the mesial tooth (Modified from Bakker et al. 1988 #22; Unordered): (0) subcircular, ovoid or elliptical; (1) lanceolate, with acute and well-developed distal carina and mesial margin convex; (2) Salinon-shaped, with labial margin convex and lingual margin biconcave; (3) D-shaped or J-shaped, with lingual margins strongly convex and labial margins convex or sigmoid; (5) U-shaped, with mesial and distal margin subparalell and lingual margin planar or weakly convex; (6), lenticular, with acute and well-developed distal and mesial carinae
42. Mesial teeth, concave surface adjacent to the carina: (**New**; Unordered): (0) absent; (1) on the labial surface and adjacent to the distal carina; (2) on the lingual surface and adjacent to both carinae; (3) on the lingual surface and adjacent to the mesial carina only; (4) on the lingual surface and adjacent to the distal carina only.

Carinae

43. Mesial teeth, mesial carina (**New**): (0) absent; (1) present.
44. Mesial teeth, mesial carina (Modified from Senter et al. 2004 #20): (0) non-serrated; (1) serrated.
45. Mesial teeth, distal carina (**New**): (0) serrated; (1) non-serrated.
46. Mesial teeth, mesial carina (**New**; Unordered): (0) not twisted at all; (1) twisted, curves onto the lingual surface.
47. Mesial teeth, mesial carina (Modified from Currie 1995 #2; Unordered): (0) facing mesially; (1) facing mesiolabially or labially; (2) facing mesiolingually; (3) facing entirely lingually.
48. Mesial teeth, distal carina (**New**; Unordered): (0) centrally positioned on the crown and facing distally or labiodistally; (1) labially displaced and facing distally or labiodistally; (2) labially displaced and facing lingually or linguodistally.
49. Mesial teeth, axis passing through both carinae at mid-crown (**New**; Unordered): (0) sub-parallel to long axis of skull; (1) diagonally oriented from long axis of skull; (2) perpendicular to long axis of skull.
50. Mesial teeth, mesial carina, and if serrated, basalmost serration of the mesial carina (Modified from Benson 2009 #89; Unordered): (0) terminates well-above the cervix; (1) extends to the cervix or just above it; (2) terminates well beneath the cervix.

Denticles

51. Mesial teeth, average number of denticles per five mm on mesial carina at two thirds of the crown (MC) in subadult/adult (Modified from Russell and Dong 1993 #20; Unordered): (0) > 19; (1) 14-19; (2) 9-13; (3) 1-8.
52. Mesial teeth, average number of mid-crown denticles per five mm on distal carina (DC) in subadult/adult (Modified from Russell and Dong 1993 #20; Unordered): (0) > 19; (1) 14-19; (2) 9-13; (3) 1-8.
53. Mesial teeth, denticle size (except in embryos and hatchlings; **New**; **Ordered**): (0) minute denticles, more than 250 denticles along the crown; (1) normal in height, between 15 to 250 denticles along the crown; (2) very larges denticles, less than 15 denticles along the crown.
54. Mesial teeth, denticles on mesial carina (Modified from Norell et al. 2001 #88; Unordered): (0) rounded and symmetrically convex; (1) rounded and asymmetrically convex; (2) strongly hooked/pointed, denticles with a tip pointing apically.
55. Mesial teeth, denticles on distal carina (Modified from Senter et al. 2004 #23; Unordered): (0) rounded and symmetrically convex; (1) rounded and asymmetrically convex; (2) strongly hooked/pointed, denticles with a tip pointing apically.
56. Mesial teeth, size of mesial denticles relative to distal denticles (i.e., DSDI; Rauhut and Werner 1995; Unordered): (0) mesial and distal denticles of same size, 0.8 < DSDI <1.2; (1) mesial denticles larger than distal ones, DSDI < 0,8 (2) distal denticles larger than mesial ones, DSDI > 1,2.
57. Mesial teeth, denticles contiguous over tip (Modified from Harris 1998 #45): (0) present; (1) absent.
58. Mesial teeth, interdenticular sulci (Modified from Benson 2009 #90; Unordered): (0) absent; (1) present, short; (2) present, long and well-developed.

Ornamentations

59. Mesial teeth, flutes (i.e., subparallel longitudinal grooves separated by acute ridges) on the crown (Modified from Sereno et al. 1998 #18; Charig and Milner 1997; Unordered): (0) absent; (1) present on the lingual surface only; (2) present on both labial and lingual surfaces; (3) present on the labial surface only.
60. Mesial teeth, longitudinal groove on the labial and/or lingual side of the crown (**New**; Unordered): (0) absent; (1) present, a single groove centrally positioned; (2) present, a single groove mesially positioned.
61. Mesial teeth, elongated, large, longitudinal and rounded ridge, different from acute ridges of fluted surface, on the lingual side of the crown (**New**; Unordered): (0) absent; (1) present, a single ridge centrally positioned; (2) present, two ridges or more.
62. Mesial teeth, basal striations, different of flutes, on both lingual and labial surfaces of the crown (**New**): (0) absent; (1) present.

VI. LATERAL TEETH

Crown

63. Lateral teeth, constriction between root and crown (Modified from Martin et al. 1980; Hou et al. 1996; Currie 1987; Unordered): (0) absent; (1) constriction important, base of crown occupying 85% or less of largest crown width; (2) constriction weak, base of crown occupying more than 85% of largest crown width.
64. Lateral teeth, constriction between root and crown along the tooth row (**New**): (0) present in some teeth; (1) present in all teeth.
65. Lateral teeth, height of the largest crown (CH in centimeters) in subadult/adults (**New**; **Ordered**): (0) CH ≤ 1; (1) 1 < CH ≤ 6; (2) CH > 6.
66. Lateral teeth, labiolingual compression of the crown (CBR = CBW/CBL; **New**; Unordered): (0) important, CBR ≤ 0.5, tooth strongly flattened; (1) normal, 0.5 < CBR ≤ 0.75; (2) weak, CBR > 0.75, tooth incrassate or subcircular.
67. Lateral teeth, baso-apical elongation of the crown (CHR = CH/CBL; **New**; Unordered): (0) weak, CHR ≤ 1.5; (1) normal, 1.5 < CHR ≤ 2.5; (2) important, CHR > 2.5.
68. Lateral teeth, distal margin of crown in lateral view (**New**; Unordered): (0) strongly concave; (1) slightly concave, roughly straight, or straight, apex positioned at the same level as distal profile; (2) convex, apex positioned mesial to mesial profile; (3) weakly sigmoid, basal half concave and apical half convex.
69. Lateral teeth, mesial margin of crown in lateral view (**New**): (0) strongly convex; (1) slightly convex, almost straight, apex centrally positioned.
70. Lateral teeth, mesiodistal curvature of the labial surface of the crown (**New**): (0) convex; (1) surface centrally positioned on the crown roughly flattened.
71. Lateral teeth, concave surface adjacent to carinae all along the crown (**New**; Unordered): (0) absent; (1) present on labial surface and adjacent to distal carina: (2) present on lingual surface and adjacent to distal carina; (3) present on the labial surface and adjacent to both mesial and distal carinae; (4) present on lingual surface and adjacent to both mesial and distal carinae.

72. Lateral teeth, outline of basal cross-section of the crown (**New**; Unordered): (0) subcircular; (1) lenticular or lanceolate; (2) elliptical or bean-shaped (i.e., longitudinal depression centrally positioned on one side only); (3) 8-shaped (i.e., longitudinal depression centrally positioned on both lingual and labial margins); (4) subrectangular.
73. Lateral teeth, basoapical extension of labial depression (i.e., centrally positioned depression on the basolabial surface) on the crown: (**New**; Unordered): (0) labial depression absent; (1) restricted to the crown base; (2) extends along the basal half of the crown or more apically.

Carinae

74. Lateral teeth, mesial carina (**New**): (0) present; (1) absent.
75. Lateral teeth, mesial carina (Modified from Currie 1995 #2): (0) centrally positioned on mesial margin or slightly twisted lingually towards the base; (1) sharply twisted lingually.
76. Lateral teeth, mesial carina (Modified from Senter et al. 2004 #20): (0) serrated; (1) non-serrated.
77. Lateral teeth, distal carina (**New**): (0) present; (1) absent.
78. Lateral teeth, distal carina (**New**): (0) serrated; (1) non-serrated.
79. Lateral teeth, extension of mesial carina relative to distal carina (**New**): (0) mesial carina extends at the same level or terminates more apically than the distal carina; (1) mesial carina extends more basally than the distal carina.
80. Lateral teeth, mesial carina, and if serrated, basalmost serration of the mesial carina (Modified from Benson 2009 #89; Unordered): (0) terminates around mid-height of crown or more apically; (1) extends to base of crown or slightly above the cervix; (2) terminates well beneath the cervix.
81. Lateral teeth, distal carina, and if serrated, basalmost serration of the distal carina (Modified from Benson 2009 #89): (0) extends to the cervix or just above it; (1) terminates well beneath the cervix; (2) terminates well-above the cervix.
82. Lateral teeth, profile of the distal carina on the crown in distal view (**New**): (0) straight or very slightly bowed; (1) strongly bowed or sigmoid.
83. Lateral teeth, position of distal carina on the crown in distal view (**New**): (0) centrally positioned, crown subsymmetrical; (1) strongly labially deflected on the distal margin, crown asymmetrical.

Denticles/serrations

84. Lateral teeth, average number of denticles per five mm on mesial carina at two thirds of the crown (MCA) in subadult/adult (Modified from Russell and Dong 1993 #20; Unordered): (0) > 44; (1) 30-44; (2) 16-29; (3) 9-15; (4) < 9.
85. Lateral teeth, average number of mid-crown denticles per five mm on distal carina (DC) in subadult/adult (Modified from Russell and Dong 1993 #20; Unordered): (0) > 44; (1) 30-44; (2) 16-29; (3) 9-15; (4) < 9.
86. Lateral teeth, denticle size on a single carina (except in embryos and hatchlings; **New**; **Ordered**): (0) minute denticles, more than 250 denticles; (1) normal in height, between 20 to 250 denticles; (2) very larges denticles, less than 20 denticles.
87. Lateral teeth, shape of denticles on mesial carina in lateral view (Modified from Norell et al. 2001 #88; Unordered): (0) symmetrically convex; (1) asymmetrically convex; (2) hooked/pointed.
88. Lateral teeth, shape of denticles on distal carina in lateral view (Senter et al. 2004 #23; Unordered): (0) symmetrically convex; (1) asymmetrically convex; (2) hooked/pointed.
89. Lateral teeth, shape of mesial margin of rounded denticles on mesial carina in lateral view (**New**): (0) parabolic; (1) subrectangular, with flattened surface.
90. Lateral teeth, shape of distal margin of rounded denticles on distal carina in lateral view (**New**; Unordered): (0) parabolic; (1) subrectangular, with flattened surface; (2) semi-circular.
91. Lateral teeth, shape of denticles at two thirds of the crown (MC-MA) on mesial carina in lateral view (**New**; Unordered): (0) longer apicobasally than mesiodistally, vertical subrectangular; (1) as long mediodistally as apicobasally, subquadrangular; (2) longer mediodistally than apicobasally, horizontal subrectangular.
92. Lateral teeth, shape of mid-crown denticles (DC) on distal carina in lateral view (**New**; Unordered): (0) as long mediodistally than apicobasally, subquadrangular; (1) longer mediodistally than apicobasally, horizontal subrectangular; (2) longer apicobasally than mesiodistally, vertical subrectangular.
93. Lateral teeth, denticle size along the carinae (Mateus et al. 2011): (0) regular, gradual change in denticle size; (1) irregular, sporadic change in denticle size.
94. Lateral teeth, biconvex apical denticles (i.e., biconvex external margin of denticle) on mesial carina in lateral view (**New**): (0) absent; (1) present.
95. Lateral teeth, orientation of mesiodistal axis of apical denticles on mesial carina in lateral view (**New**): (0) perpendicular to mesial margin; (1) inclined apically from mesial margin.
96. Lateral teeth, orientation of mesiodistal axis of mid-crown denticles on distal carina in lateral view (**New**): (0) perpendicular to distal margin; (1) inclined apically from distal margin.

97. Lateral teeth, average number of denticles on mesial carina (**New**; Unordered): (0) higher number of denticles basally than at the mid-crown; (1) lower number of denticles basally than at the mid-crown; (2) subequal number of denticles basally than at the mid-crown.
98. Lateral teeth, average number of denticles on mesial carina (**New**; Unordered): (0) higher number of denticles apically than at the mid-crown; (1) lower number of denticles apically than at the mid-crown; (2) subequal number of denticles apically than at the mid-crown.
99. Lateral teeth, average number of denticles on distal carina (except in embryos and hatchlings; **New**; Unordered): (0) higher number of denticles basally than at the mid-crown; (1) subequal or lower number of denticles basally than at the mid-crown.
100. Lateral teeth, average number of denticles on distal carina (**New**; Unordered): (0) higher number of denticles apically than at the mid-crown; (1) lower number of denticles apically than at the mid-crown; (2) subequal number of denticles apically than at the mid-crown.
101. Lateral teeth, size of mesial denticles relative to distal denticles (i.e., DSDI; Rauhut and Werner 1995; Unordered): (0) mesial and distal denticles of same size, 0.8 < DSDI <1.2; (1) mesial denticles larger than distal ones, DSDI < 0,8 (2) distal denticles larger than mesial ones, DSDI > 1,2.
102. Lateral teeth, distal denticles on the apex (Harris 1998 #45): (0) contiguous over tip, or very close to the apex; (1) distal denticles disappear well beneath the apex.
103. Lateral teeth, interdenticular space between mid-crown denticles on the distal carina (**New**): (0) narrow, less than one third of the denticle width; (1) broad, more than one third of the denticle width.
104. Lateral teeth, interdenticular sulci between apical denticles on the mesial carina (Modified from Benson 2009 #90; Unordered): (0) absent; (1) present, short and poorly developed; (2) present, long and well-developed.
105. Lateral teeth, interdenticular sulci between mid-crown denticles on the distal carina (Modified from Benson 2009 #90; Unordered): (0) absent; (1) present, short and poorly developed; (2) present, long and well-developed.
106. Lateral teeth, interdenticular sulci between basalmost denticles on the distal carina (Modified from Benson 2009 #90; Unordered): (0) absent; (1) present, short and poorly developed; (2) present, long and well-developed.

Ornamentations and texture

107. Lateral teeth, flutes (i.e., subparallel longitudinal grooves separated by acute ridges) on the crown (Modified from Sereno et al. 1998 #18; Charig and Milner 1997; Unordered): (0) absent; (1) present on the lingual surface; (2) present on both labial and lingual surfaces.
108. Lateral teeth, average number of flutes on the crown (**New**; Unordered): (0) 1-7; (1) >7
109. Lateral teeth, large transverse undulations on the crown in some teeth (Holtz 1998 #131; Unordered): (0) absent; (1) present, tenuous; (2) present, well visible.
110. Lateral teeth, large transverse undulations on the crown in some teeth when present (**New**): (0) present, just a few; (1) present, numerous and closely packed.
111. Lateral teeth, marginal undulations (i.e., short undulations adjacent to carinae) in some teeth (Modified from Currie and Carpenter 2000 #42; Brusatte et al. 2007; Unordered): (0) absent; (1) present and short, the mesiodistal elongation is less than twice the space separating each undulations; (2) present and elongated, the mesiodistal elongation is longer than twice the space separating each undulations.
112. Lateral teeth, marginal undulations in some teeth (**New**; Unordered): (0) present and shallow, only visible with light; (1) present and pronounced, well visible in lateral view.
113. Lateral teeth, marginal undulations in some teeth (**New**; Unordered): (0) present only on the mesial side of the crown; (1) present only on the distal side of the crown; (2) present on both mesial and distal sides.
114. Lateral teeth, marginal undulations in some teeth (**New**; Unordered): (0) present and mesio-distally oriented; (1) present and diagonally oriented.
115. Lateral teeth, longitudinal groove on the labial and/or lingual surface of the crown (**New**; Unordered): (0) absent; (1) present, a single groove centrally positioned; (2) present, a single groove adjacent to mesial carina; (3) present, two grooves.
116. Lateral teeth, elongated longitudinal and rounded ridge (different from acute ridges of fluted surface) on the lingual surface of the crown (**New**; Unordered): (0) absent; (1) present, a single ridge centrally positioned; (2) present, two or three ridges.
117. Lateral teeth, enamel surface texture (**New**; Unordered): (0) smooth or irregular (non-oriented) texture; (1) braided (oriented) texture, not clearly visible with light; (2) braided (oriented) texture, clearly visible with light; (2) deeply veined texture.
118. Lateral teeth, oriented enamel surface texture (**New**): (0) remains baso-apically oriented or slightly curved basally close to the carinae; (1) strongly curved basally close to the carinae.

VII. ENAMEL MICROSTRUCTURE

119. Enamel microstructure, enamel tubules (Hwang 2007 #12; Unordered): (0) absent or rare; (1) common only in BUL and/or inner potion of enamel; (2) common and extend throughout entire enamel thickness; (3) extremely common and forming an integral structural component of enamel.
120. Enamel microstructure, predominant enamel type (Hwang 2007 #13; Unordered): (0) parallel crystallites; (1) basal unit layer (BUL); (2) columnar.
121. Enamel microstructure, predominant enamel type, percentage of enamel thickness (Hwang 2007 #14): (0) ≥ 75%; (1) < 75%.
122. Enamel microstructure, number of enamel types present in schmelzmuster (Hwang 2007 #15; Unordered): (0) one; (1) two; (3) four.
123. Enamel microstructure, number of different module types present in schmelzmuster (Hwang 2007 #16; Unordered): (0) one; (1) two.
124. Enamel microstructure, boundary between first and second enamel types from the EDJ (Hwang 2007 #17): (0) parallel to EDJ; (1) jagged, varies in distance from EDJ.
125. Enamel microstructure, boundary between second and third enamel types from the EDJ (Hwang 2007 #18): (0) parallel to EDJ; (1) jagged, varies in distance from EDJ.
126. Enamel microstructure, basal unit layer (BUL; Hwang 2007 #19): (0) present; (1) absent.
127. Enamel microstructure, basal unit layer (BUL; Hwang 2007 #20): (0) poorly developed; (1) well-developed, with distinct planes of separation between adjacent units.
128. Enamel microstructure, basal unit layer (BUL), maximum unit diameter (Hwang 2007 #21): (0) < 10 µm; (1) ≥ 10 µm.
129. Enamel microstructure, basal unit layer (BUL; Hwang 2007 #22; Unordered): (0) < 25% of total enamel thickness; (1) 25-50% of total enamel thickness; (2) ≥ 50% of enamel thickness.
130. Enamel microstructure, incremental lines (Hwang 2007 #23; Unordered): (0) absent; (1) faint, poorly defined; (2) well-defined.
131. Enamel microstructure, incremental lines (Hwang 2007 #24; Unordered): (0) present in one section of the schmelzmuster only; (1) present in more than one section of the schmelzmuster but not throughout entire schmelzmuster; (2) present throughout entire schmelzmuster.
132. Enamel microstructure, columnar units closest to the EDJ, shape of units in cross-sections (Hwang 2007 #27; Unordered): (0) polygons with sharp corners and more than 4 sides; (1) subcircular or polygons with rounded corners and more than 4 sides; (2) triangles and/or rectangles with sharp corners.
133. Enamel microstructure, columnar units closest to the EDJ (Hwang 2007 #28): (0) extend straight and unbroken to the OES or to within 20 µm below the OES; (1) end, split, or are interrupter less than two thirds of the distance from the EDJ to OES.
134. Enamel microstructure, columnar units closest to the EDJ, maximum unit diameter (Hwang 2007 #29): (0) < 15 µm; (1) ≥ 15µm.
135. Enamel microstructure, columnar units closest to the OES (Hwang 2007 #33): (0) no dominant direction of orientation, planes of separations equally well-developed in all directions; (1) distinct longitudinal orientation, planes of separation better developed in an apicobasal (longitudinal) direction.
136. Enamel microstructure, ratio of thickest enamel type in schmelzmuster divided by second thickest enamel type (Hwang 2007 #39): (0) > 7; (1) 1.3 to 7; (2) 1 to 1.3.

VIII. ROOT

137. Root, shape in lateral view (**New**): (0) with subparallel margins; (1) with convex margins, root significantly larger than crown base.
138. Root, distal shape in lateral view (Sereno et al. 1998 #21; Charig and Milner 1997): (0) broad; (1) strongly tapered.
139. Root, outline of mid-root in cross section (**New**; Unordered): (0) oval to subcircular; (1) 8-shaped (i.e., longitudinal depression centrally positioned on both lingual and labial margins); (2) bean-shaped (i.e., longitudinal depression centrally positioned on one side only).
140. Root, form of the resorption pit (i.e., lingual depression hosting the unerupted tooth) in lingual view (**New**): (0) deep and well-delimited depression; (1) shallow concavity.
141. Root, transverse undulations below the cervix (**New**): (0) absent; (1) present.

A4.2. Character dependency

All characters are treated as independent. Although some characters states are repeated for mesial teeth and lateral teeth, their dependence is strongly limited due to the large amount of variation between mesial teeth (i.e., premaxillary teeth and mesialmost dentary teeth) and lateral teeth (pers. obs.). In fact, mesial teeth tend to be either shorter or longer and usually labio-lingually thicker than lateral teeth. In addition, they also tend to lack of serrations or bearing denticles on the distal carina only, whereas lateral teeth have serrated mesial and distal

keels in most carnivorous theropods. The number of denticles on both carinae in mesial teeth and lateral teeth can also be different in some taxa (e.g., *Ceratosaurus*, *Dubreuillosaurus*, *Duriavenator*, *Allosaurus*). Likewise, both mesial and distal carinae can strongly variate in position and orientation when compared to those of lateral teeth. The best example is the salinon-shaped, D-shaped, J-shaped or U-shaped outline of mesial crowns at their base in Abelisauridae, basal Allosauroidea, Tyrannosauridae and some dromaeosaurids, which contrast with the tear-drop/lenticular outline of lateral teeth in those taxa. Finally, mesial teeth can display several crown features like flutes (e.g., *Ceratosaurus*, *Scipionyx*, *Velociraptor*), basal striations (e.g., *Herrerasaurus*, *Proceratosaurus*) or longitudinal grooves (*Allosaurus*, *Raptorex*) that can be totally absent in lateral teeth (pers. obs.).

A4.3. Illustration of states of dentition-based characters

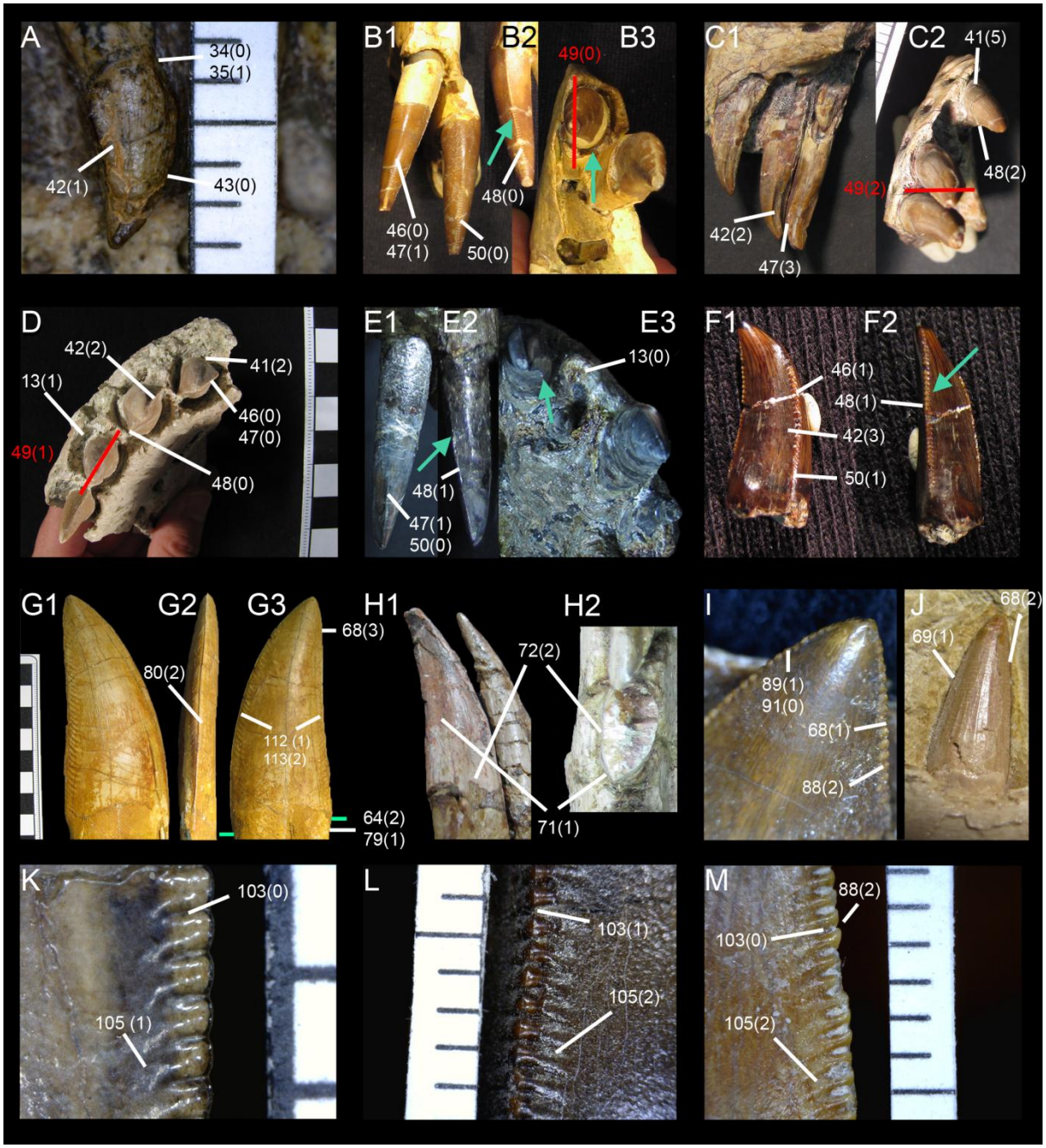

FIGURE A4.1. States of dentition-based characters. **A.** Fourth right premaxillary tooth of *Eoraptor lunensis* (PVSJ 512) in lateral view lacking a mesial carina (char. 43:0), displaying a concave area present on the labial side of the crown and adjacent to the distal carina (char. 42:1), and having an important constriction between root and crown at both mesial and distal margins (char. 35:1), giving a lanceolate shape to one of the premaxillary teeth (char. 34:0). **B.** First and second left premaxillary teeth of *Dubreuillosaurus valesdunensis* (MNHN 1998-13) in anterior (B1) and palatal (B3) views, and second left premaxillary tooth in posterior view (B2) showing a non-twisted (char. 46:0) mesial carina, facing labially (char. 47:1) and terminating well-above

the cervix (char. 50:0), as well as a distal carina facing distally (char. 48:0). The axis passing through both carinae at mid-crown in *Dubreuillosaurus* mesial teeth is subparallel to long axis of the skull (char. 49:0). The distal carinae, designated by the green arrows, are centrally positioned on the crown and not displaced labially. **C.** Premaxillary teeth of *Raptorex kriegsteini* (LH PV18) in medial (C1) and palatal (C2) views showing the U-shaped outline of mesial crowns (char. 41:5), the concave area adjacent to both carinae (char. 42:2), the mesial and distal carinae facing lingually (char. 47:3; char. 48:2), and the axis passing through both carinae at mid-crown in mesial teeth that is perpendicular to long axis of skull (char. 49:2). **D.** Right premaxilla of *Majungasaurus crenatissimus* (FMNH PR 2100) in palatal view displaying the subrectangular alveoli (char. 13:1), a salinon-shaped outline of the mesial teeth (char. 41:2), a concave area present on the lingual side of the crown and adjacent to both carina (char. 42:2), a non-twisted mesial carina (char. 46:0) facing mesially (char. 47:0), a distal carina facing distally (char. 48:0), and an axis passing through both carinae at mid-crown in mesial teeth mediolaterally oriented from long axis of skull (char. 49:1). **E.** First premaxillary tooth of *Acrocanthosaurus atokensis* (NCSM 14345) in anterior (E1) and posterior (E2) views and premaxillary teeth in palatal view (E3) showing the oval alveoli (char. 13:0), and the mesial carina facing labially (char. 47.1) and terminating well-above the cervix (char. 50:0). Unlike *Dubreuillosaurus valesdunensis*, the distal carina, pointed by the green arrows, is here strongly displaced labially (char. 48:1). **F.** Isolated premaxillary crown of *Dromaeosaurus albertensis* (AMNH 5356) in lingual (F1) and distal (F2) views showing the concave area on the lingual side of the crown and adjacent to the mesial carina only (char. 42:3), and the strongly twisted mesial carina (char. 46:1) terminating at the level of the cervix (char. 50:1). Like *Acrocanthosaurus*, the distal carina, designated by the green arrow, is strongly displaced labially (char. 48:1). **G.** Isolated lateral tooth of *Carcharodontosaurus saharicus* (UC PV6) in lingual (G1), mesial (G2) and labial (G3) views showing the weak constriction between root and crown at the lateral margin (char. 64:2), the weakly sigmoid distal profile of the crown due to the convex apical half of the tooth (char. 68:3), the pronounced and well-visible marginal undulations (char. 112:1) adjacent to both carinae (char. 113:2), and the mesial carina terminating well beneath the cervix (char. 80:2) and extending further basally than the distal carina (char. 79:1; the basal extension of carinae are represented by green bars). **H.** Lateral teeth of *Genyodectes serus* (MLP 26-39) in labiodistal (H1) and apical (H2) views showing the concave surface adjacent to the distal carina (char. 71:1) and the wide mesiodistally concave area on the basal part of the labial margin of the crown and giving a bean-shaped outline of the cross-section (char. 72:2). **I.** Tenth left maxillary tooth of *Rugops primus* (MNN IGU1) in labial views showing the slightly concave, roughly straight distal margin of the crown (char. 68:1), the apically hooked denticles on the distal carina (char. 88:2), and the parabolic margin of apical denticles on the mesial carina (char. 89:1), having a vertical subrectangular shape (char. 91:0). **J.** Maxillary tooth of *Irritator challengeri* (SMNS 58022) in labial view showing the convex, almost straight mesial (char. 69:1) and distal (char. 68:2) margins of the crown. **K.** Mid-crown denticles on the distal carina of the first left maxillary crown of *Erectopus superbus* (MNHN 2001-4) in lateral view showing the narrow interdenticular space (char. 103:0), and the short interdenticular sulci (char. 105:1) in between the denticles. **L.** Mid-crown denticles on the distal carina of the height right maxillary tooth of *Tyrannosaurus rex* (FMNH PR 2081) in laterodistal view showing the broad interdenticular space (char. 103:1) and the well-developed interdenticular sulci (char. 105:2) in between the denticles. **M.** Mid-crown denticles on the distal carina of the third right maxillary tooth of *Majungasaurus crenatissimus* (FMNH PR 2278) in lateral view showing the apically hooked denticles (char. 88:2), the narrow interdenticular space (char. 103:0), and the well-developed interdenticular sulci (char. 105:2).

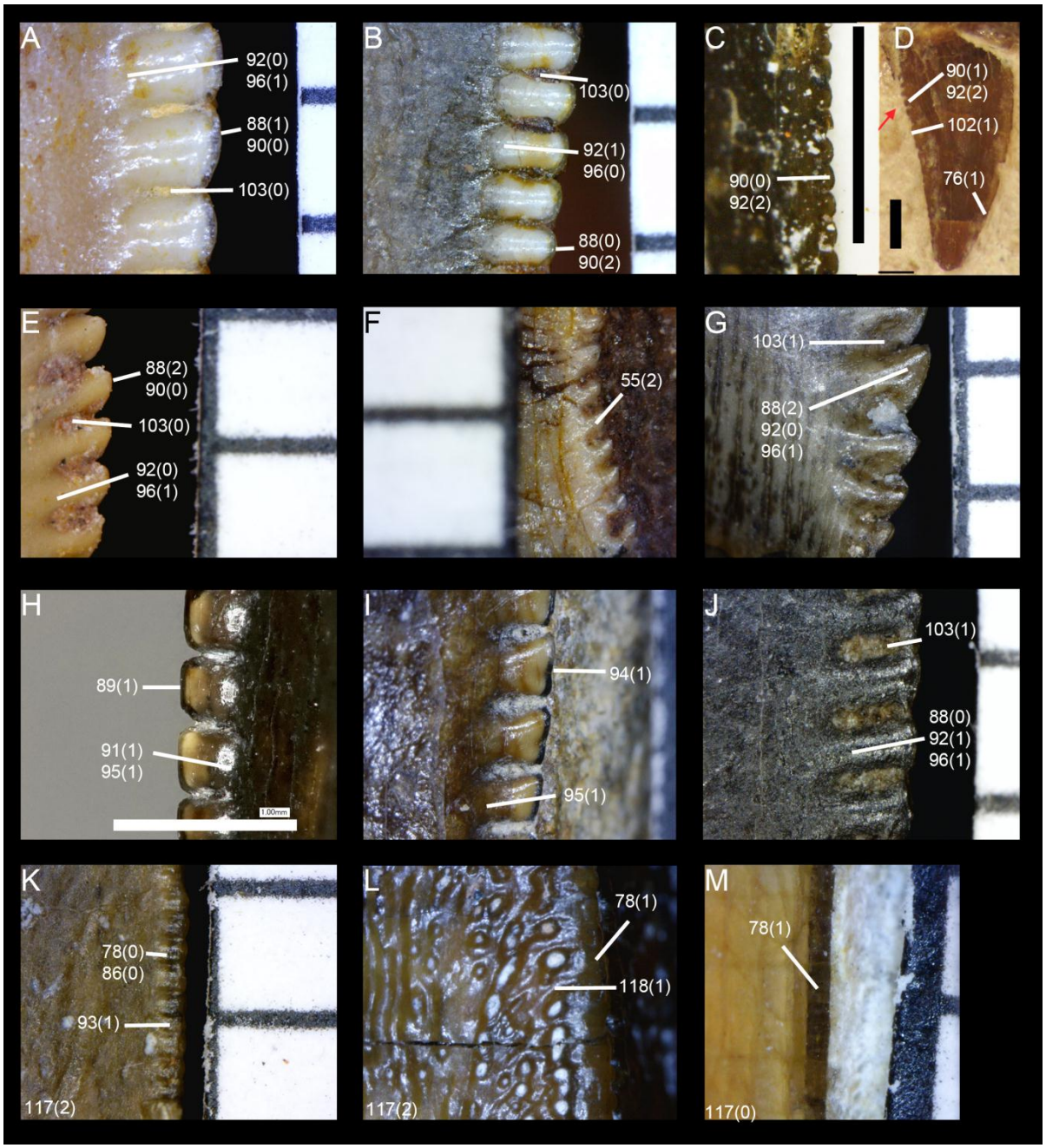

FIGURE A4.2. States of denticle-based characters. **A.** Mid-crown denticles on the distal carina of an isolated tooth of *Carcharodontosaurus saharicus* (UC unlabeled) in lateral view showing the asymmetrically convex (char. 88:1) and parabolic (char. 90:0) margin of subquadrangular (char. 92:0) and apically inclined (char. 96:1) denticles, as well as a narrow interdenticular space (char. 103:0). **B.** Mid-crown denticles on the distal carina of an isolated tooth of *Afrovenator abakensis* (UC unlabeled) in lateral view showing the symmetrically convex (char. 88:0) and semi-circular (char. 90:2) margin of horizontal subrectangular (char. 92:1) denticles, perpendicular to mesial margin (char. 96:0), as well as a narrow interdenticular space (char. 103:0). **C.** Distal denticles of the fourth left maxillary tooth of *Eodromaeus murphi* (PVSJ 561) in lateral view displaying the mid-crown denticles vertically subrectangular in shape (char. 92:2) and having a convex external margin (char. 90:0) on the distal carina. **D.** Third left maxillary tooth of *Scipionyx samniticus* in lateral view displaying an unserrated mesial carina (char. 76:1), mid-crown denticles vertically subrectangular in shape (char. 92:2) and having a flattened margin (char. 90:1) on the distal carina, and a serrated distal carina extending well-beneath the crown apex (char. 102:1). **E.** Mid-crown denticles on the distal carina of an isolated tooth belonging to an indeterminate abelisaurid (MUCPv 482) in lateral view showing apically hooked denticles (char. 88:2) with a parabolic margin (char. 90:0), subquadrangular in shape (char. 92:0) and apically inclined (char. 96:1) from the distal margin, as well as a narrow interdenticular space between the denticles (char. 103:0). **F.** Mid-crown denticles on the distal carina of the third right premaxillary tooth of *Eoraptor lunensis* (PVSJ 512) in lateral view showing the apically hooked denticles (char. 55:2). **G.** Basal and mid-crown denticles on the distal carina of an isolated tooth of

Troodon formosus (DMNH 22837) in lateral view showing subquadrangular (char. 92:0), apically hooked and strongly variable in size (char. 88:2) denticles, apically inclined (char. 96:1) from the distal margin, as well as a broad interdenticular space (char. 103:1) between them. **H.** Apical denticles on the mesial carina of an isolated tooth of *Acrocanthosaurus atokensis* (SMU 74646) in lateral view showing the subquadrangular (char. 91:1) and apically inclined (char. 95:1) denticles with a flattened margin (char. 89:1). **I.** Apical denticles on the mesial carina of an isolated lateral crown belonging to *Megalosaurus bucklandi* (NHM R234, tooth in matrix) in lateral view showing the apically inclined (char. 95:1) and biconvex denticles (char. 94:1). **J.** Mid-crown denticles on the distal carina of the ninth right maxillary tooth of *Allosaurus fragilis* (AMNH 851) in lateral view showing the symmetrically convex (char. 88:0), horizontal subrectangular (char. 92:1) and apically inclined (char. 96:1) denticles, as well as the broad interdenticular space (char. 103:1). **K.** Mid-crown denticles on the distal carina of an isolated tooth of *Suchomimus tenerensis* (MNN G73-3) in lateral view showing the serrated carina (char. 78:0) with minute denticles (char. 86:0) of irregular size along the carina (char. 93:1) and a veined enamel texture (char. 117:2). **L.** Distal carina at mid-crown in an isolated tooth of *Spinosaurus aegyptiacus* (MSNM V6422) in laterodistal view showing an unserrated carina (char. 78:1) and a deeply veined enamel surface texture (char. 117:2) curving basally in the vicinity of the carina (char. 118:1). **M.** Distal carina at mid-crown of a maxillary tooth of *Irritator challengeri* (SMNS 58022) in lateral view showing an unserrated carina (char. 78:1) and the smooth enamel surface texture (char. 117:0).

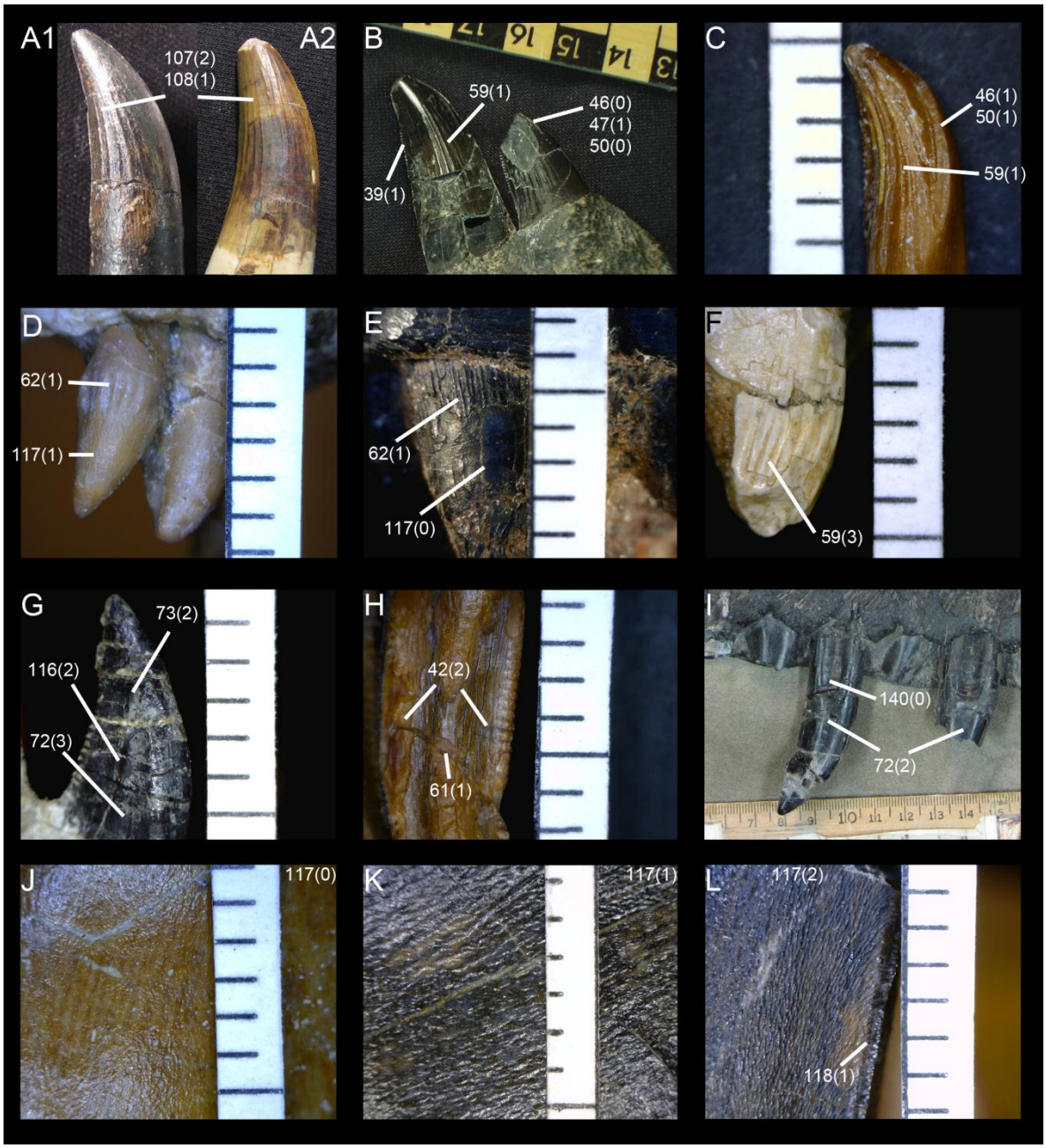

◄FIGURE A4.3. States of crown structure-based characters. **A.** Isolated teeth of *Baryonyx walkeri* (A1, NHM R9951) and *Suchomimus tenerensis* (A2, MNN G48-9) in lateral view displaying less than ten flutes (char. 108:1) present on both labial and lingual side of the crown (char. 107:2) in those taxa. **B.** First and second left dentary teeth of *Ceratosaurus nasicornis* (formerly *C. dentisulcatus*; UMNH VP 5278 = UUVP 158) in lingual view showing the weak curvature of these mesial crowns (char. 39:1), the untwisted mesial carina (char. 46:0) facing mesio-labially (char. 47:1) and terminating well-above the tooth-cervix (char. 50:0), and the fluted crown, only present on the lingual side of the tooth (char. 59:1). **C.** Isolated mesial tooth of *Masiakasaurus knopfleri* (FMNH PR 2696, small tooth) in mesio-lingual view displaying the twisted mesial carina (char. 46:1) extending to the tooth cervix (char. 50:1), as well as the flutes present only on the lingual side of the tooth (char. 59:1). **D.** First right premaxillary tooth of *Proceratosaurus bradleyi* (NHM R 4860) in labial view displaying the short longitudinal furrows/striations present at the base of the crown (char. 62:1) and the braided enamel surface texture of the crown (char. 117:1). **E.** Tenth left maxillary tooth of *Herrerasaurus ischigualastensis* (PVSJ 407) in lateral view showing the longitudinal furrows/striations present at the base of the crown (char. 62:1; also present on the mesial teeth of *H. ischigualastensis* = *Ischisaurus cattoi*, MACN 18.060), and the irregular/non-oriented enamel surface texture of the crown (char. 117:0). **F.** First right premaxillary tooth of *Velociraptor mongoliensis* (AMNH 6515) in labial view showing the flutes present on the labial side of the crows (char. 59:3). **G.** Fifth left maxillary tooth of *Bambiraptor feinbergi* (AMNH 30556) in labial view displaying the wide mesiodistally concave area on the basal part of the crown extending along two thirds of the crown (char. 73:2) and giving the 8-shaped cross-section of the crown base (char. 72:3), and the two elongated, longitudinal and rounded ridges present on the lingual side of the crown as well (char. 116:2). **H.** Third right premaxillary tooth of *Raptorex kriegsteini* (LH PV18) in lingual view showing the two concave areas on the lingual side of the crown and adjacent to both carinae (char. 42:2) and the central and longitudinal ridge on the crown (char. 61:1). **I.** Sixth and eight left maxillary teeth of *Allosaurus fragilis* (UMNH VP 5393) in medial view displaying the deep and well delimited resorption pit (char. 140:0) and the wide mesiodistally concave area on the basal part of the crown and present on the lingual side of the tooth, giving the bean-shaped cross-section of the crown base (char. 72:2) in this specimen (photo courtesy shared by Stephen Brusatte). **J.** Enamel texture of the sixth right maxillary crown of *Majungasaurus crenatissimus* (FMNH PR 2278) in lateral view showing the irregular non-oriented enamel surface texture (char. 117:0). **K.** Enamel texture of the second right maxillary tooth of *Acrocanthosaurus atokensis* (NCSM 14345) in lateral view showing the regular, oriented braided enamel surface texture of the crown (char. 117:1). **L.** Enamel texture of an isolated tooth of *Baryonyx walkeri* (NHM R9951) in lateral view showing the deeply veined enamel surface texture of the crown (char. 117:2), strongly curved basally close to the carina (char. 118:1).

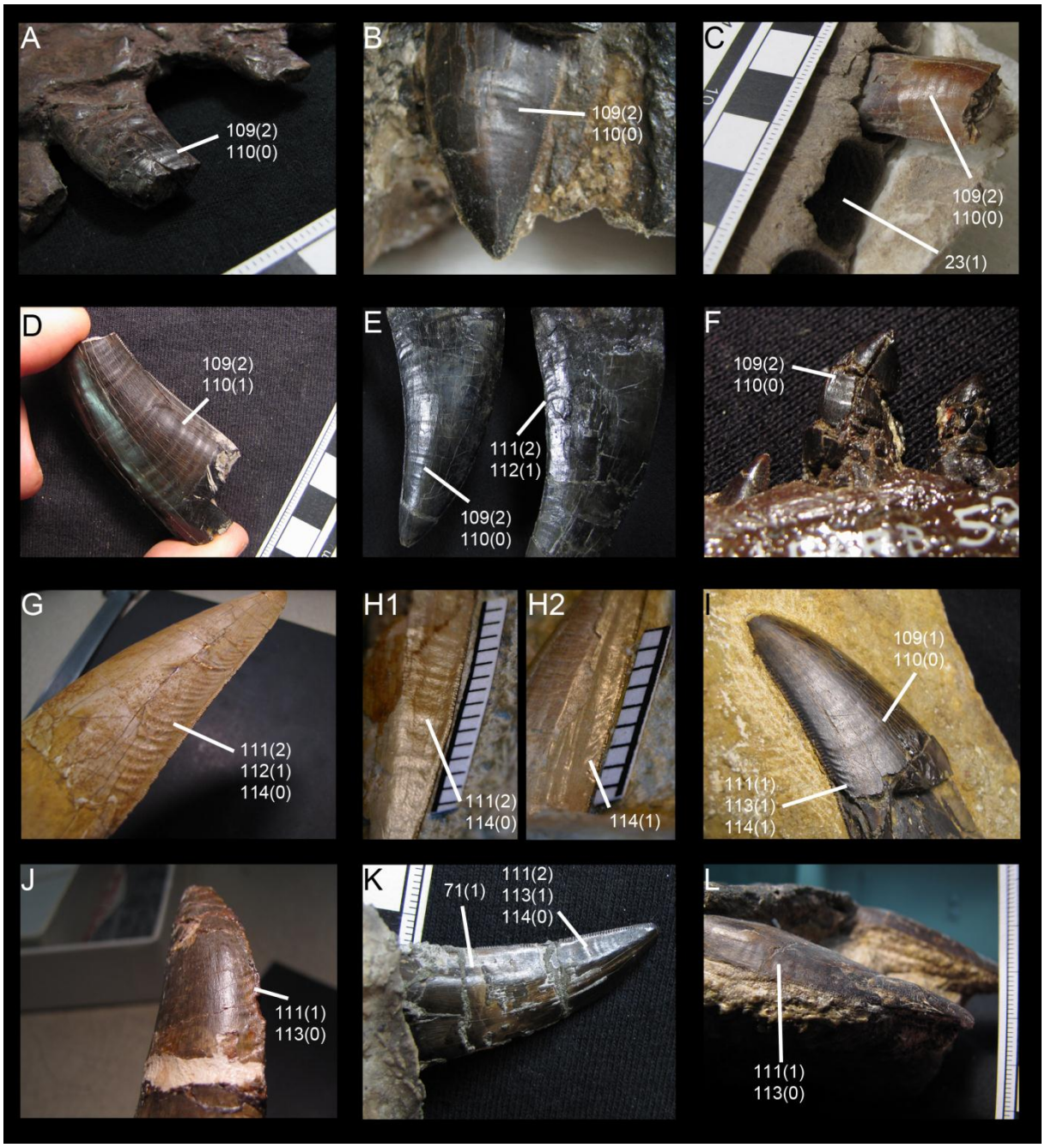

FIGURE A4.4. States of crown undulation-based characters and distribution of transverse and marginal undulations in non-avian Theropoda. **A.** Fifth? left maxillary tooth of *Herrerasaurus ischigualastensis* (formerly *Sanjuansaurus gordilloi*, PVSJ 605) in lateroventral view displaying the well-visible (char. 109:2) but few (char. 110:0) transverse undulations on the crown. **B.** Fifth or sixth left maxillary tooth of *Ceratosaurus nasicornis* (USNM 4735) in labial view displaying the well-visible (char. 109:2) but few (char. 110:0) transverse undulations on the crown. **C.** Second left maxillary tooth of *Majungasaurus crenatissimus* (FMNH PR 2278) in medioposterior view displaying the well-visible (char. 109:2) but few (char. 110:0) transverse undulations on the crown, as well as the subrectangular maxillary alveoli (char. 23:1). **D.** Isolated lateral tooth of *Megalosaurus bucklandii* (OUMNH J.29866) in lateral view displaying the well-visible (char. 109:2) and numerous and closely packed (char. 110:1) transverse undulations on the crown. **E.** Fifth and sixth right maxillary teeth of *Acrocanthosaurus atokensis* (NCSM 14345) in lateral view displaying the well-visible (char. 109:2) but few (char. 110:0) transverse undulations, that cannot be confused with the pronounced (char. 112:1) and mesiodistally elongated (char. 111:2) marginal undulations adjacent to the distal carina. **F.** Eighth left maxillary tooth of *Dromaeosaurus albertensis* (AMNH 5356) in medial view showing the well-visible (char. 109:2) but few (char. 110:0) transverse undulations on the crown. **G.** Isolated lateral tooth of *Carcharodontosaurus saharicus* (UC unnumbered) in laterodistal view showing the elongated (char. 111:2), pronounced (char. 112:1) and mesio-distally oriented (char. 114:0) marginal undulations adjacent to the distal carina. **H.** Mesial margin of

a left maxillary tooth in labialo-mesial view (H1) and distal margin of a right maxillary tooth in labialo-distal view (H2) of *Irritator challengeri* (SMNS 58022) displaying the elongated (char. 111:2) and mesio-distally oriented (char. 114:0) marginal undulations adjacent to the mesial carina, and the diagonally oriented marginal undulations (char. 114:1), adjacent to the distal carina. **I.** Isolated lateral tooth of *Megalosaurus bucklandi* (OUMNH J.23014) in laterodistal view displaying the tenuous (char. 109:2) and few (char. 110:0) transverse undulations on the crown, as well as the short (char. 111:1) and diagonally oriented (char. 114:1) marginal undulations, adjacent to the distal carina only (char. 113:1). **J.** Isolated lateral tooth of *Afrovenator abakensis* (UC UBA1) in lateromesial view displaying the short (char. 111:1) marginal undulations, adjacent to the mesial carina only (char. 113:0). **K.** Isolated lateral tooth of *Neovenator salerii* (MIWG 6348) in labial view displaying the concave surface adjacent to the distal carina (char. 71:1), the elongated (char. 111:2), mesio-distally oriented (char. 114:0) marginal undulations, adjacent to the distal carina only (char. 113:1). **L.** Fourth left maxillary tooth of *Ceratosaurus nasicornis* (USNM 4735) in mesial view showing the short (char. 111:1) marginal undulations adjacent to the mesial carina only (char. 113:0).

A4.4. Data matrix of dentition based characters

TNT file

nstates 5
xread
141 64
Eoraptor
0101000000000?000110000?02???????0100[01][12]100[01][01]10000101012[12]1100000[12]00?[01]10?[13]?0
0000000000?012210[01]00000001--001000000-0-0---0000??????????????????????
Herrerasaurus
0100000000000000110000002000100010-10[23]10000-0--0---01-0-?000010-
1[012][01][01]000[02]0000000?000221000[01]100000-???0?10000-200---0000??????????????????????
Eodromaeus
01???????????000410?000?30??10000??????????????????????????????0-
0[01]2000110[01]0000010000[01]1[01]0000[01]000020000?00000-100---0010??????????????????????
Coelophysis
010?000000000011010110000010?10010-00[012]10000-0--0---01-0-0030000-
[01][01][01]000[13]00000000[01]0??[01][01]100[01]0100000-000000000[03]00-0---001000011--1---0------
?????
Dilophosaurus
01[01]10020010100214111100120[01]11110?0-10[01]00001101???01110000000000-
111000[34]1[01]00000010002310000[01]100000?0?20?0000-0-0---00?0??????????????????00100
Ceratosaurus
00111-0000000000[34]1110001[23]001100010-10[23][12]000[01]1001100[23][23]10000010000-
[12][01]1[012]01[34]?[01]000000100133100[01]011001[01]0[12]0[02]00100[02]0-
2010[01]000102202100011020200000100
Genyodectes
0111110000000000??11000?30011000?0-20[012]000011001100221000?000000-
1[01]1[01]01[34]2[01]00000000[01]13310[01]0010001[01]-2020010[01]00-210---
0010????????????????????????
Berberosaurus
??0-
1010012310000000?01331[01][01]???1001?-1020?10000-200---0010??????????????????????
Noasaurus
??????????????????4101000??0-
01[01]1000100000001000121000000000002?2?00000-0-0---0000??????????????????????
Masiakasaurus
0?11???1?0???????10?000?30000001?210[12][01]10221[01]01011100100[02]0010000-
[01][01][12]0000100000001001[12]210[012][01]000000[01]00002000000-200---
0010??????????????????00110
Kryptops
??????????????????0?001??0-
1?1100010000000100?231[01]2[01]0000001?0?000022?0-0-0---0000?????????????????0????
Rugops
0100000?1?001000?111001?????????????0???2?11??00??????????????0-
1[01]?[12]000100000001000[23]310200000001?0?000000?0-0-0---0000????????????????????
Abelisaurus

01?000???????000????00???????????0-103[12][12]221100???12210[12]00200000-
1[01][01]1000100000001?00331[01][12]0010011100000000100-1010100000?????????????????????
Aucasaurus
01?000??1?00?00041010011???0-
1[01][01]1000100000001000331[01][12][01]01[01]011100?00000000-200---0000?????????????????0?0??
Indosuchus
0100000110001000400100l??0?10000?0-1[01]3[12][12][23][23]110[01]0011[23][23]1??0?000000-
?[01]?[12]0001000000010?0331?????????0???0??0110-0-0---0000?????????????????????
Majungasaurus
010000011[01]0010002111001120010000l0-103[12][12][23][23]110[01]0011221[12]200200000-
1[01][01][12]000100000001000[34]31[12]2000[01]0001000000001220-2010100000220210001101020000?????
Skorpiovenator
01???????????000110?00?1?????????0-10222?[23]1100???1?11???0000000-
10[01][12]00[01]10000000101033l0?0?11001[01]0?0?0?00000-0-20200000?????????????????????
Erectopus
??????????????????????000???0-
10[12]00121000000100033100[01]011010000000000100-1[01]0---0000?????????????????????
Piatnitzkysaurus
???????????????1?00000??0???000?????????????????????????????0-
1110010100000000[01]10331000[02][01]10000000000001[12]0-[12]1201000[01]0??????????????????00110
Eustreptospondylus
011110?0000?0000????000?30011000???1??10?0110?10002210l?0100000-
11?0000100000000???[34]3100[01]0000000???00000??0-0-0---0010?????????????????????
Afrovenator
??????????????????41010002???0-
2010002100000000110431[01][01][01]2010?00-0010001110-0-10000010?????????????????0?1?0
Dubreuillosaurus
011110000000000041010002300110001O-10210001100100022100l?000000-
1[01]0000010000000010022l[01][01][01]0000000-0010000110-0-0---0010??????????????????000?0
Duriavenator
0?11???0?0??00???101000??0010000?0-?02??1?110?100?[23]3100?0?00000-
1[01]100001?00000001??3310[01][01]00101[01]0-1010000110-[01]00---0010??????????????????00?10
Megalosaurus
0?????????????????41010002300100001?????????????????????????????0-
[12][01]100001000000001[01]0331[01][01][01][02]010100-1000001[12][12]0-
2110[12][01]0010?????????????????????????
Torvosaurus
011110010001000041010002301?10001??20???001100100033l???0?00000-
20200001000000001[01]0441[01][01][01]0110?00-10100[01]1220-2[01]10100010?????????????????00210
Baryonyx
0[34]11101100110120?100102?0011111010-11[12]100011001002000000010000-
121000000000000[012]1[01]011[01]00[01][01]2111000202000000[12]00-10100021?????????????????01011
Suchomimus
04111011001101200100102200111111?10-???100011001002000000000[12]0000-
1[12][12]000000000000[012]1[01]0[12][12][01]00[01][01]1010002202000000[12]00-
10[12][01]0021?????????????????????????
Irritator_Angaturama
0410001??0210121?????022?0??????1?????????????????????????????0-12[12]0100000010101100----------
--------210-101[01]0000?????????????????????
Spinosaurus
0312[01]011012101214001123201111[12]110-?[01]??1001010100[12]--------20000-
[12][12][12]010000001010[01]100----------220-0---0021?????????????????????
Sinraptor
011110201002000030010002200?100010-1?[123]1[12]2311012011?21000??00000-
[12]?1[01]00[01][23]100000000003310[01]00110?000000001?[02]?0-210---0010??????????????????00?00
Allosaurus
02111001100000003001000220001000l0-1[01][12]00[23][23]11012111221[01][01]0000[01][02]00-
[12][012][12]0000200[01]0000[01]1[01]1[23][23]1[01][01]0011001100000011[12][12]0-
20201[01]000022021100111112000000000
Neovenator

0211112011200000310000??00110001????????????????????????????0-
111001[12]20000000011[01]3[23]11100110010-0000011110-2[01]20100010??????????????????00211
Fukuiraptor
??????????????????????000??0?1?0?0?0-1[01]?00301101?1?1[01]110[01]0??00000-
[01][01][012]00??1?000000[01]010[23][23]0[01][01]000[01]0?0000000002220-
[12]020?000?????????????????????????
Australovenator
??????????????????????????1001?000?0-1[01][23]00?311012??1?[12]1?????00000-
1[01]1001[12]?000000000?[01]331?[01]?00[01]0??0-000001???0-??????001????????????????????????
Acrocanthosaurus
011111000000000031010002200110001 0-[12][01][12]100011001100[12]210000000000-
[12][01][012]0000?0000000[01]11[01][23]3[01]001[01]110111010[12]0010[01]00-
2[01]2[01]100010????????????????????????
Eocarcharia
??????????????????310?000??0-
101[03]00020000000011[01]321[01][01]0[02][12]10110-101[01]001110-100---0010????????????????????????
Carcharodontosaurus
??????????????????40010002?0?1?000????????????????????????????????20201[13]000100000012110[34][34]1110
010011[01]0000[01]001[01][01]0-[01]021200010??????????????????00110
Giganotosaurus
01111101111?0000??0?000?2001?00010-
?1?1100110[01]1111221?00?10000202[01][12][03]00010000000[12]110[34][34]1[01][01]001[01]0000000000
1[12]220-[12]0[12]0200010??????????????????00[12]10
Mapusaurus
??????????????????4101000??0???000?0-
11[23]1000110[01]?1??221??000000020[12][01][01][013]00010000000[12]110[34][34]1[01][01]00110000000
0001[12]220-0-[12][01]200010??????????????????[01]0[12]10
Proceratosaurus
01111100000000[01]0011100?2102110011100?[23]103[03]110122[12]00010020000010-
1?[01]0000[13][01]0[01]000000[01]11[12]1000000000000002000[01][01]0-0-0---
0010????????????????????????
Eotyrannus
0121110000000000??10001??0210000?0-1211[01]4311013221[12][12]10000100000-
111[01]0001000000000[01]02[23]1000000000000002000110-0-0---0010????????????????????????
Raptorex
012111000000000040010002202110001 0-?2[01]104211003221??10020000100-
?[01]100[01]0000[01]0000[01]0[01]1??100[01][02]1[01]000000000000100-100---
0010??????????????????0?100
Alioramus
??????????????????211100021021100 01????????????????????????????0-
?[01][01]00[01]0[13]10[01]0000[01]011??10000110001000000000100-210---0010??????????????????00100
Tyrannosaurus
012211000000000041110002302100 0010-223[01]04[02]11003221[23][23]10000000[01]00-
[12][12][12][01]000000[01]0000[01]001[34][34]100001[01]010002020012 2?0-2[01]0---001022021101---0-
0111200000
Compsognathus
01?????00????00?210?00?2100?100010-0?3[012]0?00-1----------00000-0[01][12]00000?1--0[01]--2??-0--0-
[01]-20--0--00-10-000-0-0---0000????????????????????10?00
Scipionyx
02?100-11122?00151000?23001100010-??2000?0-1----------10000-??[012][01]0?0?11--01--[02]??-??-0-0-
[02]0--0--?0-10-000-0-0---0000????????????????????????
Ornitholestes
011100121021?000410100023000 1000110[01]?210300-1----------00000-0110000211--0[01]--200-00-0-0-00-
-0---0-10-000-0-0---0010????????????????????????
Shuvuuia
??????????????????000100?401000000?1100?22000-1----------00?0210012000001--00----------
0-0-0---000-????????????????????0?0??
Jianchangosaurus

1----------0---00?20000-
000?211021004110000001?22??000?0011021[12]0?[03]0000000002003322200000011-2-20010000-0-0---000-
??????????????????010?0
Erlikosaurus
1----------0???00?30010?00110-
0022100110000000??2??0000000110202000000000000200??2[02][02]00020011-2-20010000-0-0---000-
??????????????????0?0??
Tsaagan
011100210021?000400?00?2[23]001000010-1?3[01][01]000-0--0---01-0-0000?00-1?1[01]0?0311--01--000-21-
0-0-10--0--00-00-000-0-0---0000????????????????????????
Velociraptor
011000110?21?000[34]10?00?2[23]001100010-0031030110120l?001?02?030?00-
001[01]0?1?2[01]000000001210000[01]0000?0022000000-0-0---0[012]00100110-00000-----1?????
Bambiraptor
01??00???? ??00004???00?230?10000??????????0-0--?---??-?-??0???0-
0[01]1000[01]32[01]0000000001[12]10[01]0001000[01]??002010000-0-0---0[02]1000000--1---12-----?????
Dromaeosaurus
0???000?10000000500100023001000010-1[01][12][01]033110121111111000100000-
[01]11000[01]3[12]010000[01]001[23]2100000[01]000100000000100-100---0000201110-000112----2?????
Saurornitholestes
01?????????????0?????????20???000?0-0221033[01]10121111[12]1[01][12]20100000-
[01]02[01]00[12]0[12][01][01]0000[01]000[12][12][12]22[12]-01000[01]00002010000-0-0---0000211110-
00020-----100100
Buitreraptor
??????????????????????002?0??0000????????????????????????????????0-0[01][01]000[01]321--1----------
---------0-0-0---[13][12]00??????????????????1?1?0
Byronosaurus
0101000110?00000021100?30100?000?1000211010-1----------0000[12]00[12][12][01]0?[01][24][01]1--1----
------------------------0-0-0---[13][12]0000000--1---22-----?????
Zanabazar
0101000000000000[01]211000401001000011100311[35]?0-1----------
0000[12]10[12][01][01]0?1[13]?[01]01000?000-32-2-0-000-1--22-1[01]0000-000---
2000????????????????????????
Troodon
01?????????????????000?010000001210121050[01][01]0000?13322200000002101[01][01]00[134]1[01][01]0
[01]0001000[34][34][12]22[12]00[01]001100000010000-100---0000110110-00020-----100110
Richardoestesia gilmorei
????????????????????????10??2?001[01]0023[12]00[01]0000000[12][12]
101000[02]000[01]0010[02]000000-0-0---000-200110-010112----0?????
ML962
????????????????????????????????0-
20100001100?0?0331?00?10000??
???????
ML327
??0-
1111000100100001?1134112[01]011001000000?00220-100---2010????????????????????????
ML966
??0-
11110001001000?1?1033111[01]01100100?000?10220-1010110010????????????????????????
ML939
??2-
001000[12]31???0000000?01?[01]?2?100?0-010?00?100-0-0---2000?????????????????????1??
;
ccode + 1 3 14 16 23 24 35 52 64 85;
;
proc/;

A4.5. Supermatrix of dentition based characters combined with 6 other datasets
The data file is available at DRYAD: http://doi.org/10.5061/dryad.33tb2.

A4.6. Results of the cladistic analyses

Cladistic analysis on the dentition based data matrix (isolated teeth excluded) and list of synapomorphies and autapomorphies for each clade.

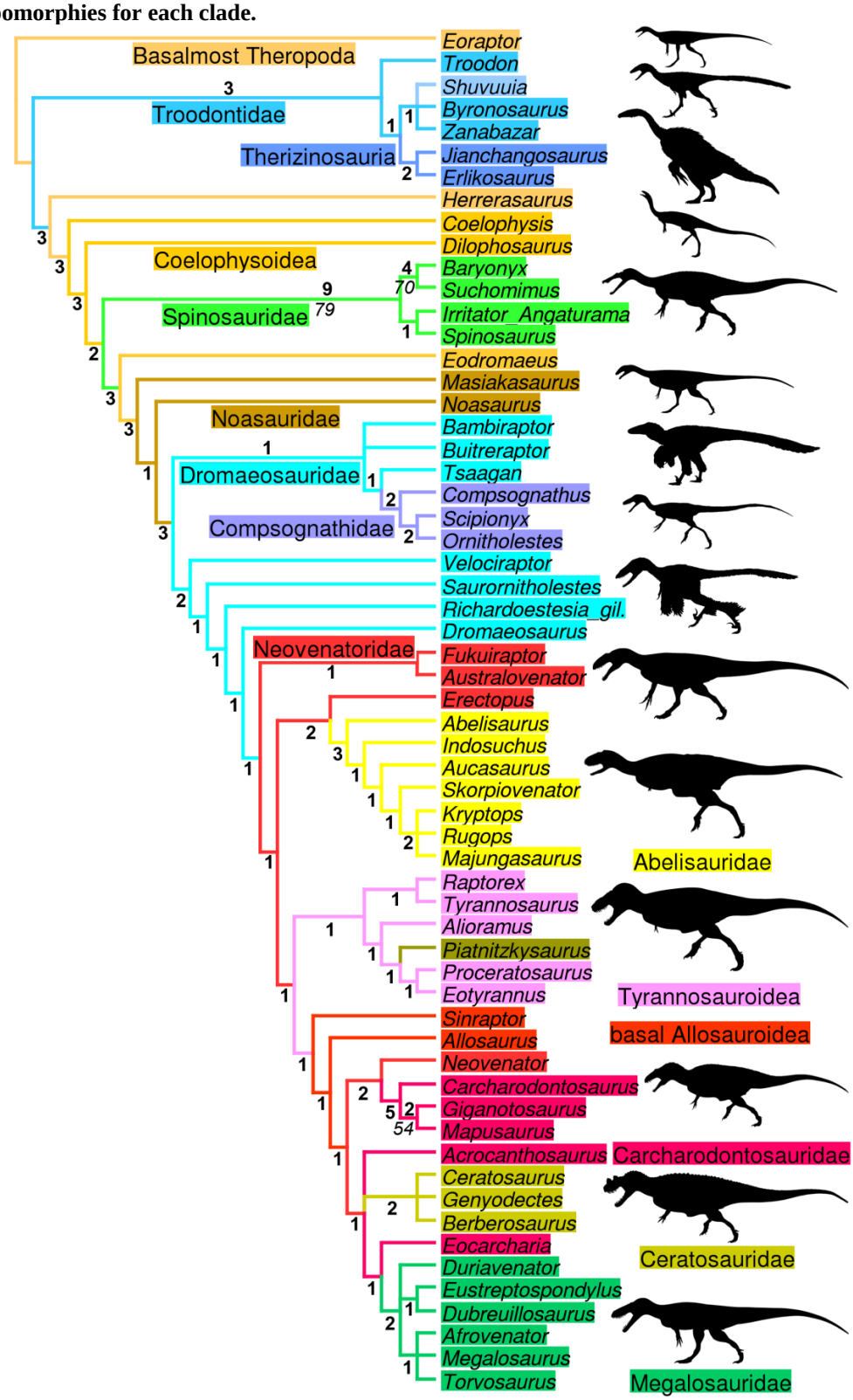

FIGURE A4.5. Strict consensus cladogram of 10 most parsimonious trees recovered from the analysis of a data matrix of dentition based characters. Initial analysis was a New Technology Search using TNT v.1.1 of a data matrix comprising 141 characters for one outgroup (*Eoraptor*) and 59 non-avian theropod taxa. Tree length = 681 steps; CI = 0.338; RI = 0.56. Bremer support values are in bold and bootstrap values are in italic. For silhouette attribution, see Appendices A1.1.

FIGURE A4.6. Strict consensus cladogram of 10 most parsimonious trees recovered from analysis of dentition based characters, with each nodes numbered (see the list of synapomorphies for each clades below). Initial analysis was a New Technology Search using TNT v.1.1 of a data matrix comprising 141 dentition-based characters for one outgroup (*Eoraptor lunensis*) and 59 non-avian theropod taxa. Tree length = 681 steps; CI = 0.338; RI = 0.56.

Eoraptor
No autapomorphies

Herrerasaurus
Char. 4: 1 --> 0
Char. 62: 0 --> 1
Char. 71: 3 --> 0
Char. 109: 0 --> 2

Eodromaeus
Char. 33: 1 --> 0
Char. 67: 1 --> 2
Char. 71: 0 --> 1
Char. 84: 1 --> 0
Char. 97: 0 --> 2
Char. 109: 0 --> 1

Coelophysis
Char. 17: 1 --> 0
Char. 25: 2 --> 0
Char. 59: 0 --> 3

Dilophosaurus
Char. 10: 0 --> 1
Char. 19: 0 --> 1
Char. 39: 1 --> 0
Char. 52: 0 --> 1
Char. 85: 1 --> 3
Char. 92: 0 --> 1
Char. 101: 0 --> 2
Char. 140: 1 --> 0

Ceratosaurus
Char. 2: 1 --> 0
Char. 59: 0 --> 1
Char. 80: 0 --> 1
Char. 111: 0 --> 1

Genyodectes
Char. 36: 1 --> 2
Char. 39: 1 --> 0
Char. 92: 1 --> 0
Char. 98: 1 --> 2
Char. 1010: 0 --> 1

Berberosaurus
Char. 71: 34 --> 2
Char. 72: 2 --> 3

Noasaurus
Char. 68: 0 --> 1
Char. 99: 0 --> 2

Masiakasaurus
Char. 28: 1 --> 0
Char. 32: 0 --> 1
Char. 34: 0 --> 2
Char. 41: 0 --> 2
Char. 42: 0 --> 2
Char. 48: 0 --> 1
Char. 83: 0 --> 1
Char. 109: 0 --> 2

Kryptops
Char. 84: 3 --> 2
Char. 104: 0 --> 2

Rugops
No autapomorphies

Abelisaurus
Char. 58: 0 --> 2
Char. 111: 0 --> 1

Aucasaurus
Char. 109: 0 --> 2

Indosuchus
Char. 106: 0 --> 1

Majungasaurus
Char. 87: 0 --> 12
Char. 104: 0 --> 1
Char. 109: 0 --> 2
Char. 111: 0 --> 1

Skorpiovenator
Char. 17: 2 --> 1
Char. 38: 3 --> 2
Char. 52: 2 --> 1
Char. 82: 0 --> 1
Char. 111: 0 --> 2
Char. 113: 1 --> 2

Erectopus
Char. 70: 0 --> 1
Char. 71: 0 --> 2

Piatnitzkysaurus
Char. 70: 0 --> 1
Char. 111: 0 --> 2

Eustreptospondylus
Char. 58: 0 --> 1
Char. 100: 1 --> 0

Afrovenator
Char. 71: 0 --> 2
Char. 90: 0 --> 2
Char. 98: 1 --> 0
Char. 113: 1 --> 0

Dubreuillosaurus
Char. 84: 3 --> 2
Char. 85: 3 --> 2

Duriavenator
Char. 29: 1 --> 0
Char. 41: 0 --> 1

Megalosaurus
Char. 29: 1 --> 0
Char. 100: 1 --> 0

Torvosaurus
Char. 67: 1 --> 2
Char. 85: 3 --> 4
Char. 91: 0 --> 1
Char. 105: 1 --> 2
Char. 106: 1 --> 2
Char. 139: 1 --> 2

Baryonyx
Char. 91: 1 --> 2
Char. 92: 0 --> 1
Char. 94: 0 --> 1

Suchomimus
Char. 97: 0 --> 2

Irritator_Angaturama
Char. 4: 1 --> 0
Char. 117: 2 --> 0

Spinosaurus
Char. 4: 1 --> 2
Char. 10: 0 --> 1
Char. 22: 0 --> 1
Char. 24: 2 --> 3

Sinraptor
Char. 7: 0 --> 2
Char. 12: 0 --> 2
Char. 40: 0 --> 12
Char. 73: 0 --> 1
Char. 105: 1 --> 02
Char. 1010: 0 --> 1

Allosaurus
Char. 2: 1 --> 2
Char. 8: 0 --> 1
Char. 28: 1 --> 0
Char. 39: 1 --> 0
Char. 83: 0 --> 1
Char. 96: 0 --> 1
Char. 117: 1 --> 0
Char. 131: 0 --> 1
Char. 139: 1 --> 0

Neovenator
Char. 2: 1 --> 2
Char. 7: 0 --> 2
Char. 20: 1 --> 0
Char. 66: 0 --> 1
Char. 70: 0 --> 1
Char. 71: 0 --> 12
Char. 139: 1 --> 2
Char. 141: 0 --> 1

Fukuiraptor
Char. 42: 3 --> 0
Char. 86: 1 --> 0

Australovenator
Char. 103: 0 --> 1

Acrocanthosaurus
Char. 89: 0 --> 1
Char. 96: 0 --> 1

Eocarcharia
Char. 85: 3 --> 2
Char. 104: 0 --> 1

Carcharodontosaurus
Char. 18: 1 --> 0
Char. 79: 0 --> 1
Char. 92: 1 --> 0
Char. 94: 0 --> 1
Char. 103: 1 --> 0
Char. 112: 0 --> 1

Giganotosaurus
Char. 40: 0 --> 1
Char. 58: 0 --> 1

Mapusaurus
No autapomorphies

Proceratosaurus
Char. 32: 0 --> 1
Char. 34: 0 --> 1
Char. 36: 1 --> 0
Char. 41: 4 --> 3
Char. 50: 1 --> 0
Char. 51: 2 --> 0
Char. 52: 2 --> 0
Char. 56: 0 --> 2
Char. 62: 0 --> 1

Eotyrannus
Char. 29: 1 --> 0
Char. 58: 0 --> 1

Raptorex

Char. 56: 0 --> 2
Char. 109: 2 --> 1

Alioramus
Char. 73: 0 --> 1
Char. 96: 0 --> 1

Tyrannosaurus
Char. 4: 1 --> 2
Char. 25: 2 --> 3
Char. 29: 1 --> 0
Char. 94: 0 --> 1
Char. 98: 0 --> 2
Char. 100: 0 --> 2
Char. 103: 0 --> 1
Char. 104: 0 --> 2
Char. 105: 1 --> 2
Char. 139: 1 --> 0

Compsognathus
Char. 8: 1 --> 0
Char. 17: 4 --> 2
Char. 25: 3 --> 1

Scipionyx
Char. 2: 1 --> 2
Char. 10: 0 --> 1
Char. 12: 1 --> 2
Char. 16: 0 --> 1
Char. 17: 4 --> 5
Char. 20: 1 --> 0
Char. 39: 1 --> 0
Char. 59: 0 --> 1

Ornitholestes
Char. 8: 1 --> 2
Char. 28: 1 --> 0
Char. 34: 0 --> 1
Char. 41: 0 --> 3
Char. 117: 0 --> 1

Shuvuuia
Char. 18: 2 --> 0
Char. 39: 1 --> 2
Char. 40: 1 --> 2
Char. 66: 12 --> 0
Char. 68: 01 --> 2

Jianchangosaurus
Char. 36: 0 --> 1
Char. 42: 0 --> 4

Erlikosaurus
Char. 27: 0 --> 1
Char. 32: 0 --> 1
Char. 39: 1 --> 2
Char. 67: 1 --> 0
Char. 92: 0 --> 2

Tsaagan
Char. 7: 1 --> 2
Char. 18: 1 --> 0
Char. 36: 0 --> 1
Char. 65: 0 --> 1

Velociraptor
Char. 29: 0 --> 1
Char. 59: 0 --> 3
Char. 100: 0 --> 2
Char. 129: 2 --> 0

Bambiraptor
Char. 103: 0 --> 1
Char. 117: 0 --> 1

Dromaeosaurus
Char. 17: 4 --> 5
Char. 25: 2 --> 3
Char. 54: 0 --> 1
Char. 66: 0 --> 1
Char. 75: 0 --> 1
Char. 83: 0 --> 1
Char. 96: 0 --> 1
Char. 121: 0 --> 1
Char. 136: 0 --> 2

Saurornitholestes
Char. 37: 0 --> 2
Char. 55: 0 --> 12
Char. 67: 1 --> 2
Char. 72: 3 --> 0
Char. 87: 0 --> 2
Char. 88: 0 --> 2
Char. 89: 0 --> 12
Char. 103: 0 --> 1
Char. 120: 0 --> 1
Char. 121: 0 --> 1

Buitreraptor
Char. 77: 0 --> 1
Char. 115: 0 --> 13
Char. 116: 0 --> 12

Byronosaurus
Char. 8: 0 --> 1
Char. 9: 0 --> 1
Char. 35: 1 --> 0
Char. 42: 0 --> 1
Char. 64: 1 --> 0
Char. 72: 0 --> 24
Char. 77: 0 --> 1
Char. 115: 0 --> 13
Char. 116: 0 --> 12

Zanabazar
Char. 38: 2 --> 3
Char. 41: 0 --> 35
Char. 71: 0 --> 1
Char. 72: 0 --> 13
Char. 115: 0 --> 2

Troodon
Char. 37: 0 --> 1
Char. 41: 0 --> 5
Char. 50: 0 --> 1
Char. 51: 1 --> 3
Char. 72: 0 --> 1
Char. 89: 0 --> 12
Char. 109: 0 --> 1
Char. 119: 0 --> 1
Char. 120: 0 --> 1
Char. 126: 1 --> 0

Richardoestesia_gil.
Char. 25: 2 --> 1
Char. 63: 0 --> 2
Char. 71: 1 --> 2
Char. 88: 0 --> 1
Char. 92: 1 --> 02
Char. 99: 0 --> 1

Node 61
Char. 55: 2 --> 0
Char. 63: 2 --> 0
Char. 65: 0 --> 1
Char. 91: 0 --> 1
Char. 96: 1 --> 0

Node 62
No synapomorphies

Node 63
Char. 15: 12 --> 0
Char. 21: 1 --> 0
Char. 25: 2 --> 3
Char. 30: 1 --> 0
Char. 65: 1 --> 0
Char. 91: 1 --> 0

Node 64
Char. 8: 0 --> 1
Char. 11: 0 --> 2
Char. 24: 1 --> 2
Char. 51: 1 --> 0
Char. 71: 3 --> 0

Node 65
Char. 12: 0 --> 1
Char. 17: 1 --> 4
Char. 24: 0 --> 1
Char. 28: 0 --> 1
Char. 43: 0 --> 1

Node 66
Char. 15: 0 --> 1
Char. 21: 0 --> 1
Char. 30: 0 --> 1
Char. 85: 2 --> 1
Char. 117: 0 --> 1

Node 67 - Ceratosauridae
Char. 19: 0 --> 1
Char. 70: 0 --> 1
Char. 71: 0 --> 34
Char. 81: 1 --> 0
Char. 82: 1 --> 0
Char. 83: 0 --> 1
Char. 105: 1 --> 0

Node 68
Char. 9: 1 --> 0
Char. 49: 1 --> 0
Char. 50: 1 --> 0
Char. 98: 0 --> 1
Char. 100: 0 --> 12

Node 69
Char. 6: 0 --> 1
Char. 41: 2 --> 0
Char. 42: 3 --> 0
Char. 47: 2 --> 1

Node 70
Char. 81: 0 --> 1
Char. 95: 0 --> 1

Node 71
Char. 72: 1 --> 2
Char. 103: 0 --> 1

Node 72
Char. 5: 0 --> 1
Char. 8: 1 --> 0
Char. 29: 0 --> 1
Char. 109: 1 --> 2

Node 73
Char. 41: 3 --> 2
Char. 51: 1 --> 2
Char. 52: 1 --> 2
Char. 71: 1 --> 0
Char. 91: 0 --> 1

Node 74
Char. 72: 3 --> 1
Char. 73: 2 --> 0
Char. 85: 2 --> 3

Node 75
Char. 84: 1 --> 3
Char. 105: 0 --> 1
Char. 109: 0 --> 1

Node 76
Char. 129: 2 --> 1
Char. 130: 0 --> 1
Char. 136: 1 --> 0

Node 77
Char. 42: 0 --> 3
Char. 48: 0 --> 1
Char. 51: 0 --> 1
Char. 52: 0 --> 1

Node 78
Char. 41: 0 --> 3
Char. 66: 1 --> 0
Char. 71: 0 --> 1
Char. 126: 1 --> 0

Node 79
Char. 72: 1 --> 3
Char. 73: 0 --> 2
Char. 80: 1 --> 0
Char. 92: 0 --> 1

Node 80
Char. 117: 1 --> 0

Node 81
Char. 29: 1 --> 0
Char. 85: 1 --> 2
Char. 101: 0 --> 2

Node 82
Char. 91: 1 --> 0
Char. 95: 1 --> 0

Node 83
Char. 17: 4 --> 2
Char. 94: 1 --> 0

Node 84
Char. 105: 1 --> 0

Node 85
Char. 109: 1 --> 0

Node 86 - Abelisauridae
Char. 68: 0 --> 1
Char. 88: 0 --> 2
Char. 95: 0 --> 1
Char. 96: 0 --> 1

Node 87
Char. 80: 0 --> 1
Char. 94: 0 --> 1

Node 88
Char. 17: 2 --> 1
Char. 106: 0 --> 1

Node 89
Char. 17: 34 --> 2
Char. 25: 2 --> 1
Char. 82: 0 --> 1
Char. 1010: 0 --> 1

Node 90 - Tyrannosauroidea
Char. 6: 0 --> 1
Char. 9: 1 --> 0
Char. 27: 0 --> 2
Char. 37: 0 --> 2
Char. 41: 2 --> 4
Char. 48: 01 --> 2
Char. 49: 1 --> 2
Char. 66: 0 --> 1

Node 91
Char. 92: 1 --> 0
Char. 94: 1 --> 0

Node 92 - Megalosauridae
Char. 17: 3 --> 4
Char. 72: 2 --> 1
Char. 91: 1 --> 0
Char. 95: 1 --> 0

Node 93
Char. 103: 1 --> 0

Node 94
Char. 65: 1 --> 2
Char. 104: 0 --> 1
Char. 111: 0 --> 1

Node 95 - Baryonychinae
Char. 5: 0 --> 1
Char. 11: 2 --> 1
Char. 25: 2 --> 0

Node 96 - Spinosauridae
Char. 2: 1 --> 34
Char. 14: 0 --> 1
Char. 20: 1 --> 0
Char. 23: 0 --> 2
Char. 47: 0 --> 1
Char. 66: 1 --> 2
Char. 81: 0 --> 1
Char. 107: 0 --> 2
Char. 117: 1 --> 2

Node 97 - Spinosaurinae
Char. 69: 0 --> 1
Char. 76: 0 --> 1
Char. 78: 0 --> 1

Node 98
Char. 10: 0 --> 1
Char. 87: 0 --> 1
Char. 88: 0 --> 1

Node 99
Char. 39: 1 --> 0

Node 100 - Carcharodontosaurinae
Char. 17: 3 --> 4
Char. 63: 0 --> 2
Char. 65: 1 --> 2

Char. 72: 2 --> 1
Char. 80: 0 --> 2
Char. 113: 1 --> 2

Node 101
Char. 95: 1 --> 0
Char. 105: 1 --> 2
Char. 106: 01 --> 2

Node 102
Char. 92: 1 --> 0
Char. 101: 0 --> 2
Char. 109: 2 --> 0

Node 103
Char. 42: 3 --> 2
Char. 46: 1 --> 0
Char. 72: 1 --> 0

Node 104
Char. 29: 0 --> 1
Char. 45: 0 --> 1
Char. 81: 0 --> 2
Char. 85: 2 --> 0
Char. 102: 0 --> 1

Node 105
Char. 73: 2 --> 1
Char. 78: 0 --> 1

Node 106
Char. 43: 1 --> 0
Char. 74: 0 --> 1
Char. 137: 0 --> 1

Node 107
Char. 9: 0 --> 1
Char. 38: 3 --> 2

Node 108
Char. 45: 0 --> 1
Char. 74: 0 --> 1

Node 109
Char. 71: 3 --> 0
Char. 100: 0 --> 2
Char. 139: 1 --> 0

Node 110
Char. 25: 2 --> 0
Char. 53: 1 --> 2
Char. 64: 0 --> 1
Char. 84: 2 --> 3
Char. 85: 2 --> 3
Char. 87: 0 --> 2
Char. 88: 0 --> 2
Char. 95: 0 --> 1

Node 111 - Therizinosauria
Char. 1: 0 --> 1
Char. 43: 0 --> 1
Char. 63: 2 --> 1
Char. 81: 0 --> 2

Cladistic analysis on a supermatrix with theropod taxa (ML teeth excluded).

FIGURE A4.7. **A**, Strict consensus cladogram of nine most parsimonious trees recovered from the analysis of a supermatrix including a dentition-based data matrix and six recent datasets based on whole theropod skeleton (i.e., Xu et al. 2009*a*; Brusatte et al. 2010*d*; Martinez et al. 2011; Senter 2011; Carrano et al. 2012; Pol and Rauhut 2012). Initial analysis was a New Technology Search using TNT v.1.1 of a supermatrix comprising 1972 characters for one outgroup (*Eoraptor*) and 59 non-avian theropod taxa. Tree length = 3583 steps; CI = 0.546; RI = 0.604; **B**, Strict consensus cladogram of four most parsimonious trees recovered from the analysis of a supermatrix after the deletion of the two wildcard taxa *Erectopus* and *Piatnitzkysaurus*. Tree length = 3529 steps; CI = 0.575; RI = 0.642.

Unambiguous and ambiguous dentition based synapomorphies and autapomorphies from a cladistic analysis on the supermatrix (ML teeth excluded)

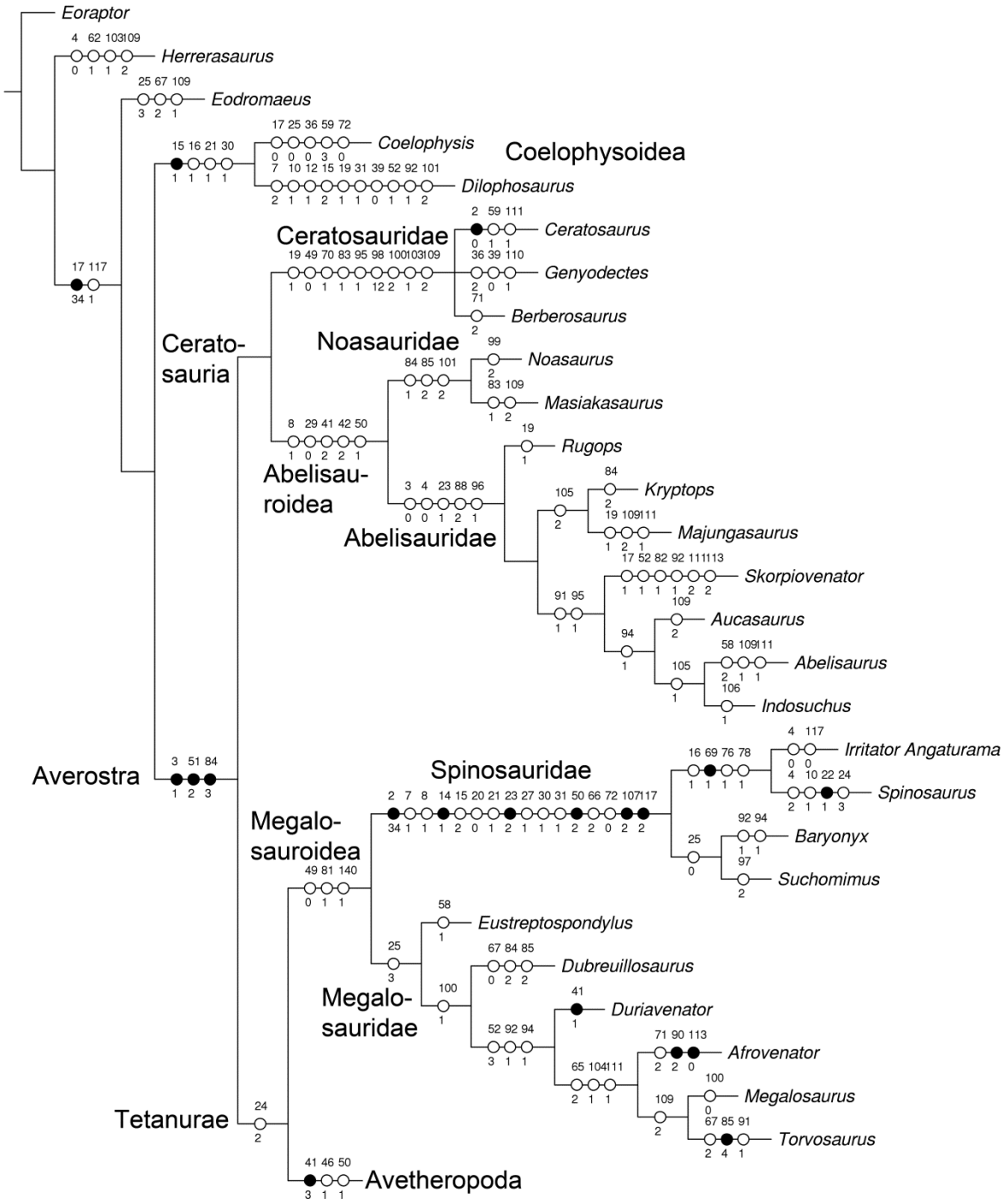

FIGURE A4.8. Strict consensus cladogram of six most parsimonious trees recovered from the analysis of a supermatrix including a dentition-based data matrix and six recent datasets based on whole theropod skeleton (i.e., Xu et al. 2009*a*; Brusatte et al. 2010*d*; Martinez et al. 2011; Senter 2011; Carrano et al. 2012; Pol and Rauhut 2012). The consensus tree was obtained after the deletion of the wildcard taxa *Erectopus* and *Piatnitzkysaurus*. Initial analysis was a Ratchet (Island Hopper) analysis using WinClada 1.00.08 of a supermatrix comprising 1972 characters for one outgroup (*Eoraptor*) and 57 non-avian theropod taxa. Tree length = 3507 steps; CI = 0.57; RI = 0.64. The same topology was obtained with TNT v.1.1 with a New Technology Search that yielded four MPTs (Tree length = 3529 steps; CI = 0.575; RI = 0.642). The unambiguous and ambiguous dentition based synapomorphies are represented by black and white circles, respectively, and the character number and character state associated with each synapomorphy are above and below the circles, respectively.

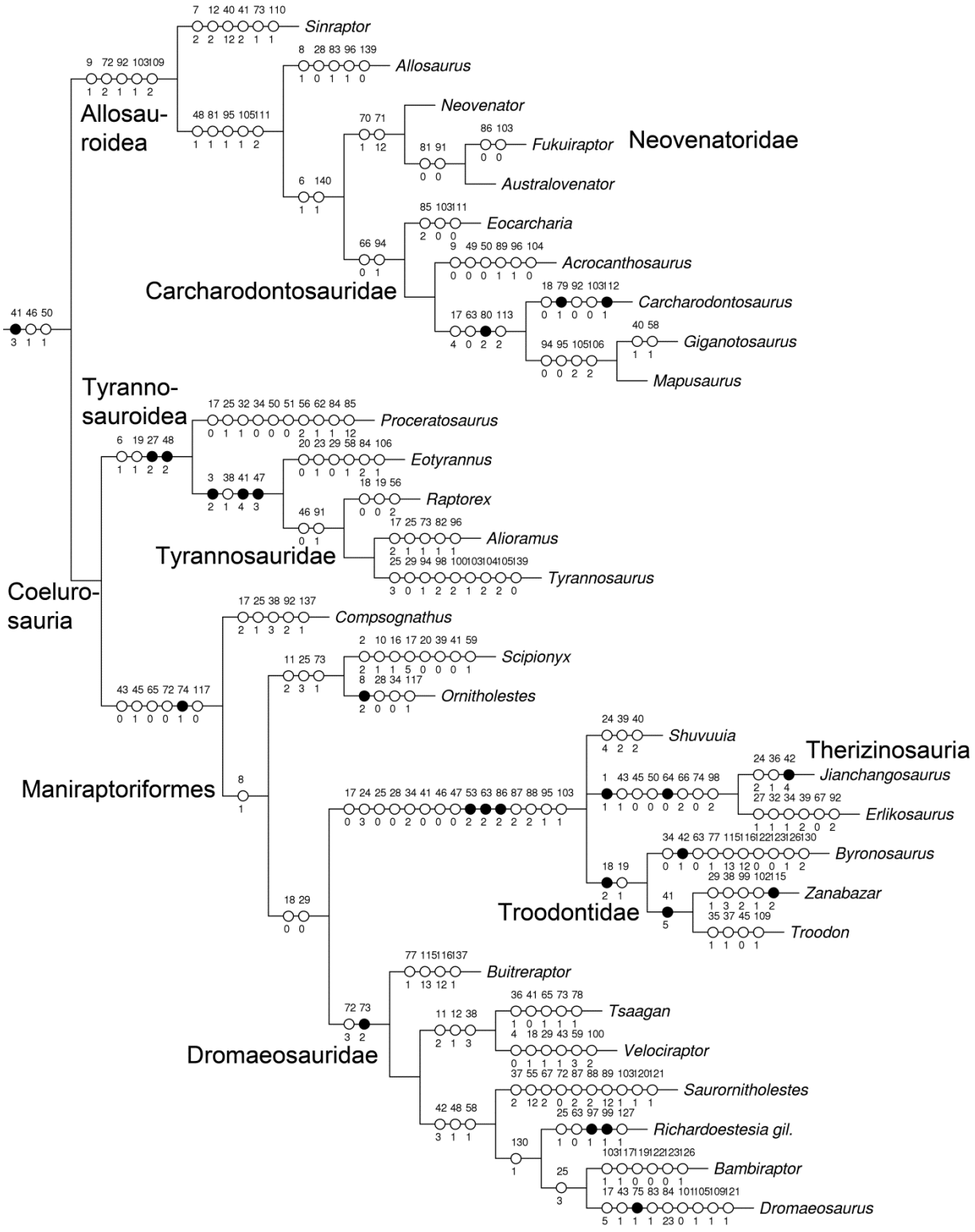

FIGURE A4.8. (Continued)

Cladistic analysis on a supermatrix with theropod taxa (ML teeth included).

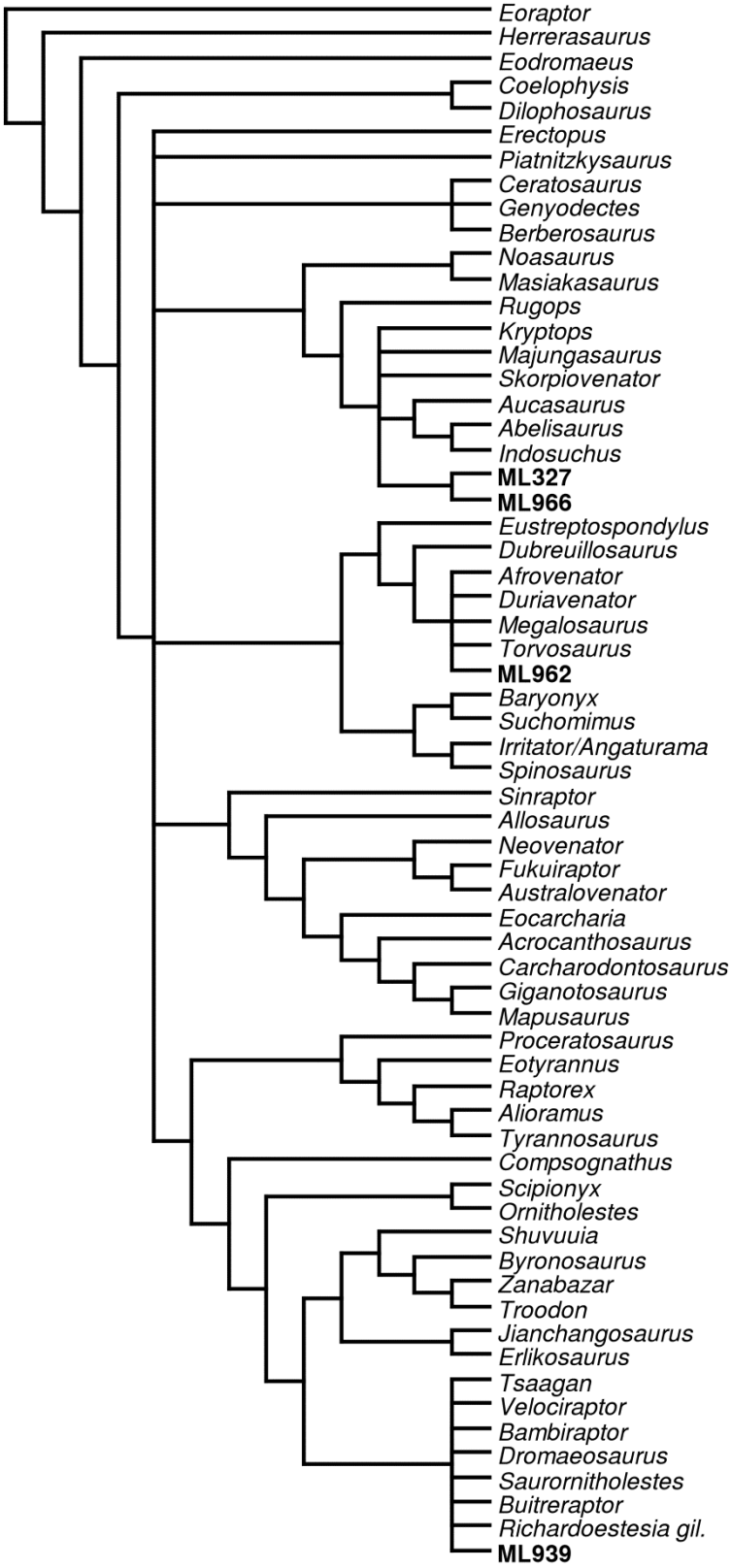

FIGURE A4.9. Strict consensus cladogram of 96 most parsimonious trees recovered from the analysis of a supermatrix including a dentition-based data matrix and six recent datasets based on whole theropod skeleton (i.e., Xu et al. 2009*a*; Brusatte et al. 2010*d*; Martinez et al. 2011; Senter 2011; Carrano et al. 2012; Pol and Rauhut 2012). Initial analysis was a New Technology Search using TNT v.1.1 of a supermatrix comprising 1972 characters for one outgroup (*Eoraptor*), 59 non-avian theropod taxa and ML 327, ML 966, ML 939 (coded as lateral teeth), and ML 962 (coded as a mesial tooth). Tree length = 3607 steps; CI = 0.529; RI = 0.58.

A5. Morphometric data on theropod teeth

Abbreviations: AL, apical length; **C/**, cast; **CBL**, crown base length; **CBR**, crown base ratio; **CBW**, crown base width; **CHR**, crow height ratio; **DC**, distocental denticles density (per 5 mm); **dt**, dentary tooth; **L**, left side of the jaw; **M**, mesial tooth; **MC**, mesiocentral denticle density (per 5 mm); **MCL**, mid-crown length; **MCR**, mid-crown ratio; **MCW**, mid-crown width; **mx**, maxillary tooth; **pmx**, premaxillary tooth; **R**, right side of the jaw.

Taxa (Genus)	Side	Position	Specimen	Source	CBL	CBW	CH	AL	CBR	CHR	MCL	MCW	MCR	MC	DC
Eoraptor	L	pmx2	PVSJ 512	Pers. Obs.	2.5	1.6	6.7	7.0	0.6	2.7	?	?	?		25
Eoraptor	L	pmx3	PVSJ 512	Pers. Obs.	2.0	2.4	5.9	6.4	1.2	3.0	?	?	?		?
Eoraptor	L	pmx4	PVSJ 512	Pers. Obs.	2.2	1.7	6.5	6.1	0.8	3.0	?	?	?		?
Eoraptor	R	pmx2	PVSJ 512	Pers. Obs.	2.2	1.6	5.0	5.4	0.7	2.3	?	?	?		30
Eoraptor	R	pmx4	PVSJ 512	Pers. Obs.	2.1	1.6	4.2	4.9	0.8	2.0	?	?	?		27.5
Eoraptor	L	mx2	PVSJ 512	Pers. Obs.	2.7	1.8	5.6	5.7	0.7	2.1	?	?	?		30
Eoraptor	L	mx4	PVSJ 512	Pers. Obs.	3.0	1.5	5.7	6.5	0.5	1.9	?	?	?	?	27.5
Eoraptor	L	mx5	PVSJ 512	Pers. Obs.	3.6	1.7	5.5	6.9	0.5	1.5	?	?	?	30	27.5
Eoraptor	L	mx9	PVSJ 512	Pers. Obs.	2.5	1.8	5.1	6.4	0.7	2.1	?	?	?	22.5	25
Eoraptor	L	mx10	PVSJ 512	Pers. Obs.	2.7	1.2	4.6	6.0	0.5	1.7	?	?	?	25	30
Eoraptor	L	mx11	PVSJ 512	Pers. Obs.	2.3	1.4	2.3	3.5	0.6	1.0	?	?	?	20	32.5
Eoraptor	L	pm02	PVSJ 512	Smith & Lamanna 2006	2.9	1.9	7.2	7.4	0.6	2.5	?	?	?	?	37.5
Eoraptor	L	pm03	PVSJ 512	Smith & Lamanna 2006	2.0	1.5	5.7	5.9	0.7	2.9	?	?	?	?	30
Eoraptor	L	pm04	PVSJ 512	Smith & Lamanna 2006	1.9	1.6	6.1	6.2	0.8	3.2	?	?	?	?	
Eoraptor	R	pm02	PVSJ 512	Smith & Lamanna 2006	2.3	1.8	5.2	5.4	0.8	2.2	?	?	?	?	35
Eoraptor	L	mx02	PVSJ 512	Smith & Lamanna 2006	2.1	1.5	5.7	5.9	0.7	2.7	?	?	?	?	
Eoraptor	L	mx04	PVSJ 512	Smith & Lamanna 2006	3.0	2.0	6.6	7.6	0.6	2.2	?	?	?	?	30
Eoraptor	L	mx06	PVSJ 512	Smith & Lamanna 2006	2.9	1.7	5.4	6.4	0.6	1.9	?	?	?	?	30
Eoraptor	L	mx07	PVSJ 512	Smith & Lamanna 2006	2.7	1.6	6.2	6.8	0.6	2.3	?	?	?	?	25
Eoraptor	L	mx09	PVSJ 512	Smith & Lamanna 2006	2.7	1.8	5.0	6.1	0.7	1.9	?	?	?	?	30
Eoraptor	L	mx10	PVSJ 512	Smith & Lamanna 2006	2.6	1.7	4.7	5.8	0.7	1.8	?	?	?	?	30
Eoraptor	R	mx02	PVSJ 512	Smith & Lamanna 2006	2.9	1.9	5.3	6.2	0.6	1.8	?	?	?	?	30
Eoraptor	R	mx04	PVSJ 512	Smith & Lamanna 2006	2.5	1.6	6.5	7.4	0.6	2.6	?	?	?	?	32.5
Eoraptor	R	mx05	PVSJ 512	Smith & Lamanna 2006	3.3	1.8	6.8	7.0	0.5	2.0	?	?	?	?	40
Eoraptor	R	mx07	PVSJ 512	Smith & Lamanna 2006	2.9	1.6	4.8	6.5	0.6	1.7	?	?	?	?	32.5
Eoraptor	R	mx08	PVSJ 512	Smith & Lamanna 2006	2.8	1.5	4.7	6.0	0.5	1.7	?	?	?	?	
Ischisaurus	R	pmx1	MACN 18.060	Pers. Obs.	8.2	4.7	14.6	17.0	0.6	1.8	5.5	?	?		?
Ischisaurus	R	pmx2	MACN 18.060	Pers. Obs.	7.5	4.4	14.5	17.1	0.6	1.9	5.5	?	?		20
Eodromaeus	L	mx3	PVSJ 561	Pers. Obs.	3.6	1.6	9.7	10.9	0.4	2.7	2.7	?	?		42.5
Coelophysis	L	pmx2	CMNH 82931	Pers. Obs.	1.7	0.5	4.0	4.8	0.3	2.4	1.2	?	?		
Coelophysis	L	pmx3	CMNH 82931	Pers. Obs.	1.8	1.0	6.8	6.8	0.6	3.8	1.6	?	?		?
Coelophysis	L	mx1	CMNH 82931	Pers. Obs.	3.0	1.5	8.2	8.7	0.5	2.7	2.4	?	?		50
Coelophysis	L	mx2	CMNH 82931	Pers. Obs.	4.1	1.4	8.9	9.6	0.3	2.2	2.3	?	?	50	47
Coelophysis	L	mx4	CMNH 82931	Pers. Obs.	4.4	1.6	11.6	12.3	0.4	2.6	4.1	?	?	40	40
Coelophysis	L	mx6	CMNH 82931	Pers. Obs.	5.5	1.7	9.7	10.8	0.3	1.8	3.1	?	?	40	40
Coelophysis	L	mx8	CMNH 82931	Pers. Obs.	5.9	1.8	9.3	13.2	0.3	1.6	2.8	?	?	40	40
Coelophysis	L	mx9	CMNH 82931	Pers. Obs.	5.4	1.7	8.6	11.6	0.3	1.6	2.9	?	?	40	?
Coelophysis	L	mx11	CMNH 82931	Pers. Obs.	5.4	1.9	7.5	10.1	0.3	1.4	3.7	?	?	40	35
Coelophysis	L	mx13	CMNH 82931	Pers. Obs.	4.7	1.6	5.5	7.8	0.3	1.2	3.0	?	?		35

Coelophysis	L	mx14	CMNH 82931	Pers. Obs.	5.2	1.7	6.2	8.7	0.3	1.2	2.9	?	?	40	40
Coelophysis	L	mx15	CMNH 82931	Pers. Obs.	3.9	1.5	5.4	7.1	0.4	1.4	2.2	?	?	40	35
Coelophysis	L	mx16	CMNH 82931	Pers. Obs.	3.3	1.1	5.0	6.2	0.3	1.5	2.0	?	?	?	40
Coelophysis	L	mx17	CMNH 82931	Pers. Obs.	3.5	1.6	4.1	6.6	0.5	1.2	2.1	?	?		35
Coelophysis	L	mx19	CMNH 82931	Pers. Obs.	3.4	1.9	3.3	3.7	0.6	1.0	1.8	?	?		40
Coelophysis	L	mx21	CMNH 82931	Pers. Obs.	3.5	0.9	3.5	5.2	0.3	1.0	1.4	?	?		40
Coelophysis	L	mx22	CMNH 82931	Pers. Obs.	3.3	0.9	3.8	4.9	0.3	1.2	1.4	?	?		40
Coelophysis	L	dt1	CMNH 82931	Pers. Obs.	1.9	1.2	5.1	5.1	0.6	2.7	1.4	?	?		
Coelophysis	L	dt3	CMNH 82931	Pers. Obs.	2.6	1.0	6.7	7.4	0.4	2.6	2.4	?	?		45
Coelophysis	L	dt4	CMNH 82931	Pers. Obs.	3.1	1.6	6.2	7.3	0.5	2.0	2.3	?	?		40
Liliensternus	?	max	MBR 21751/4	Smith et al. 2005	6.6	2.5	8.8	12.4	0.4	1.3	?	?	?	35	20
Liliensternus	?	max	MBR 21751/3	Smith et al. 2005	7.4	3.0	10.3	12.5	0.4	1.4	?	?	?	30	25
Liliensternus	L	d01	MBR 21751/8	Smith et al. 2005	5.1	3.5	8.0	9.2	0.7	1.6	?	?	?	30	25
Liliensternus	L	d04	MBR 21751/8	Smith et al. 2005	7.0	3.5	10.6	11.8	0.5	1.5	?	?	?	25	20
Liliensternus	L	d15	MBR 21751/8	Smith et al. 2005	8.3	3.5	10.5	12.6	0.4	1.3	?	?	?	25	20
Liliensternus	L	d16	MBR 21751/8	Smith et al. 2005	5.9	3.0	8.8	10.1	0.5	1.5	?	?	?	30	25
Liliensternus	R	?d19	MBR 21751/9	Smith et al. 2005	6.6	2.5	11.2	12.9	0.4	1.7	?	?	?	35	30
Dilophosaurus	R	mx3	UCMP 37303	Smith et al. 2005	16.3	9.9	24.7	30.0	0.6	1.5	?	?	?	?	15
Dilophosaurus	L	max	UCMP 37303	Smith et al. 2005	16.4	10.2	28.0	33.0	0.6	1.7	?	?	?	?	14
Dilophosaurus	L	max	UCMP 37303	Smith et al. 2005	19.1	10.4	35.2	47.5	0.5	1.8	?	?	?	?	15
Dilophosaurus	R	max	UCMP 37303	Smith et al. 2005	17.3	10.1	25.7	31.0	0.6	1.5	?	?	?	?	14
Genyodectes	R	mx6	MLP 26-39	Pers. Obs.	27.5	9.2	50.7	62.1	0.3	1.8	23.3	9.1	0.4	?	12.5
Genyodectes	L	dt2	MLP 26-39	Pers. Obs.	17.2	11.3	43.7	44.1	0.7	2.5	16.4	8.7	0.5	?	11
Genyodectes	L	dt4	MLP 26-39	Pers. Obs.	22.3	7.2	52.8	58.5	0.3	2.4	?	?	?	15	?
Genyodectes	R	dt1	MLP 26-39	Pers. Obs.	13.8	9.1	28.8	35.9	0.7	2.1	?	?	?	?	13.5
Genyodectes	R	dt2	MLP 26-39	Pers. Obs.	16.6	11.2	34.3	39.5	0.7	2.1	14.5	9.4	0.7	15	13
Genyodectes	R	dt3	MLP 26-39	Pers. Obs.	21.5	12.6	46.0	46.3	0.6	2.1	18.8	10.1	0.5	11.66	11.5
Genyodectes	R	dt5	MLP 26-39	Pers. Obs.	18.9	10.6	37.8	45.4	0.6	2.0	16.9	9.0	0.5	10.5	13
Genyodectes	R	dt7	MLP 26-39	Pers. Obs.	19.9	10.3	41.7	42.8	0.5	2.1	18.2	9.9	0.5	12.5	12
Ceratosaurus	L	dt7	NMNH 4735	Pers. Obs.	19.0	6.5	34.8	40.9	0.3	1.8	14.8	6.4	0.4	12.5	13
Ceratosaurus	L	dt9	NMNH 4735	Pers. Obs.	18.4	7.3	32.3	39.6	0.4	1.8	15.6	7.5	0.5	12.5	13.33
Ceratosaurus	L	dt10	NMNH 4735	Pers. Obs.	18.1	7.5	34.5	38.3	0.4	1.9	15.0	6.4	0.4	?	?
Ceratosaurus	R	dt6	NMNH 4735	Pers. Obs.	17.4	8.8	34.6	38.8	0.5	2.0	14.3	8.1	0.6	10	11.5
Ceratosaurus	R	dt12	NMNH 4735	Pers. Obs.	15.0	8.0	28.3	29.4	0.5	1.9	12.7	5.7	0.4	11.25	12.5
Ceratosaurus	R	dt13	NMNH 4735	Pers. Obs.	14.9	6.7	25.4	26.9	0.4	1.7	6.8	5.0	0.7	12	?
Ceratosaurus	L	pm01	UMNHVP7819	Smith et al. 2005	25.9	14.8	31.6	41.3	0.6	1.2	?	?	?	?	8
Ceratosaurus	L	pm02	UMNHVP7819	Smith et al. 2005	23.0	16.8	41.9	43.7	0.7	1.8	?	?	?	?	8
Ceratosaurus	L	pm03	UMNHVP7819	Smith et al. 2005	24.0	14.9	41.7	48.6	0.6	1.7	?	?	?	8	9
Ceratosaurus	R	pm01	UMNHVP7819	Smith et al. 2005	20.3	14.3	38.7	41.4	0.7	1.9	?	?	?	?	8
Ceratosaurus	R	pm03	UMNHVP7819	Smith et al. 2005	22.6	13.9	39.7	48.1	0.6	1.8	?	?	?	9	7
Ceratosaurus	L	mx01	UMNHVP5278	Smith et al. 2005	25.5	15.1	51.3	56.1	0.6	2.0	?	?	?	9	9
Ceratosaurus	L	mx03	UMNHVP5278	Smith et al. 2005	29.6	12.9	61.7	72.9	0.4	2.1	?	?	?	11	10
Ceratosaurus	L	mx05	UMNHVP5278	Smith et al. 2005	33.0	14.0	75.0	84.5	0.4	2.3	?	?	?	12.8	11
Ceratosaurus	L	mx08	UMNHVP5278	Smith et al. 2005	27.5	10.5	52.4	61.5	0.4	1.9	?	?	?	14	12
Ceratosaurus	L	mx10	UMNHVP5278	Smith et al. 2005	20.8	9.1	38.1	42.7	0.4	1.8	?	?	?	12	10.5
Berberosaurus	/	Isolated	MNHN Pt369	Pers. Obs.	17.8	6.4	32.3	38.4	0.4	1.8	11.7	5.3	0.5	18	15
Berberosaurus	/	Isolated	MNHN Pt369	Pers. Obs.	18.6	9.1	41.8	46.8	0.5	2.2	14.2	7.0	0.5	13.3	13.5
Noasaurus	L	mx6	PVL 4061	Pers. Obs.	3.1	1.8	3.3	4.2	0.6	1.1	?	?	?	?	20
Noasaurus	L	mx8	PVL 4061	Pers. Obs.	3.0	1.8	5.0	5.9	0.6	1.6	2.2	1.3	0.6	45	25

Masiakasaurus	M	Isolated	UA 9128	Pers. Obs.	2.4	2.6	7.7	6.3	1.1	3.2	2.8	2.3	0.8		
Masiakasaurus	M	Isolated	FMNH PR 2696	Pers. Obs.	2.2	2.5	6.6	6.5	1.1	3.0	2.5	2.0	0.8		35
Masiakasaurus	M	Isolated	FMNH PR 2182	Pers. Obs.	2.3	2.2	6.1	6.5	1.0	2.6	2.1	1.6	0.7	40	40
Masiakasaurus	L	dt1	FMNH PR 2471	Pers. Obs.	2.8	3.5	7.7	7.9	1.2	2.8	3.1	2.4	0.8	35	30
Masiakasaurus	R	dt3	UA 8680	Pers. Obs.	2.9	2.0	6.2	6.0	0.7	2.2	2.0	2.5	1.2	35	40
Masiakasaurus	R	dt7	UA 8680	Pers. Obs.	3.0	1.9	4.8	4.3	0.6	1.6	1.9	1.4	0.8	?	40
Masiakasaurus	/	Isolated	FMNH PR 2221	Pers. Obs.	5.1	2.0	8.7	10.1	0.4	1.7	3.9	1.8	0.4	27.5	18.33
Masiakasaurus	/	Isolated	FMNH PR 2476	Pers. Obs.	2.4	1.3	4.6	4.8	0.5	1.9	2.3	1.3	0.6		50
Masiakasaurus	/	Isolated	FMNH PR 2201	Pers. Obs.	6.3	3.1	11.4	13.7	0.5	1.8	4.6	2.4	0.5	20	15
Masiakasaurus	/	Isolated	UA 9091	Pers. Obs.	2.8	1.4	4.3	5.5	0.5	1.6	2.3	1.1	0.5	50	35
Masiakasaurus	/	Isolated	FMNH PR 2696	Pers. Obs.	4.6	2.5	11.8	11.4	0.5	2.6	3.7	2.1	0.6	20	15
Masiakasaurus	M	Isolated	98312-1	Smith et al. 2005	4.5	3.9	7.5	8.6	0.9	1.7	?	?	?	17	14.5
Masiakasaurus	/	Isolated	95345-1	Smith et al. 2005	5.3	2.3	7.0	8.2	0.4	1.3	?	?	?	30	25
Masiakasaurus	/	Isolated	99016	Smith et al. 2005	6.2	3.0	14.3	13.5	0.5	2.3	?	?	?	25	22.5
Masiakasaurus	/	Isolated	95358	Smith et al. 2005	2.8	2.2	5.9	6.0	0.8	2.1	?	?	?	?	?
Masiakasaurus	/	Isolated	95244-1	Smith et al. 2005	3.3	1.9	6.5	6.8	0.6	2.0	?	?	?	?	?
Masiakasaurus	/	Isolated	98313-1	Smith et al. 2005	7.1	3.5	10.4	11.7	0.5	1.5	?	?	?	17.5	18.5
Masiakasaurus	/	Isolated	98203	Smith et al. 2005	4.6	2.5	11.6	12.1	0.5	2.5	?	?	?	30	15
Masiakasaurus	/	Isolated	93086-4	Smith et al. 2005	4.9	2.4	8.6	9.5	0.5	1.7	?	?	?		20
Masiakasaurus	/	Isolated	95435	Smith et al. 2005	4.9	2.4	6.8	8.2	0.5	1.4	?	?	?	22.5	20
Masiakasaurus	/	Isolated	96068-4	Smith et al. 2005	5.5	2.2	8.9	10.2	0.4	1.6	?	?	?	26.3	16.7
Masiakasaurus	/	Isolated	MSNM V 5378	Fanti & Therrien 2007	5.2	3.0	13.3	?	1.7	0.4	?	?	?	25	15
Abelisaurus	M	Isolated	MC 1	Pers. Obs.	9.1	5.6	14.2	15.5	0.6	1.6	7.7	4.2	0.6	11	12
Abelisaurus	M	Isolated	MC 5	Pers. Obs.	11.6	6.9	22.6	23.4	0.6	2.0	10.5	5.2	0.5	10.5	10
Abelisaurus	M	Isolated	MC 267	Pers. Obs.	9.2	4.8	11.2	12.9	0.5	1.2	7.3	3.8	0.5	10	10
Abelisaurus	/	Isolated	MC 689	Pers. Obs.	19.6	9.4	24.3	26.6	0.5	1.2	12.8	8.7	0.7	10.5	10
Abelisaurus	/	Isolated	MC 709	Pers. Obs.	17.1	9.8	24.1	28.1	0.6	1.4	14.3	8.1	0.6	15	12.5
Rugops	L	mx4	MNN IGU1	Smith & Lamanna 2006	11.6	4.6	13.2	17.2	0.4	1.1	?	?	?	?	12
Indosuchus	R	pmx1	AMNH 1753	Pers. Obs.	12.9	12.9	20.0	24.1	1.0	1.6	11.9	10.4	0.9	7.5	6.66
Indosuchus	R	pmx2	AMNH 1753	Pers. Obs.	16.0	13.2	30.0	31.0	0.8	1.9	14.0	9.8	0.7	9	9
Indosuchus	L	pmx3	AMNH 1753	Pers. Obs.	16.0	10.0	27.0	29.0	0.6	1.7	14.1	8.7	0.6	8.5	10
Indosuchus	L	pmx4	AMNH 1753	Pers. Obs.	16.6	13.3	29.1	36.0	0.8	1.8	15.1	9.8	0.6	8.75	8.5
Indosuchus	L	mx08	AMNH 1753	Smith et al. 2005	19.5	9.1	29.4	31.5	0.5	1.5	?	?	?	10	12
Indosuchus	L	pm02	AMNH 1753	Smith et al. 2005	17.3	13.0	26.9	28.5	0.8	1.6	?	?	?	11.5	11
Indosuchus	L	pm03	AMNH 1753	Smith et al. 2005	16.6	10.7	27.3	29.5	0.6	1.6	?	?	?	10	11.5
Indosuchus	L	pm04	AMNH 1753	Smith et al. 2005	17.3	12.9	28.0	32.1	0.7	1.6	?	?	?	12	10
Indosuchus	R	pm01	AMNH 1753	Smith et al. 2005	13.6	10.5	26.0	29.0	0.8	1.9	?	?	?	8	10
Indosuchus	R	pm02	AMNH 1753	Smith et al. 2005	16.0	12.0	31.9	32.0	0.7	2.0	?	?	?	8	10
Majungasaurus	R	pm02	FMNHPR2008	Smith et al. 2005	13.0	9.5	30.1	31.9	0.7	2.3	?	?	?	11	11.5
Majungasaurus	R	pm02	UA 8716	Smith et al. 2005	12.4	9.3	27.1	27.8	0.7	2.2	?	?	?	10	10
Majungasaurus	R	pm04	UA 8716	Smith et al. 2005	12.5	8.3	27.7	30.7	0.7	2.2	?	?	?	10	11
Majungasaurus	L	mx04	FMNH PR2100	Smith et al. 2005	18.3	8.6	36.9	39.3	0.5	2.0	?	?	?	8.5	9
Majungasaurus	L	mx06	FMNH PR2100	Smith et al. 2005	18.4	9.2	38.1	39.9	0.5	2.1	?	?	?	9.5	9
Majungasaurus	R	mx05	FMNH PR2100	Smith et al. 2005	18.9	8.9	35.5	41.7	0.5	1.9	?	?	?	10	10
Majungasaurus	R	mx07	FMNH PR2100	Smith et al. 2005	18.2	9.1	38.7	44.2	0.5	2.1	?	?	?	9.7	9
Majungasaurus	R	mx17	FMNH PR2100	Smith et al. 2005	7.9	3.5	12.5	13.8	0.4	1.6	?	?	?	12	14
Majungasaurus	L	d01	FMNH PR2100	Smith et al. 2005	8.8	7.2	19.9	19.9	0.8	2.3	?	?	?	9	9
Majungasaurus	L	d05	FMNH PR2100	Smith et al. 2005	13.3	8.6	25.4	29.5	0.6	1.9	?	?	?	11	9.5
Majungasaurus	L	d07	FMNH PR2100	Smith et al. 2005	14.2	7.7	25.1	27.9	0.5	1.8	?	?	?	11	11

Majungasaurus	L	d12	FMNH PR2100	Smith et al. 2005	12.7	7.1	19.9	23.8	0.6	1.6	?	?	?	12	10
Majungasaurus	L	d13	FMNH PR2100	Smith et al. 2005	12.5	6.7	19.2	24.3	0.5	1.5	?	?	?	11.7	10.5
Majungasaurus	L	d14	FMNH PR2100	Smith et al. 2005	12.3	6.7	17.9	23.4	0.5	1.5	?	?	?	12	11.3
Majungasaurus	L	d15	FMNH PR2100	Smith et al. 2005	11.7	6.3	16.2	21.5	0.5	1.4	?	?	?	12.8	10.5
Majungasaurus	L	d17	FMNH PR2100	Smith et al. 2005	9.3	5.4	14.5	17.9	0.6	1.6	?	?	?	15	11
Majungasaurus	R	d02	FMNH PR2100	Smith et al. 2005	10.9	8.5	22.9	20.8	0.8	2.1	?	?	?	8	8.5
Majungasaurus	R	d03	FMNH PR2100	Smith et al. 2005	13.5	8.3	22.9	26.0	0.6	1.7	?	?	?	9.5	9
Majungasaurus	R	d04	FMNH PR2100	Smith et al. 2005	13.9	7.9	24.1	26.1	0.6	1.7	?	?	?	9.5	10
Majungasaurus	R	d06	FMNH PR2100	Smith et al. 2005	13.5	7.8	25.8	27.5	0.6	1.9	?	?	?	9.5	10.5
Majungasaurus	R	d10	FMNH PR2100	Smith et al. 2005	12.8	8.6	23.8	27.7	0.7	1.9	?	?	?	10.8	10
Majungasaurus	R	d11	FMNH PR2100	Smith et al. 2005	13.2	7.1	23.0	26.0	0.5	1.7	?	?	?	11	9.5
Majungasaurus	R	d15	FMNH PR2100	Smith et al. 2005	11.3	5.8	18.7	22.5	0.5	1.7	?	?	?	11.5	11.5
Majungasaurus	R	d16	FMNH PR2100	Smith et al. 2005	12.9	5.3	18.7	23.1	0.4	1.5	?	?	?	12.2	11.7
Majungasaurus	R	mx02	FMNH PR 2278	Smith et al. 2005	16.9	8.7	37.6	40.2	0.5	2.2	?	?	?	10	9.3
Majungasaurus	R	mx03	FMNH PR 2278	Smith et al. 2005	17.1	8.8	35.0	41.0	0.5	2.0	?	?	?	12	10
Aucasaurus	/	Isolated	MCF-PVPH-236	Pers. Obs.	18.0	11.3	36.4	37.8	0.6	2.0	13.4	7.2	0.5	13	15
Aucasaurus	R	last	MCF-PVPH-236	Pers. Obs.	14.6	4.5	18.4	23.7	0.3	1.3	10.9	4.8	0.4	13.5	12.5
Skorpiovenator	/	Isolated	MMCH-PV 48	Pers. Obs.	13.6	8.5	28.1	27.7	0.6	2.1	11.9	6.3	0.5	13	15
Skorpiovenator	/	Isolated	MMCH-PV 48	Pers. Obs.	18.8	6.7	41.0	43.0	0.4	2.2	?	?	?	13.5	13.5
Carnotaurus	L	dt3	MACN-CH 894	Pers. Obs.	13.9	9.9	30.1	30.6	0.7	2.2	?	?	?	?	?
Carnotaurus	L	dt6	MACN-CH 894	Pers. Obs.	15.0	8.9	33.2	30.2	0.6	2.2	?	?	?	?	?
Carnotaurus	L	dt10	MACN-CH 894	Pers. Obs.	13.5	8.8	27.0	29.3	0.6	2.0	?	?	?	?	?
Carnotaurus	L	dt11	MACN-CH 894	Pers. Obs.	11.8	7.8	22.2	27.8	0.7	1.9	?	?	?	?	?
Abelisauridae	/	Isolated	MUCPv 641	Pers. Obs.	11.0	4.6	19.3	22.6	0.4	1.8	9.0	4.2	0.5	13.5	13
Abelisauridae	/	Isolated	MUCPv 482	Pers. Obs.	10.5	4.2	19.6	18.8	0.4	1.9	9.1	4.0	0.4	13.5	13.5
Abelisauridae	R	mx6	UCPC 10	Pers. Obs.	11.4	6.1	22.0	26.0	0.5	1.9	8.7	4.9	0.6	12.5	13
Abelisauridae	/	Isolated	MGUP MEGA002	Smith & Lamanna 2006	13.0	6.7	16.6	21.0	0.5	1.3	?	?	?	10	13
Abelisauridae	/	Isolated	MCPM 13693	Smith & Vechia 2006	16.2	9.8	27.5	29.5	0.6	1.7	?	?	?	12.5	8.5
Erectopus	L	mx01	MNHN 2001-4	Pers. Obs.	16.2	7.5	45.0	49.0	0.5	2.8	13.2	6.6	0.5	15	14
Erectopus	L	mx02	MNHN 2001-4	Pers. Obs.	18.7	7.4	48.3	55.3	0.4	2.6	14.5	6.9	0.5	14	13
Erectopus	L	mx03	MNHN 2001-4	Pers. Obs.	21.5	10.3	49.0	56.0	0.5	2.3	16.0	7.5	0.5	13	12
Piatnitzkysaurus	/	Isolated	MACN-CH 895	Pers. Obs.	23.3	14.2	52.3	56.8	0.6	2.2	19.5	11.4	0.6	15	12
Piatnitzkysaurus	/	Isolated	MACN-CH 895	Pers. Obs.	17.3	9.0	35.3	39.6	0.5	2.0	13.8	8.1	0.6	15	12
Afrovenator	/	Isolated	UC UBA 1	Pers. Obs.	27.6	11.7	61.1	64.6	0.4	2.2	21.8	11.6	0.5	8	10
Duriavenator	R	mx03	NHM R332	Pers. Obs.	24.3	12.7	51.7	57.2	0.5	2.1	19.1	10.1	0.5	12	11
Duriavenator	R	mx06	NHM R332	Pers. Obs.	21.0	8.0	39.4	49.2	0.4	1.9	18.2	8.5	0.5	13	12.5
Duriavenator	R	mx03	NHM R332	Smith et al. 2005	24.3	12.8	51.1	57.9	0.5	2.1	?	?	?	8.5	11
Duriavenator	R	mx06	NHM R332	Smith et al. 2005	20.9	11.8	38.9	45.6	0.6	1.9	?	?	?	10.5	11
Duriavenator	/	Isolated	NHM R332	Smith et al. 2005	18.2	8.3	29.3	34.1	0.5	1.6	?	?	?	9	12
Megalosaurus	/	Isolated	NHM R15909	Ősi et al. 2010	20.0	11.0	42.6	48.4	0.6	2.1	?	?	?	16	13
Megalosaurus	/	Isolated	NHM R1997	Ősi et al. 2010	12.5	8.7	30.0	34.0	0.7	2.4	?	?	?	17	15
Megalosaurus	/	Isolated	NHM R210	Ősi et al. 2010	14.0	8.5	27.5	33.0	0.6	2.0	?	?	?	?	11
Megalosaurus	/	Isolated	NHM R39476	Pers. Obs.	18.3	10.1	35.5	38.8	0.6	1.9	15.8	8.0	0.5	?	14
Megalosaurus	/	Isolated	NHM R47152	Pers. Obs.	11.3	6.4	22.5	24.3	0.6	2.0	9.1	5.4	0.6	20.63	20
Megalosaurus	/	Isolated	NHM R234	Pers. Obs.	24.3	13.1	52.3	54.2	0.5	2.2	18.1	10.3	0.6	9.5	12
Megalosaurus	/	Isolated	NHM R31834	Pers. Obs.	17.7	6.8	28.6	33.4	0.4	1.6	13.1	6.7	0.5	12	14
Megalosaurus	/	Isolated	NHM R47963	Pers. Obs.	23.9	12.1	51.7	48.9	0.5	2.2	18.5	9.7	0.5	11	13
Megalosaurus	/	Isolated	NHM R28608	Pers. Obs.	21.4	13.7	47.4	44.9	0.6	2.2	17.3	11.7	0.7	8.5	8.75
Megalosaurus	/	Isolated	NHM R2635	Pers. Obs.	26.5	13.9	54.4	59.3	0.5	2.1	20.6	11.1	0.5	11.25	11

Megalosaurus	/	Isolated	NHM R2635	Pers. Obs.	11.4	7.7	26.6	29.8	0.7	2.3	8.6	5.6	0.7	?	13
Megalosaurus	R	dt06	OUMNH J13505	Pers. Obs.	24.1	12.8	46.5	55.8	0.5	1.9	19.3	10.2	0.5	?	10
Megalosaurus	L	mx01	OUMNH J13506	Pers. Obs.	24.8	14.9	62.7	68.0	0.6	2.5	?	?	?	8.75	?
Dubreuillosaurus	L	pmx1	MNHN 1998-13	Pers. Obs.	8.3	6.0	18.0	17.0	0.7	2.2	6.0	4.5	0.8	12	11.5
Dubreuillosaurus	L	pmx2	MNHN 1998-13	Pers. Obs.	10.5	7.7	22.0	23.6	0.7	2.1	7.7	5.2	0.7	12.5	12.5
Dubreuillosaurus	R	mx4, cast	MNHN 1998-13	Pers. Obs.	17.5	6.3	27.7	32.1	0.4	1.6	11.3	4.9	0.4	?	?
Dubreuillosaurus	R	mx5, cast	MNHN 1998-13	Pers. Obs.	17.6	7.1	39.1	37.8	0.4	2.2	14.0	5.5	0.4	?	?
Dubreuillosaurus	R	mx6, cast	MNHN 1998-13	Pers. Obs.	14.8	6.0	21.3	28.4	0.4	1.4	10.6	5.0	0.5	?	?
Dubreuillosaurus	R	mx7, cast	MNHN 1998-13	Pers. Obs.	15.7	6.5	27.7	36.0	0.4	1.8	12.2	5.6	0.5	?	?
Dubreuillosaurus	R	mx9, cast	MNHN 1998-13	Pers. Obs.	10.4	5.7	16.8	22.2	0.5	1.6	10.1	4.6	0.5	?	?
Dubreuillosaurus	L	dt6	MNHN 1998-13	Pers. Obs.	10.7	5.4	18.0	17.6	0.5	1.7	6.8	3.8	0.6	17.5	16
Dubreuillosaurus	L	dt8	MNHN 1998-13	Pers. Obs.	10.5	5.2	16.0	15.9	0.5	1.5	6.4	3.4	0.5	16.6	16
Dubreuillosaurus	/	Isolated	MNHN 1998-13	Pers. Obs.	9.9	4.3	14.1	12.8	0.4	1.4	6.3	3.2	0.5	16	16
Torvosaurus	/	Isolated	BYUVP 725 12817	Pers. Obs.	39.8	19.2	103.3	110.7	0.5	2.6	30.2	16.7	0.6	6	7
Torvosaurus	L	mx02	ML 1100	Pers. Obs.	45.5	16.4	106.4	118.6	0.4	2.3	33.1	16.8	0.5	8	8
Torvosaurus	/	Isolated	ML 1853	Pers. Obs.	24.8	13.7	43.5	46.4	0.6	1.8	21.5	11.2	0.5	9.5	9.5
Torvosaurus	M	Isolated	ML 962	Pers. Obs.	31.2	20.2	85.8	91.9	0.6	2.8				8	8
Baryonyx	R	pmx04	NHM R9951	Pers. Obs.	13.3	11.2	33.3	33.5	0.8	2.5	10.3	8.7	0.8	35	?
Baryonyx	R	pmx06	NHM R9951	Pers. Obs.	10.7	8.5	25.4	27.6	0.8	2.4	7.7	7.0	0.9	35	35
Baryonyx	R	pmx07	NHM R9951	Pers. Obs.	8.3	7.7	20.8	21.9	0.9	2.5	6.7	5.5	0.8	35	30
Baryonyx	L	mx5	NHM R9951	Pers. Obs.	18.2	13.5	32.5	38.6	0.7	1.8	14.6	10.4	0.7	30	35
Baryonyx	/	Isolated	NHM R9951	Pers. Obs.	16.9	13.6	33.3	34.0	0.8	2.0	12.1	9.7	0.8	?	35
Baryonyx	/	Isolated	NHM R9951	Pers. Obs.	12.1	10.0	26.6	26.8	0.8	2.2	9.4	7.0	0.7	35	35
Baryonyx	/	Isolated	NHM R9951	Pers. Obs.	13.4	10.4	29.4	29.0	0.8	2.2	10.7	7.7	0.7	35	35
Baryonyx	/	Isolated	NHM R9951	Pers. Obs.	15.3	11.8	33.7	33.8	0.8	2.2	11.2	9.5	0.8	35	40
Baryonyx	/	Isolated	NHM R9951	Pers. Obs.	9.0	8.4	20.8	21.1	0.9	2.3	7.7	6.0	0.8	35	35
Baryonyx	/	Isolated	NHM R9951	Pers. Obs.	11.2	11.2	25.8	26.8	1.0	2.3	9.0	7.8	0.9	?	35
Baryonyx	/	Isolated	NHM R9951	Pers. Obs.	11.8	10.7	24.2	26.8	0.9	2.0	9.6	7.6	0.8	30	35
Baryonyx	/	Isolated	NHM R9951	Pers. Obs.	8.8	7.5	16.9	18.0	0.9	1.9	8.0	5.9	0.7	?	35
Baryonyx	/	Isolated	NHM R9951	Pers. Obs.	9.3	8.0	17.9	18.0	0.9	1.9	7.9	6.3	0.8	?	35
Baryonyx	/	Isolated	NHM R9951	Pers. Obs.	9.3	7.3	20.4	19.6	0.8	2.2	7.4	6.1	0.8	45	35
Baryonyx	/	Isolated	NHM R9951	Pers. Obs.	15.8	13.3	36.5	37.7	0.8	2.3	12.4	9.7	0.8	40	35
Baryonyx	/	Isolated	NHM R9951	Pers. Obs.	17.1	14.3	30.9	33.3	0.8	1.8	13.5	10.5	0.8	35	?
Baryonyx	/	Isolated	NHM R9951	Pers. Obs.	19.3	14.4	42.8	41.7	0.7	2.2	14.3	10.7	0.7	30	30
Baryonyx	R	pm04	NHM R9951	Smith et al. 2005	13.1	11.2	31.4	32.3	0.9	2.4	?	?	?	35	35
Baryonyx	R	pm06	NHM R9951	Smith et al. 2005	10.5	7.9	23.7	24.8	0.8	2.3	?	?	?	35	35
Baryonyx	/	Isolated	NHM R9951a	Smith et al. 2005	11.7	11.2	28.7	29.2	1.0	2.5	?	?	?	35	35
Baryonyx	/	Isolated	NHM R9951d	Smith et al. 2005	15.8	12.1	34.8	37.4	0.8	2.2	?	?	?	35	35
Baryonyx	/	Isolated	NHM R9951e	Smith et al. 2005	13.2	10.9	29.7	30.5	0.8	2.3	?	?	?	35	35
Baryonyx	/	Isolated	NHM R9951f	Smith et al. 2005	12.1	10.4	27.2	30.5	0.9	2.2	?	?	?	35	35
Baryonyx	/	Isolated	NHM R9951h	Smith et al. 2005	16.4	15.2	38.6	43.9	0.9	2.3	?	?	?	35	35
Baryonyx	/	Isolated	NHM R9951n	Smith et al. 2005	16.5	13.7	34.1	38.1	0.8	2.1	?	?	?	35	35
Suchomimus	/	Isolated	UC G69-5	Pers. Obs.	18.2	14.2	54.0	57.8	0.8	3.0	13.2	10.4	0.8	?	?
Suchomimus	/	Isolated	UC G67-1	Pers. Obs.	18.6	14.9	48.5	53.0	0.8	2.6	13.6	9.2	0.7	35	25
Suchomimus	/	Isolated	UC G67-8	Pers. Obs.	12.4	8.2	32.6	33.3	0.7	2.6	8.4	5.7	0.7	?	?
Suchomimus	/	Isolated	UC G35-9	Pers. Obs.	15.0	11.3	40.4	42.4	0.8	2.7	10.7	6.8	0.6	30	?
Suchomimus	/	Isolated	UC G35-9	Pers. Obs.	15.2	11.3	32.4	34.0	0.7	2.1	10.6	7.5	0.7	30	30
Suchomimus	/	Isolated	UC G43-4	Pers. Obs.	18.0	14.4	36.9	46.5	0.7	2.1	13.6	9.8	0.7	?	?
Suchomimus	/	Isolated	UC G26-5	Pers. Obs.	15.9	10.8	41.7	47.8	0.7	2.6	11.6	7.8	0.7	30	25

Suchomimus	/	Isolated	UC G73-3	Pers. Obs.	15.1	9.8	41.2	43.1	0.6	2.7	10.8	6.8	0.6	25	25
Suchomimus	/	Isolated	UC G73-3	Pers. Obs.	9.4	7.8	26.5	28.6	0.8	2.8	7.9	6.2	0.8	?	?
Suchomimus	/	Isolated	UC G34-12	Pers. Obs.	13.4	9.7	39.3	41.0	0.7	2.9	9.5	6.7	0.7	27.5	25
Suchomimus	/	Isolated	UC G100-4	Pers. Obs.	14.5	9.5	37.3	39.0	0.7	2.6	10.6	6.7	0.6	30	32.5
Suchomimus	/	Isolated	UC G22-7	Pers. Obs.	12.8	9.8	38.5	39.5	0.8	3.0	9.0	6.6	0.7	?	35
Suchomimus	/	Isolated	UC G34-12	Pers. Obs.	17.2	11.6	38.8	38.0	0.7	2.3	10.5	7.9	0.8	?	32.5
Suchomimus	/	Isolated	UC G34-7	Pers. Obs.	9.0	8.3	18.2	19.5	0.9	2.0	6.5	5.4	0.8	30	30
Suchomimus	/	Isolated	UC G34-7	Pers. Obs.	8.0	7.0	23.8	21.4	0.9	3.0	6.0	4.9	0.8	?	?
Suchomimus	/	Isolated	UC G54-4	Pers. Obs.	19.9	15.0	47.6	47.8	0.8	2.4	14.7	10.6	0.7	25	25
Suchomimus	/	Isolated	UC G89-5	Smith et al. 2005	18.9	15.2	62.9	70.6	0.8	3.3	?	?	?	?	27.5
Suchomimus	/	Isolated	UC G54-4	Smith et al. 2005	20.8	18.1	56.9	64.2	0.9	2.7	?	?	?	?	27
Suchomimus	/	Isolated	UC G48-9	Smith et al. 2005	18.7	13.3	52.7	60.2	0.7	2.8	?	?	?	?	35
Suchomimus	/	Isolated	UC G67-1	Smith et al. 2005	19.2	14.4	54.3	55.6	0.8	2.8	?	?	?	?	29
Irritator	R	mx3rd last	SMNS 58022	Pers. Obs.	8.2	7.1	21.0	19.8	0.9	2.6	6.4	5.2	0.8		
Spinosaurus	/	Isolated	SMA 0173	Pers. Obs.	27.8	23.9	81.6	86.0	0.9	2.9	22.6	17.3	0.8		
Spinosaurus	/	Isolated	MSNM V6422	Pers. Obs.	26.3	23.3	55.2	59.0	0.9	2.1	?	?	?		
Spinosaurus	/	Isolated	MSNM V3976	Pers. Obs.	18.1	17.1	45.6	50.4	0.9	2.5	14.5	12.1	0.8		
Allosaurus	R	pm02	YPM 4944	Smith et al. 2005	12.5	6.0	28.7	25.5	0.5	2.3	?	?	?	10	10
Allosaurus	R	pm03	YPM 4944	Smith et al. 2005	12.0	11.1	20.7	25.6	0.9	1.7	?	?	?	10	10
Allosaurus	R	pm05	YPM 4944	Smith et al. 2005	13.0	9.3	27.0	30.4	0.7	2.1	?	?	?	10	11
Allosaurus	L	pm03	SDSM 25248	Smith et al. 2005	20.4	12.3	49.6	54.0	0.6	2.4	?	?	?	9	9
Allosaurus	L	pm05	SDSM 25248	Smith et al. 2005	16.0	8.2	34.1	39.7	0.5	2.1	?	?	?	16	12.5
Allosaurus	L	mx04	UMNHVP9211	Smith et al. 2005	15.0	7.3	30.0	37.5	0.5	2.0	?	?	?	11.5	10
Allosaurus	L	mx06	UMNHVP9211	Smith et al. 2005	15.2	7.0	33.5	37.9	0.5	2.2	?	?	?	11	11
Allosaurus	R	mx07	UMNHVP9275	Smith et al. 2005	12.1	7.5	25.4	30.5	0.6	2.1	?	?	?	14	17.5
Allosaurus	R	mx07	UMNHVP9273	Smith et al. 2005	14.1	7.6	28.5	32.1	0.5	2.0	?	?	?	13.5	14
Allosaurus	R	mx06	UMNHVP9273	Smith et al. 2005	14.8	7.2	25.5	29.8	0.5	1.7	?	?	?	12.5	15
Allosaurus	L	mx01	UMNHVP9218	Smith et al. 2005	17.3	13.0	38.3	42.2	0.8	2.2	?	?	?	9.5	11.5
Allosaurus	R	d06	UMNHVP9369	Smith et al. 2005	11.8	8.3	25.8	29.1	0.7	2.2	?	?	?	18	13.5
Allosaurus	R	d02	UMNHVP9365	Smith et al. 2005	10.6	9.8	24.6	27.6	0.9	2.3	?	?	?	10	11
Allosaurus	R	pm05	UMNHVP1251	Smith et al. 2005	16.1	13.8	40.9	40.6	0.9	2.5	?	?	?	10	11
Allosaurus	R	mx1	USNM 8335	Pers. Obs.	16.7	13.4	34.1	45.0	0.8	2.0	15.3	8.9	0.6	12	11
Allosaurus	R	mx10	USNM 8335	Pers. Obs.	18.7	6.9	31.9	35.0	0.4	1.7	14.5	7.4	0.5	13	13.33
Allosaurus	R	pmx	CMNH 11844	Pers. Obs.	17.9	17.3	39.5	39.2	1.0	2.2	14.2	11.2	0.8	10	12
Allosaurus	/	Isolated	CMNH 11844	Pers. Obs.	18.2	14.4	50.8	56.2	0.8	2.8	18.0	10.7	0.6	?	?
Allosaurus	L	pm02	CMNH 21703	Pers. Obs.	12.6	14.5	33.8	34.8	1.2	2.7	12.6	9.8	0.8	10	10
Allosaurus	L	pm03	CMNH 21703	Pers. Obs.	15.6	12.6	33.3	37.0	0.8	2.1	11.4	9.4	0.8	?	?
Allosaurus	L	pm04	CMNH 21703	Pers. Obs.	15.5	12.8	34.8	35.1	0.8	2.2	12.4	8.8	0.7	10.5	11
Allosaurus	L	pm02	CMNH 21703	Smith et al. 2005	14.1	12.5	34.3	34.8	0.9	2.4	?	?	?	10	10
Allosaurus	L	pm03	CMNH 21703	Smith et al. 2005	12.8	10.5	34.2	36.5	0.8	2.7	?	?	?	9.5	10
Allosaurus	L	pm04	CMNH 21703	Smith et al. 2005	13.7	10.7	33.2	35.5	0.8	2.4	?	?	?	10.5	11
Allosaurus	R	pmx03	AMNH851	Pers. Obs.	18.0	17.7	36.4	38.0	1.0	2.0	13.5	12.2	0.9	10	9.5
Allosaurus	R	mx09	AMNH851	Pers. Obs.	22.2	9.7	43.7	48.8	0.4	2.0	19.6	9.7	0.5	10	11
Allosaurus	C/	pm01	LACM 46030	Smith et al. 2005	16.1	15.3	33.9	36.7	1.0	2.1	?	?	?	9.5	10
Allosaurus	C/	pm02	LACM 46030	Smith et al. 2005	16.0	14.6	33.9	36.0	0.9	2.1	?	?	?	9.3	10.3
Allosaurus	C/	pm03	LACM 46030	Smith et al. 2005	15.5	14.9	36.8	38.3	1.0	2.4	?	?	?	9.5	10
Allosaurus	C/	pm04	LACM 46030	Smith et al. 2005	16.3	13.5	37.7	39.0	0.8	2.3	?	?	?	9.8	10
Allosaurus	L	pm05	LACM 46030	Smith et al. 2005	17.5	12.8	38.9	40.3	0.7	2.2	?	?	?	11	11
Megaraptor	L	mx5	MUCPv 595	Pers. Obs.	8.1	3.8	14.2	16.5	0.5	1.8	6.8	2.9	0.4		17.5

Megaraptor	R	mx2	MUCPv 595	Pers. Obs.	6.2	3.2	11.4	11.3	0.5	1.8	5.7	3.3	0.6		?
Megaraptor	R	mx5	MUCPv 595	Pers. Obs.	8.1	3.9	13.7	15.3	0.5	1.7	6.4	3.4	0.5		15
Megaraptor	R	mx7	MUCPv 595	Pers. Obs.	7.4	3.6	12.4	13.7	0.5	1.7	6.4	3.2	0.5		17.5
Megaraptor	R	mx9	MUCPv 595	Pers. Obs.	7.7	3.7	10.6	13.7	0.5	1.4	5.9	3.4	0.6		?
Megaraptor	R	mx10	MUCPv 595	Pers. Obs.	7.7	3.5	11.2	13.9	0.5	1.5	6.6	3.2	0.5		17.5
Aerosteon	C/	Isolated	MCNA-PV-3137	Pers. Obs.	16.5	8.4	33.3	34.8	0.5	2.0	13.4	6.4	0.5	15	14
Neovenator	/	Isolated	MIWG 6348	Pers. Obs.	14.3	7.7	24.9	29.0	0.5	1.7	12.2	6.1	0.5	15	15
Neovenator	/	Isolated	MIWG 6348	Pers. Obs.	13.7	7.8	20.6	23.0	0.6	1.5	9.5	5.4	0.6	15	18
Neovenator	/	Isolated	MIWG 6348	Pers. Obs.	18.1	9.8	40.2	36.6	0.5	2.2	13.9	8.6	0.6	15	14.5
Fukuiraptor	/	Isolated	NDC-P0001	Molnar et al. 2009	16.8	6.2	34.8	40.4	0.4	2.1	?	?	?	?	?
Australovenator	M	Isolated	AODF 604-341	Hocknull et al. 2009	7.2	5.1	13.8	14.5	0.7	1.9	5.5	?	?	?	?
Australovenator	M	Isolated	AODF 604-42	Hocknull et al. 2009	6.8	5.3	14.6	16.7	0.8	2.1	6.0	?	?	?	?
Australovenator	/	Isolated	AODF 604-343a	Hocknull et al. 2009	8.3	4.0	12.5	16.3	0.5	1.5	6.3	?	?	?	?
Australovenator	/	Isolated	AODF 604-343b	Hocknull et al. 2009	11.1	5.9	20.9	23.7	0.5	1.9	10.0	?	?	?	?
Australovenator	/	Isolated	AODF 604-342	Hocknull et al. 2009	9.3	5.0	17.2	20.1	0.5	1.9	8.2	?	?	?	?
Australovenator	/	Isolated	AODF 604-344	Hocknull et al. 2009	10.8	6.4	22.0	25.6	0.6	2.0	9.3	?	?	?	?
Acrocanthosaurus	/	Isolated	SMU Acrocan.	Pers. Obs.	30.7	19.0	95.4	89.5	0.6	3.1	24.2	16.1	0.7	10	12
Acrocanthosaurus	/	Isolated	SMU 73417	Pers. Obs.	23.1	10.6	58.9	60.8	0.5	2.5	17.6	9.3	0.5	20	14
Acrocanthosaurus	R	pm01	NCSM 14345	Pers. Obs.	21.1	16.2	49.1	50.4	0.8	2.3	15.6	13.5	0.9	18	11.5
Acrocanthosaurus	R	pm03	NCSM 14345	Pers. Obs.	28.6	16.6	63.4	62.9	0.6	2.2	18.0	13.0	0.7	18	13.33
Acrocanthosaurus	L	pm01	NCSM 14345	Pers. Obs.	20.6	20.8	49.5	49.2	1.0	2.4	15.7	13.8	0.9	19	13
Acrocanthosaurus	L	pm03	NCSM 14345	Pers. Obs.	24.1	16.6	63.4	59.5	0.7	2.6	18.2	12.6	0.7	17	12
Acrocanthosaurus	L	mx01	NCSM 14345	Pers. Obs.	26.0	16.9	51.8	63.6	0.6	2.0	17.9	10.1	0.6	16	13.33
Acrocanthosaurus	L	mx02	NCSM 14345	Pers. Obs.	38.9	20.3	90.1	93.6	0.5	2.3	27.6	16.4	0.6	15	13
Acrocanthosaurus	C/	pm01	NCSM 14345	Smith et al. 2005	21.7	16.3	52.2	55.2	0.7	2.4	?	?	?	15.1	14.1
Acrocanthosaurus	C/	pm03	NCSM 14345	Smith et al. 2005	26.8	16.6	72.4	77.5	0.6	2.7	?	?	?	12.4	13.7
Acrocanthosaurus	C/	mx01	NCSM 14345	Smith et al. 2005	26.7	17.6	62.6	71.3	0.7	2.3	?	?	?	12	14.2
Acrocanthosaurus	C/	mx02	NCSM 14345	Smith et al. 2005	35.2	20.6	79.2	90.0	0.6	2.2	?	?	?	12.3	13.4
Acrocanthosaurus	C/	mx04	NCSM 14345	Smith et al. 2005	36.6	20.6	87.1	97.5	0.6	2.4	?	?	?	12.1	13.6
Acrocanthosaurus	C/	mx05	NCSM 14345	Smith et al. 2005	42.1	20.7	93.1	107.9	0.5	2.2	?	?	?	12.8	12.9
Acrocanthosaurus	L	mx13	NCSM 14345	Smith et al. 2005	22.4	10.9	33.8	41.9	0.5	1.5	?	?	?	15	16
Acrocanthosaurus	C/	mx14	NCSM 14345	Smith et al. 2005	17.1	8.6	25.0	32.1	0.5	1.5	?	?	?	18	15
Acrocanthosaurus	R	mx03	NCSM 14345	Smith et al. 2005	37.2	21.4	90.8	101.5	0.6	2.4	?	?	?	11	15.3
Acrocanthosaurus	R	mx06	NCSM 14345	Smith et al. 2005	40.8	17.9	82.3	90.3	0.4	2.0	?	?	?	13	12
Acrocanthosaurus	R	mx08	NCSM 14345	Smith et al. 2005	31.9	16.7	66.8	76.6	0.5	2.1	?	?	?	11.3	14.9
Acrocanthosaurus	R	mx09	NCSM 14345	Smith et al. 2005	29.1	14.4	55.0	64.0	0.5	1.9	?	?	?	13	13.3
Acrocanthosaurus	R	mx11	NCSM 14345	Smith et al. 2005	26.6	11.8	39.4	46.5	0.4	1.5	?	?	?	15.5	13.8
Acrocanthosaurus	L	d01	NCSM 14345	Smith et al. 2005	14.4	11.8	29.5	35.4	0.8	2.0	?	?	?	13.4	13.3
Acrocanthosaurus	C/	d02	NCSM 14345	Smith et al. 2005	23.9	17.1	58.6	63.6	0.7	2.4	?	?	?		13
Acrocanthosaurus	L	d03	NCSM 14345	Smith et al. 2005	29.6	17.6	72.2	79.2	0.6	2.4	?	?	?	13.55	15
Acrocanthosaurus	C/	d04	NCSM 14345	Smith et al. 2005	29.1	19.3	70.6	77.8	0.7	2.4	?	?	?	13.3	11.5
Acrocanthosaurus	L	d05	NCSM 14345	Smith et al. 2005	30.6	18.8	60.5	68.8	0.6	2.0	?	?	?	13.3	13
Acrocanthosaurus	C/	d07	NCSM 14345	Smith et al. 2005	31.1	17.2	64.9	76.1	0.6	2.1	?	?	?	15.9	16.5
Acrocanthosaurus	L	d08	NCSM 14345	Smith et al. 2005	26.1	16.6	43.0	58.1	0.6	1.6	?	?	?	15	13.3
Acrocanthosaurus	L	d10	NCSM 14345	Smith et al. 2005	28.3	14.4	47.5	55.5	0.5	1.7	?	?	?	17	14.5
Acrocanthosaurus	L	d12	NCSM 14345	Smith et al. 2005	25.0	13.2	39.0	49.0	0.5	1.6	?	?	?	17	15.5
Acrocanthosaurus	L	d14	NCSM 14345	Smith et al. 2005	20.4	11.5	33.1	38.9	0.6	1.6	?	?	?	10	15
Acrocanthosaurus	L	d17	NCSM 14345	Smith et al. 2005	15.4	9.1	16.0	22.6	0.6	1.0	?	?	?	12.5	16.7
Acrocanthosaurus	R	d05	NCSM 14345	Smith et al. 2005	29.0	16.5	68.2	72.2	0.6	2.4	?	?	?	17.5	17.5

Acrocanthosaurus	R	d06	NCSM 14345	Smith et al. 2005	31.4	16.7	62.2	73.0	0.5	2.0	?	?	?	14	12.8
Eocarcharia	/	Isolated	MNN GAD14	Pers. Obs.	24.0	11.5	42.0	45.3	0.5	1.8	16.1	8.9	0.6	14	16
Eocarcharia	/	Isolated	MNN GAD14	Sereno & Brusatte 2008	24.0	11.0	48.0	57.0	0.5	2.0	?	?	?	?	?
Carcharodontosaurus	R	mx03	SGM Din-1	Smith et al. 2005	41.5	15.2	71.0	82.3	0.4	1.7	?	?	?	8	9
Carcharodontosaurus	R	mx05	SGM Din-1	Smith et al. 2005	41.0	14.9	74.0	80.6	0.4	1.8	?	?	?	7.7	9
Carcharodontosaurus	R	mx06	SGM Din-1	Smith et al. 2005	41.2	14.9	73.2	79.5	0.4	1.8	?	?	?	8.9	9
Carcharodontosaurus	R	mx08	SGM Din-1	Smith et al. 2005	39.9	14.5	74.0	80.0	0.4	1.9	?	?	?	8	8.2
Carcharodontosaurus	/	Isolated	SGM Din-1	Smith et al. 2005	41.5	15.1	80.7	89.8	0.4	1.9	?	?	?	8	10
Carcharodontosaurus	/	Isolated	SGM Din-1	Smith et al. 2005	46.7	16.9	97.6	102.3	0.4	2.1	?	?	?	8	9
Carcharodontosaurus	R	mx03	SGM Din-1	Pers. Obs.	40.6	17.1	72.0	81.0	0.4	1.8	29.4	15.9	0.5	7	8.5
Carcharodontosaurus	R	mx05	SGM Din-1	Pers. Obs.	41.4	16.6	73.0	75.0	0.4	1.8	32.5	15.6	0.5	8	9.5
Carcharodontosaurus	R	mx06	SGM Din-1	Pers. Obs.	41.1	15.5	69.0	77.0	0.4	1.7	30.0	12.4	0.4	8	9
Carcharodontosaurus	/	Isolated	SGM Din-1	Pers. Obs.	40.4	15.9	80.9	93.4	0.4	2.0	32.8	13.6	0.4	7.5	10
Carcharodontosaurus	/	Isolated	UCRC PV6	Pers. Obs.	45.1	16.8	102.6	113.0	0.4	2.3	37.1	16.1	0.4	8	8.5
Carcharodontosaurus	/	Isolated	MNN IGV6	Pers. Obs.	43.8	22.6	85.0	89.9	0.5	1.9	32.6	16.1	0.5	9	10.5
Carcharodontosaurus	/	Isolated	MNN IGV10	Pers. Obs.	30.1	19.3	60.6	67.8	0.6	2.0	25.1	15.4	0.6	9.5	11.5
Carcharodontosaurus	/	Isolated	MNN GAD12	Pers. Obs.	32.1	18.2	67.4	76.6	0.6	2.1	24.5	15.9	0.6	10	14
Giganotosaurus	L	dt3	MUCPV-CH-1	Pers. Obs.	33.8	22.8	81.6	88.5	0.7	2.4	28.9	18.5	0.6	8.5	9.5
Giganotosaurus	L	dt7	MUCPV-CH-1	Pers. Obs.	37.3	20.3	79.3	86.9	0.5	2.1	30.7	16.2	0.5	9	9.5
Giganotosaurus	/	Isolated	MUCPV-CH-1	Pers. Obs.	37.8	21.1	96.0	97.7	0.6	2.5	33.3	17.5	0.5	7.5	8.5
Giganotosaurus	/	Isolated	MUCPV-CH-1	Pers. Obs.	30.9	19.4	70.4	72.5	0.6	2.3	24.9	16.0	0.6	7.5	10
Giganotosaurus	/	Isolated	MUCPV-CH-1	Pers. Obs.	34.9	14.6	72.6	72.4	0.4	2.1	29.7	13.5	0.5	9.5	10
Giganotosaurus	/	Isolated	MUCPV-CH-1	Pers. Obs.	33.2	21.6	70.2	76.0	0.6	2.1	25.1	17.1	0.7	?	9
Giganotosaurus	/	Isolated	MUCPV-CH-1	Pers. Obs.	27.8	11.8	45.5	50.8	0.4	1.6	21.3	9.2	0.4	10	10
Mapusaurus	M	Isolated	MCF-PVPH-108.166	Pers. Obs.	21.5	17.3	42.7	40.8	0.8	2.0	18.6	13.6	0.7	10	11.5
Mapusaurus	/	Isolated	MCF-PVPH-108.8	Pers. Obs.	33.0	19.7	65.4	69.8	0.6	2.0	25.6	18.1	0.7	10	?
Mapusaurus	/	Isolated	MCF-PVPH-108.9	Pers. Obs.	32.6	17.1	74.0	75.7	0.5	2.3	28.4	13.7	0.5	10	12.5
Mapusaurus	/	Isolated	MCF-PVPH-108.171	Pers. Obs.	28.9	15.4	55.1	58.6	0.5	1.9	24.7	12.6	0.5	10	12
Mapusaurus	/	Isolated	MCF-PVPH-108.10	Pers. Obs.	23.9	13.2	40.3	48.8	0.6	1.7	21.5	11.5	0.5	12	13
Mapusaurus	/	Isolated	MCF-PVPH-108.141	Pers. Obs.	23.8	12.3	38.7	46.8	0.5	1.6	20.0	9.1	0.5	?	?
Mapusaurus	/	Isolated	MCF-PVPH-108.103	Pers. Obs.	19.8	8.6	22.6	24.9	0.4	1.1	18.5	7.9	0.4	12	12
Eotyrannus	/	pmx	MIWG 1997.550	Pers. Obs.	5.7	7.0	14.8	14.7	1.2	2.6	4.6	5.4	1.2	15	14.16
Raptorex	R	pmx1	LH PV18	Pers. Obs.	2.5	4.2	6.8	7.1	1.7	2.7	2.7	2.6	1.0	20	18
Raptorex	R	pmx3	LH PV18	Pers. Obs.	3.5	5.0	9.0	9.0	1.4	2.6	3.5	3.2	0.9	19	17
Raptorex	R	pmx4	LH PV18	Pers. Obs.	3.5	4.6	8.8	7.6	1.3	2.5	3.3	3.0	0.9	20	17.5
Raptorex	M	7pxm	LH PV18	Pers. Obs.	2.7	4.6	9.4	9.5	1.7	3.5	2.0	2.5	1.3	?	17.5
Raptorex	L	mx2	LH PV18	Pers. Obs.	9.5	4.8	16.8	20.0	0.5	1.8	6.9	4.3	0.6	18	14
Raptorex	L	mx6	LH PV18	Pers. Obs.	9.8	4.2	19.4	22.3	0.4	2.0	7.2	3.5	0.5	18.33	16
Raptorex	L	mx8	LH PV18	Pers. Obs.	9.8	3.8	18.7	19.9	0.4	1.9	8.0	3.6	0.5	?	?
Raptorex	L	mx10	LH PV18	Pers. Obs.	8.1	3.3	10.0	11.3	0.4	1.2	4.8	2.4	0.5	18	18.5
Raptorex	R	dt5	LH PV18	Pers. Obs.	7.4	3.4	11.0	13.5	0.5	1.5	6.1	3.2	0.5	19	20
Raptorex	R	dt8	LH PV18	Pers. Obs.	9.6	3.8	14.3	17.4	0.4	1.5	8.0	3.6	0.5	20	18.33
Raptorex	R	dt9	LH PV18	Pers. Obs.	8.9	3.1	14.0	14.5	0.3	1.6	?	?	?	19	18
Raptorex	/	Isolated1	LH PV18	Pers. Obs.	10.7	4.0	19.1	20.3	0.4	1.8	7.6	4.1	0.5	15.5	15
Raptorex	/	Isolated2	LH PV18	Pers. Obs.	10.3	4.7	21.2	23.8	0.5	2.1	7.1	3.7	0.5	16.5	17
Raptorex	/	Isolated3	LH PV18	Pers. Obs.	8.0	4.9	18.8	18.0	0.6	2.4	6.1	3.9	0.6	16	15.5
Raptorex	/	Isolated4	LH PV18	Pers. Obs.	9.0	3.6	13.4	19.0	0.4	1.5	5.8	3.1	0.5	?	16.66
Raptorex	/	Isolated5	LH PV18	Pers. Obs.	7.0	4.2	14.2	16.4	0.6	2.0	5.2	3.2	0.6	18	15
Raptorex	/	Isolated6	LH PV18	Pers. Obs.	8.7	3.0	12.0	14.6	0.3	1.4	5.9	2.7	0.5	18	18.5

Alioramus	L	dt5	IGM 100-1844	Pers. Obs.	12.4	6.7	22.9	24.4	0.5	1.8	10.6	5.3	0.5	14	13.5
Alioramus	L	dt12	IGM 100-1844	Pers. Obs.	12.0	6.0	18.7	22.1	0.5	1.6	9.2	4.2	0.5	14.5	15
Alioramus	L	dt13	IGM 100-1844	Pers. Obs.	12.0	5.6	18.2	22.8	0.5	1.5	10.3	5.0	0.5	15	15
Alioramus	R	mx05	IGM 100-1844	Pers. Obs.	18.0	8.4	39.8	37.4	0.5	2.2	12.8	7.1	0.6	13.5	13
Alioramus	L	mx07	IGM 100-1844	Pers. Obs.	16.6	6.3	31.7	31.5	0.4	1.9	12.7	6.0	0.5	13.5	14
Alioramus	L	mx09	IGM 100-1844	Pers. Obs.	15.8	6.0	26.5	26.8	0.4	1.7	12.2	5.4	0.4	15	14
Alioramus	L	mx11	IGM 100-1844	Pers. Obs.	15.5	5.8	24.2	25.5	0.4	1.6	12.3	5.4	0.4	15	16
Alioramus	L	mx13	IGM 100-1844	Pers. Obs.	12.7	4.9	19.9	26.1	0.4	1.6	9.6	4.5	0.5	15	16
Alioramus	L	mx14	IGM 100-1844	Pers. Obs.	10.9	4.6	16.1	18.2	0.4	1.5	8.9	4.0	0.4	16	15
Alioramus	/	Isolated1	IGM 100-1844	Pers. Obs.	13.5	6.7	23.4	24.9	0.5	1.7	10.5	5.9	0.6	15	14
Alioramus	/	Isolated2	IGM 100-1844	Pers. Obs.	12.1	7.2	25.8	26.0	0.6	2.1	9.0	5.8	0.6	15	13.5
Alioramus	/	Isolated3	IGM 100-1844	Pers. Obs.	13.1	5.6	23.0	24.3	0.4	1.8	10.2	5.3	0.5	17	16
Alioramus	/	Isolated4	IGM 100-1844	Pers. Obs.	12.5	5.5	20.4	24.5	0.4	1.6	9.9	4.8	0.5	15.5	16
Alioramus	/	Isolated5	IGM 100-1844	Pers. Obs.	12.3	5.5	19.7	20.8	0.4	1.6	9.9	4.9	0.5	17	14
Alioramus	/	Isolated6	IGM 100-1844	Pers. Obs.	9.6	4.5	13.0	15.9	0.5	1.4	8.1	4.0	0.5	18	19
Gorgosaurus	R	d02	ROM1247	Smith et al. 2005	12.4	11.6	25.5	26.0	0.9	2.1	?	?	?		11
Gorgosaurus	R	d03	ROM1247	Smith et al. 2005	17.8	14.3	42.2	42.4	0.8	2.4	?	?	?	10	12.5
Gorgosaurus	R	d04	ROM1247	Smith et al. 2005	21.3	10.8	39.7	45.9	0.5	1.9	?	?	?	12	11
Gorgosaurus	R	d06	ROM1247	Smith et al. 2005	21.2	12.9	43.8	53.4	0.6	2.1	?	?	?	11	12
Gorgosaurus	R	d08	ROM1247	Smith et al. 2005	20.0	13.6	43.3	44.0	0.7	2.2	?	?	?	10.5	14
Gorgosaurus	R	d09	ROM1247	Smith et al. 2005	17.8	7.7	31.9	32.8	0.4	1.8	?	?	?	12	12.5
Gorgosaurus	R	d11	ROM1247	Smith et al. 2005	18.5	11.4	37.0	41.4	0.6	2.0	?	?	?	10	13
Gorgosaurus	R	d13	ROM1247	Smith et al. 2005	17.7	9.2	31.3	41.5	0.5	1.8	?	?	?	10	15
Gorgosaurus	R	d15	ROM1247	Smith et al. 2005	13.7	8.8	22.2	24.9	0.6	1.6	?	?	?		14
Gorgosaurus	R	mx04	ROM1247	Smith et al. 2005	26.5	13.4	54.9	58.8	0.5	2.1	?	?	?	9	11.5
Gorgosaurus	R	mx09	ROM1247	Smith et al. 2005	20.6	10.6	40.3	36.9	0.5	2.0	?	?	?	12.5	11
Gorgosaurus	L	d03	USNM 12814	Pers. Obs.	22.2	15.8	40.0	45.1	0.7	1.8	16.4	13.4	0.8	9.5	10
Gorgosaurus	L	d07	USNM 12814	Pers. Obs.	20.6	14.6	38.9	45.0	0.7	1.9	18.2	12.1	0.7	11	10.5
Gorgosaurus	L	d09	USNM 12814	Pers. Obs.	20.3	14.9	42.5	45.1	0.7	2.1	17.1	11.4	0.7	11	10
Gorgosaurus	L	d11	USNM 12814	Pers. Obs.	16.6	12.4	29.6	35.6	0.7	1.8	16.2	10.7	0.7	11	11
Gorgosaurus	L	d12	USNM 12814	Pers. Obs.	17.9	12.6	27.0	33.1	0.7	1.5	13.4	7.9	0.6	11	11.5
Gorgosaurus	L	d13	USNM 12814	Pers. Obs.	12.7	7.9	14.5	19.1	0.6	1.1	8.9	5.8	0.7	?	?
Daspletosaurus	R	d04	NHM R4863	Smith et al. 2005	28.8	19.8	56.0	59.0	0.7	1.9	?	?	?	11	10
Daspletosaurus	R	d08	NHM R4863	Smith et al. 2005	26.4	17.7	44.6	51.3	0.7	1.7	?	?	?	13	10
Daspletosaurus	R	d10	NHM R4863	Smith et al. 2005	24.5	18.5	53.4	57.3	0.8	2.2	?	?	?	10	10
Daspletosaurus	R	d04	NHM R4863	Pers. Obs.	29.0	20.3	56.2	60.6	0.7	1.9	18.0	12.5	0.7	12.5	10
Daspletosaurus	R	d08	NHM R4863	Pers. Obs.	26.8	18.2	43.8	51.8	0.7	1.6	20.7	13.1	0.6	11	12
Daspletosaurus	R	d10	NHM R4863	Pers. Obs.	25.9	18.3	54.4	57.3	0.7	2.1	19.6	12.5	0.6	11.5	10.5
Daspletosaurus	R	d12	NHM R4863	Pers. Obs.	16.6	11.4	23.1	24.2	0.7	1.4	13.5	8.8	0.7	18.33	15
Daspletosaurus	/	Isolated	NHM R4863	Pers. Obs.	26.9	20.4	60.8	62.2	0.8	2.3	20.5	14.7	0.7	10.5	10
Daspletosaurus	L	mx02	AMNH 5346	Smith et al. 2005	27.0	22.6	74.8	80.9	0.8	2.8	?	?	?	12	11
Daspletosaurus	R	d02	MOR 590	Smith et al. 2005	18.0	12.7	36.4	39.5	0.7	2.0	?	?	?	12	11.2
Daspletosaurus	R	d03	MOR 590	Smith et al. 2005	22.9	17.8	52.6	56.5	0.8	2.3	?	?	?	11.3	10
Daspletosaurus	R	d05	MOR 590	Smith et al. 2005	22.9	17.3	54.6	57.9	0.8	2.4	?	?	?	10.5	10.7
Daspletosaurus	R	d07	MOR 590	Smith et al. 2005	22.5	16.6	49.6	49.8	0.7	2.2	?	?	?	10	9
Daspletosaurus	R	d08	MOR 590	Smith et al. 2005	22.3	12.3	46.8	50.7	0.6	2.1	?	?	?	12.8	10
Daspletosaurus	R	d10	MOR 590	Smith et al. 2005	19.2	12.2	34.9	35.7	0.6	1.8	?	?	?	13.8	11
Albertosaurus	/	Isolated	DMNH 22019	Pers. Obs.	22.8	13.0	45.9	49.8	0.6	2.0	12.3	11.6	0.9	13	11
Tyrannosaurus	L	pm03	FMNH PR2081	Smith 2005	36.1	24.0	63.7	72.0	0.7	1.8	?	?	?	7	7.1

Tyrannosaurus	L	mx05	FMNH PR2081	Smith 2005	45.5	32.6	94.1	108.4	0.7	2.1	?	?	?	6.5	7.5
Tyrannosaurus	L	mx07	FMNH PR2081	Smith 2005	39.4	27.2	75.8	86.3	0.7	1.9	?	?	?	7.5	8.3
Tyrannosaurus	L	mx08	FMNH PR2081	Smith 2005	38.6	26.2	72.6	83.4	0.7	1.9	?	?	?	7	8.8
Tyrannosaurus	R	mx01	FMNH PR2081	Smith 2005	44.9	32.6	91.1	101.6	0.7	2.0	?	?	?	6	7
Tyrannosaurus	R	mx02	FMNH PR2081	Smith 2005	47.7	37.6	105.3	117.6	0.8	2.2	?	?	?	7	7
Tyrannosaurus	R	mx03	FMNH PR2081	Smith 2005	46.7	37.2	108.8	123.0	0.8	2.3	?	?	?	6	7
Tyrannosaurus	R	mx10	FMNH PR2081	Smith 2005	35.7	23.5	61.0	71.7	0.7	1.7	?	?	?	7	9
Tyrannosaurus	R	mx11	FMNH PR2081	Smith 2005	27.9	18.2	46.0	49.9	0.7	1.6	?	?	?	11	10
Tyrannosaurus	R	mx12	FMNH PR2081	Smith 2005	19.0	13.2	29.7	32.2	0.7	1.6	?	?	?	9	12
Tyrannosaurus	C/	d02	FMNH PR2081	Smith 2005	40.8	24.5	75.0	81.3	0.6	1.8	?	?	?	7	7
Tyrannosaurus	C/	d12	FMNH PR2081	Smith 2005	26.5	19.1	44.3	47.7	0.7	1.7	?	?	?	7.5	10.5
Tyrannosaurus	L	d03	FMNH PR2081	Smith 2005	52.1	32.7	87.4	96.0	0.6	1.7	?	?	?	6.5	6.5
Tyrannosaurus	L	d05	FMNH PR2081	Smith 2005	48.7	33.9	88.9	93.9	0.7	1.8	?	?	?	7.3	7
Tyrannosaurus	L	d06	FMNH PR2081	Smith 2005	40.2	27.4	78.1	84.2	0.7	1.9	?	?	?	9	9
Tyrannosaurus	L	d08	FMNH PR2081	Smith 2005	34.5	25.7	66.3	74.7	0.7	1.9	?	?	?	7	8
Tyrannosaurus	L	d09	FMNH PR2081	Smith 2005	34.7	24.5	63.6	66.8	0.7	1.8	?	?	?	8.8	9
Tyrannosaurus	R	mx10	MOR 1125	Smith 2005	34.2	21.3	60.7	68.0	0.6	1.8	?	?	?	8.5	9.5
Tyrannosaurus	L	mx07	MOR 555	Smith 2005	42.9	28.4	72.7	80.2	0.7	1.7	?	?	?	11.1	11
Tyrannosaurus	L	mx08	MOR 555	Smith 2005	37.3	22.8	65.1	70.5	0.6	1.7	?	?	?	9.3	10.4
Tyrannosaurus	L	mx09	MOR 555	Smith 2005	33.7	24.4	55.1	56.7	0.7	1.6	?	?	?	8.8	10.8
Tyrannosaurus	L	d03	MOR 008	Smith 2005	46.1	33.8	91.0	93.0	0.7	2.0	?	?	?	8	7
Tyrannosaurus	L	d05	MOR 008	Smith 2005	39.3	31.3	78.0	79.5	0.8	2.0	?	?	?	9	9
Tyrannosaurus	C/	d06	MOR 008	Smith 2005	38.2	27.1	75.0	76.5	0.7	2.0	?	?	?	8.3	8.5
Tyrannosaurus	R	d08	MOR 008	Smith 2005	35.0	26.6	65.0	67.0	0.8	1.9	?	?	?		9
Tyrannosaurus	R	d10	MOR 008	Smith 2005	31.5	21.0	55.0	56.5	0.7	1.7	?	?	?	9	8.5
Tyrannosaurus	C/	pm01	BHI 3033	Smith 2005	27.4	14.3	44.2	50.2	0.5	1.6	?	?	?	9.5	9.9
Tyrannosaurus	C/	pm03	BHI 3033	Smith 2005	34.9	21.8	58.7	60.0	0.6	1.7	?	?	?	9.1	9.8
Tyrannosaurus	R	pm02	BHI 3033	Smith 2005	31.8	18.0	50.1	56.3	0.6	1.6	?	?	?	9	8.5
Tyrannosaurus	R	pm04	BHI 3033	Smith 2005	30.1	19.0	52.8	53.9	0.6	1.8	?	?	?	9	8.7
Tyrannosaurus	C/	mx01	BHI 3033	Smith 2005	45.9	35.0	93.7	98.8	0.8	2.0	?	?	?	8	7.7
Tyrannosaurus	C/	mx02	BHI 3033	Smith 2005	52.0	34.2	102.2	108.0	0.7	2.0	?	?	?	7.5	7.2
Tyrannosaurus	C/	mx03	BHI 3033	Smith 2005	48.6	33.0	115.3	118.8	0.7	2.4	?	?	?	7	8.2
Tyrannosaurus	C/	mx04	BHI 3033	Smith 2005	49.7	29.6	103.4	110.8	0.6	2.1	?	?	?	8.3	8
Tyrannosaurus	C/	mx05	BHI 3033	Smith 2005	48.2	31.5	94.9	99.4	0.7	2.0	?	?	?	8	7
Tyrannosaurus	C/	mx06	BHI 3033	Smith 2005	38.5	27.2	73.7	79.4	0.7	1.9	?	?	?	4.7	4.5
Tyrannosaurus	C/	mx08	BHI 3033	Smith 2005	29.3	19.0	48.6	56.4	0.6	1.7	?	?	?	10.3	10.2
Tyrannosaurus	C/	mx09	BHI 3033	Smith 2005	32.1	21.9	55.3	56.6	0.7	1.7	?	?	?	9.5	9.9
Tyrannosaurus	L	mx11	BHI 3033	Smith 2005	21.3	14.6	32.0	32.1	0.7	1.5	?	?	?	15.1	14
Tyrannosaurus	R	mx07	BHI 3033	Smith 2005	40.2	23.6	66.3	69.9	0.6	1.6	?	?	?	8.5	9
Tyrannosaurus	C/	d01	BHI 3033	Smith 2005	26.2	18.3	45.2	46.3	0.7	1.7	?	?	?	9	8.9
Tyrannosaurus	C/	d02	BHI 3033	Smith 2005	40.7	26.4	72.0	78.0	0.6	1.8	?	?	?	7	8.2
Tyrannosaurus	C/	d03	BHI 3033	Smith 2005	46.2	32.7	95.0	96.0	0.7	2.1	?	?	?	7	7
Tyrannosaurus	C/	d04	BHI 3033	Smith 2005	46.3	31.9	89.0	90.9	0.7	1.9	?	?	?	7.3	7.7
Tyrannosaurus	C/	d06	BHI 3033	Smith 2005	37.7	27.7	62.0	66.1	0.7	1.6	?	?	?	7.7	8
Tyrannosaurus	C/	d07	BHI 3033	Smith 2005	33.4	23.2	50.5	53.5	0.7	1.5	?	?	?	8.5	9.4
Tyrannosaurus	C/	d09	BHI 3033	Smith 2005	30.6	21.4	46.8	50.6	0.7	1.5	?	?	?	8.9	9.2
Tyrannosaurus	C/	d10	BHI 3033	Smith 2005	28.1	20.4	41.6	45.0	0.7	1.5	?	?	?	9.9	10.4
Tyrannosaurus	L	d13	BHI 3033	Smith 2005	15.0	9.2	15.9	17.4	0.6	1.1	?	?	?	13.6	15.7
Tyrannosaurus	R	d05	BHI 3033	Smith 2005	45.9	32.2	77.7	79.0	0.7	1.7	?	?	?	8	7

Tyrannosaurus	R	d08	BHI 3033	Smith 2005	33.1	24.8	54.1	56.5	0.7	1.6	?	?	?	9	10
Tyrannosaurus	R	d11	BHI 3033	Smith 2005	23.6	16.6	30.3	33.1	0.7	1.3	?	?	?	11	10.9
Tyrannosaurus	R	d12	BHI 3033	Smith 2005	18.5	13.6	21.9	24.3	0.7	1.2	?	?	?	14.1	14
Tyrannosaurus	C/	pm01	AMNH 5027	Smith 2005	29.8	16.5	42.6	50.2	0.6	1.4	?	?	?	9.1	9.6
Tyrannosaurus	C/	pm03	AMNH 5027	Smith 2005	30.9	19.5	45.4	58.3	0.6	1.5	?	?	?	8.5	9.5
Tyrannosaurus	R	pm02	AMNH 5027	Smith 2005	29.9	16.9	43.6	54.3	0.6	1.5	?	?	?	8.2	8
Tyrannosaurus	R	pm04	AMNH 5027	Smith 2005	31.9	21.2	54.6	60.0	0.7	1.7	?	?	?	9	8.9
Tyrannosaurus	C/	mx01	AMNH 5027	Smith 2005	38.9	31.6	85.5	93.1	0.8	2.2	?	?	?	7.5	8.4
Tyrannosaurus	C/	mx03	AMNH 5027	Smith 2005	41.5	30.6	104.0	109.3	0.7	2.5	?	?	?	6.9	7.8
Tyrannosaurus	C/	mx05	AMNH 5027	Smith 2005	48.6	31.2	102.4	104.8	0.6	2.1	?	?	?	7	7.5
Tyrannosaurus	C/	mx06	AMNH 5027	Smith 2005	38.4	24.4	77.6	88.3	0.6	2.0	?	?	?	8	7.4
Tyrannosaurus	C/	mx07	AMNH 5027	Smith 2005	40.0	25.3	79.7	84.2	0.6	2.0	?	?	?	8.6	7.4
Tyrannosaurus	C/	mx08	AMNH 5027	Smith 2005	37.5	26.1	82.1	84.0	0.7	2.2	?	?	?	8.3	8.3
Tyrannosaurus	R	mx11	AMNH 5027	Smith 2005	25.9	16.5	37.6	42.7	0.6	1.4	?	?	?	10	10.5
Tyrannosaurus	L	mx04	AMNH 5027	Smith 2005	50.0	33.9	104.1	115.5	0.7	2.1	?	?	?	8.5	8
Tyrannosaurus	L	mx01	SDSM 12047	Smith 2005	49.5	34.8	100.9	103.7	0.7	2.0	?	?	?	7	6.5
Tyrannosaurus	L	mx02	SDSM 12047	Smith 2005	36.8	28.7	81.6	88.3	0.8	2.2	?	?	?	7	7
Tyrannosaurus	L	mx03	SDSM 12047	Smith 2005	47.2	32.8	117.1	120.7	0.7	2.5	?	?	?	7	7.5
Tyrannosaurus	L	mx04	SDSM 12047	Smith 2005	46.7	36.7	108.5	116.4	0.8	2.3	?	?	?	7	6.7
Tyrannosaurus	C/	mx08	SDSM 12047	Smith 2005	43.6	27.5	87.9	105.7	0.6	2.0	?	?	?	8	8
Tyrannosaurus	L	mx10	SDSM 12047	Smith 2005	42.5	26.7	91.3	103.5	0.6	2.1	?	?	?	8	7.8
Tyrannosaurus	C/	mx11	SDSM 12047	Smith 2005	31.0	20.2	51.1	57.9	0.7	1.7	?	?	?	7.8	8.5
Tyrannosaurus	R	mx06	SDSM 12047	Smith 2005	48.0	33.1	105.5	116.9	0.7	2.2	?	?	?		7
Tyrannosaurus	R	mx12	SDSM 12047	Smith 2005	22.5	12.8	32.1	39.3	0.6	1.4	?	?	?	9	9
Tyrannosaurus	L	d04	SDSM 12047	Smith 2005	44.9	32.9	105.6	115.9	0.7	2.4	?	?	?		6.7
Tyrannosaurus	C/	d05	SDSM 12047	Smith 2005	42.4	28.1	96.3	98.9	0.7	2.3	?	?	?	6.9	7.5
Tyrannosaurus	C/	d06	SDSM 12047	Smith 2005	40.2	28.4	82.2	93.0	0.7	2.0	?	?	?	7	7
Tyrannosaurus	L	d07	SDSM 12047	Smith 2005	39.1	26.5	74.7	80.2	0.7	1.9	?	?	?	8	9
Tyrannosaurus	C/	d08	SDSM 12047	Smith 2005	34.8	25.6	68.2	75.9	0.7	2.0	?	?	?	7.5	7.5
Tyrannosaurus	C/	d09	SDSM 12047	Smith 2005	30.9	20.6	55.6	63.5	0.7	1.8	?	?	?	8	8.5
Tyrannosaurus	R	d03	SDSM 12047	Smith 2005	46.1	31.0	99.0	109.1	0.7	2.1	?	?	?	7.2	7
Tyrannosaurus	L	d2	CMNH 9380	Pers. Obs.	30.6	44.5	82.8	103.2	1.5	2.7	26.4	28.7	1.1	6.5	8
Tyrannosaurus	L	d4	CMNH 9380	Pers. Obs.	43.4	37.6	93.5	99.6	0.9	2.2	30.0	25.9	0.9	6.5	6.5
Tyrannosaurus	L	d6	CMNH 9380	Pers. Obs.	38.4	32.6	77.0	85.1	0.8	2.0	29.4	24.1	0.8	6.5	8
Tyrannosaurus	L	d7	CMNH 9380	Pers. Obs.	34.2	28.3	66.9	67.9	0.8	2.0	26.3	19.5	0.7	7.5	8
Tyrannosaurus	L	d12	CMNH 9380	Pers. Obs.	20.2	15.8	26.2	28.3	0.8	1.3	14.6	9.9	0.7	11	12
Tyrannosaurus	R	d1	CMNH 9380	Pers. Obs.	16.5	23.6	37.2	36.2	1.4	2.3	13.6	15.5	1.1	?	8
Tyrannosaurus	R	d3	CMNH 9380	Pers. Obs.	38.1	48.6	95.6	112.3	1.3	2.5	30.6	30.2	1.0	6.5	7
Tyrannosaurus	R	d5	CMNH 9380	Pers. Obs.	40.4	42.1	87.7	84.4	1.0	2.2	29.4	24.2	0.8	7	7.5
Tyrannosaurus	R	d7	CMNH 9380	Pers. Obs.	35.7	31.7	67.7	74.8	0.9	1.9	27.4	21.7	0.8	8	9
Tyrannosaurus	R	d8	CMNH 9380	Pers. Obs.	34.8	62.4	67.8	66.0	1.8	1.9	26.7	18.4	0.7	9.5	9
Tyrannosaurus	R	d10	CMNH 9380	Pers. Obs.	29.1	22.1	46.4	52.0	0.8	1.6	22.4	15.1	0.7	9	9
Tyrannosaurus	L	d02	CMNH 9380	Smith 2005	42.3	30.9	86.6	87.8	0.7	2.0	?	?	?		9.7
Tyrannosaurus	L	d04	CMNH 9380	Smith 2005	51.1	38.0	92.1	104.1	0.7	1.8	?	?	?		9
Tyrannosaurus	L	d06	CMNH 9380	Smith 2005	46.9	35.4	82.0	87.0	0.8	1.7	?	?	?	9	10
Tyrannosaurus	C/	d07	CMNH 9380	Smith 2005	41.7	31.3	70.9	78.1	0.8	1.7	?	?	?	9	8.5
Tyrannosaurus	L	d12	CMNH 9380	Smith 2005	21.5	16.3	34.1	37.1	0.8	1.6	?	?	?	10	13
Tyrannosaurus	R	d01	CMNH 9380	Smith 2005	25.6	18.1	35.0	40.0	0.7	1.4	?	?	?	9.5	11
Tyrannosaurus	R	d03	CMNH 9380	Smith 2005	48.5	37.5	97.5	102.3	0.8	2.0	?	?	?	8	7.5

Tyrannosaurus	R	d05	CMNH 9380	Smith 2005	47.3	37.2	96.1	100.5	0.8	2.0	?	?	?	8.5	9
Tyrannosaurus	R	d08	CMNH 9380	Smith 2005	39.1	28.7	68.0	72.0	0.7	1.7	?	?	?	8	11
Tyrannosaurus	R	d10	CMNH 9380	Smith 2005	30.2	23.9	51.9	62.8	0.8	1.7	?	?	?	9	12.5
Tyrannosaurus	L	d07	NHM R7994	Pers. Obs.	35.7	25.6	59.3	72.7	0.7	1.7	26.1	19.8	0.8	9	?
Tyrannosaurus	L	d08	NHM R7994	Pers. Obs.	38.5	29.2	61.1	71.1	0.8	1.6	29.6	21.4	0.7	9	7
Tyrannosaurus	L	d09	NHM R7994	Pers. Obs.	32.3	26.8	56.5	60.1	0.8	1.8	26.0	19.8	0.8	7.5	?
Tyrannosaurus	L	d11	NHM R7994	Pers. Obs.	23.9	17.2	31.5	38.7	0.7	1.3	18.7	11.9	0.6	10	10.5
Tyrannosaurus	L	d12	NHM R7994	Pers. Obs.	17.8	12.1	16.4	24.5	0.7	0.9	13.0	8.8	0.7	11	11
Tyrannosaurus	L	d07	NHM R7994	Smith 2005	40.5	28.6	76.1	86.3	0.7	1.9	?	?	?	6.8	7.7
Tyrannosaurus	L	d08	NHM R7994	Smith 2005	38.9	33.1	65.2	79.9	0.9	1.7	?	?	?	7	7.5
Tyrannosaurus	L	d09	NHM R7994	Smith 2005	32.6	27.0	56.6	62.7	0.8	1.7	?	?	?	8.3	8
Tyrannosaurus	L	d11	NHM R7994	Smith 2005	30.5	22.1	45.6	52.6	0.7	1.5	?	?	?	10.3	9
Tyrannosaurus	L	d12	NHM R7994	Smith 2005	24.0	16.1	32.4	37.1	0.7	1.4	?	?	?	12	10.5
Tyrannosaurus	L	d13	NHM R7994	Smith 2005	18.4	10.4	22.5	26.9	0.6	1.2	?	?	?	10.5	14
Tyrannosaurus	L	mx06	LACM 150167	Smith 2005	42.1	25.8	88.8	92.4	0.6	2.1	?	?	?	8	8.5
Tyrannosaurus	R	d03	LACM 150167	Smith 2005	38.1	23.9	73.4	86.7	0.6	1.9	?	?	?	8	10
Tyrannosaurus	R	d04	LACM 150167	Smith 2005	42.1	28.9	76.0	87.9	0.7	1.8	?	?	?	8	8.5
Tyrannosaurus	R	d13	LACM 150167	Smith 2005	16.2	11.0	17.8	19.9	0.7	1.1	?	?	?	12	14
Tyrannosaurus	R	mx01	LACM 23844	Smith 2005	46.0	33.7	79.1	88.2	0.7	1.7	?	?	?		8.5
Tyrannosaurus	R	mx03	LACM 23844	Smith 2005	54.5	34.4	117.1	138.9	0.6	2.1	?	?	?	6.5	8
Tyrannosaurus	R	mx05	LACM 23844	Smith 2005	47.8	32.6	100.5	110.9	0.7	2.1	?	?	?	6.5	10
Tyrannosaurus	C/	d02	LACM 23844	Smith 2005	38.8	27.4	68.9	77.7	0.7	1.8	?	?	?		9.5
Tyrannosaurus	L	d04	LACM 23844	Smith 2005	47.1	35.1	88.0	107.4	0.7	1.9	?	?	?		10.5
Tyrannosaurus	R	d05	LACM 23844	Smith 2005	47.6	33.9	96.9	102.2	0.7	2.0	?	?	?	7.5	7
Tyrannosaurus	C/	d07	LACM 23844	Smith 2005	37.2	27.1	61.0	71.9	0.7	1.6	?	?	?	8.5	8
Tyrannosaurus	L	d08	LACM 23844	Smith 2005	41.2	28.5	85.3	96.9	0.7	2.1	?	?	?		9.5
Tyrannosaurus	L	d11	LACM 23844	Smith 2005	20.0	15.9	21.8	27.3	0.8	1.1	?	?	?		12.5
Tyrannosaurus	R	mx07	UCMP 118742	Smith 2005	45.4	35.0	83.1	94.8	0.8	1.8	?	?	?		10
Tyrannosaurus	R	mx08	UCMP 118742	Smith 2005	42.0	30.5	71.4	78.3	0.7	1.7	?	?	?	8	9
Tyrannosaurus	R	mx09	UCMP 118742	Smith 2005	41.3	33.5	73.0	88.3	0.8	1.8	?	?	?	8	10
Tyrannosaurus	R	mx11	UCMP 118742	Smith 2005	28.8	19.0	48.3	54.5	0.7	1.7	?	?	?	8	13
Tyrannosaurus	R	mx12	UCMP 118742	Smith 2005	19.1	14.0	27.0	34.3	0.7	1.4	?	?	?	11	14
Nuthetes	/	Isolated	NHM 48208	Pers. Obs.	7.7	3.6	15.0	19.2	0.5	1.9	6.0	3.4	0.6		30
Nuthetes	/	Isolated	NHM 48208	Pers. Obs.	5.4	2.7	15.5	15.0	0.5	2.9	3.9	2.2	0.6	40	35
Nuthetes	M?	Isolated	NHM 48208	Pers. Obs.	3.2	3.5	7.2	6.7	1.1	2.2	3.0	2.8	0.9	42.5	37.5
Nuthetes	/	Isolated	NHM 48208	Pers. Obs.	3.7	1.4	5.0	6.0	0.4	1.4	2.9	1.2	0.4	37.5	37.5
Nuthetes	/	Isolated	NHM 48208	Pers. Obs.	3.9	1.3	4.5	6.2	0.3	1.2	3.0	1.2	0.4	30	27.5
Nuthetes	/	Isolated	NHM 48208	Pers. Obs.	3.6	1.8	8.3	8.3	0.5	2.3	2.8	1.5	0.5	55	35
Nuthetes	/	Isolated	NHM 48208	Pers. Obs.	3.2	1.6	4.7	5.7	0.5	1.5	2.6	1.5	0.6		35
Nuthetes	/	Isolated	NHM 48208	Pers. Obs.	3.0	1.0	4.9	5.4	0.3	1.6	2.1	0.9	0.4	60	42.5
Nuthetes	/	Isolated	NHM 48208	Pers. Obs.	6.3	4.3	12.9	15.3	0.7	2.1	5.1	3.2	0.6	31.66	30
Bambiraptor	C/	d06	KUVP129737	Smith et al. 2005	2.4	1.4	5.3	7.3	0.6	2.2	?	?	?		25
Bambiraptor	C/	d08	KUVP129737	Smith et al. 2005	2.3	1.4	5.0	6.5	0.6	2.1	?	?	?		25
Bambiraptor	L	d09	KUVP129737	Smith et al. 2005	2.1	1.4	4.8	5.3	0.7	2.3	?	?	?		
Bambiraptor	R	d05	KUVP129737	Smith et al. 2005	2.4	1.6	4.9	6.8	0.7	2.1	?	?	?		30
Bambiraptor	R	d07	KUVP129737	Smith et al. 2005	2.5	1.2	5.6	6.4	0.5	2.3	?	?	?		30
Bambiraptor	L	mx04	KUVP129737	Smith et al. 2005	2.6	1.4	6.0	7.1	0.5	2.3	?	?	?		25
Bambiraptor	L	mx06	KUVP129737	Smith et al. 2005	2.4	1.2	5.9	6.9	0.5	2.5	?	?	?		24.2
Bambiraptor	L	mx09	KUVP129737	Smith et al. 2005	2.5	1.0	4.6	5.1	0.4	1.8	?	?	?		32.5

Bambiraptor	/	Isolated	KUVP129737	Smith et al. 2005	3.2	1.4	5.7	7.0	0.4	1.8	?	?	?		23.7
Bambiraptor	M?	Isolated	KUVP129737	Smith et al. 2005	2.2	1.6	4.0	4.4	0.7	1.9	?	?	?		
Deinonychus	L	d01	YPM 5232 66-11	Smith et al. 2005	5.1	3.0	8.9	10.4	0.6	1.7	?	?	?	24.8	17.2
Deinonychus	L	d12	YPM 5232 66-11	Smith et al. 2005	7.1	3.2	10.1	12.3	0.5	1.4	?	?	?	29.5	17.5
Deinonychus	C/	d13	YPM 5232 66-11	Smith et al. 2005	6.8	2.9	9.6	12.3	0.4	1.4	?	?	?	27.5	16.3
Deinonychus	R	d14	YPM 5232 612	Smith et al. 2005	6.7	2.8	9.1	11.8	0.4	1.4	?	?	?	29.5	17.8
Deinonychus	R	d16	YPM 5232 612	Smith et al. 2005	5.4	2.4	6.5	8.4	0.5	1.2	?	?	?	29	17.5
Deinonychus	R	d07	YPM 5232 557	Smith et al. 2005	7.2	3.2	11.0	13.5	0.5	1.5	?	?	?	28.5	17.5
Deinonychus	R	d07	YPM 5232 557	Smith et al. 2005	7.2	3.2	11.0	13.5	0.5	1.5	?	?	?	28.5	17.5
Deinonychus	R	d08	YPM 5232 557	Smith et al. 2005	6.4	3.1	10.4	12.1	0.5	1.6	?	?	?	28.5	
Deinonychus	R	d10	YPM 5232 557	Smith et al. 2005	7.0	3.2	12.2	14.2	0.5	1.7	?	?	?	27.5	17.5
Deinonychus	R	mx01	YPM 5232 557	Smith et al. 2005	7.1	4.0	13.6	16.1	0.6	1.9	?	?	?	25	15
Deinonychus	R	pm01	YPM 5232 557	Smith et al. 2005	5.7	3.2	11.8	10.8	0.6	2.1	?	?	?	20	20
Deinonychus	L	mx03	MCZ8791	Smith et al. 2005	6.1	2.6	8.8	13.7	0.4	1.4	?	?	?	28	17.3
Dromaeosaurus	L	mx3	AMNH 5356	Pers. Obs.	8.0	4.8	18.0	21.7	0.6	2.3	6.7	4.5	0.7	17.5	18.75
Dromaeosaurus	R	mx3	AMNH 5356	Pers. Obs.	6.9	4.2	12.3	15.5	0.6	1.8	5.7	3.4	0.6	13.75	16.66
Dromaeosaurus	L	dt2	AMNH 5356	Pers. Obs.	6.0	4.5	12.8	14.0	0.7	2.1	4.8	3.3	0.7	17.5	20
Dromaeosaurus	L	dt3	AMNH 5356	Pers. Obs.	6.2	4.0	13.8	13.9	0.6	2.2	5.6	3.4	0.6	16.66	15.83
Dromaeosaurus	L	dt5	AMNH 5356	Pers. Obs.	7.2	4.1	14.8	15.3	0.6	2.0	5.9	3.3	0.6	?	?
Dromaeosaurus	L	dt8	AMNH 5356	Pers. Obs.	5.6	3.3	10.1	11.1	0.6	1.8	5.2	2.9	0.6	15	20
Dromaeosaurus	L	dt9	AMNH 5356	Pers. Obs.	6.2	3.5	10.0	11.4	0.6	1.6	5.5	2.9	0.5	?	22.5
Dromaeosaurus	M	Isolated	AMNH 5356	Pers. Obs.	4.5	4.2	10.9	11.3	0.9	2.4	3.6	3.4	0.9	15	14.5
Dromaeosaurus	M	Isolated	AMNH 5356	Pers. Obs.	5.0	6.0	13.2	12.7	1.2	2.6	4.3	4.4	1.0	14	15
Dromaeosaurus	M	Isolated	AMNH 5356	Pers. Obs.	4.2	4.2	9.0	11.0	1.0	2.1	3.5	3.3	1.0	13	14
Dromaeosaurus	C/	mx03	AMNH 5356	Smith et al. 2005	7.2	4.1	12.9	15.8	0.6	1.8	?	?	?	13.8	17
Dromaeosaurus	C/	mx04	AMNH 5356	Smith et al. 2005	6.8	3.7	11.6	14.0	0.5	1.7	?	?	?	16	20
Dromaeosaurus	L	mx05	AMNH 5356	Smith et al. 2005	7.6	4.0	12.4	16.4	0.5	1.6	?	?	?	17.5	17.5
Dromaeosaurus	C/	mx06	AMNH 5356	Smith et al. 2005	6.3	3.1	10.7	12.4	0.5	1.7	?	?	?	18.8	20
Dromaeosaurus	R	mx02	AMNH 5356	Smith et al. 2005	6.7	3.3	11.0	12.9	0.5	1.6	?	?	?	17.5	17.5
Dromaeosaurus	R	mx07	AMNH 5356	Smith et al. 2005	5.7	3.1	9.7	11.0	0.5	1.7	?	?	?		
Dromaeosaurus	L	d02	AMNH 5356	Smith et al. 2005	5.5	4.0	9.4	10.5	0.7	1.7	?	?	?	15	
Dromaeosaurus	L	d03	AMNH 5356	Smith et al. 2005	6.1	3.8	11.6	12.3	0.6	1.9	?	?	?	13.8	15
Dromaeosaurus	L	d04	AMNH 5356	Smith et al. 2005	6.5	3.9	11.2	13.1	0.6	1.7	?	?	?	17	17.5
Dromaeosaurus	L	d05	AMNH 5356	Smith et al. 2005	6.6	3.9	11.3	13.0	0.6	1.7	?	?	?	17	17.5
Dromaeosaurus	L	d08	AMNH 5356	Smith et al. 2005	5.6	3.3	8.5	10.7	0.6	1.5	?	?	?	17	17.5
Dromaeosaurus	/	Isolated	TMP 1999.055.0328	Sankey et al. 2002	3.9	2.3	8.5	?	0.6	2.2	?	?	?		20
Dromaeosaurus	/	Isolated	TMP 1989.077.0006	Sankey et al. 2002	4.5	2.9	11.5	?	0.6	2.6	?	?	?		16.3
Dromaeosaurus	/	Isolated	TMP 1989.077.0006	Sankey et al. 2002	4.7	2.8	11.0	?	0.6	2.3	?	?	?		17.5
Dromaeosaurus	/	Isolated	TMP 1992.077.0002	Sankey et al. 2002	5.9	3.9	10.5	?	0.7	1.8	?	?	?		20
Dromaeosaurus	/	Isolated	TMP 1985.068.0032	Sankey et al. 2002	5.3	4.2	14.5	?	0.8	2.7	?	?	?		17.5
Dromaeosaurus	/	Isolated	TMP 1987.153.0056	Sankey et al. 2002	5.7	3.9	9.5	?	0.7	1.7	?	?	?		17.5
Dromaeosaurus	/	Isolated	TMP 1985.036.0332	Sankey et al. 2002	3.6	2.3	6.4	?	0.6	1.8	?	?	?		25
Dromaeosaurus	/	Isolated	TMP 1995.143.0045	Sankey et al. 2002	4.1	2.8	9.0	?	0.7	2.2	?	?	?		20
Dromaeosaurus	/	Isolated	TMP 1980.008.0298	Sankey et al. 2002	4.3	2.7	9.8	?	0.6	2.3	?	?	?		15
Dromaeosaurus	/	Isolated	TMP 1980.008.0308	Sankey et al. 2002	4.9	2.7	8.5	?	0.6	1.7	?	?	?		17.5
Dromaeosaurus	/	Isolated	TMP 1981.016.0281	Sankey et al. 2002	5.0	3.2	10.0	?	0.6	2.0	?	?	?		15
Dromaeosaurus	/	Isolated	TMP 1995.406.0004	Sankey et al. 2002	5.0	3.5	11.4	?	0.7	2.3	?	?	?		17.5
Dromaeosaurus	/	Isolated	TMP 1986.130.0218	Sankey et al. 2002	5.1	3.1	10.8	?	0.6	2.1	?	?	?		16.25
Dromaeosaurus	/	Isolated	TMP 1986.130.0211	Sankey et al. 2002	5.2	3.1	9.5	?	0.6	1.8	?	?	?	15.2	15

Dromaeosaurus	/	Isolated	TMP 1981.026.0175	Sankey et al. 2002	5.4	3.2	11.0	?	0.6	2.0	?	?	?	19.8	17.5
Dromaeosaurus	/	Isolated	TMP 1998.093.0172	Sankey et al. 2002	5.4	2.9	10.5	?	0.5	1.9	?	?	?		17.5
Dromaeosaurus	/	Isolated	TMP 1981.014.0060	Sankey et al. 2002	5.5	3.7	11.5	?	0.7	2.1	?	?	?		17.5
Dromaeosaurus	/	Isolated	TMP 1995.171.0040	Sankey et al. 2002	5.5	3.7	12.3	?	0.7	2.2	?	?	?		20
Dromaeosaurus	/	Isolated	TMP 1995.171.0040	Sankey et al. 2002	6.2	3.5	14.0	?	0.6	2.3	?	?	?		20
Dromaeosaurus	/	Isolated	TMP 1966.025.0016	Sankey et al. 2002	5.7	3.3	14.0	?	0.6	2.5	?	?	?	18.6	16.25
Dromaeosaurus	/	Isolated	TMP 1979.008.0732	Sankey et al. 2002	6.1	3.9	13.0	?	0.6	2.1	?	?	?		17.5
Dromaeosaurus	/	Isolated	TMP 1980.016.2094	Sankey et al. 2002	7.1	4.0	13.5	?	0.6	1.9	?	?	?		17.5
Dromaeosaurus	/	Isolated	TMP1981.027.0066	Sankey et al. 2002	7.0	4.5	13.5	?	0.6	1.9	?	?	?		15
Dromaeosaurus	/	Isolated	TMP 1982.018.0137	Sankey et al. 2002	6.4	4.0	11.0	?	0.6	1.7	?	?	?		16.25
Dromaeosaurus	/	Isolated	TMP 1983.067.0038	Sankey et al. 2002	7.8	4.1	13.2	?	0.5	1.7	?	?	?		15
Dromaeosaurus	/	Isolated	TMP 1984.067.0115	Sankey et al. 2002	6.0	3.2	12.0	?	0.5	2.0	?	?	?	17.4	17.5
Dromaeosaurus	/	Isolated	TMP 1984.089.0048	Sankey et al. 2002	6.0	3.5	14.5	?	0.6	2.4	?	?	?		22.5
Dromaeosaurus	/	Isolated	TMP 1986.018.0099	Sankey et al. 2002	6.0	3.7	13.5	?	0.6	2.3	?	?	?		16.25
Dromaeosaurus	/	Isolated	TMP 1986.076.0011	Sankey et al. 2002	7.9	5.1	17.2	?	0.6	2.2	?	?	?		17.5
Dromaeosaurus	/	Isolated	TMP1989.155.0002	Sankey et al. 2002	7.9	4.0	14.5	?	0.5	1.8	?	?	?		16.25
Dromaeosaurus	/	Isolated	TMP 1989.036.0354	Sankey et al. 2002	6.1	3.7	13.0	?	0.6	2.1	?	?	?		15
Dromaeosaurus	/	Isolated	TMP 1993.036.0460	Sankey et al. 2002	5.4	4.0	16.5	?	0.7	3.1	?	?	?		15
Dromaeosaurus	/	Isolated	TMP 1993.036.0462	Sankey et al. 2002	6.5	3.7	13.5	?	0.6	2.1	?	?	?		17.5
Dromaeosaurus	/	Isolated	TMP 1993.036.0472	Sankey et al. 2002	6.5	4.0	13.0	?	0.6	2.0	?	?	?		18.75
Dromaeosaurus	/	Isolated	TMP 1994.012.0241	Sankey et al. 2002	7.2	3.9	15.5	?	0.5	2.2	?	?	?		18.75
Dromaeosaurus	/	Isolated	TMP 1994.012.0247	Sankey et al. 2002	7.1	4.3	15.5	?	0.6	2.2	?	?	?		15
Dromaeosaurus	/	Isolated	TMP 1994.012.0652	Sankey et al. 2002	6.4	4.3	12.5	?	0.7	2.0	?	?	?		18.75
Dromaeosaurus	/	Isolated	TMP 1994.172.0039	Sankey et al. 2002	5.6	3.9	12.0	?	0.7	2.1	?	?	?		15
Dromaeosaurus	/	Isolated	TMP 1995.127.0026a	Sankey et al. 2002	6.3	3.6	10.5	?	0.6	1.7	?	?	?		15
Dromaeosaurus	/	Isolated	TMP 1995.137.0001	Sankey et al. 2002	6.1	3.3	10.5	?	0.5	1.7	?	?	?		25
Dromaeosaurus	/	Isolated	TMP 1996.012.0362	Sankey et al. 2002	6.3	3.9	13.5	?	0.6	2.1	?	?	?		16.25
Dromaeosaurus	/	Isolated	TMP 1995.151.0010	Sankey et al. 2002	6.8	3.3	13.0	?	0.5	1.9	?	?	?		18.75
Dromaeosaurus	/	Isolated	TMP 1979.014.1000	Sankey et al. 2002	4.2	2.7	8.8	?	0.6	2.1	?	?	?		15
Dromaeosaurus	/	Isolated	TMP 1979.015.0002	Sankey et al. 2002	5.5	3.9	13.0	?	0.7	2.4	?	?	?		15
Dromaeosaurus	/	Isolated	TMP 1981.016.0161	Sankey et al. 2002	4.0	3.0	10.5	?	0.8	2.6	?	?	?		15
Dromaeosaurus	/	Isolated	TMP 1981.022.0093	Sankey et al. 2002	3.5	2.7	7.8	?	0.8	2.2	?	?	?		17.5
Dromaeosaurus	/	Isolated	TMP 1984.089.0047	Sankey et al. 2002	5.0	4.1	11.0	?	0.8	2.2	?	?	?		16.25
Dromaeosaurus	/	Isolated	TMP 1985.036.0336	Sankey et al. 2002	4.9	3.5	11.0	?	0.7	2.2	?	?	?		20
Dromaeosaurus	/	Isolated	TMP 1985.052.0010	Sankey et al. 2002	3.8	2.0	6.5	?	0.5	1.7	?	?	?		22.5
Dromaeosaurus	/	Isolated	TMP 1985.059.0081	Sankey et al. 2002	5.5	3.4	12.0	?	0.6	2.2	?	?	?		16.25
Dromaeosaurus	/	Isolated	TMP 1985.068.0047	Sankey et al. 2002	4.9	2.5	9.8	?	0.5	2.0	?	?	?		16.25
Dromaeosaurus	/	Isolated	TMP 1986.054.0067	Sankey et al. 2002	3.8	2.8	8.0	?	0.7	2.1	?	?	?		17.5
Dromaeosaurus	/	Isolated	TMP 1988.050.0127	Sankey et al. 2002	4.1	2.5	10.0	?	0.6	2.4	?	?	?		17.5
Dromaeosaurus	/	Isolated	TMP 1990.145.0001	Sankey et al. 2002	5.8	3.9	10.7	?	0.7	1.8	?	?	?		15
Dromaeosaurus	/	Isolated	TMP 1994.012.0266	Sankey et al. 2002	3.8	2.9	9.2	?	0.8	2.4	?	?	?		15
Dromaeosaurus	/	Isolated	TMP 1995.134.0005	Sankey et al. 2002	5.1	4.2	11.0	?	0.8	2.2	?	?	?		17.5
Dromaeosaurus	/	Isolated	TMP 1995.151.0008	Sankey et al. 2002	4.3	3.1	10.5	?	0.7	2.4	?	?	?		17.5
Dromaeosaurus	/	Isolated	TMP 1995.181.0009	Sankey et al. 2002	3.0	2.1	7.3	?	0.7	2.4	?	?	?		20
Dromaeosaurus	/	Isolated	Bobs site	Sankey et al. 2002	6.0	4.6	13.0	?	0.8	2.2	?	?	?		15
Dromaeosaurus	/	Isolated	TMP 1980.008.0214	Longrich 2008	5.0	3.1	9.0	?	0.6	1.8	?	?	?		25.1
Dromaeosaurus	/	Isolated	TMP 1985.066.0056	Longrich 2008	5.2	3.0	11.0	?	0.6	2.1	?	?	?	14.2	15.2
Dromaeosaurus	/	Isolated	TMP 2001.012.0181	Longrich 2008	7.3	4.5	12.5	?	0.6	1.7	?	?	?	15.2	14.7
Velociraptor	L	pmx1	AMNH 6515	Pers. Obs.	3.7	1.5	6.2	7.3	0.4	1.7	3.2	1.7	0.5		35

Velociraptor	L	pmx4	AMNH 6515	Pers. Obs.	3.9	1.8	5.9	6.3	0.5	1.5	2.7	1.1	0.4		30
Velociraptor	L	mx04	AMNH 6515	Pers. Obs.	4.8	1.8	7.9	9.6	0.4	1.7	3.8	1.5	0.4		30
Velociraptor	L	dt01	AMNH 6515	Pers. Obs.	2.7	1.2	5.1	5.7	0.4	1.9	2.3	0.9	0.4		32.5
Velociraptor	R	mx02	AMNH 6515	Pers. Obs.	2.9	1.2	2.9	4.5	0.4	1.0	1.9	1.2	0.6		30
Velociraptor	R	mx05	AMNH 6515	Pers. Obs.	4.5	2.0	8.0	10.2	0.4	1.8	2.1	?	?		?
Velociraptor	R	mx08	AMNH 6515	Pers. Obs.	4.3	1.7	7.8	9.3	0.4	1.8	3.4	1.7	0.5		27.5
Velociraptor	L	pm01	AMNH 6515	Smith et al. 2005	3.6	1.5	5.9	6.8	0.4	1.6	?	?	?		30
Velociraptor	L	pm03	AMNH 6515	Smith et al. 2005	3.3	1.5	4.4	5.9	0.5	1.3	?	?	?		30
Velociraptor	R	mx02	AMNH 6515	Smith et al. 2005	4.2	1.5	6.7	8.4	0.3	1.6	?	?	?		27.5
Velociraptor	R	mx04	AMNH 6515	Smith et al. 2005	4.4	2.2	7.9	9.5	0.5	1.8	?	?	?	37.5	30
Velociraptor	R	mx06	AMNH 6515	Smith et al. 2005	4.0	1.6	6.9	9.1	0.4	1.8	?	?	?	37.5	25
Velociraptor	R	mx08	AMNH 6515	Smith et al. 2005	3.1	0.8	4.7	5.1	0.3	1.5	?	?	?	40	30
Velociraptor	L	d01	AMNH 6515	Smith et al. 2005	2.4	1.2	4.3	5.0	0.5	1.8	?	?	?		30
Velociraptor	L	mx01	uncat, IGM	Smith et al. 2005	4.5	2.8	7.6	9.2	0.6	1.7	?	?	?		25
Velociraptor	L	mx03	uncat, IGM	Smith et al. 2005	6.1	2.5	9.9	12.5	0.4	1.6	?	?	?		25
Velociraptor	L	mx05	uncat, IGM	Smith et al. 2005	6.0	2.4	9.9	12.9	0.4	1.7	?	?	?		20
Velociraptor	L	mx06	uncat, IGM	Smith et al. 2005	4.7	1.6	6.8	9.1	0.3	1.4	?	?	?		22.5
Velociraptor	R	mx05	uncat, IGM	Smith et al. 2005	4.7	2.0	9.4	10.3	0.4	2.0	?	?	?		
Velociraptor	R	mx08	uncat, IGM	Smith et al. 2005	4.6	2.0	9.3	10.5	0.4	2.0	?	?	?		25
Unpublished dromaeosaurid	R	pmx1	uncat, UC	Pers. Obs.	4.8	7.4	12.1	16.6	1.5	2.5	5.7	3.8	0.7		17.5
Unpublished dromaeosaurid	R	pmx2	uncat, UC	Pers. Obs.	8.6	6.2	20.7	19.8	0.7	2.4	6.6	4.1	0.6		16.66
Unpublished dromaeosaurid	R	pmx3	uncat, UC	Pers. Obs.	8.8	5.8	18.4	19.3	0.7	2.1	6.1	3.6	0.6		16
Unpublished dromaeosaurid	R	mx1	uncat, UC	Pers. Obs.	12.1	5.1	21.0	35.8	0.4	1.7	9.1	5.2	0.6		16
Unpublished dromaeosaurid	R	mx3	uncat, UC	Pers. Obs.	14.3	5.8	30.0	36.8	0.4	2.1	9.8	4.5	0.5	17.5	16.25
Unpublished dromaeosaurid	R	mx4	uncat, UC	Pers. Obs.	10.5	5.5	23.0	27.0	0.5	2.2	8.1	4.0	0.5	17.5	15
Unpublished dromaeosaurid	R	mx5	uncat, UC	Pers. Obs.	13.1	5.7	26.0	33.5	0.4	2.0	11.3	6.4	0.6	20	13.75
Unpublished dromaeosaurid	R	mx6	uncat, UC	Pers. Obs.	11.0	5.3	20.5	22.7	0.5	1.9	6.7	3.8	0.6	20	17
Unpublished dromaeosaurid	R	mx7	uncat, UC	Pers. Obs.	11.1	4.8	25.0	28.0	0.4	2.3	8.7	4.3	0.5	?	14.5
Saurornitholestes	/	Isolated	TMP 1995.177.0048c	Sankey et al. 2002	2.1	0.9	3.4	?	0.4	1.6	?	?	?		35
Saurornitholestes	/	Isolated	TMP 1995.180.0004	Sankey et al. 2002	2.1	0.7	3.5	?	0.3	1.7	?	?	?		25
Saurornitholestes	/	Isolated	TMP 1995.092.0027	Sankey et al. 2002	2.8	1.4	6.5	?	0.5	2.3	?	?	?		22.5
Saurornitholestes	/	Isolated	TMP 1987.154.0063	Sankey et al. 2002	3.4	1.9	8.1	?	0.6	2.4	?	?	?		21.25
Saurornitholestes	/	Isolated	TMP 1987.154.0064	Sankey et al. 2002	4.2	2.0	8.5	?	0.5	2.0	?	?	?		22.5
Saurornitholestes	/	Isolated	TMP 1987.079.0090	Sankey et al. 2002	4.4	1.9	8.5	?	0.4	1.9	?	?	?		20
Saurornitholestes	/	Isolated	TMP 1995.177.0048a	Sankey et al. 2002	2.9	1.5	6.0	?	0.5	2.1	?	?	?		20
Saurornitholestes	/	Isolated	TMP 1995.177.0048b	Sankey et al. 2002	1.9	1.0	4.7	?	0.5	2.5	?	?	?		27.5
Saurornitholestes	/	Isolated	TMP 1995.092.0016	Sankey et al. 2002	5.0	2.2	12.5	?	0.4	2.5	?	?	?		20
Saurornitholestes	/	Isolated	TMP 1995.092.0016	Sankey et al. 2002	5.0	2.2	13.5	?	0.4	2.7	?	?	?		22.5
Saurornitholestes	/	Isolated	TMP 1987.153.0055	Sankey et al. 2002	6.0	2.9	12.0	?	0.5	2.0	?	?	?		20
Saurornitholestes	/	Isolated	TMP 1987.077.0120	Sankey et al. 2002	5.3	3.2	11.3	?	0.6	2.1	?	?	?		18.75

Saurornitholestes	/	Isolated	TMP 1995.092.0054	Sankey et al. 2002	6.9	3.1	13.0	?	0.4	1.9	?	?	?		20
Saurornitholestes	/	Isolated	TMP 1995.092.0028	Sankey et al. 2002	2.0	1.1	5.0	?	0.6	2.5	?	?	?		25
Saurornitholestes	/	Isolated	TMP 1987.062.0087	Sankey et al. 2002	4.4	2.3	10.3	?	0.5	2.3	?	?	?		20
Saurornitholestes	/	Isolated	TMP 1988.121.0039	Currie & Varricchio 2004	5.1	2.3	9.0	?	0.5	1.8	?	?	?	30	20
Saurornitholestes	/	Isolated	TMP 2003.012.0083	Longrich 2008	5.0	2.5	7.9	?	0.5	1.6	?	?	?	31	26.3
Saurornitholestes	/	Isolated	TMP 2000.057.0080	Longrich 2008	3.8	2.3	7.9	?	0.6	2.1	?	?	?		19.4
Saurornitholestes	/	Isolated	TMP 2002.079.0004	Longrich 2008	5.1	2.1	9.0	?	0.4	1.8	?	?	?	29.9	19.5
Saurornitholestes	/	Isolated	TMP 2002.079.0003	Longrich 2008	5.3	2.1	9.1	?	0.4	1.7	?	?	?	30.7	25.3
Saurornitholestes	/	Isolated	TMP 1974.010.0001	Larson & Currie 2013	4.2	2.3	8.5	?	0.5	2.0	?	?	?	32.5	20
Saurornitholestes	/	Isolated	TMP 1974.010.0001	Larson & Currie 2013	4.0	2.0	7.9	?	0.5	2.0	?	?	?	35.5	22
Saurornitholestes	/	Isolated	TMP 1987.158.0078	Sankey et al. 2002	2.7	1.1	4.2	?	0.4	1.6	?	?	?		32.5
Saurornitholestes	/	Isolated	TMP 1987.019.0068	Sankey et al. 2002	2.0	1.0	4.6	?	0.5	2.3	?	?	?		30
Saurornitholestes	/	Isolated	TMP 1987.031.0054	Sankey et al. 2002	2.4	1.1	4.8	?	0.5	2.0	?	?	?		27.5
Saurornitholestes	/	Isolated	TMP 1987.004.0047	Sankey et al. 2002	2.2	0.7	4.1	?	0.3	1.9	?	?	?		35
Saurornitholestes	/	Isolated	TMP 1987.048.0077	Sankey et al. 2002	4.6	1.7	6.7	?	0.4	1.5	?	?	?		25
Saurornitholestes	/	Isolated	TMP 1995.127.0025c	Sankey et al. 2002	3.7	1.8	6.7	?	0.5	1.8	?	?	?		21.25
Saurornitholestes	/	Isolated	TMP 1995.147.0026	Sankey et al. 2002	1.9	0.7	2.8	?	0.4	1.5	?	?	?		32.5
Saurornitholestes	/	Isolated	TMP 1995.151.0010	Sankey et al. 2002	2.4	0.9	3.9	?	0.4	1.6	?	?	?		32.5
Saurornitholestes	/	Isolated	TMP 1995.181.0011	Sankey et al. 2002	1.9	1.0	5.0	?	0.5	2.6	?	?	?		25
Saurornitholestes	/	Isolated	TMP 1996.012.0366	Sankey et al. 2002	4.2	1.5	6.3	?	0.4	1.5	?	?	?		22.5
Saurornitholestes	/	Isolated	TMP 1987.158.0080	Sankey et al. 2002	3.9	1.9	9.0	?	0.5	2.3	?	?	?		21.25
Saurornitholestes	/	Isolated	TMP 1987.158.0081	Sankey et al. 2002	4.3	2.0	11.2	?	0.5	2.6	?	?	?		25
Saurornitholestes	/	Isolated	TMP 1987.033.0055	Sankey et al. 2002	4.0	2.1	9.9	?	0.5	2.5	?	?	?		20
Saurornitholestes	/	Isolated	TMP 1987.036.0392	Sankey et al. 2002	5.5	2.2	13.0	?	0.4	2.4	?	?	?		20
Saurornitholestes	/	Isolated	TMP 1987.051.0023	Sankey et al. 2002	3.8	1.4	8.2	?	0.4	2.2	?	?	?		25
Saurornitholestes	/	Isolated	TMP 1987.072.0023	Sankey et al. 2002	4.9	2.2	9.6	?	0.4	2.0	?	?	?		20
Saurornitholestes	/	Isolated	TMP 1987.072.0026	Sankey et al. 2002	5.0	2.3	13.0	?	0.5	2.6	?	?	?		20
Saurornitholestes	/	Isolated	TMP 1987.072.0004	Sankey et al. 2002	5.4	2.5	13.0	?	0.5	2.4	?	?	?		20
Saurornitholestes	/	Isolated	TMP 1995.012.0109	Sankey et al. 2002	5.9	2.8	13.0	?	0.5	2.2	?	?	?		18.75
Saurornitholestes	/	Isolated	TMP 1995.126.0029	Sankey et al. 2002	5.0	2.1	12.0	?	0.4	2.4	?	?	?		25
Saurornitholestes	/	Isolated	TMP 1995.127.0025a	Sankey et al. 2002	5.3	2.3	11.8	?	0.4	2.2	?	?	?		21.25
Saurornitholestes	/	Isolated	TMP 1995.127.0025b	Sankey et al. 2002	4.5	1.8	7.8	?	0.4	1.7	?	?	?		23.75
Saurornitholestes	/	Isolated	TMP 1995.127.0025d	Sankey et al. 2002	4.2	1.7	7.5	?	0.4	1.8	?	?	?		20
Saurornitholestes	/	Isolated	TMP 1995.129.0002	Sankey et al. 2002	4.9	2.2	9.6	?	0.4	2.0	?	?	?		20
Saurornitholestes	/	Isolated	TMP 1995.131.0012	Sankey et al. 2002	5.1	2.1	9.5	?	0.4	1.9	?	?	?		20
Saurornitholestes	/	Isolated	TMP 1995.137.0002a	Sankey et al. 2002	5.0	2.3	9.2	?	0.5	1.8	?	?	?		20
Saurornitholestes	/	Isolated	TMP 1995.137.0002b	Sankey et al. 2002	4.9	2.1	10.5	?	0.4	2.1	?	?	?		20
Saurornitholestes	/	Isolated	TMP 1995.179.0003	Sankey et al. 2002	4.7	2.2	10.4	?	0.5	2.2	?	?	?		21.25
Saurornitholestes	/	Isolated	TMP 1995.019.0004	Sankey et al. 2002	4.2	1.5	8.0	?	0.4	1.9	?	?	?		22.5
Saurornitholestes	/	Isolated	TMP 1995.002.0018	Sankey et al. 2002	4.2	2.5	10.5	?	0.6	2.5	?	?	?		18.75
Saurornitholestes	/	Isolated	TMP 1995.406.0005	Sankey et al. 2002	4.7	2.0	10.3	?	0.4	2.2	?	?	?		25
Saurornitholestes	/	Isolated	TMP 1996.012.0361	Sankey et al. 2002	5.9	2.7	13.0	?	0.5	2.2	?	?	?		20
Saurornitholestes	/	Isolated	TMP 1996.012.0363	Sankey et al. 2002	4.8	2.0	9.2	?	0.4	1.9	?	?	?		20
Saurornitholestes	/	Isolated	TMP 1996.012.0038	Sankey et al. 2002	5.1	2.1	11.7	?	0.4	2.3	?	?	?		25
Saurornitholestes	/	Isolated	TMP 1987.036.0011	Sankey et al. 2002	4.5	2.4	9.5	?	0.5	2.1	?	?	?		20
Saurornitholestes	/	Isolated	TMP 1987.043.0005	Sankey et al. 2002	5.7	2.1	11.2	?	0.4	2.0	?	?	?		22.5
Saurornitholestes	/	Isolated	TMP 1987.046.0053	Sankey et al. 2002	4.8	2.2	9.4	?	0.5	2.0	?	?	?		20
Saurornitholestes	/	Isolated	TMP 1996.012.0102	Sankey et al. 2002	5.5	3.2	11.2	?	0.6	2.0	?	?	?		25
Saurornitholestes	/	Isolated	TMP 1996.012.0104	Sankey et al. 2002	5.6	2.6	10.8	?	0.5	1.9	?	?	?		20

Saurornitholestes	/	Isolated	TMP 1996.012.0112	Sankey et al. 2002	7.9	2.8	16.0	?	0.4	2.0	?	?	?		18.75
Saurornitholestes	/	Isolated	TMP 1996.012.0115	Sankey et al. 2002	5.5	2.7	14.0	?	0.5	2.5	?	?	?		21.25
Saurornitholestes	/	Isolated	TMP 1996.012.0118	Sankey et al. 2002	5.1	2.2	9.0	?	0.4	1.8	?	?	?		27.5
Saurornitholestes	/	Isolated	TMP 1996.012.0034	Sankey et al. 2002	6.4	2.6	13.0	?	0.4	2.0	?	?	?		18.75
Saurornitholestes	/	Isolated	TMP 1996.012.0360	Sankey et al. 2002	5.0	1.9	9.0	?	0.4	1.8	?	?	?		21.25
Saurornitholestes	/	Isolated	TMP 1996.012.0364	Sankey et al. 2002	5.3	2.1	9.0	?	0.4	1.7	?	?	?		20
Saurornitholestes	/	Isolated	TMP 1995.182.0021	Sankey et al. 2002	3.5	1.7	7.6	?	0.5	2.2	?	?	?		20
Saurornitholestes	/	Isolated	TMP 1995.184.0023	Sankey et al. 2002	3.7	1.9	8.3	?	0.5	2.2	?	?	?		20
Saurornitholestes	/	Isolated	TMP 1995.021.0005	Sankey et al. 2002	4.7	2.4	9.2	?	0.5	2.0	?	?	?		18.75
Saurornitholestes	/	Isolated	TMP 1987.112.0010	Sankey et al. 2002	3.8	1.6	8.7	?	0.4	2.3	?	?	?		30
Saurornitholestes	/	Isolated	TMP 1987.112.0021	Sankey et al. 2002	5.6	1.4	6.3	?	0.3	1.1	?	?	?		23.75
Saurornitholestes	/	Isolated	TMP 1987.112.0009	Sankey et al. 2002	4.2	2.0	8.1	?	0.5	1.9	?	?	?		21.25
Saurornitholestes	/	Isolated	TMP 1987.112.0028	Sankey et al. 2002	5.5	2.2	11.5	?	0.4	2.1	?	?	?		21.25
Saurornitholestes	/	Isolated	TMP 1987.050.0100	Sankey et al. 2002	5.2	2.2	8.2	?	0.4	1.6	?	?	?		21.25
Saurornitholestes	/	Isolated	TMP 1987.036.0184	Sankey et al. 2002	3.5	1.9	7.5	?	0.5	2.1	?	?	?		21.25
Saurornitholestes	/	Isolated	TMP 1987.036.0418	Sankey et al. 2002	4.1	2.6	9.5	?	0.6	2.3	?	?	?		22.5
Saurornitholestes	/	Isolated	TMP 1987.036.0070	Sankey et al. 2002	4.1	2.4	9.5	?	0.6	2.3	?	?	?		20
Saurornitholestes	/	Isolated	TMP 1987.036.0093	Sankey et al. 2002	5.3	2.5	11.8	?	0.5	2.2	?	?	?		23.75
Saurornitholestes	/	Isolated	TMP 1995.012.0031	Sankey et al. 2002	5.0	2.4	10.5	?	0.5	2.1	?	?	?		20
Saurornitholestes	/	Isolated	TMP 1995.012.0033	Sankey et al. 2002	6.0	2.3	13.0	?	0.4	2.2	?	?	?		17.5
Saurornitholestes	/	Isolated	TMP 1995.012.0038	Sankey et al. 2002	5.7	2.2	11.0	?	0.4	1.9	?	?	?		18.75
Saurornitholestes	/	Isolated	TMP 1995.012.0040	Sankey et al. 2002	3.5	2.0	7.8	?	0.6	2.2	?	?	?		18.75
Saurornitholestes	/	Isolated	TMP 1995.012.0042	Sankey et al. 2002	2.9	1.7	7.0	?	0.6	2.4	?	?	?		22.5
Saurornitholestes	/	Isolated	TMP 1995.012.0043	Sankey et al. 2002	5.0	2.3	12.0	?	0.5	2.4	?	?	?		20
Saurornitholestes	/	Isolated	TMP 1995.012.0074a	Sankey et al. 2002	5.1	2.4	10.2	?	0.5	2.0	?	?	?		20
Saurornitholestes	/	Isolated	TMP 1995.012.0074b	Sankey et al. 2002	3.8	1.6	6.3	?	0.4	1.7	?	?	?		22.5
Saurornitholestes	/	Isolated	TMP 1995.012.0074c	Sankey et al. 2002	4.9	2.2	9.4	?	0.4	1.9	?	?	?		26.25
Saurornitholestes	/	Isolated	TMP 1995.124.0004	Sankey et al. 2002	3.3	1.5	6.2	?	0.5	1.9	?	?	?		21.25
Saurornitholestes	/	Isolated	TMP 1987.036.0068	Sankey et al. 2002	5.7	2.4	11.2	?	0.4	2.0	?	?	?		22.5
Saurornitholestes	/	Isolated	TMP 1987.050.0038	Sankey et al. 2002	6.3	2.4	14.2	?	0.4	2.3	?	?	?		20
Saurornitholestes	/	Isolated	TMP 2005.049.0096	Longrich 2008	4.7	2.3	8.0	?	0.5	1.7	?	?	?	34.3	17.9
Saurornitholestes	/	Isolated	TMP 2005.049.0119	Longrich 2008	6.0	2.5	11.7	?	0.4	1.9	?	?	?	29.2	22.9
Saurornitholestes	/	Isolated	TMP 2005.049.0120	Longrich 2008	5.8	2.5	11.3	?	0.4	1.9	?	?	?		27.7
Saurornitholestes	/	Isolated	TMP 2005.049.0074	Longrich 2008	4.4	2.5	9.2	?	0.6	2.1	?	?	?		21.4
Saurornitholestes	/	Isolated	TMP 2005.049.0023	Longrich 2008	4.9	2.5	8.7	?	0.5	1.8	?	?	?	27.5	19.1
Saurornitholestes	/	Isolated	TMP 2005.039.0007	Longrich 2008	4.3	2.0	7.2	?	0.5	1.7	?	?	?	35.1	21.6
Saurornitholestes	/	Isolated	TMP 2005.039.0001	Longrich 2008	5.3	2.4	10.8	?	0.5	2.0	?	?	?	25.9	18.9
Saurornitholestes	/	Isolated	TMP 2005.012.0028	Longrich 2008	3.9	1.8	5.7	?	0.5	1.4	?	?	?		21.9
Saurornitholestes	/	Isolated	TMP 2005.009.0047	Longrich 2008	5.2	2.8	10.8	?	0.5	2.1	?	?	?		20.2
Saurornitholestes	/	Isolated	TMP 2004.116.0026	Longrich 2008	5.7	2.7	11.6	?	0.5	2.0	?	?	?		21.4
Saurornitholestes	/	Isolated	TMP 2004.103.0017	Longrich 2008	3.7	1.6	4.4	?	0.4	1.2	?	?	?		18.4
Saurornitholestes	/	Isolated	TMP 2004.012.0019	Longrich 2008	5.1	2.4	8.2	?	0.5	1.6	?	?	?	30.5	20.3
Saurornitholestes	/	Isolated	TMP 2003.012.0132	Longrich 2008	5.4	2.4	9.2	?	0.4	1.7	?	?	?	30.9	21
Saurornitholestes	/	Isolated	TMP 2002.060.0006	Longrich 2008	6.5	3.7	9.7	?	0.6	1.5	?	?	?	30.5	17.9
Saurornitholestes	/	Isolated	TMP 2001.012.0183	Longrich 2008	4.7	2.2	7.7	?	0.5	1.6	?	?	?	42.1	21.7
Saurornitholestes	/	Isolated	TMP 2001.012.0180	Longrich 2008	5.6	2.5	8.3	?	0.4	1.5	?	?	?	43.2	27.2
Saurornitholestes	/	Isolated	TMP 2002.060.0008	Longrich 2008	5.6	2.4	10.0	?	0.4	1.8	?	?	?		20.2
Saurornitholestes	/	Isolated	TMP 2000.012.0111	Longrich 2008	5.8	2.4	11.0	?	0.4	1.9	?	?	?	34.4	22.5
Saurornitholestes	/	Isolated	TMP 2000.057.0006	Longrich 2008	5.8	3.2	11.5	?	0.5	2.0	?	?	?		19.1

Saurornitholestes	/	Isolated	TMP 2000.012.0116	Longrich 2008	4.7	2.6	10.1	?	0.6	2.2	?	?	?		24
Saurornitholestes	/	Isolated	TMP 2000.012.0114	Longrich 2008	4.8	2.4	7.6	?	0.5	1.6	?	?	?	24.4	21.5
Saurornitholestes	/	Isolated	TMP 2005.012.??	Longrich 2008	7.5	3.7	12.9	?	0.5	1.7	?	?	?		24.5
Saurornitholestes	/	Isolated	TMP 2004.012.0018	Longrich 2008	7.1	3.1	8.4	?	0.4	1.2	?	?	?		26.8
Saurornitholestes	/	Isolated	TMP 2003.012.0189	Longrich 2008	5.3	2.8	10.1	?	0.5	1.9	?	?	?		19.4
Saurornitholestes	/	Isolated	TMP 1983.036.0236	Longrich 2008	3.8	1.8	7.5	?	0.5	2.0	?	?	?	41.7	30.5
Saurornitholestes	/	Isolated	TMP 1995.012.0026	Longrich 2008	1.7	0.8	2.2	?	0.5	1.3	?	?	?	30.6	27.1
Atrociraptor	?	?	TMP1995.166.0001	Currie & Varricchio 2004	5.0	3.5	10.0	?	0.7	2.0	?	?	?	13.5	11.5
Atrociraptor	?	?	TMP1995.166.0001	Currie & Varricchio 2004	5.5	3.5	12.0	?	0.6	2.2	?	?	?	17.5	15
Atrociraptor	?	?	TMP1995.166.0001	Currie & Varricchio 2004	5.2	2.8	7.5	?	0.5	1.4	?	?	?	25	20
Atrociraptor	?	?	TMP1995.166.0001	Currie & Varricchio 2004	5.2	2.6	7.0	?	0.5	1.3	?	?	?	40	20
Atrociraptor	/	Isolated	TMP 1993.012.0021	Larson & Currie 2013	5.0	2.5	7.7	?	0.5	1.5	?	?	?	15.5	14
Atrociraptor	/	Isolated	TMP 2005.007.0003	Larson & Currie 2013	5.2	2.4	8.4	?	0.5	1.6	?	?	?	26	16
Atrociraptor	/	Isolated	TMP 1990.082.0018	Larson & Currie 2013	5.8	2.9	9.1	?	0.5	1.6	?	?	?	25	16
Atrociraptor	/	Isolated	TMP 1990.082.0108	Larson & Currie 2013	5.2	2.8	9.4	?	0.5	1.8	?	?	?	14.5	14
Atrociraptor	/	Isolated	TMP 1990.082.0017	Larson & Currie 2013	4.7	2.4	7.6	?	0.5	1.6	?	?	?	25.5	17.5
Atrociraptor	/	Isolated	TMP 1990.082.0021	Larson & Currie 2013	4.7	2.4	6.6	?	0.5	1.4	?	?	?	29	15.25
Atrociraptor	/	Isolated	TMP 1986.064.0003	Larson & Currie 2013	5.1	2.6	9.6	?	0.5	1.9	?	?	?	25	17
Atrociraptor	/	Isolated	TMP 1986.064.0002	Larson & Currie 2013	3.2	1.6	4.1	?	0.5	1.3	?	?	?	26	15
Atrociraptor	/	Isolated	TMP 1985.012.0002	Larson & Currie 2013	3.2	1.7	5.1	?	0.5	1.6	?	?	?	25	15
Atrociraptor	/	Isolated	TMP 1985.098.0002	Larson & Currie 2013	5.5	2.6	9.5	?	0.5	1.7	?	?	?	27	17.5
Atrociraptor	/	Isolated	TMP 1984.064.0003	Larson & Currie 2013	4.3	1.9	5.5	?	0.4	1.3	?	?	?	38.5	23.5
Atrociraptor	/	Isolated	TMP 1984.064.0012	Larson & Currie 2013	4.5	2.3	7.3	?	0.5	1.6	?	?	?	26	17.5
Atrociraptor	/	Isolated	TMP 1984.079.0004	Larson & Currie 2013	5.6	2.6	8.0	?	0.5	1.4	?	?	?	25.5	16.5
Atrociraptor	/	Isolated	TMP 1965.016.0150	Larson & Currie 2013	4.7	2.6	7.2	?	0.5	1.5	?	?	?		18.5
Atrociraptor	/	Isolated	TMP 1999.050.0117	Larson & Currie 2013	4.1	2.0	6.4	?	0.5	1.6	?	?	?	28.5	17.5
Atrociraptor	/	Isolated	TMP 2000.045.0035	Larson & Currie 2013	3.9	2.1	5.8	?	0.5	1.5	?	?	?	27	20
Atrociraptor	/	Isolated	TMP 2000.045.0103	Larson & Currie 2013	4.9	2.4	10.2	?	0.5	2.1	?	?	?	22.5	15.5
Atrociraptor	/	Isolated	TMP 2003.045.0049	Larson & Currie 2013	4.2	2.2	6.6	?	0.5	1.6	?	?	?	23	20
Zapsalis	/	Isolated	AMNH FR 3953	Cope 1876	6.5	3.0	12.0	?	0.5	1.8	?	?	?		15.15
Zapsalis	/	Isolated	TMP 1984.163.0080	Sankey et al. 2002	6.1	2.4	10.0	?	0.4	1.6	?	?	?		16.25
Zapsalis	/	Isolated	TMP 1980.016.0833	Sankey et al. 2002	6.3	3.2	11.0	?	0.5	1.7	?	?	?		17.5
Zapsalis	/	Isolated	TMP 1982.019.0458	Sankey et al. 2002	5.7	2.5	12.5	?	0.4	2.2	?	?	?		17.5
Zapsalis	/	Isolated	TMP 1982.019.0458	Sankey et al. 2002	5.8	2.5	13.0	?	0.4	2.2	?	?	?		17.5
Zapsalis	/	Isolated	TMP 1982.019.0007	Sankey et al. 2002	7.2	3.2	15.0	?	0.4	2.1	?	?	?		15
Zapsalis	/	Isolated	TMP 1985.058.0065	Sankey et al. 2002	5.4	2.5	10.5	?	0.5	1.9	?	?	?		17.5
Zapsalis	/	Isolated	TMP 1985.006.0002	Sankey et al. 2002	6.5	3.0	13.0	?	0.5	2.0	?	?	?		16.25
Zapsalis	/	Isolated	TMP 1986.077.0112	Sankey et al. 2002	7.9	3.1	14.0	?	0.4	1.8	?	?	?		16.25
Zapsalis	/	Isolated	TMP 1987.036.0005	Sankey et al. 2002	6.6	3.0	15.5	?	0.5	2.3	?	?	?		16.25
Zapsalis	/	Isolated	TMP 1989.036.0312	Sankey et al. 2002	6.4	3.1	11.5	?	0.5	1.8	?	?	?		16.25
Zapsalis	/	Isolated	TMP 1994.012.0268	Sankey et al. 2002	5.8	2.5	11.0	?	0.4	1.9	?	?	?		18.75
Zapsalis	/	Isolated	TMP 1997.133.0002	Sankey et al. 2002	6.3	3.4	12.0	?	0.5	1.9	?	?	?		17.5
Zapsalis	/	Isolated	TMP 1979.015.0003	Sankey et al. 2002	6.3	3.0	15.5	?	0.5	2.5	?	?	?		15
Zapsalis	/	Isolated	TMP 1984.091.0040	Sankey et al. 2002	6.0	3.0	12.5	?	0.5	2.1	?	?	?		16.25
Zapsalis	/	Isolated	TMP 1984.091.0040	Sankey et al. 2002	6.4	3.0	12.0	?	0.5	1.9	?	?	?		15
Zapsalis	/	Isolated	TMP 1985.006.0131	Sankey et al. 2002	6.3	2.4	11.2	?	0.4	1.8	?	?	?		17.5
Zapsalis	/	Isolated	TMP 1985.006.0133	Sankey et al. 2002	6.4	3.0	11.7	?	0.5	1.8	?	?	?		16.25
Zapsalis	/	Isolated	TMP 1986.036.0425	Sankey et al. 2002	7.0	3.0	12.0	?	0.4	1.7	?	?	?		15
Zapsalis	/	Isolated	TMP 1987.050.0008	Sankey et al. 2002	6.8	3.3	13.7	?	0.5	2.0	?	?	?		15

Zapsalis	/	Isolated	TMP 1989.050.0202	Sankey et al. 2002	5.3	2.1	9.3	?	0.4	1.8	?	?	?		16.25
Zapsalis	/	Isolated	TMP 1990.050.0208	Sankey et al. 2002	5.8	2.6	11.5	?	0.4	2.0	?	?	?		17.5
Zapsalis	/	Isolated	TMP 1990.053.0021	Sankey et al. 2002	5.0	2.3	11.0	?	0.5	2.2	?	?	?		17.5
Zapsalis	/	Isolated	TMP 1991.050.0060	Sankey et al. 2002	6.4	2.5	14.0	?	0.4	2.2	?	?	?		15
Troodon	/	Isolated	Fukui 22	Larson & Currie 2013	5.7	2.6	8.7	?	0.5	1.5	?	?	?	11	12
Troodon	/	Isolated	p7412	Farlow et al. 1991	6.2	3.4	9.0	?	0.5	1.5	?	?	?	4.7	7.8
Troodon	/	Isolated	TMP 2000.012.0117	Longrich 2008	4.5	2.2	6.7	?	0.5	1.5	?	?	?	12	11.2
Troodon	/	Isolated	TMP 1996.012.0072	Longrich 2008	5.0	2.6	8.6	?	0.5	1.7	?	?	?	10	8.9
Troodon	/	Isolated	TMP 1995.012.0011	Longrich 2008	5.4	2.7	8.0	?	0.5	1.5	?	?	?		10.8
Troodon	/	Isolated	TMP 1995.021.0010	Longrich 2008	5.0	2.8	6.9	?	0.6	1.4	?	?	?	9.2	10
Troodon	/	Isolated	TMP 1989.089.0004	Longrich 2008	3.0	1.5	3.9	?	0.5	1.3	?	?	?		16.9
Troodon	/	Isolated	TMP 1987.050.0034	Longrich 2008	3.3	1.8	4.6	?	0.5	1.4	?	?	?		10.3
Troodon	/	Isolated	TMP 1986.216.0004	Longrich 2008	4.9	2.3	6.6	?	0.5	1.3	?	?	?		10.5
Troodon	/	Isolated	TMP 1987.036.0139	Longrich 2008	5.9	2.7	8.4	?	0.5	1.4	?	?	?	13.2	11.3
Troodon	/	Isolated	TMP 1989.050.0129	Longrich 2008	4.0	2.0	4.2	?	0.5	1.0	?	?	?		9.9
Troodon	/	Isolated	TMP 1986.177.0008	Longrich 2008	3.5	1.6	3.4	?	0.4	1.0	?	?	?		14.9
Troodon	/	Isolated	TMP 1985.066.0073	Longrich 2008	3.3	1.7	4.6	?	0.5	1.4	?	?	?		12.1
Troodon	/	Isolated	TMP 1989.116.0063	Longrich 2008	3.4	1.8	4.5	?	0.5	1.3	?	?	?	11.7	10.8
Troodon	/	Isolated	TMP 1984.089.0275	Longrich 2008	5.2	2.4	8.8	?	0.5	1.7	?	?	?	11.4	9.8
Troodon	/	Isolated	TMP 1986.023.0091	Longrich 2008	2.9	1.3	3.6	?	0.4	1.2	?	?	?		16.1
Troodon	/	Isolated	TMP 1986.008.0093	Longrich 2008	3.6	1.7	3.3	?	0.5	0.9	?	?	?		14.8
Troodon	/	Isolated	TMP 1986.130.0016	Longrich 2008	5.0	2.4	7.4	?	0.5	1.5	?	?	?	15.2	12.7
Troodon	/	Isolated	TMP 1983.036.0214	Longrich 2008	4.3	2.7	6.5	?	0.6	1.5	?	?	?	7	8.2
Troodon	/	Isolated	TMP 1985.056.0182	Longrich 2008	5.9	3.3	10.4	?	0.6	1.8	?	?	?	12.1	9.6
Troodon	/	Isolated	TMP 1985.056.0179	Longrich 2008	5.8	2.9	7.7	?	0.5	1.3	?	?	?		10.2
Troodon	/	Isolated	TMP 1986.054.0066	Longrich 2008	1.5	1.1	2.3	?	0.7	1.5	?	?	?	13.8	11
Troodon	/	Isolated	TMP 1987.036.0301	Longrich 2008	4.2	1.9	5.2	?	0.5	1.3	?	?	?	7.1	8.1
Troodon	/	Isolated	TMP 1987.077.0135	Longrich 2008	3.6	1.7	3.5	?	0.5	1.0	?	?	?		14.7
Troodon	/	Isolated	TMP 1995.127.0027	Park 2000	5.2	2.8	7.6	?	0.5	1.5	?	?	?	10	10
Troodon	/	Isolated	TMP 1990.034.0001	Larson & Currie 2013	4.7	2.0	6.0	?	0.4	1.3	?	?	?		12
Troodon	/	Isolated	TMP 1986.202.0005	Larson & Currie 2013	2.5	1.3	3.1	?	0.5	1.2	?	?	?		20
Troodon	M	Isolated	DMNH 22837	Pers. Obs.	4.5	4.5	9.8	9.4	1.0	2.2	4.3	3.6	0.8	5.5	7
Troodon	/	Isolated	DMNH 22670	Pers. Obs.	5.1	3.8	8.8	9.6	0.7	1.7	4.2	2.8	0.7	8	7
Troodon	/	Isolated	DMNH 22337	Pers. Obs.	5.7	4.2	9.8	10.7	0.7	1.7	6.0	3.5	0.6	11	9.25
Troodon	/	Isolated	MOR 553	Smith et al. 2005	4.9	2.4	7.2	8.7	0.5	1.5	?	?	?	20	11.3
Troodon	/	Isolated	MOR 553	Smith et al. 2005	6.0	3.0	9.4	10.4	0.5	1.6	?	?	?	10	8.8
Troodon	/	Isolated	MOR 553	Smith et al. 2005	5.6	2.7	8.5	8.9	0.5	1.5	?	?	?	10	12.5
Troodon	/	Isolated	MOR 553	Smith et al. 2005	5.2	2.3	7.8	9.7	0.4	1.5	?	?	?	12.5	12.5
Troodon	/	Isolated	MOR 553	Smith et al. 2005	4.5	1.6	7.3	7.4	0.4	1.6	?	?	?	12.5	12.5
Zanabazar	L	mx04	IGM 100-1	Smith et al. 2005	3.6	2.7	5.0	6.9	0.7	1.4	?	?	?		15
Zanabazar	L	mx06	IGM 100-1	Smith et al. 2005	3.7	2.7	5.5	7.8	0.7	1.5	?	?	?		10
Zanabazar	L	mx07	IGM 100-1	Smith et al. 2005	4.3	2.5	5.6	7.4	0.6	1.3	?	?	?		10
Zanabazar	L	mx12	IGM 100-1	Smith et al. 2005	3.8	2.5	6.5	8.5	0.7	1.7	?	?	?		15
Zanabazar	C/	mx14	IGM 100-1	Smith et al. 2005	4.1	2.5	6.4	7.2	0.6	1.6	?	?	?		
Zanabazar	C/	mx16	IGM 100-1	Smith et al. 2005	3.8	2.3	6.2	8.0	0.6	1.7	?	?	?		12.5
Zanabazar	R	mx05	IGM 100-1	Smith et al. 2005	3.0	2.5	4.3	5.3	0.8	1.4	?	?	?		10
Zanabazar	R	mx09	IGM 100-1	Smith et al. 2005	4.1	2.6	6.3	6.6	0.6	1.5	?	?	?		10
Pectinodon	/	Isolated	UCMP187076	Sankey 2008	2.2	1.0	3.0	?	0.5	1.4	?	?	?		20
Pectinodon	/	Isolated	UCMP187075	Sankey 2008	2.7	1.0	4.5	?	0.4	1.7	?	?	?		18.75

Pectinodon	/	Isolated	UCMP187073	Sankey 2008	2.9	1.1	4.3	?	0.4	1.5	?	?	?		17.5
Pectinodon	/	Isolated	UCMP187074	Sankey 2008	2.7	1.1	4.2	?	0.4	1.6	?	?	?		20
Pectinodon	/	Isolated	UCMP187067	Sankey 2008	2.7	1.0	3.8	?	0.4	1.4	?	?	?		17.5
Pectinodon	/	Isolated	UCMP187068	Sankey 2008	2.6	1.0	3.1	?	0.4	1.2	?	?	?		22.5
Pectinodon	/	Isolated	UCMP187069	Sankey 2008	2.7	1.0	4.1	?	0.4	1.5	?	?	?		20
Pectinodon	/	Isolated	UCMP187066	Sankey 2008	3.0	1.0	3.5	?	0.3	1.2	?	?	?		15
Pectinodon	/	Isolated	UCMP187063	Sankey 2008	2.4	0.9	3.9	?	0.4	1.6	?	?	?		20
Pectinodon	/	Isolated	UCMP187065	Sankey 2008	2.0	1.0	4.1	?	0.5	2.1	?	?	?		15
Pectinodon	/	Isolated	UCMP187059	Sankey 2008	2.1	0.8	3.2	?	0.4	1.5	?	?	?		25
Pectinodon	/	Isolated	UCMP214059	Sankey 2008	1.9	1.3	3.4	?	0.7	1.8	?	?	?		15
Pectinodon	/	Isolated	UCMP186886	Sankey 2008	3.2	1.0	4.0	?	0.3	1.3	?	?	?		15
Pectinodon	/	Isolated	AMNH5731 #2	Longrich 2008	2.5	1.1	4.4	?	0.4	1.8	?	?	?		9.6
Pectinodon	/	Isolated	AMNH5731 #1	Longrich 2008	2.4	0.9	3.9	?	0.4	1.6	?	?	?		10.1
Pectinodon	/	Isolated	AMNH5731 #3	Longrich 2008	2.4	1.0	4.2	?	0.4	1.8	?	?	?		9.9
Pectinodon	/	Isolated	AMNH5728.1	Longrich 2008	2.5	1.1	4.9	?	0.5	2.0	?	?	?	25.3	14.5
Pectinodon	/	Isolated	AMNH5728.2	Longrich 2008	2.9	1.1	5.0	?	0.4	1.7	?	?	?		16
Pectinodon	/	Isolated	AMNH5728.3	Longrich 2008	2.9	1.1	4.9	?	0.4	1.7	?	?	?	32.4	15.9
Pectinodon	/	Isolated	AMNH5719.1	Longrich 2008	2.7	1.0	3.9	?	0.4	1.4	?	?	?		15.3
Pectinodon	/	Isolated	AMNH5719.2	Longrich 2008	2.5	0.9	3.3	?	0.3	1.3	?	?	?		18.7
Pectinodon	/	Isolated	AMNH5719.3	Longrich 2008	2.6	0.8	3.2	?	0.3	1.2	?	?	?		16.4
Pectinodon	/	Isolated	AMNH5502.1	Longrich 2008	2.7	1.2	5.6	?	0.4	2.0	?	?	?		17
Pectinodon	/	Isolated	AMNH5502.2	Longrich 2008	2.6	1.2	4.8	?	0.4	1.8	?	?	?	29.7	16.9
Pectinodon	/	Isolated	AMNH5502.3	Longrich 2008	2.5	1.2	4.3	?	0.5	1.7	?	?	?	57.9	19.1
Pectinodon	/	Isolated	AMNH5733.1	Longrich 2008	2.3	0.9	4.3	?	0.4	1.8	?	?	?		10
Pectinodon	/	Isolated	AMNH5706.1	Longrich 2008	2.2	0.6	2.6	?	0.3	1.2	?	?	?		19.8
Pectinodon	/	Isolated	AMNH5706.2	Longrich 2008	2.4	0.6	2.7	?	0.3	1.2	?	?	?		20.2
Pectinodon	/	Isolated	AMNH5706.3	Longrich 2008	2.4	0.7	2.6	?	0.3	1.1	?	?	?		19.5
Pectinodon	/	Isolated	AMNH5489.1	Longrich 2008	3.1	1.5	5.6	?	0.5	1.8	?	?	?		7.8
Pectinodon	/	Isolated	AMNH5489.2	Longrich 2008	2.9	1.2	4.4	?	0.4	1.5	?	?	?		10.5
Pectinodon	/	Isolated	AMNH5489.3	Longrich 2008	2.6	1.1	4.5	?	0.4	1.8	?	?	?		8.7
Pectinodon	/	Isolated	AMNH5725.1	Longrich 2008	2.7	1.1	3.7	?	0.4	1.4	?	?	?		14.4
Pectinodon	/	Isolated	AMNH5725.2	Longrich 2008	2.5	1.1	3.1	?	0.4	1.2	?	?	?		18.7
Pectinodon	/	Isolated	UCMP186904	Sankey 2008	2.0	0.7	3.0	?	0.4	1.5	?	?	?		17.5
Pectinodon	/	Isolated	UCMP128845	Sankey 2008	3.2	1.1	4.6	?	0.3	1.4	?	?	?		20
Pectinodon	/	Isolated	UCMP128787	Sankey 2008	3.6	1.7	4.6	?	0.5	1.3	?	?	?		12.5
Pectinodon	/	Isolated	UCMP186868	Sankey 2008	2.2	0.9	2.9	?	0.4	1.3	?	?	?		20
Pectinodon	/	Isolated	UCMP186885	Sankey 2008	2.1	0.7	3.0	?	0.3	1.4	?	?	?		22.5
Richardoestesia	/	Isolated	TMP 1983.036.0233	Sankey et al. 2002	4.7	2.3	12.3	?	0.5	2.6	?	?	?		26.3
Richardoestesia	/	Isolated	TMP 1983.036.0242	Sankey et al. 2002	3.7	1.6	8.3	?	0.4	2.2	?	?	?		35
Richardoestesia	/	Isolated	TMP 1984.092.0268	Sankey et al. 2002	3.5	1.5	5.5	?	0.4	1.6	?	?	?		35
Richardoestesia	/	Isolated	TMP 1986.023.0090	Sankey et al. 2002	4.0	1.7	10.0	?	0.4	2.5	?	?	?		35
Richardoestesia	/	Isolated	TMP 1988.091.0028	Sankey et al. 2002	2.9	1.0	5.3	?	0.3	1.8	?	?	?		35
Richardoestesia	/	Isolated	TMP 1989.076.0063	Sankey et al. 2002	2.8	0.9	5.2	?	0.3	1.9	?	?	?		35
Richardoestesia	/	Isolated	TMP 1990.106.0006	Sankey et al. 2002	1.7	0.7	4.0	?	0.4	2.4	?	?	?		47.5
Richardoestesia	/	Isolated	TMP 1995.157.0029	Sankey et al. 2002	1.4	0.7	2.8	?	0.5	2.0	?	?	?		55
Richardoestesia	/	Isolated	TMP 1982.024.0078	Longrich 2008	3.4	1.3	4.9	?	0.4	1.4	?	?	?	38.3	33.1
Richardoestesia	/	Isolated	TMP 1984.084.0247	Longrich 2008	3.1	1.5	6.1	?	0.5	2.0	?	?	?		35.2
Richardoestesia	/	Isolated	TMP 1986.023.0105	Longrich 2008	2.2	1.2	4.8	?	0.5	2.2	?	?	?		46.3
Richardoestesia	/	Isolated	TMP 1987.099.0048	Longrich 2008	2.0	1.0	5.4	?	0.5	2.7	?	?	?		47.3

Richardoestesia	/	Isolated	TMP 1987.114.0005	Longrich 2008	2.8	1.1	4.4	?	0.4	1.6	?	?	?		39.1
Richardoestesia	/	Isolated	TMP 1989.076.0083	Longrich 2008	2.9	1.2	3.4	?	0.4	1.2	?	?	?	43.9	36.5
Richardoestesia	/	Isolated	TMP 1986.171.0009	Longrich 2008	2.1	1.2	3.8	?	0.5	1.8	?	?	?		36.8
Richardoestesia	/	Isolated	TMP 1989.036.0355	Sankey et al. 2002	3.8	2.0	10.0	?	0.5	2.6	?	?	?		35
Richardoestesia	/	Isolated	TMP 1986.159.0062	Sankey et al. 2002	3.5	1.5	7.5	?	0.4	2.1	?	?	?		32.5
Richardoestesia	/	Isolated	TMP 1990.079.0031	Sankey et al. 2002	2.8	1.3	6.8	?	0.5	2.4	?	?	?		40
Richardoestesia	/	Isolated	TMP 1995.177.0049a	Sankey et al. 2002	3.2	1.2	8.5	?	0.4	2.7	?	?	?		50
Richardoestesia	/	Isolated	TMP 1995.180.0005a	Sankey et al. 2002	1.9	0.9	5.2	?	0.5	2.7	?	?	?		60
Richardoestesia	/	Isolated	TMP 1995.180.0005b	Sankey et al. 2002	1.7	0.9	4.2	?	0.5	2.5	?	?	?		0
Richardoestesia	/	Isolated	TMP 1996.048.0011	Sankey et al. 2002	2.5	1.3	5.0	?	0.5	2.0	?	?	?		40
Richardoestesia	/	Isolated	TMP 1996.062.0030a	Sankey et al. 2002	3.6	1.7	12.5	?	0.5	3.5	?	?	?		30
Richardoestesia	/	Isolated	TMP 1989.103.0025	Sankey et al. 2002	3.9	2.5	5.4	?	0.6	1.4	?	?	?		37.5
Richardoestesia	/	Isolated	TMP 1995.177.0079	Sankey et al. 2002	1.9	0.7	3.0	?	0.4	1.6	?	?	?		60
Richardoestesia	/	Isolated	TMP 1986.172.0053	Sankey et al. 2002	1.9	0.7	2.9	?	0.4	1.5	?	?	?		60
Richardoestesia	/	Isolated	TMP 1984.001.0012	Sankey et al. 2002	4.5	2.1	11.0	?	0.5	2.4	?	?	?		30
Richardoestesia	/	Isolated	TMP 1986.023.0105	Sankey et al. 2002	2.3	1.1	5.8	?	0.5	2.5	?	?	?		42.5
Richardoestesia	/	Isolated	TMP 1986.033.0054	Sankey et al. 2002	2.1	1.1	4.5	?	0.5	2.1	?	?	?		40
Richardoestesia	/	Isolated	TMP 1986.045.0046	Sankey et al. 2002	2.3	1.2	5.5	?	0.5	2.4	?	?	?		50
Richardoestesia	/	Isolated	TMP 1988.036.0199	Sankey et al. 2002	3.7	1.7	9.5	?	0.5	2.6	?	?	?		35
Richardoestesia	/	Isolated	TMP 1995.181.0010	Sankey et al. 2002	3.0	1.6	7.2	?	0.5	2.4	?	?	?		35
Richardoestesia	/	Isolated	TMP 1996.142.0019	Sankey et al. 2002	3.1	1.5	9.7	?	0.5	3.1	?	?	?		35
Richardoestesia	/	Isolated	TMP 1987.158.0076	Sankey et al. 2002	2.4	0.8	3.3	?	0.3	1.4	?	?	?		50
Richardoestesia	/	Isolated	TMP 1984.092.0205	Sankey et al. 2002	2.0	0.7	2.7	?	0.4	1.4	?	?	?		60
Richardoestesia	/	Isolated	TMP 1986.021.0068	Sankey et al. 2002	2.0	1.0	3.7	?	0.5	1.9	?	?	?		60
Richardoestesia	/	Isolated	TMP 1995.174.0052	Sankey et al. 2002	1.8	0.7	2.3	?	0.4	1.3	?	?	?		60
Richardoestesia	/	Isolated	TMP 1995.181.0010c	Sankey et al. 2002	2.2	0.8	3.3	?	0.4	1.5	?	?	?		60
Richardoestesia	/	Isolated	TMP 1995.181.0060e	Sankey et al. 2002	1.4	0.6	2.4	?	0.4	1.7	?	?	?		60
Richardoestesia	/	Isolated	TMP 1995.181.0060f	Sankey et al. 2002	1.9	0.7	2.5	?	0.4	1.3	?	?	?		60
Richardoestesia	/	Isolated	p8219366	Farlow et al. 1991	3.1	1.8	6.0	?	0.6	1.9	?	?	?		22
Richardoestesia	/	Isolated	LSUMG489:6237	Sankey et al. 2005	2.0	0.9	2.5	?	0.5	1.3	?	?	?		50
Richardoestesia	/	Isolated	LSUMG489:6235	Sankey et al. 2005	1.7	0.7	3.0	?	0.4	1.8	?	?	?		55
Richardoestesia	/	Isolated	LSUMG489:6050	Sankey et al. 2005	1.7	1.0	3.5	?	0.6	2.1	?	?	?		50
Richardoestesia	/	Isolated	LSUMG741:5933	Sankey et al. 2005	1.8	0.9	2.3	?	0.5	1.3	?	?	?		45
Richardoestesia	/	Isolated	LSUMG113:5939	Sankey et al. 2005	2.0	1.0	4.0	?	0.5	2.0	?	?	?		60

A6. Function of quadrate sub-entities.

Anatomical component	Nature	Anatomical sub-entity	Function	Theropod clades involved	Publication
Quadrate diverticulum	Tympanic sinus, mandibular arch pneumatic system	Lateral, medial and posterior pneumatic foramina	Auditory function?	All Theropoda	Witmer 1990; Kundrát and Janáček 2007; Tahara and Larsson 2011
Siphoneal diverticulum	Tympanic sinus, mandibular arch pneumatic system	Ventromedial pneumatic foramen?	Auditory function?	Allosauroidea? Tyrannosauroidea?	Tahara and Larsson 2011
Dorsal tympanic diverticulum	Tympanic sinus	Cotylus, separated into otic and squamosal capitula	Auditory function	Neognathae	Witmer 1990
Musculus Protractor Pterygoideus MPPt	Orbitotemporal muscle	Medial surface of the pterygoid ramus	Insertion for the MPPt	All Theropoda	Holliday 2009
Musculus Adductor Mandibulae Externus Medialis MAMEM	Temporal muscle	Quadrate body between otic and orbital processes	Origin for the MAMEM	Avian and non-avian? Theropoda	Sedlmayr 2002
Musculus Adductor Mandibulae Externus Superficialis MAMES	Temporal muscle	Ootic process	Origin for the MAMES	Avian and non-avian? Theropoda	Sakamoto 2008
Musculus Adductor Mandibulae Posterior MAMP	Palatal muscle	Lateral surface of the pterygoid ramus	Origin for the MAMP	All Theropoda	Molnar 1998; Sakamoto 2008; Holliday 2009
Musculus Pterygoideus Ventralis MPTv	Palatal muscle	Lateral surface of the pterygoid ramus	Insertion for the MPTv	Tyrannosauridae?	Sakamoto 2008; Holliday 2009
Musculus Pseudotemporalis Profundus MPsTP	Palatal muscle	Anterior surface of the ootic process	Origin for the MPsTP	Neornithes	Holliday and Witmer 2008; Sakamoto 2008; Holliday 2009
Otic joint	Synovial joint	Otic process of cotylus	Articulation with squamosal	All Theropoda	Holliday and Witmer 2008
Articular process of quadrate	Synovial joint	Mandibular condyles	Articulation with mandible	All Theropoda	Holliday and Witmer 2008
Intercondylar sulcus	Synovial joint	Groove between ectocondyle and entocondyle	Ventral or ventrolateral displacement of mandible rami	All Theropoda	Molnar 1991; Bakker 1998; Hendrickx and Buffetaut 2008
Branches of maxillomandibular vessels	Neurovascular bundle	Quadrate foramen	Neurovasculature transmission between the occiput and adductor chamber	Some Theropoda	Sampson and Witmer 2007

A7. Analyses on the non-avian theropod quadrate (Chapter 7)

A7.1: Character list.

I. QUADRATE

1. Quadrate, ventrodorsal elongation (ratio between the lateromedial width of the mandibular articulation and the ventrodorsal height of the quadrate body): (0) strongly elongated, <0.35; (1) moderately elongated, 0.35-0.5; (2) short, >0.5 (**Ordered**; Based on Currie & Carpenter, 2000 #20)
2. Quadrate, position of the quadrate head relative to the orbit height: (0) positioned at 80% or less of the orbit height; (1) positioned at more than 80% of the orbit height (Modified from Sereno et al. 1994)
3. Quadrate, position of the mandibular articulation relative to the quadrate head, when the quadrate is articulated within the cranium: (0) entirely posterior; (1) approximately aligned; (2) entirely anterior (**Ordered**; Modified from Gauthier, 1986)
4. Quadrate, ventral extension relative to the alveolar margin of the maxilla in lateral view: (0) projects well-ventral to the alveolar margin of the maxilla; (1) level with the alveolar margin of the maxilla; (2) well-dorsal to the alveolar margin of the maxilla (**Ordered**; Holtz, 1994)

II. QUADRATE BODY

Margins

5. Quadrate body, outline of the posterior margin in lateral view (mandibular articulation and quadrate head excluded): (0) strongly concave; (1) roughly straight; (2) convex; (3) sigmoid, convex dorsally and straight or concave ventrally; (4) sigmoid, concave dorsally and convex ventrally (Unordered; New)
6. Quadrate body, posterior surface at one half of the quadrate height in posterior view: (0) lateromedially concave; (1) lateromedially convex (New)
7. Quadrate body, outline of the ventromedial extremity in posterior view: (0) rounded; (1) angular (New)
8. Quadrate body, shallow groove on the posterior surface, medial to the quadrate foramen and extending on the first third of the quadrate height: (0) absent; (1) present (New)
9. Quadrate body, protuberant ridge dorsal to the ectocondyle, at one fourth of the quadrate height: (0) absent; (1) present (New)

Quadrate ridge

10. Quadrate ridge, shape at mid-height of the quadrate in posterior view: (0) prominent and well-delimited; (1) shallow and poorly delimited; (2) ridge absent (Unordered; New)
11. Quadrate ridge at mid-height of the quadrate, shape in posterior view (ratio: lateromedial width of ridge/lateromedial width of quadrate body, pterygoid excluded): (0) narrow crest (< 0.1); (1) rod-shaped (0.1-0.7); (2) very broad shaft (>0.7). (**Ordered**; New)
12. Quadrate ridge, lateroposterior inclination in posterior view: (0) present; (1) absent, subvertical ridge (New)
13. Quadrate ridge, ventral extension in posterior view: (0) extending well-dorsal to the entocondyle; (1) extending directly dorsal to the entocondyle; (2) reaching the entocondyle (Unordered; New)
14. Quadrate ridge, dorsal extension in posterior view: (0) extending to the quadrate head or directly ventral to it; (1) extending at two third of the quadrate height; (2) extending at mid-height of the quadrate (Unordered; New)
15. Quadrate ridge, bifurcation of the ventral extremity: (0) absent; (1) present (New)
16. Quadrate ridge, separation of the ridge at two-third of the quadrate height in dorsal view: (0) absent, ridge unique; (1) present, groove separating the ridge; (2) present, ridge fading away at two-third of the quadrate height and reappearing more dorsally (Unordered; New)
17. Quadrate ridge, protuberance at two third of the quadrate height in lateral view: (0) absent; (1) present (**New**)

III. MANDIBULAR ARTICULATION

General shape

18. Mandibular articulation, ratio between the lateromedial width and the anteroposterior length (perpendicular and at midlength): (0) <2; (1) 2-3; (2) 3-4; (3) >4 (**Ordered**; New)
19. Mandibular articulation, number of condyles: (0) two; (1) three (Chiappe, 2001 #21)
20. Mandibular articulation, step between the mandibular condyles and the quadrate body in lateral view: (0) absent; (1) present and weak, limit between mandibular condyles and quadrate body shallowly concave; (2) present and important, limit between mandibular condyles and quadrate body deeply concave (**Ordered**; New)
21. Mandibular condyles, ventral margin in posterior view: (0) biconvex, limit between the two condyles angular or slightly concave; (1) biconvex, very large concavity separating the two condyles; (2) W-shaped, ventral margin of condyles roughly flattened and angular roughly convex (Unordered; New)

22. Mandibular condyles, posterior margin in ventral view: (0) strongly biconvex; (1) very slightly biconvex, almost uniquely convex (New)
23. Mandibular condyles, size in ventral view (ratio: longest length ectocondyle/longest length entocondyle): (0) longer entocondyle (<0.9); (1) subequal in size (0.9-1.1); (2) longer ectocondyle (1.1-1.9); (3) much longer ectocondyle (>1.9). (**Ordered**; New)
24. Mandibular condyles, intercondylar notch in between the ecto- and entocondyles: (0) absent; (1) present on the anterior margin of the mandibular articulation; (2) present on the posterior margin of the mandibular articulation (Unordered; New)

Ectocondyle

25. Ectocondyle, ratio: width/length in ventral view: (0) >0.55, oval to subcircular; (1) 0.3-0.55, elliptical; (2) 0.3-0.55, parabolic; (3) <0.3, parabolic to sigmoid (Unordered; New)
26. Ectocondyle, concavity on the anterior side in anterior view: (0) absent; (1) present, shallow; (2) present, deep (Unordered; New)
27. Ectocondyle, ventral margin in anterior view: (0) convex; (1) sigmoid (New)
28. Ectocondyle, extension of the articular surface on the posterior surface of the quadrate body (ratio: width/length of articular surface in posterior view): (0) limited, <0.3; (1) moderately extended, 0.3-0.5; (2) important, >0.5 (Unordered; New)

Entocondyle

29. Entocondyle, ratio: width/length in ventral view: (0) >0.4, oval to subcircular; (1) 0.3-0.4, elliptical and moderately elongated; (2) <0.3, elliptical and strongly elongated (**Ordered**; New)
30. Entocondyle, shape in ventral view: (0) not protruding anteriorly, or very slightly; (1) strongly protruding anteriorly (New)
31. Entocondyle, extension of the articular surface on the quadrate body (ratio: width/length of articular surface in posterior view): (0) <0.25, limited; (1) 0.25-0.6, moderately extent; (2) >0.6, important (Unordered; New)

Intercondylar sulcus

32. Intercondylar sulcus in ventral view: (0) well-delimited by the mandibular condyles; (1) shallow (New)
33. Intercondylar sulcus in ventral view: (0) narrow, narrower than the entocondyle width; (1) wide, same width or larger than the entocondyle width (New)
34. Intercondylar sulcus, angle between main axis of sulcus and long axis of mandibular articulation in ventral view: (0) >135°; (1) <135° (New)

IV. QUADRATE HEAD

35. Quadrate head, exposure in lateral view: (0) quadrate head entirely or almost entirely exposed; (1) quadrate head partially exposed; (2) quadrate head completely obscured (Unordered; Sereno and Novas 1994)
36. Quadrate head size relative to mandibular articulation (ratio: mediolateral width of quadrate head/mediolateral width of mandibular articulation in posterior view): (0) >0.31; (1) 0.29-0.31; (2) 0.28-0.24; (3) < 0.24 (Unordered; New)
37. Quadrate head, shape in dorsal view: (0) one single condyle, the squamosal capitulum; (1) two slightly differentiated condyles on the top of the columnar body of the quadrate; (2) two very distinct condyles, one large and laterally positioned, the squamosal capitulum, and one smaller and ventromedially positioned, the otic capitulum (Unordered; Modified from Gauthier, 1986 and Chiappe, 1995)
38. Quadrate head (otic and squamosal capitula included), shape in dorsal view: (0) subtriangular; (1) oval or subcircular; (2) subquadrangular to subrectangular (Unordered; Modified from Sereno et al. 1998 #27)
39. Quadrate head, outline in posterior view: (0) convex or roughly flattened quadrate head; (1) strongly convex, conical and pointed quadrate head; (2) concave (Unordered; New)

V. CONTACTS

Lateral contact, general shape

40. Laterodorsal contact in lateral view: (0) only or mostly contacting quadratojugal; (1) mostly contacting squamosal; (2) contacting postorbital and squamosal (Unordered; New)
41. Lateral contacts, ratio: anteroposterior width of dorsal contact/anteroposterior width of ventral contact in lateral view: (0) <0.2; (1) 0.2-0.5; (2) >0.5 (Unordered; New)

Dorsal quadratojugal/squamosal/postorbital contact

42. Dorsal contact, shape in lateral view: (0) elongated line; (1) drop-shaped; (2) drop-shaped reversed; (3) elliptical; (4) subrectangular (Unordered; New)

43. Dorsal contact: (0) facing anteriorly; (1) facing laterally; (2) facing posterolaterally or completely posteriorly (Unordered; New)
44. Dorsal contact, surface: (0) roughly smooth; (1) irregular; (2) with two longitudinal furrows separated by a ridge; (3) with one longitudinal furrow (Unordered; New)
45. Dorsal contact, delimitation: (0) not delimited by any margin; (1) delimited posteriorly by a longitudinal ridge; (2) delimited by anterior and posterior margins (Unordered; New)
46. Dorsal contact, dorsal extension: (0) well-beneath the quadrate head; (1) almost reaching or reaching the quadrate head (New)
47. Dorsal contact, ventral projection bounding the quadrate foramen: (0) absent; (1) present, ventrodorsally short projection; (2) present, ventrodorsally tall process (**Ordered**; New)

Ventral quadratojugal contact

48. Ventral quadratojugal contact, shape in posterior view: (0) concave; (1) straight; (2) convex (Unordered; New)
49. Ventral quadratojugal contact: (0) facing posterolaterally, contact overlapping the posteroventral part of the quadrate body; (1) facing laterally; (2) facing anterolaterally (Unordered; New)
50. Ventral quadratojugal contact, shape in lateral view: (0) ovoid to D-shaped; (1) drop-shaped to d-shaped; (2) semi-circular; (3) subrectangular; (4) elongated ellipse (Unordered; New)
51. Ventral quadratojugal contact, surface: (0) with radiating ridges; (1) roughly smooth; (2) irregular and weakly grooved; (3) heavily and deeply grooved (Unordered; New)
52. Ventral quadratojugal contact, surface: (0) not delimited by any upper margin; (1) delimited by upper margins (New)
53. Ventral quadratojugal contact, extension on lateral surface of ectocondyle: (0) limited, occupies only part of the surface; (1) extensive, covers entire lateral surface of the ectocondyle Brusatte et al. 2010 #108)
54. Ventral quadratojugal contact, anterior projection in ventral view: (0) absent; (1) present, short; (2) present, elongated (Unordered; New)
55. Ventral quadratojugal contact, ventrolateral projection in ventral view: (0) absent; (1) present (New)
56. Ventral quadratojugal contact, small perforation: (0) absent; (1) present (New)
57. Ventral quadratojugal contact, dorsal projection bounding the quadrate foramen: (0) absent; (1) present (New)

Pterygoid contact

58. Pterygoid contact, in posterior view: (0) contact on the pterygoid flange; (1) contact on the ventromedial or anteroventral side of the quadrate body (New)
59. Contact of the epipterygoid and the pterygoid flange, in medial view: (0) present; (1) absent, quadrate and epipterygoid remains separated (New)

Braincase contact

60. Braincase (opisthotic/exoccipital/paroccipital process) contact on the dorsal and/or medial part of the quadrate: (0) absent; (1) present (New)

VI. FORAMINA

Quadrate foramen

61. Quadrate foramen: (0) present; (1) absent (Modified from Novas, 1989 and Sereno et al. 1996 #36)
62. Quadrate foramen, position: (0) completely enclosed within the quadrate; (1) mostly delimited by the quadrate, only lateral margin of foramen bordered by quadratojugal; (2) developed as a distinct opening between the quadrate and quadratojugal. Lateral margin of the foramen formed by the quadratojugal and ventral and dorsal margins formed by both quadrate and quadratojugal; (3) developed as a distinct opening between the quadrate and postorbital. (**Ordered**; Modified from Novas, 1989)
63. Quadrate foramen, position in posterior view: (0) situated more ventrally than the mid-height of the quadrate, or covering most of the ventral part of the quadrate; (1) situated at mid-height of the quadrate (Modified from Holtz, 2000)
64. Quadrate foramen, position in lateral view: (0) facing posterolaterally and visible in lateral view; (1) facing posteriorly and not visible in lateral view (New)
65. Quadrate foramen, shape in posterior view: (0) subcircular; (1) strongly ventrodorsally elongated and elliptical or bean-shaped; (2) strongly ventrodorsally elongated and lenticular or tear drop shaped; (3) strongly lateromedially elongated (Unordered; New)
66. Quadrate foramen, size in posterior view: (0) minute, long axis less than 7% of the ventrodorsal height of the quadrate; (1) small, long axis between 7 to 15% of the ventrodorsal height of the quadrate; (2) large quadrate

fenestra, long axis greater than 15% of the ventrodorsal height of the quadrate (**Ordered**; Holtz,1998 #67; Carr and Williamson 2010 #123)

67. Inclination of the main axis of the quadrate foramen: (0) absent, main axis parallel to quadrate ridge; (1) present, foramen strongly medially inclined; (2) present, foramen perpendicular to quadrate ridge (Unordered; New)

Medial foramen

68. Medial foramen, at the ventralmost part of the pterygoid flange: (0) absent; (1) present (Benson, 2009 #57)

VII. FLANGE & PROCESS

Pterygoid flange

69. Pterygoid flange, anterior extension in medial view (ratio between the anteroposterior length of the pterygoid flange/ventrodorsal height of the quadrate body): (0) >0.65; (1) 0.57-0.65; (2) 0.4-0.57; (3) <0.4 (**Ordered**; New)
70. Pterygoid flange, position of the anteriormost point: (0) at two-third of the quadrate height or more dorsally; (1) at mid-height of the quadrate; (2) at one-third of the quadrate height or more ventrally (Unordered; New)
71. Pterygoid flange, outline in medial view: (0) subtrapezoidal, formed by 3 distinct sides, the anteriormost one being ventrodorsally short; (1) subrectangular, formed by 3 distinct sides, the anteriormost one being ventrodorsally long; (2) roughly parabolic, formed by 3 poorly-defined sides, the anterior one being convex; (3) Semi-oval; (4) roughly M-shaped; (5) subtriangular, formed by two distinct sides (Unordered; Modified from Chiappe, 2001 #18)
72. Pterygoid flange, shape and orientation of the anteriormost side in medial view: (0) straight and inclined posteriorly from the long axis of the quadrate body; (1) straight and subparalell to long axis of quadrate body, or inclined anteriorly; (2) rounded or sigmoid (Unordered; New)
73. Pterygoid flange, angle between the main axis of the ventral margin and the main axis of the quadrate body in medial view: (0) < 55°; (1) 55° - 75°; (2) > 75° (**Ordered**; New)
74. Pterygoid flange, position of the ventralmost point in medial view (ratio between the distance separating the dorsal margin of entocondyle and ventral end of flange and the ventrodorsal height of the quadrate body): (0) well dorsal to the mandibular articulation (>0.1); (1) directly dorsal to the mandibular articulation (0.02-0.1); (2) reaching the mandibular articulation (<0.02). (**Ordered**; New)
75. Pterygoid flange, medial curvature in ventral view: (0) absent or weak, flange projecting mostly anteriorly; (1) present and important, flange curving anteromedially (New)
76. Pterygoid flange, curvature of the ventroposterior part at the level of the quadrate body in anterior view: (0) present, important; (1) present, short; (2) absent (Unordered; New)
77. Pterygoid flange, ventral shelf on the anteroventral margin in medial view: (0) absent; (1) present (New)
78. Pterygoid flange, posteromedial projection of the ventral part in posterior view: (0) absent; (1) present (New)

Lateral process

79. Lateral process: (0) present; (1) absent (Currie, 1995 and Sereno et al. 1996 #58)
80. Lateral process, ventral extension: (0) process extending to the quadrate foramen or at mid-height of the bone; (1) process extending below the mid-height of the bone, just above the ectocondyle or reaching it. (New)
81. Lateral process, maximum width: (0) large, >40% the lateromedial length of the mandibular articulation; (1) short, <40% the lateromedial length of the mandibular articulation (Modified from Forster 1999)
82. Lateral process, outline of lateral margin: (0) angular; (1) parabolic (New)
83. Lateral process, main orientation: (0) lateral; (1) anterolateral; (2) anterior (Unordered; New)
84. Lateral process, dorsal extension: (0) reaching the quadrate head; (1) not reaching the quadrate head (New)
85. Lateral process, extension of the dorsal contact: (0) contact extending entirely along the lateral process; (1) contact restricted to the ventral part of the lateral process; (2) contact restricted to the dorsal part of the lateral process (Unordered; New)

VIII. QUADRATE FOSSAE

Medial fossae

86. Medial fossa between pterygoid flange and quadrate body (pneumatic fossa excluded), in medial view: (0) shallow fossa; (1) deep depression (New)
87. Small fossa on the ventralmost part to the pterygoid flange, dorsal to the entocondyle, in medial view: (0) absent; (1) present (New)

Posterior fossa

88. Posterior fossa, in posterior view: (0) absent; (1) present and separated from the quadrate foramen; (2) present, and leading to or surrounding the quadrate foramen (Unordered; New)
89. Posterior fossa, shape in posterior view: (0) small oval and poorly delimited depression; (1) ventrodorsally tall, diagonally oriented, and poorly delimited depression; (2) ventrodorsally oriented, tall, and well-delimited depression (Unordered; New)

Anterior fossa

90. Anterior fossa, at one third of the quadrate height, lateral to the ventral extremity of the pterygoid flange in anterior view: (0) absent or shallow concavity; (1) present, deep depression (New)

IX. PNEUMACITY

91. Quadrate, pneumaticity: (0) absent; (1) present (Gauthier, 1986; Molnar, 1991)
92. Pneumatic foramen on the posterior surface of the quadrate body, within the posterior fossa, in posterior view: (0) absent; (1) present and ventral to the quadrate foramen; (2) present and at the same level or dorsal to the quadrate foramen; (3) present and at the same level than the quadrate foramen (Unordered; New)
93. Posterior pneumatic foramen, size (ratio between the maximum length of the pneumatic foramen and the lateromedial width of the mandibular articulation): (0) large, >30%; (1) small, <30% (New)
94. Pneumatic depression on the medial side, in medial view: (0) absent; (1) present, with no septum; (2) present and divided by a septum (Unordered; New)
95. Medial pneumatic foramen, size (ratio between the maximum length of the pneumatic foramen and the lateromedial width of the mandibular articulation): (0) small, <20%; (1) large, >20% (New)
96. Pneumatic foramen on the anteroventral margin of the quadrate body, in ventral view: (0) absent; (1) present, small circular pneumatic foramen; (2) present, large pneumatic recess (Unordered; New)
97. Pneumatic foramen on the anterodorsal surface of the quadrate body, ventral to the quadrate head, in anterior view: (0) absent; (1) present (New)
98. Pneumatic foramen on the lateral surface of the quadrate body, dorsal to the ectocondyle: (0) absent; (1) present (New)

A7.2: Illustration of States of Quadrate-based Characters

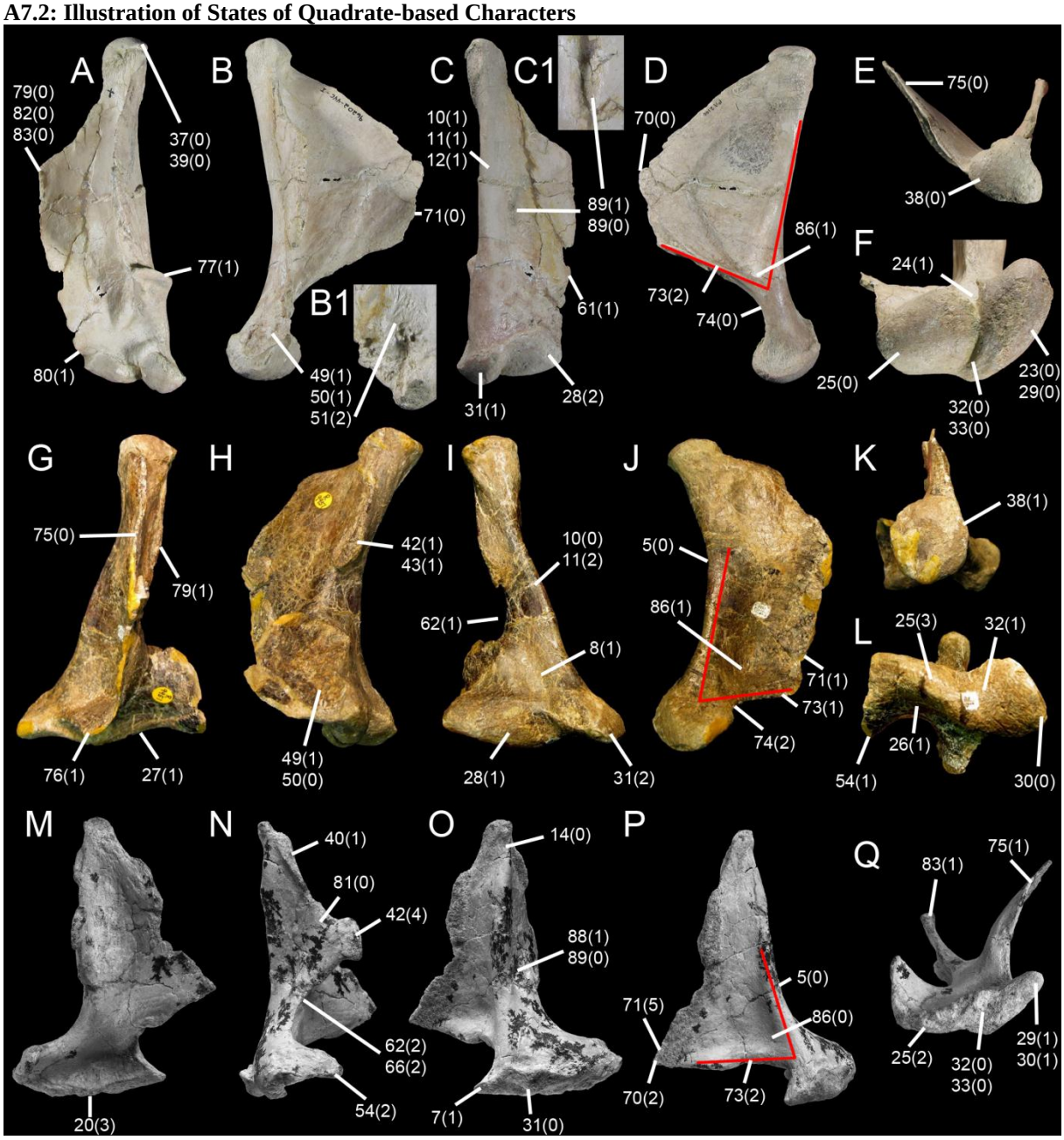

FIGURE A7.1. States of quadrate-based characters. **A–F**, Right quadrate of *Majungasaurus crenatissimus* (FMNH PR 2100) in **A**, anterior; **B**, lateral; **C**, posterior; **D**, medial; **E**, dorsal; and **F**, ventral views (courtesy of Lawrence Witmer); with detail on **B1**, the ventral quadratojugal contact; and **C1**, posterior fossa of the left quadrate (FMNH PR 2100). In posterior view, the quadrate display a lateral process (char. 79:0) with an angular outline (char. 82:0), oriented mainly laterally (char. 83:0) and reaching the mandibular articulation (char. 80:1), as well as a quadrate head with a convex dorsal margin (char. 39:0) and made of a single condyle (char. 37:0). A ventral shelf is seen on the ventral margin of the pterygoid flange (char. 77:1). In lateral view, the ventral quadratojugal contact is drop-shaped (char. 50:1), faces laterally (char. 49:1), and its surface is irregular and weakly grooved (char. 51:2). The pterygoid flange is subtrapezoidal, with a short anterior sides (char. 71:0), and the quadrate ridge is poorly delimited (char. 10:1), rod-shaped (char. 11:1) and subvertical (char. 12:1). The quadrate shows, in dorsal view, a posterior fossa, centrally positioned on the quadrate body and not connected to the quadrate foramen (C1, char. 88:1), and relatively poorly delimited and oval in outline (char. 89:0). There is no quadrate foramen (char. 61:1), and the entocondyle moderately extends on the body (char. 31:1) whereas the ectocondyle strongly extend on the posterior margin of the quadrate (char. 28:2). The pterygoid flange gets attached to the quadrate body well above the mandibular articulation (char. 74:0) and its ventral margin makes an angle of more than 75° with the main axis of the dorsal part of the quadrate body (char. 73:2). The anteriormost point of the pterygoid flange is located at two-third of the quadrate (char. 70:0), and the medial fossa corresponds to a deep depression (char. 86:1). In dorsal view, the pterygoid flange does not show any

medial curvature and only projects anteriorly (char. 75:0) and the quadrate head has a subtriangular outline (char. 38:0). In ventral view, the mandibular articulation of *Majungasaurus* displays an ovoid/subcircular ectocondyle with a width/length ratio of more than 0.55 (char. 25:0), a longer entocondyle (char. 23:0) with an ovoid outline (char. 29:0), a well-delimited (char. 32:0) and narrow (char. 33:0) intercondylar sulcus, and an intercondylar notch on the anterior margin of the mandibular articulation (char. 24:1). **G–L**, Left quadrate of *Baryonyx walkeri* (NHM R9951) in **G**, anterior; **H**, lateral; **I**, posterior; **J**, medial; **K**, dorsal; and **L**, ventral views. The pterygoid flange of *Baryonyx* projects anteriorly and the anterior part does not curve medially (char. 75:0), contrarily to the ventral margin of the flange that bends medially (char. 76:1). There is no lateral process on the lateral surface of the quadrate body (char. 79:1) and the ventral margin of the ectocondyle is sigmoid in anterior view (char. 27:1). The dorsal quadratojugal contact is drop-shaped (char. 42:1) and faces laterally (char. 43:1), whereas the ventral quadratojugal contact is D-shaped (char. 49:1) and also faces laterally (char. 50:0). In posterior view, the quadrate foramen is mostly delimited by the quadrate (char. 62:1), the quadrate ridge is broad (char. 11:2), prominent and well-delimited (char. 10:0), and a shallow furrow curving basally from the foramen towards the mandibular articulation is seen on the ventral half of the quadrate body (char. 8:1). The ectocondyle moderately extends on the posterior margin of the quadrate body (char. 28:1), while the posterior extension of the entocondyle is important (char. 31:2). In medial view, the posterior margin of the quadrate body is concave (char. 5:0), the medial fossa is deep (char. 86:1), and the pterygoid flange consists of a subrectangular ala with a long anterior side (char. 71:1), reaching the quadrate body at the level of the mandibular articulation (char. 74:2), and whose the ventral margin makes an angle of 55° to 75° with the main axis of the quadrate body (char. 73:1). In dorsal view, the quadrate head is subcircular in outline (char. 38:1) and, in ventral view, the ventral quadratojugal contact projects anteriorly (char. 54:1) while the mandibular articulation corresponds to a sigmoid ectocondyle (char. 25:2) separated from a non-protruding entocondyle (char. 30:0) by a shallow intercondylar sulcus (char. 32:1); **M–Q**, Right quadrate of *Tsaagan mangas* (IGM 100-1015) in **M**, anterior; **N**, lateral; **O**, posterior; **P**, medial; and **Q**, ventral views (courtesy of Mick Ellison © AMNH). The ventral margin of the mandibular articulation of *Tsaagan* is roughly convex in anterior/posterior view (char. 30:3), and the laterodorsal contact of the quadrate body mostly contact the squamosal (char. 40:1) in lateral view. Tsaagan quadrate shows a large lateral process (char. 80:0) terminated anteriorly by a subrectangular dorsal quadratojugal contact (char. 42:4). The quadrate foramen is equally delimited by the quadrate and quadratojugal (char. 62:2) and corresponds to a large fenestra (char. 66:2). The ventral quadratojugal contact well projects anteriorly and the anterior process is well-developed (char. 54:2). In posterior view, the quadrate ridge reaches the quadrate head dorsally (char. 14:0) and the posterior surface of the quadrate display a small oval posterior fossa (char. 89:1) centrally positioned on the quadrate body and not leading to or surrounding the quadrate foramen (char. 88:1). The medioventral corner of the quadrate body is pointed and angular (char. 7:1) and the extension of the entocondyle on the posterior surface of the quadrate is relatively limited (char. 31:0). In medial view, the pterygoid flange corresponds to a subtriangular wing (char. 71:5) in which the anteriormost point is located at one third of the quadrate body (char. 70:2). The ventral margin of the pterygoid flange makes an angle of more than 75° with the main axis passing through the quadrate body (char. 73:2). The medial fossa of the pterygoid wing is shallow (char. 86:0) and the posterior margin of the quadrate body is strongly concave (char. 5:0). In ventral view, the lateral process extends anterolaterally (char. 83:1) whereas the pterygoid flange curves anteromedially (char. 75:1). The ectocondyle of the mandibular articulation is parabolic (char. 25:2), while the entocondyle is moderately elongated (char. 29:1) and strongly protrudes anteriorly (char. 30:1). A narrow (char. 33:0) and well-delimited (char. 32:0) intercondylar sulcus separates the two condyles.

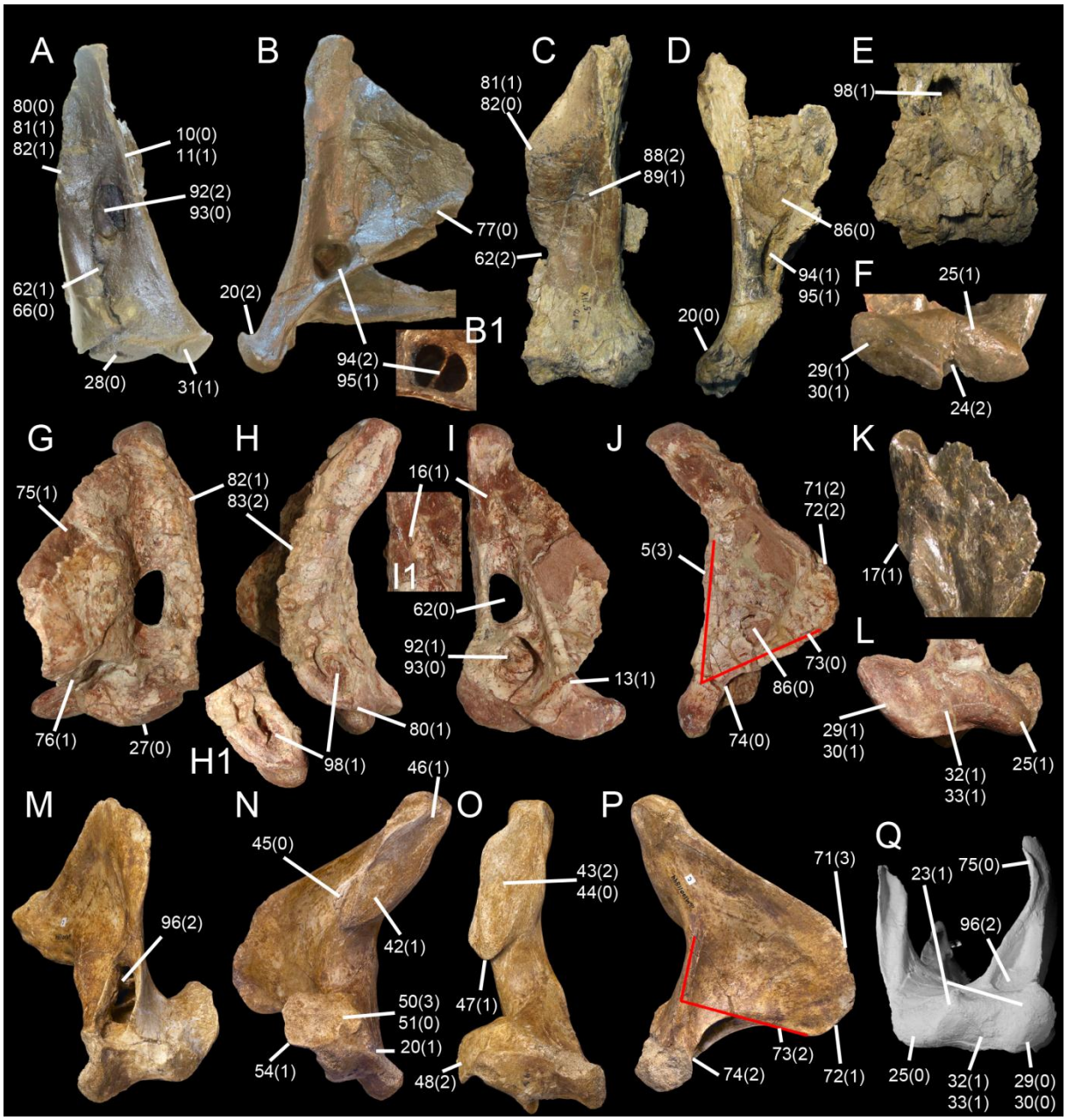

FIGURE A7.2. States of quadrate-based characters. **A–B**, Left coosified quadrate and quadratojugal of *Acrocanthosaurus atokensis* (NCSM 14345) in **A**, posterior; and **B**, medial views; with **B1**, details on the medial pneumatic foramen of the right quadrate in medial view (courtesy of Drew Eddy). In posterior view, the quadrate of *Acrocanthosaurus* displays a short lateral process (char. 81:1) with an angular lateral margin (char. 82:0), and extending ventrally to the quadrate foramen (char. 80: 0). The quadrate ridge is prominent, well-delimited (char. 10:0) and rod-shaped (char. 11:1), while the posterior pneumatic foramen is large (char. 93:0) and dorsal to the quadrate foramen (char. 92:2). The latter is mostly delimited by the quadrate bone (char. 62:1) and relatively small in size (char. 66:0). The extension of the entocondyle on the posterior surface of the quadrate is limited whereas the entocondyle extends moderately on the quadrate body. In medial view, there is a deep concavity delimiting the mandibular articulation from the rest of the quadrate body (char. 20:2). The medial pneumatic foramen is a large opening (char. 95:1) divided by a septum (char. 94:2), and there is a medial shelf (char. 77:1) at the ventral margin of the pterygoid flange; **C–E**, Left quadrate of *Mapusaurus roseae* (MCFPVPH-108.102) in **C**, posterior; **D**, medial; and **E**, anterior (ventral part) views. As seen in *Acrocanthosaurus*, the lateral process of *Mapusaurus* is short (char. 81:1) and its lateral margin is angular (char. 82:0). Nevertheless, the quadrate foramen is developed as distinct opening equally delimited by the quadrate and quadratojugal (char. 62:2), and the posterior fossa corresponds to a ventrodorsally elongated and poorly delimited depression (char. 89:1) leading to the quadrate foramen (char. 88:2). In medial and anterior views, there is no concavity delimiting the mandibular articulation from the rest of the quadrate body (char. 20:0). The medial fossa is shallow (char. 86:0), the medial pneumatic foramen is large (char. 95:1) with no septum (char. 94:1) dividing it, and the anterior

pneumatic foramen corresponds to a small aperture (char. 98:1) ventral to the pterygoid flange; **F, K**, Left quadrate of *Allosaurus* '*jimmadseni*' (SMA 005/02) in **F**, ventral; and **K**, medial (dorsal part) views. The mandibular articulation of *Allosaurus* includes an elliptical entocondyle (char. 29:1) that does not protrude anteriorly (char. 30:1), an elliptical entocondyle as well having a width/length ratio between 0.3 and 0.55 (char. 25:1), and an intercondylar notch on the posterior margin of the quadrate (char. 24:2). In medial view, the quadrate ridge of *Allosaurus* displays a marked protuberance at two-third of the quadrate body (char. 17:1); **G–J**, **L**, Left quadrate of *Aerosteon riocoloradensis* (MCNA-PV-3137) in **G**, anterior; **H**, lateral; **I**, posterior; **J**, medial; and **L**, ventral views; with **H1**, details on the lateral pneumatic foramen in lateral view; and **I1**, the quadrate ridge groove in posterior view (courtesy of Martin Ezcurra). In anterior view, the anterior part of the pterygoid flange extends anteromedially (char. 75:1), and the medial curvature of the ventral margin of the flange is relatively short (char. 76:1). The ventral margin of the ectocondyle is convex in anterior view (char. 27:0) and, in lateral view, the lateral process projects anterior (char. 83:2) and reaches the ectocondyle ventrally (char. 80:1), and its anterior margin is parabolic in outline (char. 82:1). There is a lateral depression corresponding to a lateral pneumatic foramen (char. 98:1) on the ventral part of the lateral process, just above the ectocondyle. In posterior view, the quadrate ridge almost reaches the entocondyle ventrally (char. 13:1), and its posterior surface is separated by a narrow groove (char. 16:1), just below the quadrate head. The quadrate foramen is enclosed within the quadrate body (char. 62:0) and a large pneumatic foramen (char. 93:0) occurs beneath the quadrate foramen (char. 92:1). In medial view, the pterygoid flange corresponds to a parabolic ala (char. 71:2) in which the anteriormost side is rounded (char. 72:2). The ventral margin of the pterygoid flange reaches the quadrate body well above the mandibular articulation (char. 74:0) and makes an angle of less than 55° with the main axis of the quadrate ridge. The quadrate body is sigmoid in outline (char. 5:3) and the medial fossa is shallow (char. 86:0). The mandibular articulation of *Aerosteon* encompasses an elliptical and moderately elongated entocondyle (char. 29:1) protruding anteriorly (char. 30:1), and an elliptical ectocondyle as well (char. 25:1). The condyles are separated by a shallow, poorly delimited (char. 32:1) and lateromedially wide (char. 33:1) intercondylar sulcus; **M–P**, Left quadrate of *Alioramus altai* (IGM 100-1844) in **M**, anteroventral; **N**, lateral; **O**, posterior; and **P**, medial views (courtesy of Mick Ellison © AMNH). The quadrate of *Alioramus* displays a large anteroventral pneumatic recess (char. 96:2) in the ventral part of the pterygoid flange in anteroventral view and, in lateral view, the dorsal quadratojugal contact is tear-drop shaped (char. 42:1) and not delimited by margins anteriorly or posteriorly (char. 45:0). The ventral quadratojugal is D-shaped (char. 50:3), with a smooth surface (char. 51:0) and a short anterior projection (char. 54:1). A small concavity delimiting the mandibular articulation from the rest of the quadrate body is visible in *Alioramus* quadrate (char. 20:1). In posterior view, the dorsal quadratojugal contact also shows a smooth surface (char. 44:0) as well as a small ventral projection (char. 47:1), and this articulating surface faces posterolaterally (char. 43:2). The ventral quadratojugal contact is convex in posterior view; **Q**, Right quadrate of *Tyrannosaurus rex* (cast of BHI 3033) in ventral view (Larson 2008*b*). The mandibular articulation of *Tyrannosaurus* is typical of tyrannosaurids by having subsymmetrical mandibular condyles (char. 23:1) separated by a large (char. 33:1) and shallow (char. 32:1) intercondylar sulcus. Both ecto- and entocondyle are ovoid (char. 25:0; char. 29:0) and the entocondyle does not protrude anteriorly (char. 30:0). The pterygoid flange mostly extends anteriorly (char. 75:0), and its ventral part is separated into two laminae delimiting a large anteroventral pneumatic recess (char. 96:2).

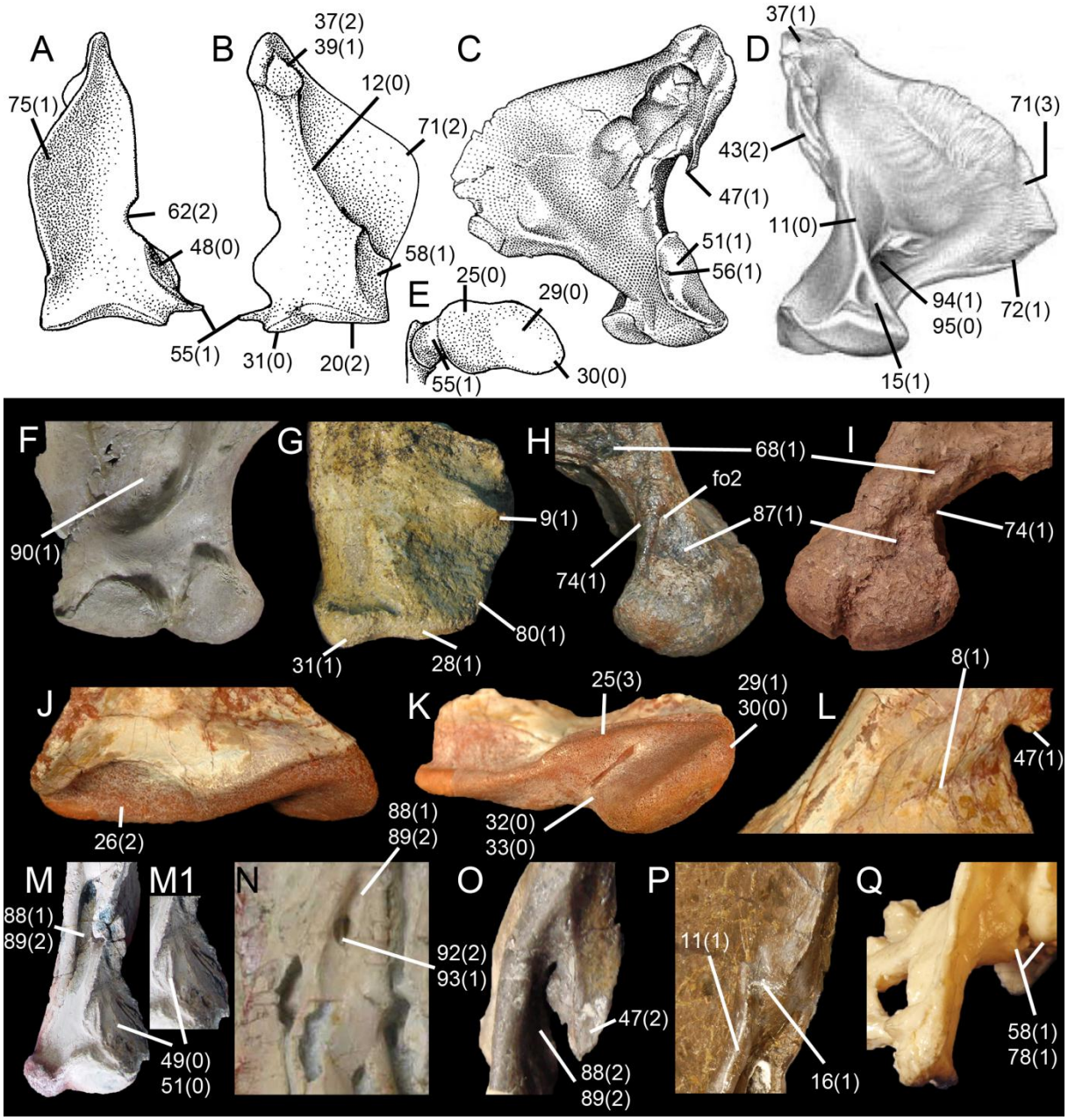

FIGURE A7.3. States of quadrate-based characters. **A–B, E**, Left quadrate of an indeterminate Oviraptoridae (based on specimens IGM A, B, ZPAL MgD-I/95, 96) in **A**, anterior; **B**, posterior; and **E**, ventral views (modified from Maryańska & Osmólska, 1997: fig. 3A-C). In some oviraptorids, the anterior part of the pterygoid ala curves anteromedially (char. 75:1) and the quadrate foramen is equally delimited by the quadrate and quadratojugal (char. 62:2). The ventral quadratojugal contact is concave (char. 48:0) in anterior view and shows a ventral projection extending laterally (char. 55:1) dorsal to the ectocondyle. In posterior view, the quadrate head is conical and pointed (char. 39:1) and includes two very distinct condyles, an otic and squamosal capitula (char. 37:2). The quadrate ridge is strongly inclined laterally (char. 12:0), and the anterior margin of the pterygoid flange is parabolic (char. 71:2). In oviraptorids, the pterygoid contacts the quadrate on the medioventral side of the quadrate body (char. 58:1). The entocondyles has a limited extension on the posterior surface of the quadrate body (char. 28:0; char. 31:0), and the ventral margin of the mandibular articulation is 'W-shaped' in posterior view (char. 20:2). Both ecto- and entocondyle are oval in ventral view (char. 25:0; char. 29:0) and the entocondyle does not protrude anteriorly (char. 30:0); **C**, Left quadrate of *Daspletosaurus* jimmadseni (TMP 94.143.1) in lateral view (Currie, 2003). The dorsal quadratojugal contact shortly projects ventrally (char. 47:1), and the surface of the ventral quadratojugal contact is smooth (char. 51:1) and pierced by small foramina (char. 56:1); **D**, Left quadrate of *Albertosaurus sarcophagus* (TMP 81.10.1) in posteromedial view (Currie, 2003). The quadrate head of *Albertosaurus* has two slightly differentiated condyles (char. 37:1), and the dorsal quadratojugal contact faces posterolaterally (char. 43:2). The quadrate ridge corresponds to a narrow crest (char. 11:0) bifurcating ventrally (char. 15:1) into two ridges separated by an oval concavity. The

pterygoid flange is semi-oval (char. 71:3) with the anteriormost side inclined anteriorly (char. 72:1). There is a medial pneumatic foramen lacking of a septum (char. 94:1) in the posteroventral corner of the pterygoid flange, and this pneumatic opening is relatively small (char. 95:0); **F**, Ventral parts of the right quadrate of *Majungasaurus crenatissimus* (FMNH PR 2100) in anterior view showing the deep anterior fossa (char. 90:1) lateral to the ventral part of the pterygoid flange; G, Right quadrate of *Ilokelesia aguadagrandensis* (MCF-PVPH 35) in posterior view displaying a pronounced ridge on the lateroventral part of the quadrate body (char. 9:1), a lateral process terminating to the mandibular articulation ventrally (char. 80:1), and the ecto- and entocondyle extending moderately on the posterior surface of the quadrate (char. 31:1; char. 28:1); **H**, Ventral parts of right quadrate of *Torvosaurus tanneri* (BYUVP 9246); and **I**, left quadrate of *Afrovenator abakensis* (UC OBA1) in medial views. The quadrates of these two megalosaurids possess a medial foramen located within the posteroventral corner of the pterygoid flange (char. 68:1), as well as small fossa dorsal to the entocondyle (char. 87:1) that includes a second small foramen (fo2) in *Torvosaurus*. The pterygoid flange of both quadrates join the quadrate body just above the mandibular articulation without reaching it (char. 74:1); **J–L**, Right quadrate of an indeterminate Spinosauridae (WDC-CSG uncatalogued) in **J**, anterior; **K**, ventral; and **L**, posterior view; with **J–K**, details on the mandibular articulation; and **L**, the quadrate ridge and quadrate foramen. The mandibular articulation of some spinosaurid display a deep concavity on the anterior surface of the ectocondyle (char. 26:2), a strongly sigmoid ectocondyle (char. 25:3), and an elliptical and moderately entocondyle (29:1) which does not protrude anteriorly (char. 30:0). The ridge of some spinosaurids also shows a small furrow on the posterior surface of the quadrate, medial to the quadrate foramen (char. 8:1), as well as a ventral projection of the dorsal quadratojugal contact (char. 47:1); **M**, Ventral part of right quadrate of *Sinraptor dongi* (IVPP 10600) in posterior view; with details on **M1**, the ventral quadratojugal contact. There is a deep and strongly ventrodorsally elongated posterior fossa (char. 89:2) centrally positioned on the posterior surface of the quadrate body and not leading to the quadrate foramen (char. 88:1) in *Sinraptor*. The ventral quadratojugal contact faces posterolaterally (char. 49:0) and there are radiating ridges on its surface (char. 51:0); **N**, Central part of left quadrate of *Sinornithomimus dongi* (IVPP−V11797−31) in posterior view showing the well-delimited, ventrodorsally elongated (char. 89:2) and centrally positioned (char. 88:1) posterior fossa, as well as the small posterior pneumatic foramen (93:1) within the fossa, well dorsal to the quadrate foramen (char. 92:2); **O**, Posterior parts of right quadrates of *Falcarius utahensis* (UMNH VP 16022) with details on the ventrodorsally elongated, well-delimited posterior fossa (char. 89:2) surrounding the quadrate foramen (char. 88:2), as well as the elongated projection of the dorsal quadratojugal contact (char. 47:2); **P**, Right quadrate of *Allosaurus* '*jimmadseni*' (SMA 005/02) in posterior views showing the quadrate ridge groove (char. 16:1) passing through the rod-shaped quadrate ridge (char. 11:1); **Q**, Left quadrate of *Avimimus portensus* (cast of PIN 3907/1) in lateral view with the ventral part of the pterygoid flange projecting posteromedially (char. 58:1) to contact the basisphenoid.

A7.3: Character Scoring for Taxa
A7.3.1 Data matrix of quadrate based characters.
TNT file
"?"–unknown; "[]"–polymorphic character state; "-"–inapplicable character.

nstates 5
xread
98 56
Eoraptor
?02100?000?1?0?00??0??????????????0???00?????00?1???0???0???0101000??????????000100???0-?0-------
Herrerasaurus
000110000010000001000010100[01]2011010?0000?????0001???[01]1??000101010000110010010000001000000-00-------
Eodromaeus
0???0?00?0100000010000201002[12]0210[01]?1000????????000200000???????????0????100??0???????????00-------
Tawa
0??10?00???100000100002?3001??1?00000?0000?????010000100?0?????????021001001007??????00???0----------
Liliensternus
????3000?01011000??1????????001??0?1??0???1???01?00-------
Megapnosaurus
0101000000010000?010??0???1??1???100?10??1??0001???0???00??0111000?????????00000100??10?0----------
Dilophosaurus

1101200000100000020000203201[12]01111?0000?10110?11112001000?10101302020002011000000010?002200-------
Cryolophosaurus
10010000-0100?001?0?0??????????????0??0??1??0011???1???001?0111100?00?02000?01------10???0-------
Ceratosaurus
0101000000110000000101102001001011010100101000-11[01]101000-0111------020010001100000010100-00-------
Noasaurus
????00?0?11100000?0001000000?1??0???010?????????????????0?????????021010001000l??01?00??00-------
Masiakasaurus
01??10000111000000000010000?0011001?10?00??????-111101000-0??1------0????2001?0010?0???0??00-------
Abelisaurus
?00100???11102000?010?00?0??0??0??0[01]0?0?????????1????????010???????000010101000???01??0??10----------
Ilokelesia
????1?001111000000010100000100110l?[01]0000??1??0-122101000?0?????????0?????1????010?01??0??00----------
Carnotaurus
0102000001110000000001010001011001O?0?00??0??1-?????100?-0?01------?2001101000010011010O-10-------
Aucasaurus
????000000110000000201000O?2012101?0010????????111200000???????????0?????0????01??01???1000-------
Majungasaurus
000100000111000000020101000201100100000000l000-111201000-0101------020012000100100010101010----------
Monolophosaurus
10010?0000102?000?0?0?????????????0?0??0??1???001???????00?00101220?200110??100011011100-00-------
Eustreptospondylus
11??10000110100001010020300?11?000?00100001100-010111100-0?01------020010100001------000-00-------
Afrovenator
11011000001010001100000010121121O0?0010?101100-010200100-0??1------120010100001------010-00-------
Torvosaurus
11?10000001010000101002031110110O0?00100101100-021201000-0??1------1?????1?0??1------?10-00-------
Baryonyx
2???0101002010000300003032110021O0?001001112001010211000O??011112002011120000l------100-00----------
Suchomimus
2???01?000201000030000?2???1???????000001111001010111001O0??01111200?????2?0??1------?00-00-------
Irritator
?020??????????????????????????????????0200??1??0?11???????0??00101100???????????1------?????0-------
Spinosaurine morphotype I
2???010[01]00201[01]0[02]02000030311210[12][01]00?00[12]00111[02][02]01110[23]0110000??0101110030111210001------100-00-------
Spinosaurine morphotype II
?????10100201?0??3000030320110200?????02?1[02]2?11132001000???01011000?????2?0??1------100-00----------
Allosaurus fragilis
1000000000102001110100221001111000110100100111101000000010100111110031220011101------100-00----------
Allosaurus europaeus
?00000?00010???1?????????????????????0?0??0??0??0101???0?000010011111O??122000110001101110220O------
Allosaurus jimmadseni
10?0100000101001110100221001111000?10100?00??1101???000010?00101110021l?10101000110111022O0------
Aerosteon
1???300000001001110000201001111110?10101201001001310010O-0??001112002122001000011121?000-01100--02

Sinraptor
0000000000101001010200201001001000210100101011000100010010100111100031220110100011010001200-------
Acrocanthosaurus
1000000000100001020200203000001000120100??1??0000???0???001001012000212201O?100011011002101202100?
Shaochilong
1???0?000010000002010020300120110O?2010????????010200000?0?????????03122010000???????00??00----------
Giganotosaurus
1???000000100000020000202002121100O?2010021110001100010000??02012000?????1?0?0001?01?0021010-10000
Mapusaurus
1???000000100000O?000??0??0????????10100221100011020000?0?0??010120002l?2111000001001100210l0-11100
Ornitholestes
?101?00000112?0??10100101000201011????0??00?002???????0?10??0101??002122[12]00??0000111???22?0-------
Bicentenaria
??01?00000112?0??10000201001001001?????????????0101100001???01?1??00????220000???????10??00--------
Zuolong
1?0?000000111000020000101O?1201011?00?00??0??0201????10000??01112210220021000000010010022?0----------
Proceratosaurus
1?2030000010000O0?000??????????????????0???????00???0???00?00211110?013??11?001------000-00-------
Eotyrannus
?????00000100?0??10000101001110001????????110?00002001000???02???2?00?????1?1??1------100-00-------
Xiongguanlong
1020000000102?0?0100001010010010112?0100??2????10???010?00??0211220???????0?001------?00-?0-------
Alioramus
1000300000002210O?0[01]00?0?001?0?1???00100212001120310010000?10101220011312201001------000-010-0-200
Albertosaurus
2001300000002210O?0000???001??0???2?1?00212020100310010100?10111221001312 2??001------100-010-10210
Daspletosaurus
2001300000002210010000100O0?10?0112?01001020011?1010010110?10111?200013?2201001------100-010-??200
Tyrannosaurus
2001300000002010010000100001001111201100232100100020010010l?01112200013222010 01------000-010-0-210
Garudimimus
002030000[01]110?000?010??????1??1??1000100??1??0001?20000000??02012100112?120??01------??12?121?????
Sinornithomimus
0?21000??[01]110?000?000?????????????????0?00??1???000???0?0?00??0201210?2????2???01------??12?121?????
Shuvuuia
012100000011000002000020 2??0000101202?22??0??10?2???100?00?10310120031221 01?000001012000-?0----------
Falcarius
1???10000110200O0?01102010020020l1?001002110212010200000000??01111200314211110000110O?0022010-10000
Erlikosaurus
10104000011l2?0001100020????00?1010?0??120132?00142000000O?10211120?2242101000001100100O-?0----------
Avimimus
101?100002-------0000010100010011l??2??110110?02112011000l?10??????0?122?11?011------100-00-------
Oviraptoridae

10[01]000100010002000002000000100010120201010110000012010100111020 02[12]1011[02]01210001------
000-0[01]0-[01]1000
Buitreraptor
1?2100100111200 00?010020?0?0000????00?0???1???00112100000 0??02112200??????????100000???0-
?121?????
Bambiraptor
1021001001110000030130203000000100231 0?00100001101002000 0??0200?2000250200200000000?000-
00-------
Tsaagan
2020001001110000020130203000110000230 1011[14]1000001010020000?00200220002502011000000101001
000-------
Dromaeosaurus
1020001001110000030110?0??0101000020010110110002102000 00?0100201220021501002000010011000-
00-------
Troodontidae
1020001?0[01]110?000301101010010001012 00?00?01?000001100100 00?10[12]10?2?03[12]2210?1?01------
000-0[01]210--00
;
ccode + 0 2 3 10 17 19 22 28 61 65 68 73;
proc/;

A7.3.2 Supermatrix of quadrate related characters combined with 6 other datasets.
TNT file available at https://drive.google.com/file/d/0B_-0b-kZatHiZ1RxdXREZEMwRXM/edit?usp=sharing

A7.4: Results of the Cladistic Analysis
Cladistic analysis perform on the data matrix of quadrate based characters.

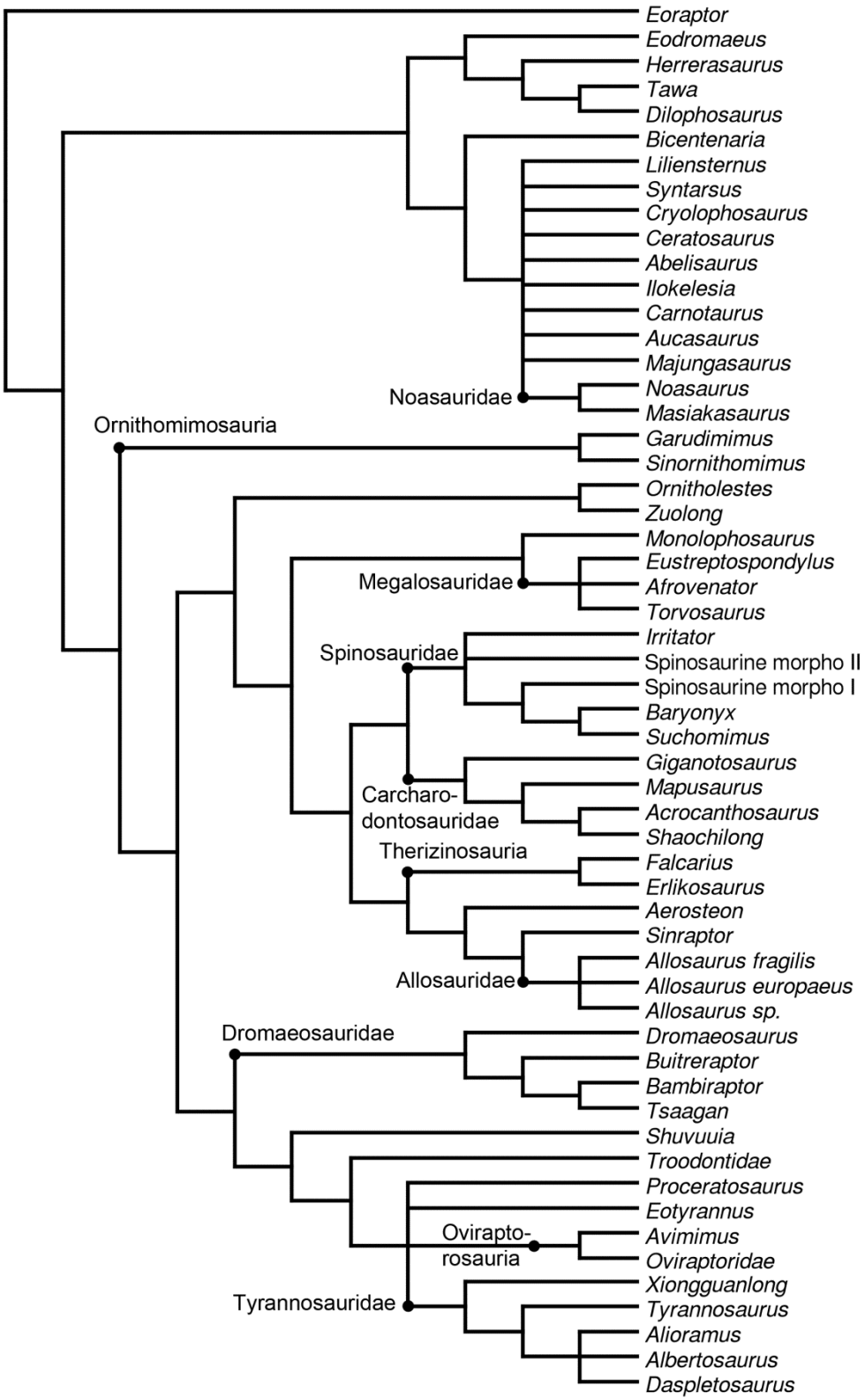

FIGURE A7.4. Strict consensus cladogram from 40 most parsimonious trees. Initial analysis was a New Technology Search using TNT v.1.1 of a data matrix comprising 98 quadrate based characters combined with one outgroup (*Eoraptor lunensis*) and 55 nonavian theropod taxa. Tree length = 592 steps; CI = 0.271; RI = 0.536.

Cladistic analysis perform on the supermatrix.

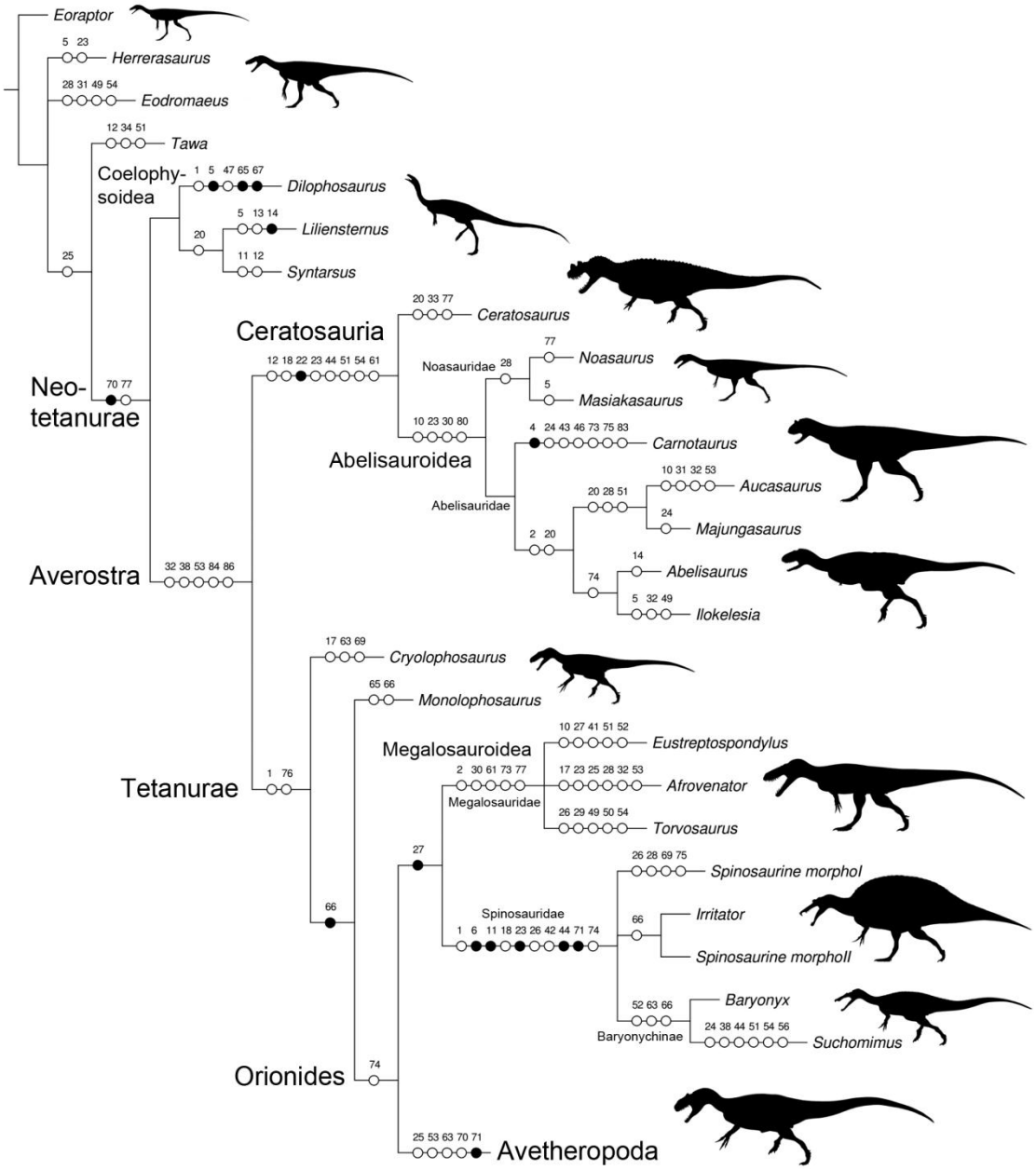

FIGURE A7.5A. Strict consensus cladogram of 36 most parsimonious trees. Initial analysis was a New Technology Search using TNT v.1.1 of a data matrix comprising 98 quadrate based characters combined with six recent datasets on the whole skeleton (Brusatte et al. 2010*d*; Choiniere et al. 2010*b*; Martinez et al. 2011; Carrano et al. 2012; Pol and Rauhut 2012) for one outgroup (*Eoraptor lunensis*) and 55 non-avian theropod taxa. Tree length = 3616 steps; CI = 0.562; RI = 0.631. The unambiguous and ambiguous quadrate based synapomorphies are represented by black and white circles, respectively, and the character number associated with each synapomorphy is above the circles.

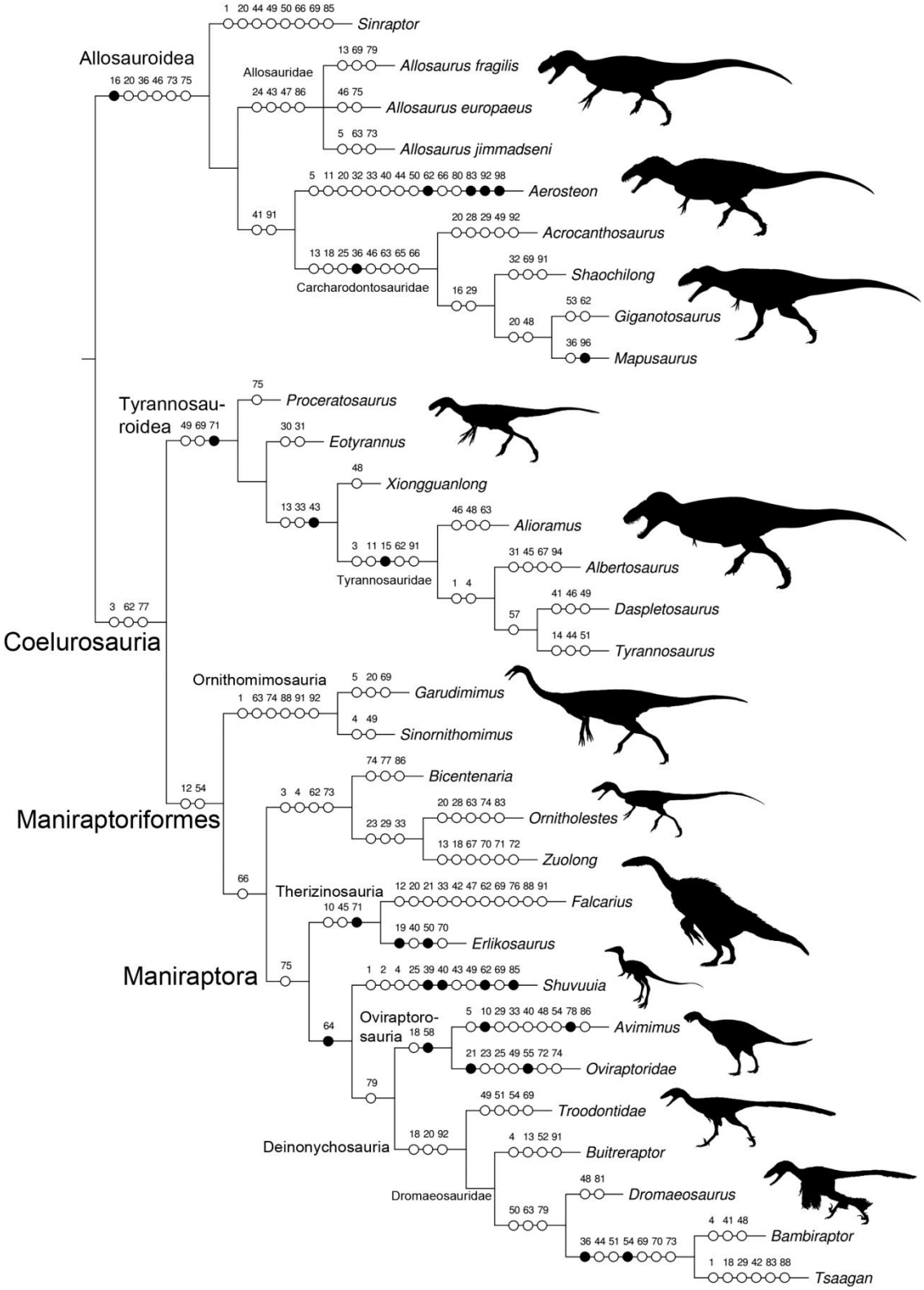

FIGURE A7.5B. (Continued).

A7.5: Illustration of Landmarks for the Phylogenetic Morphometric Analysis

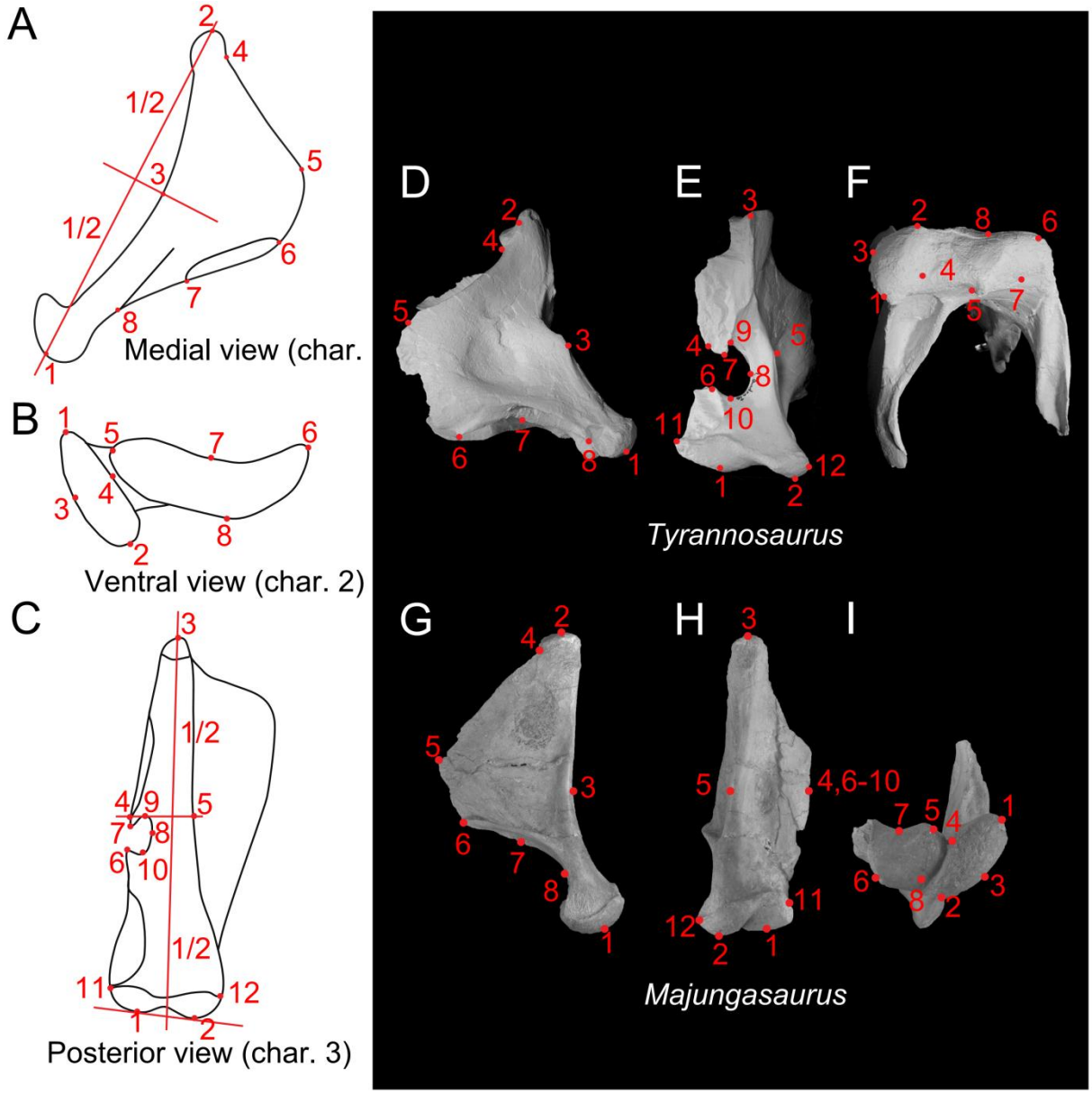

FIGURE A7.6. Phylogenetic morphometrics landmark locations and examples. **A–C**, Hypothetical quadrate in **A**, medial view; **B**, ventral view; and **C**, posterior view; **D–G**, the resulting landmark configurations correspond to characters 1, 2, and 3, respectively; **D–F**, *Tyrannosaurus* quadrate in **D**, medial; **E**, posterior; and **F**, ventral views and the corresponding landmark locations on each view forming therefore a landmark configuration thus, character; **G–I**, *Majungasaurus* quadrate in **G**, medial; **H**, posterior; and **I**, ventral views. The absence of a quadrate foramen implies a specific organization of landmarks 4, 6-10 in character 3 (figure 8).

A7.6: TNT files of the phylogenetic morphometric analysis
Quadrate in medial view
xread
1 23
& [landmark 2d]
Tawa -0.393379,-0.363027 0.030871,0.494995 -0.099922,0.034209 0.095770,0.410704 0.240327,0.055161 0.252247,-0.155153 0.042896,-0.250473 -0.168809,-0.226416
Acrocanthosaurus -0.347851,-0.372605 0.064049,0.454228 -0.129651,0.030656 0.086559,0.377745 0.332817,0.076521 0.268293,-0.091671 -0.031051,-0.179041 -0.243165,-0.295832
Aerosteon -0.330502,-0.339433 0.006116,0.542885 -0.082190,0.078341 0.073417,0.440501 0.248078,-0.021938 0.214597,-0.213055 0.033620,-0.237495 -0.163136,-0.249806

Afrovenator -0.317782,-0.409878 0.044241,0.488695 -0.155718,0.053133 0.091950,0.427828 0.324932,-0.021360 0.202490,-0.133618 0.002617,-0.169229 -0.192729,-0.235572
Allosaurus_fragilis -0.373657,-0.423068 0.099659,0.446464 -0.128198,0.008971 0.135785,0.392038 0.277109,0.165119 0.185009,-0.114792 0.002690,-0.212743 -0.198396,-0.261989
Bambiraptor -0.278910,-0.318253 -0.043199,0.574985 -0.106330,0.109591 0.008940,0.494961 0.298554,-0.211952 0.242902,-0.243588 0.035657,-0.193141 -0.157613,-0.212604
Baryonyx -0.325118,-0.332576 0.038011,0.483921 -0.089595,0.056640 0.108911,0.421752 0.344402,0.182231 0.081729,-0.230561 -0.000108,-0.302492 -0.158233,-0.278915
Allosaurus_jimmadseni. -0.383948,-0.387309 0.083620,0.426610 -0.162140,0.029601 0.093109,0.376991 0.332825,0.133744 0.239706,-0.085431 -0.003290,-0.249564 -0.199882,-0.244642
Ceratosaurus_dentisulcatus -0.406391,-0.423291 0.076669,0.444680 -0.159697,-0.001862 0.113533,0.387656 0.300400,0.061212 0.242128,-0.075908 0.034870,-0.135694 -0.201512,-0.256792
Ceratosaurus_magnicornis -0.377604,-0.383236 0.059158,0.422494 -0.139449,0.015676 0.108359,0.363167 0.345451,0.096021 0.276476,-0.048708 -0.006060,-0.165918 -0.266330,-0.299496
Dilophosaurus -0.430510,-0.368257 0.058452,0.399213 -0.193359,0.026841 0.095194,0.351027 0.331982,0.082015 0.327973,-0.032344 ? -0.242083,-0.277175
Eustreptospondylus -0.333681,-0.389891 0.050350,0.490386 -0.134473,0.048712 0.108051,0.420804 0.289401,-0.006978 0.214875,-0.107432 0.004566,-0.163626 -0.199089,-0.291974
Falcarius -0.292259,-0.372774 0.089411,0.508849 -0.100318,0.064938 0.104489,0.466756 0.250721,0.029336 0.124453,-0.103134 -0.005458,-0.300058 -0.171040,-0.293914
Giganotosaurus -0.439289,-0.425809 0.096641,0.431695 -0.176710,0.000314 0.144277,0.337092 ? ? ? -0.240508,-0.297850
Majungasaurus -0.317048,-0.394642 0.040925,0.500737 -0.122645,0.047431 0.092083,0.434958 0.311627,0.004114 0.179358,-0.168037 0.005615,-0.172104 -0.189915,-0.252455
Masiakasaurus -0.330711,-0.386602 0.090842,0.460793 -0.167200,0.039820 0.111380,0.411775 ? ? ? -0.194187,-0.252939
Oviraptoridae -0.348556,-0.341898 0.053853,0.455543 -0.152191,0.061371 0.124301,0.339907 0.259494,0.122775 0.309898,-0.105011 0.055531,-0.207009 -0.302332,-0.325678
Shaochilong -0.327703,-0.397807 0.079713,0.505791 -0.099231,0.045422 0.129980,0.416180 0.262057,0.112648 0.129885,-0.165009 -0.010664,-0.226369 -0.164038,-0.290855
Sinraptor -0.320705,-0.372504 0.058710,0.493063 -0.106836,0.047984 0.100197,0.447441 0.271319,0.061080 0.185202,-0.186872 -0.019947,-0.212228 -0.167940,-0.277964
Spinosaurinae_morphoI -0.316729,-0.355880 0.103613,0.474022 -0.063714,0.035556 0.101397,0.443775 0.314260,0.230764 0.041325,-0.219714 -0.021927,-0.303130 -0.158224,-0.305392
Torvosaurus -0.417646,-0.454881 0.118029,0.463426 -0.119705,-0.028078 0.165537,0.397299 ? ? ? -0.226565,-0.308099
Tsaagan -0.293354,-0.316888 -0.016823,0.536914 -0.116529,0.101890 0.020909,0.504520 0.273643,-0.182841 0.269108,-0.192841 0.032114,-0.220458 -0.169069,-0.230296
Tyrannosaurus -0.336384,-0.303823 0.014658,0.472741 -0.118755,0.053683 0.059230,0.398866 0.358495,0.125098 0.222479,-0.255952 0.009612,-0.217283 -0.209333,-0.273330
;

Quadrate in posterior view
xread
1 23
& [landmark 2d]
Tawa 0.023888,-0.274110 0.210722,-0.265792 -0.133421,0.752203 -0.110409,0.215758 0.071896,0.249426 -0.058885,-0.094335 -0.056505,-0.003903 -0.029194,-0.037576 -0.040803,0.002815 -0.045755,-0.076486 -0.062606,-0.240083 0.231071,-0.227917
Acrocanthosaurus 0.012428,-0.290145 0.246361,-0.277328 -0.088901,0.680540 -0.183063,0.181942 0.080680,0.204930 -0.055772,-0.026106 -0.067918,0.007360 -0.040582,0.010029 -0.058635,0.017817 -0.055809,-0.026026 -0.081889,-0.270151 0.293099,-0.212862
Aerosteon 0.028165,-0.336047 0.271439,-0.295344 -0.107656,0.580106 -0.169869,0.096919 0.117138,0.138522 -0.129006,0.057858 -0.128935,0.058828 0.008523,0.079085 -0.076058,0.139378 -0.035399,-0.020055 -0.120749,-0.262117 0.342407,-0.237134
Afrovenator 0.066015,-0.343904 0.245400,-0.352224 -0.163238,0.566721 -0.080950,0.102022 0.080088,0.137411 -0.080740,0.099694 -0.080608,0.101508 -0.079766,0.100868 -0.080335,0.101912 -0.080593,0.099883 -0.020021,-0.300222 0.274748,-0.313669

Allosaurus_fragilis 0.011834,-0.349177 0.277691,-0.325771 -0.141951,0.569229 -0.142640,0.174572 0.051994,0.208544 -0.062744,0.030465 -0.067773,0.047959 -0.035040,0.053709 -0.057911,0.091325 -0.037666,0.013405 -0.107392,-0.242491 0.311598,-0.271770
Bambiraptor 0.024545,-0.286390 0.275900,-0.220804 -0.035558,0.641438 -0.161154,0.166439 0.155973,0.189613 -0.172090,-0.193351 -0.155566,0.143320 0.011165,0.011265 -0.072573,0.113052 -0.053830,-0.113844 -0.134530,-0.285027 0.317718,-0.165712
Baryonyx -0.013952,-0.324187 0.311699,-0.284159 -0.149628,0.570796 -0.053273,0.128242 0.068642,0.142662 -0.102209,-0.025183 -0.071956,0.132243 -0.036914,0.052039 -0.062471,0.140155 -0.057069,-0.021334 -0.183773,-0.269628 0.350903,-0.241645
Allosaurus_jimmadseni. 0.012501,-0.342776 0.263913,-0.321825 -0.142172,0.574733 -0.098343,0.115041 0.071511,0.140566 -0.059500,0.023154 -0.092918,0.111760 -0.042234,0.080813 -0.082256,0.129302 -0.048105,0.020529 -0.108312,-0.286174 0.325917,-0.245122
Ceratosaurus_dentisulcatus 0.073402,-0.357246 0.239552,-0.330516 -0.120229,0.594176 -0.087696,0.089953 0.094634,0.132326 -0.087297,0.087952 -0.087205,0.089216 -0.086619,0.088770 -0.087015,0.089497 -0.086879,0.088020 -0.039769,-0.328490 0.275120,-0.243657
Ceratosaurus_magnicornis 0.057922,-0.357020 0.247213,-0.330440 -0.135307,0.574643 -0.084150,0.098644 0.075522,0.130620 -0.083696,0.096367 -0.083591,0.097805 -0.082924,0.097297 -0.083375,0.098125 -0.083220,0.096444 -0.028917,-0.322061 0.284523,-0.280423
Dilophosaurus -0.002188,-0.332170 0.229958,-0.333839 -0.221817,0.613796 -0.155836,0.126101 0.068178,0.172541 -0.034463,0.037218 -0.036321,0.041590 0.015733,0.100735 -0.016178,0.073015 0.002026,0.052457 -0.123175,-0.277568 0.274083,-0.273876
Eustreptospondylus 0.057959,-0.368416 0.280762,-0.295216 -0.090014,0.586647 -0.092720,0.089099 0.075689,0.118685 -0.093365,0.087360 -0.093275,0.088600 -0.092699,0.088162 -0.093088,0.088876 -0.092955,0.087427 -0.058366,-0.323634 0.292073,-0.247591
Falcarius -0.010253,-0.355998 0.243283,-0.314837 -0.192219,0.586555 -0.082378,0.122856 0.066754,0.153862 -0.029976,-0.042204 -0.073795,0.113959 -0.014088,0.039623 -0.069091,0.274199 -0.018107,-0.030247 -0.090292,-0.290814 0.270161,-0.256956
Giganotosaurus 0.002003,-0.311181 0.237612,-0.296558 -0.121036,0.645278 -0.121227,0.155161 0.051534,0.181855 -0.054496,-0.007695 -0.062975,0.051402 -0.048461,0.027187 -0.057640,0.052169 -0.050132,-0.000909 -0.104438,-0.274855 0.329254,-0.221854
Majungasaurus 0.099024,-0.339532 0.272242,-0.316177 -0.042762,0.577528 -0.127056,0.085753 0.120598,0.133298 -0.126932,0.082461 -0.126762,0.084793 -0.125680,0.083970 -0.126411,0.085313 -0.126160,0.082587 0.002510,-0.294227 0.307389,-0.265767
Masiakasaurus 0.091113,-0.327294 0.253669,-0.292511 -0.005101,0.596734 -0.140255,0.073489 0.158005,0.162417 -0.140895,0.067911 -0.140658,0.071143 -0.139159,0.070002 -0.140172,0.071863 -0.139824,0.068085 0.033314,-0.320626 0.309962,-0.241212
Oviraptoridae -0.025136,-0.310625 0.193592,-0.255300 -0.130330,0.634953 -0.066994,0.171316 0.105996,0.195535 -0.112837,-0.123470 -0.065468,0.136367 -0.046556,0.025949 -0.054251,0.138879 -0.086676,-0.078925 -0.039911,-0.306165 0.328570,-0.228515
Shaochilong 0.017622,-0.343527 0.276639,-0.300141 -0.143293,0.606636 -0.081323,0.115986 0.056261,0.139048 -0.051471,0.032257 -0.069160,0.093674 -0.060194,0.060931 -0.068159,0.093084 -0.051749,0.029716 -0.131637,-0.289280 0.306463,-0.238384
Sinraptor 0.015004,-0.336593 0.188983,-0.323739 -0.196693,0.650400 -0.123755,0.144438 0.018799,0.176253 -0.065233,0.043940 0.003597,0.020437 -0.001774,0.070966 -0.015648,0.104658 -0.021597,0.029946 -0.053620,-0.320158 0.251937,-0.260547
Spinosaurinae_morphoI 0.014599,-0.304523 0.287253,-0.275502 -0.084159,0.643305 -0.118931,0.154071 0.096792,0.176022 -0.104744,-0.065452 -0.092440,0.059253 -0.036257,0.012202 -0.067604,0.081091 -0.078858,-0.065362 -0.159020,-0.231238 0.343368,-0.183867
Torvosaurus 0.066384,-0.312031 0.310572,-0.350556 -0.120196,0.527992 -0.100853,0.096682 0.091892,0.130708 -0.100235,0.093577 -0.100091,0.095538 -0.100106,0.095016 -0.100721,0.096145 -0.100510,0.093853 -0.095361,-0.254839 0.349225,-0.312085
Tsaagan -0.021163,-0.326065 0.236268,-0.230804 -0.127302,0.645777 -0.070085,0.161908 0.122438,0.175539 -0.121135,-0.159638 -0.080653,0.184843 -0.007217,-0.002548 -0.039114,0.111327 -0.055292,-0.114945 -0.171108,-0.287916 0.334363,-0.157478
Tyrannosaurus -0.004194,-0.320605 0.294005,-0.265460 -0.114374,0.613546 -0.167962,0.128312 0.078535,0.155846 -0.108608,-0.043052 -0.069656,0.085598 0.029187,0.050303 -0.072327,0.131975 -0.018494,-0.054362 -0.168194,-0.264560 0.322081,-0.217541
;

Quadrate in medial view

xread
1 23
& [landmark 2d]
Tawa -0.464489,0.116176 -0.023970,-0.232866 -0.318547,-0.168238 -0.158595,0.048151 -0.124170,0.213977 0.596220,-0.028899 0.301808,0.121968 0.191744,-0.070269
Acrocanthosaurus -0.432153,0.123473 -0.032635,-0.208255 -0.302894,-0.138827 -0.176459,0.048779 -0.193505,0.170150 0.644601,-0.034614 0.277339,0.126262 0.215706,-0.086967
Aerosteon -0.494234,0.143456 0.011661,-0.214962 -0.321330,-0.153061 -0.177685,0.035283 -0.117259,0.157430 0.569638,-0.061088 0.303482,0.164450 0.225727,-0.071508
Afrovenator -0.518297,0.204136 0.049576,-0.291341 -0.345897,-0.189691 -0.163377,0.056306 -0.118179,0.161330 0.576952,-0.013944 0.255974,-0.077890 0.263248,0.151094
Allosaurus_fragilis -0.458156,0.130333 0.002849,-0.177182 -0.326445,-0.145232 -0.203823,0.029355 -0.090362,0.168071 0.634774,0.002972 0.280282,0.147470 0.160881,-0.155787
Bambiraptor -0.422093,0.160801 -0.036247,-0.156368 -0.319435,-0.131978 -0.172433,0.048943 -0.218974,0.150053 0.667119,0.083687 0.272167,0.002342 0.229897,-0.157481
Baryonyx -0.389248,0.127314 -0.075976,-0.220962 -0.313834,-0.131841 -0.159977,0.015696 -0.260645,0.234471 0.598531,0.021290 0.318131,0.076945 0.283019,-0.122913
Allosaurus_jimmadseni -0.497871,0.135941 0.064919,-0.229350 -0.320044,-0.176788 -0.163265,0.069501 -0.103574,0.206528 0.568997,-0.058819 0.284870,0.164846 0.165969,-0.111858
Ceratosaurus_dentisulcatus -0.438566,0.226949 0.070832,-0.311251 -0.321897,-0.201864 -0.104747,0.001422 -0.193434,0.239815 0.557789,-0.044235 0.259861,0.172292 0.170161,-0.083128
Ceratosaurus_magnicornis -0.418052,0.234891 0.026183,-0.316629 -0.353723,-0.203537 -0.117064,0.006618 -0.129073,0.224423 0.555172,0.065259 0.285554,0.126580 0.151003,-0.137605
Dilophosaurus -0.439368,0.146150 -0.031261,-0.233712 -0.287253,-0.138233 -0.180410,0.022163 -0.181168,0.222383 0.610898,0.016447 0.287771,0.086566 0.220791,-0.121765
Eustreptospondylus -0.455742,0.201997 -0.027289,-0.244244 -0.296984,-0.131572 -0.159681,0.053811 -0.188417,0.155885 0.600698,0.096668 0.279211,0.015790 0.248204,-0.148333
Falcarius -0.421929,0.058159 -0.162755,-0.225253 -0.414150,-0.244350 -0.214662,0.024311 0.073116,0.226813 0.521634,-0.016482 0.384042,0.207239 0.234703,-0.030436
Giganotosaurus -0.524450,0.138561 0.019481,-0.177997 -0.310622,-0.119446 -0.197408,0.059989 -0.107774,0.136560 0.581747,0.017456 0.319724,0.068951 0.219301,-0.124075
Majungasaurus -0.492128,0.211120 0.041819,-0.321744 -0.348417,-0.194278 -0.105881,0.049621 -0.033734,0.199570 0.501004,0.006431 0.249403,0.252058 0.187934,-0.202779
Masiakasaurus -0.535751,0.194571 0.100893,-0.277631 -0.330561,-0.295874 -0.129582,0.093324 -0.020571,0.237944 0.480331,-0.080462 0.310916,0.190240 0.124325,-0.062112
Oviraptoridae -0.523617,0.160491 0.025144,-0.355843 -0.399898,-0.280510 -0.060073,0.065909 0.051864,0.253321 0.445016,-0.047314 0.342087,0.227737 0.119477,-0.023791
Shaochilong -0.455568,0.174560 0.045420,-0.199899 -0.302979,-0.136574 -0.188634,0.048861 -0.191284,0.186538 0.613706,0.033727 0.266961,0.057411 0.212377,-0.164624
Sinraptor -0.492616,0.113184 -0.015966,-0.242545 -0.338943,-0.162879 -0.142788,0.036502 -0.053343,0.203982 0.565829,-0.032094 0.307480,0.192839 0.170346,-0.108989
Spinosaurinae_MorphoI -0.445947,0.152836 -0.047449,-0.200774 -0.331024,-0.135508 -0.175562,0.032535 -0.136129,0.171821 0.621545,0.077712 0.284126,0.041544 0.230441,-0.140167
Torvosaurus -0.487335,0.157126 -0.017826,-0.221727 -0.337676,-0.135715 -0.152719,0.062997 -0.103433,0.137419 0.584630,0.041485 0.280290,0.102202 0.234069,-0.143787
Tsaagan -0.506605,0.186508 -0.029755,-0.211724 -0.298369,-0.107450 -0.191987,0.077072 -0.112285,0.109430 0.588528,0.129073 0.296071,-0.001390 0.254402,-0.181519
Tyrannosaurus -0.420497,0.121775 -0.155857,-0.246915 -0.403823,-0.190452 -0.196052,0.002755 0.027429,0.165579 0.537503,0.048744 0.348481,0.186010 0.262816,-0.087496
;

Quadrate in all views
xread
3 23
& [landmark 2d]
Tawa -0.393379,-0.363027 0.030871,0.494995 -0.099922,0.034209 0.095770,0.410704 0.240327,0.055161 0.252247,-0.155153 0.042896,-0.250473 -0.168809,-0.226416
Acrocanthosaurus -0.347851,-0.372605 0.064049,0.454228 -0.129651,0.030656 0.086559,0.377745 0.332817,0.076521 0.268293,-0.091671 -0.031051,-0.179041 -0.243165,-0.295832

Aerosteon -0.330502,-0.339433 0.006116,0.542885 -0.082190,0.078341 0.073417,0.440501 0.248078,-0.021938 0.214597,-0.213055 0.033620,-0.237495 -0.163136,-0.249806
Afrovenator -0.317782,-0.409878 0.044241,0.488695 -0.155718,0.053133 0.091950,0.427828 0.324932,-0.021360 0.202490,-0.133618 0.002617,-0.169229 -0.192729,-0.235572
Allosaurus_fragilis -0.373657,-0.423068 0.099659,0.446464 -0.128198,0.008971 0.135785,0.392038 0.277109,0.165119 0.185009,-0.114792 0.002690,-0.212743 -0.198396,-0.261989
Bambiraptor -0.278910,-0.318253 -0.043199,0.574985 -0.106330,0.109591 0.008940,0.494961 0.298554,-0.211952 0.242902,-0.243588 0.035657,-0.193141 -0.157613,-0.212604
Baryonyx -0.325118,-0.332576 0.038011,0.483921 -0.089595,0.056640 0.108911,0.421752 0.344402,0.182231 0.081729,-0.230561 -0.000108,-0.302492 -0.158233,-0.278915
Allosaurus_jimmadseni -0.383948,-0.387309 0.083620,0.426610 -0.162140,0.029601 0.093109,0.376991 0.332825,0.133744 0.239706,-0.085431 -0.003290,-0.249564 -0.199882,-0.244642
Ceratosaurus_dentisulcatus -0.406391,-0.423291 0.076669,0.444680 -0.159697,-0.001862 0.113533,0.387656 0.300400,0.061212 0.242128,-0.075908 0.034870,-0.135694 -0.201512,-0.256792
Ceratosaurus_magnicornis -0.377604,-0.383236 0.059158,0.422494 -0.139449,0.015676 0.108359,0.363167 0.345451,0.096021 0.276476,-0.048708 -0.006060,-0.165918 -0.266330,-0.299496
Dilophosaurus -0.430510,-0.368257 0.058452,0.399213 -0.193359,0.026841 0.095194,0.351027 0.331982,0.082015 0.327973,-0.032344 ? -0.242083,-0.277175
Eustreptospondylus -0.333681,-0.389891 0.050350,0.490386 -0.134473,0.048712 0.108051,0.420804 0.289401,-0.006978 0.214875,-0.107432 0.004566,-0.163626 -0.199089,-0.291974
Falcarius -0.292259,-0.372774 0.089411,0.508849 -0.100318,0.064938 0.104489,0.466756 0.250721,0.029336 0.124453,-0.103134 -0.005458,-0.300058 -0.171040,-0.293914
Giganotosaurus -0.439289,-0.425809 0.096641,0.431695 -0.176710,0.000314 0.144277,0.337092 ? ? ? -0.240508,-0.297850
Majungasaurus -0.317048,-0.394642 0.040925,0.500737 -0.122645,0.047431 0.092083,0.434958 0.311627,0.004114 0.179358,-0.168037 0.005615,-0.172104 -0.189915,-0.252455
Masiakasaurus -0.330711,-0.386602 0.090842,0.460793 -0.167200,0.039820 0.111380,0.411775 ? ? ? -0.194187,-0.252939
Oviraptoridae -0.348556,-0.341898 0.053853,0.455543 -0.152191,0.061371 0.124301,0.339907 0.259494,0.122775 0.309898,-0.105011 0.055531,-0.207009 -0.302332,-0.325678
Shaochilong -0.327703,-0.397807 0.079713,0.505791 -0.099231,0.045422 0.129980,0.416180 0.262057,0.112648 0.129885,-0.165009 -0.010664,-0.226369 -0.164038,-0.290855
Sinraptor -0.320705,-0.372504 0.058710,0.493063 -0.106836,0.047984 0.100197,0.447441 0.271319,0.061080 0.185202,-0.186872 -0.019947,-0.212228 -0.167940,-0.277964
Spinosaurinae_morphoI -0.316729,-0.355880 0.103613,0.474022 -0.063714,0.035556 0.101397,0.443775 0.314260,0.230764 0.041325,-0.219714 -0.021927,-0.303130 -0.158224,-0.305392
Torvosaurus -0.417646,-0.454881 0.118029,0.463426 -0.119705,-0.028078 0.165537,0.397299 ? ? ? -0.226565,-0.308099
Tsaagan -0.293354,-0.316888 -0.016823,0.536914 -0.116529,0.101890 0.020909,0.504520 0.273643,-0.182841 0.269108,-0.192841 0.032114,-0.220458 -0.169069,-0.230296
Tyrannosaurus -0.336384,-0.303823 0.014658,0.472741 -0.118755,0.053683 0.059230,0.398866 0.358495,0.125098 0.222479,-0.255952 0.009612,-0.217283 -0.209333,-0.273330

& [landmark 2d]
Tawa -0.464489,0.116176 -0.023970,-0.232866 -0.318547,-0.168238 -0.158595,0.048151 -0.124170,0.213977 0.596220,-0.028899 0.301808,0.121968 0.191744,-0.070269
Acrocanthosaurus -0.432153,0.123473 -0.032635,-0.208255 -0.302894,-0.138827 -0.176459,0.048779 -0.193505,0.170150 0.644601,-0.034614 0.277339,0.126262 0.215706,-0.086967
Aerosteon -0.494234,0.143456 0.011661,-0.214962 -0.321330,-0.153061 -0.177685,0.035283 -0.117259,0.157430 0.569638,-0.061088 0.303482,0.164450 0.225727,-0.071508
Afrovenator -0.518297,0.204136 0.049576,-0.291341 -0.345897,-0.189691 -0.163377,0.056306 -0.118179,0.161330 0.576952,-0.013944 0.255974,-0.077890 0.263248,0.151094
Allosaurus_fragilis -0.458156,0.130333 0.002849,-0.177182 -0.326445,-0.145232 -0.203823,0.029355 -0.090362,0.168071 0.634774,0.002972 0.280282,0.147470 0.160881,-0.155787
Bambiraptor -0.422093,0.160801 -0.036247,-0.156368 -0.319435,-0.131978 -0.172433,0.048943 -0.218974,0.150053 0.667119,0.083687 0.272167,0.002342 0.229897,-0.157481
Baryonyx -0.389248,0.127314 -0.075976,-0.220962 -0.313834,-0.131841 -0.159977,0.015696 -0.260645,0.234471 0.598531,0.021290 0.318131,0.076945 0.283019,-0.122913
Allosaurus_jimmadseni -0.497871,0.135941 0.064919,-0.229350 -0.320044,-0.176788 -0.163265,0.069501 -0.103574,0.206528 0.568997,-0.058819 0.284870,0.164846 0.165969,-0.111858

Ceratosaurus_dentisulcatus -0.438566,0.226949 0.070832,-0.311251 -0.321897,-0.201864 -0.104747,0.001422 -0.193434,0.239815 0.557789,-0.044235 0.259861,0.172292 0.170161,-0.083128
Ceratosaurus_magnicornis -0.418052,0.234891 0.026183,-0.316629 -0.353723,-0.203537 -0.117064,0.006618 -0.129073,0.224423 0.555172,0.065259 0.285554,0.126580 0.151003,-0.137605
Dilophosaurus -0.439368,0.146150 -0.031261,-0.233712 -0.287253,-0.138233 -0.180410,0.022163 -0.181168,0.222383 0.610898,0.016447 0.287771,0.086566 0.220791,-0.121765
Eustreptospondylus -0.455742,0.201997 -0.027289,-0.244244 -0.296984,-0.131572 -0.159681,0.053811 -0.188417,0.155885 0.600698,0.096668 0.279211,0.015790 0.248204,-0.148333
Falcarius -0.421929,0.058159 -0.162755,-0.225253 -0.414150,-0.244350 -0.214662,0.024311 0.073116,0.226813 0.521634,-0.016482 0.384042,0.207239 0.234703,-0.030436
Giganotosaurus -0.524450,0.138561 0.019481,-0.177997 -0.310622,-0.119446 -0.197408,0.059989 -0.107774,0.136560 0.581747,0.017456 0.319724,0.068951 0.219301,-0.124075
Majungasaurus -0.492128,0.211120 0.041819,-0.321744 -0.348417,-0.194278 -0.105881,0.049621 -0.033734,0.199570 0.501004,0.006431 0.249403,0.252058 0.187934,-0.202779
Masiakasaurus -0.535751,0.194571 0.100893,-0.277631 -0.330561,-0.295874 -0.129582,0.093324 -0.020571,0.237944 0.480331,-0.080462 0.310916,0.190240 0.124325,-0.062112
Oviraptoridae -0.523617,0.160491 0.025144,-0.355843 -0.399898,-0.280510 -0.060073,0.065909 0.051864,0.253321 0.445016,-0.047314 0.342087,0.227737 0.119477,-0.023791
Shaochilong -0.455568,0.174560 0.045420,-0.199899 -0.302979,-0.136574 -0.188634,0.048861 -0.191284,0.186538 0.613706,0.033727 0.266961,0.057411 0.212377,-0.164624
Sinraptor -0.492616,0.113184 -0.015966,-0.242545 -0.338943,-0.162879 -0.142788,0.036502 -0.053343,0.203982 0.565829,-0.032094 0.307480,0.192839 0.170346,-0.108989
Spinosaurinae_morphoI -0.445947,0.152836 -0.047449,-0.200774 -0.331024,-0.135508 -0.175562,0.032535 -0.136129,0.171821 0.621545,0.077712 0.284126,0.041544 0.230441,-0.140167
Torvosaurus -0.487335,0.157126 -0.017826,-0.221727 -0.337676,-0.135715 -0.152719,0.062997 -0.103433,0.137419 0.584630,0.041485 0.280290,0.102202 0.234069,-0.143787
Tsaagan -0.506605,0.186508 -0.029755,-0.211724 -0.298369,-0.107450 -0.191987,0.077072 -0.112285,0.109430 0.588528,0.129073 0.296071,-0.001390 0.254402,-0.181519
Tyrannosaurus -0.420497,0.121775 -0.155857,-0.246915 -0.403823,-0.190452 -0.196052,0.002755 0.027429,0.165579 0.537503,0.048744 0.348481,0.186010 0.262816,-0.087496

& [landmark 2d]
Tawa 0.023888,-0.274110 0.210722,-0.265792 -0.133421,0.752203 -0.110409,0.215758 0.071896,0.249426 -0.058885,-0.094335 -0.056505,-0.003903 -0.029194,-0.037576 -0.040803,0.002815 -0.045755,-0.076486 -0.062606,-0.240083 0.231071,-0.227917
Acrocanthosaurus 0.012428,-0.290145 0.246361,-0.277328 -0.088901,0.680540 -0.183063,0.181942 0.080680,0.204930 -0.055772,-0.026106 -0.067918,0.007360 -0.040582,0.010029 -0.058635,0.017817 -0.055809,-0.026026 -0.081889,-0.270151 0.293099,-0.212862
Aerosteon 0.028165,-0.336047 0.271439,-0.295344 -0.107656,0.580106 -0.169869,0.096919 0.117138,0.138522 -0.129006,0.057858 -0.128935,0.058828 0.008523,0.079085 -0.076058,0.139378 -0.035399,-0.020055 -0.120749,-0.262117 0.342407,-0.237134
Afrovenator 0.066015,-0.343904 0.245400,-0.352224 -0.163238,0.566721 -0.080950,0.102022 0.080088,0.137411 -0.080740,0.099694 -0.080608,0.101508 -0.079766,0.100868 -0.080335,0.101912 -0.080593,0.099883 -0.020021,-0.300222 0.274748,-0.313669
Allosaurus_fragilis 0.011834,-0.349177 0.277691,-0.325771 -0.141951,0.569229 -0.142640,0.174572 0.051994,0.208544 -0.062744,0.030465 -0.067773,0.047959 -0.035040,0.053709 -0.057911,0.091325 -0.037666,0.013405 -0.107392,-0.242491 0.311598,-0.271770
Bambiraptor 0.024545,-0.286390 0.275900,-0.220804 -0.035558,0.641438 -0.161154,0.166439 0.155973,0.189613 -0.172090,-0.193351 -0.155566,0.143320 0.011165,0.011265 -0.072573,0.113052 -0.053830,-0.113844 -0.134530,-0.285027 0.317718,-0.165712
Baryonyx -0.013952,-0.324187 0.311699,-0.284159 -0.149628,0.570796 -0.053273,0.128242 0.068642,0.142662 -0.102209,-0.025183 -0.071956,0.132243 -0.036914,0.052039 -0.062471,0.140155 -0.057069,-0.021334 -0.183773,-0.269628 0.350903,-0.241645
Allosaurus_jimmadseni 0.012501,-0.342776 0.263913,-0.321825 -0.142172,0.574733 -0.098343,0.115041 0.071511,0.140566 -0.059500,0.023154 -0.092918,0.111760 -0.042234,0.080813 -0.082256,0.129302 -0.048105,0.020529 -0.108312,-0.286174 0.325917,-0.245122
Ceratosaurus_dentisulcatus 0.073402,-0.357246 0.239552,-0.330516 -0.120229,0.594176 -0.087696,0.089953 0.094634,0.132326 -0.087297,0.087952 -0.087205,0.089216 -0.086619,0.088770 -0.087015,0.089497 -0.086879,0.088020 -0.039769,-0.328490 0.275120,-0.243657

Ceratosaurus_magnicornis 0.057922,-0.357020 0.247213,-0.330440 -0.135307,0.574643 -0.084150,0.098644 0.075522,0.130620 -0.083696,0.096367 -0.083591,0.097805 -0.082924,0.097297 -0.083375,0.098125 -0.083220,0.096444 -0.028917,-0.322061 0.284523,-0.280423
Dilophosaurus -0.002188,-0.332170 0.229958,-0.333839 -0.221817,0.613796 -0.155836,0.126101 0.068178,0.172541 -0.034463,0.037218 -0.036321,0.041590 0.015733,0.100735 -0.016178,0.073015 0.002026,0.052457 -0.123175,-0.277568 0.274083,-0.273876
Eustreptospondylus 0.057959,-0.368416 0.280762,-0.295216 -0.090014,0.586647 -0.092720,0.089099 0.075689,0.118685 -0.093365,0.087360 -0.093275,0.088600 -0.092699,0.088162 -0.093088,0.088876 -0.092955,0.087427 -0.058366,-0.323634 0.292073,-0.247591
Falcarius -0.010253,-0.355998 0.243283,-0.314837 -0.192219,0.586555 -0.082378,0.122856 0.066754,0.153862 -0.029976,-0.042204 -0.073795,0.113959 -0.014088,0.039623 -0.069091,0.274199 -0.018107,-0.030247 -0.090292,-0.290814 0.270161,-0.256956
Giganotosaurus 0.002003,-0.311181 0.237612,-0.296558 -0.121036,0.645278 -0.121227,0.155161 0.051534,0.181855 -0.054496,-0.007695 -0.062975,0.051402 -0.048461,0.027187 -0.057640,0.052169 -0.050132,-0.000909 -0.104438,-0.274855 0.329254,-0.221854
Majungasaurus 0.099024,-0.339532 0.272242,-0.316177 -0.042762,0.577528 -0.127056,0.085753 0.120598,0.133298 -0.126932,0.082461 -0.126762,0.084793 -0.125680,0.083970 -0.126411,0.085313 -0.126160,0.082587 0.002510,-0.294227 0.307389,-0.265767
Masiakasaurus 0.091113,-0.327294 0.253669,-0.292511 -0.005101,0.596734 -0.140255,0.073489 0.158005,0.162417 -0.140895,0.067911 -0.140658,0.071143 -0.139159,0.070002 -0.140172,0.071863 -0.139824,0.068085 0.033314,-0.320626 0.309962,-0.241212
Oviraptoridae -0.025136,-0.310625 0.193592,-0.255300 -0.130330,0.634953 -0.066994,0.171316 0.105996,0.195535 -0.112837,-0.123470 -0.065468,0.136367 -0.046556,0.025949 -0.054251,0.138879 -0.086676,-0.078925 -0.039911,-0.306165 0.328570,-0.228515
Shaochilong 0.017622,-0.343527 0.276639,-0.300141 -0.143293,0.606636 -0.081323,0.115986 0.056261,0.139048 -0.051471,0.032257 -0.069160,0.093674 -0.060194,0.060931 -0.068159,0.093084 -0.051749,0.029716 -0.131637,-0.289280 0.306463,-0.238384
Sinraptor 0.015004,-0.336593 0.188983,-0.323739 -0.196693,0.650400 -0.123755,0.144438 0.018799,0.176253 -0.065233,0.043940 0.003597,0.020437 -0.001774,0.070966 -0.015648,0.104658 -0.021597,0.029946 -0.053620,-0.320158 0.251937,-0.260547
Spinosaurinae_morphoI 0.014599,-0.304523 0.287253,-0.275502 -0.084159,0.643305 -0.118931,0.154071 0.096792,0.176022 -0.104744,-0.065452 -0.092440,0.059253 -0.036257,0.012202 -0.067604,0.081091 -0.078858,-0.065362 -0.159020,-0.231238 0.343368,-0.183867
Torvosaurus 0.066384,-0.312031 0.310572,-0.350556 -0.120196,0.527992 -0.100853,0.096682 0.091892,0.130708 -0.100235,0.093577 -0.100091,0.095538 -0.100106,0.095016 -0.100721,0.096145 -0.100510,0.093853 -0.095361,-0.254839 0.349225,-0.312085
Tsaagan -0.021163,-0.326065 0.236268,-0.230804 -0.127302,0.645777 -0.070085,0.161908 0.122438,0.175539 -0.121135,-0.159638 -0.080653,0.184843 -0.007217,-0.002548 -0.039114,0.111327 -0.055292,-0.114945 -0.171108,-0.287916 0.334363,-0.157478
Tyrannosaurus -0.004194,-0.320605 0.294005,-0.265460 -0.114374,0.613546 -0.167962,0.128312 0.078535,0.155846 -0.108608,-0.043052 -0.069656,0.085598 0.029187,0.050303 -0.072327,0.131975 -0.018494,-0.054362 -0.168194,-0.264560 0.322081,-0.217541
;

A7.7: Results of the Phylogenetic Morphometric Analysis

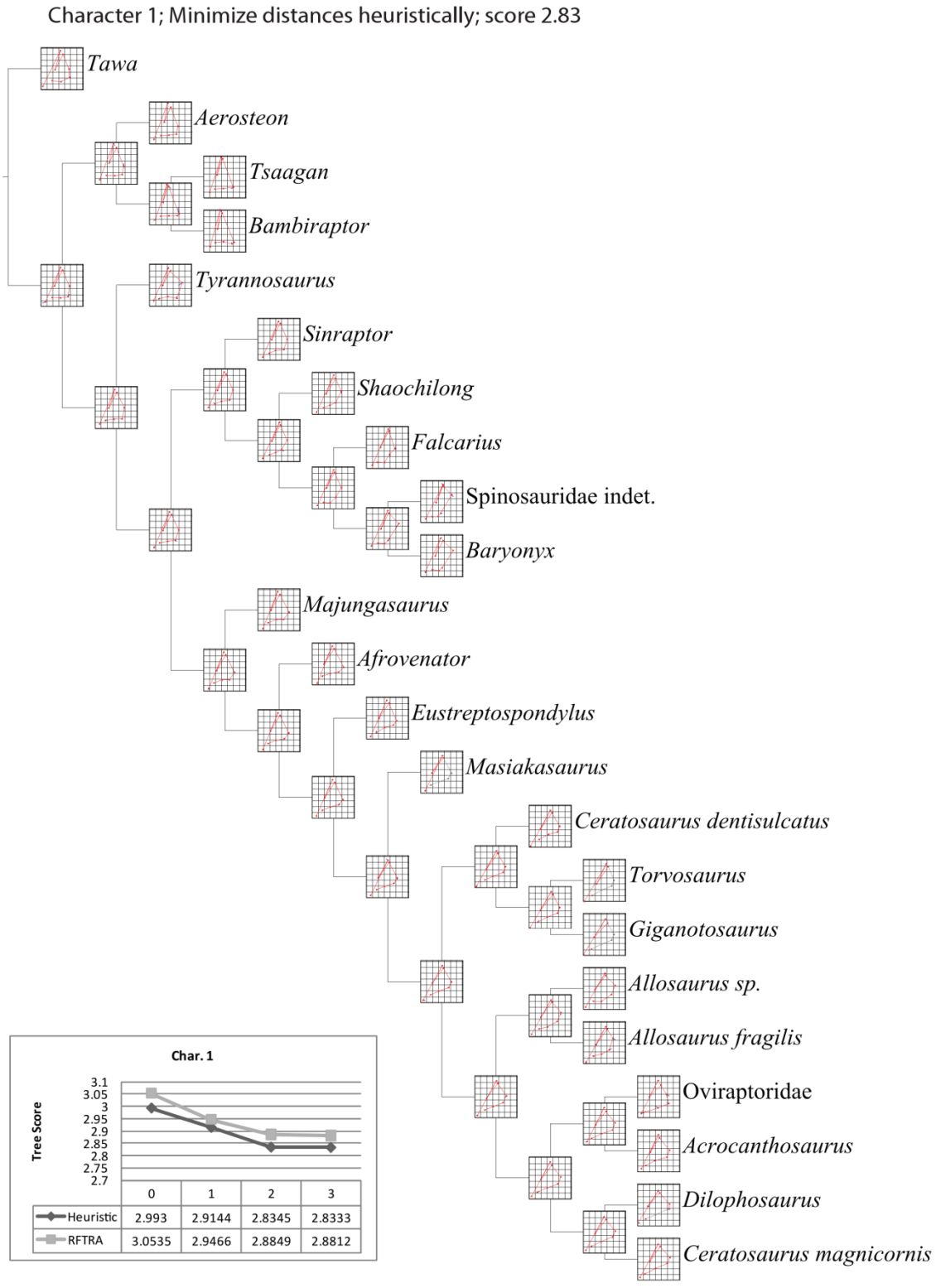

FIGURE A7.7. Quadrate in medial view (char.1) phylogenetic morphometrics results. The graphic shows on the y axis the tree score versus the level of thoroughness of the analysis (x axis), level 3 being more thorough.

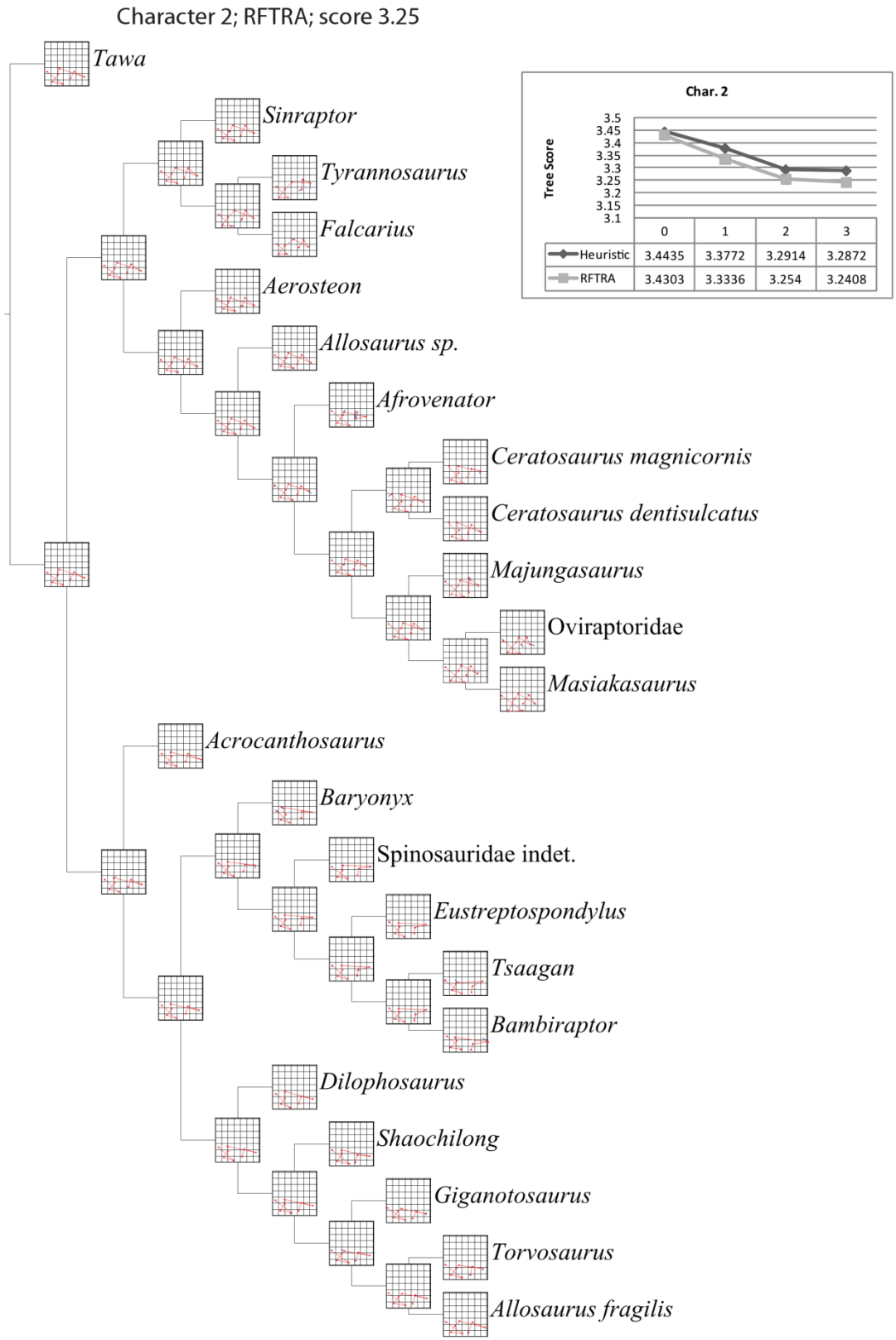

FIGURE A7.8. Phylogenetic morphometrics results of the quadrate in ventral view (char. 2). The graphic shows on the y axis the tree score versus the level of thoroughness of the analysis (x axis), level 3 being more thorough.

FIGURE A7.9. Phylogenetic morphometrics results of the quadrate in posterior view (char. 3). The graphic shows on the y axis the tree score versus the level of thoroughness of the analysis (x axis), level 3 being more thorough.

A8. Analyses on the *Spinosaurus* quadrate (Chapter 8)

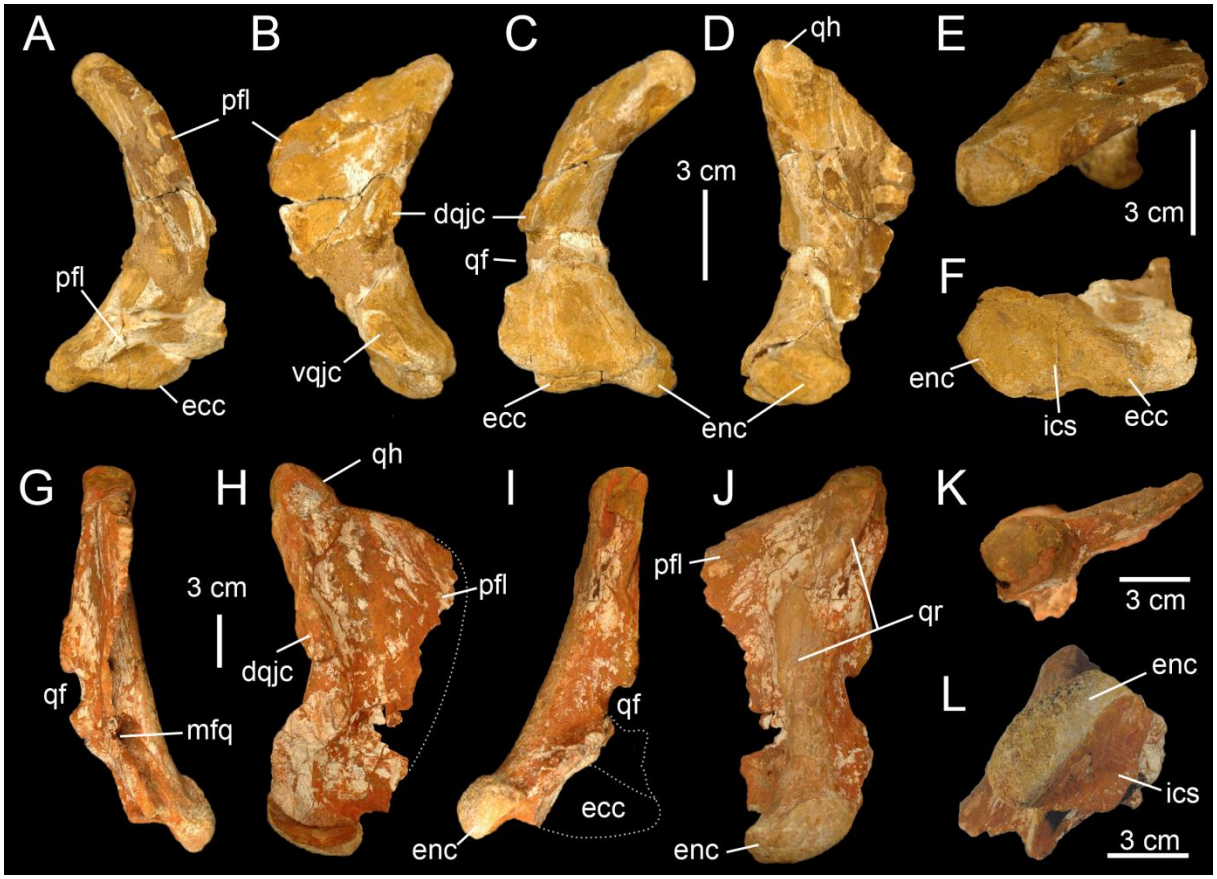

FIGURE A8.1. Quadrates of Morphotype 1 referred to *Spinosaurus aegyptiacus*. **A–N**, Left quadrates of specimen MHNM.KK377 and right quadrate of specimen MHNM.KK378 in **A, G**, anterior; **B, H**, lateral; **C, I**, posterior; **D**, medial; **J**, posteromedial; **E, K**, dorsal; and **F, L**, ventral views, with reconstructed parts in dotted line. **Abbreviations**: **dqjc**, dorsal quadratojugal contact; **ecc**, ectocondyle; **enc**, entocondyle, **ics**, intercondylar sulcus; **mfq**, medial fossa; **pfl**, pterygoid flange; **qf**, quadrate foramen; **qh**, quadrate head; **qr**, quadrate ridge; **vqjc**, ventral quadratojugal contact.

A8.1. Cladistic analysis on the non-avian theropod quadrate (supermatrix)
TNT file available at https://drive.google.com/file/d/0B_-0b-kZatHiUGtCN0ZrWlhaWDA/edit?usp=sharing

A8.2. Morphometric analysis on the mandibular articulation in non-avian theropods
MorphoJ file available at
https://drive.google.com/file/d/0B_-0b-kZatHiVG1WWktJMHBKY28/edit?usp=sharing

A8.3. Phylogenetic morphometric analysis on the mandibular articulation in non-avian theropods
TNT file
xread
2378 37
& [landmark 2d]
Herrerasaurus 0.129297,0.157989 0.058195,0.172355 -0.215019,0.121665 -0.552419,-0.107629 -0.164084,-0.093845 -0.209355,-0.174951 -0.022836,-0.274862 0.393198,-0.072945 0.390294,0.217945 0.192730,0.054278
Eodromaeus 0.116611,0.198612 0.042508,0.211269 -0.211653,0.121048 -0.533806,-0.076591 -0.295294,-0.132790 -0.097379,-0.174529 0.043818,-0.273251 0.371343,-0.081158 0.376633,0.184046 0.187220,0.023343
Tawa 0.157620,0.196927 0.111849,0.211633 -0.328042,0.027810 -0.505236,-0.085209 -0.219726,-0.132557 -0.197498,-0.138550 0.060512,-0.178562 0.357430,-0.094445 0.440659,0.160204 0.122432,0.032748
Dilophosaurus 0.231251,0.190602 0.145236,0.176421 -0.397721,-0.064541 -0.496790,0.030284 -0.333935,-0.146110 -0.098055,-0.164175 0.057286,-0.209766 0.346641,-0.022212 0.358973,0.155754 0.187113,0.053742

Ceratosaurus 0.218866,0.206912 0.126162,0.212120 -0.265849,0.111628 -0.493000,-0.123412 -0.165315,-0.106353 -0.280196,-0.176235 -0.009002,-0.297162 0.377429,-0.078582 0.351553,0.221815 0.139351,0.029269
Masiakasaurus 0.096786,0.136851 0.005784,0.229076 -0.359561,0.132114 -0.424232,-0.086130 -0.100667,-0.109740 -0.175885,-0.202341 -0.030018,-0.270513 0.353845,-0.205149 0.466665,0.246450 0.167281,0.129381
Ilokelesia 0.143078,0.181696 0.015513,0.163087 -0.262885,0.105439 -0.455936,-0.034027 -0.126615,-0.128410 -0.283326,-0.208145 -0.006954,-0.285452 0.401985,-0.126900 0.417762,0.285707 0.157379,0.047007
Carnotaurus 0.065363,0.137840 0.018533,0.222708 -0.322418,0.178183 -0.368001,-0.128340 -0.068748,-0.092338 -0.254175,-0.197545 -0.103287,-0.313834 0.420083,-0.172370 0.511956,0.277358 0.100694,0.088337
Aucasaurus 0.077410,0.196001 0.015319,0.210633 -0.256895,0.159208 -0.453452,-0.063749 -0.129978,-0.084393 -0.192090,-0.275566 -0.027020,-0.327026 0.368418,-0.140086 0.430029,0.259133 0.168259,0.065846
Majungasaurus 0.085327,0.118629 0.044457,0.139738 -0.308333,0.200552 -0.481171,-0.043910 -0.094051,-0.189203 -0.147949,-0.234069 -0.075721,-0.286968 0.372257,-0.136992 0.427700,0.253360 0.177486,0.178863
Eustreptospondylus 0.197118,0.148441 0.134291,0.116828 -0.334358,-0.040518 -0.491600,0.029186 -0.365306,-0.147941 -0.152446,-0.153375 0.054859,-0.211020 0.370036,-0.000779 0.382507,0.210088 0.204898,0.049091
Afrovenator 0.151681,0.179705 0.102536,0.161795 -0.351462,0.080179 -0.471944,-0.069844 -0.264366,-0.070285 -0.063019,-0.185194 0.019612,-0.242915 0.331099,-0.143174 0.443626,0.278045 0.102236,0.011690
Torvosaurus 0.141383,0.129226 0.084813,0.143351 -0.406041,0.052998 -0.533688,-0.023794 -0.158715,-0.136105 -0.083082,-0.171392 0.012503,-0.184480 0.330988,-0.103791 0.445526,0.206466 0.166314,0.087522
Baryonyx 0.176735,0.175902 0.147271,0.172773 -0.275330,0.076498 -0.588975,-0.092567 -0.438274,-0.145200 0.008039,-0.043981 0.148334,-0.193757 0.370604,-0.041616 0.362675,0.165970 0.088922,-0.074021
*Spinosaurus*_morphoI 0.241747,0.205416 0.175389,0.205103 -0.254304,0.020428 -0.576788,-0.057543 -0.344604,-0.192777 -0.083532,-0.153605 0.046984,-0.188100 0.292301,-0.071013 0.351786,0.189675 0.151021,0.042416
*Spinosaurus*_morphoII 0.253533,0.207798 0.187821,0.194787 -0.273093,0.049195 -0.668769,-0.151934 -0.252493,-0.110987 -0.057197,-0.122907 0.032692,-0.170951 0.272543,-0.064019 0.347632,0.147200 0.157329,0.021818
Allosaurus 0.186628,0.165102 0.047290,0.197669 -0.372830,0.073637 -0.497507,-0.096827 -0.238525,-0.169557 -0.052467,-0.074459 -0.022645,-0.217369 0.352971,-0.104724 0.432467,0.161785 0.164619,0.064741
Aerosteon 0.119928,0.142828 0.039315,0.163831 -0.220560,0.160726 -0.558581,-0.139515 -0.182856,-0.123974 -0.228907,-0.160287 0.053868,-0.239460 0.329209,-0.082031 0.419986,0.184353 0.228598,0.093528
Acrocanthosaurus 0.196136,0.125513 0.047224,0.142653 -0.303084,0.069454 -0.588249,-0.105231 -0.244487,-0.111403 -0.114758,-0.100112 0.027438,-0.200317 0.393007,-0.023384 0.382176,0.118045 0.204599,0.084782
Shaochilong 0.186073,0.157721 0.128237,0.148034 -0.281859,0.006732 -0.505594,-0.035792 -0.403981,-0.156034 -0.079300,-0.163460 -0.009037,-0.175496 0.391748,-0.014856 0.389750,0.178230 0.183963,0.054921
Giganotosaurus 0.100078,0.123635 0.058593,0.127173 -0.333803,0.042754 -0.490921,-0.041229 -0.288428,-0.143369 -0.083042,-0.154179 -0.028152,-0.175997 0.385884,-0.031805 0.485303,0.173213 0.194487,0.079803
Bicentenaria 0.263895,0.197831 0.119591,0.279828 -0.289161,0.150683 -0.591330,-0.224684 -0.174254,-0.086783 -0.085611,-0.165982 -0.000024,-0.236633 0.271325,-0.116218 0.377613,0.129359 0.107956,0.072599
Guanlong 0.163052,0.136727 0.100988,0.173993 -0.281475,0.078429 -0.574997,-0.083526 -0.192100,-0.117368 -0.284300,-0.147807 0.146998,-0.205558 0.350399,-0.027210 0.385783,0.153793 0.185651,0.038528
Eotyrannus 0.075460,0.162014 0.053335,0.168631 -0.281835,0.107289 -0.503387,-0.100181 -0.212963,-0.082815 -0.120789,-0.196014 -0.002224,-0.243114 0.334636,-0.116340 0.472211,0.211897 0.185556,0.088633
Qianzhousaurus 0.158223,0.142958 -0.008501,0.148314 -0.308162,0.093045 -0.474535,-0.063085 -0.253736,-0.130260 -0.126921,-0.145561 0.008845,-0.222605 0.365940,-0.098330 0.456025,0.237462 0.182822,0.038063
Tyrannosaurus 0.015122,0.134363 -0.071410,0.165630 -0.324666,0.133975 -0.486395,-0.027124 -0.221167,-0.109054 -0.182477,-0.129903 0.166684,-0.242521 0.474223,-0.068616 0.420408,0.125851 0.209678,0.017400

Ornitholestes 0.093244,0.219877 -0.015546,0.259851 -0.312797,0.123760 -0.500548,-0.173815 -0.179321,-0.064865 -0.077162,-0.142182 -0.008189,-0.240930 0.334497,-0.131643 0.484774,0.127332 0.181048,0.022614
Gallimimus 0.127105,0.145953 -0.100012,0.135845 -0.404447,-0.026405 -0.594825,0.174689 -0.196028,-0.198163 0.014905,-0.151944 0.179442,-0.190551 0.390791,-0.086333 0.399683,0.140269 0.183385,0.056641
Shuvuuia 0.015632,0.104301 -0.028941,-0.016330 -0.323904,0.088615 -0.548034,-0.088327 -0.318495,-0.183838 -0.036292,-0.109217 0.007497,0.001682 0.368926,-0.073103 0.575324,0.129866 0.288287,0.146351
Falcarius 0.030929,0.141373 -0.114663,0.208160 -0.384380,0.129377 -0.474320,-0.081488 -0.248334,-0.042651 -0.110872,-0.099984 0.215135,-0.219575 0.469654,-0.140215 0.418283,0.085448 0.198567,0.019554
Avimimus 0.149461,0.197496 0.084484,0.152940 -0.300175,0.106860 -0.509369,-0.081231 -0.188698,-0.116653 -0.207297,-0.163758 0.044830,-0.248002 0.355408,-0.103284 0.394448,0.228799 0.176909,0.026833
Ingenia 0.036132,0.240990 -0.022559,0.250266 -0.352679,0.157908 -0.371566,-0.117576 -0.090344,-0.060658 -0.211409,-0.182860 0.013095,-0.308436 0.453274,-0.200599 0.498362,0.184041 0.047693,0.036925
Citipati 0.164853,0.194854 -0.003808,0.234632 -0.315952,0.144594 -0.478321,-0.084199 -0.204881,-0.132576 -0.117697,-0.208422 0.014079,-0.247258 0.414125,-0.080566 0.400464,0.124204 0.127137,0.054736
Bambiraptor 0.117618,0.131571 0.006007,0.132322 -0.401097,-0.023536 -0.518013,0.029799 -0.398146,-0.161745 0.007194,-0.103297 0.137851,-0.127682 0.349677,-0.063340 0.427816,0.129101 0.271094,0.056808
Tsaagan 0.162451,0.106001 0.129459,0.112806 -0.350609,-0.067377 -0.496184,0.073447 -0.434986,-0.164711 -0.017929,-0.161674 0.057433,-0.180161 0.327972,-0.026752 0.437366,0.240262 0.185026,0.068158
Dromaeosaurus 0.082805,0.114110 -0.023405,0.120996 -0.229627,0.088482 -0.513607,-0.003698 -0.350531,-0.164905 -0.087722,-0.152966 0.071721,-0.227633 0.425428,-0.090494 0.401686,0.193118 0.223251,0.122990
Troodontidae 0.046712,0.117491 -0.094723,0.103478 -0.317700,0.083855 -0.536270,-0.120451 -0.245213,-0.172422 -0.032532,-0.111097 0.014024,-0.034870 0.305174,-0.183827 0.590018,0.135362 0.270512,0.182481

& [num]
Herrerasaurus
0001100000100000010000010100[01]2011010?0000?????0001???[01]1??000101010000110010010000
00100000-00-------??000000?00??100----???0010-00000000000????0?00000001?201000000000-0--01100--
0010000??-?00?0-00?00??00?1?????000?0?0000?0????0??000??1?1?0?0?0-000????0??????????0??1?000-
0?0011???????010?000??????????1010?000?010000000???0?000??00-
0000100?0????0010?001000?000000000000000000100?0??1??0?00000???200000000?000?0000?????????00????
?????0??0-00?1010?00110?1000010??0100?0?00001?0??010000?10000011000?11100000???0000?0-
0??0????00-00001001????00??1010???00000?0101????00-1?1?0-??010000?2000000000000000?0000----
0?0??100????001000000??00?0-0?00?000?000?01000100?10000000000101010010000?110000-
1000000011000010010010000010?001120011101100001000010000000000000100110010100100000000000000
000000010001000000000002100000000000000000000100100[01]000000000000000?000000000000000000100
000000000000000001000000000000000[01]001000000100000000?000000000001100?000000000010000000000
000000000000000000000000?000000000000000000001000000000????0?0001000?0?0?00000?0000100??00120
1000000000000?000001000000010?00000?10??00000000?000000?10000?0?0000?000010010000?0?0100000
000000-00?000010?-
0000000000000000?0?1000000?0000000000000??001??00?1?011?0??000101000000100000101000100000000000
0010000000?000000000000?0?001000000?00000??000010000000000000001??-
0100001000000000000000000??
??
??
??
??
??
??
??
??
??
??
??
??
Eodromaeus
0???0?00?0100000010000201002[12]0210[01]?1000????????000200000???????????0????100??0????
???????00-------
??
??
??
??

????????????

00?0000002001010000001??0??0?????20110001000?1000000[01]10000000100000101011 01??000111001000
00101100000000000010101000010000201??10000100000010010011010000001010001?111011000100010010
00110000110011 0[01]000?10000010001?00100110[01]000000000001000211002100001010110100011000?0?
??
??
??
000000000000100000?00000000??000000?011002?001001000000000?00?0???????000000000000000100000000??
??????000000000000100000000000000000000000000000100100001300000000001100100100000000000000
0?000?0000000?0??????2000000000000000000010000010 0?10100000000000000100000000100000000100 0
000000000000000000000000000000002000000000000000000000010000000001000010000000000000000
000000000000000?00000?1100000100100000100000000000001?001001?????0100000?????0001000 00?
000000000101010010000131000100001 0?000100000000?????????00?0000000000?0?000100000000100001100
000000010000010001000100 10010?000000000000000000000000000000000001000100???0?0000??0000010000
000110??02?10100110000001000?000??000001000000000000100100000000?00?000000000000000000?01000
00??00000000
Ceratosaurus 0101000000110000000101102001001011010100101000-11[01]101000-0111------
02001000110000001010 0-00-------??10100010001100---00?00?0100000001000010001111010101101-
100000001110?11100--001001000000010-
011101010010000?00?0??1000?02??01??000?0??1?1???10?00???0???????????1????000-???0???0-
10?001000?0??????100?100??000?11000?0000??0?0?0??00-
0000111?1101100000001 1??0?00101?00100????10000011011004001?0?1?000?01000?0?01000010??10000??
???????00010?01001000?????????????????10001100101????0100?100010101110??1??????2????1100??0000???
?1?000001001000000000-000101000100100000010-00000-
0?1100000000001101100011101111 0?0?0000?1000???00100001 1????????????000?????????01001000010000
011111100101111100000-
1100000011111010010011 1?0100?0112111110?131001000120001000000001000?100021001111011000 00-
?1111???111??000012001000000001000000000101002010000000000000000000000011?11000011101110011
11010110000111112111111210000 00[01]120000110111 0?1?000010020000010000011111[01]000010100?1111
??01000?111111010[01]11011011011111100010???021010001000000000000000001010001012 0?00000020200
11000000010000111111000101010101000000001101000011100 00?100010000001??100000010010001000001
0100100011021?0100010000000021100000010100001010211??10000210?0100001101011110100100110000?
???0??1??1?01?00010?010?11100?0000111011110110100000 1[01]0001001100110[01]00110210001010020021
11010010 21??1?0001??10??
??
??
??
??
??
??
??
??
??
??
??
??
Masiakasaurus 01??10000111000000000 10000?0011001?10?00?????-111101000-0??1------
0????2001?0010?0???0??00-------????????????????0--??100???0-
00???0100??10000????????????????????????????????????0-
??1?110-01?11100-
1000?????????????0-??????????0?00?0?00?000?00010100-0???????1101-10??00?0-
1?2110?0???01??00001??00010?01?0???01?0?110?0020????0??0?0?????????????????????00010???????????100
?1001???110?0100000
0?????????????????????0100100010000100100011101011000000?????????1??100111100?????000?0??00?????
00??
??00?1?00?111?0?????00000000????000010001 00?0?0010?????????
???11?1001???????10?1110000110011?0?12?0111121111100111210011101011110011 1000?0111?010111110
10?????110?1111?11010??1110110111210?1111111111111111010?????0???0010010000100001000???0????
?????10???????????0??20101?10?????????0????000?0001??00???0100?????????11101000011-
0??00?000100000000???0020001102?0011001001100011 1?000000101000000002011110001011?0100001?01
011111001110100001?????????????????????001001?1000000011?1111111201000010010 01??10011010011021
000101002102?1111112021111?0011??1101???
??

??
??
??
??
??
??
??
??
??
??
Ilokelesia ????1?0011110000000101000001001101?[01]0000??1??0-
122101000?0?????????0?????1????010?01??0??00-------
??
??
??
??
??
??
??
??1????????????????????????
?11101111010?1????????????????????1????????????????????????????????????1???????2210010101201l0?111???????
?1??112?011??111????????????????????????
??
??
??
??
??
??
??
??
??
??
??
??
Carnotaurus 0102000001110000000001010001011001 0?0?00??0??1-?????100?-0?01------
?2001101000010011010-10-------??10000000001000---
0??00?0100001000100011???1?1001110??200000000?00-10101000--?10-
110000001?1101100101000000???0????1000??2??0????0????00?1001??0?0?????????????1101100??00?010
00-100?01000??0?1110100010100??01000000?0?0000000???0-
000010101101?10?00??11102?10100?00100?10?10000111?110040?11?0??????00????0?????0000???0??????0
0--0?0000-?01001010?221?0110?200000-000111000----??????????????????????????????11000-
0000?????0000??00??0?00000100????1000000100?000?0-00000-
??000?10000?0111011??011?00?110?0??
??
??????????????????111112111?02111011011111210111111101110011101110111111111111011???100111?111?111
111111111110?10100012?1111121110111012010011111111111111111?1?101111011011111111211111?11111111
11111?11110?1111????11????1??
??
??
??
??
??
??
??
??
??
??
??
??
??
??

Aucasaurus
????0000001100000002010000?2012101?0010????????111200000???????????0?????0????01??01???
1000-------
??

0000000100000010100001000 10?0?01?000-
0101001000000010001000100000111000000011000000001000 11??0??????0000010000?0010????????????????
??
??
??
????????????????????????1???2000001 1?01100000010120?1???0???????100200001??????10?10001?1??00000?
??10??1001000100?11000012??????????00110111????????????00000?0?0100000100110 01???0110100100011
011000001001100010 1?100??1?0000????1????????111?0???0121210?00?????????????????????0011010110
0011?011300?2?1?000001010100?111111000011000010000211110 1?110102111??1001??000????????????????
??
??
??
??
??
??
??
??
????????????????
Afrovenator 1101100000101000110000001012112100?0010?101100-010200100-0??1------
120010100001------010-00-------
?????0???????1?101001??0??110101001 10?00000?1???????0?201100??0?01010011100--00????????00010-
01??0????01000????????0?0???
??????????????02000100000???????0100-0110110?10-
1?0001?1?11???0100?[01]?1010?????1?00?????0???????????0???0??0?0?0?100???????11?00????????????????
??????????0??0?01??????00?????????1???011?1?0?????12100?2???0100000001001 00??0???00?00100001 00?
000000-0?0?01???0001001001 1010000-
?0?0?11000100010001 00????0?0??????001????00?0000100?111???0?110????01????2????????????????????????
??
??
??
????????????????????????????????00101011000001001 20011000?????0?000201001?011001011000?????????00?0
??0000000001?????10?11001?0?011000010001101100
001?001?000001???????100000???1?01010??????????0121?????00?0?????0?31001111?100001?10?011010 11?
011?2012?1?00?00101110001110110000110000100002 1?11010110???111011?011100??1?????????????????????
??
??
??
??
??
??
??
??
????????
Torvosaurus 11?10000001010000101002031110110 00?00100101100-021201000-0??1------1?????1?0??1-
-----?10-00-------??001010???????0-
?????????1100????0000010 1??????????1?2??10000??0101??1100???00?????????0010-
00??0?0-???????0-
????????????????????????00??0??0?0001?00?0????1????010000???1?10-
1000?1?1?11????10002?10100????11000??1?0??03??????????1?02??0?0??0?1??????11?0??????????0??0-
0000??????2?0??0201?00?0200?1?01001?????01111?0?10?01?????0????10????00100110??0????00?0000000?
????000?0-00???0000000100?10?00-1?0?0-
???0??1????0?010?0??0??0??00111???0?0?????00???011000111?????????????010????????????????????????
??
??
??
????????????????????00???100?0010??1101100010120 00??????00?10120000 1?011111011000?[01]??????????0

????????????????????????????????????010?0?????????????00000100010010010011011010210010010001121100001100011000101110000011100000??010?10100111000000012121100000010 0?0[12]???0011011010000010101101011101130 00[12]?1000002001010001110?10000110000100002121101011010211 0?1001??0????????????????????????????????????

??
??
??
??
??
??
*Spinosaurus*_morphoII

?????10100201?0??300003032011020000?????02?1[02]2?11132001000???01011000?????2?0??1------100-00-------

??

0000000000000000000000010000000000100000000000000000000000000000000000000000000000000000000000000000
00000
Aerosteon 1???3000000010011100002010011111110?10101201001001310010 0-
0??00111200212200100001112 1?000-01100--
02??0??10-
??
??????????????????000?0?????????01?100?????0?11111?00???????????001201?0010001111?0?01001?03?????
??0??10??????1?????????????????????100??
?????????????1101000001 00?0010?00000100?000?010100?011--
00??
??
??
??
??01?000?111??
??110121???????11?01001
?1?000100010110101111?????2?110??0?????????0101100121?????????????????????????????0101101001022
11101102012 01?120?????????????????????????1001?412????01112021110????????????????????????????
??
??
??
??
??
??
??
??
??
????????
Acrocanthosaurus
1000000000100001020200203000001000120100??1??0000???0???00100101200021220 10?10001101
1002101202100????010100?0??101?0??10?0?10-?0?1?0110001001000?0?0?0112011??0?0001010??1110--
?11?0?????01101111?00??10110?020?0??1?0??0?????010?0???1?0101?0?10000????10-????????0????200-
?0000-
?10???0?10111???0??0?0??101??00002100 1?00?0?0??1?0???1000?1??1?111110??001?11??0?10??2?1??01???
?10?1?00??01?0?1?????????0?02??????10?1?0????1?010?????????0???1?101?10?0?100000??10???02??00?10 1
??0?0??01111?0?10100220002??100?0???00???10?????????????10??????????101010??0?0[01]0??0????00?1 1
?10?00???01012?1001?011?0??00100?101?????0?0?????0??0??100????00?000-
00??0?110??2?010??
??
??
??020?1100?0000001111000000211111100010?0000
0021110121110002021201 1?1121111020110121000001001101000120111 11?1100210010102001 0?11111?00
0100010000010011012?00110011?00?00121100010001100112111 10?0021000000101?1?11011012001200121
0?0010111100001131101111110 00???010?10??1110110201201?120?2011110002201110111100001100103 1
2?1010?1110?1??01210111001?1??
??
??
??
??
??
??
??
??
??
??
??
Shaochilong
1???0?000010000002010020300120 1100?2010????????010200000?0?????????03122010000???????0
0??00-------
??
??

????????????

????????????

????????????????????0?1?????????????0?0?????????????????????00??0?0??????0000?10??01???00??1?1?????
????????????????????????????0?0?0?000????????000?????????????????????????????????????0???00?????????
???0?0???00?????00???00??00?00??11??0?0?????01?111?00?0?????00????11?0??0??1?0?0??0?0??0?00?????
????????????????????????1??????1??000??0?00?0???00??????????
Qianzhousaurus
10003000000022100?0[01]00?0?001?0?1???001002120011203100100000?10101220011312201001-------000-010-0-
200??
??
??
??
??
??
??
??
??
??
??
????????????001011??2?????000001111011110?0111012011010120121010102111010111000100001020000
1000010010111001132011110110121001111111111?1011100100111010001101101111110110111110111100101111212211110??10000????000001000001111110?11011?21011111?????????????????????????1?111110110?
????????21?11?10111121??00?11111?11?01??
??
??
??
??
??
??
??
Tyrannosaurus
2001300000002010010000100001001111201100232100100020010010 1?01112200013222010 01------000-010-0-210??10?0000000110101011100110-
000000010000010111011010002011001100111101110110?11110100-
011?10011201110110103?000010000001001011 0?0010000010010-0?010?010-?0-1000000011000-00000-00-
1000010111?0111001010101000010200000000000000000010100000111010-
11?00000011?000100010000000000100000010010031000 00?0100001000000200000 00-
100110???101??000100101000000110001001 2?000100010010 01?0?0000101000----03200021--
00000?000100101011100000001200011000000101011000101000010000000102100101011012001210010001
000100010111?0010?0??0?0100020001101 00?0011000 01-
100020000??
??
??
??
??
??
??
??
??
??
??
????????????

Ornitholestes

?101?00000112?0??10100101000201011????0??00?002???????0?10??0101??002122[12]00??0000111???22?0-------??00?0000?01?00101011100??10000?01101000000000?0?00111000110000010-10011100--00101?000?10000-000201000?0000[23]0????100000???0?0???0?00111101?100-????-?????????????0010?10-?0010-00-100?00-011100011010001012011102101-001000000?010100-????????10-1?101200011??1111?11?101??01001??1001010100?0??10?0?10?0020000?10?0???????????1?1?????????????????????010?0100001001?0??0?0?0?0?????0?????????????????????????????????1?0101??0100000?0001001100000011????010?0100001 0?010001?10000-0?????????????10?0?10?????????????????00??0?????????????00??????0?100??0?0?0?10?????????????????????????????????

011101012001111000?30---1--11-00000-0000----22000-010011112-
20010010 1???0??1???101?001??????10111211011010000011000102-
1000?0011??
??
??
????????

????????????

??1100000011011101201?10011001001111001100013200110110111111000?110001110?1220010001??011011000111100020210102100?1?000101110101101?????1??
???1?????????110110100000?110?110?01?1101??201??????02???00?11?1011101013000?010?00100000011001
10?011200100000010000001000000001000000001000000110010?1100?0101?02?011?000??0?0?10?2000110??
??11?1?11000100?00010?100101010000000001000?00?00100000001000000?011001001001??221000111111
0001011?100132100011000001100011022112 0?011001011?1?3??????101100110010111100 1??20???0021001
11?011111?010000100?11000001110021100?110220?0??1010010?1101000000100?0000010000000010010110
?000000000??0???0101011010100111010100 1??????10????010?00101101001010000000000000000100??????1
??101?000000010110010000001??00000100?10?01?1110?0?10??

Bambiraptor

102100100111000003013020300000010023010?00100001101002000??0200?200025020020000000?000-00-------

??

?0??0??00?0?0000???0?0??00010013?0001000001?1???0?0?0???
??0???1?????0???????0??
Dromaeosaurus
1020001001110000030110?0??0101000020010110110002102000000?0100201220021501002000010011000-00-------?????????2?0??1??1?1??100????0???0?010??10100??0????011???100??011??????1???????0-121111???????0??0????????031???0?0??0001000010000000??0011?11010000-1110-10-1000000011000-00000-00-0-000100111010111101010?000110?000?00000000000?0100-0???????????0?????????????????????????????????????0???

A9. Phylogenetic analysis including *Torvosaurus gurneyi* (ML 1100)

A9.1. Character list

Characters 1-351 are from Carrano et al. (2012), with the modification of character 26. Character 352 and 353 were created and coded for each taxa.

26. Maxilla, development of maxillary 'fenestra': absent (0), deep and well-delimited fossa (1), shallow and poorly delimited fossa (2), fenestra (3).
352. Maxilla, shape of interdental plates (separated or fused): rectangular (0), subpentagonal (1), triangular or trapezoidal (2).
353. Maxilla, neurovascular opening on the dorsomedial edge of the jugal ramus: absent (0), present as one foramen (1), present as several foramina (2).

A9.2. Data matrix

nstates 5
xread
353 62
Eoraptor
00010000?00000??????0101000?0?0010000?0000100??0001?0000001000000?0000000000?10?00??0?001000
?0000?0??????0??00?0?10100000?0?0000?00?0000?0?00?000100000000000-0?????????-
000000000000000?0?000000000000000?0000001?0010000?000001000000101000000000?00100000100000000
00010000000?00000000000??000?0000000?00000?0000?000?000000000???-000000000000000000000000??
Herrerasaurus
00001000000000????0?0001000?0?0?00000?0000100??00120100000000000?000001000000000?0?000010?0
0000?10??00000000?000000?10000?0?0000?000010010000?0?0100000000000-00?000010?-
000000000000000?0?1000000?0000000000000??001??00?1?011?0??000101000000100000101000100000000000
0010000000?00000000000?0?001000000?00000??000010000000000000001??-010000100000000000000000000
Acrocanthosaurus
020?1100?000000111100000031111110001 0?000002111012111000202120 11?112111020110?02??1101210
000010011010001201111 1?11002100101020010?11111?000100010000010011012?00110011?00?001211000
100011001121111 0?0021000000101?1?1101101200120012 10?00101111000011311011111 1000????010?10??
111011020120 1?120?201111000220111011110000110010312?1010?1110?1??01210111001?100
Aerosteon
??01?000?111?????????10000200????????????????
??110121???????11?01001?1?000100010110101 11??
????2?110??0?????????0101100121?????????????????????????????????0101101001022111011020 1201?120????
?????????????????????1001?412????01112021110?????????????
Afrovenator
?????????0010101100000100120011000?????0?000201001?011001011000?????????00?001111001?????????
??0000000001?????10?11001?0?011000010001101100001?001?0
00001??????100000???1?01010??????????0121?????00?0?????0?31001111?100001?10?0110101 1?011?2012?
1?00?00101110001110110000110000100002 1?11010110???111011?011100??110
Allosaurus
00101[01]000001000101010000031111110001101100002[01]2[01]00101100000001011111000110200000020
011011000110100100102012011111111112000100110201111111110000100011020010011001100110010[01]1
000001011000100001000101111000011?000000010 1?1101101200120012101011000010001113100111111000
011101001021111011020120 1?1100200111000[12]101110111100001100102122101011110211012101110010
0110
Angaturama
11???201?1121?11???0?????????????0??
??????????????????1?0??????????????????1101117013 11???
??
??
Australovenator
??
??????????????????00001???????????10000100011 0???
???????0?????????????????????????????00010101????01?1111??101?????????????????????????????????2
20121011110001110011412210101112121110121 1????010???
Baryonyx

111?02010112101l0?0000???02???1??01????0?001202011?0??????0??0?1111100??????0?1101101000101l?0
1??010210?011??????????001101010?[12]101???1??0100101100013001011100[12]?10010010010001101111l
0100011000101010?0???000?00??1??1?00??0?1?0100012111100010011010????????????10?0?11010?101?111
0110[01]0?2?1?0????0011000????1????00110100????????110?0?????????????0????????1?
Carcharodontosaurus
??????0??000000111100001031101110101111000?02?1?0??111100??2121121l?211????0????????110121?0??
0100??01121121???1???????2?10?????????????1000020000?????10?110?2?????0??01?0?00101?0???1????0?
?????????????100?0???1???1???1??1???????11?????0?????
0??11?????22??1101111??01?100???????010?????????????????????[01]0
Ceratosaurus
021010001000000000000000001010001012l?000000202001100000001000011111100010100100100010101l0
000000011010000111000l?100010000001??100000010010001000001010010001102l?0100010000000021100
000010100001010211??10000210?0100001101011110100100110000????0??1??1?01?00010?010?11100?0000
11101111011010000l[01]000100110011l[01]0011021000101002002111010010?1??1?0001??10???00
Chilantaisaurus
??
??
??????????????????????????0120110000?????????????????????11??????10????2110?????????????????????????22?
?111???1000?1100??41221????1?????????2101??0??????
Chuandongocoelurus
??
??0??????????????????0?????????????0?????????
0??00???0011101011???1?0?????0?????????????00
?101000100000?1000041?2121011???21110?100??100?????
Coelophysis_bauri
0010121100001l????0?011010100?0000000?0000101??000000000000000?0?000001101101000l?0000000?
0?2??1????0??1?0?0?0?00??00110?0?0000?00?000000001000l?000000000110l?100011000?000001011000000
0?000000001000000000011?1100?01?000001002000101000000?0[01]?00101110101000000100100011000011
1011110100?1000000100001000011l[01]00?00?000?0100011000210000001011110001100000?0
Megapnosaurus_rhodesiensis
00???211000010???00?01101100?00000000?020010100001[01]00000000?000100000000?0110?000000000000
00000200100?000?100000000010001000000000000000010000000010000000011011?000110000000001011
0000000?000000001000?0000?11?1100001?000001002000101000?0010[01]000110110101000000100100011
000111011110000?1000?011100010000111[01]001102000?0100?110002100000010111100011010000020
Compsognathus
00???100000100????0?010003100?1??0000?0000000??00000?000?00?00????1?00????????0??0????0??00????
?0??0?0??????1?1????1?0000?00??0??100??10100?0000?0??0000100?100[12]???????100?001??001100?000?
???0000??1??0??000?0?00?1?0?0111?011100?0??[12]??0???0???0??01?1310011????0?000??010?11??110011
?20?201?011?11?10??002???111?????????1?0???????01011???????01??0?11?01010?
Concavenator
?????0???????0??????001003??0?1?00?1111?10102010000?110??10??2????1?????????????????????????????
??1020?0??????[01]0??100?????????????????[12]?1??10????1???
0211?1?1??[01]100?000????1?111110?10?1??0?1??10??0?1010001?????????????0?0?0?10?11??111011020??
??????02011???1?22??1100?????????????[12]2??0?0?1?1?????0???0?1?00?????
Condorraptor
??
??????????????????????????????????????0010001????????01001????????0000?00101?00001000?2001?011101
001?0002???01??101???0?1??01?01010????????0????0???0000110
0????????0??01000001?00??11?????????????????1?01???0?????
Cryolophosaurus
??????????????????00?????????1??00?1001?01010?000?0111??0?00[01]0?1?10000?10??000000??100010000
01??1?0010????0??????1??0?????????????10?000000000?0?01??????0?01000????????00?0?000?0?1000??0010
00??010?0?????000200????0?01?????????????????????0?10001?????????????00???00???0?????011??0????0
???0?0??10011001?0?00110100000000?2??????01001011??0?????????????
Dilophosaurus
01?11211000010000000001000100000000?100200100??00?200100001?0001001000?1101101000000000?000
0002001010000001??0??0?????201100010000?1000000[01]10000000100000101011101??000111001000001011
0000000000001010100001000020l??10000100000010010011010000001010001?11101100010001001000l100
001100110[01]000?10000010001?00100110[01]000000000001000211002100001010110100011000?0?[01]0
Dubreuillosaurus

01???100?0010101?000001001[12]0001??0??0??0??002??001?0????1011?001011?000000??????????10??2011
100?0??110010??0??????010?0110111??201??????0000000?0100000100?1001?????????0??????????0?00??0?
1??????1???????1??000?10????0110?????0???
??????????????????11????0?0???????????1?01?????????????????1??????1?
Duriavenator
00???100??0101011000?0?0?120?1???0??
??????????????????????110101???????????0000010?0??0?00100????????????????????????????????????
??
??12
Elaphrosaurus
??
??0110[12]????????00100000?01100000?0000000002
111?0000011??010???????0???11?01110100001000?????????????????????0001110000001?111111100?[12]?????
?0?0?0000110011?00110??00010000210??21?0?????111?001???1??????
Eocarcharia
????????0000001110010100311111?0?????????????????????01?00201111???1?????????????????????????
??1000010?01?????10??
??
??10
Eustreptospondylus
?1???20000011?0110000010120?1???0???????100200001??????10?10001?1??00000???0111100010??100100
0100?11000012??????????00110111?????????????00000?0?0100000100110010???0110100100011011000001001
1100010?100??1?0000????1????????111?0???0121210?00?????????????????????00110101100011?011300
??2?1?000001010100?1111110000110000100002111101?110102111??1001??000??1?
Fukuiraptor
??????????????????0?0?0???
??????????????????0?????????????????1000010?0110????00110?[12]????????1?????????0????0????????11??
??????????????????????????????12001211101?001?1010?????????????10?????10?????????????????????????
????2101210?1100011??01??12????01112121??012?1???0??????
Giganotosaurus
02???000??0?00?11?100001031101???10?1110100021110????????2021211??11211??0??1?00020?110121???0
0100?0011211?1??????111??201010?????1?1111110?0020000??000100110l2?01?0??111001?01?1?00?100?1
1001?21?2??????2?00000???1??0?10??0???01?0?????????????????????????????00?110100102111101102012
01?120020111100022011101??1?0???1001?3122101O?10?????????????????00
Irritator
?????2????02?0???????01100200?100010??0000010?201110010000??00011?11000????0?0???11?10??10?100
10001021000?101?10?????0?????????????10?11?0???1101?1-
??????1??
??1??
?0
Leshansaurus
???????????1?1?1?001??1?0????1????????????????????????????????????10000????????????00000001002100
1??00????0????????????????????????????????00???0????????[01]0?1100?1?0010??0110000121?0000??0????00
0001100??1?????????????0?0??????0110?0111011?[12]0??????
??0??0??????[01]????100001???1?10???211110?0?????????????????0????0
Lourinhanosaurus
??
??1100?????????0??????1?1?000?000?0?00???1?1?0??
1100000?????0?111??00?01010?1011111011?2?????1???0?001100
??11011101?0110?????01?21?2101?????????????????????????
Magnosaurus
????????????????????????????????0???
??????????????????110?11???????????0000000?0????????0???0????????????????????????0????????????
?00??0???01??1?????????????????0??0?????????1??
?????0?110?001000?21?????0?11?????????????????????
Majungasaurus
021010001000000100000001001000001112O?10020000?10120000002020201 2?1111011011000010001010O?0
0000010?01101?1000000010101100101001100100010010100000001000010001102100110010011000121100
000010100000010 21?111001201?01000011?1011?10?01110200001O??????0?????????????0??0011100000001
111111?????0???1?????????0????100110?1000101002102111111110211 11?0001??1101?00

Mapusaurus
??????0???0000011110000100110?10101111010002111 0??1111102?2121121????????[02]01?000?0????????
????????????????????????????0020101 0?01001??????1000020000?0???10011012???01???1??0?0010??0001??01
?00102012?????210000?????????1?11012?0????1???10?10???????0????1????????000???0?0?102?1110110[12
]?????????0?011?100022??1101111?00?1100??31221010110??2111012101??0010?10
Marshosaurus
000??000000001001000110201100 1?000010?000??????????0?1001?10000????1000000?10?0?01?0100020000
001001?0?00?1?0???????????10001??0???1?011??001001000100000100110 01?01111100010000121100000000
012001101?1?????????????????10???????0?1????????????1?????????????????????????00?110100101011?0110010
201?0000?00111000?????1?????????????????????21???????0?????????????????10
Masiakasaurus
0?????0???001001000001000010000???0?????????10???????????0??20101?10?????????0?001??00????000?000
1??00???0100?????????11101000011-
0??00?000100000000???002000110 2?001100100110001 11?000000101000000002011110001011?0100001?01
011111001110100001?????????????????????001001?1000000011?11111112010000100100 1??10011010011021
000101002102?111111202111 1?0011??1101?10
Megalosaurus
?????????0000?01101100?001?0?1?000?????????????????1?111???
??????????????????????000101?????0?011000010010?01??00?100???01????????0??????1?????0?1????10002011
100001?0000???010?????01110?000001212110?000010000?????????????00101010110101110113?00[12]???
???0?10??1?001110110000 1?000010000221??0?0?1????1????1001??00???00
Megaraptor
??
??11012????????11?0100121?0????????1?????????????
?110?0????????1?111011?0121?????????????0101011?2?0101111111 0??????????????????????2??????????????
??2?11?????????
Metriacanthosaurus
??
??1001?????????0??0??1?1?00011?00?00012111?????
1?000?0???1????1???00??10100101111?011??012?1?0?00?101?01
?111??110?11110001??0???21?????????????????????????????
Monolophosaurus
001?1000?00100??????000003000?100011101300100?-
0012[01]1100011001 0?11110001?021000000??1000100000010?????0????01?1??????0010000100201 00?0?0?0?
0?0010?0??000010111001 0?001001001 0?0010110000000?10000101?10?0?1?000?00?010?????????????????
????????????????????????????0011000101010111011?00?[12]0100???0001000?0?????????????????????????????
????????????????????????
Neovenator
00???100000100010101000003100 1???10110110??
???????????1?????????110000????????????1000010001?020010011012?1?????111101001211000100011010 1
0110?0???2100001???1?10?10?1011?0120?????????????????????????????01?110100102211101102012 01?
12000001?1011020?110111100011100113122101 0?10???1????210111?010?10
Ornitholestes
000??000?00000??????0000011 00?1?000010000010 10?0012?11000001000?1??10001?020?00??0??1000?00??
?0????0??0?????????????00000?0??0?0?0?0100111?000000??00001001100[12]?????????0100101?0?000?000
1000000010100??1?00010??010??11?????????00111100000000???01??11??111??1??00?0001011121111011
020????????010010000021??211??0100001???????2??0?0????????????2001??0??????
Piatnitzkysaurus
??????????000?0100001002011 0?1???0????????????????????????????????1???0?????????????10?0100000010
?1101000?10????????????2010?1????????????0010010?01?????0000100 1?00111100010000121100001000 1200
?1011100001?000?0??010?????01011?1120012111011 00??100?1?????????????001?10100101011?011?0002?
100000000110000 11?11100001000001000022121010?10???1????1001??0????10
Piveteausaurus
??011?000?????????????1000?0?1002100?
?1002?110??
??
??
Poekilopleuron
??
??1

00?0??1?????111??????????012??10110001000001????0?11????0??
??????????????10???2????0?01111021?10????????000???
Proceratosaurus
000??000?00100??????000003100?1??0????????0???????201100000?????????????1??20??0??0??????????????
?????0??????????????00[02]00?0??0???00??1?1?110000?0??0000000?????????????????????????????????????
??
??
??1?
Saurophaganax
??0????????????????????0????????????????????
??1100?1??????????0?001?1?000?0??0??????11??????
??00??0????????10??????????012?0101100?????????????????????00001?1010010?????????20?[12]01?1?00??01
?????210?110??01???011001?21?????????????????????00??????????
Shaochilong
??????????000??11?10100100110111?00???1????????????????????????????1?011?????0?00020011???1?00001
00?0011??120????????????????????????????????1??
??
??
??00
Shidaisaurus
??0??11000????????????110?0??????????0
??0??0?00???????????0??0110000???????1????001?00????01211010
0001?00???????0??00??0?1??1???111011020?[12]0??00??20?
?0??0??
Siamotyrannus
??
??0[12]????????????????????????????0????1101000
?0?000????010???00201010010 2?11101122012110000??1011
01??
Sinosaurus
?0?0?000?0010???????000203??0?1??0??101300100??000?00?00?01?000???1??0?????1?0????????????????????
??????????????????????????00??0?00???1?????????0??0?0??????10?0100[12]?1?00??00010000?00100000100?0
00001??000?1000020??01?010??010001?000112111000000010001???1010111?000000?0101?0000111011?[0
1]002010000?2000101110011100001010 00?10000220010 10?0????0???110011100??110
Sinraptor_dongi
000010000000000000000100031111110001101000021100001110001000100 1?1100001120010002001101100
0010010010011201001 11?111110000001100200111110000000010?0?100001001100110110001001000012110 0
011000110012110 10?0?1?000?000010???1?01011100?????????????????????2????????11?0002010100101011
101122012111000021011010111011101111000011000022121010110102111012101110010110
Sinraptor_hepingensis
00001000000000??????010003111?1?000110110000211000011100010001001?1100001120010000??11?12000
?00?????01??????1?1?1??????0000001?00?001???1?000?00?000?100001001100110110001001000012110001 10
001?001211?1100011000100?0101?1100101110 0?0????????????????????????????????0000101001 01?111011
2[12]00211101002101 10?10110?1101111?00????????????????????????????????????
Spinosaurus
110?1201011210????0??0000020??1??0?????0??
??????????????????00110?0??011????????010110111-
01311?101100[12]??????????1000??21?0100?00???0?02010?00????000?0??0????????????????????????????
??
?????????2?
Streptospondylus
??
??1100[12]????????0??0?01??1?0000010?1?0???010??
?????000?0??0?0???0??1?000????????
0??????????01000?01????2???????1101021 11?????????????????
Suchomimus
1111020101121 01?0?00000100200?1??0?????0????????????????????????????1???????????110110?????????????
??????????????????????110??????1????????0100101 10?013001011100[12]???????100?0001121?11101000110
00201?10?0???00000???1001?0001011?0100012111100010011010?????????????100011?010?10001111011000?
[12]?0?00?000011?00?11??1101001101001 00??41211010?102021??0?1???????????10
S._zigongensis

??
??00?0??1?????00?1100[12]?????0010??0000121100010000?1?00?011?
1??0??000?100?????????01011?0???011021001000010001??2?00111111??0000101O?10??1110110101[12]0?1
00?020011011111?1??0??110?000?00??211[12]10?0??010?????????????????????
Torvosaurus_tanneri
00???100?0010??11011000102000O??00????00?10120000l?011111011000?[01]??????????001111?01????????
????????????????????????????010?0?????????????000001000100100100110110102100100100011211000011100
1100010111000011100O0??010?1010011100000001212110000000100?0[12]???001101101000001010110101110113000[12]?1000002001010001110?10000110000100002121101011010211O?1001??0????11
Torvosaurus_gurneyi
???????????10001101000010200000O?0??
??0?00010001?????20??
??1??
??01
Tyrannotitan
????????????????????????????????1?????????????????1111??
??????????????????20?010?0?????????1??0?20?0????????01101?1???????1???1001?1?00??00?1?001?2?1???
????000??0??????????11????01???0????0?201?????20?????
0?220?1?01111?0?01???????2?????????????????????????010???
Xuanhanosaurus
??
??1100?????????0??????1??????000?0??00??11???????
1?????????????????0?1???1?200?2111?0100001000110O?001101?100??
??
Yangchuanosaurus
0000?000000000??????000003111?1?000110110000O?100001110001O?010?1?1??0?0?120???0?0????????????
?????????????0111???1??00000?1?00???1???1?0???00?0?0??00001001100[12]?0110001?01000012110001000
?1?000111010000?0000100?010??000000100101?111011010
120?100?020011?11111??0101?110????100??211??0101101021??0??????????????
CV00214
??
??1100[12]?0110001??10000121100010000???000[12]11??0?????00?1?????????????????????????012010?0?00101000??0??000???????000?0010?10?????0110[12]0?[12]0??00?0?001???1?[12]1?10111?110?00???0???1???0?0?1???????01???????0?0???
;
proc/;

A9.3. Morphological variations in the interdental plates of *Dilophosaurus wetherilli*

Two distinct morphotypes of the interdental plates can be seen in the specimens referred to the taxon *Dilophosaurus wetherilli*. The holotype UCMP 37302 and the paratype UCMP 37303, both juvenile individuals, possess fully fused and subrectangular interdental plates with an anteroposterior axis of elongation and straight ventral margins of the plates. On the other hand, the juvenile specimen TMM 43646-1 and the adult individual UCMP 77270 display separated interdental plates that are subquadrangular to subrectangular, with a long axis directed ventrodorsally and strongly 'V-shaped' ventral margins (Tykoski 2005; pers. obs.). As far as we know, such variability of interdental plates is unique among theropods and cannot be explained by ontogeny, therefore the existence of two taxa of *Dilophosaurus* in the Kayenta Formation, as previously suggested by Welles (1984), seems highly plausible to us. In fact, a second species of *Dilophosaurus*, *D.* '*breedorum*' was named by Welles and Pickering (1995) based on the specimen UCMP 77270 in a controversial paper, but the name does not follow the condition of the ICZN to be recognized as valid (see http://theropoddatabase.blogspot.com.ar/2010/05/pickerings-taxa-6-dilophosaurus.html for more information). UCMP 77270 consists of an incomplete skull and skeleton discovered in 1964 that was initially referred to a larger specimen of *D. wetherilli* (Welles 1970) then thought to be a new genus closely related to *D. wetherilli* (Welles 1984). Despite the fact that some differences between UCMP 77270 and the type specimens were noted by Welles and Pickering (1995), and later by Tykoski (2005) and Irmis (2007), the scientific literature only recognizes the existence of one species of *Dilophosaurus* from the Kayenta Formation hitherto (e.g., Madsen and Welles 2000; Gay 2005; Tykoski 2005; Irmis 2007; Sampson and Witmer 2007; Carrano and Sampson 2008; Carrano et al. 2012).

The stratigraphic level from which the type and paratype specimens came, as well as UCMP 77270 collected in Moenkopi Wash, does not seem to be well established, and there is some potential uncertainty with correlating the exact position of UCMP 77270 with those from Gold Spring like TMM 43646-1 (Tykoski, pers.

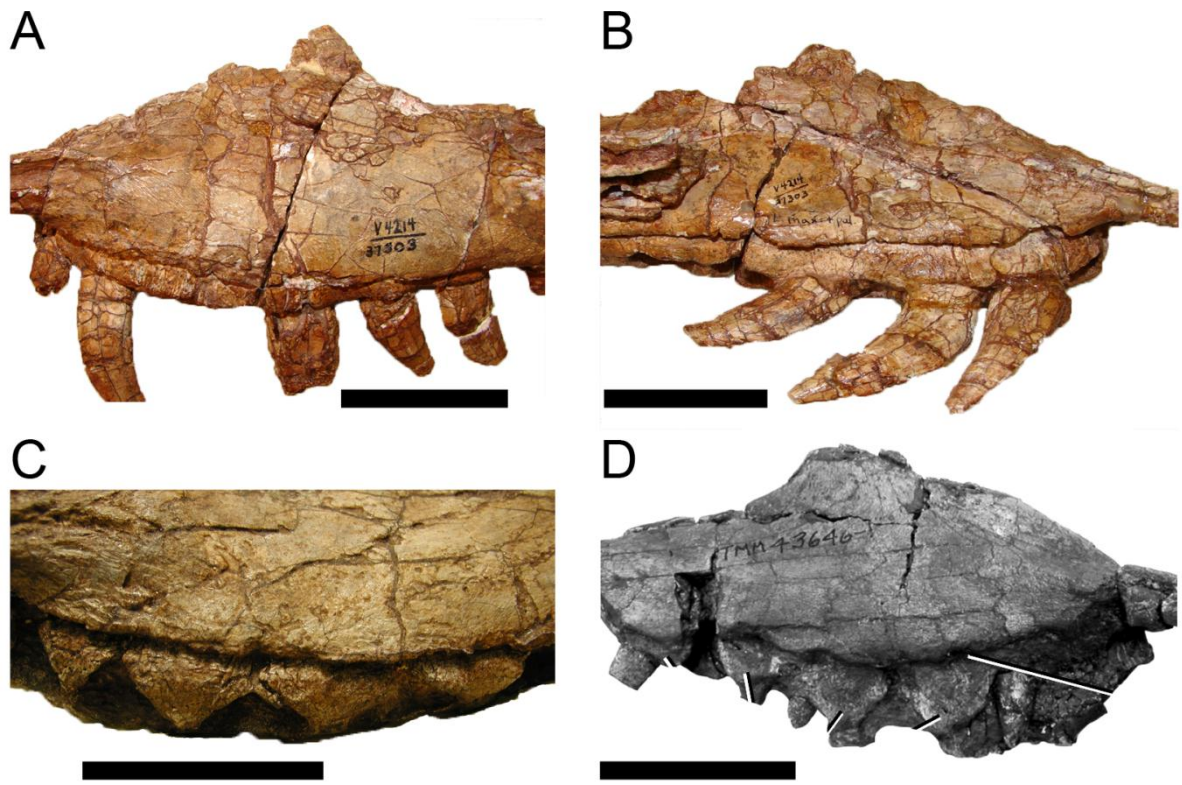

FIGURE A9.1. Morphological variations in the interdental plates of *Dilophosaurus*. **A-B**, Right and left maxillae of the juvenile specimen UCMP 37303 (paratype) of *Dilophosaurus wetherilli* in medial views representing a first morphotype of interdental plates (courtesy of Martín Ezcurra); **C-D**, Interdental plates of left maxilla (**C**) of adult specimen UCMP 77270 referred to *Dilophosaurus* '*breedorum*' by Welles and Pickering (1995; courtesy of Ronald Tykoski); and **D**, partial left maxilla of juvenile specimen TMM 43646-1 (from Tykoski 2005:figure 36B) referred to *Dilophosaurus wetherilli* in medial views and representing morphotype II of interdental plates. Scale bars = 5 cm.

comm.). According to Welles (1954, 1970), the type locality is listed at an elevation of 1402 meters near the base of the Kayenta Formation, slightly above the contact with the Moenave Formation and about 38 meters (126 feet) above the top of the Chinle Formation. However, the Texas *Dilophosaurus* quarry is actually closer to 1550 meters in elevation and clearly in the middle third of the Kayenta Formation, certainly not near the contact with the Moenave Formation. This is also the case for TMM 43646-1 that was discovered in the middle third of the Kayenta Formation near Gold Spring (Tykoski, pers. comm.). Although no one has been able to work out the stratigraphic separation between the type specimen, UCMP 77270 and TMM 43646-1, and the amount of time separating them, it may be possible that there is enough time represented in the section to capture evolutionary change to the species level (Tykoski, pers. comm.).

Given the important difference in the interdental plates between the type specimens and UCMP 77270 and TMM 43646-1, accompanied by difference in the maxillary and dentary tooth count and, in UCMP 77270, the participation of the prefrontal in the nasal crest, the presence of a groove along the posteroventral edge of the postorbital, a posterolateral sulcus in the quadratojugal, and closed dorsal and proximal caudal neurovascular suture (Welles and Pickering 1995), all features that seem to be autapomorphies, we tentatively accept the existence of two species of *Dilophosaurus* in the Kayenta Formation, pending on a thorough description of UCMP 77270 and TMM 43646-1 to support the erection of a new species of *Dilophosaurus*.

TABLE A9.1. Morphology of interdental plates in non-maniraptoriforms theropods. Fusion of interdental plates: fused (0), separated (1); ventral extension of interdental plates relative to lateral wall of maxilla: fall short (0), well dorsal (1); Shape of interdental plates: rectangular with a straight ventral margin (0), subpentagonal with a V-shaped ventral margin (1); triangular or trapezoidal (2). * specimens UCMP 77270 and TMM 43646-1.

Taxa	Fusion	Ventral extension	Shape
Abelisaurus comahuensis	0	0	0
Acrocanthosaurus atokensis	0	0	0
Afrovenator abakensis	1	0	1
Albertosaurus sarcophagus	1	1	1
Alioramus altai	1	0	1
Allosaurus fragilis	0	1	1
Aucasaurus garridoi	0	0	0
Baryonyx walkeri	1	0	1
Carcharodontosaurus iguidensis	0	0	1
Carcharodontosaurus saharicus	0	0	0
Ceratosaurus nasicornis	0	0	0
Compsognathus longipes	1	0	0
Daspletosaurus torosus	1	1	1
Dilophosaurus wetherilli	0	0	0
*Dilophosaurus 'breedorum'**	1	0	1
Dubreuillosaurus valesdunensis	1	0	1
Duriavenator hesperis	1	0	1
Eocarcharia dinops	0	0	1
Eodromaeus murphi	1	0	0
Eotyrannus lengi	0	0	1
Eustreptospondylus oxoniensis	1	0	1
Frenguellisaurus ischigualastensis	0	0	0
Genyodectes serus	0	0	0
Giganotosaurus carolinii	0	0	0
Gorgosaurus libratus	1	0	1
Guanlong wucaii	1	1	1
Indosuchus raptorius	0	0	1
Kileskus aristotocus	1	0	1
Kryptops palaïos	0	0	0
Leshansaurus qianweiensis	1	0	?
Majungasaurus crenatissimus	0	0	0
Mapusaurus roseae	0	0	1
Marshosaurus bicentesimus	1	0	1
Masiakasaurus knopfleri	0	0	1
Megalosaurus bucklandii	1	1	0
Megapnosaurus rhodesiensis	1	0	2
Neovenator salerii	0	1	1
Noasaurus leali	0	0	0
Piatnitzkysaurus floresi	1	0	1
Proceratosaurus bradleyi	1	0	1
Raptorex kriegsteini	1	0	1
Rugops primus	0	0	1
Scipionyx samnicicus	1	0	0
Shaochilong maortuensis	0	0	0
Sinosaurus triassicus	1	0	1
Sinraptor dongi	1	0	1
Spinosaurus aegyptiacus	1	0	2
Suchomimus tenerensis	1	0	1
Tarbosaurus bataar	1	1	1
Torvosaurus gurneyi	**0**	**0**	**0**
Torvosaurus tanneri	0	1	1
Tyrannosaurus rex	1	1	1
Zuolong sallei	1	0	1

A10. Phylogenetic analysis including *Torvosaurus* embryos (ML 1188)

A10.1. Character list

Characters 1-352 are from Carrano et al. (2012), with the modification of character 12, 28 and 146.

12. Maxilla, development of anterior ramus in adults: anteroposteriorly short or absent (0), moderate (1), anteroposteriorly long (2). As noticed by Carr (1999), Rauhut & Fechner (2005), Loewen (2012), the relative proportion of the anterior ramus changes through ontogeny, therefore this ontogenetic feature was coded for adults only.
28. Maxilla, dimensions of promaxillary fenestra opening in lateral view: small foramen (0), small fenestra, smaller than maxillary fenestra (1), large fenestra, larger than maxillary fenestra.
146. Teeth, maxillary and dentary, serrations in adults: present (0), absent (1). Absence of denticles on the crown occurs in embryonic specimens of theropods with serrated carinae (Varricchio et al. 2002; pers. obs.), therefore this ontogenetic feature was coded for adults only.
352. Maxilla, medial antorbital fossa in medial view: absent (0), present (1).
353. Maxilla, maxillary fenestra in medial view: absent (0), present as a crescentic aperture in the anteriormost corner of the medial antorbital fossa (1), present as a large maxillary recess/antrum (2), present as a fenestra (3).
354. Maxilla, promaxillary fenestra in medial view: absent (0), present as a promaxillary recess/antrum (1), present as a fenestra (2).
355. Maxilla, shape of promaxillary fenestra in lateral view: circular (0), subtrapezoidal (1), bean-shaped (2), D-shaped (3) drop-shaped (4).
356. Maxilla, position of the most posterior point of anteromedial process: on the anterior part of the anterior ramus (0), on the posterior part of the anterior ramus (1) at the level of the antorbital fenestra (2).
357. Maxilla, angle formed by the main axis of the base of the ascending ramus with the ventral margin of the maxilla: > 50° (0), 50°-35° (1); 34°-15 (2); <15°(3).
358. Maxilla, dorsal and ventral margins of the jugal ramus: slightly convergent, subparallel (0), strongly convergent (1).
359. Maxilla, shape of posterior part of jugal ramus: elongated and tapering process (0), large tongue-like process (1).
360. Maxillary teeth, number of teeth borne by the anterior ramus (anterior to the antorbital fenestra) in medial view: <6 (0), 6 (1), 7 or 8 (2) >8 (3)
361. Maxillary and dentary teeth, baso-apical elongation of the most elongated crown (CHR = CH/CBL): < 2.5(0), >2.5 (1).
362. Dentary, anteriormost paradental plates of the dentary, when unfused: wider than tall, horizontal subrectangular outline (0); as tall as high, subquadrangular outline (1); taller than wide, vertical subrectangular outline (2).
363. Dentary, number of teeth along the tooth row, from the anteriormost point of the mandibular symphysis to the anteriormost point of the Meckelian fossa: <10 (0); 10 – 15 (1); >15 (2).

TABLE A10.1. Number of maxillary and dentary teeth and angle of the ascending ramus in non-maniraptoriform theropods.

Taxa	Number of maxillary teeth borne by the anterior ramus (anterior to the antorbital fenestra)	Number of dentary teeth, from the anteriormost point of the mandibular symphysis to the Meckelian fossa	Angle formed by the main axis of the base of the ascending ramus with the anteroventral margin of the maxilla.
Eoraptor	6	?	68°
Herrerasaurus	5	?	55°
Acrocanthosaurus	7	12-13	39°
Aerosteon	?	?	?
Afrovenator	6	?	32°
Allosaurus	8	11-14	55-41°
Angaturama	?	?	?
Australovenator	?	13	?
Baryonyx	>8	>18	?
Carcharodontosaurus	6	?	47°
Ceratosaurus	5	10	44°
Chilantaisaurus	?	?	?

Chuandongocoelurus	?	?	?
Coelophysis bauri	7	?	57°
Compsognathus	9	>15	45°
Concavenator	?	?	44°
Condorraptor	?	?	?
Cryolophosaurus	?	?	?
D. sinensis	5	?	46°
Dilophosaurus	5	11	44°
Dubreuillosaurus	5	8	38°
Duriavenator	6	11	39°
Elaphrosaurus	?	?	?
Eocarcharia	6	?	52°
Eustreptospondylus	6	6	50°
Fukuiraptor	?	?	?
Giganotosaurus	?	11	65°
Irritator	>8	?	12°
Leshansaurus	5	?	41°
Lourinhanosaurus	?	?	?
Magnosaurus	?	9	?
Majungasaurus	5	12	59°
Mapusaurus	6	?	36°
Marshosaurus	6	14	40°
Masiakasaurus	3	8	?
Megalosaurus	5	5	40°
Megapnosaurus rhodesiensis	7-8?	?	50°
Megaraptor	?	?	?
Metriacanthosaurus	?	?	?
Monolophosaurus	6	?	45°
Neovenator	8	?	51°
Ornitholestes	?	?	?
Piatnitzkysaurus	7-8?	?	40°
Piveteausaurus	?	?	?
Poekilopleuron	?	?	?
Proceratosaurus	10	?	37°
Saurophaganax	?	?	?
Shaochilong	4-5	?	58°
Shidaisaurus	?	?	?
Siamotyrannus	?	?	?
Sinraptor dongi	6	12	52°
Sinraptor hepingensis	7	?	41°
Spinosaurus	11	>15	42°
Streptospondylus	?	?	?
Suchomimus	17	>18	~0°
S. zigongensis	?	?	?
Torvosaurus	6	?	27-31°
Tyrannotitan	?	11-12	?
Xuanhanosaurus	?	?	?
Yangchuanosaurus	6-7	?	52°
CV00214	?	?	?
ML1188	4-5	7	30°
IPFUB_Gui_Th_4	7	?	51°
ML565_122	7-8	?	52°

A10.2. Data matrix

We here present a copy of the TNT matrix used in this chapter. An excel spreadsheet, with characters and taxa separated into columns and rows, is available from the authors by request.

nstates 5
xread

363 64
Eoraptor
00010000?00000??????0101000-
0?0010000?0000100??0001?000000100000?0000000000?10?00??0?001000?0000?0??????0??00?0?10100000?0?0000?00?0000?0?00?000100000000000-0?????????-
000000000000000?0?000000000000000?0000001?0010000?000001000000101000000000?00100000100000000000010000000?00000000000??000?0000000?00000?0000?000?000000000???-
000000000000000000000000000?00-?00010??
Herrerasaurus
00001000000000????0?0001000-
0?0?00000?0000100??001201000000000000?000001000000000020?000010?00000?10??00000000?000000?10000?0?0000?000010010000?0?0100000000000-00?000010?-
000000000000000?0?1000000?000000000000??001??00?1?011?0??000101000000100000101000100000000001000000000?00000000000?0?001000000?00000??000010000000000001??-
010000100000000000000000000-000000-?
Acrocanthosaurus
020?1100?000000111100000021111110001 0?000000211101211100020212011?112111102011 0?02??1101210000010011010001201111 1?11002100101020010?11111?000100010000010011012?00110011?00?00121100010001100112111110?00210000000101?1?1101101200120012 10?001011110000113110111111000????010?10??1110110201201?120?2011110002201110111100001100103 12?1010?1110?1??012101110 01?11123110021-1
Aerosteon
??01?000?111?????????10000200???110121???????11?01001?1?000100010110101 11??2?110??0?????????0101100121?????????????????????????????????0101101001022111011020120 1?120????????????????????????1001?412????01112021110?????????????????-????????
Afrovenator
?????????0010101100000100120011000?????0?000201001?011001011000?????????00?00111100 1???0000000001?????10?11001?0?011000010001101100001?001?000001??????100000???1?01010??????????0121?????00?0?????0?31001111?100001?10?0110101 1?011?2012?1?00?00101110001110110000110000100002 1?11010110???111011?011100??1110-02101???
Allosaurus
00101[01]000001000101000000021111110001101100002[01]2[01]00101100000001011111000110200000020011011000110100100102012011111111120001001102011111111100001000110200100110011001100 10[01]1000001011000100001000101111000011?000000101?1101101200120012101011000010001113100111111000011101001021111011020120 1?1100200111000[12]10111011110000110010212210101111021110121011100101131-1[01][01]021-1
Angaturama
11???201?1121?11???0?????????????0???1?0?????????????????1101117013 11??

11101111010100001[01]0001001100110[01]0011021000101002002111010010 21??1?0001??10???000-011000-1

Chilantaisaurus

????????????

00???100??0101011000?0?0?120?1???0??
????????????????????110101???????????0000010?0??0?00100??
??
??110-011?1001

Elaphrosaurus

??
??0110[12]????????00100000?01100001?0000000002
111?0000011??010???????0???11?01110100001000?????????????????????00011100000?111111100?[12]?????
?0?0?00001100110?00110??00010000210??21?0??????111?001???1???????-????????

Eocarcharia

????????00000011100101002121111?0?????????????????????01?00201111???1?????????????????????????
??1000010?01?????10??
??
??1323?0001???

Eustreptospondylus

?1???20000011?01100000010120?1???0???????100200001??????10?10001?1??00000???0111100010??100100
0100?11000012??????????00110111????????????00000?0?0100000100110011???011010010001101100000100
11000101?100??1?0000????1????????111?0???0121210?00?????????????????????00110101100011?011300
?2?1?000001010100?11111100001100001000021111O1?110102111??1001??000??000-01??1?00

Fukuiraptor

??????????????????0?0?0???
????????????????????0?????????????????1000010?0110????00110?[12]????????1?????????0????0????????11??
????????????????????????????12001211101?001?1010?????????????10?????10?????????????????????????????
????21012101?1100011??01??12????01112121??012?1???0???????-????????

Giganotosaurus

02???000??0?00?11?100001001101???10?11101000211l0????????2021211??11211??0??1?00020?110121???0
0100?0011211?1??????111??201010?????1?1111110?0020000??000100110l2?01?0??111001?01?1?00?100?1
1001?21?2??????2?00000???1??0?10??0???01?0??????????????????????????????00?11010010211110110201
201?120020111100022011101??1?0???1001?31221010?10?????????????????121-?00??0-1

Irritator

?????2????02?0???????01100200?100010??0000010?201110010000??00011?11000????0?0???11?10??10?100
10001021000?101?10?????0?????????????10?11?0???1101?1-
??????1??
??1??
?3?-?30031??

Leshansaurus

???????????1?1?1?001??1?0[01]???1????????????????????????????????????10000????????????000000010021
001??00????0????????????????????????????????00???0????????[01]0?1100?1?0010??0110000121?0000??0????
000001100??1?????????????0?0??????0110?0111011?[12]0????
????0??0??????[01]????100001???1?10???211110?0?????????????????0???110-0110?0??

Lourinhanosaurus

??
??1100?????????0??????1?1?000?000?0?00???1?1?0??
1100000?????0?111??00?01010?101111101l?2?????1???0?001100
??11011101?0110?????01?21?2101????????????????????????????-????????

Magnosaurus

????????????????????????????????????0??
????????????????????110?11????????????0000000?0????????0???0????????????????????????????0????????????
?00??0???01??1?????????????????0??0?????????1??
?????0?110?001000?21?????0?11?????????????????????-??????10

Majungasaurus

021010001000000100000001001000001112O?10020000?10120000002020201l?111101101100001000101O0?0
0000010?01101?100000001010110010100110010001001010000000100001000110210011001001100012110O
000010100000001021?111100120l?0100001l?1011?10?01110200001O??????0?????????????0??0011100000001
111111?????0???1?????????0????100110?100010100210211111111021111?0001??1101?000-100100-1

Mapusaurus

??????0???000001111000010011O1?10101111010002111O??1111102?2121121????????[02]01?000?0????????
????????????????????????????00201010?01001??????1000020000?0???10011012???01???1??0?0010??0001??01
?00102012?????210000?????????1?11012?0????1???10?10???????0????1????????000???0?0?102?1110110[12
]?????????0?011?100022??1101111?00?1100??31221010110??2111012101??0010?121-011?10-?

Marshosaurus
000??000000001001000110201100 1?000010?000??????????0?1001?10000????1000000?10?0?01?0100020000
001001?0?00?1?0???????????10001??0???1?011??001001000100000100110 01?011110001000012110000000
012001101?1?????????????10???????0?1????????????1?????????????????????????00?110100101011?0110010
201?0000?00111000?????1?????????????????????21???????0?????????????????110-010011[01]1
Masiakasaurus
0?????0???001001000001000010 00???0?????????10???????????0??20101?10????????0?001??00????000?000
1??00???0100?????????11101000011-
0??00?001100000000???0020001102?001100100110001 11?000000101000000002011110001011?0100001?01
011111001110100001?????????????????????001001?1000000011?1111111201000010010 01??10011010011021
000101002102?111111202111 1?0011??1101?000-0?0?0?-0
Megalosaurus
?????????0000?0110110 0?00110?1?000?????????????????1?111?????????????????????????????????????
?????????????????????000101?????0?01100001001 0?01??00?100???01????????0??????1?????0?1????10002011
100001?0000???010?????01110?000001212110?000010000?????????????001010101101011011 0113?00[12]???
???0?10??1?001110110000 1?000010000221??0?0?1????1????1001??00???010-011001[12]0
Megaraptor
???
???11012????????11?0100121?0????????1?????????????
?110?0????????1?111011?0121???????????????0101011?2?0101111111 0??????????????????????2?????????????????
???2?11??????????-????????
Metriacanthosaurus
???
???1001?????????0??0??1?1?00011?00?00012111?????
1?000?0???1????1???00??10100101111?011??012?1?0?00?101?01
?111??110?11110001??0???21?????????????????????????????????-????????
Monolophosaurus
001?1000?00100?????0000020-0?100011101300100?-
0012[01]1100011001 0?11110001?021000000??1000100000010?????0????01?1??????00100001002010 0?0??0
0?0010?0??000010111001 0?001001001 0?001011000000?10000101?10?0?1?000?00?010?????????????????
?????????????????????????????001100010101011101 1?00?[12]0100???0001000?0?????????????????????????
?????????????????????????3?-?10?1???
Neovenator
00???10000010001010100000 21001???10110110???
????????????1?????????110000?????????????1000010001?020010011012?1?????111101001211000100011010 1
0110?0???2100001???1?10?10?1011?0120?????????????????????????????01?11010010221110110201201?
12000001?1011020?1101111000111001131221010?10???1????210111?010??31-101?2?-?
Ornitholestes
000??000?00000??????000002100?1?000010000010 10?0012?11000001000?1??10001?020?00??0??1000?00??
?0????0??0?????????????00000?0??0?0?0?0100111?000000??00001001100[12]????????0100101?0?000?000
1000000010100??1?00010??010??11?????????00111100000000???01??11??111??1??00?0001011121111011
020????????010010000021??211??0100001???????2??0?0???????????2001??0???????-???0??-?
Piatnitzkysaurus
??????????000?0100001002011 0?1???0?????????????????????????????????1???0?????????????10?0100000010
?1101000?10????????????2010?1?????????????0010010?01?????0000100 1?00111100010000121100001000 1200
?1011100001?000?0??010?????01011?1120012111011 00??100?1?????????????001?10100101011?011?0002?
1000000001100001 1?11100001000001000022121010?10???1????1001??0????110-011?2?1?
Piveteausaurus
???011?000?????????????1000?0?1002100?
?1002?110???
???
???-????????
Poekilopleuron
???
???1
00?0??1?????111?????????012??1011000100000 1????0?11????0???
??????????????10???2????0?01111021?10????????000????-????????
Proceratosaurus
000??000?00100?????000002100?1??0????????0???????201100000?????????????1??20??0??0??????????????
?????0??????????????00[02]00?0??0???00??1?1?110000?0??0000000?????????????????????????????????????

????????????

????????????????????????????????1?????????????????1111??
????????????????????20?010?0??????????1??0?20?0????????01101?1???????1???1001?1?00??00?1?001?2?1???
????000??0??????????11????01??0????0?201?????20?????
0?220?1?01111?0?01???????2?????????????????????????010????-??????-1
Xuanhanosaurus
??
??1100?????????0??????1??????000?0??00??11???????
1?????????????????0?1???1?200?2111?010000100011102?001101?100??
??-????????
Yangchuanosaurus
0000?000000000?????0000021?1?000110110000 2?10000111000 10?010?1?1??0?0?120???0?0????????????
????????????0111???1??00000?1?00???1???1?0???00?0?0??00001001100[12]?0110001?0100001211000 1000
?1?000111010000?0000100?010??0000001001 01?111011010
120?100?020011?11111??0101?110????100??211??0101101021??0?????????????21?010[12]1??
CV00214
??
??1100[12]?0110001??10000121100010 00???000[12]1 1
1??0?????00?1?????????????????????????012010?0?00101000??0??000???????000?0010?10????0110[12]0?[12]0
??00?0?001???1?[12]1?10111?110?00???0???1???0?0?1???????01???????0?0????-????????
ML1188
???????????-
0001100???0??????01??
???????0????1????????????000000?0-
???????00??
??
??000-02110120
IPFUB_Gui_Th_4
???????????-
00??01???000?2111111?0??
????????????????????????????????0-
??????10??
??
??132000002???
ML565
???????????-
00??????0000?212?????0??
???????00001-????????????0??0000?-
???????00??
??
?????4?01?20??
;
proc/;

A10.3. Synapomorphy list from phylogenetic analysis (50% Majority Rule):

Eoraptor:
No autapomorphies

Herrerasaurus:
Char. 53: 0 --> 1
Char. 59: 1 --> 0
Char. 82: 0 --> 2
Char. 116: 1 --> 0
Char. 118: 0 --> 1
Char. 219: 0 --> 1

Acrocanthosaurus:
Char. 6: 0 --> 1
Char. 37: 1 --> 0
Char. 39: 1 --> 0
Char. 100: 0 --> 1
Char. 104: 2 --> 0
Char. 121: 0 --> 1

Aerosteon:
Char. 219: 1 --> 0

Afrovenator:
Char. 166: 0 --> 1
Char. 168: 1 --> 0
Char. 177: 2 --> 0
Char. 283: 0 --> 1
Char. 357: 1 --> 2

Allosaurus:
No autapomorphies

Angaturama:
No autapomorphies

Australovenator:
Char. 240: 1 --> 0

Baryonyx:
Char. 177: 2 --> 0
Char. 193: 2 --> 1

Carcharodontosaurus:
Char. 169: 1 --> 0
Char. 184: 0 --> 1
Char. 204: 0 --> 1

Ceratosaurus:

Char. 29: 0 --> 1
Char. 45: 0 --> 2
Char. 51: 2 --> 1
Char. 72: 1 --> 0
Char. 76: 1 --> 0
Char. 107: 0 --> 1
Char. 108: 0 --> 1
Char. 116: 1 --> 0
Char. 142: 0 --> 1
Char. 150: 0 --> 1
Char. 171: 1 --> 0
Char. 193: 0 --> 1
Char. 227: 0 --> 1
Char. 231: 1 --> 0
Char. 234: 0 --> 1
Char. 284: 2 --> 1
Char. 296: 0 --> 1
Char. 323: 1 --> 0
Char. 358: 0 --> 1

Chilantaisaurus:
Char. 232: 1 --> 0
Char. 237: 1 --> 0
Char. 276: 1 --> 0
Char. 307: 0 --> 1

Chuandongocoelurus:
Char. 269: 0 --> 1
Char. 322: 2 --> 4

Coelophysis_bauri:
Char. 138: 1 --> 0
Char. 142: 0 --> 1
Char. 160: 1 --> 0
Char. 282: 0 --> 1
Char. 357: 1 --> 0

Megapnosaurus_rhodesiensis:
Char. 26: 0 --> 1
Char. 27: 1 --> 0
Char. 72: 1 --> 0
Char. 248: 1 --> 0
Char. 273: 0 --> 1
Char. 294: 0 --> 1
Char. 305: 0 --> 1
Char. 310: 0 --> 1
Char. 347: 0 --> 1

Compsognathus:
Char. 6: 0 --> 1
Char. 22: 0 --> 1
Char. 37: 1 --> 0
Char. 54: 1 --> 0
Char. 180: 0 --> 1
Char. 216: 1 --> 0
Char. 276: 1 --> 0
Char. 293: 0 --> 1

Concavenator:
Char. 23: 0 --> 1
Char. 41: 0 --> 1
Char. 43: 0 --> 1
Char. 141: 0 --> 1
Char. 143: 1 --> 2
Char. 159: 1 --> 0
Char. 182: 0 --> 1
Char. 183: 1 --> 0
Char. 192: 1 --> 0
Char. 202: 2 --> 01
Char. 218: 0 --> 1
Char. 231: 2 --> 1
Char. 265: 1 --> 0
Char. 271: 0 --> 1
Char. 308: 1 --> 0
Char. 357: 0 --> 1

Condorraptor:
Char. 171: 1 --> 0
Char. 177: 2 --> 0
Char. 199: 0 --> 1

Cryolophosaurus:
Char. 40: 03 --> 1
Char. 45: 0 --> 1
Char. 55: 0 --> 1
Char. 95: 0 --> 1
Char. 160: 1 --> 0
Char. 180: 0 --> 1
Char. 317: 1 --> 0

D._sinensis:
Char. 24: 0 --> 2
Char. 39: 0 --> 1
Char. 186: 0 --> 1
Char. 266: 0 --> 1
Char. 292: 0 --> 2
Char. 298: 0 --> 1
Char. 305: 0 --> 1
Char. 323: 1 --> 2
Char. 336: 1 --> 0

Dilophosaurus:
Char. 2: 0 --> 1
Char. 4: 0 --> 1
Char. 37: 0 --> 1
Char. 54: 0 --> 1
Char. 100: 0 --> 1
Char. 118: 0 --> 2
Char. 139: 0 --> 1
Char. 155: 0 --> 1
Char. 193: 0 --> 1
Char. 253: 0 --> 1
Char. 296: 0 --> 1
Char. 309: 1 --> 0
Char. 324: 0 --> 1

Dubreuillosaurus:
Char. 30: 1 --> 0
Char. 89: 1 --> 2
Char. 91: 0 --> 1
Char. 93: 0 --> 1
Char. 104: 0 --> 1
Char. 311: 1 --> 0

Duriavenator:
No autapomorphies

Elaphrosaurus:
Char. 180: 0 --> 1
Char. 207: 2 --> 1
Char. 226: 0 --> 1
Char. 343: 0 --> 1

Eocarcharia:
Char. 21: 0 --> 1
Char. 23: 0 --> 1
Char. 28: 1 --> 2
Char. 360: 2 --> 1

Eustreptospondylus:
Char. 6: 1 --> 2
Char. 13: 0 --> 1
Char. 24: 0 --> 1

Fukuiraptor:
Char. 302: 2 --> 1

Giganotosaurus:
Char. 165: 1 --> 0

Irritator:
Char. 11: 1 --> 0
Char. 23: 0 --> 1
Char. 353: 1 --> 3

Leshansaurus:
Char. 20: 0 --> 1
Char. 85: 1 --> 0
Char. 89: 1 --> 0
Char. 170: 0 --> 1
Char. 175: 1 --> 0
Char. 195: 1 --> 0
Char. 315: 0 --> 1

Lourinhanosaurus:
Char. 312: 0 --> 1

Magnosaurus:
Char. 362: 0 --> 1

Majungasaurus:
Char. 24: 0 --> 1
Char. 34: 0 --> 1
Char. 124: 0 --> 1
Char. 140: 0 --> 1
Char. 203: 0 --> 1
Char. 208: 1 --> 0
Char. 233: 1 --> 2
Char. 356: 0 --> 1

Mapusaurus:
Char. 56: 0 --> 1
Char. 194: 1 --> 0

Marshosaurus:
Char. 17: 0 --> 1
Char. 22: 0 --> 1
Char. 89: 1 --> 2
Char. 163: 0 --> 1
Char. 282: 0 --> 1
Char. 297: 0 --> 1

Masiakasaurus:
Char. 13: 0 --> 1
Char. 22: 0 --> 1
Char. 44: 0 --> 1
Char. 67: 1 --> 0
Char. 85: 1 --> 0
Char. 120: 0 --> 1
Char. 139: 0 --> 1
Char. 153: 1 --> 2
Char. 177: 2 --> 1
Char. 198: 1 --> 0
Char. 207: 2 --> 0
Char. 226: 0 --> 1
Char. 333: 1 --> 2
Char. 343: 0 --> 1
Char. 363: 1 --> 0

Megalosaurus:
Char. 12: 1 --> 0
Char. 27: 2 --> 1
Char. 52: 0 --> 1
Char. 121: 1 --> 0
Char. 140: 0 --> 1
Char. 193: 1 --> 2
Char. 323: 1 --> 2

Megaraptor:
No autapomorphies

Metriacanthosaurus:
Char. 196: 0 --> 1
Char. 312: 0 --> 1

Monolophosaurus:
Char. 27: 1 --> 0
Char. 35: 0 --> 1
Char. 39: 0 --> 1
Char. 58: 0 --> 1
Char. 62: 0 --> 1
Char. 131: 1 --> 0
Char. 155: 0 --> 1
Char. 161: 1 --> 0
Char. 193: 0 --> 1
Char. 296: 1 --> 0

Neovenator:
Char. 6: 0 --> 1
Char. 12: 0 --> 1
Char. 20: 0 --> 1
Char. 28: 1 --> 0
Char. 34: 0 --> 1
Char. 121: 0 --> 1
Char. 162: 0 --> 1
Char. 196: 1 --> 0
Char. 208: 0 --> 1
Char. 292: 2 --> 0
Char. 301: 2 --> 0

Ornitholestes:
Char. 12: 1 --> 0
Char. 43: 0 --> 1
Char. 135: 1 --> 0

Piatnitzkysaurus:
Char. 323: 1 --> 2

Piveteausaurus:
Char. 104: 0 --> 2

Poekilopleuron:
Char. 216: 0 --> 1
Char. 237: 0 --> 1

Proceratosaurus:
Char. 153: 1 --> 0

Saurophaganax:
Char. 310: 1 --> 0
Char. 342: 1 --> 0

Shaochilong:
Char. 21: 0 --> 1
Char. 77: 1 --> 0

Shidaisaurus:
Char. 89: 1 --> 0
Char. 147: 1 --> 0
Char. 168: 1 --> 0
Char. 296: 1 --> 0
Char. 299: 1 --> 0

Siamotyrannus:
Char. 202: 1 --> 0
Char. 272: 1 --> 2
Char. 287: 1 --> 0

*Sinraptor*_dongi:
Char. 40: 1 --> 0
Char. 189: 0 --> 1
Char. 273: 1 --> 0
Char. 299: 1 --> 0
Char. 360: 2 --> 1

Sinraptor_hepingensis:
Char. 89: 1 --> 2
Char. 198: 0 --> 1
Char. 283: 1 --> 0
Char. 289: 0 --> 1
Char. 300: 1 --> 0
Char. 355: 1 --> 2
Char. 357: 0 --> 1

Spinosaurus:
No autapomorphies

Streptospondylus:
No autapomorphies

Suchomimus:
Char. 272: 1 --> 0
Char. 286: 1 --> 0

S._zigongensis:
Char. 153: 1 --> 0
Char. 203: 1 --> 0
Char. 231: 2 --> 1
Char. 232: 1 --> 0
Char. 233: 1 --> 2
Char. 281: 2 --> 1
Char. 316: 1 --> 0

Torvosaurus:
No autapomorphies

Tyrannotitan:
Char. 203: 1 --> 0

Xuanhanosaurus:
Char. 183: 1 --> 0
Char. 221: 0 --> 1
Char. 225: 0 --> 1
Char. 255: 1 --> 0

Yangchuanosaurus:
Char. 193: 02 --> 1
Char. 203: 1 --> 0
Char. 281: 2 --> 1
Char. 305: 1 --> 0
CV00214:
Char. 232: 1 --> 0
Char. 234: 1 --> 0
Char. 240: 0 --> 1
Char. 253: 1 --> 0
Char. 305: 1 --> 0
Char. 307: 0 --> 1

ML1188:
No autapomorphies

IPFUB_Gui_Th_4:
No autapomorphies

ML565:
Char. 355: 1 --> 4
Char. 361: 1 --> 0

Node 65:
No synapomorphies

Node 66:
Char. 2: 0 --> 2
Char. 19: 0 --> 1
Char. 40: 1 --> 0
Char. 48: 0 --> 1
Char. 58: 1 --> 2
Char. 60: 0 --> 2
Char. 61: 0 --> 1
Char. 124: 0 --> 1
Char. 171: 1 --> 0
Char. 191: 0 --> 1
Char. 223: 1 --> 2
Char. 246: 1 --> 0
Char. 251: 0 --> 1
Char. 299: 1 --> 0

Node 67:
Char. 62: 1 --> 2
Char. 71: 0 --> 1
Char. 77: 0 --> 1
Char. 125: 1 --> 0
Char. 159: 0 --> 1
Char. 160: 1 --> 2
Char. 169: 0 --> 1
Char. 173: 0 --> 1
Char. 187: 0 --> 1
Char. 202: 1 --> 2
Char. 240: 0 --> 1
Char. 273: 1 --> 2
Char. 302: 1 --> 2
Char. 322: 2 --> 34

Node 68:
Char. 356: 0 --> 1

Node 69: Allosauria
Char. 18: 0 --> 1
Char. 28: 2 --> 1

Node 70: Allosauroidea
Char. 12: 1 --> 0
Char. 28: 0 --> 2
Char. 29: 0 --> 1
Char. 39: 0 --> 1
Char. 40: 0 --> 1
Char. 52: 0 --> 1
Char. 58: 0 --> 1
Char. 62: 0 --> 1
Char. 86: 0 --> 1
Char. 88: 0 --> 1
Char. 124: 0 --> 1
Char. 133: 0 --> 1
Char. 194: 0 --> 1
Char. 214: 0 --> 1
Char. 237: 0 --> 1
Char. 249: 13 --> 2
Char. 298: 0 --> 1
Char. 300: 0 --> 1
Char. 342: 0 --> 1
Char. 357: 1 --> 0
Char. 361: 0 --> 1

Node 71:
Char. 59: 1 --> 0
Char. 216: 0 --> 1
Char. 264: 1 --> 0
Char. 273: 0 --> 1
Char. 281: 0 --> 2
Char. 287: 0 --> 1
Char. 303: 1 --> 0
Char. 308: 0 --> 1
Char. 316: 0 --> 1
Char. 341: 1 --> 2
Char. 349: 0 --> 1

Node 72:
Char. 3: 1 --> 0
Char. 43: 1 --> 0
Char. 134: 0 --> 1
Char. 267: 0 --> 1
Char. 268: 1 --> 0
Char. 301: 0 --> 1
Char. 302: 0 --> 1
Char. 305: 0 --> 1
Char. 311: 0 --> 1

Node 73:
Char. 156: 0 --> 1
Char. 176: 0 --> 1
Char. 178: 0 --> 1
Char. 270: 0 --> 1
Char. 272: 0 --> 1
Char. 295: 0 --> 1
Char. 310: 1 --> 0
Char. 331: 0 --> 1
Char. 360: 0 --> 1

Node 74: Tetanurae
Char. 12: 0 --> 1
Char. 26: 0 --> 2
Char. 31: 0 --> 1
Char. 37: 0 --> 1
Char. 54: 0 --> 1
Char. 138: 1 --> 0
Char. 231: 1 --> 2
Char. 232: 0 --> 1
Char. 234: 0 --> 1
Char. 254: 0 --> 1
Char. 255: 0 --> 1
Char. 256: 0 --> 1
Char. 296: 0 --> 1
Char. 341: 0 --> 1
Char. 353: 0 --> 3

Node 75: Averostra
Char. 65: 0 --> 1
Char. 85: 0 --> 1
Char. 99: 0 --> 1
Char. 167: 1 --> 0
Char. 220: 0 --> 1
Char. 276: 0 --> 1
Char. 284: 0 --> 2
Char. 299: 0 --> 1
Char. 310: 0 --> 1
Char. 317: 0 --> 1
Char. 336: 0 --> 1

Node 76: Neotheropoda
Char. 3: 0 --> 1
Char. 24: 1 --> 0
Char. 27: 0 --> 1
Char. 64: 0 --> 1
Char. 73: 0 --> 1
Char. 75: 0 --> 1
Char. 76: 0 --> 1
Char. 106: 0 --> 1
Char. 157: 0 --> 1
Char. 160: 0 --> 1
Char. 179: 0 --> 1
Char. 197: 0 --> 1
Char. 212: 0 --> 1
Char. 213: 1 --> 0
Char. 217: 0 --> 1
Char. 242: 0 --> 1
Char. 249: 0 --> 1
Char. 250: 0 --> 1
Char. 264: 0 --> 1
Char. 274: 0 --> 1
Char. 275: 0 --> 1
Char. 278: 0 --> 1
Char. 279: 0 --> 1
Char. 322: 0 --> 2
Char. 337: 0 --> 1
Char. 338: 0 --> 1
Char. 340: 0 --> 1
Char. 344: 0 --> 1
Char. 345: 0 --> 1
Char. 357: 0 --> 1

Node 77:
Char. 228: 0 --> 1

Node 78:
Char. 244: 0 --> 1
Char. 252: 0 --> 1
Char. 333: 1 --> 2
Char. 343: 0 --> 1

Node 79: Megalosauridae
Char. 17: 0 --> 1
Char. 65: 1 --> 0
Char. 78: 0 --> 1
Char. 81: 0 --> 1
Char. 102: 1 --> 0
Char. 196: 0 --> 1
Char. 293: 0 --> 1
Char. 297: 0 --> 1
Char. 358: 0 --> 1

Node 80:
Char. 184: 0 --> 1
Char. 312: 0 --> 1

Node 81:
Char. 175: 0 --> 1

Node 82: Megalosauroidea
Char. 26: 2 --> 1
Char. 37: 1 --> 0
Char. 73: 1 --> 0
Char. 107: 0 --> 1
Char. 353: 3 --> 1

Node 83: Allosauridae
Char. 58: 1 --> 0
Char. 233: 1 --> 0
Char. 236: 0 --> 1
Char. 263: 0 --> 1

Node 84: Spinosaurinae
Char. 141: 0 --> 1
Char. 146: 0 --> 1
Char. 151: 0 --> 1
Char. 152: 0 --> 1
Char. 154: 0 --> 1

Node 85: Spinosauridae
Char. 1: 0 --> 1
Char. 2: 0 --> 1
Char. 8: 0 --> 1
Char. 10: 0 --> 1
Char. 11: 0 --> 1
Char. 12: 1 --> 2
Char. 13: 0 --> 1
Char. 15: 0 --> 1
Char. 26: 1 --> 0
Char. 44: 0 --> 1
Char. 49: 0 --> 1
Char. 83: 0 --> 1
Char. 129: 0 --> 1
Char. 139: 0 --> 1
Char. 142: 0 --> 1
Char. 144: 0 --> 1
Char. 145: 0 --> 1
Char. 149: 0 --> 1
Char. 150: 0 --> 3
Char. 181: 0 --> 1
Char. 193: 0 --> 2
Char. 356: 0 --> 2
Char. 360: 1 --> 3
Char. 363: 1 --> 2

Node 86:
Char. 334: 0 --> 1

Node 87: Baryonychinae
Char. 3: 0 --> 1
Char. 5: 1 --> 0
Char. 155: 0 --> 1
Char. 180: 0 --> 1
Char. 182: 0 --> 1

Node 88:
Char. 34: 0 --> 1
Char. 108: 0 --> 1

Node 89:
Char. 24: 0 --> 1
Char. 26: 2 --> 0
Char. 103: 0 --> 1

Node 90:
Char. 178: 0 --> 1
Char. 261: 0 --> 1
Char. 281: 0 --> 1
Char. 291: 0 --> 1
Char. 319: 0 --> 1

Node 91: Ceratosauria
Char. 186: 0 --> 1
Char. 197: 1 --> 2
Char. 198: 0 --> 1
Char. 199: 0 --> 1
Char. 200: 0 --> 1
Char. 208: 0 --> 1
Char. 225: 0 --> 1
Char. 266: 0 --> 1
Char. 280: 0 --> 1
Char. 339: 0 --> 1
Char. 347: 0 --> 1

Node 92:
Char. 22: 0 --> 1
Char. 25: 0 --> 1
Char. 45: 0 --> 1
Char. 51: 2 --> 0
Char. 59: 1 --> 0
Char. 208: 0 --> 1
Char. 254: 0 --> 1
Char. 277: 0 --> 1
Char. 280: 0 --> 1
Char. 293: 0 --> 1
Char. 298: 0 --> 1
Char. 322: 2 --> 1
Char. 333: 1 --> 0
Char. 339: 0 --> 1
Char. 360: 0 --> 2

Node 93: Coelophysoidea
Char. 6: 0 --> 2
Char. 7: 0 --> 1
Char. 8: 0 --> 1
Char. 13: 0 --> 1
Char. 23: 0 --> 1
Char. 89: 1 --> 0
Char. 95: 0 --> 2
Char. 120: 0 --> 1
Char. 166: 0 --> 1
Char. 177: 0 --> 1
Char. 180: 0 --> 1
Char. 261: 0 --> 1
Char. 269: 0 --> 1
Char. 318: 0 --> 1
Char. 361: 0 --> 1

Node 94:
Char. 178: 1 --> 0
Char. 271: 0 --> 1
Char. 296: 1 --> 0
Char. 301: 1 --> 2
Char. 307: 0 --> 1

Node 95: Coelurosauria
Char. 188: 1 --> 0
Char. 218: 0 --> 1

Node 96:
Char. 156: 1 --> 0
Char. 184: 0 --> 1

Node 97: Piatnitzkysauridae
Char. 12: 1 --> 0
Char. 21: 0 --> 1
Char. 24: 0 --> 2
Char. 140: 0 --> 1
Char. 166: 0 --> 1
Char. 167: 0 --> 1
Char. 168: 1 --> 0
Char. 192: 0 --> 1
Char. 193: 0 --> 1
Char. 236: 0 --> 1

Node 98:
Char. 2: 0 --> 1
Char. 124: 0 --> 1
Char. 218: 0 --> 1

Node 99: Megalosaurinae
Char. 42: 0 --> 1
Char. 193: 0 --> 1
Char. 296: 1 --> 0
Char. 352: 1 --> 0
Char. 363: 1 --> 0

Node 100:
Char. 60: 0 --> 2
Char. 97: 0 --> 1
Char. 119: 0 --> 1
Char. 122: 0 --> 1
Char. 125: 1 --> 0
Char. 165: 0 --> 1
Char. 172: 0 --> 1
Char. 176: 0 --> 1
Char. 206: 0 --> 1
Char. 329: 0 --> 1
Char. 331: 0 --> 1
Char. 332: 0 --> 1
Char. 348: 0 --> 1

Node 101: *Megalosaurus* + *Torvosaurus*
Char. 120: 1 --> 0
Char. 223: 1 --> 0
Char. 264: 1 --> 0
Char. 361: 0 --> 1
Char. 362: 0 --> 2

Node 102:
Char. 22: 0 --> 1
Char. 78: 0 --> 1
Char. 184: 0 --> 1
Char. 280: 0 --> 2
Char. 285: 0 --> 1
Char. 293: 0 --> 1
Char. 323: 1 --> 2

Node 103:
Char. 139: 0 --> 1

Node 104: *Torvosaurus*
Char. 30: 1 --> 0
Char. 357: 1 --> 2
Char. 359: 0 --> 1


Polystyrene model of *Torvosaurus gurneyi*.

CHRISTOPHE HENDRICKX

Museu da Lourinhã
Rua João Luis de Moura, 95
2530-157 Lourinhã, Portugal
Cell: +351.91.333.66.06
Email: christophe.hendrickx@hotmail.com
Website: http://sites.google.com/site/hendrickxchristophe/

PERSONAL INFORMATION

Born: 4th of May 1983, Uccle, Belgium.
Citizenship: Belgium, France.

EDUCATION

Universidade Nova de Lisboa, Lisbon, Portugal.
PhD in Vertebrate Palaeontology. 2010-2015.
Thesis: Evolution of teeth and quadrate in nonavian Theropoda (Dinosauria: Saurischia), with the description of *Torvosaurus* remains from Portugal. 613 pp. **Ten article-based thesis**.
Supervisor: Octávio Mateus.

University of Bristol, Bristol, United Kingdom.
MSc in Palaeobiology. 2007-2008.
Thesis: Diversity and disparity in sauropod dinosaurs. 113 pp.
Supervisors: Steve Brusatte, Mark Young, Emily Rayfield, Marcello Ruta and Paul Barrett.

University of Queensland, Brisbane, Australia.
General English (Advanced level). 02/2007-04/2007.

Université de Liège, Liège, Belgium.
Licence in Geology. 2001-2006.
Thesis: Morphofunctional analysis of spinosaurid quadrates. 194 pp.
Supervisors: Eric Buffetaut, Edouard Poty and Jean-Marie Cordy.

HONORS AND AWARDS

2008 Winner of the competition for the best poster from the M level unit on Dinosaurs, University of Bristol.
2006 Winner of the AGAB (Association des Géologues Amateurs de Belgique) price for the best final thesis.

FUNDING

2013	Fundação para a Ciência e a Tecnologia	PhD Grant	11760 €
2012	Fundação para a Ciência e a Tecnologia	PhD Grant	12810 €
2011	The Palaeontological Society	Travel Grants	100 £
2011	Fundação para a Ciência e a Tecnologia	PhD Grant	12810 €
2010	Fundação para a Ciência e a Tecnologia	Supplemental Training Activities	893 €
2010	European Science Foundation	Short Visit Grant	722 €
2010	Fundação para a Ciência e a Tecnologia	PhD Grant	13810 €
2006	Association des Géologues Amateurs de Belgique	Thesis Award	1000 €
2005	Europalia.Russia	Travel Award	2500 €

PUBLICATIONS

Monographic Work

Hendrickx, C. and Mateus, O. 2014. Abelisauridae (Dinosauria: Theropoda) from the Late Jurassic of Portugal and dentition-based phylogeny as a contribution for the identification of isolated theropod teeth. *Zootaxa* 3759 (1): 1–74.

Published Articles

Hendrickx, C., Mateus, O. and Araújo, R. 2014. The dentition of megalosaurid theropods. *Acta Palaeontologica Polonica*: 1–45. DOI:10.4202/app.00056.2013 (in press).

Hendrickx, C. and Mateus, O. 2014. *Torvosaurus gurneyi* n. sp., the largest terrestrial predator from Europe, and a proposed terminology of the maxilla anatomy in nonavian theropods. *PLoS ONE* 9 (3): e88905. 1–25.

Araújo, R., Castanhinha, R., Martins, R. M. S., Mateus, O., **Hendrickx, C.**, Beckmann, F., Schell, N. and Alves, L. C. 2013. Filling the gaps of dinosaur eggshell phylogeny: Late Jurassic theropod clutch with embryos from Portugal. *Scientific Reports* 3 (1924): 1–8.

In Press/In Review

Hendrickx, C., Mateus, O. and Araújo, R. in press. A proposed terminology of theropod teeth (Saurischia: Dinosauria). *Journal of Vertebrate Paleontology*.

Hendrickx, C., Hartman, S. and Mateus, O. in press. An overview on non-avian theropod discoveries and classification. *PalArch's Journal of Vertebrate Palaeontology*.

Hendrickx, C., Mateus, O and Buffetaut, E. in review (accepted). Morphofunctional analysis of the quadrate of Spinosauridae (Dinosauria: Theropoda) and the first definitive evidence of two cohabiting *Spinosaurus* in the Upper Cretaceous of Northern Africa. *PLoS ONE*.

Hendrickx, C., Araújo, R. and Mateus, O. in review (accepted). The nonavian theropod quadrate I: standardized terminology and overview of the anatomy, function and ontogeny. *PeerJ*. (*PeerJ PrePrints* 2:e379v1. http://dx.doi.org/10.7287/peerj.preprints.379v1).

Hendrickx, C., Araújo, R. and Mateus, O. in review (accepted). The nonavian theropod quadrate II: systematic usefulness, major trends and cladistic and phylogenetic morphometrics analyses. *PeerJ*. (*PeerJ Preprints*. 2:e380v1. http://dx.doi.org/10.7287/peerj.preprints.380v1).

Hendrickx, C., Mateus, O. and Araújo, R. in review (accepted). The distribution of dental features in non-avian theropods. *Palaeontologia Electronica*.

In Preparation

Hendrickx, C., Ezcurra, M. and Mateus, O. in prep. On the tooth of *Aerosteon* (Theropoda: Megaraptora) and the dentition of Megaraptoridae.

Published Oral Presentations

Hendrickx, C., Mateus, O. and Araújo, R. 2014. The dentition of megalosaurids, with a proposed terminology on theropod teeth. In: Delfino, M., Carnevale, G., and Pavia, M. (Eds.). *Abstract Book and Field Trip Guide, XII Annual Meeting of the European Association of Vertebrate Palaeontologists. Museo Regionale di Scienze Naturali, Torino*, p. 75.

Hendrickx, C. and Mateus, O. 2012. Ontogenetical changes in the quadrate of basal tetanurans. In: Royo-Torres, R., Gascó, F. and Alcalá, L. (editors). *10th Annual Meeting of the European Association of Vertebrate Palaeontologists, Terruel, Spain. ¡Fundamental!*, p. 101-104.

Hendrickx, C. and Mateus, O., 2012. Deducting behaviour of dinosaurs: spinosaur theropods feeding. *9th National Congress of Ethology.* (12th-13th of April 2012, Lisbon, Portugal). p. 26-27.

Hendrickx, C. and Buffetaut, E. 2008. Functional interpretation of spinosaurid quadrates (Dinosauria: Theropoda) from the Mid Cretaceous of Morocco. In: *56th Annual Symposium of Vertebrate Palaeontology and Comparative Anatomy, Dublin, Ireland.* (September 2nd-6th 2008). p. 25-26.

Published Poster Presentations

Hendrickx, C., Mateus, O. and Araújo, R. 2014. The distribution of dental features in non-avian theropods and a proposed terminology of theropod teeth. *74th Annual Meeting of the Society of Vertebrate Paleontology, Berlin, Germany.* (November 5-8, 2014). p. 146.

Hendrickx, C., Araújo, R. and Mateus, O., 2012. The nonavian theropod quadrate : systematic usefulness, major trends and phylogenetic morphometrics analysis. *72nd Annual Meeting of the Society of Vertebrate Paleontology, Raleigh, USA.* (October 17-20, 2012). p. 110.

Hendrickx, C. and Mateus, O., 2011. Using dentition-based phylogeny of nonavian theropod teeth for resolving isolated teeth identification to the genus level. *55th Annual Meeting of The Palaeontological Association, Plymouth, U.K.* (17th-20th December 2011).

Hendrickx, C. and Buffetaut, E., 2009. Morphofunctional analysis of spinosaurid quadrates. *EAVP Extraordinary Meeting, Brussels, Belgium.* (February 9th-14th, 2009).

Hendrickx, C., Brusatte, S., Young, M., Rayfield, E., Ruta, M. and Barrett, P., 2009. Diversity and disparity in sauropod dinosaurs. *EAVP Extraordinary Meeting, Brussels, Belgium.* (February 9th-14th, 2009).

TEACHING EXPERIENCE

05/2013	**A Short Introduction on Feeding Mechanisms in Tetrapods**. Class given as part of the Master Program in Paleontology, Universidade Nova de Lisboa.
12/2012	**A Short Introduction on Cladistics**. Class given as part of the Master Program in Paleontology, Universidade Nova de Lisboa.
11/2012	**A Short Introduction on Phylogenetic Morphometric**. Class given as part of the Master Program in Paleontology, Universidade Nova de Lisboa.

ATTENDED COURSES

10/2010	**Digitalized Imagery and FEA in Paleontology** by Dr. Mike Polcyn and Ricardo Araújo (SMU), Southern Methodist University, Texas, U.S.
04/2010	**Paleohistology Short Course** by Prof. Martin Sander (University of Bonn), University of Bonn, Bonn, Germany.
03/2010	**Geometric Morphometrics and Phylogeny** by Dr. Chris Klingenberg (University of Manchester), Transmitting Science, Universitat Autònoma de Barcelona, Barcelona, Spain.

INVITED TALKS, PRESS ARTICLES AND INTERVIEWS

TV News and Documentaries

02/2015	"Les Indiana Jones d'aujourd'hui". Tout s'explique, RTL-TVI (Belgian TV Show).
06/2014	"Belgische dino in Antwerpen". Ketnet (Belgian TV Show for children).
06/2014	"Vleesetende dinosaurus die we nog niet kennen in Antwerpen Centraal". VRT (Belgian TV News; 06/23/14).
06/2014	"Grootste Europese roofdier op Dino-expo". VTM (Belgian TV News; 06/23/14).
06/2014	" Le cousin du T-rex au Jurassic Park d'Hanovre et bientôt à Anvers". RTBF (Belgian TV News; 06/18/14).

Radio Interviews and Press Articles

09/2014 "L'ADN de… Christophe Hendrickx, paléontologue". ATHENA n°303 (Belgian newspaper).
08/2014 "Belge, scientifique et expatrié". Daily Science (Online Media; 08/07/2014).
08/2014 "Le plus grand prédateur de l'histoire est à Anvers". Le Soir Magazine (Belgian newspaper).
07/2014 "*Torvosaurus gurneyi*, the European T-rex". This View of Live (Online newspaper; 07/21/2014).
06/2014 "Un dinosaure belge exposé à Anvers". BEL RTL (Belgian radio; 06/24/2014).
06/2014 "Les dinosaures sont à nos portes". Vers l'Avenir (Belgian newspaper and Webdoc; 06/21/2014).
03/2014 "The largest terrestrial predator from Europe". BBC1 (English radio; 03/05/2014).

Invited talks

03/2013 "What's new in the world of theropods?". 10° Mini Symposium on Paleontology, Museu da Lourinhã, Portugal.
10/2010 "Evolution of teeth and tooth-bearing bones in nonavian theropods". Southern Methodist University, Texas, USA.
01/2010 "Evolution of teeth and feeding related bones in nonavian theropods". PhD Program Presentation, Departamento de Ciências da Terra, Universidade Nova de Lisboa, Portugal.
01/2010 "The diversity and disparity in sauropod dinosaurs". 9° Mini Symposium on Paleontology, Museu da Lourinhã, Portugal.
01/2010 "A Short Introduction on Evolution" (Part I and II)." 8° Mini Symposium on Paleontology, Museu da Lourinhã, Portugal.
10/2009 "Les dinosaures théropodes, témoins de l'évolution." Festival des Petits Explorateurs, Vannes, France.
10/2009 "The Big Lizard Story." (Café des Sciences) Festival des Petits Explorateurs, Vannes, France.
08/2009 "Spinosauridae, these fish-eating dinosaurs." 7° Mini Simposium on Paleontology, Museu da Lourinhã, Portugal.
03/2009 "Les Spinosauridae, des dinosaures géants mangeurs de poissons." Association des Géologues Amateurs de Belgique, Centre Culturel de Chênée, Belgium.

RESEARCH INTERESTS

My current research interests can be divided into four main themes:

1. **The systematic usefulness of theropod teeth.**
2. **The evolution and ontogeny of teeth, and quadrate in nonavian theropods.**
3. **The functional anatomy of spinosaurid mandibular articulation.**
4. **The theropod fauna of Late Jurassic ecosystems of Portugal.**

PROFESSIONAL EXPERIENCE

02/2006-03/2006 Professional work placement of two weeks in the «Bureau Conseil en Géologie », Namur (Belgium) managed by Benoît André. The work consisted of geophysical prospecting to resolve hydrogeological questions.

10/2005-04/2006 Engaged by the University of Liège (Belgium) to enforce and inform smokers about new regulations established by the University.

Several student jobs in different sectors including agricultural and café work.

MUSEUM EXPERIENCE

07/2014 Scientific adviser at Dino Expo Adventure in Antwerpen, Belgium.

09/2008 - 2009	Scientific adviser at the Festival des Petits Explorateurs in Vannes, France.
06/2008	Scientific adviser at the Explore-at-Bristol Museum in Bristol, England.

FIELD EXPERIENCE

2009 - 2013	Lourinhã Formation, Lourinhã, Portugal, Late Jurassic. Dinosaurs, pterosaurs, crocodiles, turtles.
2010 - 2011	Grès de Silves Formation, Algarve, Portugal, Late Triassic. Temnospondyls.
2005	Udurchukan Formation, Blagoveschensk, Russia, Late Cretaceous. Lambeosaurinae.
2001 - 2002	Marnes Rouges Inférieures Formation, Département de l'Aude, France, Late Cretaceous. Dinosaurs.

JOURNALS REFEREED

- PLoS ONE.
- Palaeogeography, Palaeoclimatology, Palaeoecology.
- Acta Palaeontologica Polonica.
- Journal of African Earth Sciences.
- Scottish Journal of Geology.

PROFESSIONAL MEMBERSHIPS

- European Association of Vertebrate Paleontologists.
- Palaeontological Association.
- Society of Vertebrate Paleontology.
- The Paleontological Society.

LANGUAGES

- French native language.
- Fluent in English (IELTS Overall Band Score 6.5).
- Basic knowledge of Dutch and Portuguese.

COMPUTER KNOWLEDGE

Proficient in all Microsoft Office packages (Windows, Word, Excel, Power Point, Photo Editor, Paint etc...) as well as Corel Draw, ArcView, Adobe Illustrator, Adobe Photoshop, Inkscape, Gingko, StanMode, Matlab, Paup*, TNT, WinClada, Minitab, Mesquite, Tps, MorphoJ, and Past3.

Able to perform:

- **Cladistic analysis** (Mesquite, TNT, WinClada).
- **Geometric morphometric analysis** (MorphoJ).
- **Phylogenetic morphometric analysis** (TNT).
- **Discriminant and cluster analyses** (Past3).
- **Disparity analysis** (Gingko, RARE).

INTERESTS

- **Palaeontology**: Interested in dinosaurs and palaeontology since the age of six. French ambassador on an expedition to excavate dinosaur bones in Siberia organised by the Royal Belgian Institute of Natural Sciences and conducted by the Belgian palaeontologist Pascal Godefroit. Visited the palaeontological collections of 30 scientific institutions of Europe, U.S., Argentina, and Qatar.

- **Sciences and History:** General interest in natural sciences, astronomy and archaeology.
- **Travel**: Have visited Eastern Europe as well as Russia, U.S., Chile, Argentina, Qatar, Australia, Madagascar, Morocco, Mauritius, South Africa, and Tanzania (Kilimanjaro climbing).
- **Sports and health**: Currently enjoy running and swimming on a leisurely basis. I have practised a lot of other sports such as surfing, cycling, tennis, tennis table, badminton and rowing. I'm a non-smoker.
- **Scientific websites for the general public**: Have created several articles on dinosaurs on the French Wikipedia[1] and an all-comprehensive website on Spinosauridae[2].

REFERENCES

Stephen Brusatte, PhD
School of GeoSciences,
University of Edinburgh,
The King's Buildings,
James Hutton Road
Edinburgh EH9 3FE
United Kingdom
Stephen.Brusatte@ed.ac.uk

Octávio Mateus, PhD
Departamento de Ciências da Terra,
Faculdade de Ciências e Tecnologia,
Universidade Nova de Lisboa,
Caparica, 2829-516
Portugal
omateus@fct.unl.pt

Ricardo Araújo, PhD
Huffington Department of Earth Sciences,
Southern Methodist University,
PO Box 750395,
Dallas, 75275-0395
Texas, USA
rmaraujo@smu.edu

[1] e.g., http://fr.wikipedia.org/wiki/Spinosaurus (**featured article**) and http://fr.wikipedia.org/wiki/Spinosauridae
[2] http://spinosauridae.fr.gd/